SITE-SELECTIVE REACTIONS VIA SCAFFOLDING CATALYSIS & SYNTHESIS AND BINDING STUDY OF 1,2-AZABORINES

Author: Hyelee Lee

Boston College

The Graduate School of Arts and Sciences

Department of Chemistry

SITE-SELECTIVE REACTIONS VIA SCAFFOLDING CATALYSIS &

SYNTHESIS AND BINDING STUDY OF 1,2-AZABORINES

A dissertation

by

HYELEE LEE

submitted in partial fulfillment of the requirements

for the degree of

Doctor of Philosophy

April 2017

SITE-SELECTIVE REACTIONS VIA SCAFFOLDING CATALYSIS &

SYNTHESIS AND BINDING STUDY OF 1,2-AZABORINES

by

HYELEE LEE

Dissertation Advisors:

Dr. Kian L. Tan and Professor Shih-Yuan Liu

Abstract

Chapter 1. In the Tan laboratory, we developed synthetic methods to control reaction selectivity (regio-, stereo-, and site-selectivity) using scaffolding catalysis. Our strategy utilizes directing groups that induce intramolecularity through the formation of a labile covalent bond between the substrate and a binding site in a catalytic system. In the first part, we described site-selective functionalization of various carbohydrates and complex polyhydroxylated molecules which contain *cis*-1,2-diol motif using a chiral organic scaffold. In the second part, *meta*-selective C–H functionalization of arenes was demonstrated. High *meta*-selectivity was achieved by the use of a nitrile-based silyl tether which is cleavable and recyclable.

Chapter 2. In the Liu laboratory, we focuses on studies of boron-nitrogen containing heterocycles. In this chapter, synthesis of 1,2-azaborines and their binding study with T4 lysozyme mutants were described. Specifically, we directly compared binding of NH-containing 1,2-azaborines and their carbonaceous analogs to probe hydrogen bonding

interaction between the NH group of azaborine and a carbonyl oxygen of protein residue. Structural and thermodynamic analysis provided us the first evidence of H-bonding of azaborines with a biological macromolecule.

Chapter 3. Described are the synthesis of regioisomers of ethyl-substituted 1,2-azaborines and their binding thermodynamics to T4 lysozyme mutants. To access the azaborine ligands used in the binding study, we developed synthetic methods for regioselective functionalization of six positions of 1,2-azaborines. Isothermal titration calorimetry experiments showed differences in binding free energy for regioisomers to the L99A T4 lysozyme. This result could originate from electronic differences of the isosteric ligands inducing dipole-dipole interaction between ligand and surrounding protein residues or it may be from local dipolar interactions.

Chapter 4. A general method for late-stage *N*-functionalization of 1,2-azaborines is described to afford libraries of BN-containing complex molecules. The chemical transformations include electrophilic substitution reactions, N–C(sp^2) bond forming reactions under Buchwald-Hartwig amination conditions, and N–C(*sp*) bond forming reactions using copper-catalyzed *N*-alkynylation. As applications in materials science and medicinal chemistry, synthesis of the first parental BN isostere of *trans*-stilbene and lisdexamfetamine derivative is described utilizing the methodology developed in this work.

List of Abbreviations

Å	Angstrom
Ac	Acetyl
atm	Atmosphere(s)
B_2pin_2	bis-Pinacolatodiboron
Bn	Benzyl
Boc	*tert*-Butoxycarbonyl
br	Broad
Bu	Butyl
COD	1,5-Cyclooctadiene
Cy	Cyclohexyl
d	Doublet
DART	Direct analysis in real time
dba	Dibenzylideneacetone
dd	Doublet of doublets
DIPEA	Diisopropylethylamine
DMF	*N*,*N*-Dimethylformamide
dt	Doublet of triplets
DTBP	Di-*tert*-butyl peroxide
dtbpy	4,4'-Di-*tert*-butyl-2,2'-bipyridyl
EDTA	Ethylenediaminetetraacetic acid
ee	Enantiomeric excess
Et	Ethyl

eq	Equation
equiv	Equivalent(s)
GC	Gas chromatography
h	Hour(s)
HPLC	High performance liquid chromatography
HRMS	High resolution mass spectrometry
i-	Iso
IPTG	Isopropyl-β-D-thiogalactopyranoside
IR	Infrared
LB	Luria–Bertani
m	Multiplet
M	Molar
*m*CPBA	*meta*-Chloroperbenzoic acid
Me	Methyl
Mes	Mesityl
min	Minute(s)
Ms	Mesyl
MTBE	*tert*-Butylmethyl ether
n-	Normal
NMI	*N*-Methylimidazole
NMO	*N*-Methylmorpholine *N*-oxide
NMR	Nuclear magnetic resonance
OD	Optical density

Pd/C	Palladium on carbon
Ph	Phenyl
PMP	1,2,2,6,6-Pentamethylpiperidine
ppm	Parts per million
PPTS	Pyridinium *para*-toluene sulfonic acid
Pr	Propyl
p-TsOH	*para*-Toluenesulfonic acid
q	Quartet
RT	Room temperature
s	Singlet
t	Triplet
t-	Tertiary
TBAF	*tetra*-Butylammonium fluoride
TBS	*tert*-Butyl dimethyl silyl
TES	Triethyl silyl
THF	Tetrahydrofuran
TLC	Thin layer chromatography
TMS	Trimethylsilyl
UV	Ultraviolet

Table of Contents

Chapter 1: Site-Selective Reactions *via* Scaffolding Catalysis

1.1 Introduction

There are growing demands to improve efficiency of synthesis by avoiding pre-functionalization. As a consequence, selective functionalization is desired to synthesize complex molecules in shorter steps (i.e. by involving late-stage modification). However, controlling reaction selectivity (site-, regio-, and stereo-) still remains one of the main challenges for synthetic chemists when the precursor to the target compound displays multiple similarly reactive sites. Creating strategies and methodologies that robustly solve selectivity issues offers to solve synthetic challenges in an array of chemical space. For example, traditional methods for site-selective functionalization of carbohydrates typically feature protection-deprotection sequences; a representative four-step protocol to monoacetylate α-D-galactose (**1.1**) at the C2-OH position (Scheme 1.1) amply demonstrates the inefficiency inherent to this approach.[1] It requires several purification steps and results in loss of overall yield.

[1] Barili, P. L.; Berti, G.; Catelani, G.; Colonna, F.; Marra, A. *Tetrahedron Lett.* **1986**, *27*, 2307–2310.

Scheme 1.1 Traditional method for acetylation of methyl α-D-galactose C2-OH

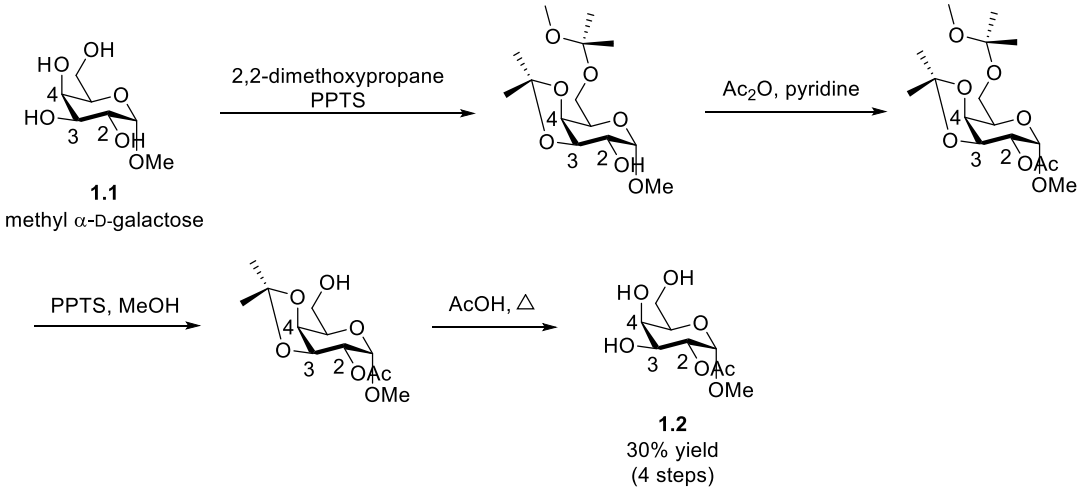

Similarly, selective activation of a specific arene C–H bond would enable more streamlined syntheses of drugs and natural products. Early methods relied on substrate control in the form of electronic and steric differences among *ortho*-, *meta*-, and *para*-positions induced by the substituents already present. More recent developments in directing group-assisted and catalyst- and ligand-controlled reactions have paved the way to control reaction selectivity. This approach obviates use of protecting group strategy or functional group manipulation. A recent example by Baran and Yu demonstrates the power of site-selective functionalization to enable more efficient syntheses.[2] The authors reported a short synthesis of (+)-hongoquercin A (**1.4**) through consecutive late-stage C–H alkylation and oxidation of compound **1.3a**, which can be accessed from (+)-sclareolide in seven steps (Scheme 1.2, eq. 1). This new method avoids the need for pre-functionalized

[2] Rosen, B. R.; Simke, L. R.; Thuy-Boun, P. S.; Dixon, D. D.; Yu, J.-Q.; Baran, P. S. *Angew. Chem. Int. Ed.* **2013**, *52*, 7317–7320.

starting materials such as **1.5**, which had been used in previous syntheses.[3] Direct C–H functionalization also allows diversity-oriented synthesis to prepare analogs of (+)-hongoquercin A; thus, in addition to methylation, compound **1.3a** or **1.3b** can undergo a range of other *ortho*-directed C–H functionalization reactions, including longer-chain alkylation, lactonization, oxidation, vinylation, amination, arylation, and carbonylation (Scheme 1.2, eq. 2).

[3] For previous syntheses of (+)-hongoquercin A, see: a) Tsujimori, H.; Bando, M.; Mori, K. *Eur. J. Org. Chem*. **2000**, 297–302. b) Kurdyumov, A. V.; Hsung, R. P. *J. Am. Chem. Soc.* **2006**, *128*, 6272–6273.

Scheme 1.2 Synthesis of (+)-hongoquercin A and its analogs by C–H functionalization

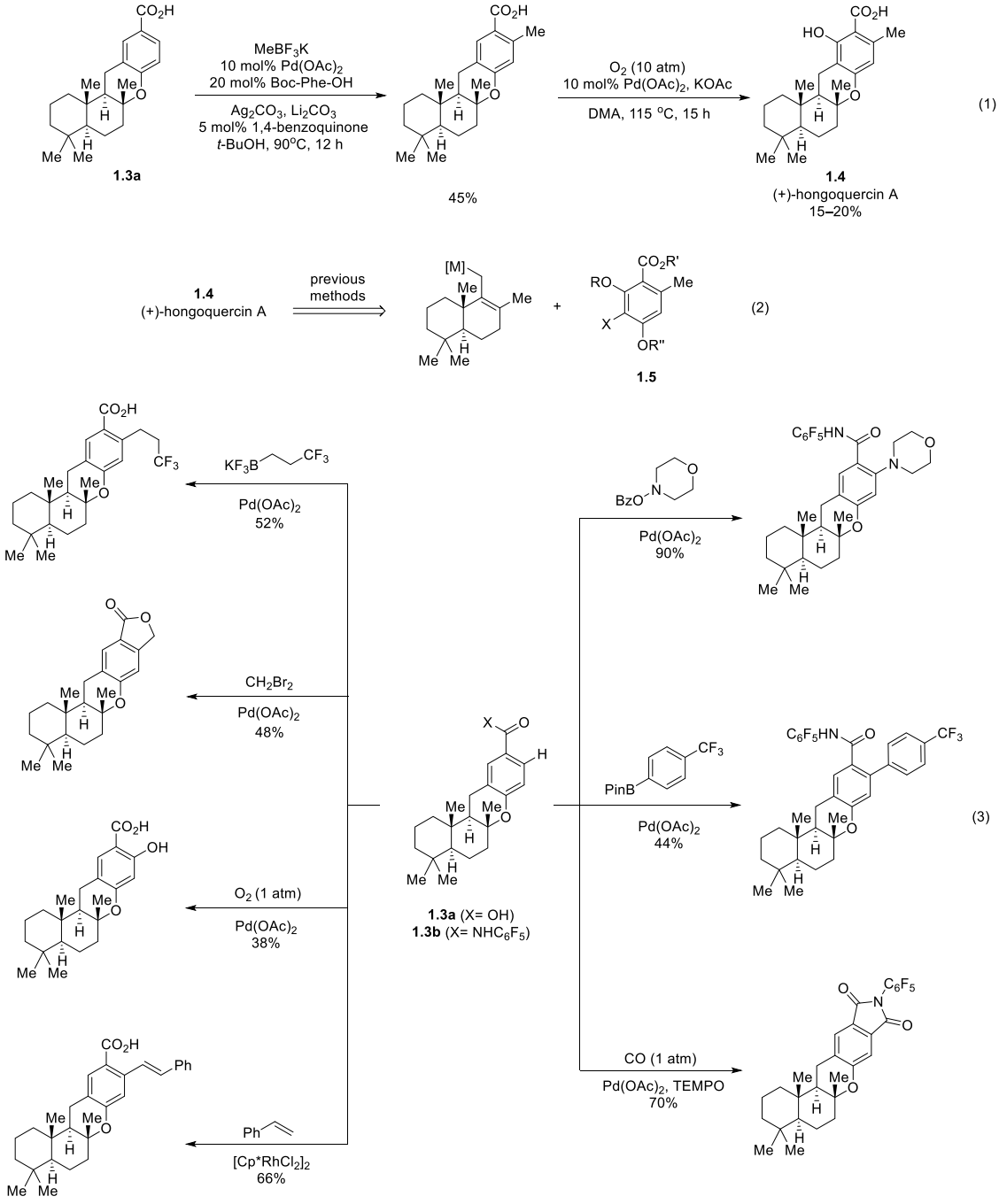

1.2 Background

1.2.1 Directing Groups in Site-Selective Functionalization

In 1973, Breslow demonstrated the feasibility of using a stoichiometric directing group covalently and irreversibly bound to the substrate to control the reaction selectivity.[4] Specifically, he employed a remote benzophenone group to achieve selective dehydrogenation of the C14–C15 bond in steroid derivative **1.6**; the reaction selectivity is believed to derive from the structural rigidity of **1.6** during photoloysis as this maintains the required proximity of the benzophenone unit to the C14–C15 bond (Scheme 1.3).

Scheme 1.3 Selective oxidation of steroid ester using benzophenone as a directing group

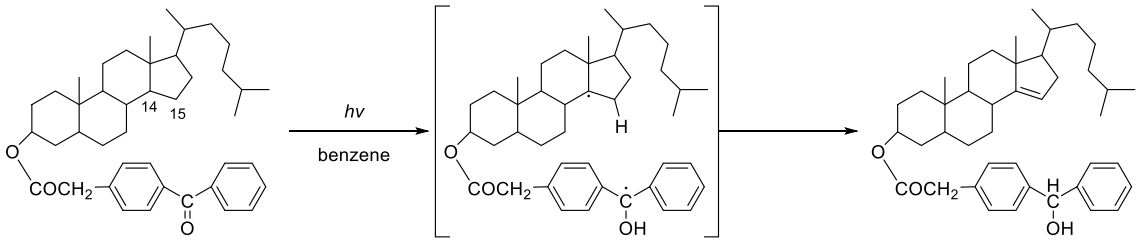

1.6 **1.7** 55% yield

More recently, there have been intensive studies of directed reactions through metal complexation for geometric pre-organization of reaction components. Through the complex formation selective functionalization at a desired site can be achievable. In this process, the use of a proximal directing group plays a key role in controlling selectivity.

[4] Breslow, R.; Baldwin, S.; Flechtner, T.; Kalicky, P.; Liu, S.; Washburn, W. *J. Am. Chem. Soc.* **1973**, *95*, 3251–3262.

The Sharpless epoxidation of allylic alcohols serves as a classic example of this strategy (Scheme 1.4).[5] The chemoselectivity arises from geometric control exerted by coordination of the titanium catalyst to the allylic alcohol and *t*-butylhydroperoxide. The enantioselectivity observed in product **1.9** is the result of (+)-diethyl tartrate inducing a chiral environment for the peroxide oxygen atom to approach from the *Re* face of the alkene.

Scheme 1.4 Sharpless epoxidation of allylic alcohol

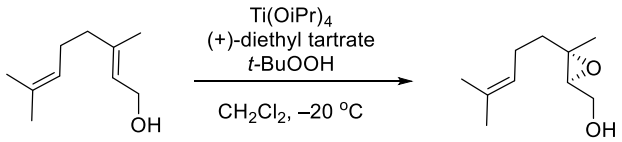

1.8 **1.9** 77% yield 95% ee

C–H activation has been the focus of intense research efforts for the past several decades and generally requires some form of directing group to achieve site-selectivity. Notably, the directing groups most commonly used in arene C–H activation reactions, pyridine, amide, carboxylate, imine, oxime, and oxazoline, involve coordination of one or more heteroatoms to a catalytic metal center.[6] One of the early examples of pyridine used for directing effect can be found in Moore's regioselective acylation of the aromatic C–H

[5] Katsuki, T.; Sharpless, K. B. *J. Am. Chem. Soc.* **1980**, *102,* 5974–5976.

[6] For selected reviews on C–H activation, see: (a) Shilov, A. E.; Shul'pin, G. B. *Chem. Rev.* **1997**, *97*, 2879–2932. (b) Davies, H. M. L.; Beckwith, R. E. J. *Chem. Rev.* **2003**, *103*, 2861–2903. (c) Omae, I. *Coord. Chem. Rev.* **2004**, *248*, 995–1023. (d) Colby, D. A.; Bergman, R. G.; Ellman, J. A. *Chem. Rev.* **2010**, *110*, 624–655. (e) Yeung, C. S.; Dong, V. M. *Chem. Rev.* **2011**, *111*, 1215–1292. (f) Kuhl, N.; Hopkinson, M. N.; Wencel-Delord, J.; Glorius, F. *Angew. Chem. Int. Ed.* **2012**, *51*, 10236–10254. (g) Lyons, T. W.; Sanford, M. S. *Chem. Rev.* **2010**, *110*, 1147–1169. (h) Giri, R.; Shi, B.-F.; Engle, K. M.; Maugel, N.; Yu, J.-Q. *Chem. Soc. Rev*. **2009**, *38*, 3242–3272.

bond *ortho* to the pyridyl nitrogen. The recation afforded the desired *ortho*-functionalized product **1.11** in 65% yield with 93:7 linear:branched selectivity for carbonyl insertion (Scheme 1.5, eq. 1).[7] A plausible mechanism involves the nucleophlic attack of pyridine on the metal center and *ortho*-metalation to form a bridged intermediate and successive olefin coordination and insertion. Murai reported a direct, site-selective alkylation of arenes using a ketone directing group.[8] Catalyst insertion takes place exclusively at the *ortho* C–H bond of the benzene ring in **1.12**. The coordination of the substrate's carbonyl oxygen to the ruthenium metal center enforces the proximity of the catalyst to the *ortho* C–H bond, subsequently leading to formation of a metallacycle through oxidative insertion (Scheme 1.5, eq. 2).

[7] Moore, E.J.; Pretzer, W. R.; O'Connell, T. J.; Harris, J.; LaBounty, L.; Chou, L.; Grimmer, S. S. *J. Am. Chem. Soc*. **1992**, *114*, 5888–5980.
[8] Murai, S.; Kakiuchi, F.; Sekine, S.; Tanaka, Y.; Kamatani, A.; Sonoda, M.; Chatani, N. *Nature* **1993**, *366*, 529–531.

Scheme 1.5 Directing groups in metal-catalyzed selective C–H activation

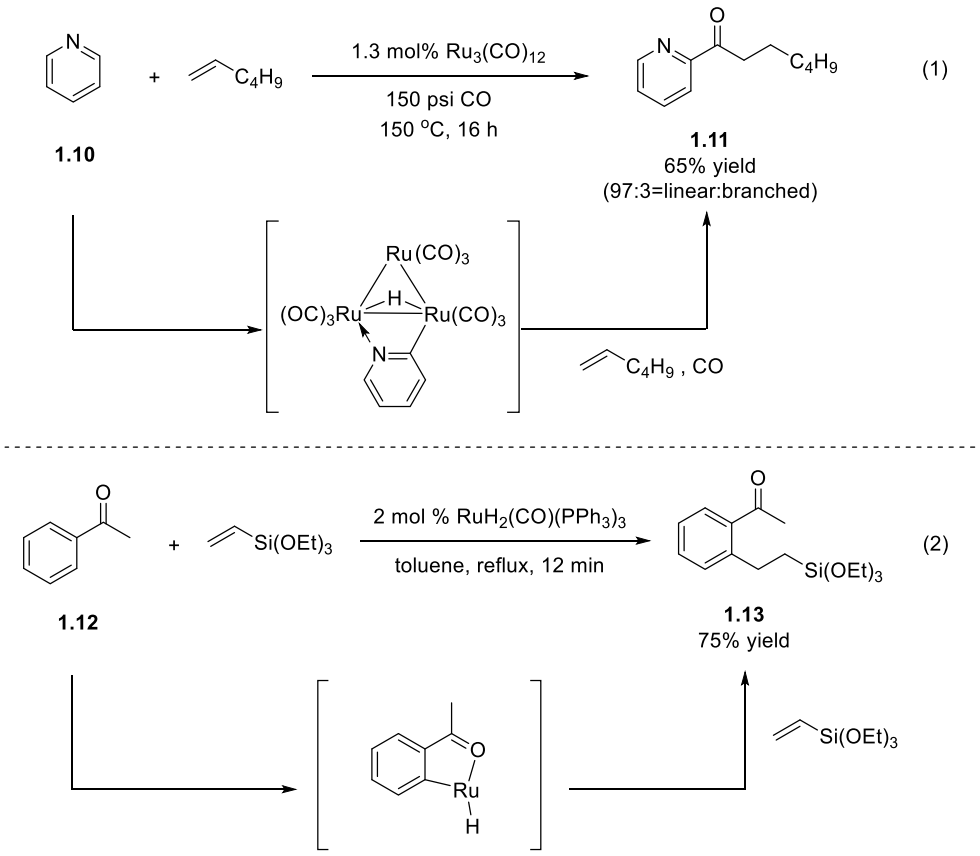

1.2.2 Site-Selective Functionalization of Complex Molecules

Controlling selectivity in natural product synthesis and late-stage derivatization of complex molecules is crucial in terms of synthetic efficiency and biological application. The Miller group has demonstrated remarkable progress in catalyst-controlled functionalization of complex, multi-functional, natural products, most notably erythromycin A, vancomycin, and teicoplanin.[9] In 2006, using peptide-based chiral catalyst 1.15, they achieved selective acetylation of erythromycin A (**1.14**)'s C11-OH to

[9] (a) Lewis, C. A.; Miller, S. J. *Angew. Chem. Int. Ed*. **2006**, *45*, 5616–5619. (b) Pathak, T. P.; Miller, S. J. *J. Am. Chem. Soc*. **2012**, *134*, 6120–6123. (c) Han, S.; Miller, S. J. *J. Am. Chem. Soc.* **2013**, *135*, 12414–12421.

afford **1.16** in 58% yield (Scheme 1.6, eq. 1).[9a] More recently, they demonstrated site-selective phosphorylation of teicoplanin using three distinct peptide-based catalysts (**1.17a–c**) to target three different hydroxyl groups (Scheme 1.6, eq. 2).[9c] The key interaction in this example is mutiple hydrogen bonds between the substrate and the side chain from the peptide-based catalyst. Structural rigidity of the catalyst induced by internal hydrogen bonding also contributes to spatial control for selective functionalization.

Scheme 1.6 Catalyst-controlled site-selective derivatization of complex molecules

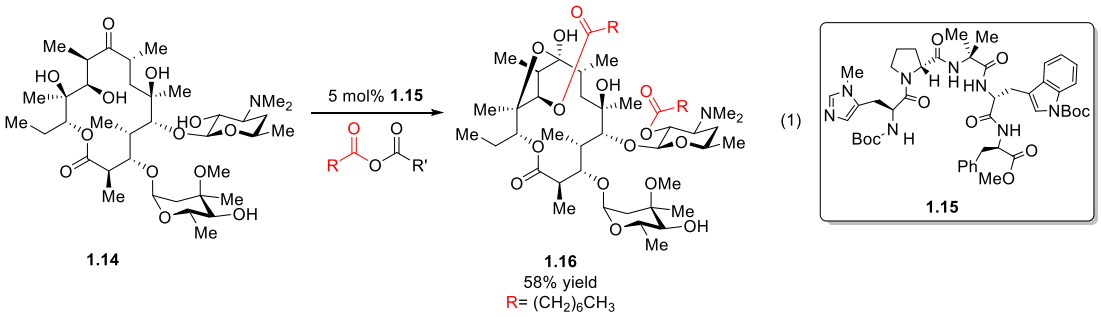

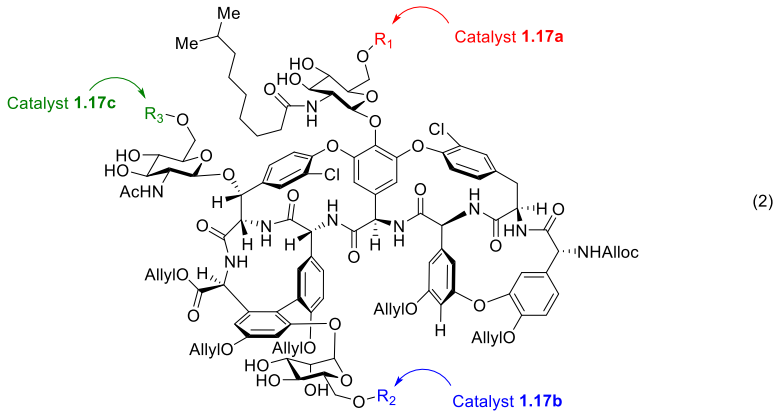

substrate: R_1, R_2, R_3 = H
product: **1.18** 42% yield (R_1= PO(OPh)$_2$, R_2, R_3 = H) with 10 mol% **1.17a**
1.19 23% yield (R_2= PO(OPh)$_2$, R_1, R_3 = H) with 20 mol% **1.17b**
1.20 41% yield (R_3= PO(OPh)$_2$, R_1, R_2 = H) with 30 mol% **1.17c**

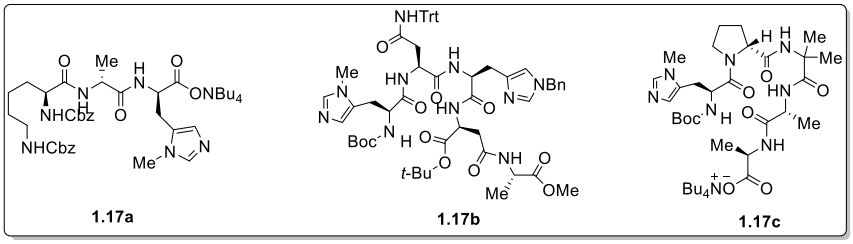

Late-stage functionalization of unactivated C–H bonds in complex molecules has been a rapidly growing research area in the last decade.[10] The White group in 2007 demonstrated

[10] For selected examples, see: (a) Godula, K.; Sames, D. *Science* **2006**, *312*, 67–72. (b) Yamaguchi, J.; Yamaguchi, A. D.; Itami, K. *Angew. Chem. Int. Ed.* **2012**, *51*, 8960–9009. (c) Y. Ishihara and P. S. Baran, *Synlett*, **2010**, *12*, 1733–1745. (d) McMurray, L.; O'Hara, F.; Gaunt, M. J. *Chem. Soc. Rev.* **2011**, *40*, 1885–

that both steric and electronic factors contribute to predictable selectivity in iron-catalyzed aliphatic C–H oxidation of complex molecules.[11] The authors anticipated site-selective oxidation of (+)-artemisinin (**1.21**) would occur at the C10 position, which is electron-rich and less sterically hindered compared to other tertiary C–H bonds in the molecule. As predicted, reaction with hydrogen peroxide (H_2O_2) in the presence of electrophilic iron catalyst (**1.22**) afforded (+)-10β-hydroxyartemisinin (**1.23**) (Scheme 1.7, eq. 1). In contrast, when they subjected (–)-α-dihydropicrotoxinin (**1.24**) to the same oxidation conditions, 92% of the starting material was recovered, which can be rationalized by deactivation of the isopropyl tertiary C–H bond due to both electronic and steric factors (Scheme 1.7, eq. 2).

1898. (e) Wencel-Delord, J.; Glorius, F. *Nature. Chem.* **2013**, *5*, 369–375. (f) Davies, H. M. L.; Denton, J. R. *Chem. Soc. Rev*. **2009**, *38*, 3061–3071. (g) Gutekunst, W. R.; Baran, P. S. *Chem. Soc. Rev*. **2011**, *40*, 1976–1991. (h) Dai, H.-X.; Stepan, A. F.; Plummer, M. S.; Zhang, Y.-H.; Yu, J.-Q. *J. Am. Chem. Soc.* **2011**, *133*, 7222–7228. (i) Gormisky, P. E.; White, M. C. *J. Am. Chem. Soc*. **2013**, *135*, 14052–14055. (j) Larsen, M. A.; Hartwig, J. F. *J. Am. Chem. Soc.* **2014**, *136*, 4287–4299. (k) White, K. L; Movassaghi, M. *J. Am. Chem. Soc.* **2016**, *138*, 11383–11389. (l) He, J.; Hamann, L.G.; Davies, H. M. L.; Beckwith, R. E. J. *Nat. Commun.* **2015**, *6*, 5943.

[11] Chen, M. S.; White, M. C. *Science* **2007**, *318*, 783–787.

Scheme 1.7 Selective aliphatic C–H bond oxidations with **1.22** of natural products

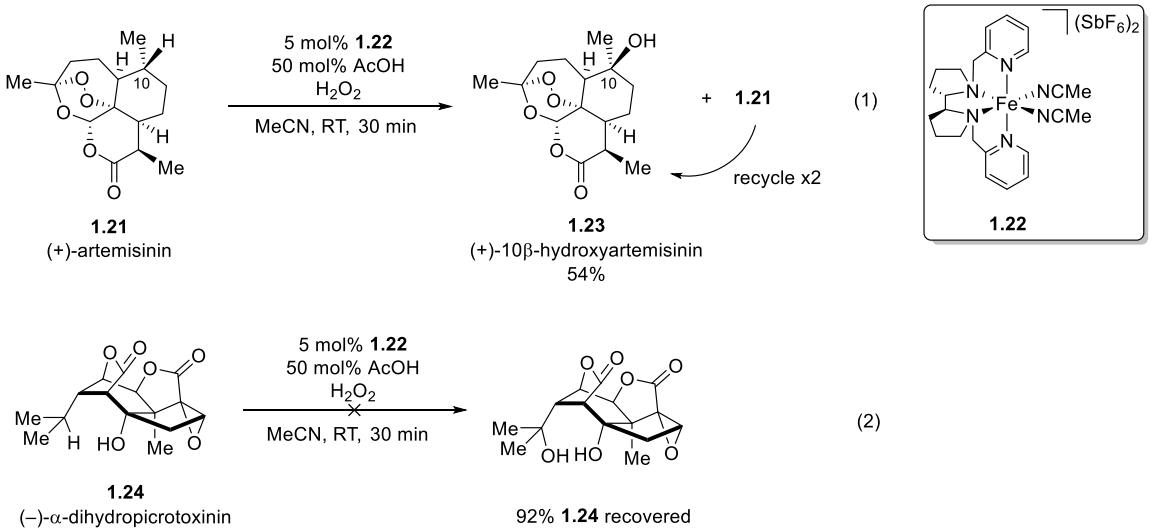

In 2009, the Baran group reported a highly efficient site-selective oxidation of primary and secondary C–H bonds to synthesize a series of eudesmane terpenes.[12] Inspired by terpene biosynthesis, they designed and succesfully demonstrated site-selective oxidation by innate and guided C–H functionalization logic.[13] Installation of the trifluoroethyl carbamate directing group on the C3–OH of dihydrojunenol (**1.25**) afforded a common precursor (Scheme 1.8, **1.26**). Site-specific C1–H oxidation was achieved to afford the corresponding oxidized product **1.27** by reaction with methyl(trifluoromethyl)dioxirane (TFDO). The origin of site-selectivity was later experimentally explained by strain release effects due to the presence of a 1,3-diaxial interaction.[14] Basic hydrolysis led to the final desired product, 4-epiajanol (**1.28**). Dihydroxyeudesmane (**1.30**) was accessed by site-selective halogenation at C5 position, followed by cyclization and hydrolysis of the

[12] Chen, K.; Baran, P. S. *Nature* **2009**, *459*, 824–828.
[13] Brückl, T.; Baxter, R. D.; Ishihara, Y.; Baran, P. S. *Acc. Chem. Res*. **2012**, *45*, 826–839.
[14] Chen, K.; Eschenmoser, A.; Baran, P. S. *Angew. Chem. Int. Ed.* **2009**, *48*, 9705–9708.

brominated intermediate (**1.29**). Site-selective bromination occurs at C5 position because geometric constraints prevents the directing group from reaching C1 position (Scheme 1.8).

Scheme 1.8 Total syntheses of 4-epiajanol and dihydroxyeudesmane *via* site-specific C–H oxidations

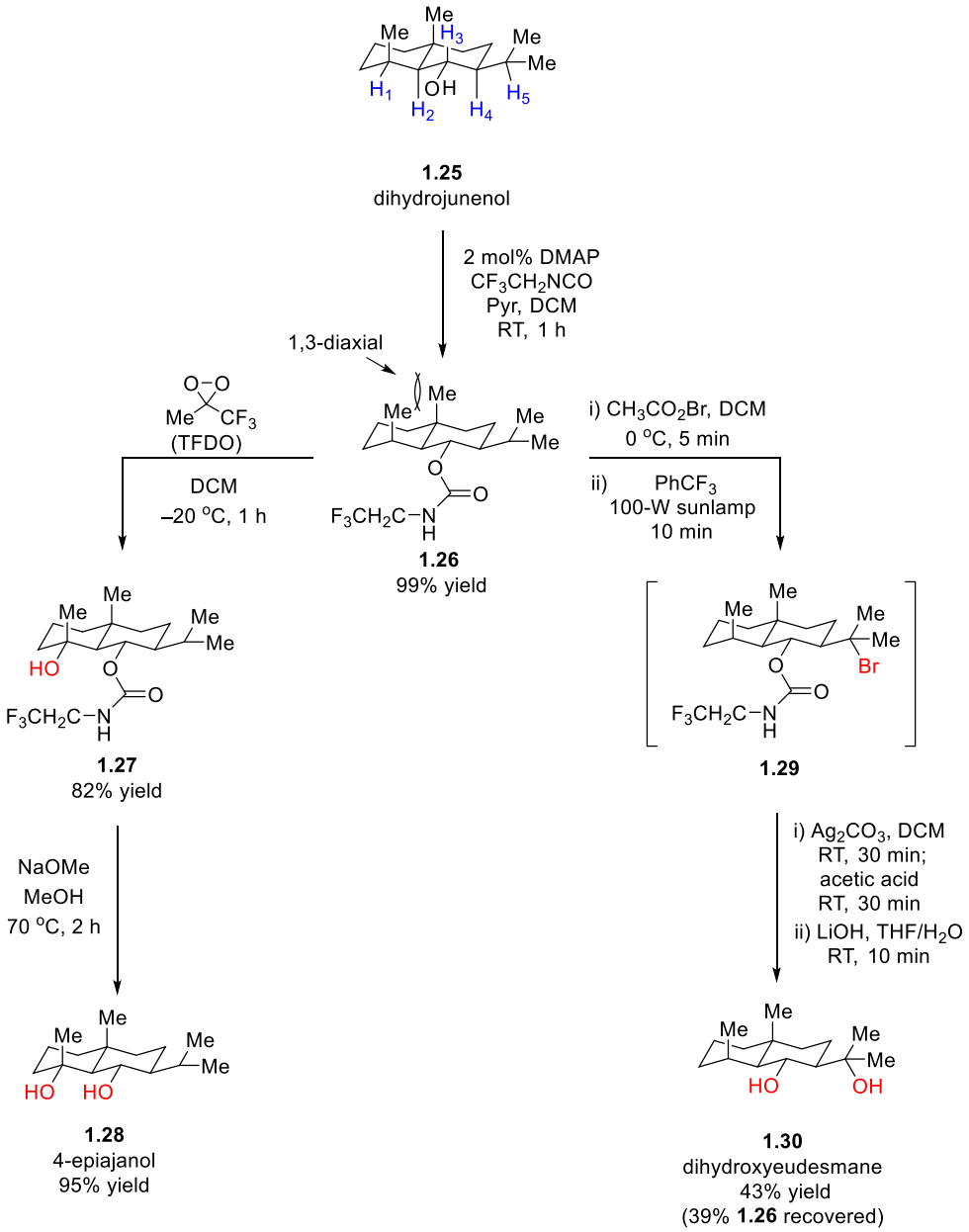

1.2.3 Catalyst-Controlled Selective Functionalization of Carbohydrates

1.2.3.1 Metal-Catalyzed Reactions

Selective functionalization or temporary protection of carbohydrates can be achieved *via* complexation of a diol unit within the substrate to a metal species. It typically proceeds through selective activation of one of the hydroxyl groups coordinated to the metal center. This strategy has been found most commonly effective using tin reagents.[15] In 2000, Matsumura demonstrated regioselective monobenzoylation of the C2-hydroxyl group of glucose derivative **1.31** using a catalytic amount of Me_2SnCl_2 (Scheme 1.9, eq. 1).[16] Tin coordination to the *cis*-1,2-diol motif comprising C1-OMe and C2-OH leads to benzoylation at the equatorial C2 position. More recently, Muramatsu reported chemo- and regioselective functionalization of unprotected carbohydrates also using tin-based catalysts.[17] An anomeric mixture of methyl D-glucoside (**1.33** and **1.34**) underwent benzoylation with high chemo- and regioselectivity to produce either C2- or C6-functionalized products depending on the alkyl substituents on the tin catalyst (Scheme 1.9, eq. 2). The reaction was found to proceed well with various acylating and sulfonylating electrophiles. When Bu_2SnCl_2 is used as catalyst, formation of intermediate **1.37** from methyl α-D-glucoside **1.33** is kinetically favored (Figure 1.1a); which undergoes functionalization at the C2-OH to form the desired product **1.35**. The other possible intermediates **1.38** and **1.39** are destabilized by 1,3-diaxial interactions between the Sn-Bu

[15] (a) Wagner, D.; Verheyden, J. P. H.; Moffatt, J. G. *J. Org. Chem*. **1974**, *39*, 24–30. (b) Munavu, R. M.; Szmant, H. H. *J. Org. Chem*. **1976**, *41*, 1832–1836. (c) Nashed, M. A.; Anderson, L. *Tetrahedron Lett.* **1976**, *17*, 3503–3506. (d) Tsuda, Y.; Haque, M. E.; Yoshimoto, K. *Chem. Pharm. Bull.* **1983**, *31*, 1612–1624. (e) Nicolaou, K. C.; van Delft, F. L.; Conley, S. R.; Mitchell, H. J.; Jin, Z.; Rodrı´guez, R. M. *J. Am. Chem. Soc.* **1997**, *119*, 9057–9058.

[16] Iwasaki, F.; Maki, T.; Onomura, O,; Nakashima, W.; Matsumura, W. *J. Org. Chem.* **2000**, *65*, 996–1002.

[17] Muramatsu, W.; Takemoto, Y. *J. Org. Chem*. **2013**, *78*, 2336–2345.

group and the axial C4 and C6 protons (Figure 1.1b). The reaction with Me_2SnCl_2 occurs selectively at the sterically less hindered hydroxyl group at C6 of methyl β-D-glucoside **1.34** through the intermediate **1.38**. The origin of the selectivity was explained by anomeric effect as depicted in Figure 1.1c. They rationalized that nucleophilicity of C6-OH in the minor isomer **1.39** is weakened by anomeric effect compared to the case in the major isomer **1.38** (Figure 1.1c). This chemistry is one of the very few examples wherein catalyst control affords reactivity at the more sterically hindered secondary alcohol in the presence of primary alcohol.

Scheme 1.9 Chemo- and regioselective functionalization of carbohydrates using tin reagents

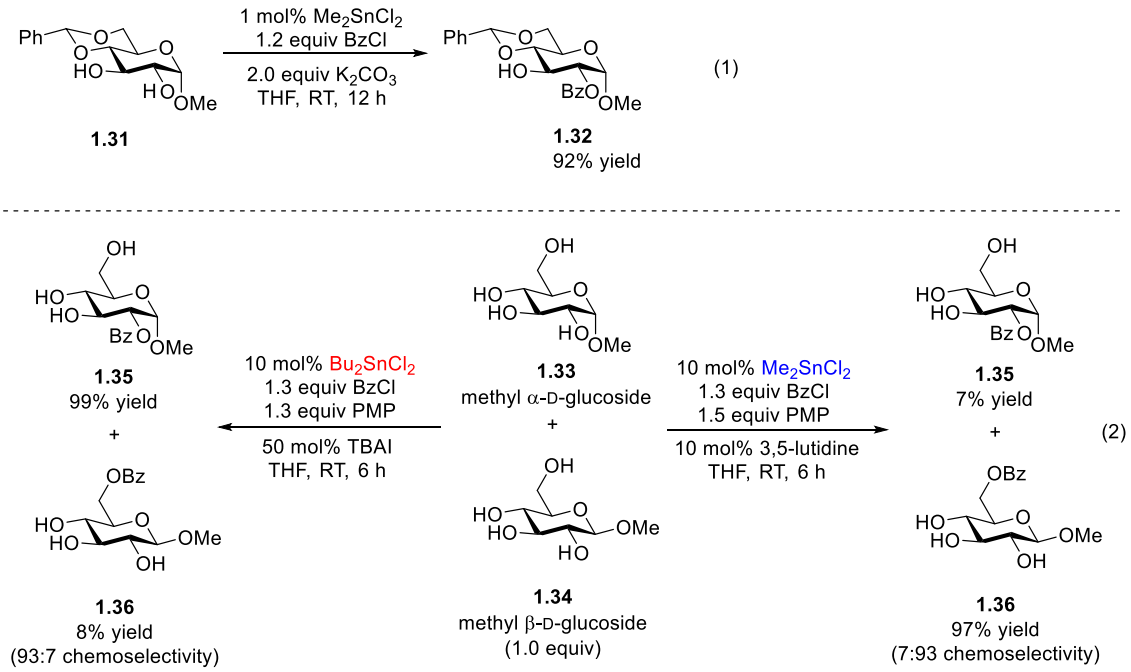

Figure 1.1 Rationale for chemo- and regioselectivity

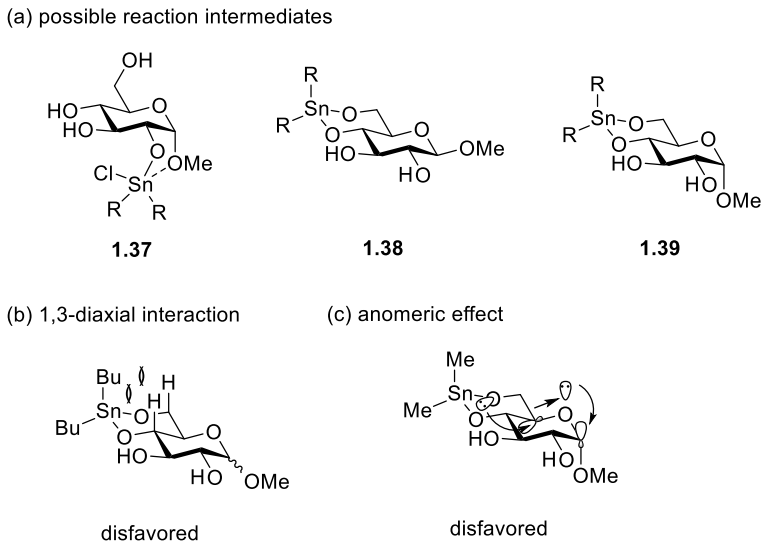

1.2.3.2 Organocatalyst-Controlled Reactions

Regioselective functionalization of carbohydrates has also been accomplished using organocatalysts. The Taylor group employed diarylborinic acid derivatives to selectively control the reactivity of carbohydrate secondary hydroxyl groups through specific catalyst binding of substrate *cis*-1,2-diol units. [18] Specifically, they reported selective transformation with a variety of electrophiles to afford C3-functionalized methyl α-L-fucopyranosides (Scheme 1.10). [19] Diphenylborinic acid **1.41** forms tetra-coordinated organoboron complex **1.42** with the substrate C3 and C4-OH groups; of these two activated hydroxyls, the equatorial C3-OH is more reactive and therefore undergoes subsequent

[18] (a) Chan, L.; Taylor, M. S. *Org. Lett*., **2011**, *13*, 3090–3093. (b) Dimitrijevic, E; Taylor, M. S. *ACS Catal*. **2013**, *3*, 945–. (c) Taylor, M. S. *Acc. Chem. Res*. **2015**, *48*, 295–305. (d) Tanveer, K.; Jarrah, K.; Taylor, M. S. *Org. Lett*. **2015**, *17*, 3482–3485. (e) Mancini, R. S.; Lee, J. B.; Taylor, M. S. *Org. Biomol. Chem*. **2017**, *15*, 132–143.

[19] (a) Lee, D.; Taylor, M. S. *J. Am. Chem. Soc*. **2011**, *133*, 3724–3727. (b) Lee, D.; Williamson, C. L.; Chan, L.; Taylor, M. S. *J. Am. Chem. Soc*. **2012**, *134*, 8260–8267.

functionalization. This chemistry was further developed to achieve glycosylation of carbohydrates for efficient oligosaccharide synthesis and derivatization of complex molecules.[20]

Scheme 1.10 Regioselective functionalization of carbohydrates using a diarylborinic acid-derived catalyst

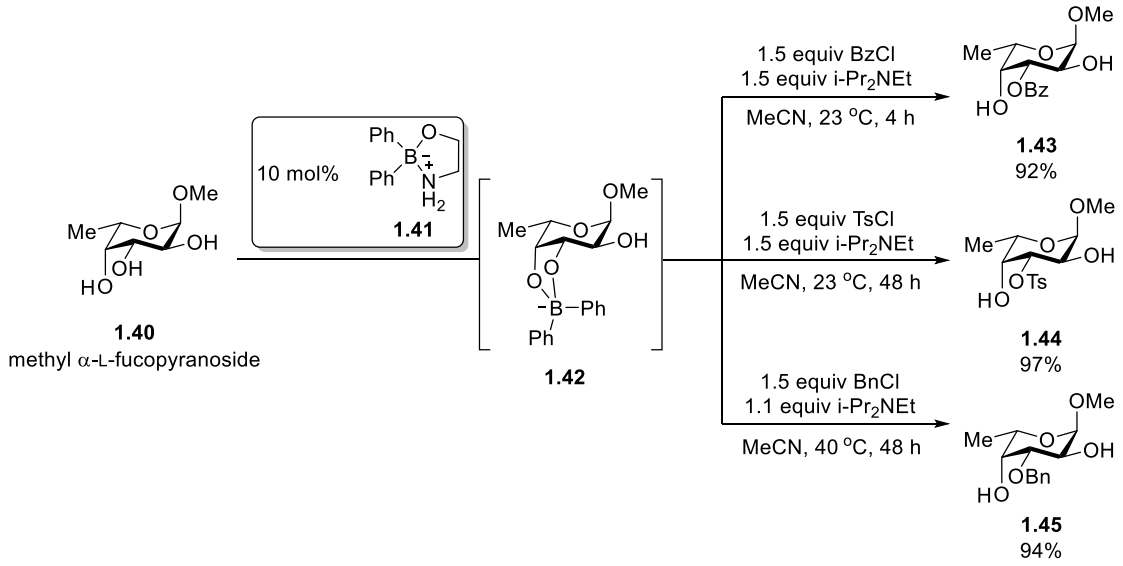

Inspired by enzyme-catalyzed reactions, the Miller group developed peptide-based catalysts for use in various asymmetric chemical transformations including site-selective functionalization of diols and carbohydrates.[21] The catalyst's peptide residues form

[20] (a) Gouliaras, C.; Lee, D.; Chan, L.; Taylor, M. S. *J. Am. Chem. Soc*. **2011**, *133*, 13926–13929. (b) Beale, T. M.; Taylor, M. S. *Org. Lett.* **2013**, *15*, 1358–1361. (c) McClary, C. A.; Taylor, M. S. *Carbohydrate Res*. **2013**, *381*,112–122. (d) Beale, T. M.; Moon, P. J.; Taylor, M. S. *Org. Lett*. **2014**, *16,* 3604–3607. (e) Mancini, R. S.; McClary, C. A.; Anthonipillai, S.; Taylor, M. S. *J. Org. Chem*. **2015**, *80*, 8501–8510. (f) D'Angelo, K. A.; Taylor, M. S. *J. Am. Chem. Soc*. **2016**, *138*, 11058–11066.

[21] For selected examples, see: (a) Jarvo, E. R.; Miller, S. J. *Tetrahedron* **2002**, *58*, 2481–2495. (b) Colby Davie, E.; Mennen, S. M.; Xu, Y.; Miller, S. J. *Chem. Rev*. **2007**, *107*, 5759–5812. (c) Giuliano, M. W.; Miller, S. J. *Top. Curr. Chem*. **2016**, *372*, 157–201. (d) Miller, S. J.; Copeland, G. T.; Papaioannou, N.; Horstmann, T. E.; Ruel, E. M. *J. Am. Chem. Soc.* **1998**, *120*, 1629–1630. (e) Lewis, C. A.; Sculimbrene, B. R.; Xu, Y.; Miller, S. J. *Org. Lett.* **2005**, *7*, 3021–3023.

multiple hydrogen bonds with the substrate of interest to achieve a specific reaction geometry that selectively brings one substrate functional unit into proximity of the catalysts' activating group. C3-acetylation of glucosamine analog **1.46** was achieved using penta-peptide **1.47** with good conversion and excellent selectivity (Scheme 1.11).[22] Variation of the peptide sequence facilitated expansion of the substrate scope to include molecules bearing polyol functionality as discussed in section 1.2.2.[9]

Scheme 1.11 Miller's peptide-based catalyst in controlling site-selectivity of acetylation

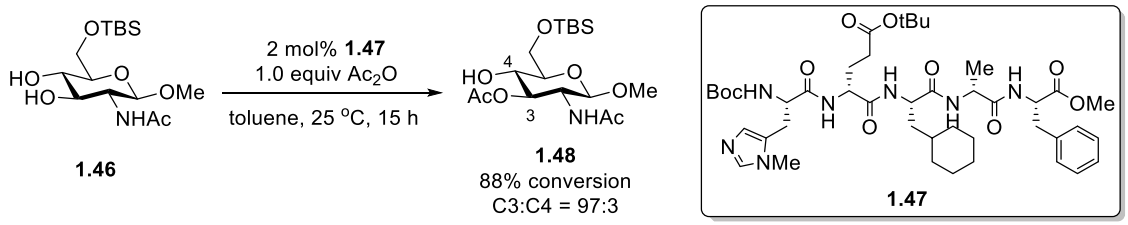

Kawabata's C_2-symmetric DMAP catalyst provides another example of an organocatalyst-controlled reaction.[23] Specifically, chiral catalyst **1.50** afforded site-selective acylation at C4-OH of octyl β-D-glucopyranoside (**1.49**) (Scheme 1.12). They achieved high regioselectivity for this position (C2:C3:C4:C6= 0:<1:>99:0) even in the presence of the more reactive primary hydroxyl group at C6. The authors' rationale for this selectivity involves a hydrogen bond between the primary C6 hydroxyl group and the catalyst's amide carbonyl group. This molecular interaction consequently brings C4

[22] Griswold, K.S.; Miller, S. J. *Tetrahedron* **2003**, *59*, 8869–8875.
[23] (a) Kawabata, T.; Muramatsu, W.; Nishio, T.; Shibata, T.; Schedel, H. *J. Am. Chem. Soc*. **2007**, *129*, 12890–12895. (b) Yoshida, K.; Furuta, T.; Kawabata, T. *Tetrahedron Lett.* **2010**, *51*, 4830–4832.

hydroxyl into close proximity to the acyl pyridinium catalytic site. Additional hydrogen bonding of substrate C3-OH with the NH group of the catalyst indole moiety also contributes to the regioselectivity by further constraining the catalyst-bound substrate to a specific orientation (Figure 1.2).

Scheme 1.12 Kawabata's C_2-symmetric DMAP-derived catalyst in regioselective C4-functionalization

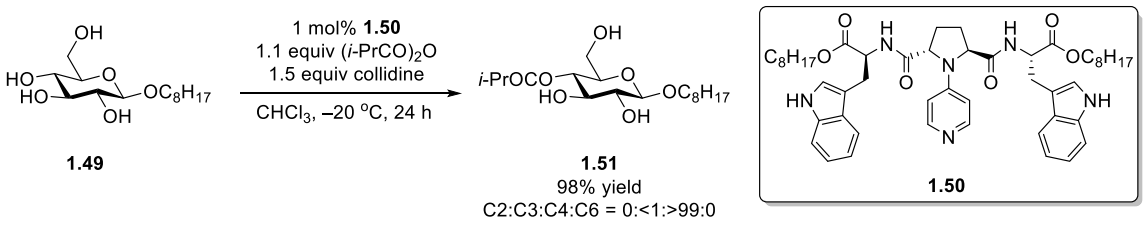

Figure 1.2 Transition state that rationalizes the C4 regioselectivity

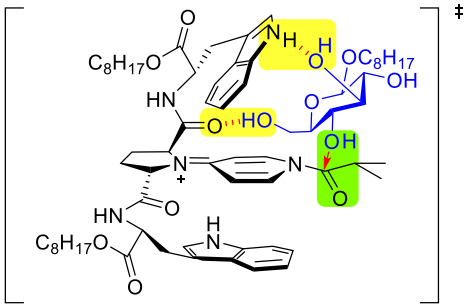

1.2.4 Scaffolding Catalysis

1.2.4.1 Catalyst Mode of Action

To address similar synthetic problems, the Tan group developed catalysts to control reaction selectivity through reversible, covalent substrate binding. The general proposed

cycle for these catalysts is shown in Figure 1.3.[24] Well-defined, rigid catalyst-substrate interactions *via* a single binding point induces a state of temporary intramolecularity between the substrate molecule and an activating residue on the catalyst. This proximity in turn accelerates a specific chemical transformation to lead to the product of interest. Dissociation of the converted product regenerates the catalyst, thus rendering the directing group catalytic.

Figure 1.3 Proposed catalytic cycle for a scaffolding catalyst

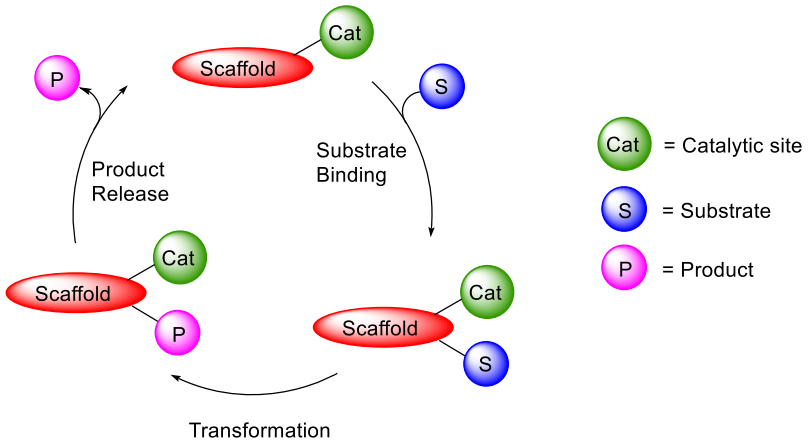

1.2.4.2 Desymmetrization of *meso*-1,2 -Diols

One of the Tan group's initial applications of scaffolding catalysis featured the desymmetrization of *meso*-1,2-diols. Enantioselective desymmetrization of *meso*-1,2-diols has previously been reported by other groups using various catalytic functionalizations

[24] (a) Tan, K. L. *ACS Catal*. **2011**, *1*, 877–886. (b) Tan, K. L.; Sun, X.; Worthy, A. D. *Synlett* **2012**, *23*, 321–325.

including acylation, sulfonylation, phosphorylation, and silylation.[25] In 2001, Ishikawa reported the first example of asymmetric silylation of secondary alcohols by using chiral guanidine derivatives.[25f] Kinetic resolution of indanol **1.52** was achieved by silyl transfer with a stoichiometric amount of the chiral base **1.53** to yield 79% silylated (*R*)-indanol **1.54** in 58% ee (Scheme 1.13).

Scheme 1.13 Asymmetric silylation of indanol using a chiral guanidine

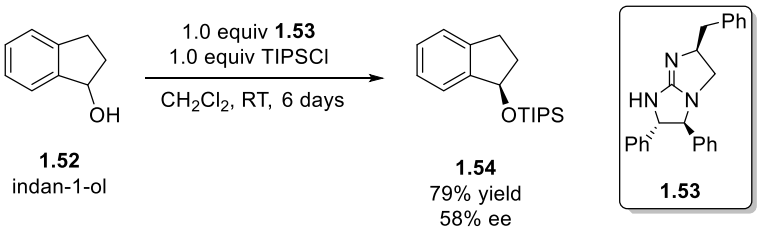

In 2006, Hoveyda and Snapper demonstrated effective enantioselective silylation of 1,2- and 1,3-diols using peptide-based catalysts, with enantioselectivities up to 96% ee (Scheme 1.14).[25h] They proposed that hydrogen bonding interactions between the diol substrate and the side chains of the catalyst leads to one enantiotopic diol substrate selectively undergoing silylation (Figure 1.4). In their initial mechanistic model, the role

[25] (a) Oriyama, T.; Imai, K.; Sano, T.; Hosoya, T. *Tet. Lett.* **1998**, *39*, 3529–3532. (b) Spivey, A. C.; Arseniyadis, S. *Top. Curr. Chem.* **2010**, *291*, 233–280. (c) Sculimbrene, B.; Morgan, A.; Miller, S. *J. Am. Chem. Soc*. **2002**, *124*, 11653–11656. (d) Jordan, P. A.;Kayser-Bricker, K. J.; Miller, S. J. *Proc. Natl. Acad. Sci. U. S. A.* **2010**, *107*, 20620–20624. (e) Fiori, K. W.; Puchlopek, A. L. A.; Miller, S. J. *Nat. Chem*. **2009**, *1*, 630–634. (f) Isobe, T.; Fukuda, K.; Araki, Y.; Ishikawa, T. *Chem. Commun*. **2001**, 243–244. (g) Zhao, Y.; Mitra, A. W.; Hoveyda, A. H.; Snapper, M. L. *Angew. Chem. Int. Ed*. **2007**, *46*, 8471–8474. (h) Zhao, Y.; Rodrigo, J.; Hoveyda, A. H.; Snapper, M. L. *Nature* **2006**, *443*, 67–70. (i) You, Z.; Hoveyda, A. H.; Snapper, M. L. *Angew. Chem., Int. Ed*. **2009**, *48*, 547–550. (j) Rodrigo, J. M.; Zhao, Y.; Hoveyda, A. H.; Snapper, M. L. *Org. Lett*. **2011**, *13*, 3778–3781. (k) Mannville, N.; Alite, H.; Haeffner, F.; Hoveyda, A. H.; Snapper, M. L. *Nature Chem.* **2013**, *5*, 768–774. (l) Weickgenannt, A.; Mewald, M.; Oestreich, M. *Org. Biomol. Chem*. **2010**, *8*, 1497–1504.

of the *N*-methylimidazole group was hypothesized to consist mainly of activating the silyl chloride. Based on their observation of the original reaction to be second-order in peptide catalyst, the catalytic system was further developed to enhance reaction efficiency by the aid of an achiral co-catalyst, 2-ethylthiotetrazole.[25k] In this example of dual catalysis, computational study suggested that deprotonated tetrazole serves as a nucleophilic co-catalyst to activate silyl chloride while the imidazole unit of the chiral catalyst is involved in deprotonation of alcohol substrate acting as a Brønsted base (Figure 1.5).

Scheme 1.14 Hoveyda-Snapper's peptide-based chiral catalyst in desymmetrization of alcohols

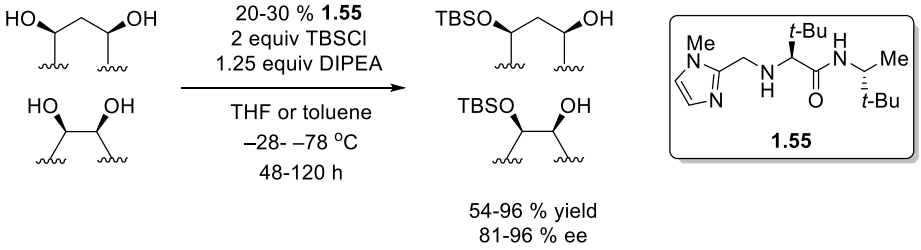

Figure 1.4 Initially proposed transition state model for enantioselective silylation using a peptide-based catalyst

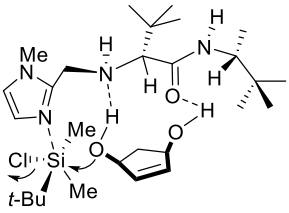

Figure 1.5 Proposed transition state model for enantioselective silylation in dual catalysis

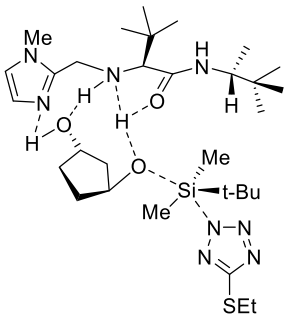

In 2011, we reported desymmetrization of *cis*-1,2-diols using scaffolding catalysts.[26] The catalyst was designed to benefit from induced temporal intramolecularity as discussed in section 1.2.4.1. It contains three main features: 1) oxazoline-based *N*,*O*-acetal substrate binding site to exchange with alcohol, 2) *N*-methylimidazole as a catalytic site, 3) amino alcohol-based chiral backbone to control stereoselectivity (Figure 1.6). We envisioned that inducing temporary intramolecularity during a reaction through a reversible covalent bond would result in both rate acceleration and high enantioselectivity.

Figure 1.6 Key features of scaffolding catalyst

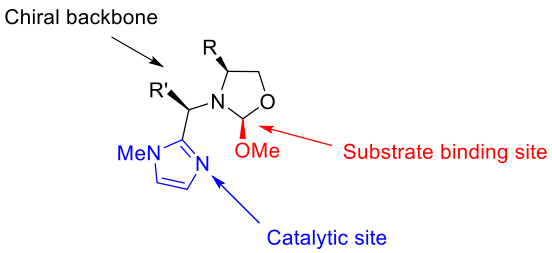

[26] Sun, X.; Worthy, A. D.; Tan, K. L. *Angew. Chem. Int. Ed.* **2011**, *50*, 8167–8171.

The chiral catalyst **(–)-1.56** successfully afforded desymmetrization of various *meso*-1,2-diols *via* silyl transfer with high yields and enantioselectivities under mild conditions (Table 1.1). We proposed that a reversible covalent bond between the chiral catalyst and the diol substrate is essential for high enantioselectivity. To rule out the possibility of the catalyst operating by alternative mechanisms involving non-covalent interactions with substrate, we attempted silylation of 1,2-cyclopentane diol with control catalyst **1.68** which lacks the ability to covalently bind substrates (Scheme 1.15). Both reaction yield and enantioselectivity suffered with **1.68** as compared to results with catalyst **(–)-1.56**, consistent with our hypothesis that covalent catalyst-substrate bonding plays a major role in achieving high reactivity and stereoselectivity.

Table 1.1 Desymmetrization of *meso*-1,2-diols using scaffolding catalysts

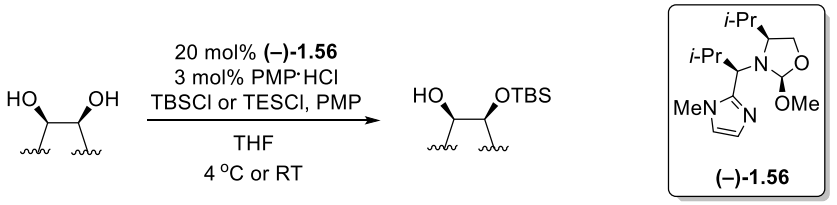

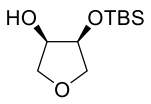	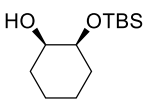	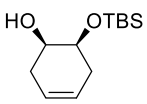	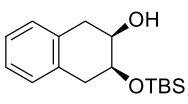	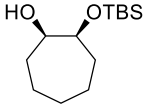
1.57 79% yield 89% ee	**1.58** 86% yield 92% ee	**1.59** 87% yield 90% ee	**1.60** 88% yield 95% ee	**1.61** 82% yield 90% ee
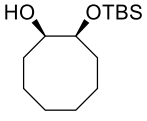	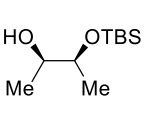	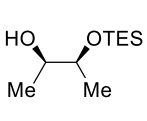	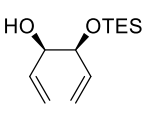	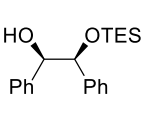
1.62 93% yield 86% ee	**1.63** 78% yield 90% ee	**1.64** 84% yield 92% ee	**1.65** 82% yield 92% ee	**1.66** 70% yield 88% ee

Scheme 1.15 Silyl transfer reaction of 1,2-cyclopentane diol using a control catalyst

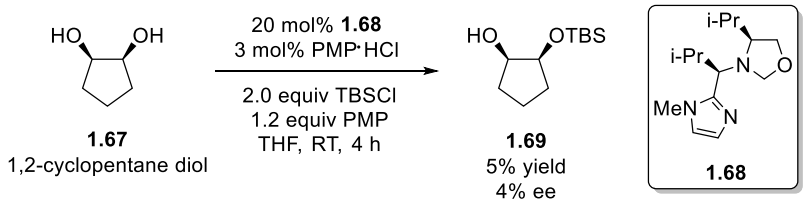

1.3 Site-Selective Functionalization of 1,2-Diols of Carbohydrates[27]

1.3.1 Importance of Polyhydroxylated Molecules

Polyhydroxylated moieties are conspicuously prevalent molecules that participate in critical biological processes (Figure 1.7). More specifically, species featuring carbohydrate groups in particular have been found to frequently play significant roles in the processes associated with cell growth, intercellular communication, and immune responses.[28] Carbohydrates also notably compose the core structures of numerous antimicrobial and anticancer agents.

[27] Sun, X.; Lee, H.; Lee, S.; Tan, K. L. *Nature Chem.* **2013**, *5*, 790–795.
[28] (a) van Kooyk, Y.; Rabinovich, G. A. *Nature Immunol.* **2008**, *9*, 593–601. (b) Feizi, T. *Nature* **1985**, *314*, 53–57. (c) Crocker, P. R.; Feizi, T. *Curr. Opin. Struct. Biol.* **1996**, *6*, 679–691. (d) Liedtke, S.; Geyer, H.; Wuhrer, M.; Geyer, R.; Frank, G.; Gerardy-Schahn, R.; Zahringer, U.; Schachner, M. *Glycobiology* **2001**, *11*, 373–384. (e) Almkvist, J.; Karlsson, A. *Glycoconjugate* J. **2004**, *19*, 575–581.

Figure 1.7 Polyhydroxylated molecules found in nature

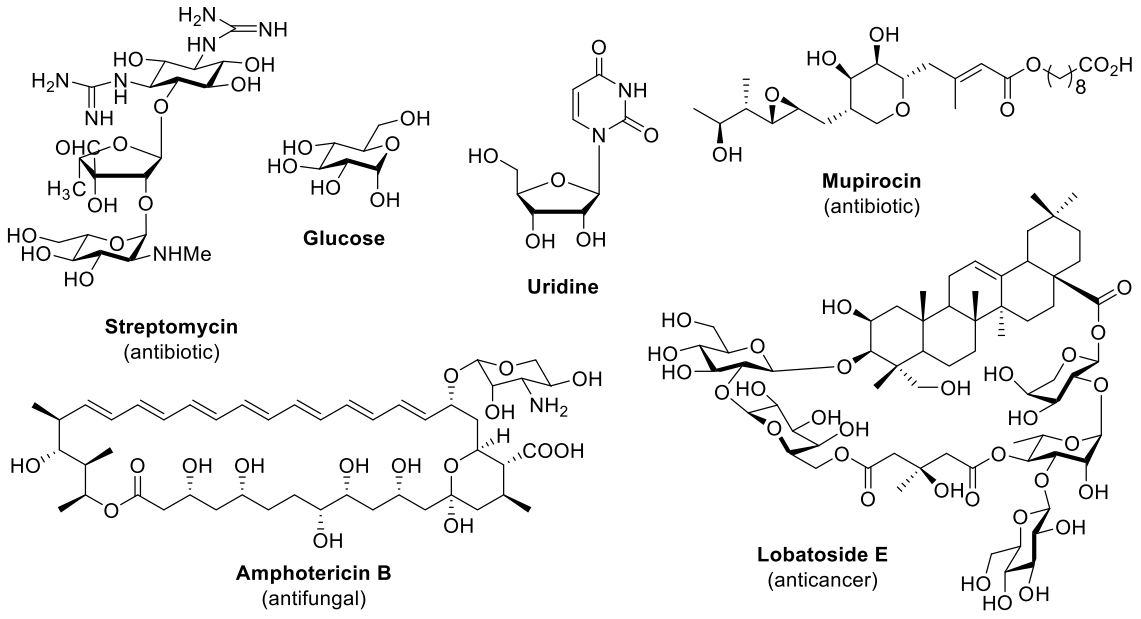

1.3.2 Motivation for Study

To expand the scope and solve unmet problems, we decided to examine our catalytic system in more complex substrates such as carbohydrates and natural products. An unsolved site-selective functionalization of carbohydrate is the reaction at axial hydroxyl groups. This challenging issue has been addressed by enzymatic systems. Kre2p/Mnt1p, a Golgi α-1,2-mannosyltransferase, catalyzes transfer of mannose from GDP-mannose to an α-mannoside.[29] During the transfer, surrounding protein residues are engaged in multiple hydrogen bonds and van der Waals interactions for pre-organization of substrate in the active site (Figure 1.8). Through this mode of activation, the axial C2 hydroxyl group of methyl α-D-mannose is selectively functionalized.

[29] Lobsanov, Y. D.; Romero, P. A.; Sleno, B.; Yu, B.; Yip, P.; Herscovics, A.; Howell, P. L. *J. Biol. Chem.* **2004**, *279*, 17921–17931.

Figure 1.8 Schematic representation of the interactions in the active site of Kre2p/Mnt1p and methyl α-D-mannose

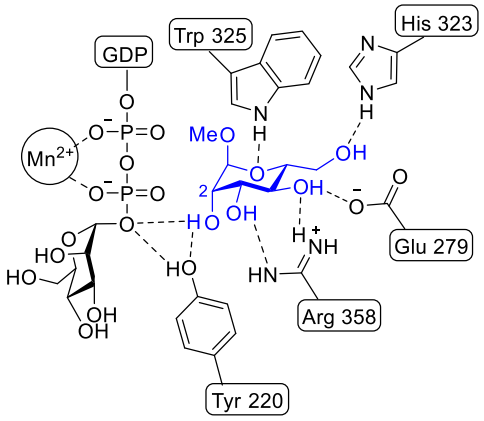

We envisioned that with our catalytic system the number of interactions required for effective localization of substrate can be minimized through a single reversible covalent bond. In addition, as described in 1.2.4.2, our scaffolding catalysts have unique recognition of *cis*-1,2-diols. By employing this feature, site-selective functionalization of polyhydroxylated molecules is achievable, in which display *cis*-1,2-diol moiety within the structure. During the activation of mannose derivative, the chiral catalyst recognizes *cis*-1,2-diol of C2 and C3 positions in the matched case and functionalization occurs at the C2-axial hydroxyl group (Figure 1.9). It resembles pre-organization of substrate by the surrounding chiral information as we observe in the enzymatic system shown in Figure 1.8. However, our catalyst is not limited to a specific substrate but rather applicable in a wide range of polyols in selective functionalization due to its unique recognition ability of *cis*-1,2-diol motif.

Figure 1.9 Proposed mode of activation of mannose derivative catalyzed by scaffolding catalyst

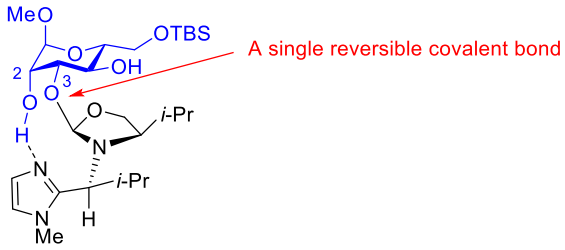

1.3.3 Synthesis of Catalysts

The required catalysts can be synthesized in two steps from readily available materials. Imine formation between valinol and isopropyl aldehyde, followed by reaction with *in situ*-generated 2-lithiated *N*-methylimidazole afforded intermediate **1.71** with good diastereoselectivity. Oxazoline ring formation was achieved by cyclization with DMF·DMA; the desired catalysts could be obtained as a single isomer after recrystallization. The use of simple amino alcohols and aldehydes as starting materials affords significant modularity with respect to the substituents of the catalysts' chiral backbone. With different alkyl groups, one can access derivatives of chiral catalysts (Scheme 1.16).[30]

[30] Worthy, A. D.; Sun, X.; Tan, K. L. *J. Am. Chem. Soc*. **2012**, *134*, 7321–7324.

Scheme 1.16 Synthesis of scaffolding catalysts

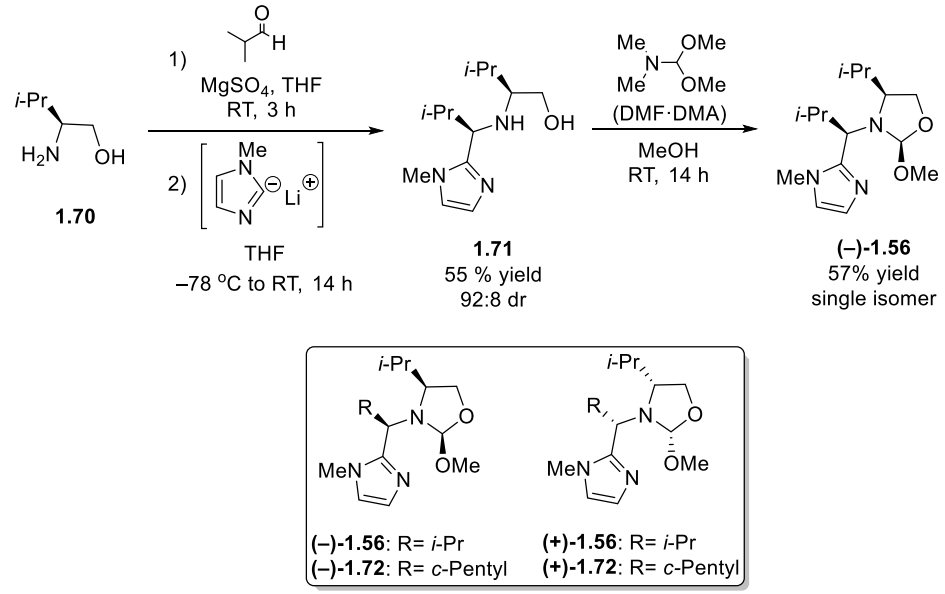

1.3.4 Substrate Scope

With an array of catalysts in hand, we first examined site-selective functionalization of a C6-OH silyl-protected methyl α-D-mannose derivative (**1.73**). A control reaction using 20 mol% *N*-methylimidazole as a catalyst revealed the C3-OH to possess the highest innate reactivity (C2:C3:C4= 5:78:17 in Table 1.2, entry 1). In a reaction with 20 mol% scaffolding catalyst **(+)-1.56**, however, the reaction selectivity was reversed to give C2-OH functionalized mannose as the major product (Table 1.2, entry 2). This result demonstrates that the scaffolding catalyst's ability to override the substrate's inherent reactivity bias. When **(–)-1.72** was used as catalyst, the reaction exclusively gave C3-OH silylated product in quantitative yield, reflecting an enhancement of the inherent reactivity of the C3-OH (Table 1.2, entry 3). As in previous work,[26] reaction with a control catalyst (i.e. **1.68**), which lacks a covalent substrate binding site, gave poor yields and similar

selectivities to those of the NMI-catalyzed reaction. This supports again our hypothesis that a covalent bond between catalyst and substrate has a critical role in both reactivity and selectivity. Depending on the choice of catalyst, selective acylation or sulfonylation can also be achieved for either the C2 or C3 hydroxyl group (Table 1.2, entries 4-9).

Table 1.2 Site-selective functionalization of methyl α-D-mannose derivative

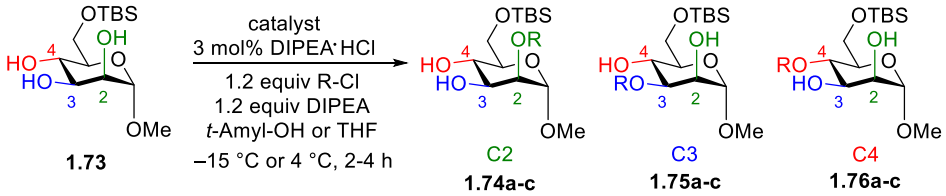

a: R= TES, **b**: R= Ac, **c**: R= Ms

entry	R-Cl	catalyst	C2:C3:C4	yield (%)[a,b]
1	TESCl	20 mol% NMI	5:78:17	77
2		20 mol% **(+)-1.56**	90:10:-	84 (76)
3		5 mol% **(–)-1.72**	-:100:-	(>98)
4	AcCl	20 mol% NMI	9:84:7	39
5		20 mol% **(+)-1.56**	84:15:1	74
6		5 mol% **(–)-1.72**	1:99:-	(96)
7	MsCl	20 mol% NMI	22:56:22	68
8		20 mol% **(+)-1.56**	91:8:1	(80)
9		5 mol% **(–)-1.72**	-:100:-	(97)

[a]Isolated yield of the isomeric mixture. [b]Yields in parentheses are of the isolated major isomer. NMI = *N*-methylimidazole.

The catalysts are also applicable to site-selective functionalization of a variety of other monosaccharides. Methyl α-L-rhamnose bears a *cis*-1,2-diol motif between C2 and C3 positions with the opposite absolute stereochemistry of D-mannose. Therefore, for axial C2-OH functionalization, the enantiomer of catalyst **(–)-1.72** was required (Table 1.3, entries 2,5, and 8). Silylation, acylation, and sulfonylation occurred in overall good yield and high site-selectivity. For functionalization at the equatorial C3-OH position, catalyst

loading can be reduced to 5 mol% probably due to the pre-existing inherent bias being the most reactive site (Table 1.3, entries 3,6, and 9).

Table 1.3 Site-selective functionalization of methyl α-L-rhamnose

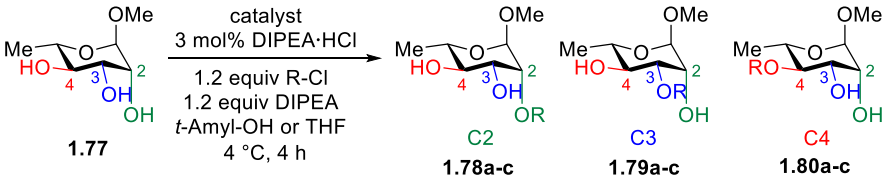

a: R= TES, **b**: R= Ac, **c**: R= Ms

entry	R-Cl	catalyst	C2:C3:C4	yield (%)[a,b]
1	TESCl	20 mol% NMI	7:79:14	78
2		20 mol% **(–)-1.72**	89:11:-	88
3		5 mol% **(+)-1.56**	-:100:-	(>98)
4	AcCl	20 mol% NMI	12:79:9	83
5		20 mol% **(–)-1.72**	84:14:2	73
6		5 mol% **(+)-1.56**	1:99:-	(98)
7	MsCl	20 mol% NMI	24:57:19	72
8		20 mol% **(–)-1.72**	92:8:-	(82)
9		5 mol% **(+)-1.56**	1:99:-	(>98)

[a]Isolated yield of the isomeric mixture. [b]Yields in parentheses are of the isolated major isomer. NMI =*N*-methylimidazole.

The catalytic system could be further adopted to methyl β-L-arabinose, in which *cis*-1,2-diol is located at C3 and C4 positions. With (–)-1.56 functionalization occurred selectively at the axial C4 hydroxyl group, whereas with the enantiomeric catalyst (+)-1.56 reversed selectivity was observed to yield the C3-OH functionalized product as the major isomer (Table 1.4). Notably, during C4 modification higher selectivity was obtained when the catalyst **(–)-1.56** was used instead of **(–)-1.72**. This might be ascribed to slight differences in sterics around substrate. Therefore it was necessary to have different alkyl groups on the catalyst to achieve high level of site-selectivity depending on substrate.

Table 1.4 Site-selective functionalization of methyl β-L-arabinose

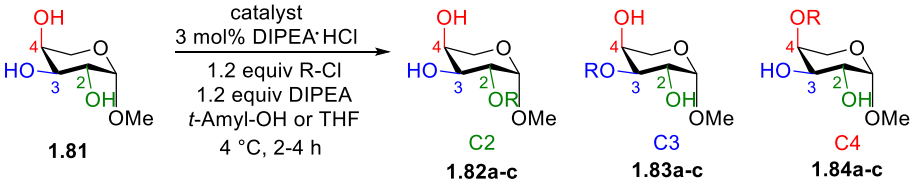

a: R= TES, **b**: R= Ac, **c**: R= Ms

entry	R-Cl	catalyst	C2:C3:C4	yield (%)[a,b]
1	TESCl	20 mol% NMI	27:14:59	39
2		20 mol% **(–)-1.56**	-:3:97	(92)
3		5 mol% **(+)-1.56**	-:98:2	(97)
4	AcCl	20 mol% NMI	22:72:6	6
5		20 mol% **(–)-1.56**	5:9:86	61
6		5 mol% **(+)-1.56**	3:96:1	(83)
7	MsCl	20 mol% NMI	68:23:9	27
8		20 mol% **(–)-1.56**	3:10:87	93
9		5 mol% **(+)-1.56**	1:92:7	(91)

[a]Isolated yield of the isomeric mixture. [b]Yields in parentheses are of the isolated major isomer. NMI = *N*-methylimidazole.

Methyl α-D-galactose derivative (**1.85**) was also efficiently functionalized at the C3 equatorial position with all three electrophiles (TESCl, AcCl, and MsCl) using the catalyst **(+)-1.56** (Table 1.5). Unfortunately, attempts to functionalize the C4 axial position gave poor results, possibly due to added congestion around the C4-OH resulting from the adjacent C6-OTBS group. Functionalization at the C4 position of galactose could still be achieved, however, by reaction of conformationally constrained 1,6-anhydro-β-D-galactose (**1.89**), in which the C4-OH is in an equatorial position instead (Table 1.6).

Table 1.5 Site-selective functionalization of methyl α-D-galactose derivative

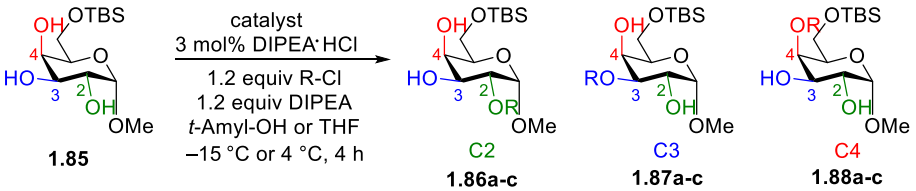

1.85 | **1.86a-c** | **1.87a-c** | **1.88a-c**

a: R= TES, **b**: R= Ac, **c**: R= Ms

entry	R-Cl	catalyst	C2:C3:C4	yield (%)[a,b]
1	TESCl	20 mol% NMI	86:14:-	77
2		20 mol% **(+)-1.56**	6:94:-	95
3	AcCl	20 mol% NMI	42:58:-	26
4		20 mol% **(+)-1.56**	19:81:-	96
5	MsCl	20 mol% NMI	76:24:-	62
6		20 mol% **(+)-1.56**	-:100:-	(74)

[a]Isolated yield of the isomeric mixture. [b]Yields in parentheses are of the isolated major isomer. NMI = *N*-methylimidazole.

Table 1.6 Site-selective functionalization of 1,6-anhydro-β-D-galactose

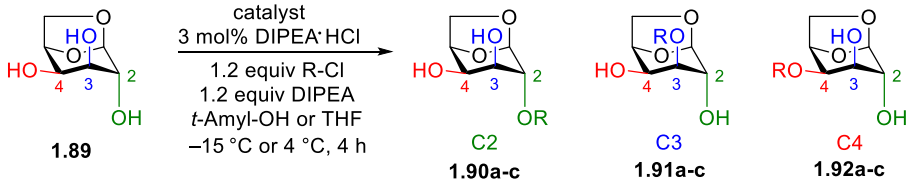

1.89 | **1.90a-c** | **1.91a-c** | **1.92a-c**

a: R= TES, **b**: R= Ac, **c**: R= Ms

entry	R-Cl	catalyst	C2:C3:C4	yield (%)[a,b]
1	TESCl	20 mol% NMI	91:-:9	51
2		5 mol% **(–)-1.72**	1:-:99	(98)
3	AcCl	20 mol% NMI	75:8:17	53
4		5 mol% **(–)-1.72**	-:3:97	(93)
5	MsCl	20 mol% NMI	75:6:19	50
6		5 mol% **(–)-1.72**	-:1:99	(88)

[a]Isolated yield of the isomeric mixture. [b]Yields in parentheses are of the isolated major isomer. NMI = *N*-methylimidazole.

1.3.5 Origin of Axial Functionalization

One of the main advantages of our catalytic system is that it overturns inherent substrate reactivity favoring functionalization at the equatorial position and furnishes the axially

derivatized product instead. We investigated the origin of this preference for axial functionalization by studying the reaction of the C3-OH in 1,6-anhydro-β-D-galactose. With 20 mol% **(+)-1.72**, acetylation proceeded with good site-selectivity (Figure 1.10). Since the substrate is conformationally locked, catalyst-bound intermediate **1.93a** cannot undergo chair-flip to form the less stable conformer **1.93b** wherein the C3-OH is in an equatorial position. Therefore, the axially acetylated product **1.91b** is believed to derive directly from the intermediate **1.93a**.

Figure 1.10 Fixed chair conformation in 1,6-anhydro-β-D-galactose

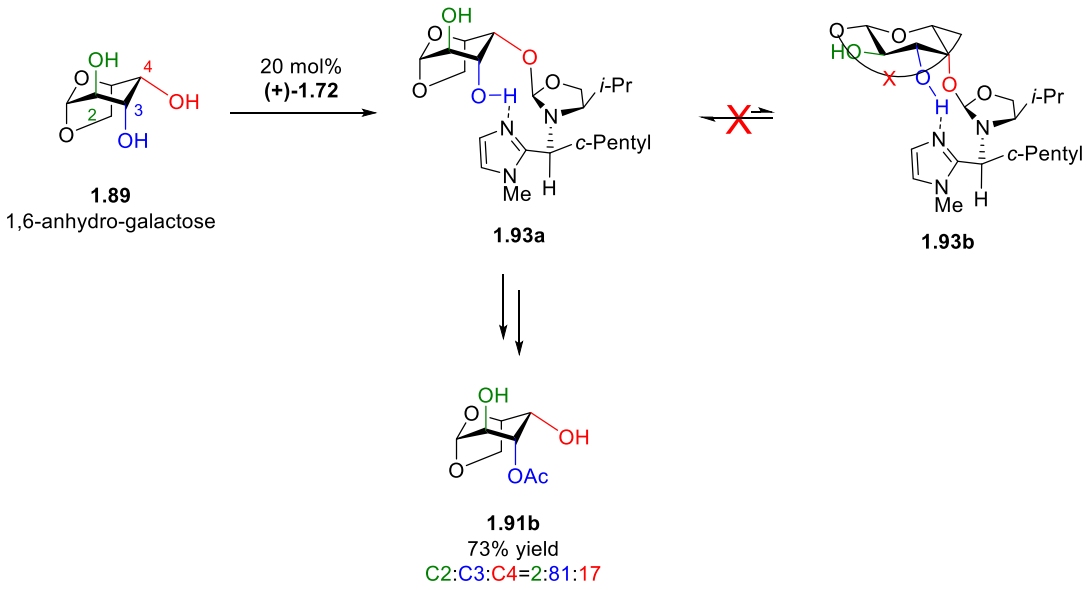

The above results do not rule out the possibility of chair-flipped intermediates being relevant to the reaction of unconstrained carbohydrates. Figure 1.11 shows potential chair-flip mechanism in acetylation of the axial C2 position of methyl α-D-mannose derivative. The reaction can be initiated by the formation of the catalyst-bound intermediate, in which

the catalyst binding site is covalently bonded to the equatorial C3-OH group. The intermediate can undergo ring-flip to form a less stable axially bound intermediate **1.94b**. After acyl transfer followed by dissociation of catalyst, equatorially functionalized product **1.74b'** can proceed through a second ring-flip to generate the observed thermodynamically more stable product **1.74b**.

Figure 1.11 Potential chair-flip mechanism in unconstrained carbohydrates

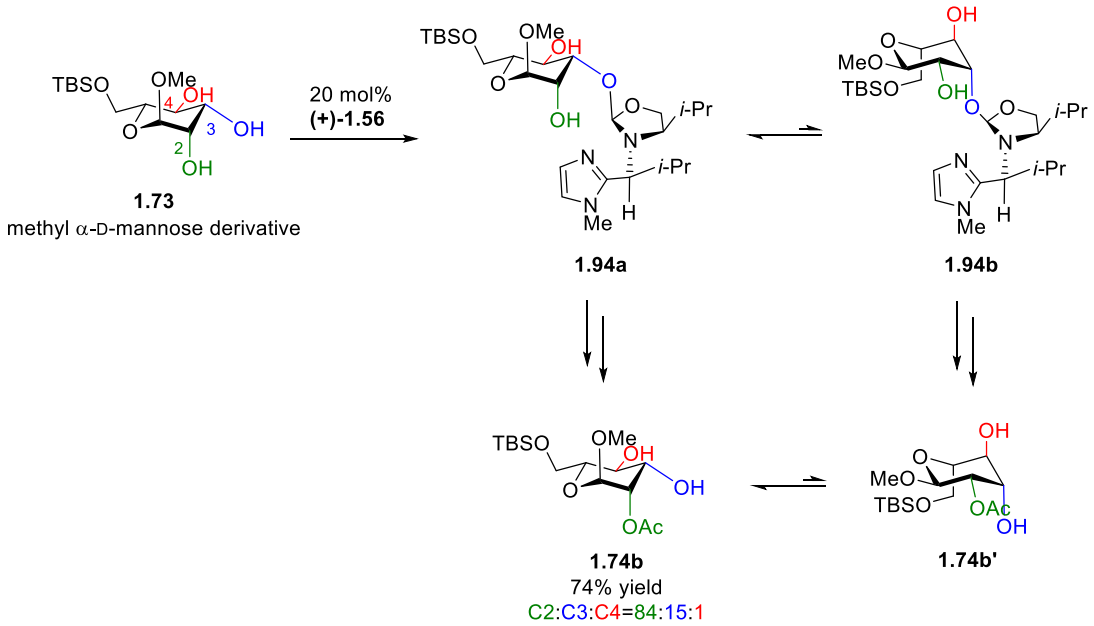

1.3.6 Application to Complex Molecules

The scaffolding catalysts' ability to specifically recognize *cis*-1,2-diol units was also tested in other complex systems. Selective protection of one of the secondary hydroxyl groups on ribonucleosides would be advantageous to overcome limitation of low yielding

automated RNA synthesis.[31] As an example, 4,4'-dimethoxytrityl (DMTr)-protected uridine **1.95** underwent selective silyl protection at the C3-OH using the scaffolding catalyst **(+)-1.56**, leaving C2-OH available for elongation of the RNA strand. By switching the catalyst to **(–)-1.72**, protection occurred at C2-OH exclusively to give the desired silyl protected product **1.97** (Scheme 1.17).[32]

Scheme 1.17 Selective silyl protection of ribonucleoside, uridine derivative

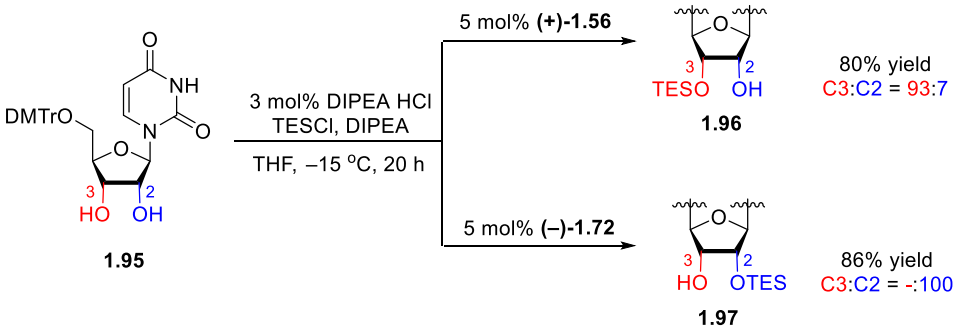

Mupirocin (an antibiotic for skin infections) and digoxin (a treatment for cardiovascular disease) both display multiple hydroxyl groups at disparate sites within their molecular frameworks. Site-selective derivatization of such complex molecules would be useful towards the preparation of structurally diversified analogs for use in medicinal chemistry or biochemical assays. Using scaffolding catalysis, we were able to selectively activate both the C6 and C7 hydroxyl groups of mupirocin methyl ester (**1.98**) (Scheme 1.18, eq. 1). Digoxin has four other hydroxyl groups besides those at α and β positions. The

[31] Somoza, A. *Chem. Soc. Rev*. **2008**, *37*, 2668–2675.
[32] Blaisdell, T. P.; Lee, S.; Kasaplar, P.; Sun, X.; Tan, K. L. *Org. Lett.*, **2013**, *15*, 4710–4713.

acetylated products (**1.102** and **1.103** in Scheme 1.18, eq. 2) are also used to treat heart failure. Site-selective acetylation with enantiomers of catalyst provided each of these target molecules in good yield (Scheme 1.18, eq. 2).

Scheme 1.18 Selective functionalization of mupirocin methyl ester and digoxin using scaffolding catalysis

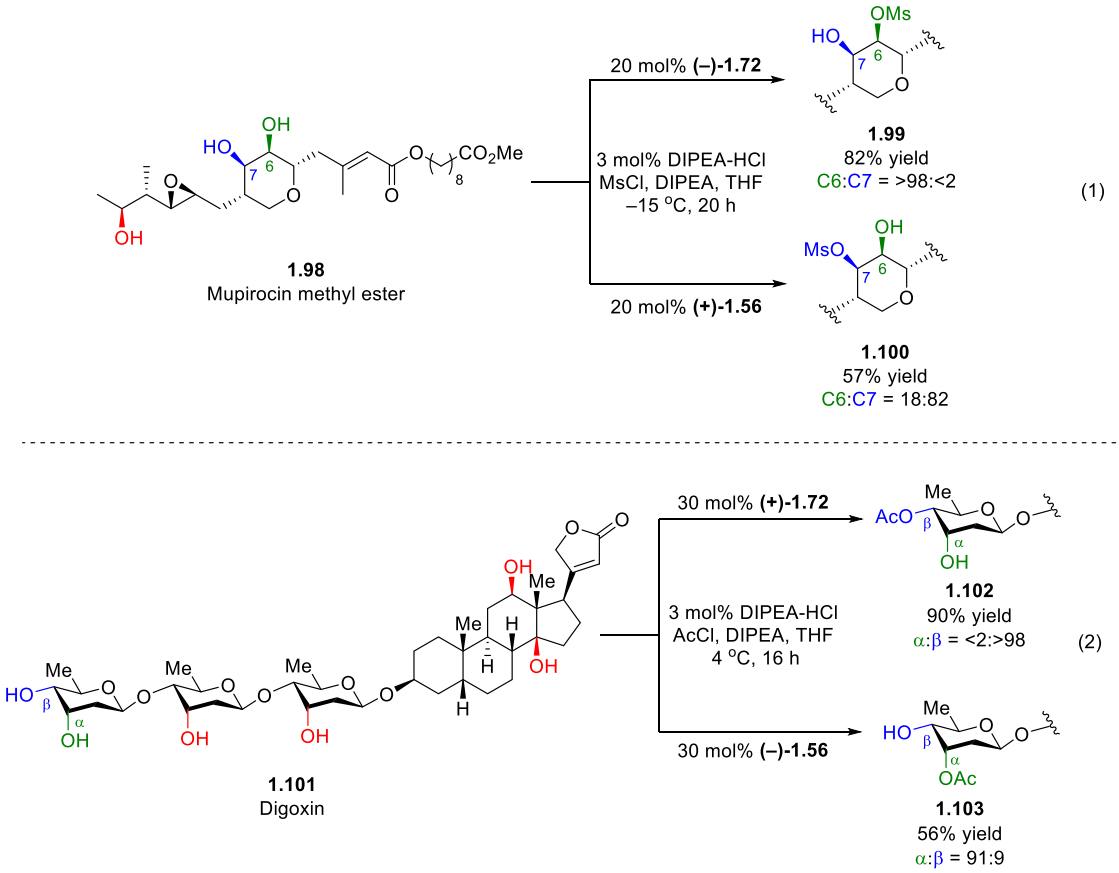

1.4 Si-Based Scaffold Enabling *meta*-Selective C–H Activation[33]

1.4.1 Importance of Functionalized Arenes

Arenes are a prevalent motif in therapeutically important molecules. As shown in Figure 1.12, all the current best-selling drugs feature at least one (hetero) aryl unit. This can be partially explained by its readily functionalizable characteristics for further derivatization to build structural complexity found in drugs.[34]

Figure 1.12 Arenes as a phamacophore

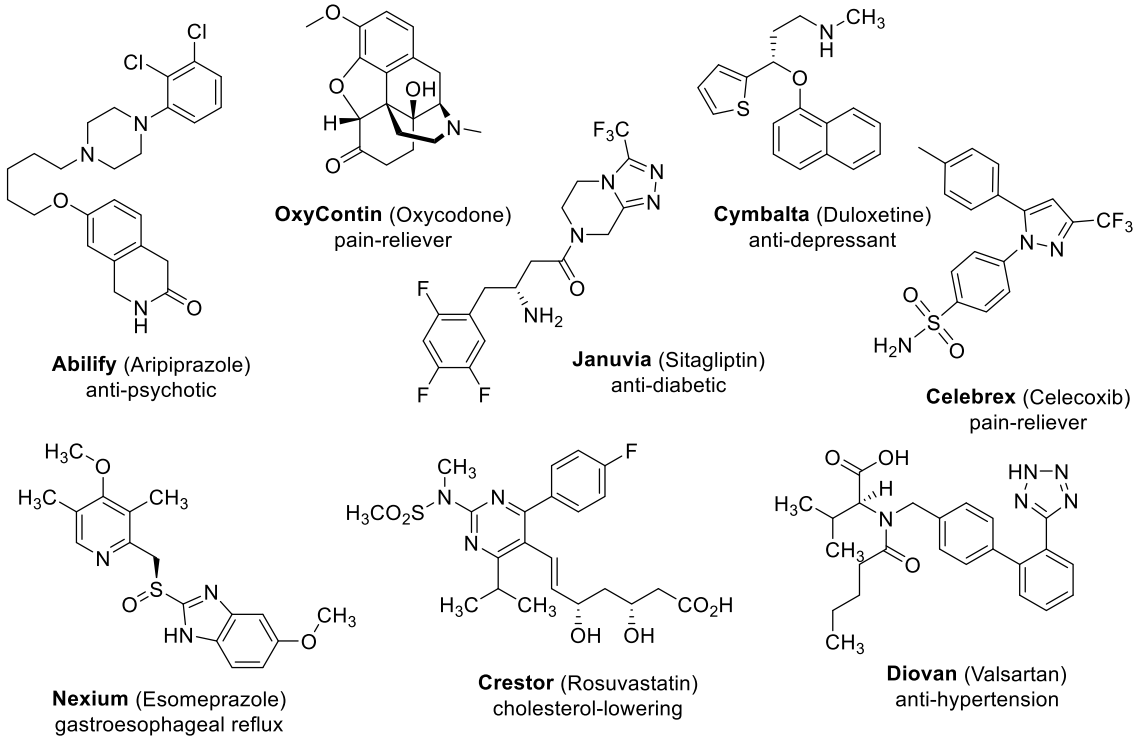

[33] Lee, S.; Lee, H.; Tan, K. L. *J. Am. Chem. Soc*. **2013**, *135*, 18778–18781.
[34] Roughley, S. D.; Jordan, A. M. *J. Med. Chem*. **2011**, *54*, 3451–3479.

1.4.2 Template-Assisted Remote C–H Activation of Arenes

Enormous progress in site-selective C–H activation of arenes has been made in the last several decades.[35] Due to the advantageous features that *ortho* position has, such as propensity to form 6- or 7-membered metallocycle with a neighboring *ortho* substituent, proximity-driven C–H activation at this position is well developed.[36] In sharp contrast, reports of remote C–H activation at the *meta* or *para* positions have been limited until very recently.[37]

In 2012, the Yu group used metal coordination by nitrile group to direct palladium-catalyzed *meta*-selective olefination of toluene and hydrocinnamic acid derivatives.[38] They initially proposed that end-on palladium coordination by the nitrile group of a template leads to a macrocyclic cyclophane-like pre-transition state. Later in 2014, however, a

---

[35] For selected reviews, see: (a) Ryabov, A. D. *Chem. Rev*. **1990**, *90*, 403–424. (b) Arndtsen, B. A.; Bergman, R. G.; Mobley, T. A.; Peterson, T. H. *Acc. Chem. Res*. **1995**, *28*, 154–162. (c) Kakiuchi, F.; Murai, S. *Acc. Chem. Res*. **2002**, *35*, 826–834. (d) Ritleng, V.; Sirlin, C.; Pfeffer, M. *Chem. Rev*. **2002**, *102*, 1731–1770. (e) Labinger, J. A.; Bercaw, J. E. *Nature* **2002**, *417*, 507–514. (f) Dupont, J.; Consorti, C. S.; Spencer, J. *Chem. Rev*. **2005**, *105*, 2527–2571. (g) Alberico, D.; Scott, M. E.; Lautens, M. *Chem. Rev*. **2007**, *107*, 174–238. (h) Chen, X.; Engle, K. M.; Wang, D.-H.; Yu, J.-Q. *Angew. Chem. Int. Ed.* **2009**, *48*, 5094–5115.

[36] For selected examples, see: (a) Miura, M.; Tsuda, T.; Satoh, T.; Pivsa-Art, S.; Nomura, M. *J. Org. Chem*. **1998**, *63*, 5211–5215. (b) Boele, M. D. K.; van Strijdonck, G. T. P. F.; de Vries, A. H. M.; Kamer, P. C. J.; de Vries, J. G.; van Leeuwen, P. W. N. M. *J. Am. Chem. Soc.* **2002**, *124*, 1586–1587. (c) Zaitsev, V. G.; Daugulis, O. *J. Am. Chem. Soc*. **2005**, *127*, 4156–4157. (d) Cai, G.; Fu, Y.; Li, Y.; Wan, X.; Shi, Z. *J. Am. Chem. Soc*. **2007**, *129*, 7666–7673. (e) Wang, J.-R.; Yang, C.-T.; Liu, L.; Guo, Q.-X. *Tetrahedron Lett.* **2007**, *48*, 5449–5453. (f) Li, J.-J.; Mei, T.-S.; Yu, J.-Q. *Angew. Chem., Int. Ed.* **2008**, *47*, 6452–6455. (g) Houlden, C. E.; Bailey, C. D.; Ford, J. G.; Gagne´, M. R.; Lloyd-Jones, G. C.; Booker-Milburn, K. I. *J. Am. Chem. Soc*. **2008**, *130*, 10066–10067. (h) Cho, S. H.; Hwang, S. J.; Chang, S. *J. Am. Chem. Soc*. **2008**, 130, 9254–9256.

[37] For recent developments on remote C–H functionalizations, see: (a) Topczewski, J. J.; Cabrera, P. J.; Saper, N. I.; Sanford, M. S. *Nature* **2016**, *531*, 220–224. (b) Patra, T.; Watile, R.; Agasti, S.; Naveen, T.; Maiti, D. *Chem. Commun*. **2016**, *52*, 2027–2030. (c) Shen, P.-X.; Wang, X.-C.; Wang, P.; Zhu, R.-Y.; Yu, J.-Q. *J. Am. Chem. Soc.* **2015**, *137*, 11574–11577. (d) Wang, X.-C.; Gong, W.; Fang, L.-Z.; Zhu, R.-Y.; Li, S.; Engle, K. M.; Yu, J.-Q. *Nature* **2015**, *519*, 334–338. (e) Bera, M.; Maji, A.; Sahoo, S. K.; Maiti, D. *Angew. Chem. Int. Ed*. **2015**, *54*, 8515–8519. (f) Kuninobu, Y.; Ida, H.; Nishi, M.; Kanai, M. *Nat. Chem*. **2015**, *7*, 712–717. (g) Dong, Z.; Wang, J.; Dong, G. *J. Am. Chem. Soc.* **2015**, *137*, 5887–5890. (h) Bag, S.; Patra, T.; Modak, A.; Deb, A.; Maity, S.; Dutta, U.; Dey, A.;Kancherla, R.; Maji, A.; Hazra, A.; Bera, M.; Maiti, D. *J. Am. Chem. Soc.* **2015**, *137*, 11888–11891. (i) Yang, G.; Lindovska, P.; Zhu, D.; Kim, J.; Wang, P.; Tang, R. Y.; Movassaghi, M.; Yu, J.-Q. *J. Am. Chem. Soc*. **2014**, *136*, 10807–10813. (j) Bera, M.; Modak, A.; Patra, T.; Maji, A.; Maiti, D. *Org. Lett*. **2014**, *16*, 5760–5763.

[38] Leow, D.; Li, G.; Mei, T.-S.; Yu, J.-Q. *Nature* **2012**, *486*, 518–522.

computational study examining the origin of the observed *meta*-selectivity indicated that the reaction occurs *via* Pd−Ag heterodimeric transition states (**1.105)** (Scheme 1.19).[39] Olefination of template-tethered benzyl alcohol **1.104** afforded *meta*-functionalized products (**1.106** and **1.107)** in high selectivity.

Scheme 1.19 Template-directed *meta*-selective olefination of toluene

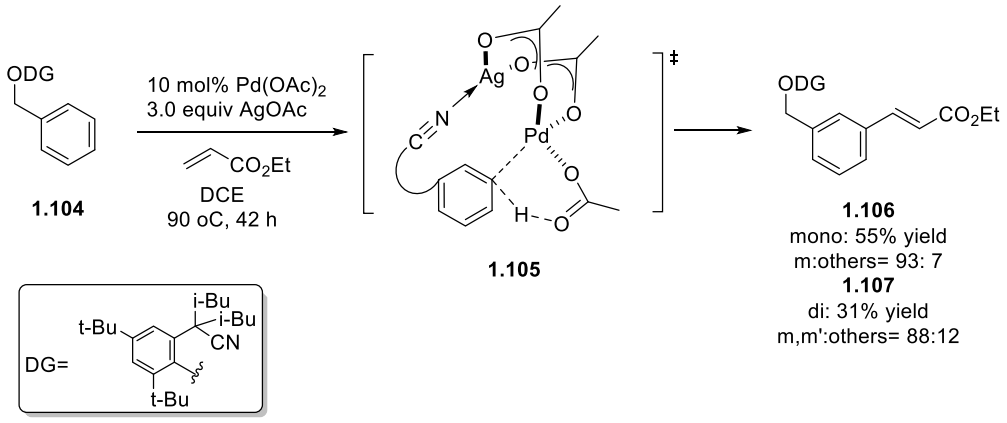

A modified nitrile-based template was developed and applied to *meta*-selective olefination of phenols (Scheme 1.20).[40] This method was applied to functionalization of drug molecules containing an α-phenoxyacetic acid motif. The nitrile directing group can be removed by hydrolysis to afford *meta*-substituted α-phenoxyacetic acids. In addition, removal of acetic acid moiety can be achieved by treatment with diphenylphosphoryl azide (DPPA) to give functionalized phenols. A similar strategy was also employed in the *meta*-

[39] Yang, Y.-F.; Cheng, G.-J.; Liu, P.; Leow, D.; Sun, T.-Y.; Chen, P.; Zhang, X.; Yu, J.-Q.; Wu, Y.-D.; Houk, K. N. *J. Am. Chem. Soc.* **2014**, 136, 344–355.
[40] Dai, H.-X.; Li, G.; Zhang, X.-G.; Stepan, A. F.; Yu, J.-Q. *J. Am. Chem. Soc.* **2013**, *135*, 7567–7571.

selective olefination and acetoxylation of tetrahydroquinolines and N-methylanilines.[41] Recent developments in *meta*-selective functionalization by other groups have also expanded the reaction scope beyond olefination and acetoxylation to include hydroxylation, arylation, alkylation, and halogenation.[42]

Scheme 1.20 *meta*-Olefination of phenol derivative **1.108**

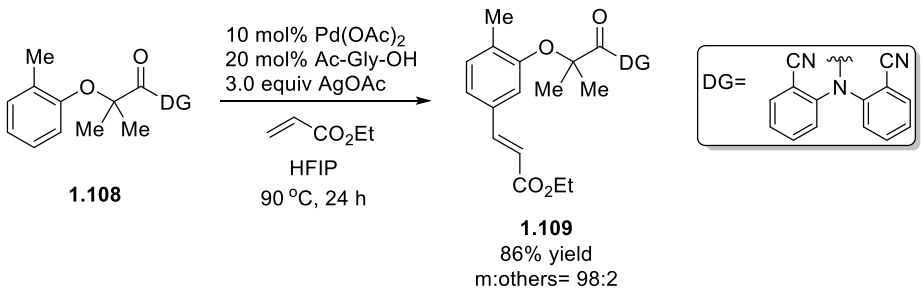

1.4.3 Silicon-Tethered Template Design and Optimization

As an extension of our scaffolding catalysis concept, we investigated controlling site-selectivity in C–H activation of arenes. Removal of the Yu group's nitrile template (Scheme 1.19) by hydrogenolysis ultimately results in formation of methyl substituted products wherein the initial olefin substituent has also been reduced (Scheme 1.21). Thus,

---

[41] Tang, R.-Y.; Li, G.; Yu, J.-Q. *Nature* **2014**, *507*, 215–220.

[42] (a) Li, S.; Cai, L.; Ji, H.; Yang, L.; Li, G. *Nat. Commun*. **2016**, *7*, 10443. (b) Maji, A.; Bhaskararao, B.; Singha, S.; Sunoj, R. B.; Maiti, D. *Chem. Sci*. **2016***, 7*, 3147–3153. (c) Phipps, R. J.; Gaunt, M. J. *Science* **2009**, *323*, 1593–1597. (d) Cornella, J.; Righi, M.; Larrosa, I. *Angew. Chem. Int. Ed*. **2011**, *50*, 9429–9432. (e) Wan, L.; Dastbaravardeh, N.; Li, G.; Yu, J.-Q. *J. Am. Chem. Soc*. **2013**, *135*, 18056–18059. (f) Luo, J.; Preciado, S.; Larrosa, I. *J. Am. Chem. Soc*. **2014**, *136*, 4109–4112. (g) Luo, J.; Preciado, S.; Larrosa, I. *Chem. Commun*. **2015**, *51*, 3127–3130. (h) Luo, J.; Preciado, S.; Araromi, S. O.; Larrosa, I. *Chem. Asian J.* **2016**, *11*, 347–350. (i) Teskey, C. J.; Lui, A. Y. W.; Greaney, M. F. *Angew. Chem., Int. Ed*. **2015**, *54*, 11677–11680. (j) Chu, L.; Shang, M.; Tanaka, K.; Chen, O.; Pissarnitski, N.; Streckfuss, E.; Yu, J.-Q. *ACS Cent. Sci.* **2015**, *1*, 394–399.

we considered the possibility to obtain olefinated benzyl alcohols instead as final products, by designing a directing group which would be readily cleavable under mild conditions so as to avoid cleavage of the O–C_{benzyl} bond (Scheme 1.21).

Scheme 1.21 Products after removal of directing group of functionalized arene

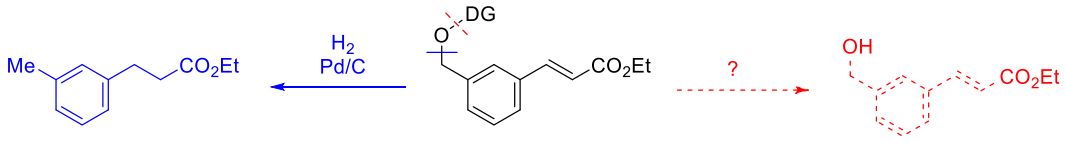

We initially designed a template which could be rendered catalytic through reversible formation of a Si–O bond. Therefore, we introduced a silicon atom as an alcohol exchange site. Exchange at the silicon center of a template prototype (**1.110**) between the starting ethoxy substituent and the benzyl alcohol substrate was observed under acidic conditions using either *p*-toluenesulfonic acid (PTSA) or pyridinium *p*-toluenesulfonate (PPTS) (Scheme 1.22). Unfortunately, however, under the actual oxidative conditions of C–H olefination of **1.112**, we observed oxidation of the free alcohols to give benzaldehyde (Scheme 1.23).

Scheme 1.22 Alcohol exchange experiments with Si-containing template

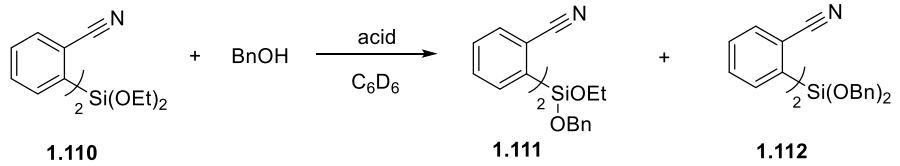

1.110 **1.111** **1.112**

	1.110 :	**1.111** :	**1.112**
with PTSA at 50 °C, 1 h	95 :	5 :	0
4 h	82 :	15 :	3
16 h	44 :	38 :	18
with PPTS at 50 °C, 1 h	100 :	0 :	0
4 h	98 :	2 :	0
80 °C, 1 h	93 :	7 :	0
4 h	76 :	21 :	3
16 h	30 :	43 :	27

Scheme 1.23 Initial attempt at C–H olefination of **1.112**

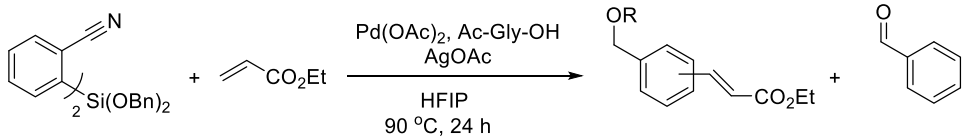

1.112

1.113
29%
(o:m:p= 38:42:20)

observed

We then turned our attention to design a directing group-bearing template using a silicon tether (Figure 1.13, **1.114**). We hypothesized that the silicon tether could be easily removed after the reaction through standard silyl deprotection methods. Similar to our organocatalysts, the template incorporates three interconnected: a substrate binding site, a catalytically active site and a rigid scaffold in between (Figure 1.13).

Figure 1.13 Template design

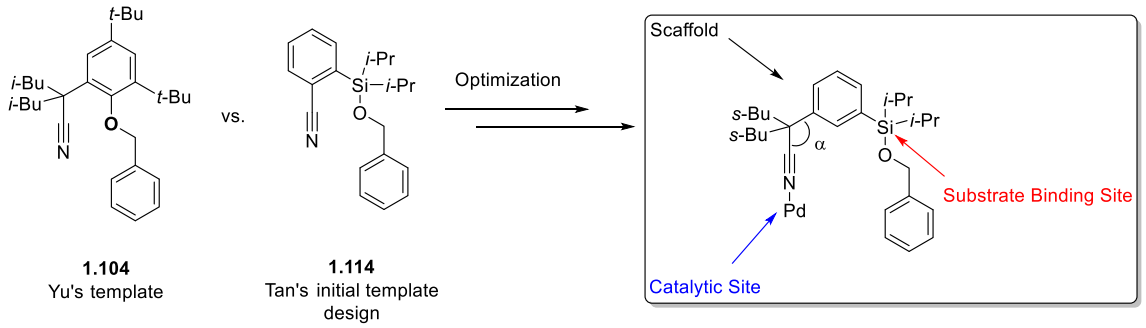

1.104
Yu's template

1.114
Tan's initial template design

Several structural refinements of our initial template design were required in order to achieve the desired *meta*-selectivity, as summarized in Table 1.7. Indeed, the initial template **1.114** itself showed preference for *ortho* functionalization (o:m:p=56:29:14). By adjusting the bond angle (α) between the phenyl ring and nitrile, we expected that it will affect site-selectivity by changing the distance between catalytic site and functionalization position on the substrate. When the chelating nitrile unit was moved to the *para*-position relative to the silicon substituent, *meta*-selective functionalization became slightly preferred (**1.115**). With a 1,3 relationship between the two groups, however, we observed higher than 80% *meta*-selectivity (**1.116**). We finally discovered the *s*-butyl substituted optimized template (**1.119** giving o:m:p=4:92:4 selectivity) upon further modification on the alkyl group between the nitrile and phenyl ring.

Table 1.7 Template optimization for *meta*-selective olefination

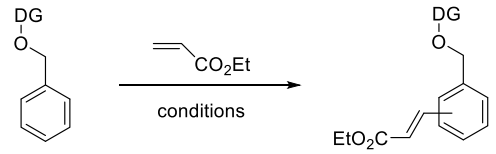

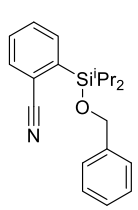

1.114
20% yield
o:m:p=56:29:14

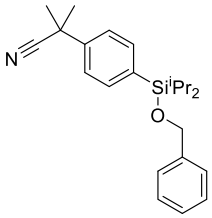

1.115
8% yield
o:m:p= 22:43:35

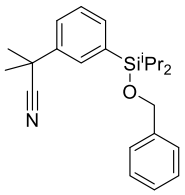

1.116
36% yield
o:m:p= 7:81:12

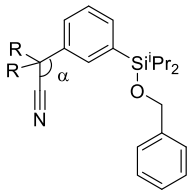

	yield	o:m:p
R= Et (**1.117**)	38%	6:88:6
i-Pr (**1.118**)	39%	4:90:6
***s*-Bu (1.119)**	**54%**	**2:96:2**
c-Hx (**1.120**)	42%	6:90:4
-CH_2CH_2- (**1.121**)	43%	6:81:13
-$CH_2CH_2CH_2$- (**1.122**)	37%	6:83:11
-$CH_2CH_2CH_2CH_2$- (**1.123**)	35%	5:86:9

1.4.4 Preparation of Template-Bound Substrates

The optimized template can be synthesized starting from commercially available 2-(3-bromophenyl)-acetonitrile (**1.124**). Deprotonation with potassium *t*-butoxide and subsequent dialkylation with *s*-butyl iodide, followed by lithium-halogen exchange and subsequent quenching with diisopropylchlorosilane affords arylsilane **1.126**. Chlorination using trichloroisocyanuric acid provided the optimized template **1.127** in good yield. Installation of template was achieved by silylation of various benzyl alcohols to give desired template-bound substrates (Scheme 1.24).

Scheme 1.24 Synthesis of template-bound substrates

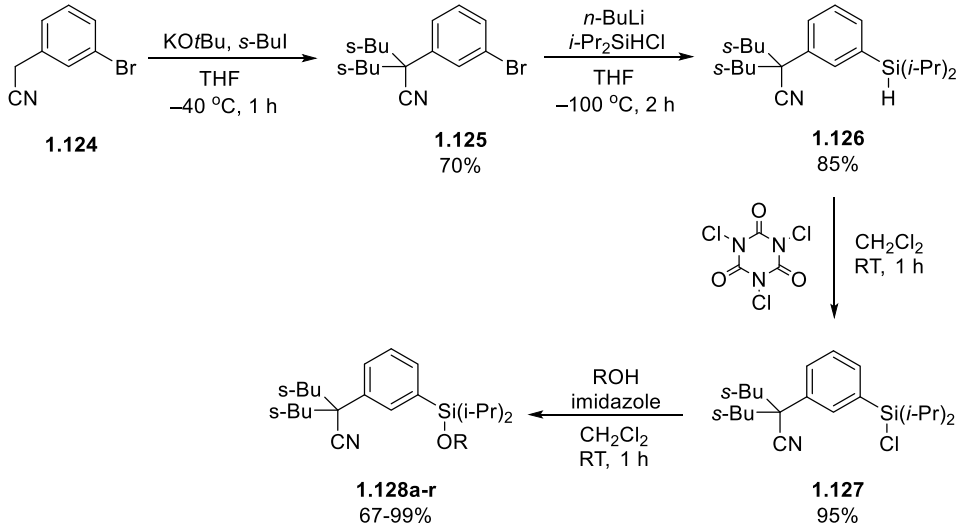

1.4.5 Substrate Scope

Under the optimized conditions, we investigated scope of benzyl alcohols, amenable to *meta*-olefination (Table 1.8). Mono- or bis-functionalization (at the two available *meta* positions) of benzyl alcohols afforded products with high *meta*-selectivity. Subsequent deprotection to remove the Si-containing directing group afforded free olefinated benzyl alcohols. C–H activation of benzyl alcohols with a wide range of substitution patterns at the *ortho*- (**1.128a-c**), *meta*- (**1.128d-k**), or *para*-positions (**1.128l-n**) resulted in desired *meta*-selectivity regardless of the electronic nature of the substituents. An ester group at the *meta* position did not negatively impact selectivity (**1.129k**, m:others= 91:9), whereas an acetyl group diminished *meta*-selectivity presumably due to the acetyl group's *ortho*-directing ability (**1.129j**, m:others= 78:22). Reaction of a naphthyl group occurred at the C3 position selectively (**1.129o'**). Similar reaction selectivity and yield were achieved when used secondary benzyl alcohols (**1.128p-r**) as substrates.

Table 1.8 Olefination with various benzyl alcohol-bound templates

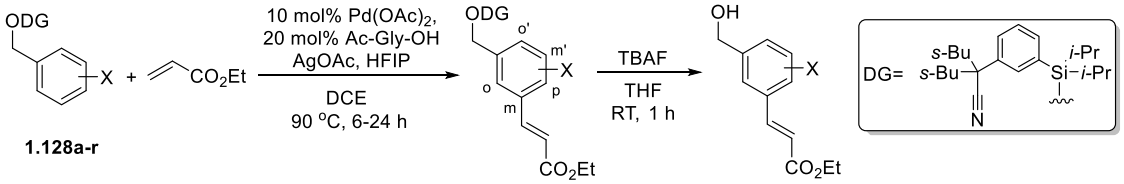

1.128a-r **1.129a-r** **1.129a'-r'**

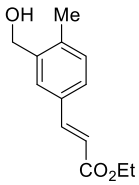

1.129a'$_{mono}$
51% yield
m:others= 95:5
1.129a'$_{di}$
28% yield
mm':others= 92:8

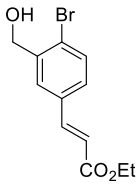

1.129b'$_{mono}$
46% yield
m:others= 93:7
1.129b'$_{di}$
26% yield
mm':others= 80:20

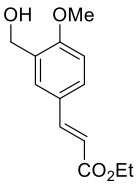

1.129c'$_{mono}$
57% yield
m:others= 94:6
1.129c'$_{di}$
trace
mm':others= -

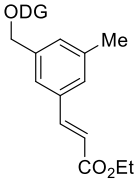

1.129d$_{mono}$
81% yield
m:others= 95:5
1.129d'$_{mono}$
75% yield
m:others= 95:5

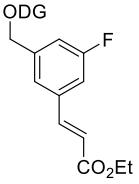

1.129e$_{mono}$
72% yield
m:others= 86:14

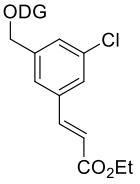

1.129f$_{mono}$
78% yield
m:others= 91:9

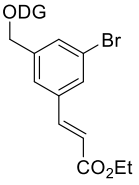

1.129g$_{mono}$
63% yield
m:others= 91:9

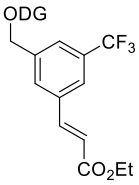

1.129h$_{mono}$
50% yield
m:others= 97:3

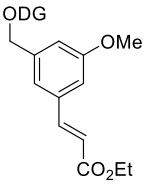

1.129i$_{mono}$
71% yield
m:others= 87:13

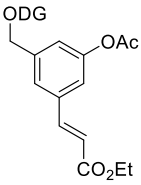

1.129j$_{mono}$
73% yield
m:others= 78:22

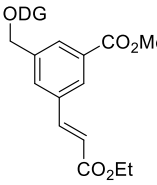

1.129k$_{mono}$
75% yield
m:others= 91:9

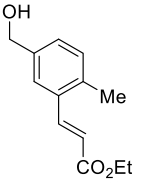

1.129l'$_{mono}$
46% yield
m:others= 91:9
1.129l'$_{di}$
26% yield
mm':others= 91:9

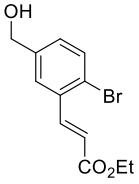

1.129m'$_{mono}$
37% yield
m:others= 84:16
1.129m'$_{di}$
8% yield
mm':others= -[a]

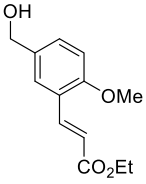

1.129n'$_{mono}$
51% yield
m:others= 98:2
1.129n'$_{di}$
9% yield
mm':others= 78:22

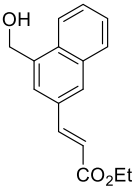

1.129o'$_{mono}$
53% yield
m:others= 96:4

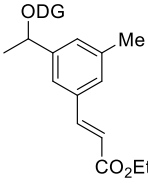

1.129p$_{mono}$
75% yield
m:others= 97:3

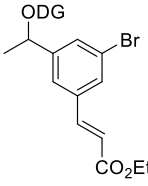

1.129q$_{mono}$
60% yield
m:others= 92:8

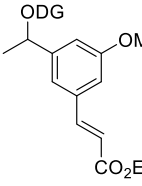

1.129r$_{mono}$
77% yield
m:others= 91:9

[a]Inseparable mixture with side product from metal–halogen exchange.

We then examined C–H activation of template-bound substrate **1.129d** with various olefins besides ethyl acrylate under the optimized conditions (Table 1.9). C–H functionalization with a diverse array of olefins terminally substituted with amide, ketone, sulfone groups, as well as a 1,2-disubstituted alkene, gave high *meta*-selectivity.

Table 1.9 Reaction with various olefins

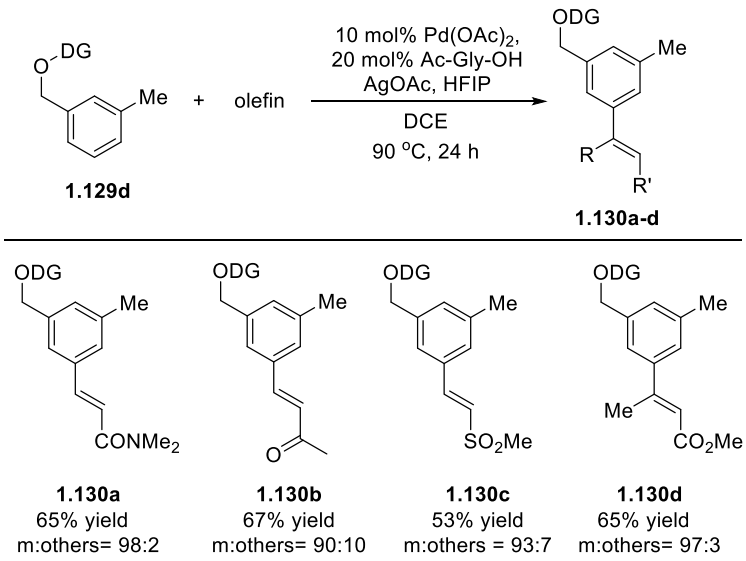

1.130a
65% yield
m:others= 98:2

1.130b
67% yield
m:others= 90:10

1.130c
53% yield
m:others = 93:7

1.130d
65% yield
m:others= 97:3

1.4.6 Kinetic Isotope Effect

An intermolecular competition experiment was performed to probe the reaction mechanism. A 1:1 mixture of hydrogenated and deuterated template-bound starting material was subjected to the standard reaction conditions. Removal of the silicon tether allowed for determination of a kinetic isotope effect of 2.5 (Scheme 1.25). The result is consistent with Yu's mechanistic study on nitrile directed *meta* C–H activation, which suggests that C–H bond activation is the rate determining step.[38]

Scheme 1.25 Intermolecular competition experiment

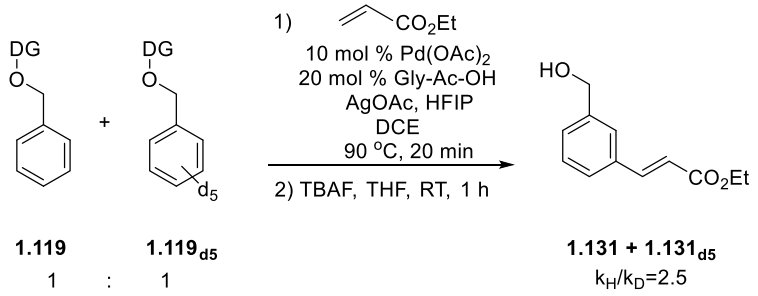

1.4.7 Recyclability of Template

One of the benefits of our strategy is that the template is recyclable after removal. Acidic hydrolysis of the template-bound functionalized product **1.129d** afforded the directing group-free benzyl alcohol **1.129d'** and cleaved silanol directing group **1.132** in 83% yield (Scheme 1.26). The resulting silanol can be reused to form the corresponding template-bound substrate **1.128d** in moderate yield.

Scheme 1.26 Reusable directing group

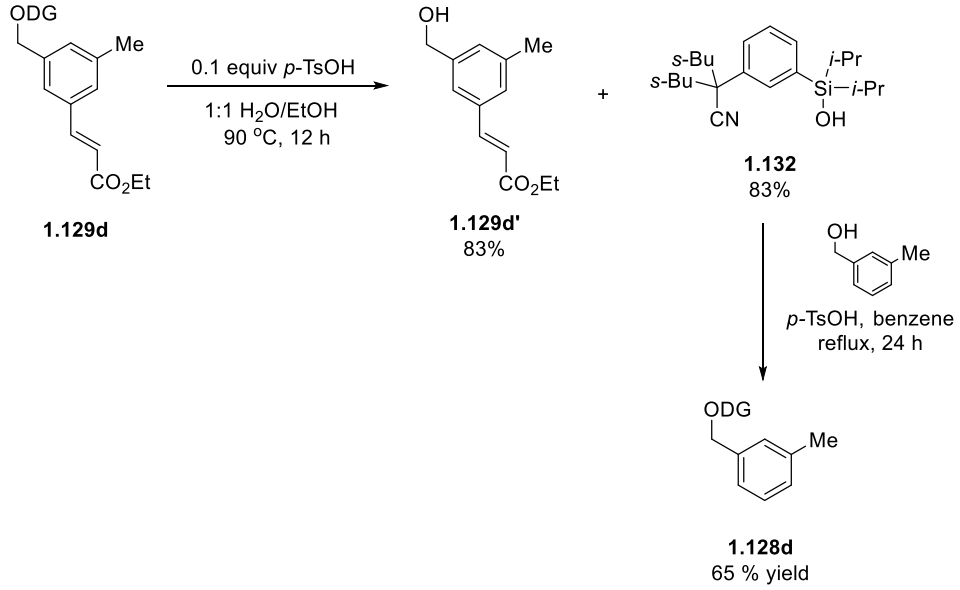

1.5 Conclusions

In the Tan laboratory, we developed scaffolding catalysts to control reaction selectivity (regio-, stereo-, and site-selectivity). This strategy utilizes directing groups that induce intramolecularity before the key reaction step. This was achieved through the formation of a labile covalent bond between the substrate and a binding site in a catalytic system. By this approach, we were able to develop 1) highly site-selective functionalization of polyhydroxylated molecules using a chiral organic scaffold, and 2) *meta*-selective C–H functionalization using a nitrile-based cleavable silyl tether.

In the first part, we demonstrated the catalyst's recognition of *cis*-1,2-diol motif, within complex polyol frameworks and functionalization of a single hydroxyl group therein in a predictable manner. The reaction was controlled by chiral catalysts which are similar to enzymatic systems in terms of preorganization of substrate. However, our catalytic system

has broader substrate scope due to the catalysts' ability to specifically recognize *cis*-1,2-diol.

In the second part, we introduced a removable silicon tether for *meta*-selective olefination of benzyl alcohols. The reaction was compatible with various substituents on the aryl portion of the substrate, including both electron-deficient and electron-rich groups, to give high *meta*-selectivity. Several different olefins also efficiently afforded the desired functionalized products. The key features of this work are easy removal of the directing group by standard silyl deprotection methods and recyclability of template.

1.6 Experimental

1.6.1 Site-Selective Functionalization of 1,2-Diols of Carbohydrates

1.6.1.1 General Information

Unless otherwise noted, all reagents were obtained from commercial suppliers and used without further purification. N,N-Diisopropylethylamine, chlorotriethylsilane, acetyl chloride, and methanesulfonyl chloride were purchased from Sigma Aldrich and distilled over CaH_2 before use. Flash column chromatography was performed using EMD Silica Gel 60 (230-400 mesh) and ACS grade solvents as received from Fisher Scientific. All experiments were performed in oven or flame dried glassware under an atmosphere of nitrogen or argon using standard syringe techniques, except where otherwise noted. All reactions were run with dry, degassed solvents dispensed from a Glass Contour Solvent Purification System (SG Water, USA LLC).

^{1}H, ^{13}C, and gCOSY NMR were performed on a Varian Gemini 400 MHz, Varian Gemini 500 MHz or a Varian Unity Inova 500 MHz spectrometer. Deuterated solvents were purchased from Cambridge Isotope Labs and stored over 3Å molecular sieves. All NMR chemical shifts are reported in ppm relative to residual solvent for ^{1}H and ^{13}C NMR. Signals are quoted as singlet (s), doublet (d), triplet (t), quartet (q), multiplet (m), and broad singlet (br s). Coupling constants are reported in Hz. All IR spectra were gathered on a Bruker Alpha FT-IR equipped with a single crystal diamond ATR module and values are reported in cm^{-1}. All GC analyses were performed on an SHIMADZU GC-2014 System. HRMS data were generated in Boston College facilities.

Methyl α-L-rhamnose, methyl β-L-arabinose, and 1,6-anhydro-β-D-galactose were purchased from Carbosynth and used as received. Digoxin was purchased from Carbosynth and dried under vacuum at 100 °C overnight before use. The following compounds were prepared following the previously reported procedures: Methyl-6-(*tert*-butyldimethylsilyloxy)-α-D-mannose [43], methyl-6-(*tert*-butyldimethylsilyloxy)-α-D-galactose[43][43], 5-dimethoxytrityloxy-uridine[44] and mupirocin methyl ester[45].

1.6.1.2 Experimental Procedures and Characterization

Catalyst Synthesis:

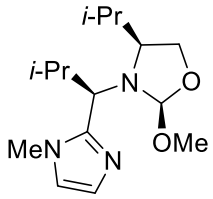

(–)-1.56

To a stirring solution of L-valinol (25.3 g, 250 mmol) in anhydrous THF (188 mL) under nitrogen atmosphere was added a solution of isobutyraldehyde (18.1 g, 250 mmol). $MgSO_4$ (15.1 g, 125 mmol) was added, and the reaction was stirred at room temperature for 3 hours (^{1}H NMR analysis showed oxazolidine formed). In another oven-dried glass reaction flask, to the solution of *N*-methylimidazole (45.2 g, 550 mmol) in anhydrous THF (250 mL) under nitrogen atmosphere was added butyllithium (55 mL of 10 M in hexanes, 550 mmol) slowly at –78 °C. The solution was stirred at –78 °C for 30 minutes, and the formed oxazolidine solution was slowly cannula transferred into the *N*-methylimidazolium lithium solution at –78 °C. The resulting mixture was stirred overnight and gradually warmed to room

[43] Lee, D.; Taylor, M. S *J. Am. Chem. Soc*. **2011**, *133*, 3724–3727.
[44] Xu, Y.; Ishizuka, T.; Kimura, T.; Komiyama, M. *J. Am. Chem. Soc*. **2010**, *132*, 7231–7233.
[45] Scott, R. W.; Murphy, A. C.; Wu, J.; Hothersall, J.; Cox, R. J.; Simpson, T. J.; Thomas, C. M.; Willis, C. L. *Tetrahedron* **2011**, *67*, 5098–5106.

temperature. Aqueous NH_4Cl (50 mL) was added slowly to quench the reaction at 0 °C. $MgSO_4$ (15 g) was added. The mixture was stirred at room temperature for 15 minutes, filtered and concentrated. Excess *N*-methylimidazole was distilled off (150 °C at 1.0 mmHg). Flash column chromatography (Hex/EtOAc = 2:1 to pure EtOAc) afforded the pure product **1.71** as colorless oil (32.8 g, 55 %). ^{1}H NMR ($CDCl_3$, 500 MHz) δ 6.93 (d, 1H, *J* = 1.2), 6.78 (d, 1H, *J* = 1.2), 3.568-3.560 (m, 4H), 3.35 (d, 1H, *J* = 1.2), 3.35 (d, 1H, *J* = 3.9), 2.17-2.13 (m, 1H), 1.93-1.86 (m, 1H), 1.68-1.61 (m, 1H), 0.98 (d, 3H, *J* = 6.8), 0.93 (d, 3H, *J* = 6.8), 0.89 (d, 3H, *J* = 2.9), 0.87 (d, 3H, *J* = 2.9); ^{13}C NMR ($CDCl_3$, 125 MHz) δ 151.7, 127.0, 121.3, 64.2, 62.9, 60.4, 34.0, 32.9, 31.7, 20.2, 19.5, 19.4, 17.7; IR: 2956, 2871, 1488, 1468, 1280, 1045, 725 cm^{-1}; HRMS (DART-TOF) calcd. for $C_{13}H_{26}N_3O$ $[M+H]^+$: 240.20759, found: 240.20870. Optical rotation: $[a]^{25}_D$ 40 (c = 1.0, CH_2Cl_2). To a solution of **1.71** (8.4 g, 35 mmol) in anhydrous methanol (70 mL) under nitrogen atmosphere was added *N*,*N*-dimethylformamide dimethyl acetal (24 mL, 70 mmol). The reaction was stirred at 50 °C overnight (^{1}H NMR analysis showed all substrate consumed and product formed). Solvent was removed under vacuum, and the residue was redissolved in anhydrous methanol (70 mL). The reaction was stirred at 50 °C for 2 hours, and solvent was removed under vacuum. Impurities were distilled off (100 °C at 0.05 mmHg). Kugelrohr distillation (130 °C at 0.05 mmHg), followed by recrystallization with pentane (20 mL, 3 mL/g) at -40 °C overnight afforded the pure product **(–)-1.56** as a white solid (5.6 g, 57 %). ^{1}H NMR (C_6D_6, 500 MHz) δ 7.12 (d, 1H, *J* =1.2), 6.80 (s, 1H), 6.20 (d, 1H, *J* =1.2), 3.72 (dd, 1H, *J* =9.0, 8.1), 3.53 (dd, 1H, *J* =7.8, 7.1), 3.29 (s, 3H), 3.22 (d, 1H, *J* = 10.8), 2.78 (s, 3H), 2.64-2.55 (m, 2H), 1.72-1.63 (m, 1H), 1.34 (d, 3H, *J* =6.4), 0.86 (d, 3H, *J* = 6.8), 0.67 (d, 3H, *J* = 6.8), 0.63 (d, 3H, *J* = 6.6); ^{13}C NMR (C_6D_6, 125 MHz) δ 148.8,

128.7, 120.1, 112.4, 66.1, 65.8, 60.5, 52.7, 33.7, 32.2, 29.5, 21.6, 21.0, 20.2, 16.9; IR: 2956, 1470, 1281, 1052, 964 cm^{-1}; HRMS (DART-TOF) calcd. for $C_{14}H_{24}N_3O$ $[M-OMe]^+$: 250. 19194, found: 250.19264. Optical rotation: $[a]^{26}_D$ -57 (c = 1.0, CH_2Cl_2).

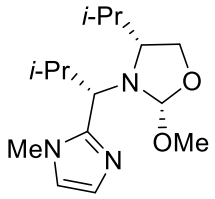

(+)-1.56

Catalysts **(+)-1.56** was prepared following the same procedures to synthesize **(–)-1.50**. D-valinol and isobutraldehyde were used.

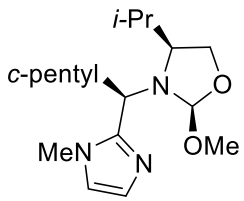

(–)-1.72

Catalysts **(–)-1.72** was prepared according to literature procedures[30] from L-valinol and cyclopentene.

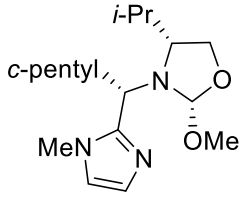

(+)-1.72

Catalysts **(+)-1.72** was prepared according to literature procedures[30] from D-valinol and cyclopentene.

Site-Selective Functionalization of Mannose (Table 1.2):

General Procedure A (Table 1.2, Entry1):

In a dry box, a solution of **1.73** (62 mg, 0.20 mmol), catalyst (*N*-methylimidazole, 3.2 μL, 0.040 mmol, 20 mol %), and *N,N*-diisopropylethylamine hydrochloride (1.0 mg, 0.0060 mmol, 3 mol %) in anhydrous *tert*-amyl alcohol (1.0 mL) was prepared in an oven-dried

glass reaction vial. The solution was brought out of the dry box, *N,N*-diisopropylethylamine (42 μL, 0.24 mmol, 1.2 eq) was added to the stirring reaction at room temperature. The reaction was stirred at 4 °C for 10 minutes, followed by dropwise addition of chlorotriethylsilane (40 μL, 0.24 mmol, 1.2 eq). The reaction was stirred at 4 °C for 2 hours. MeOH (50 μL) was added to quench the reaction. The mixture was filtered through a Pasteur pipette packed with silica gel, followed by flush with EtOAc (15 mL). The solvent was removed under reduced pressure. Column chromatography (Hexane/EtOAc = 20:1 to 5:1) afforded a mixture of mono-functionalized products (65 mg, 77%). ^{1}H NMR of the mixture afforded the selectivity (C2:C3:C4 = 5:78:17).

Table 1.2, Entry 2.

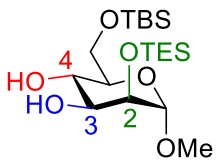

1.74a

The general procedure A was followed using **(+)-1.56** (11 mg, 0.040 mmol, 20 mol %) as the catalyst. Column chromatography (Hexane/EtOAc = 20:1 to 1:1) afforded the bis-silylated product (10 mg, 9%), the substrate **3** (3 mg, 5%), and a mixture of mono-functionalized products (71 mg, 84%). ^{1}H NMR of the mixture afforded the selectivity (C2:C3:C4 = 90:10:-). A second column chromatography was performed to isolate the pure product **1.74a** (64 mg, 76%). ^{1}H NMR ($CDCl_3$, 500 MHz) δ 4.57 (d, 1H, *J* = 1.5), 3.90 (dd, 1H, *J* = 2.9, 1.7), 3.88 (dd, 1H, *J* = 10.5, 5.1), 3.85 (dd, 1H, *J* = 9.0, 3.2), 3.72-3.69 (m, 2H), 3.53-3.50 (m, 1H), 3.43 (s, 3H), 2.88 (br s, 1H), 2.11 (br s, 1H), 0.96 (t, 9H, *J* = 8.1), 0.90 (s, 9H), 0.63 (q, 6H, *J* = 7.8), 0.089 (s, 3H), 0.086 (s, 3H). ^{13}C NMR ($CDCl_3$, 125 MHz) δ 106.9, 83.0, 82.7, 82.4, 75.8, 69.9, 60.4, 31.5, 23.9, 12.4, 10.6, 0.3, 0.2. IR: 3428,

2953, 2927, 2878, 1251, 1139, 1110, 1048, 1005, 833, 776, 728 cm^{-1}. HRMS (DART-TOF) calcd. for $C_{19}H_{42}O_6Si_2$: $[M+H]^+$: 423.2598, found: 423.2591.

Table 1.2, Entry 3.

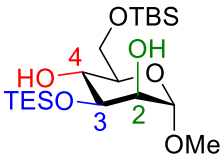

1.75a

The general procedure A was followed using **(–)-1.72** (3.1 mg, 0.010 mmol, 5 mol %) as the catalyst. ^1H NMR of the crude mixture afforded the selectivity (C2:C3:C4 = -:100:-). Column chromatography afforded the pure product **1.75a** (84 mg, >98%). ^1H NMR ($CDCl_3$, 500 MHz) δ 4.71 (d, 1H, *J* = 1.5), 3.87 (d, 1H, *J* = 1.0), 3.86 (d, 1H, *J* = 0.5), 3.84 (dd, 1H, *J* = 8.8, 3.7), 3.75-3.73 (m, 1H), 3.70 (td, 1H, *J* = 9.5, 2.0), 3.58-3.54 (m, 1H), 3.56 (s, 3H), 2.69 (d, 1H, *J* = 2.0), 2.57 (d, 1H, *J* = 1.5), 0.98 (t, 9H, *J* = 8.1), 0.90 (s, 9H), 0.67 (qd, 6H, *J* = 7.3, 2.5), 0.089 (s, 3H), 0.087 (s, 3H). ^{13}C NMR ($CDCl_3$, 125 MHz) δ 106.7, 83.9, 83.6, 83.2, 79.4, 71.4, 61.3, 32.4, 24.8, 13.3, 11.4, 1.1, 1.0. IR: 3506, 2953, 2929, 2878, 1252, 1137, 1106, 1054, 977, 834, 778, 742, 729 cm^{-1}. HRMS (DART-TOF) calcd. for $C_{19}H_{42}O_6Si_2$: $[M+NH_4]^+$: 440.2864, found: 440.2874.

General Procedure B (Table 1.2, Entry 4):

In a dry box, a solution of **1.73** (62 mg, 0.20 mmol), catalyst (*N*-methylimidazole, 3.2 μL, 0.040 mmol, 20 mol %), and *N,N*-diisopropylethylamine hydrochloride (1.0 mg, 0.0060 mmol, 3 mol %) in anhydrous THF (3.0 mL) was prepared in an oven-dried glass reaction vial. The solution was brought out of the dry box, *N,N*-diisopropylethylamine (42 μL, 0.24 mmol, 1.2 eq) was added to the stirring reaction at room temperature. The reaction was stirred at 4 °C for 10 minutes, followed by dropwise addition of acetyl chloride (17 μL,

0.24 mmol, 1.2 eq). The reaction was stirred at 4 °C for 4 hours. MeOH (50 μL) was added to quench the reaction. The mixture was filtered through a Pasteur pipette packed with silica gel, followed by flush with EtOAc (15 mL). The solvent was removed under reduced pressure. 1,3,5-trimethoxybenzene (50 μL of 0.40 M in $CDCl_3$, 0.020 mmol, 10 mol %) was added as standard. ^1H NMR of the crude mixture afforded yield (39%) and selectivity (C2:C3:C4 = 9:84:7).

Table 1.2, Entry 5.

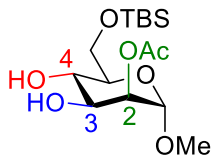

1.74b

The general procedure B was followed using **(+)-1.56** (11 mg, 0.040 mmol, 20 mol %) as the catalyst. ^1H NMR of the crude mixture afforded selectivity (C2:C3:C4 = 84:15:1). Column chromatography (Hexane/EtOAc = 5:1 to 2:1) afforded the mixture of mono-functionalized products with **1.74b** as the major product (52 mg, 74%, C2:C3:C4 = 84:15:1). ^1H NMR ($CDCl_3$, 500 MHz) δ 5.07 (dd, 1H, J = 3.4, 1.5), 4.68 (d, 1H, J = 1.5), 3.99 (d, 1H, J = 9.0), 3.92 (dd, 1H, J = 10.8, 4.9), 3.85 (dd, 1H, J = 10.5, 5.4), 3.81 (t, 1H, J = 9.5), 3.60-3.56 (m, 1H), 3.36 (s, 3H), 3.15 (br s, 1H), 2.44 (br s, 1H), 2.11 (s, 3H), 0.91 (s, 9H), 0.11 (s, 3H), 0.10 (s, 3H). ^{13}C NMR ($CDCl_3$, 125 MHz) δ 171.0, 87.8, 72.0, 71.0, 70.5, 70.2, 64.5, 55.2, 26.0, 21.1, 18.4, -5.23, -5.25. IR: 3412, 2952, 2929, 2856, 1748, 1725, 1375, 1251, 1237, 1139, 1078, 1048, 836, 777 cm^{-1}. HRMS (DART-TOF) calcd. for $C_{15}H_{30}O_7Si$: $[M-OH]^+$: 333.1733, found: 333.1743.

Table 1.2, Entry 6.

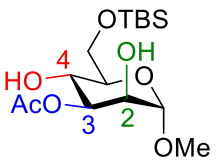

1.75b

The general procedure B was followed using **(–)-1.72** (3.1 mg, 0.010 mmol, 5 mol %) as the catalyst. ^{1}H NMR of the crude mixture afforded the selectivity (C2:C3:C4 = -:100:-). Column chromatography (Hexane/EtOAc = 5:1 to 2:1) afforded the pure product **1.75b** (67 mg, 96%). ^{1}H NMR ($CDCl_3$, 500 MHz) δ 5.08 (dd, 1H, J = 9.8, 3.2), 4.68 (d, 1H, J = 1.7), 4.00-3.98 (m, 1H), 3.96 (t, 1H, J = 9.5), 3.91 (dd, 1H, J = 10.5, 4.9), 3.86 (dd, 1H, J = 10.5, 5.6), 3.67-3.63 (m, 1H), 3.38 (s, 3H), 3.07 (br s, 1H), 2.18 (br s, 1H), 2.15 (s, 3H), 0.89 (s, 9H), 0.090 (s, 3H), 0.088 (s, 3H). ^{13}C NMR ($CDCl_3$, 125 MHz) δ 171.2, 100.8, 74.6, 71.5, 69.3, 68.2, 64.7, 55.2, 26.0, 21.3, 18.4, -5.3. IR: 3438, 2953, 2929, 1716, 1369, 1249, 1107, 1048, 969, 833, 776, 732 cm^{-1}. HRMS (DART-TOF) calcd. for $C_{15}H_{30}O_7Si$: $[M+H]^+$: 351.1839, found: 351.1844.

General Procedure C (Table 1.2, Entry 7):

In a dry box, a solution of **1.73** (62 mg, 0.20 mmol), catalyst (*N*-methylimidazole, 3.2 μL, 0.040 mmol, 20 mol %), and *N,N*-diisopropylethylamine hydrochloride (1.0 mg, 0.0060 mmol, 3 mol %) in anhydrous THF (1.0 mL) was prepared in an oven-dried glass reaction vial. The solution was brought out of the dry box, *N,N*-diisopropylethylamine (42 μL, 0.24 mmol, 1.2 eq) was added to the stirring reaction at room temperature. The reaction was stirred at -15 °C for 10 minutes, followed by dropwise addition of methanesulfonyl chloride (19 μL, 0.24 mmol, 1.2 eq). The reaction was stirred at -15 °C for 4 hours. MeOH (50 μL) was added to quench the reaction. The mixture was filtered through a Pasteur pipette packed with silica gel, followed by flush with EtOAc (15 mL). The solvent was removed

under reduced pressure. Column chromatography (Hexane/EtOAc = 5:1 to 2:1) afforded a mixture of mono-functionalized products (53 mg, 68%). GC Analysis (Shimazu SHRXI-5MS 15 m, 150 °C for 3 min, 10 °C/min to 200 °C, 200°C for 6 min, 15 psi., t_{C2} = 10.50 min, t_{C3} = 11.04 min, t_{C4} = 9.50 min) of the mixture afforded selectivity (C2:C3:C4 = 22:56:22).

Table 1.2, Entry 8.

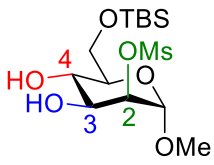

1.74c

The general procedure C was followed using **(+)-1.56** (11 mg, 0.040 mmol, 20 mol %) as the catalyst. GC Analysis of the crude mixture afforded selectivity (C2:C3:C4 = 91:8:1). Column chromatography (Hexane/EtOAc = 5:1 to 2:1) afforded the pure product **1.74c** (62 mg, 80%). ^{1}H NMR ($CDCl_3$, 500 MHz) δ 4.81 (d, 1H, *J* = 1.7), 4.78 (dd, 1H, *J* = 3.2, 1.7), 4.00 (dd, 1H, *J* = 9.5, 3.2), 3.91 (dd, 1H, *J* = 10.3, 4.9), 3.83 (dd, 1H, *J* = 10.5, 6.4), 3.78 (t, 1H, 9.3), 3.60-3.56 (m, 1H), 3.38 (s, 3H), 3.13 (s, 3H), 0.90 (s, 9H), 0.11 (s, 3H), 0.10 (s, 3H). ^{13}C NMR ($CDCl_3$, 125 MHz) δ 99.2, 7.5, 71.0, 70.6, 69.6, 65.0, 55.4, 38.6, 26.0, 18.4, -5.3. IR: 3457, 2928, 2856, 1352, 1175, 1138, 1069, 962, 907, 833, 777, 523 cm^{-1}. HRMS (DART-TOF) calcd. for $C_{14}H_{30}O_8SSi$: $[M+H]^+$: 387.1509, found: 387.1510.

Table 1.2, Entry 9.

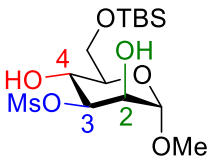

1.75c

The general procedure C was followed using **(–)-1.72** (3.1 mg, 0.010 mmol, 5 mol %) as the catalyst. GC Analysis of the crude mixture afforded selectivity (C2:C3:C4 = -:100:-). Column chromatography (Hexane/EtOAc = 5:1 to 2:1) afforded the pure product **1.75c** (75 mg, 97%). ^{1}H NMR ($CDCl_3$, 500 MHz) δ 4.79 (dd, 1H, *J* = 9.5, 3.2), 4.72 (d, 1H, *J* = 1.7), 4.14-

4.12 (m, 1H), 4.07 (td, 1H, J = 9.5, 2.0), 3.95 (dd, 1H, J = 10.3, 4.9), 3.85 (dd, 1H, J = 10.0, 7.1), 3.68-3.63 (m, 1H), 3.49 (d, 1H, J = 2.2), 3.38 (s, 3H), 3.18 (s, 3H), 2.57 (d, 1H, J = 4.7), 0.90 (s, 9H), 0.111 (s, 3H), 0.107 (s, 3H). ^{13}C NMR ($CDCl_3$, 125 MHz) δ 100.7, 82.7, 70.5, 10.1, 68.9, 65.5, 55.3, 38.6, 26.0, 18.4, -5.3, -5.4. IR: 3497, 2930, 2857, 1350, 1253, 1175, 1135, 1109, 1058, 963, 837, 779 cm^{-1}. HRMS (DART-TOF) calcd. for $C_{14}H_{30}O_8SSi$: $[M+H]^+$: 387.1509, found: 387.1500.

Site-Selective Functionalization of Rhamnose (Table 1.3):

General Procedure D (Table 1.3, Entry 1):

In a dry box, a solution of **1.77** (36 mg, 0.20 mmol), catalyst (*N*-methylimidazole, 3.2 μL, 0.040 mmol, 20 mol %), and *N,N*-diisopropylethylamine hydrochloride (1.0 mg, 0.0060 mmol, 3 mol %) in anhydrous *tert*-amyl alcohol (1.0 mL) was prepared in an oven-dried glass reaction vial. The solution was brought out of the dry box, and *N,N*-diisopropylethylamine (42 μL, 0.24 mmol, 1.2 eq) was added to the stirring reaction at room temperature. The reaction was stirred at 4 °C for 10 minutes, followed by dropwise addition of chlorotriethylsilane (40 μL, 0.24 mmol, 1.2 eq). The reaction was stirred at 4 °C for 4 hours. MeOH (50 μL) was added to quench the reaction. The mixture was filtered through a Pasteur pipette packed with silica gel, followed by flushing with EtOAc (15 mL). The solvent was removed under reduced pressure. Column chromatography (Hexane/EtOAc = 10:1 to 3:1) afforded a mixture of mono-functionalized products (46 mg, 78%). Selectivity of the mixture was determined by ^{1}H NMR (C2:C3:C4 = 7:79:14).

Table 1.3, Entry 2.

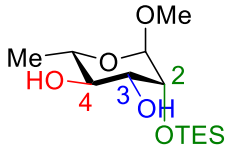

1.78a

The general procedure D was followed using **(–)-1.72** (12 mg, 0.040 mmol, 20 mol %) as the catalyst. Column chromatography (Hexane/EtOAc = 10:1 to 3:1) afforded a mixture of mono-functionalized products with **1.78a** as the major product (52 mg, 88%). ^{1}H NMR of the mixture afforded the selectivity (C2:C3:C4 = 89:11:-). A second column chromatography was performed for characterization of the pure product. ^{1}H NMR ($CDCl_3$, 500 MHz) δ 4.54 (d, 1H, *J* = 1.5), 3.91 (dd, 1H, *J* = 3.7, 1.7), 3.62-3.58 (m, 2H), 3.38 (t, 1H, *J* = 9.3), 3.34 (s, 3H), 2.29 (br s, 1H), 2.03 (d, 1H, *J* = 10.5), 1.31 (d, 3H, *J* = 6.4), 0.97 (t, 9H, *J* = 6.0), 0.64 (q, 6H, *J* = 8.1). ^{13}C NMR ($CDCl_3$, 125 MHz) δ 101.4, 74.0, 72.2, 72.1, 67.9, 55.0, 17.8, 6.9, 5.1. IR: 3416, 2953, 2877, 2831, 1458, 1239, 1052, 1005, 829, 727, 630 cm^{-1}. HRMS (DART-TOF) calcd. for $C_{13}H_{28}O_5Si$: $[M+NH_4]^+$: 310.2050, found: 310.2049.

Table 1.3, Entry 3.

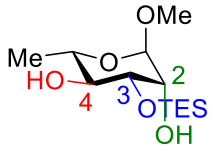

1.79a

The general procedure D was followed using **(+)-1.56** (2.8 mg, 0.010 mmol, 5 mol %) as the catalyst. The reaction was stirred at 4 °C for 20 hours. Selectivity was determined by ^{1}H NMR of the crude reaction mixture (C2:C3:C4 = -:100:-). Column chromatography (Hexane/EtOAc = 10:1 to 3:1) afforded the pure product **1.79a** (59 mg, >98%). ^{1}H NMR ($CDCl_3$, 500 MHz) δ 4.68 (d, 1H, *J* = 1.2), 3.80 (dd, 1H, *J* = 8.8, 3.7), 3.78 (dd, 1H, *J* = 3.7, 1.5), 3.65-3.62 (m, 1H), 3.46 (td, 1H, *J* = 9.1, 2.9), 3.36 (s, 3H), 2.54 (d, 1H, *J* = 1.5), 2.04 (d, 1H, *J* = 3.4), 1.32 (d, 3H, *J* = 6.4), 0.98 (t, 9H, *J* = 8.1), 0.67 (q, 6H, *J* = 8.1). ^{13}C NMR ($CDCl_3$, 125 MHz) δ 100.4,

73.4, 73.3, 71.8, 67.5, 55.0, 17.8, 6.9, 5.1. IR: 3477, 2954, 2911, 2833, 1458, 1238, 1107, 972, 852, 727, 616 cm^{-1}. HRMS (DART-TOF) calcd. for $C_{13}H_{28}O_5Si$: $[M+H]^+$: 293.1784, found: 293.1780.

General Procedure E (Table 1.3, Entry 4):

In a dry box, a solution of **1.77** (36 mg, 0.20 mmol), catalyst (*N*-methylimidazole, 3.2 μL, 0.040 mmol, 20 mol %), and *N,N*-diisopropylethylamine hydrochloride (1.0 mg, 0.0060 mmol, 3 mol %) in anhydrous THF (1.0 mL) was prepared in an oven-dried glass reaction vial. The solution was brought out of the dry box, and *N,N*-diisopropylethylamine (42 μL, 0.24 mmol, 1.2 eq) was added to the stirring reaction at room temperature. The reaction was stirred at 4 °C for 10 minutes, followed by dropwise addition of acetyl chloride (17 μL, 0.24 mmol, 1.2 eq). The reaction was stirred at 4 °C for 4 hours. MeOH (50 μL) was added to quench the reaction. The mixture was filtered through a Pasteur pipette packed with silica gel, followed by flushing with EtOAc (15 mL). The solvent was removed under reduced pressure. Column chromatography (Hexane/EtOAc = 5:1 to 1:1) afforded a mixture of mono-functionalized products (37 mg, 83%). Selectivity of the mixture was determined by ^1H NMR (C2:C3:C4 = 12:79:9).

Table 1.3, Entry 5.

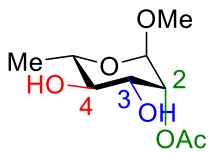

1.78b

The general procedure E was followed using **(–)-1.72** (12 mg, 0.040 mmol, 20 mol %) as the catalyst in anhydrous THF (3.0 mL). Column chromatography (Hexane/EtOAc = 5:1 to 1:1) afforded the mixture of

mono-functionalized products (32 mg, 73%) with **1.78b** as the major product. Selectivity was determined by ^{1}H NMR of the isolated mixture (C2:C3:C4 = 84:14:2). ^{1}H NMR ($CDCl_3$, 500 MHz) δ 5.08 (dd, 1H, *J* = 3.4, 1.5), 4.63 (d, 1H, *J* = 1.5), 3.92 (dd, 1H, *J* = 9.5, 3.4), 3.67-3.63 (m, 1H), 3.45 (t, 1H, *J* = 9.5), 3.37 (s, 3H), 3.16 (br s, 2H), 2.14 (s, 3H), 1.34 (d, 3H, *J* = 6.1). ^{13}C NMR ($CDCl_3$, 125 MHz) δ 171.3, 98.7, 73.3, 72.6, 70.3, 68.1, 55.2, 21.2, 17.7. IR: 3409, 2934, 2837, 1747, 1726, 1376, 1237, 1135, 1076, 1054, 973, 838, 803 cm^{-1}. HRMS (DART-TOF) calcd. for $C_9H_{16}O_6$: $[M+NH_4]^+$: 238.1291, found: 238.1294.

Table 1.3, Entry 6.

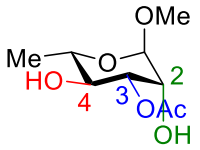

1.79b

The general procedure E was followed using **(+)-1.56** (2.8 mg, 0.010 mmol, 5 mol %) as the catalyst in anhydrous THF (3.0 mL). ^{1}H NMR of the crude reaction mixture afforded the selectivity (C2:C3:C4 = 1:99:-). Column chromatography (Hexane/EtOAc = 5:1 to 1:1) afforded the pure product **1.79b** (43 mg, 98%). ^{1}H NMR ($CDCl_3$, 500 MHz) δ 5.04 (dd, 1H, *J* = 9.8, 3.2), 4.68 (d, 1H, *J* = 1.7), 4.05-4.03 (m, 1H), 3.74-3.71 (m, 1H), 3.64 (td, 1H, *J* = 9.5, 5.4), 3.41 (s, 3H), 2.21 (d, 1H, *J* = 5.6), 2.19 (s, 3H), 2.04 (d, 1H, *J* = 5.1), 1.37 (d, 3H, *J* = 6.1). ^{13}C NMR ($CDCl_3$, 125 MHz) δ 171.6, 100.6, 75.2, 71.7, 69.9, 68.6, 55.2, 21.4, 17.8. IR: 3437, 2922, 2837, 1717, 1450, 1372, 1249, 1132, 1056, 987, 973, 805 cm^{-1}. HRMS (DART-TOF) calcd. for $C_9H_{16}O_6$: $[M+NH_4]^+$: 238.1291, found: 238.1283.

General Procedure F (Table 1.3, Entry 7):

In a dry box, a solution of **1.77** (36 mg, 0.20 mmol), catalyst (*N*-methylimidazole, 3.2 μL, 0.040 mmol, 20 mol %), and *N,N*-diisopropylethylamine hydrochloride (1.0 mg, 0.0060 mmol, 3 mol %) in anhydrous THF (1.0 mL) was prepared in an oven-dried glass reaction vial. The solution was brought out of the dry box, and *N,N*-diisopropylethylamine (42 μL, 0.24 mmol, 1.2 eq) was added to the stirring reaction at room temperature. The reaction was stirred at 4 °C for 10 minutes, followed by dropwise addition of methanesulfonyl chloride (19 μL, 0.24 mmol, 1.2 eq). The reaction was stirred at 4 °C for 4 hours. MeOH (50 μL) was added to quench the reaction. The mixture was filtered through a Pasteur pipette packed with silica gel, followed by flushing with EtOAc (15 mL). The solvent was removed under reduced pressure. Column chromatography (Hexane/EtOAc = 5:1 to 1:1) afforded a mixture of mono-functionalized products (37 mg, 72%). Selectivity of the mixture was determined by GC analysis (Shimazu SHRXI-5MS 15 m, 120 °C for 2 min, 1 °C/min to 140 °C, 10 °C/min to 200 °C, 200°C for 2 min, 15 psi., t_{C2} = 15.07 min, t_{C3} = 16.30 min, t_{C4} = 14.46 min) (C2:C3:C4 = 24:57:19).

Table 1.3, Entry 8.

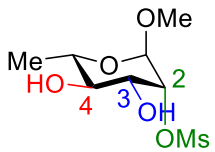

1.78c

The general procedure F was followed using **(–)-1.72** (11 mg, 0.040 mmol, 20 mol %) as the catalyst. The reaction was stirred at -15 °C for 4 hours. Selectivity was determined by GC analysis of the crude reaction mixture (C2:C3:C4 = 92:8:-). Column chromatography (Hexane/EtOAc = 5:1 to 1:1) afforded the pure product **1.78c** (42 mg, 82%). ^{1}H NMR ($CDCl_3$, 500 MHz) δ 4.82 (dd, 1H, *J* = 3.2, 1.7), 4.79 (d, 1H, *J* = 1.7), 3.93 (d, 1H, *J* = 9.5), 3.68-3.62 (m, 1H),

3.44 (t, 1H, J = 9.5), 3.38 (s, 3H), 3.15 (s, 3H), 3.03 (br s, 1H), 2.74 (br s, 1H), 1.33 (d, 3H, J = 6.4). ^{13}C NMR ($CDCl_3$, 125 MHz) δ 99.0, 79.0, 73.2, 69.8, 68.3, 55.3, 38.7, 17.6. IR: 3454, 2935, 2842, 1451, 1346, 1173, 1133, 1051, 963, 907, 855, 637, 529 cm^{-1}. HRMS (DART-TOF) calcd. for $C_8H_{16}O_7S$: $[M+NH_4]^+$: 274.0961, found: 274.0974.

Table 1.3, Entry 9.

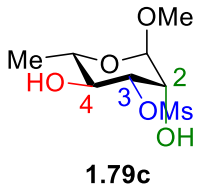

1.79c

The general procedure F was followed using **(+)-1.56** (2.8 mg, 0.010 mmol, 5 mol %) as the catalyst. Selectivity was determined by GC analysis of the crude reaction mixture (C2:C3:C4 = 1:99:-). Column chromatography (Hexane/EtOAc = 5:1 to 1:1) afforded the pure product **1.79c** (51 mg, >98%). ^{1}H NMR ($CDCl_3$, 500 MHz) δ 4.76 (dd, 1H, J = 9.1, 3.2), 4.70 (d, 1H, J = 1.7), 4.19 (br s, 1H), 3.77-3.70 (m, 2H), 3.40 (s, 3H), 3.18 (s, 3H), 2.73 (br s, 1H), 2.71 (br s, 1H), 1.38 (d, 3H, J = 5.9). ^{13}C NMR ($CDCl_3$, 125 MHz) δ 100.6, 82.8, 70.8, 70.5, 68.4, 55.2, 38.6, 17.8. IR: 3462, 2936, 2839, 1452, 1348, 1198, 1150, 1055, 959, 860, 799, 530, 513 cm^{-1}. HRMS (DART-TOF) calcd. for $C_8H_{16}O_7S$: $[M+NH_4]^+$: 274.0961, found: 274.0964.

Site-Selective Functionalization of Arabinose (Table 1.4):

General Procedure G (Table 1.4, Entry 1):

In a dry box, a solution of **1.81** (33 mg, 0.20 mmol), catalyst (*N*-methylimidazole, 3.2 μL, 0.040 mmol, 20 mol %), and *N,N*-diisopropylethylamine hydrochloride (1.0 mg, 0.0060 mmol, 3 mol %) in anhydrous *tert*-amyl alcohol (1.0 mL) was prepared in an oven-dried

glass reaction vial. The solution was brought out of the dry box, and *N,N*-diisopropylethylamine (42 μL, 0.24 mmol, 1.2 eq) was added to the stirring reaction at room temperature. The reaction was stirred at 4 °C for 10 minutes, followed by dropwise addition of chlorotriethylsilane (40 μL, 0.24 mmol, 1.2 eq). The reaction was stirred at 4 °C for 4 hours. MeOH (50 μL) was added to quench the reaction. The mixture was filtered through a Pasteur pipette packed with silica gel, followed by flush with EtOAc (15 mL). The solvent was removed under reduced pressure. 1,3,5-trimethoxybenzene (50 μL of 0.40 M in $CDCl_3$, 0.020 mmol, 10 mol %) was added as standard. ^1H NMR of the crude mixture afforded the yield (39%) and selectivity (C2:C3:C4 = 27:14:59).

Table 1.4, Entry 2.

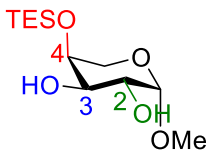

1.84a

The general procedure G was followed using **(–)-1.72** (11 mg, 0.040 mmol, 20 mol %) as the catalyst. Reaction was performed in anhydrous *tert*-amyl alcohol (3.0 mL). ^1H NMR of the crude mixture afforded the selectivity (C2:C3:C4 = -:3:97). Column chromatography (Hexane/EtOAc = 4:1 to 3:1) afforded the pure product **1.84a** (51 mg, 92%). ^1H NMR ($CDCl_3$, 500 MHz) δ 4.75 (d, 1H, J = 3.2), 4.00 (dd, 1H, J = 5.6, 3.4), 3.79-3.78 (m, 1H), 3.74-3.72 (m, 2H), 3.57 (dd, 1H, J = 12.2, 3.4), 3.42 (s, 3H), 2.27 (d, 1H, J = 6.1), 2.23 (br s, 1H), 0.97 (t, 9H, J = 8.1), 0.63 (q, 6H, J = 7.8). ^{13}C NMR ($CDCl_3$, 125 MHz) δ 100.0, 70.8, 70.3, 69.8, 63.6, 55.9, 6.9, 5.1. IR: 3422, 2952, 2911, 2875, 1070, 1045, 1002, 890, 877, 798, 725 cm^{-1}. HRMS (DART-TOF) calcd. for $C_{12}H_{26}O_5Si$: $[M+H]^+$: 279.1628, found: 279.1625.

Table 1.4, Entry 3.

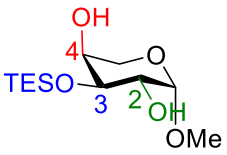

1.83a

The general procedure G was followed using **(+)-1.56** (2.8 mg, 0.010 mmol, 5mol %) as the catalyst. ^{1}H NMR of the crude mixture afforded the selectivity (C2:C3:C4 = -:98:2).Column chromatography (Hexane/EtOAc = 4:1 to 3:1) afforded the pure product **1.83a** (54 mg, 97%). ^{1}H NMR ($CDCl_3$, 500 MHz) δ 4.75 (d, 1H, *J* = 3.7), 3.82 (dd, 1H, *J* = 8.8, 3.7), 3.79 (t, 1H, *J* = 1.5), 3.75 (td, 1H, *J* = 8.6, 3.4), 3.72 (d, 2H, *J* = 1.7), 3.41 (s, 3H), 2.65 (s, 1H), 1.93 (d, 1H, *J* = 8.3), 0.98-0.95 (m, 9H), 0.68-0.63 (m, 6H). ^{13}C NMR ($CDCl_3$, 125 MHz) δ 100.2, 71.9, 70.0, 69.9, 61.7, 55.7, 6.9, 5.1. IR: 3458, 2952, 2911, 2875, 1062, 998, 848, 742 cm^{-1}. HRMS (DART-TOF) calcd. for $C_{12}H_{26}O_5Si$: $[M+H]^+$: 279.1628, found: 279.1624.

General Procedure H (Table 1.4, Entry 4):

In a dry box, a solution of **1.81** (33 mg, 0.20 mmol), catalyst (*N*-methylimidazole, 3.2 μL, 0.040 mmol, 20 mol %), and *N,N*-diisopropylethylamine hydrochloride (1.0 mg, 0.0060 mmol, 3 mol %) in anhydrous THF (3.0 mL) was prepared in an oven-dried glass reaction vial. The solution was brought out of the dry box, and *N,N*-diisopropylethylamine (42 μL, 0.24 mmol, 1.2 eq) was added to the stirring reaction at room temperature. The reaction was stirred at 4 °C for 10 minutes, followed by dropwise addition of acetyl chloride (17 μL, 0.24 mmol, 1.2 eq). The reaction was stirred at 4 °C for 4 hours. MeOH (50 μL) was added to quench the reaction. The mixture was filtered through a Pasteur pipette packed with silica gel, followed by flush with EtOAc (15 mL). The solvent was removed under

reduced pressure. 1,3,5-trimethoxybenzene (50 μL of 0.40 M in $CDCl_3$, 0.020 mmol, 10 mol %) was added as standard. ^{1}H NMR of the crude mixture afforded the yield (6%) and selectivity (C2:C3:C4 = 22:72:6).

Table 1.4, Entry 5.

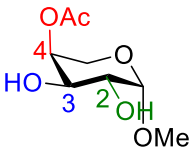

1.84b

The general procedure H was followed using **(–)-1.72** (11 mg, 0.040 mmol, 20 mol %) as the catalyst. Reaction was stirred for 8 hours. ^{1}H NMR of the crude mixture afforded the selectivity (C2:C3:C4 = 5:9:86).Column chromatography (CH_2Cl_2/MeOH = 100:1 to 20:1) afforded the mixture of mono-functionalized products with **1.84b** as the major product (25 mg, 61%). ^{1}H NMR (acetone-d6, 500 MHz) δ 5.08-5.07 (m, 1H), 4.69 (d, 1H, *J* = 3.4), 3.88 (dd, 1H, *J* = 9.8, 3.4), 3.80 (dd, 1H, *J* = 12.7, 1.5), 3.72 (dd, 1H, *J* = 9.8, 2.9), 3.57 (dd, 1H, *J* = 12.7, 2.4), 3.35 (s, 3H), 2.04 (s, 3H). ^{13}C NMR (acetone-d6, 125 MHz) δ 170.9, 101.6, 72.7, 70.8, 69.1, 61.4, 55.8, 21.1. IR: 3429, 2937, 1734, 1241, 1077, 1038, 997 cm^{-1}. HRMS (DART-TOF) calcd. for $C_8H_{14}O_6$: $[M+H]^+$: 207.0869, found: 207.0861.

Table 1.4, Entry 6.

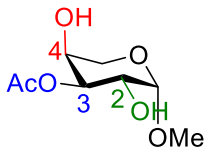

1.83b

The general procedure H was followed using **(+)-1.56** (2.8 mg, 0.010 mmol, 5 mol %) as the catalyst. ^{1}H NMR of the crude mixture afforded the selectivity (C2:C3:C4 = 3:96:1). Column chromatography (Hex/EtOAc = 2:1 to 1:2) afforded the pure product **1.83b** (34 mg, 83%). ^{1}H NMR (acetone-d6, 500 MHz) δ 4.96 (dd, 1H, *J* = 10.3, 3.4), 4.70 (d, 1H, *J* = 3.7), 4.12 (d, 1H, *J* = 3.2), 4.00 (s, 1H), 3.98-3.96 (m, 1H), 3.79 (dd, 1H, *J* = 12.5, 1.5), 3.56 (dd, 1H, *J* = 12.2, 2.4), 3.52 (d, 1H, *J* = 8.8), 3.37 (s, 3H), 2.02 (s, 3H). ^{13}C NMR (acetone-d6, 125 MHz) δ

171.1, 101.8, 74.0, 68.2, 67.6, 63.7, 55.6, 21.1. IR: 3436, 2927, 1737, 1716, 1240, 1141, 1057, 997cm^{-1}. HRMS (DART-TOF) calcd. for $C_8H_{14}O_6$: $[M+H]^+$: 207.0869, found: 207.0878.

General Procedure I (Table 1.4, Entry 7):

In a dry box, a solution of **1.81** (33 mg, 0.20 mmol), catalyst (*N*-methylimidazole, 3.2 μL, 0.040 mmol, 20 mol %), and *N,N*-diisopropylethylamine hydrochloride (1.0 mg, 0.0060 mmol, 3 mol %) in anhydrous THF (1.0 mL) was prepared in an oven-dried glass reaction vial. The solution was brought out of the dry box, and *N,N*-diisopropylethylamine (42 μL, 0.24 mmol, 1.2 eq) was added to the stirring reaction at room temperature. The reaction was stirred at 4 °C for 10 minutes, followed by dropwise addition of methanesulfonyl chloride (19 μL, 0.24 mmol, 1.2 eq). The reaction was stirred at 4 °C for 4 hours. MeOH (50 μL) was added to quench the reaction. The mixture was filtered through a Pasteur pipette packed with silica gel, followed by flush with EtOAc (15 mL). The solvent was removed under reduced pressure. Column chromatography (Hex/EtOAc = 1:1 to 1:3) afforded the mixture of mono-functionalized products (13 mg, 27%). ^{1}H NMR of the mixture afforded the selectivity (C2:C3:C4 = 68:23:9).

Table 1.4, Entry 8.

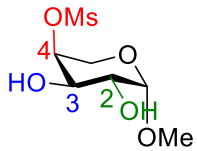

1.84c

The general procedure I was followed using **(–)-1.72** (11 mg, 0.040 mmol, 20 mol %) as the catalyst. Column chromatography (Hex/EtOAc = 1:1 to 1:3) afforded the mixture of mono-functionalized products (45 mg, 93%). ^{1}H NMR of the mixture afforded the selectivity (C2:C3:C4 = 3:10:87). A second column chromatography (Hex/EtOAc = 1:1 to 1:3) afforded **1.84c** for

characterizations. ^{1}H NMR (acetone-d6, 500 MHz) δ 4.88-4.87 (m, 1H), 4.71 (d, 1H, *J* = 3.4), 3.96 (dd, 1H, *J* = 10.0, 3.4), 3.91 (dd, 1H, *J* = 13.0, 1.0), 3.74 (dd, 1H, *J* = 13.0, 2.2), 3.69 (dd, 1H, *J* = 10.0, 3.7), 3.36 (s, 3H), 3.15 (s, 3H). ^{13}C NMR (acetone-d6, 125 MHz) δ 101.5, 81.5, 70.3, 69.0, 62.2, 55.9, 38.6. IR: 3439, 2939, 1337, 1173, 1076, 975, 925, 895 cm^{-1}. HRMS (DART-TOF) calcd. for $C_7H_{14}O_7S$: $[M+NH_4]^+$: 260.0804, found: 260.0809.

Table 1.4, Entry 9.

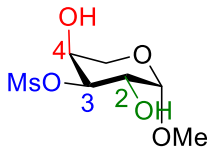

1.83c

The general procedure I was followed using **(+)-1.56** (2.8 mg, 0.010 mmol, 5 mol %) as the catalyst. ^{1}H NMR of the crude mixture afforded the selectivity (C2:C3:C4 = 1:92:7). Column chromatography (Hex/EtOAc = 1:1 to 1:3) afforded the pure product **1.83c** (44 mg, 91%). ^{1}H NMR (acetone-d6, 500 MHz) δ 4.75 (d, 1H, *J* = 3.2), 4.66 (dd, 1H, *J* = 9.0, 3.2), 4.47 (d, 1H, *J* = 2.7), 4.13 (s, 1H), 4.04-4.02 (m, 2H), 3.82 (dd, 1H, *J* = 12.2, 1.2), 3.61 (dd, 1H, *J* = 12.5, 2.2), 3.38 (s, 3H), 3.14 (s, 3H). ^{13}C NMR (acetone-d6, 125 MHz) δ 72.1, 52.8, 39.8, 38.0, 34.1, 26.0, 9.0. IR: 3460, 1334, 1171, 1140, 1061, 1018, 972, 860 cm^{-1}. HRMS (DART-TOF) calcd. for $C_7H_{14}O_7S$: $[M+NH_4]^+$: 260.0804, found: 260.0802.

Site-Selective Functionalization of Galactose (Table 1.5):

General Procedure J (Table 1.5, Entry 1):

In a dry box, a solution of **1.85** (62 mg, 0.20 mmol), catalyst (*N*-methylimidazole, 3.2 μL, 0.040 mmol, 20 mol %), and *N,N*-diisopropylethylamine hydrochloride (1.0 mg, 0.0060 mmol, 3 mol %) in anhydrous *tert*-amyl alcohol (1.0 mL) was prepared in an oven-dried

glass reaction vial. The solution was brought out of the dry box, and *N,N*-diisopropylethylamine (42 μL, 0.24 mmol, 1.2 eq) was added to the stirring reaction at room temperature. The reaction was stirred at 4 °C for 10 minutes, followed by dropwise addition of chlorotriethylsilane (40 μL, 0.24 mmol, 1.2 eq). The reaction was stirred at 4 °C for 4 hours. MeOH (50 μL) was added to quench the reaction. The mixture was filtered through a Pasteur pipette packed with silica gel, followed by flush with EtOAc (15 mL). The solvent was removed under reduced pressure. 1,3,5-trimethoxybenzene (50 μL of 0.40 M in $CDCl_3$, 0.020 mmol, 10 mol %) was added as standard. ^1H NMR of the crude mixture afforded yield (77%) and selectivity (C2:C3:C4 = 86:14:-).

Table 1.5, Entry 2.

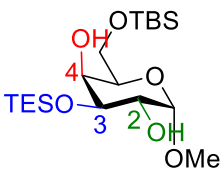

1.87a

The general procedure J was followed using **(+)-1.56** (11 mg, 0.040 mmol, 20 mol %) as the catalyst. ^1H NMR of the crude mixture afforded selectivity (C2:C3:C4 = 6:94:-). Column chromatography (Hexane/EtOAc = 20:1 to 5:1) afforded the pure product **1.87a** (80 mg, 95%). ^1H NMR ($CDCl_3$, 500 MHz) δ 4.78 (d, 1H, J = 3.2), 3.88-3.84 (m, 2H), 3.80-3.74 (m, 3H), 3.41 (s, 3H), 2.58 (s, 1H), 1.87 (dd, 1H, J = 5.1, 3.7), 0.97 (t, 9H, J = 8.1), 0.89 (s, 9H), 0.66 (qd, 6H, J = 7.6, 3.4), 0.08 (s, 6H). ^{13}C NMR ($CDCl_3$, 125 MHz) δ 99.8, 72.7, 70.4, 70.0, 69.9, 62.5, 55.4, 26.0, 18.5, 7.0, 5.1, -5.1, -5.3. IR: 3566, 2953, 2930, 2877, 1250, 1086, 1053, 835, 744 cm^{-1}. HRMS (DART-TOF) calcd. for $C_{19}H_{42}O_6Si_2$: $[M+H]^+$: 423.2598, found: 423.2612.

General Procedure K (Table 1.5, Entry 3):

In a dry box, a solution of **1.85** (62 mg, 0.20 mmol), catalyst (*N*-methylimidazole, 3.2 μL, 0.040 mmol, 20 mol %), and *N,N*-diisopropylethylamine hydrochloride (1.0 mg, 0.0060 mmol, 3 mol %) in anhydrous THF (3.0 mL) was prepared in an oven-dried glass reaction vial. The solution was brought out of the dry box, and *N,N*-diisopropylethylamine (42 μL, 0.24 mmol, 1.2 eq) was added to the stirring reaction at room temperature. The reaction was stirred at 4 °C for 10 minutes, followed by dropwise addition of acetyl chloride (17 μL, 0.24 mmol, 1.2 eq). The reaction was stirred at 4 °C for 4 hours. MeOH (50 μL) was added to quench the reaction. The mixture was filtered through a Pasteur pipette packed with silica gel, followed by flush with EtOAc (15 mL). The solvent was removed under reduced pressure. 1,3,5-trimethoxybenzene (50 μL of 0.40 M in $CDCl_3$, 0.020 mmol, 10 mol %) was added as standard. ^{1}H NMR of the crude mixture afforded yield (26%) and selectivity (C2:C3:C4 = 42:58:-).

Table 1.5, Entry 4.

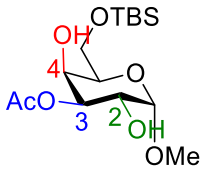

1.87b

The general procedure K was followed using **(+)-1.56** (11 mg, 0.040 mmol, 20 mol %) as the catalyst. ^{1}H NMR of the crude mixture afforded selectivity (C2:C3:C4 = 19:81:-). Column chromatography (Hexane/EtOAc = 5:1 to 2:1) afforded the mixture of mono-functionalized products with **1.87b** as the major product (67 mg, 96%). ^{1}H NMR ($CDCl_3$, 500 MHz) δ 5.03 (dd, 1H, *J* = 10.0, 2.9), 4.84 (d, 1H, *J* = 3.9), 4.18 (s, 1H), 4.06 (td, 1H, *J* = 10.8, 3.9), 3.91 (dd, 1H, *J* = 10.8, 4.9), 3.87 (dd, 1H, *J* = 10.8, 4.2), 3.76 (t, 1H, *J* = 4.6), 3.43 (s, 3H), 3.25 (d, 1H, *J* = 2.0), 2.16 (s, 1H), 1.99 (d, 1H, *J* = 11.0), 0.89 (s, 9H), 0.09 (s, 3H), 0.08 (s, 3H). ^{13}C

NMR ($CDCl_3$, 125 MHz) δ 171.3, 100.0, 73.7, 69.6, 69.3, 67.5, 64.0, 55.6, 26.0, 21.4, 18.4, -5.3, -5.4. IR: 3428, 2953, 2929, 2856, 1739, 1721, 1248, 1146, 1083, 1050, 836, 776 cm^{-1}. HRMS (DART-TOF) calcd. for $C_{15}H_{30}O_7Si$: $[M-OH]^+$: 333.1733, found: 333.1743.

General Procedure L (Table 1.5, Entry 5):

In a dry box, a solution of **1.85** (62 mg, 0.20 mmol), catalyst (*N*-methylimidazole, 3.2 μL, 0.040 mmol, 20 mol %), and *N,N*-diisopropylethylamine hydrochloride (1.0 mg, 0.0060 mmol, 3 mol %) in anhydrous THF (1.0 mL) was prepared in an oven-dried glass reaction vial. The solution was brought out of the dry box, and *N,N*-diisopropylethylamine (42 μL, 0.24 mmol, 1.2 eq) was added to the stirring reaction at room temperature. The reaction was stirred at -15 °C for 10 minutes, followed by dropwise addition of methanesulfonyl chloride (19 μL, 0.24 mmol, 1.2 eq). The reaction was stirred at -15 °C for 4 hours. MeOH (50 μL) was added to quench the reaction. The mixture was filtered through a Pasteur pipette packed with silica gel, followed by flush with EtOAc (15 mL). The solvent was removed under reduced pressure. Column chromatography (Hexane/EtOAc = 5:1 to 2:1) afforded the mixture of mono-functionalized products (48 mg, 62%). ^1H NMR of the mixture afforded the selectivity (C2:C3:C4 = 76:24:-).

Table 1.5, Entry 6.

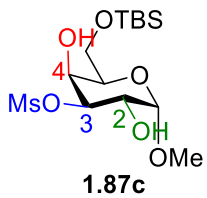

1.87c

The general procedure L was followed using **(+)-1.56** (11 mg, 0.040 mmol, 20 mol %) as the catalyst. ^1H NMR of the crude mixture afforded selectivity (C2:C3:C4 = -:100:-). Column chromatography

(Hexane/EtOAc = 5:1 to 2:1) afforded the pure product **1.87c** (57 mg, 74%). ^{1}H NMR ($CDCl_3$, 500 MHz) δ 4.85 (d, 1H, *J* = 4.2), 4.73 (dd, 1H, *J* = 10.0, 2.9), 4.30 (s, 1H), 4.12 (td, 1H, *J* = 10.0, 4.2), 3.89 (dd, 1H, *J* = 10.8, 5.4), 3.85 (dd, 1H, *J* = 10.8, 4.9), 3.76 (t, 1H, *J* = 5.1), 3.43 (s, 3H), 3.25 (d, 1H, *J* = 2.4), 3.18 (s, 3H), 2.39 (d, 1H, *J* = 10.3), 0.88 (s, 9H), 0.08 (s, 6H). ^{13}C NMR ($CDCl_3$, 125 MHz) δ 99.8, 82.3, 70.0, 69.7, 67.3, 63.3, 55.6, 39.0, 26.0, 18.4, -5.31, -5.32. IR: 3468, 2952, 2929, 2856, 1350, 1172, 1084, 1047, 961, 834, 776, 731, 526, 489 cm^{-1}. HRMS (DART-TOF) calcd. for $C_{14}H_{30}O_8SSi$: $[M+H]^+$: 387.1509, found: 387.1505.

Site-Selective Functionalization of 1,6-Anhydro-Galactose (Table 1.6):

General Procedure M (Table 1.6, Entry 1):

In a dry box, a solution of **1.89** (32 mg, 0.20 mmol), catalyst (*N*-methylimidazole, 3.2 μL, 0.040 mmol, 20 mol %), and *N,N*-diisopropylethylamine hydrochloride (1.0 mg, 0.0060 mmol, 3 mol %) in anhydrous *tert*-amyl alcohol (1.0 mL) was prepared in an oven-dried glass reaction vial. The solution was brought out of the dry box, and *N,N*-diisopropylethylamine (42 μL, 0.24 mmol, 1.2 eq) was added to the stirring reaction at room temperature. The reaction was stirred at 4 °C for 10 minutes, followed by dropwise addition of chlorotriethylsilane (40 μL, 0.24 mmol, 1.2 eq). The reaction was stirred at 4 °C for 4 hours. MeOH (50 μL) was added to quench the reaction. The mixture was filtered through a Pasteur pipette packed with silica gel, followed by flush with EtOAc (15 mL). The solvent was removed under reduced pressure. 1,3,5-trimethoxybenzene (50 μL of 0.40

M in $CDCl_3$, 0.020 mmol, 10 mol %) was added as standard. ^1H NMR of the crude mixture afforded the yield (51%) and selectivity (C2:C3:C4 = 91:-:9).

Table 1.6, Entry 2.

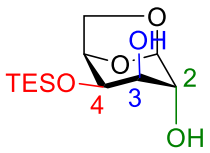

1.92a

The general procedure M was followed using **(–)-1.72** (3.1 mg, 0.010 mmol, 5 mol %) as the catalyst. ^1H NMR of the crude mixture afforded the selectivity (C2:C3:C4 = 1:-:99). Column chromatography (Hexane/EtOAc = 3:1) afforded the pure product **1.92a** (54 mg, 98%). ^1H NMR ($CDCl_3$, 500 MHz) δ 5.36 (t, 1H, *J* = 1.5), 4.24 (d, 2H, *J* = 7.1), 4.06 (t, 1H, *J* = 4.7), 3.86-3.85 (m, 1H), 3.83 (d, 1H, *J* = 8.3), 3.63 (dd, 1H, *J* = 6.4, 5.9), 2.88 (s, 1H), 2.32 (d, 1H, *J* = 8.6), 0.96 (t, 9H, *J* = 8.1), 0.65 (q, 6H, *J* = 7.7). ^{13}C NMR ($CDCl_3$, 125 MHz) δ 101.6, 74.7, 71.6, 71.2, 65.8, 63.9, 6.8, 4.9. IR: 3430, 2956, 2878, 1240, 1136, 1099, 1051, 1011, 938, 847, 809, 765, 744, 456 cm^{-1}. HRMS (DART-TOF) calcd. for $C_{12}H_{24}O_5Si$: $[M+H]^+$: 277.1471, found: 277.1474.

General Procedure N (Table 1.6, Entry 3):

In a dry box, a solution of **1.89** (32 mg, 0.20 mmol), catalyst (*N*-methylimidazole, 3.2 μL, 0.040 mmol, 20 mol %), and *N,N*-diisopropylethylamine hydrochloride (1.0 mg, 0.0060 mmol, 3 mol %) in anhydrous THF (3.0 mL) was prepared in an oven-dried glass reaction vial. The solution was brought out of the dry box, and *N,N*-diisopropylethylamine (42 μL, 0.24 mmol, 1.2 eq) was added to the stirring reaction at room temperature. The reaction was stirred at 4 °C for 10 minutes, followed by dropwise addition of acetyl chloride (17

μL, 0.24 mmol, 1.2 eq). The reaction was stirred at 4 °C for 4 hours. MeOH (50 μL) was added to quench the reaction. The mixture was filtered through a Pasteur pipette packed with silica gel, followed by flush with EtOAc (15 mL). The solvent was removed under reduced pressure. 1,3,5-trimethoxybenzene (50 μL of 0.40 M in $CDCl_3$, 0.020 mmol, 10 mol %) was added as standard. ^{1}H NMR of the crude mixture afforded the yield (53%) and selectivity (C2:C3:C4 = 75:8:17).

Table 1.6, Entry 4.

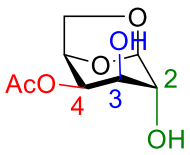

1.92b

The general procedure N was followed using **(–)-1.72** (3.1 mg, 0.010 mmol, 5 mol %) as the catalyst. ^{1}H NMR of the crude mixture afforded the selectivity (C2:C3:C4 = -:3:97). Column chromatography (Hexane/EtOAc = 1:1 to 1:2) afforded the pure product **1.92b** (38 mg, 93%). ^{1}H NMR (acetone-d6, 500 MHz) δ 5.26 (s, 1H), 5.00 (br s, 1H), 4.41 (dd, 2H, J = 6.9, 3.2), 4.25 (d, 1H, J = 6.9), 4.07 (t, 2H, J = 1.0), 3.68 (d, 1H, J = 6.9), 3.54 (t, 1H, J = 5.9), 2.04 (s, 3H). ^{13}C NMR (acetone-d6, 125 MHz) δ 170.4, 103.1, 73.9, 73.1, 70.8, 68.9, 64.8, 20.9. IR: 3432, 2961, 2905, 1727, 1432, 1373, 1238, 1132, 1050, 975, 928, 852, 700, 463 cm^{-1}. HRMS (DART-TOF) calcd. for $C_8H_{12}O_6$: $[M+H]^+$: 205.0712, found: 205.0717.

General Procedure O (Table 1.6, Entry 5):

In a dry box, a solution of **1.89** (32 mg, 0.20 mmol), catalyst (*N*-methylimidazole, 3.2 μL, 0.040 mmol, 20 mol %), and *N,N*-diisopropylethylamine hydrochloride (1.0 mg, 0.0060 mmol, 3 mol %) in anhydrous THF (3.0 mL) was prepared in an oven-dried glass reaction

vial. The solution was brought out of the dry box, and *N,N*-diisopropylethylamine (42 μL, 0.24 mmol, 1.2 eq) was added to the stirring reaction at room temperature. The reaction was stirred at -15 °C for 10 minutes, followed by dropwise addition of methanesulfonyl chloride (19 μL, 0.24 mmol, 1.2 eq). The reaction was stirred at -15 °C for 4 hours. MeOH (50 μL) was added to quench the reaction. The mixture was filtered through a Pasteur pipette packed with silica gel, followed by flush with EtOAc (15 mL). The solvent was removed under reduced pressure. 1,3,5-trimethoxybenzene (50 μL of 0.40 M in $CDCl_3$, 0.020 mmol, 10 mol %) was added as standard. ^{1}H NMR of the crude mixture afforded the yield (50%) and selectivity (C2:C3:C4 = 75:6:19).

Table 1.6, Entry 6.

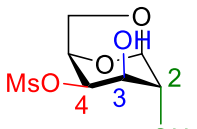

1.92c

The general procedure O was followed using **(–)-1.72** (3.1 mg, 0.010 mmol, 5 mol %) as the catalyst. ^{1}H NMR of the crude mixture afforded the selectivity (C2:C3:C4 = -:1:99). Column chromatography (Hexane/EtOAc = 1:1 to 1:2) afforded the pure product **1.92c** (42 mg, 88%). ^{1}H NMR (acetone-d6, 500 MHz) δ 5.28 (t, 1H, *J* = 1.5), 4.88 (t, 1H, *J* = 4.4), 4.56 (t, 1H, *J* = 4.2), 4.44 (d, 1H, *J* = 7.1), 4.38-4.37 (m, 2H), 4.15 (br s, 1H), 3.75 (br s, 1H), 3.60 (td, 1H, *J* = 5.1, 0.5), 3.22 (s, 3H). ^{13}C NMR (acetone-d6, 125 MHz) δ 103.3, 75.0, 74.5, 74.0, 71.8, 64.9, 38.8. IR: 3458, 2937, 1340, 1172, 1132, 1055, 1000, 970, 901, 818, 525, 459 cm^{-1}. HRMS (DART-TOF) calcd. for $C_7H_{12}O_7S$: $[M+NH_4]^+$: 258.0648, found: 258.0652.

Axial Hydroxyl Functionalization (Figure 1.10):

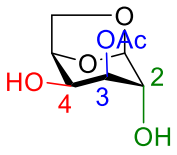

1.91b

The general procedure N was followed using **(+)-1.72** (12 mg, 0.040 mmol, 20 mol %) as the catalyst. ^{1}H NMR of the crude mixture afforded the selectivity (C2:C3:C4 = 2:81:17). Column chromatography (Hexane/EtOAc = 1:1 to 1:2) afforded the mixture of mono-functionalized products with **1.91b** as the major product (30 mg, 73%, C2:C3:C4 = 2:81:7). ^{1}H NMR ($CDCl_3$, 500 MHz) δ 5.22 (t, 1H, *J* = 1.2), 5.03 (dq, 1H, *J* = 5.1, 1.2), 4.39 (d, 1H, *J* = 7.1), 4.32 (d, 2H, *J* = 6.4), 4.24 (d, 1H, *J* = 7.1), 4.15-4.12 (m, 1H), 3.56-3.53 (m, 2H), 2.03 (s, 3H). ^{13}C NMR ($CDCl_3$, 125 MHz) δ 170.7, 102.2, 75.7, 73.4, 71.5, 64.8, 64.1, 21.1. IR: 3418, 2963, 2904, 1723, 1435, 1240, 1137, 1066, 1040, 971, 852, 696, 438 cm^{-1}. HRMS (DART-TOF) calcd. for $C_8H_{12}O_6$: $[M+H]^+$: 205.0712, found: 205.0721.

Site-Selective Silylation of Uridine and Characterization of Products (Scheme 1.17):

In a dry box, a mixture of **1.95** (112 mg, 0.20 mmol), **(+)-1.56** (2.8 mg, 0.01 mmol, 5 mol %), and *N*,*N*-diisopropylethylamine hydrochloride (1.5 mg, 0.006 mmol, 3 mol %) in anhydrous THF (1 mL) was prepared in an oven-dried round-bottom flask. The mixture was brought out of the dry box, and *N*,*N*-diisopropylethylamine (42 µL, 0.24 mmol, 1.2 eq) was added to the stirring reaction at room temperature, followed by dropwise addition of triethylsilyl chloride (40 µL, 0.24 mmol, 1.2 eq). The reaction was stirred at room temperature for 4 hours. MeOH (50 µL) was added to quench the reaction. The reaction mixture was put through a plug of silica gel and washed with 15 mL of EtOAc. The solvent was removed under reduced pressure. Column chromatography

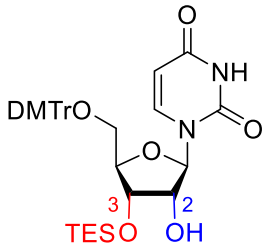

1.96

(Dichloromethane/Methanol = 99.5:0.5 to 99:1) on silica gel afforded the desired product (**1.96**) as a white solid (106 mg, 80%, C3:C2 = 93:7). ^{1}H NMR ($CDCl_3$, 400 MHz) δ 8.36 (br s, 1H), 7.82 (d, 1H, *J* = 10), 7.35–7.22 (m, 9H), 6.82 (dd, 4H, *J* = 2, 11), 5.96 (d, 1H, *J* = 5.5), 5.36 (dd, 1H, *J* = 10, 3), 4.36–4.34 (m, 1H), 4.16–4.12 (m, 1H), 4.05–4.03 (m, 1H), 3.78 (s, 6H), 3.58 (dd, *J* = 13.5, 3, 1H), 3.30 (dd, 1H, *J* = 13.5, 3), 2.89 (d, 1H, *J* = 8), 0.87 (t, 9H, *J* = 10), 0.57–0.46 (m, 6H). ^{13}C NMR ($CDCl_3$, 100 MHz) δ 163.3, 159.0, 150.6, 144.2, 140.4, 135.3, 135.2, 130.3, 128.4, 128.2, 127.4, 113.5, 113.4, 102.7, 89.5, 87.3, 84.2, 75.4, 71.2, 62.4, 55.4, 6.8, 4.8. IR: 3441, 3170, 3058, 2954, 2911, 2875, 2836, 1692, 1608 1581, 1508, 1459, 1415, 1389, 1300, 1250, 1176, 1150, 1112, 1066, 1035, 1002, 910, 829, 729, 704, 676, 648, 633, 585, 427 cm^{-1}. HRMS (DART-ESI+) calcd. for $C_{36}H_{44}N_2O_8NaSi$: $[M+Na]^+$: 683.27710, found: 683.275914.

In a dry box, a mixture of **1.95** (112 mg, 0.20 mmol), **(–)-1.72** (3.1 mg, 0.01 mmol, 5 mol %), and *N*,*N*-diisopropylethylamine hydrochloride (1.5 mg, 0.006 mmol, 3 mol %) in anhydrous THF (1 mL) was prepared in an oven-dried round-bottom flask. The mixture was brought out of the dry box, and *N*,*N*-diisopropylethylamine (42 µL, 0.24 mmol, 1.2 eq) was added to the stirring reaction at room temperature, followed by dropwise addition of triethylsilyl chloride (40 µL, 0.24 mmol, 1.2 eq). The reaction was stirred at room temperature for 4 hours. MeOH (50 µL) was added to quench the reaction. The reaction mixture was put through a plug of silica gel and washed with 15 mL of EtOAc. The solvent was removed under reduced pressure. Column chromatography (Dichloromethane/Methanol = 99.5:0.5 to 99:1) on silica gel afforded the desired product

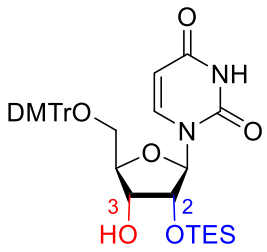

1.97

(**1.97**) as a white solid (114 mg, 86%, 2':3' = >98:<2). ^{1}H NMR ($CDCl_3$, 500 MHz) δ 8.67 (br s, 1H), 7.94 (d, 1H, J = 8), 7.37 (m, 2H), 7.27 (m, 7H), 6.84 (d, 4H, J = 9), 5.94 (d, 1H, J = 3), 5.29 (dd, 1H, J = 8.3, 2.3), 4.37–4.33(m, 2H), 4.13–4.10 (m, 1H), 3.80 (s, 6H), 3.53–3.46 (m, 2H), 2.66–2.64 (m, 1H), 0.98 (t, 9H, J = 8), 0.70 (q, 6H, J = 8). ^{13}C NMR ($CDCl_3$, 100 MHz) δ 163.5, 158.9, 158.9, 150.5, 144.5, 140.5, 135.4, 135.2, 130.4, 130.3, 128.3, 128.2, 127.4, 113.5,113.5, 102.5, 88.9, 87.4, 83.7, 76.2, 70.6, 62.5, 55.4, 6.7, 4.7 IR: 3197, 3058, 2955, 2912, 2876, 2836, 1680, 1607, 1582, 1508, 1458, 1413, 1381, 1332, 1299, 1249, 1175, 1114, 1087, 1062, 1033, 1005, 912, 876, 827, 791, 729, 701, 583, 557, 419 cm^{-1}. HRMS (DART-ESI+) calcd. For $C_{36}H_{44}N_2O_8NaSi$: $[M+Na]^+$: 683.27700, found: 683.275914.

Site-Selective Mesylation of Mupirocin and Characterization of Products (Scheme 1.18, eq. 1):

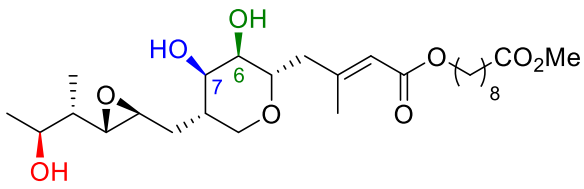

1.98
Mupirocin methyl ester

A modified method was adopted from the previously reported procedure.[45] To a solution of mupirocin (2.0 g, 4.0 mmol) in anhydrous toluene (16 mL) and anhydrous MeOH (4.0 mL) was added trimethylsilyldiazomethane (2.0 M in Et_2O, 2.4 mL, 4.8 mmol) dropwise at room temperature. After stirring for 1 h, the reaction mixture was diluted with EtOAc (15 mL) and AcOH (10% aqueous, 10 mL) was added. The aqueous phase was extracted with EtOAc (3x15 mL) and the organic layers were combined, washed with brine

(25 mL), dried with $MgSO_4$, filtered and the solvent was removed under reduced pressure. The resulting crude product (colorless oil) was dissolved in a mixture of hexane (10 mL) and Et_2O (20 mL) and crystallized out in an ice bath as a white solid (1.84 g, 92%). Note: Trimethylsilyldiazomethane is highly toxic and potentially fatal if inhaled. ^{1}H NMR ($CDCl_3$, 500 MHz) δ 5.75 (s, 1H), 4.07 (t, 2H, J = 6.6), 3.92 (d, 1H, J = 2.9), 3.87 (dd, 1H, J = 12, 3.2), 3.82 (t, 1H, J = 6.6), 3.75 (td, 1H, J = 8.6, 3.2), 3.67 (s, 3H), 3.55 (dd, 1H, J = 12, 2.7), 3.47 (td, 1H, J = 7.8, 2.9), 2.80 (td, 1H, J = 6.8, 2.2), 2.69 (dd, 1H, J = 8.1, 2.2), 2.58 (dd, 1H, J = 14, 2.7), 2.43 (d, 1H, J = 3.2), 2.32-2.27 (m, 5H), 2.21 (s, 3H), 2.02-1.99 (m, 1H), 1.78-1.68 (m, 2H), 1.66-1.60 (m, 4H), 1.36-1.31 (m, 9H), 1.22 (d, 3H, J = 6.4), 0.94 (d, 3H, J = 7.1). ^{13}C NMR ($CDCl_3$, 125 MHz) δ 211.9, 198.8, 174.6, 166.9, 156.8, 117.9, 75.0, 71.6, 70.7, 69.3, 65.5, 64.0, 61.6, 55.8, 51.7, 43.1, 39.7, 34.3, 31.8, 29.3, 29.2, 28.9, 26.2, 25.1, 21.0, 19.3, 13.0. IR: 3444, 2931, 2859, 1736, 1714, 1647, 1437, 1346, 1224, 1150, 1109, 1053, 943, 869 cm^{-1}. HRMS (DART-TOF) calcd. for $C_{27}H_{46}O_9$: $[M+H]^+$: 515.3220, found: 515.3229.

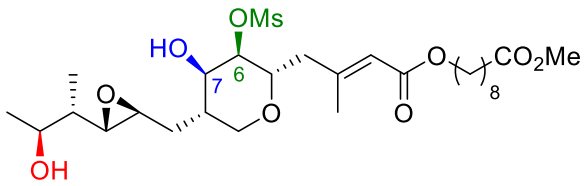

1.99

In a dry box, a solution of mupirocin methyl ester (51 mg, 0.10 mmol), catalyst **(–)-1.72** (6.1 mg, 0.020 mmol, 20 mol %), and *N,N*-diisopropylethylamine hydrochloride (0.5 mg, 0.0030 mmol, 3 mol %) in anhydrous THF (0.5 mL) was prepared in an oven-dried glass reaction vial. The solution was brought out of the dry box, and *N,N*-diisopropylethylamine (21 μL, 0.12 mmol, 1.2 eq) was added to the stirring reaction at room temperature. The reaction was stirred at -15 °C for 10 minutes, followed by dropwise

addition of methanesulfonyl chloride (9.3 μL, 0.12 mmol, 1.2 eq). The reaction was stirred at -15 °C for 20 hours. MeOH (25 μL) was added to quench the reaction. The mixture was filtered through a Pasteur pipette packed with silica gel, followed by flushing with EtOAc (8 mL). The solvent was removed under reduced pressure. Selectivity of the reaction was determined by ^{1}H NMR in the crude reaction mixture (C6:C7 = >98:<2). Column chromatography (Hexane/EtOAc = 1:1 to 1/2) afforded the pure product **1.99** (49 mg, 82%). ^{1}H NMR δ 5.73 (s, 1H), 4.53 (dd, 1H, *J* = 7.8, 2.5), 4.23-4.22 (m, 1H), 4.09-4.03 (m, 3H), 3.92 (dd, 1H, *J* = 12, 3.4), 3.84-3.81 (m, 1H), 3.67 (s, 3H), 3.59 (dd, 1H, *J* = 12, 3.4), 3.11 (s, 3H), 2.80-2.78 (m, 1H), 2.72 (dd, 1H, *J* = 7.8, 2.0), 2.56 (d, 1H, *J* = 3.9), 2.44 (dd, 1H, *J* = 14, 3.4), 2.36-2.30 (m, 3H), 2.24 (d, 1H, *J* = 3.4), 2.20 (d, 3H, *J* = 1.0), 2.13-2.11 (m, 1H), 1.85-1.80 (m, 1H), 1.69 (q, 1H, *J* = 7.4), 1.64-1.60 (m, 4H), 1.36-1.31 (m, 9H), 1.21 (d, 3H, *J* = 6.4), 0.95 (d, 3H, *J* = 7.3). ^{13}C NMR ($CDCl_3$, 125 MHz) δ 174.5, 166.7, 154.9, 118.6, 79.2, 72.4, 71.5, 69.3, 65.8, 64.1, 61.5, 55.7, 51.7, 43.1, 42.6, 39.8, 39.1, 34.3, 31.9, 29.4, 29.3, 29.2, 28.9, 26.2, 25.1, 20.9, 19.0, 13.0. IR: 3500, 2933, 2858, 1714, 1649, 1455, 1438, 1353, 1226, 1175, 1152, 1116, 965, 942, 856, 529 cm^{-1}. HRMS (DART-TOF) calcd. for $C_{28}H_{48}O_{11}S$: $[M+H]^+$: 593.2996, found: 593.2977.

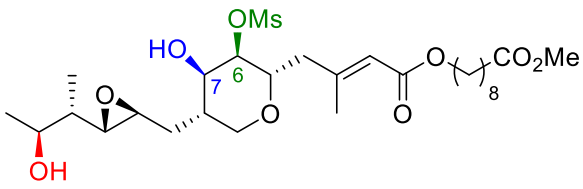

1.100

In a dry box, a solution of mupirocin methyl ester (618 mg, 1.2 mmol), catalyst **(+)-1.56** (68 mg, 0.24 mmol, 20 mol %), and *N,N*-diisopropylethylamine hydrochloride (6.0 mg, 0.036 mmol, 3 mol %) in anhydrous THF (6.0 mL) was prepared in an oven-dried glass reaction vial. The solution was brought out of the dry box, and *N,N*-

diisopropylethylamine (251 μL, 1.44 mmol, 1.2 eq) was added to the stirring reaction at room temperature. The reaction was stirred at -15 °C for 10 minutes, followed by dropwise addition of methanesulfonyl chloride (111 μL, 1.44 mmol, 1.2 eq). The reaction was stirred at -15 °C for 20 hours. MeOH (300 μL) was added to quench the reaction. The mixture was filtered through a Pasteur pipette packed with silica gel, followed by flushing with EtOAc (90 mL). The solvent was removed under reduced pressure. Selectivity of the reaction was determined by ^{1}H NMR in the crude reaction mixture (C6:C7 = 18:82). Column chromatography (Hexane/EtOAc = 1:1 to 2/5) afforded the pure product **1.100** (403 mg, 57%). ^{1}H NMR ($CDCl_3$, 500 MHz) δ 5.75 (s, 1H), 5.04 (br s, 1H), 4.07 (t, 2H, *J* = 6.9), 3.86-3.82 (m, 2H), 3.70-3.3.65 (m, 5H), 3.61-3.59 (m, 1H), 3.15 (s, 3H), 2.81 (td, 1H, *J* = 5.9, 2.0), 2.78 (dd, 1H, *J* = 7.3, 2.5), 2.65 (d, 1H, *J* = 14), 2.36 (d, 1H, *J* = 6.8), 2.32-2.26 (m, 4H), 2.21 (s, 3H), 1.85-1.81 (m, 1H), 1.79-1.74 (m, 1H), 1.65-1.60 (m, 4H), 1.45 (q, 1H, *J* = 6.8), 1.38-1.28 (m, 9H), 1.24 (d, 3H, *J* = 6.4), 0.93 (d, 3H, *J* = 6.9). ^{13}C NMR ($CDCl_3$, 125 MHz) δ 174.5, 166.8, 156.1, 118.1, 81.4, 75.4, 71.6, 67.6, 65.8, 64.1, 61.0, 54.8, 51.7, 42.9, 42.6, 39.6, 38.8, 34.3, 32.0, 29.3, 29.2, 29.1, 29.0, 26.2, 25.1, 21.3, 19.5, 12.6. IR: 3496, 2401, 2930, 2861, 1736, 1714, 1649, 1457, 1352, 1225, 1174, 1151, 1112, 968, 874, 548 cm^{-1}. HRMS (DART-TOF) calcd. for $C_{28}H_{48}O_{11}S$: $[M+H]^+$: 593.2996, found: 593.2980.

Site-Selective Acylation of Digoxin and Characterization of Products (Scheme 1.18, eq. 2):

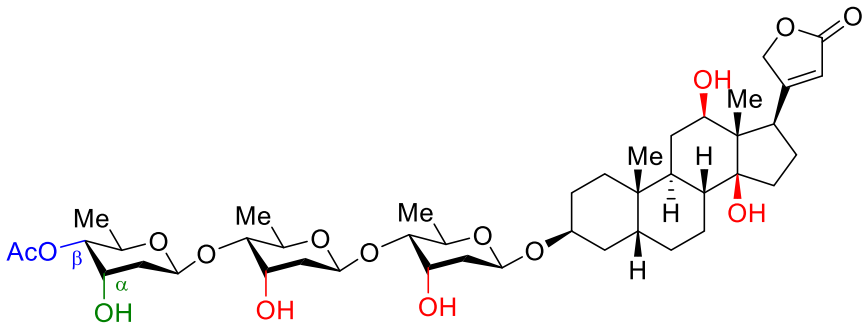

1.102

In a dry box, a suspension of digoxin (39 mg, 0.050 mmol), catalyst **(+)-1.72** (4.6 mg, 0.015 mmol, 30 mol %), and *N,N*-diisopropylethylamine hydrochloride (0.3 mg, 0.0015 mmol, 3 mol %) in anhydrous THF (2.5 mL) was prepared in an oven-dried round-bottom flask. The suspension was brought out of the dry box, and *N,N*-diisopropylethylamine (11 μL, 0.060 mmol, 1.2 eq) was added to the stirring reaction at room temperature. The reaction was stirred at 4 °C for 10 minutes, followed by dropwise addition of acetyl chloride (4.3 μL, 0.060 mmol, 1.2 eq). The reaction was stirred at 4 °C for 16 hours. MeOH (12 μL) was added to quench the reaction. The solvent was removed under reduced pressure. Column chromatography (CH_2Cl_2/MeOH = 50:1 to 30:1) afforded the pure product β-acetyldigoxin **1.102** (37 mg, 90%, no α-acetyldigoxin observed). ^{1}H NMR ($CDCl_3$, 500 MHz) δ 5.95 (s, 1H), 5.05-5.00 (m, 2H), 4.98-4.93 (m, 3H), 4.47 (dd, 1H, *J* = 9.8, 2.9), 4.31-4.28 (m, 3H), 4.24-4.22 (m, 1H), 4.10-4.05 (m, 2H), 3.91-3.82 (m, 2H), 3.43 (dd, 1H, *J* = 12.0, 4.2), 3.38 (d, 1H, *J* = 9.5, 6.1), 3.31 (dd, 1H, *J* = 9.5, 2.9), 3.27 (dd, 1H, *J* = 9.5, 2.9), 2.22-2.14 (m, 1H), 2.13 (s, 3H), 2.09-1.61 (m, 19H), 1.56-1.48 (m, 4H), 1.27 (d, 3H, *J* = 6.1), 1.25 (d, 3H, *J* = 6.4), 1.21 (d, 3H, *J* = 6.4), 1.00 (s, 3H), 0.83 (s, 3H). ^{13}C NMR ($CDCl_3$, 125 MHz) δ 178.6, 177.4, 172.2, 117.9, 100.8, 100.7, 97.1, 86.9, 83.9, 83.8, 76.8, 75.8, 75.6, 74.6,

69.6, 68.6, 68.5, 66.4, 57.4, 47.2, 42.4, 39.4, 39.1, 38.7, 38.1, 36.3, 33.8, 33.7, 31.6, 31.1, 31.0, 28.5, 27.9, 27.6, 24.4, 22.9, 21.0, 18.63, 18.60, 18.4, 10.0 IR: 3433, 2932, 2880, 1734, 1370, 1239, 1164, 1084, 1069, 1016, 866 cm^{-1}. HRMS (DART-TOF) calcd. for $C_{43}H_{66}O_{15}$: $[M+Na]^+$: 845.4294, found: 845.4280.

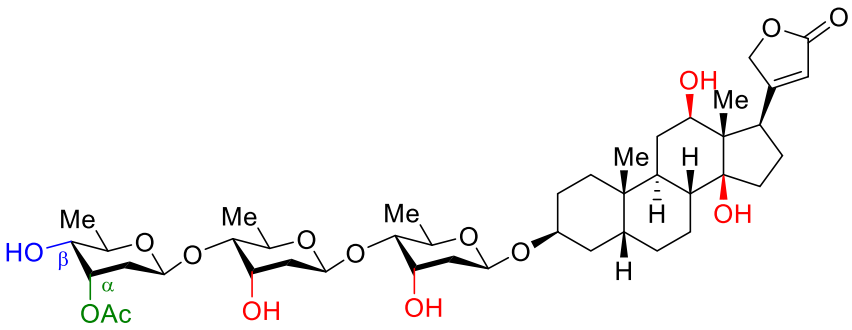

1.103

The same procedure to produce α-acetyldigoxin was followed using (–)-**1.56** (4.2 mg, 0.015 mmol, 30 mol %) as the catalyst. Column chromatography (CH_2Cl_2/MeOH = 50:1 to 30:1) afforded the mixture of mono-acylated products with α-acetyldigoxin **1.103** as the major product (23 mg, 56%, α:β = 91:9). ^{1}H NMR ($CDCl_3$, 500 MHz) δ 5.94 (s, 1H), 5.26 (d, 1H, *J* = 3.2), 5.03-4.89 (m, 6H), 4.30-4.27 (m, 2H), 4.05 (d, 1H, *J* = 2.2), 3.90-3.80 (m, 3H), 3.42 (dd, 1H, *J* = 11.7, 4.2), 3.37 (dd, 1H, *J* = 9.0, 5.6), 3.31 (dd, 1H, *J* = 9.5, 2.9), 3.26 (dd, 1H, *J* = 9.5, 2.9), 2.19-2.15 (m, 1H), 2.12-1.63 (m, 20H), 1.52-1.50 (m, 3H), 1.34-1.32 (m, 2H), 1.30 (d, 3H, *J* = 6.4), 1.29-1.27 (m, 2H), 1.24 (d, 3H, *J* = 1.7), 1.23 (d, 3H, *J* = 1.5), 0.99 (s, 3H), 0.82 (s, 3H). ^{13}C NMR ($CDCl_3$, 125 MHz) δ 179.2, 178.0, 173.0, 118.4, 101.3, 101.2, 97.6, 87.5, 84.5, 84.2, 76.4, 76.2, 75.2, 73.4, 72.9, 72.3, 70.2, 69.2, 69.0, 58.0, 47.8, 42.9, 39.6, 39.2, 38.7, 37.8, 36.9, 34.3, 34.2, 32.1, 31.7, 31.6, 29.1, 28.5, 28.2, 24.9, 23.5, 21.8, 19.3, 19.2, 10.6. IR: 3412, 2931, 2882, 1736, 1371, 1241, 1163, 1068, 1017m 866 cm^{-1}. HRMS (DART-TOF) calcd. for $C_{43}H_{66}O_{15}$: $[M+Na]^+$: 845.4294, found: 845.4303.

1.6.2 Template-Assisted *Meta*-Selective C–H Activation

1.6.2.1 General Information

Unless otherwise noted, all reagents were obtained from commercial suppliers and used without further purification. Flash column chromatography was performed using EMD Silica Gel 60 (230-400 mesh) and ACS grade solvents as received from Fisher Scientific. All experiments were performed in oven or flame dried glassware under an atmosphere of nitrogen or argon using standard syringe techniques, except where otherwise noted. All reactions were run with dry, degassed solvents dispensed from a Glass Contour Solvent Purification System (SG Water, USA LLC).

^{1}H, ^{13}C, and NOE NMR were performed on a Varian Gemini 400 MHz, Varian Gemini 500 MHz, Varian Gemini 600 MHz or a Varian Unity Inova 500 MHz spectrometer. Deuterated solvents were purchased from Cambridge Isotope Labs and stored over 3Å molecular sieves. All NMR chemical shifts are reported in ppm relative to residual solvent for ^{1}H and ^{13}C NMR. Signals are quoted as singlet (s), doublet (d), triplet (t), quartet (q), multiplet (m), and broad singlet (br s). Coupling constants are reported in Hz. All IR spectra were gathered on a Bruker Alpha FT-IR equipped with a single crystal diamond ATR module and values are reported in cm^{-1}. HRMS data were generated in Boston College facilities.

1.6.2.2 Experimental Procedures and Characterization

Procedure for preparation of substrate:

General procedure A (Scheme 1.24):

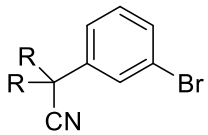

To a stirred solution of 2-(3-bromophenyl)-acetonitrile (1.0 eq) was added potassium *tert*-butoxide (2.2 eq) portionwise at –40 ºC under nitrogen atmosphere. After being stirred for 15 min at –40 ºC, alkyl iodide (2.45 eq) was added. The mixture was warmed to room temperature and stirred further for 1h. The white solid was filtered off though a short pad of Celite and filtrate was concentrated under reduced pressure. A column chromatography on silica gel gave the product as colorless oil.

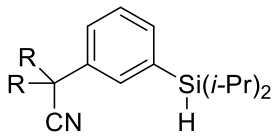

To a stirred solution of arylbromide (1.0 eq) in tetrahydrofuran (0.3 M) was added *n*-BuLi (1.0 eq) at –100 ºC in liquid nitrogen/acetone bath. After being stirred for 30min at the same temperature, chlorodiisopropylsilane (1.0 eq) was added. The mixture was allowed to warm room temperature without more liquid nitrogen. With further 2 h of stirring, silica gel was added to quench the reaction and column chromatography afforded the product as colorless oil.

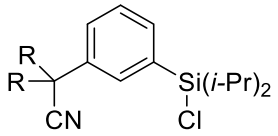

To a suspension of trichloroisocyanuric acid (0.33 eq) in dichloromethane (0.3 M) was added previously synthesized silane in dichloromethane (0.5 M) at 0 ºC under nitrogen atmosphere. After being stirred for 1h at room temperature, white solid was filtered off through a short pad of Celite and the filtrate was concentrated under reduced pressure. Short path distillation gave the product as colorless oil (when R= *s*Bu, bp=220 ºC at 0.05 mmHg).

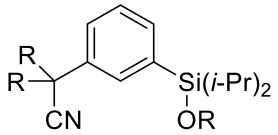

To a mixture of corresponding alcohol (1.0 eq) and imidazole (1.2 eq) in dichloromethane (0.3 M) was added a solution of chlorosilane (1.1 eq) in dichloromethane (0.5 M) at 0 ºC under N_2 atmosphere. The mixture was warmed to room temperature and stirred for 1 h. After filtering off the white solid, the

filtrate was concentrated and purified using flash column chromatography to give a product as colorless oil.

General procedure B (Scheme 1.27):

Scheme 1.27 General procedure B for preparation of substrate

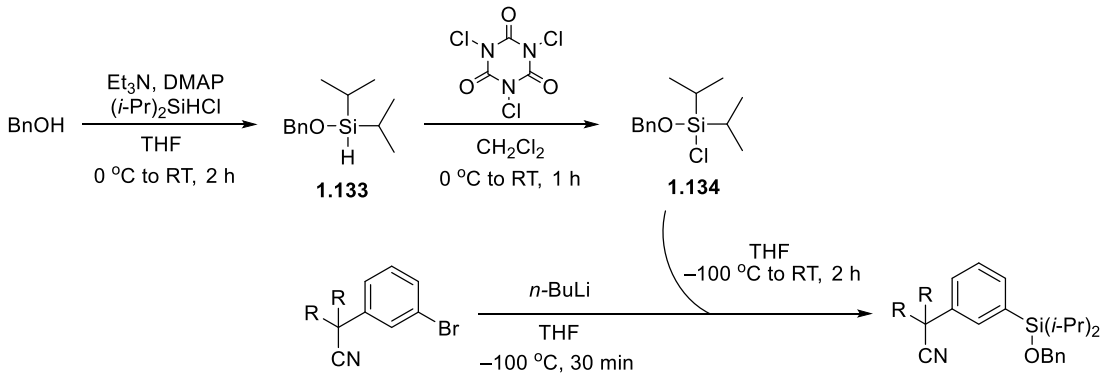

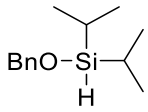

1.133

Chlorodiisopropylsilane (1.7 mL, 10.0 mmol, 1.0 eq) was added to a mixture of benzyl alcohol (1.0 mL, 10.0 mml, 1.0 eq) and DMAP (122 mg, 1.0 mmol, 0.1 eq) in tetrahydrofuran (0.3 M) at 0 °C under nitrogen atmosphere. Triethylamine (2.8 mL, 20.0 mmol, 2.0 eq) was added dropwise and the reaction mixture was stirred for overnight at room temperature. White solid was filtered off and the filtrate was concentrated under reduced pressure. Column chromatography on silica gel (EA/Hx=1/20) gave the product as a colorless liquid (1.7 g, 76%) ^{1}H NMR ($CDCl_3$, 500 MHz) 7.29-7.41 (m, 4H), 7.21-7.29 (m, 1H), 4.81 (s, 2H), 4.25 (s, 1H), 0.98-1.12 (m, 14H). ^{13}C NMR ($CDCl_3$, 125 MHz) δ 141.1, 128.5, 127.3, 126.6, 67.6, 17.7, 17.6, 12.7 IR: 2942,

2864, 2091, 1461, 1094, 1064, 880, 837, 817, 800, 729, 694, 667 cm^{-1}. HRMS (DART-ESI+) calcd. for $C_{13}H_{23}O_1Si_1$: $[M+H]^+$: 221.1362, found: 221.1363.

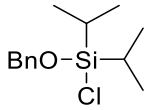

1.134

To a suspension of trichloroisocyanuric acid (640 mg, 2.75 mmol, 0.33 eq) in dichloromethane (0.3 M) was added previously synthesized silane (1.7 g, 7.6 mmol, 1.0 eq) in dichloromethane (0.5 M) at 0 °C under nitrogen atmosphere. After being stirred for 1h at room temperature, precipitated white solid was filtered off through short pad of Celite and the filtrate was concentrated under reduced pressure. Short path distillation gave the product as colorless oil (1.82 g, 93%, 150 °C at 0.3 mmHg). ^{1}H NMR ($CDCl_3$, 500 MHz) δ 7.31-7.43 (m, 4H), 7.21-7.31 (m, 1H), 4.90 (s, 2H), 1.16-1.30 (m, 2H), 1.12 (d, *J*=8.1 Hz, 6H), 1.11 (d, *J*=8.1 Hz, 6H). ^{13}C NMR ($CDCl_3$, 125 MHz) δ (ppm) 140.2, 128.5, 127.5, 126.6, 65.8, 17.1, 16.9, 15.3. IR: 2948, 2868, 1463, 1093, 1062, 1027, 1001, 883, 827, 730, 694, 620 cm^{-1}. LRMS (EI) calcd. for $C_{13}H_{22}Cl_1O_1Si_1$: 256.11, found: 256.10.

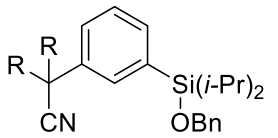

To a stirred solution of arylbromide (1.0 eq) in tetrahydrofuran (0.3 M) was added *n*-BuLi (1.0 eq) at –100 °C in liquid nitrogen/acetone bath. After being stirred for 30 min at the same temperature, (benzyloxy)chlorodiisopropylsilane (1.0 eq) was added. The mixture was allowed to warm to room temperature. With additional 2 h stirring, silica gel was added to quench the reaction and column chromatography gave a product as colorless oil.

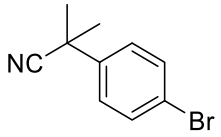

The general procedure A was followed for the dialkylation in 20 mmol scale using 2-(4-bromophenyl)-acetonitrile (3.4 g, 76%). ^{1}H NMR ($CDCl_3$, 500 MHz) δ 7.48-7.55 (m, 2H), 7.31-7.38 (m, 2H), 1.71 (s, 6H). ^{13}C NMR ($CDCl_3$,

125 MHz) δ 140.7, 132.2, 127.1, 124.2, 122.0, 37.1, 29.2. IR: 2982, 1489, 1398, 1101, 1074, 1008, 820, 714, 579, 520. cm^{-1}. HRMS (DART-ESI+) calcd. for $C_{10}H_{11}Br_1N_1$: $[M+H]^+$: 224.0075, found: 224.0066.

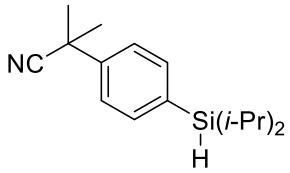

The general procedure A was followed for silyl group introduction in 7.0 mmol scale (1.56 g, 86%). ^1H NMR ($CDCl_3$, 500 MHz) δ 7.50-7.55 (m, 2H), 7.41-7.47 (m, 2H), 3.95 (t, *J*=3.2 Hz, 1H), 1.73 (s, 6H), 1.19-1.28 (m, 2H), 1.07 (d, *J*=7.3 Hz, 6H), 0.99 (d, *J*=7.3 Hz, 6H). ^{13}C NMR ($CDCl_3$, 125 MHz) δ 142.3, 136.3, 134.1, 124.7, 124.5, 37.4, 29.3, 18.8, 18.7, 10.9. IR: 2941, 2863, 2099, 1461, 1086, 1001, 880, 798, 660, 536 cm^{-1}. HRMS (DART-ESI+) calcd. for $C_{16}H_{26}N_1Si_1$: $[M+H]^+$: 260.1835, found: 260.1841.

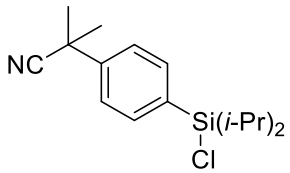

The general procedure A was followed for chlorination in 6.0 mmol scale (1.43 g, 81%). ^1H NMR ($CDCl_3$, 500 MHz) δ 7.62 (m, 2H), 7.50 (m, 2H), 1.74 (s, 6H), 1.39-1.45 (m, 2H), 1.09 (d, *J*=7.3 Hz, 6H), 1.01 (d, *J*=7.3 Hz, 6H). ^{13}C NMR ($CDCl_3$, 125 MHz) δ 143.3, 135.2, 132.3, 124.8, 124.5, 37.4, 29.2, 17.2, 16.9, 14.0. IR: 2948, 2868, 1463, 1396, 1086, 994, 882, 822, 733, 673, 649, 550 cm^{-1}. HRMS (DART-ESI+) calcd. for $C_{16}H_{25}Cl_1N_1Si_1$: $[M+H]^+$: 294.1445, found: 294.1456.

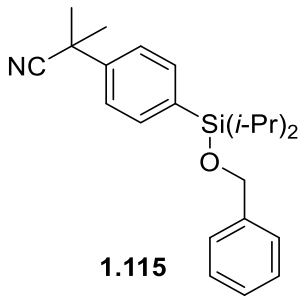

1.115

The general procedure A was followed for an introduction of alcohol in 1.0 mmol scale using benzyl alcohol (547 mg, 100 %). ^1H NMR ($CDCl_3$, 500 MHz) δ 7.55-7.63 (m, 2H), 7.42-7.50 (m, 2H), 7.32-7.42 (m, 4H), 7.24-7.30 (m, 1H), 4.90 (s, 2H), 1.74 (s, 6H), 1.36 (sept, *J*=7.4 Hz, 2H), 1.10 (d, *J*=7.3 Hz, 6H), 1.05 (d,

J=7.3 Hz, 6H). ^{13}C NMR ($CDCl_3$, 125 MHz) δ 142.5, 141.3, 135.5, 134.2, 128.5, 127.2, 126.1, 124.7, 124.5, 65.7, 37.4, 29.2, 17.7, 17.5, 12.4. IR: 2942, 2864, 1460, 1377, 1206, 1085, 993, 881, 820, 730, 695, 669, 631, 583, 537 cm^{-1}. HRMS (DART-ESI+) calcd. for $C_{23}H_{32}N_1O_1Si_1$: $[M+H]^+$: 366.2253, found: 366.2248.

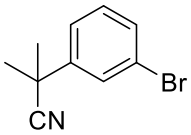

The general procedure A was followed for the dialkylation in 20 mmol scale (4.0 g, 90 %). ^{1}H NMR ($CDCl_3$, 500 MHz) δ 7.60 (t, *J*=2.0 Hz, 1H), 7.40-7.48 (m, 2H), 7.27 (t, *J*=8.0 Hz, 1H), 1.72 (s, 6H). ^{13}C NMR ($CDCl_3$, 125 MHz) δ 143.9, 131.2, 130.7, 128.5, 124.1, 124.0, 123.2, 37.2, 29.2. IR: 2983, 2937, 2237, 1594, 1567, 1476, 1418, 1369, 1239, 1091, 785, 693 cm^{-1}. HRMS (DART-ESI+) calcd. for $C_{10}H_{10}Br_1N_1Na_1$: $[M+Na]^+$: 245.9889, found: 245.9883.

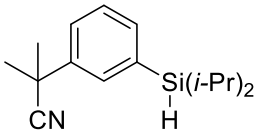

The general procedure A was followed for silyl group introduction in 20 mmol scale (1.46 g, 80 %). ^{1}H NMR ($CDCl_3$, 500 MHz) δ 7.60 (d, *J*=2.0 Hz, 1H), 7.44-7.50 (m, 2H), 7.37 (t, *J*=7.3 Hz, 1H), 3.97 (t, *J*=3.2 Hz, 1H), 1.74 (s, 6H), 1.20-1.30 (m, 2H), 1.08 (d, *J*=7.3 Hz, 6H), 1.00 (d, *J*=7.3 Hz, 6H). ^{13}C NMR ($CDCl_3$, 125 MHz) δ 140.8, 135.6, 135.0, 132.1, 128.3, 126.0, 124.8, 37.4, 29.4, 18.8, 18.7, 10.8. IR: 2940, 2863, 2102, 1461, 1397, 1127, 880, 783, 705, cm^{-1}. HRMS (DART-ESI+) calcd. for $C_{16}H_{25}N_1Si_1Na_1$: $[M+Na]^+$: 282.1649, found: 282.1649.

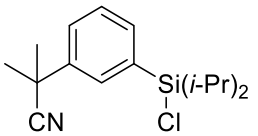

The general procedure A was followed for chlorination in 5.4 mmol scale (1.3 g, 82 %). ^{1}H NMR ($CDCl_3$, 500 MHz) δ 7.65-7.71 (m, 1H), 7.55 (dd, *J*=7.8, 1.5 Hz, 2H), 7.43 (t, *J*=7.8 Hz, 1H), 1.74 (s, 6H), 1.43 (sept, *J*= 7.3 Hz, 2H), 1.09 (d, *J*=7.3 Hz, 3H), 1.01 (d, *J*=7.3 Hz, 3H). ^{13}C NMR ($CDCl_3$, 125 MHz) δ 141.1, 133.9, 133.7, 130.9, 128.6, 127.0, 124.6, 37.4, 29.4, 17.2, 16.9, 14.0. IR: 2948, 2868, 1463,

1398, 1128, 994, 882, 794, 750, 674, 639, 526 cm^{-1}. HRMS (DART-ESI+) calcd. for $C_{16}H_{25}Cl_1N_1Si_1$: $[M+H]^+$: 294.1445, found: 294.1451.

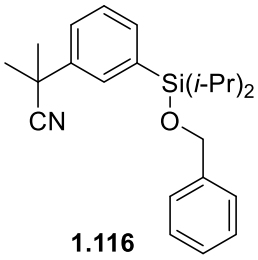

1.116

The general procedure A was followed for introduction of alcohol in 1.0 mmol scale (321 mg, 88 %). ^{1}H NMR ($CDCl_3$, 500 MHz) δ 7.60-7.64 (m, 1H), 7.51 (dd, *J*=7.3, 1.5 Hz, 2H), 7.33-7.42 (m, 5H), 7.24-7.29 (m, 1H), 4.90 (s, 2H), 1.65 (s, 6H), 1.40-1.34 (m, 2H), 1.11 (d, *J*=7.3 Hz, 3H), 1.05 (d, *J*=7.3 Hz, 3H). ^{13}C NMR ($CDCl_3$, 125 MHz) δ 141.3, 140.8, 135.6, 134.2, 131.1, 128.5, 128.4, 127.2, 126.4, 126.0, 124.8, 65.7, 37.4, 29.3, 17.7, 17.5, 12.4. IR: 2942, 2865, 1462, 1397, 1205, 1097, 1068, 993, 882, 795, 732, 707, 676, 617, 491 cm^{-1}. HRMS (DART-ESI+) calcd. for $C_{23}H_{32}N_1O_1Si_1$: $[M+H]^+$: 388.2067, found: 388.2076.

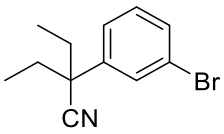

The general procedure A was followed for the dialkylation in 10.0 mmol scale (2.47 g, 98 %). ^{1}H NMR ($CDCl_3$, 500 MHz) δ 7.51 (t, *J*=1.7 Hz, 1H), 7.45 (d, *J*=7.8 Hz, 1H), 7.34 (d, *J*=7.8 Hz, 1H), 7.26 (t, *J*=8.3 Hz, 1H), 1.99-2.10 (m, 2H), 1.85-1.92 (m, 2H), 0.91 (t, *J*=7.3 Hz, 6H). ^{13}C NMR ($CDCl_3$, 125 MHz) δ 140.8, 131.1, 130.5, 129.3, 125.2, 123.3, 121.9, 49.9, 34.0, 9.9. IR: 2971, 2937, 1594, 1567, 1475, 1419, 1383, 1075, 997, 879, 778, 715, 694 cm^{-1}. HRMS (DART-ESI+) calcd. for $C_{12}H_{15}Br_1N_1Na_1$: $[M+H]^+$: 274.0202, found: 274.0205.

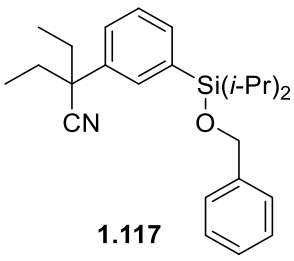

1.117

The general procedure B was followed for the introduction of silyl group in 1.5 mmol scale (506 mg, 86 %). ^{1}H NMR ($CDCl_3$, 500 MHz) δ 7.47-7.54 (m, 2H), 7.42-7.45 (m, 1H), 7.33-7.41 (m, 5H), 7.24-7.29 (m, 1H), 4.90 (s, 2H), 1.92-2.00 (m, 2H), 1.74-

1.84 (m, 2H), 1.31-1.41 (m, 2H), 1.10 (d, *J*=7.3 Hz, 6H), 1.04 (d, *J*=7.3 Hz, 6H), 0.86 (t, *J*=7.3 Hz, 6H). ^{13}C NMR ($CDCl_3$, 125 MHz) δ 141.4, 137.4, 135.2, 134.0, 132.0, 128.5, 128.3, 127.7, 127.2, 125.9, 122.5, 65.7, 49.9, 33.9, 17.7, 17.5, 12.4, 9.9. IR: 2940, 2865, 1462, 1381, 1097, 1068, 993, 882, 797, 732, 708, 672, 492 cm^{-1}. HRMS (DART-ESI+) calcd. for $C_{25}H_{35}N_1O_1Si_1Na_1$: $[M+Na]^+$: 416.2380, found: 416.2385.

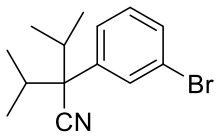

The general procedure A was followed for the dialkylation (2.67 g, 95 %). ^{1}H NMR ($CDCl_3$, 500 MHz) δ 7.52 (br. s., 1H), 7.46 (d, *J*=7.8 Hz, 1H), 7.30-7.36 (m, 1H), 7.21-7.27 (m, 1H), 2.41-2.49 (m, 2H), 1.03 (d, *J*=6.8 Hz, 6H), 0.88 (d, *J*=6.8 Hz, 6H). ^{13}C NMR ($CDCl_3$, 125 MHz) δ (ppm) 137.4, 131.1, 131.0, 129.8, 127.1, 122.7, 121.5, 58.0, 32.8, 19.0, 17.8. IR: 2970, 2837, 1593, 1562, 1472, 1416, 1390, 1374, 1173, 1096, 1077, 996, 782, 719, 699 cm^{-1}. HRMS (DART-ESI+) calcd. for $C_{12}H_{19}Br_1N_1$: $[M+H]^+$: 280.0701, found: 280.0698.

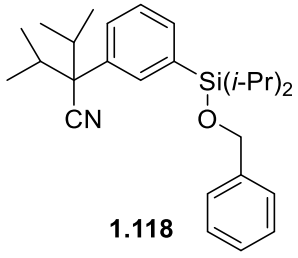

1.118

The general procedure B was followed for the introduction of silyl group in 1.5 mmol scale (414 mg, 65%). ^{1}H NMR ($CDCl_3$, 500 MHz) δ 7.50-7.52 (m, 1H), 7.49 (br. s, 1H), 7.45 (d, *J*=7.8 Hz, 1H), 7.39-7.42 (m, 2H), 7.33-7.39 (m, 3H), 7.24-7.29 (m, 1H), 4.92 (s, 2H), 2.36 (sept, *J*= 6.8 Hz, 2H), 1.37 (sept, *J*= 7.4 Hz, 2H), 1.10 (d, *J*=7.3 Hz, 6H), 1.04 (d, *J*=7.3 Hz, 6H), 0.99 (d, *J*=6.8 Hz, 6H), 0.80 (d, *J*=6.8 Hz, 6H). ^{13}C NMR ($CDCl_3$, 125 MHz) δ 141.4, 134.2, 134.0, 133.9, 133.7, 129.9, 128.5, 127.7, 127.1, 125.8, 122.1, 65.6, 58.1, 32.6, 19.0, 17.8, 17.7, 17.5, 12.4. IR: 2966, 2865, 1463, 1389, 1098, 1068, 993, 882, 791, 731, 712, 695, 671 cm^{-1}. HRMS (DART-ESI+) calcd. for $C_{27}H_{40}N_1O_1Si_1$: $[M+H]^+$: 422.2879, found: 422.2887.

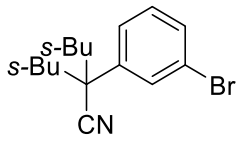

1.125

The general procedure A was followed for the dialkylation in 20 mmol scale (6.54 g, 70 %). ^{1}H NMR ($CDCl_3$, 500 MHz) δ 7.51 (br. s., 1H), 7.41-7.46 (m, 1H), 7.31 (d, *J*=6.8 Hz, 1H), 7.22 (t, *J*=7.8 Hz, 1H), 2.06-2.22 (m, 2H), 1.69-1.83 (m, 1H), 1.31-1.45 (m, 1H), 0.70-1.08 (m, 14H). ^{13}C NMR ($CDCl_3$, 125 MHz) δ 138.4, 138.3, 138.2, 131.0, 131.0, 130.9, 130.8, 129.8, 126.8, 122.7, 122.7, 122.1, 122.0, 121.8, 58.4, 58.1, 57.9, 39.9, 39.8, 39.5, 39.4, 25.9, 25.6, 24.8, 24.4, 15.1, 14.8, 13.9, 13.3, 12.5, 12.3, 12.3 IR: 2968, 2936, 2877, 1593, 1563, 1475, 1384, 1077, 996, 785, 727, 700. cm^{-1}. HRMS (DART-ESI+) calcd. for $C_{16}H_{23}Br_1N_1$: $[M+H]^+$: 308.1014, found: 308.1016.

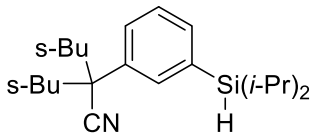

1.126

The general procedure A was followed for silyl group introduction in 32.0 mmol scale (8.76 g, 85 %). ^{1}H NMR ($CDCl_3$, 500 MHz) δ 7.47 (br. s., 1H), 7.44 (d, *J*=7.3 Hz, 1H), 7.35-7.42 (m, 1H), 7.32 (t, *J*=7.3 Hz, 1H), 3.95 (t, *J*=2.9 Hz, 1H), 2.08-2.27 (m, 2H), 1.82-1.76 (m, 0.5H), 1.30-1.48 (m, 0.5H), 1.17-1.29 (m, 2H), 0.74-1.10 (m, 27H). ^{13}C NMR ($CDCl_3$, 125 MHz) δ 134.9, 134.9, 134.8, 134.7, 134.6, 134.5, 134.3, 129.1, 127.6, 127.6, 122.7, 122.6, 122.4, 58.5, 58.2, 58.0, 40.0, 39.7, 39.4, 39.3, 26.1, 25.7, 25.0, 24.4, 18.8, 18.8, 18.6, 18.6, 15.1, 14.7, 13.8, 13.1, 12.6, 12.6, 12.4, 12.4, 10.9, 10.8. IR: 2962, 2939, 2863, 2102, 1461, 1396, 1384, 1003, 880, 804, 783, 711, 657 cm^{-1}. HRMS (DART-ESI+) calcd. for $C_{22}H_{38}N_1Si_1$: $[M+H]^+$: 344.2774, found: 344.2768.

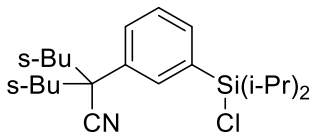

1.127

The general procedure A was followed for chlorination in 25.4 mmol scale (8.5 g, 89%). ^{1}H NMR ($CDCl_3$, 500 MHz) δ 7.50-7.57 (m, 2H), 7.42-7.50 (m, 1H), 7.39 (t, *J*=7.8 Hz, 1H), 2.05-

2.29 (m, 2H), 1.72-1.87 (m, 1H), 1.25-1.49 (m, 3H), 0.68-1.11 (m, 26H). ^{13}C NMR ($CDCl_3$, 125 MHz) δ 135.2, 135.0, 135.0, 133.8, 133.8, 133.8, 133.4, 132.4, 130.1, 127.9, 127.9, 122.4, 122.2, 58.5, 58.3, 58.1, 40.0, 39.7, 39.4, 39.3, 26.2, 25.7, 25.1, 24.4, 17.2, 17.1, 16.9, 15.1, 14.7, 14.0, 13.9, 13.8, 13.1, 12.6, 12.5, 12.4, 12.4. IR: 2962, 2868, 1463, 1384, 1123, 994, 882, 794, 751, 711, 672, 636, 529 cm^{-1}. HRMS (DART-ESI+) calcd. for $C_{22}H_{40}Cl_1N_2Si_1$: $[M+NH_4]^+$: 395.2649, found: 395.2654.

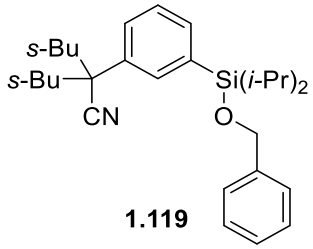

1.119

The general procedure A was followed for an introduction of alcohol in 5.0 mmol scale (2.0 g, 89%). ^{1}H NMR ($CDCl_3$, 500 MHz) δ 7.48-7.53 (m, 2H), 7.45 (d, *J*=7.3 Hz, 1H), 7.38-7.42 (m, 2H), 7.33-7.38 (m, 3H), 7.24-7.29 (m, 1H), 4.92 (s, 2H), 2.01-2.21 (m, 2H), 1.69-1.82 (m, 1H), 1.21-1.43 (m, 3H), 0.68-1.12 (m, 26H). ^{13}C NMR ($CDCl_3$, 125 MHz) δ 141.3, 134.9, 134.7, 134.7, 134.2, 134.0, 133.9, 133.6, 129.6, 128.5, 128.5, 128.3, 127.7, 127.2, 127.1, 125.9, 125.9, 125.8, 122.7, 122.6, 122.4, 65.6, 65.6, 58.5, 58.3, 58.1, 39.9, 39.7, 39.3, 39.2, 26.1, 25.7, 25.0, 24.4, 17.7, 17.7, 17.5, 17.5, 15.1, 14.7, 13.8, 13.1, 12.5, 12.5, 12.4, 12.4, 12.4, 12.4. IR: 2962, 2940, 2865, 1461, 1382, 1205, 1097, 1068, 1027, 993, 881, 809, 795, 749, 730, 713, 695, 680, 669, 496 cm^{-1}. HRMS (DART-ESI+) calcd. for $C_{29}H_{44}N_1O_1Si_1$: $[M+H]^+$: 450.3192, found: 450.3200.

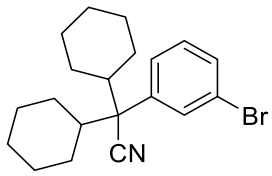

The general procedure A was followed for the dialkylation in 10.0 mmol scale (955 mg, 27%). ^{1}H NMR ($CDCl_3$, 500 MHz) δ 7.49 (br. s, 1H), 7.41-7.46 (m, 1H), 7.27-7.31 (m, 1H), 7.22 (t, *J*=7.8 Hz, 1H), 2.07 (tt, *J*=11.9, 3.0 Hz, 2H), 1.92 (d, *J*=12.7 Hz, 2H), 1.76-1.86 (m, 2H), 1.69-1.76 (m, 2H), 1.64 (d, *J*=13.2 Hz, 2H), 1.54 (d, *J*=12.2 Hz, 2H), 1.25-1.35 (m, 2H), 1.14-1.25 (m,

2H), 0.98-1.12 (m, 4H), 0.88-0.98 (m, 2H). ^{13}C NMR ($CDCl_3$, 100 MHz) δ 138.1, 131.0, 130.9, 129.8, 126.8, 122.7, 122.1, 57.4, 41.9, 29.2, 27.9, 26.6, 26.3. IR: 2930, 2853, 1592, 1564, 1476, 1447, 1414, 1313, 1078, 996, 889, 800, 780, 743, 714, 695, 667 cm^{-1}. HRMS (DART-ESI+) calcd. for $C_{20}H_{27}Br_1N_1$: $[M+H]^+$: 360.1327, found: 360.1336.

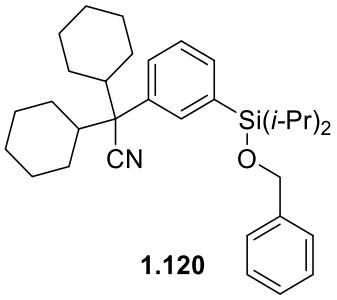

1.120

The general procedure B was followed for the introduction of silyl group in 1.5 mmol scale (650 mg, 86%). ^{1}H NMR ($CDCl_3$, 400 MHz) δ 7.45-7.51 (m, 2H), 7.43 (d, *J*=7.8 Hz, 1H), 7.37-7.41 (m, 2H), 7.31-7.37 (m, 3H), 7.22-7.28 (m, 1H), 4.91 (s, 2H), 1.96-2.06 (m, 2H), 1.88 (d, *J*=12.5 Hz, 2H), 1.75 (d, *J*=13.3 Hz, 2H), 1.62 (t, *J*=15.7 Hz, 4H), 1.45 (d, *J*=12.5 Hz, 2H), 1.36 (sept, *J*=7.3 Hz, 2H), 1.18-1.31 (m, 2H), 0.85-1.13 (m, 20H). ^{13}C NMR ($CDCl_3$, 100 MHz) δ 141.4, 134.7, 134.0, 133.9, 133.4, 129.8, 128.5, 127.7, 127.2, 125.8, 122.6, 65.6, 57.4, 41.8, 29.2, 27.9, 26.6, 26.4, 17.7, 17.5, 12.4. IR: 2930, 2855, 1450, 1098, 1067, 993, 882, 805, 785, 730, 714, 694, 667, 493 cm^{-1}. HRMS (DART-ESI+) calcd. for $C_{33}H_{48}N_1O_1Si_1$: $[M+H]^+$: 502.3505, found: 502.3510.

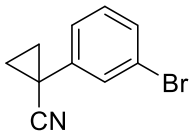

The biphasic mixture of 2-(3-bromophenyl)-acetonitrile (1.0 eq., 10 mmol, 1.96 g) and 1,2-dibromoethane (1.5 eq., 1.3 mL) in toluene/water (0.5 M) was vigorously stirred for 4 h at room temperature. After dilution with water, the mixture was extracted with ethyl acetate. The organic phase was dried over anhydrous magnesium sulfate and concentrated under reduced pressure. A flash chromatography on silica gel gave the product as yellowish oil (959 mg, 43%). ^{1}H NMR ($CDCl_3$, 500 MHz) δ 7.36-7.48 (m, 2H), 7.17-7.31 (m, 2H), 1.70-1.78 (m, 2H), 1.38-1.44 (m, 2H). ^{13}C NMR

($CDCl_3$, 125 MHz) δ 138.5, 131.0, 130.6, 129.0, 124.8, 123.2, 122.1, 18.6, 13.8. IR: 2958, 2236, 1596, 1566, 1478, 1424, 1073, 949, 876, 780, 718, 687 cm^{-1}. HRMS (DART-ESI+) calcd. for $C_{10}H_9Br_1N_1$: $[M+H]^+$: 221.9918, found: 221.9921.

The general procedure B was followed for the introduction of silyl group in 1.5 mmol scale (478 mg, 88%). ^1H NMR ($CDCl_3$, 500 MHz) δ 7.44-7.51 (m, 1H), 7.31-7.43 (m, 7H), 7.24-7.31 (m, 1H), 4.89 (s, 2H), 1.64 - 1.70 (m, 2H), 1.31-1.41 (m, 2H), 1.24-1.31 (m, 2H), 1.10

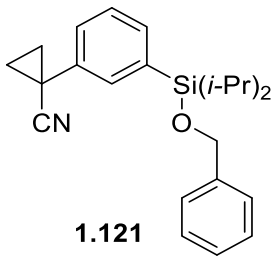

1.121

(dd, *J*=7.3, 1.5 Hz, 6H), 1.04 (dd, *J*=7.6, 1.7 Hz, 6H). ^{13}C NMR ($CDCl_3$, 125 MHz) δ 141.3, 135.6, 135.4, 134.0, 131.5, 128.5, 128.4, 127.3, 127.2, 126.0, 122.8, 65.7, 18.3, 17.7, 17.5, 14.0, 12.4. IR: 2944, 2865, 2236, 1462, 1377, 1097, 1068, 993, 882, 789, 733, 703, 672, 578, 491 cm^{-1}. HRMS (DART-ESI+) calcd. for $C_{23}H_{30}N_1O_1Si_1$: $[M+H]^+$: 364.2097, found: 364.2104.

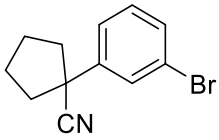

The same procedure was followed with 1-(3-bromophenyl)cyclopropane-1-carbonitrile except using 1,4-dibromobutane. Product as yellowish oil (1.98 mg, 79%). ^1H NMR ($CDCl_3$, 500 MHz) δ 7.54-7.62 (m, 1H), 7.45 (dd, *J*=7.8, 1.0 Hz, 1H), 7.40 (dd, *J*=7.8, 1.0 Hz, 1H), 7.25 (t, *J*=7.8 Hz, 1H), 2.40-2.55 (m, 2H), 2.00-2.11 (m, 4H), 1.84-2.00 (m, 2H). ^{13}C NMR ($CDCl_3$, 125 MHz) δ 142.3, 131.2, 130.6, 129.4, 125.0, 124.0, 123.2, 47.7, 40.7, 24.4. IR: 2965, 2876, 2233, 1592, 1566, 1476, 1418, 1078, 996, 878, 782, 691 cm^{-1}. HRMS (DART-ESI+) calcd. for $C_{12}H_{13}Br_1N_1$: $[M+H]^+$: 250.0231, found: 250.0228.

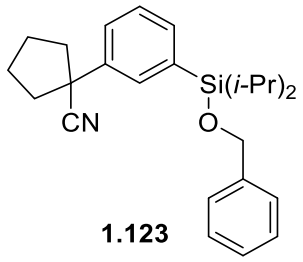

1.123

The general procedure B was followed for the introduction of silyl group in 1.5 mmol scale (512 mg, 87 %). ^{1}H NMR ($CDCl_3$, 500 MHz) δ 7.55-7.58 (m, 1H), 7.47-7.52 (m, 2H), 7.33-7.42 (m, 5H), 7.24-7.29 (m, 1H), 4.90 (s, 2H), 2.35-2.45 (m, 2H), 1.89-2.03 (m, 4H), 1.79-1.89 (m, 2H), 1.36 (sept, *J*= 7.5 Hz, 2H), 1.10 (d, *J*= 7.5 Hz, 6H), 1.05 (d, *J*= 7.5 Hz, 6H). ^{13}C NMR ($CDCl_3$, 100 MHz) δ 141.4, 139.2, 135.4, 134.1, 132.0, 128.5, 128.3, 127.4, 127.2, 126.0, 124.7, 65.7, 47.9, 40.6, 24.4, 17.7, 17.5, 12.4. IR: 2945, 2865, 1453, 1378, 1096, 1068, 993, 882, 794, 732, 707, 492 cm^{-1}. HRMS (DART-ESI+) calcd. for $C_{25}H_{34}N_1O_1Si_1$: $[M+H]^+$: 392.2410, found: 392.2402.

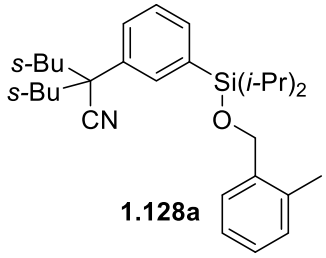

1.128a

The general procedure A was followed for an introduction of alcohol in 1.0 mmol scale using 2-methylbenzyl alcohol (461 mg, 99 %). ^{1}H NMR ($CDCl_3$, 500 MHz) δ 7.55-7.65 (m, 1H), 7.40-7.55 (m, 3H), 7.36 (t, *J*= 7.8 Hz, 1H), 7.26 (t, *J*= 7.3 Hz, 1H), 7.20 (t, *J*= 7.1 Hz, 1H), 7.15 (d, *J*=7.3 Hz, 1H), 4.88 (s, 2H), 2.20-2.27 (m, 3H), 1.99-2.17 (m, 2H), 1.67-1.80 (m, 1H), 1.22-1.46 (m, 3H), 0.73-1.14 (m, 26H). ^{13}C NMR ($CDCl_3$, 125 MHz) δ 139.1, 134.9, 134.7, 134.7, 134.3, 133.9, 133.8, 133.5, 130.0, 129.6, 127.7, 127.7, 127.1, 127.1, 127.0, 126.1, 126.1, 126.0, 125.9, 125.8, 122.7, 122.5, 122.4, 63.9, 58.5, 58.3, 58.0, 39.8, 39.6, 39.2, 39.2, 26.1, 25.6, 24.9, 24.3, 18.7, 18.6, 18.6, 17.7, 17.7, 17.6, 17.6, 15.1, 14.7, 13.7, 13.1, 12.5, 12.5, 12.4, 12.3, 12.3. IR: 2939, 2865, 1462, 1383, 1122, 1083, 993, 881, 812, 745, 712, 669, 594, 494 cm^{-1}. HRMS (DART- ESI+) calcd. for $C_{30}H_{46}N_1O_1Si_1$: $[M+H]^+$: 464.3349, found: 464.3332.

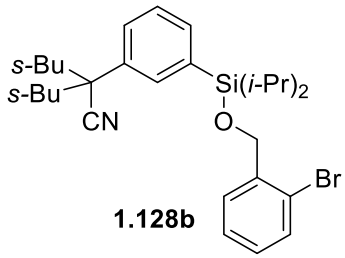

1.128b

The general procedure A was followed for an introduction of alcohol in 1.0 mmol scale using 2-bromobenzyl alcohol (484 mg, 92%). ^{1}H NMR ($CDCl_3$, 500 MHz) δ 7.76 (d, *J*=8.3 Hz, 1H), 7.42-7.53 (m, 4H), 7.34-7.42 (m, 2H), 7.15 (td, *J*=7.3, 1.0 Hz, 1H), 4.89 (s, 1H), 2.00-2.16 (m, 2H), 1.70-1.77 (m, 1H), 1.21-1.46 (m, 3H), 1.72-1.15 (m, 26H). ^{13}C NMR ($CDCl_3$, 125 MHz) δ 140.2, 135.0, 134.8, 134.8, 133.9, 133.9, 133.8, 133.8, 133.8, 133.5, 132.3, 129.8, 128.5, 128.5, 128.5, 127.8, 127.8, 127.7, 127.5, 127.4, 122.6, 122.5, 122.4, 121.1, 65.5, 58.5, 58.3, 58.0, 39.8, 39.6, 39.3, 39.2, 26.0, 25.6, 24.9, 24.3, 17.7, 17.7, 17.5, 17.5, 15.1, 14.7, 13.7, 13.2, 12.5, 12.5, 12.5, 12.4, 12.4, 12.4, 12.3. IR: 2963, 2865, 1463, 1383, 1203, 1120, 1097, 1026, 993, 881, 813, 749, 712, 669, 620, 449 cm^{-1}. HRMS (DART- ESI+) calcd. for $C_{29}H_{43}Br_1N_1O_1Si_1$: $[M+H]^+$: 528.2297, found: 528.2292.

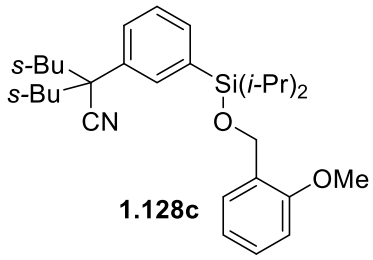

1.128c

The general procedure A was followed for an introduction of alcohol in 1.0 mmol scale using 2-methoxybenzyl alcohol (478 mg, 99 %). ^{1}H NMR ($CDCl_3$, 500 MHz) δ 7.68 (d, *J*=6.8 Hz, 1H), 7.42-7.54 (m, 3H), 7.35 (t, *J*=7.3 Hz, 1H), 7.25 (td, *J*=7.7, 1.7 Hz, 1H), 7.03 (t, *J*=7.3 Hz, 1H), 6.84 (d, *J*=7.8 Hz, 1H), 4.90-4.95 (m, 2H), 3.76-3.81 (m, 3H), 1.99-2.16 (m, 2H), 1.71-1.78 (m, 1H), 1.21-1.45 (m, 3H), 0.71-1.14 (m, 26H). ^{13}C NMR ($CDCl_3$, 100 MHz) δ 156.0, 134.7, 134.6, 134.6, 134.4, 134.4, 134.3, 133.9, 133.9, 133.4, 129.9, 129.8, 129.8, 127.8, 127.7, 127.7, 127.7, 126.4, 126.3, 126.2, 122.7, 122.6, 122.4, 120.7, 109.6, 61.1, 61.0, 58.5, 58.2, 58.0, 55.2, 39.8, 39.6, 39.2, 39.1, 26.1, 25.6, 24.9, 24.3, 17.7, 17.7, 17.6, 17.5, 15.1, 14.7, 13.7, 13.0, 12.5, 12.4, 12.4.

IR: 2940, 2865, 1491, 1462, 1382, 1239, 1122, 1085, 882, 752, 712, 669, 494 cm^{-1}. HRMS (DART- ESI+) calcd. for $C_{30}H_{46}N_1O_2Si_1$: $[M+H]^+$: 480.3298, found: 480.3278.

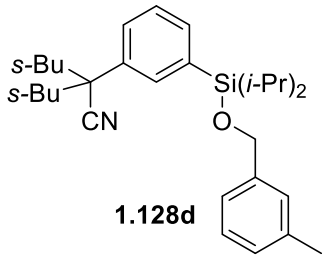

1.128d

The general procedure A was followed for an introduction of alcohol in 3.0 mmol scale using 3-methylbenzyl alcohol (1.32 g, 95%). ^1H NMR ($CDCl_3$, 500 MHz) δ 7.48-7.53 (m, 2H), 7.43-7.48 (m, 1H), 7.36 (t, *J*=7.8 Hz, 1H), 7.25 (t, *J*=7.8 Hz, 1H), 7.17-7.23 (m, 2H), 7.08 (d, *J*=7.3 Hz, 1H), 4.88 (s, 2H), 2.37 (s, 3H), 2.02-2.18 (m, 2H), 1.68-1.83 (m, 1H), 1.24-1.48 (m, 3H), 0.79-1.12 (m, 26H). ^{13}C NMR ($CDCl_3$, 125 MHz) δ 141.3, 138.0, 134.8, 134.7, 134.7, 134.3, 134.0, 133.9, 133.5, 129.7, 128.5, 128.4, 128.4, 127.9, 127.7, 126.6, 126.5, 123.0, 123.0, 122.9, 122.7, 122.6, 122.4, 65.6, 65.6, 58.5, 58.3, 58.1, 39.9, 39.7, 39.3, 39.2, 26.1, 25.7, 25.0, 24.4, 21.7, 17.7, 17.7, 17.5, 17.5, 15.1, 14.7, 13.8, 13.1, 12.5, 12.5, 12.4, 12.4, 12.3. IR: 2964, 2866, 1462, 1383, 1157, 1104, 993, 882, 815, 771, 713, 669, 495 cm^{-1}. HRMS (DART-ESI+) calcd. for $C_{30}H_{46}N_1O_1Si_1$: $[M+H]^+$: 464.3349, found: 464.3363.

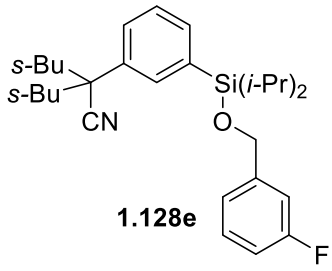

1.128e

The general procedure A was followed for an introduction of alcohol in 1.0 mmol scale using 3-fluorobenzyl alcohol (462 mg, 99%). ^1H NMR ($CDCl_3$, 500 MHz) δ 7.40-7.53 (m, 3H), 7.36 (t, *J*=7.3 Hz, 1H), 7.28-7.33 (m, 1H), 7.10-7.17 (m, 2H), 6.95 (td, *J*=8.6, 2.4 Hz, 1H), 4.89 (s, 2H), 2.03-2.18 (m, 2H), 1.70-1.77 (m, 1H), 1.24-1.43 (m, 3H), 0.71-1.12 (m, 26H). ^{13}C NMR ($CDCl_3$, 100 MHz) δ 164.5, 162.1, 144.2, 144.1, 135.0, 134.8, 134.8, 133.9, 133.9, 133.8, 133.5, 130.0, 129.9, 129.8, 127.8, 122.6, 122.5, 122.4, 121.2, 121.2, 121.2, 121.1, 121.1, 114.0, 113.8, 112.9, 112.8, 112.6, 112.6, 65.0,

64.9, 64.9, 58.5, 58.3, 58.0, 39.9, 39.7, 39.3, 39.2, 26.1, 25.7, 24.9, 24.4, 17.7, 17.6, 17.5, 17.5, 15.1, 14.7, 13.7, 13.1, 12.5, 12.5, 12.4, 12.3, 12.3. IR: 2963, 2866, 1592, 1462, 1383, 1253, 1136, 1101, 1065, 993, 924, 881, 779, 713, 682, 496 cm^{-1}. HRMS (DART-ESI+) calcd. for $C_{29}H_{43}F_1N_1O_1Si_1$: $[M+H]^+$: 468.3098, found: 468.3094.

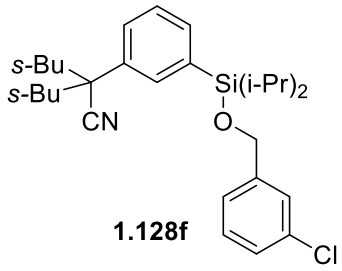

1.128f

The general procedure A was followed for an introduction of alcohol in 1.0 mmol scale using 3-chlorobenzyl alcohol (475 mg, 98%). ^1H NMR ($CDCl_3$, 500 MHz) δ 7.43-7.65 (m, 3H), 7.40 (s, 1H), 7.36 (t, *J* = 7.0, 1H), 7.22-7.32 (m, 3H), 4.88 (s, 2H), 1.98-2.20 (m, 2H), 1.69-1.82 (m, 1H), 1.24-1.44(m, 3H), 0.68-1.12 (m, 26H). ^{13}C NMR ($CDCl_3$, 125 MHz) δ 143.5, 143.5, 135.0, 134.9, 134.8, 134.5, 133.9, 133.9, 133.5, 129.8, 129.8, 127.8, 127.3, 126.0, 125.9, 123.9, 123.9, 123.8, 122.5, 122.4, 64.9, 64.9, 58.5, 58.3, 58.1, 39.9, 39.7, 39.3, 39.2, 26.1, 25.7, 25.0, 24.4, 17.7, 17.6, 17.5, 17.5, 15.1, 14.7, 13.8, 13.1, 12.5, 12.5, 12.4, 12.3. IR: 2963, 2940, 2866, 1600, 1462, 1384, 1200, 1108, 994, 882, 810, 775, 681, 496 cm^{-1}. HRMS (DART-ESI+) calcd. for $C_{29}H_{43}Cl_1N_1O_1Si_1$: $[M+H]^+$: 484.2802, found: 484.2791.

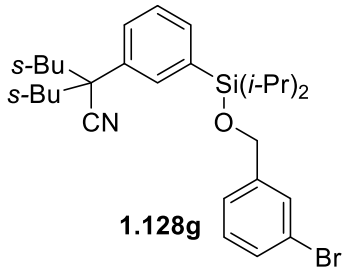

1.128g

The general procedure A was followed for an introduction of alcohol in 1.0 mmol scale using 3-bromobenzyl alcohol (464 mg, 88 %). ^1H NMR ($CDCl_3$, 500 MHz) δ 7.56 (s, 1H), 7.42-7.53 (m, 3H), 7.40 (d, *J*=8.3 Hz, 1H), 7.36 (t, *J*=7.8 Hz, 1H), 7.31 (d, *J*=7.8 Hz, 1H), 7.22 (t, *J*=7.8 Hz, 1H), 4.87 (s, 2H), 2.00-2.23 (m, 2H), 1.70-1.77 (m, 1H), 1.24-1.44 (m, 3H), 0.73-1.12 (m, 26H). ^{13}C NMR ($CDCl_3$, 125 MHz) δ 143.7, 143.7, 135.0, 134.9, 134.8, 133.9, 133.8, 133.5, 130.2, 130.1, 129.9, 128.9, 128.8, 127.8,

124.4, 124.4, 124.3, 122.7, 122.6, 122.5, 122.4, 64.8, 64.8, 58.5, 58.3, 58.1, 39.9, 39.7, 39.3, 39.2, 26.1, 25.7, 25.0, 24.4, 17.7, 17.6, 17.5, 17.5, 15.1, 14.7, 13.8, 13.1, 12.5, 12.5, 12.4, 12.3, 12.3. IR: 2963, 2865, 1571, 1461, 1383, 1197, 1107, 993, 881, 810, 772, 712, 681, 495 cm^{-1}. HRMS (DART-ESI+) calcd. for $C_{29}H_{43}Br_1N_1O_1Si_1$: $[M+H]^+$: 528.2297, found: 528.2296.

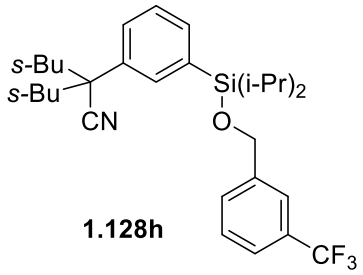

1.128h

The general procedure A was followed for an introduction of alcohol in 1.0 mmol scale using 3-trifluoromethylbenzyl alcohol (508 mg, 98 %). ^1H NMR ($CDCl_3$, 500 MHz) δ 7.66 (s, 1H), 7.58 (d, *J* = 7.8, 1H), 7.53 (d, *J* =7.8, 1H), 7.42-7.51 (m, 4H), 7.36 (t, *J* = 7.8, 1H), 4.95 (s, 2H), 2.02-2.18 (m, 2H), 1.70 - 1.80 (m, 1H), 1.24-1.44 (m, 3H), 1.68-1.13 (m, 26H). ^{13}C NMR ($CDCl_3$, 125 MHz) δ 142.3, 135.0, 134.9, 134.8, 133.9, 133.8, 133.5, 131.0, 130.7, 129.8, 129.1, 129.0, 127.8, 125.8, 124.0, 124.0, 123.1, 122.6, 122.6, 122.4, 65.0, 65.0, 58.5, 58.3, 58.1, 39.9, 39.7, 39.3, 39.2, 26.1, 25.7, 25.0, 24.4, 17.7, 17.6, 17.5, 17.5, 15.1, 14.7, 13.7, 13.0, 12.5, 12.5, 12.4, 12.3. IR: 2965, 2942, 2867, 1463, 1330, 1164, 1126, 1073, 882, 793, 702, 495 cm^{-1}. HRMS (DART-ESI+) calcd. for $C_{30}H_{43}F_3N_1O_1Si_1$: $[M+H]^+$: 518.3066, found: 518.3087.

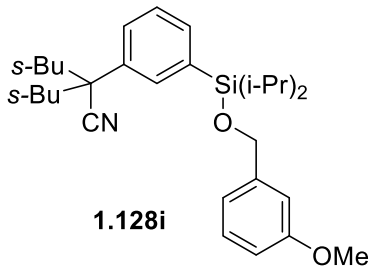

1.128i

The general procedure A was followed for an introduction of alcohol in 1.0 mmol scale using 3-methoxybenzyl alcohol (400 mg, 83%). ^1H NMR ($CDCl_3$, 500 MHz) δ 7.40-7.59 (m, 3H), 7.35 (t, *J* = 7.8, 1H), 7.26 (t, *J* = 7.8, 1H), 7.00 (s, 1H), 6.95 (d, *J* = 7.8, 1H), 6.81 (dd, *J* = 7.8, 2.9, 1H), 4.89 (s, 2H), 3.82 (s, 3H), 1.99-2.23 (m, 2H), 1.65-1.80 (m, 1H), 1.22-1.44 (m, 3H), 1.69-1.12 (m, 26H). ^{13}C NMR

($CDCl_3$, 125 MHz) δ 160.1, 143.1, 134.9, 134.8, 134.7, 134.2, 134.0, 133.9, 133.5, 129.8, 129.5, 127.7, 122.6, 122.4, 118.1, 118.1, 117.9, 112.6, 112.6, 112.5, 111.5, 111.4, 111.2, 65.5, 65.4, 58.5, 58.3, 58.1, 55.4, 39.9, 39.7, 39.3, 39.2, 26.1, 25.7, 24.9, 24.4, 17.7, 17.7, 17.5, 17.5, 15.1, 14.7, 13.7, 13.1, 12.5, 12.5, 12.4, 12.4, 12.3. IR: 2962, 2940, 2866, 1603, 1462, 1383, 1283, 1152, 1105, 882, 795, 713, 690, 496 cm^{-1}. HRMS (DART-ESI+) calcd. for $C_{30}H_{46}N_1O_2Si_1$: $[M+H]^+$: 480.3298, found: 480.3296.

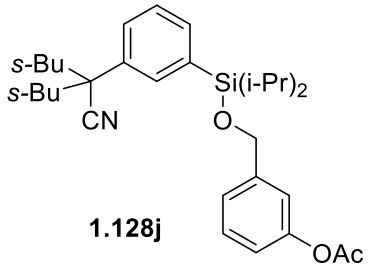

1.128j

The general procedure A was followed for an introduction of alcohol in 1.0 mmol scale using 3-(hydroxymethyl)phenyl acetate (339 mg, 67%).^{1}H NMR ($CDCl_3$, 500 MHz) δ 7.46-7.54 (m, 2H), 7.44 (d, *J*=5.9 Hz, 1H), 7.32-7.39 (m, 2H), 7.25 (d, *J*=7.8 Hz, 1H), 7.13 (s, 1H), 6.99 (d, *J*=8.3 Hz, 1H), 4.90 (s, 2H), 2.30 (s, 3H), 2.05-2.19 (m, 2H), 1.69-1.82 (m, 1H), 1.23-1.44 (m, 4H), 0.79-1.11 (m, 26H). ^{13}C NMR ($CDCl_3$, 100 MHz) δ 169.6, 151.0, 143.2, 143.2, 134.9, 134.8, 134.7, 134.0, 133.9, 133.9, 133.6, 129.7, 129.4, 127.8, 123.2, 123.1, 122.6, 122.5, 122.4, 120.3, 119.0, 118.9, 65.1, 58.5, 58.2, 58.0, 39.9, 39.6, 39.3, 39.2, 26.1, 25.6, 25.0, 24.3, 21.4, 17.6, 17.6, 17.5, 17.5, 15.1, 14.7, 13.7, 13.0, 12.5, 12.5, 12.3, 12.3. IR: 2963, 2940, 2866, 1768, 1462, 1369, 1204, 1139, 1102, 1072, 881 cm^{-1}. HRMS (DART- ESI+) calcd. for $C_{31}H_{46}N_1O_3Si_1$: $[M+H]^+$: 508.3247, found: 508.3245.

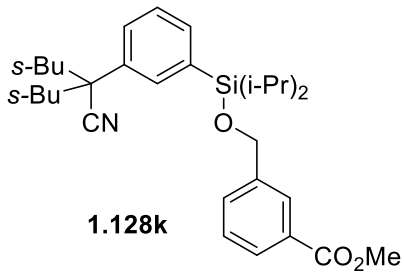

1.128k

The general procedure A was followed for an introduction of alcohol in 1.0 mmol scale using methyl 3-(hydroxymethyl)benzoate (476 mg, 94%). ^{1}H NMR ($CDCl_3$, 500 MHz) δ 8.04 (s, 1H), 7.95 (d, *J* = 7.3, 1H),

7.64 (d, J =7.3, 1H), 7.41-7.54 (m, 4H), 7.35 (t, J = 8.3, 1H), 4.94 (s, 2H), 3.92 (s, 3H), 2.01-2.16 (m, 2H), 1.70-1.79 (m, 1H), 1.24-1.42 (m, 3H), 0.68-1.13 (m, 26H). ^{13}C NMR ($CDCl_3$, 125 MHz) δ 167.3, 141.8, 141.8, 134.9, 134.8, 134.8, 134.0, 133.9, 133.6, 130.5, 130.5, 130.4, 129.8, 128.7, 128.5, 127.8, 127.1, 127.0, 122.6, 122.5, 122.4, 65.2, 65.2, 58.5, 58.3, 58.0, 52.3, 39.9, 39.7, 39.3, 39.2, 26.1, 26.7, 25.0, 24.6, 17.7, 17.6, 17.5, 17.5, 15.1, 14.7, 13.7, 13.1, 12.5, 12.5, 12.4, 12.3. IR: 2963, 2942, 2866, 1725, 1462, 1287, 1200, 1106, 882, 747, 496 cm^{-1}. HRMS (DART-ESI+) calcd. for $C_{31}H_{46}N_1O_3Si_1$: $[M+H]^+$: 508.3247 found: 508.3253.

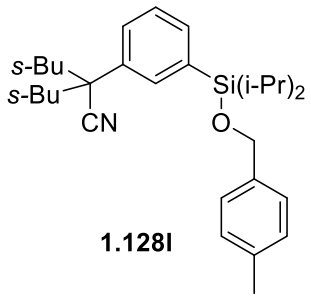

1.128l

The general procedure A was followed for an introduction of alcohol in 1.0 mmol scale using 4-methylbenzyl alcohol (350 mg, 76%). ^{1}H NMR ($CDCl_3$, 500 MHz) δ 7.48-7.56 (m, 2H), 7.46 (d, J=7.3 Hz, 1H), 7.36 (t, J=7.3 Hz, 1H), 7.30 (d, J=7.8 Hz, 2H), 7.17 (d, J=7.8 Hz, 2H), 4.88 (s, 2H), 2.36 (s, 3H), 2.04-2.19 (m, 2H), 1.75-1.81 (m, 1H), 1.24-1.45 (m, 3H), 0.73-1.12 (m, 26H). ^{13}C NMR ($CDCl_3$, 125 MHz) δ 138.3, 136.7, 136.6, 134.8, 134.7, 134.7, 134.3, 134.3, 134.0, 133.9, 133.6, 129.6, 129.2, 129.1, 127.7, 127.7, 126.0, 126.0, 125.8, 122.7, 122.6, 122.4, 65.5, 65.5, 58.5, 58.3, 58.0, 39.9, 39.7, 39.3, 39.2, 26.1, 25.7, 24.9, 24.4, 21.3, 17.7, 17.7, 17.5, 17.5, 15.1, 14.7, 13.8, 13.1, 12.5, 12.5, 12.4, 12.4, 12.3. IR: 2940, 2865, 1462, 1383, 1092, 993, 881, 793, 749, 713, 669, 615, 479 cm^{-1}. HRMS (DART-ESI+) calcd. for $C_{30}H_{46}N_1O_1Si_1$: $[M+H]^+$: 464.3349, found: 464.3343.

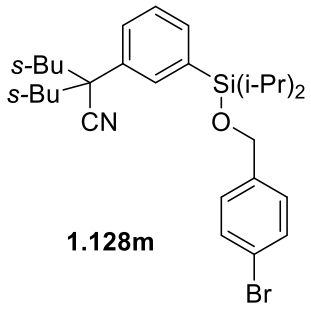

1.128m

The general procedure A was followed for an introduction of alcohol in 1.0 mmol scale using 4-bromolbenzyl alcohol (526 mg, 99%). ^{1}H NMR ($CDCl_3$, 500 MHz) δ 7.46-7.55 (m, 4H), 7.44 (d, *J*= 7.3 Hz, 1H), 7.35 (t, *J*= 7.3 Hz, 1H), 7.28 (d, *J*= 8.8 Hz, 2H), 4.85 (s, 2H), 2.05-2.17 (m, 2H), 1.70-1.77 (m, 1H), 1.25-1.44 (m, 3H), 0.70-1.11 (m, 26H). ^{13}C NMR ($CDCl_3$, 125 MHz) δ 140.4, 140.3, 134.9, 134.8, 134.8, 134.0, 133.9, 133.8, 133.7, 131.6, 129.6, 127.8, 127.7, 127.7, 127.6, 127.5, 122.6, 122.5, 122.3, 120.9, 65.0, 65.0, 58.5, 58.3, 58.0, 39.9, 39.7, 39.3, 39.2, 26.1, 25.7, 24.9, 24.4, 17.7, 17.6, 17.5, 17.5, 15.1, 14.7, 13.8, 13.1, 12.5, 12.5, 12.4, 12.3. IR: 2962, 2865, 1486, 1462, 1383, 1098, 1010, 881, 795, 712, 670, 606, 505 cm^{-1}. HRMS (DART-ESI+) calcd. for $C_{29}H_{43}Br_1N_1O_1Si_1$: $[M+H]^+$: 528.2297, found: 528.2292.

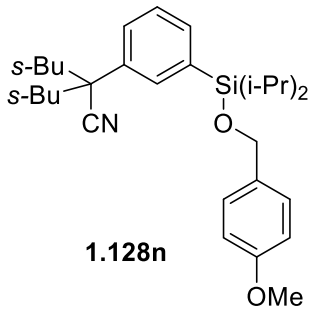

1.128n

The general procedure A was followed for an introduction of alcohol in 1.0 mmol scale using 4-methoxybenzyl alcohol (431 mg, 90%). ^{1}H NMR ($CDCl_3$, 500 MHz) δ 7.47 - 7.54 (m, 2H), 7.45 (d, *J*=6.8 Hz, 1H), 7.35 (t, *J*=7.3 Hz, 1H), 7.32 (d, *J*=8.8 Hz, 2H), 6.90 (d, *J*=8.8 Hz, 2H), 4.85 (s, 2H), 3.82 (s, 3H), 2.03 - 2.19 (m, 2H), 1.71 - 1.84 (m, 1H), 1.24 - 1.47 (m, 3H), 0.71 - 1.11 (m, 26H). ^{13}C NMR ($CDCl_3$, 100 MHz) δ 158.9, 134.8, 134.7, 134.6, 134.4, 134.3, 134.3, 134.0, 133.9, 133.6, 133.5, 129.6, 127.7, 127.4, 127.3, 127.2, 122.7, 122.6, 122.4, 113.9, 65.3, 65.3, 58.5, 58.2, 58.0, 55.5, 55.4, 39.9, 39.7, 39.3, 39.2, 26.1, 25.6, 24.9, 24.4, 17.7, 17.6, 17.5, 17.5, 15.1, 14.7, 13.8, 13.1, 12.5, 12.5, 12.4, 12.3. IR: 2940, 2865, 1613, 1512, 1462, 1382, 1300,

1246, 1169, 1091, 1037, 881, 820, 745, 713, 669, 500 cm^{-1}. HRMS (DART- ESI+) calcd. for $C_{30}H_{46}N_1O_2Si_1$: $[M+H]^+$: 480.3298, found: 480.3291.

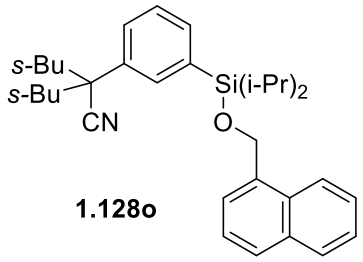

1.128o

The general procedure A was followed for an introduction of alcohol in 1.0 mmol scale using 1-naphthylmethanol (478 mg, 96 %). ^1H NMR ($CDCl_3$, 500 MHz) δ 7.86-7.96 (m, 2H), 7.80 (d, J = 8.3, 1H), 7.76 (d, J = 6.8, 1H), 7.41-7.56 (m, 6H), 7.35 (t, J = 6.8, 1H), 5.38 (s, 2H), 1.95-2.10 (m, 2H), 1.65-1.75 (m, 1H), 1.36-1.49 (m, 2H), 1.18-1.32 (m, 1H), 0.63-1.17 (m, 26H). ^{13}C NMR ($CDCl_3$, 125 MHz) δ 136.6, 134.9, 134.8, 134.7, 134.2, 134.0, 133.9, 133.9, 133.7, 133.5, 130.7, 130.6, 129.8, 128.9, 128.9, 127.8, 127.8, 127.7, 127.7, 126.2, 126.1, 125.8, 125.7, 125.7, 123.5, 123.3, 123.1, 123.1, 123.0, 122.7, 122.6, 122.4, 64.1, 64.0, 58.5, 58.2, 58.0, 39.8, 39.6, 39.2, 39.1, 26.0, 25.6, 24.9, 24.3, 17.8, 17.7, 17.6, 17.6, 15.0, 14.7, 13.6, 13.0, 12.5, 12.5, 12.4, 12.3. IR: 3051, 2962, 2940, 2865, 1462, 1384, 1167, 920, 792, 713, 670, 488 cm^{-1}. HRMS (DART-ESI+) calcd. for $C_{33}H_{46}N_1O_1Si_1$: $[M+H]^+$: 500.3349, found: 500.3356.

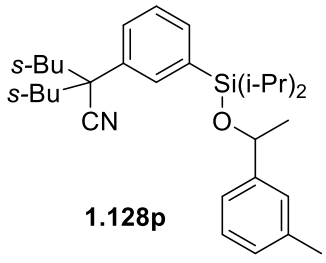

1.128p

The general procedure A was followed for an introduction of alcohol in 1.0 mmol scale using α-methyl-3-methylbenzyl alcohol (437 mg, 92%). ^1H NMR ($CDCl_3$, 500 MHz) δ 7.37-7.52 (m, 3H), 7.31 (t, J = 7.3 Hz, 1H), 7.15-7.23 (m, 3H), 7.05 (d, J = 7.3 Hz, 1H), 4.98 (q, J=6.0 Hz, 1H), 2.35 (s, 3H), 1.98-2.17 (m, 2H), 1.70-1.81 (m, 1H), 1.49 (d, J=6.4 Hz, 3H), 1.21-1.43 (m, 3H), 0.68-1.08 (m, 26H). ^{13}C NMR ($CDCl_3$, 100Hz) δ 159.8, 159.8, 159.8, 148.8, 148.7, 134.9, 134.8, 134.7, 134.6, 134.5, 133.9, 133.9, 133.6, 129.6, 129.4, 129.4, 127.5, 127.5, 122.7, 122.6, 122.5, 117.9, 117.8, 117.8, 112.5,

112.4, 112.4, 112.3, 111.1, 111.0, 111.0, 110.8, 71.7, 71.6, 71.6, 58.5, 58.3, 58.3, 58.1, 55.3, 40.0, 39.9, 39.7, 39.6, 39.3, 39.2, 39.2, 39.1, 28.0, 26.2, 26.1, 25.7, 25.6, 25.0, 25.0, 24.4, 17.6, 17.6, 17.5, 17.4, 17.4, 15.1, 15.1, 14.7, 14.7, 13.8, 13.7, 13.1, 12.6, 12.5, 12.5, 12.5, 12.5, 12.5, 12.4, 12.4, 12.3. IR: 2965, 2865, 1462, 1383, 1161, 1092, 1037, 994, 882, 703, 667, 598, 504 cm^{-1}. HRMS (DART- ESI+) calcd. for $C_{31}H_{48}N_1O_1Si_1$: $[M+H]^+$: 478.3505, found: 478.3513.

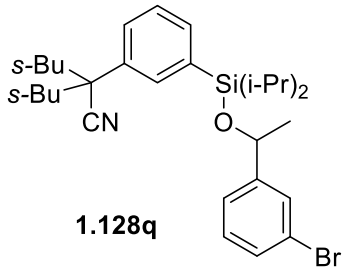

1.128q

The general procedure A was followed for an introduction of alcohol in 1.0 mmol scale using α-methyl-3-bromobenzyl alcohol (541 mg, 99%). ^1H NMR ($CDCl_3$, 500 MHz) δ 7.53 (s, 1H), 7.39-7.50 (m, 3H), 7.37 (d, *J* = 7.8 Hz, 1H), 7.27-7.35 (m, 2H), 7.16-7.22 (m, 1H), 4.97 (m, 1H), 1.97-2.21 (m, 2H), 1.68-1.85 (m, 1H), 1.48 (d, *J* = 6.4 Hz, 3H), 1.24-1.45 (m, 3H), 0.67 1.08 (m, 26H). ^{13}C NMR ($CDCl_3$, 100 MHz) δ 149.4, 149.3, 134.8, 134.7, 134.6, 134.6, 134.5, 134.5, 133.9, 133.8, 133.7, 130.2, 130.1, 129.5, 128.6, 128.6, 128.6, 127.6, 124.1, 124.0, 124.0, 122.7, 122.6, 122.4, 71.2, 71.1, 71.1, 58.5, 58.3, 58.3, 58.1, 40.0, 39.9, 39.7, 39.7, 39.4, 39.2, 39.2, 39.2, 27.9, 26.2, 26.1, 25.7, 25.6, 25.0, 25.0, 24.4, 17.5, 17.5, 17.5, 17.5, 17.4, 17.4, 17.4, 15.1, 14.7, 14.7, 13.8, 13.7, 13.1, 12.6, 12.6, 12.5, 12.5, 12.5, 12.4, 12.4, 12.4, 12.4, 12.4. IR: 2965, 2866, 1570, 1463, 1383, 1200, 1117, 1094, 1034, 994, 960, 882, 818, 786, 712, 695, 667, 504 cm^{-1}. HRMS (DART-ESI+) calcd. for $C_{30}H_{45}Br_1N_1O_1Si_1$: $[M+H]^+$: 542.2454, found: 542.2471.

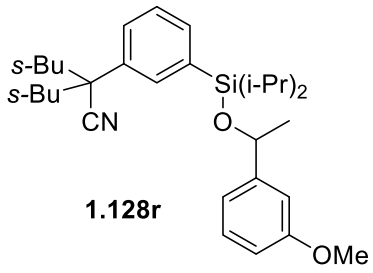

1.128r

The general procedure A was followed for an introduction of alcohol in 1.0 mmol scale using α-methyl-3-methoxybenzyl alcohol (492 mg, 99%). ^{1}H NMR ($CDCl_3$, 500 MHz) δ 7.37-7.51 (m, 3H), 7.31 (t, *J* = 7.3 Hz, 1H), 7.23 (td, *J* = 7.8, 1.5 Hz, 1H), 6.98 (s, 1H), 6.90-6.96 (m, 1H), 6.78 (dd, *J* = 7.8, 2.4 Hz, 1H), 5.00 (q, *J* = 6.4 Hz, 1H), 3.80 (s, 3H), 1.99-2.19 (m, 2H), 1.69-1.82 (m, 1H), 1.50 (d, *J* = 6.4 Hz, 3H), 1.20-1.44 (m, 3H), 0.77-1.07 (m, 26H). ^{13}C NMR ($CDCl_3$, 100Hz) δ 146.9, 137.9, 137.8, 135.0, 134.9, 134.7, 134.5, 134.5, 133.9, 133.9, 133.6, 129.5, 128.3, 127.8, 127.8, 127.5, 127.5, 126.1, 126.1, 126.1, 122.7, 122.6, 122.5, 122.5, 122.5, 122.4, 71.8, 71.8, 71.7, 58.5, 58.3, 58.3, 58.1, 40.0, 39.9, 39.6, 39.4, 39.2, 39.2, 39.2, 28.0, 26.2, 26.2, 25.7, 25.6, 25.1, 25.0, 24.4, 24.4, 21.7, 17.6, 17.5, 17.5, 17.5, 17.4, 17.4, 15.1, 14.7, 14.7, 13.8, 13.7, 13.1, 12.6, 12.5, 12.5, 12.5, 12.5, 12.5, 12.4, 12.4, 12.4. IR: 2964, 2866, 1602, 1462, 1383, 1256, 1157, 1092, 1036, 994, 968, 881, 782, 713, 698, 667, 504 cm^{-1}. HRMS (DART-ESI+) calcd. for $C_{31}H_{48}N_1O_2Si_1$: $[M+H]^+$: 494.3454, found: 494.3464.

C-H Activation:

General procedure for C-H activation reaction (

Table 1.7):

To a 4 mL vial, substrate (0.1 mmol), 2.2 mg $Pd(OAc)_2$ (0.1 eq., 0.01 mmol), 2.3 mg acetyl glycine (0.2 eq., 0.02 mmol), 36.0 mg AgOAc (2.0 eq., 0.2 mmol) were measured in glove box. The reaction vial was taken out from glove box and 16 μL olefin (1.5 eq., 0.15 mmol), 1.0 mL 1,2-dichloroethane were added. The reaction mixture was heated at 90 °C for 24 h

with a screw cap. The silver and palladium precipitates were removed by filtering through a short pad of celite and washed with ethyl acetate. The solvent was evaporated under reduced pressure and column chromatography on silica gel gave the product as sticky oil.

Determination of regioselectivity:

Regioselectivity was determined by ^{1}H NMR experiment based on known chemical shifts for 2-, 3-, and 4- substituted free benzyl alcohol.[46]

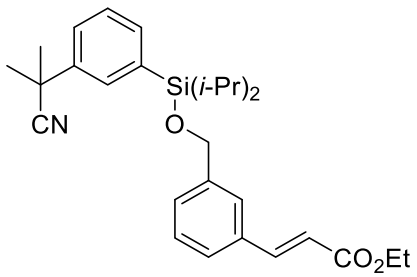

16.8 mg, 36%, o:m:p=7:81:12. ^{1}H NMR ($CDCl_3$, 500 MHz) δ 7.72 (d, *J* = 16.1 Hz, 1H), 7.63-7.66 (m, 1H), 7.58 (s, 1H), 7.51-7.55 (m, 2H), 7.38-7.48 (m, 4H), 6.46 (d, *J* = 16.1 Hz, 1H), 4.93 (s, 2H), 4.30 (q, *J* = 7.2 Hz, 2H), 1.68 (s, 6H), 1.37-1.43 (m, 2H), 1.37 (t, *J* = 7.1 Hz, 3H), 1.13 (d, *J* = 7.3 Hz, 6H), 1.08 (d, *J* = 7.3 Hz, 6H). ^{13}C NMR ($CDCl_3$, 100 MHz) δ 167.2, 144.9, 142.1, 140.9, 135.4, 134.7, 134.2, 131.1, 129.1, 128.5, 128.0, 126.9, 126.5, 125.6, 124.7, 118.6, 65.4, 60.7, 37.4, 29.3, 17.7, 17.5, 14.6, 12.3. IR: 2942, 2865, 1711, 1637, 1462, 1367, 1308, 1265, 1160, 1103, 991, 882, 792, 707, 678, 490 cm^{-1}. HRMS (DART-ESI+) calcd. for $C_{28}H_{37}N_1O_3Na_1Si_1$: $[M+H]^+$: 486.2435, found: 486.2438.

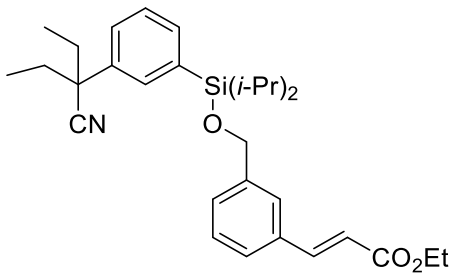

18.4 mg, 38%, o:m:p=6:88:6. ^{1}H NMR ($CDCl_3$, 500 MHz) δ 7.73 (d, *J*=16.1 Hz, 1H), 7.57 (s, 1H), 7.50 - 7.54 (m, 2H), 7.38 - 7.48 (m, 5H), 6.47 (d, *J*=16.1 Hz,

[46] Ortho: Xia, W., Shao, Y., Gui, W. & Yang, C. *Chem. Commun.* **2011,** 11098–11100. Meta: Kurita, T.; Aoki, F.; Mizumoto, T.; Maejima, T.; Esaki, H.; Maegawa, T.; Monguchi, Y.; Sajiki, H. *Chem. Eur. J.* **2008**, *14*, 3371–3379. Para: Hirono, Shuichi; Shiozawa, Shunichi. EP1445249 A1, 2004

1H), 4.93 (s, 2H), 4.30 (q, *J*=7.2 Hz, 2H), 1.94 - 2.04 (m, 2H), 1.79 - 1.86 (m, 2H), 1.34 - 1.44 (m, 2H), 1.37 (t, *J*=7.1 Hz, 3H), 1.13 (d, *J*=7.3 Hz, 6H), 1.07 (d, *J*=7.3 Hz, 6H), 0.89 (t, *J*=7.6 Hz, 6H). ^{13}C NMR ($CDCl_3$, 125 MHz) δ 167.2, 144.8, 142.1, 137.4, 134.9, 134.7, 134.0, 132.0, 129.1, 128.4, 127.9, 127.8, 126.9, 125.6, 122.5, 118.6, 65.3, 60.7, 49.9, 33.9, 17.7, 17.5, 14.5, 12.3, 9.8. IR: 2938, 2864, 1711, 1637, 1461, 1308, 1264, 1176, 1159, 1129, 1103, 1081, 1041, 991, 882, 786, 708, 674 cm^{-1}. HRMS (DART-ESI+) calcd. for $C_{30}H_{41}N_1O_3Si_1$: $[M+H]^+$: 514.2748, found: 514.2754.

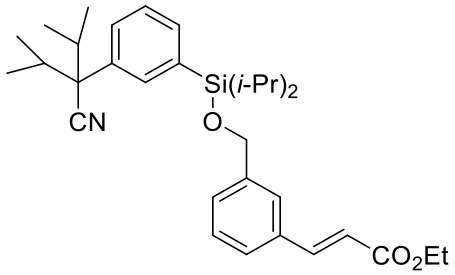

20.1 mg, 39%, o:m:p=4:90:6. ^{1}H NMR ($CDCl_3$, 500 MHz) δ 7.70 (d, *J* = 15.7 Hz, 1H), 7.56 (s, 1H), 7.46-7.51 (m, 2H), 7.41-7.46 (m, 2H), 7.41 (s, 1H), 7.34-7.40 (m, 2H), 6.44 (d, *J* = 15.7 Hz, 1H), 4.91 (s, 2H), 4.27 (q, *J* = 7.2 Hz, 2H), 2.34 (sept, *J* = 6.7 Hz, 2H), 1.30-1.43 (m, 5H), 1.10 (d, *J* = 7.3 Hz, 6H), 1.04 (d, *J* = 7.3 Hz, 6H), 0.97 (d, *J* = 6.8 Hz, 6H), 0.78 (d, *J* = 6.8 Hz, 6H). ^{13}C NMR ($CDCl_3$, 125 MHz) δ 167.2, 144.8, 142.2, 134.7, 134.0, 133.9, 133.8, 133.7, 130.0, 129.1, 127.8, 127.8, 126.9, 125.5, 122.1, 118.5, 65.2, 60.7, 58.1, 32.6, 19.0, 17.8, 17.7, 17.6, 14.6, 12.4. IR: 2966, 2941, 2865, 1713, 1638, 1463, 1369, 1308, 1264, 1176, 1160, 1102, 1082, 882, 810, 789, 712 cm^{-1}. HRMS (DART-ESI+) calcd. for $C_{32}H_{46}N_1O_3Si_1$: $[M+H]^+$: 520.3247, found: 520.3246.

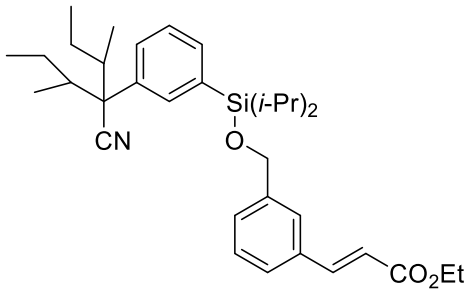

29.6 mg, 54%, o:m:p=2:96:2. ^{1}H NMR ($CDCl_3$, 500 MHz) δ 7.70 (d, *J* = 16.1 Hz, 1H), 7.55 (s, 1H), 7.47-7.51 (m, 2H), 7.42-7.47 (m, 2H), 7.41 (s, 1H), 7.32-7.40 (m, 2H), 6.44 (d, *J* = 16.1 Hz, 1H), 4.91 (s, 2H),

4.27 (q, J = 7.3 Hz, 2H), 1.98-2.19 (m, 2H), 1.65-1.82 (m, 1H), 1.19-1.43 (m, 6H), 069-1.12 (m, 26H). ^{13}C NMR ($CDCl_3$, 100 MHz) δ 167.2, 144.8, 142.2, 142.1, 134.9, 134.8, 134.8, 134.7, 134.0, 134.0, 133.9, 133.9, 133.5, 129.8, 129.1, 127.9, 127.8, 127.8, 127.8, 127.8, 126.9, 126.9, 126.9, 125.6, 125.5, 125.4, 122.6, 122.5, 122.4, 118.5, 65.3, 60.7, 58.5, 58.3, 58.0, 39.9, 39.7, 39.3, 39.2, 26.1, 25.7, 25.0, 24.4, 17.7, 17.7, 17.5, 17.5, 15.1, 14.7, 14.6, 13.8, 13.1, 12.5, 12.5, 12.4, 12.4, 12.4. IR: 2963, 2866, 1713, 1638, 1462, 1383, 1308, 1264, 1159, 1103, 992, 882, 792, 713, 681, 496 cm^{-1}. HRMS (DART-ESI+) calcd. for $C_{34}H_{50}N_1O_3Si_1$: $[M+H]^+$: 548.3560, found: 548.3567.

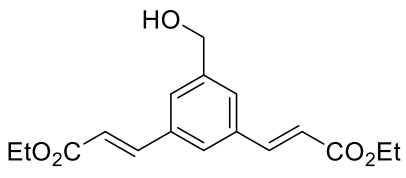

20.3 mg, 31%, mm:others=85:15 (structure and regioselectivity were confirmed after deprotection). ^{1}H NMR ($CDCl_3$, 500 MHz) δ 7.67 (d, J = 16.1 Hz, 2H), 7.56 (s, 1H), 7.54 (s, 2H), 6.48 (d, J = 16.1 Hz, 2H), 4.75 (d, J = 4.9 Hz, 2H), 4.27 (q, J = 7.0 Hz, 4H), 1.84 (t, J = 5.9 Hz, 1H), 1.34 (t, J = 7.1 Hz, 6H). ^{13}C NMR ($CDCl_3$, 125 MHz) δ 166.9, 143.7, 142.6, 135.7, 127.8, 127.1, 119.8, 64.7, 60.9, 14.5. IR: 3454, 2924, 1708, 1637, 1463, 1443, 1391, 1367, 1306, 1286, 1267, 1177, 1164, 1095, 1036, 981, 852 cm^{-1}. HRMS (DART-ESI+) calcd. for $C_{17}H_{21}O_5$: $[M+H]^+$: 305.1389, found: 305.1396.

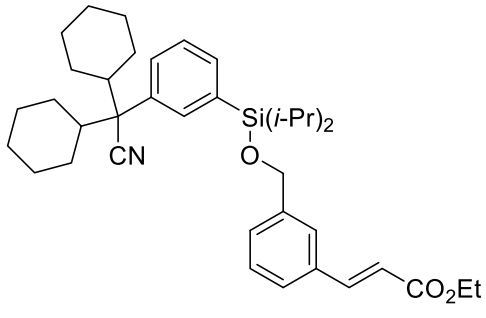

25.1 mg, 42 %, o:m:p=6:90:4. ^{1}H NMR ($CDCl_3$, 500 MHz) δ 7.70 (d, J = 16.1 Hz, 1H), 7.56 (s, 1H), 7.49 (d, J = 7.3 Hz, 1H), 7.33-7.46 (m, 6H), 6.44 (d, J = 16.1 Hz, 1H), 4.91 (s, 2H), 4.27 (q, J = 6.8 Hz, 2H), 1.96-2.04 (m, 2H), 1.88 (d, J = 12.7 Hz, 2H), 1.75 (d, J = 12.2 Hz, 2H), 1.56-1.68 (m, 4H), 1.45 (d, J = 12.2 Hz, 2H), 1.30-1.42 (m,

5H), 1.15-1.30 (m, 2H), 0.83-1.13 (m, 20H). ^{13}C NMR ($CDCl_3$, 100 MHz) δ 167.2, 144.8, 142.2, 134.8, 134.7, 133.9, 133.7, 133.4, 129.8, 129.1, 127.8, 127.7, 126.9, 125.4, 122.6, 118.6, 65.2, 60.7, 57.4, 41.9, 29.2, 27.9, 26.6, 26.3, 17.7, 17.5, 14.6, 12.4. IR: 2931, 2857, 1714, 1462, 1450, 1307, 1264, 1176, 1159, 1100, 1069, 992, 882, 806, 786, 730, 715, 667, 493 cm^{-1}. HRMS (DART-ESI+) calcd. for $C_{38}H_{54}N_1O_3Si_1$: $[M+H]^+$: 600.3873, found: 600.3858.

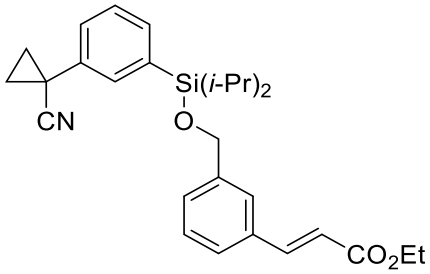

20.0 mg, 43%, o:m:p=6:81:13. ^{1}H NMR ($CDCl_3$, 500 MHz) δ 7.70 (d, *J* = 16.1 Hz, 1H), 7.54 (s, 1H), 7.43-7.49 (m, 2H), 7.32-7.43 (m, 5H), 6.44 (d, *J* = 16.1 Hz, 1H), 4.89 (s, 2H), 4.27 (q, *J* = 7.2 Hz, 2H), 1.65-1.70 (m, 2H), 1.31-1.41 (m, 5H), 1.27-1.31 (m, 2H), 1.10 (d, *J* = 7.8 Hz, 6H), 1.04 (d, *J* = 7.8 Hz, 6H). ^{13}C NMR ($CDCl_3$, 125 MHz) δ 167.2, 144.8, 142.1, 135.4, 134.8, 134.0, 131.6, 129.1, 128.5, 128.3, 128.0, 127.2, 127.0, 125.6, 122.8, 118.6, 65.4, 60.7, 18.4, 17.7, 17.5, 14.6, 14.1, 12.3. IR: 2942, 2865, 1712, 1637, 1637, 1462, 1367, 1308, 1265, 1177, 1103, 882, 787, 704 cm^{-1}. HRMS (DART-ESI+) calcd. for $C_{28}H_{36}N_1O_3Si_1$: $[M+H]^+$: 462.2464, found: 462.2454.

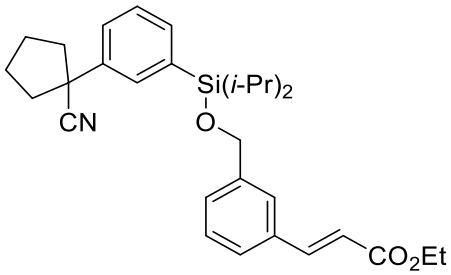

17.1 mg, 35 %, o:m:p=5:86:9. ^{1}H NMR ($CDCl_3$, 500 MHz) δ 7.70 (d, *J* = 16.1 Hz, 1H), 7.56 (d, *J* = 2.0 Hz, 1H), 7.55 (s, 1H), 7.45-7.52 (m, 2H), 7.41-7.45 (m, 1H), 7.35-7.41 (m, 3H), 6.44 (d, *J* = 16.1 Hz, 1H), 4.90 (s, 2H), 4.27 (q, *J* = 7.0 Hz, 2H), 2.33-2.46 (m, 2H), 1.90-2.06 (m, 4H), 1.79-1.90 (m, 2H), 1.29-1.42 (m, 5H), 1.11 (d, *J* = 7.3 Hz, 6H), 1.05 (d, *J* = 7.3 Hz, 6H). ^{13}C NMR ($CDCl_3$,

100 MHz) δ 167.2, 144.8, 142.1, 139.3, 135.2, 134.7, 134.1, 131.9, 129.1, 128.4, 127.9, 127.5, 126.9, 125.6, 124.6, 118.6, 65.3, 60.7, 47.9, 40.7, 24.4, 17.7, 17.5, 14.6, 12.4. IR: 2943, 2865, 1710, 1637, 1461, 1366, 1307, 1174, 1157, 1097, 1080, 886, 788, 681, 490 cm^{-1}. HRMS (DART-ESI+) calcd. for $C_{30}H_{40}N_1O_3Si_1$: $[M+H]^+$: 490.2777, found: 490.2800.

General procedure for C-H activation reaction (Table 1.8 and Table 1.9):

To a 4 mL vial, substrate (0.1 mmol), 2.2 mg $Pd(OAc)_2$ (0.1 eq., 0.01 mmol), 2.3 mg acetyl glycine (0.2 eq., 0.02 mmol), 50.0 mg AgOAc (3.0 eq., 0.3 mmol) were measured in glove box. The reaction vial was taken out from glove box and 16 μL olefin (1.5 eq., 0.15 mmol), 50 μL 1,1,1,3,3,3-hexafluoro-2-propanol, and 1.0 mL 1,2-dichloroethane were added. The reaction mixture was heated at 90 ºC for 24 h with a screw cap. The silver and palladium precipitates were removed by filtering through a short pad of Celite and washed with ethyl acetate. The solvent was evaporated under reduced pressure and column chromatography on silica gel gave the product as sticky oil.

Deprotection procedure:

After filter off solid residues, the reaction mixture was concentrated and re-dissolved in 3.0 mL tetrahydrofuran. 0.2 mL of 1.0 M tetrabutylammonium fluoride in THF was subjected and the reaction mixture was stirred for 1h at room temperature. The solvent was evaporated and purification using column chromatography on silica gel gave the product.

Determination of regioselectivity:

Structure of **1.129a′** to **1.129c′** and **1.129l′** to **1.129n′** was confirmed by 1D NOE experiments.

Structure of **1.129d** to **1.129k**, **1.129p** to **1.129r**, **1.130a** to **1.130d**, was confirmed by observation of at least 2 singlets in aromatic region (if necessary, after deprotection).

Structure of **1.129o** was determined by observation of 2 singlets in aromatic region after deprotection.

Stereochemistry of **1.130d** was confirmed by 2D NOESY experiment.

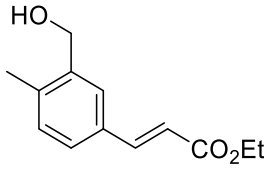

1.129a'mono

11.3 mg, 51 %, m:others=95:5 (structure and regioselectivity were confirmed after deprotection). ^{1}H NMR ($CDCl_3$, 500 MHz) δ 7.66 (d, *J* = 16.1 Hz, 1H), 7.55 (s, 1H), 7.36 (dd, *J* = 7.8, 2.0 Hz, 1H), 7.18 (d, *J* = 7.8 Hz, 1H), 6.42 (d, *J* = 16.1 Hz, 1H), 4.71 (s, 2H), 4.25 (q, *J* = 7.0 Hz, 2H), 2.36 (s, 3H), 1.45 (br. s, 1H), 1.33 (t, *J* = 7.1 Hz, 3H). ^{13}C NMR ($CDCl_3$, 100 MHz) δ 167.4, 144.7, 139.5, 138.8, 132.6, 131.1, 127.6, 127.1, 117.7, 63.4, 60.7, 18.9, 14.5. IR: 3412, 2979, 1707, 1634, 1415, 1391, 1367, 1317, 1270, 1228, 1201, 1177, 1160, 1123, 1095, 1037, 983, 819 cm^{-1}. HRMS (DART-ESI+) calcd. for $C_{13}H_{17}O_3$: $[M+H]^+$: 221.1178, found: 221.1178.

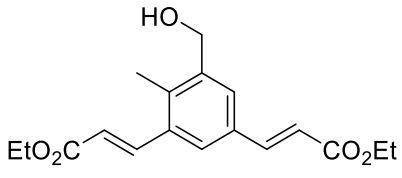

1.129a'$_{di}$

9.0 mg, 28%, mm:others=92:8 (structure and regioselectivity were confirmed after deprotection). ^{1}H NMR (acetone-d_6, 500 MHz) δ 8.01 (d, *J* = 15.7 Hz, 1H), 7.65 (d, *J* = 16.1 Hz, 1H), 7.60 (s, 2H), 6.46 (d, *J* = 15.7 Hz, 1H), 6.35 (d, *J* = 15.7 Hz, 1H), 4.75 (s, 2H), 4.21-4.32 (m, 4H), 2.40 (s, 3H), 1.79 (br. s, 1H), 1.31-1.38 (m, 6H). ^{13}C NMR ($CDCl_3$, 100 MHz) δ 167.1, 166.9, 143.9, 142.2, 140.4, 137.9, 135.3, 132.6, 128.3, 126.1, 121.3, 118.7, 63.7, 60.9, 60.8, 15.0, 14.5. IR: 3445, 2925, 1709, 1635, 1464, 1367, 1268, 1177, 1135, 1094, 1036, 981, 856 cm^{-1}. HRMS (DART-ESI+) calcd. for $C_{18}H_{23}O_5$: $[M+H]^+$: 319.1546, found: 319.1545.

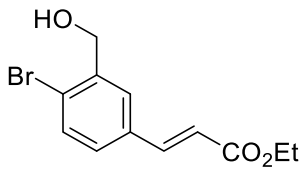

1.129b'$_{mono}$

13.0 mg, 46%, m:others=97:3 (structure and regioselectivity were confirmed after deprotection). ^{1}H NMR ($CDCl_3$, 500 MHz) δ 7.67 (d, *J* = 2.0 Hz, 1H), 7.63 (d, *J* = 16.1 Hz, 1H), 7.55 (d, *J* = 8.3 Hz, 1H), 7.30 (dd, *J* = 8.3, 2.4 Hz, 1H), 6.46 (d, *J* = 16.1 Hz, 1H), 4.77 (s, 2H), 4.26 (q, *J* = 7.3 Hz, 2H), 2.04 (br. s, 1H), 1.34 (t, *J* = 7.1 Hz, 3H). ^{13}C NMR ($CDCl_3$, 125 MHz) δ 166.9, 143.4, 140.6, 134.3, 133.3, 128.4, 128.1, 124.3, 119.5, 64.9, 60.9, 14.5. IR: 3410, 2927, 1710, 1637, 1467, 1406, 1315, 1268, 1215, 1179, 1021, 982, 864 cm^{-1}. HRMS (DART-ESI+) calcd. for $C_{12}H_{14}Br_1O_3$: $[M+H]^+$: 285.0126, found: 285.0133.

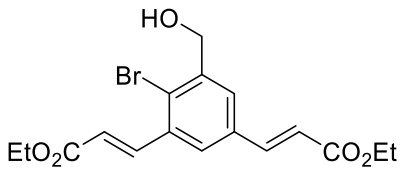

1.129b'$_{di}$

10.0 mg, 26%, mm:others=80:20 (structure and regioselectivity were confirmed after deprotection). ^{1}H NMR ($CDCl_3$, 500 MHz) δ 8.08 (d, *J* = 16.1 Hz, 1H), 7.71 (d, *J* = 2.0 Hz, 1H), 7.65 (d, *J* = 16.1 Hz, 1H), 7.61-

7.63 (m, 1H), 6.51 (d, J = 16.1 Hz, 1H), 6.40 (d, J = 16.1 Hz, 1H), 4.80 (d, J = 4.9 Hz, 2H), 4.24-4.33 (m, 4H), 2.11 (t, J = 6.1 Hz, 1H), 1.32-1.37 (m, 6H). ^{13}C NMR ($CDCl_3$, 100 MHz) δ 166.7, 166.4, 142.9, 142.7, 142.0, 136.1, 134.3, 128.4, 126.4, 126.3, 122.5, 120.2, 65.1, 61.1, 61.0, 14.5. IR: 3446, 2925, 1711, 1637, 1268, 1179, 1094, 1072, 1035, 980, 860 cm^{-1}. HRMS (DART-ESI+) calcd. for $C_{17}H_{20}Br_1O_5$: $[M+H]^+$: 383.0494, found: 383.0496.

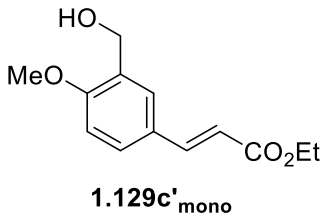

1.129c'$_{mono}$

13.5 mg, 57%, m:others=94:6 (structure and regioselectivity were confirmed after deprotection). ^{1}H NMR ($CDCl_3$, 500 MHz) δ 7.63 (d, J = 15.7 Hz, 1H), 7.51 (d, J = 2.0 Hz, 1H), 7.43 (dd, J = 8.6, 2.2 Hz, 1H), 6.88 (d, J = 8.8 Hz, 1H), 6.32 (d, J = 15.7 Hz, 1H), 4.69 (s, 2H), 4.24 (q, J = 7.3 Hz, 2H), 3.89 (s, 3H), 2.24 (br. s, 1H), 1.32 (t, J = 7.1 Hz, 3H). ^{13}C NMR ($CDCl_3$, 100 MHz) δ 167.5, 159.2, 144.3, 129.9, 129.7, 128.2, 127.4, 116.3, 110.6, 61.8, 60.6, 55.8, 14.5. IR: 3435, 2933, 1702, 1631, 1604, 1499, 1463, 1442, 1423, 1392, 1368, 1301, 1250, 1210, 1177, 1160, 1124, 1095, 982, 859, 813, cm^{-1}. HRMS (DART-ESI+) calcd. for $C_{13}H_{17}O_4$: $[M+H]^+$: 237.1127, found: 237.1131.

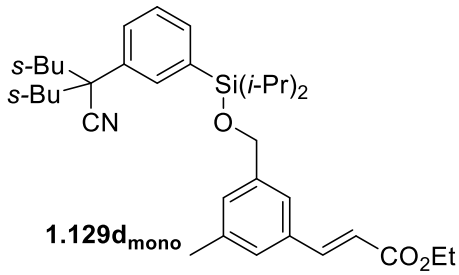

1.129d$_{mono}$

29.5 mg, 54%, m:others=95:5. ^{1}H NMR ($CDCl_3$, 600 MHz) δ 7.67 (d, J = 15.8 Hz, 1H), 7.41-7.52 (m, 3H), 7.36 (t, J = 7.6 Hz, 2H), 7.25 (s, 1H), 7.22 (s, 1H), 6.42 (d, J = 15.8 Hz, 1H), 4.87 (s, 2H), 4.26 (q, J = 7.0 Hz, 2H), 2.38 (s, 3H), 1.99-2.15 (m, 2H), 1.68-1.83 (m, 1H), 1.33 (t, J = 7.0 Hz, 3H), 1.21-1.41 (m, 3H), 0.69-1.12 (m, 26H). ^{13}C NMR (CD_3OD, 125 MHz) δ 168.7, 146.4, 146.4, 143.5, 140.2, 136.2, 136.0, 136.0, 136.0, 135.9, 135.9, 135.3, 135.1, 134.9, 130.9, 129.9, 129.9, 129.8, 128.9, 128.9, 128.9, 128.8, 128.8, 128.7, 123.9, 123.8, 123.7, 123.4,

123.3, 119.1, 119.1, 66.3, 61.8, 59.8, 59.5, 59.3, 41.0, 40.8, 40.4, 40.3, 27.3, 26.9, 26.1, 25.6, 21.6, 18.1, 18.1, 18.1, 18.1, 17.9, 15.5, 15.2, 14.8, 14.3, 13.7, 13.5, 13.5, 13.5, 12.8, 12.7, 12.5. IR: 2939, 2865, 1713, 1638, 1462, 1383, 1264, 1158, 1101, 983, 881, 848, 795, 713, 680, 495 cm^{-1}. HRMS (DART-ESI+) calcd. for $C_{35}H_{52}N_1O_3Si_1$: $[M+H]^+$: 562.3716, found: 562.3692.

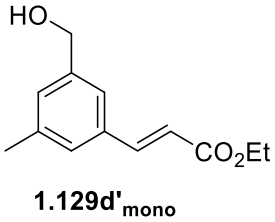

1.129d'$_{mono}$

16.5 mg, 75%, m:others=95:5. ^1H NMR ($CDCl_3$, 500 MHz) δ 7.65 (d, *J* = 16.1 Hz, 1H), 7.33 (s, 1H), 7.26 (s, 1H), 7.20 (s, 1H), 6.43 (d, *J* = 15.7 Hz, 1H), 4.68 (s, 2H), 4.25 (q, *J* = 7.3 Hz, 2H), 2.37 (s, 3H), 1.80 (br s. 1H), 1.33 (t, *J* = 7.1 Hz, 3H). ^{13}C NMR ($CDCl_3$, 125 MHz) δ 167.2, 144.7, 141.7, 139.1, 134.9, 129.8, 128.3, 123.9, 118.6, 65.2, 60.7, 21.5, 14.5. IR: 3401, 2923, 1707, 1636, 1446, 1392, 1367, 1325, 1305, 1257, 1177, 1163, 1095, 1039, 981, 848 cm^{-1}. HRMS (DART-ESI+) calcd. for $C_{13}H_{17}O_3$: $[M+H]^+$: 221.1178, found: 221.1179.

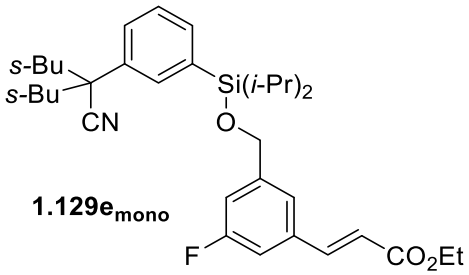

1.129e$_{mono}$

40.9 mg, 72%, mm:others=86:14. ^1H NMR ($CDCl_3$, 500 MHz) δ 7.63 (d, *J* = 16.1 Hz, 1H), 7.42-7.51 (m, 3H), 7.36 (t, *J* = 7.8 Hz, 1H), 7.28 (s, 1H), 7.16 (d, *J* = 9.3 Hz, 1H), 7.12 (d, *J* = 9.3 Hz, 1H), 6.42 (d, *J* = 16.1 Hz, 1H), 4.89 (s, 2H), 4.27 (q, *J* = 7.3 Hz, 1H), 2.01-2.19 (m, 2H), 1.70-1.77 (m, 1H), 1.21-1.44 (m, 3H), 1.34 (t, *J* = 7.3 Hz, 3H), 0.75 (m, 26H). ^{13}C NMR ($CDCl_3$, 100 MHz) δ 166.8, 164.7, 162.2, 144.8, 144.8, 143.5, 143.5, 136.8, 136.7, 135.0, 134.9, 134.9, 133.9, 133.8, 133.7, 133.6, 129.8, 127.9, 122.6, 122.5, 122.3, 121.3, 121.3, 121.3, 121.2, 121.2, 120.0, 119.9, 114.7, 114.6, 114.5, 114.4, 113.0, 113.0, 112.8, 64.7, 64.7, 60.9, 58.5,

58.3, 39.9, 39.7, 39.3, 39.3, 26.1, 25.7, 25.0, 24.4, 17.6, 17.5, 17.5, 17.5, 14.7, 15.1, 14.5, 13.8, 13.1, 12.5, 12.5, 12.4, 12.3. IR: 2940, 2866, 1715, 1641, 1592, 1462, 1368, 1272, 1177, 1099, 981, 881, 852, 795, 713, 671 cm^{-1}. HRMS (DART-ESI+) calcd. for $C_{34}H_{49}F_1N_1O_3Si_1$: $[M+H]^+$: 566.3466, found: 566.3438.

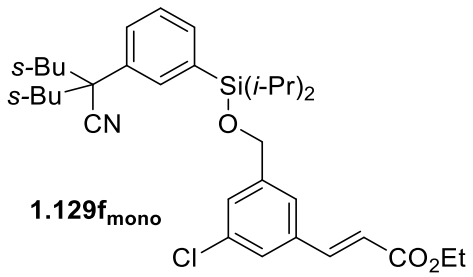

1.129f$_{mono}$

45.2 mg, 78%, mm:others=91:9. ^1H NMR ($CDCl_3$, 500 MHz) δ 7.61 (d, *J* =15.7, 1H), 7.34-7.51 (m, 7H), 6.43 (d, *J* = 15.7, 1H), 4.87 (s, 2H), 4.27 (q, *J* = 7.3, 2H), 2.03-2.19 (m, 2H), 1.70-1.80 (m, 1H), 1.25-1.42 (m, 3H), 1.34 (t, *J* = 7.1, 3H), 0.68-1.13 (m, 26H). ^{13}C NMR ($CDCl_3$, 125 MHz) δ 166.8, 144.1, 144.1, 143.2, 136.4, 135.2, 135.0, 134.9, 134.9, 133.9, 133.6, 133.6, 129.9, 128.0, 128.0, 127.5, 127.4, 126.5, 126.4, 123.7, 123.6, 122.6, 122.5, 122.3, 120.0, 64.7, 64.6, 60.9, 58.5, 58.3, 58.0, 39.9, 39.7, 39.3, 39.2, 26.1, 25.7, 25.0, 24.4, 17.7, 17.6, 17.6, 17.5, 17.5, 14.7, 15.1, 14.5, 13.8, 13.0, 12.5, 12.5, 12.3, 12.3. IR: 2962, 2940, 2866, 1714, 1640, 1575, 1462, 1367, 1267, 1176, 1096, 881, 851, 713, 671, 495 cm^{-1}. HRMS (DART-ESI+) calcd. for $C_{34}H_{48}NO_3NaSiCl$: $[M+Na]^+$: 604.2984, found: 604.2984.

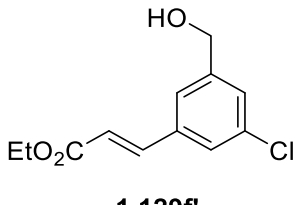

1.129f'$_{mono}$

The structure of regioisomer was confirmed after deprotection. ^1H NMR (CD_3OD, 500 MHz) δ 7.65 (d, *J* = 16.1, 1H), 7.54 (s, 1H), 7.52 (s, 1H), 7.43 (s, 1H), 6.58 (d, *J* = 16.1, 1H), 4.64 (s, 2H), 4.27 (q, *J* = 7.2, 2H), 1.35 (t, *J* = 7.3, 3H). ^{13}C NMR (CD_3OD, 125 MHz) δ 168.4, 146.3, 144.5, 137.9, 136.1, 129.5, 127.7, 125.8, 120.9, 64.2, 61.9, 14.7. IR: 3411, 2981, 2932, 2872, 1706, 1639, 1574, 1435, 1368, 1316, 1178, 1036, 979, 850,

672, 639, 593 cm^{-1}. HRMS (DART-ESI+) calcd. for $C_{12}H_{13}O_3Na_1Cl_1$: $[M+Na]^+$: 263.0445, found: 263.0454.

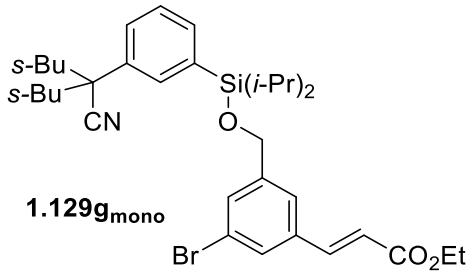

1.129g$_{mono}$

39.2 mg, 63%, m:others=91:9. ^{1}H NMR ($CDCl_3$, 500 MHz) δ 7.60 (d, *J*=15.7Hz, 1H), 7.57 (s, 1H), 7.55 (s, 1H), 7.41 - 7.50 (m, 4H), 7.37 (t, *J*=7.3 Hz, 1H), 6.42 (d, *J*=16.1 Hz, 1H), 4.87 (s, 2H), 4.27 (q, *J*=7.3 Hz, 2H), 2.01 - 2.17 (m, 2H), 1.67 - 1.80 (m, 1H), 1.34 (t, J=7.3 Hz, 3H), 1.26 - 1.43 (m, 3H), 0.72 - 1.12 (m, 26H). ^{13}C NMR ($CDCl_3$, 100 MHz) δ 166.7, 144.3, 143.1, 136.7, 135.0, 134.9, 134.9, 133.9, 133.6, 133.5, 130.4, 130.4, 130.2, 130.0, 129.4, 129.4, 129.4, 127.9, 124.1, 124.1, 124.0, 123.2, 122.6, 122.5, 122.3, 120.0, 64.6, 58.5, 58.3, 58.0, 39.9, 39.7, 39.3, 39.2, 17.6, 17.6, 17.5, 17.5, 14.5, 15.1, 14.7, 13.8, 13.1, 12.6, 12.5, 12.3, 12.3). . IR: 2963, 2939, 2866, 1715, 1639, 1461, 1383, 1367, 1312, 1267, 1177, 1113, 1096, 1040, 992, 980, 881, 796, 712, 670 cm^{-1}. HRMS (DART-ESI+) calcd. for $C_{34}H_{49}Br_1N_1O_3Si_1$: $[M+H]^+$: 626.2665, found: 626.2679.

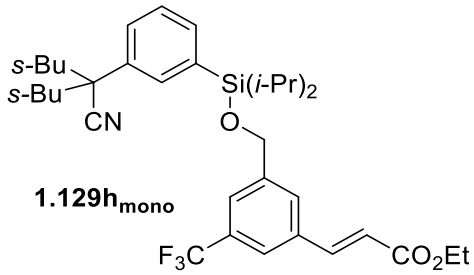

1.129h$_{mono}$

30.9 mg, 50%, m:others=97:3. ^{1}H NMR (CD_3OD, 500 MHz) δ 7.90 (s, 1H), 7.84 (s, 1H), 7.81 (s, 1H), 7.77 (d, *J* =16.1, 1H), 7.56 (d, *J* = 6.8, 2H), 7.49 (br s, 1H), 7.45 (t, *J* = 6.8, 1H), 6.64 (dt, *J* = 15.8, 1.7, 1H), 5.05 (s, 2H), 4.28 (q, *J* = 6.8, 2H), 2.02-2.22 (m, 2H), 1.68-1.80 (m, 1H), 1.25-1.50 (m, 3H), 1.35 (t, *J* = 6.8, 3H), 0.64-1.20 (m, 26H). ^{13}C NMR ($CDCl_3$, 125 MHz) δ 166.6, 143.3, 143.0, 135.6, 135.0, 134.9, 133.9, 133.6, 131.9, 131.6, 129.9, 128.4, 128.3, 127.9, 125.1, 124.1, 124.0, 123.4, 123.3, 123.0, 122.4, 122.3, 120.5, 64.7, 61.0, 58.5, 58.3, 58.0,

56.7, 39.9, 39.7, 39.3, 39.2, 26.1, 25.6, 25.0, 24.4, 17.6, 17.6, 17.6, 17.5, 17.5, 14.7, 15.1, 14.5, 13.7, 13.0, 12.5, 12.5, 12.4, 12.3. IR: 2963, 2941, 2867, 1715, 1643, 1463, 1368, 1216, 1156, 1127, 882, 795, 696, 496 cm^{-1}. HRMS (DART-ESI+) calcd. for $C_{35}H_{48}N_1O_3F_3Na_1Si_1$: $[M+Na]^+$: 638.3248, found: 638.3252.

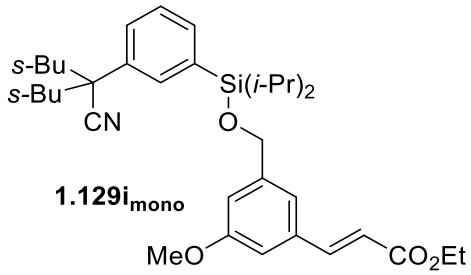

1.129i$_{mono}$

41.1 mg, 71 %, m:others=87:13. ^{1}H NMR ($CDCl_3$, 500 MHz) δ 7.65 (d, *J* = 16.1, 1H), 7.41-7.52 (m, 3H), 7.36 (t, *J* = 7.3, 1H), 7.12 (s, 1H), 7.02 (s, 1H), 6.95 (s, 1H), 6.42 (d, *J* = 16.1, 1H), 4.88 (s, 2H), 4.26 (q, *J* = 7.3, 2H), 3.84 (s, 3H), 2.00-2.17 (m, 2H), 1.69-1.79 (m, 1H), 1.20-1.42 (m, 3H), 1.34 (t, *J* = 7.1, 3H), 0.67-1.15 (m, 26H). ^{13}C NMR ($CDCl_3$, 125 MHz) δ 167.2, 160.3, 144.8, 143.7, 135.9, 134.9, 134.8, 134.8, 133.9, 133.5, 129.8, 127.8, 122.6, 122.5, 122.4, 118.8, 118.2, 118.2, 118.1, 113.7, 113.6, 113.5, 111.7, 111.6, 111.5, 65.2, 65.1, 60.7, 58.5, 58.3, 58.0, 55.5, 39.9, 39.7, 39.3, 39.2, 26.1, 25.6, 24.9, 24.4, 17.7, 17.7, 17.5, 17.5, 14.7, 15.1, 14.5, 13.7, 13.1, 12.5, 12.5, 12.4, 12.4, 12.3. IR: 2962, 2939, 2866, 1712, 1593, 1461, 1278, 1163, 1103, 882, 810, 713, 495 cm^{-1}. HRMS (DART-ESI+) calcd. for $C_{35}H_{51}N_1O_4Na_1Si_1$: $[M+Na]^+$: 600.3480 found: 600.3481.

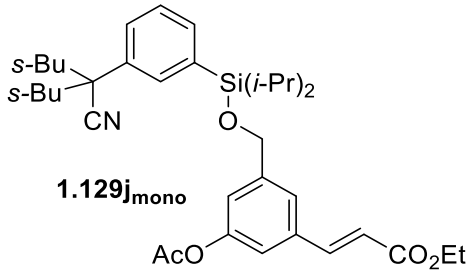

1.129j$_{mono}$

44.5 mg, 73%, m:others=78:22. ^{1}H NMR ($CDCl_3$, 500 MHz) δ 7.65 (d, *J* = 16.1 Hz, 1H), 7.40 - 7.51 (m, 3H), 7.39 (s, 1H), 7.36 (t, *J* = 7.8 Hz, 1H), 7.16 (s, 2H), 6.42 (d, *J* = 16.1 Hz, 1H), 4.89 (s, 2H), 4.26 (q, *J* = 7.3 Hz, 2H), 2.31 (s, 3H), 2.01-2.18 (m, 2H), 1.72-1.77 (m, 1H), 1.34 (t, *J* = 7.3 Hz, 3H), 1.27-1.44 (m, 3H), 0.76-1.14 (m, 26H). ^{13}C NMR ($CDCl_3$, 100 MHz) δ 169.4, 166.9,

151.4, 143.8, 143.8, 138.1, 135.0, 134.9, 134.8, 133.9, 133.8, 133.3, 129.8, 127.8, 123.0, 122.9, 122.6, 122.5, 122.4, 120.8, 120.8, 119.6, 119.5, 64.8, 60.8, 58.5, 58.3, 58.1, 39.9, 39.7, 39.3, 39.2, 26.2, 25.7, 25.0, 24.4, 21.4, 17.6, 17.6, 17.5, 17.5, 14.5, 15.1, 14.7, 13.8, 13.1, 12.5, 12.5, 12.4, 12.3. IR: 2962, 2940, 2866, 1770, 1714, 1639, 1462, 1368, 1269, 1200, 1177, 1139, 1101, 1037, 993, 881, 713 cm^{-1}. HRMS (DART-ESI+) calcd. for $C_{36}H_{52}N_1O_5Si_1$: $[M+H]^+$: 606.3615, found: 606.3614.

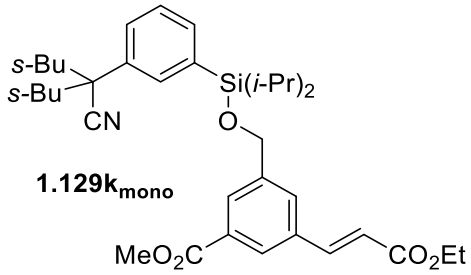

1.129k$_{mono}$

45.5 mg, 75%, m:others=91:9. ^1H NMR ($CDCl_3$, 500 MHz) δ 8.12 (s, 1H), 8.04 (s, 1H), 7.76 (s, 1H), 7.72 (d, *J* =16.1, 1H), 7.41-7.52 (m, 3H), 7.36 (t, *J* = 7.8, 1H), 6.52 (d, *J* = 16.1, 1H), 4.94 (s, 2H), 4.28 (q, *J* = 6.8, 2H), 3.94 (s, 3H), 2.01-2.18 (m, 2H), 1.69-1.80 (m, 1H), 1.20-1.42 (m, 3H), 1.34 (t, *J* = 7.1, 3H), 0.66 - 1.16 (m, 26H). ^{13}C NMR ($CDCl_3$, 125 MHz) δ 166.9, 166.7, 143.7, 142.7, 142.7, 135.2, 135.0, 134.9, 134.9, 133.9, 133.7, 131.2, 129.7, 129.6, 128.6, 128.5, 127.9, 127.8, 122.6, 122.5, 122.3, 119.9, 64.9, 60.9, 58.5, 58.3, 58.0, 52.5, 39.9, 39.7, 39.3, 39.2, 26.1, 25.7, 25.0, 24.4, 17.7, 17.7, 17.5, 17.5, 14.7, 15.1, 14.5, 13.7, 13.1, 12.5, 12.5, 12.4, 12.3. IR: 2961, 2941, 2866, 1716, 1641, 1461, 1266, 1212, 1160, 1097, 982, 795, 713, 671, 497 cm^{-1}. HRMS (DART-ESI+) calcd. for $C_{36}H_{51}N_1O_5Na_1Si_1$: $[M+Na]^+$: 628.3429, found: 628.3434.

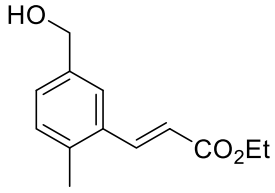

1.129l'$_{mono}$

10.1 mg, 46 %, m:others=91:9 (structure and regioselectivity were confirmed after deprotection). ^1H NMR ($CDCl_3$, 500 MHz) δ 7.96 (d, *J* = 16.1 Hz, 1H), 7.56 (d, *J* = 1.5 Hz, 1H), 7.28 (dd, *J*=7.6, 1.7 Hz, 1H), 7.20 (d, *J* = 7.3 Hz, 1H), 6.39 (d, *J* = 15.7 Hz, 1H), 4.68

(s, 2H), 4.27 (q, J = 7.0 Hz, 2H), 2.43 (s, 3H), 1.69 (br. s, 1H), 1.34 (m, J = 14.7 Hz, 3H). ^{13}C NMR ($CDCl_3$, 100 MHz) δ 167.2, 142.3, 139.1, 137.2, 133.8, 131.2, 128.8, 125.2, 119.8, 65.1, 60.7, 19.7, 14.5. IR: 3431, 2926, 1708, 1632, 1611, 1495, 1446, 1391, 1367, 1313, 1269, 1230, 1176, 1104, 1034, 980, 863, 822 cm^{-1}. HRMS (DART-ESI+) calcd. for $C_{13}H_{17}O_3$: $[M+H]^+$: 221.1178, found: 221.1177.

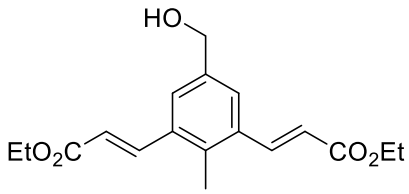

1.129l'$_{di}$

8.3 mg, 26 %, mm:others=91:9 (structure and regioselectivity were confirmed after deprotection). ^{1}H NMR ($CDCl_3$, 500 MHz) δ 8.03 (d, J = 16.1 Hz, 2H), 7.54 (s, 2H), 6.34 (d, J = 16.1 Hz, 2H), 4.70 (s, 2H), 4.27 (q, J = 7.3 Hz, 4H), 2.45 (s, 3H), 1.77 (br. s, 1H), 1.34 (t, J = 7.3 Hz, 6H). ^{13}C NMR ($CDCl_3$, 125 MHz) δ 166.9, 142.5, 139.1, 136.0, 135.3, 126.9, 121.3, 64.8, 60.9, 14.5. IR: 3469, 2924, 1709, 1629, 1449, 1391, 1367, 1311, 1264, 1174, 1095, 1068, 1031, 978, 929, 860 cm^{-1}. HRMS (DART-ESI+) calcd. for $C_{18}H_{23}O_5$: $[M+H]^+$: 319.1546, found: 319.1545.

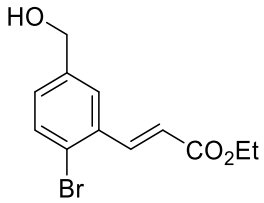

1.129m'$_{mono}$

10.5 mg, 37%, m:others=84:16 (structure and regioselectivity were confirmed after deprotection). ^{1}H NMR ($CDCl_3$, 500 MHz) δ 8.03 (d, J = 16.1 Hz, 1H), 7.61 (d, J = 2.4 Hz, 1H), 7.59 (d, J = 8.3 Hz, 1H), 7.22 (dd, J = 8.3, 2.4 Hz, 1H), 6.41 (d, J = 16.1 Hz, 1H), 4.68 (s, 2H), 4.28 (q, J = 7.2 Hz, 2H), 1.87 (br. s, 1H), 1.34 (t, J = 7.2 Hz, 1H). ^{13}C NMR ($CDCl_3$, 100 MHz) δ 166.6, 143.0, 140.8, 134.8, 133.7, 129.8, 126.2, 124.4, 121.6, 64.5, 61.0, 14.5. IR: 3432, 2926, 1711, 1635, 1465, 1315, 1270, 1180, 1025, 980, 820 cm^{-1}. HRMS (DART-ESI+) calcd. for $C_{12}H_{14}Br_1O_3$: $[M+H]^+$: 285.0126, found: 285.0127.

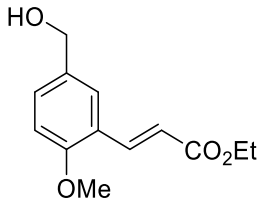

1.129n'mono

12.0 mg, 51%, m:others=98:2 (structure and regioselectivity were confirmed after deprotection). ^{1}H NMR ($CDCl_3$, 500 MHz) δ 7.96 (d, J = 16.1 Hz, 1H), 7.50 (d, J = 2.0 Hz, 1H), 7.34 (dd, J = 8.3, 2.0 Hz, 1H), 6.90 (d, J = 8.3 Hz, 1H), 6.53 (d, J = 16.1 Hz, 1H), 4.63 (s, 2H), 4.25 (q, J = 7.6 Hz, 2H), 3.88 (s, 3H), 1.79 (br. s, 1H), 1.33 (t, J = 7.6 Hz, 3H). ^{13}C NMR ($CDCl_3$, 100 MHz) δ 167.7, 158.1, 139.9, 133.3, 130.5, 128.0, 123.6, 119.3, 111.5, 64.9, 60.6, 55.9, 14.6. IR: 3399, 2932, 1701, 1628, 1497, 1463, 1367, 1310, 1269, 1247, 1159, 1115, 1095, 1026, 985, 862, 813 cm^{-1}. HRMS (DART-ESI+) calcd. for $C_{13}H_{17}O_4$: $[M+H]^+$: 237.1127, found: 237.1131.

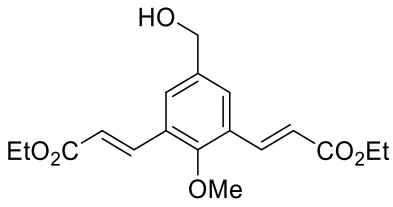

1.129n'di

2.0 mg, 9%, mm:others=78:22 (structure and regioselectivity were confirmed after deprotection). ^{1}H NMR ($CDCl_3$, 500 MHz) δ 8.02 (d, J = 16.1 Hz, 2H), 7.54 (s, 2H), 6.35 (d, J = 16.1 Hz, 2H), 4.70 (s, 2H), 4.28 (q, J = 7.3 Hz, 4H), 2.45 (s, 3H), 1.77 (br. s, 1H), 1.34 (t, J = 7.3 Hz, 6H). ^{13}C NMR ($CDCl_3$, 125 MHz) δ 167.1, 157.7, 138.7, 137.4, 129.2, 128.2, 120.8, 64.6, 63.4, 60.9, 29.9, 14.5. IR: 3434, 2924, 2852, 1712, 1633, 1466, 1426, 1391, 1368, 1312, 1261, 1219, 1176, 1096, 1038, 996, 863 cm^{-1}. HRMS (DART-ESI+) calcd. for $C_{18}H_{23}O_6$: $[M+H]^+$: 335.1495, found: 335.1496.

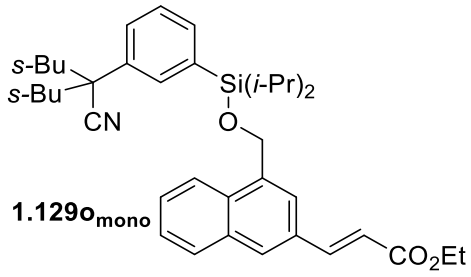

1.129omono

(structure and regioselectivity were confirmed after deprotection). ^{1}H NMR ($CDCl_3$, 500 MHz) δ 7.82-8.01 (m, 5H), 7.41-7.57 (m, 5H), 7.36 (t, J = 7.3, 1H), 6.56 (dd, J = 16.1, 1.5, 1H), 5.35 (s, 2H), 4.30

(q, J = 7.2, 2H), 1.90-2.09 (m, 2H), 1.64-1.74 (m, 1H), 1.39-1.49 (m, 2H), 1.36 (t, J = 6.8, 3H), 0.60-1.20 (m, 26H). ^{13}C NMR ($CDCl_3$, 125 MHz) δ 167.3, 145.0, 137.5, 135.0, 134.9, 134.8, 133.9, 133.9, 133.8, 133.7, 133.7, 133.7, 133.4, 131.8, 131.6, 131.6, 131.5, 129.9, 129.7, 129.7, 129.6, 127.9, 127.8, 127.5, 126.7, 123.2, 123.1, 123.0, 122.6, 122.5, 122.4, 121.1, 121.0, 121.0, 118.6, 63.9, 63.8, 60.7, 58.5, 58.2, 58.0, 39.7, 39.6, 39.2, 39.2, 26.0, 25.6, 24.8, 24.3, 17.8, 17.7, 17.7, 17.6, 17.6, 14.7, 15.0, 14.6, 13.6, 13.1, 12.5, 12.5, 12.5, 12.4, 12.2. IR: 2962, 2939, 2866, 1711, 1635, 1462, 1306, 1265, 1174, 1114, 883, 750, 713, 595, 497 cm^{-1}. HRMS (DART-ESI+) calcd. for $C_{38}H_{51}N_1O_3Na_1Si_1$: $[M+Na]^+$: 620.3530, found: 620.3536.

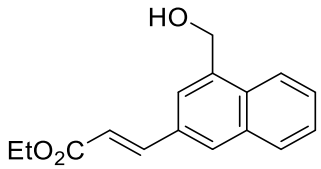

1.129o'$_{mono}$

13.7 mg, 53%, 3:others=96:4. ^{1}H NMR ($CDCl_3$, 500 MHz) δ 8.06 (d, J = 8.3, 1H), 7.87 (d, J = 7.8, 1H), 7.85 (s, 1H), 7.81 (d, J = 16.1, 1H), 7.72 (s, 1H), 7.49-7.61 (m, 2H), 6.55 (d, J = 16.1, 1H), 5.15 (s, 2H), 4.27 (q, J = 7.3, 2H), 2.08 (br s, 1H), 1.35 (t, J = 7.3, 3H). ^{13}C NMR ($CDCl_3$, 125 MHz) δ 167.3, 144.6, 137.4, 133.9, 132.2, 131.7, 130.5, 129.6, 127.8, 126.9, 123.8, 122.7, 118.8, 63.7, 60.8, 14.6 IR: 3426, 2980, 2938, 1706, 1634, 1368, 1308, 1268, 1177, 1038, 980, 853, 751, 617 cm^{-1}. HRMS (DART-ESI+) calcd. for $C_{16}H_{16}O_3Na_1$: $[M+Na]^+$: 279.0992, found: 279.0993.

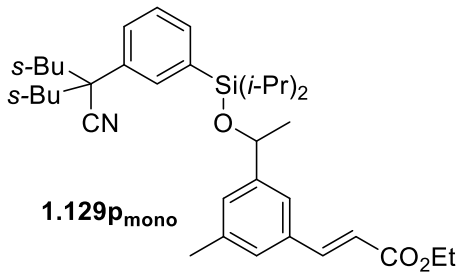

1.129p$_{mono}$

43.3 mg, 75%, m:others=97:3. ^{1}H NMR ($CDCl_3$, 500 MHz) δ 7.66 (d, J = 16.1 Hz, 1H), 7.39-7.49 (m, 3H), 7.34 (s, 1H), 7.32 (t, J = 7.8 Hz, 1H), 7.23 (s, 1H), 7.20 (s, 1H), 6.42 (d, J = 16.1 Hz, 1H), 4.94-5.03 (m, 1H), 4.26 (q, J = 7.2 Hz, 2H), 2.36 (s, 3H), 2.00-2.18 (m, 2H), 1.70-1.82 (m, 1H), 1.50 (d,

J = 6.4 Hz, 3H), 1.33 (t, J = 7.3 Hz, 3H), 1.22-1.42 (m, 3H), 0.76-1.07 (m, 26H). ^{13}C NMR ($CDCl_3$, 100 MHz) δ 167.3, 147.7, 145.1, 138.6, 138.6, 134.7, 134.7, 134.7, 134.6, 134.6, 134.6, 134.5, 134.3, 133.9, 133.9, 133.9, 133.6, 129.5, 128.3, 128.3, 128.3, 127.8, 127.6, 127.6, 127.6, 122.7, 122.6, 122.5, 122.4, 122.4, 118.2, 71.5, 71.5, 71.4, 60.6, 58.5, 58.3, 58.2, 58.0, 40.0, 39.9, 39.7, 39.7, 39.4, 39.3, 39.2, 39.2, 28.0, 26.2, 26.2, 25.7, 25.6, 25.1, 25.0, 24.4, 21.6, 17.6, 17.5, 17.5, 17.5, 17.4, 17.4, 17.4, 14.5, 15.1, 14.7, 13.8, 13.8, 13.0, 12.6, 12.6, 12.5, 12.5, 12.4, 12.4, 12.4, 12.4, 12.4, 12.3. IR: 2964, 2939, 1713, 1462, 1265, 1160, 1109, 1044, 981, 881, 853, 775, 712, 693, 679, 503 cm^{-1}. HRMS (DART-ESI+) calcd. for $C_{36}H_{54}N_1O_3Si_1$: $[M+H]^+$: 576.3873, found: 576.3860.

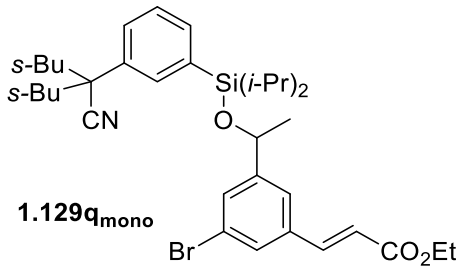

1.129q$_{mono}$

38.5 mg, 60%, m:others=92:8. ^{1}H NMR ($CDCl_3$, 500 MHz) δ 7.59 (d, J = 15.7 Hz, 1H), 7.55 (s, 1H), 7.53 (s, 1H), 7.37-7.49 (m, 4H), 7.33 (t, J = 7.3 Hz, 1H), 6.42 (d, J = 16.1 Hz, 1H), 4.91-5.02 (m, 1H), 4.26 (q, J = 6.8 Hz, 2H), 2.00-2.21 (m, 2H), 1.68-1.83 (m, 1H), 1.49 (d, J = 6.4 Hz, 3H), 1.22-1.45 (m, 6H), 0.74 (m, 26H). ^{13}C NMR ($CDCl_3$, 100 MHz) δ 166.7, 149.9, 143.2, 136.7, 136.7, 134.9, 134.8, 134.7, 134.3, 134.3, 134.3, 133.9, 133.9, 133.9, 133.6, 130.2, 130.1, 129.6, 129.4, 129.4, 127.7, 123.9, 123.8, 123.8, 123.1, 122.6, 122.5, 122.4, 120.0, 71.0, 70.9, 70.9, 60.9, 58.5, 58.3, 58.3, 58.1, 40.0, 39.9, 39.7, 39.7, 39.4, 39.3, 39.2, 39.2, 27.8, 26.2, 26.2, 25.7, 25.7, 25.1, 25.0, 24.4, 17.6, 17.6, 17.5, 17.4, 17.4, 17.4, 14.5, 15.2, 14.7, 13.8, 13.8, 13.1, 13.1, 12.6, 12.6, 12.5, 12.5, 12.5, 12.4, 12.4. IR: 2964, 2939, 2866, 1715, 1462, 1311, 1266, 1225, 1176, 1163, 1120, 1094, 1038, 993, 980, 881, 712, 684 cm^{-1}. HRMS (DART-ESI+) calcd. for $C_{35}H_{51}Br_1N_1O_3Si_1$: $[M+H]^+$: 640.2822, found: 640.2790.

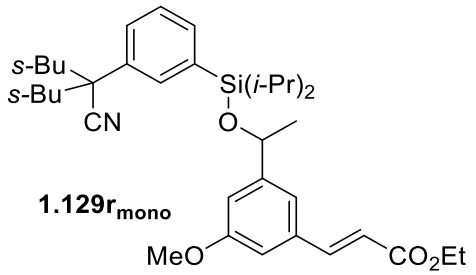

1.129r$_{mono}$

45.4 mg, 77%, m:others=91:9. ^{1}H NMR ($CDCl_3$, 500 MHz) δ 7.64 (d, *J*=16.1 Hz, 1H), 7.36 - 7.52 (m, 3H), 7.32 (t, *J*=7.3 Hz, 1H), 7.10 (s, 1H), 6.98 - 7.03 (m, 1H), 6.92 - 6.95 (m, 1H), 6.38 - 6.44 (m, 1H), 4.94 - 5.04 (m, 1H), 4.26 (q, *J*=7.3 Hz, 2H), 3.83 (s, 3H), 1.99 - 2.17 (m, 2H), 1.70 - 1.77 (m, 1H), 1.50 (d, *J*=6.4 Hz, 3H), 1.20 - 1.43 (m, 6H), 0.72 - 1.07 (m, 26H). ^{13}C NMR ($CDCl_3$, 100 MHz) δ 167.1, 160.2, 160.2, 160.2, 149.4, 149.4, 144.8, 135.8, 135.8, 134.8, 134.7, 134.6, 134.6, 134.6, 133.9, 133.9, 133.6, 129.6, 127.6, 127.6, 122.7, 122.6, 122.4, 118.7, 118.1, 118.0, 117.9, 113.5, 113.4, 113.4, 113.2, 111.6, 111.5, 111.5, 111.4, 71.4, 71.4, 71.3, 60.7, 58.5, 58.2, 58.1, 55.5, 40.0, 39.9, 39.7, 39.7, 39.3, 39.2, 39.2, 27.9, 26.2, 26.1, 25.7, 25.6, 25.0, 25.0, 24.4, 24.4, 17.6, 17.6, 17.5, 17.4, 17.4, 17.4, 15.1, 15.1, 14.7, 14.5, 13.8, 13.1, 13.0, 12.6, 12.5, 12.5, 12.5, 12.5, 12.4, 12.4, 12.4, 12.4, 12.3. IR: 2964, 2939, 2866, 1715, 1592, 1461, 1276, 1162, 1108, 1093, 1061, 1040, 992, 982 cm^{-1}. HRMS (DART-ESI+) calcd. for $C_{36}H_{54}N_1O_4Si_1$: $[M+H]^+$: 592.3822, found: 592.3795.

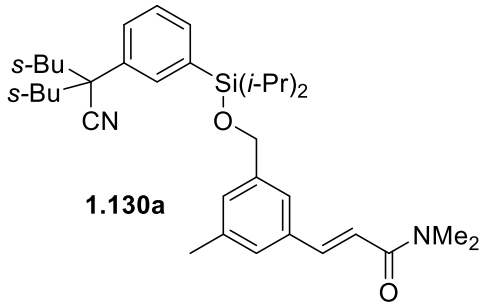

1.130a

33.3 mg, 62%, mm:others=98:2. ^{1}H NMR ($CDCl_3$, 500 MHz) δ 7.65 (d, *J*=15.7 Hz, 1H), 7.41 - 7.51 (m, 3H), 7.38 (s, 1H), 7.35 (t, *J*=7.8 Hz, 1H), 7.24 (s, 1H), 7.17 (s, 1H), 6.89 (d, *J*=15.7 Hz, 1H), 4.88 (s, 2H), 3.16 (s, 3H), 3.06 (s, 3H), 2.37 (s, 3H), 1.97 - 2.17 (m, 2H), 1.62 - 1.82 (m, 1H), 1.19 - 1.43 (m, 3H), 0.75 - 1.14 (m, 26H). ^{13}C NMR ($CDCl_3$, 125 MHz) δ 166.9, 142.7, 141.9, 138.6, 135.6, 134.8, 134.7, 134.0, 133.9, 133.9, 133.6, 129.7, 127.9, 127.8, 127.8, 127.5, 127.4, 127.4, 122.6, 122.5, 122.4, 122.4,

122.2, 117.4, 117.4, 65.3, 65.3, 65.2, 58.5, 58.2, 58.0, 39.9, 39.7, 39.3, 39.2, 37.6, 36.1, 26.1, 25.6, 25.0, 24.4, 21.6, 17.7, 17.7, 17.5, 17.5, 15.1, 14.7, 13.8, 13.1, 12.5, 12.5, 12.4, 12.4, 12.4, 12.3. IR: 2938, 2865, 1653, 1613, 1462, 1392, 1261, 1104, 980, 882, 841, 796, 713, 679, 605 cm^{-1}. HRMS (DART-ESI+) calcd. for $C_{35}H_{53}N_2O_2Si_1$: $[M+H]^+$: 561.3871, found: 561.3863.

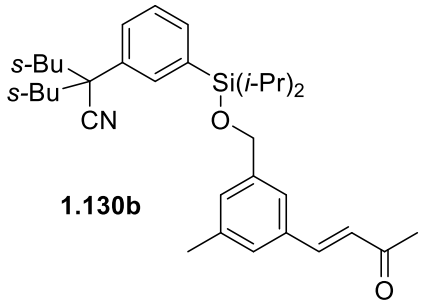

1.130b

33.7 mg, 63%, m:others=92:8. ^1H NMR ($CDCl_3$, 500 MHz) δ 7.46-7.55 (m, 3H), 7.43 (br. s, 1H), 7.39 (s, 1H), 7.36 (t, *J* = 7.3. Hz, 1H), 7.27 (s, 1H), 7.23 (s, 1H), 6.71 (d, *J* = 16.1 Hz, 1H), 4.88 (s, 2H), 2.39 (s, 3H), 2.38 (s, 3H), 1.98-2.17 (m, 2H), 1.70-1.78 (m, 1H), 1.24-1.44 (m, 4H), 0.76-1.14 (m, 25H). ^{13}C NMR ($CDCl_3$, 125 MHz) δ 198.6, 143.9, 142.2, 142.2, 138.9, 134.9, 134.8, 134.8, 134.7, 134.0, 134.0, 133.9, 133.9, 133.7, 129.7, 129.0, 128.9, 127.8, 127.8, 127.8, 127.7, 127.2, 123.2, 123.1, 123.0, 122.6, 122.5, 122.4, 65.3, 65.2, 58.5, 58.3, 58.0, 39.9, 39.7, 39.3, 39.2, 27.7, 26.1, 25.7, 25.0, 24.4, 21.6, 17.7, 17.7, 17.5, 17.5, 15.1, 14.7, 13.8, 13.1, 12.6, 12.5, 12.4, 12.4. IR: 2939, 2865, 1669, 1613, 1461, 1382, 1254, 1156, 1103, 992, 882, 795, 713, 681, 597, 496 cm^{-1}. HRMS (DART-ESI+) calcd. for $C_{34}H_{50}N_1O_2Si_1$: $[M+H]^+$: 532.3611, found: 532.3610.

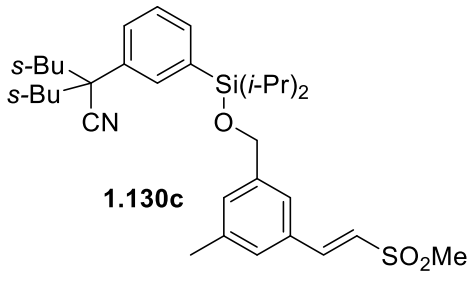

1.130c

33.2 mg, 58%, m:others=94:6. ^1H NMR ($CDCl_3$, 500 MHz) δ 7.61 (d, *J* = 15.2 Hz, 1H), 7.53 (br. s, 1H), 7.48 (d, *J* = 6.8 Hz, 1H), 7.42 (d, *J*=6.4 Hz, 1H), 7.32-7.39 (m, 2H), 7.27 (s, 1H), 7.23 (s, 1H), 6.91 (d, *J* = 15.2 Hz, 1H), 4.87 (s, 2H), 3.03 (s, 3H), 2.39 (s, 3H), 2.00-2.19 (m, 2H), 1.57-

1.80 (m, 1H), 1.20-1.43 (m, 3H), 0.77-1.12 (m, 26H). ^{13}C NMR ($CDCl_3$, 125 MHz) δ 144.4, 142.4, 139.1, 134.9, 134.8, 134.8, 133.9, 133.9, 133.9, 133.8, 132.4, 129.8, 129.8, 129.7, 129.5, 128.1, 128.1, 128.1, 127.8, 126.2, 123.4, 123.3, 123.2, 122.5, 122.3, 65.1, 65.1, 58.5, 58.2, 58.0, 43.5, 39.9, 39.7, 39.3, 39.2, 26.1, 25.6, 25.0, 24.4, 21.5, 17.7, 17.7, 17.5, 17.5, 15.1, 14.7, 13.8, 13.1, 12.5, 12.5, 12.4, 12.3. IR: 2938, 1462, 1310, 1134, 966, 882, 798, 713, 501 cm^{-1}. HRMS (DART-ESI+) calcd. for $C_{33}H_{50}N_1O_3S_1Si_1$: $[M+H]^+$: 568.3281, found: 568.3275.

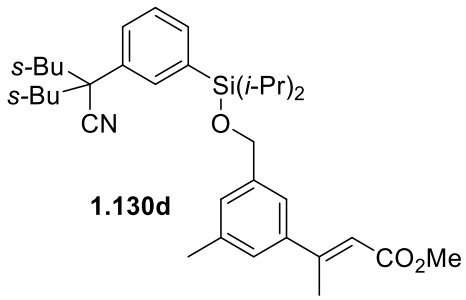

1.130d

36.4 mg, 65%, m:others=97:3. ^{1}H NMR ($CDCl_3$, 500 MHz) δ 7.48-7.56 (m, 2H), 7.46 (d, J = 6.8 Hz, 1H), 7.36 (t, J = 7.3 Hz, 1H), 7.31 (s, 1H), 7.21 (s, 1H), 7.19 (s, 1H), 6.14 (s, 1H), 4.89 (s, 2H), 3.75 (s, 3H), 2.58 (s, 3H), 2.39 (s, 3H), 2.01-2.18 (m, 2H), 1.69-1.79 (m, 1H), 1.26-1.45 (m, 3H), 0.77-1.13 (m, 26H). ^{13}C NMR ($CDCl_3$, 125 MHz) δ 167.5, 156.4, 156.3, 156.3, 142.5, 142.4, 142.4, 141.6, 141.6, 138.4, 138.4, 134.9, 134.8, 134.7, 134.0, 134.0, 133.9, 133.4, 129.7, 127.8, 127.8, 127.4, 127.3, 125.9, 122.6, 122.5, 122.3, 121.1, 121.0, 116.7, 116.7, 65.4, 65.4, 58.5, 58.3, 58.0, 51.3, 39.9, 39.7, 39.3, 39.2, 26.1, 25.7, 25.0, 24.4, 21.7, 21.7, 18.3, 18.2, 17.7, 17.7, 17.5, 17.5, 15.1, 14.7, 13.8, 13.1, 12.5, 12.5, 12.4, 12.4, 12.4, 12.3. IR: 2941, 2865, 1717, 1628, 1462, 1382, 1214, 1161, 1109, 881, 796, 713 cm^{-1}. HRMS (DART-ESI+) calcd. for $C_{35}H_{52}N_1O_3Si_1$: $[M+H]^+$: 562.3716, found: 562.3729.

Hydrolytic deprotection of directing group:

To a stirred mixture of **1.129d** (28 mg, 0.05 mmol) in 2 mL of wet ethanol (ethanol:water=3:1) was added 0.1 equiv *para*-toluenesulfonic acid at room temperature. After heating at 90 ºC for 12 h, the mixture was diluted with ethyl acetate and dried over anhydrous magnesium sulfate. The solvent was evaporated under reduced pressure and column chromatography on silica gel gave the alcohol **1.129d′** (9.2 mg, 83%) and silanol **1.132** (15.0 mg, 83%).

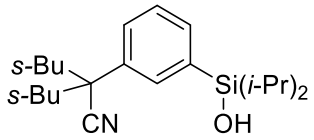

1.132

15.0 mg, 83%. ^{1}H NMR ($CDCl_3$, 500 MHz) δ 7.44-7.56 (m, 2H), 7.37-7.44 (m, 1H), 7.34 (t, J = 7.3 Hz, 1H), 2.06-2.27 (m, 2H), 2.03 (s, 1H), 1.71-1.85 (m, 1H), 1.29-1.51 (m, 1H), 1.13-1.28 (m, 2H), 0.74-1.09 (m, 26H). ^{13}C NMR ($CDCl_3$, 125 MHz) δ 135.4, 134.5, 134.4, 134.3, 133.3, 133.3, 133.2, 133.1, 129.1, 127.4, 127.4, 122.5, 122.4, 122.2, 58.3, 58.1, 57.8, 39.8, 39.5, 39.2, 39.1, 25.9, 25.5, 24.8, 24.2, 17.1, 16.9, 14.9, 14.5, 13.6, 12.9, 12.4, 12.4, 12.4, 12.3. IR: 3482, 2939, 2864, 1462, 1384, 1123, 993, 882, 838, 793, 747, 712, 667, 613, 494 cm^{-1}. HRMS (DART-ESI+) calcd. for $C_{22}H_{38}N_1O_1Si_1$: $[M+H]^+$: 360.2723, found: 360.2739.

1.6.3 Spectral Data

HO
HO
4
3
2
OTBS
OTES
O
OMe
8
7
6
5
4
3
2
1
-0
ppm

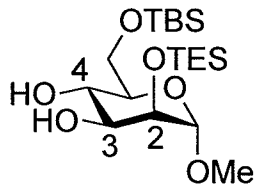
OTBS
OTES
4
HO
HO
3
2
O
OMe

133
220
200
180
160
140
120
100
80
60
40
20
0
ppm

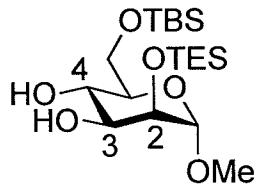
OTBS
OTES
4
HO
O
HO
3
2
OMe

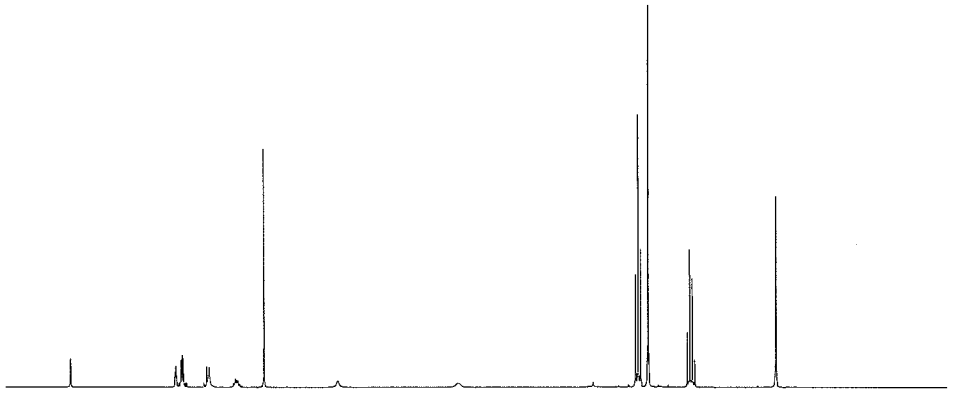

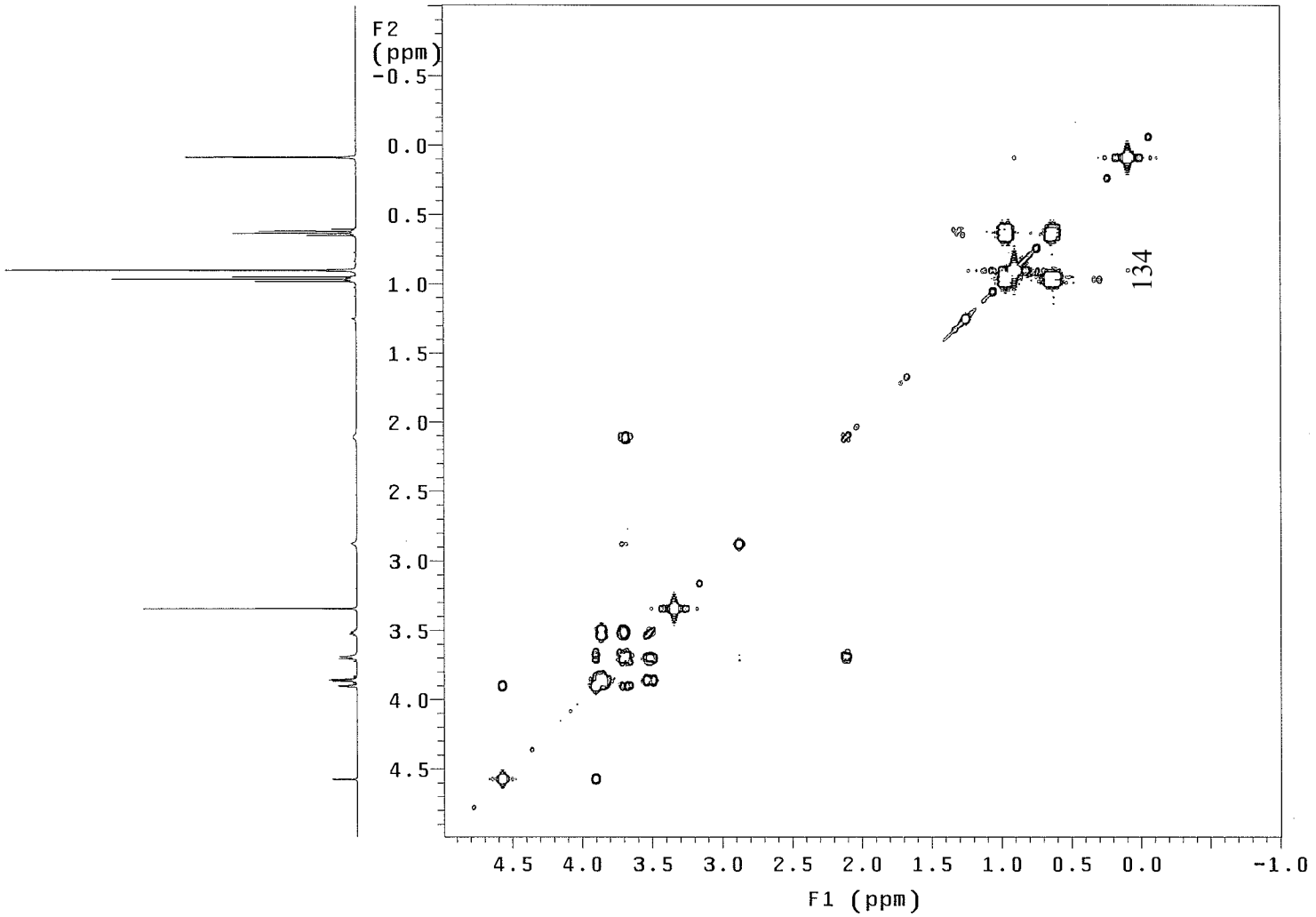
F2
(ppm)
-0.5
0.0
0.5
1.0
1.5
2.0
2.5
3.0
3.5
4.0
4.5
134
4.5
4.0
3.5
3.0
2.5
2.0
1.5
1.0
0.5
0.0
-1.0
F1 (ppm)

OTBS
OH
O
OMe
HO
TESO
4
3
2
8
7
6
5
4
3
2
1
-0
ppm

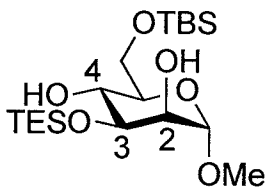
OTBS
OH
4
HO
O
TESO
3
2
OMe

136
220
200
180
160
140
120
100
80
60
40
20
0 ppm

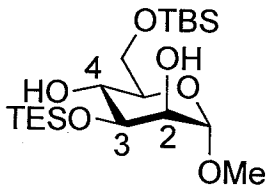
OTBS
OH
4
HO
O
TESO
3
2
OMe

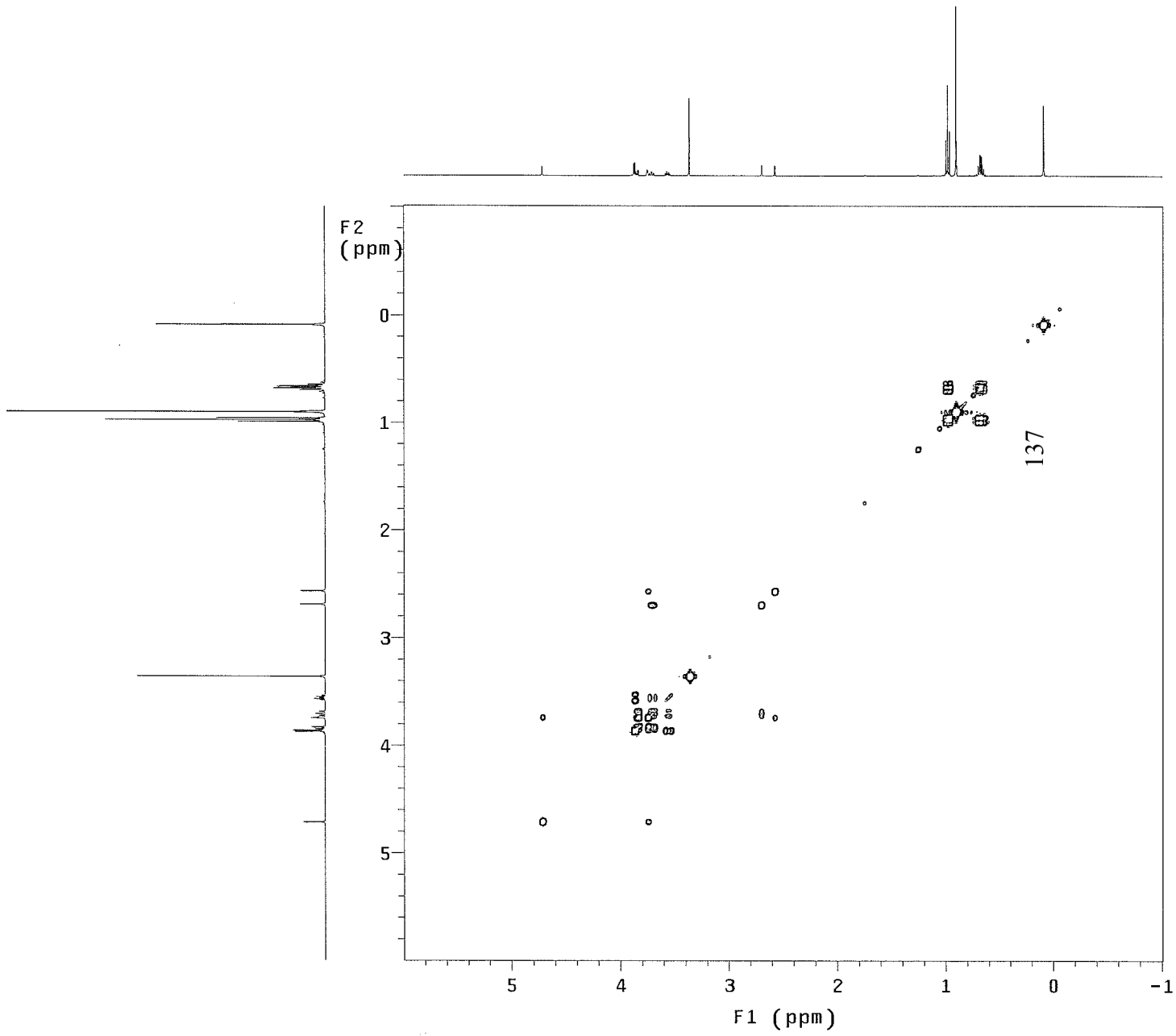
F2
(ppm)
0
1
2
3
4
5
137
5
4
3
2
1
0
-1
F1 (ppm)

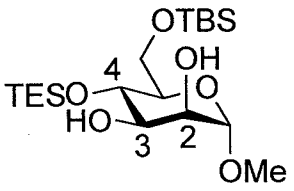
OTBS
OH
4
TESO
O
HO
3
2
OMe

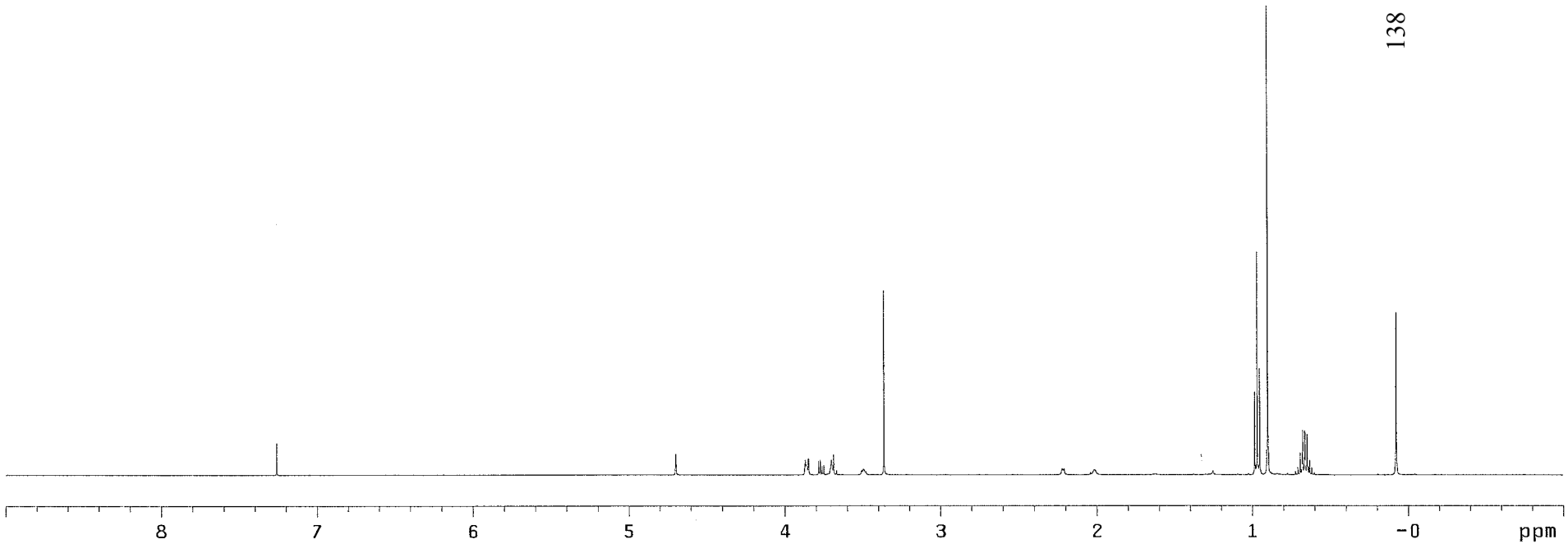
138
8
7
6
5
4
3
2
1
-0
ppm

TESO
HO
4
3
2
OTBS
OH
O
OMe
220
200
180
160
140
120
100
80
60
40
20
0
ppm

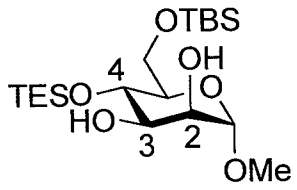
OTBS
OH
4
TESO
O
HO
3
2
OMe

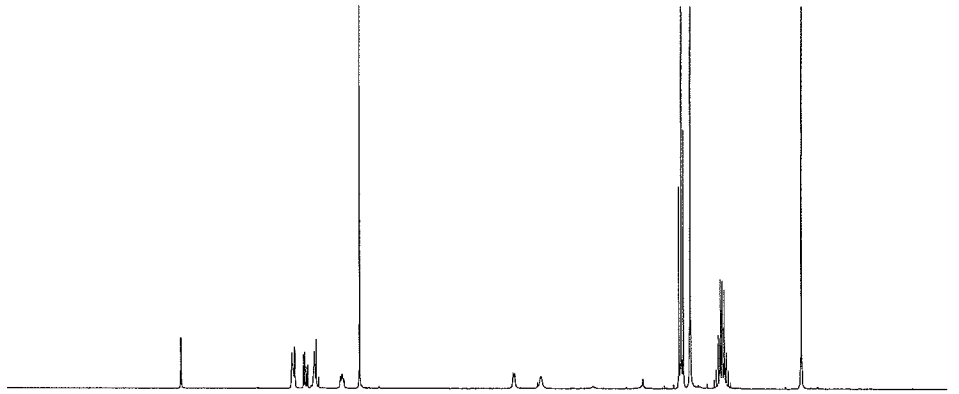

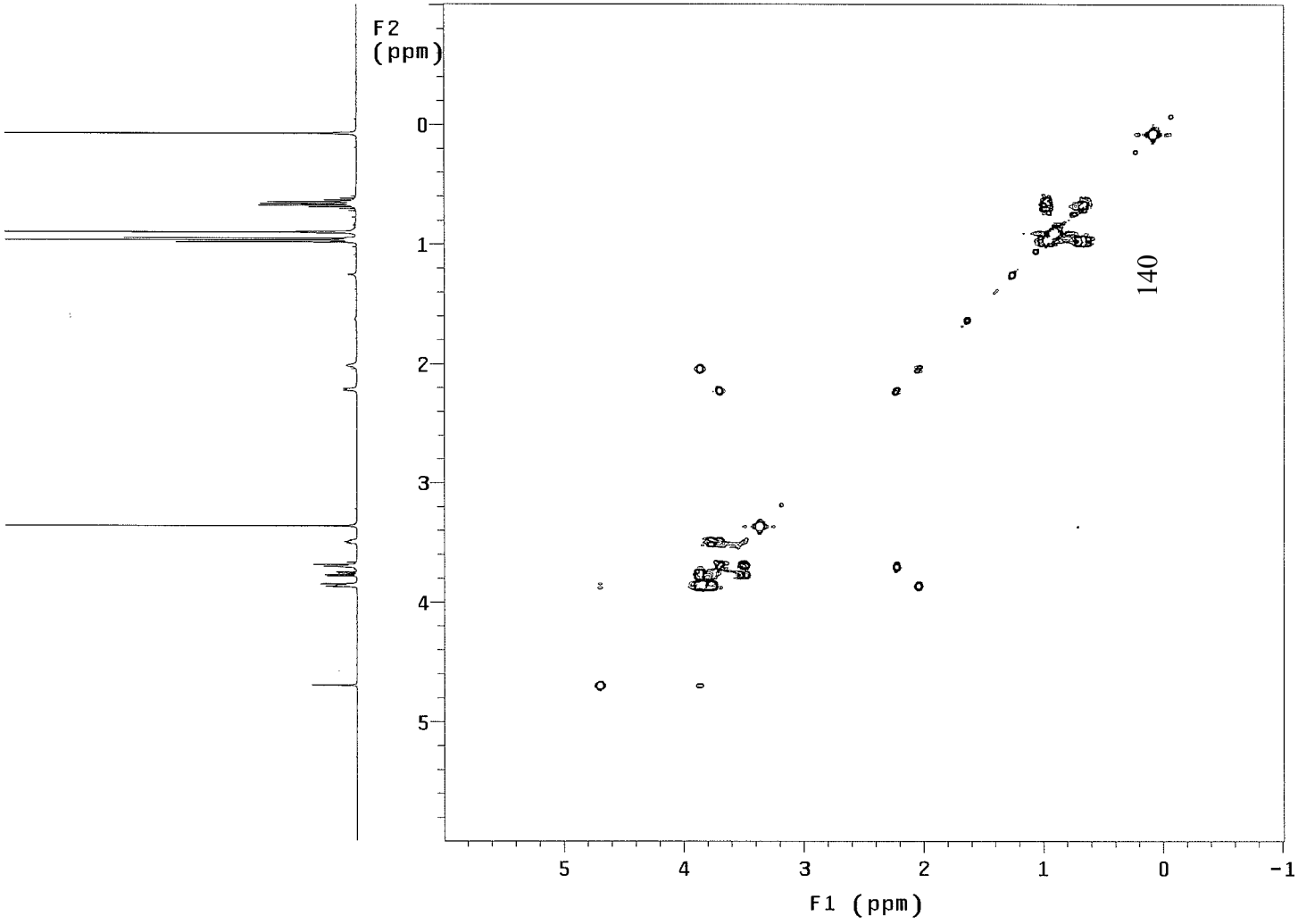
F2
(ppm)
0
1
2
3
4
5
140
5
4
3
2
1
0
-1
F1 (ppm)

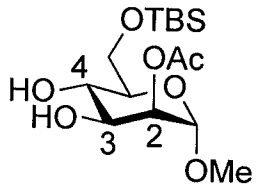
OTBS
OAc
4
HO
O
HO
3
2
OMe

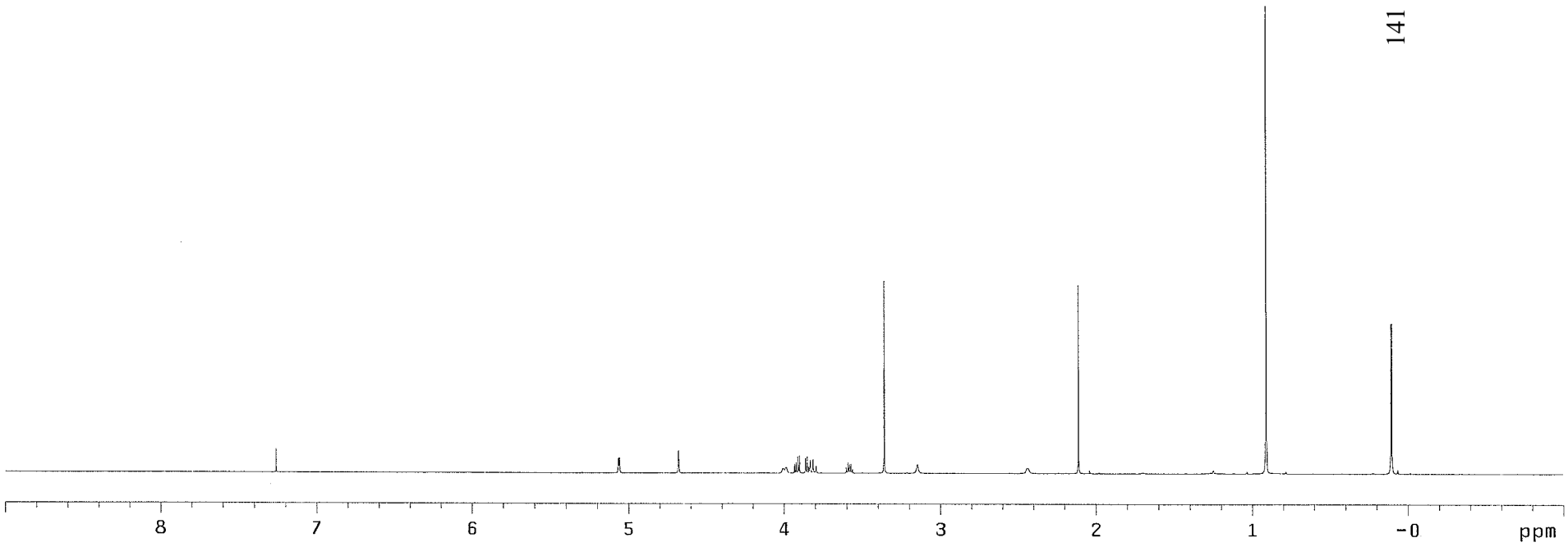
141
8
7
6
5
4
3
2
1
-0
ppm

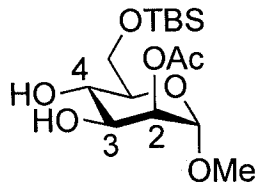

142

220 200 180 160 140 120 100 80 60 40 20 0 ppm

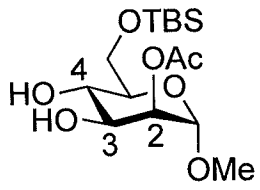
OTBS
OAc
4
HO
HO
3
2
O
OMe

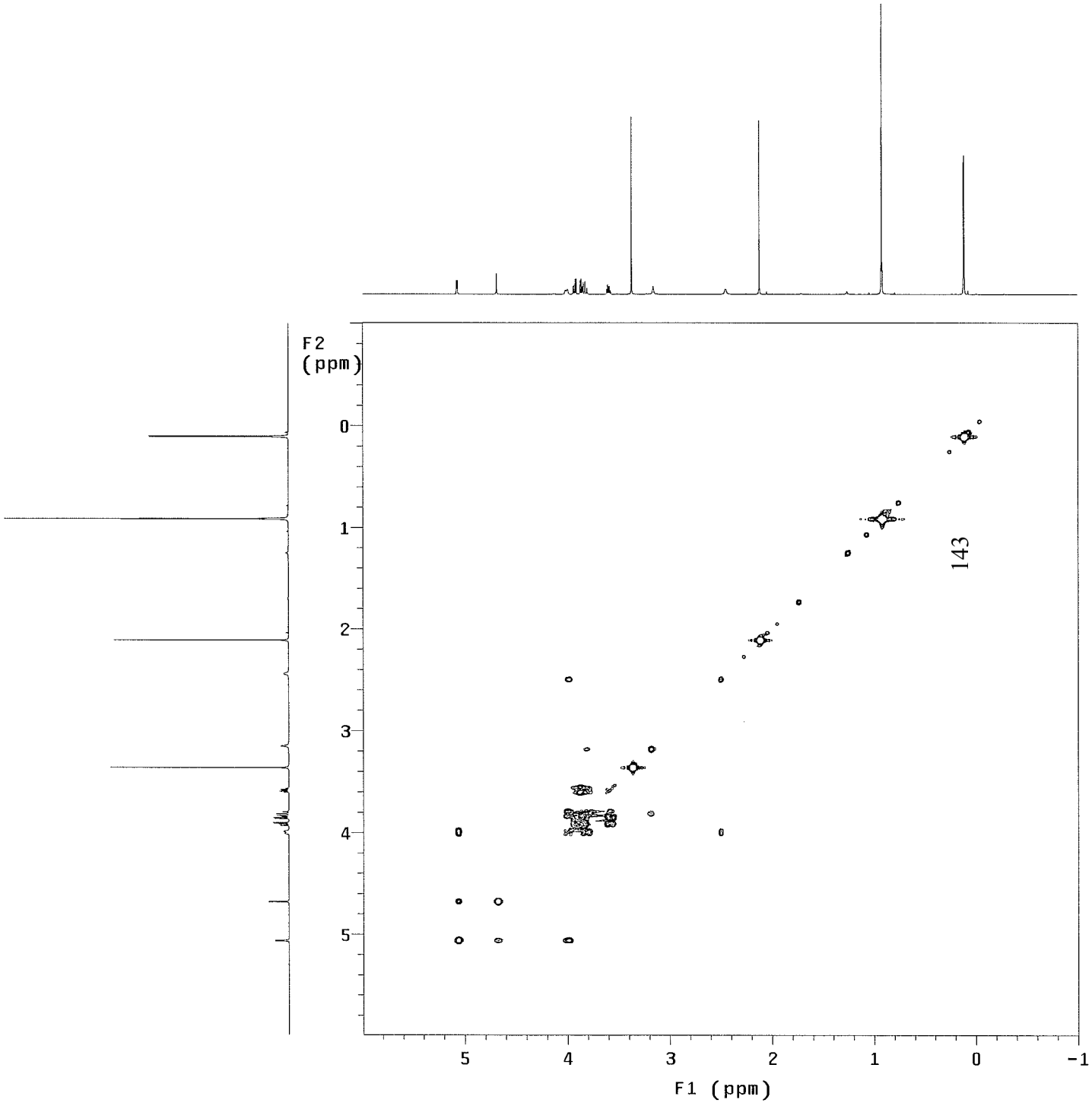
F2
(ppm)
0
1
2
3
4
5
143
5
4
3
2
1
0
-1
F1 (ppm)

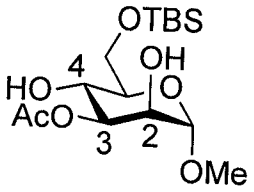

144

8 7 6 5 4 3 2 1 -0 ppm

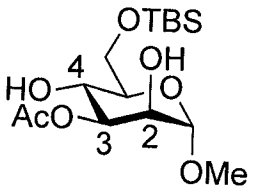
OTBS
OH
4
HO
O
AcO
3
2
OMe

145
220
200
180
160
140
120
100
80
60
40
20
0
ppm

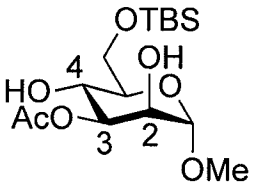
OTBS
OH
4
HO
O
AcO
3
2
OMe

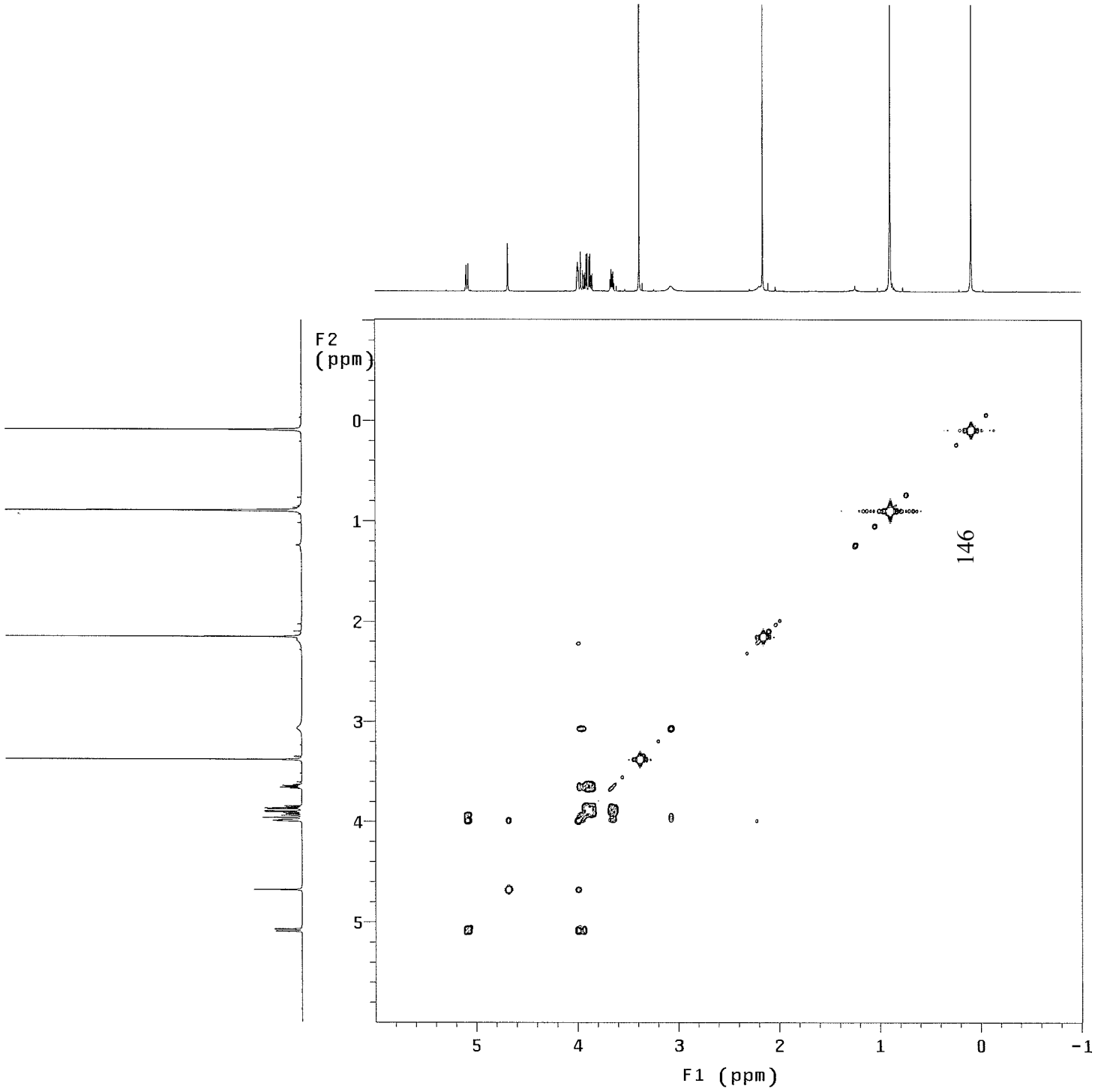
F2
(ppm)
0
1
2
3
4
5
146
5
4
3
2
1
0
-1
F1 (ppm)

AcO
HO
4
3
2
OH
O
OTBS
OMe

8
7
6
5
4
3
2
1
0
ppm

AcO
HO
4
3
2
OTBS
OH
O
OMe
220
200
180
160
140
120
100
80
60
40
20
0
ppm

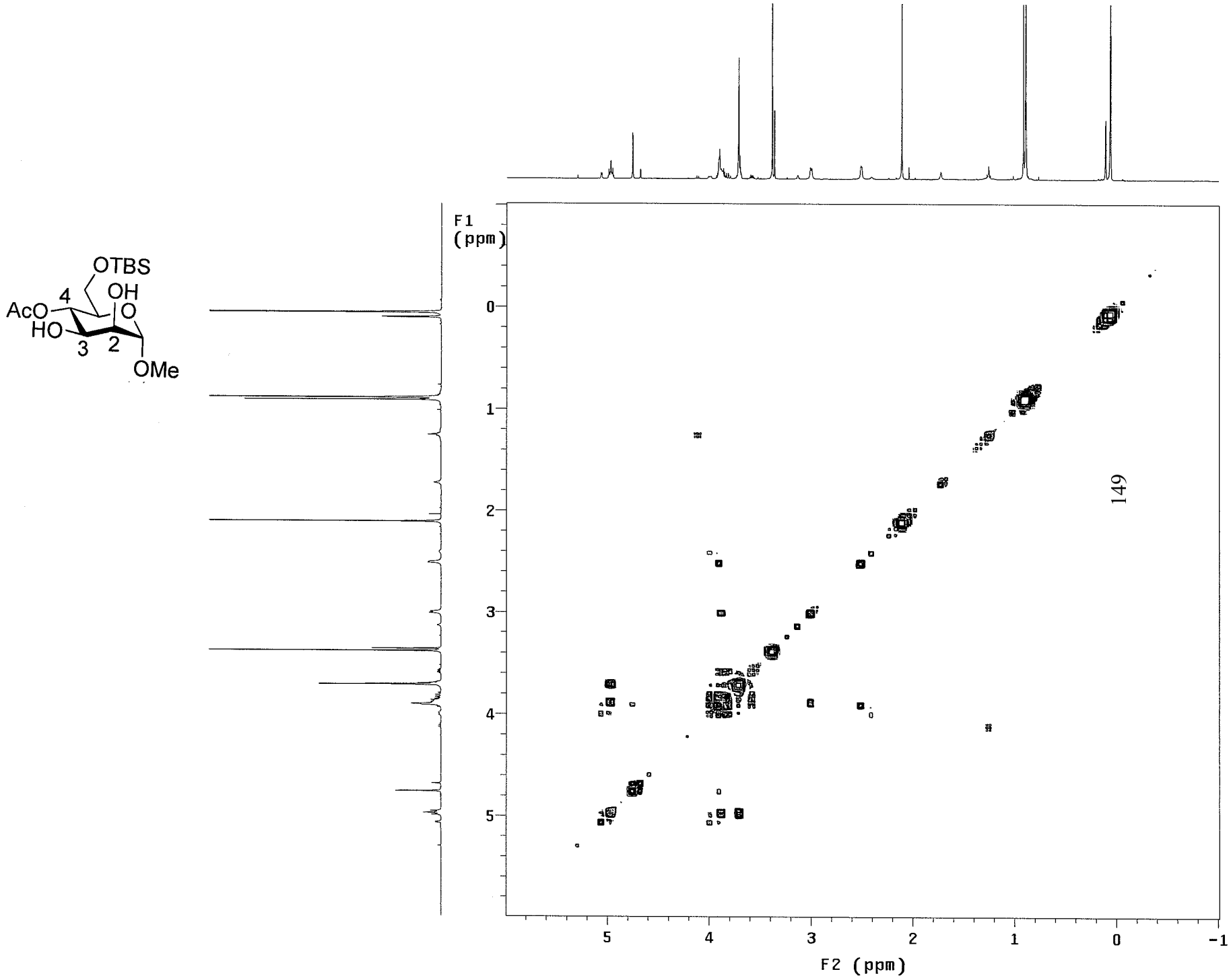
OTBS
OH
AcO
O
HO
4
3
2
OMe
F1
(ppm)
0
1
2
3
4
5
5
4
3
2
1
0
-1
F2 (ppm)

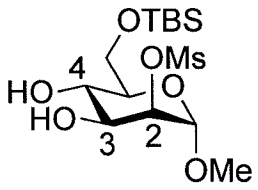
OTBS
OMs
4
HO
O
HO
3
2
OMe

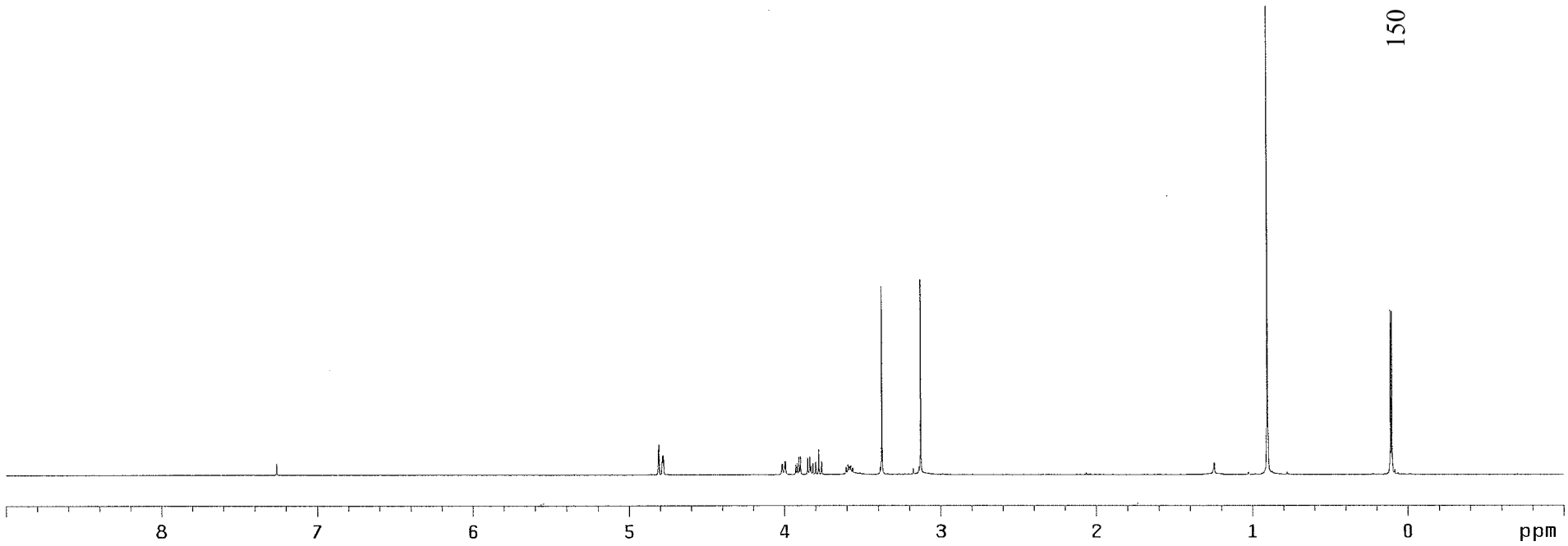
150
8
7
6
5
4
3
2
1
0
ppm

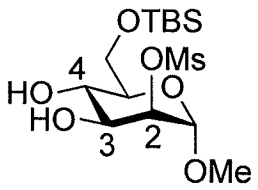
OTBS
OMs
4
HO
HO
3
2
O
OMe

151
220
200
180
160
140
120
100
80
60
40
20
0
ppm

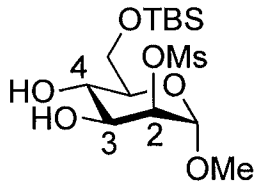
OTBS
OMs
4
HO
HO
3
2
O
OMe

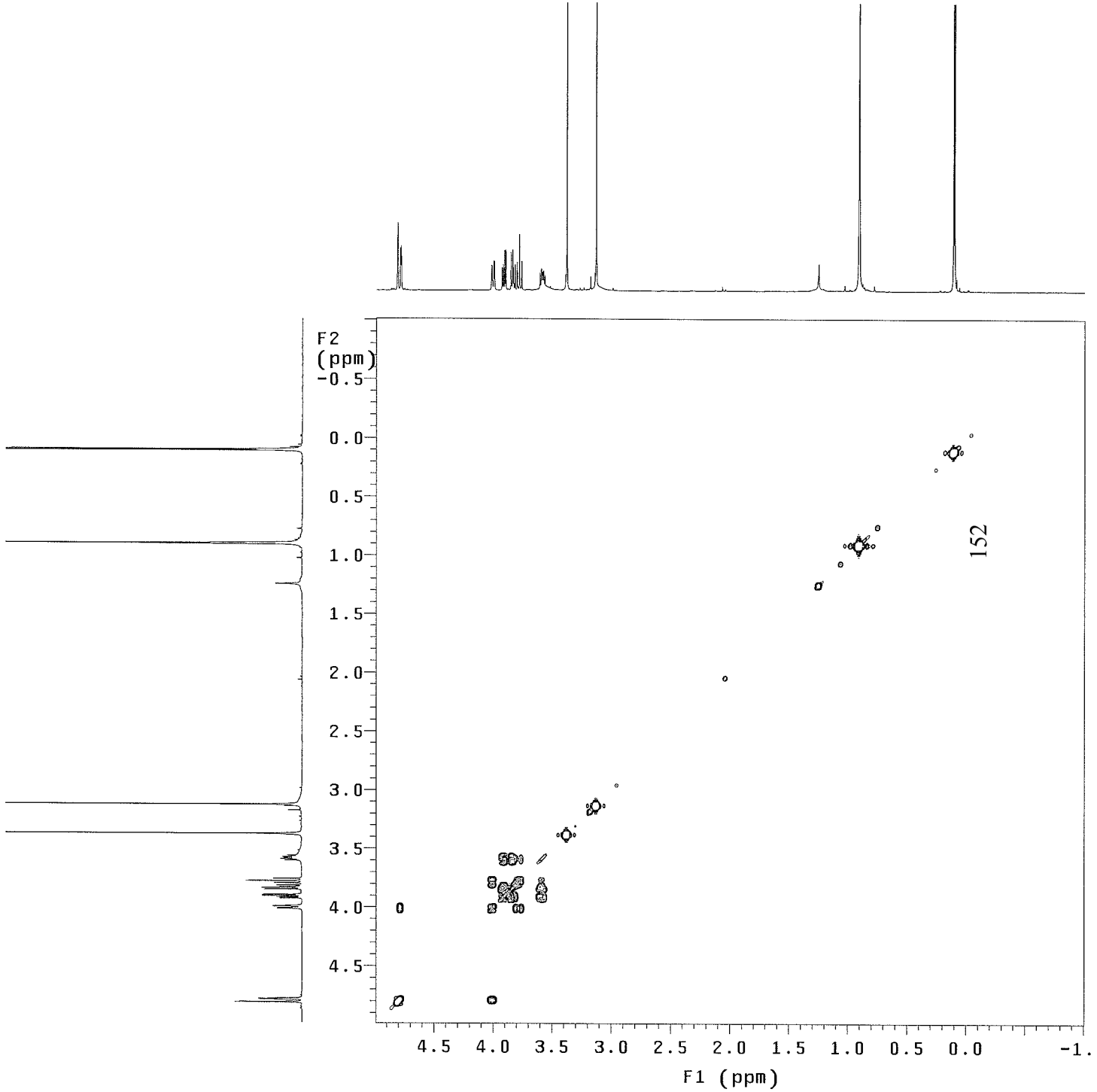
F2
(ppm)
-0.5
0.0
0.5
1.0
1.5
2.0
2.5
3.0
3.5
4.0
4.5
4.5
4.0
3.5
3.0
2.5
2.0
1.5
1.0
0.5
0.0
-1.0
F1 (ppm)
152

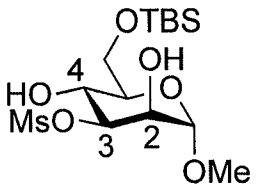
OTBS
OH
4
HO
O
MsO
3
2
OMe

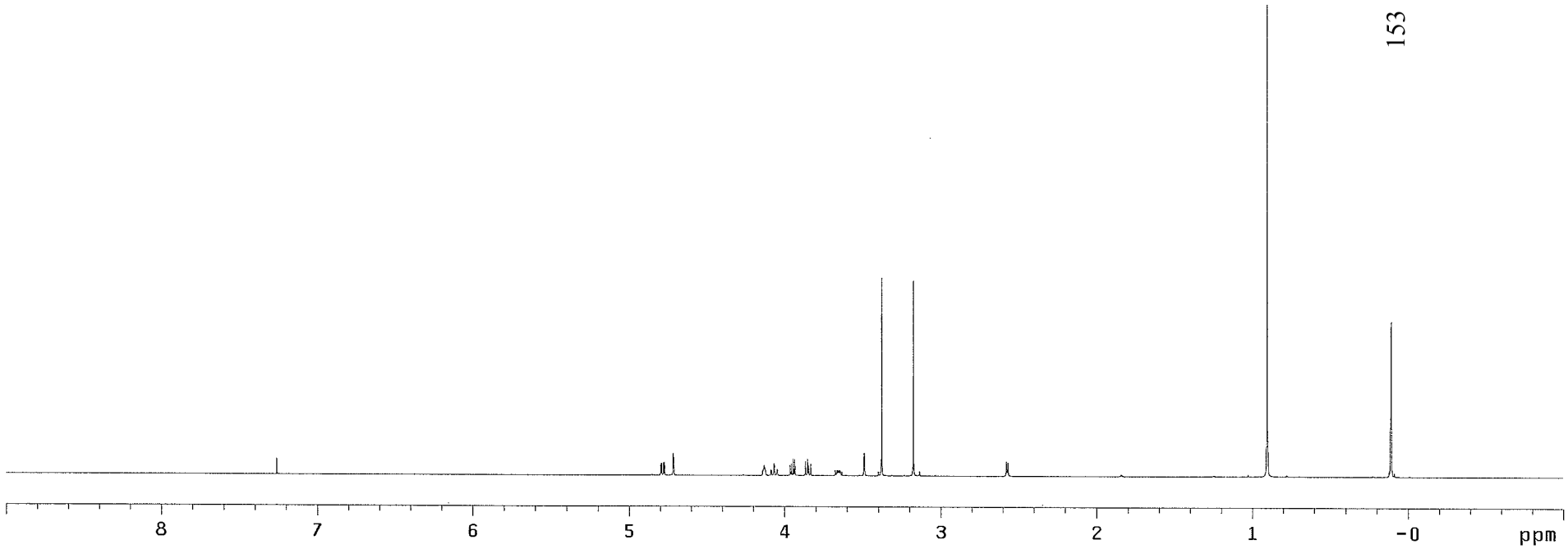
153
8
7
6
5
4
3
2
1
-0
ppm

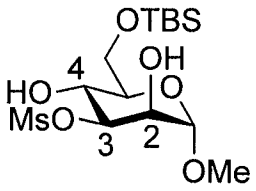

154

220 200 180 160 140 120 100 80 60 40 20 0 ppm

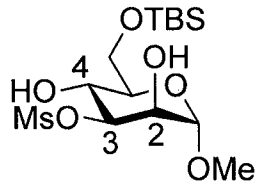
OTBS
OH
4
HO
O
MsO
3
2
OMe

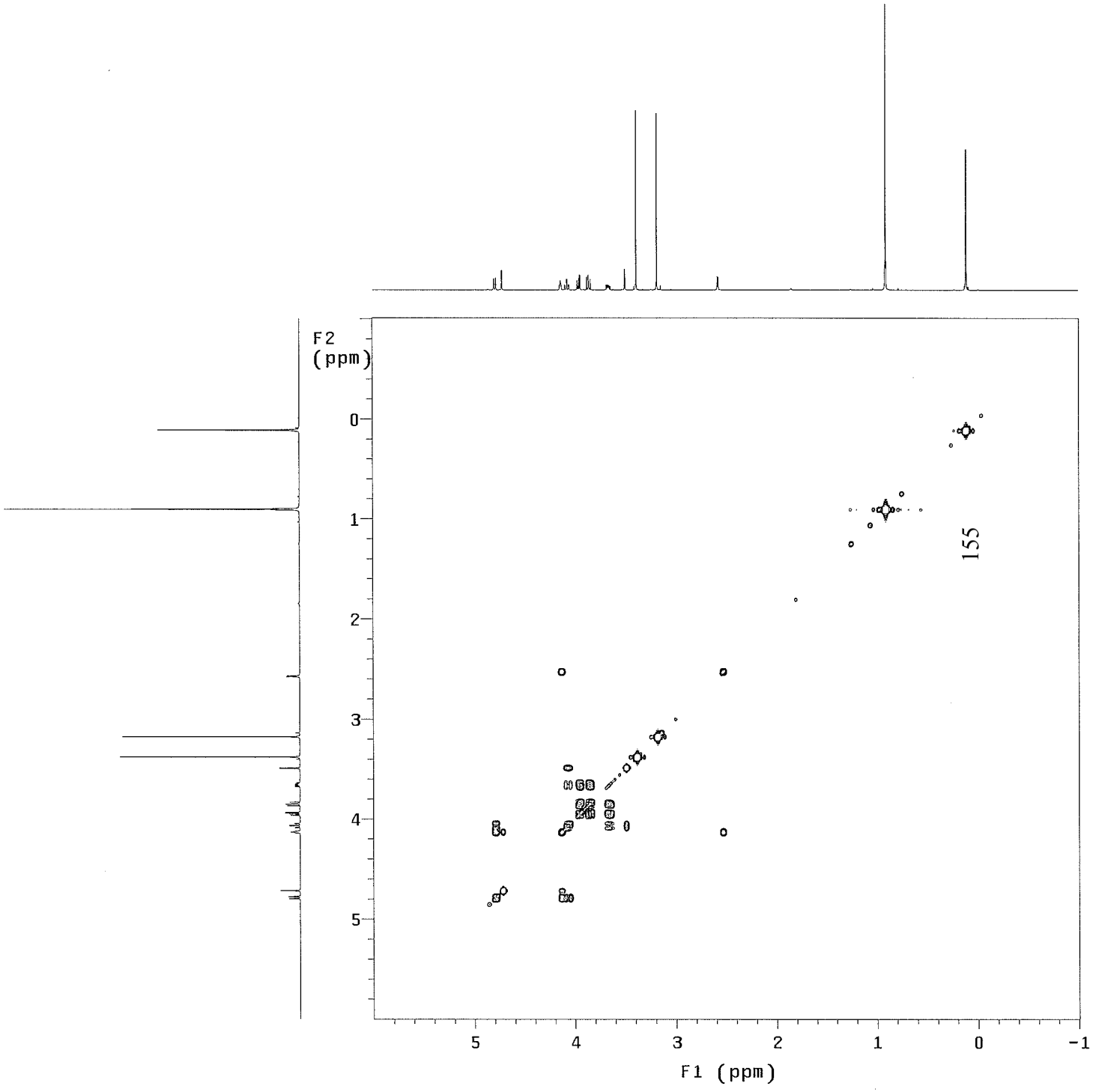
F2
(ppm)
0
1
2
3
4
5
155
5
4
3
2
1
0
-1
F1 (ppm)

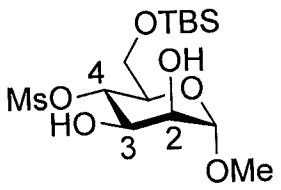
OTBS
OH
4
MsO
O
HO
3
2
OMe

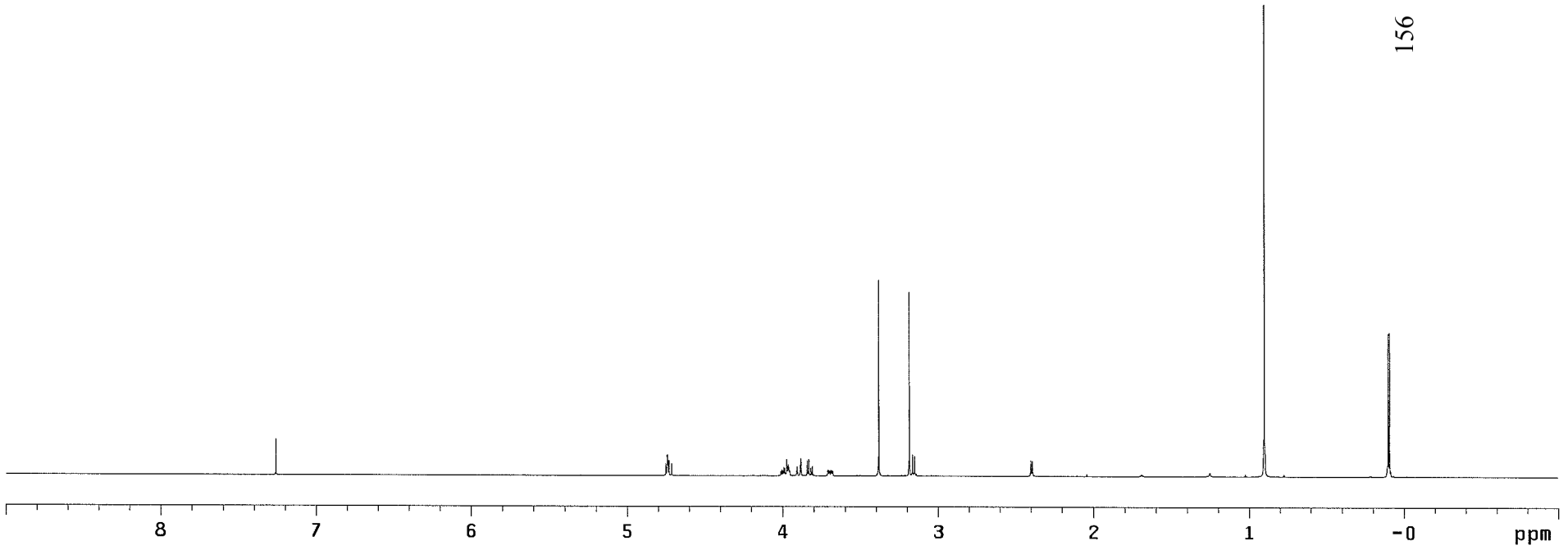
156
8
7
6
5
4
3
2
1
-0
ppm

MsO
HO
4
3
2
OTBS
OH
O
OMe
220
200
180
160
140
120
100
80
60
40
20
0
ppm

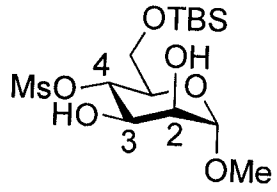
OTBS
OH
4
MsO
O
HO
3
2
OMe

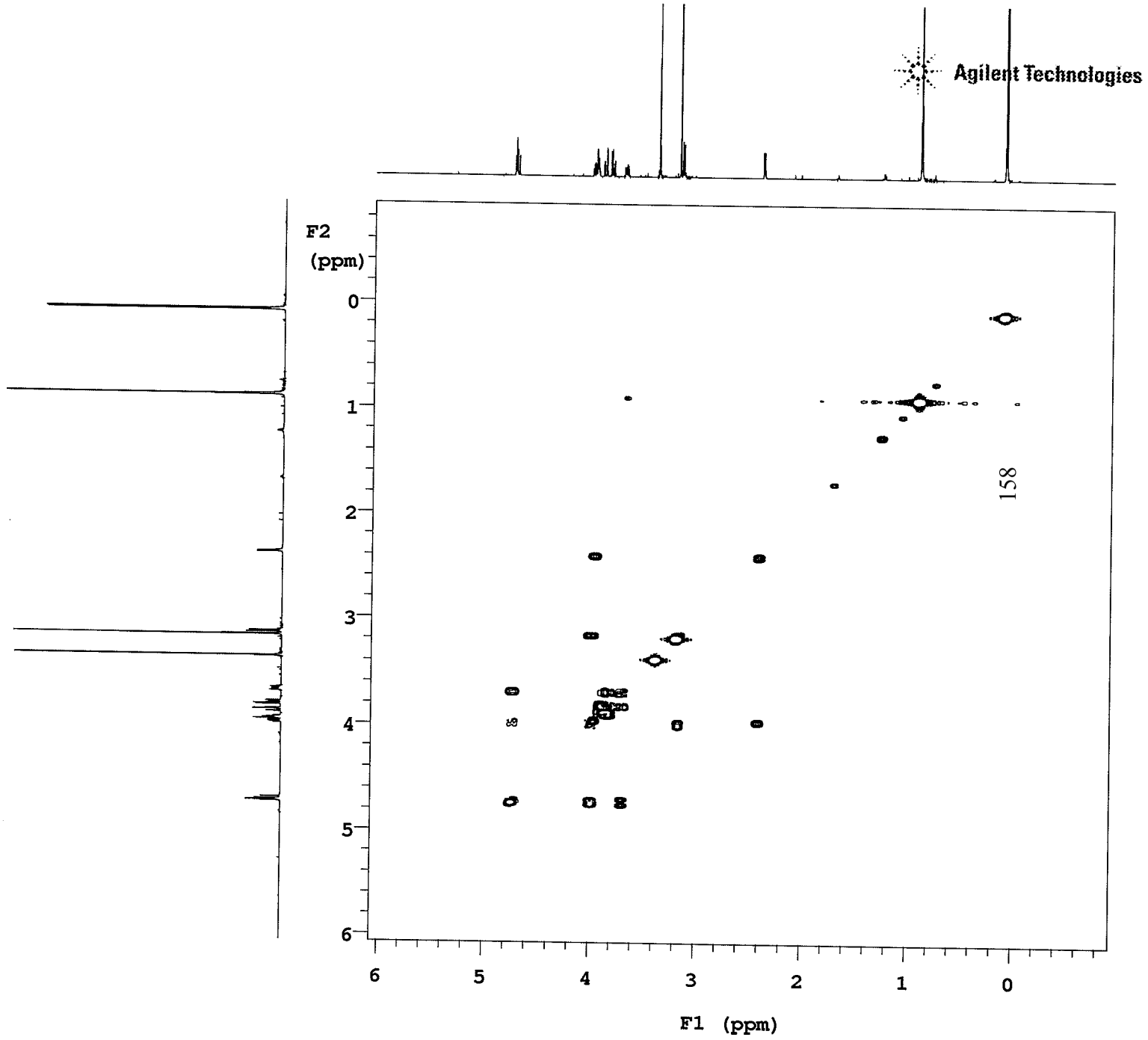
Agilent Technologies
F2
(ppm)
0
1
2
3
4
5
6
158
F1 (ppm)

Me
HO
4
O
3
2
OMe
OH
OTES
9
8
7
6
5
4
3
2
1
ppm

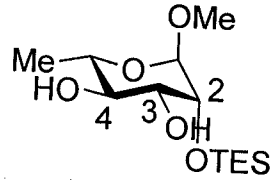
OMe
Me
O
HO
2
4
3
OH
OTES

160
220
200
180
160
140
120
100
80
60
40
20
0
ppm

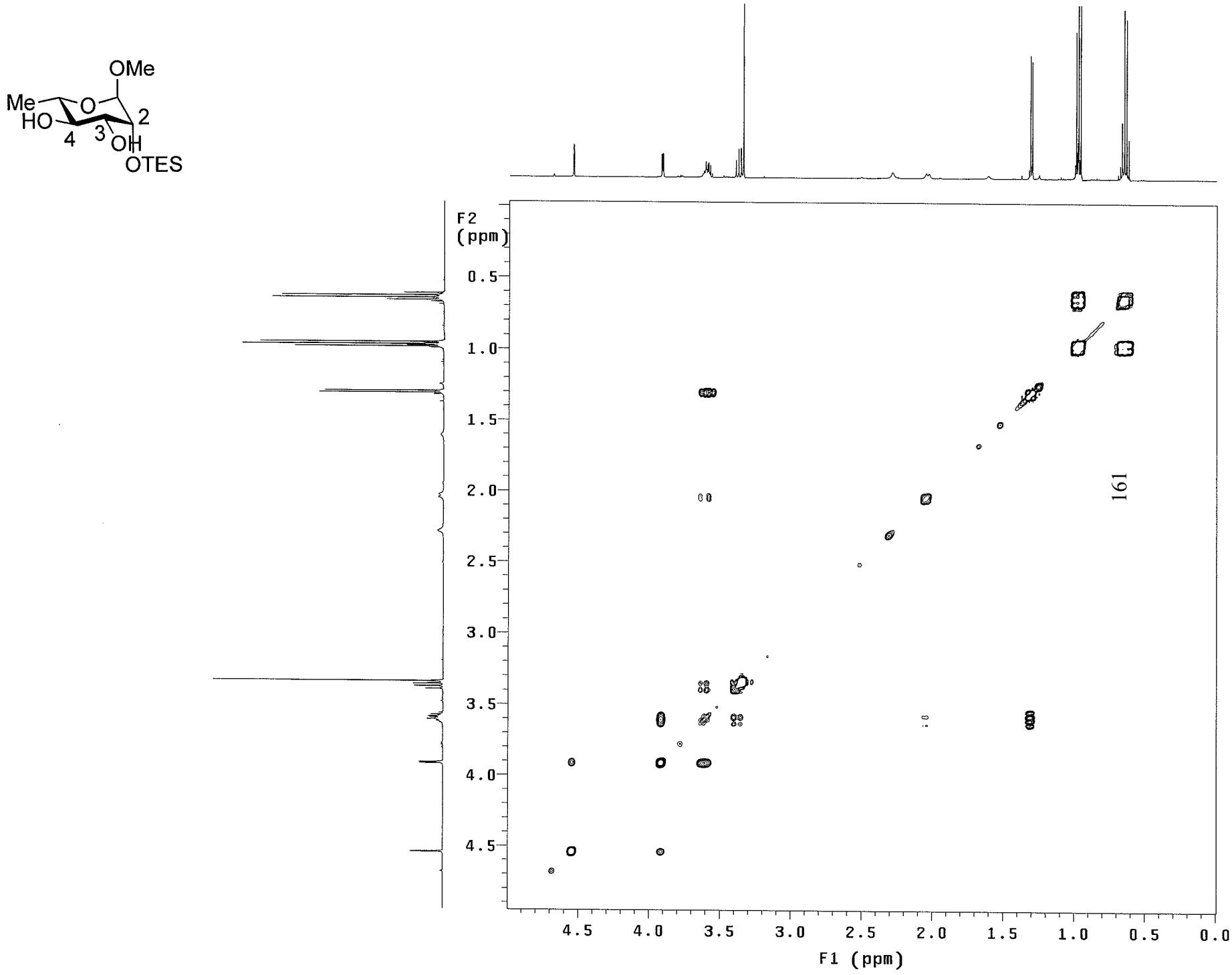
OMe
Me
O
HO
2
4
3
OH
OTES
F2 (ppm)
0.5
1.0
1.5
2.0
2.5
3.0
3.5
4.0
4.5
4.5
4.0
3.5
3.0
2.5
2.0
1.5
1.0
0.5
0.0
F1 (ppm)
161

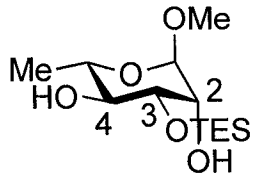
OMe
Me
O
HO
2
4
3
OTES
OH

162
9
8
7
6
5
4
3
2
1
ppm

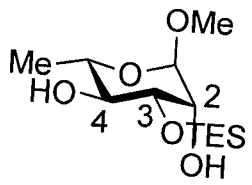
OMe
Me
O
HO
2
4
3
OTES
OH

163
220
200
180
160
140
120
100
80
60
40
20
0
ppm

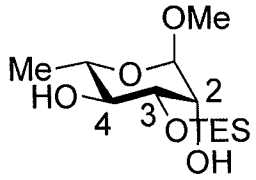
OMe
Me
O
HO
2
4
3
OTES
OH

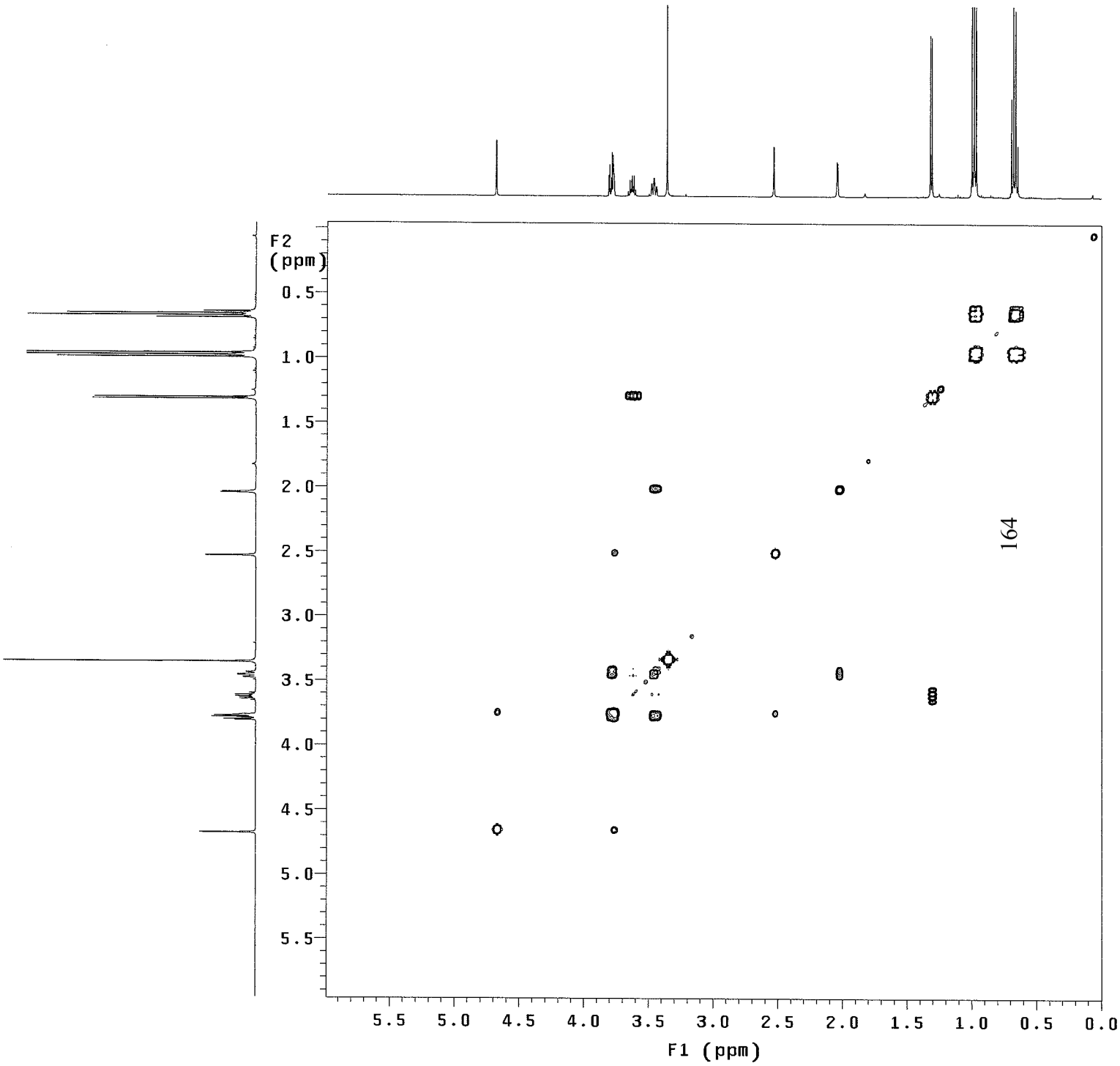
F2 (ppm)
0.5
1.0
1.5
2.0
2.5
3.0
3.5
4.0
4.5
5.0
5.5
5.5 5.0 4.5 4.0 3.5 3.0 2.5 2.0 1.5 1.0 0.5 0.0
F1 (ppm)
164

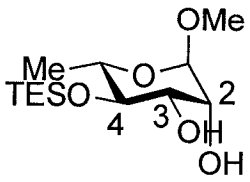
OMe
Me
O
TESO
2
4
3
OH
OH

1.65
9
8
7
6
5
4
3
2
1
ppm

Me
TESO
4
O
3
OH
2
OMe
OH
220
200
180
160
140
120
100
80
60
40
20
0
ppm

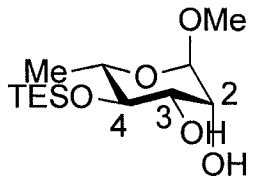
OMe
Me
O
TESO
2
4
3
OH
OH

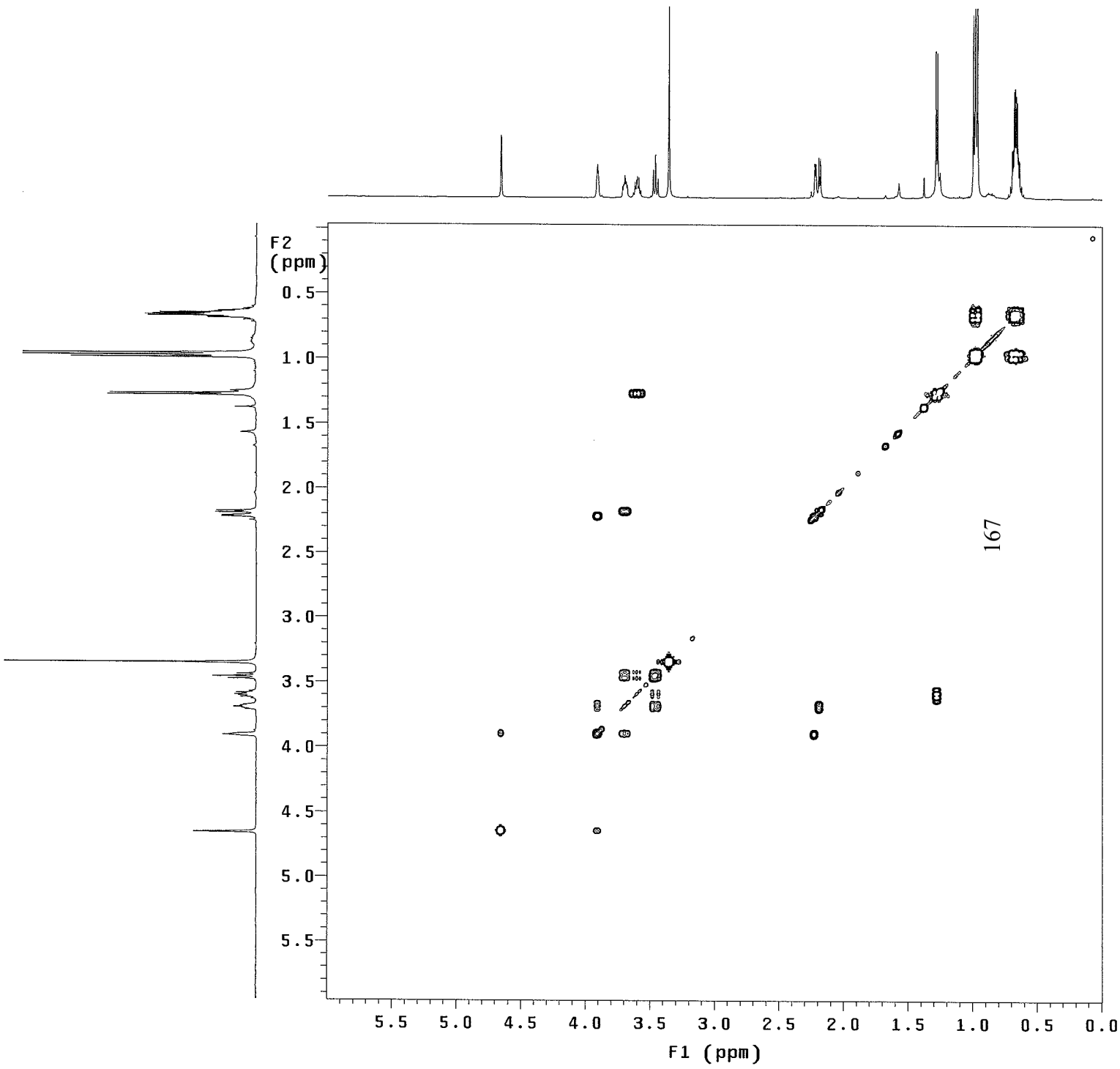
F2 (ppm)
0.5
1.0
1.5
2.0
2.5
3.0
3.5
4.0
4.5
5.0
5.5
5.5 5.0 4.5 4.0 3.5 3.0 2.5 2.0 1.5 1.0 0.5 0.0
F1 (ppm)
167

Me
HO
4
O
3
OH
OAc
2
OMe
9
8
7
6
5
4
3
2
1
ppm

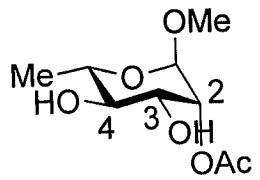
OMe
Me
O
HO
2
4
3
OH
OAc

169
220
200
180
160
140
120
100
80
60
40
20
0
ppm

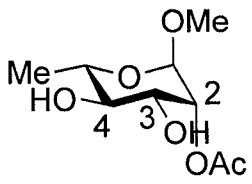
OMe
Me
O
HO
2
4
3
OH
OAc

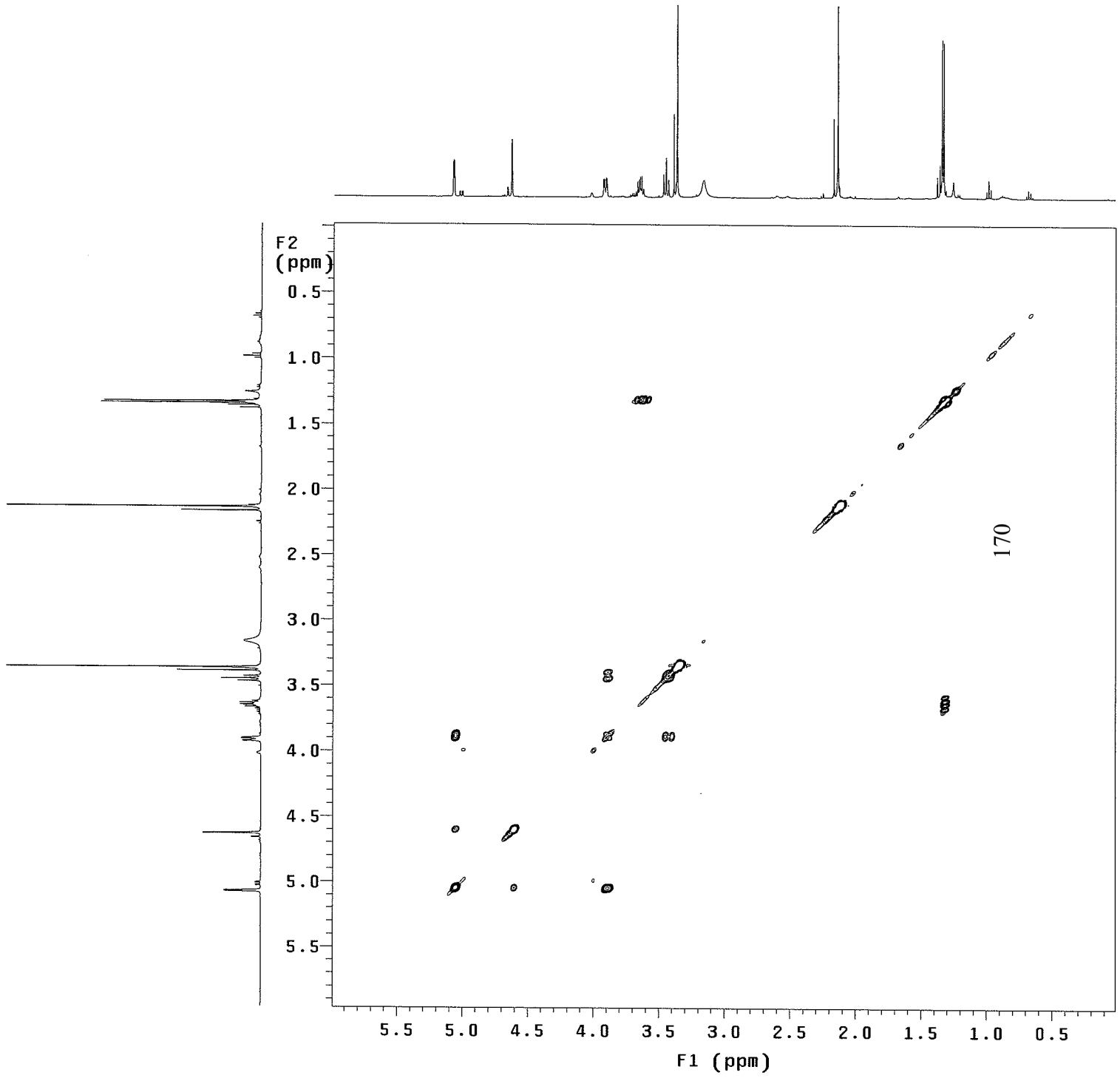
F2
(ppm)
0.5
1.0
1.5
2.0
2.5
3.0
3.5
4.0
4.5
5.0
5.5
5.5
5.0
4.5
4.0
3.5
3.0
2.5
2.0
1.5
1.0
0.5
F1 (ppm)
170

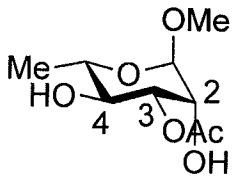

171

Me
HO
4
3
OAc
OH
2
OMe
220
200
180
160
140
120
100
80
60
40
20
0
ppm

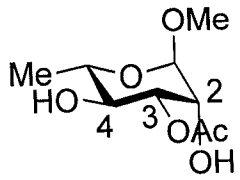
OMe
Me
O
HO
2
4
3
OAc
OH

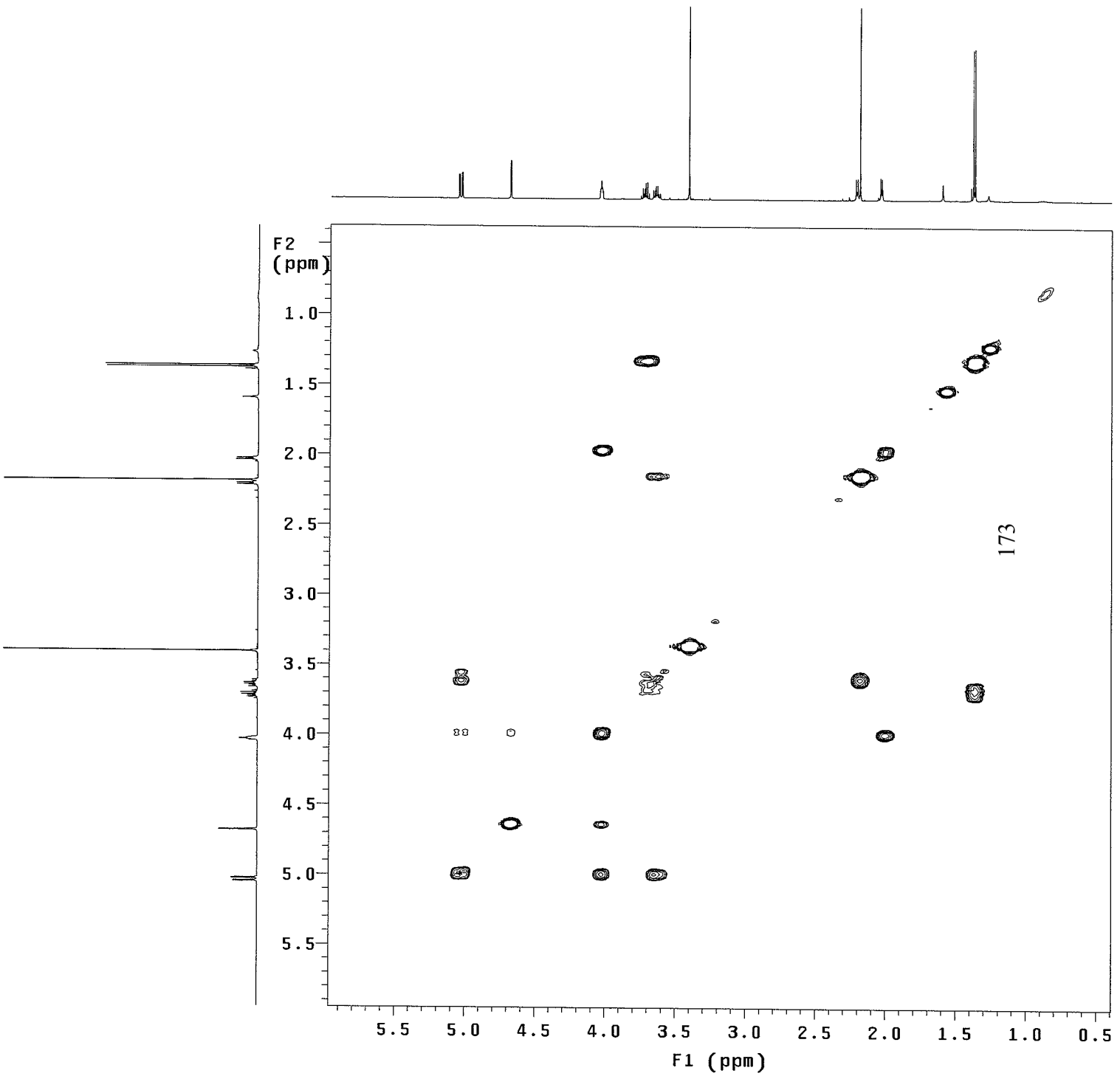
F2
(ppm)
1.0
1.5
2.0
2.5
3.0
3.5
4.0
4.5
5.0
5.5
5.5
5.0
4.5
4.0
3.5
3.0
2.5
2.0
1.5
1.0
0.5
F1 (ppm)
173

Me
AcO
4
3
OH
OH
2
O
OMe
9
8
7
6
5
4
3
2
1
ppm

Me
AcO
4
O
3
OH
2
OMe
OH

220
200
180
160
140
120
100
80
60
40
20
0
ppm

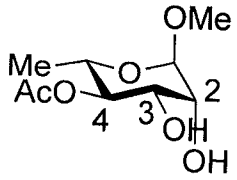
OMe
Me
O
AcO
2
4
3
OH
OH

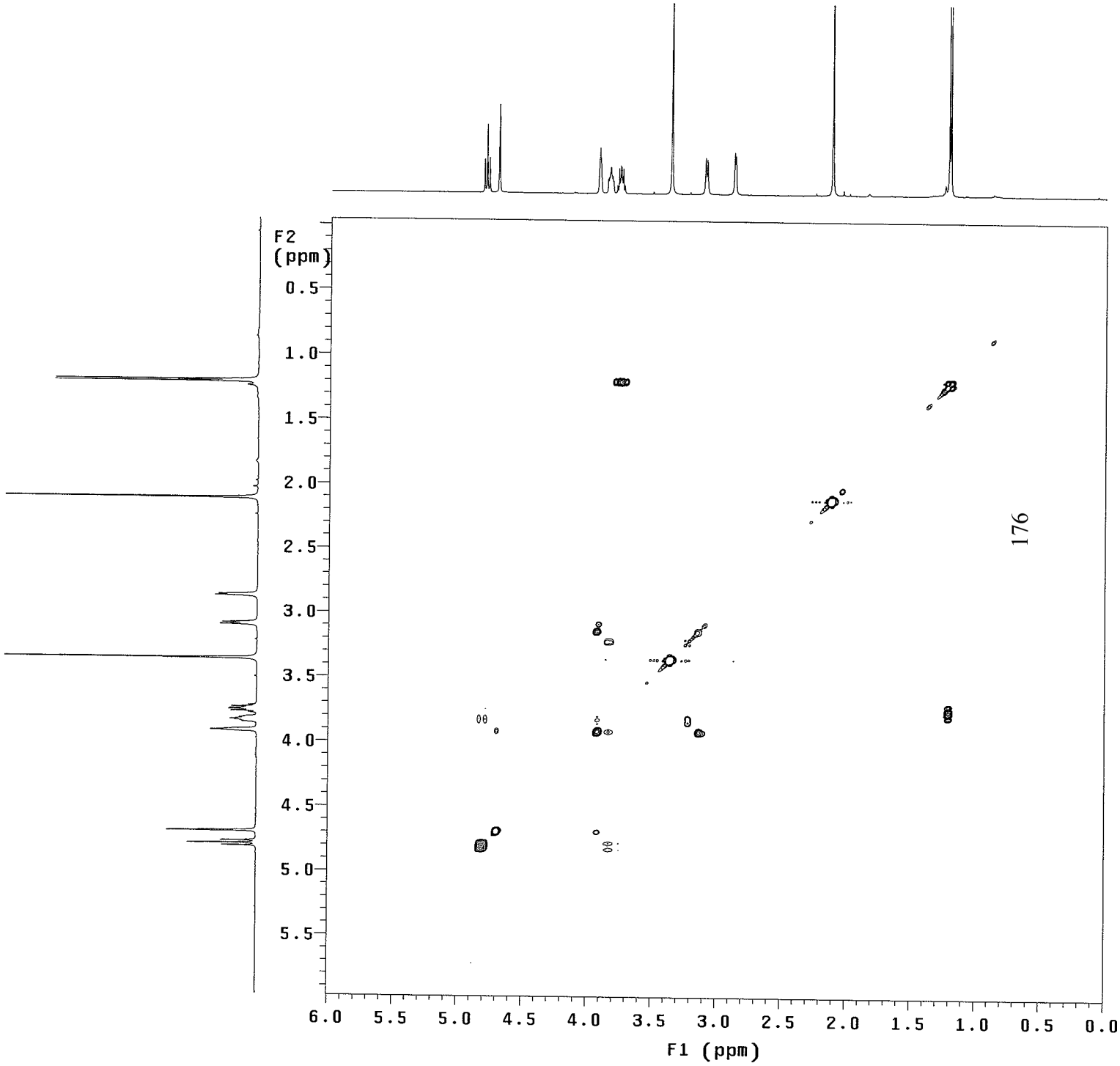
F2 (ppm)
0.5
1.0
1.5
2.0
2.5
3.0
3.5
4.0
4.5
5.0
5.5
6.0
5.5
5.0
4.5
4.0
3.5
3.0
2.5
2.0
1.5
1.0
0.5
0.0
F1 (ppm)

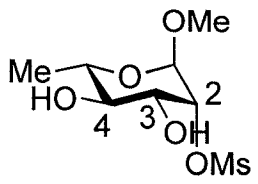

177

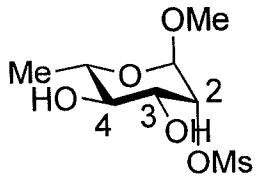
OMe
Me
O
HO
2
4
3
OH
OMs

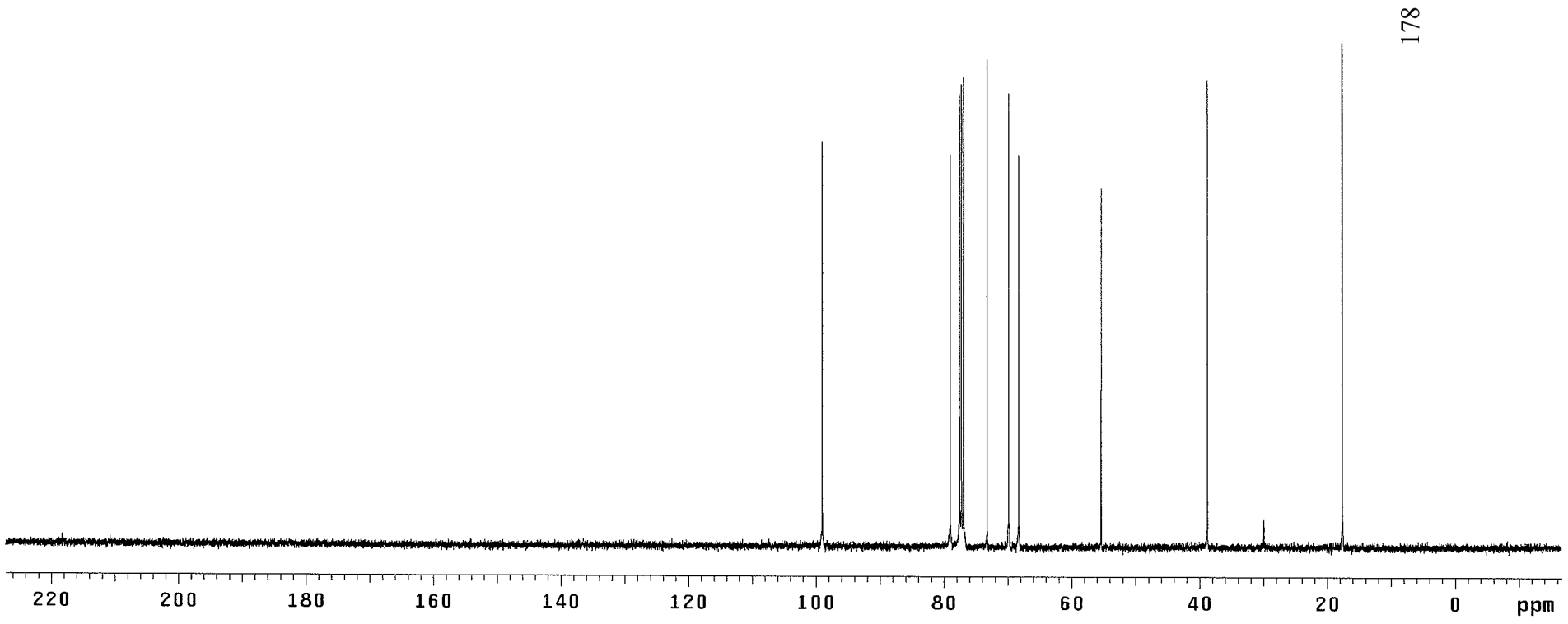
178
220
200
180
160
140
120
100
80
60
40
20
0
ppm

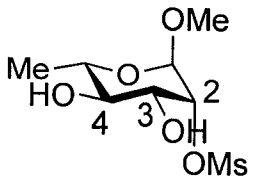
OMe
Me
O
HO
2
4
3
OH
OMs

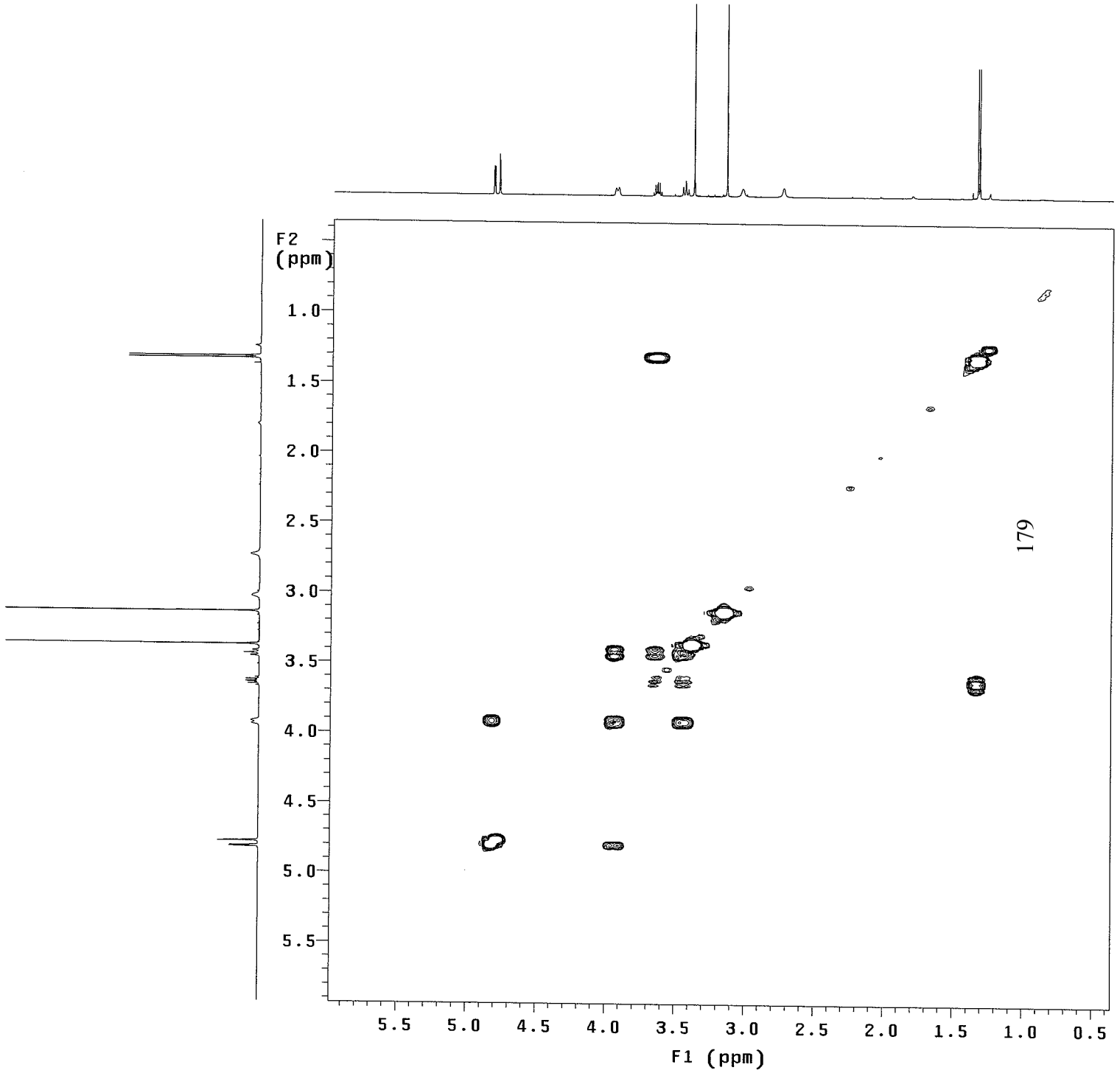
F2
(ppm)
1.0
1.5
2.0
2.5
3.0
3.5
4.0
4.5
5.0
5.5
5.5
5.0
4.5
4.0
3.5
3.0
2.5
2.0
1.5
1.0
0.5
F1 (ppm)
179

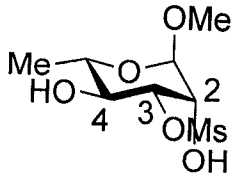

180

9 8 7 6 5 4 3 2 1 ppm

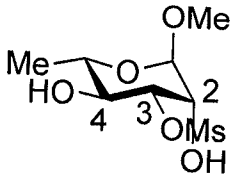

181

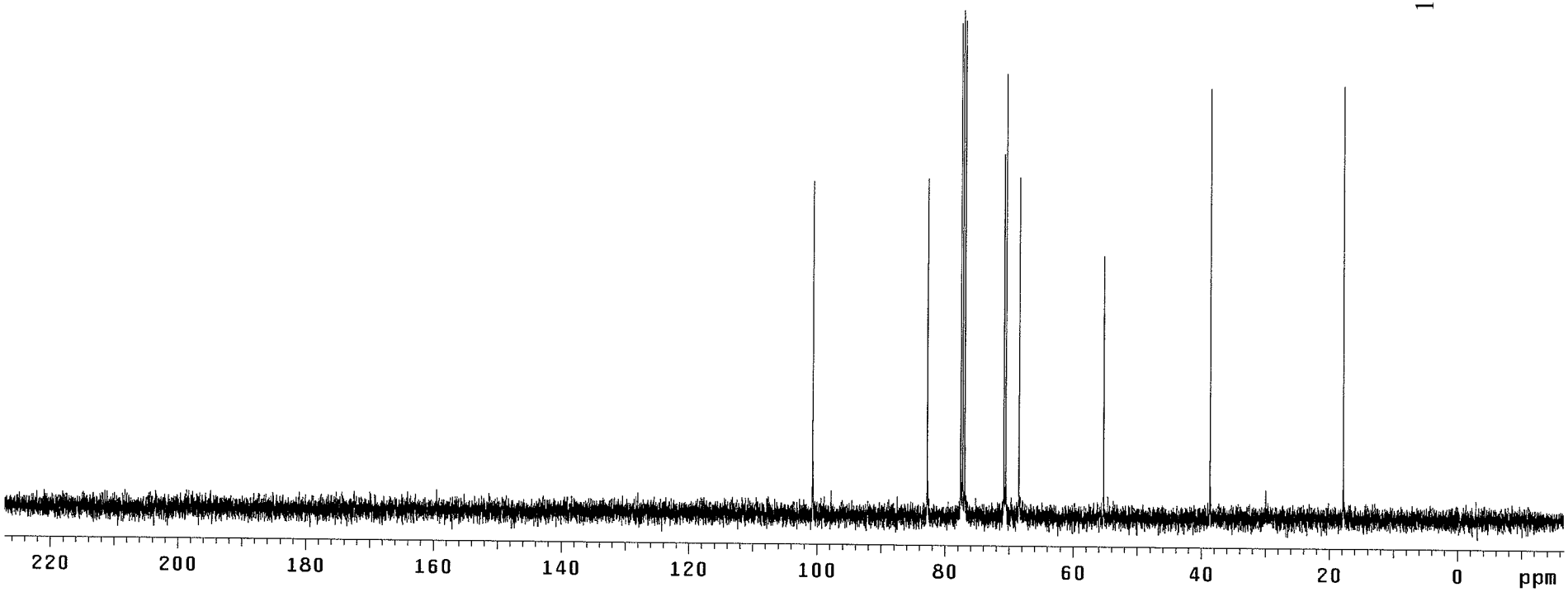

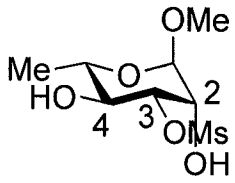
OMe
Me
O
HO
2
4
3
OMs
OH

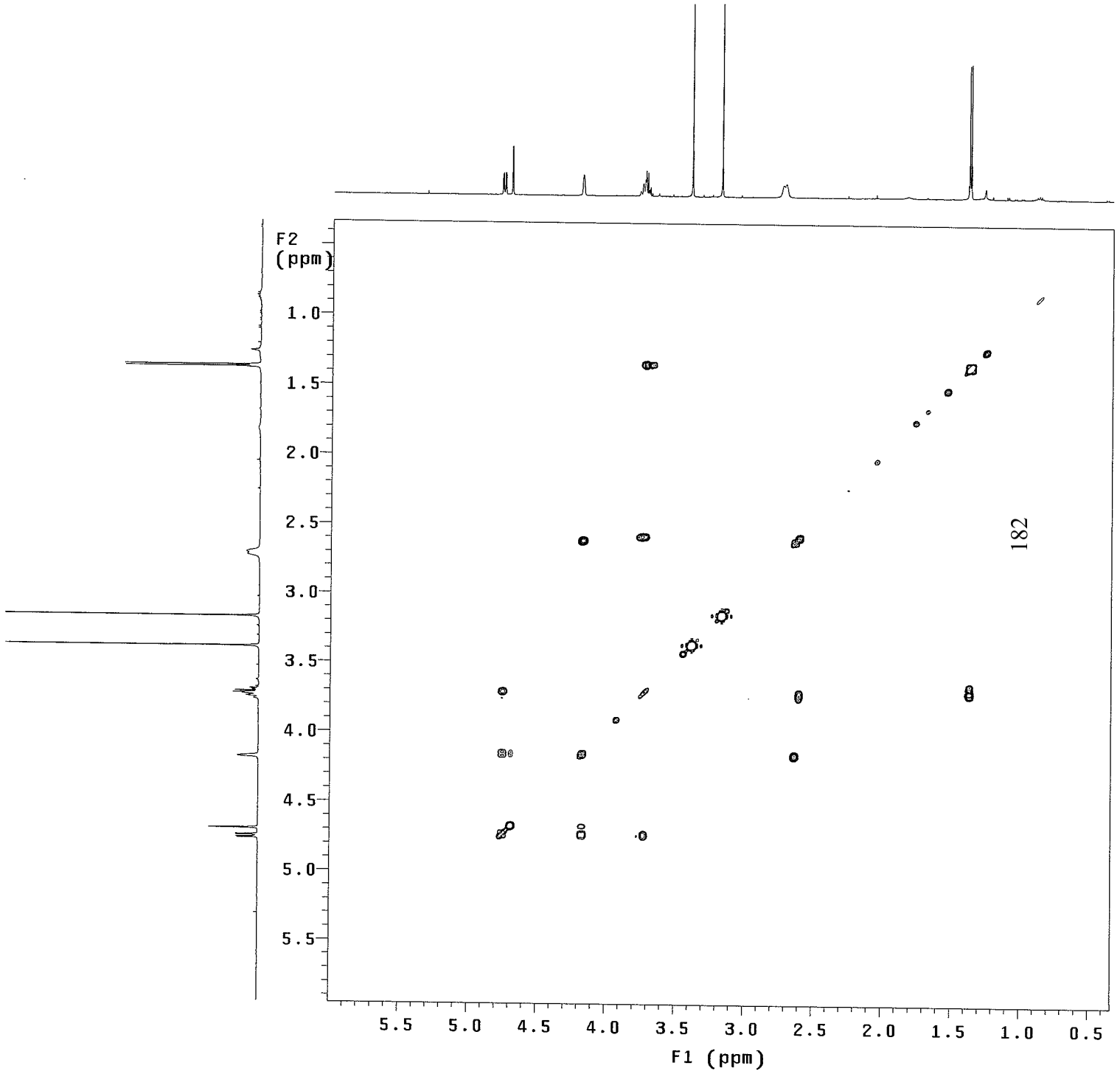
F2
(ppm)
1.0
1.5
2.0
2.5
3.0
3.5
4.0
4.5
5.0
5.5
5.5
5.0
4.5
4.0
3.5
3.0
2.5
2.0
1.5
1.0
0.5
F1 (ppm)
182

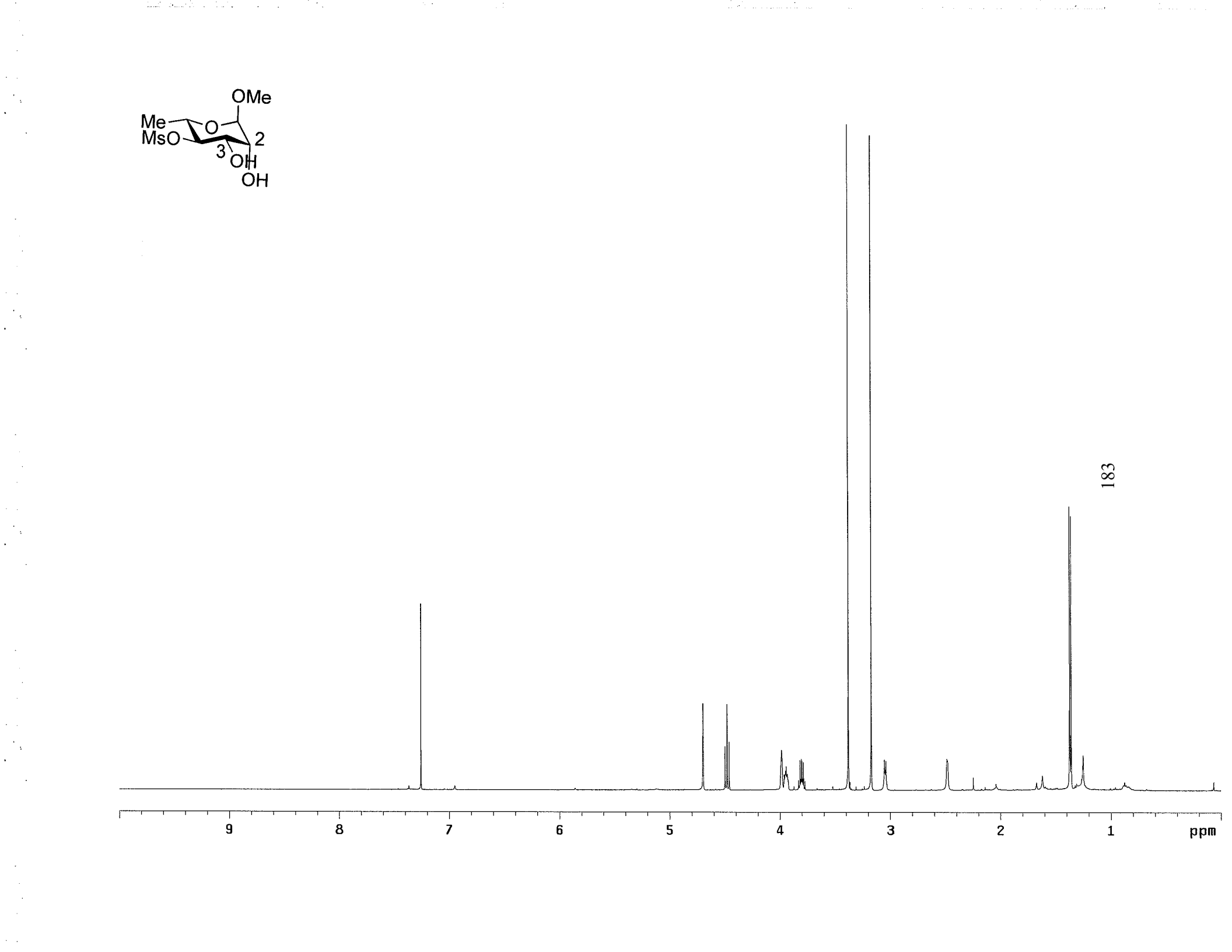
OMe
Me
O
MsO
2
3
OH
OH
183
9
8
7
6
5
4
3
2
1
ppm

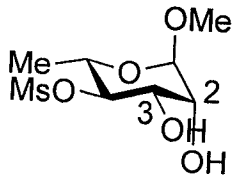

184

220 200 180 160 140 120 100 80 60 40 20 0 ppm

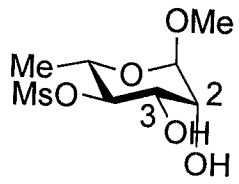
OMe
Me
O
MsO
2
3
OH
OH

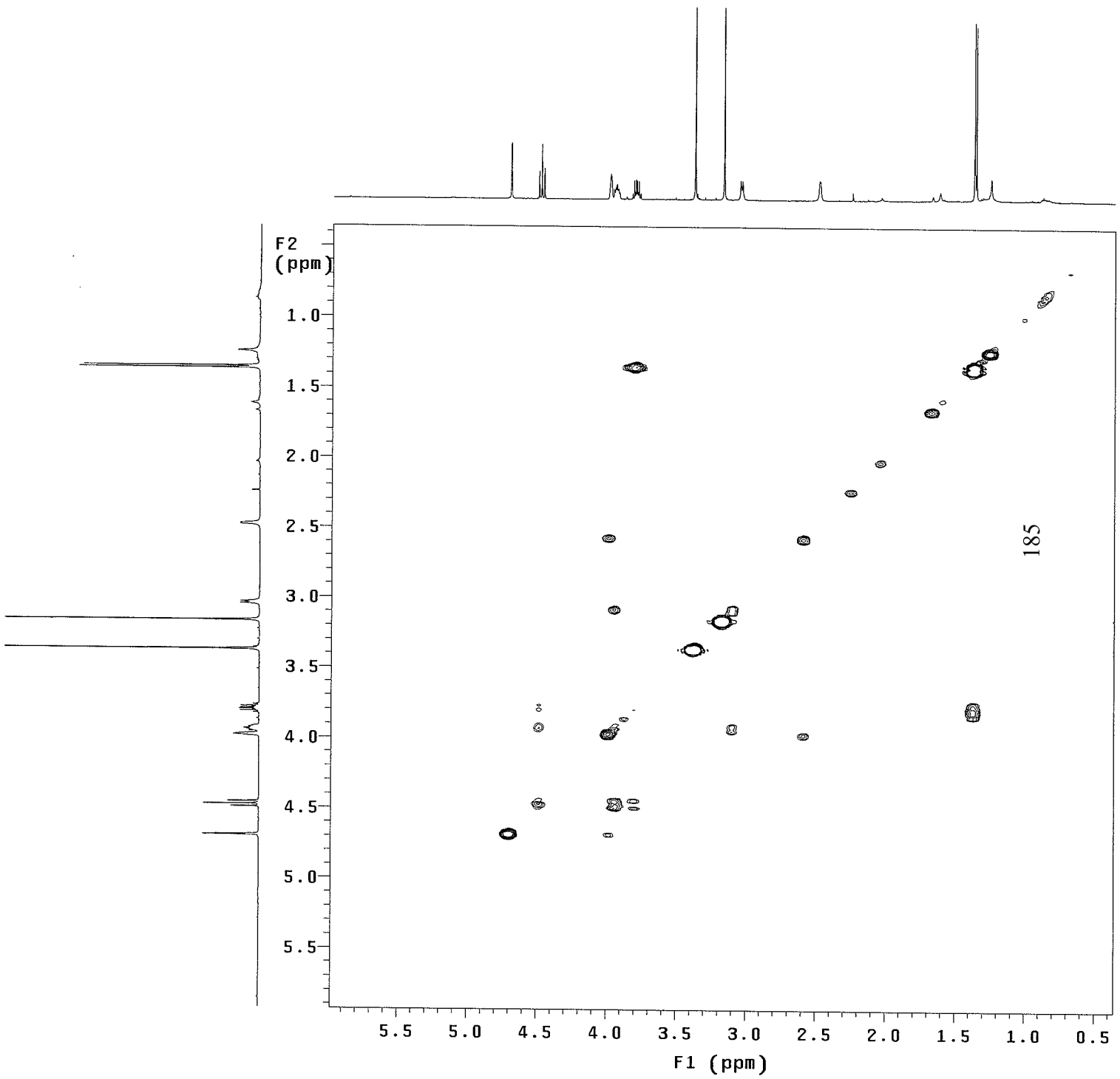
F2
(ppm)
1.0
1.5
2.0
2.5
3.0
3.5
4.0
4.5
5.0
5.5
5.5
5.0
4.5
4.0
3.5
3.0
2.5
2.0
1.5
1.0
0.5
F1 (ppm)
185

HO
4
HO
3
2
O
OTES
OMe
9
8
7
6
5
4
3
2
1
ppm

HO
4
HO
3
2
O
OTES
OMe
200
180
160
140
120
100
80
60
40
20
0
ppm

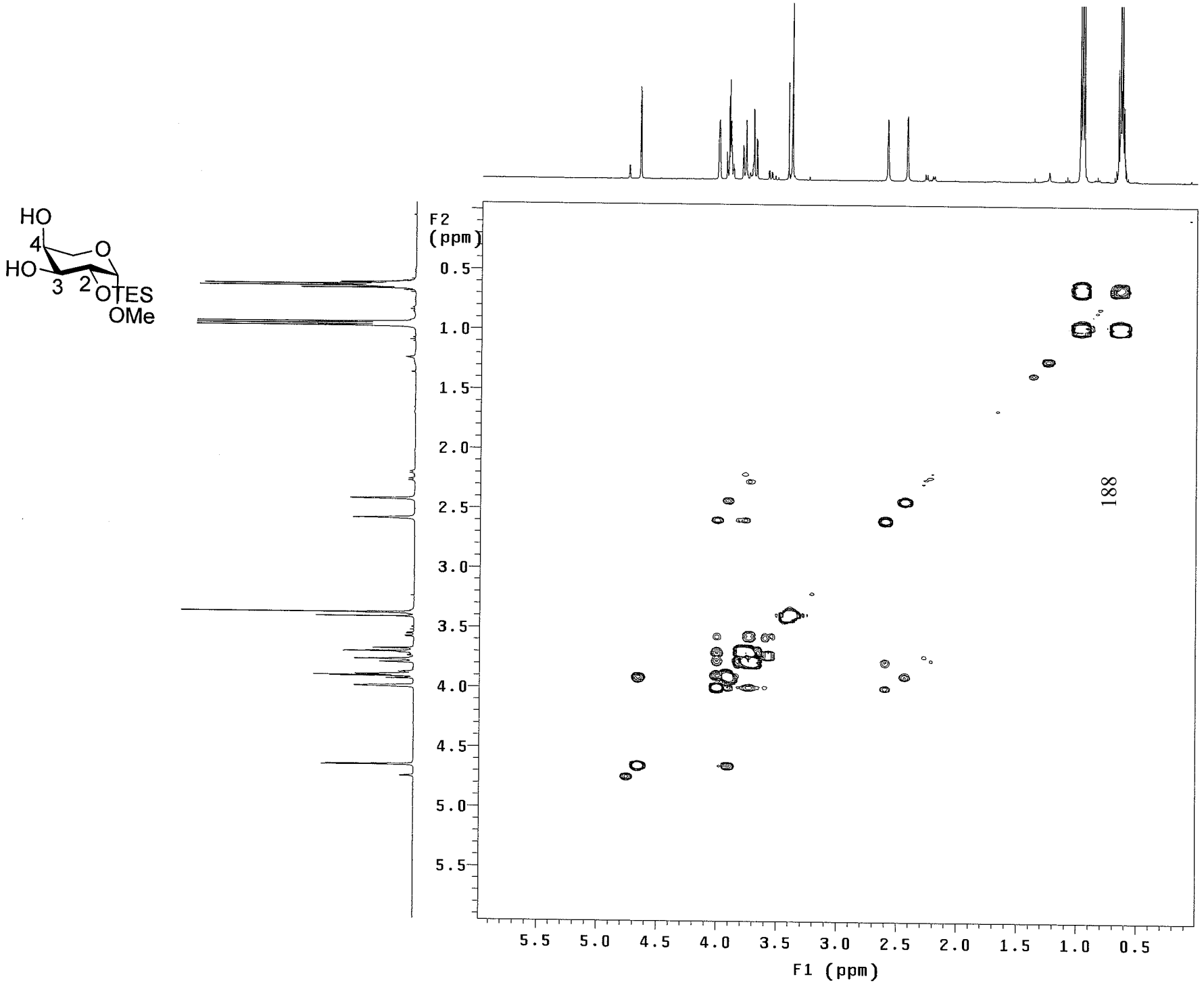
HO
4
O
HO
3
2
OTES
OMe
F2
(ppm)
0.5
1.0
1.5
2.0
2.5
3.0
3.5
4.0
4.5
5.0
5.5
188
5.5
5.0
4.5
4.0
3.5
3.0
2.5
2.0
1.5
1.0
0.5
F1 (ppm)

HO
4
TESO
3
2
O
OH
OMe
8
7
6
5
4
3
2
1
0
ppm

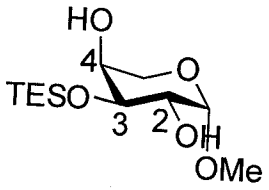
HO
4
O
TESO
3
2
OH
OMe

190
220
200
180
160
140
120
100
80
60
40
20
0
ppm

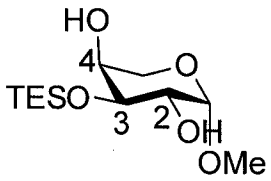
HO
4
O
TESO
3
2
OH
OMe

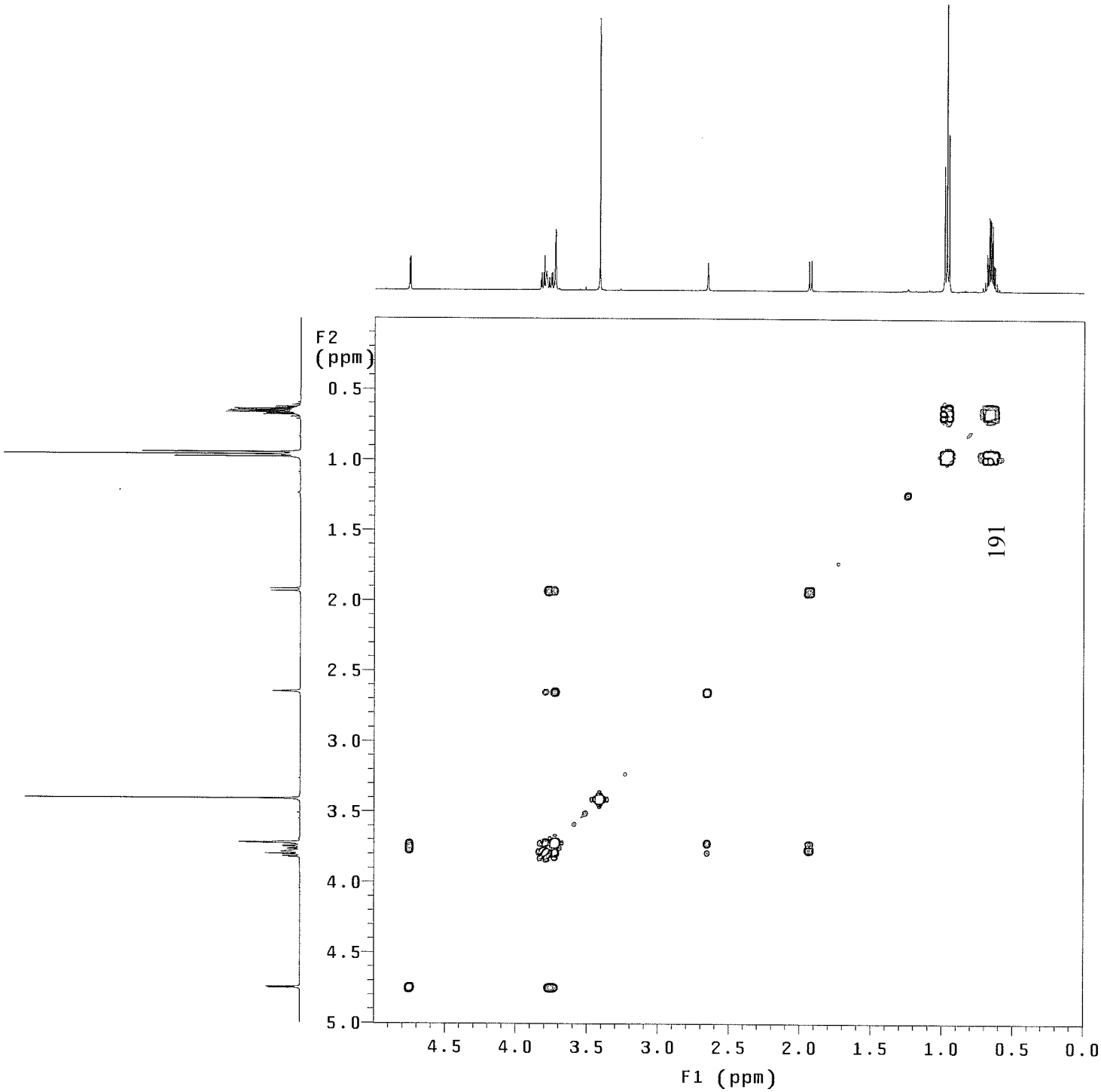
F2
(ppm)
0.5
1.0
1.5
2.0
2.5
3.0
3.5
4.0
4.5
5.0
4.5
4.0
3.5
3.0
2.5
2.0
1.5
1.0
0.5
0.0
F1 (ppm)
191

OTES
HO
4
3
2
O
OH
OMe
9
8
7
6
5
4
3
2
1
ppm

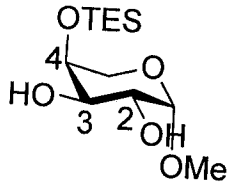
OTES
4
O
HO
3
2
OH
OMe

193
220
200
180
160
140
120
100
80
60
40
20
0
ppm

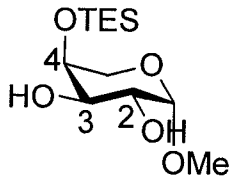
OTES
4
O
HO
3
2
OH
OMe

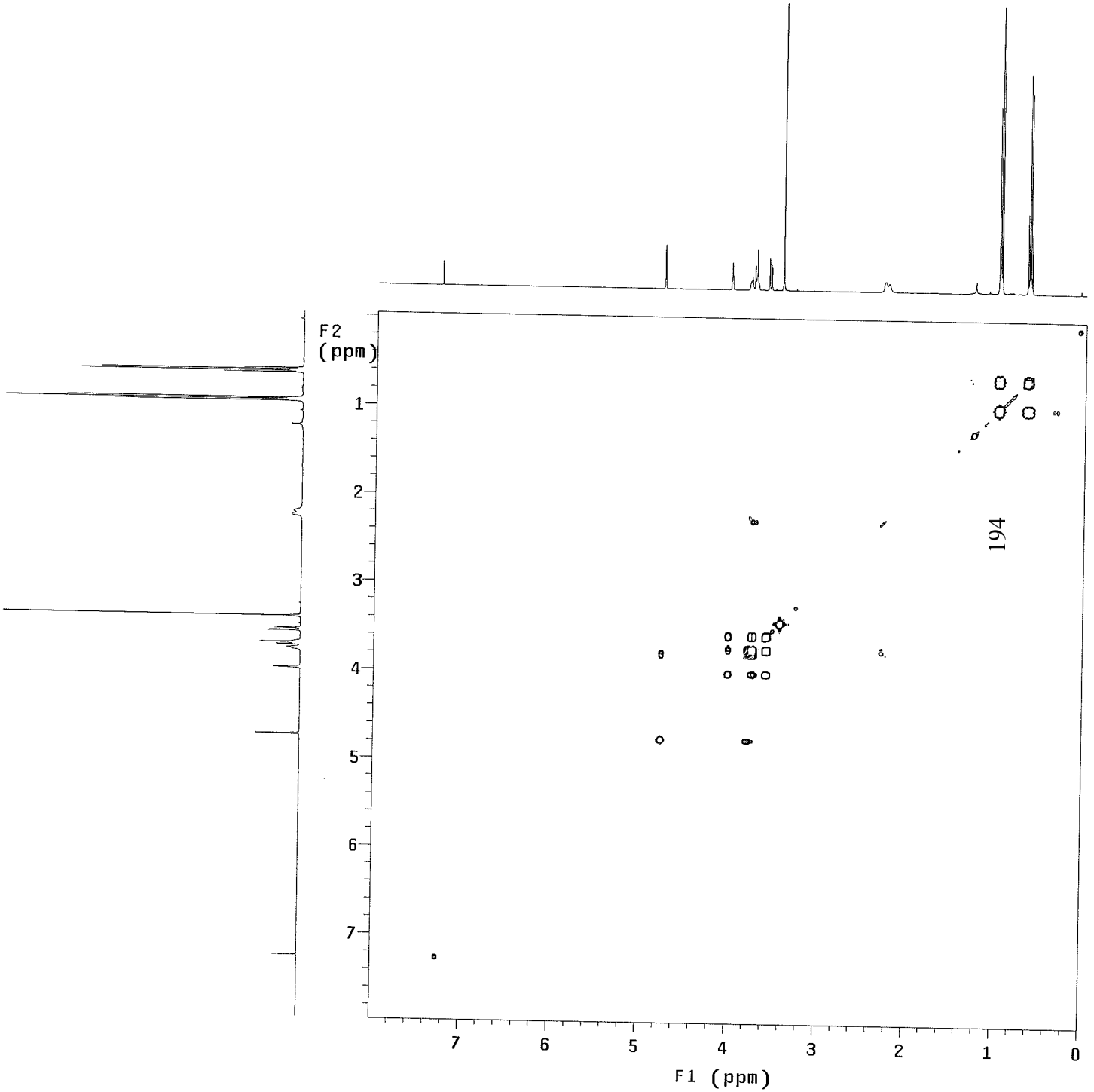
F2
(ppm)
1
2
3
4
5
6
7
194
7
6
5
4
3
2
1
0
F1 (ppm)

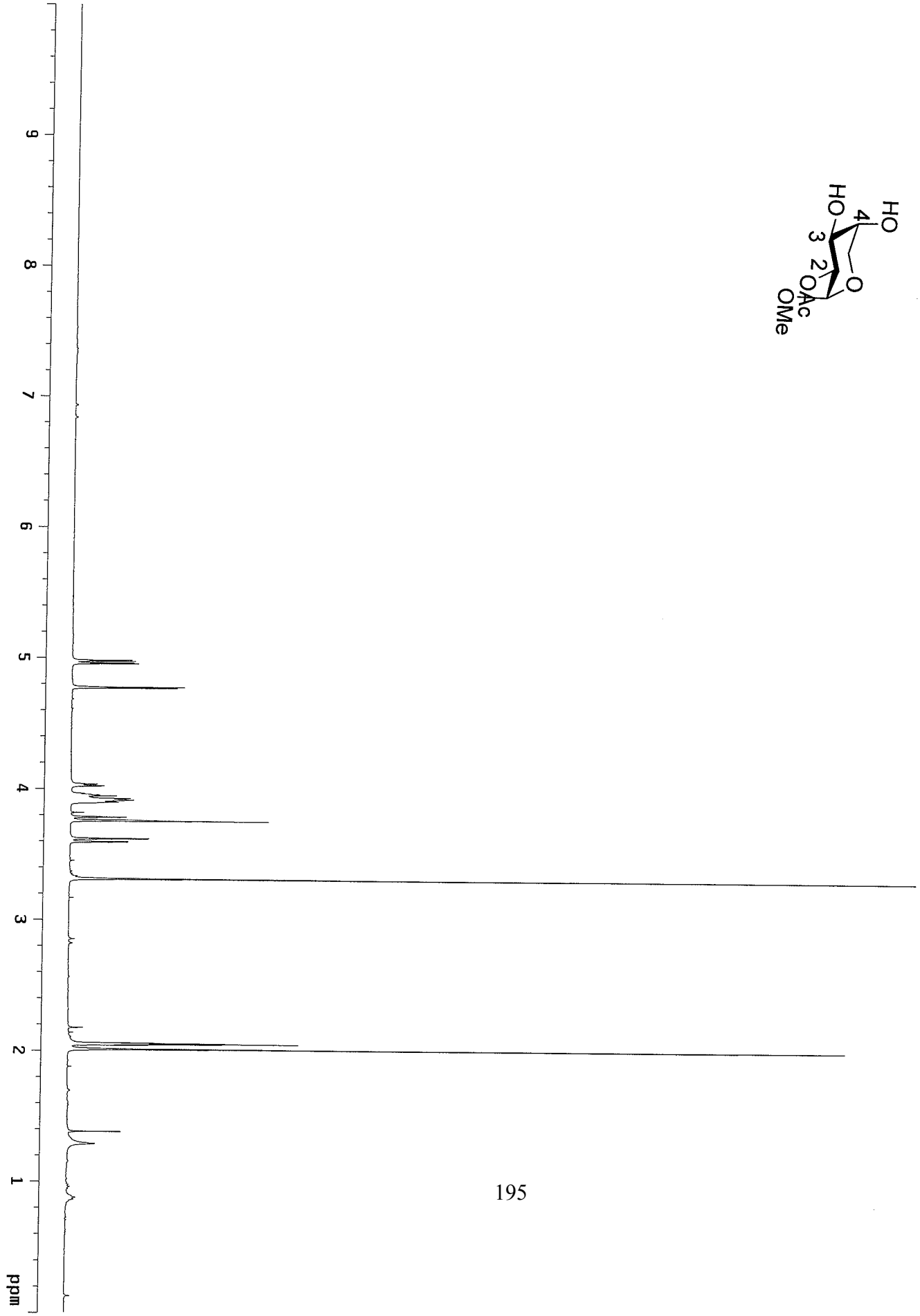
HO
HO
4
3
2
O
OAc
OMe
O
9
8
7
6
5
4
3
2
1
ppm

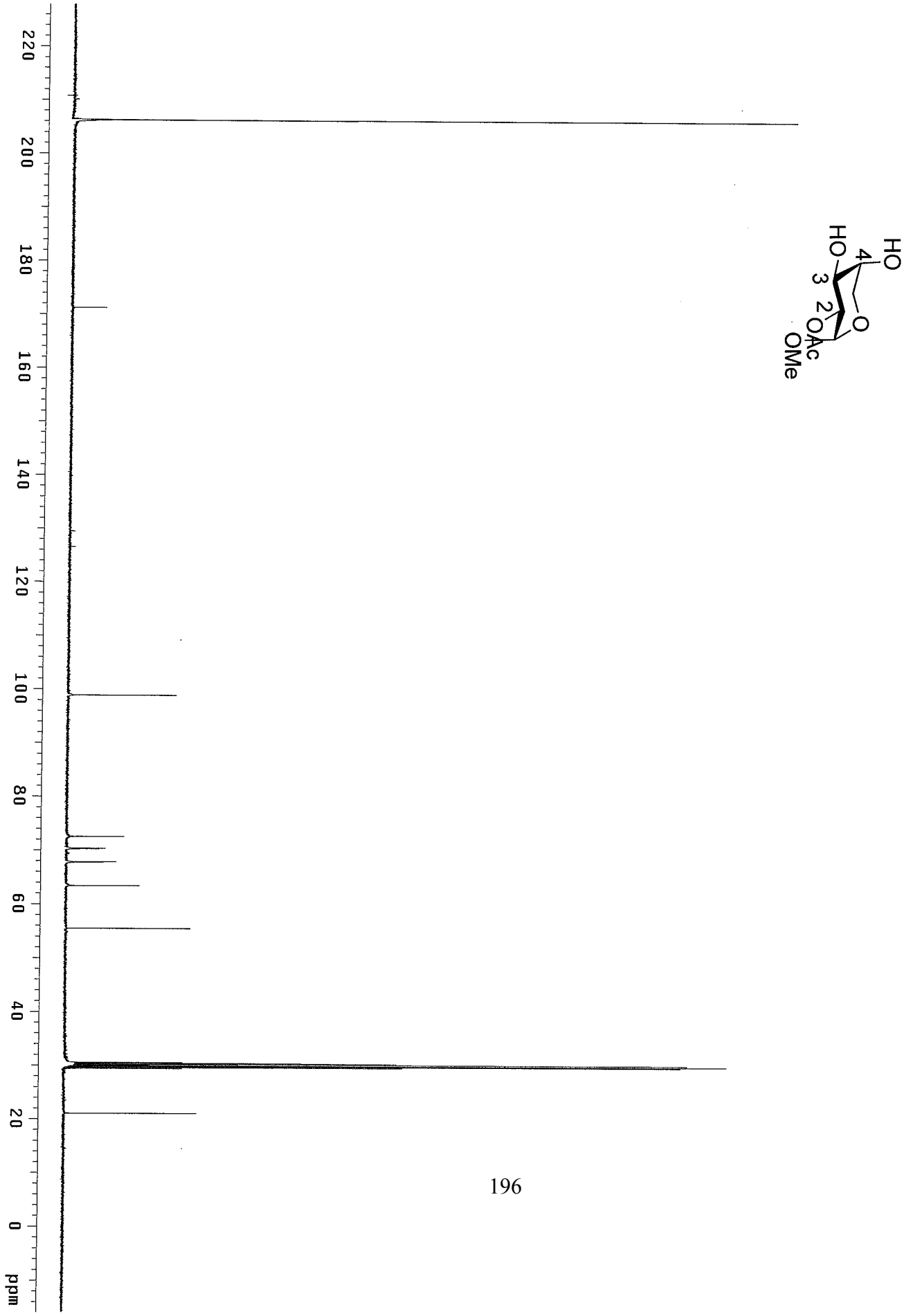
220
200
180
160
140
120
100
80
60
40
20
0
ppm
HO
4
HO
3
2
O
OAc
OMe

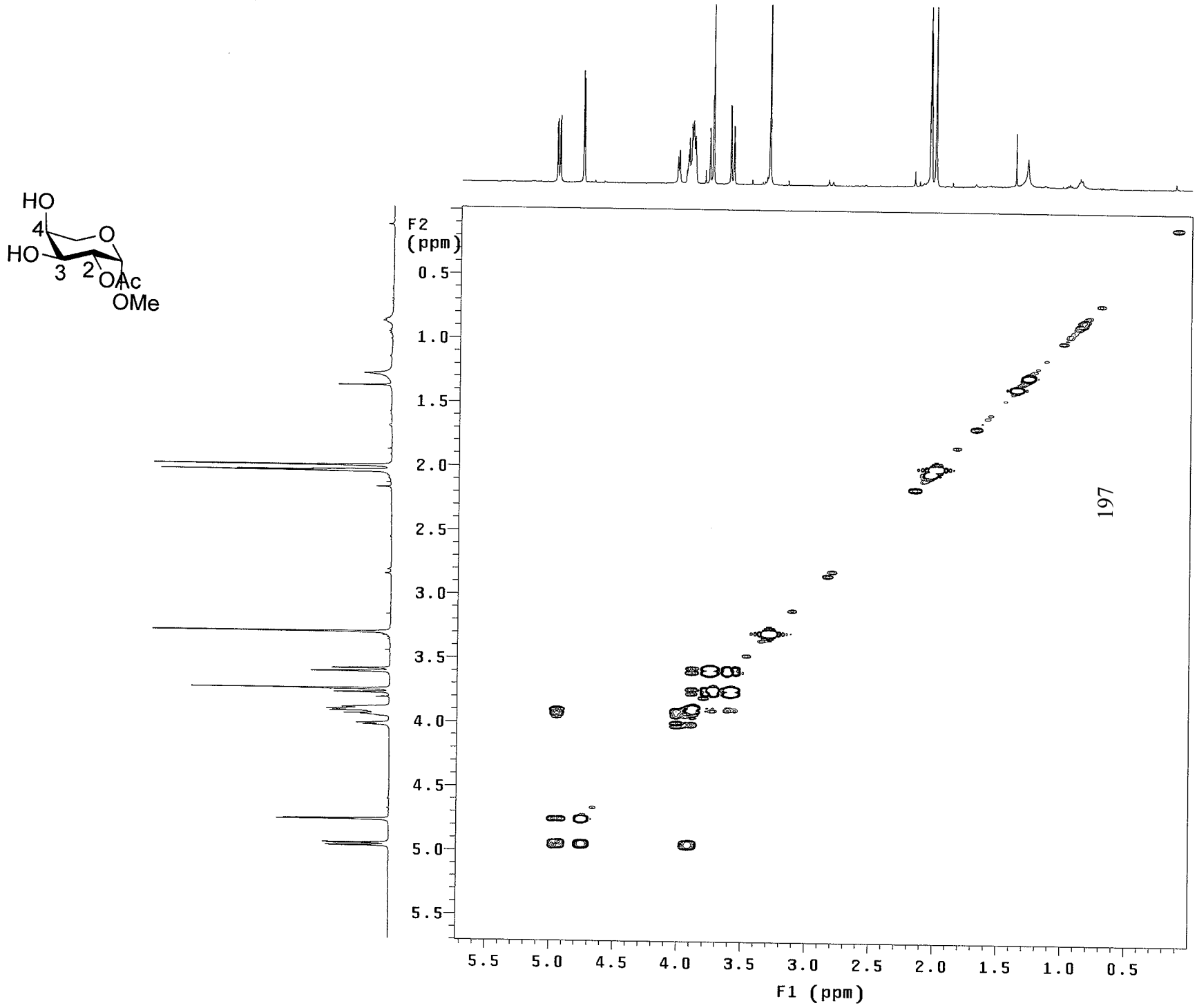
HO
4
O
HO
3
2
OAc
OMe
F2
(ppm)
0.5
1.0
1.5
2.0
2.5
3.0
3.5
4.0
4.5
5.0
5.5
5.5
5.0
4.5
4.0
3.5
3.0
2.5
2.0
1.5
1.0
0.5
F1 (ppm)
197

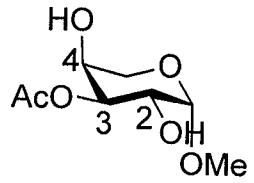

198

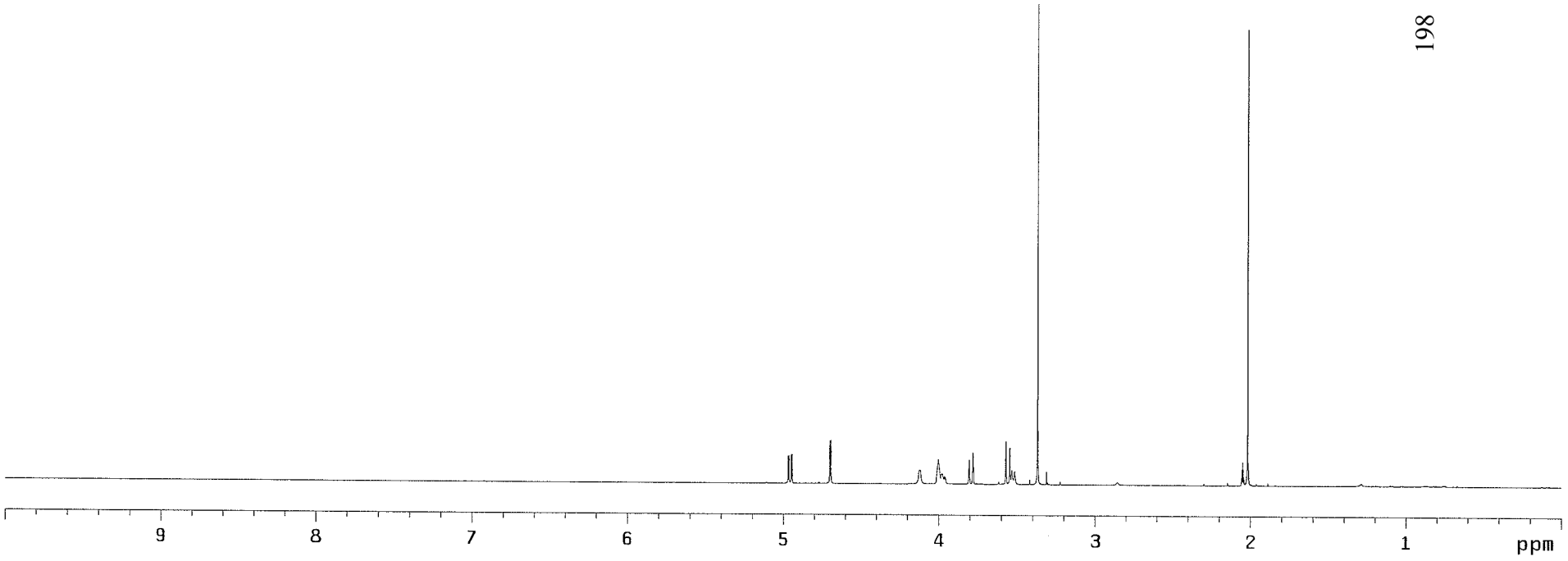

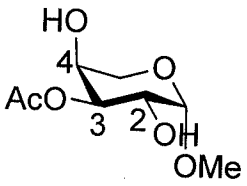

199

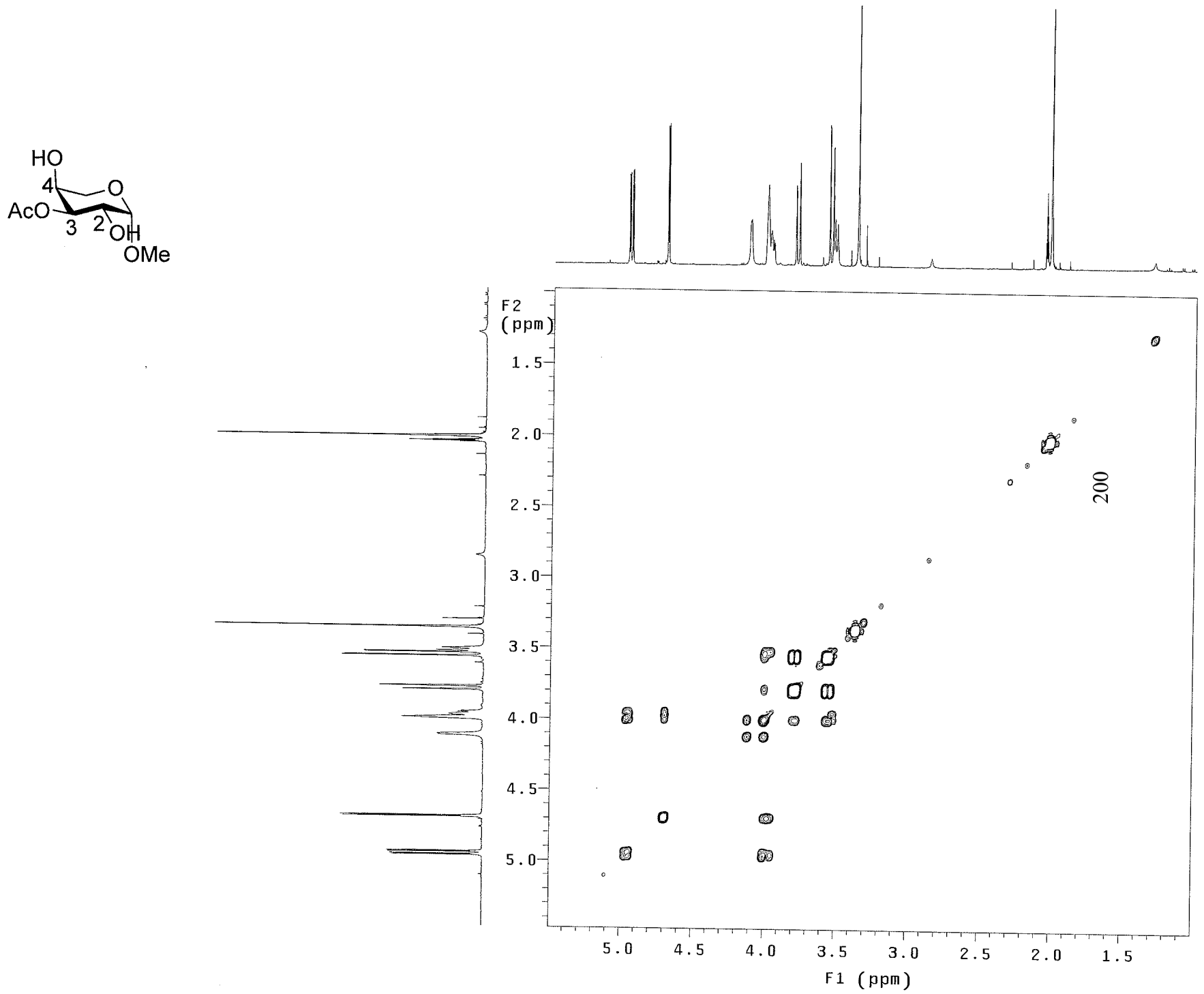
HO
4
O
AcO
3
2
OH
OMe
F2
(ppm)
1.5
2.0
2.5
3.0
3.5
4.0
4.5
5.0
200
5.0
4.5
4.0
3.5
3.0
2.5
2.0
1.5
F1 (ppm)

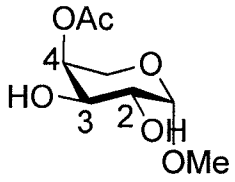

201

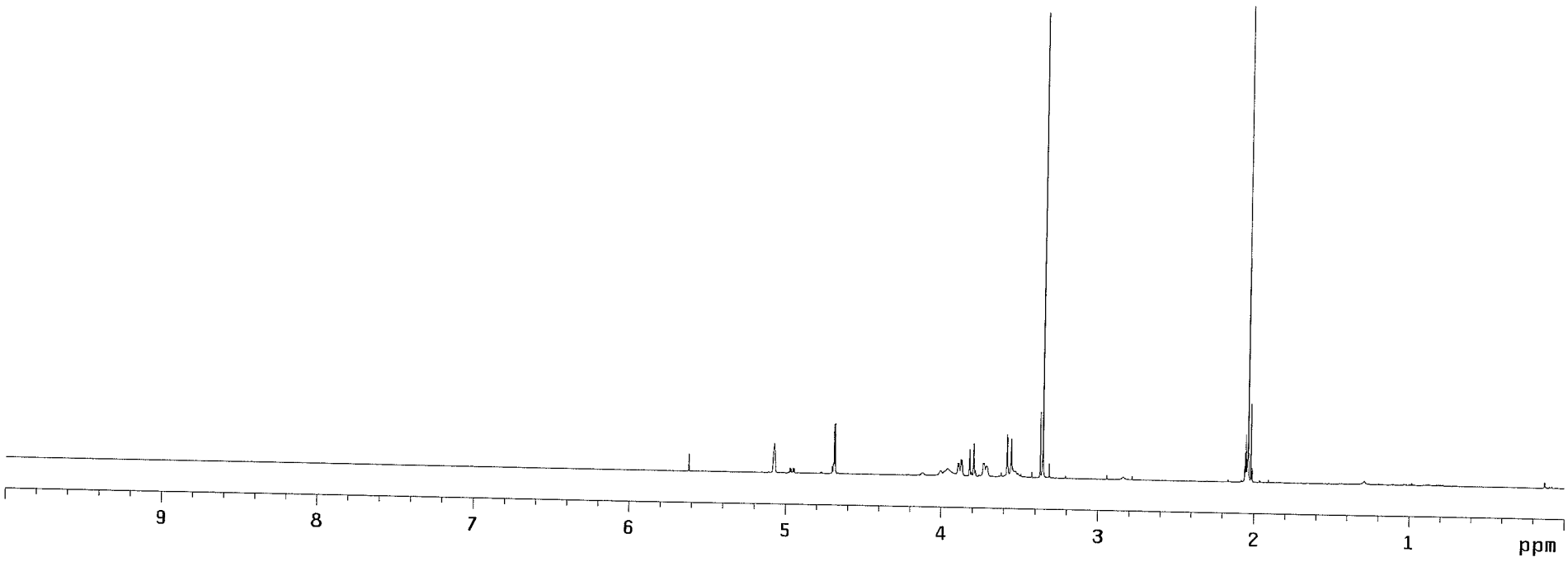

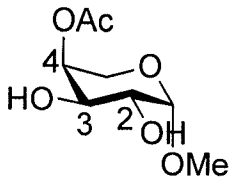

202

220 200 180 160 140 120 100 80 60 40 20 0 ppm

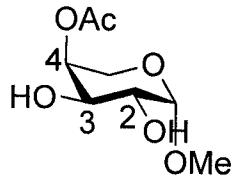
OAc
4
O
HO
3
2
OH
OMe

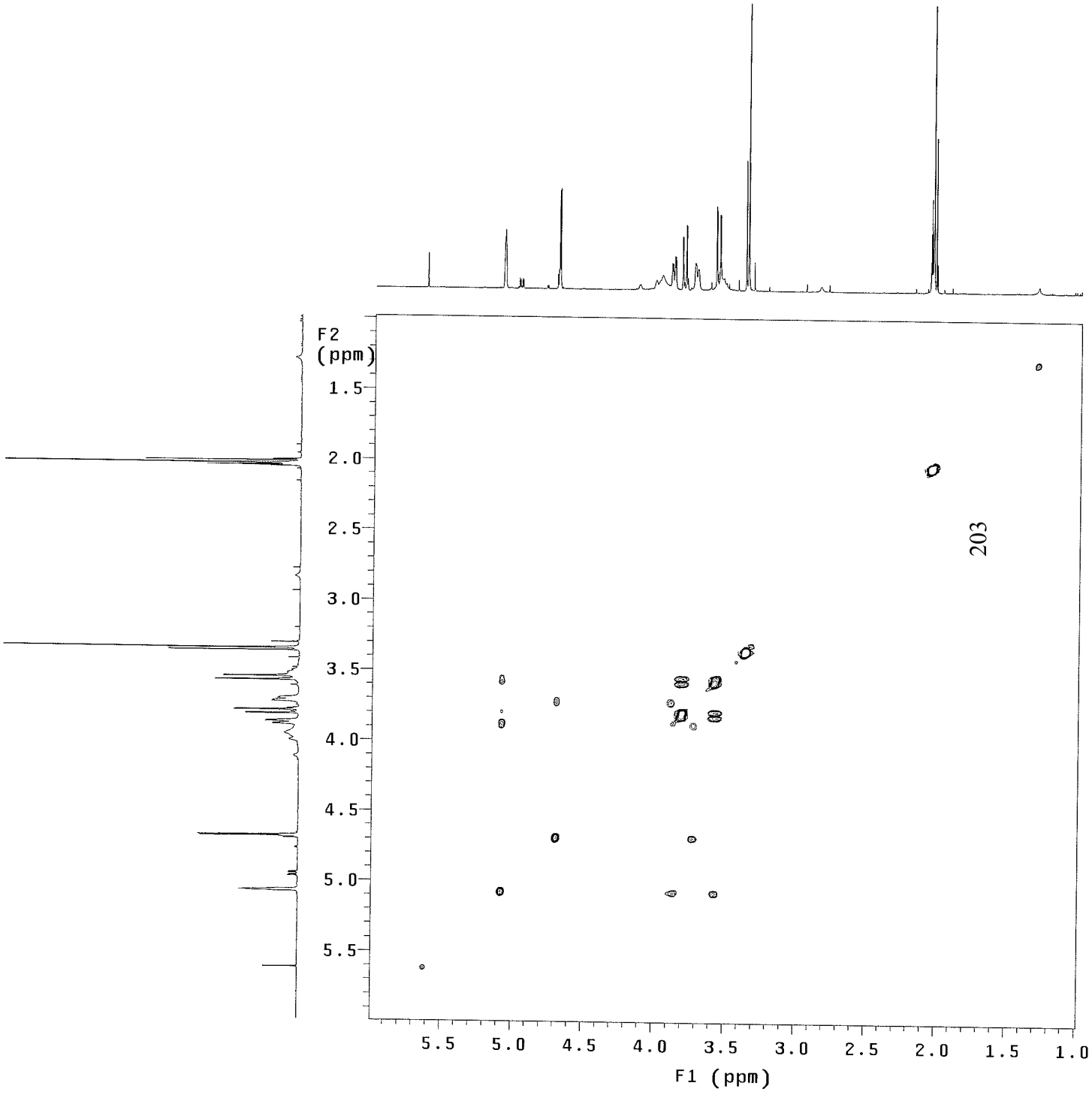
F2
(ppm)
1.5
2.0
2.5
3.0
3.5
4.0
4.5
5.0
5.5
203
5.5
5.0
4.5
4.0
3.5
3.0
2.5
2.0
1.5
1.0
F1 (ppm)

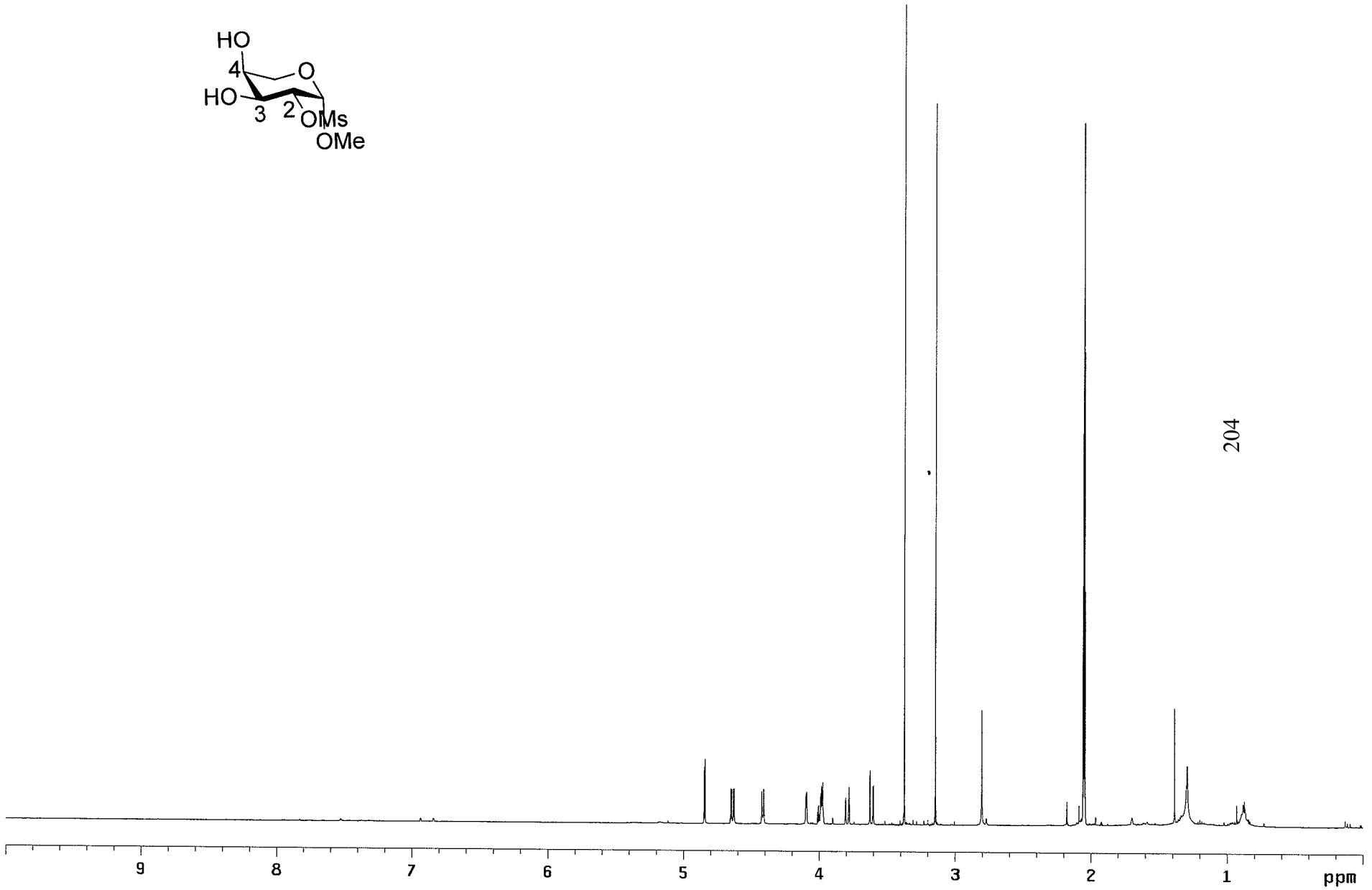
HO
4
O
HO
3
2
OMs
OMe
204
9
8
7
6
5
4
3
2
1
ppm

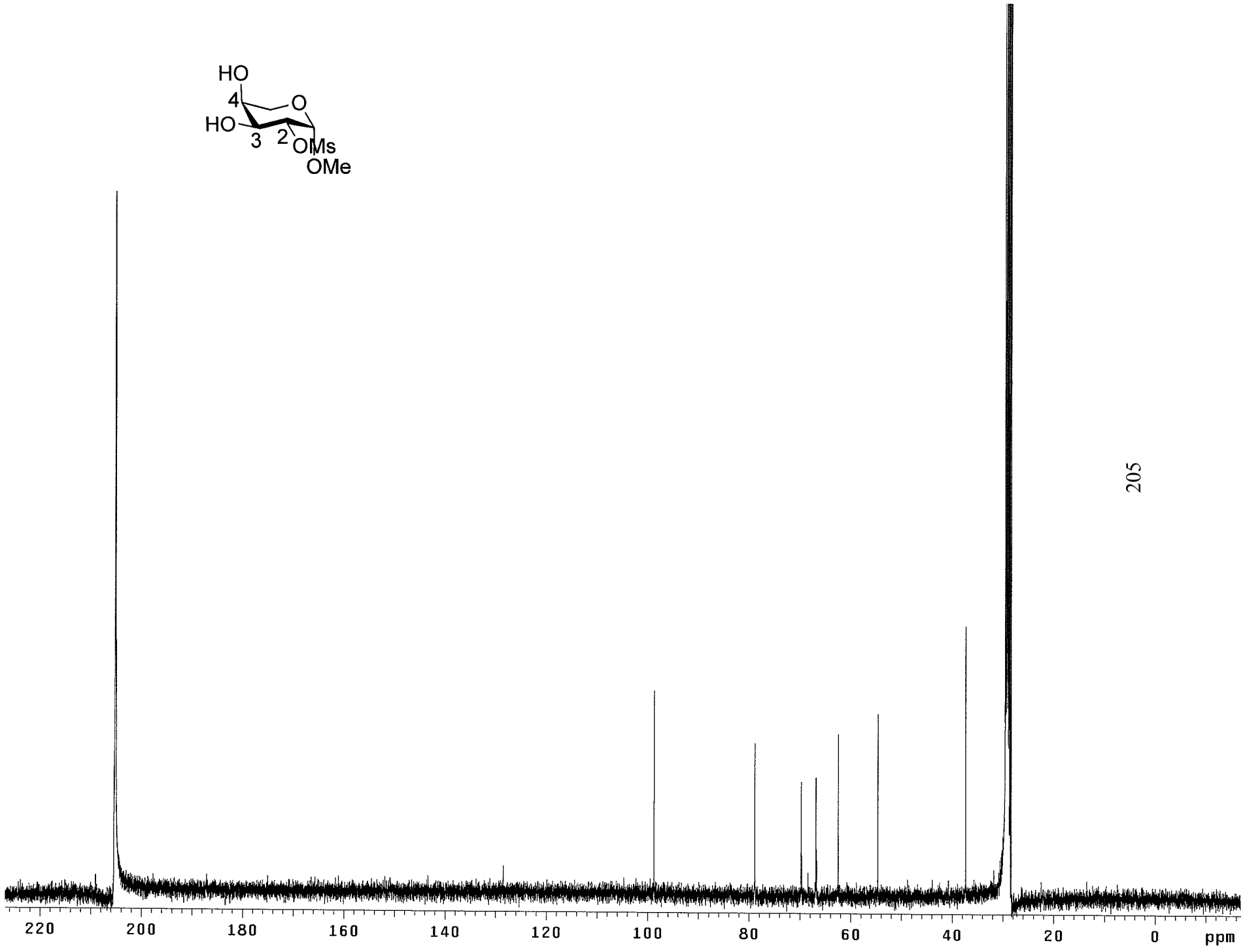
HO
4
O
HO
3
2
OMs
OMe
205
220
200
180
160
140
120
100
80
60
40
20
0
ppm

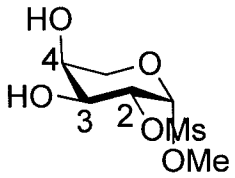
HO
4
O
HO
3
2
OMs
OMe

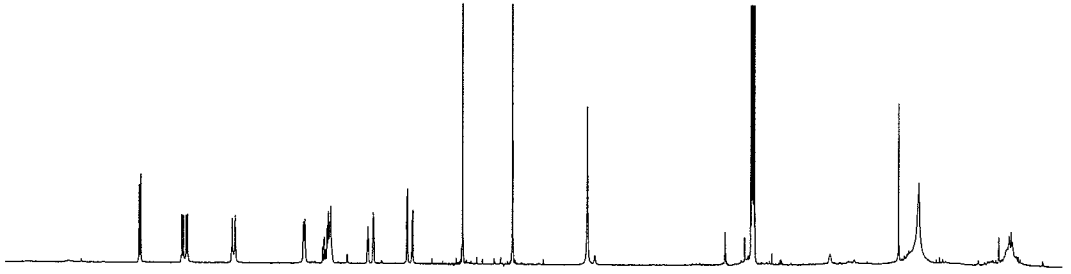

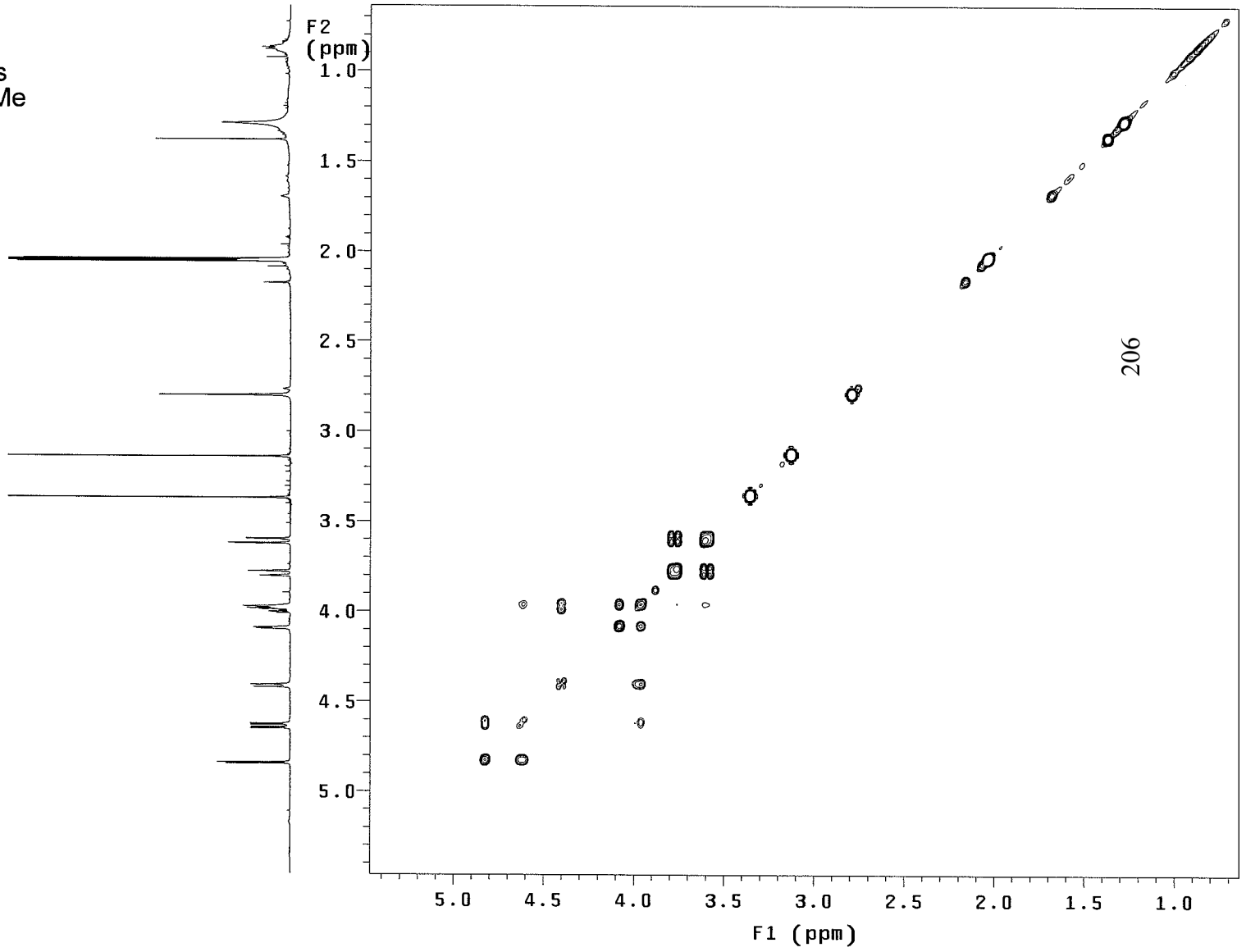
F2
(ppm)
1.0
1.5
2.0
2.5
3.0
3.5
4.0
4.5
5.0
5.0
4.5
4.0
3.5
3.0
2.5
2.0
1.5
1.0
F1 (ppm)
206

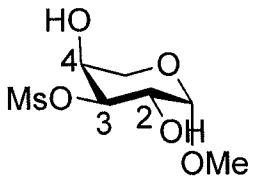

207

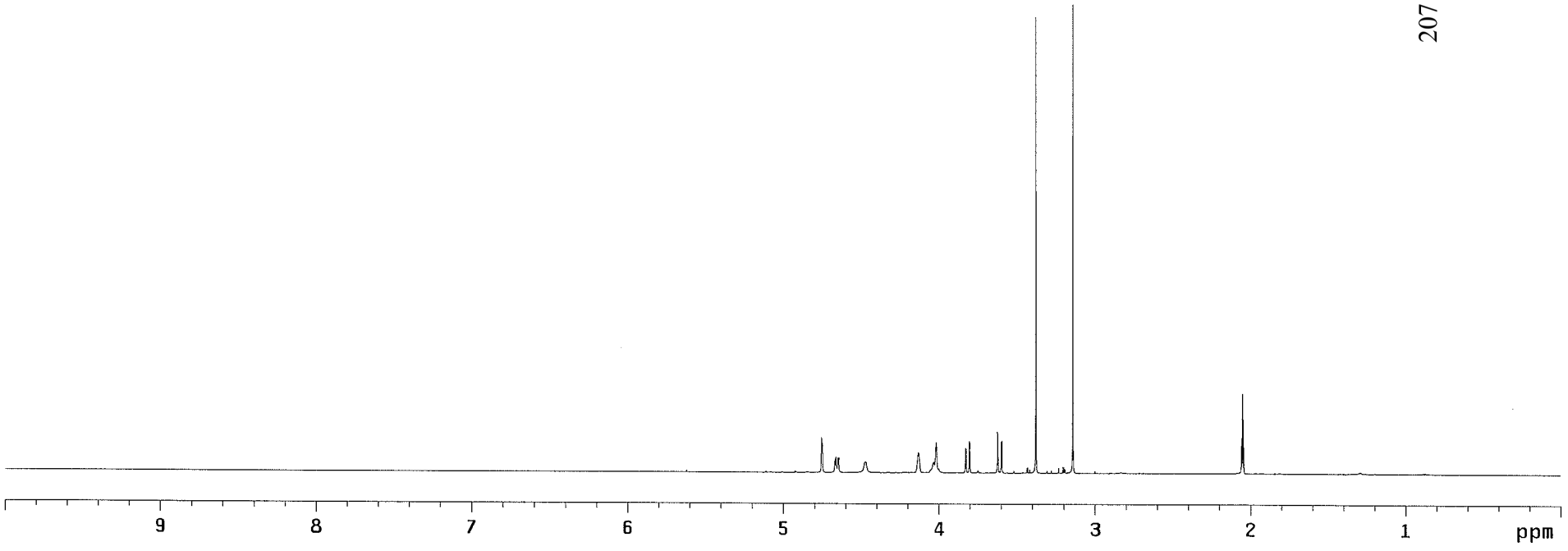

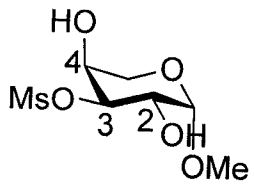

208

180 160 140 120 100 80 60 40 20 0 -20 ppm

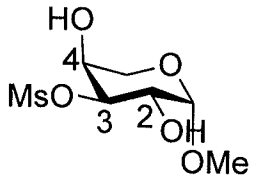
HO
4
O
MsO
3
2
OH
OMe

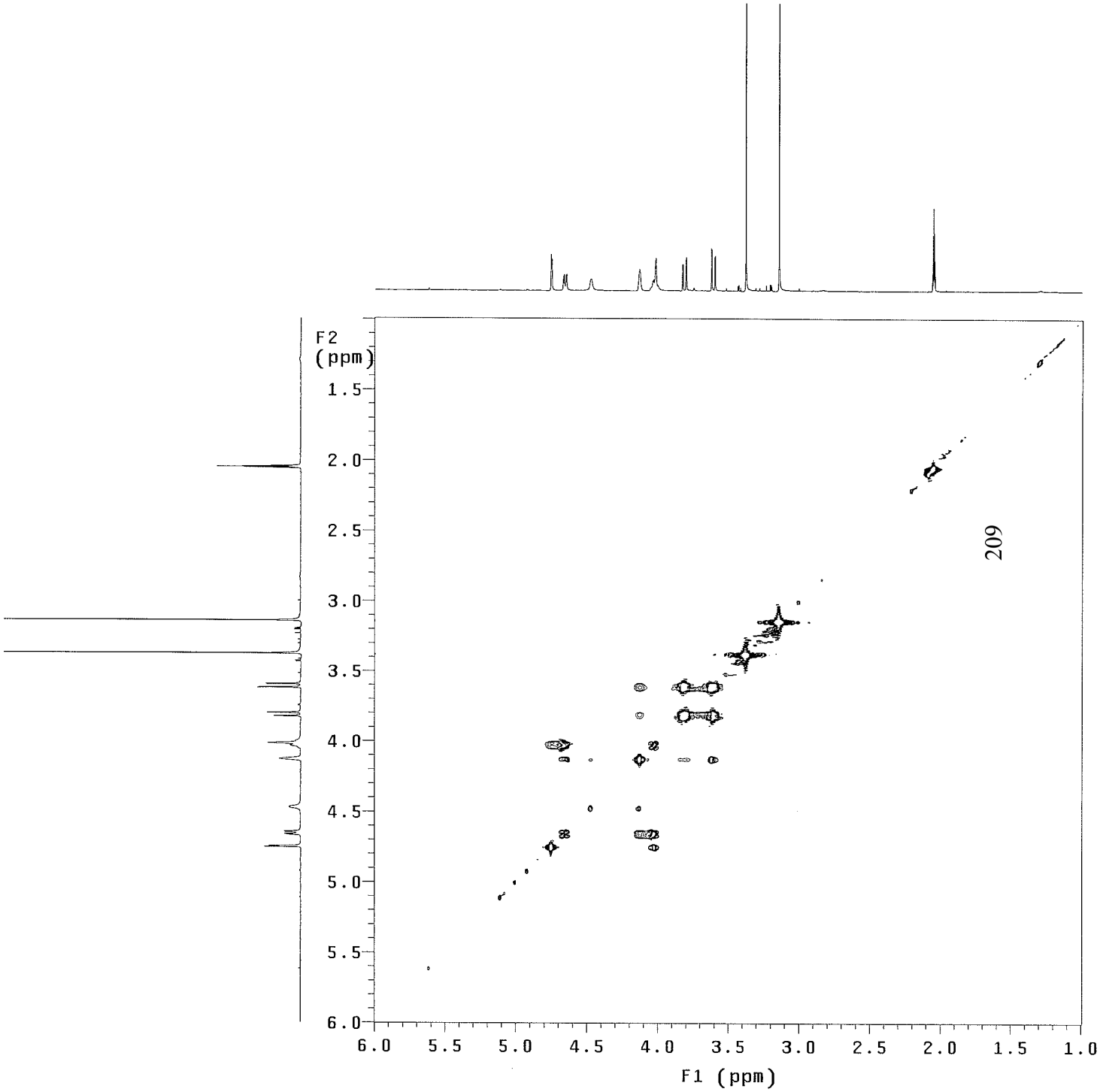
F2
(ppm)
1.5
2.0
2.5
3.0
3.5
4.0
4.5
5.0
5.5
6.0
6.0
5.5
5.0
4.5
4.0
3.5
3.0
2.5
2.0
1.5
1.0
F1 (ppm)
209

OMs
HO
4
3
2
O
OH
OMe

9
8
7
6
5
4
3
2
1
ppm

OMs
4
HO
3
2
O
OH
OMe
220
200
180
160
140
120
100
80
60
40
20
0
ppm

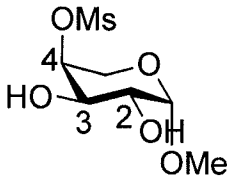
OMs
4
O
HO
3
2
OH
OMe

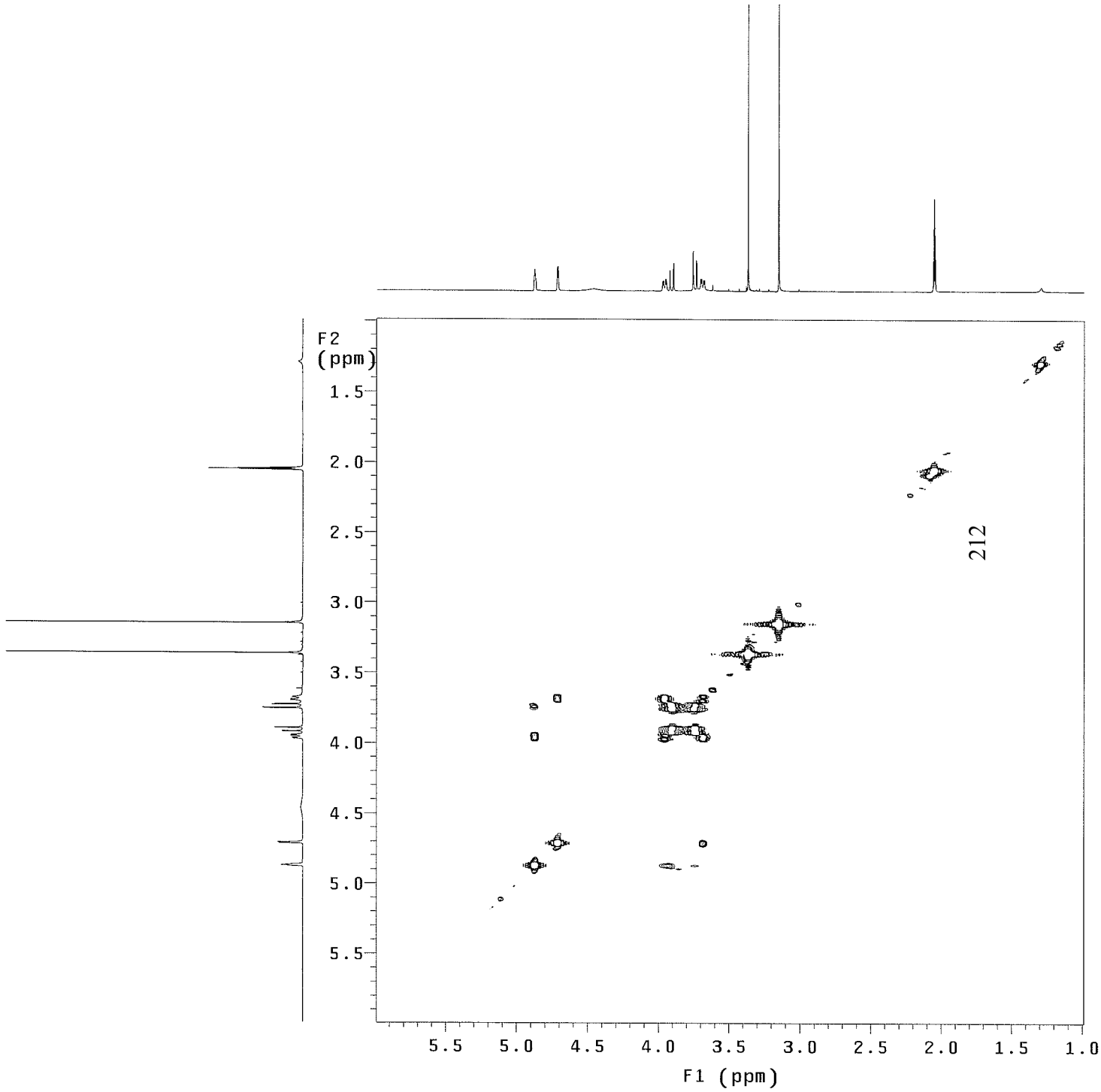
F2
(ppm)
1.5
2.0
2.5
3.0
3.5
4.0
4.5
5.0
5.5
212
5.5
5.0
4.5
4.0
3.5
3.0
2.5
2.0
1.5
1.0
F1 (ppm)

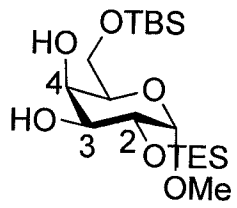

213

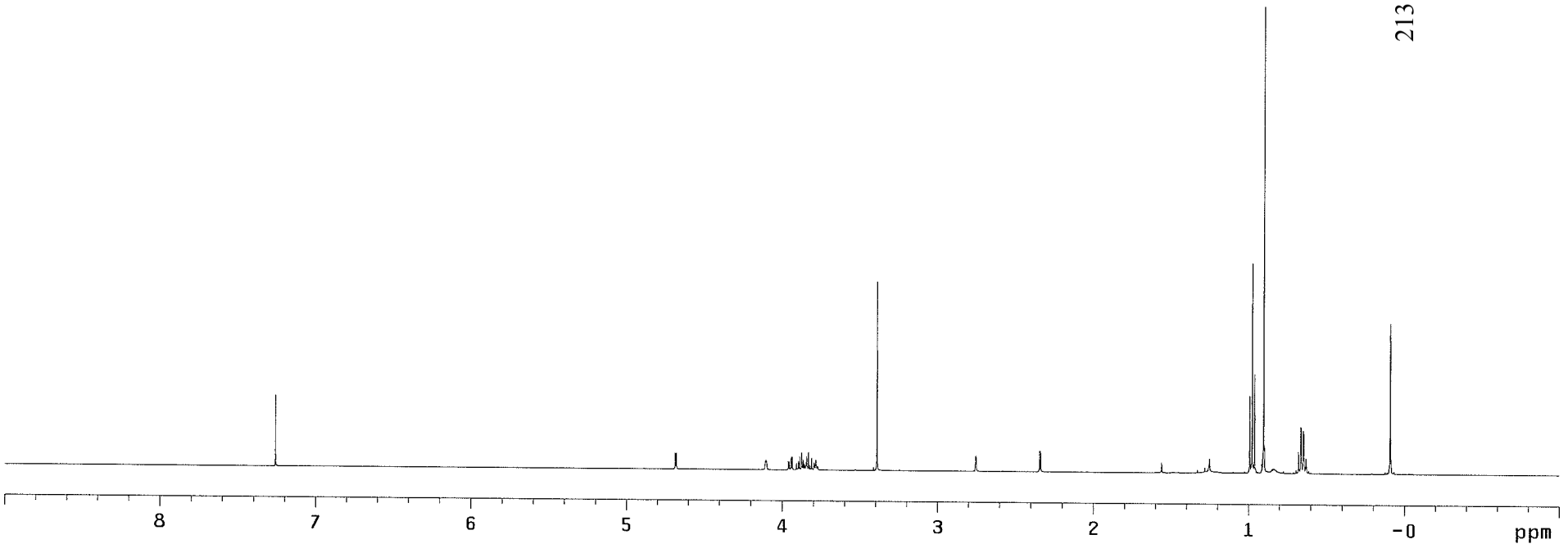

HO
OTBS
4
HO
3
2
O
OTES
OMe
220
200
180
160
140
120
100
80
60
40
20
0
ppm

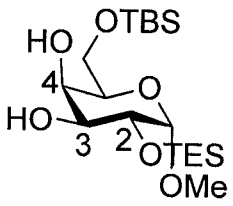
HO
OTBS
4
O
HO
3
2
OTES
OMe

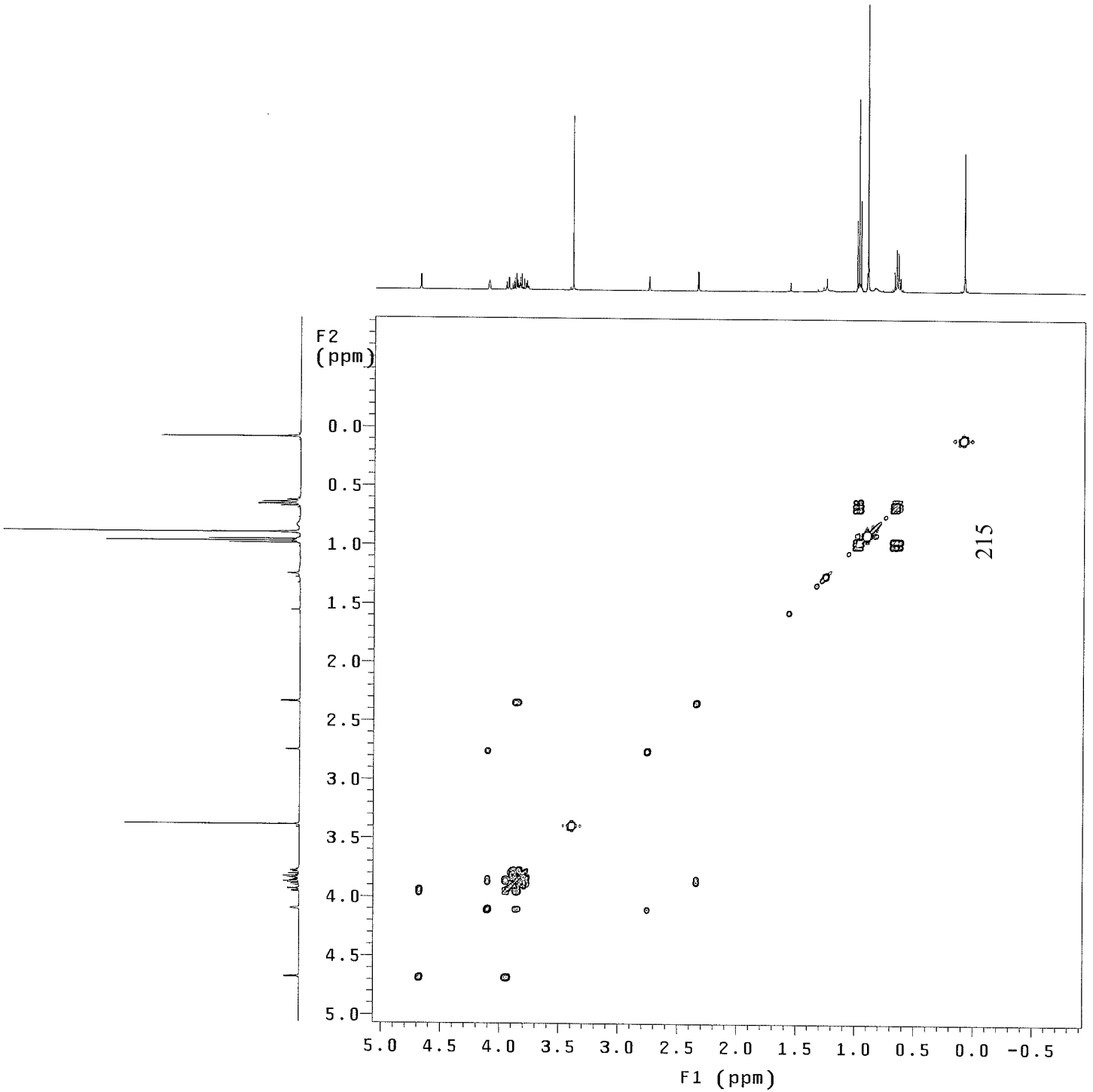
F2
(ppm)
0.0
0.5
1.0
1.5
2.0
2.5
3.0
3.5
4.0
4.5
5.0
5.0 4.5 4.0 3.5 3.0 2.5 2.0 1.5 1.0 0.5 0.0 -0.5
F1 (ppm)
215

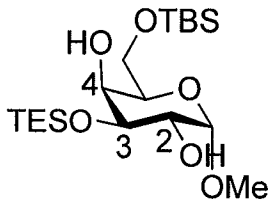
OTBS
HO
4
O
TESO
3
2
OH
OMe

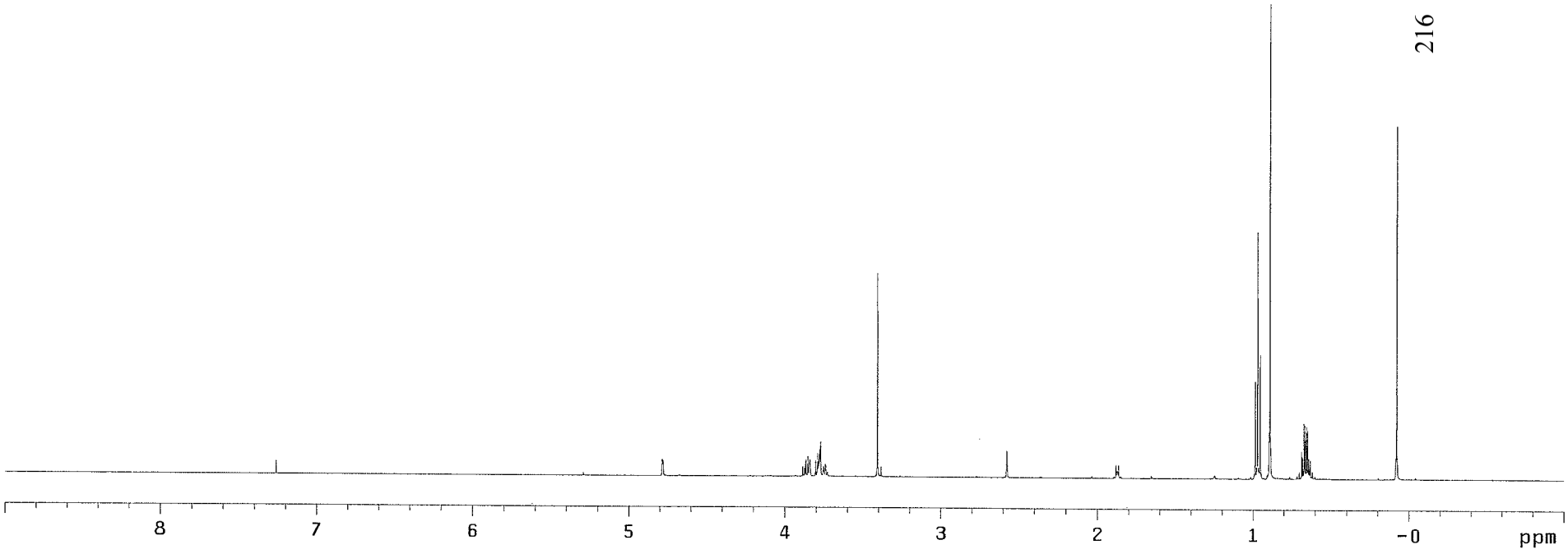
216
8
7
6
5
4
3
2
1
-0
ppm

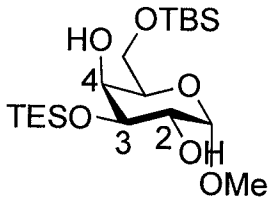
HO
OTBS
4
O
TESO
3
2
OH
OMe

217
220
200
180
160
140
120
100
80
60
40
20
0
ppm

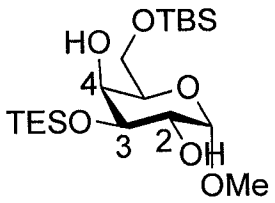
OTBS
HO
4
O
TESO
3
2
OH
OMe

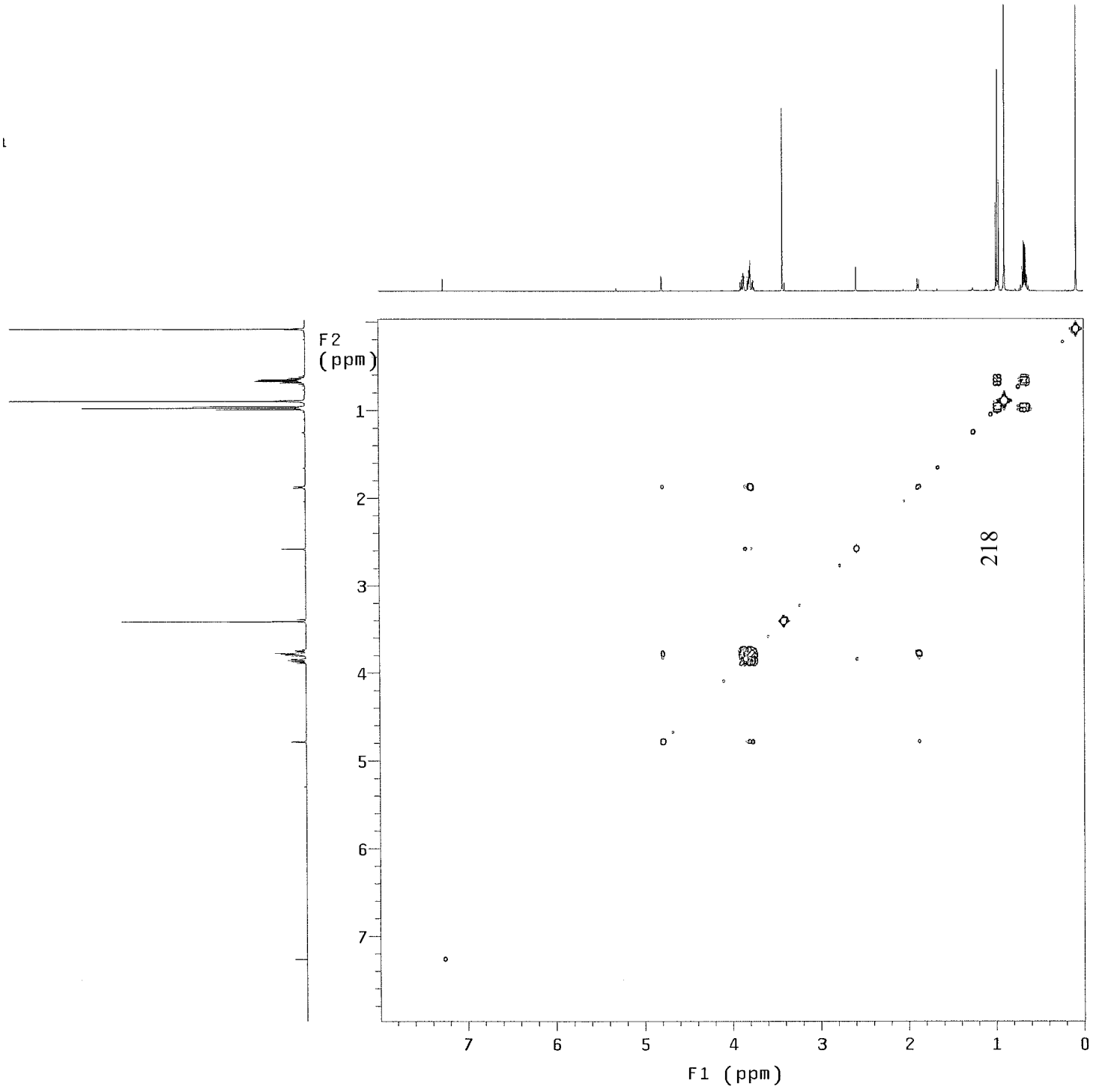
F2
(ppm)
1
2
3
4
5
6
7
218
7
6
5
4
3
2
1
0
F1 (ppm)

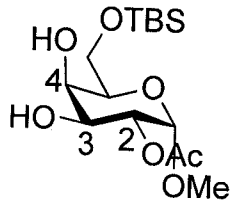
HO
OTBS
4
O
HO
3
2
OAc
OMe

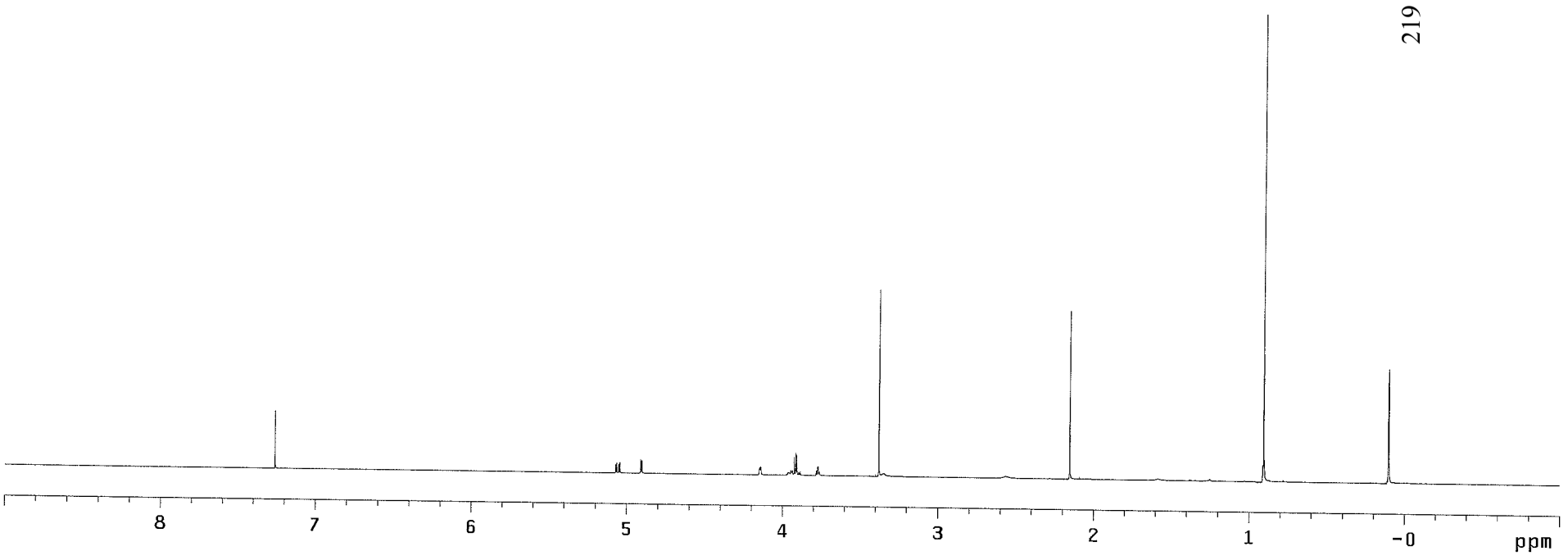
219
8
7
6
5
4
3
2
1
-0
ppm

HO
OTBS
4
HO
3
2
O
OAc
OMe
220
200
180
160
140
120
100
80
60
40
20
0
ppm

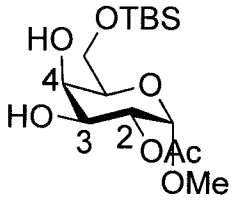
OTBS
HO
4
O
HO
3
2
OAc
OMe

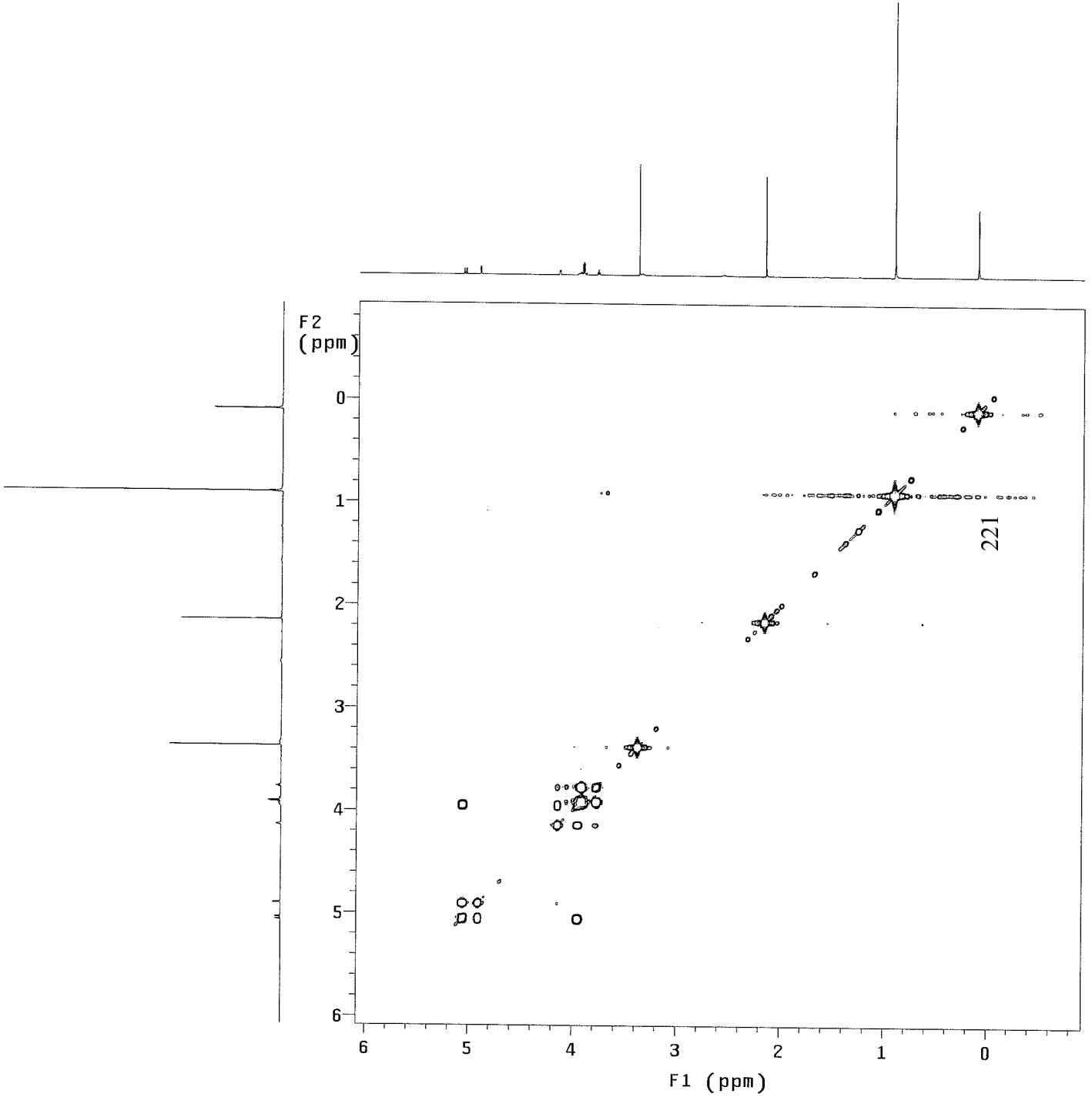
F2
(ppm)
0
1
2
3
4
5
6
221
6
5
4
3
2
1
0
F1 (ppm)

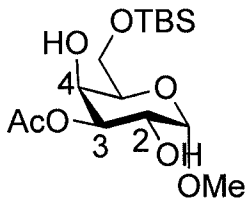
HO
OTBS
4
O
AcO
3
2
OH
OMe

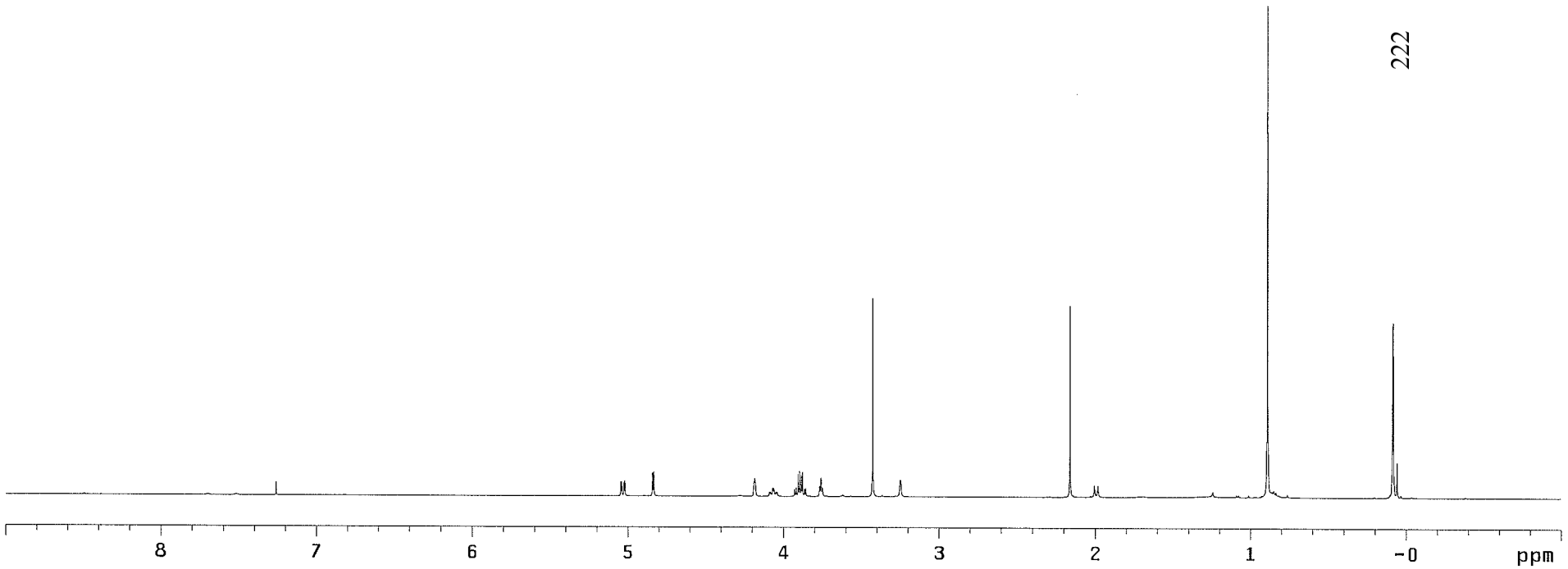
222
8
7
6
5
4
3
2
1
-0
ppm

220
200
180
160
140
120
100
80
60
40
20
0
ppm

HO
OTBS
4
AcO
3
2
O
OH
OMe

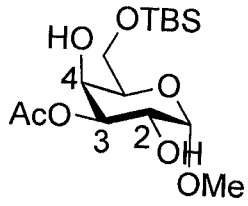
HO
OTBS
4
O
AcO
3
2
OH
OMe

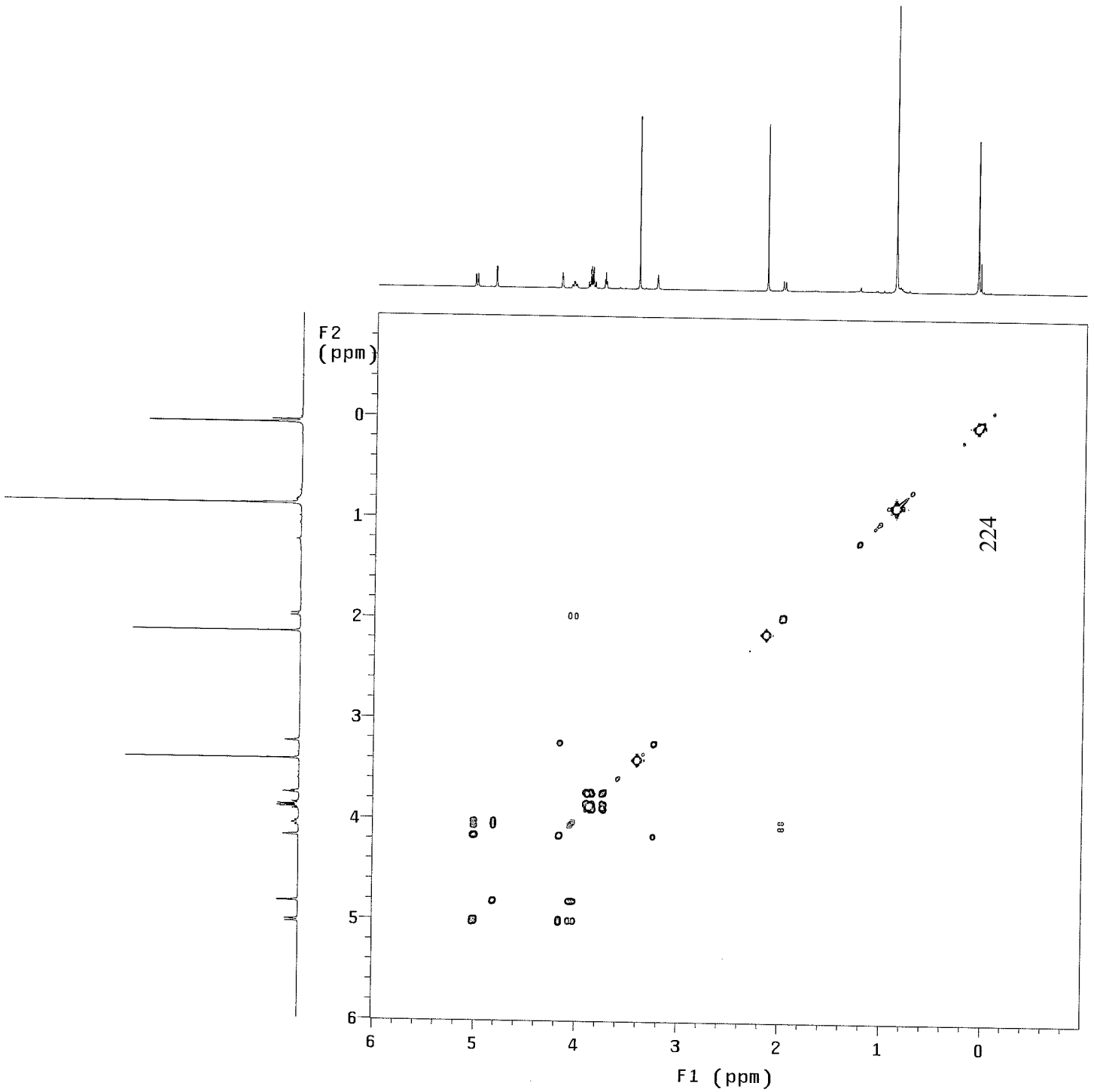
F2
(ppm)
0
1
2
3
4
5
6
224
F1 (ppm)

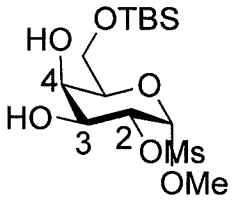
OTBS
HO
4
O
HO
3
2
OMs
OMe

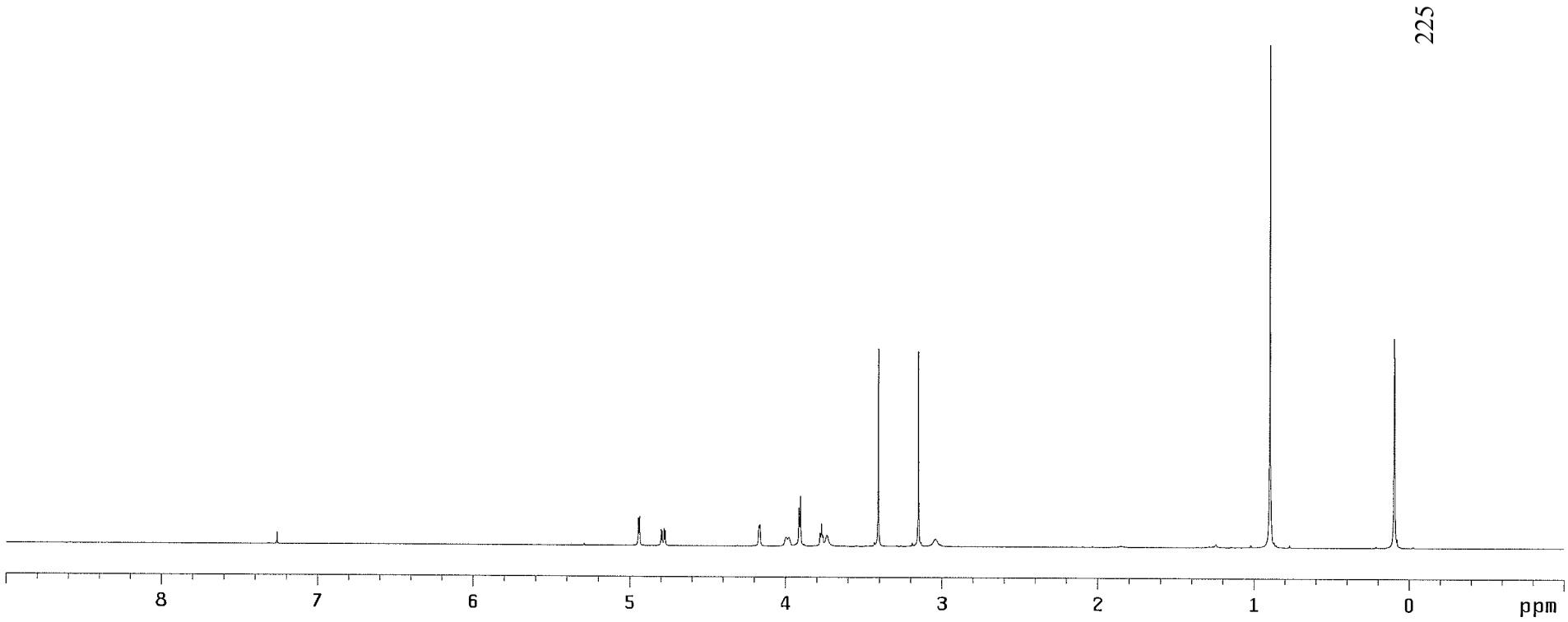
225
8
7
6
5
4
3
2
1
0
ppm

HO
OTBS
4
HO
3
2
O
OMs
OMe
220
200
180
160
140
120
100
80
60
40
20
0
ppm

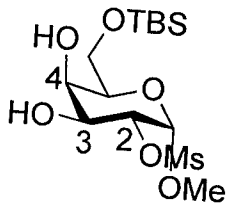
HO
OTBS
4
O
HO
3
2
OMs
OMe

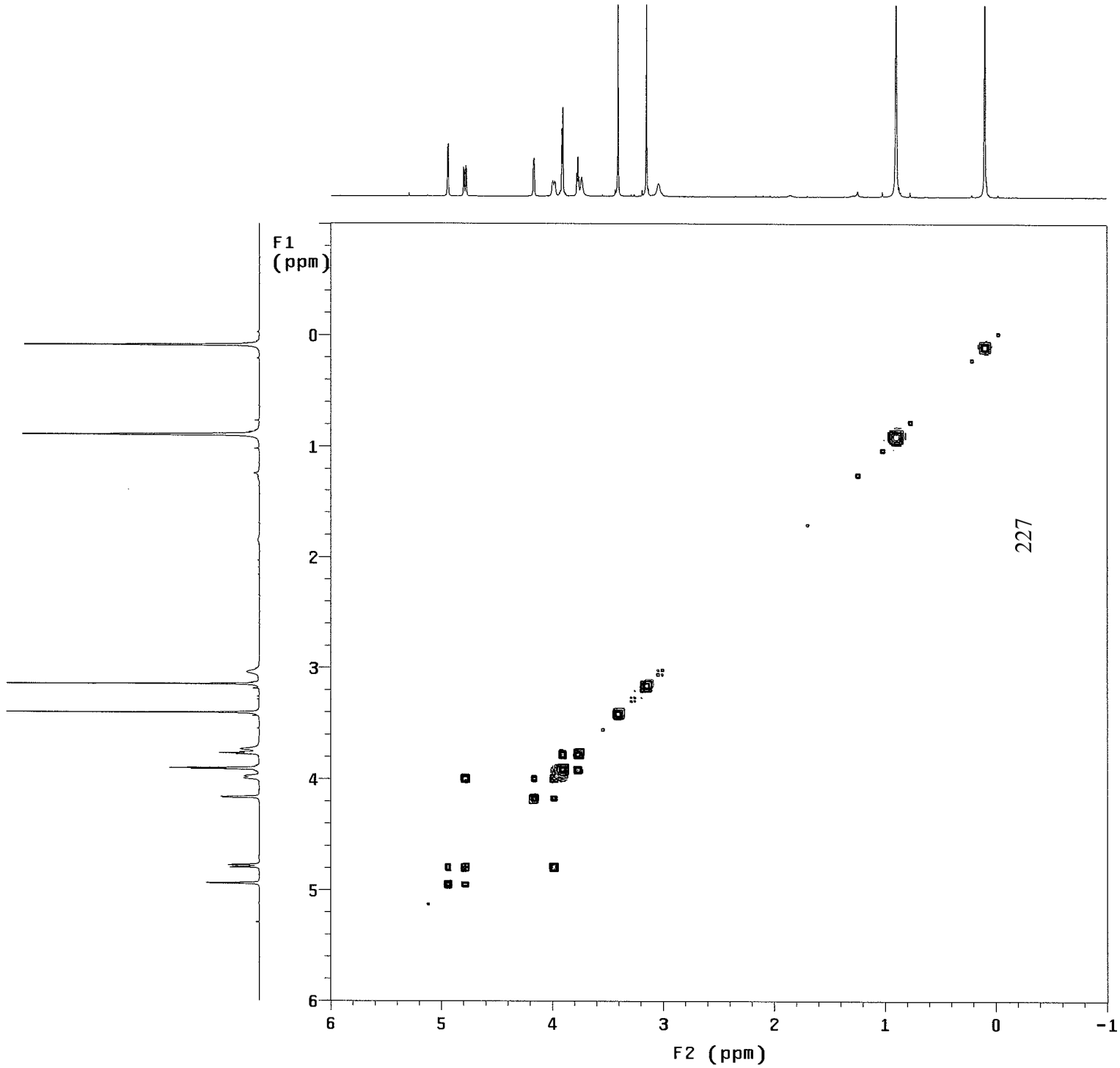
F1
(ppm)
0
1
2
3
4
5
6
F2 (ppm)
6
5
4
3
2
1
0
-1
227

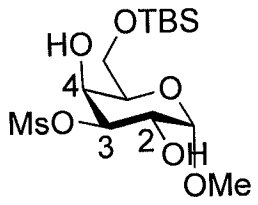
OTBS
HO
4
O
MsO
3
2
OH
OMe

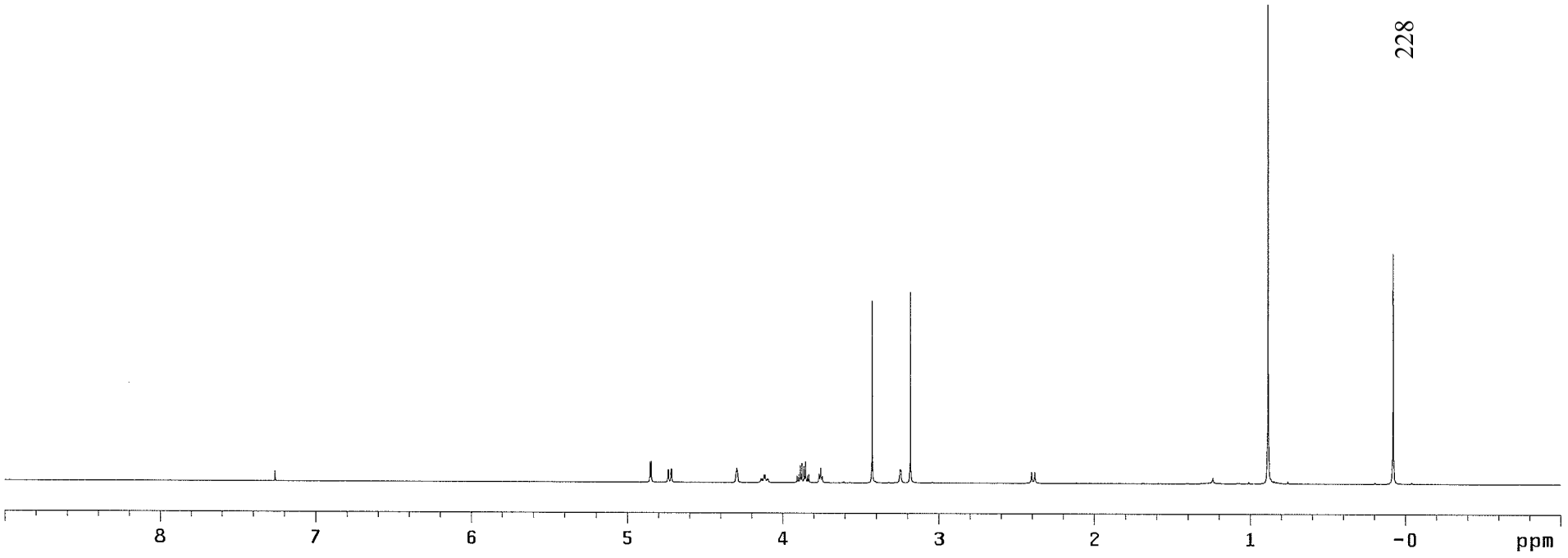
228
8
7
6
5
4
3
2
1
-0
ppm

MsO
HO
OTBS
OMe
O
4
3
2
OH
H
220
200
180
160
140
120
100
80
60
40
20
0
ppm

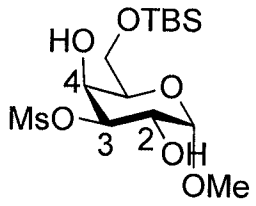
OTBS
HO
4
O
MsO
3
2
OH
OMe

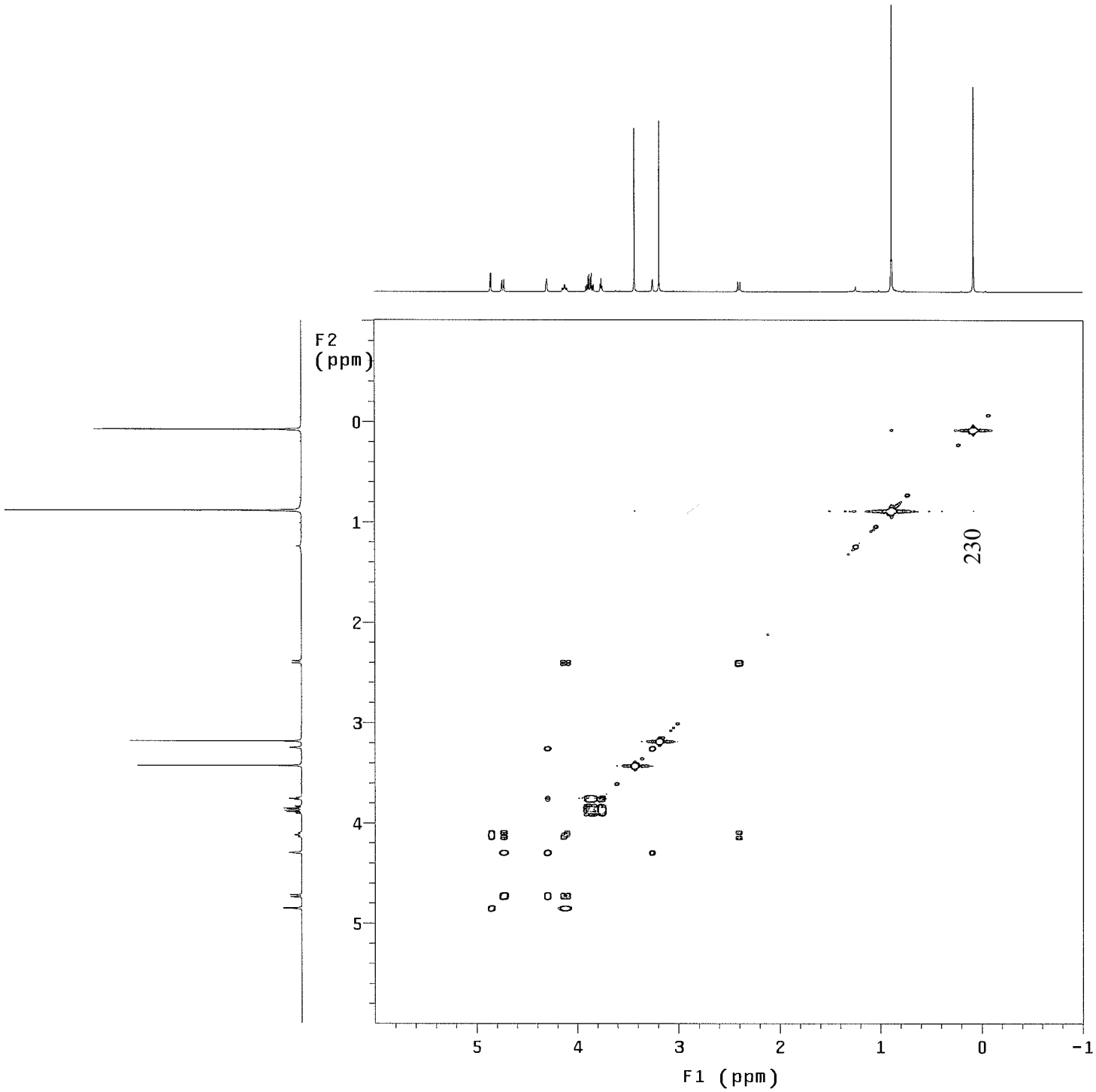
F2
(ppm)
0
1
2
3
4
5
230
5
4
3
2
1
0
-1
F1 (ppm)

HO
HO
4
3
2
OTES
9
8
7
6
5
4
3
2
1
ppm

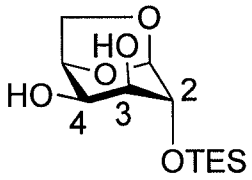
O
HO
O
HO
2
4
3
OTES

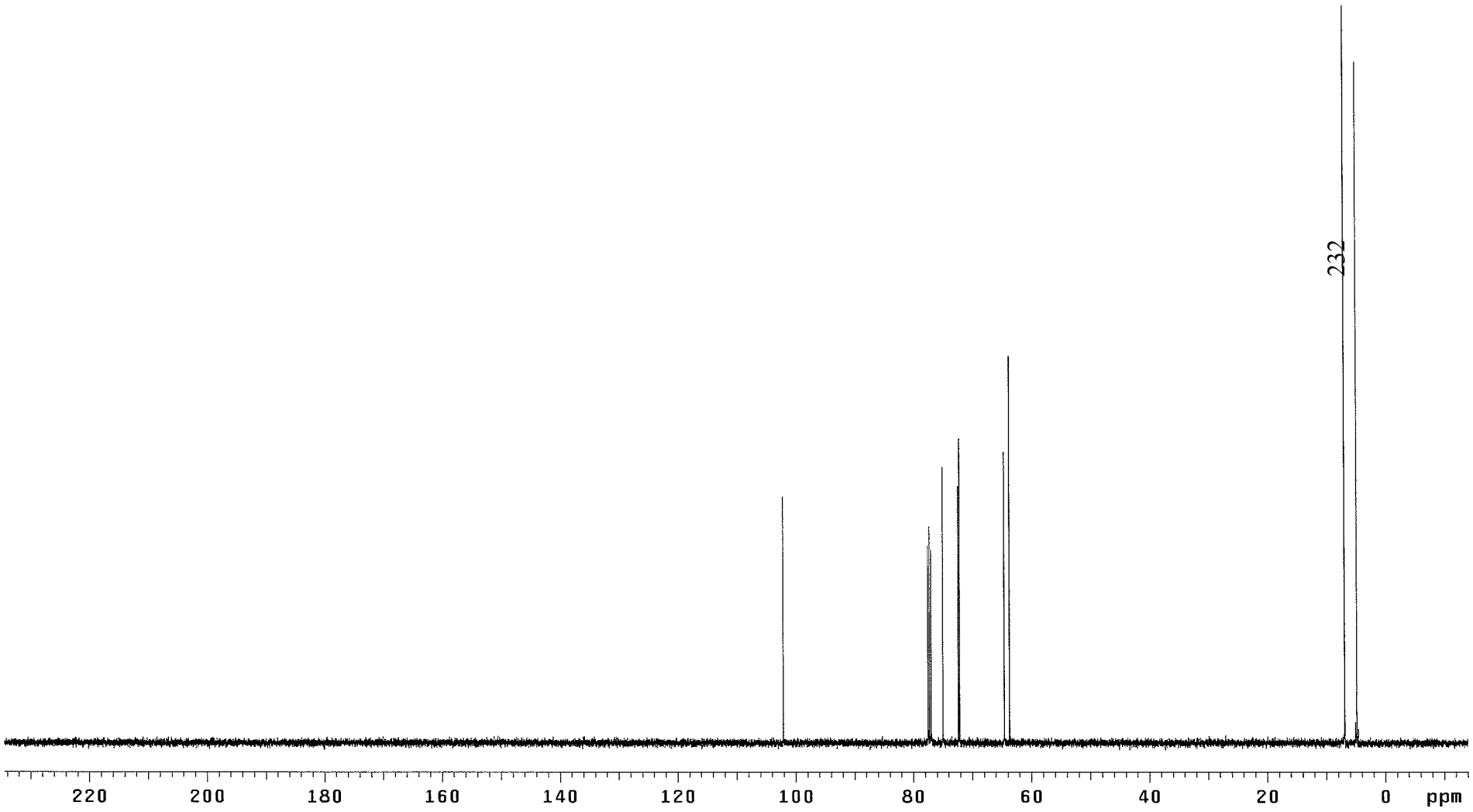
232
220
200
180
160
140
120
100
80
60
40
20
0
ppm

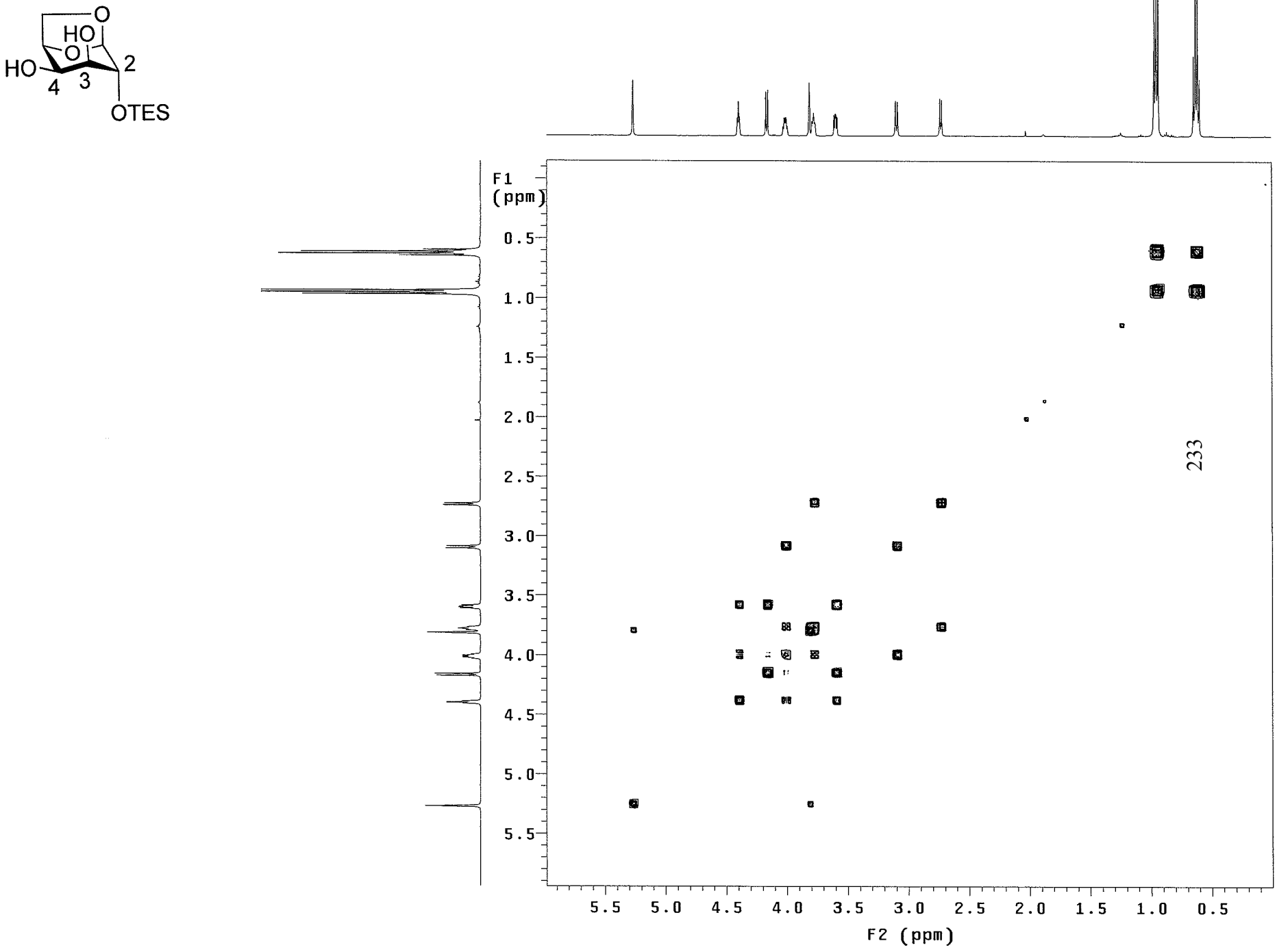
O
HO
O
HO
2
4
3
OTES
F1
(ppm)
0.5
1.0
1.5
2.0
2.5
3.0
3.5
4.0
4.5
5.0
5.5
5.5
5.0
4.5
4.0
3.5
3.0
2.5
2.0
1.5
1.0
0.5
F2 (ppm)
233

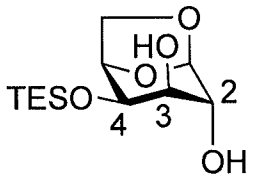

234

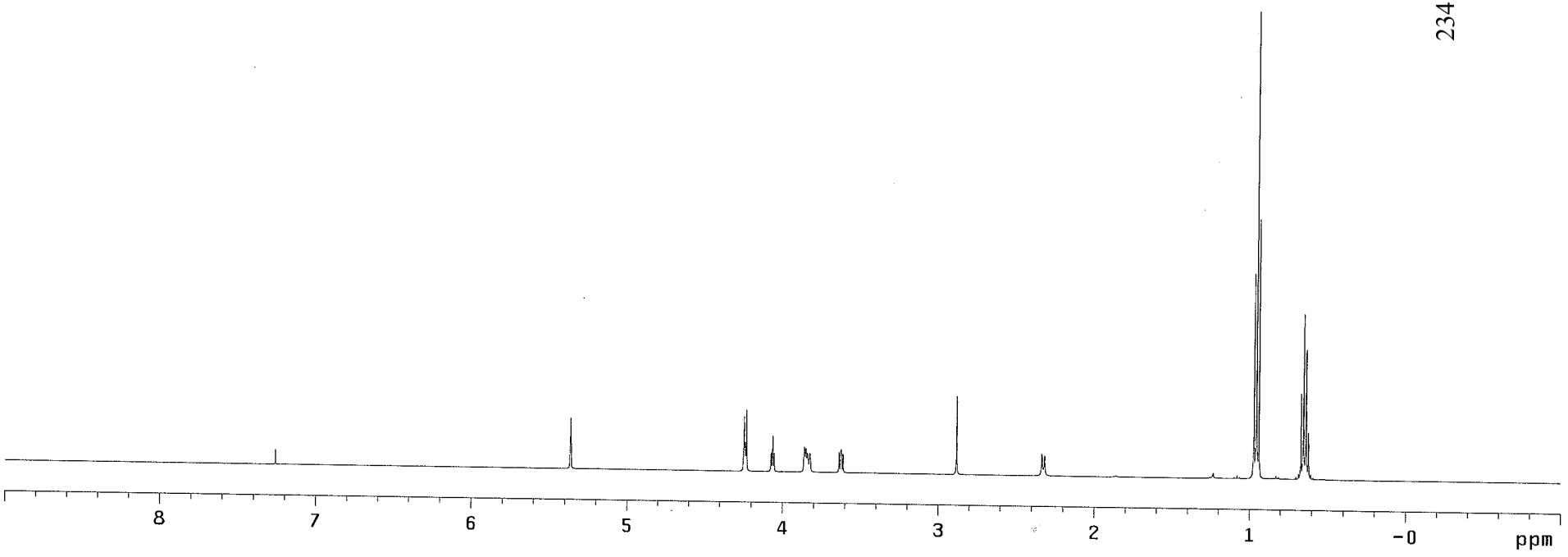

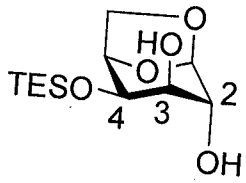
O
HO
O
TESO
4
3
2
OH

235
220
200
180
160
140
120
100
80
60
40
20
0
ppm

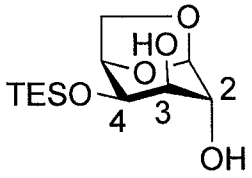
O
HO
O
TESO
2
4
3
OH

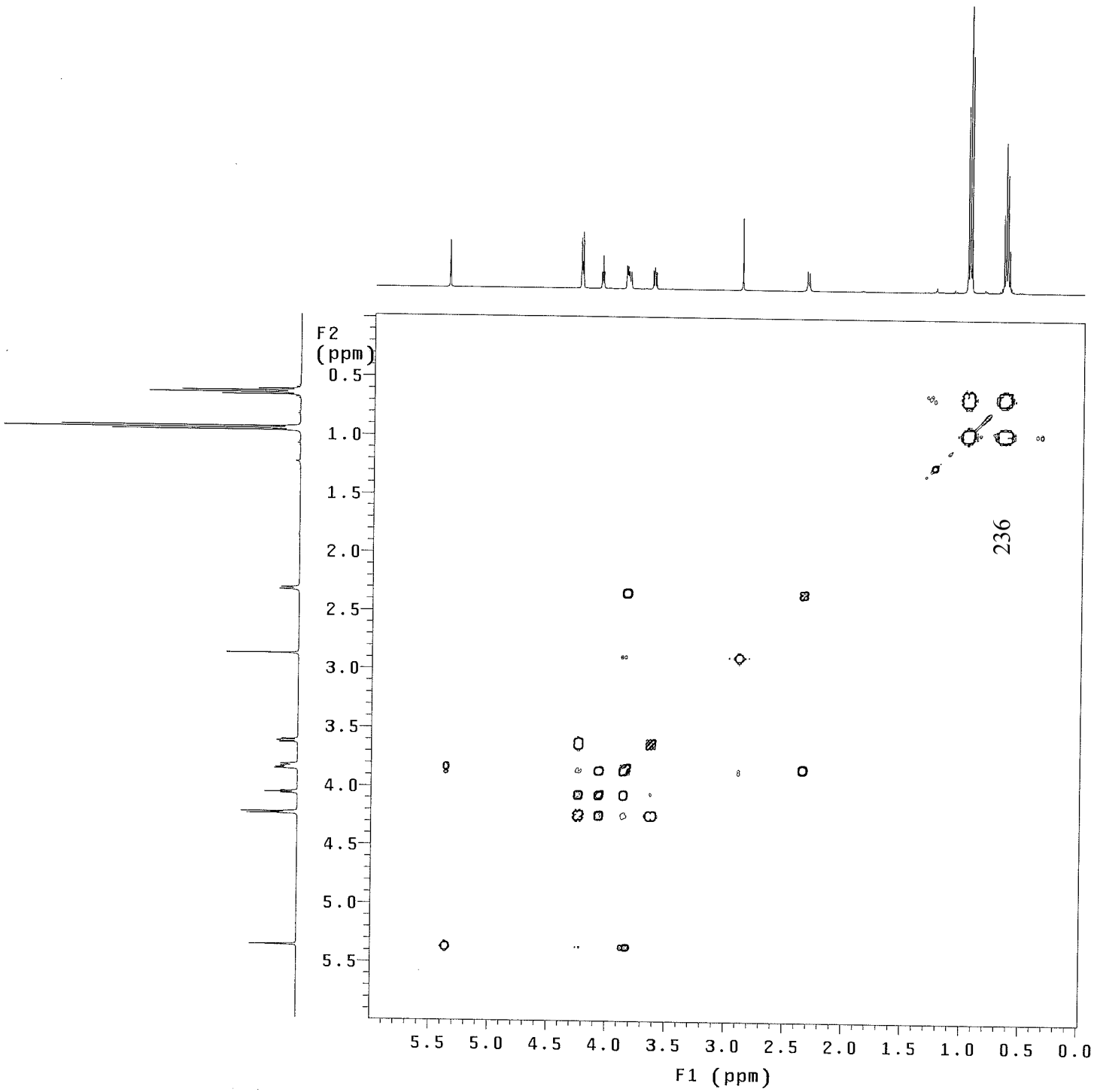
F2
(ppm)
0.5
1.0
1.5
2.0
2.5
3.0
3.5
4.0
4.5
5.0
5.5
5.5 5.0 4.5 4.0 3.5 3.0 2.5 2.0 1.5 1.0 0.5 0.0
F1 (ppm)
236

HO
HO
O
4
3
2
OAc

9
8
7
6
5
4
3
2
1
ppm

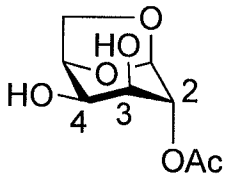

238

220 200 180 160 140 120 100 80 60 40 20 0 ppm

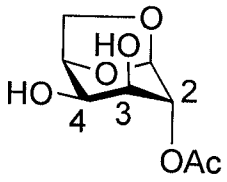
O
HO
O
HO
4
3
2
OAc

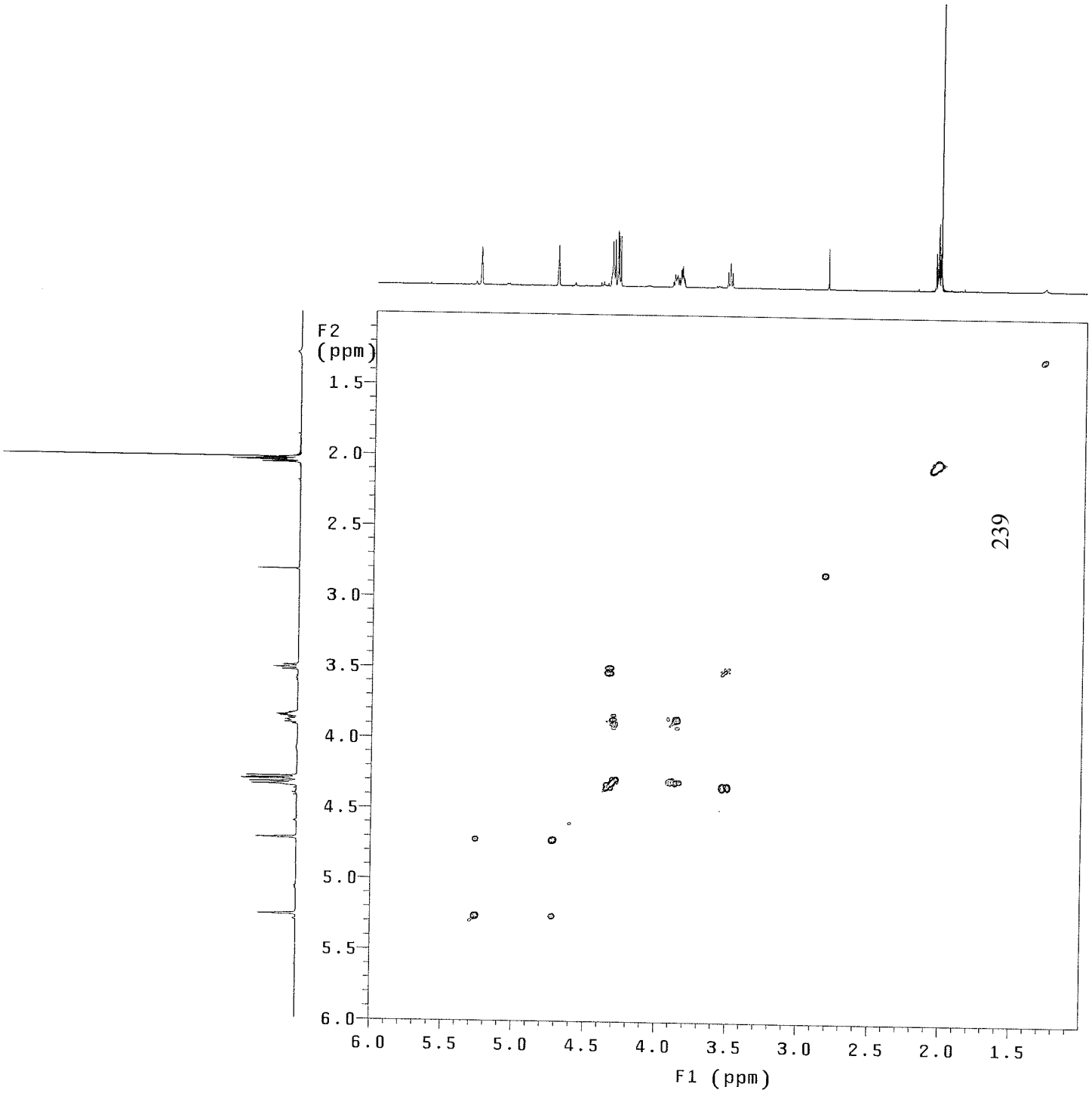
F2
(ppm)
1.5
2.0
2.5
3.0
3.5
4.0
4.5
5.0
5.5
6.0
6.0
5.5
5.0
4.5
4.0
3.5
3.0
2.5
2.0
1.5
F1 (ppm)
239

HO
4
3
2
OAc
OH
O
O
ppm
9
8
7
6
5
4
3
2
1

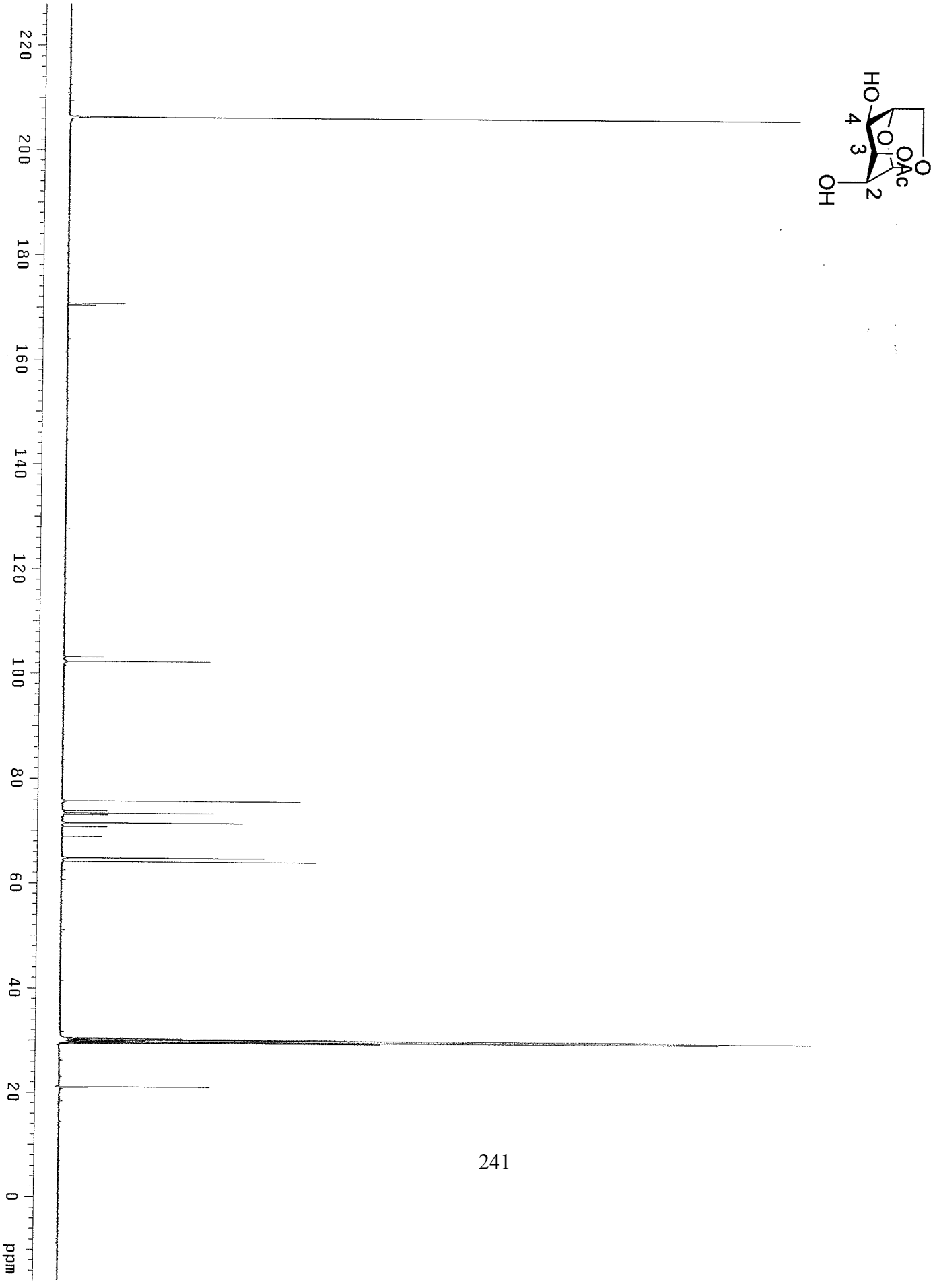
220
200
180
160
140
120
100
80
60
40
20
0
ppm
HO
4
3
O
OAc
2
OH

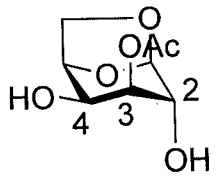
O
OAc
O
HO
2
4
3
OH

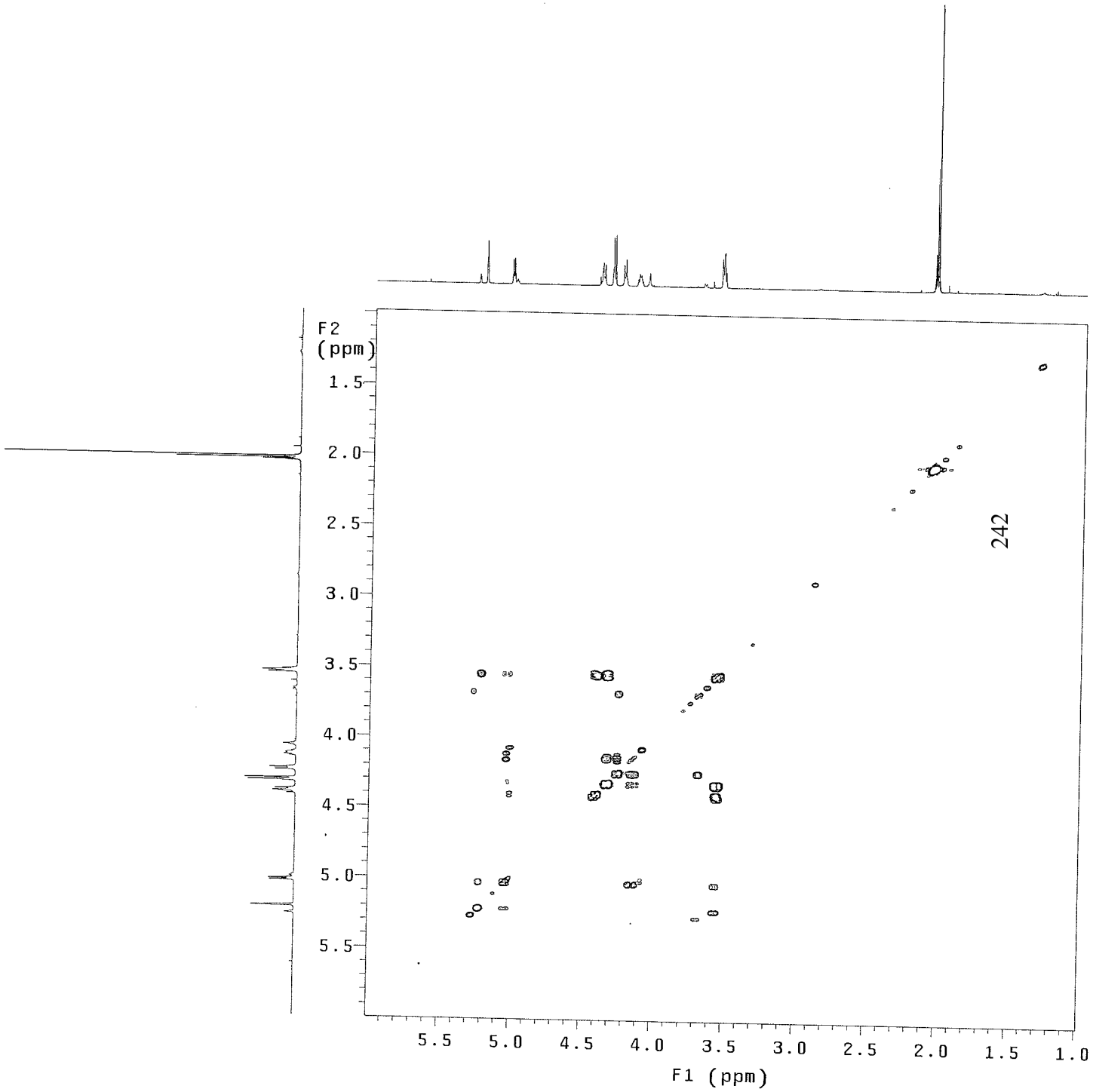
F2
(ppm)
1.5
2.0
2.5
3.0
3.5
4.0
4.5
5.0
5.5
5.5
5.0
4.5
4.0
3.5
3.0
2.5
2.0
1.5
1.0
F1 (ppm)
242

AcO
4
3
HO
O
O
2
OH

9
8
7
6
5
4
3
2
1
ppm

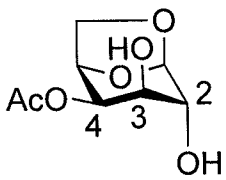

244

220 200 180 160 140 120 100 80 60 40 20 0 ppm

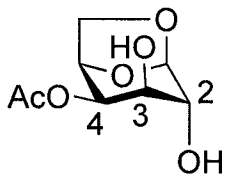
O
HO
O
AcO
2
4
3
OH

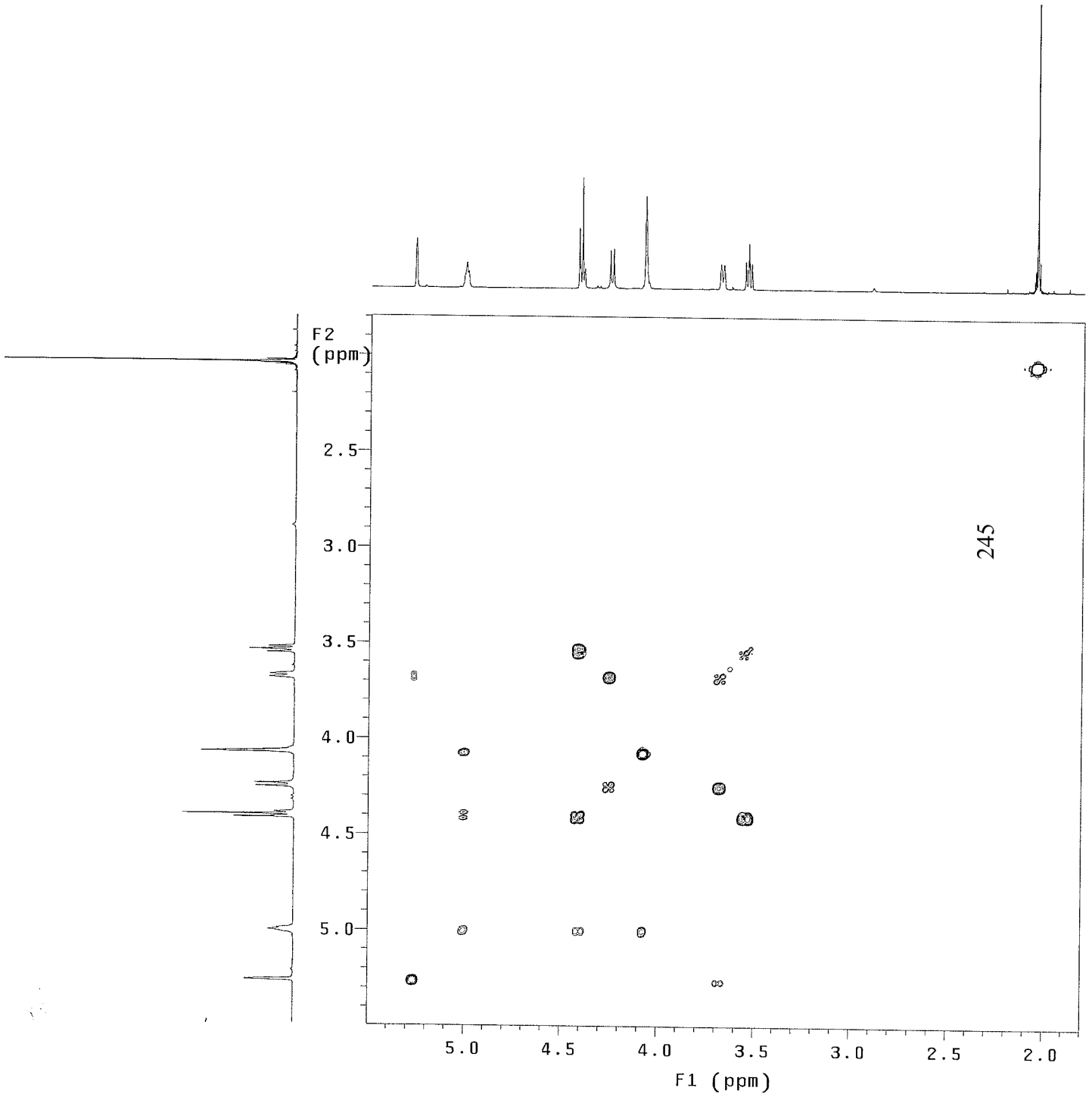
F2
(ppm)
2.5
3.0
3.5
4.0
4.5
5.0
245
5.0
4.5
4.0
3.5
3.0
2.5
2.0
F1 (ppm)

HO
4
3
HO
O
O
2
OMs

9
8
7
6
5
4
3
2
1
ppm

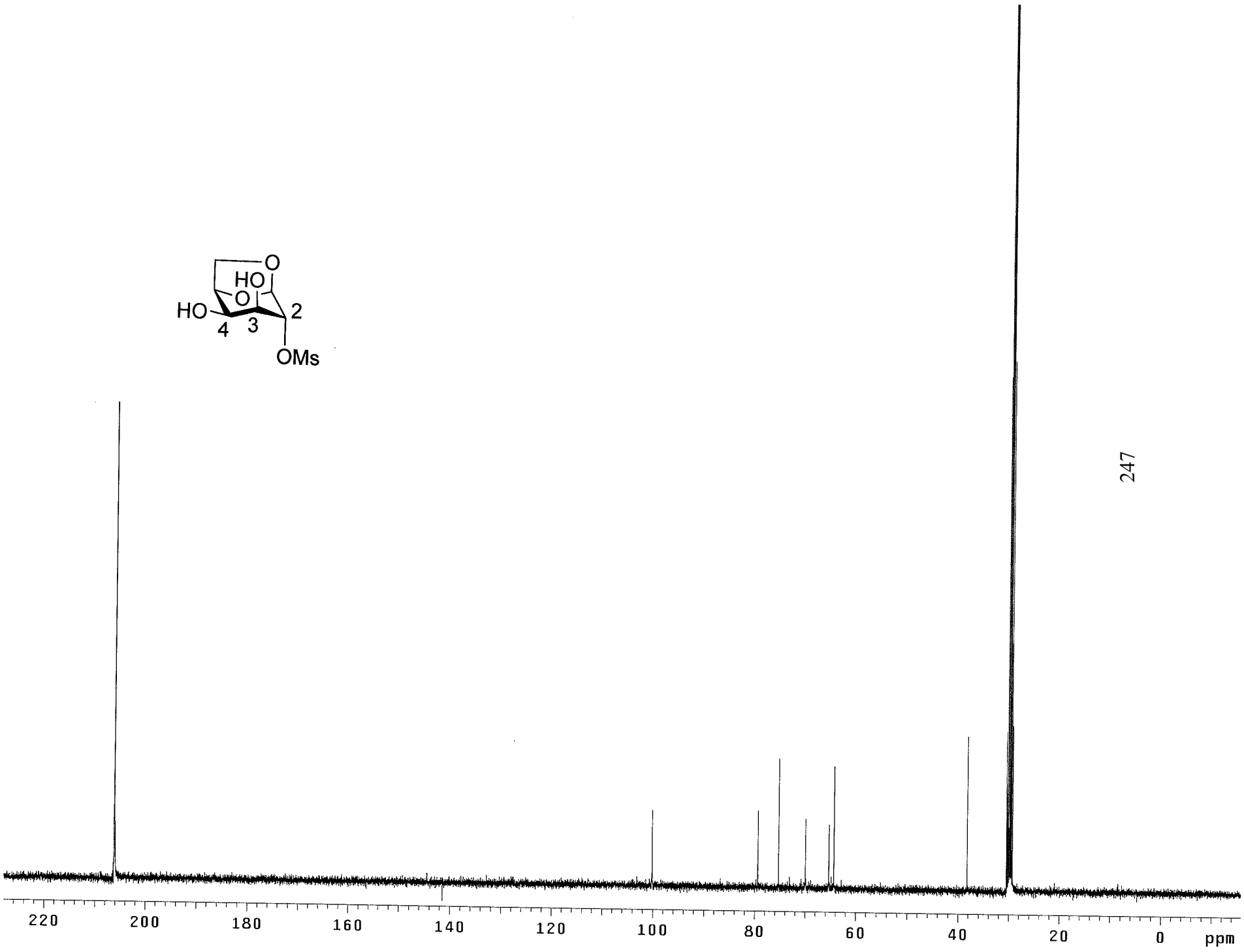
O
HO
O
HO
2
4
3
OMs
247
220
200
180
160
140
120
100
80
60
40
20
0
ppm

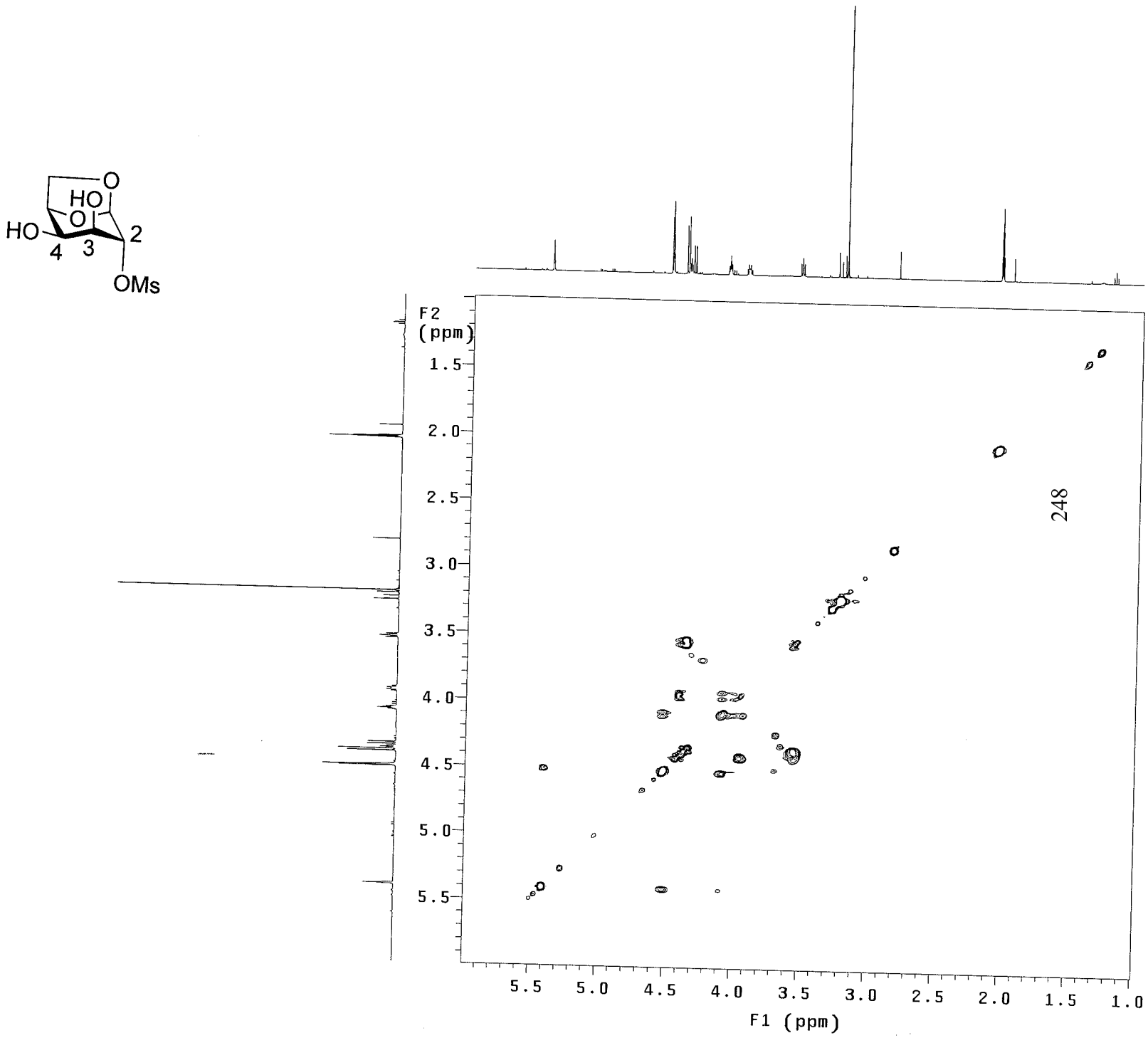
O
HO
O
HO
2
4
3
OMs
F2
(ppm)
1.5
2.0
2.5
3.0
3.5
4.0
4.5
5.0
5.5
5.5
5.0
4.5
4.0
3.5
3.0
2.5
2.0
1.5
1.0
F1 (ppm)
248

HO
4
3
O
OMs
2
OH

ppm
9
8
7
6
5
4
3
2
1

HO
O
4
3
O
OMs
2
OH
220
200
180
160
140
120
100
80
60
40
20
0
ppm

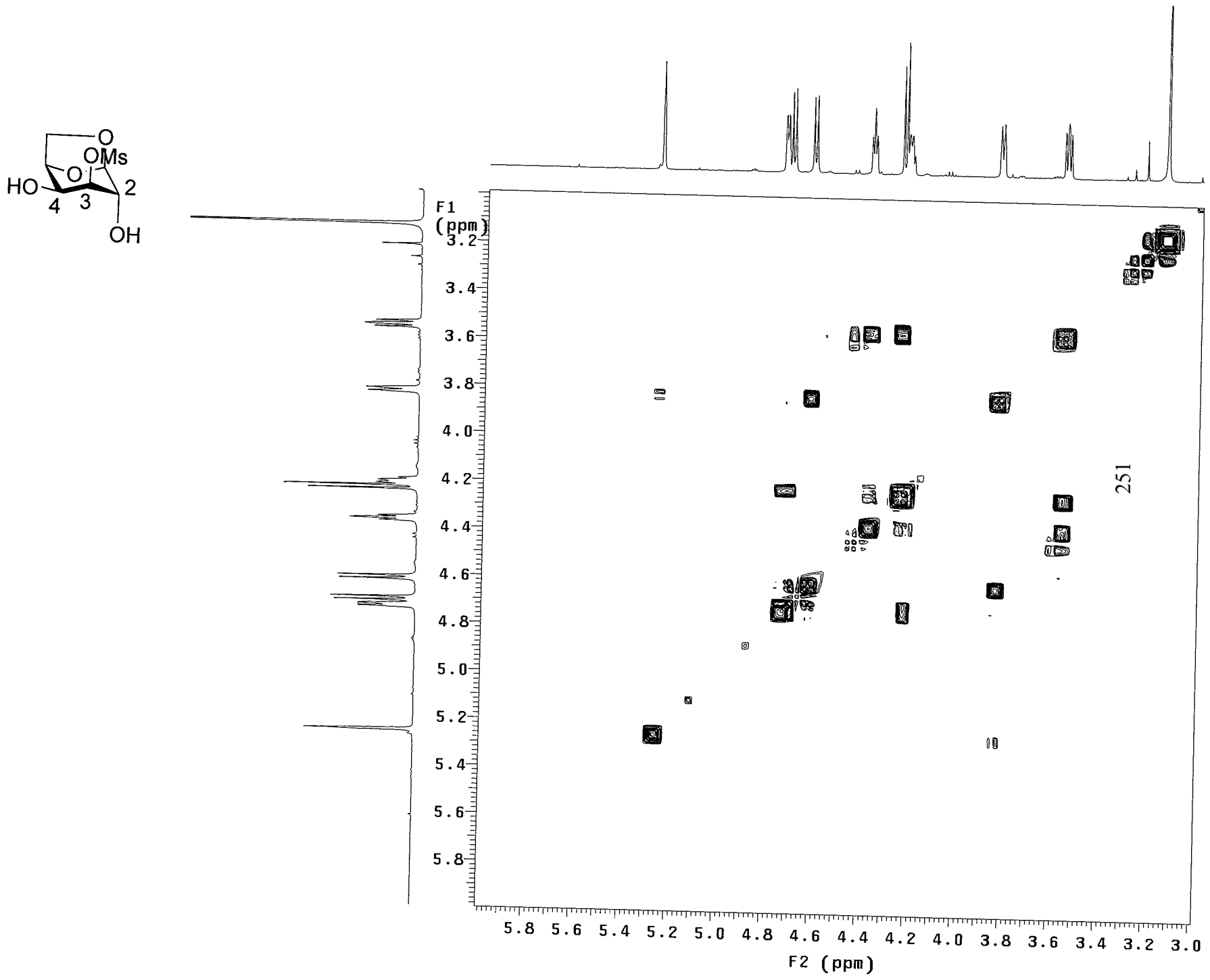
O
OMs
HO
O
2
4
3
OH
F1
(ppm)
3.2
3.4
3.6
3.8
4.0
4.2
4.4
4.6
4.8
5.0
5.2
5.4
5.6
5.8
5.8 5.6 5.4 5.2 5.0 4.8 4.6 4.4 4.2 4.0 3.8 3.6 3.4 3.2 3.0
F2 (ppm)
251

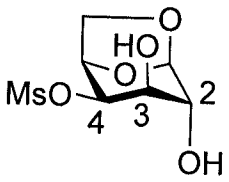

252

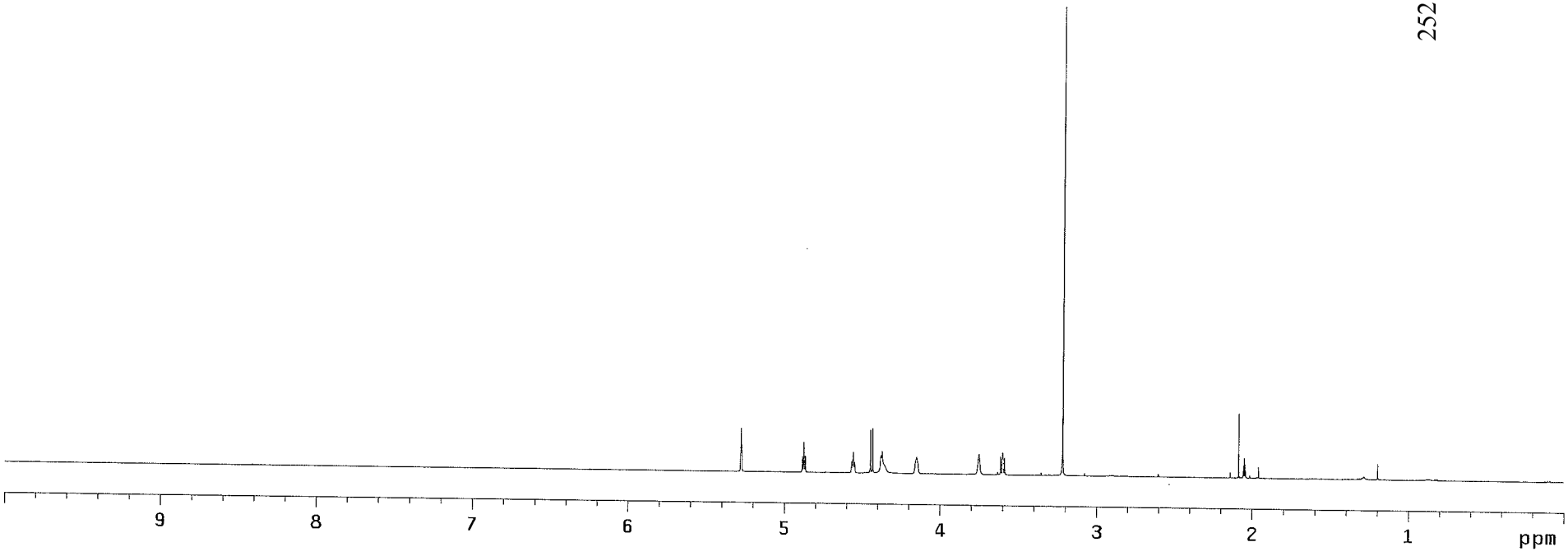

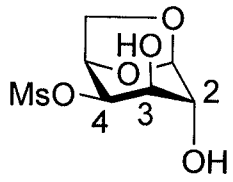

253

220 200 180 160 140 120 100 80 60 40 20 0 ppm

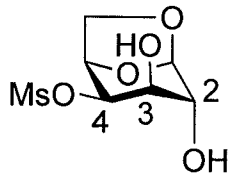
O
HO
O
MsO
4
3
2
OH

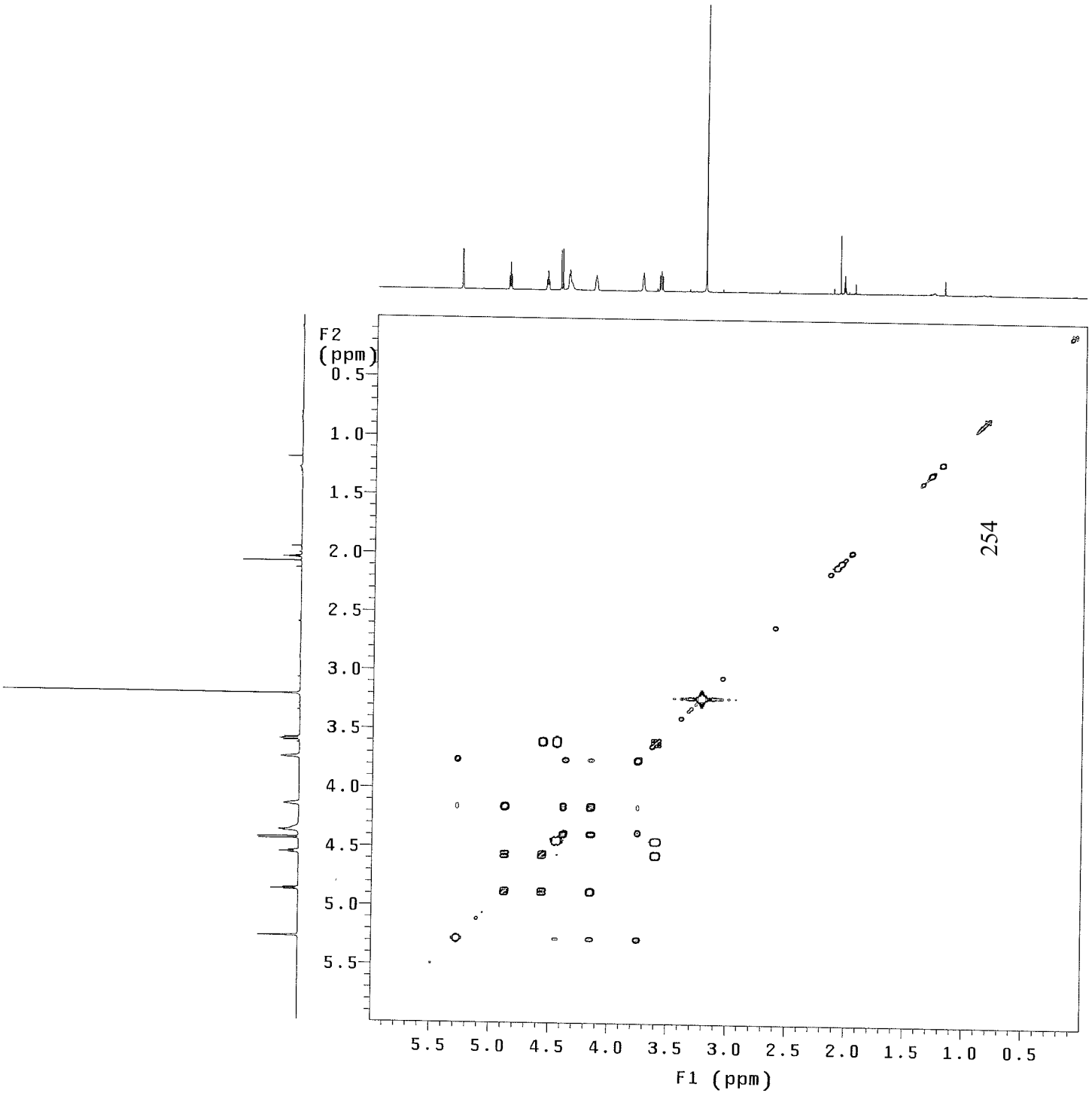
F2
(ppm)
0.5
1.0
1.5
2.0
2.5
3.0
3.5
4.0
4.5
5.0
5.5
5.5 5.0 4.5 4.0 3.5 3.0 2.5 2.0 1.5 1.0 0.5
F1 (ppm)
254

Table 1.2, entry 1
C2:C3:C4 = 5:78:17

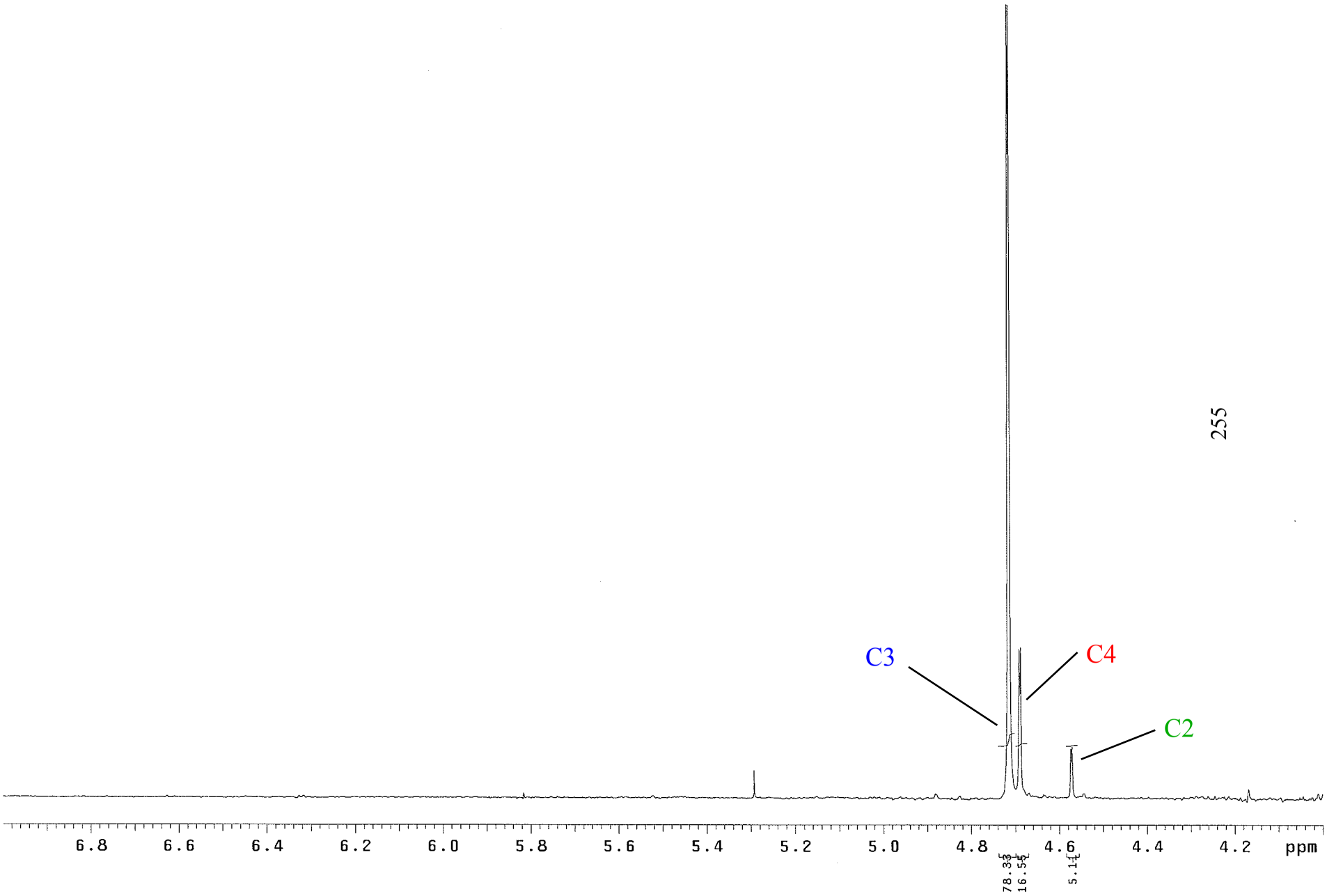

Table 1.2, entry 2
C2:C3:C4 = 90:10:-

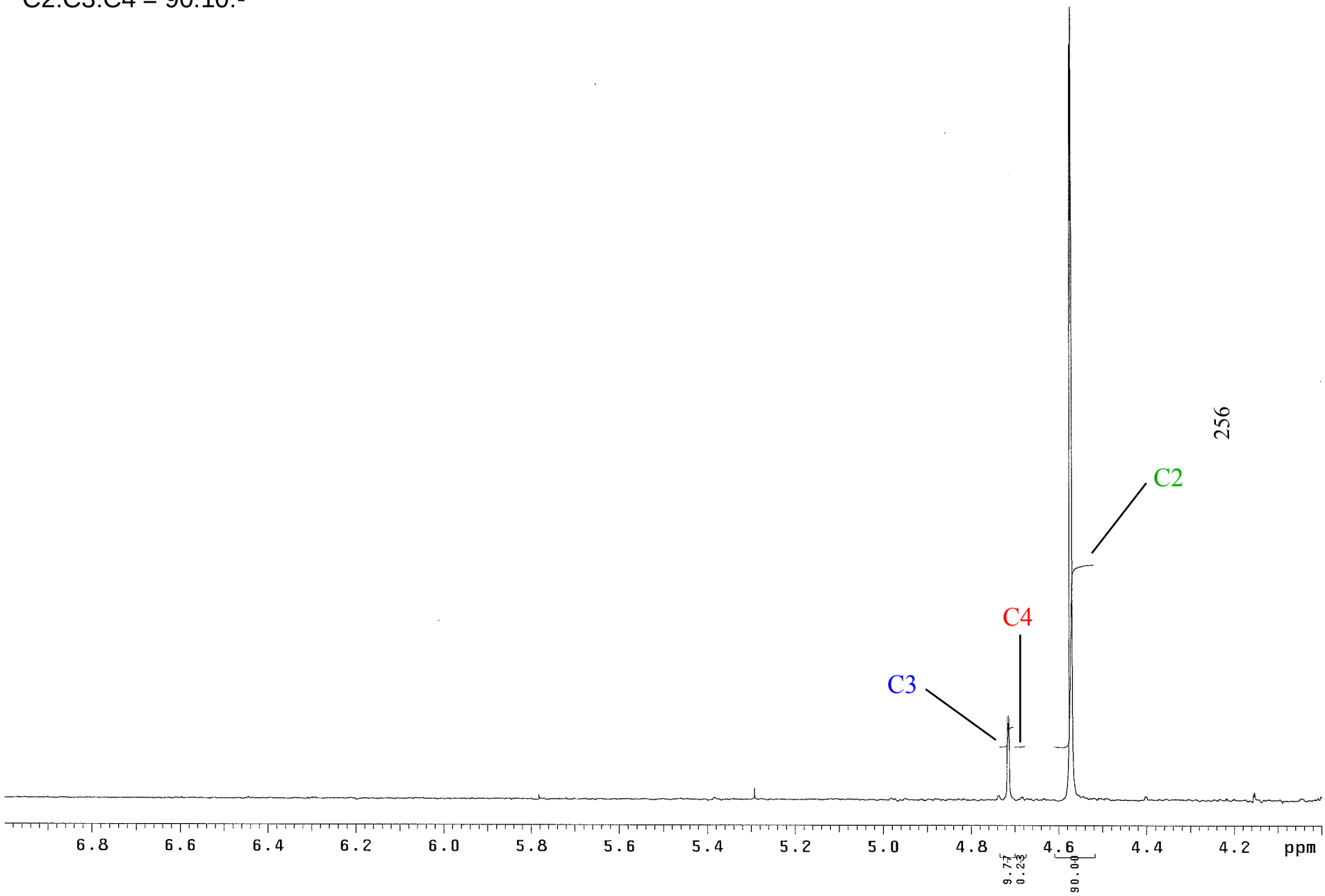

Table 1.2, entry 3
C2:C3:C4 = -:100:-

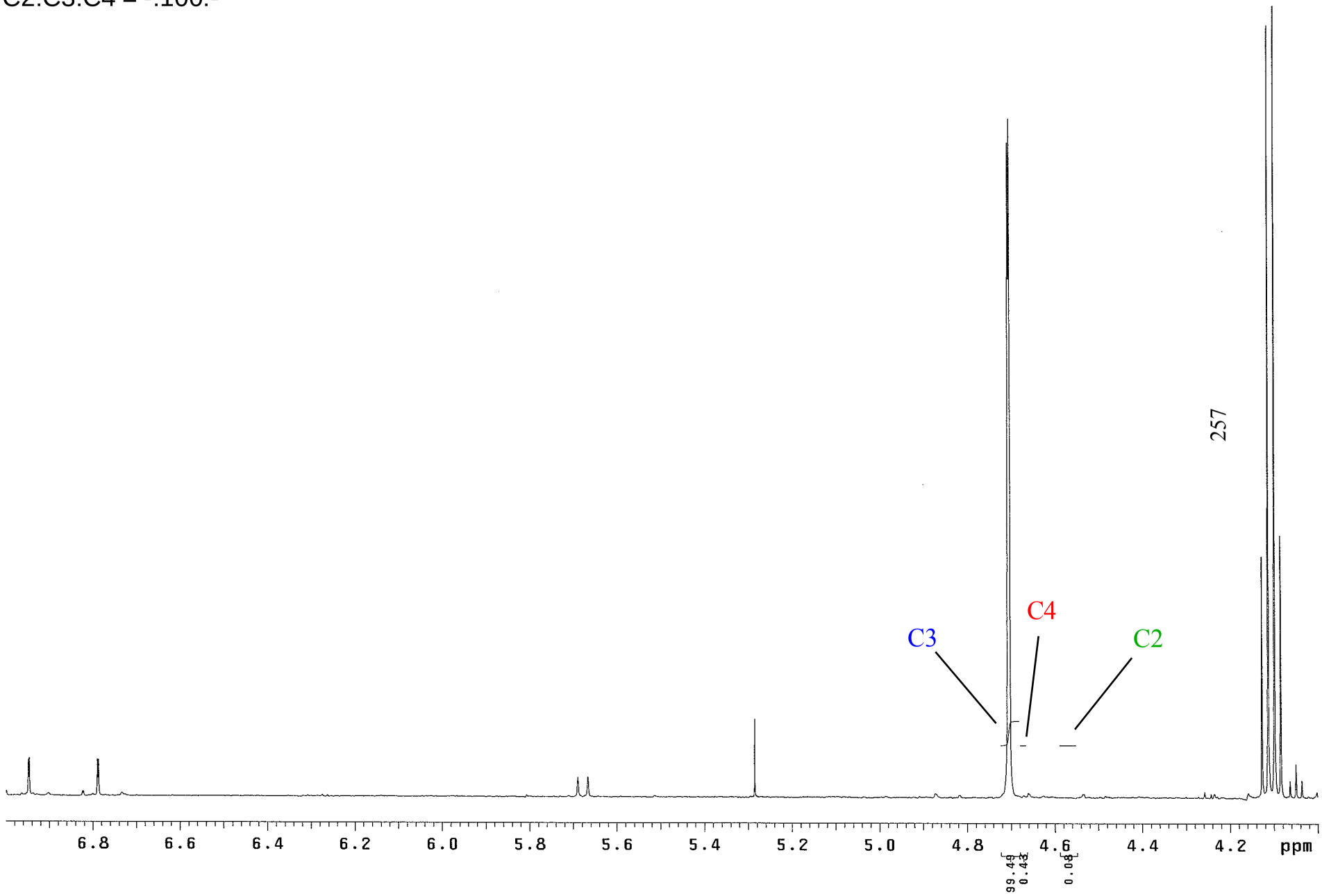

Table 1.2, entry 4
C2:C3:C4 = 9:84:7

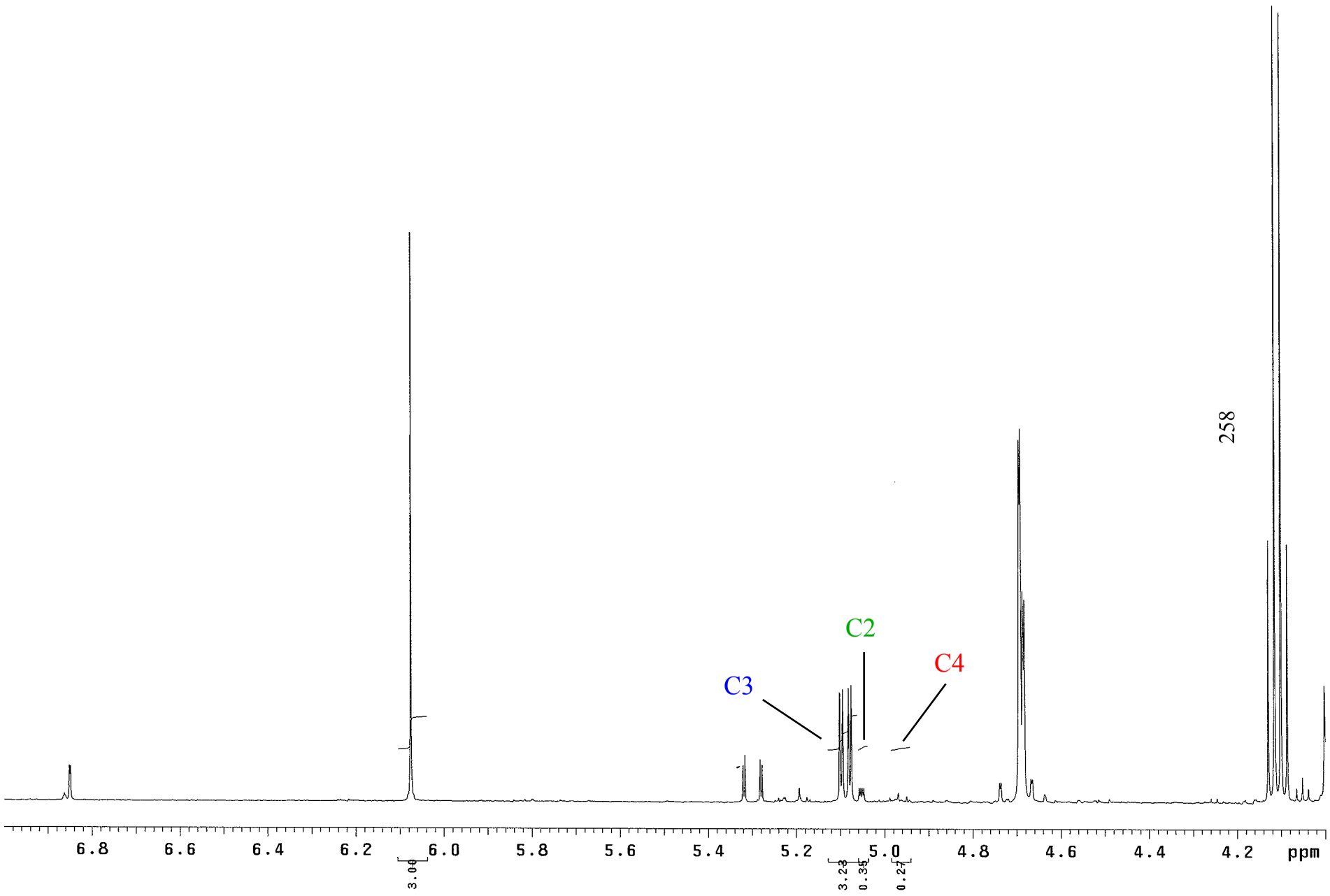

Table 1.2, entry 5
C2:C3:C4 = 84:15:1

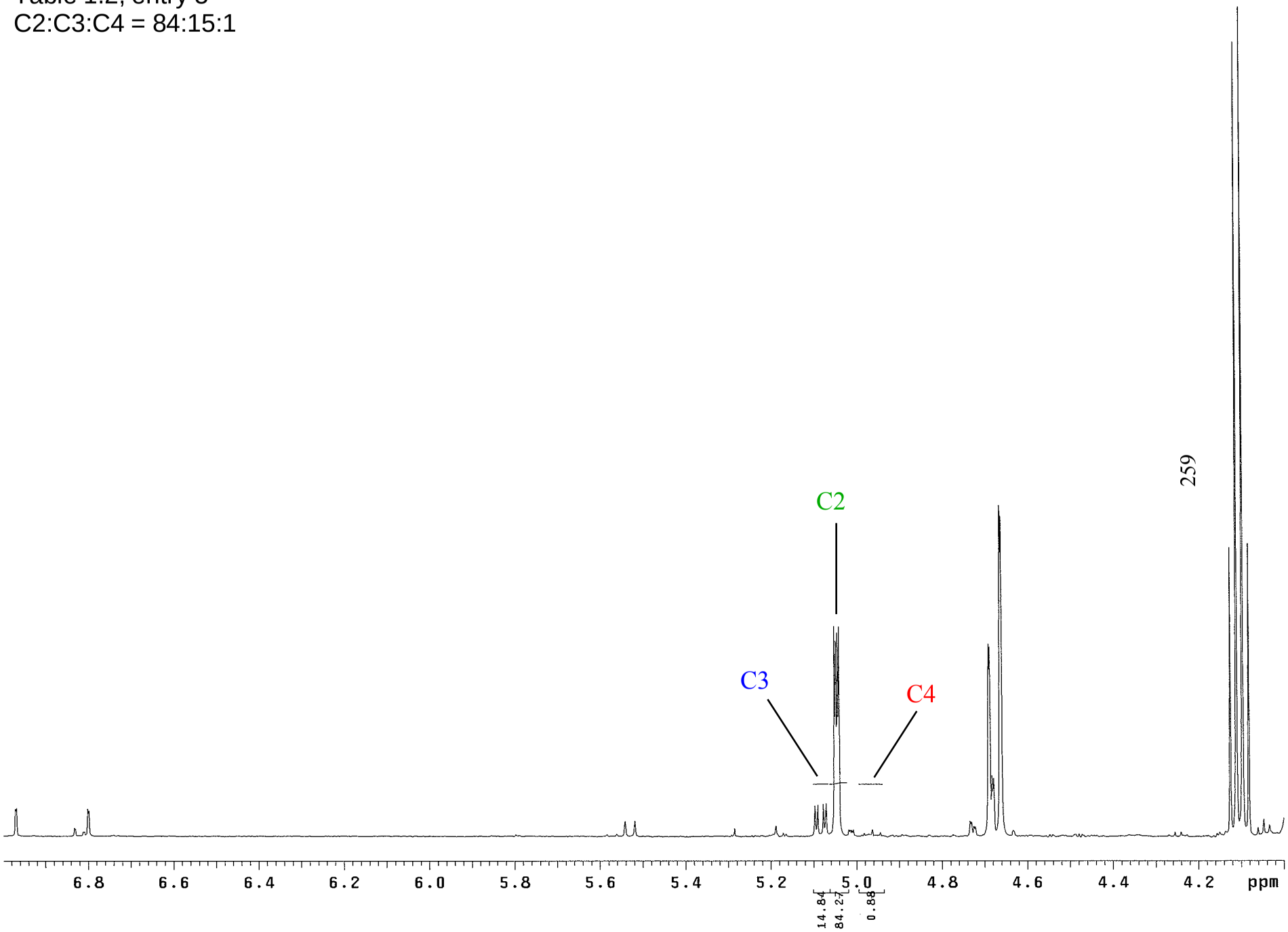

Table 1.2, entry 6
C2:C3:C4 = 1:99:-

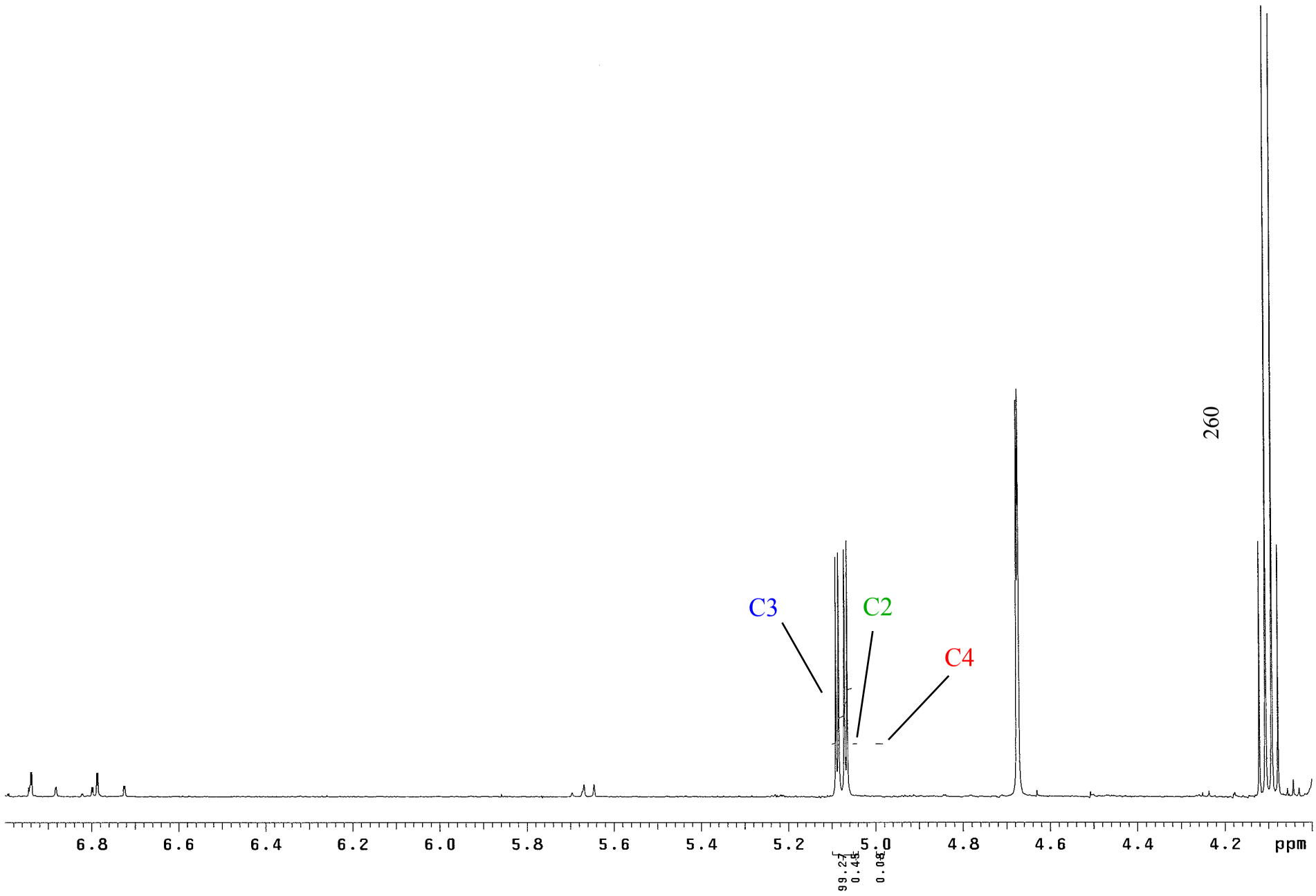

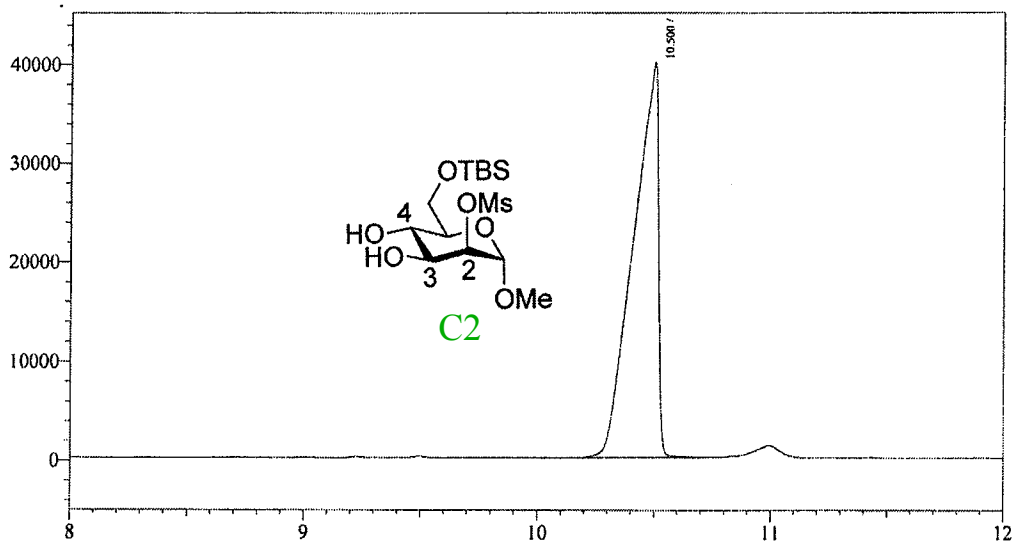
40000
30000
20000
10000
0
8
9
10
11
12
10.506
OTBS
OMs
4
HO
HO
O
3
2
OMe
C2

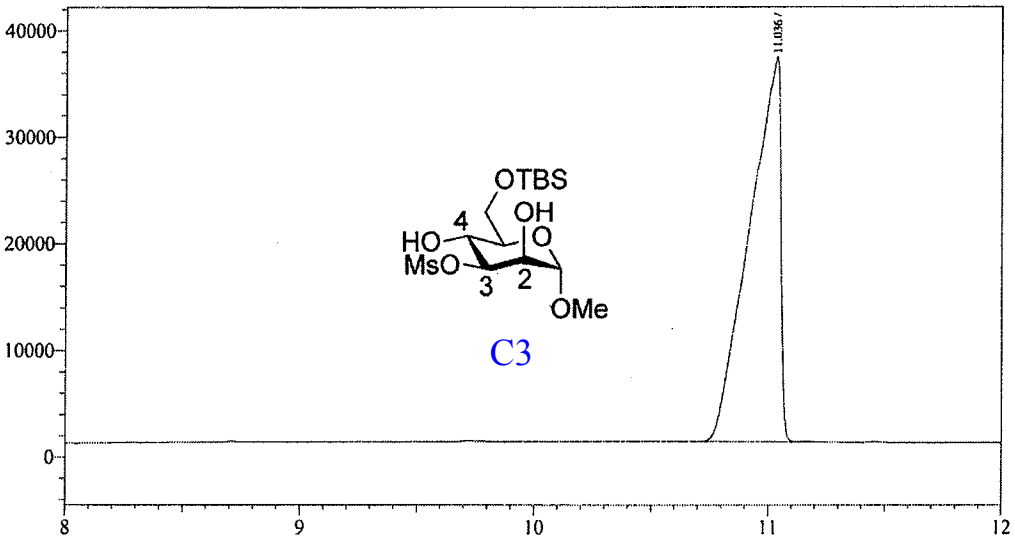
40000
30000
20000
10000
0
8
9
10
11
12
11.036
OTBS
OH
4
HO
MsO
O
3
2
OMe
C3

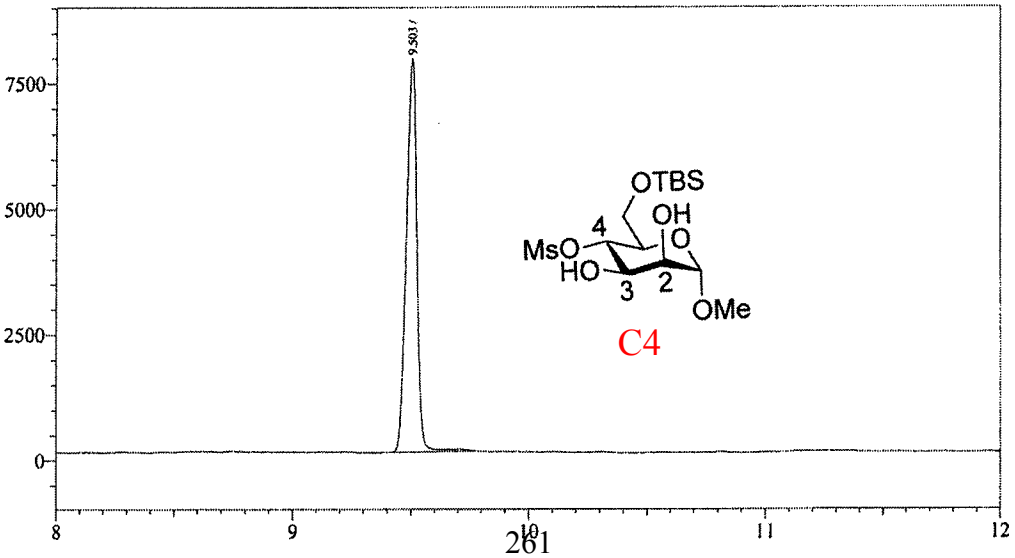
7500
5000
2500
0
8
9
10
11
12
9.503
OTBS
OH
4
MsO
HO
O
3
2
OMe
C4

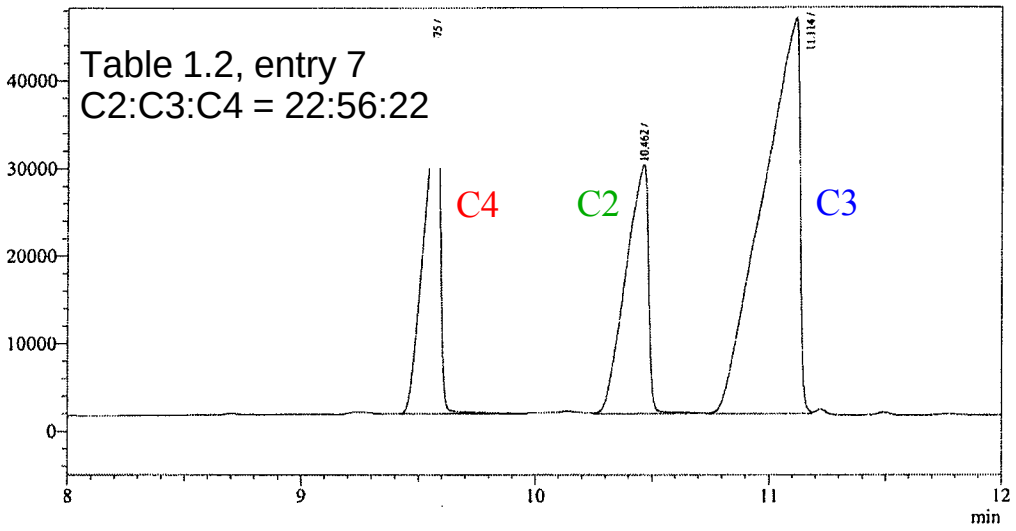

Peak#	Ret.Time	Area	Height	Conc.	Unit	Mark	ID#	Cmpd Name
1	9.575	189627	40877	21.735				
2	10.462	190976	28420	21.890				
3	11.114	491830	45209	56.375				

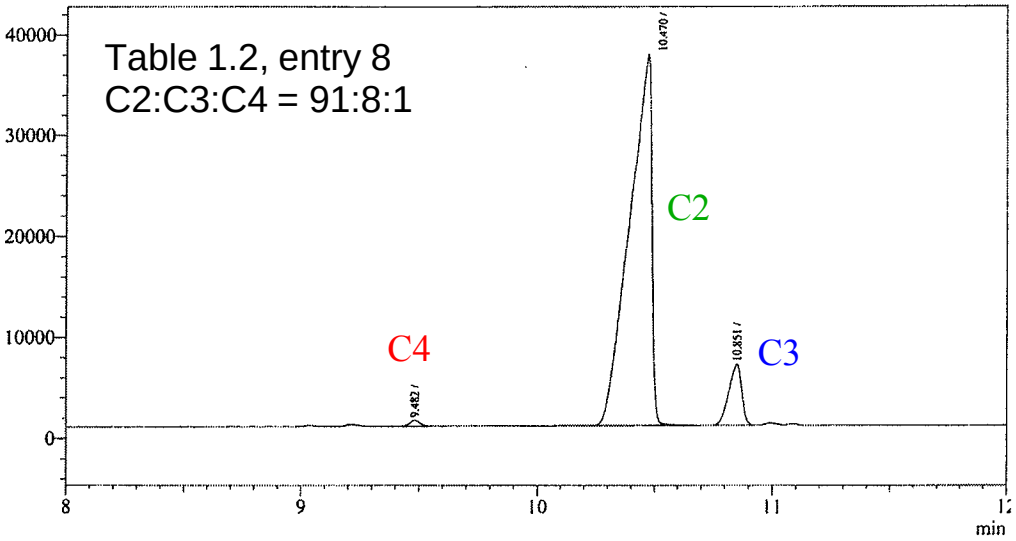

Peak#	Ret.Time	Area	Height	Conc.	Unit	Mark	ID#	Cmpd Name
1	9.482	1725	559	0.650				
2	10.470	241042	36677	90.876				
3	10.851	22476	5974	8.474				

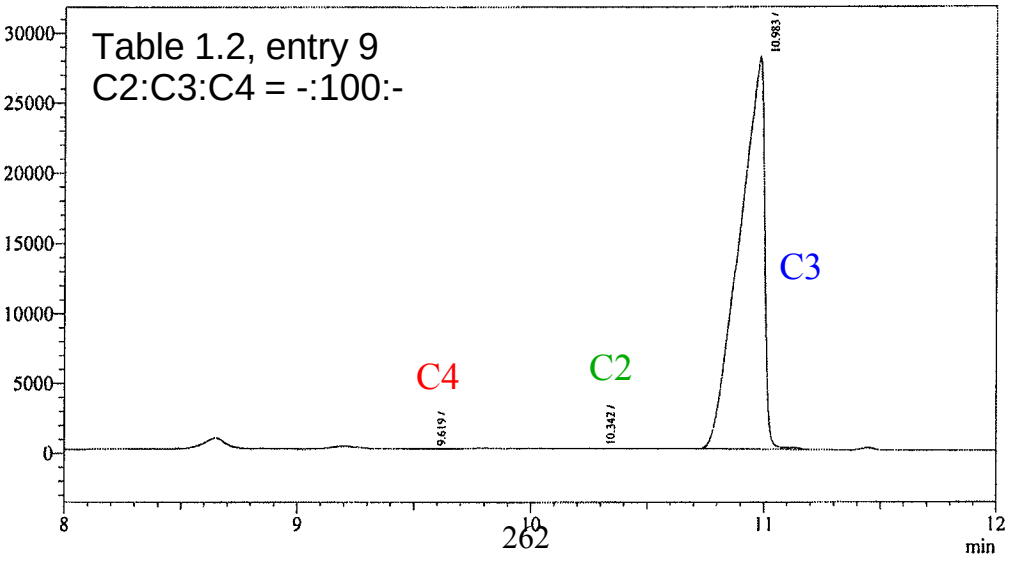

Peak#	Ret.Time	Area	Height	Conc.	Unit	Mark	ID#	Cmpd Name
1	9.619	-74	0	-0.036				
2	10.342	-35	6	-0.017				
3	10.983	206555	28014	100.052				

Table 1.3, entry 1
C2:C3:C4 = 7:79:14

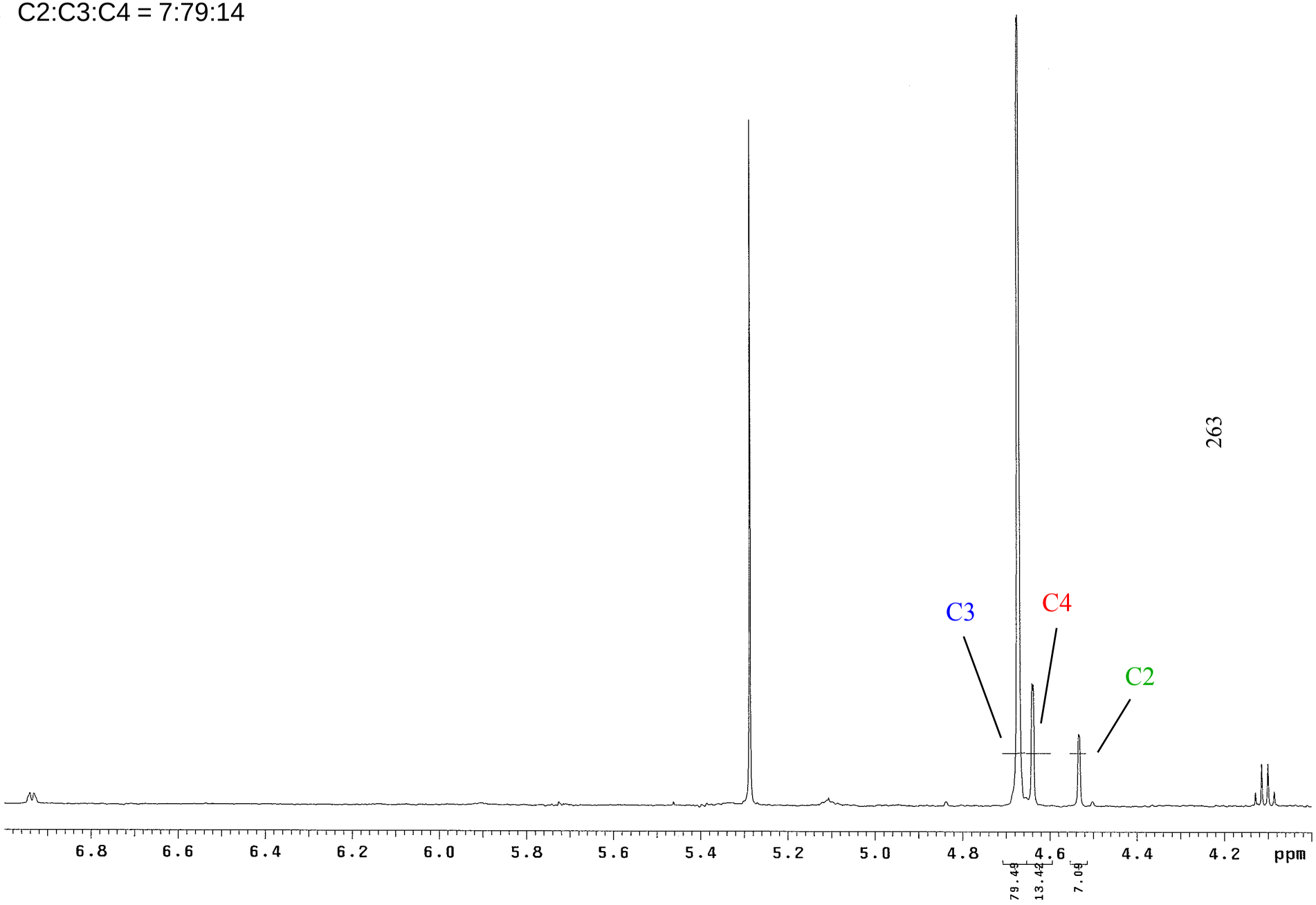

Table 1.3, entry 2
C2:C3:C4 = 89:11:-

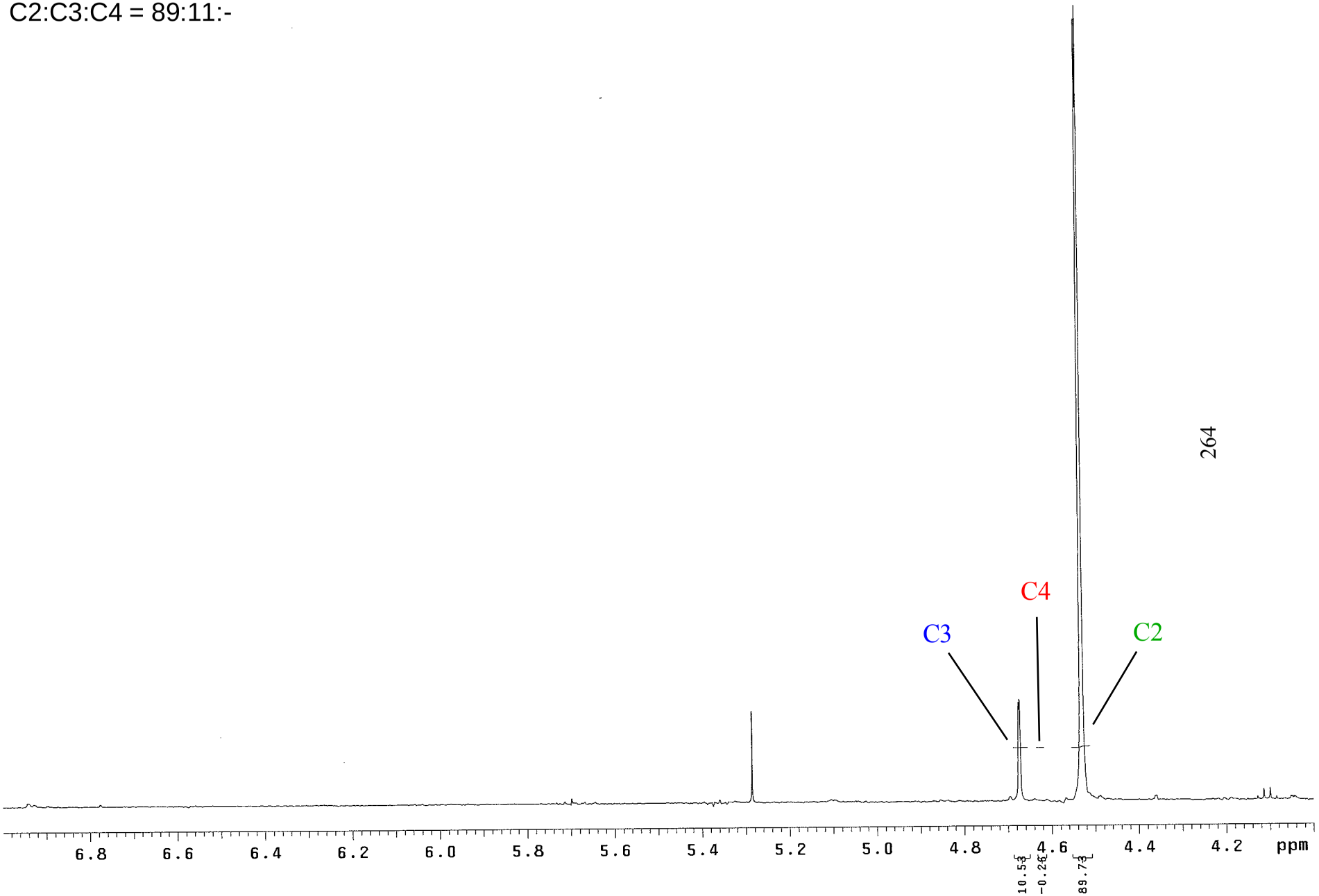

Table 1.3, entry 3
C2:C3:C4 = -:100:-

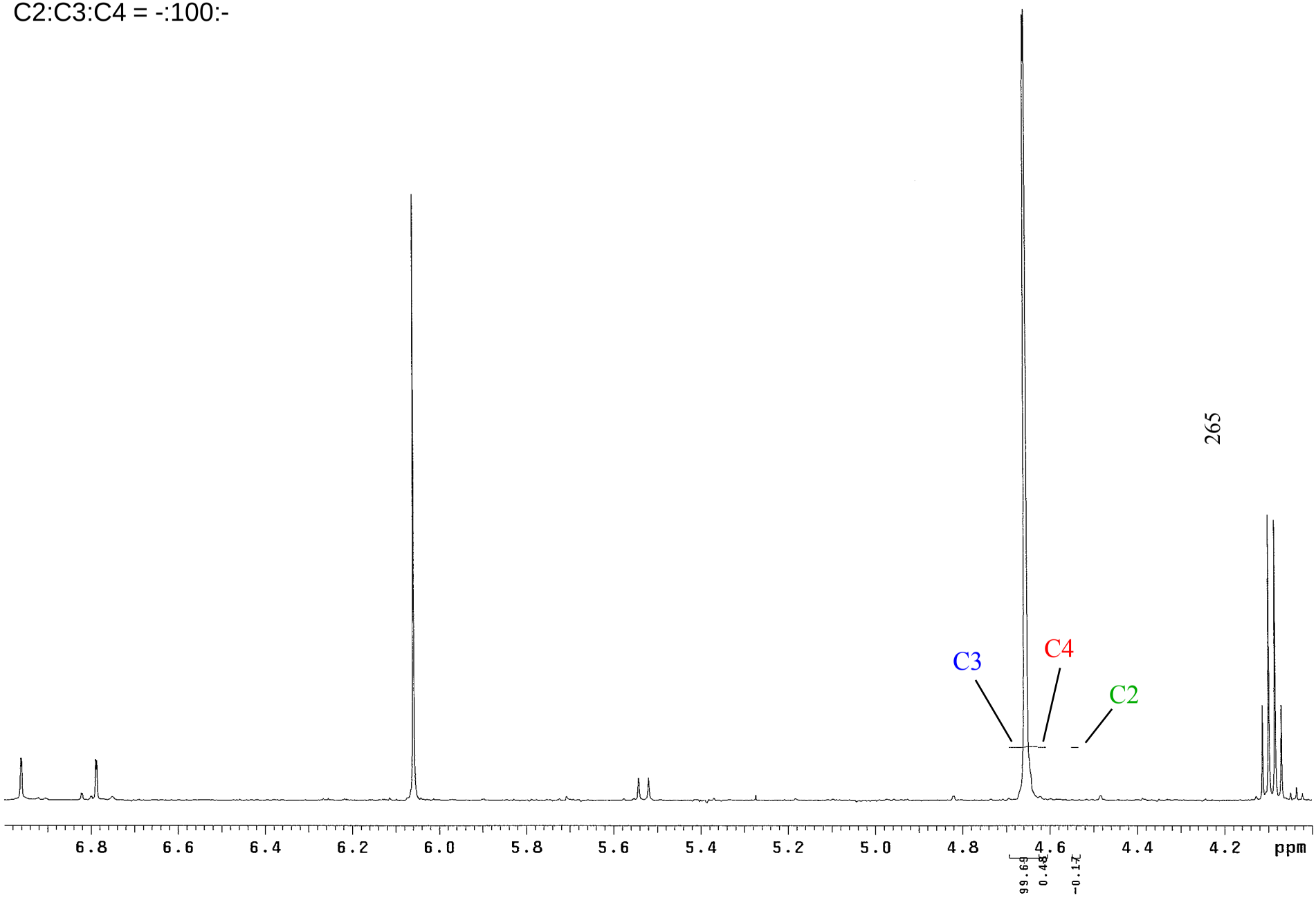

Table 1.3, entry 4
C2:C3:C4 = 12:79:9

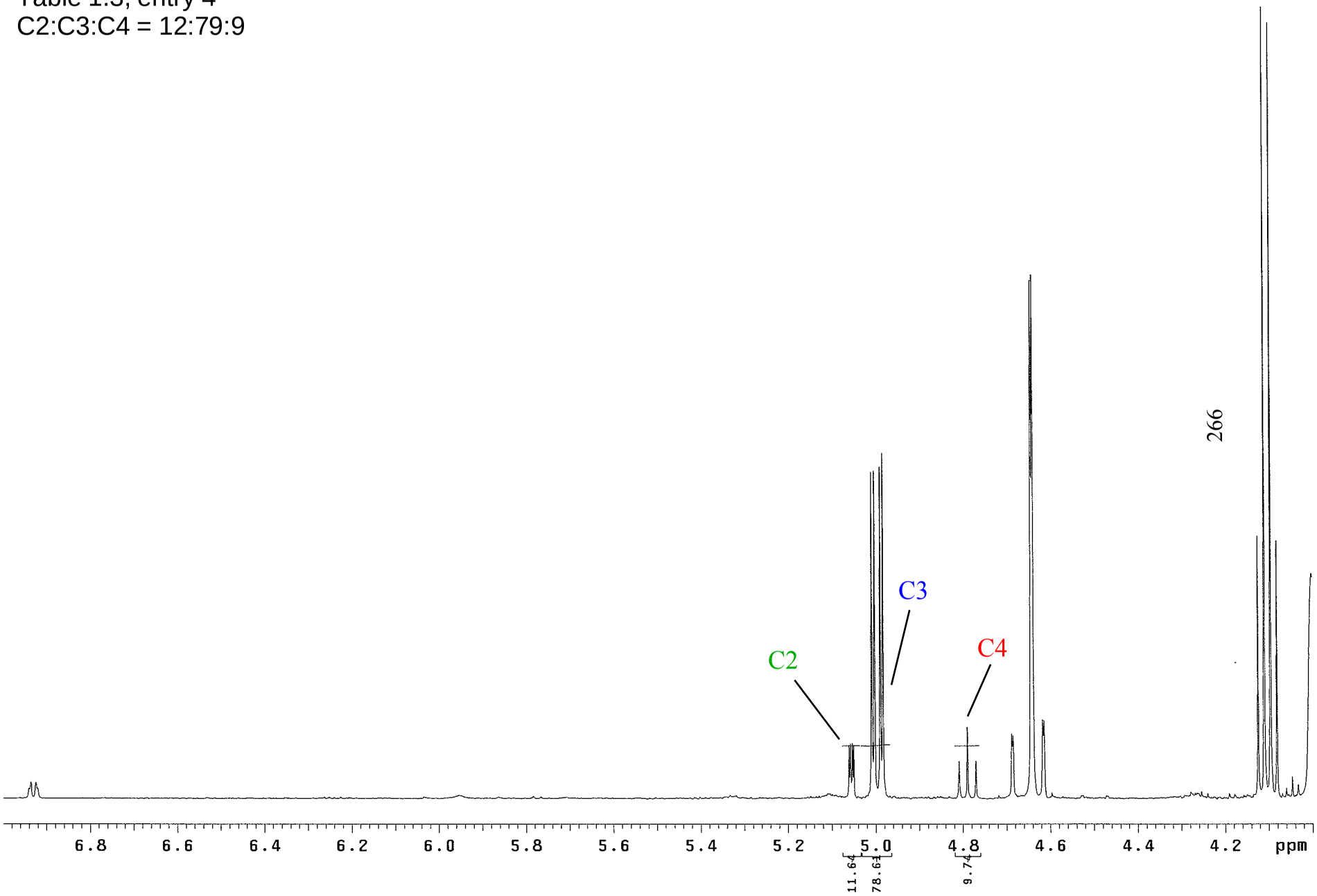

Table 1.3, entry 5
C2:C3:C4 = 84:14:2

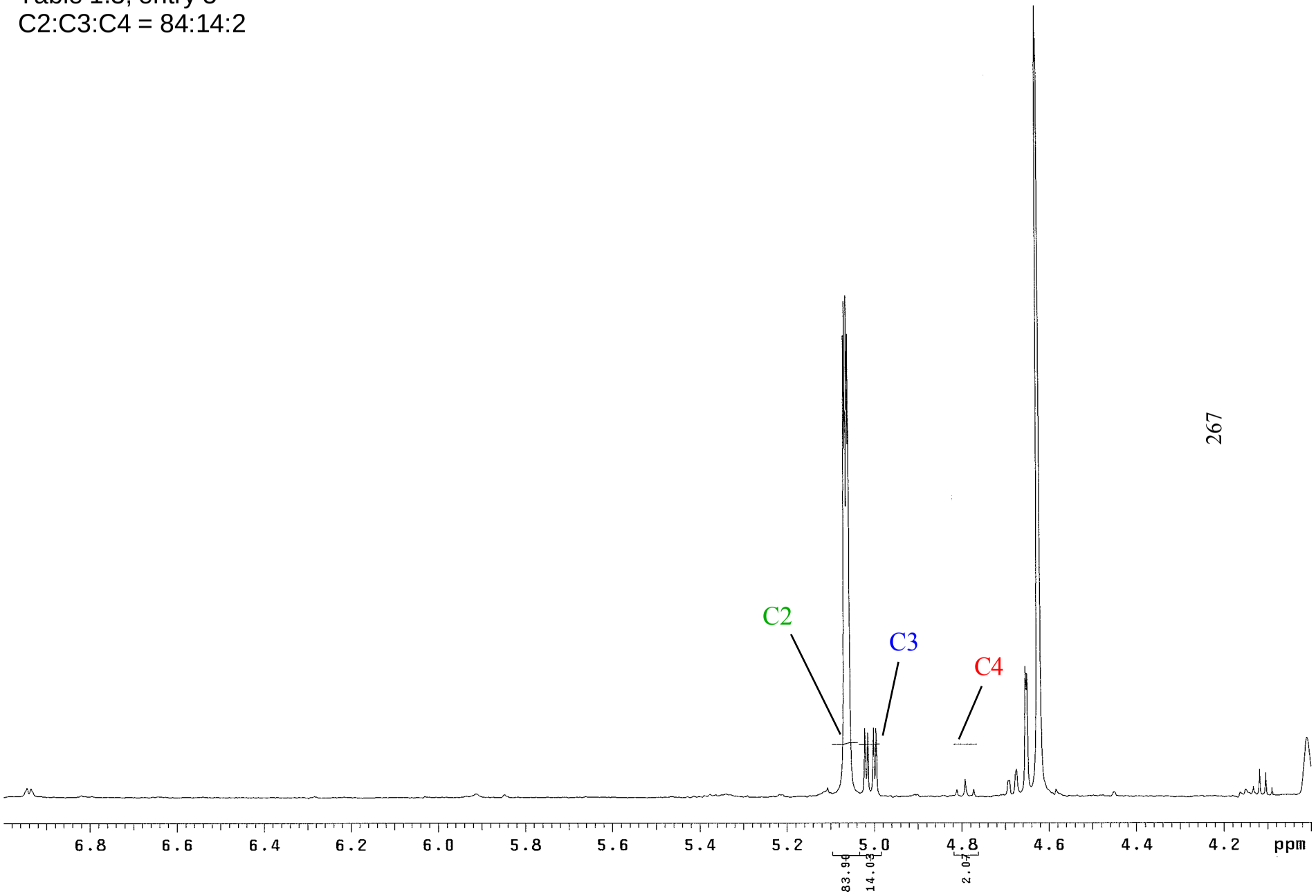

Table 1.3, entry 6
C2:C3:C4 = 1:99:-

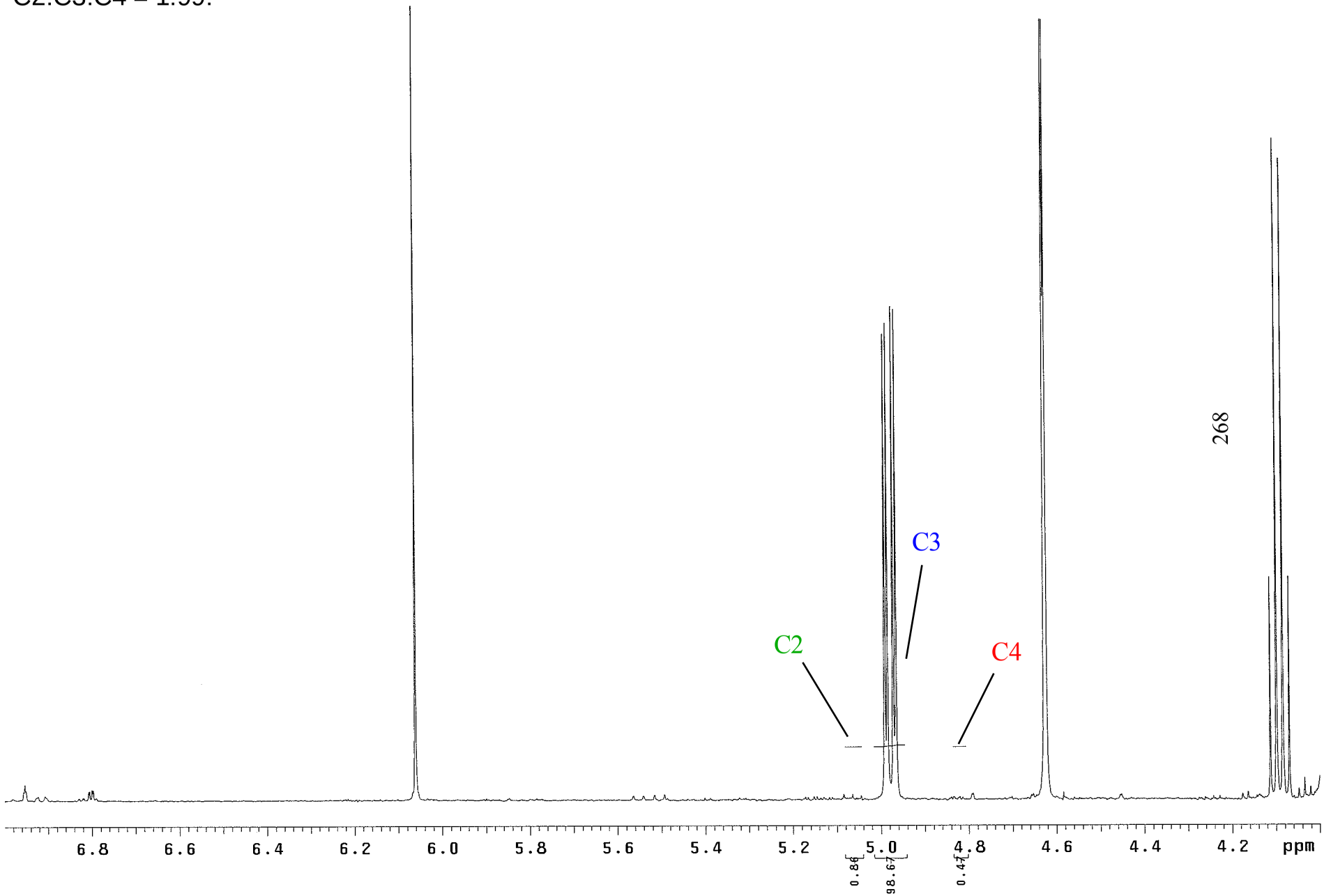

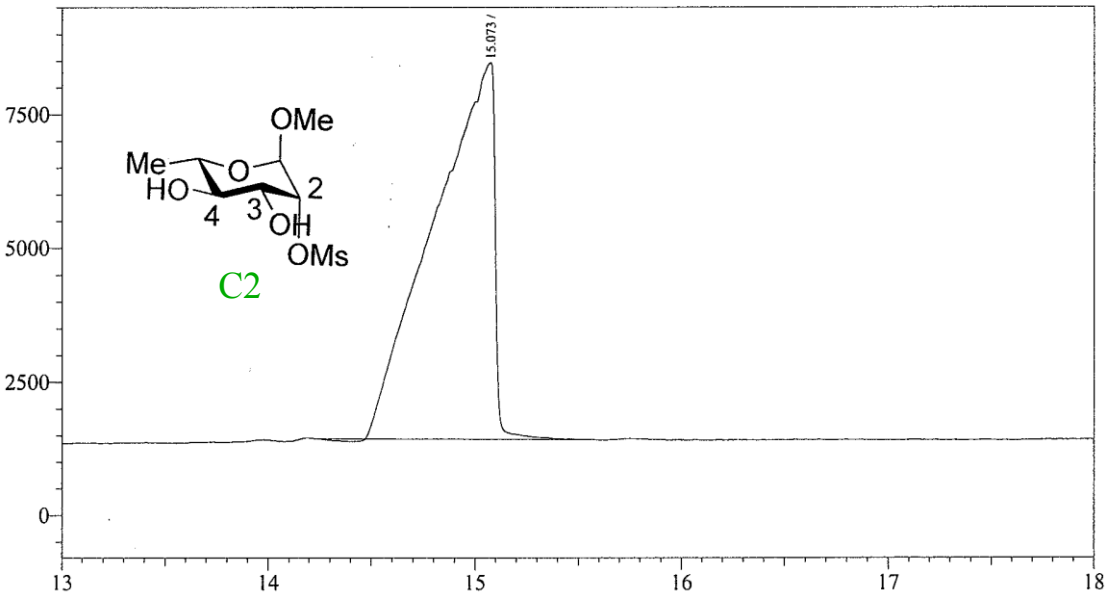
15.073
7500
5000
2500
0
13
14
15
16
17
18
OMe
Me
O
HO
2
4
3
OH
OMs
C2

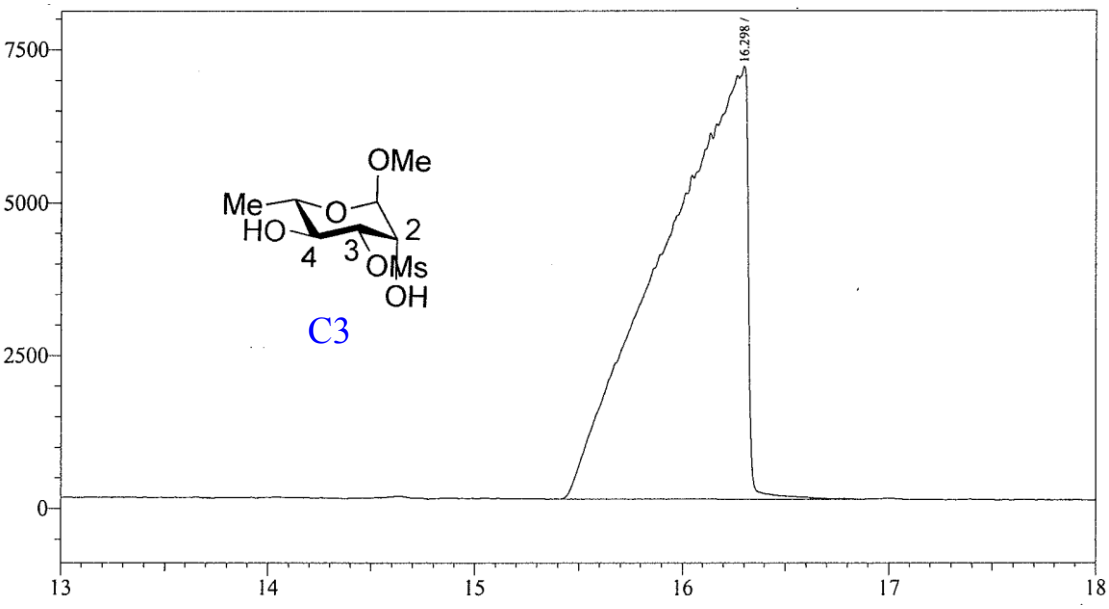
16.298
7500
5000
2500
0
13
14
15
16
17
18
OMe
Me
O
HO
2
4
3
OMs
OH
C3

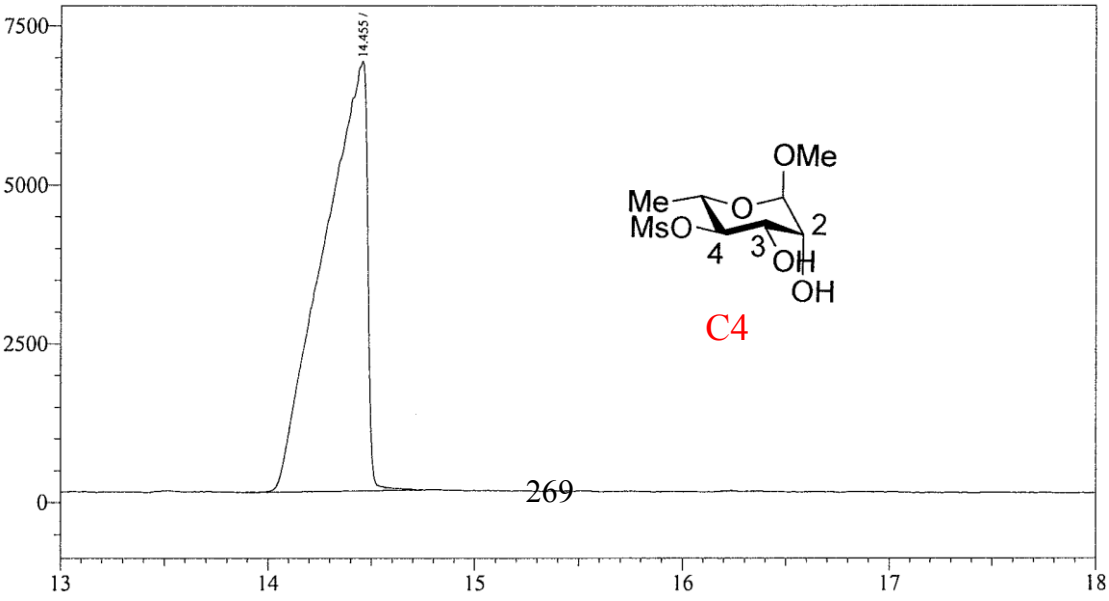
14.455
7500
5000
2500
0
13
14
15
16
17
18
OMe
Me
O
MsO
2
4
3
OH
OH
C4

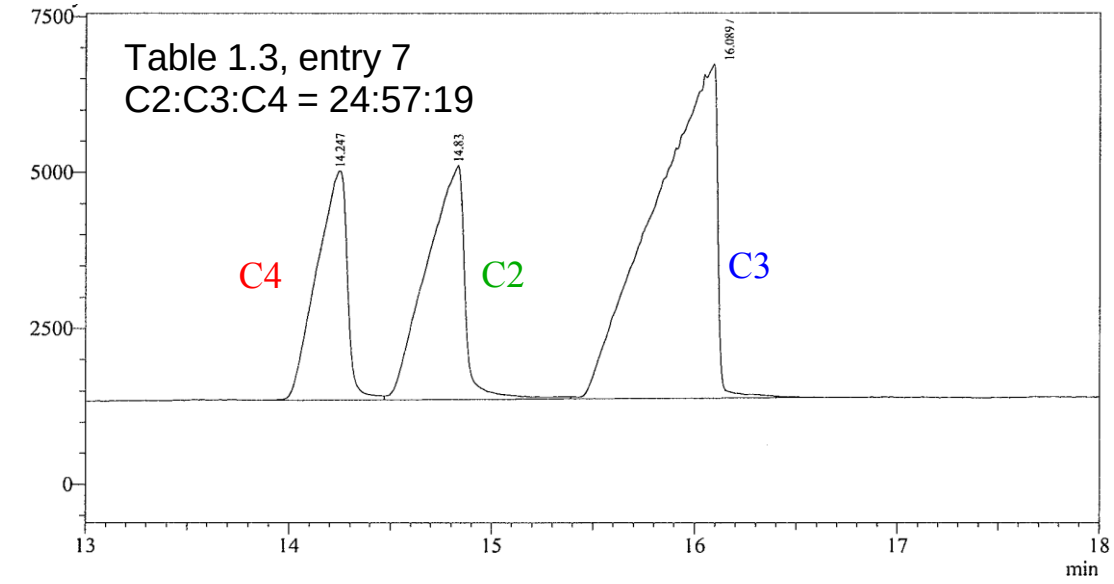

Peak#	Ret.Time	Area	Height	Conc.	Unit	Mark	ID#	Cmpd Name
1	14.247	38196	3668	18.816				
2	14.832	49663	3734	24.464		V		
3	16.089	115146	5342	56.721		V		
Total		203005	12744					

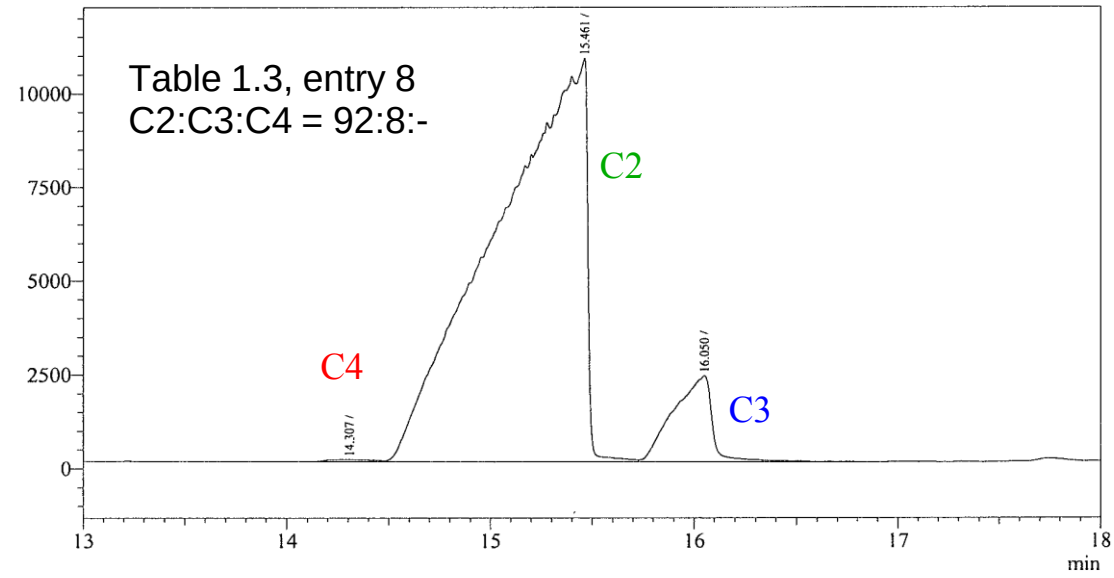

Peak#	Ret.Time	Area	Height	Conc.	Unit	Mark	ID#	Cmpd Name
1	14.307	839	55	0.229				
2	15.461	335292	10716	91.493		V		
3	16.050	30337	2290	8.278		V		
Total		366468	13061					

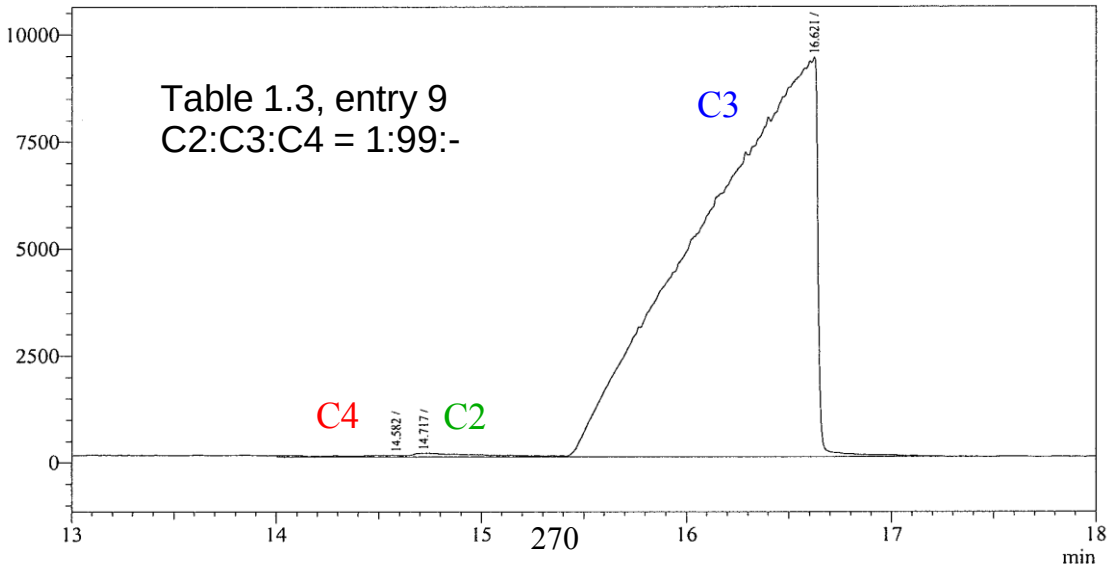

Peak#	Ret.Time	Area	Height	Conc.	Unit	Mark	ID#	Cmpd Name
1	14.582	1120	41	0.303				
2	14.717	2316	94	0.627		V		
3	16.621	365789	9320	99.070		V		
Total		369225	9455					

Table 1.3, entry 1
C2:C3:C4 = 27:14:59

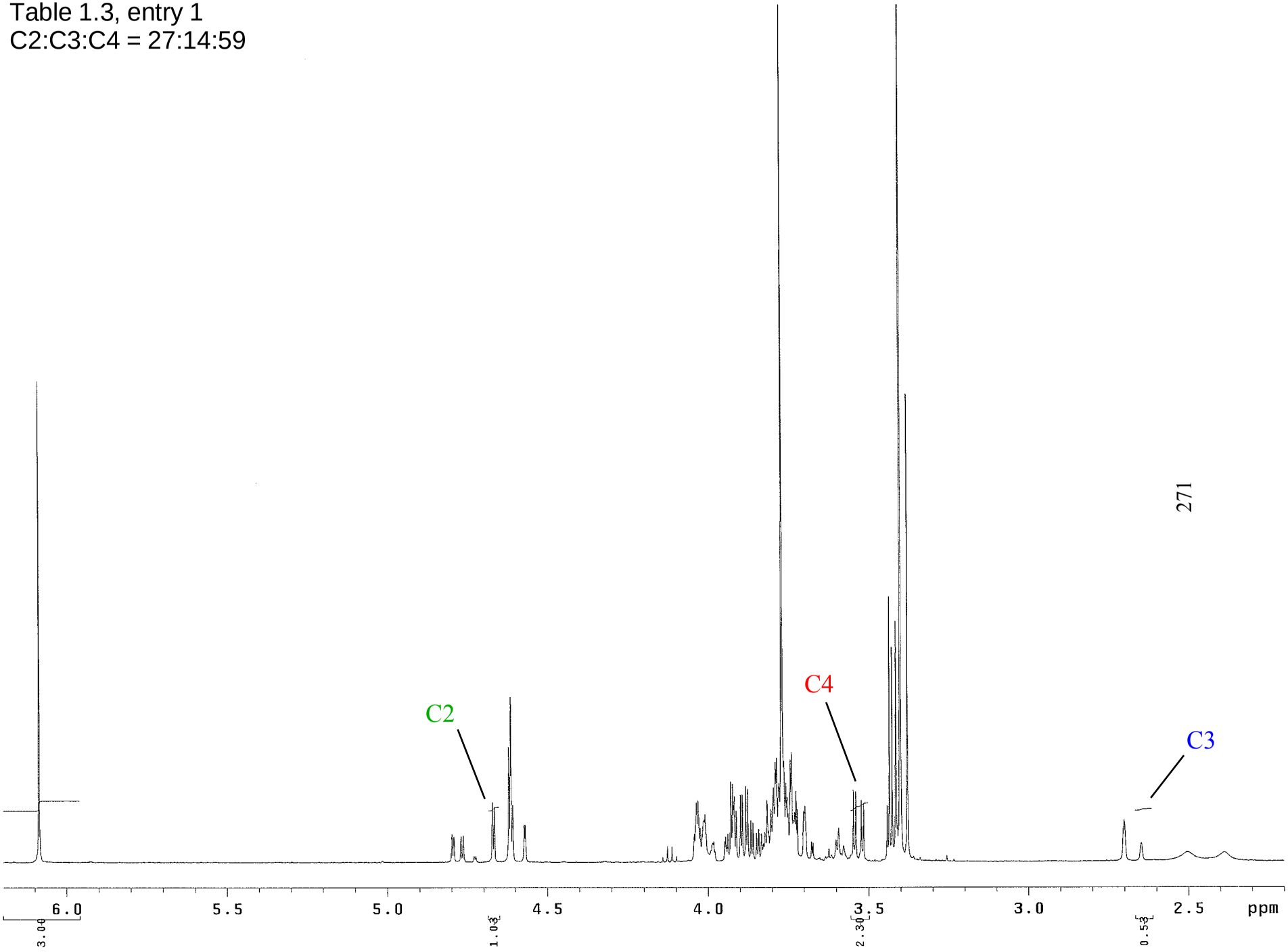

Table 1.4, entry 2
C2:C3:C4 = -:3:97

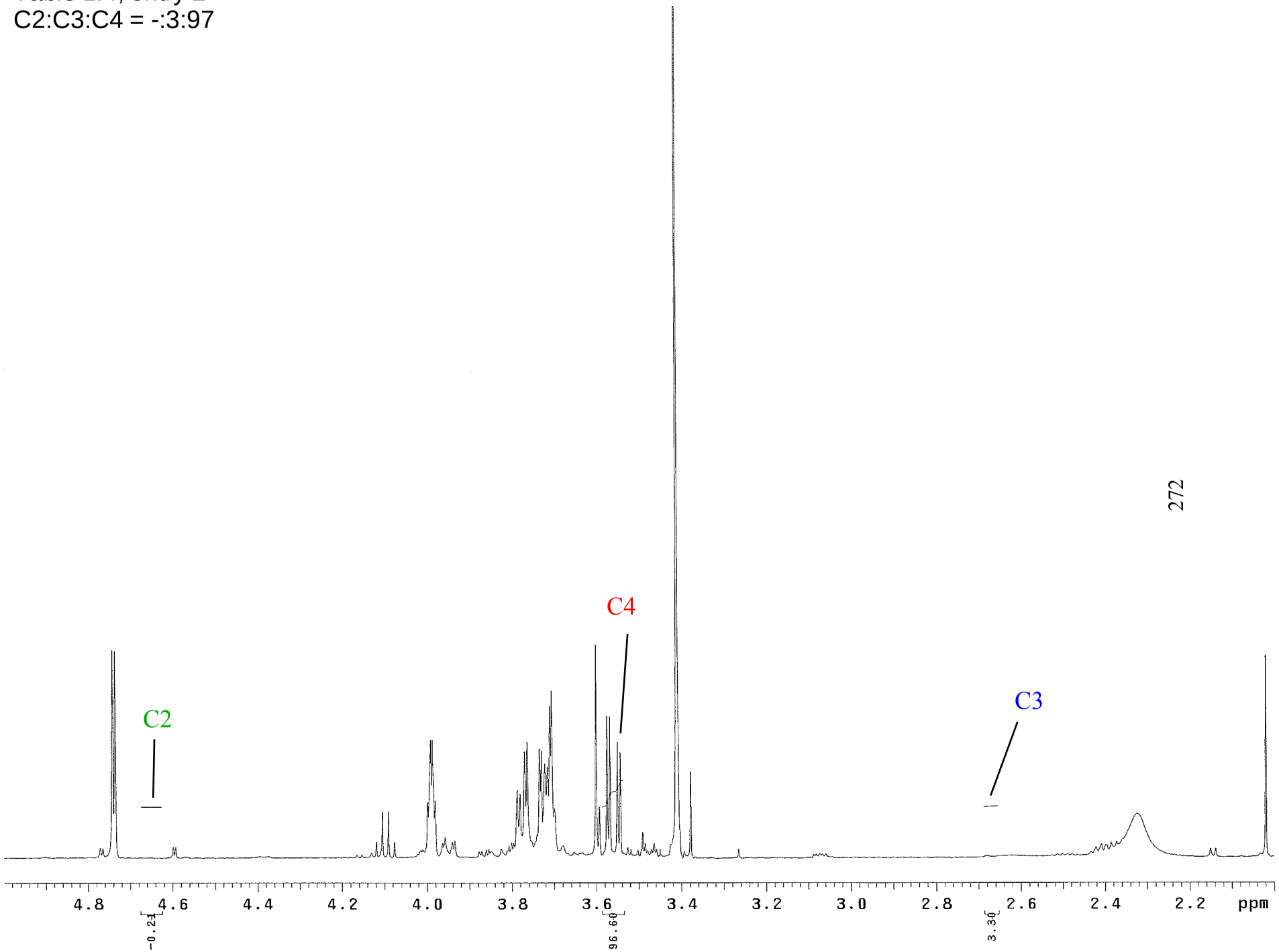

Table 1.4, entry 3
C2:C3:C4 = -:98:2

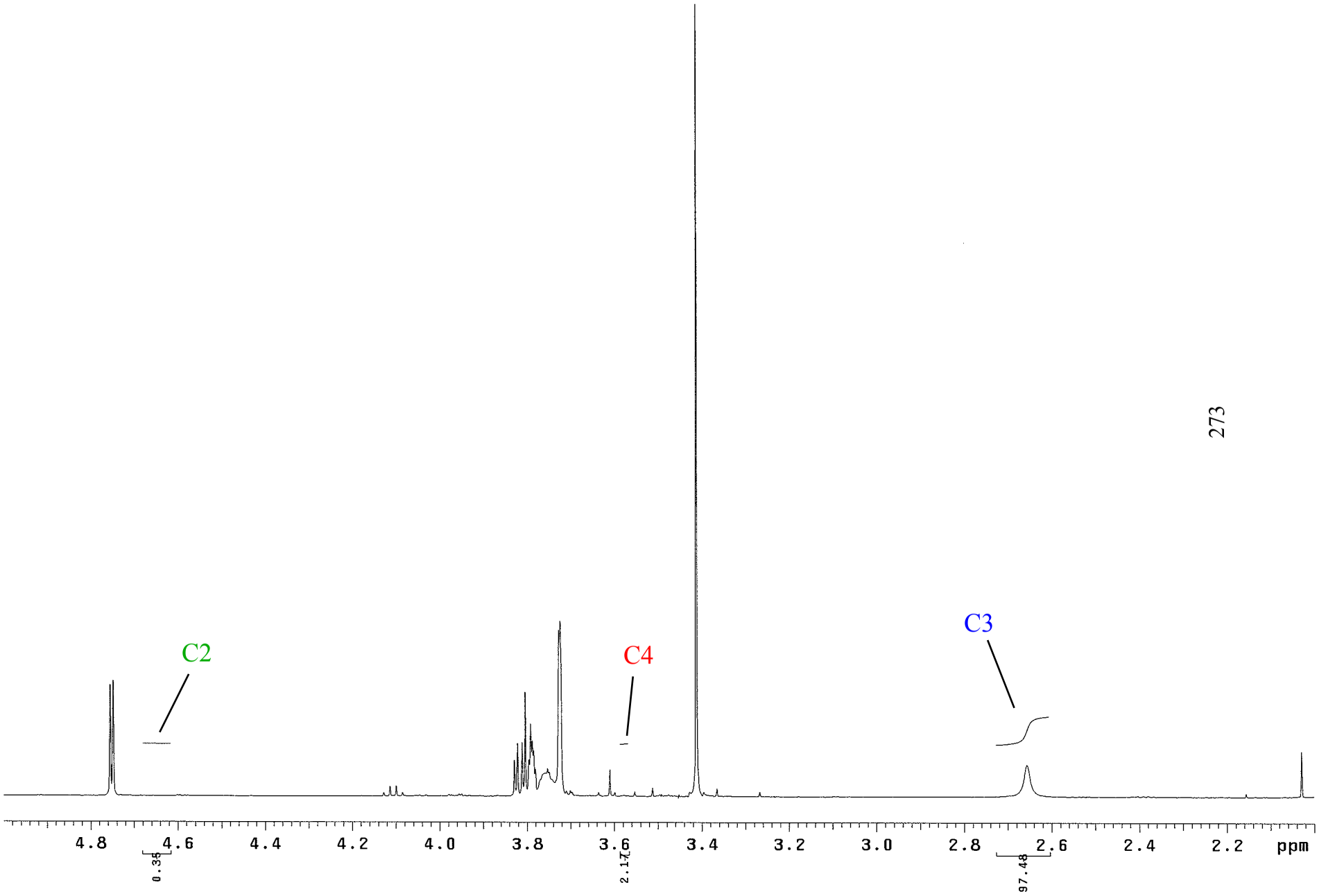

Table 1.4, entry 4
C2:C3:C4 = 22:72:6

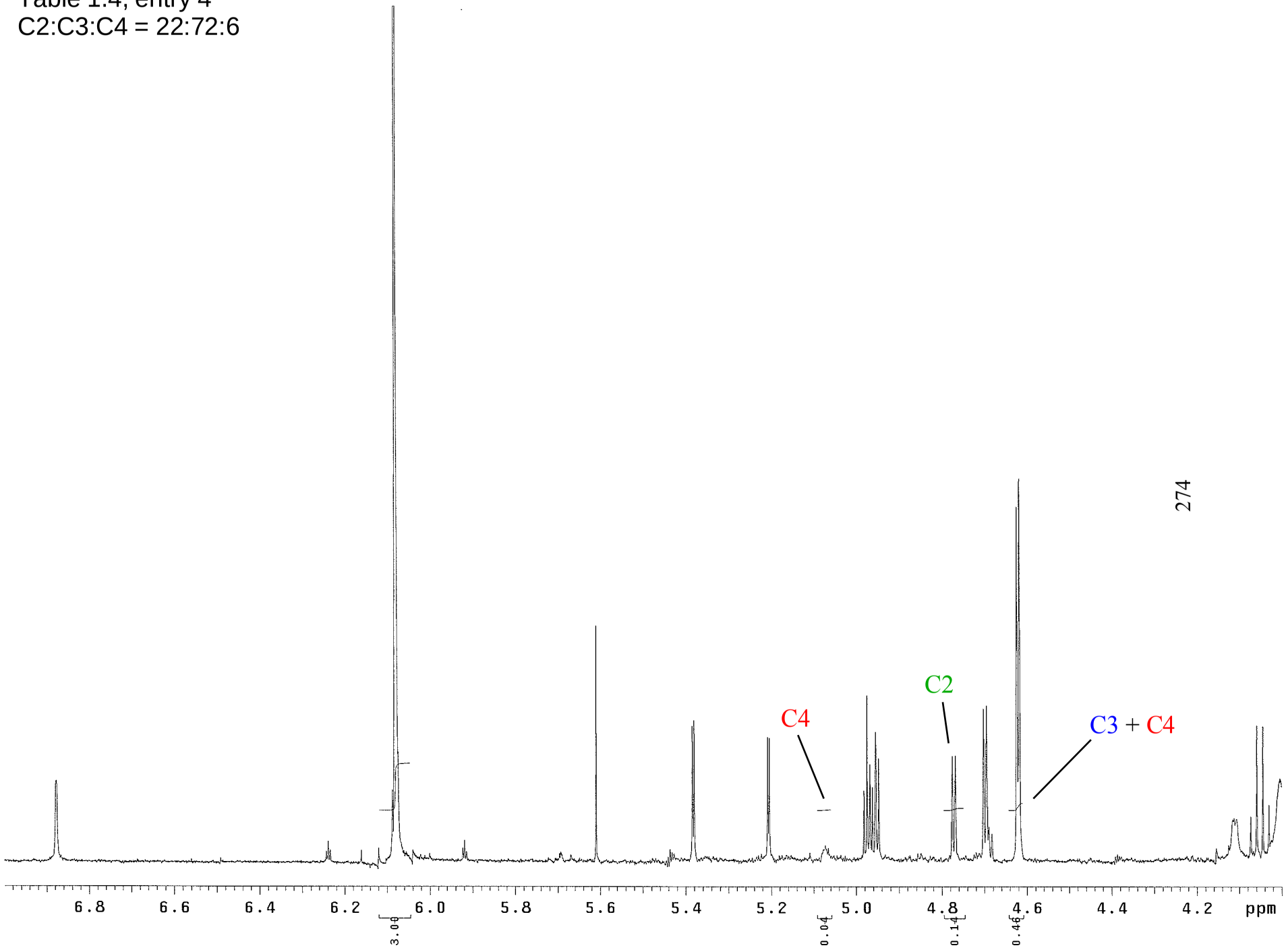

Table 1.4, entry 5
C2:C3:C4 = 5:9:86

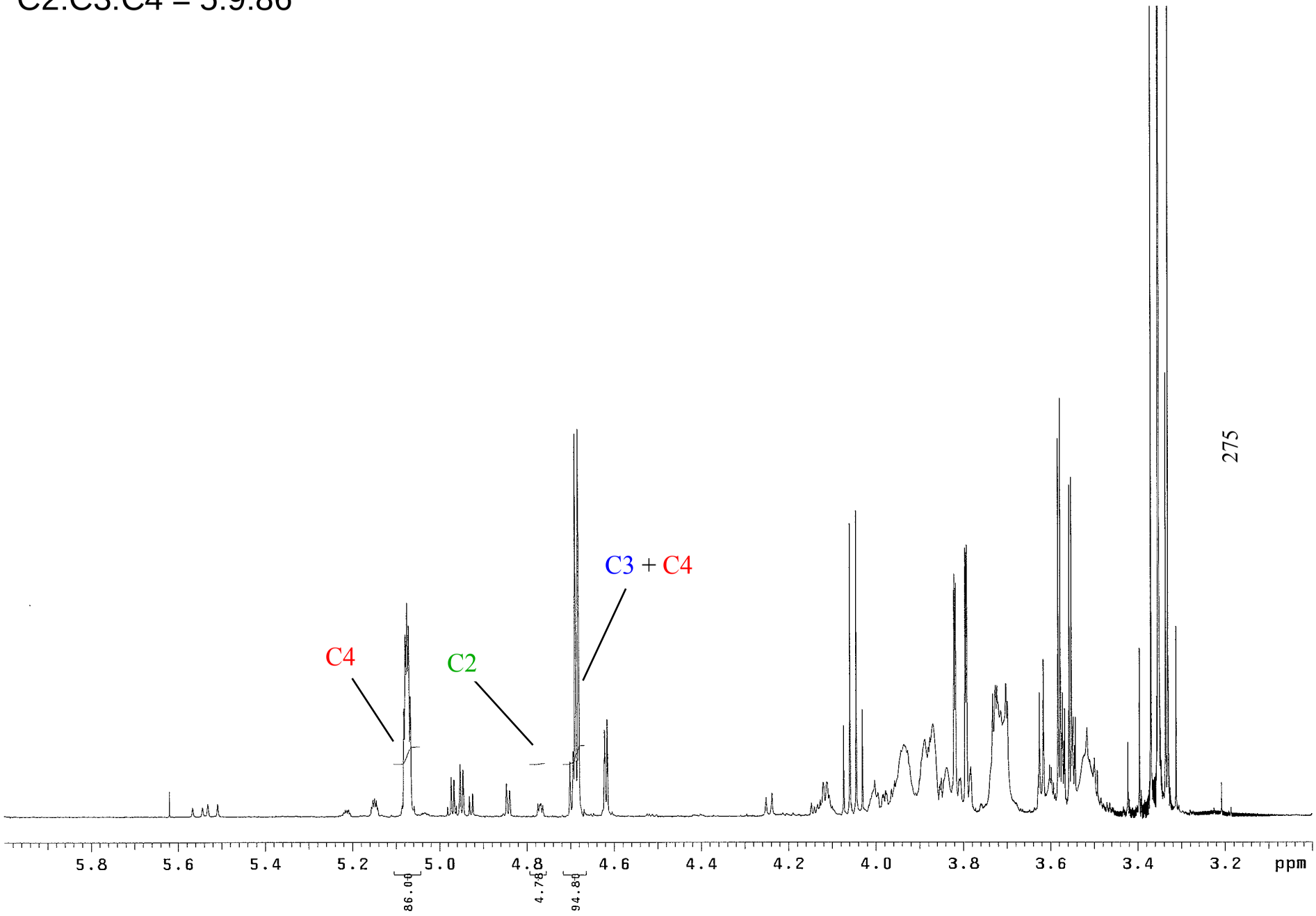

Table 1.4, entry 6
C2:C3:C4 = 3:96:1

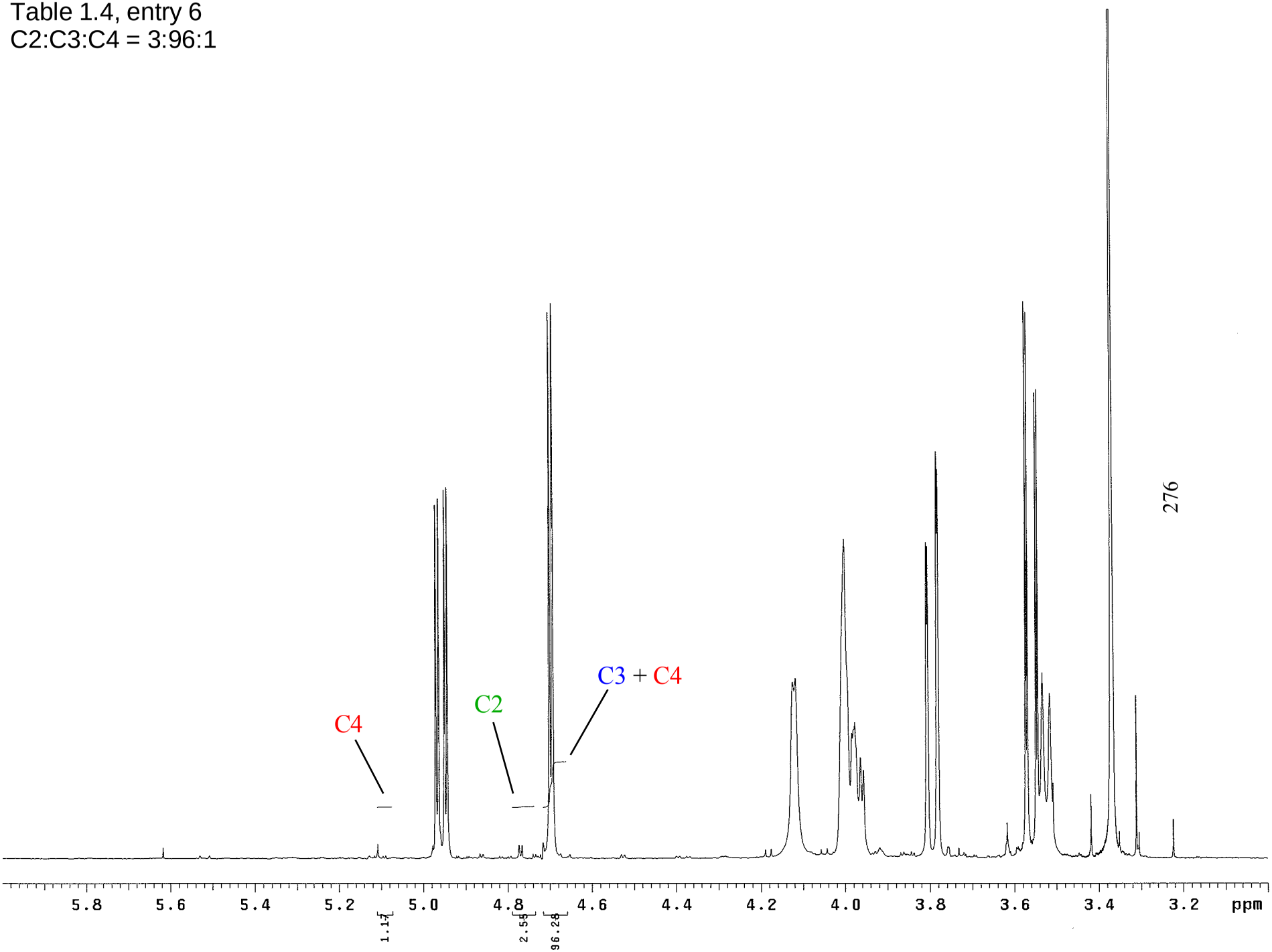

Table 1.4, entry 7
C2:C3:C4 = 68:23:9

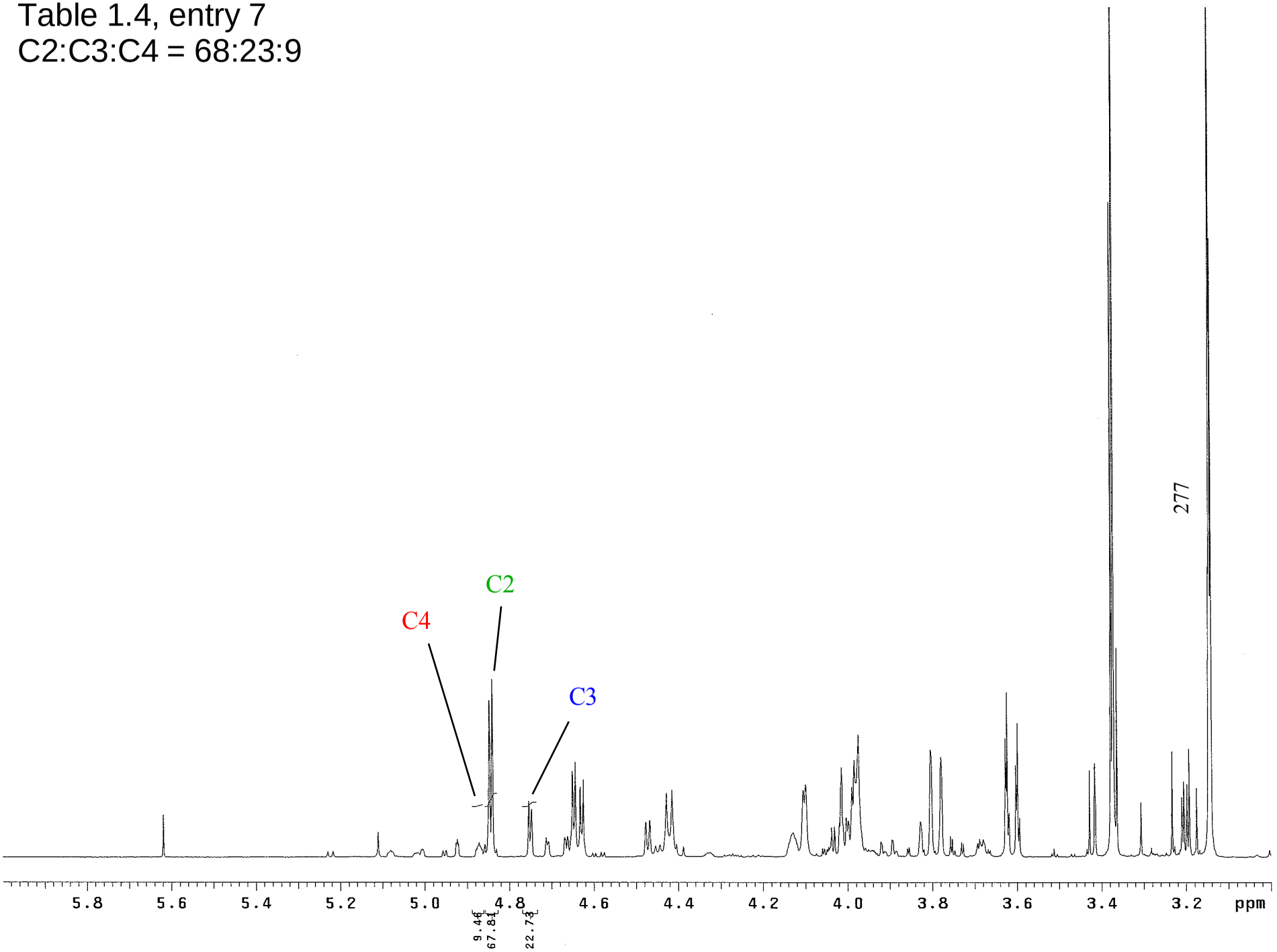

Table 1.4, entry 8
C2:C3:C4 = 3:10:87

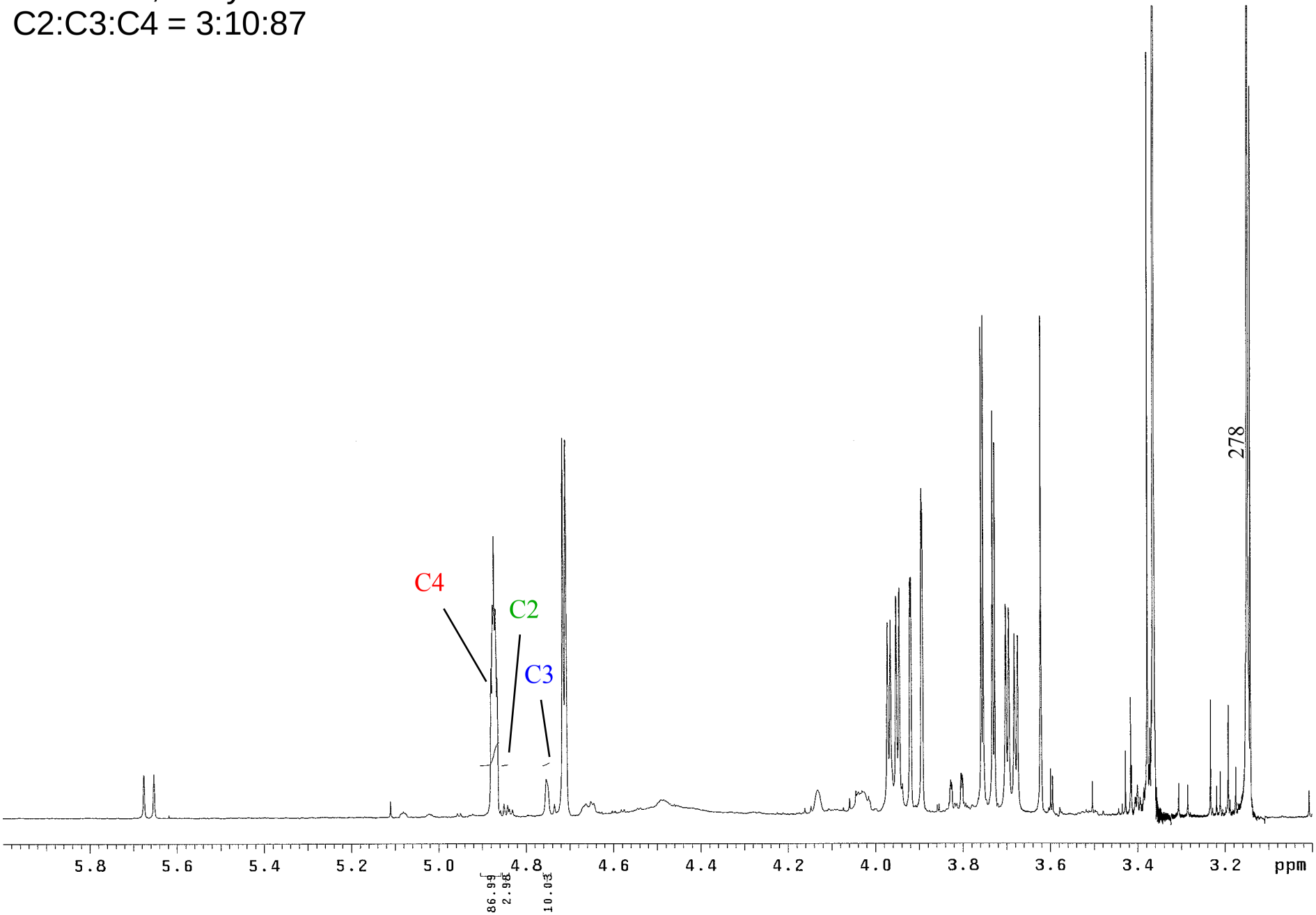

Table 1.4, entry 9
C2:C3:C4 = 1:92:7

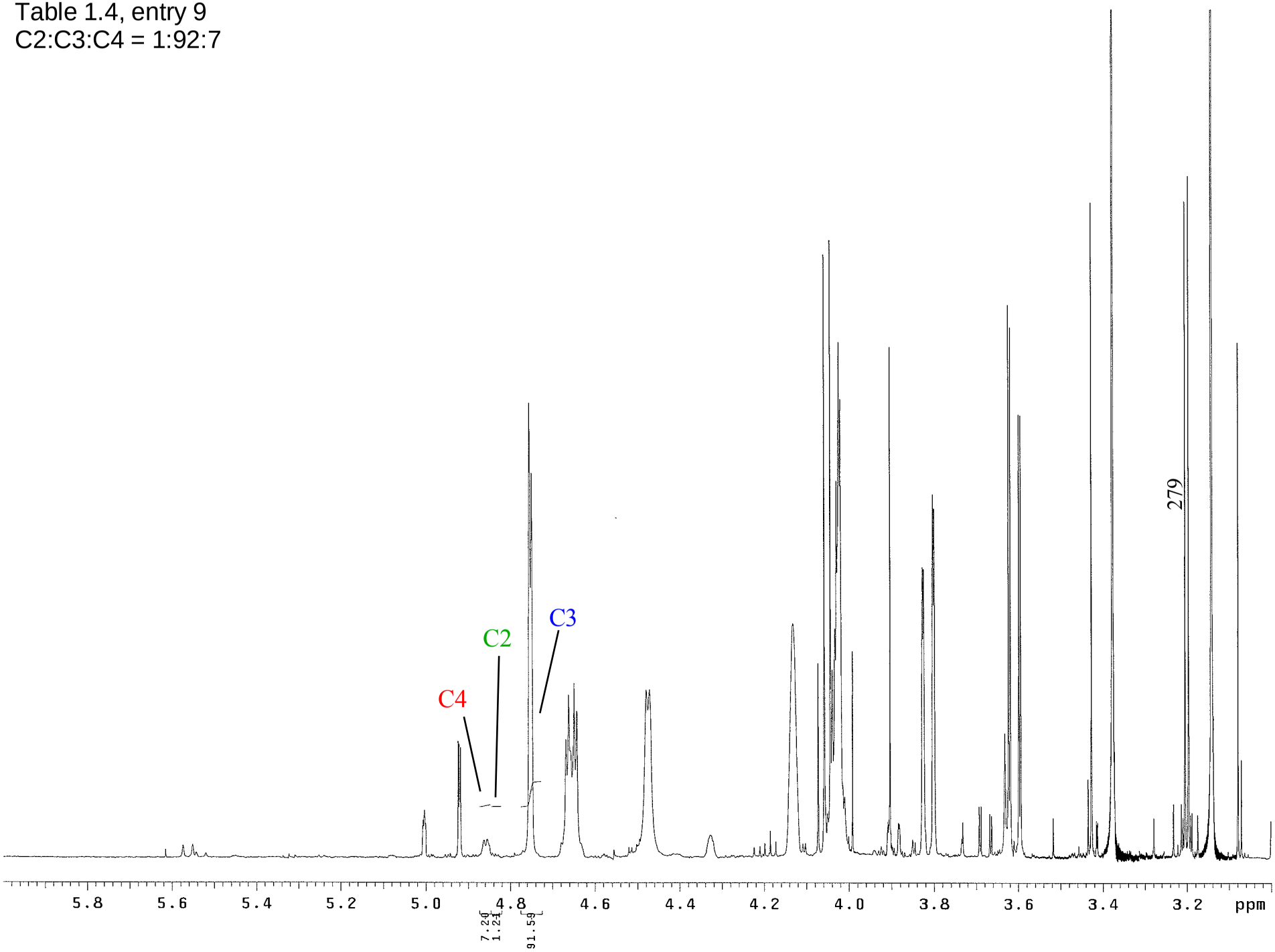

Table 1.5, entry 1
C2:C3:C4 = 86:14:-

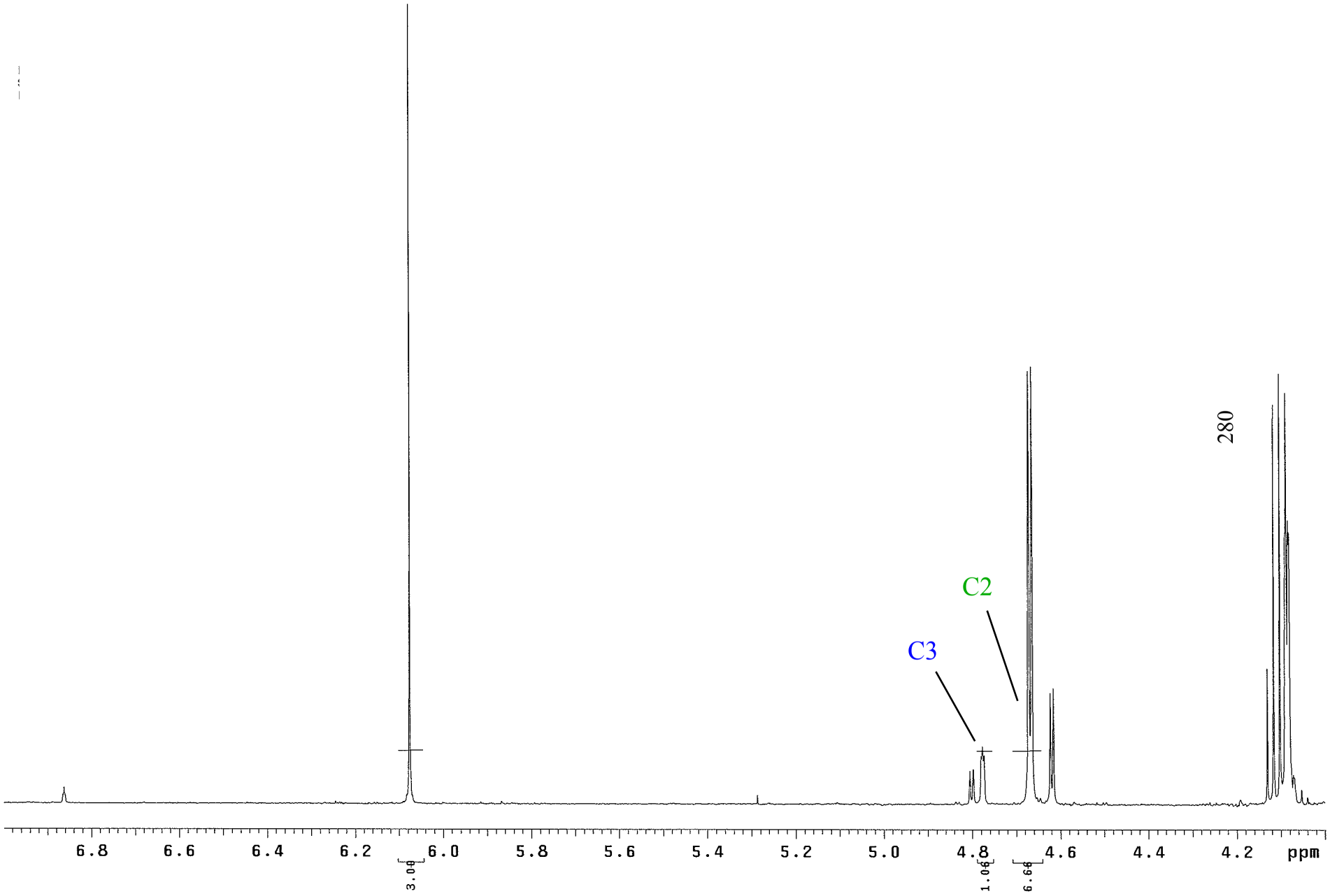

Table 1.5, entry 2
C2:C3:C4 = 6:94:-

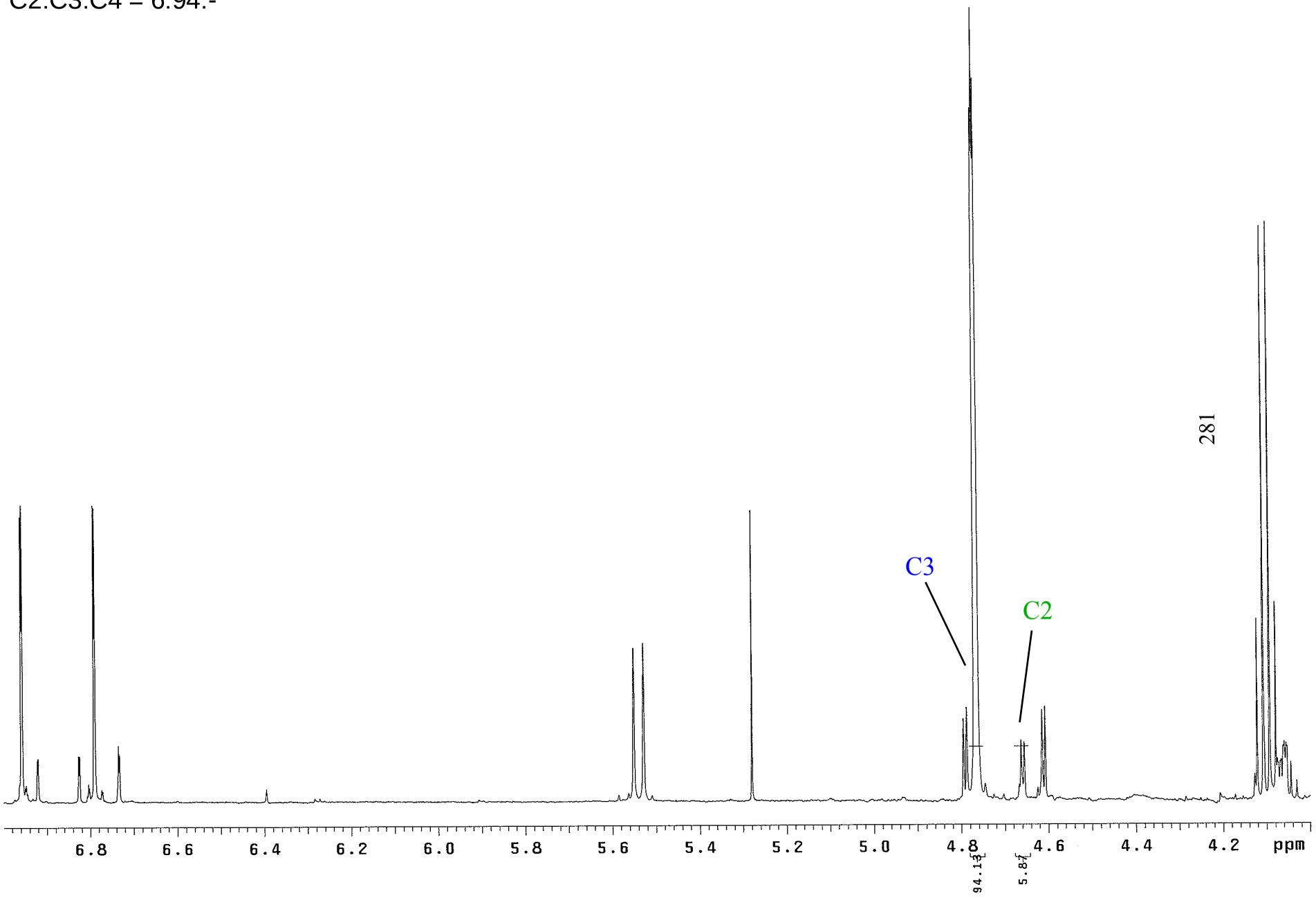

Table 1.5, entry 3
C2:C3:C4 = 42:58:-

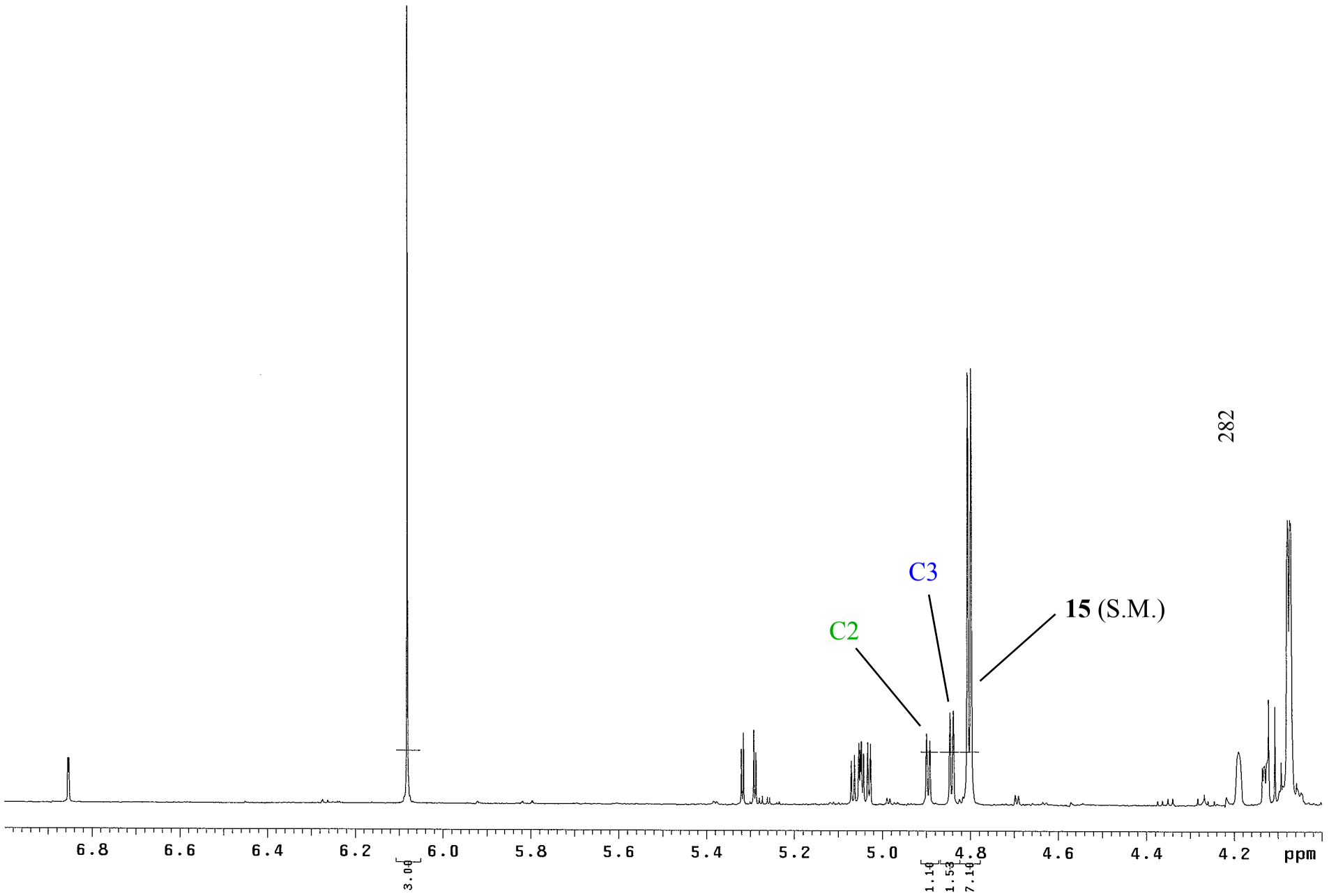

Table 1.5, entry 4
C2:C3:C4 = 19:81:-

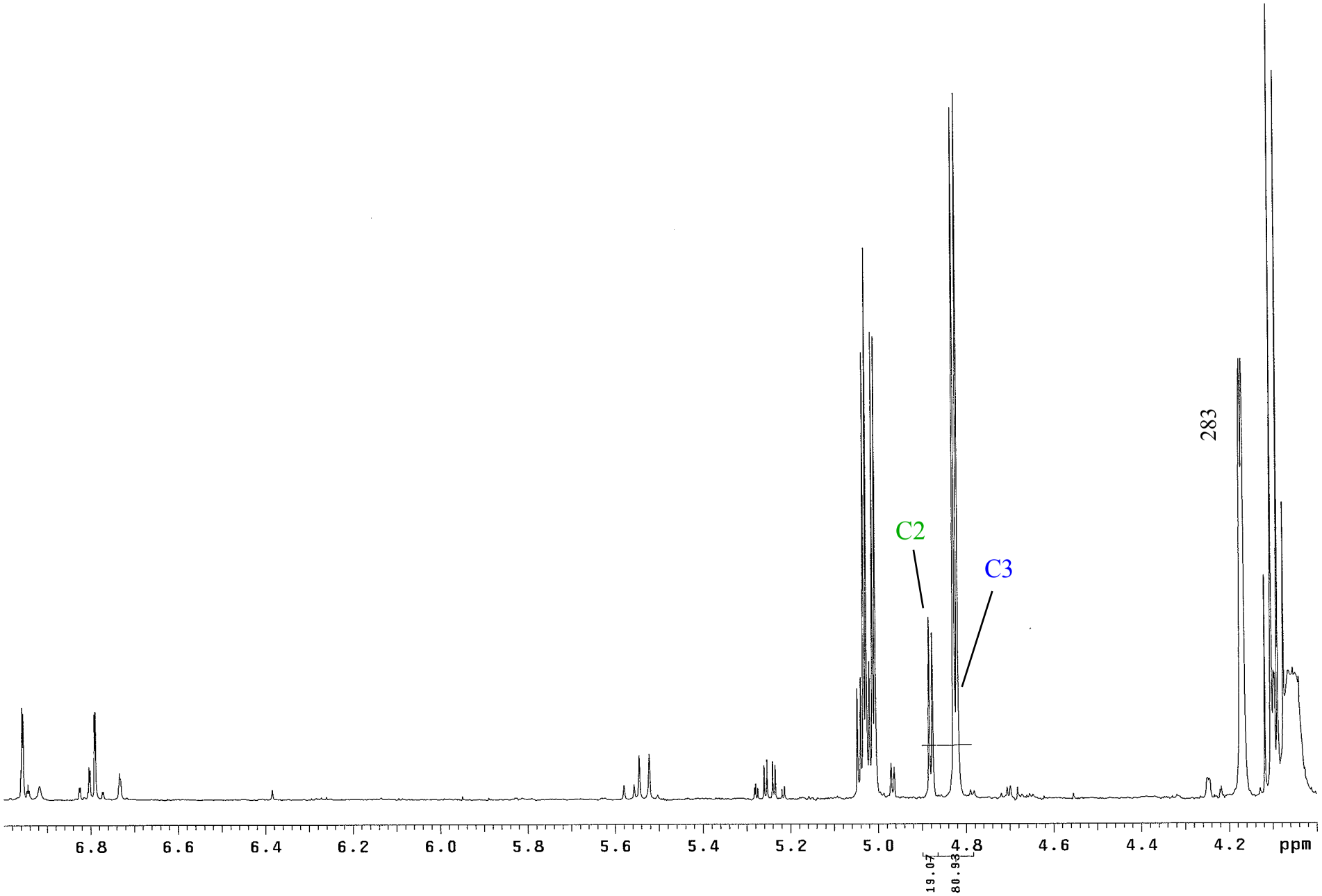

Table 1.5, entry 5.
C2:C3:C4 = 76:24:-

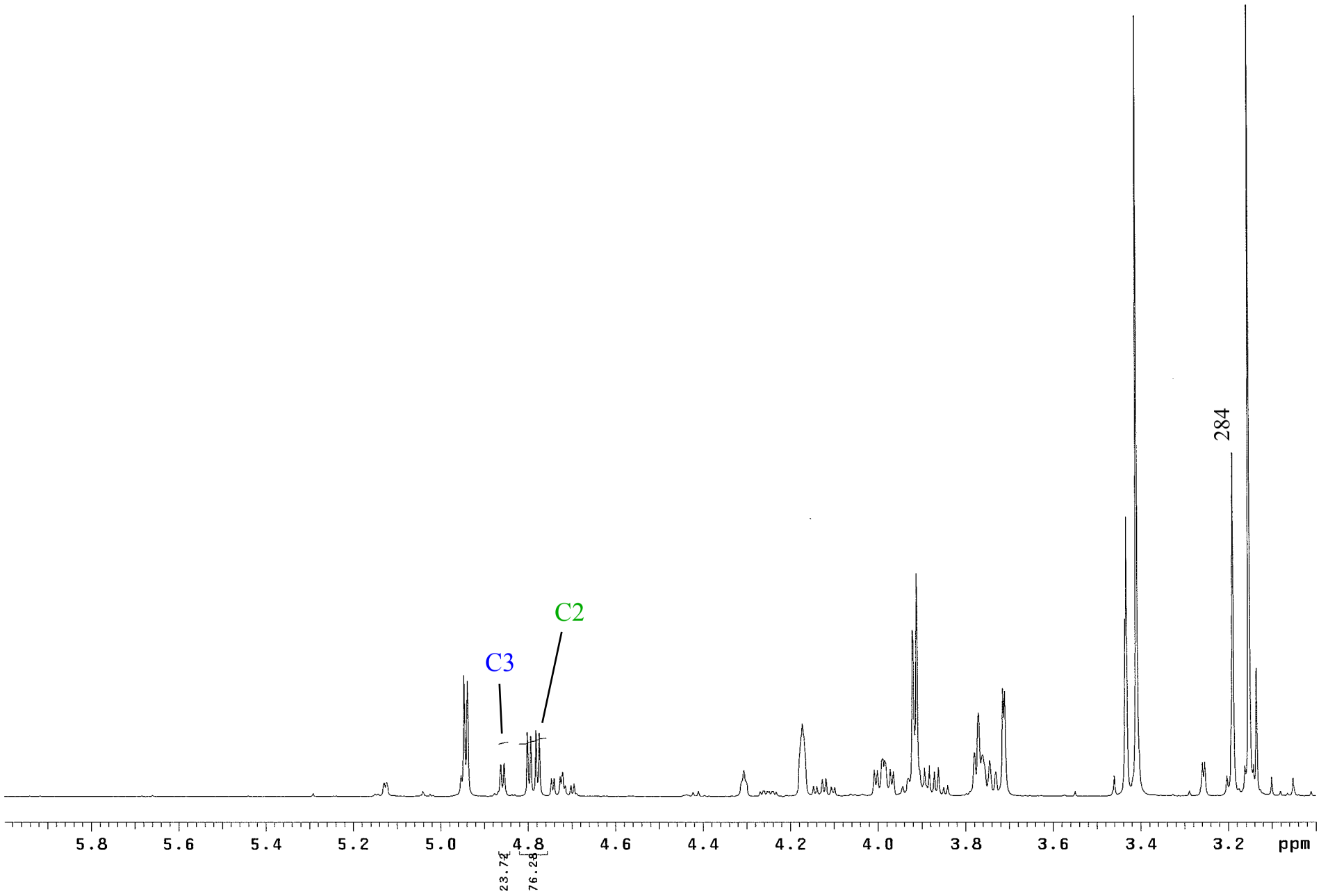

Table 1.5, entry 6
C2:C3:C4 = -:100:-

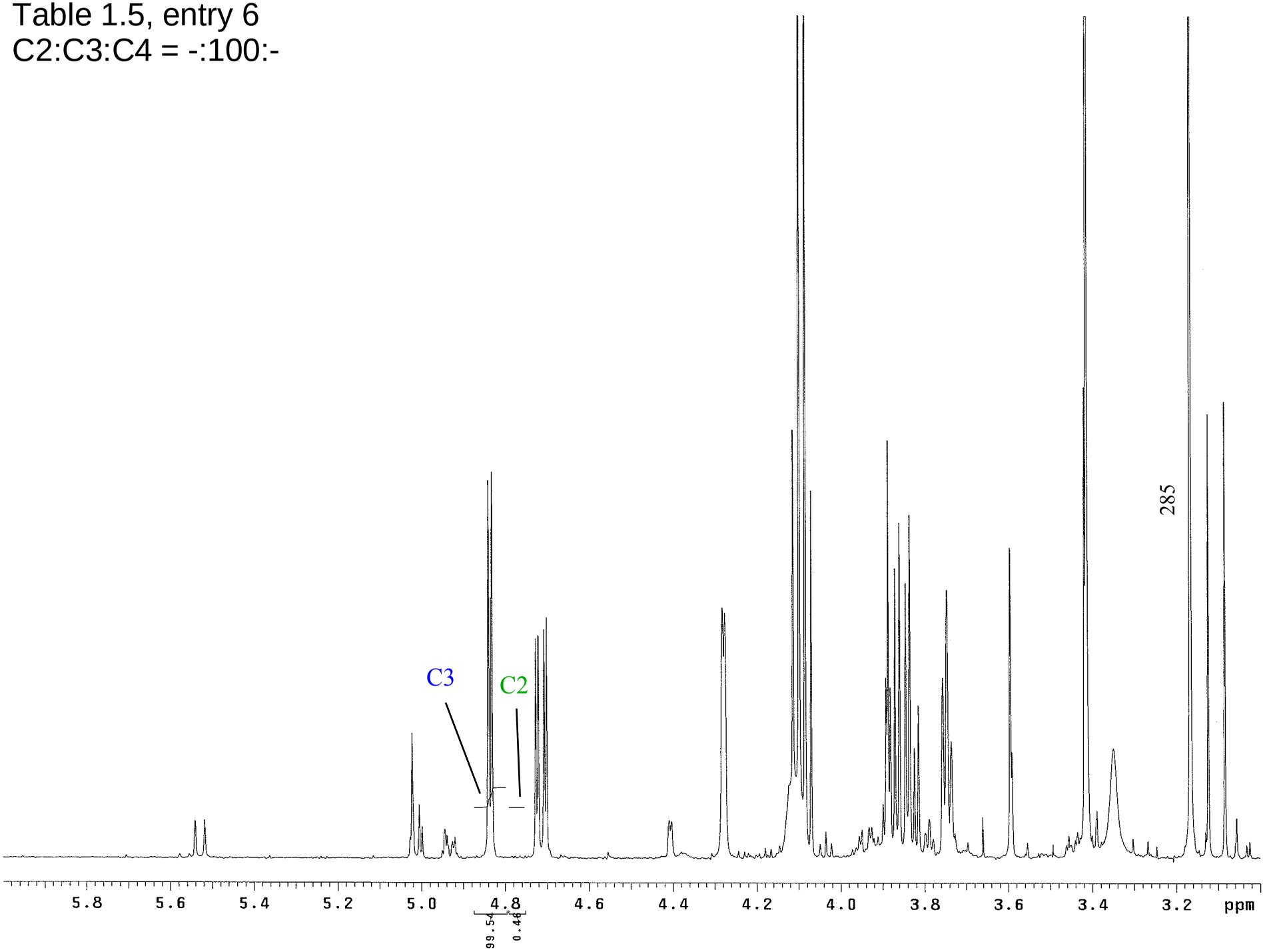

Table 1.6, entry 1
C2:C3:C4 = 91:-:9

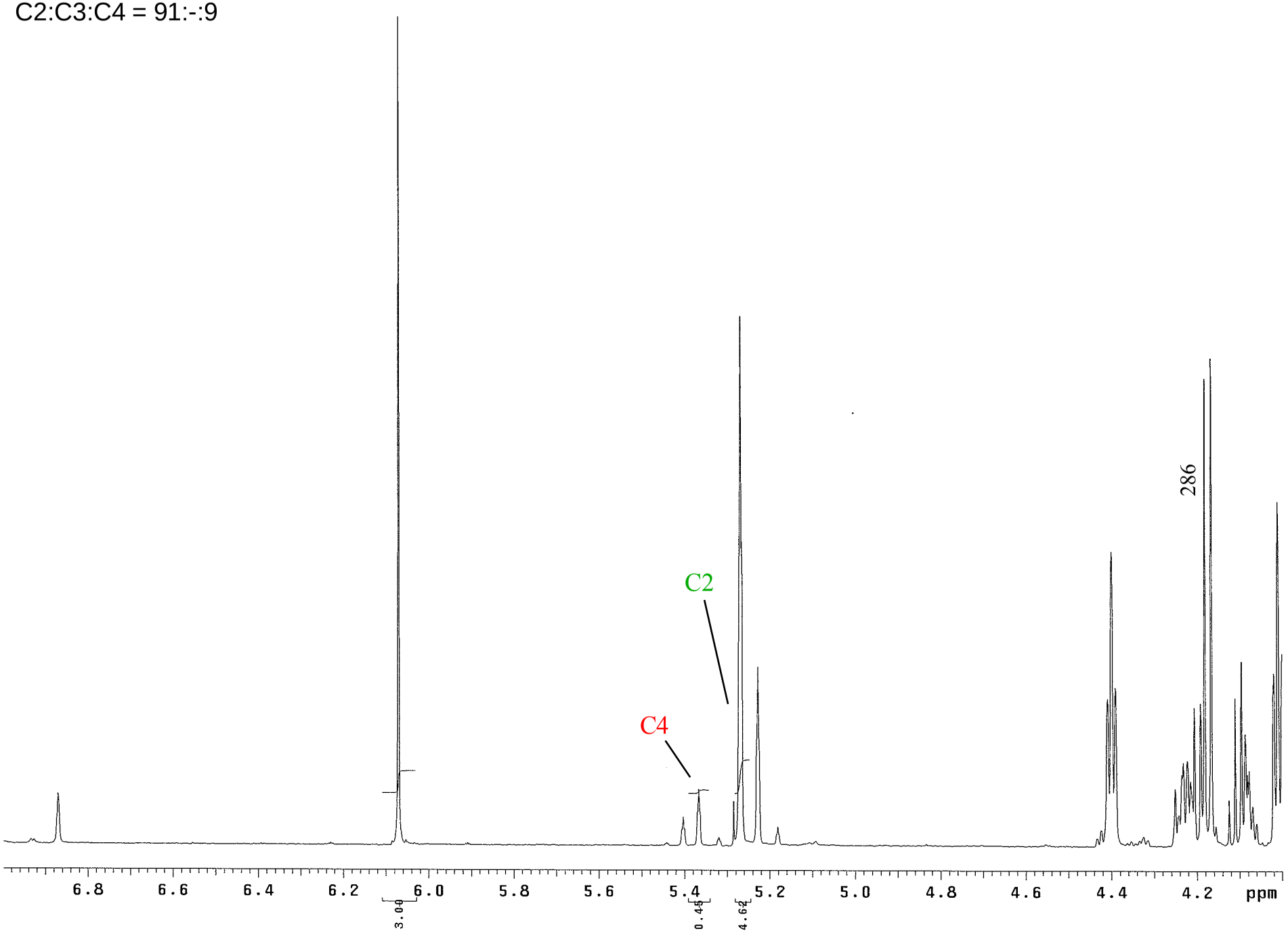

Table 1.6, entry 2
C2:C3:C4 = 1:-:99

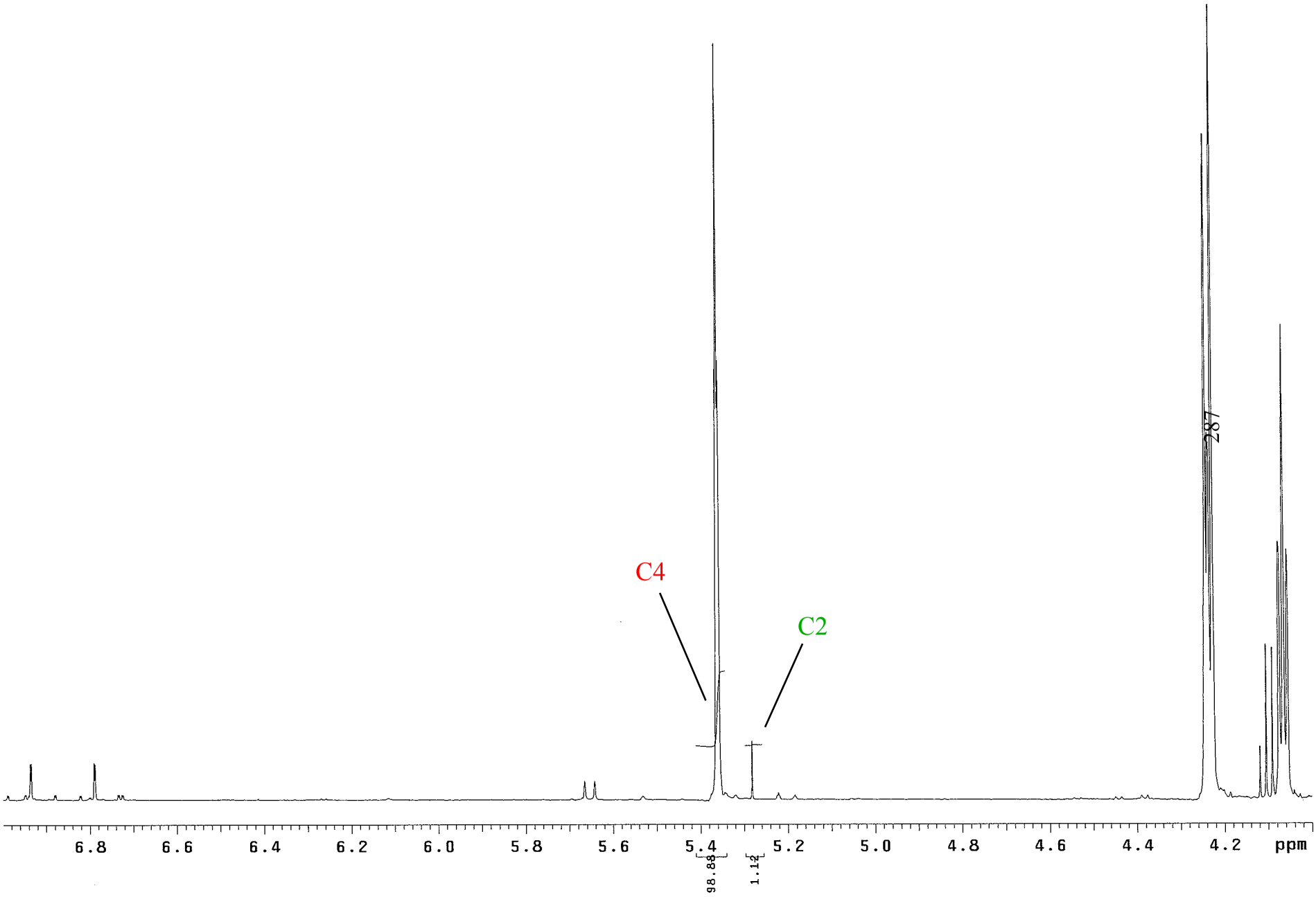

Table 1.6, entry 3
C2:C3:C4 = 75:8:17

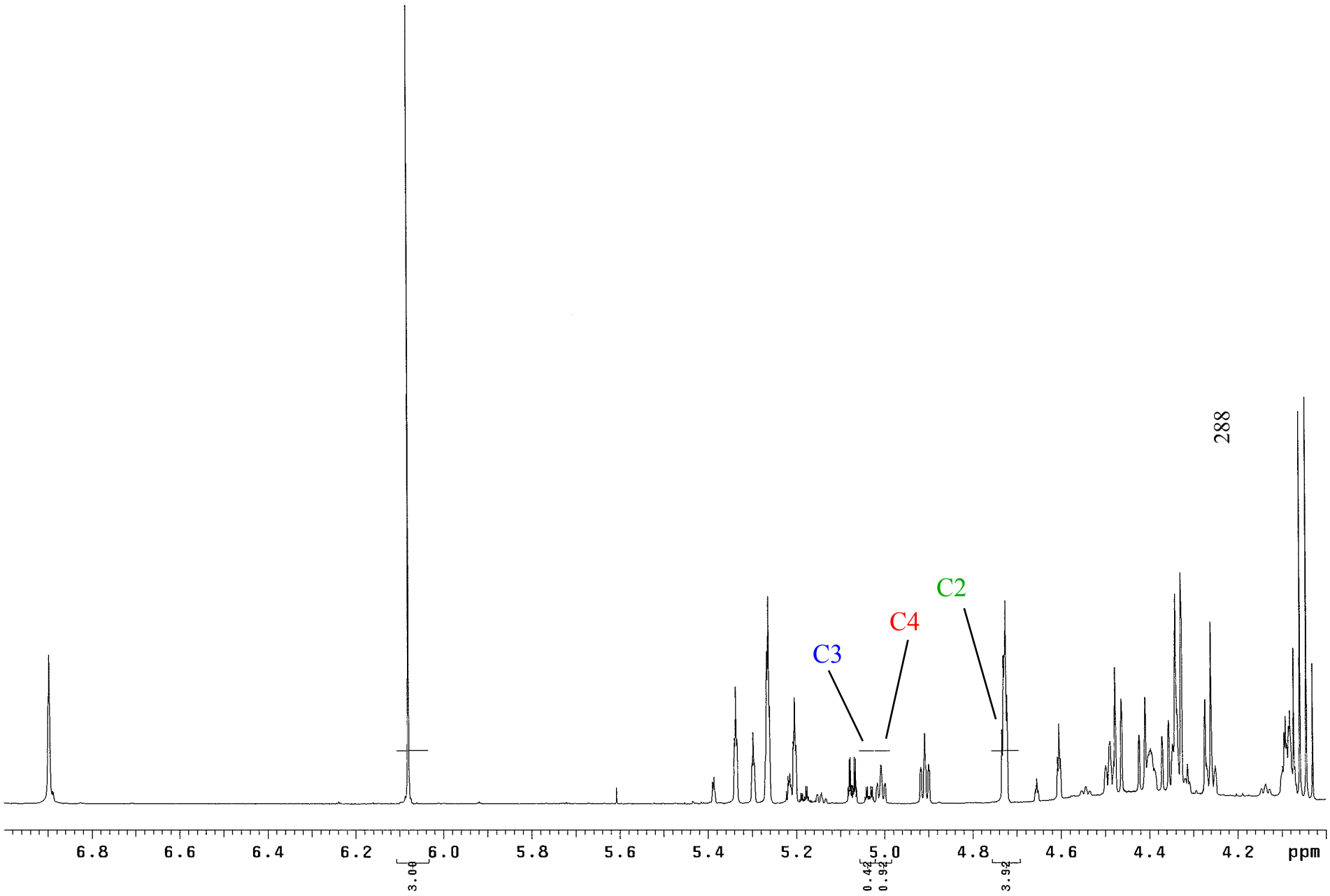

Table 1.6, entry 4
C2:C3:C4 = -:3:97

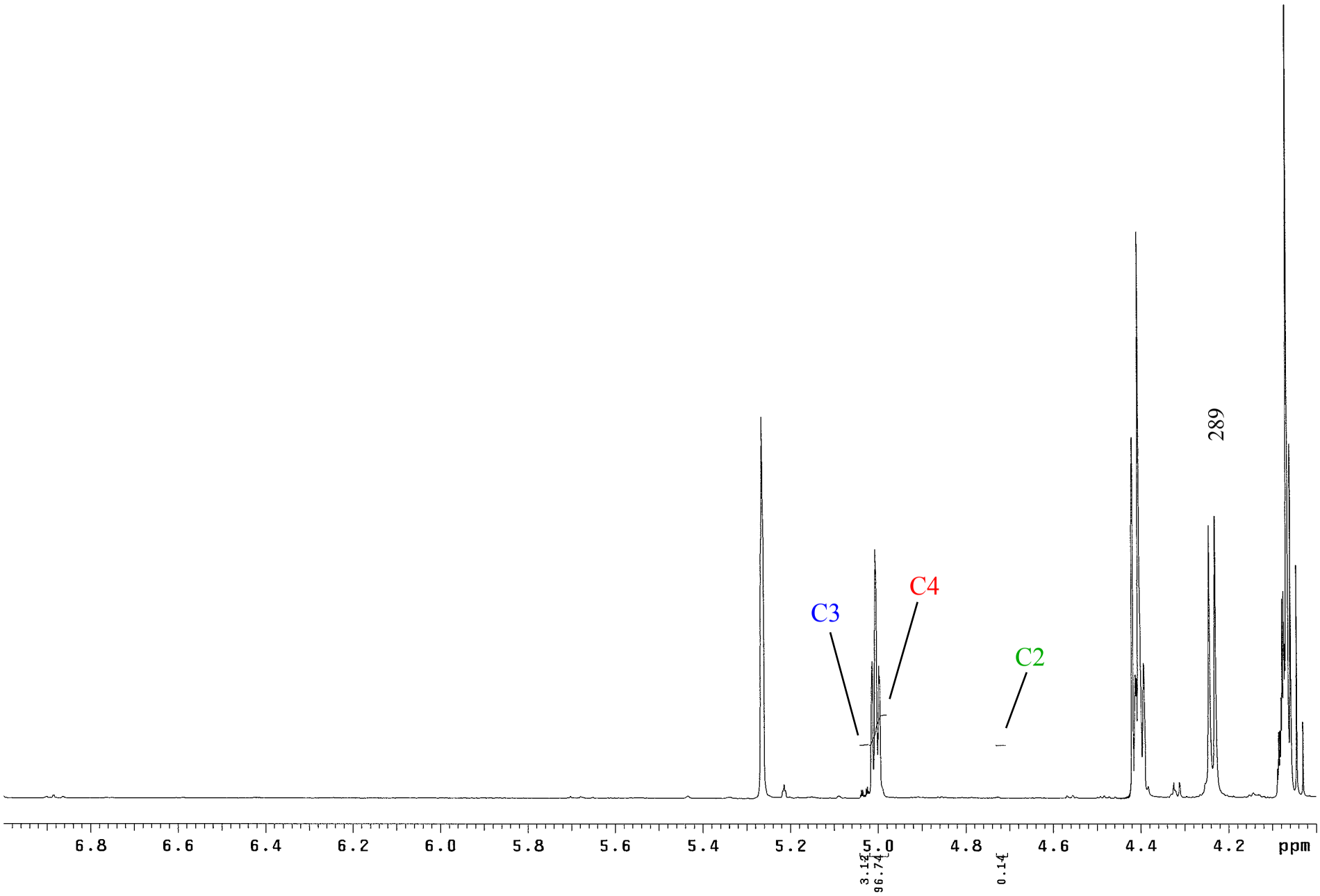

Table 1.6, entry 5
C2:C3:C4 = 75:6:19

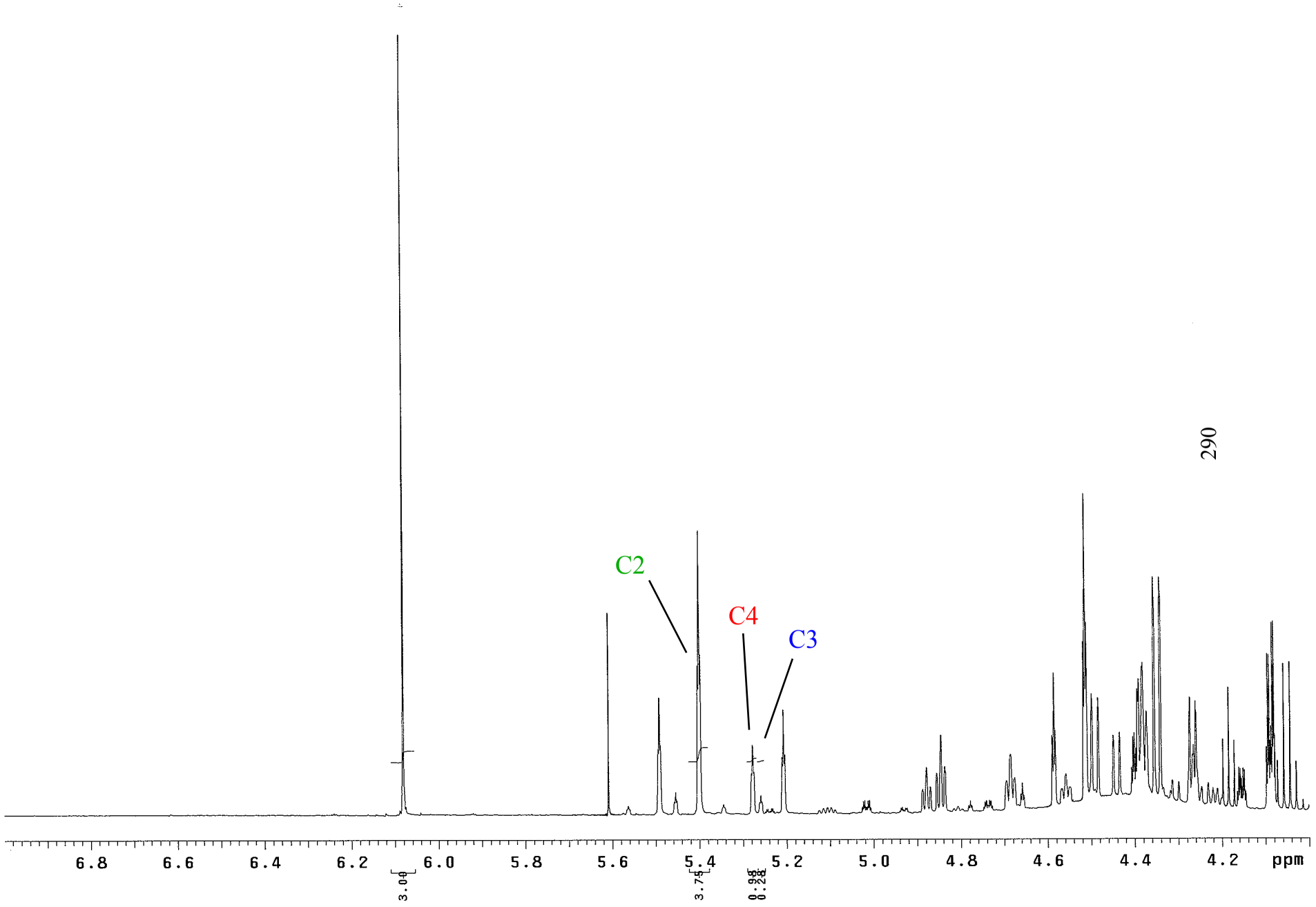

Table 1.6, entry 6
C2:C3:C4 = -:1:99

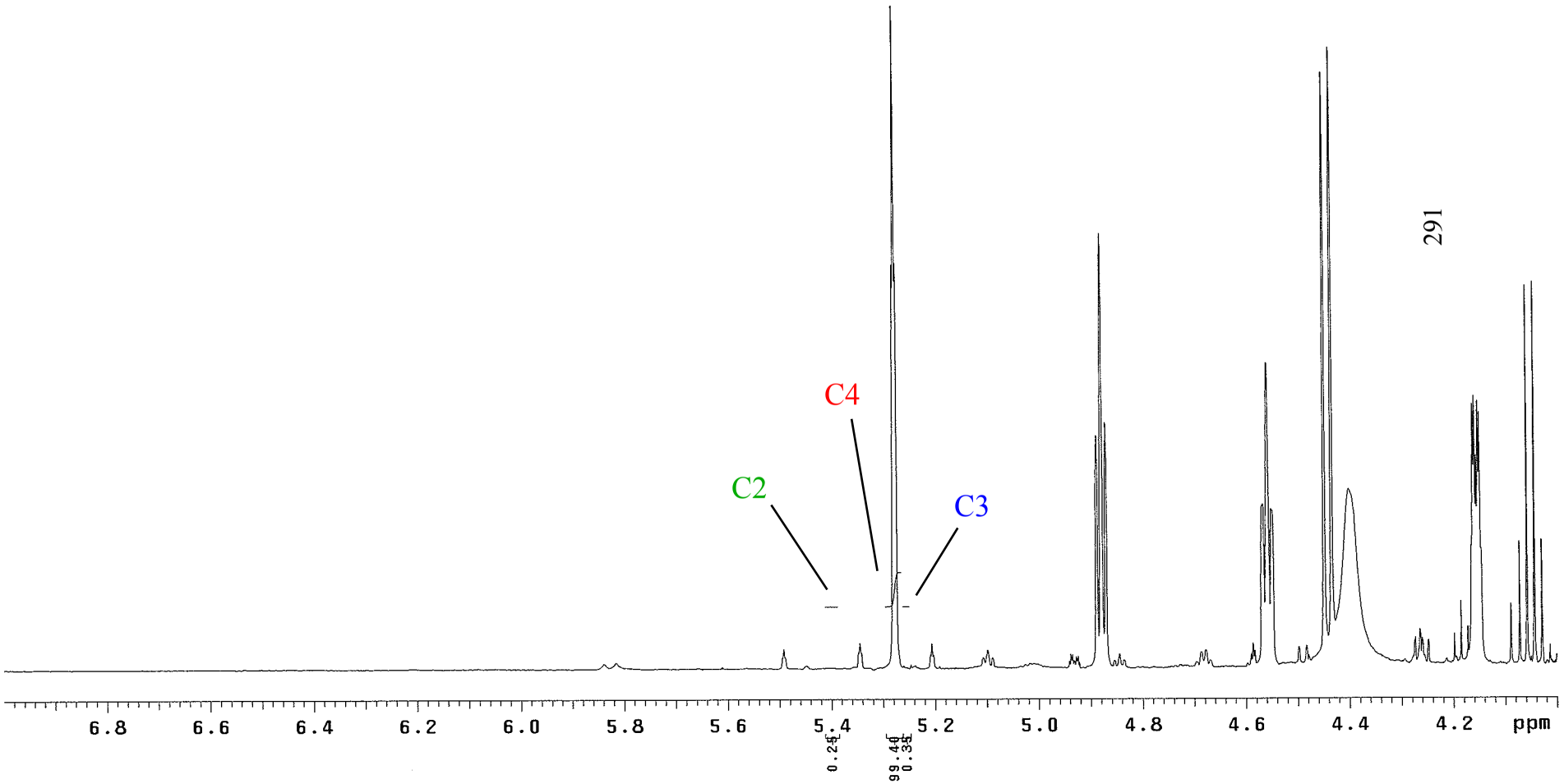

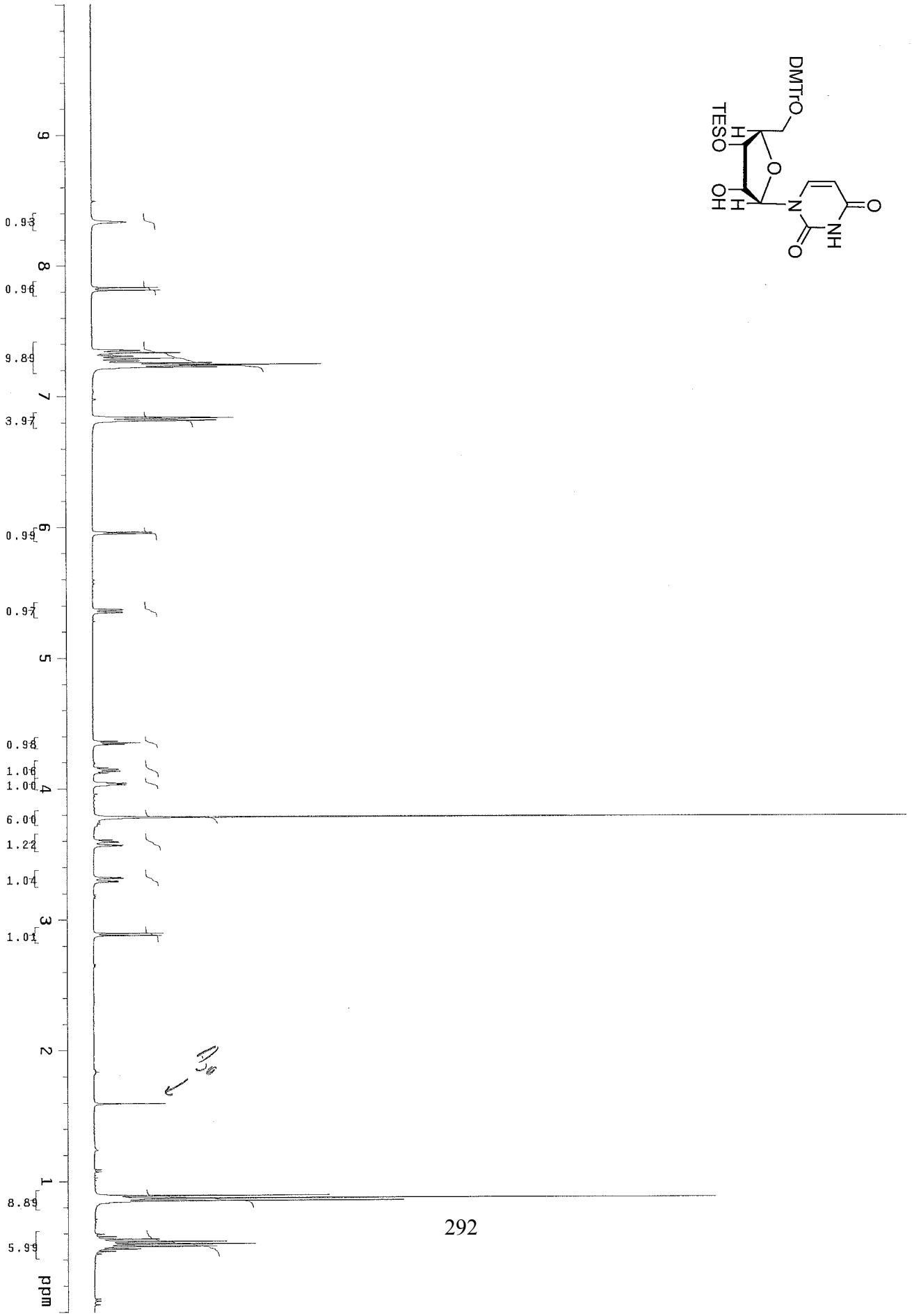
DMTrO
TESO
H
OH
H
O
N
NH
O
O
9
8
7
6
5
4
3
2
1
ppm
0.93
0.96
9.89
3.97
0.99
0.97
0.98
1.06
1.00
6.00
1.22
1.04
1.01
8.89
5.99

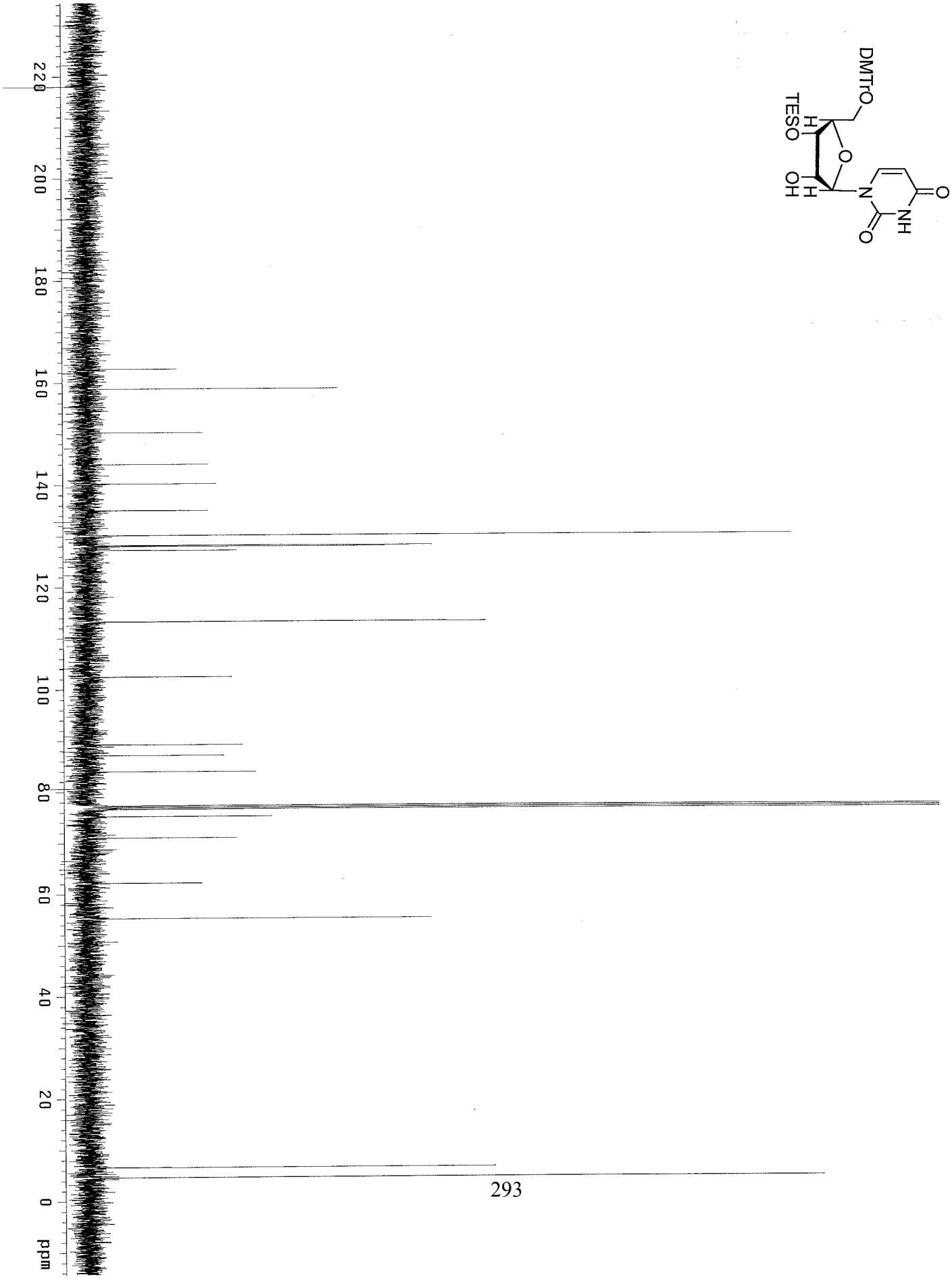
DMTrO
TESO
H
OH
H
O
N
NH
O
O
220
200
180
160
140
120
100
80
60
40
20
0
ppm

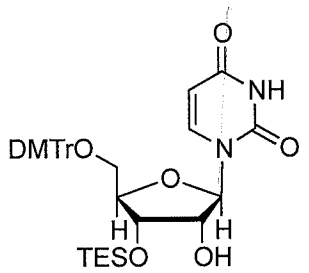
O
NH
N
O
DMTrO
O
H
TESO
OH
H

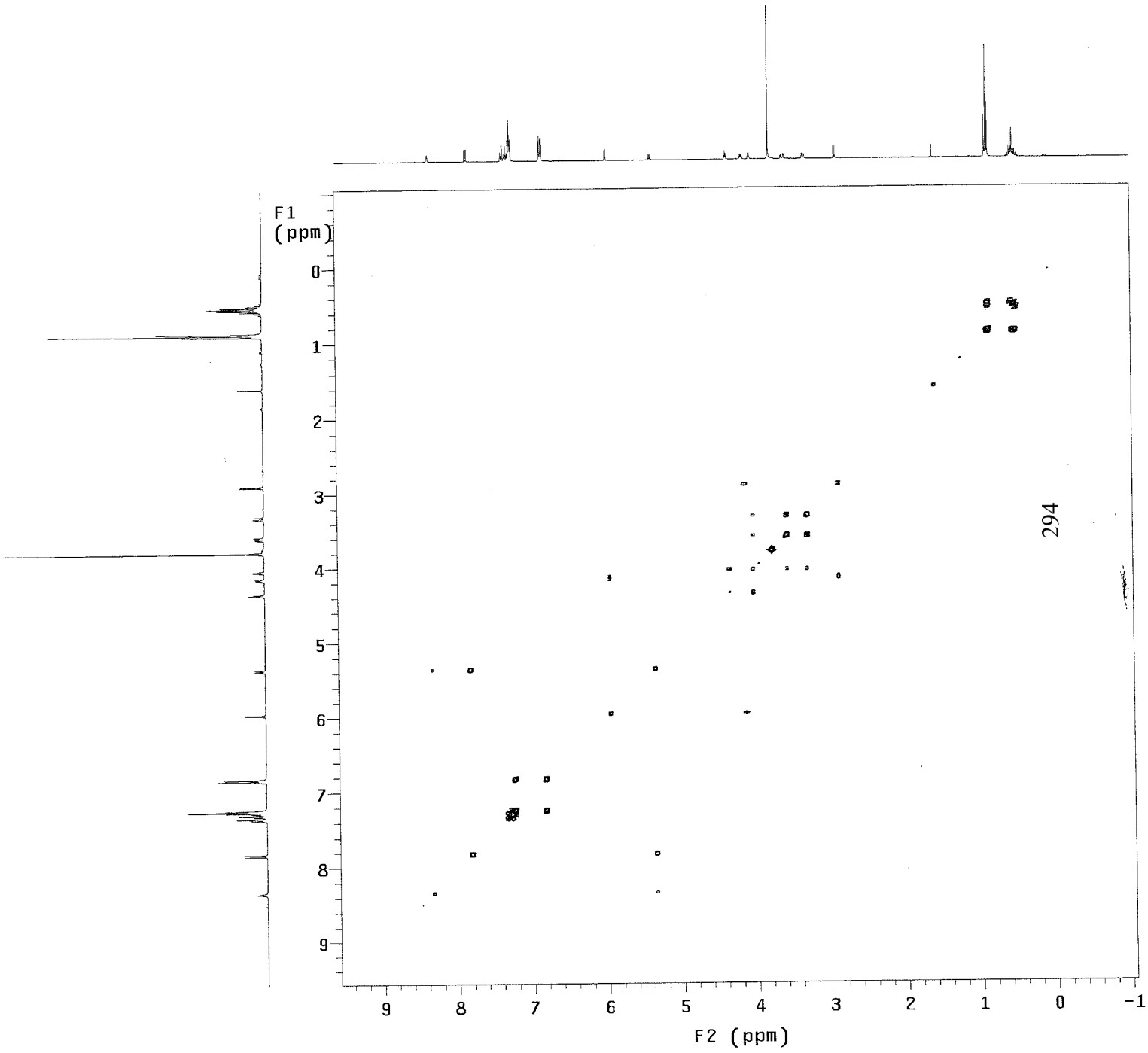
F1
(ppm)
0
1
2
3
4
5
6
7
8
9
9
8
7
6
5
4
3
2
1
0
-1
F2 (ppm)
294

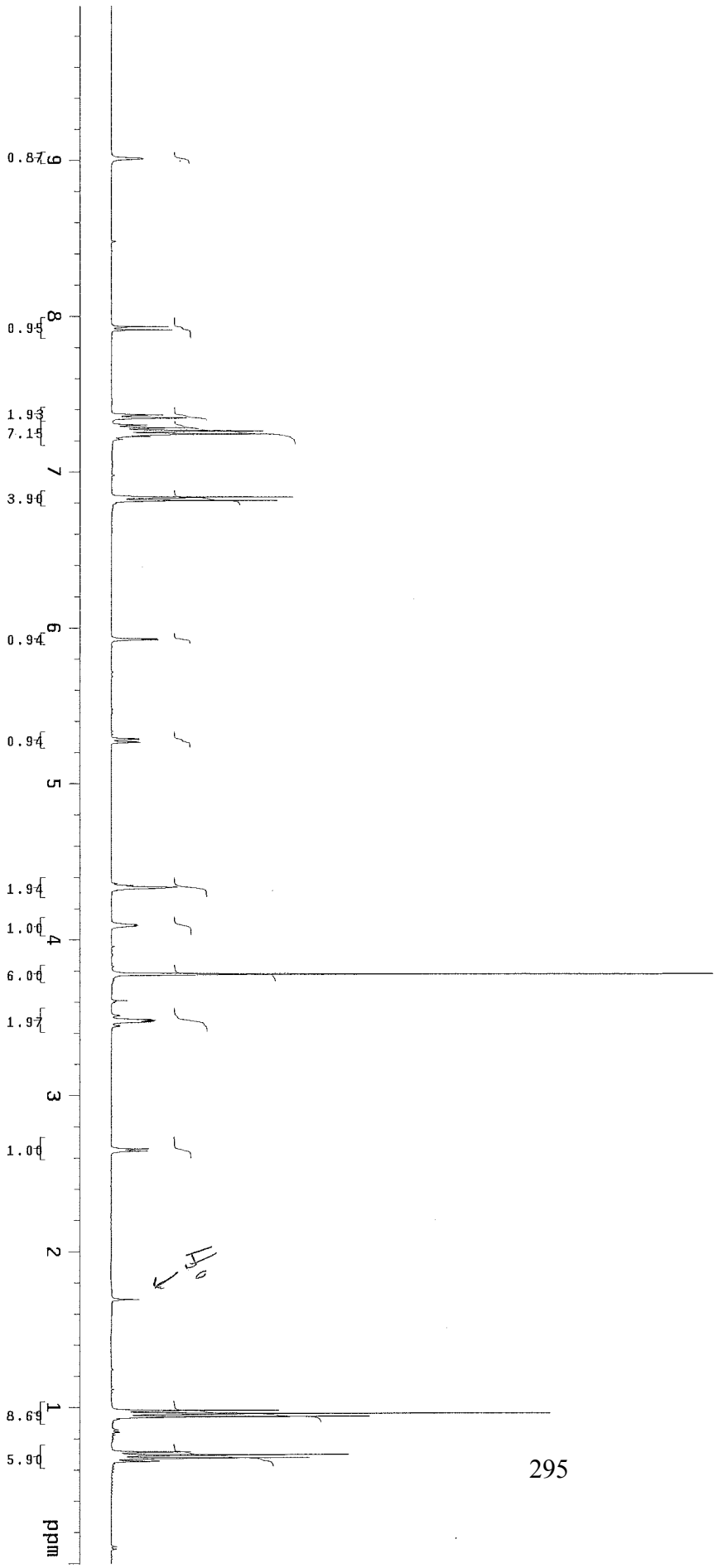
DMTrO
H
OH
OTES
H
O
N
O
NH
O
0.87
0.95
1.93
7.15
3.96
0.94
0.94
1.94
1.00
6.00
1.97
1.00
8.69
5.90
9
8
7
6
5
4
3
2
1
ppm

DMTrO
H
OH
O
H
OTES
N
O
NH
O

220
200
180
160
140
120
100
80
60
40
20
0
ppm

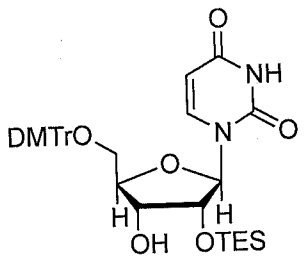
O
NH
N
O
DMTrO
O
H
H
OH
OTES

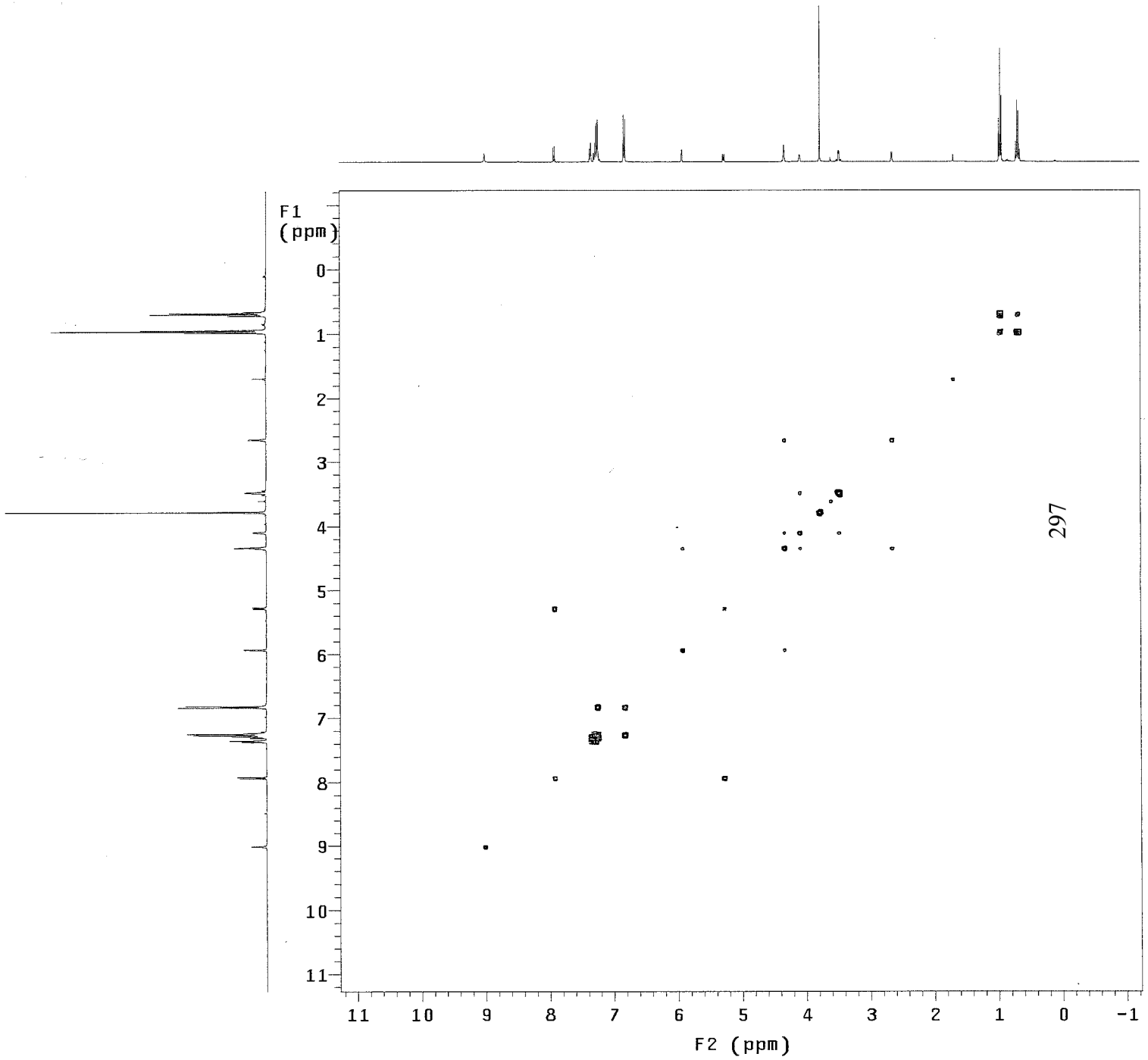
F1
(ppm)
0
1
2
3
4
5
6
7
8
9
10
11
11
10
9
8
7
6
5
4
3
2
1
0
-1
F2 (ppm)
297

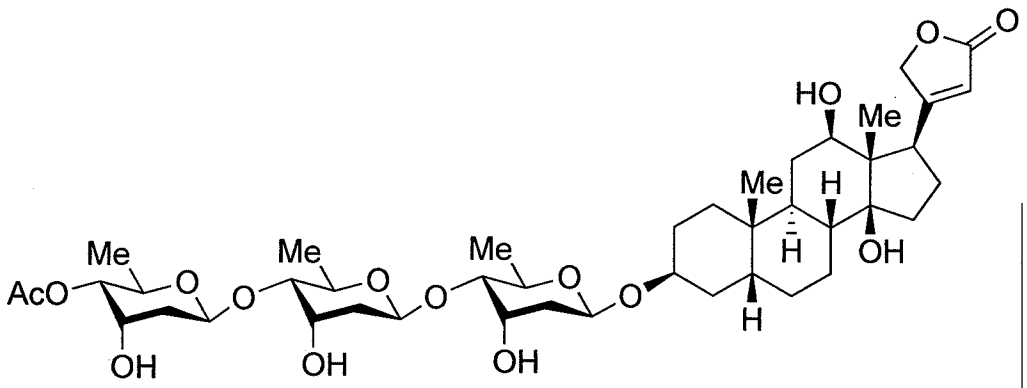

β-Acetyldigoxin ^{1}H NMR

α:β = <2:>98

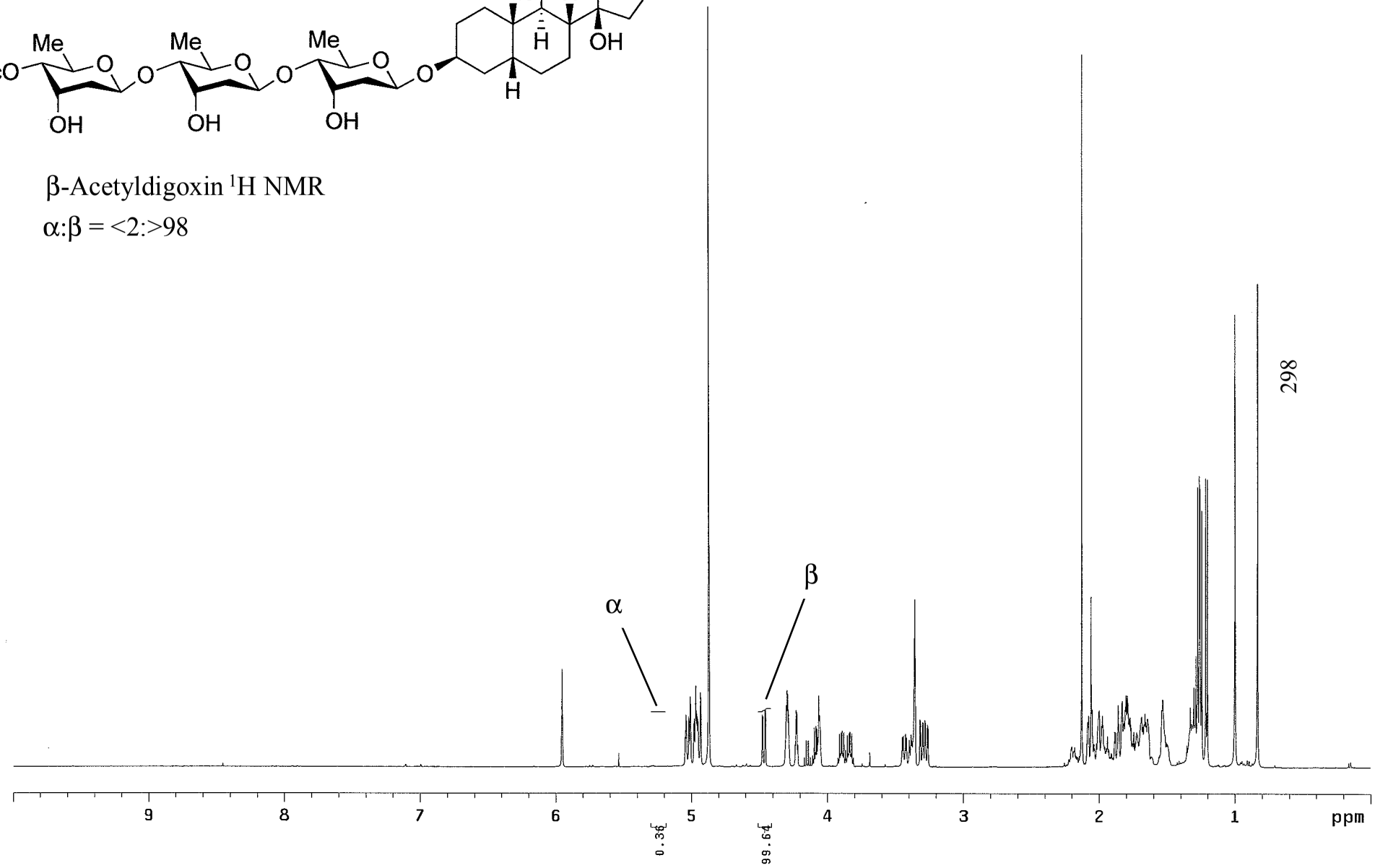

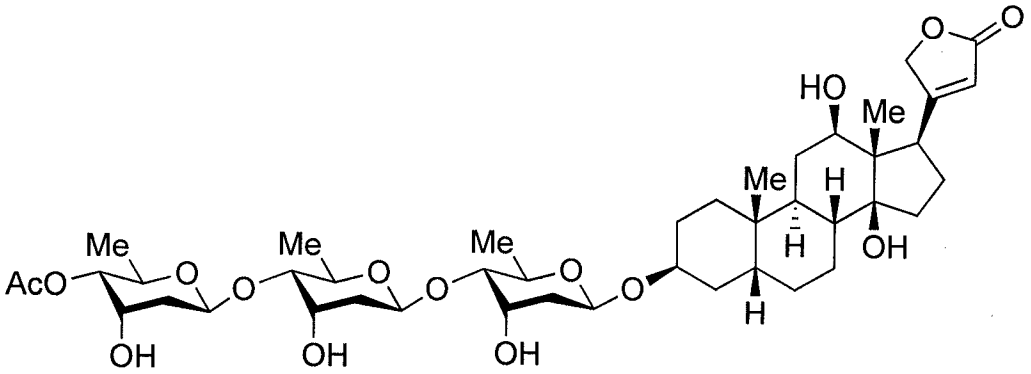

β-Acetyldigoxin ^{13}C NMR

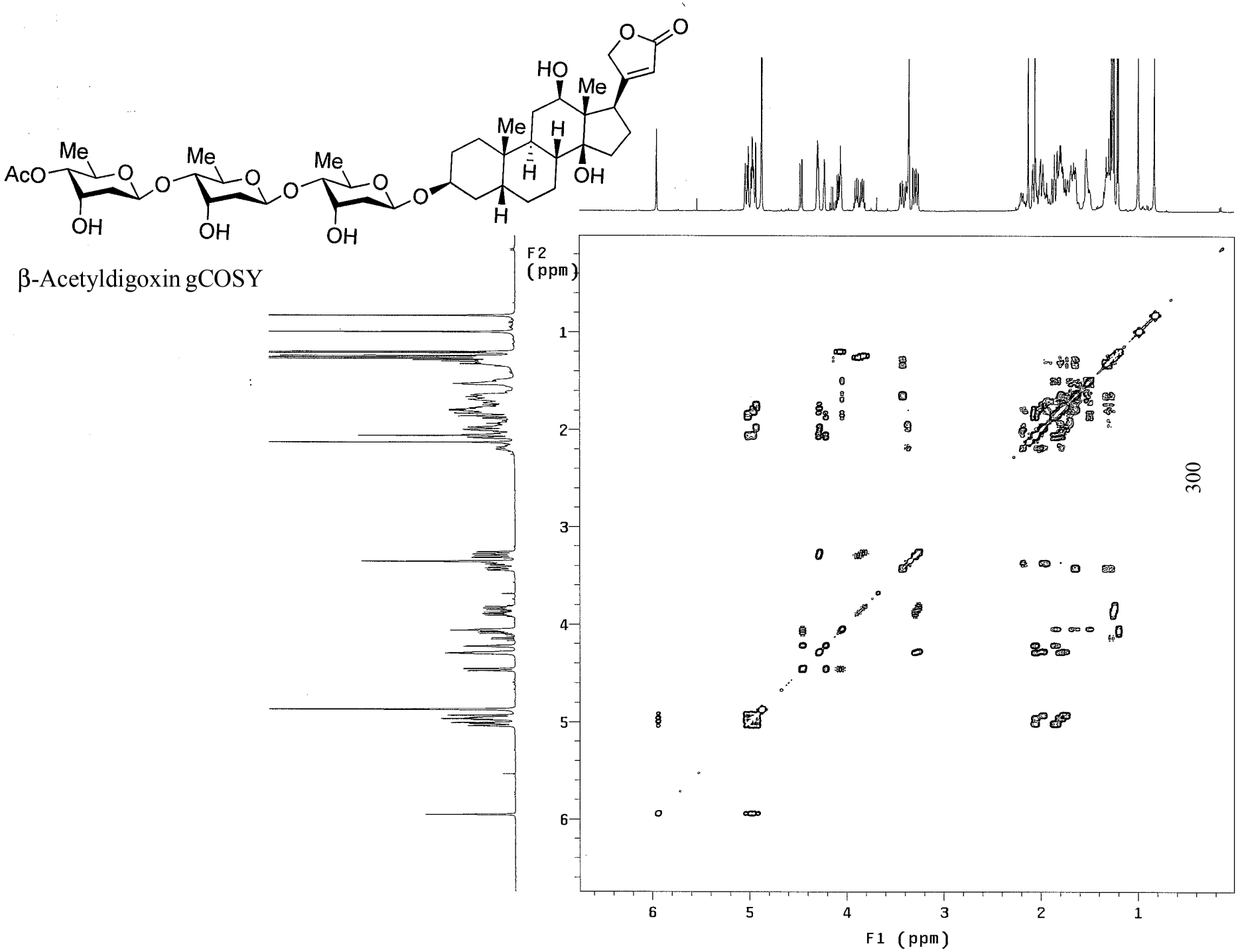

β-Acetyldigoxin gCOSY

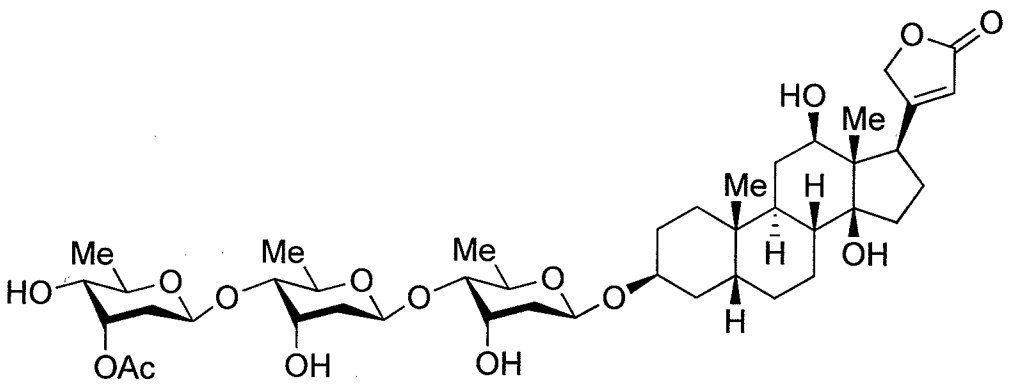

α-Acetyldigoxin ^{1}H NMR

α:β = 91:9

Notebook PHAMHE2-007-EXP058
Project Kian Tan Project

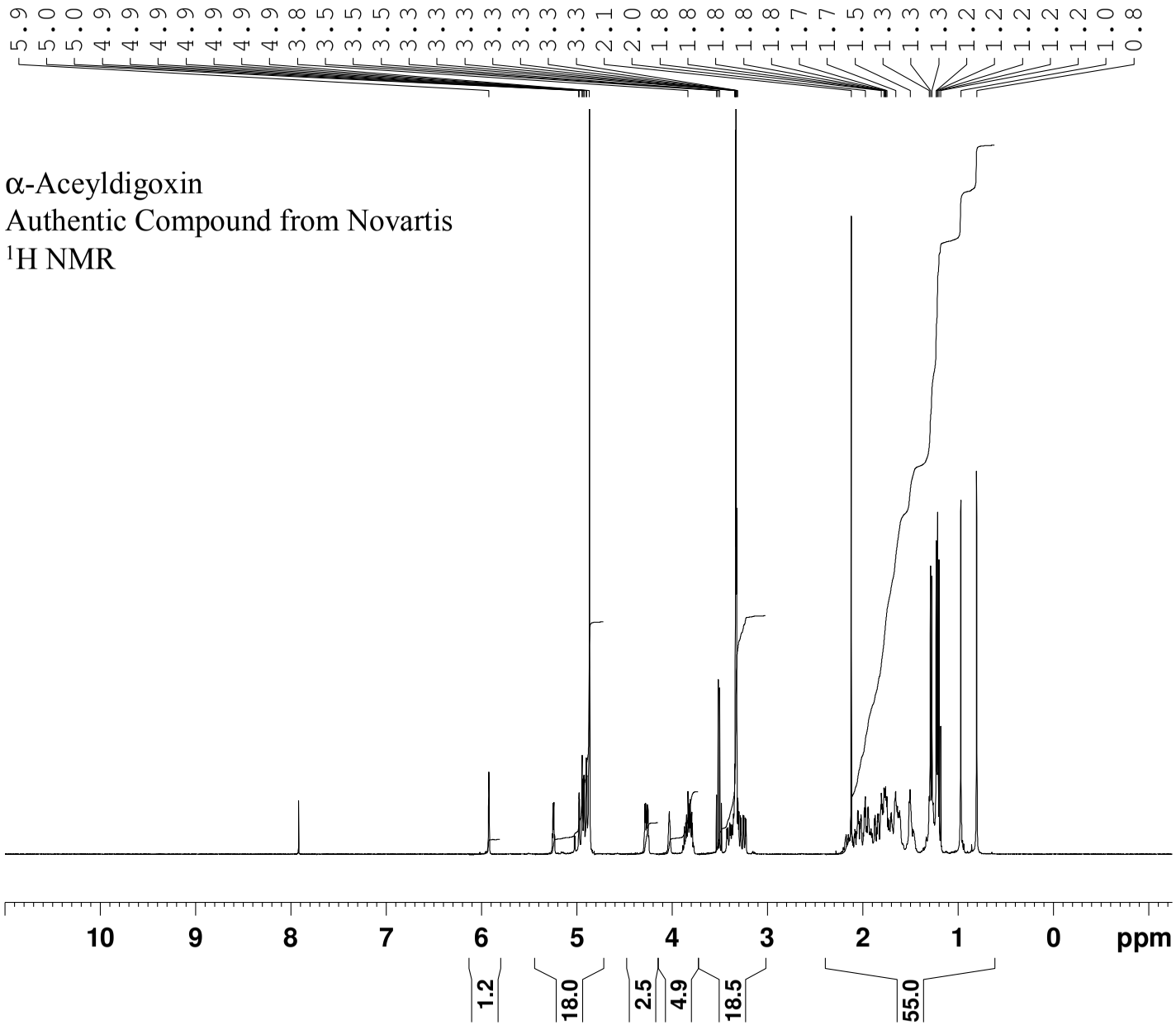

NAME	Feb13-2013	
EXPNO	370	
PROCNO	1	
Date_	20130213	
Time	15.28	
INSTRUM	av400e	
PROBHD	5 mm PABBO BB-	
PULPROG	zg30	
TD	32768	
SOLVENT	MeOD	
NS	32	
DS	2	
SWH	8278.146	Hz
FIDRES	0.252629	Hz
AQ	1.9792372	sec
RG	322.5	
DW	60.400	usec
DE	6.50	usec
TE	298.0	K
D1	1.00000000	sec
TD0	1	
======== CHANNEL f1 ========		
NUC1	1H	
P1	14.38	usec
PL1	0.00	dB
PL1W	12.48407555	W
SFO1	400.1324710	MHz
SI	16384	
SF	400.1300000	MHz
WDW	EM	
SSB	0	
LB	0.30	Hz
GB	0	
PC	1.00	

302

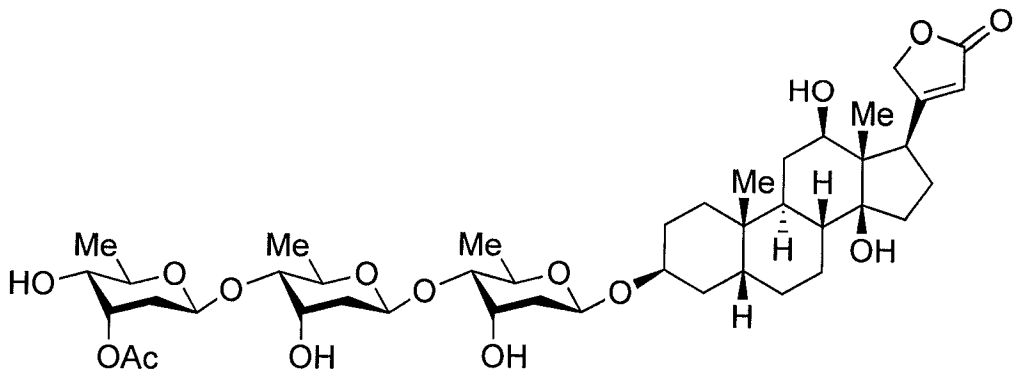

α-Acetyldigoxin ^{13}C NMR

Notebook PHAMHE2-007-EXP058
Project Kian Tan Project

178.53
177.34
172.32

117.73
100.59
100.53
96.94
86.83
83.79
83.48
75.68
75.46
74.45
72.67
72.15
71.55
69.47
68.48
68.29
66.91
57.30
49.65
49.43
49.22
49.01
48.79
48.58
48.37
47.06
42.21
38.95
38.49
37.99
37.10
36.21
33.61
33.53
31.42
30.99
30.84
28.37
27.79
27.47
24.22
22.80

α-Aceyldigoxin
Authentic Compound from Novartis
^{13}C NMR

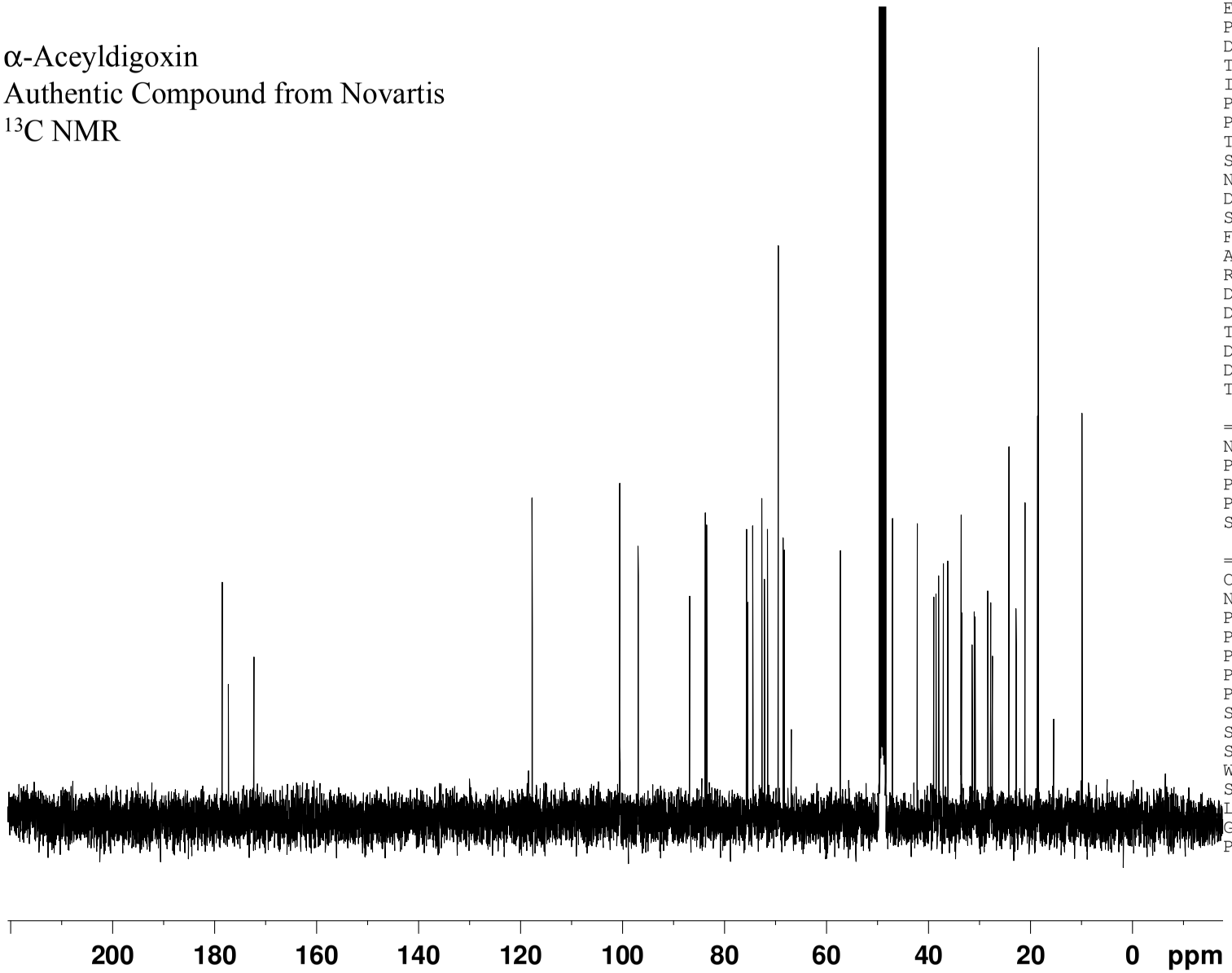

NAME	Feb13-2013
EXPNO	371
PROCNO	1
Date_	20130213
Time	21.01
INSTRUM	av400e
PROBHD	5 mm PABBO BB-
PULPROG	zgdc
TD	65536
SOLVENT	MeOD
NS	2048
DS	4
SWH	23980.814 Hz
FIDRES	0.365918 Hz
AQ	1.3664756 sec
RG	8192
DW	20.850 usec
DE	6.50 usec
TE	300.0 K
D1	2.00000000 sec
D11	0.03000000 sec
TD0	1
======== CHANNEL f1 ========	
NUC1	13C
P1	10.00 usec
PL1	-0.42 dB
PL1W	37.07701874 W
SFO1	100.6228298 MHz
======== CHANNEL f2 ========	
CPDPRG2	waltz16
NUC2	1H
PCPD2	70.00 usec
PL2	0.00 dB
PL12	13.98 dB
PL2W	12.48407555 W
PL12W	0.49929410 W
SFO2	400.1316005 MHz
SI	32768
SF	100.6126261 MHz
WDW	EM
SSB	0
LB	1.00 Hz
GB	0
PC	1.40

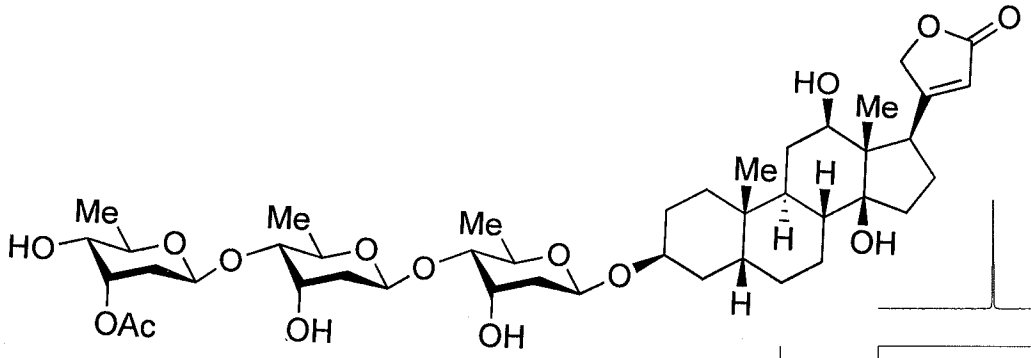

α-Acetyldigoxin gCOSY

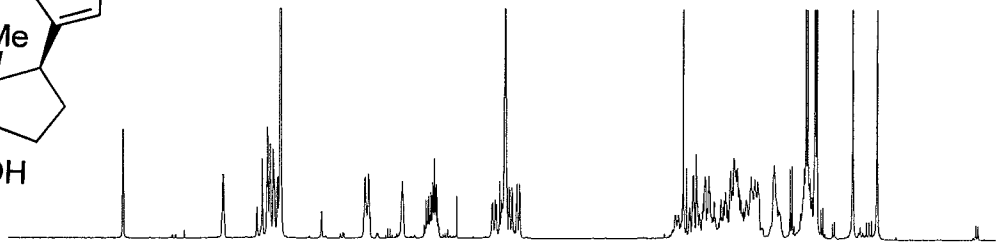

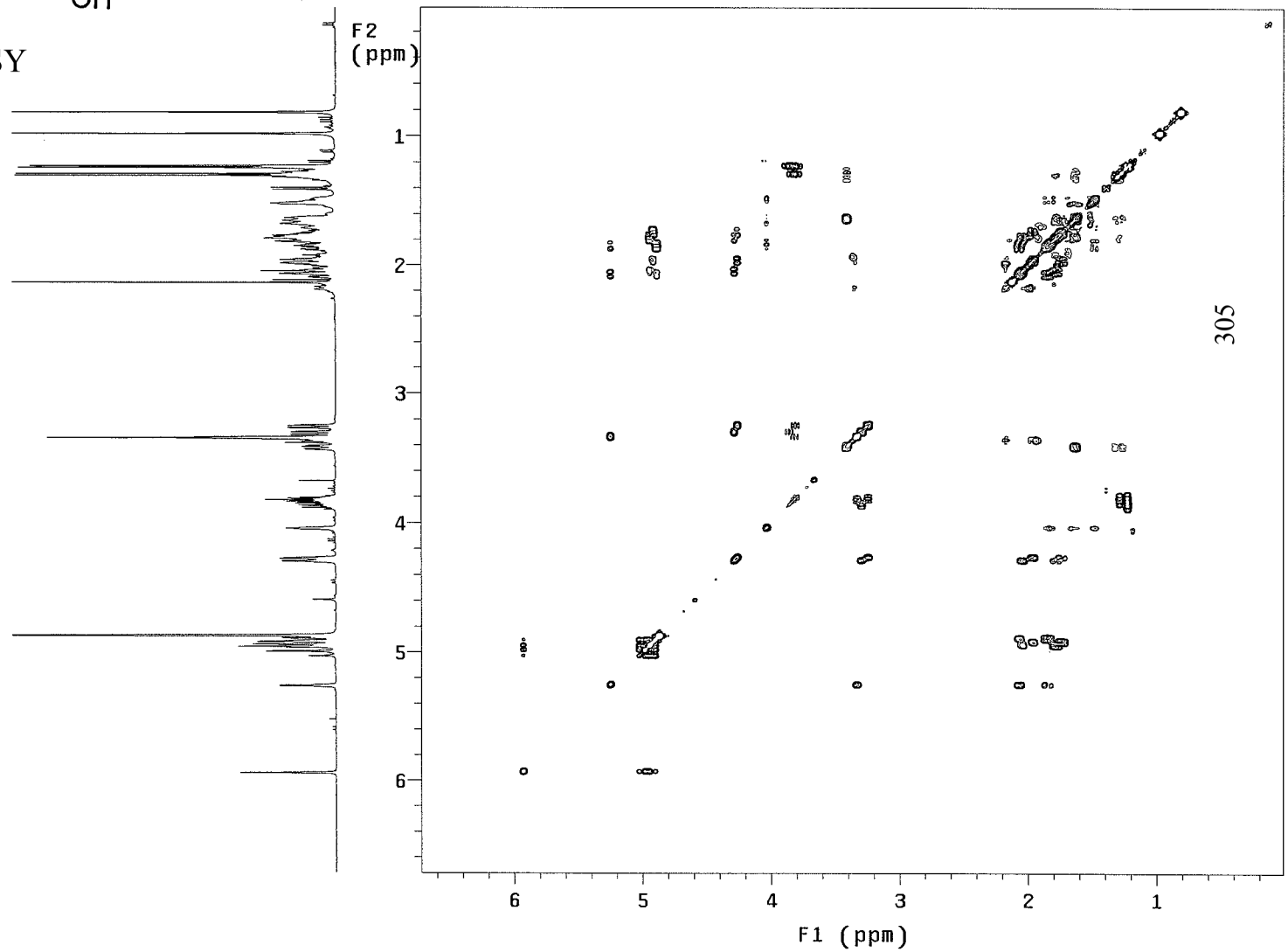

Notebook PHAMHE2-007-EXP058
Project Kian Tan Project

α-Aceyldigoxin
Authentic Compound from Novartis
gCOSY

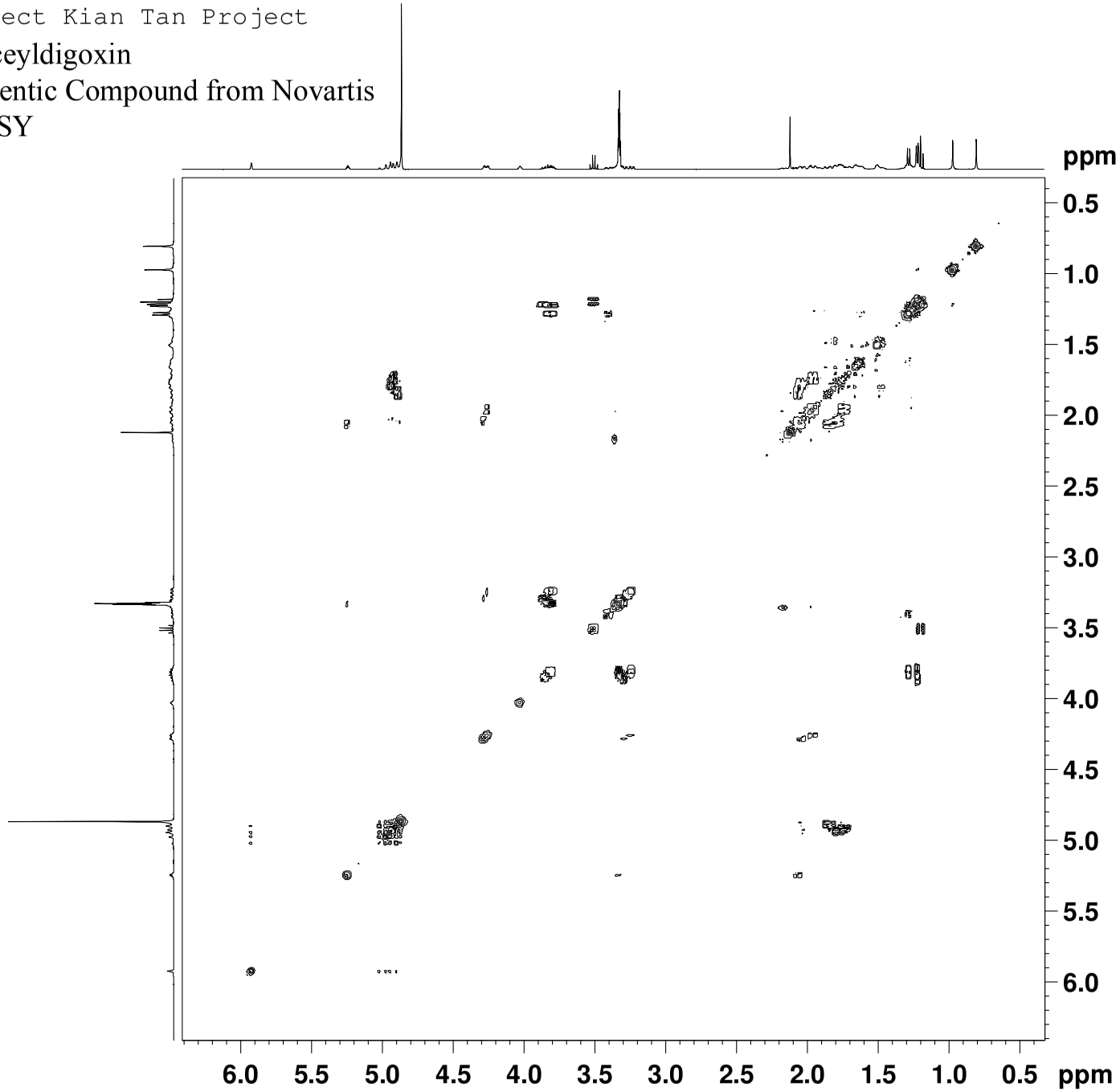

BRUKER

NAME	Feb13-2013
EXPNO	373
PROCNO	1
Date_	20130213
Time	21.06
INSTRUM	av400e
PROBHD	5 mm PABBO BB-
PULPROG	cosygpqf
TD	2048
SOLVENT	MeOD
NS	1
DS	8
SWH	2436.647 Hz
FIDRES	1.189769 Hz
AQ	0.4202996 sec
RG	161.3
DW	205.200 usec
DE	6.50 usec
TE	298.0 K
D0	0.00000300 sec
D1	1.25874496 sec
D13	0.00000400 sec
D16	0.00020000 sec
IN0	0.00041040 sec
======== CHANNEL f1 ========	
NUC1	1H
P0	14.38 usec
P1	14.38 usec
PL1	0.00 dB
PL1W	12.48407555 W
SFO1	400.1313476 MHz
====== GRADIENT CHANNEL =====	
GPNAM1	SINE.100
GPZ1	10.00 %
P16	1000.00 usec
ND0	1
TD	128
SFO1	400.1313 MHz
FIDRES	19.036306 Hz
SW	6.090 ppm
FnMODE	QF
SI	1024
SF	400.1300000 MHz
WDW	SINE
SSB	0
LB	0.00 Hz
GB	0
PC	1.40
SI	1024
MC2	QF
SF	400.1300000 MHz
WDW	SINE
SSB	0
LB	0.00 Hz
GB	0

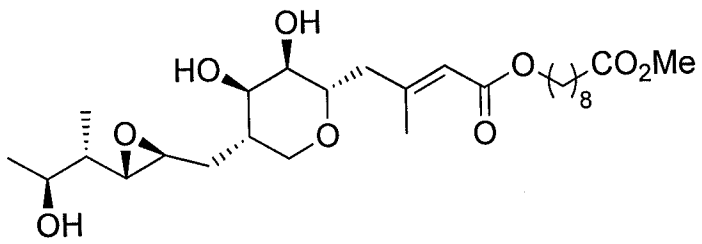

Mupirocin Methyl Ester

^{1}H NMR

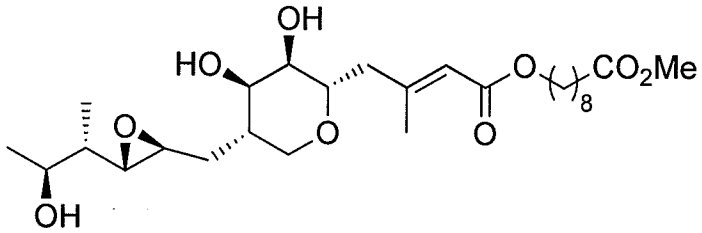

Mupirocin Methyl Ester

^{13}C NMR

308

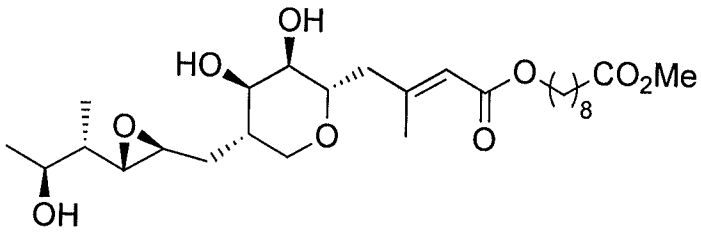

Mupirocin Methyl Ester
gCOSY

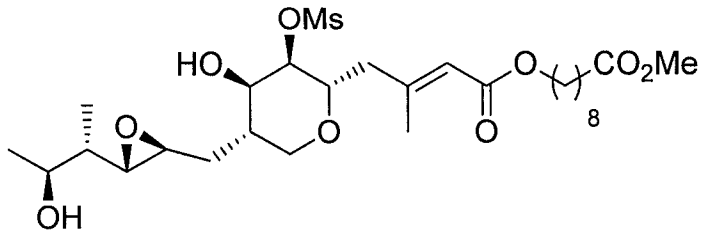

C6:C7 = >98:<2

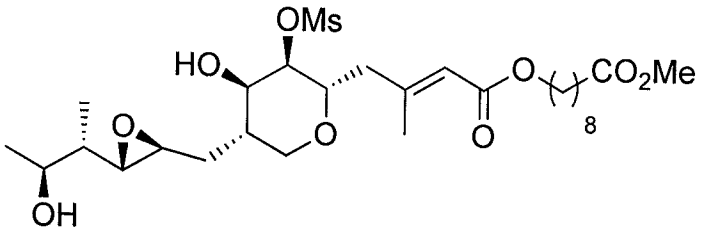

311

9 8 7 6 5 4 3 2 1 ppm

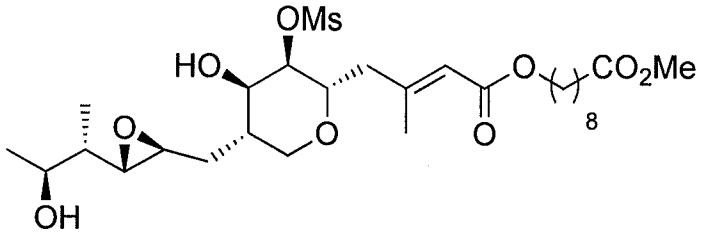

312

220 200 180 160 140 120 100 80 60 40 20 0 ppm

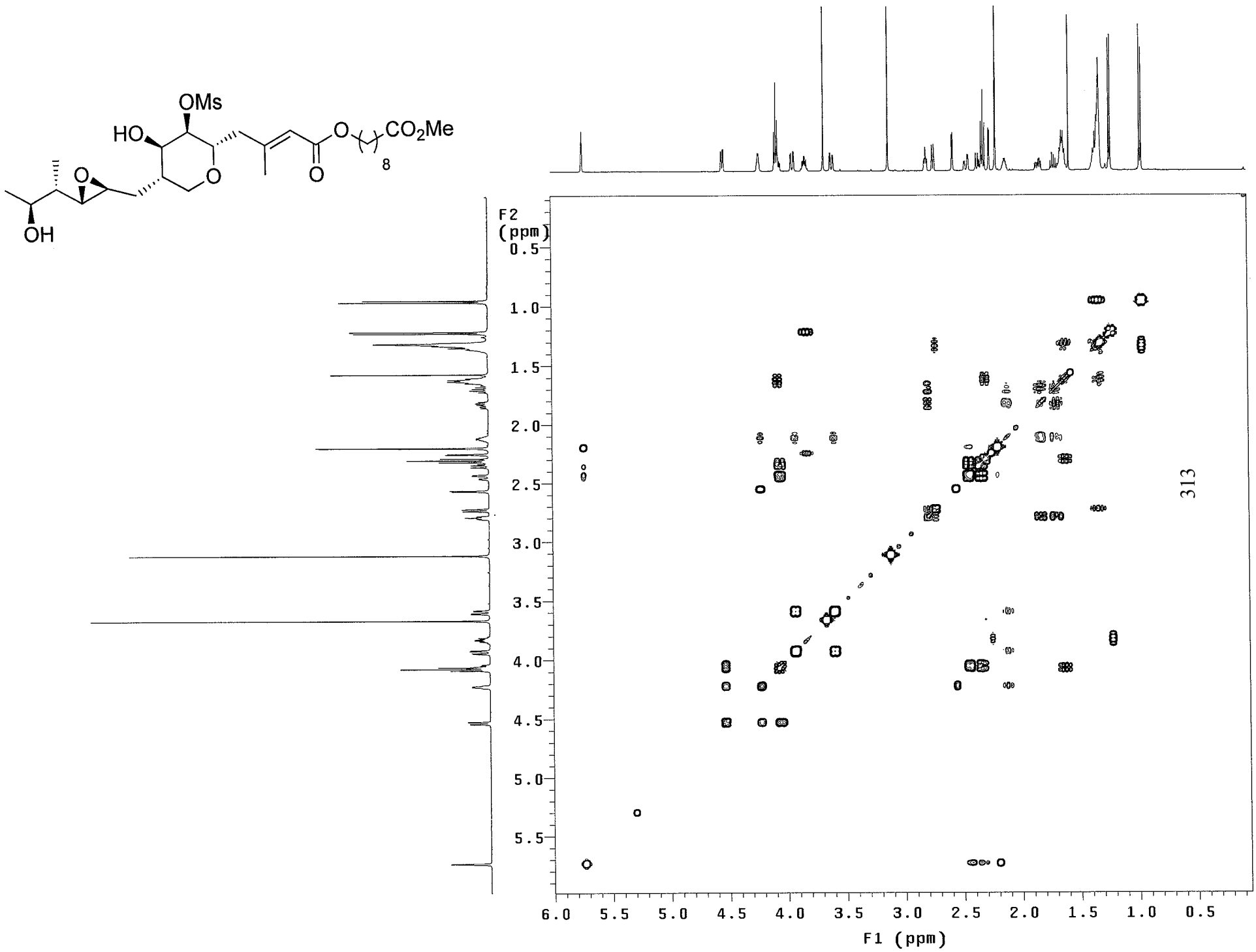
OMs
HO
O
O
O
8
CO2Me
O
OH
F2
(ppm)
0.5
1.0
1.5
2.0
2.5
3.0
3.5
4.0
4.5
5.0
5.5
6.0
5.5
5.0
4.5
4.0
3.5
3.0
2.5
2.0
1.5
1.0
0.5
F1 (ppm)
313

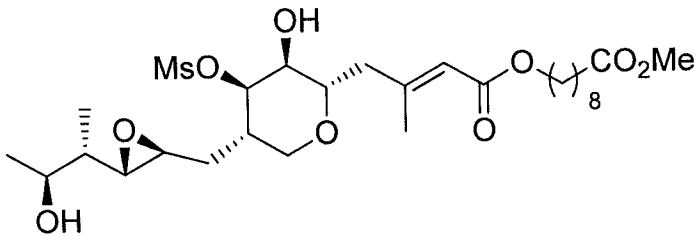
OH
MsO
O
O
O
O
8
CO2Me
O
OH

C6:C7 = 18:82

314
C7
C6
5.5
5.0
4.5
4.0
3.5
3.0
2.5
ppm
81.77
18.23

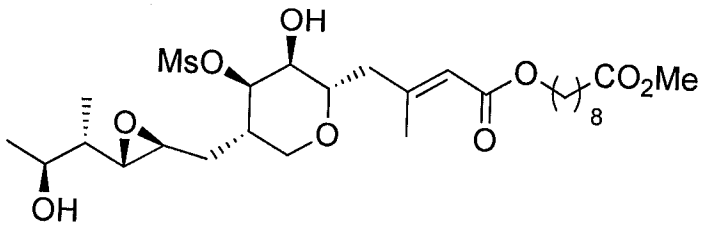

315

9 8 7 6 5 4 3 2 1 ppm

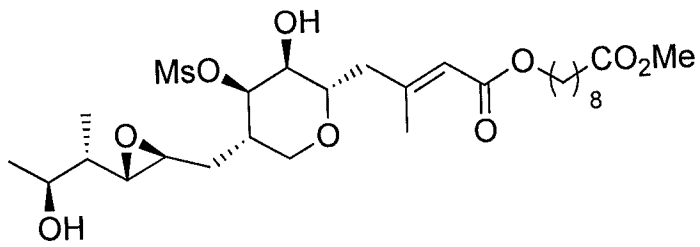
OH
MsO
O
O
O
O
8
CO2Me
O
OH

220
200
180
160
140
120
100
80
60
40
20
0
ppm

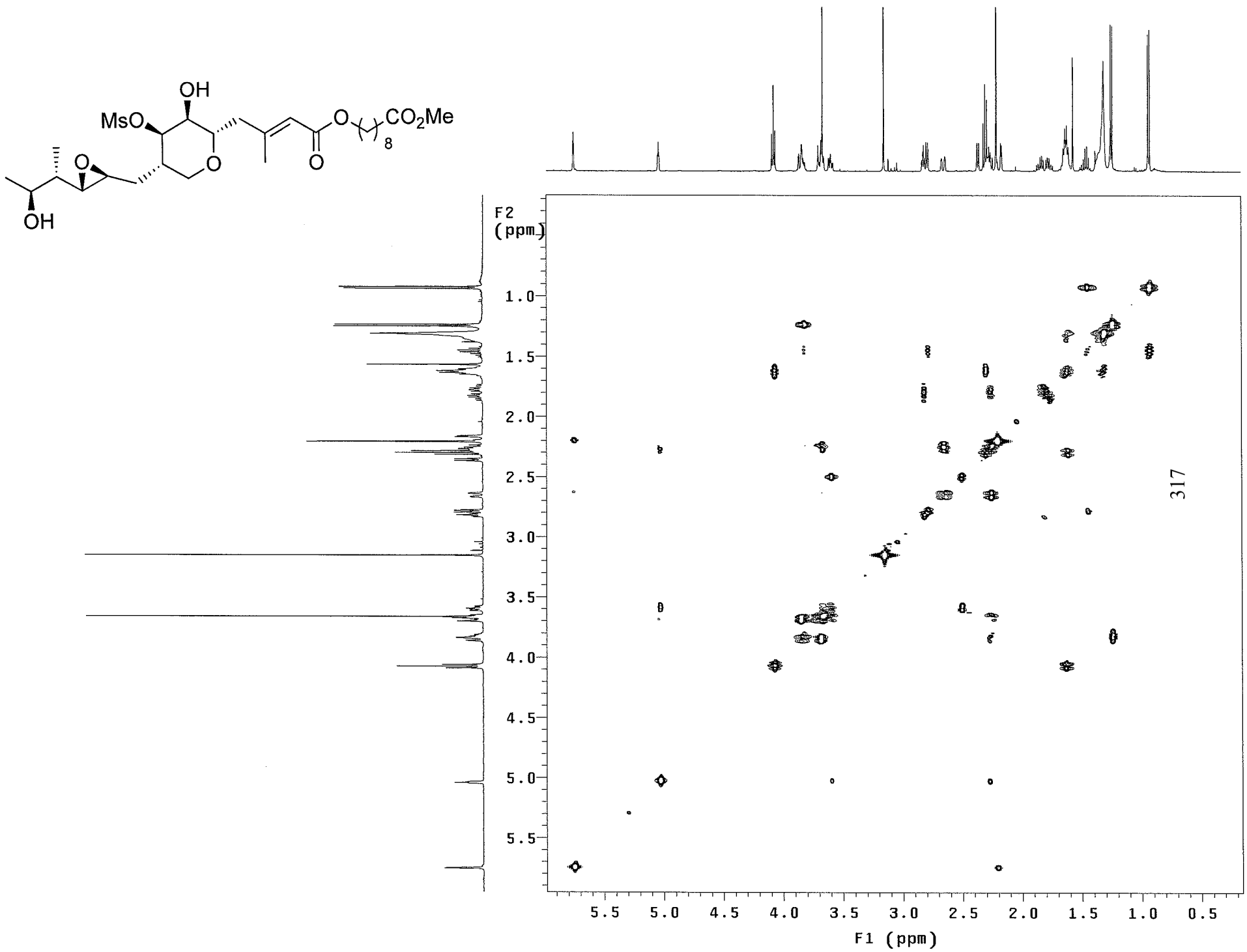
OH
MsO
O
O
O
O
8
CO2Me
OH
F2
(ppm)
1.0
1.5
2.0
2.5
3.0
3.5
4.0
4.5
5.0
5.5
5.5
5.0
4.5
4.0
3.5
3.0
2.5
2.0
1.5
1.0
0.5
F1 (ppm)
317

SG-2-211-H

Sample Name:
SG-2-211-H
Data Collected on:
nmr18-vnmrs500
Archive directory:

Sample directory:

FidFile: PROTON

Pulse Sequence: PROTON (s2pul)
Solvent: cdcl3
Data collected on: Feb 26 2013

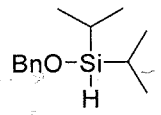

SG-2-211-C

Sample Name:
SG-2-211-C
Data Collected on:
nmr18-vnmrs500
Archive directory:

Sample directory:

FidFile: CARBON

Pulse Sequence: CARBON (s2pul)
Solvent: cdcl3
Data collected on: Feb 26 2013

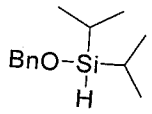

SG-2-212-distil-H

Sample Name:
SG-2-212-distil-H
Data Collected on:
nmr18-vnmrs500
Archive directory:

Sample directory:

FidFile: PROTON

Pulse Sequence: PROTON (s2pul)
Solvent: cdcl3
Data collected on: Feb 28 2013

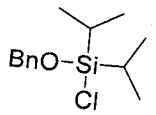

SG-2-212-distil-C

Sample Name:
SG-2-212-distil-C
Data Collected on:
nmr18-vnmrs500
Archive directory:

Sample directory:

FidFile: CARBON

Pulse Sequence: CARBON (s2pul)
Solvent: cdcl3
Data collected on: Feb 28 2013

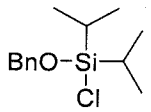

SG-2-203-H

Sample Name:
SG-2-203-H
Data Collected on:
nmr18-vnmrs500
Archive directory:

Sample directory:

FidFile: PROTON

Pulse Sequence: PROTON (s2pul)
Solvent: cdcl3
Data collected on: Jul 29 2013

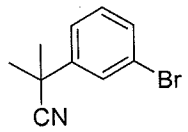

SG-2-203-recolumn-C

Sample Name:
SG-2-203-recolumn-C
Data Collected on:
nmr18-vnmrs500
Archive directory:

Sample directory:

FidFile: CARBON

Pulse Sequence: CARBON (s2pul)
Solvent: cdcl3
Data collected on: Jul 29 2013

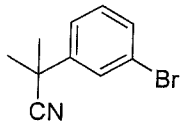

SG-2--207-SiH-H

Sample Name:
SG-2-207-SiH-H
Data Collected on:
nmr18-vnmrs500
Archive directory:

Sample directory:

FidFile: SG-2-207-SiH-H

Pulse Sequence: PROTON (s2pul)
Solvent: cdcl3
Data collected on: Sep 24 2013

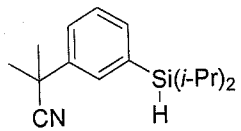

SG-2-207-SiH-C

Sample Name:
SG-2-207-SiH-C
Data Collected on:
nmr18-vnmrs500
Archive directory:

Sample directory:

FidFile: SG-2-207-SiH-C

Pulse Sequence: CARBON (s2pul)
Solvent: cdcl3
Data collected on: Sep 24 2013

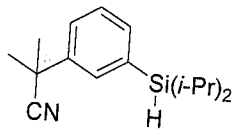

SG-2-214-H

Sample Name:
SG-2-214-H
Data Collected on:
nmr18-vnmrs500
Archive directory:

Sample directory:

FidFile: SG-2-214-H

Pulse Sequence: PROTON (s2pul)
Solvent: cdcl3
Data collected on: Sep 25 2013

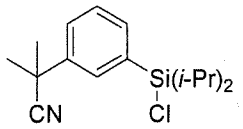

SG-2-214-distil-C

Sample Name:
SG-2-214-distil-C
Data Collected on:
nmr18-vnmrs500
Archive directory:

Sample directory:

FidFile: CARBON

Pulse Sequence: CARBON (s2pul)
Solvent: cdcl3
Data collected on: Feb 26 2013

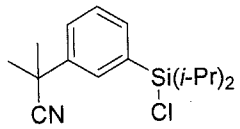

SG-2-215-Bn-H

Sample Name:
SG-2-215-Bn-H
Data Collected on:
nmr18-vnmrs500
Archive directory:

Sample directory:

FidFile: PROTON

Pulse Sequence: PROTON (s2pul)
Solvent: cdcl3
Data collected on: Feb 27 2013

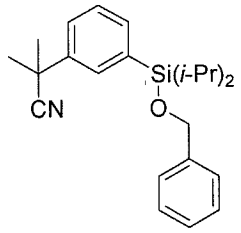

SG-2-215-Bn-C

Sample Name:
SG-2-215-Bn-C
Data Collected on:
nmr18-vnmrs500
Archive directory:

Sample directory:

FidFile: CARBON

Pulse Sequence: CARBON (s2pul)
Solvent: cdcl3
Data collected on: Feb 27 2013

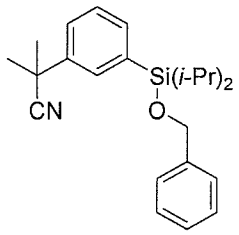

SG-2-243-2-column1-H

Sample Name:
SG-2-243-2-column1-H
Data Collected on:
nmr18-vnmrs500
Archive directory:

Sample directory:

FidFile: PROTON

Pulse Sequence: PROTON (s2pul)
Solvent: cdcl3
Data collected on: Mar 27 2013

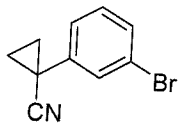

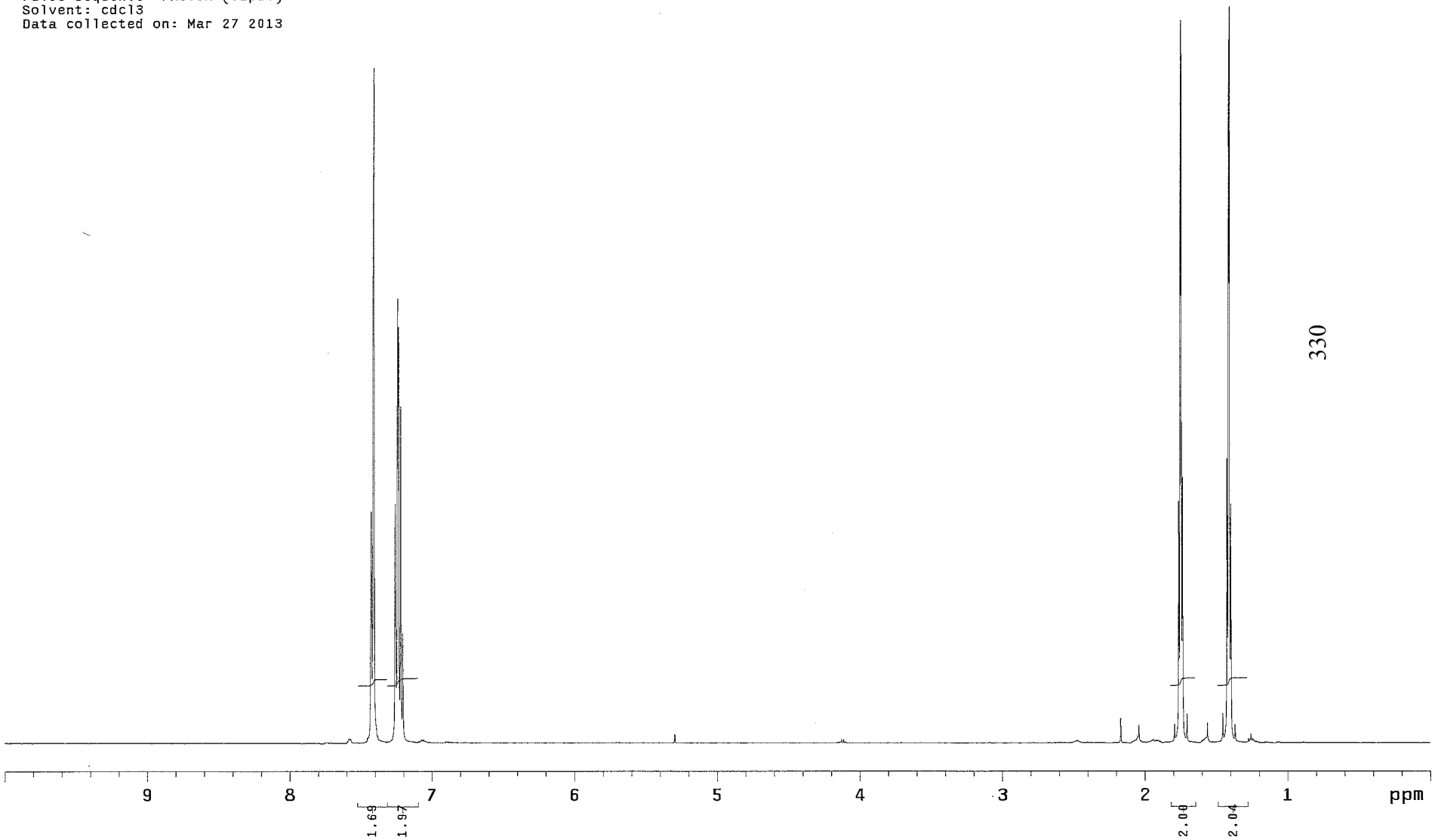

SG-2-243-2-column1-C

Sample Name:
SG-2-243-2-column1-C
Data Collected on:
nmr18-vnmrs500
Archive directory:

Sample directory:

FidFile: CARBON

Pulse Sequence: CARBON (s2pul)
Solvent: cdcl3
Data collected on: Mar 27 2013

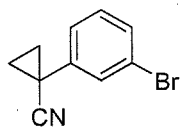

SG-2-256-3-H

Sample Name:
SG-2-256-3-H
Data Collected on:
nmr18-vnmrs500
Archive directory:

Sample directory:

FidFile: SG-2-256-3-H

Pulse Sequence: PROTON (s2pul)
Solvent: cdcl3
Data collected on: Aug 2 2013

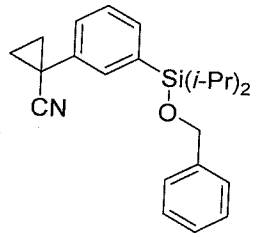

SG-2-256-3-H

Sample Name:
SG-2-256-3-H
Data Collected on:
nmr18-vnmrs500
Archive directory:

Sample directory:

FidFile: SG-2-256-3-C

Pulse Sequence: CARBON (s2pul)
Solvent: cdcl3
Data collected on: Aug 2 2013

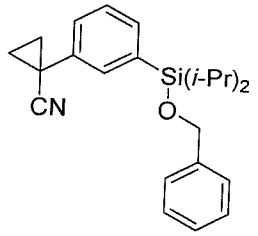

SG-2-243-4-column1-H

Sample Name:
SG-2-243-4-column1-H
Data Collected on:
nmr18-vnmrs500
Archive directory:

Sample directory:

FidFile: PROTON

Pulse Sequence: PROTON (s2pul)
Solvent: cdcl3
Data collected on: Mar 27 2013

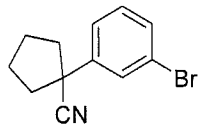

SG-2-243-4-column1-C

Sample Name:
SG-2-243-4-column1-C
Data Collected on:
nmr18-vnmrs500
Archive directory:

Sample directory:

FidFile: CARBON

Pulse Sequence: CARBON (s2pul)
Solvent: cdcl3
Data collected on: Mar 27 2013

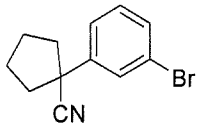

SG-2-256-5-H

Sample Name:
SG-2-256-5-H
Data Collected on:
nmr18-vnmrs500
Archive directory:

Sample directory:

FidFile: SG-2-256-5-H

Pulse Sequence: PROTON (s2pul)
Solvent: cdcl3
Data collected on: Aug 2 2013

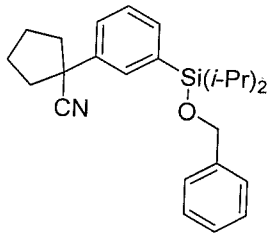

Sample Name:
SG-2-256-4
Data Collected on:
nmr14-vnmrs400
Archive directory:
/home/Robot/vnmrsys/data
Sample directory:
SG-2-256-4_20130802_01
FidFile: CARBON_01

Pulse Sequence: CARBON (s2pul)
Solvent: cdcl3
Data collected on: Aug 2 2013

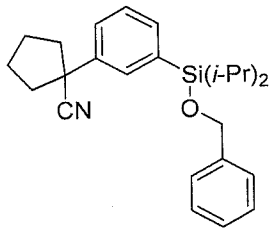

SG-2-227-Et-H

Sample Name:
SG-2-227-Et-H
Data Collected on:
nmr18-vnmrs500
Archive directory:

Sample directory:

FidFile: PROTON

Pulse Sequence: PROTON (s2pul)
Solvent: cdcl3
Data collected on: Mar 20 2013

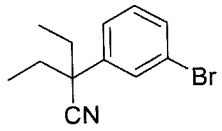

SG-2-227-Et-C

Sample Name:
SG-2-227-Et-C
Data Collected on:
nmr18-vnmrs500
Archive directory:

Sample directory:

FidFile: CARBON

Pulse Sequence: CARBON (s2pul)
Solvent: cdcl3
Data collected on: Mar 20 2013

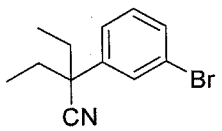

339

160 140 120 100 80 60 40 20 ppm

SG-2-256-Et-H

Sample Name:
SG-2-256-Et-H
Data Collected on:
nmr18-vnmrs500
Archive directory:

Sample directory:

FidFile: SG-2-256-Et-H

Pulse Sequence: PROTON (s2pul)
Solvent: cdcl3
Data collected on: Aug 2 2013

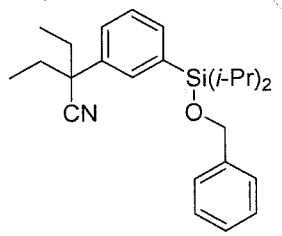

SG-2-256-Et-C

Sample Name:
SG-2-256-Et-C
Data Collected on:
nmr18-vnmrs500
Archive directory:

Sample directory:

FidFile: SG-2-256-Et-C

Pulse Sequence: CARBON (s2pul)
Solvent: cdcl3
Data collected on: Aug 2 2013

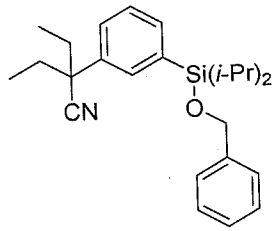

SG-2-227-iPr-H

Sample Name:
SG-2-227-iPr-H
Data Collected on:
nmr18-vnmrs500
Archive directory:

Sample directory:

FidFile: PROTON

Pulse Sequence: PROTON (s2pul)
Solvent: cdcl3
Data collected on: Mar 20 2013

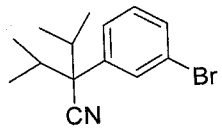

SG-2-227-iPr-C

Sample Name:
SG-2-227-iPr-C
Data Collected on:
nmr18-vnmrs500
Archive directory:

Sample directory:

FidFile: CARBON

Pulse Sequence: CARBON (s2pul)
Solvent: cdcl3
Data collected on: Mar 20 2013

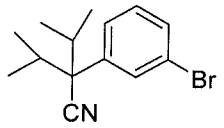

SG-2-256-iPr-H

Sample Name:
SG-2-256-iPr-H
Data Collected on:
nmr18-vnmrs500
Archive directory:

Sample directory:

FidFile: SG-2-256-iPr-H

Pulse Sequence: PROTON (s2pul)
Solvent: cdcl3
Data collected on: Aug 1 2013

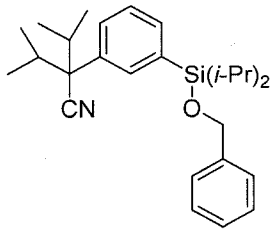

SG-2-256-iPr-C

Sample Name:
SG-2-256-iPr-C
Data Collected on:
nmr18-vnmrs500
Archive directory:

Sample directory:

FidFile: SG-2-256-iPr-C

Pulse Sequence: CARBON (s2pul)
Solvent: cdcl3
Data collected on: Aug 1 2013

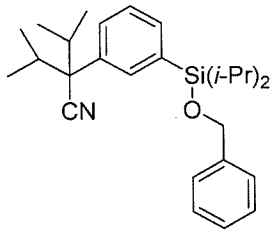

SG-3-010-Br-H

Sample Name:
SG-3-010-Br-H
Data Collected on:
nmr18-vnmrs500
Archive directory:

Sample directory:

FidFile: SG-3-010-Br-H

Pulse Sequence: PROTON (s2pul)
Solvent: cdcl3
Data collected on: Aug 2 2013

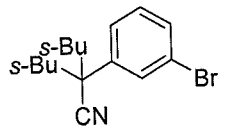

SG-3-010-1step-br-C

Sample Name:
SG-3-010-1step-br-C
Data Collected on:
nmr18-vnmrs500
Archive directory:
/home/Tan/vnmrsys/data
Sample directory:
CS-2-58-frac1_20130715_01
FidFile: CARBON

Pulse Sequence: CARBON (s2pul)
Solvent: cdcl3
Data collected on: Jul 16 2013

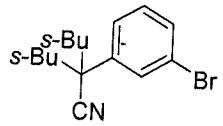

SG-3-010-SiH-H

Sample Name:
SG-3-010-SiH-H
Data Collected on:
nmr18-vnmrs500
Archive directory:

Sample directory:

FidFile: SG-3-010-SiH-H

Pulse Sequence: PROTON (s2pul)
Solvent: cdcl3
Data collected on: Aug 2 2013

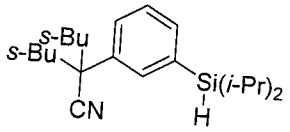

SG-3-010-SiH-H

Sample Name:
SG-3-010-SiH-H
Data Collected on:
nmr18-vnmrs500
Archive directory:

Sample directory:

FidFile: SG-3-010-SiH-C

Pulse Sequence: CARBON (s2pul)
Solvent: cdcl3
Data collected on: Aug 2 2013

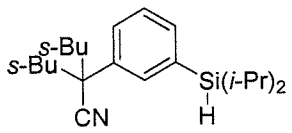

SG-3-011-SiCl-H

Sample Name:
SG-3-011-SiCl-H
Data Collected on:
nmr18-vnmrs500
Archive directory:

Sample directory:

FidFile: SG-3-011-SiCl-H

Pulse Sequence: PROTON (s2pul)
Solvent: cdcl3
Data collected on: Aug 8 2013

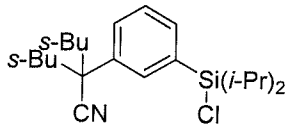

SG-3-011-SiCl-C

Sample Name:
SG-3-011-SiCl-C
Data Collected on:
nmr18-vnmrs500
Archive directory:

Sample directory:

FidFile: SG-3-011-SiCl-C

Pulse Sequence: CARBON (s2pul)
Solvent: cdcl3
Data collected on: Aug 8 2013

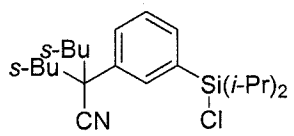

SG-3--nosub-H

Sample Name:
SG-3--nosub-H
Data Collected on:
nmr18-vnmrs500
Archive directory:

Sample directory:

FidFile: PROTON

Pulse Sequence: PROTON (s2pul)
Solvent: cdcl3
Data collected on: Jul 15 2013

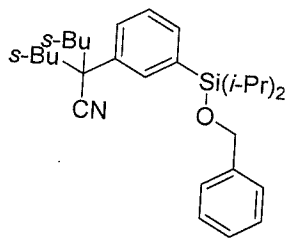

SG-3-nosub-C

Sample Name:
SG-3-nosub-C
Data Collected on:
nmr18-vnmrs500
Archive directory:

Sample directory:

FidFile: CARBON

Pulse Sequence: CARBON (s2pul)
Solvent: cdcl3
Data collected on: Jul 15 2013

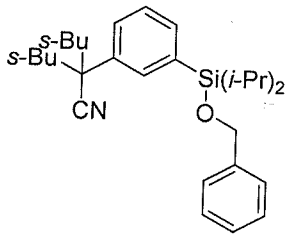

SG-2-263-cHx-H

Sample Name:
SG-2-263-cHx-H
Data Collected on:
nmr18-vnmrs500
Archive directory:

Sample directory:

FidFile: SG-2-263-cHx-H

Pulse Sequence: PROTON (s2pul)
Solvent: cdcl3
Data collected on: Jul 31 2013

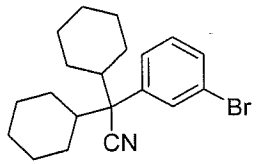

ErrorLog:
auto_20130731_02 loc:8 (night)
Findz0 failed - low S/N

Sample Name:
SG-2-263-cHx
Data Collected on:
nmr14-vnmrs400
Archive directory:
/home/Robot/vnmrsys/data
Sample directory:
SG-2-263-cHx_20130731_01
FidFile: CARBON_01

Pulse Sequence: CARBON (s2pul)
Solvent: cdcl3
Data collected on: Jul 31 2013

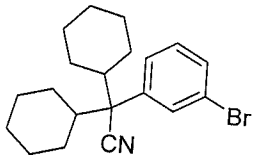

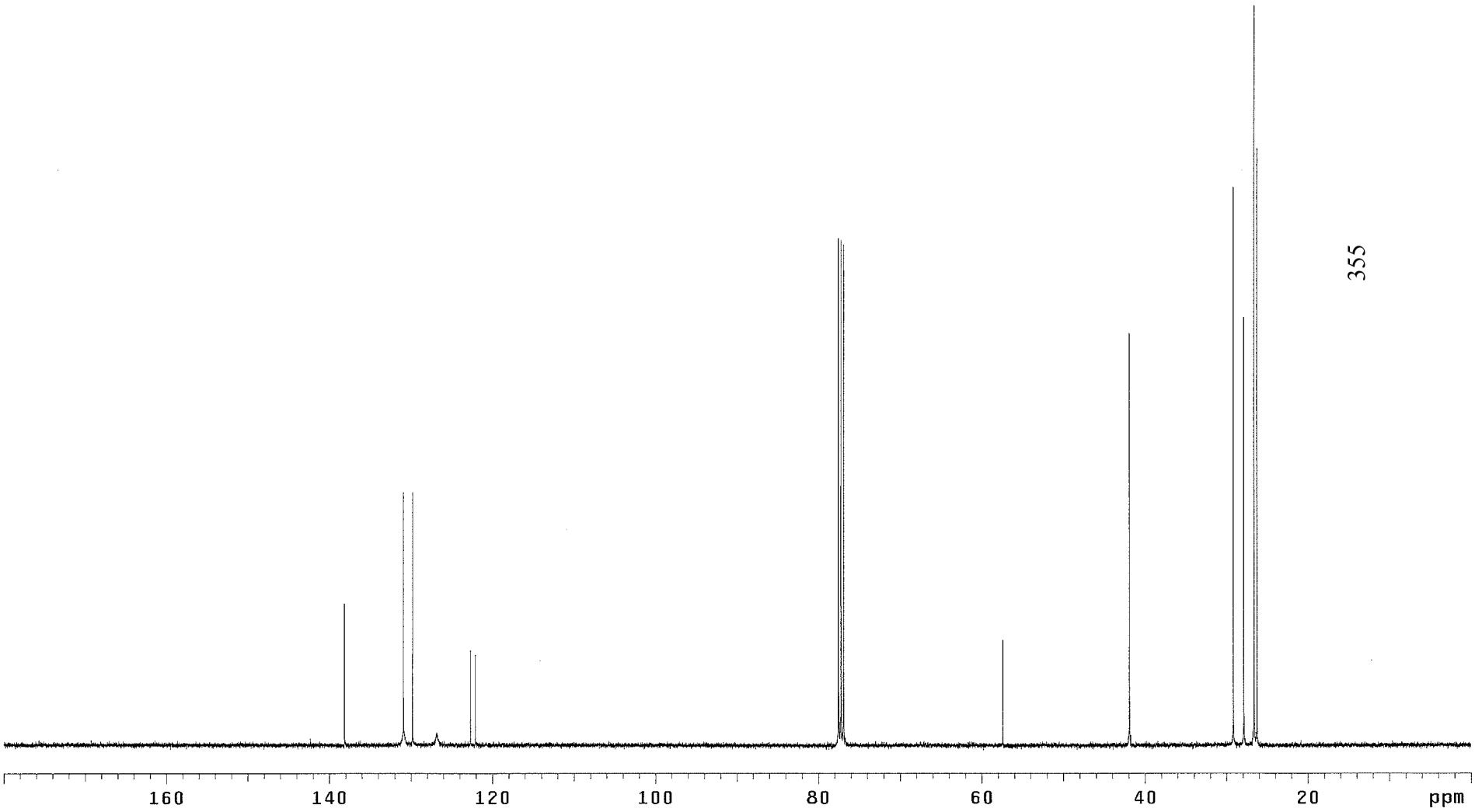

Sample Name:
SG-2-256-cHX
Data Collected on:
nmr14-vnmrs400
Archive directory:
/home/Robot/vnmrsys/data
Sample directory:
SG-2-256-cHX_20130802_01
FidFile: PROTON_01

Pulse Sequence: PROTON (s2pul)
Solvent: cdcl3
Data collected on: Aug 2 2013

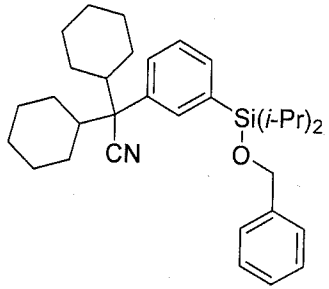

ErrorLog:
auto_20130802_01 loc:7 (night)
Findz0 failed - low S/N

Sample Name:
SG-2-256-cHX
Data Collected on:
nmr14-vnmrs400
Archive directory:
/home/Robot/vnmrsys/data
Sample directory:
SG-2-256-cHX_20130802_01
FidFile: CARBON_01

Pulse Sequence: CARBON (s2pul)
Solvent: cdcl3
Data collected on: Aug 2 2013

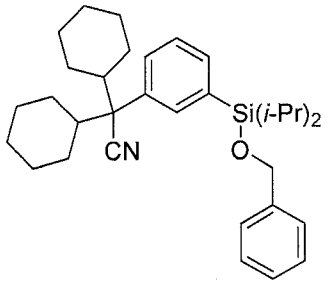

SG-2-246-H

Sample Name:
SG-2-246-H
Data Collected on:
nmr18-vnmrs500
Archive directory:

Sample directory:

FidFile: PROTON

Pulse Sequence: PROTON (s2pul)
Solvent: cdcl3
Data collected on: Oct 8 2013

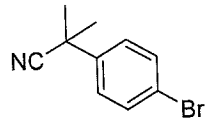

SG-2-246-C

Sample Name:
SG-2-246-C
Data Collected on:
nmr18-vnmrs500
Archive directory:

Sample directory:

FidFile: CARBON

Pulse Sequence: CARBON (s2pul)
Solvent: cdcl3
Data collected on: Oct 8 2013

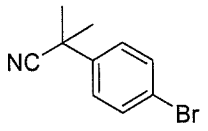

SG-2-246-H

Sample Name:
SG-2-249-H
Data Collected on:
nmr18-vnmrs500
Archive directory:

Sample directory:

FidFile: PROTON

Pulse Sequence: PROTON (s2pul)
Solvent: cdcl3
Data collected on: Oct 8 2013

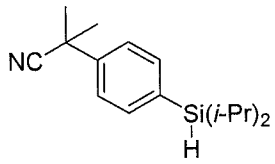

SG-2-249-c

Sample Name:
SG-2-249-c
Data Collected on:
nmr18-vnmrs500
Archive directory:

Sample directory:

FidFile: CARBON

Pulse Sequence: CARBON (s2pul)
Solvent: cdcl3
Data collected on: Oct 8 2013

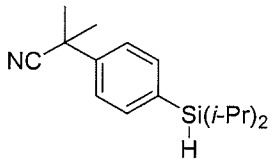

SG-2-249-2step-H

Sample Name:
SG-2-249-2step-H
Data Collected on:
nmr18-vnmrs500
Archive directory:

Sample directory:

FidFile: PROTON

Pulse Sequence: PROTON (s2pul)
Solvent: cdcl3
Data collected on: Mar 28 2013

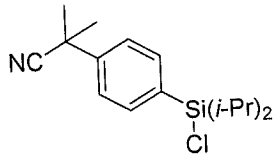

362

SG-2-249-2step-C

Sample Name:
SG-2-249-2step-C
Data Collected on:
nmr18-vnmrs500
Archive directory:

Sample directory:

FidFile: CARBON

Pulse Sequence: CARBON (s2pul)
Solvent: cdcl3
Data collected on: Mar 28 2013

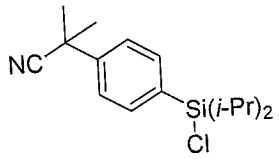

SG-2-252-H-Bn

Sample Name:
SG-2-252-H-Bn
Data Collected on:
nmr18-vnmrs500
Archive directory:

Sample directory:

FidFile: PROTON

Pulse Sequence: PROTON (s2pul)
Solvent: cdcl3
Data collected on: Oct 9 2013

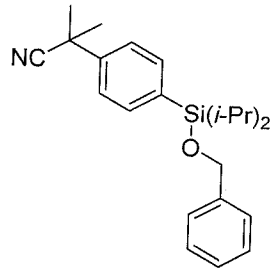

SG-2-252-C-Bn

Sample Name:
SG-2-252-C-Bn
Data Collected on:
nmr18-vnmrs500
Archive directory:

Sample directory:

FidFile: CARBON

Pulse Sequence: CARBON (s2pul)
Solvent: cdcl3
Data collected on: Oct 9 2013

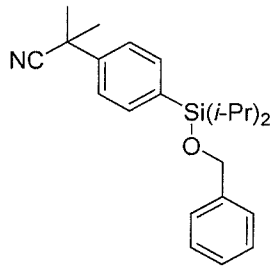

SG-3-020-2-Me-H

Sample Name:
SG-3-020-2-Me-H
Data Collected on:
nmr18-vnmrs500
Archive directory:

Sample directory:

FidFile: PROTON

Pulse Sequence: PROTON (s2pul)
Solvent: cdcl3
Data collected on: Sep 22 2013

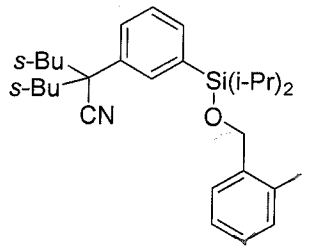

SG-3-020-2-Me-C

Sample Name:
SG-3-020-2-Me-C
Data Collected on:
nmr18-vnmrs500
Archive directory:

Sample directory:

FidFile: CARBON

Pulse Sequence: CARBON (s2pul)
Solvent: cdcl3
Data collected on: Sep 24 2013

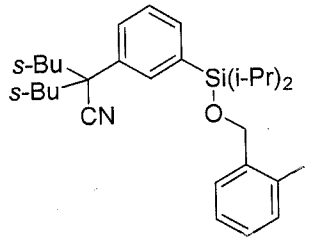

SG-3-020-2-Br-H

Sample Name:
SG-3-020-2-Br-H
Data Collected on:
nmr18-vnmrs500
Archive directory:

Sample directory:

FidFile: PROTON

Pulse Sequence: PROTON (s2pul)
Solvent: cdcl3
Data collected on: Sep 22 2013

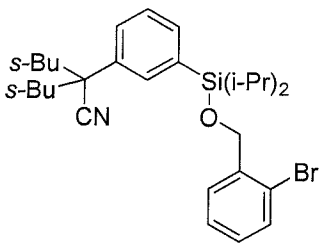

SG-3-020-2-Br-C

Sample Name:
SG-3-020-2-Br-C
Data Collected on:
nmr18-vnmrs500
Archive directory:

Sample directory:

FidFile: CARBON

Pulse Sequence: CARBON (s2pul)
Solvent: cdcl3
Data collected on: Sep 23 2013

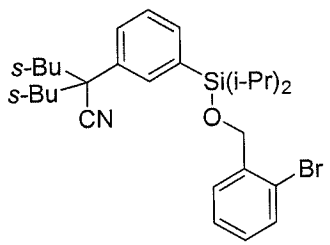

SG-3-020-2-MeO-H

Sample Name:
SG-3-020-2-MeO-H
Data Collected on:
nmr18-vnmrs500
Archive directory:

Sample directory:

FidFile: PROTON

Pulse Sequence: PROTON (s2pul)
Solvent: cdcl3
Data collected on: Sep 22 2013

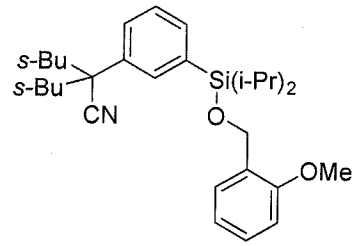

Sample Name:
SG-3-020-2-MeO-C
Data Collected on:
nmr14-vnmrs400
Archive directory:
/home/Robot/vnmrsys/data
Sample directory:
SG-3-020-2-MeO-C_20130923_01
FidFile: CARBON_01

Pulse Sequence: CARBON (s2pul)
Solvent: cdcl3
Data collected on: Sep 23 2013

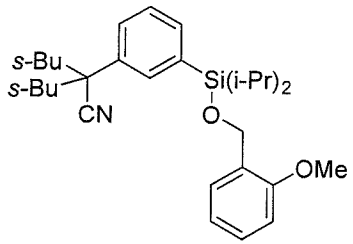

SG-3-017-3-Me-H

Sample Name:
SG-3-017-3-Me-H
Data Collected on:
nmr18-vnmrs500
Archive directory:

Sample directory:

FidFile: PROTON

Pulse Sequence: PROTON (s2pul)
Solvent: cdcl3
Data collected on: Sep 26 2013

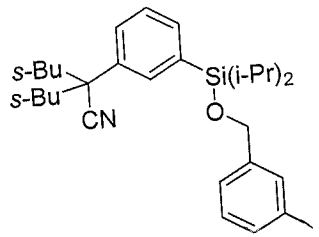

SG-3-017-3-Me-C

Sample Name:
SG-3-017-3-Me-C
Data Collected on:
nmr18-vnmrs500
Archive directory:

Sample directory:

FidFile: CARBON

Pulse Sequence: CARBON (s2pul)
Solvent: cdcl3
Data collected on: Sep 26 2013

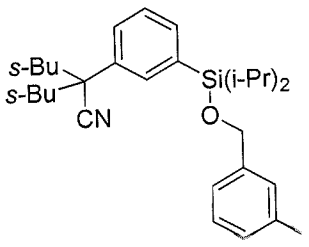

SG-3-020-3-F-H

Sample Name:
SG-3-020-3-F-H
Data Collected on:
nmr18-vnmrs500
Archive directory:

Sample directory:

FidFile: PROTON

Pulse Sequence: PROTON (s2pul)
Solvent: cdcl3
Data collected on: Sep 25 2013

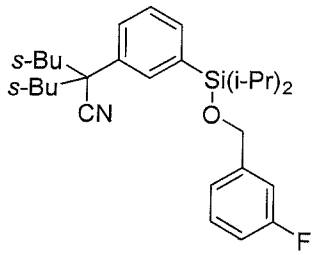

```
ErrorLog:
   auto_20130923_01 loc:33 (night)
Findz0 failed - low S/N

 Sample Name:
   SG-3-020-3-F-C
 Data Collected on:
   nmr14-vnmrs400
 Archive directory:
   /home/Robot/vnmrsys/data
 Sample directory:
   SG-3-020-3-F-C_20130923_01
 FidFile: CARBON_01

Pulse Sequence: CARBON (s2pul)
Solvent: cdcl3
Data collected on: Sep 23 2013
```

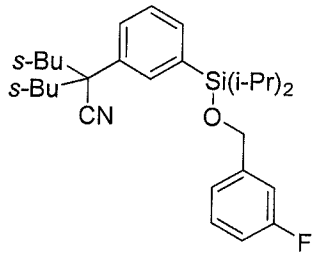

Sample Name:
HL-2-114
Data Collected on:
nmr18-vnmrs500
Archive directory:

Sample directory:

FidFile: HL-2-114

Pulse Sequence: PROTON (s2pul)
Solvent: cdcl3
Data collected on: Jul 18 2013

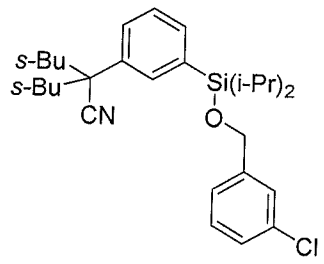

Sample Name:
HL-2-114-13C
Data Collected on:
nmr14-vnmrs400
Archive directory:
/home/Robot/vnmrsys/data
Sample directory:
HL-2-114-13C_20130718_01
FidFile: CARBON_02

Pulse Sequence: CARBON (s2pul)
Solvent: cdcl3
Data collected on: Jul 19 2013

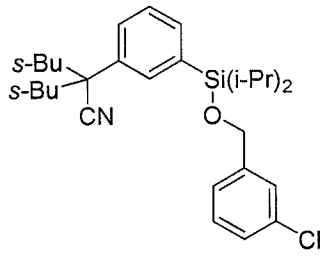

SG-3-020-3-Br-H

Sample Name:
SG-3-020-3-Br-H
Data Collected on:
nmr18-vnmrs500
Archive directory:

Sample directory:

FidFile: PROTON

Pulse Sequence: PROTON (s2pul)
Solvent: cdcl3
Data collected on: Sep 22 2013

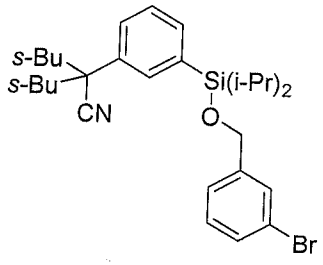

SG-3-020-3-Br-C

Sample Name:
SG-3-020-3-Br-C
Data Collected on:
nmr18-vnmrs500
Archive directory:

Sample directory:

FidFile: SG-3-020-3-Br-C

Pulse Sequence: CARBON (s2pul)
Solvent: cdcl3
Data collected on: Sep 23 2013

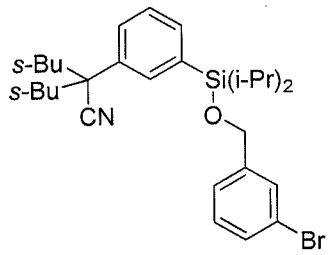

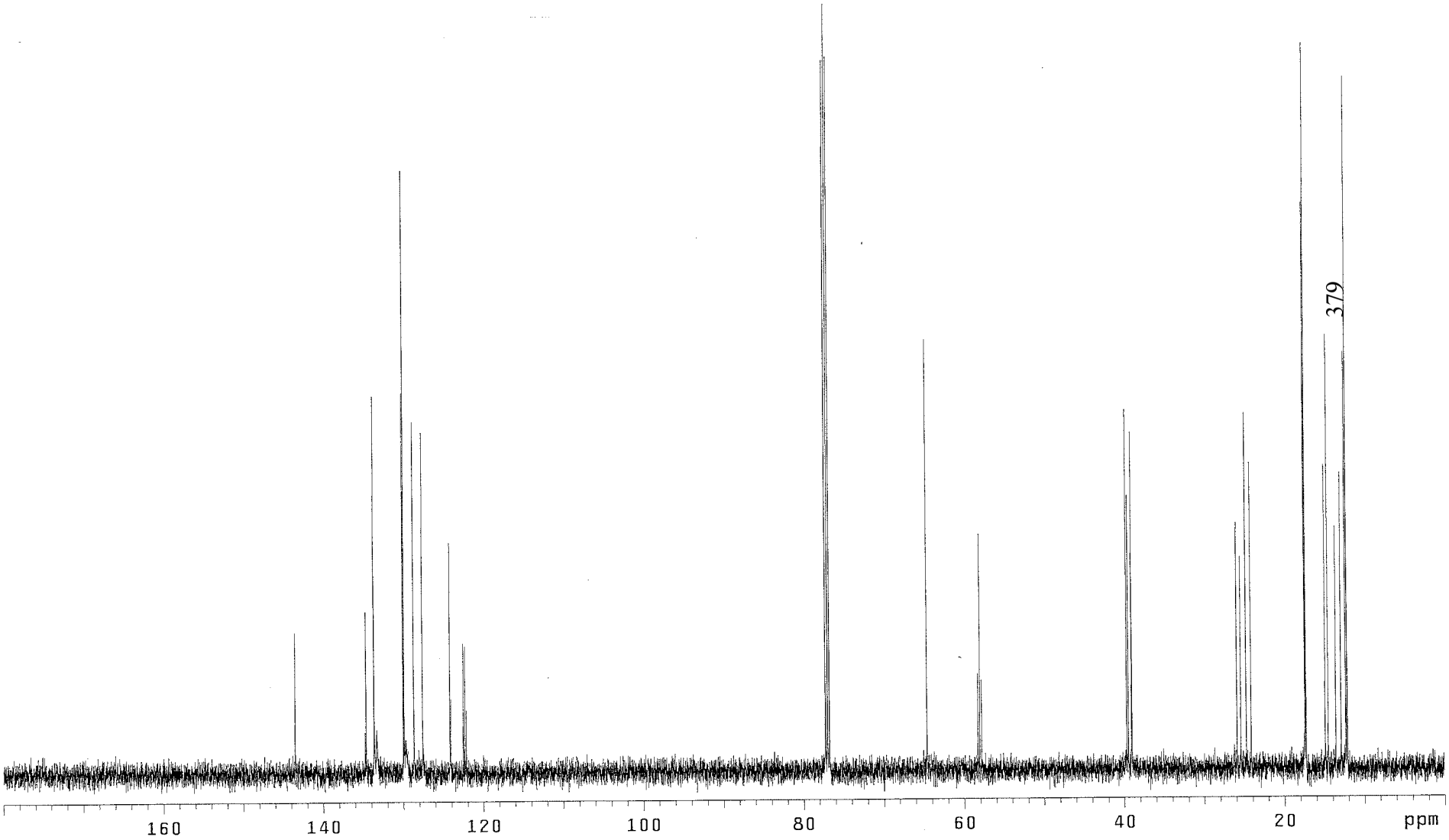

Sample Name:
HL-2-136
Data Collected on:
nmr18-vnmrs500
Archive directory:

Sample directory:

FidFile: HL-2-136

Pulse Sequence: PROTON (s2pul)
Solvent: cdcl3
Data collected on: Jul 18 2013

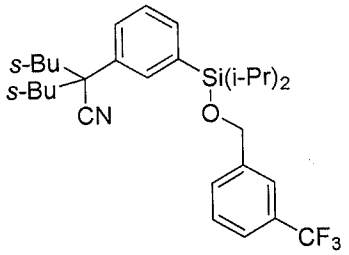

Sample Name:
HL-2-136-13C
Data Collected on:
nmr14-vnmrs400
Archive directory:
/home/Robot/vnmrsys/data
Sample directory:
HL-2-136-13C_20130719_01
FidFile: CARBON_01

Pulse Sequence: CARBON (s2pul)
Solvent: cdcl3
Data collected on: Jul 19 2013

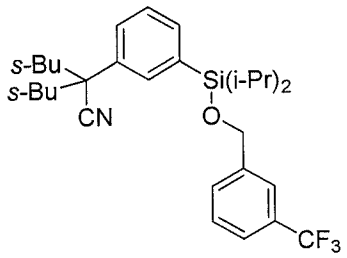

Sample Name:
SG-3-020
Data Collected on:
nmr18-vnmrs500
Archive directory:

Sample directory:

FidFile: SG-3-020

Pulse Sequence: PROTON (s2pul)
Solvent: cdcl3
Data collected on: Jul 18 2013

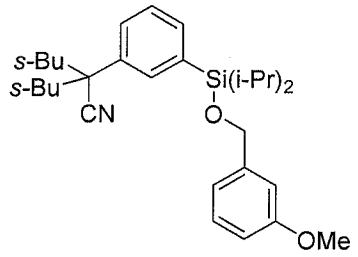

382

9 8 7 6 5 4 3 2 1 ppm

1.79 0.92 1.04 1.60 0.84 0.89 0.84 1.87 2.74 2.00 0.86 3.16 26.77

Sample Name:
SG-3-020-13C
Data Collected on:
nmr14-vnmrs400
Archive directory:
/home/Robot/vnmrsys/data
Sample directory:
SG-3-020-13C_20130718_01
FidFile: CARBON_01

Pulse Sequence: CARBON (s2pul)
Solvent: cdcl3
Data collected on: Jul 18 2013

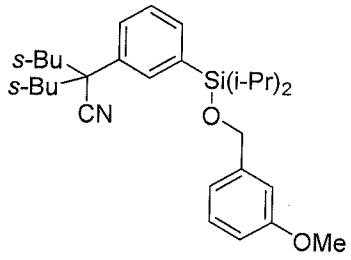

Sample Name:
HL-2-127
Data Collected on:
nmr18-vnmrs500
Archive directory:

Sample directory:

FidFile: HL-2-127

Pulse Sequence: PROTON (s2pul)
Solvent: cdcl3
Data collected on: Jul 19 2013

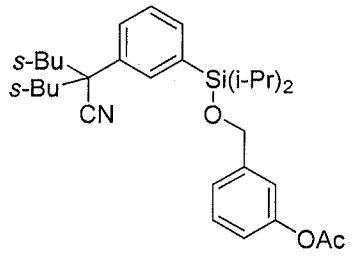

Sample Name:
HL-2-127-3-OAc-C
Data Collected on:
nmr14-vnmrs400
Archive directory:
/home/Robot/vnmrsys/data
Sample directory:
HL-2-127-3-OAc-C_20130923_01
FidFile: CARBON_01

Pulse Sequence: CARBON (s2pul)
Solvent: cdcl3
Data collected on: Sep 23 2013

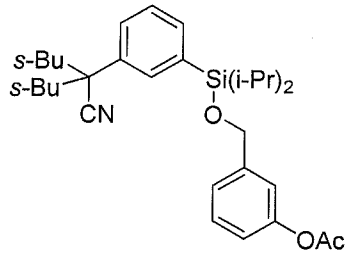

Sample Name:
HL-2-126
Data Collected on:
nmr18-vnmrs500
Archive directory:

Sample directory:

FidFile: HL-2-126

Pulse Sequence: PROTON (s2pul)
Solvent: cdcl3
Data collected on: Jul 19 2013

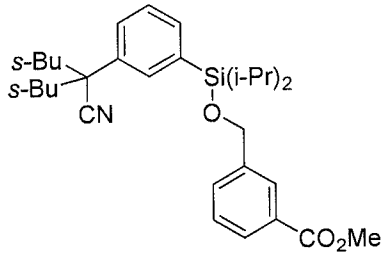

386

9 8 7 6 5 4 3 2 1 ppm

0.84 0.83 0.91 1.83 1.85 1.01 1.95 2.73 2.00 0.93 3.27 26.24

Sample Name:
HL-2-126-13C
Data Collected on:
nmr14-vnmrs400
Archive directory:
/home/Robot/vnmrsys/data
Sample directory:
HL-2-126-13C_20130719_01
FidFile: CARBON_01

Pulse Sequence: CARBON (s2pul)
Solvent: cdcl3
Data collected on: Jul 19 2013

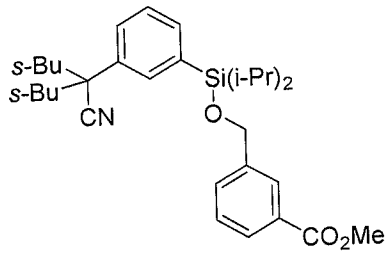

SG-3-020-4-Me-H

Sample Name:
SG-3-020-4-Me-H
Data Collected on:
nmr18-vnmrs500
Archive directory:

Sample directory:

FidFile: PROTON

Pulse Sequence: PROTON (s2pul)
Solvent: cdcl3
Data collected on: Sep 22 2013

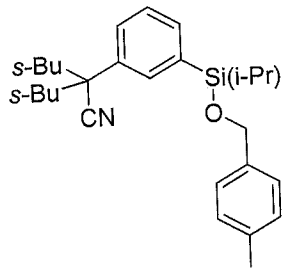

SG-3-020-4-Me-C

Sample Name:
SG-3-020-4-Me-C
Data Collected on:
nmr18-vnmrs500
Archive directory:

Sample directory:

FidFile: CARBON

Pulse Sequence: CARBON (s2pul)
Solvent: cdcl3
Data collected on: Sep 24 2013

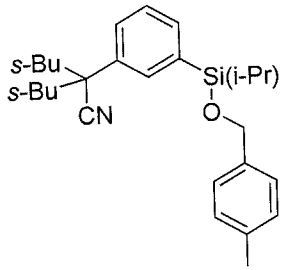

SG-3-020-4-Br-H

Sample Name:
SG-3-020-4-Br-H
Data Collected on:
nmr18-vnmrs500
Archive directory:

Sample directory:

FidFile: PROTON

Pulse Sequence: PROTON (s2pul)
Solvent: cdcl3
Data collected on: Sep 22 2013

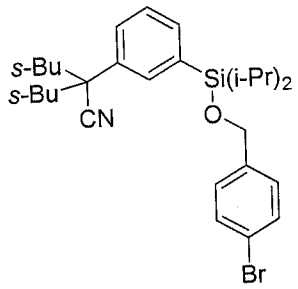

SG-3-020-4-Br-C

Sample Name:
SG-3-020-4-Br-C
Data Collected on:
nmr18-vnmrs500
Archive directory:

Sample directory:

FidFile: CARBON

Pulse Sequence: CARBON (s2pul)
Solvent: cdcl3
Data collected on: Sep 24 2013

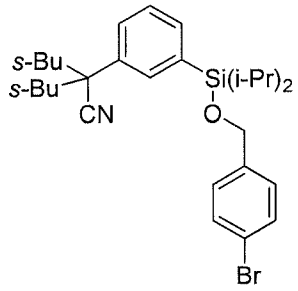

SG-3-020-4-MeO-H

Sample Name:
SG-3-020-4-MeO-H
Data Collected on:
nmr18-vnmrs500
Archive directory:

Sample directory:

FidFile: SG-3-020-4-MeO-H

Pulse Sequence: PROTON (s2pul)
Solvent: cdcl3
Data collected on: Sep 22 2013

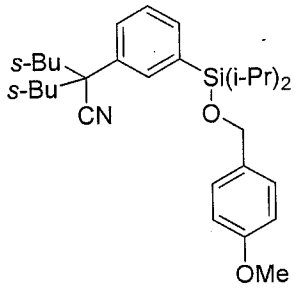

Sample Name:
SG-3-020-4-MeO-C
Data Collected on:
nmr14-vnmrs400
Archive directory:
/home/Robot/vnmrsys/data
Sample directory:
SG-3-020-4-MeO-C_20130923_01
FidFile: CARBON_01

Pulse Sequence: CARBON (s2pul)
Solvent: cdcl3
Data collected on: Sep 23 2013

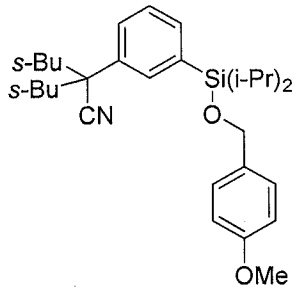

Sample Name:
HL-2-115
Data Collected on:
nmr18-vnmrs500
Archive directory:

Sample directory:

FidFile: HL-2-115

Pulse Sequence: PROTON (s2pul)
Solvent: cdcl3
Data collected on: Jul 18 2013

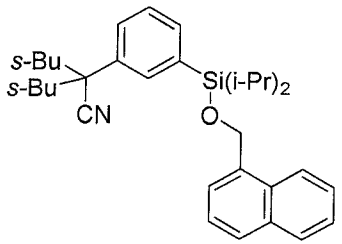

Sample Name:
HL-2-115-13C
Data Collected on:
nmr14-vnmrs400
Archive directory:
/home/Robot/vnmrsys/data
Sample directory:
HL-2-115-13C_20130719_01
FidFile: CARBON_03

Pulse Sequence: CARBON (s2pul)
Solvent: cdcl3
Data collected on: Jul 19 2013

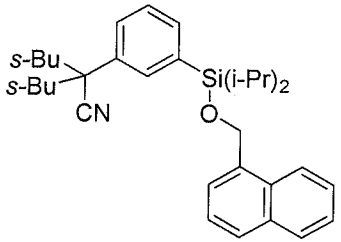

SG-3-065-Me-H

Sample Name:
SG-3-065-Me-H
Data Collected on:
nmr18-vnmrs500
Archive directory:

Sample directory:

FidFile: PROTON

Pulse Sequence: PROTON (s2pul)
Solvent: cdcl3
Data collected on: Jul 22 2013

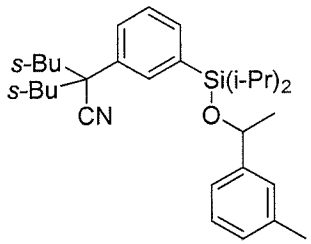

396

Sample Name:
SG-3-065-3-Me-C
Data Collected on:
nmr14-vnmrs400
Archive directory:
/home/Robot/vnmrsys/data
Sample directory:
SG-3-065-3-Me-C_20130928_01
FidFile: CARBON_01

Pulse Sequence: CARBON (s2pul)
Solvent: cdcl3
Data collected on: Sep 28 2013

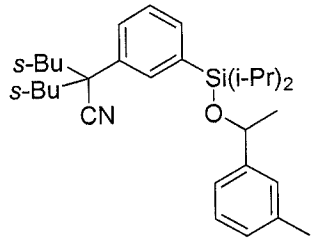

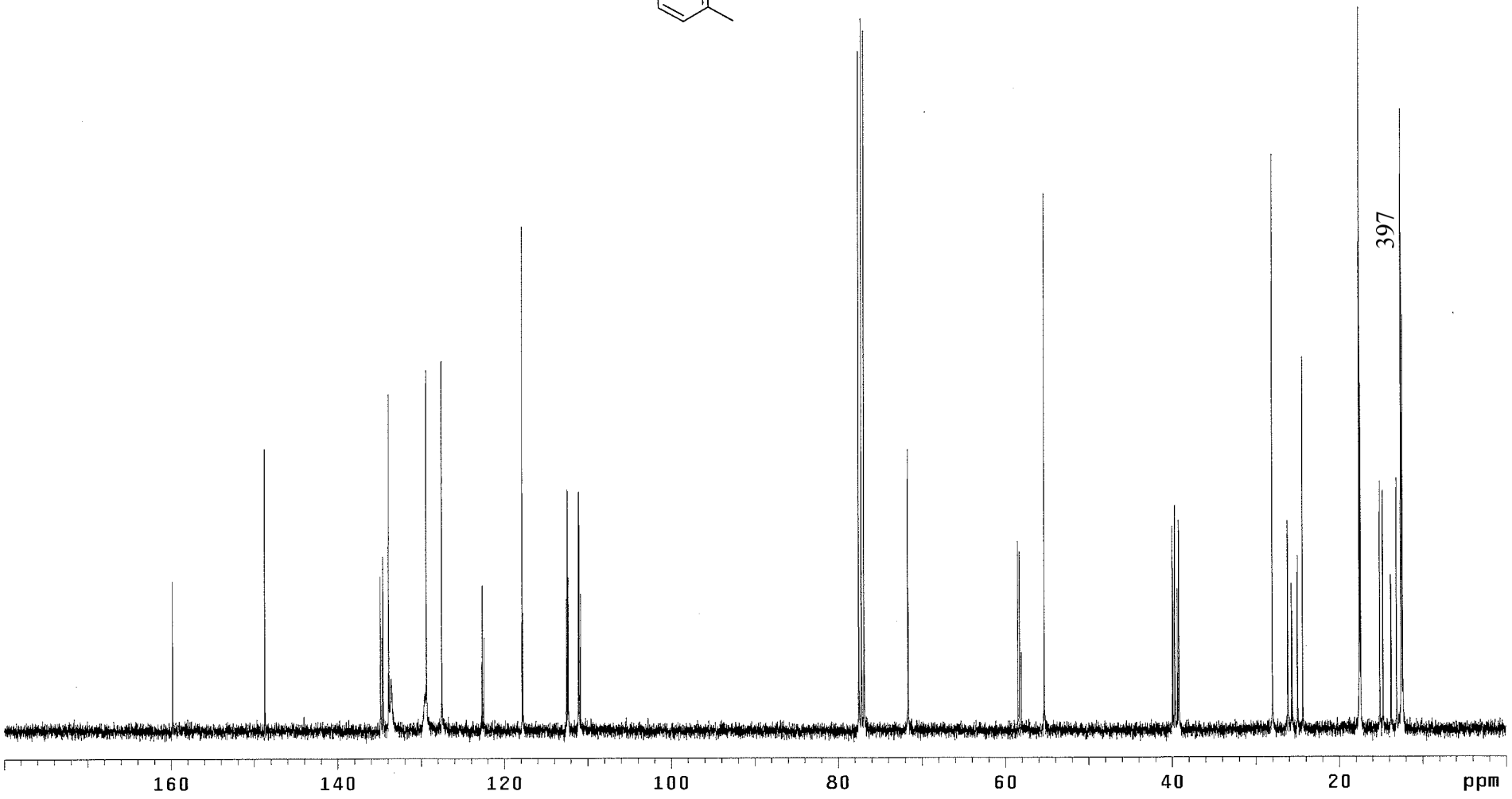

SG-3-065-Br-H

Sample Name:
SG-3-065-Br-H
Data Collected on:
nmr18-vnmrs500
Archive directory:

Sample directory:

FidFile: PROTON

Pulse Sequence: PROTON (s2pul)
Solvent: cdcl3
Data collected on: Jul 22 2013

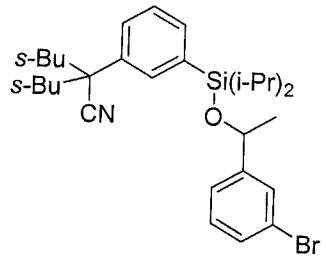

Sample Name:
SG-3-067-3-Br-pd-C
Data Collected on:
nmr14-vnmrs400
Archive directory:
/home/Robot/vnmrsys/data
Sample directory:
SG-3-067-3-Br-pd-C_20130920_01
FidFile: CARBON_01

Pulse Sequence: CARBON (s2pul)
Solvent: cdcl3
Data collected on: Sep 20 2013

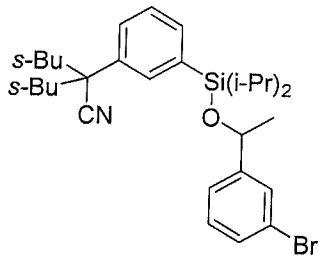

SG-3-065-OMe-H

Sample Name:
SG-3-065-OMe-H
Data Collected on:
nmr18-vnmrs500
Archive directory:

Sample directory:

FidFile: PROTON

Pulse Sequence: PROTON (s2pul)
Solvent: cdcl3
Data collected on: Jul 22 2013

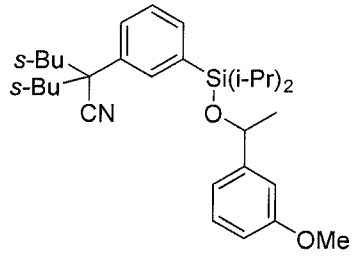

Sample Name:
SG-3-065-3-MeO-C
Data Collected on:
nmr14-vnmrs400
Archive directory:
/home/Robot/vnmrsys/data
Sample directory:
SG-3-065-3-MeO-C_20130928_01
FidFile: CARBON_01

Pulse Sequence: CARBON (s2pul)
Solvent: cdcl3
Data collected on: Sep 28 2013

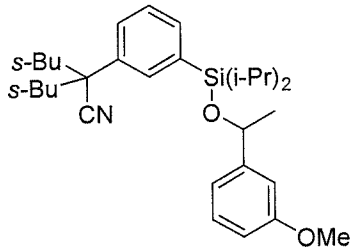

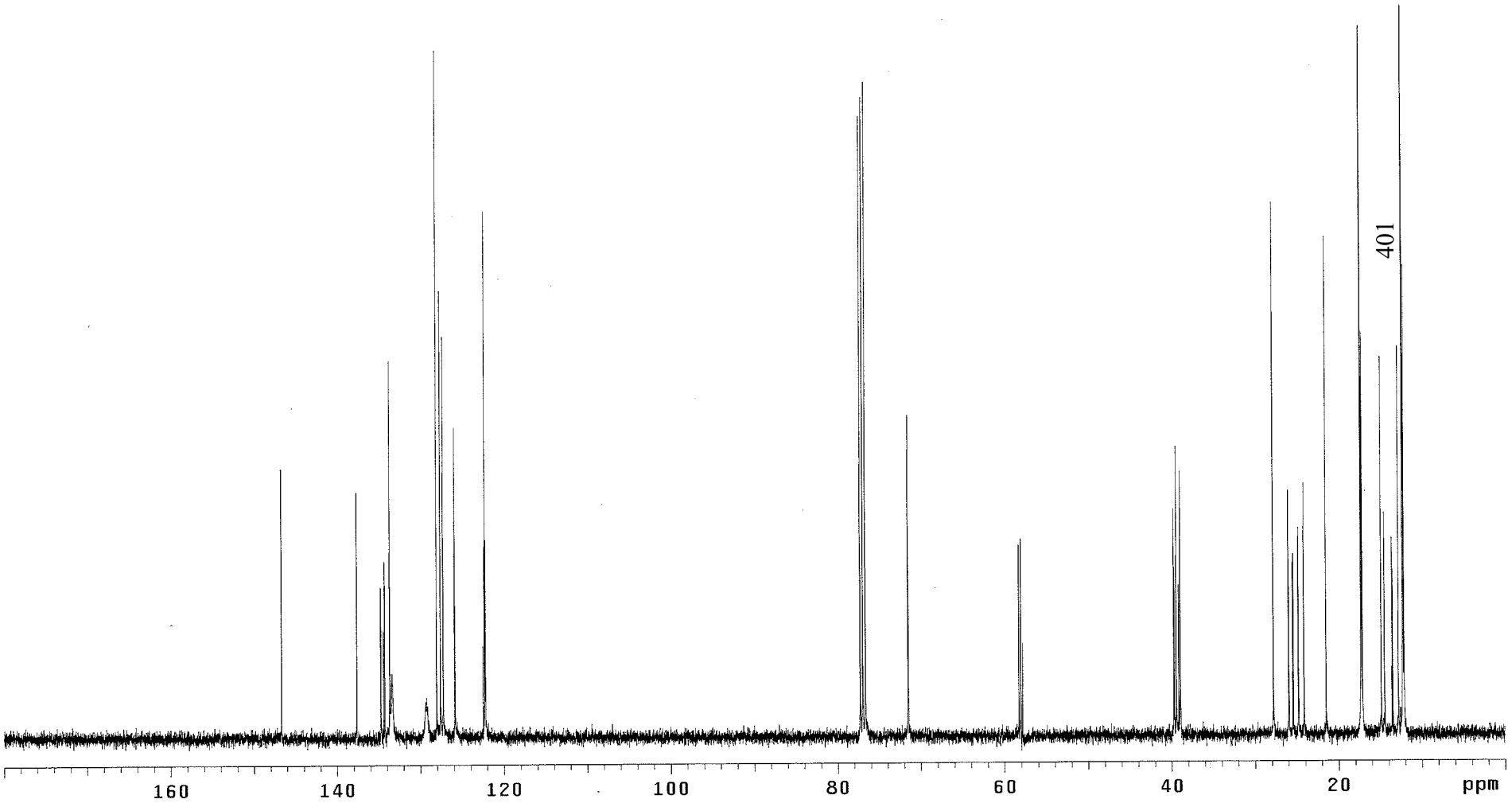

SG-2-216-pd-H

Sample Name:
SG-2-216-pd-H
Data Collected on:
nmr11-inova500
Archive directory:

Sample directory:

FidFile: SG-2-216-pd-H

Pulse Sequence: PROTON (s2pul)
Solvent: cdcl3
Data collected on: Aug 5 2013

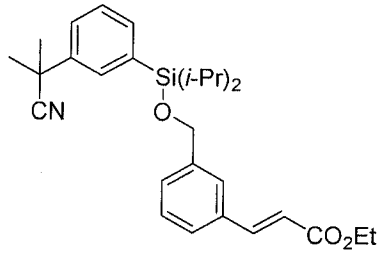

402

Sample Name:
SG-2-216
Data Collected on:
nmr14-vnmrs400
Archive directory:
/home/Robot/vnmrsys/data
Sample directory:
SG-2-216_20130811_01
FidFile: CARBON_01

Pulse Sequence: CARBON (s2pul)
Solvent: cdcl3
Data collected on: Aug 11 2013

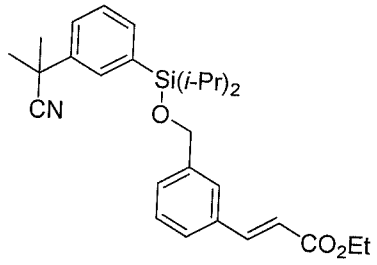

SG-2-258-Et-pd-H

Sample Name:
SG-2-258-Et-pd-H
Data Collected on:
nmr11-inova500
Archive directory:

Sample directory:

FidFile: SG-2-258-Et-pd-H

Pulse Sequence: PROTON (s2pul)
Solvent: cdcl3
Data collected on: Aug 5 2013

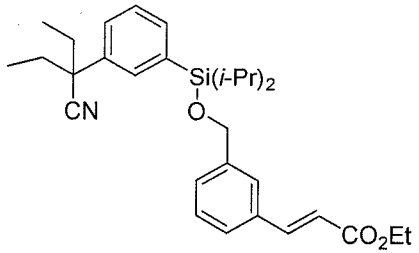

SG-2-258-Et-C

Sample Name:
SG-2-258-Et-C
Data Collected on:
nmr18-vnmrs500
Archive directory:

Sample directory:

FidFile: SG-2-258-Et-C

Pulse Sequence: CARBON (s2pul)
Solvent: cdcl3
Data collected on: Aug 10 2013

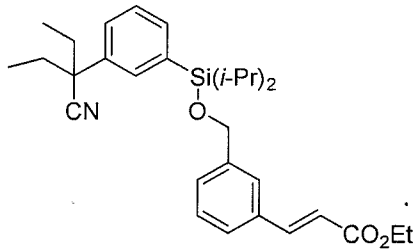

SG-2-258-iPr-H

Sample Name:
SG-2-258-iPr-H
Data Collected on:
nmr18-vnmrs500
Archive directory:

Sample directory:

FidFile: SG-2-258-iPr-H

Pulse Sequence: PROTON (s2pul)
Solvent: cdcl3
Data collected on: Aug 6 2013

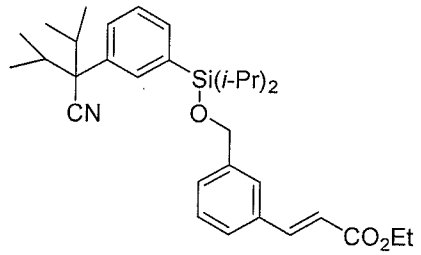

SG-2-258-iPr-H

Sample Name:
SG-2-258-iPr-H
Data Collected on:
nmr18-vnmrs500
Archive directory:

Sample directory:

FidFile: SG-2-258-iPr-C

Pulse Sequence: CARBON (s2pul)
Solvent: cdcl3
Data collected on: Aug 6 2013

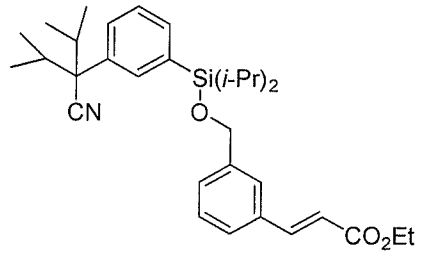

SG-2-268-sBu-H

Sample Name:
SG-2-268-sBu-H
Data Collected on:
nmr18-vnmrs500
Archive directory:

Sample directory:

FidFile: SG-2-268-sBu-H

Pulse Sequence: PROTON (s2pul)
Solvent: cdcl3
Data collected on: Aug 14 2013

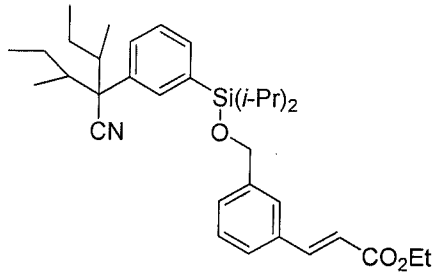

Sample Name:
SG-2-268-sBu
Data Collected on:
nmr14-vnmrs400
Archive directory:
/home/Robot/vnmrsys/data
Sample directory:
SG-2-268-sBu_20130814_02
FidFile: CARBON_01

Pulse Sequence: CARBON (s2pul)
Solvent: cdcl3
Data collected on: Aug 14 2013

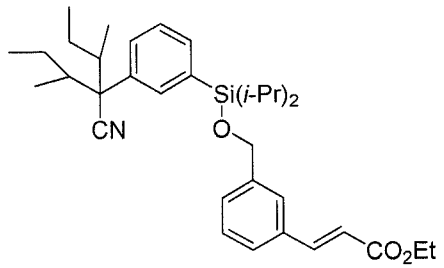

SG-3-004-pd-di-hydro-H

Sample Name:
SG-3-004-pd-di-hydro-H
Data Collected on:
nmr18-vnmrs500
Archive directory:

Sample directory:

FidFile: SG-3-004-pd-di-hydro-H

Pulse Sequence: PROTON (s2pul)
Solvent: cdcl3
Data collected on: Sep 26 2013

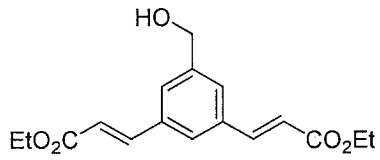

SG-3-004-pd-di-hydro-H

Sample Name:
SG-3-004-pd-di-hydro-H
Data Collected on:
nmr18-vnmrs500
Archive directory:

Sample directory:

FidFile: CARBON

Pulse Sequence: CARBON (s2pul)
Solvent: cdcl3
Data collected on: Sep 26 2013

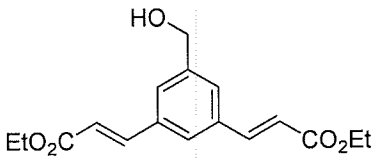

(500Mhz, CDCl3)

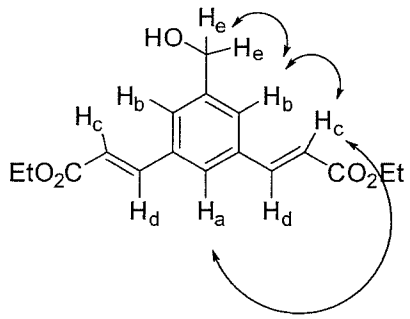

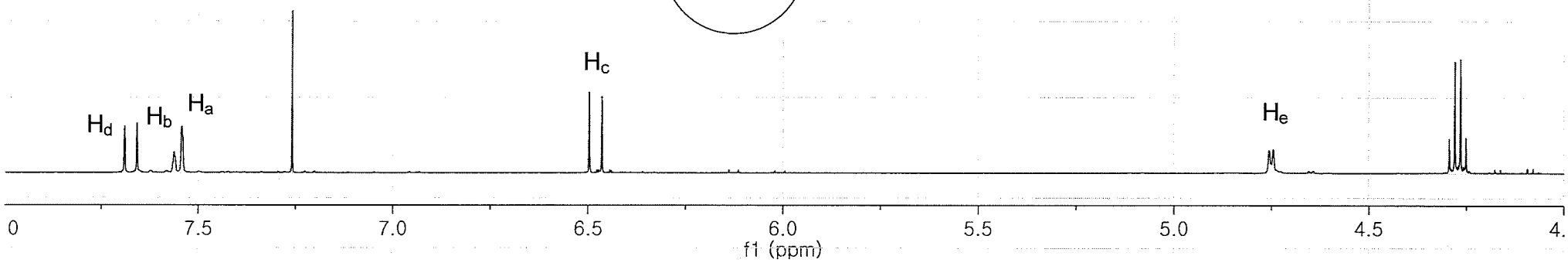

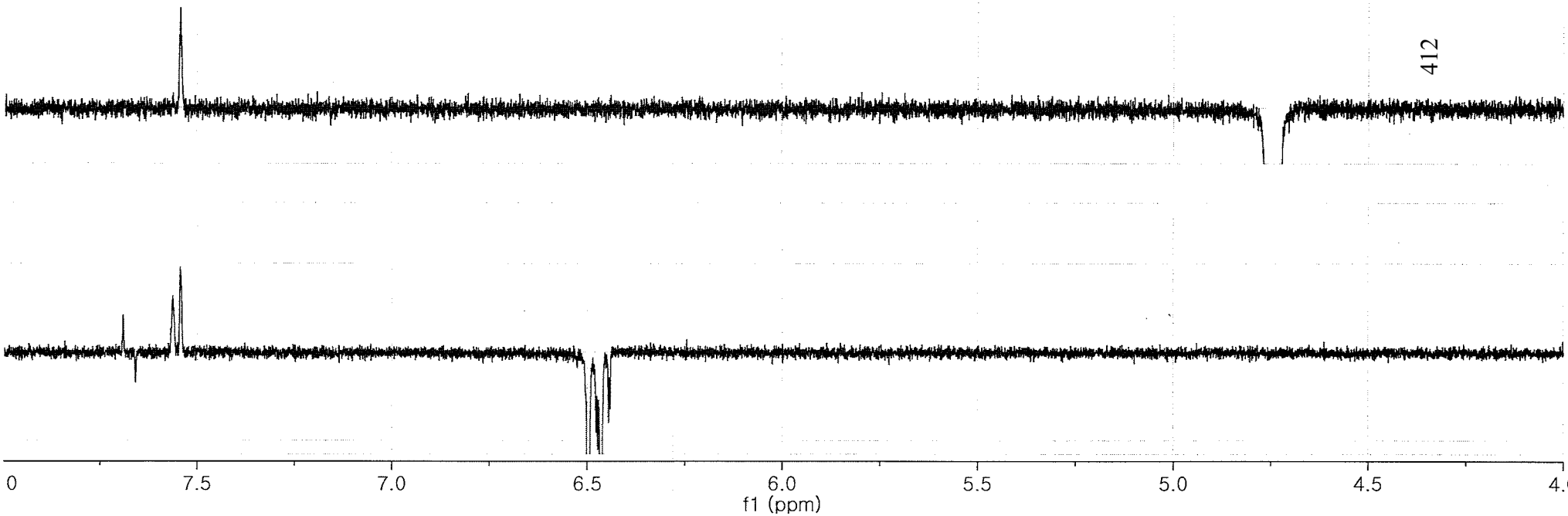

SG-2-268-cHx-H

Sample Name:
SG-2-268-cHx-H
Data Collected on:
nmr18-vnmrs500
Archive directory:

Sample directory:

FidFile: SG-2-268-cHx-H

Pulse Sequence: PROTON (s2pul)
Solvent: cdcl3
Data collected on: Aug 14 2013

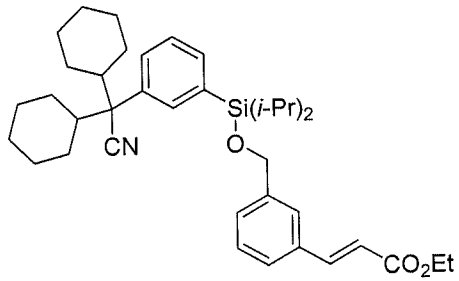

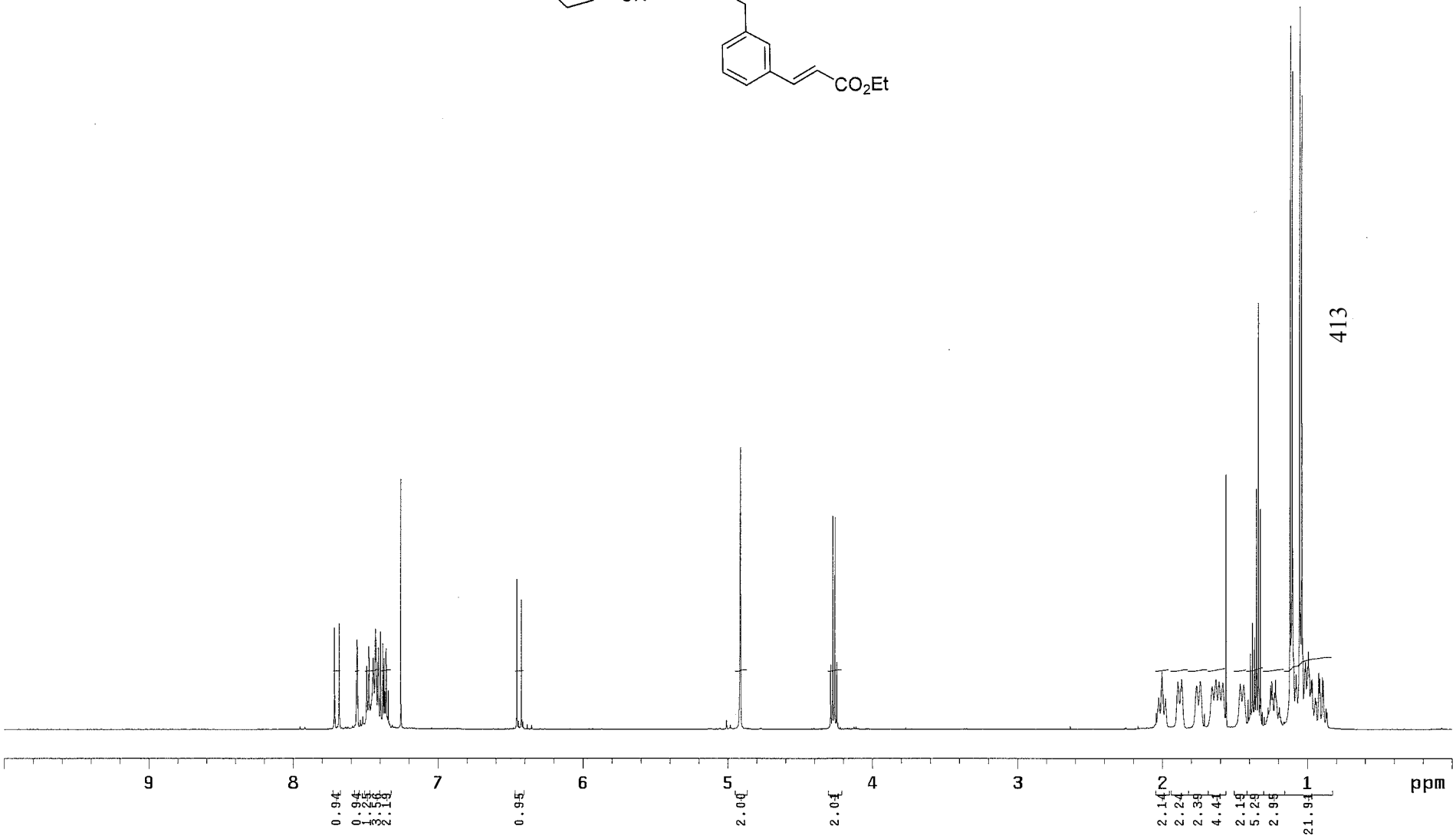

Sample Name:
SG-2-268-cHx
Data Collected on:
nmr14-vnmrs400
Archive directory:
/home/Robot/vnmrsys/data
Sample directory:
SG-2-268-cHx_20130814_01
FidFile: CARBON_01

Pulse Sequence: CARBON (s2pul)
Solvent: cdcl3
Data collected on: Aug 14 2013

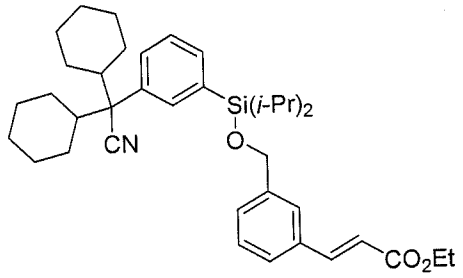

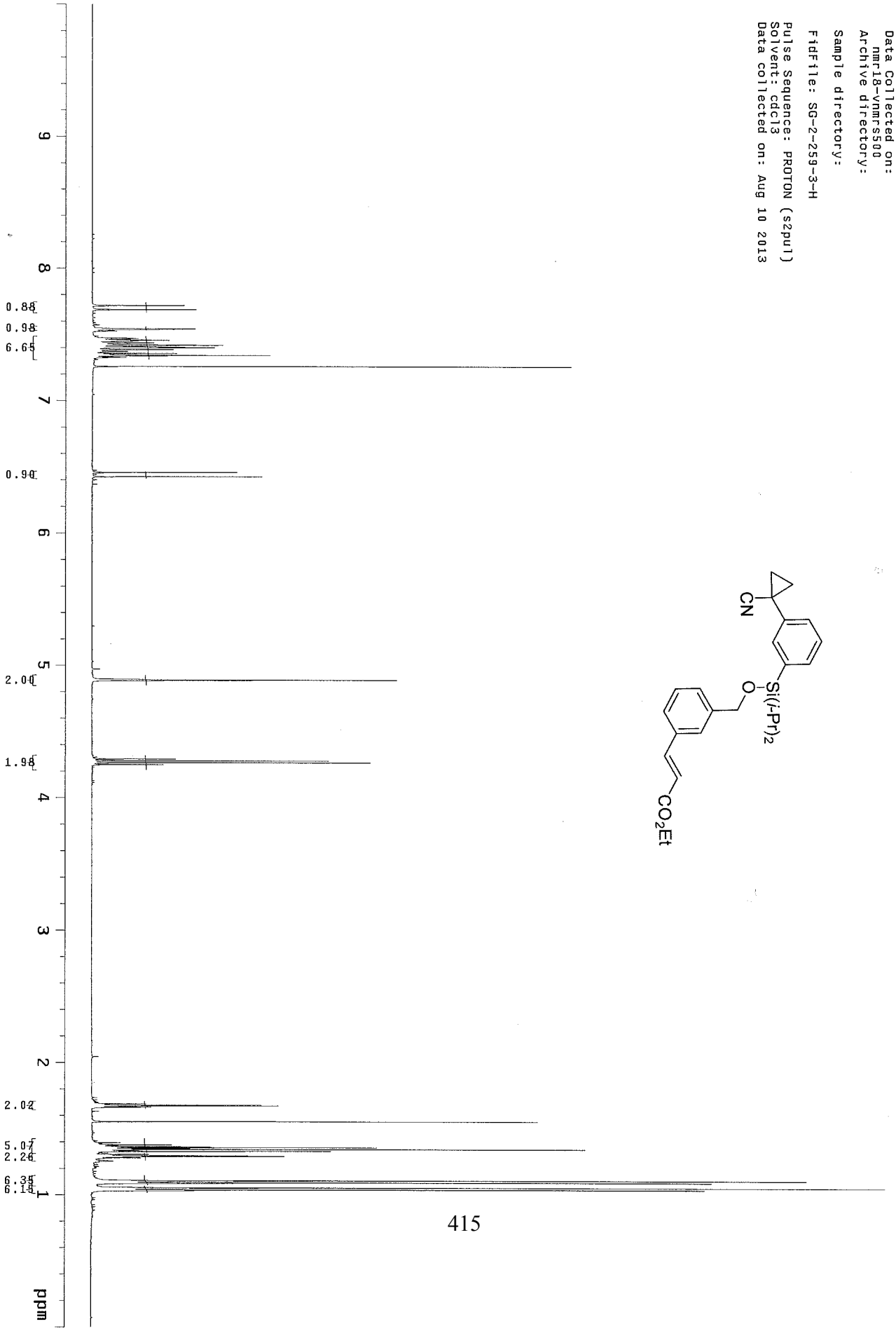
SG-2-259-3-H
Sample Name:
SG-2-259-3-H
Data Collected on:
nmr18-vnmrs500
Archive directory:
Sample directory:
FidFile: SG-2-259-3-H
Pulse Sequence: PROTON (s2pul)
Solvent: cdcl3
Data collected on: Aug 10 2013
CN
Si(i-Pr)2
O
CO2Et
0.88
0.98
6.65
0.90
2.00
1.98
2.02
5.07
2.26
6.35
6.15
9
8
7
6
5
4
3
2
1
ppm

SG-2-259-3-C

Sample Name:
SG-2-259-3-C
Data Collected on:
nmr18-vnmrs500
Archive directory:

Sample directory:

FidFile: SG-2-259-3-C

Pulse Sequence: CARBON (s2pul)
Solvent: cdcl3
Data collected on: Aug 13 2013

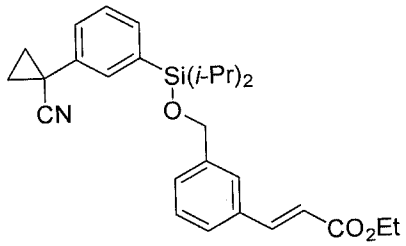

SG-2-259-5-H

Sample Name:
SG-2-259-5-H
Data Collected on:
nmr18-vnmrs500
Archive directory:

Sample directory:

FidFile: SG-2-259-5-H

Pulse Sequence: PROTON (s2pul)
Solvent: cdcl3
Data collected on: Aug 10 2013

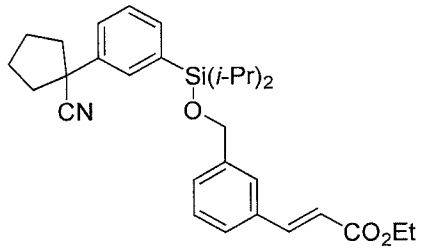

Sample Name:
SG-2-259-5-pd-C
Data Collected on:
nmr14-vnmrs400
Archive directory:
/home/Robot/vnmrsys/data
Sample directory:
SG-2-259-5-pd-C_20130928_01
FidFile: CARBON_01

Pulse Sequence: CARBON (s2pul)
Solvent: cdcl3
Data collected on: Sep 28 2013

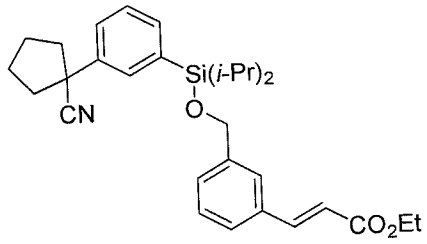

SG-3-107-2-Me-pd-m-H

Sample Name:
SG-3-107-2-Me-pd-m-H
Data Collected on:
nmr15-vnmrs500
Archive directory:

Sample directory:

FidFile: PROTON

Pulse Sequence: PROTON (s2pul)
Solvent: cdcl3
Data collected on: Sep 10 2013

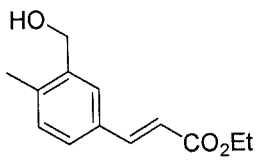

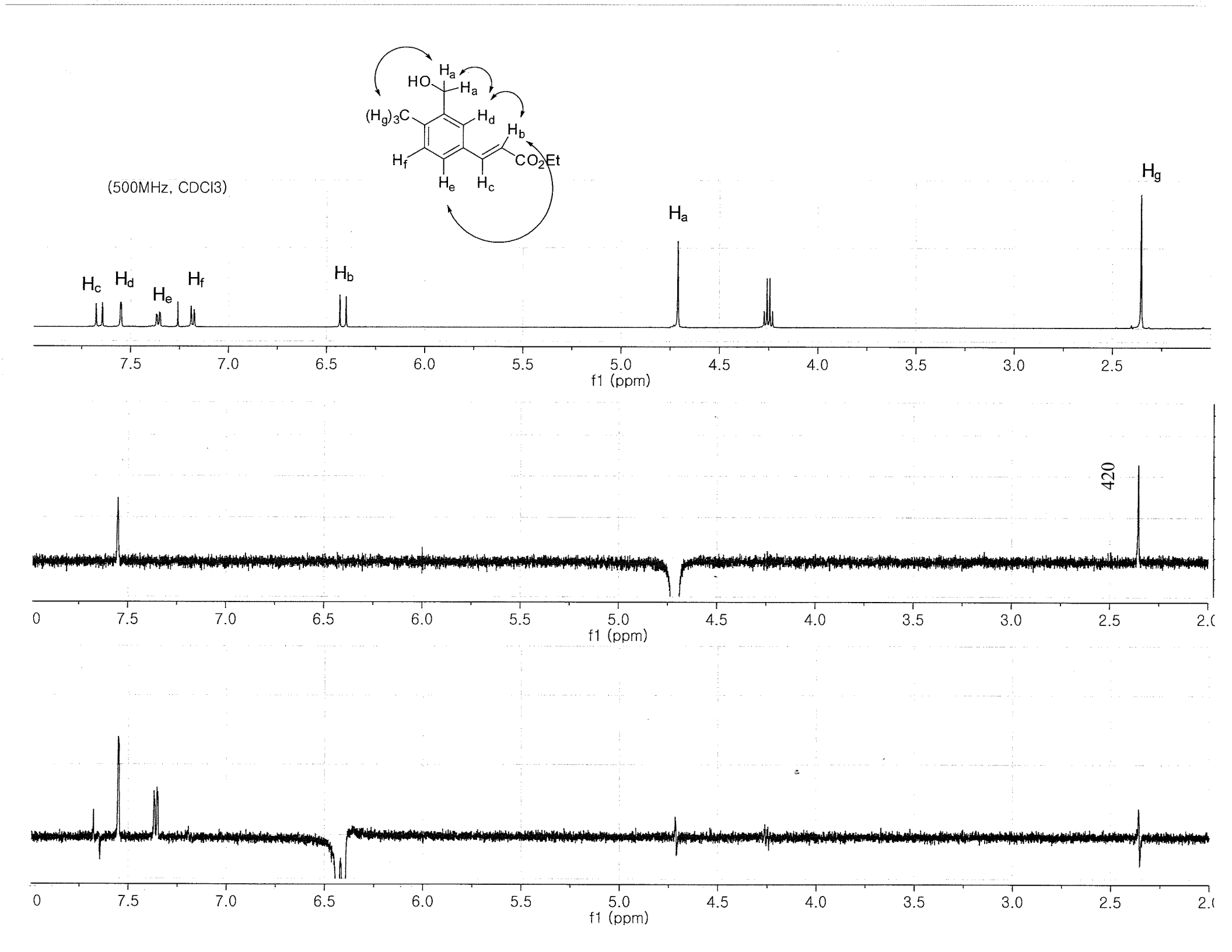
(500MHz, CDCl3)
HO
Ha
Ha
(Hg)3C
Hd
Hb
Hf
CO2Et
He
Hc
Hc
Hd
He
Hf
Hb
Ha
Hg
f1 (ppm)
420
f1 (ppm)
f1 (ppm)

SG-3-107-2-Me-pd-di-H

Sample Name:
SG-3-107-2-Me-pd-di-H
Data Collected on:
nmr15-vnmrs500
Archive directory:

Sample directory:

FidFile: PROTON

Pulse Sequence: PROTON (s2pul)
Solvent: cdcl3
Data collected on: Sep 11 2013

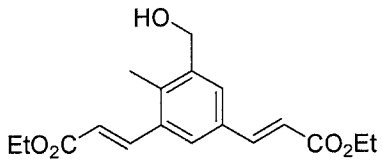

SG-3-107-2-Me-pd-m-C

Sample Name:
SG-3-107-2-Me-pd-m-C
Data Collected on:
nmr15-vnmrs500
Archive directory:

Sample directory:

FidFile: CARBON

Pulse Sequence: CARBON (s2pul)
Solvent: cdcl3
Data collected on: Sep 10 2013

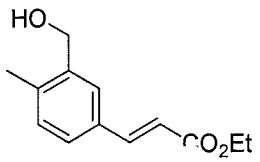

Sample Name:
SG-3-107-2-Me-di-C
Data Collected on:
nmr14-vnmrs400
Archive directory:
/home/Robot/vnmrsys/data
Sample directory:
SG-3-107-2-Me-di-C_20130911_01
FidFile: CARBON_01

Pulse Sequence: CARBON (s2pul)
Solvent: cdcl3
Data collected on: Sep 11 2013

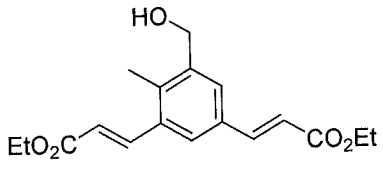

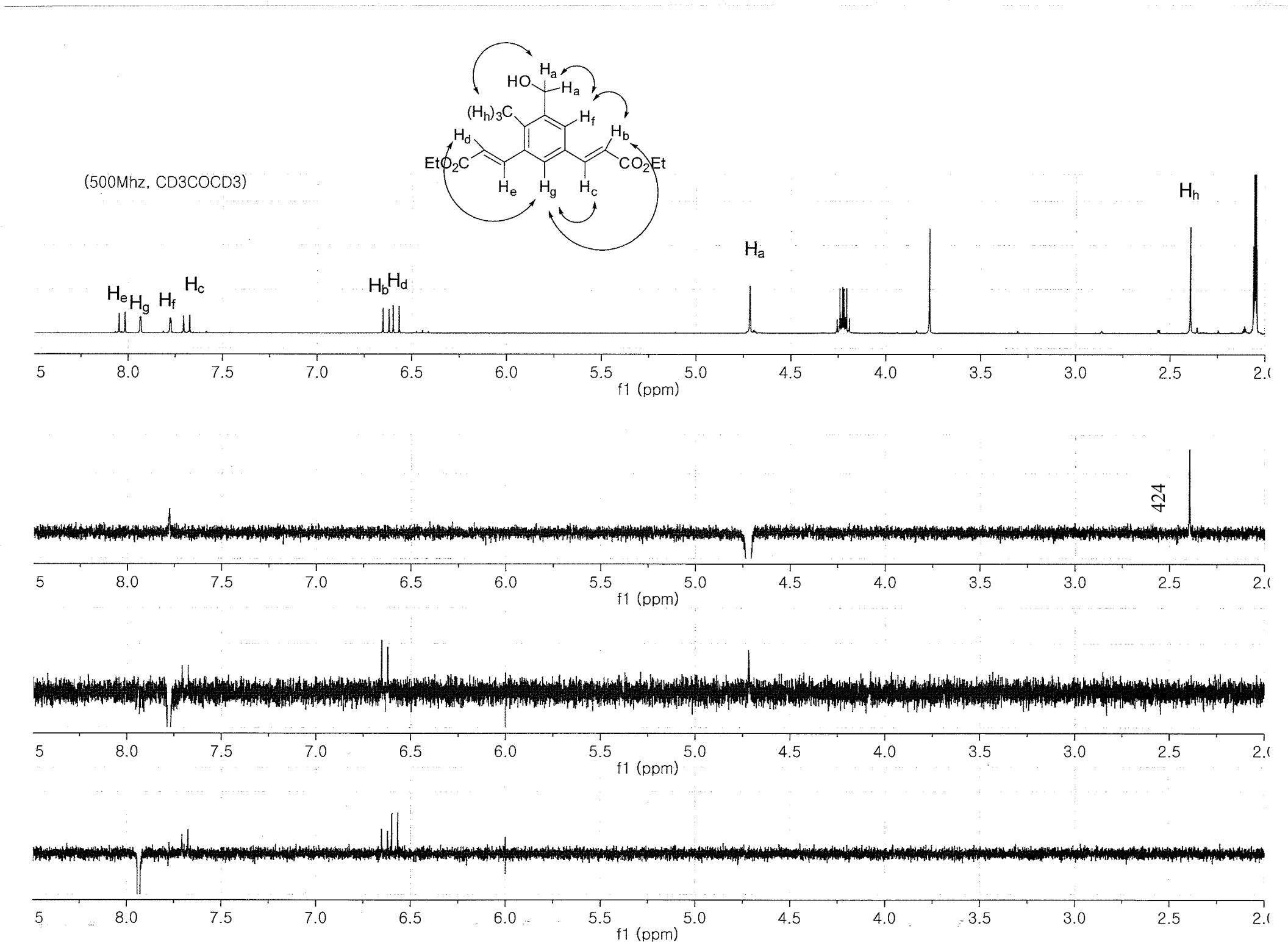
(500Mhz, CD3COCD3)
HO
H_a
H_a
$(H_h)_3C$
H_f
H_d
H_b
EtO_2C
CO_2Et
H_e
H_g
H_c
H_e H_g H_f H_c
H_b H_d
H_a
H_h
424
5 8.0 7.5 7.0 6.5 6.0 5.5 5.0 4.5 4.0 3.5 3.0 2.5 2.0
f1 (ppm)

SG-3-054-2-Br-pd-m-H

Sample Name:
SG-3-054-2-Br-pd-m-H
Data Collected on:
nmr18-vnmrs500
Archive directory:

Sample directory:

FidFile: PROTON

Pulse Sequence: PROTON (s2pul)
Solvent: cdcl3
Data collected on: Sep 20 2013

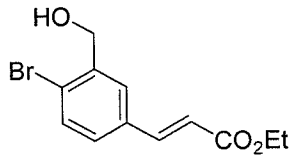

425

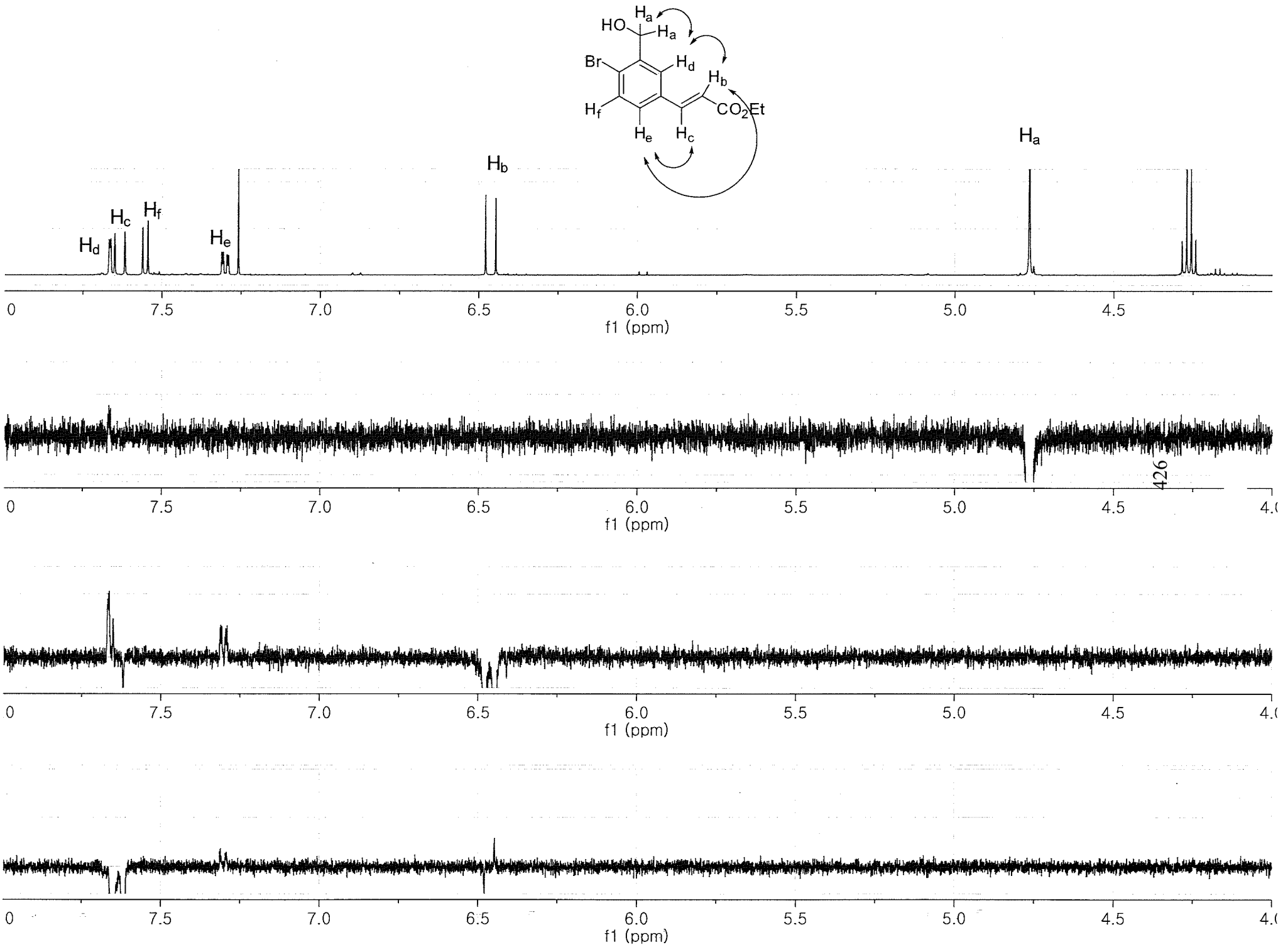
Ha
HO
Ha
Br
Hd
Hb
Hf
CO2Et
He
Hc
Ha
Hb
Hc
Hf
Hd
He
0
7.5
7.0
6.5
6.0
5.5
5.0
4.5
f1 (ppm)
426

SG-3-054-2-Br-pd-m-C

Sample Name:
SG-3-054-2-Br-pd-m-C
Data Collected on:
nmr18-vnmrs500
Archive directory:

Sample directory:

FidFile: CARBON

Pulse Sequence: CARBON (s2pul)
Solvent: cdcl3
Data collected on: Sep 20 2013

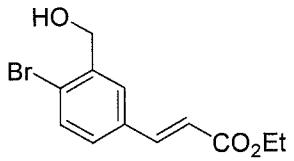

SG-3-054-2-br-pd-di-4

Sample Name:
SG-3-054-2-br-pd-di-4
Data Collected on:
nmr18-vnmrs500
Archive directory:

Sample directory:

FidFile: PROTON

Pulse Sequence: PROTON (s2pul)
Solvent: cdcl3
Data collected on: Oct 11 2013

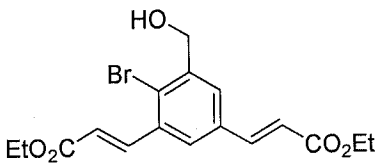

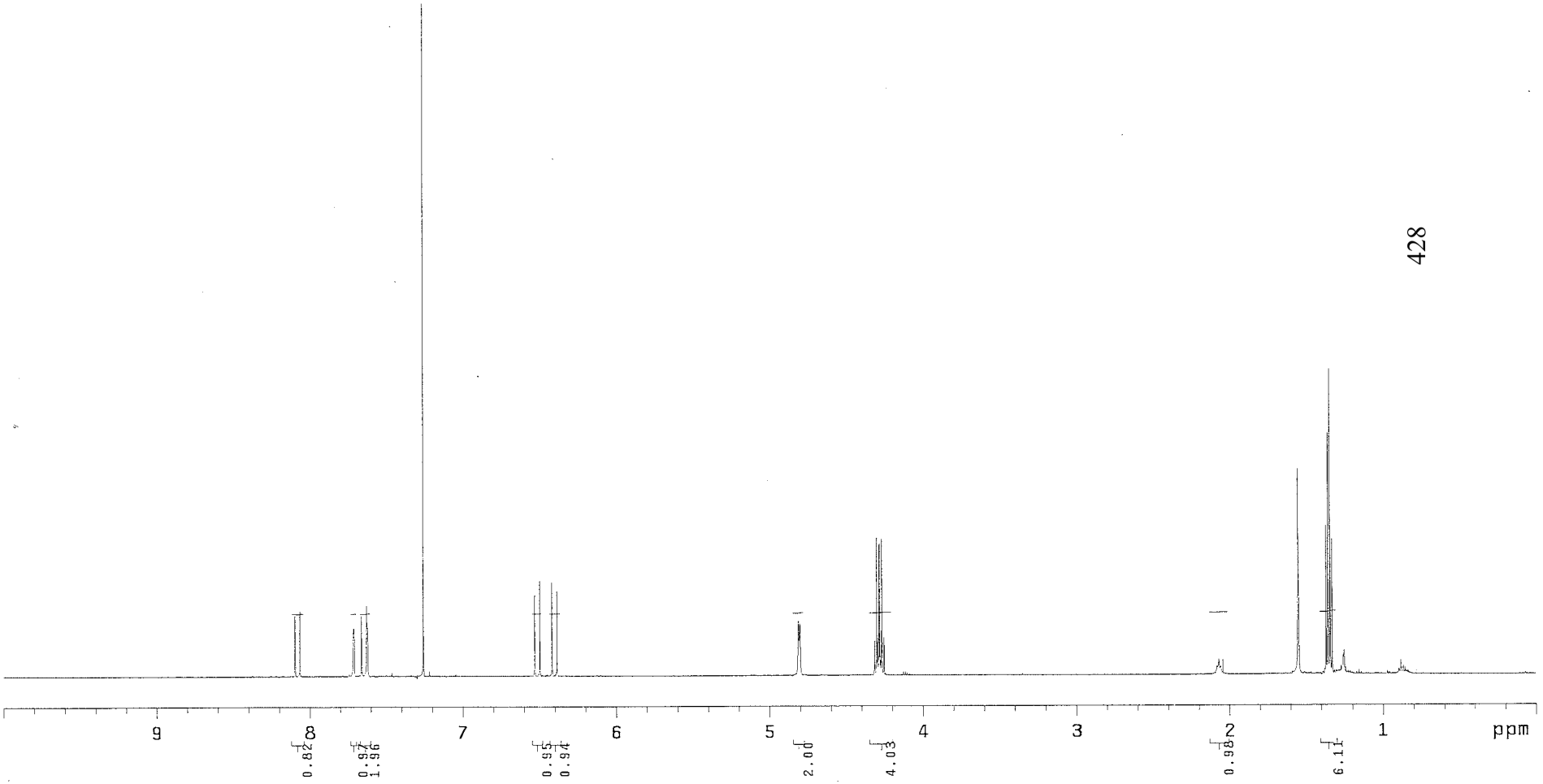

Sample Name:
SG-3-054-2-br-di-C
Data Collected on:
nmr14-vnmrs400
Archive directory:
/home/Robot/vnmrsys/data
Sample directory:
SG-3-054-2-br-di-C_20131011_01
FidFile: CARBON_01

Pulse Sequence: CARBON (s2pul)
Solvent: cdcl3
Data collected on: Oct 11 2013

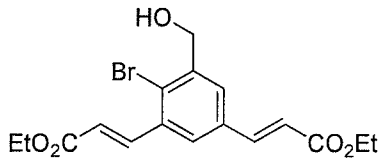

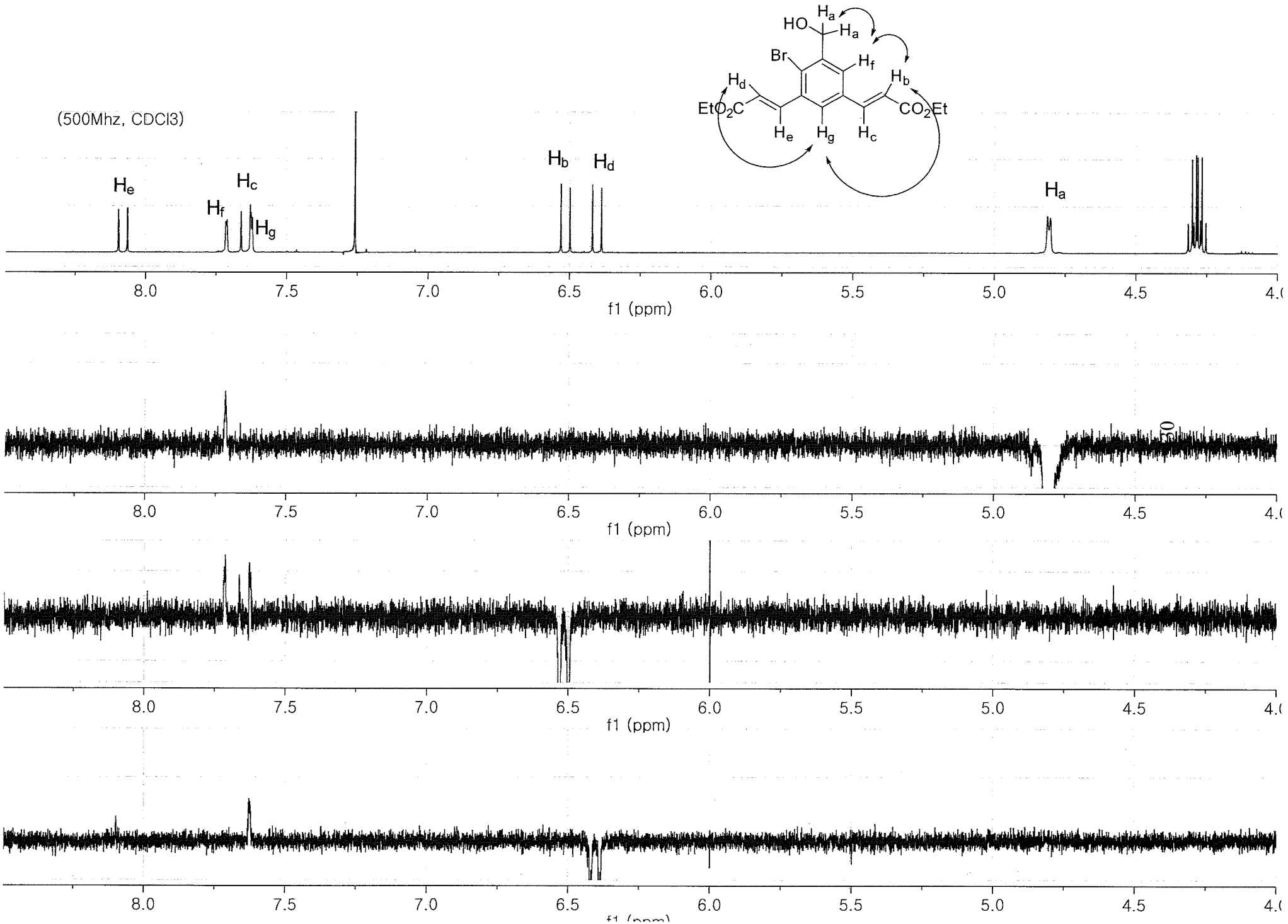
(500Mhz, CDCl3)
H_e
H_f
H_c
H_g
H_b
H_d
H_a
HO
Br
EtO_2C
CO_2Et
8.0
7.5
7.0
6.5
6.0
5.5
5.0
4.5
f1 (ppm)

Sample Name:
SG-3-069-OMe-NOE-H
Data Collected on:
nmr18-vnmrs500
Archive directory:

Sample directory:

FidFile: SG-3-069-OMe-NOE-H

Pulse Sequence: PROTON (s2pul)
Solvent: cdcl3
Data collected on: Aug 1 2013

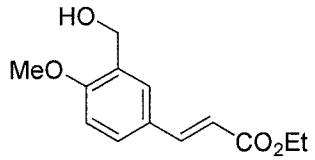

SG-3-069-2-OMe-Pd-C

Sample Name:
SG-3-069-2-OMe-Pd-C
Data Collected on:
nmr18-vnmrs500
Archive directory:

Sample directory:

FidFile: CARBON

Pulse Sequence: CARBON (s2pul)
Solvent: cdcl3
Data collected on: Aug 1 2013

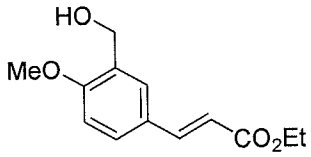

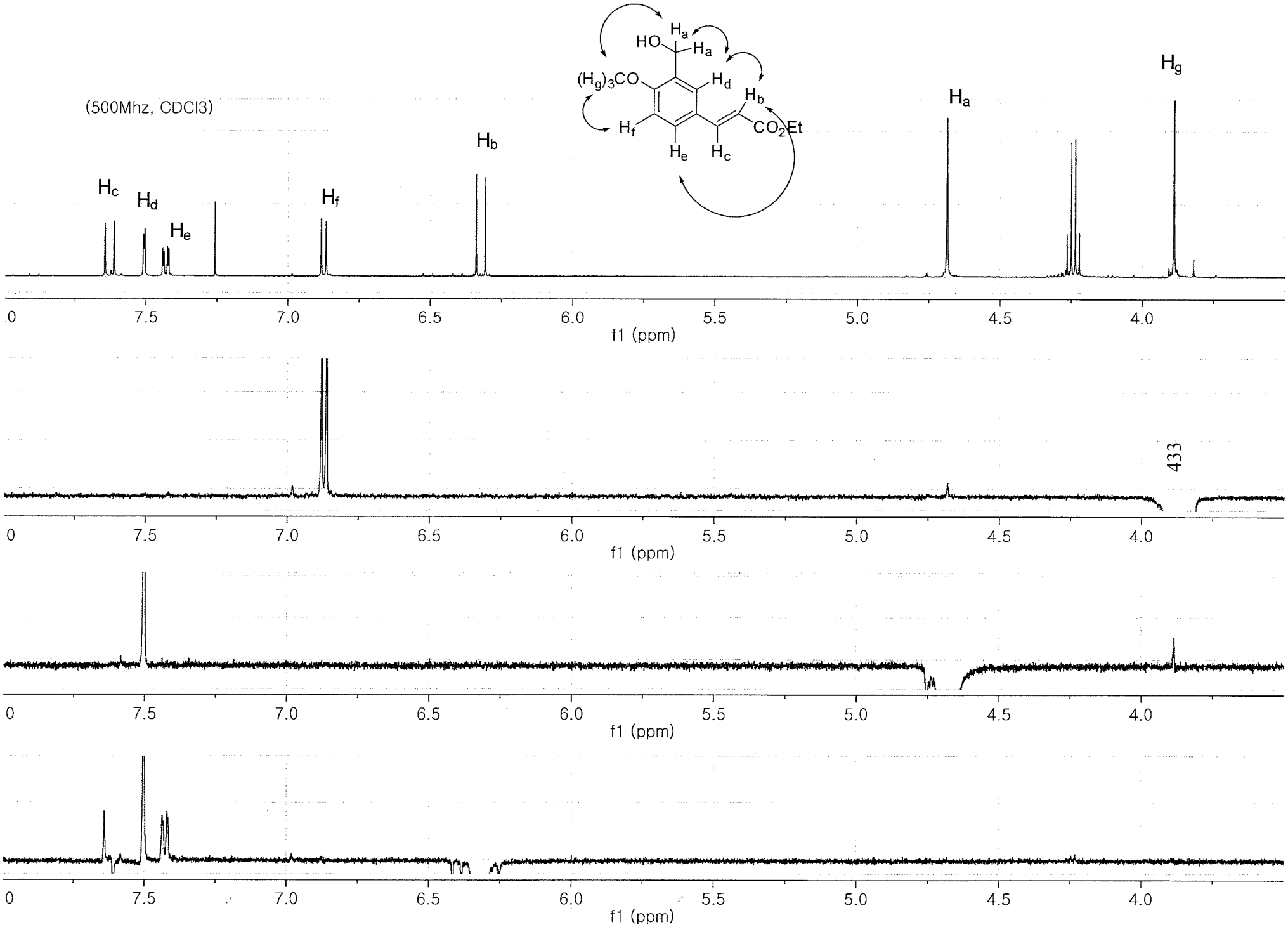
(500Mhz, CDCl3)
Hc
Hd
He
Hf
Hb
Ha
Hg
HO
Ha
(Hg)3CO
Hd
Hb
Hf
CO2Et
He
Hc
433
0
7.5
7.0
6.5
6.0
5.5
5.0
4.5
4.0
f1 (ppm)

SG-3-033-5-2_2-CD3OD-H

Sample Name:
SG-3-033-5-2_2-CD3OD-H
Data Collected on:
nmr18-vnmrs500
Archive directory:

Sample directory:

FidFile: CARBON

Pulse Sequence: CARBON (s2pul)
Solvent: cd3od
Data collected on: Jul 18 2013

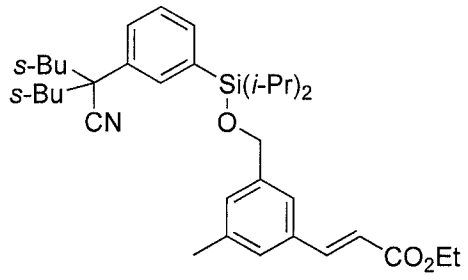

STANDARD 1H OBSERVE - profile

Sample Name:

Data Collected on:
nmr19-vnmrs600
Archive directory:

Sample directory:

FidFile: SG-3-033-5-2.2eq-H

Pulse Sequence: PROTON (s2pul)
Solvent: cdcl3
Data collected on: Jul 17 2013

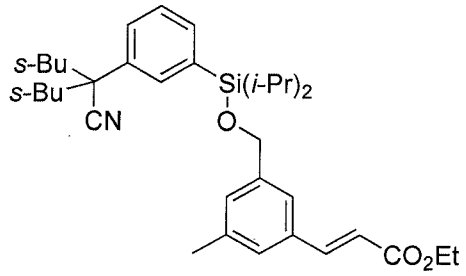

SG-3-083-pd-H

Sample Name:
SG-3-083-pd-H
Data Collected on:
nmr18-vnmrs500
Archive directory:

Sample directory:

FidFile: SG-3-083-pd-H

Pulse Sequence: PROTON (s2pul)
Solvent: cdcl3
Data collected on: Aug 16 2013

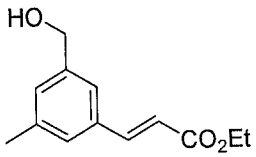

SG-3-083-pd-H

Sample Name:
SG-3-083-pd-H
Data Collected on:
nmr18-vnmrs500
Archive directory:

Sample directory:

FidFile: CARBON

Pulse Sequence: CARBON (s2pul)
Solvent: cdcl3
Data collected on: Aug 16 2013

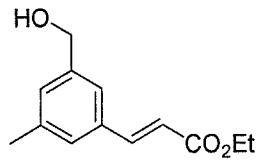

Sample Name:
SG-3-069-3-F-Pd-C
Data Collected on:
nmr14-vnmrs400
Archive directory:
/home/Robot/vnmrsys/data
Sample directory:
SG-3-069-3-F-Pd-C_20130920_01
FidFile: CARBON_01

Pulse Sequence: CARBON (s2pul)
Solvent: cdcl3
Data collected on: Sep 20 2013

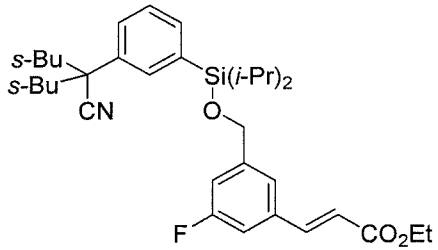

Sample Name:
HL-2-139-1H
Data Collected on:
nmr18-vnmrs500
Archive directory:

Sample directory:

FidFile: HL-2-139-1H

Pulse Sequence: PROTON (s2pul)
Solvent: cdcl3
Data collected on: Jul 24 2013

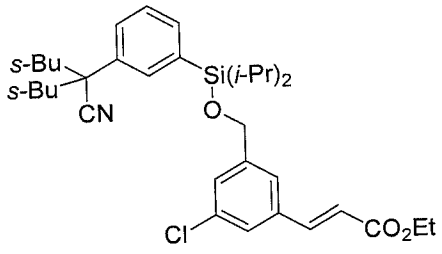

SG-3-069-3-F-pd-H

Sample Name:
SG-3-069-3-F-pd-H
Data Collected on:
nmr18-vnmrs500
Archive directory:

Sample directory:

FidFile: PROTON

Pulse Sequence: PROTON (s2pul)
Solvent: cdcl3
Data collected on: Sep 19 2013

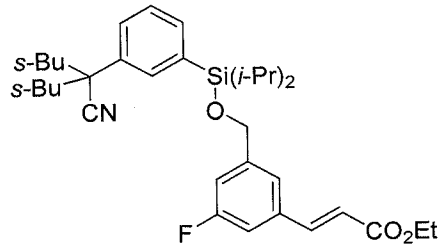

Sample Name:
HL-2-139-13C
Data Collected on:
nmr14-vnmrs400
Archive directory:
/home/Robot/vnmrsys/data
Sample directory:
HL-2-139-13C_20130724_01
FidFile: CARBON_03

Pulse Sequence: CARBON (s2pul)
Solvent: cdcl3
Data collected on: Jul 24 2013

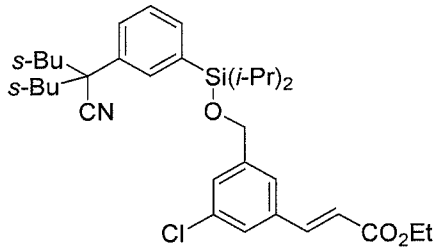

Sample Name:
HL-2-133-1H
Data Collected on:
nmr18-vnmrs500
Archive directory:

Sample directory:

FidFile: HL-2-133-1H-methanol

Pulse Sequence: PROTON (s2pul)
Solvent: cd3od
Data collected on: Jul 24 2013

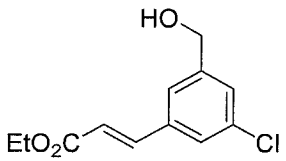

Sample Name:
HL-2-133-13C-methanol
Data Collected on:
nmr18-vnmrs500
Archive directory:

Sample directory:

FidFile: HL-2-133-13C-methanol

Pulse Sequence: CARBON (s2pul)
Solvent: cd3od
Data collected on: Jul 25 2013

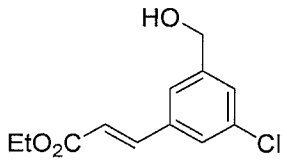

SG-3-036-3-Br-pd

Sample Name:
SG-3-036-3-Br-pd
Data Collected on:
nmr18-vnmrs500
Archive directory:

Sample directory:

FidFile: PROTON

Pulse Sequence: PROTON (s2pul)
Solvent: cdcl3
Data collected on: Sep 19 2013

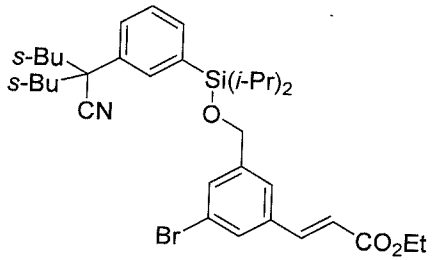

```
ErrorLog:
   auto_20130919_01 loc:22 (day)
Findz0 failed - low S/N

 Sample Name:
   SG-3-036-3-Br-pd-C
 Data Collected on:
   nmr14-vnmrs400
 Archive directory:
   /home/Robot/vnmrsys/data
 Sample directory:
   SG-3-036-3-Br-pd-C_20130919_01
 FidFile: CARBON_01

Pulse Sequence: CARBON (s2pul)
Solvent: cdcl3
Data collected on: Sep 19 2013
```

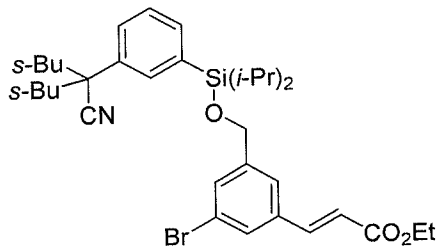

Sample Name:
HL-2-138-1H-methanol
Data Collected on:
nmr18-vnmrs500
Archive directory:

Sample directory:

FidFile: HL-2-138-1H-methanol

Pulse Sequence: PROTON (s2pul)
Solvent: cd3od
Data collected on: Jul 24 2013

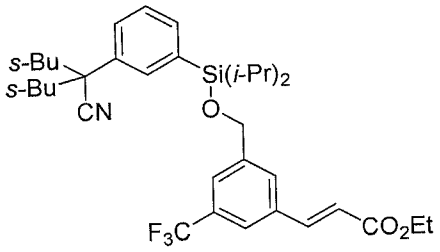

446

9 8 7 6 5 4 3 2 1 ppm

0.95 0.96 0.89 0.96 2.05 1.12 1.03 0.90 1.90 2.00 2.45 1.20 7.55 30.20

Sample Name:
HL-2-138-2-13C
Data Collected on:
nmr18-vnmrs500
Archive directory:

Sample directory:

FidFile: HL-2-138-2-13C

Pulse Sequence: CARBON (s2pul)
Solvent: cdcl3
Data collected on: Jul 22 2013

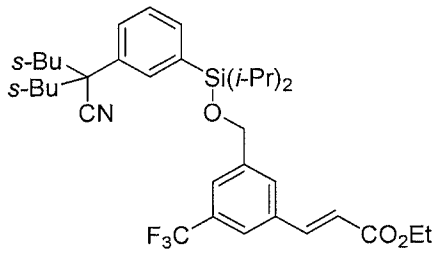

Sample Name:
HL-2-118-1H
Data Collected on:
nmr18-vnmrs500
Archive directory:

Sample directory:

FidFile: HL-2-118-1H

Pulse Sequence: PROTON (s2pul)
Solvent: cdcl3
Data collected on: Jul 23 2013

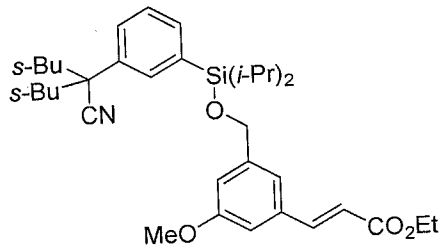

Sample Name:
HL-2-118-13C
Data Collected on:
nmr14-vnmrs400
Archive directory:
/home/Robot/vnmrsys/data
Sample directory:
HL-2-118-13C_20130724_01
FidFile: HL-2-118-13C

Pulse Sequence: CARBON (s2pul)
Solvent: cdcl3
Data collected on: Jul 24 2013

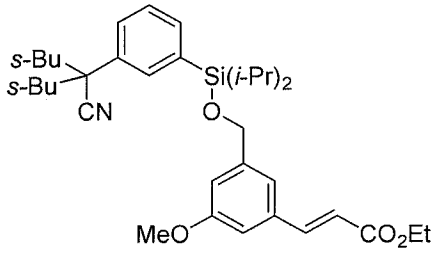

HL-2-132-3-OAc-pd-H

Sample Name:
HL-2-132-3-OAc-pd-H
Data Collected on:
nmr18-vnmrs500
Archive directory:

Sample directory:

FidFile: PROTON

Pulse Sequence: PROTON (s2pul)
Solvent: cdcl3
Data collected on: Sep 19 2013

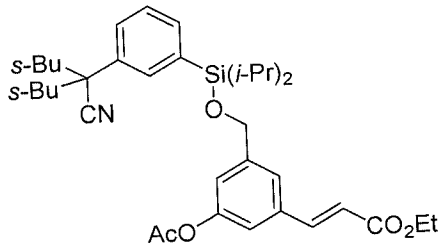

Sample Name:
HL-2-132-3-OAc-pd-C
Data Collected on:
nmr14-vnmrs400
Archive directory:
/home/Robot/vnmrsys/data
Sample directory:
HL-2-132-3-OAc-pd-C_20130920_01
FidFile: CARBON_01

Pulse Sequence: CARBON (s2pul)
Solvent: cdcl3
Data collected on: Sep 20 2013

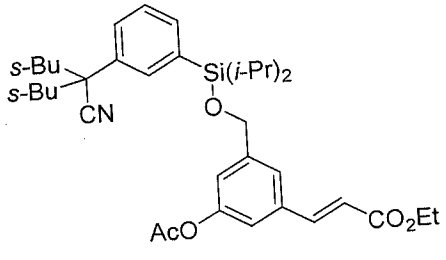

Sample Name:
HL-2-131-1H-CDCl3
Data Collected on:
nmr18-vnmrs500
Archive directory:

Sample directory:

FidFile: HL-2-131-1H-CDCl3

Pulse Sequence: PROTON (s2pul)
Solvent: cdcl3
Data collected on: Jul 25 2013

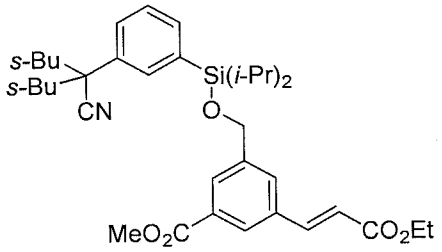

452

9 8 7 6 5 4 3 2 1 ppm

0.81 0.78 0.82 0.84 2.66 0.94 0.84 1.78 1.74 2.44 2.00 0.91 5.89 25.38

Sample Name:
HL-2-131-13C-2
Data Collected on:
nmr14-vnmrs400
Archive directory:
/home/Robot/vnmrsys/data
Sample directory:
HL-2-131-13C-2_20130725_01
FidFile: CARBON_01

Pulse Sequence: CARBON (s2pul)
Solvent: cdcl3
Data collected on: Jul 25 2013

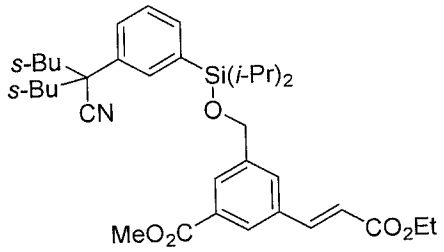

-4-Me-pd-m-H

Sample Name:
-4-Me-pd-m-H
Data Collected on:
nmr15-vnmrs500
Archive directory:

Sample directory:

FidFile: PROTON

Pulse Sequence: PROTON (s2pul)
Solvent: cdcl3
Data collected on: Sep 11 2013

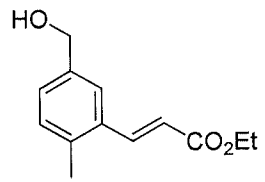

Sample Name:
SG-3-107-4-Me-pd-m2
Data Collected on:
nmr14-vnmrs400
Archive directory:
/home/Robot/vnmrsys/data
Sample directory:
SG-3-107-4-Me-pd-m2_20130911_01
FidFile: CARBON_01

Pulse Sequence: CARBON (s2pul)
Solvent: cdcl3
Data collected on: Sep 11 2013

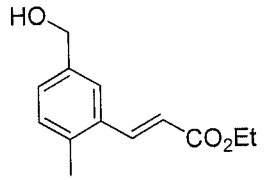

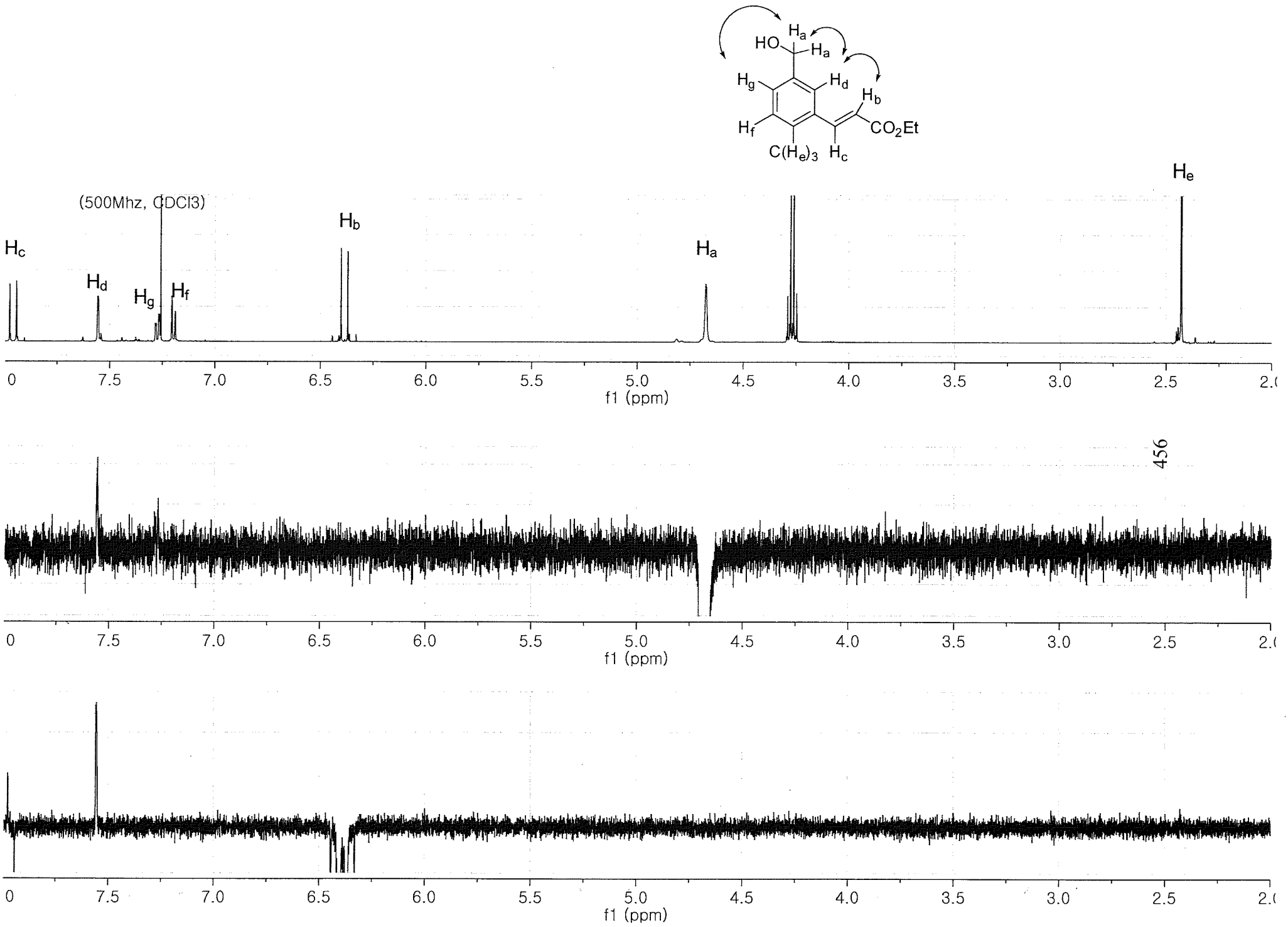
Ha
HO
Ha
Hg
Hd
Hb
Hf
CO2Et
C(He)3
Hc
(500Mhz, CDCl3)
Hc
Hd
Hg
Hf
Hb
Ha
He
0
7.5
7.0
6.5
6.0
5.5
5.0
4.5
4.0
3.5
3.0
2.5
f1 (ppm)
456

SG-3-107-4-Me-pd-d-H

Sample Name:
SG-3-107-4-Me-pd-d-H
Data Collected on:
nmr15-vnmrs500
Archive directory:

Sample directory:

FidFile: PROTON

Pulse Sequence: PROTON (s2pul)
Solvent: cdcl3
Data collected on: Sep 10 2013

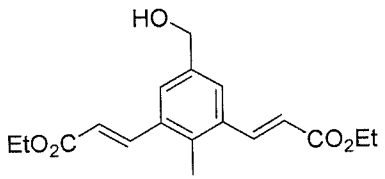

SG-3-107-4-Me-pd-d-C

Sample Name:
SG-3-107-4-Me-pd-d-C
Data Collected on:
nmr15-vnmrs500
Archive directory:

Sample directory:

FidFile: CARBON

Pulse Sequence: CARBON (s2pul)
Solvent: cdcl3
Data collected on: Sep 10 2013

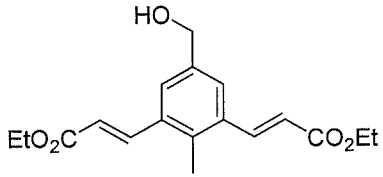

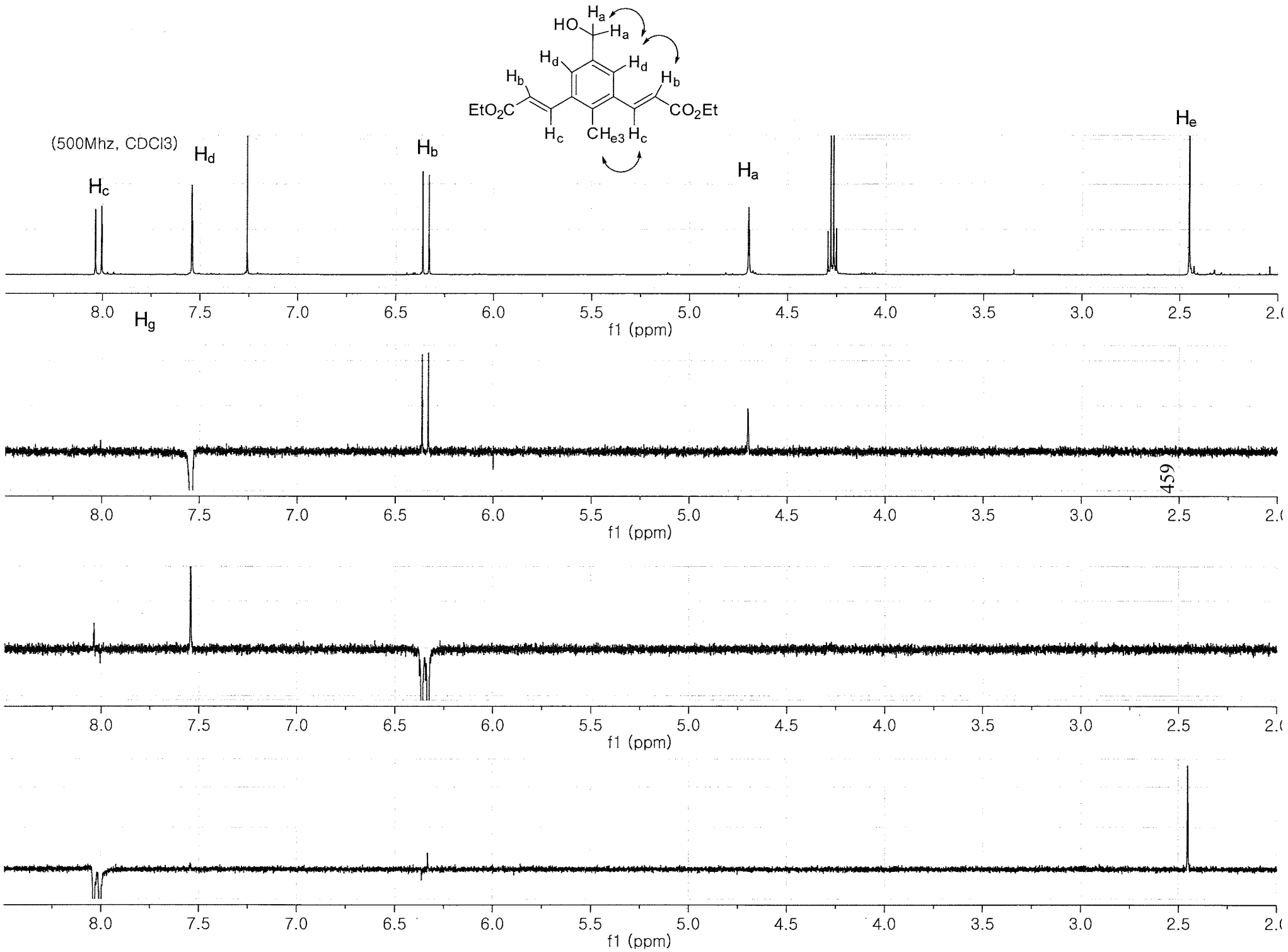
(500Mhz, CDCl3)
Hc
Hd
Hb
Ha
He
Hg
HO
Ha
Hd
Hd
Hb
Hb
EtO2C
CO2Et
Hc
CHe3
Hc
8.0
7.5
7.0
6.5
6.0
5.5
5.0
4.5
4.0
3.5
3.0
2.5
f1 (ppm)
459

SG-3-054-4-Br-pd-m-H

Sample Name:
SG-3-054-4-Br-pd-m-H
Data Collected on:
nmr18-vnmrs500
Archive directory:

Sample directory:

FidFile: PROTON

Pulse Sequence: PROTON (s2pul)
Solvent: cdcl3
Data collected on: Sep 27 2013

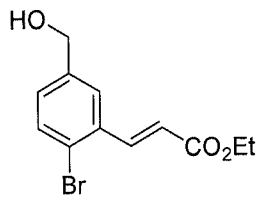

Sample Name:
SG-3-069-4-Br-pd-mono-C
Data Collected on:
nmr14-vnmrs400
Archive directory:
/home/Robot/vnmrsys/data
Sample directory:
SG-3-069-4-Br-pd-mono-C_20131010_01
FidFile: CARBON_01

Pulse Sequence: CARBON (s2pul)
Solvent: cdcl3
Data collected on: Oct 10 2013

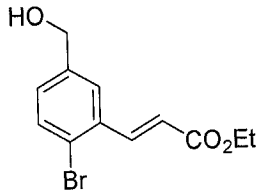

461

160 140 120 100 80 60 40 20 ppm

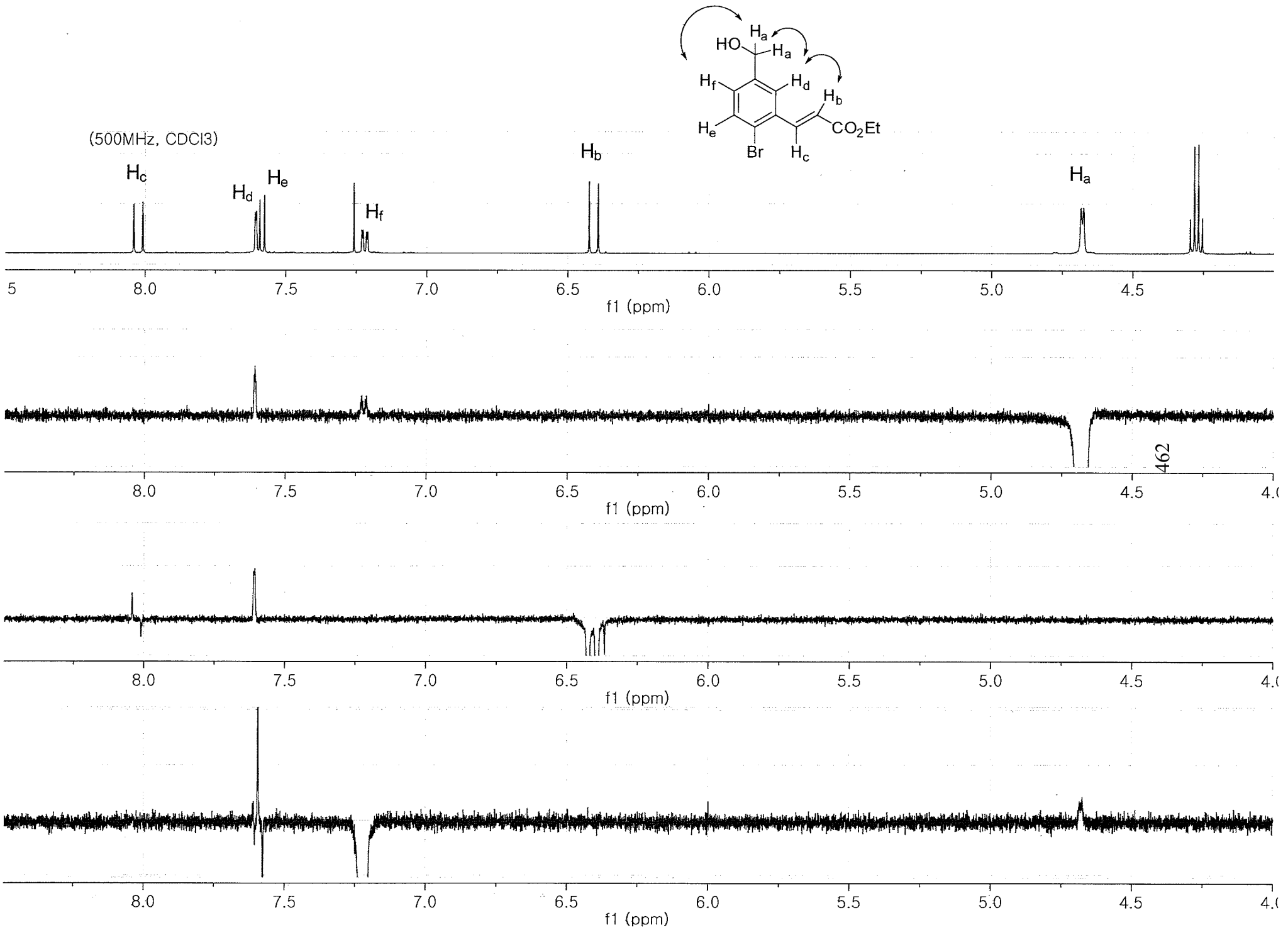
(500MHz, CDCl3)
Hc
Hd
He
Hf
Hb
Ha
HO
Ha
Hf
Hd
Hb
He
Br
Hc
CO2Et
f1 (ppm)
462

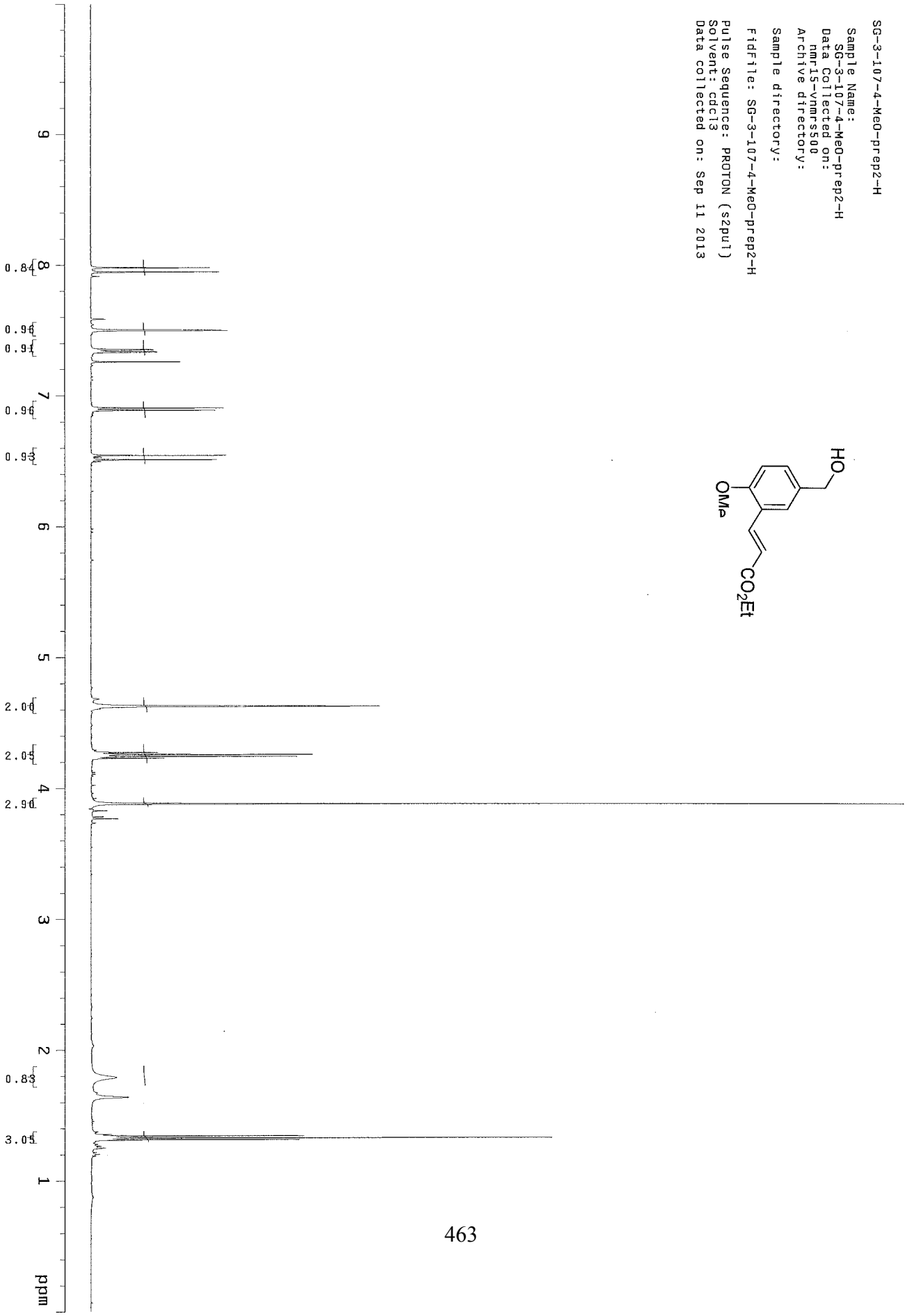
SG-3-107-4-MeO-prep2-H
Sample Name:
SG-3-107-4-MeO-prep2-H
Data Collected on:
nmr15-vnmrs500
Archive directory:
Sample directory:
FidFile: SG-3-107-4-MeO-prep2-H
Pulse Sequence: PROTON (s2pul)
Solvent: cdcl3
Data collected on: Sep 11 2013
HO
OMe
CO2Et
0.84
0.96
0.91
0.96
0.93
2.00
2.05
2.96
0.83
3.05
9
8
7
6
5
4
3
2
1
ppm

Sample Name:
SG-3-107-4-MeO-pd-m-C
Data Collected on:
nmr14-vnmrs400
Archive directory:
/home/Robot/vnmrsys/data
Sample directory:
SG-3-107-4-MeO-pd-m-C_20130911_01
FidFile: CARBON_01

Pulse Sequence: CARBON (s2pul)
Solvent: cdcl3
Data collected on: Sep 11 2013

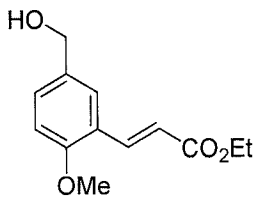

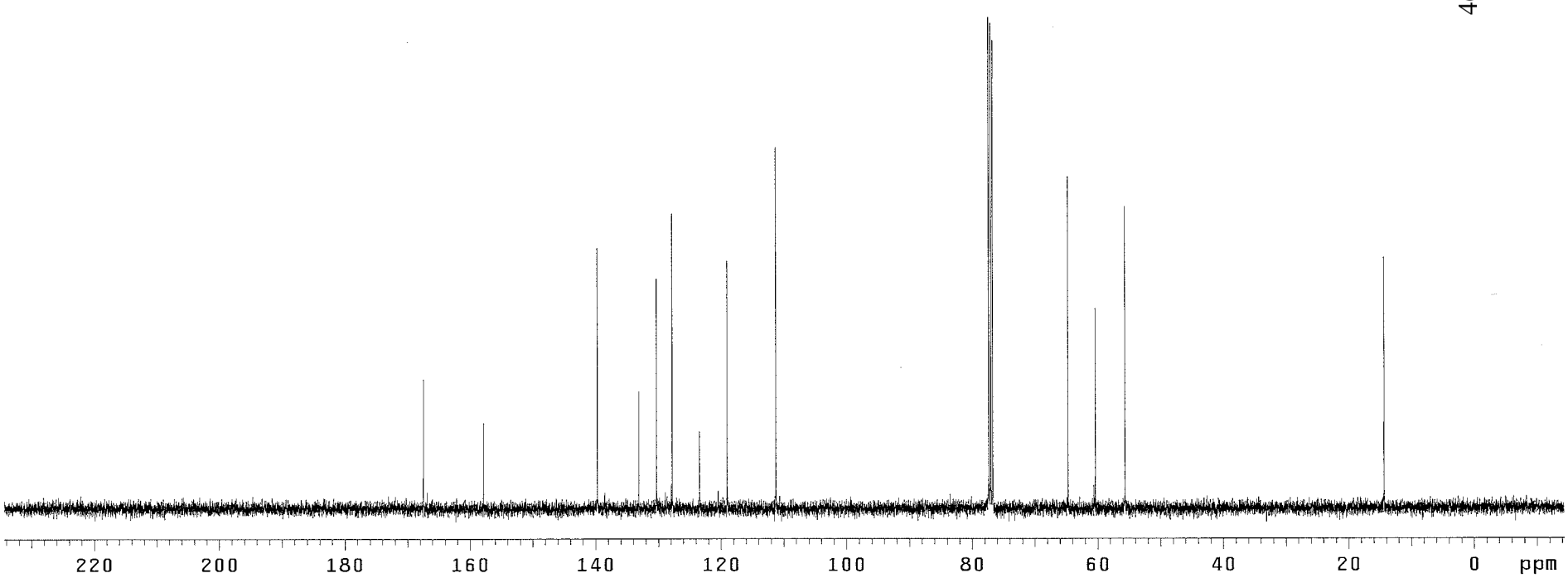

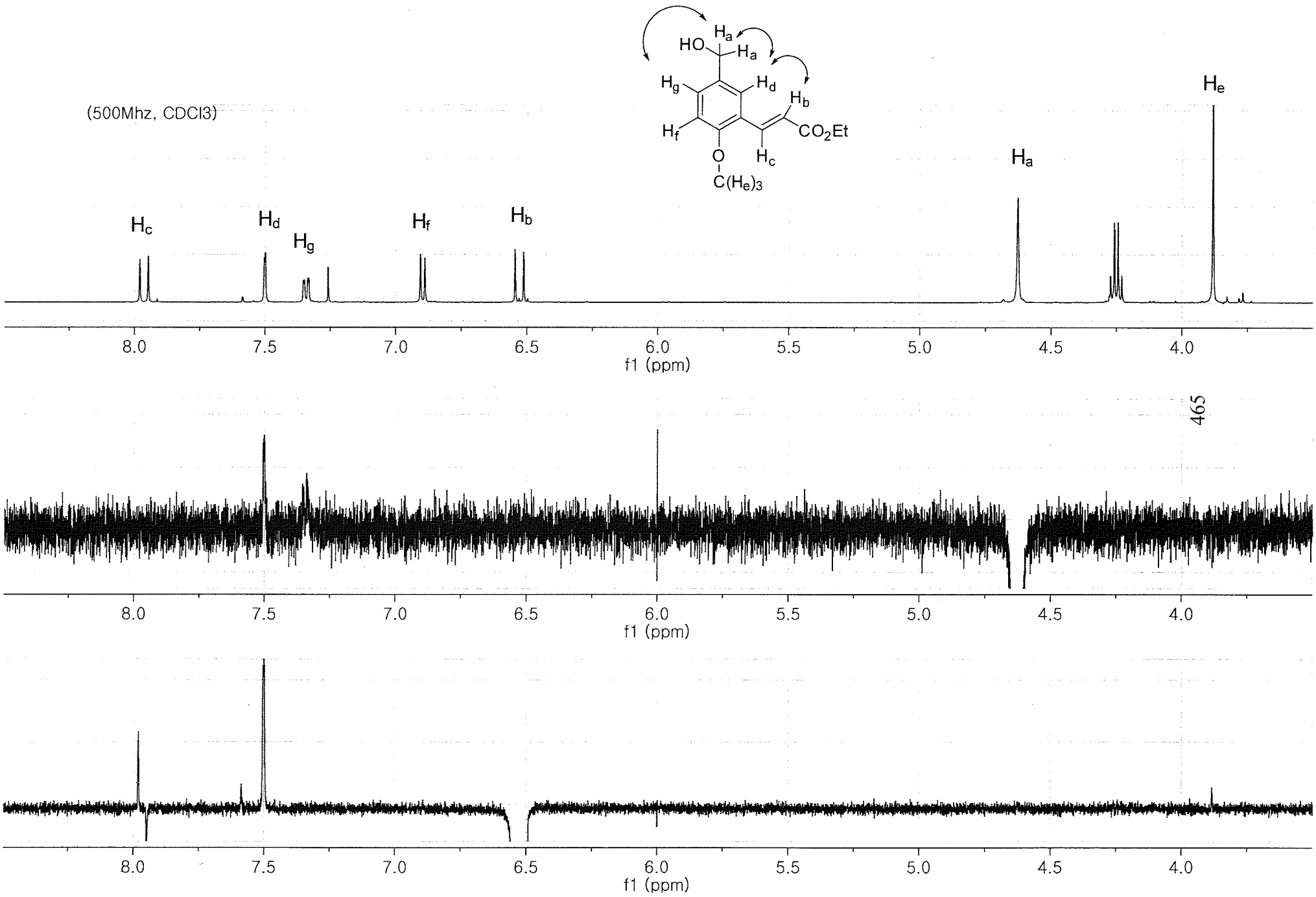
(500Mhz, CDCl3)
Ha
HO
Ha
Hg
Hd
Hb
Hf
CO2Et
Hc
O
C(He)3
Hc
Hd
Hg
Hf
Hb
Ha
He
8.0
7.5
7.0
6.5
6.0
5.5
5.0
4.5
4.0
f1 (ppm)
465

SG-3-050-4-MeO-pd-di-H

Sample Name:
SG-3-050-4-MeO-pd-di-H
Data Collected on:
nmr18-vnmrs500
Archive directory:

Sample directory:

FidFile: SG-3-050-4-MeO-pd-di-H

Pulse Sequence: PROTON.(s2pul)
Solvent: cdcl3
Data collected on: Sep 17 2013

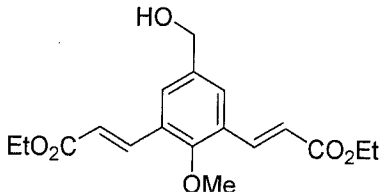

Sample Name:
SG-3-050-4-MeO-pd-di-C
Data Collected on:
nmr14-vnmrs400
Archive directory:
/home/Robot/vnmrsys/data
Sample directory:
SG-3-050-4-MeO-pd-di-C_20130919_01
FidFile: CARBON_01

Pulse Sequence: CARBON (s2pul)
Solvent: cdcl3
Data collected on: Sep 19 2013

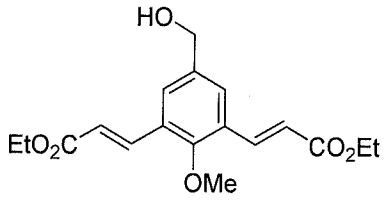

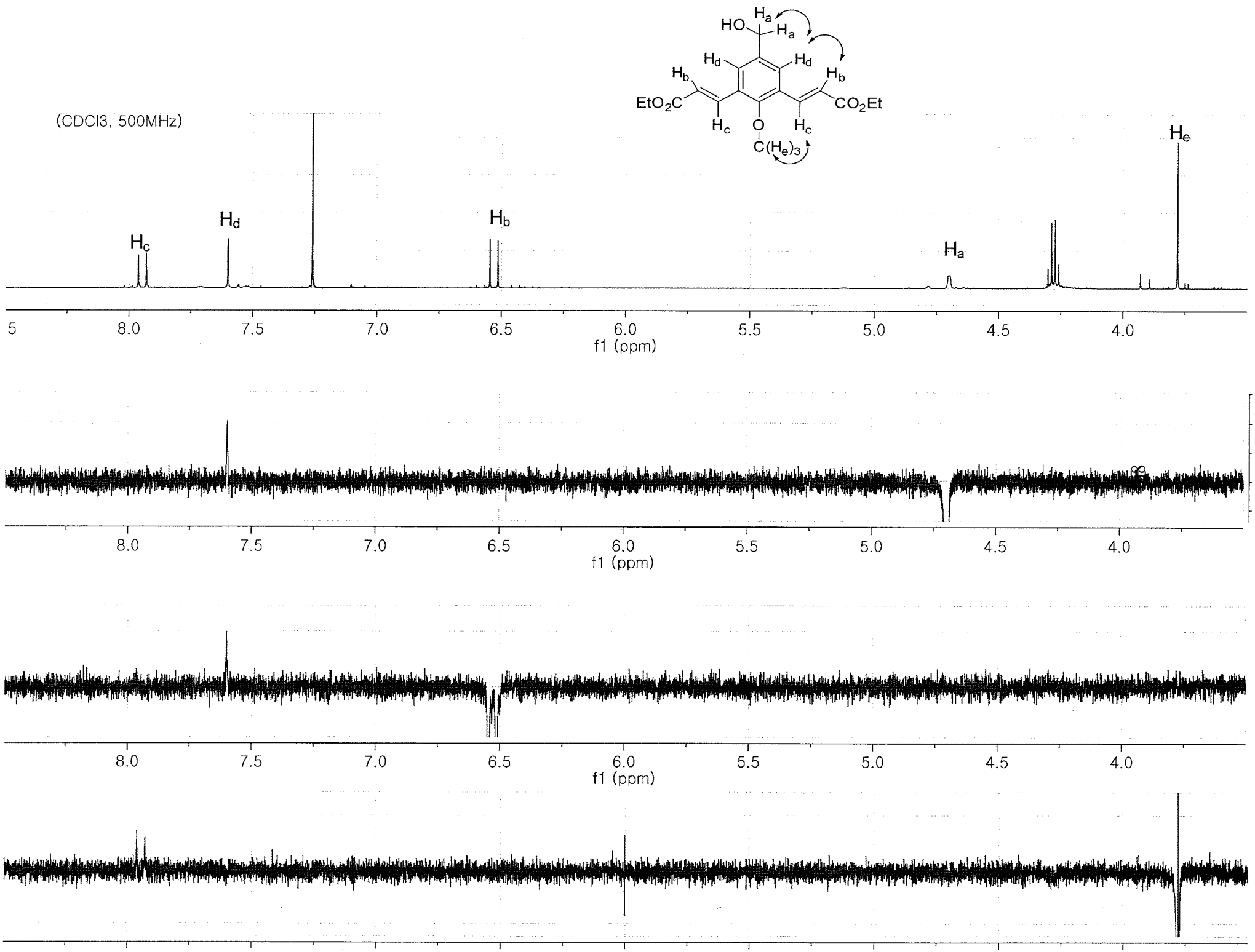
(CDCl3, 500MHz)
HO
Ha
Ha
Hd
Hd
Hb
Hb
EtO2C
CO2Et
Hc
O
Hc
C(He)3
He
Hc
Hd
Hb
Ha
5
8.0
7.5
7.0
6.5
6.0
5.5
5.0
4.5
4.0
f1 (ppm)

Sample Name:
HL-2-124-1H
Data Collected on:
nmr18-vnmrs500
Archive directory:

Sample directory:

FidFile: HL-2-124-1H

Pulse Sequence: PROTON (s2pul)
Solvent: cdcl3
Data collected on: Jul 24 2013

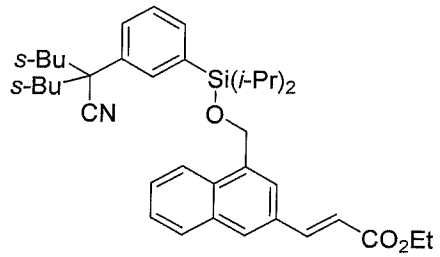

469

Sample Name:
HL-2-124-13C
Data Collected on:
nmr14-vnmrs400
Archive directory:
/home/Robot/vnmrsys/data
Sample directory:
HL-2-124-13C_20130724_01
FidFile: CARBON_01

Pulse Sequence: CARBON (s2pul)
Solvent: cdcl3
Data collected on: Jul 24 2013

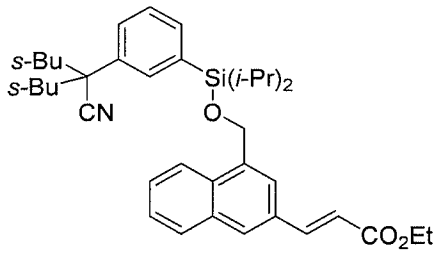

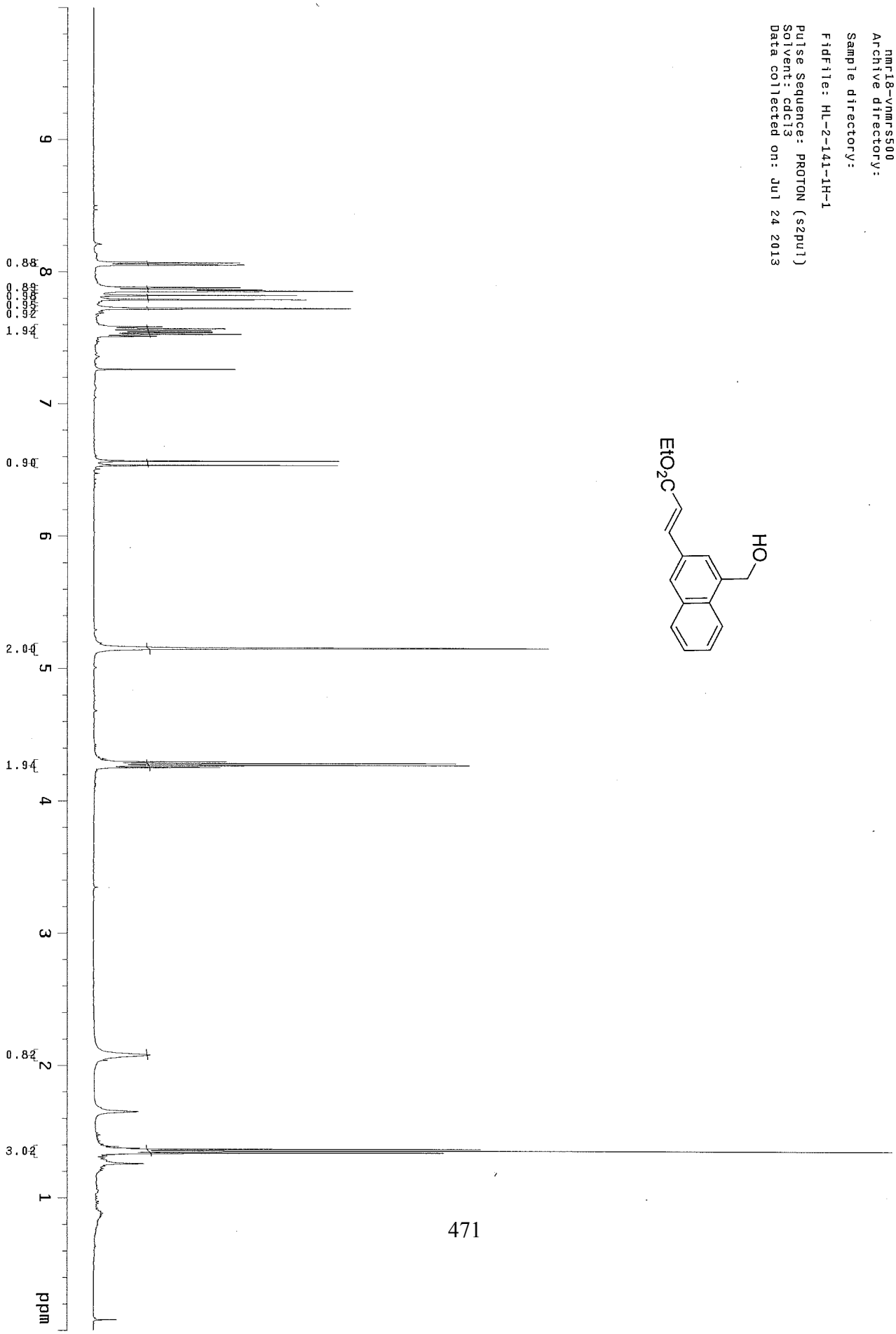
Sample Name:
HL-1-141-1
Data Collected on:
nmr18-vnmrs500
Archive directory:
Sample directory:
FidFile: HL-2-141-1H-1
Pulse Sequence: PROTON (s2pul)
Solvent: cdcl3
Data collected on: Jul 24 2013
EtO2C
HO
0.88
1.94
0.90
2.00
1.94
0.82
3.02
ppm

Sample Name:
HL-2-141-13C
Data Collected on:
nmr14-vnmrs400
Archive directory:
/home/Robot/vnmrsys/data
Sample directory:
HL-2-141-13C_20130724_01
FidFile: CARBON_04

Pulse Sequence: CARBON (s2pul)
Solvent: cdcl3
Data collected on: Jul 25 2013

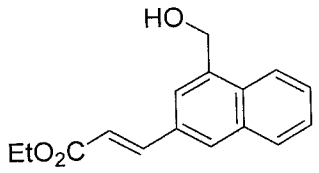

472

SG-3-067-3-MeO-H

Sample Name:
SG-3-067-3-MeO-H
Data Collected on:
nmr18-vnmrs500
Archive directory:

Sample directory:

FidFile: PROTON

Pulse Sequence: PROTON (s2pul)
Solvent: cdcl3
Data collected on: Sep 20 2013

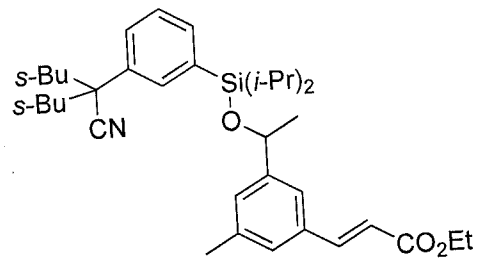

Sample Name:
SG-3-067-3-Me-pd-C
Data Collected on:
nmr14-vnmrs400
Archive directory:
/home/Robot/vnmrsys/data
Sample directory:
SG-3-067-3-Me-pd-C_20130920_01
FidFile: CARBON_01

Pulse Sequence: CARBON (s2pul)
Solvent: cdcl3
Data collected on: Sep 20 2013

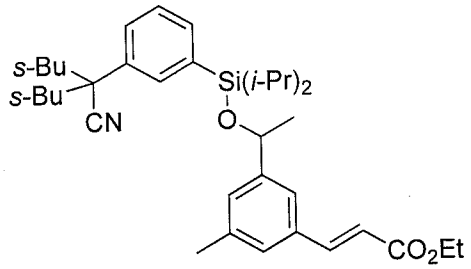

SG-3-067-3-Br-H

Sample Name:
SG-3-067-3-Br-H
Data Collected on:
nmr18-vnmrs500
Archive directory:

Sample directory:

FidFile: PROTON

Pulse Sequence: PROTON (s2pul)
Solvent: cdcl3
Data collected on: Sep 20 2013

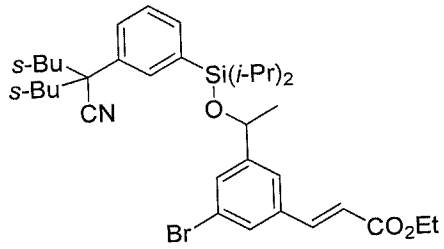

Sample Name:
SG-3-067-3-Br-pd-C
Data Collected on:
nmr14-vnmrs400
Archive directory:
/home/Robot/vnmrsys/data
Sample directory:
SG-3-067-3-Br-pd-C_20130920_01
FidFile: CARBON_01

Pulse Sequence: CARBON (s2pul)
Solvent: cdcl3
Data collected on: Sep 20 2013

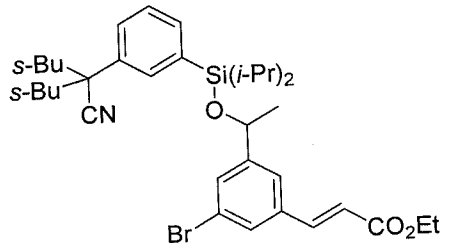

SG-3-067-3-MeO-H

Sample Name:
SG-3-067-3-MeO-H
Data Collected on:
nmr18-vnmrs500
Archive directory:

Sample directory:

FidFile: PROTON

Pulse Sequence: PROTON (s2pul)
Solvent: cdcl3
Data collected on: Sep 20 2013

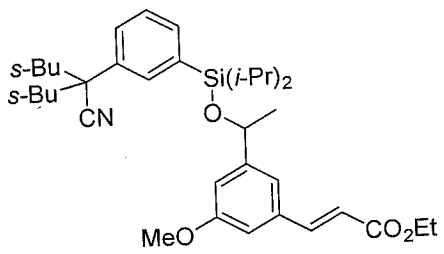

Sample Name:
SG-3-067-3-MeO-pd-C
Data Collected on:
nmr14-vnmrs400
Archive directory:
/home/Robot/vnmrsys/data
Sample directory:
SG-3-067-3-MeO-pd-C_20130921_01
FidFile: CARBON_01

Pulse Sequence: CARBON (s2pul)
Solvent: cdcl3
Data collected on: Sep 21 2013

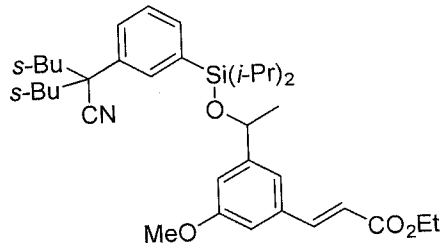

SG-3-053-NMe2-pd-H

Sample Name:
SG-3-053-NMe2-pd-H
Data Collected on:
nmr18-vnmrs500
Archive directory:

Sample directory:

FidFile: PROTON

Pulse Sequence: PROTON (s2pul)
Solvent: cdcl3
Data collected on: Sep 19 2013

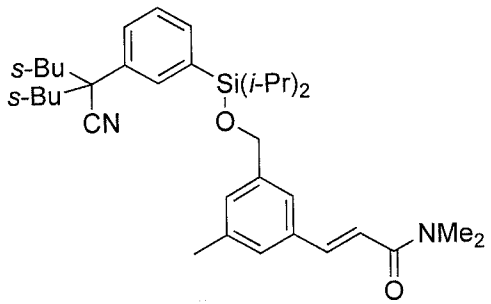

SG-3-052-NMe2-C

Sample Name:
SG-3-052-NMe2-C
Data Collected on:
nmr18-vnmrs500
Archive directory:

Sample directory:

FidFile: CARBON

Pulse Sequence: CARBON (s2pul)
Solvent: cdcl3
Data collected on: Sep 20 2013

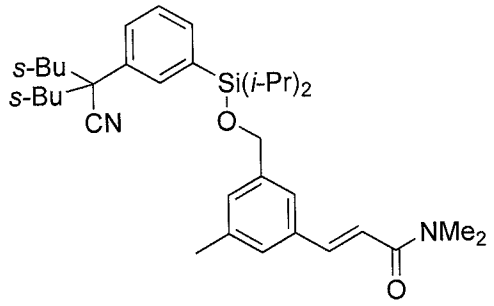

SG-3-085-ketone-pd-H

Sample Name:
SG-3-085-ketone-pd-H
Data Collected on:
nmr18-vnmrs500
Archive directory:

Sample directory:

FidFile: SG-3-085-ketone-pd-H

Pulse Sequence: PROTON (s2pul)
Solvent: cdcl3
Data collected on: Sep 17 2013

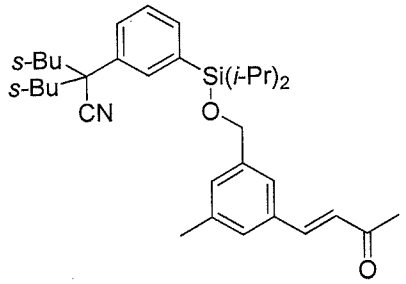

```
ErrorLog:
   auto_20130918_01 loc:23 (night)
Findz0 failed - low S/N

 Sample Name:
   SG-3-085-ketone-C
 Data Collected on:
   nmr14-vnmrs400
 Archive directory:
   /home/Robot/vnmrsys/data
 Sample directory:
   SG-3-085-ketone-C_20130918_01
 FidFile: CARBON_01

Pulse Sequence: CARBON (s2pul)
Solvent: cdcl3
Data collected on: Sep 18 2013
```

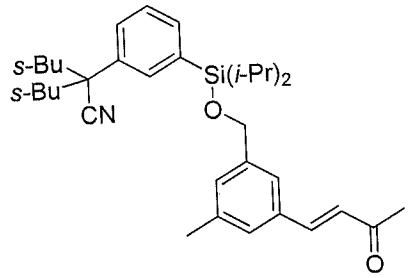

SG-3-085-sulfone-pd-H

Sample Name:
SG-3-085-sulfone-pd-H
Data Collected on:
nmr18-vnmrs500
Archive directory:

Sample directory:

FidFile: SG-3-085-sulfone-pd-H

Pulse Sequence: PROTON (s2pul)
Solvent: cdcl3
Data collected on: Sep 18 2013

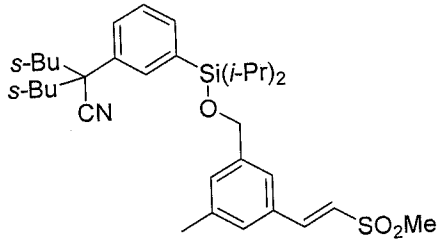

SG-3-085-sulfone-C

Sample Name:
SG-3-085-sulfone-C
Data Collected on:
nmr18-vnmrs500
Archive directory:

Sample directory:

FidFile: SG-3-085-sulfone-C

Pulse Sequence: CARBON (s2pul)
Solvent: cdcl3
Data collected on: Sep 19 2013

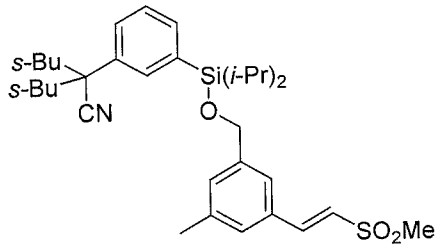

SG-3-058-croto-pd-H

Sample Name:
SG-3-058-croto-pd-H
Data Collected on:
nmr18-vnmrs500
Archive directory:

Sample directory:

FidFile: PROTON

Pulse Sequence: PROTON (s2pul)
Solvent: cdcl3
Data collected on: Sep 18 2013

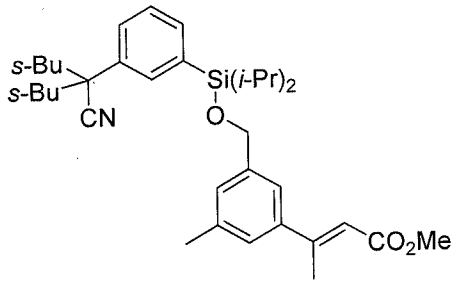

SG-3-058-croto-C

Sample Name:
SG-3-058-croto-C
Data Collected on:
nmr18-vnmrs500
Archive directory:

Sample directory:

FidFile: CARBON

Pulse Sequence: CARBON (s2pul)
Solvent: cdcl3
Data collected on: Sep 19 2013

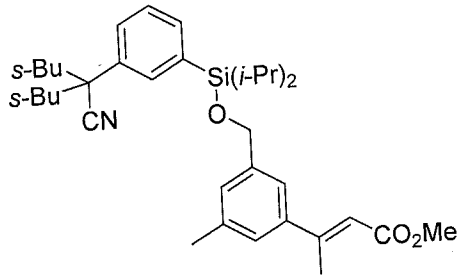

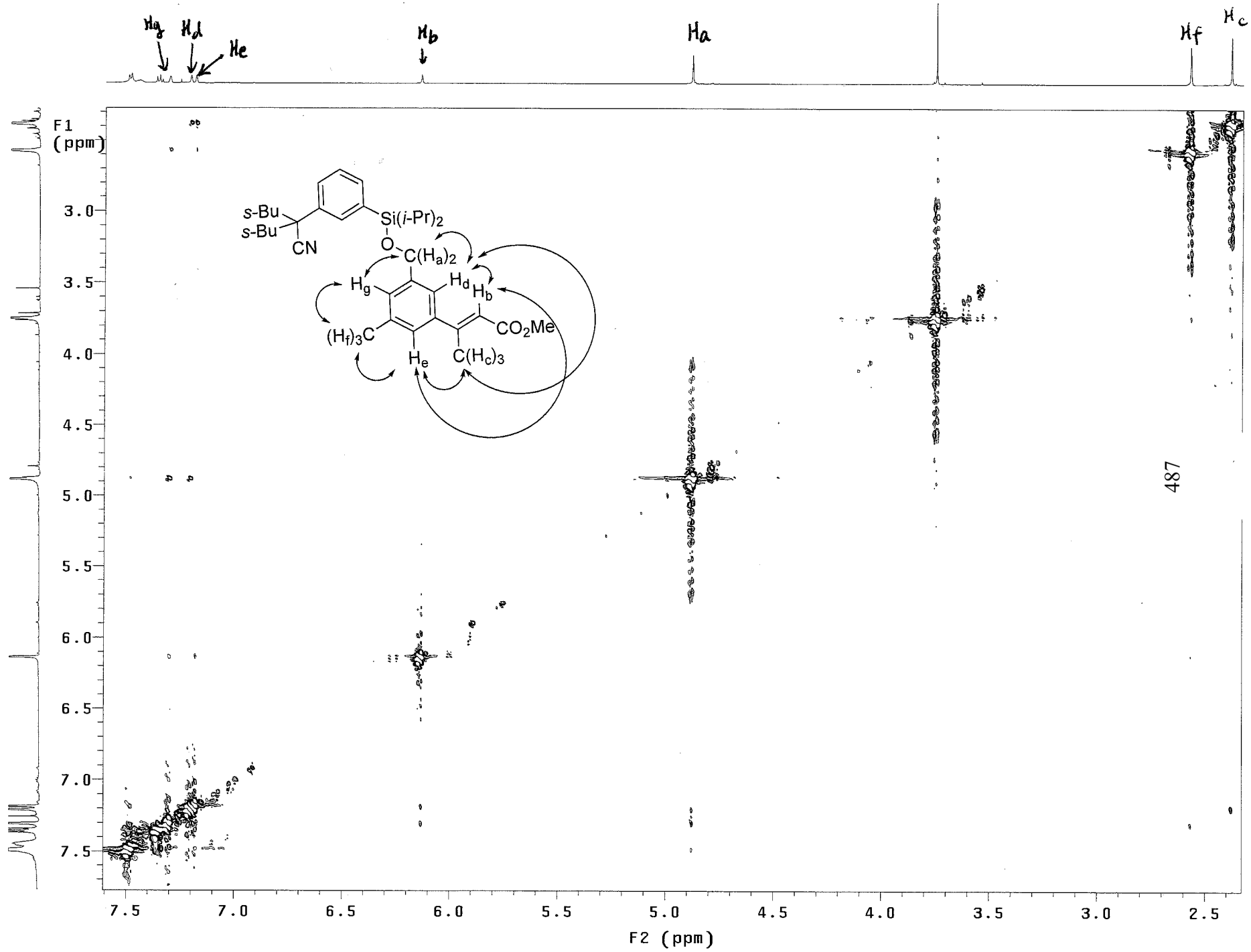
Hg
Hd
He
Hb
Ha
Hf
Hc
F1 (ppm)
3.0
3.5
4.0
4.5
5.0
5.5
6.0
6.5
7.0
7.5
s-Bu
s-Bu
CN
Si(i-Pr)2
O
C(Ha)2
Hg
Hd
Hb
(Hf)3C
CO2Me
He
C(Hc)3
7.5
7.0
6.5
6.0
5.5
5.0
4.5
4.0
3.5
3.0
2.5
F2 (ppm)

SG-3-041-H

Sample Name:
SG-3-041-H
Data Collected on:
nmr18-vnmrs500
Archive directory:

Sample directory:

FidFile: PROTON

Pulse Sequence: PROTON (s2pul)
Solvent: cdcl3
Data collected on: Sep 25 2013

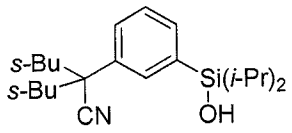

SG-3-041-C

Sample Name:
SG-3-041-C
Data Collected on:
nmr18-vnmrs500
Archive directory:

Sample directory:

FidFile: CARBON

Pulse Sequence: CARBON (s2pul)
Solvent: cdcl3
Data collected on: Sep 25 2013

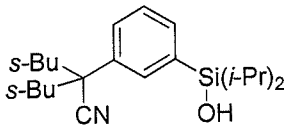

Chapter 2: Investigation of the Interactions of 1,2-Azaborines with Biomacromolecules: Hydrogen Bonding

2.1 Introduction

2.1.1 Arenes as a Pharmacophore

Aromatic rings are ubiquitous in nature, and arene-containing compounds prevail among clinically important small-molecule drugs (Figure 1.2).[1] This reflects the importance of aromatics to the fundamental key interactions involved in various molecular recognition. Because of their polarizability, aromatic molecules engage in many of non-covalent interactions, including cation–π, π–π stacking, and hydrophobic interaction.[2] Such interactions are prominent in the functional elements of receptor-type drug targets, and thus are frequently considered in rational drug designs.

2.1.2 BN/CC Isosterism

Creating structural diversity is one of the main goals for synthetic chemists, especially during the process of lead optimization efforts in medicinal chemistry.[3] In this regards, BN/CC isosterism[4] (i.e. the replacement of a carbon-carbon (CC) unit with a boron-

[1] (a) Roughley, S. D.; Jordan, A. M. *J. Med. Chem.* **2011**, *54*, 3451–3479. (b) McGrath, N. A.; Brichacek, M.; Njardarson, J. T. *J. Chem. Ed.* **2010**, *87*, 1348–1349.
[2] (a) Tewari, A. K.; Srivastava, P.; Singh, V. P.; Singh, P.; Khanna, R. S. *Res. Chem. Intermed.* **2013**, *39*, 2925–2944. (b) Tewari, A. K.; Dubey, R. *Bioorg. Med. Chem*. **2008**, *16*, 126–143. (c) Johnson, D. W.; Hof, F. Aromatic Interactions: Frontiers in Knowledge and Application 2016.
[3] Bleicher, K. H.; Böhm, H.-J.; Müller, K.; Alanine, A. I. *Nat. Rev. Drug Discov.* **2003**, *2*, 369–378. (b) Keserü, G. M.; Makara, G. M. *Drug Discov Today* **2006**, *11*, 741–748.
[4] For selected reviews, see: (a) Liu, Z.; Marder, T. B. *Angew. Chem., Int. Ed.* **2008**, *47*, 242–244. (b) Bosdet, M. J. D.; Piers, W. E. *Can. J. Chem.* **2009**, *87*, 8–29. (3) Campbell, P. G.; Marwitz, A. J. V.; Liu, S.-Y. *Angew. Chem., Int. Ed*. **2012**, *51*, 6074–6092. (d) Scriven, E.; Ramsden, C. A. *Advances in Heterocyclic Chemistry* Volume 118, Academic Press, 2016.

nitrogen (BN) unit) has recently emerged as a strategy to increase the accessible chemical space of compounds relevant to biomedical research.[5] 1,2-Dihydro-1,2-azaborine (**2.1**) is the BN isostere of benzene.[6] It has the same number of valence electrons as benzene but its electronic structure significantly differs due to the presence of the unsymmetrical BN unit (Figure 2.1). Based on DFT calculations, the dipole moment of 1,2-dihydro-1,2-azaborine is ~ 2.2 D whereas benzene has dipole moment of 0 D.[7] We anticipated these differences in polarization would lead to 1,2-azaborines exhibiting chemical and physical properties distinct from all-carbon arenes. Specifically, we anticipate to take advantage of two unique features of 1,2-azaborine in the context of medicinal chemistry: 1) The NH group in 1,2-azaborine should serve as a hydrogen bond donor that can potentially improve binding to its macromolecular target. 2) The dipolar nature of 1,2-azaborines should improve solubility and thus positively impact pharmacokinetic behavior.[8]

Figure 2.1 Electronic structure differences between benzene and 1,2-azaborine

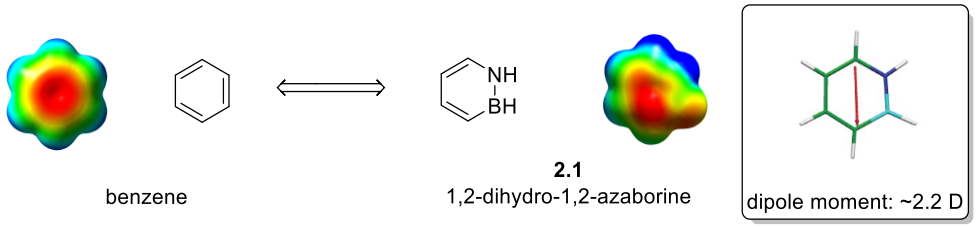

[5] (a) Zhou, H.-B.; Nettles, K. W.; Bruning, J. B.; Kim, Y.; Joachimiak, A.; Sharma, S.; Carlson, K. E.; Stossi, F.; Katzenellenbogen, B. S.; Greene, G. L.; Katzenellenbogen, *J. A. Chem. Biol.* **2007**, *14*, 659–669. (b) Ito, H.; Yumura, K.; Saigo, K. *Org. Lett*. **2010**, *12*, 3386–3389.
[6] (a) Marwitz, A. J. V.; Matus, M. H.; Zakharov, L. N.; Dixon, D. A.; Liu, S.-Y. *Angew. Chem. Int. Ed.* **2009**, *48*, 973–977. (b) Abbey, E. R.; Lamm, A. N.; Baggett, A. W.; Zakharov, L. N.; Liu, S.-Y. *J. Am. Chem. Soc.* **2013**, *135*, 12908–12913.
[7] Chrostowska, A.; Xu, S.; Lamm, A. N.; Mazière, A.; Weber, C. D.; Dargelos, A.; Baylère, P.; Graciaa, A.; Liu, S-Y. *J. Am. Chem. Soc*. **2012**, *134*, 10279–10285.
[8] Waring, M. J. *Expert Opin Drug Discov.* **2010**, *5*, 235–248.

Azaborines have a potential to expand exponentially the chemical space of arenes when they are substituted. For example, the low symmetry of the 1,2-azaborine core results in the possibility of twelve *ortho* di-substituted regioisomers. In contrast, one structural arrangement is possible for an *ortho* di-substituted benzene (Figure 2.2).

Figure 2.2 Structural diversification of an arene through BN/CC isosterism

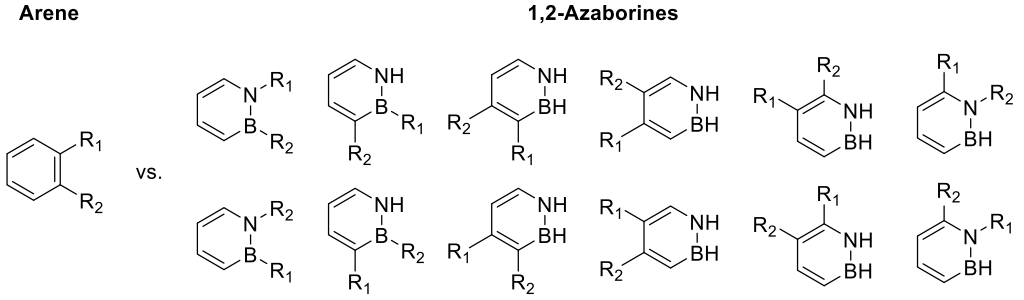

2.2 Background

2.2.1 1,2-Azaborines in Biological Systems

While recent development of synthetic methods have broadened access to structurally diversified 1,2-azaborines,[9] very little remains known about the biological behavior of these molecules. In 2013, the Liu group reported that the BN isosteres of ethylbenzene, *N*-

[9] For selected examples, see: (a) Marwitz, A. J. V.; Abbey, E. R.; Jenkins, J. T.; Zakharov, L. N.; Liu, S.-Y. *Org. Lett.* **2007**, *9*, 4905–4908. (b) Lamm, A. N.; Garner, E. B.; Dixon, D. A.; Liu, S.-Y. *Angew. Chem. Int. Ed.* **2011**, *50*, 8157–8160. (c) Rudebusch, G. E.; Zakharov, L. N.; Liu, S.-Y. *Angew. Chem., Int. Ed.* **2013**, *52*, 9316–9319. (d) Baggett, A. W.; Vasiliu, M.; Li, B.; Dixon, D. A.; Liu, S.-Y. *J. Am. Chem. Soc*. **2015**, *137*, 5536–5541. (e) Brown, A. N.; Li, B.; Liu, S.-Y. *J. Am. Chem. Soc*. **2015**, *137*, 8932–8935. (f) Amani, J.; Molander, G. A. *Org. Lett*. **2015**, *17*, 3624–3627. (g) Wisniewski, S. R.; Guenther, C. L.; Argintaru, O. A.; Molander, G. A. *J. Org. Chem.* **2014**, *79*, 365–378. (h) Braunschweig, H.; Geetharani, K.; Oscar, J.; Jimenez-Halla, C.; Schäfer, M. *Angew. Chem. Int. Ed.* **2014**, *53*, 3500–3504. (i) Couchman, S. A.; Thompson, T. K.; Wilson, D. J. D.; Duttona, J. L.; Martin, C. D. *Chem. Commun*. **2014**, *50*, 11724–11726.

and *B*-ethyl-1,2-azaborine, inhibit ethylbenzene dehydrogenase (EbDH).[10] EbDH is an oxygen-independent enzyme that catalyzes hydroxylation of alkyl-substituted aromatics (i.e. ethylbenzene) via the formation of radical and cationic intermediates.[11] Both *N*- and *B*-ethyl-1,2-azaborine (**2.2** and **2.3** in Table 2.1, respectively) showed inhibitory activity with IC_{50} values of 2.8 μM and 100 μM, respectively. Relative calculated $\Delta\Delta G$ values for formation of potential radical and carbocation intermediates from both BN isosteres of ethylbenzene are substantially higher than those for ethylbenzene (Table 2.1). Therefore, it is plausible that the energy barriers for oxidation of the azaborine compounds cannot be overcome by the enzyme, resulting in inhibition. This study clearly shows that electronic differences between the azaborine analogs and ethylbenzene can affect enzymatic activity.

[10] Knack, D. H.; Marshall, J. L.; Harlow, G. P.; Dudzik, A.; Szaleniec, M.; Liu, S.-Y.; Heider, J. *Angew. Chem., Int. Ed.* **2013**, *52*, 2599–2601.

[11] (a) Kniemeyer, O.; Heider, J. *J. Biol. Chem*. **2001**, *276*, 21381–21386. (b) Szaleniec, M.; Hagel, C.; Menke, M.; Nowak, P.; Witko, M.; Heider, J. *Biochemistry* **2007**, *46*, 7637–7646. (c) Knack, D. H.; Hagel, C.; Szaleniec, M.; Dudzik, A.; Salwinski, A.;.Heider, J. *Appl. Environ. Microbiol*. **2012**, *78*, 6475–6482. (d) Szaleniec, M.; Borowski, T.; Schuhle, K.; Witko, M.; Heider, J. *J.Am. Chem. Soc*. **2010**, *132*, 6014–6024. (e) Szaleniec, M.; Witko, M.; Heider, J. *J. Mol. Catal. A* **2008**, *286*,128–136. (f) Szaleniec, M.; Witko, M.; Tadeusiewicz, R.; Goclon, J. *J. Comput.-Aided Mol. Des.* **2006**, *20*, 145–157.

Table 2.1 Relative calculated energy levels for the formation of radical and carbocation intermediates

compound	△△ $G_{radical}$ (kJ/mol)	△△ $G_{carbocation}$ (kJ/mol)
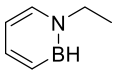 **2.2**	23.69	12.28
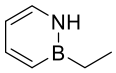 **2.3**	15.41	24.43
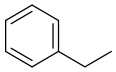 ethylbenzene	0	0

2.2.2 BN Isosteres in Medicinal Chemistry

Bioisosterism has been applied in the area of medicinal chemistry as a strategy to improve drug properties and discover new biological activities against target proteins.[12] However, there are few examples of BN isosteres being examined in drug discovery efforts. As an initial attempt, Dewar in 1964 synthesized BN isosteres of phenanthrene and naphthalene as potential agents for neutron capture therapy and as antibacterial agents.[13] Even though they exhibited improved aqueous solubility compared to their carbonaceous analogs, preliminary antibacterial activity tests showed unpromising results, with little to no increase in inhibitory effect against various bacterial strains. An *in vivo* study of potential application as boron neutron capture therapy agents also revealed that both

[12] (a) Burger, A. *Prog. Drug Res*. **1991**, *37*, 287−371. (b) Patani, G. A.; LaVoie, E. J. *Chem. Rev*. **1996**, *96*, 3147−3176. (c) Lima, L. M.; Barreiro, E. J. *Curr. Med. Chem*. **2005**, *12*, 23−49. (d) Brown, N. *Bioisosteres in Medicinal Chemistry* Wiley-VCH Verlag GmbH & Co. KGaA: Weinheim, Germany, 2012.
[13] Dewar, M. J. S.; Hashmall, J.; Kubba, V. P. *J. Org. Chem.* **1964**, *29*, 1755–1757.

intravenous (9 μg B/g) and intraperitoneal (17.5 μg B/g) injections induced instant death in mice (Figure 2.3).

Figure 2.3 BN isosteres of phenanthrene and naphthalene tested in *in vivo* studies of neutron capture therapy

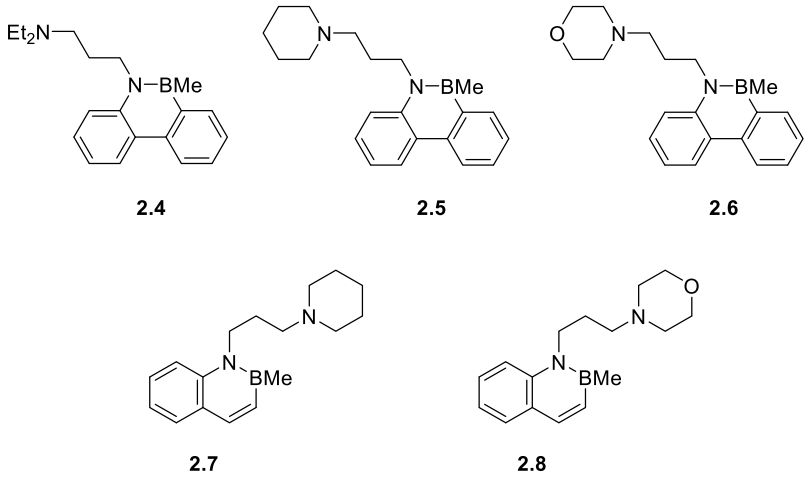

2.4 **2.5** **2.6**

2.7 **2.8**

Since Dewar's early experiments, efforts towards the application of 1,2-azaborines in biomedical research have resumed only recently. In 2015, Kilburn reported ADME (absorption, distribution, metabolism, and excretion) profiling of borazaronaphthalenes as phosphodiesterase 10A (PDE10A) inhibitors.[14] PDE10A is a potential target enzyme for the treatments of mental disorders such as Parkinson's disease, Huntington's disease, schizophrenia, and obsessive compulsive disorder (OCD). Compound **2.9a** (MP10, Table 2.2) was found to exhibit subnanomolar PDE10A inhibition with >1000-fold selectivity over other PDE's. The co-crystal structure of the active site of PDE10A, combined with structure activity relationship (SAR) analysis, revealed that one of the key binding

[14] Vlasceanu, A.; Jessing, M.; Kilburn, J. P. *Bioorg. Med. Chem*. **2015**, *23*, 4453−4461.

interactions was a hydrogen bond between the hydroxyl group of tyrosine residue (TYR693) and the nitrogen of quinoline moiety of MP10 (Figure 2.4).

Figure 2.4 Binding mode of MP10 in the active site of PDE10A

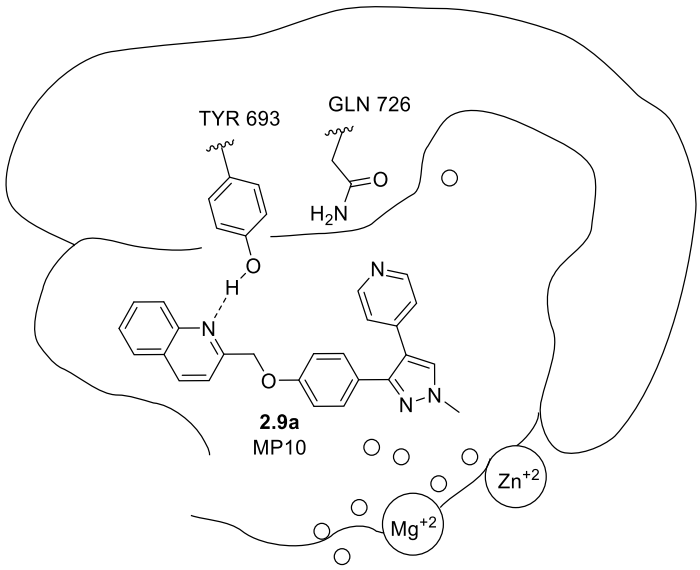

In the report, the authors described a correlation between the physical properties of the bicyclic rings (quinoline, naphthalene, and BN naphthalene) and the compounds' ability to inhibit PDE10A. Direct comparisons of IC_{50} values, lipophilicities, and clearance rates of the analogs were made (Table 2.2). The presence of the more polarized B–N bond in the BN naphthalenes (**2.10a–d**) resulted in higher inhibitory activity compared to the carbonaceous naphthalene analogs (**2.11a–d**); this activity was, however, still substantially lower than the quinoline-based compounds (**2.9a–d**). Systematic trends between lipophilicity and metabolic stability could not be identified for the compounds tested in the

study, thus highlighting the need for further refinement of structure-clearance relationship models.

Table 2.2 Potency, lipophilicity and metabolic stability of quinolinyl-, borazaronaphthyl-, and naphthyl-analogs

	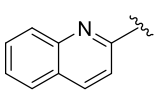	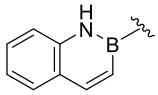	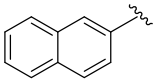
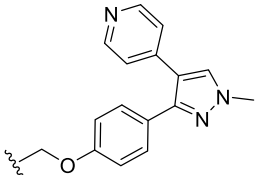	**2.9a** (MP10) IC_{50}= 2.6 *c*Log*P*= 3.84 Clint= 1.9	**2.10a** 48% inh. *c*Log*P*= 4.44 Clint= 2.5	**2.11a** 25% inh. *c*Log*P*= 5.13 Clint= 5
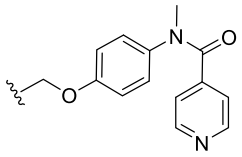	**2.9b** IC_{50}= 250 *c*Log*P*= 2.85 Clint= 0.9	**2.10b** 11% inh. *c*Log*P*= 3.44 Clint= 6.9	**2.11b** 2% at 2 µM *c*Log*P*= 4.14 Clint= 4.5
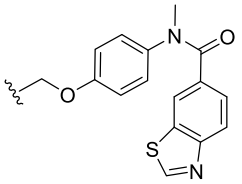	**2.9c** IC_{50}= 31 *c*Log*P*= 4.17 Clint= 1.9	**2.10c** 45% inh. *c*Log*P*= 4.76 Clint= 4.4	**2.11c** 5% inh. *c*Log*P*= 5.45 Clint= 2.9
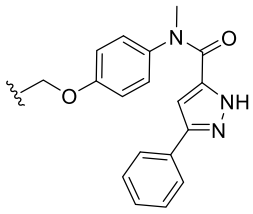	**2.9d** IC_{50}= 24 *c*Log*P*= 4.78 Clint= 1.3	**2.10d** IC_{50}= 1800 *c*Log*P*= 5.38 Clint= 0.34	**2.11d** 3% inh. *c*Log*P*= 6.07 Clint= 0.41

PDE10A potency measured as 50% inhibitory concentration (IC_{50}) in nM or given as percent inhibition at 10 µM. Lipophilicity as calculated Log*P* (*c*Log*P*). Metabolic stability as a measure of microsomal intrinsic clearance (Clint) in L/kg/h.

Another report in 2015 also examined the potential application of BN/CC isosterism to drug discovery. Two BN analogues of propranolol were synthesized and examined in both *in vitro* ADME profiles and *in vivo* pharmacokinetic studies.[15] Propranolol is an adrenergic β-receptor antagonist, used for the treatment of cardiovascular and psychiatric diseases.[16] Comparable inhibitory potency against 26 receptors was observed between the two BN-containing compounds (**2.13** and **2.14**) and propranolol (**2.12**) (Table 2.3, entries 1–4). Interestingly, both BN analogues showed improved metabolic stability in human liver microsomes (Table 2.3, entry 5).

Table 2.3 Physicochemical and *in vitro* ADME properties of **2.13** and **2.14** versus propranolol

		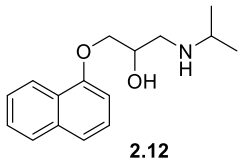 **2.12** propranolol	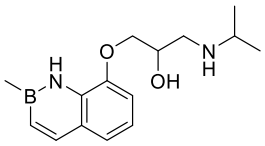 **2.13**	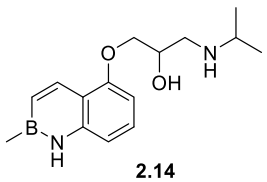 **2.14**
1	β2 pIC_{50}[a]	7.3	6.3	7.0
2	β1 pIC_{50}[a]	6.6	6.2	6.7
3	5HT1A pIC_{50}[a]	5.4	<5.3	5.7
4	23 other receptors pIC_{50} or pEC_{50}	all <5.3	all <5.3	all <5.3
5	CL_{int} h (μL/min/mg)[b]	28.8	8.7	11.0
6	CL_{int} m (μL/min/mg)[b]	61	>346	175
7	CL_{int} r (μL/min/mg)[b]	>346	289	>346

[a] cAMP quantification in hβ2-CHO cells. [b] *In vitro* clearance determined by incubation of with human (h), mouse (m), or rat (r) liver microsomes, expressed per milligram of protein.

[15] Rombouts, F. J.; Tovar, F.; Austin, N.; Tresadern, G.; Trabanco, A. A. *J. Med. Chem.* **2015**, *58*, 9287–9295.

[16] Black, J. W.; Crowther, A. F.; Shanks, R. G.; Smith, L. H.; Dornhorst, A. C. *Lancet* **1964**, *283*, 1080−1081.

Cytotoxicity tests showed that **2.13** and **2.14** display higher toxicity compared to propranolol (Table 2.4). This might originate from the formation of reactive species during the metabolic process due to the reduced aromaticity of the BN-ring system. The Ames II mutagenicity assay for all three compounds are negative, indicating low mutagenic potential for these compounds.

Table 2.4 Cytotoxicity and mutagenicity of **2.13** and **2.14** versus propranolol

	2.12	**2.13**	**2.14**
cytotoxicity (LTC, EC_{20}, μM)[a]	>100	18.7	59.0
Ames II positive	no	no	no

[a] Based on an internal analysis of 99 hepatotoxic and non-hepatotoxic compounds in the high content cytotoxicity screening, the lowest toxic concentration (LTC) for hepatotoxicity was set at 30 μM.

Table 2.5 shows a pharmacokinetic study in rats of bioavailability (C_{max} values in brain) via subcutaneous administration and brain penetration (brain/plasma AUC ratio (*K*p)). Both BN-containing compounds were bioavailable (C_{max} of 7 μM and 62 μM for **2.13** and **2.14**, respectively) and readily crossed the blood-brain barrier (*K*p of 13 and 19 for **2.13** and **2.14**, respectively).

Table 2.5 Pharmacokinetic profile of **2.13** and **2.14** versus propranolol

	2.12	**2.13**	**2.14**
C_{max} (μM)[a]	16	7	62
AUC ratio (*K*p)[b]	23	13	19

[a]The maximum concentration that the compound achieves in brain after subcutaneous administration. [b]The brain/plasma partition coefficient (permeability from blood to brain).

In their stability tests, the BN isosteres were found to be chemically stable under neutral pH, but sensitive to acidic conditions. This issue can be potentially addressed, however, with formulation technologies for oral delivery.

2.2.3 Hydrogen Bonding as a Major Contributor in Molecular Recognition

Hydrogen bonding is among the most prevalent of non-covalent interactions in chemical and biological systems, and plays a key role in molecular recognition. Hydrogen bonds provide directionality and specificity in both protein folding and protein-ligand interactions, and thus are often responsible for protein stability, functions and drug potency, respectively.[17]

2.2.3.1 Determination of Hydrogen Bond Strengths

Insight into the energy of hydrogen bonds can provide a better understanding of fundamental biological processes, and by extension, lead to more effective drug design.

[17] (a) Liu, Z.; Wang, G.; Li, Z.; Wang, R. *J. Chem. Theory Comput.* **2008**, *4*, 1959–1973. (b) Fersht, A. R.; Shi, J.-P.; Knill-Jones, J.; Lowe, D. M.; Wilkinson, A. J.; Blow, D. M.; Brick, P.; Carter, P.; Waye, M. M. Y.; Winter, G. *Nature* **1985**, *314*, 235–238.

There have been extensive studies to predict the strength of hydrogen bonds using theoretical energy calculations and molecular modeling docking experiments.[18] However, experimental determinations of hydrogen bond strengths are still limited, especially in the aqueous environment typical for drug-receptor binding interactions. This scarcity is attributed to the difficulty of dissecting the respective contributions to binding free energy of different factors (i.e. hydrophobic effect, hydrogen bonds, electrostatic interactions, lipophilicity, shape complementarity, and bulk solvent effect).[19]

Representative experimental approaches to quantify hydrogen bond strength in biological system can be found in the reports by Fersht[17b] and Williams.[20] In 1985, the Fersht group examined the contribution of hydrogen bonding to drug-receptor binding interactions using a site-directed mutagenesis strategy. They employed protein engineering of the tyrosyl-tRNA synthetase, which catalyzes the aminoacylation of tRNA when triggered by the formation of the enzyme-bound tyrosyl adenylate complex. As shown in Figure 2.5, multiple hydrogen bonding interactions between the protein side chains and tyrosyl adenylate are involved in this process.

---

[18] For selected examples, see: (a) Wendler, K.; Thar, J.; Zahn, S.; Kirchner, B. *J. Phys. Chem. A* **2010**, *114*, 9529–9536. (b) Dong, H.; Hua, W.; Li, S. *J. Phys. Chem. A* **2007**, *111*, 2941–2945. (c) Gilli, P.; Pretto, L.; Bertolasi, V.; Gilli, G. *Acc. Chem. Res.* **2009**, *42*, 33–44. (d) Sheu, S. Y.; Yang, D. Y.; Selzle, H. L.; Schlag, E. W. *Proc. Natl. Acad. Sci. U. S. A.* **2003**, *100*, 12683–12687. (e) Schwöbel, J. A. H.; Ebert, R.-U.; Kühne, R.; Schüürmann, G. *J. Phys. Org. Chem*. **2011**, *24* 1072–1080. (f) Schwöbel, J. A. H.; Ebert, R.-U.; Kühne, R.; Schüürmann, G. *J. Comput. Chem*. **2009**, *30*,1454–1464. (g) . Kollman, P. A.; Massova, I.; Reyes, C.; Kuhn, B.; Huo, S.; Chong, L.; Lee, M.; Lee, T.; Duan, Y.; Wang, W. *Acc. Chem. Res.* **2000**, *33*, 889–897.

[19] (a) Bronowska, A. K. *Thermodynamics of Ligand-Protein Interactions*: Implications for Molecular Design, Thermodynamics - Interaction Studies - Solids, Liquids and Gases. ISBN: 978-953-307-563-1, InTech, 2011. (b) Tsai, C. J.; Norel, R.; Wolfson, H. J.; Maizel, J. V. Nussinov, R. *Protein–Ligand Interactions*: Energetic Contributions and Shape Complementarity eLS, 2001.

[20] Williams, D. H.; Searle, M. S.; Mackay, J. P.; Gerhard, U.; Maple-stone, R. A. *Proc. Natl. Acad. Sci. U. S. A.* **1993**, *90*, 1172–1178.

Figure 2.5 Schematic representation of hydrogen bonding between wild-type tyrosyl-tRNA synthetase and tyrosyl adenylate

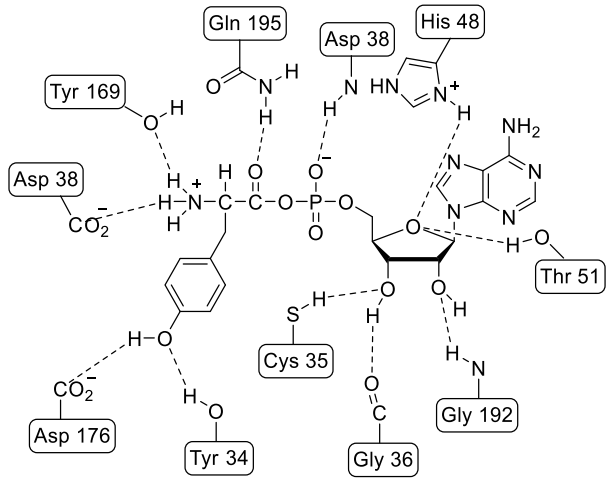

By the experimental measurement of kinetic parameters for activation of substrates, $(k_{cat}/K_M)_{mutant}$ versus $((k_{cat}/K_M)_{wild\text{-}type}$, they systematically analyzed the effect of mutation on loss and gain in hydrogen bond energy (Table 2.6). They classified the hydrogen bond interactions by two categories, hydrogen bonds with a neutral group and with a charged group. Based on their analysis, they found that a neutral-neutral hydrogen bond contributes about 0.5-1.5 kcal/mol in binding energy (equivalent to a 2- to 15-fold increase in affinity), but a hydrogen bond with a charged group contributes up to 4.5 kcal/mol (equivalent to a 3000-fold increase in affinity). For example, deletion of the hydroxyl group from Tyr34 by mutation to Phe34 resulted in only 0.52 kcal/mol loss of energy, presumably due to the relatively poor hydrogen bonding ability of tyrosyl OH with uncharged species (Table 2.6, entry 1). In contrast, mutation of Tyr169 to Phe169 resulted in loss of 3.72 kcal/mol binding energy (Table 2.6, entry 7). Deletion of the tyrosine side chain at this position

eliminates a strong hydrogen bond between the ammonium ion of the substrate and tyrosyl hydroxyl group.

Table 2.6 Comparison of binding energies of wild-type and mutant enzymes with substrates

entry	mutation	substrate	$\triangle G$ (kcal/mol)
1	Tyr 34* to Phe 34	Tyr	0.52
2	Cys 35* to Gly 35	ATP	1.14
3	Cys 51 to Ala 51	ATP	0.47
4	Asn48 to Gly 48	ATP	0.77
5	His 48* to Gly 48	ATP	0.96
6	Cys 35* to Ser 35	ATP	1.18
7	Tyr 169*† to Phe 169†	Tyr	3.72
8	Gln 195* to Gly 195	Tyr	4.49
9	Ser 35 to Gly 35	ATP	–0.04
10	Thr 51* to Ala 51	ATP	–0.44

$\triangle G = -RT \ln\{(k_{cat}/K_M)_{mutant} / (k_{cat}/K_M)_{wild\text{-}type}\}$.
*Wild-type. †truncated enzyme.

In 1993, the Williams group estimated hydrogen bond strengths by measuring the binding constants of organic molecules in aqueous media.[20] In a series of NMR studies, they investigated changes in the binding of cell wall peptide analogues to vancomycin and ristocetin derivatives, following modification of the peptide structures. Two additional factors, the hydrophobic effect and entropic costs of rotor restrictions and bimolecular associations of the antibiotics, were considered to quantify the pure hydrogen bond energy. Based on ΔG_h (the favorable free energy change due to the hydrophobic effect) and ΔG_r (the entropic penalties incurred by rotational restriction upon association) values from a comparison of the binding of peptide ligands to ristocetin A, the average neutral amide-amide hydrogen bond strengths were estimated to be –0.2 to –1.7 kcal/mol (Table 2.7). This result is in good agreement with the early works by Fersht.

Table 2.7 Estimates of amide-amide hydrogen bond strength (ΔG_p) in the binding of peptides to ristocetin A

Assumed $\triangle G_h$ (kcal/mol)	Assumed $\triangle G_r$ (kcal/mol)	Derived $\triangle G_p$ (kcal/mol)
–0.04	0.8	–1.0 ± 0.5
–0.04	1.2	–1.7 ± 0.5
–0.05	0.8	–0.2 ± 0.5
–0.05	1.2	–1.0 ± 0.5

$\triangle G = \triangle G_r + \triangle G_h + \triangle G_p$
$\triangle G$= observed binding free energy

2.2.3.2 Select Examples of Hydrogen Bond in Biology

One of the classic examples of hydrogen bonding in biological systems is base-pairing in DNA to form a stable double-helix. Hydrogen bonding also serves as the main organizing interaction for the assembly of α-helix and β-sheet, secondary protein structures. For instance, human myoglobin consists of eight α-helices that form a hydrophobic pocket around a heme molecule to enable oxygen transfer to muscle tissues. The structure of oxygenated human myoglobin is shown in Figure 2.6.[21] The α-helical structure maximizes the number of hydrogen bonding interactions along the peptide backbone, thereby directing the orientation of the side chains to create the hydrophobic core.

[21] Phillips, S. E. V. *J. Mol. Biol*. **1980**, *142*, 531–554.

Figure 2.6 α-Helical structure of oxymyoglobin (PDB: 1MBO)

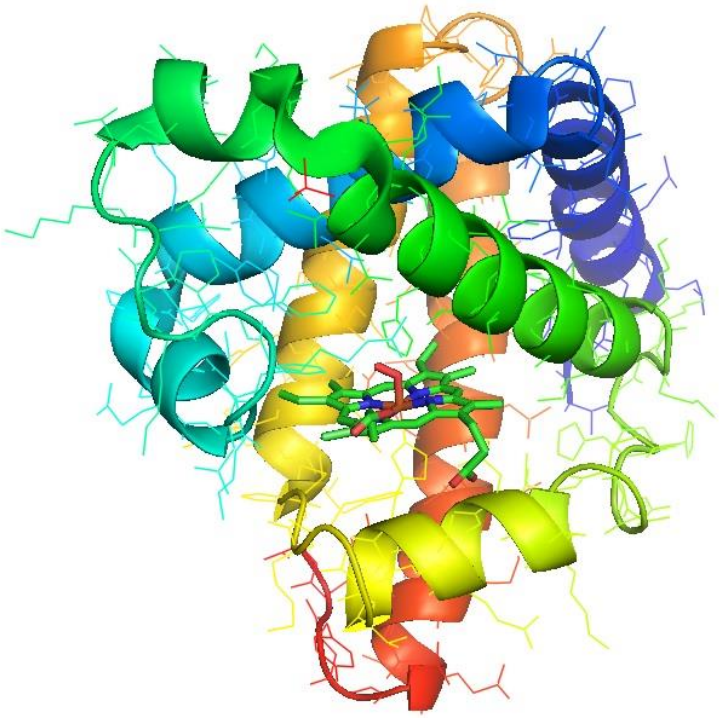

Another prevalent motif in protein structures is the β-sheet, in which peptidic amide groups form hydrogen bonds in either parallel or antiparallel series. Thioredoxin comprises five β-sheets in the central core surrounded by four α-helices; the β-strands from the N-terminus run parallel, and the β-strands from the C-terminus run antiparallel (Figure 2.7).[22] This characteristic tertiary structure of thioredoxin plays a key role in its folding and function during cellular redox processes.[23]

[22] Weichsel, A.; Gasdaska, J. R.; Powis, G.; Montfort, W. R. *Structure* **1996***, 4*, 735–751.
[23] Collet, J. F.; Messens, J. *Antioxid Redox Signal.* **2010**, *13*, 1205–1216.

Figure 2.7 Structure of human thioredoxin composed of five central β-sheets (PDB: 1ERT)

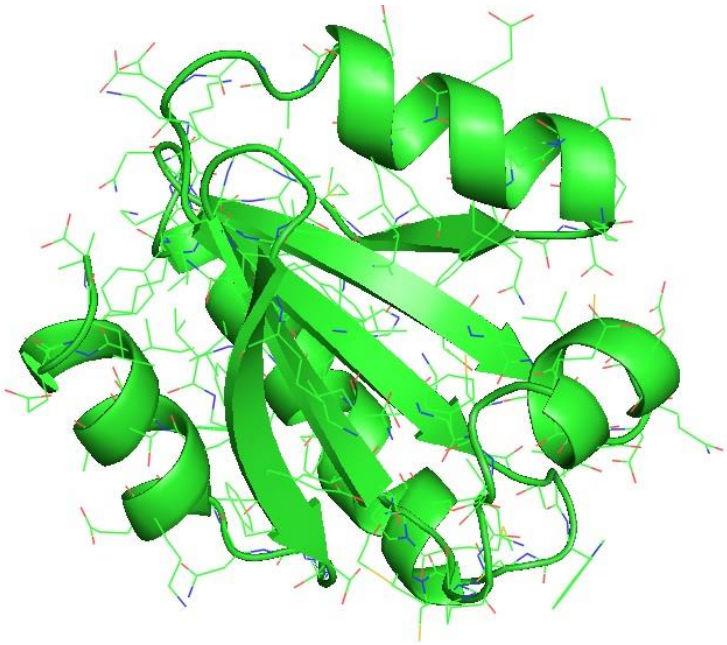

2.2.3.3 Select Examples of Hydrogen Bond in Pharmaceuticals

Hydrogen bonding interactions are often utilized in structure-activity relationship studies in drug discovery, and have been found to at times enhance the potency of drugs.[24] A well-studied example is imatinib, a strong inhibitor of the tyrosine kinase Abl.[25] Imatinib's specificity and potency are believed to arise from intermolecular hydrogen bonding interactions (as well as additional van der Waals interactions) between the

[24] For selected examples, see: (a) Gonzalez, A. Z.; Li, Z.; Beck, H. P.; Canon, J.; Chen, A.; Chow, D.; Duquette, J.; Eksterowicz, J.; Fox, B. M.; Fu, J.; Huang, X.; Houze, J.; Jin, L.; Li, Y.; Ling, Y.; Lo, M.-C.; Long, A. M.; McGee, L. R.; McIntosh, J.; Oliner, J. D.; Osgood, T.; Rew, Y.; Saiki, A. Y.; Shaffer, P.; Wortman, S.; Yakowec, P.; Yan, X.; Ye, Q.; Yu, D.; Zhao, X.; Zhou, J.; Olson, S. H.; Sun, D.; Medina, J. C. *J. Med. Chem.* **2014**, *57*, 2963–2988. (b) Verner, E.; Katz, B. A.; Spencer, J. R.; Allen, D.; Hataye, J.; Hruzewicz, W.; Hui, H. C.; Kolesnikov, A.; Li, Y.; Luong, C.; Martelli, A.; Radika, K.; Rai, R.; She, M.; Shrader, W.; Sprengeler, P. A.; Trapp, S.; Wang, J.; Young, W. B.; Mackman, R. L. *J. Med. Chem.* **2001**, *44*, 2753–2771. (c) Wang, Y.; Liu, Z.; Brunzelle, J. S.; Kovari, I. A.; Dewdney, T. G.; Reiter, S. J.; Kovari, L. C. *Biochem. Biophys. Res. Commun.* **2011**, *412*, 737–742. (d) Das, K.; Sarafianos, S. G.; Clark Jr, A. D.; Boyer, P. L; Hughes, S. H.; Arnold, E. *J. Mol. Biol.* **2007***, 365*, 77–89.

[25] Capdeville, R.; Buchdunger, E.; Zimmermann, J.; Matter, A. *Nat. Rev. Drug Discov*. **2002**, *1*, 493–502.

molecule and the protein side chains of the kinase binding site.[26] From the crystal structure of the imatinib-Abl complex, six hydrogen bonds are observed with interatomic distances of 2.7–3.2 Å (Figure 2.8).[27] Imatinib's piperazinyl group is most likely protonated, and therefore able to form hydrogen-bond contacts with the carbonyl oxygens of His361 and Ile360.[26]

Figure 2.8 Schematic diagram of the H-bonding interactions between imatinib and Abl residues

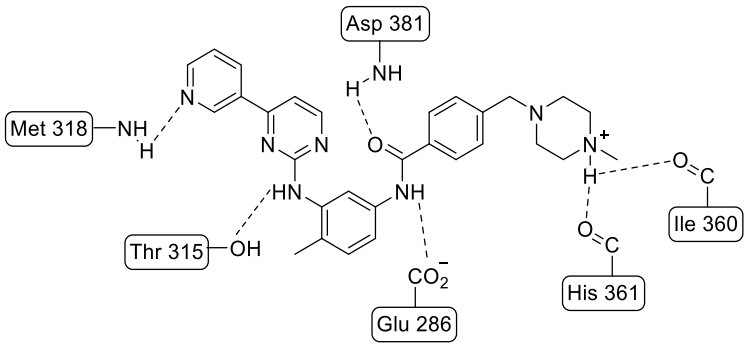

Intermolecular formation of hydrogen bonds between drugs and receptors improve drug potency by enabling specificity through the selective favorability of these local binding interactions. Intramolecular hydrogen bonds within drugs, however, can also produce notable effects, particularly with respect to membrane permeability, water solubility, and lipophilicity.[28] A systematic analysis of intramolecular hydrogen bond

[26] Lin, Y.-L.; Meng, Y.; Jiang, W.; Roux, B. *Proc. Natl. Acad. Sci. U. S. A.* **2013**, *110*, 1664–1669.
[27] Nagar, B.; Bornmann, W. G.; Pellicena, P.; Schindler, T.; Veach, D. R.; Miller, W. T.; Clarkson, B.; Kuriyan, J. *Cancer Res*. **2002**, *62*, 4236–4243.
[28] Alex, A.; Millan, D. S.; Perez, M.; Wakenhut, F.; Whitlock, G. A. *Med. Chem. Commun.* **2011**, *2*, 669–674.

effects was conducted by the discovery chemistry group at Roche.[29] The authors hypothesized that the formation of intramolecular hydrogen bond within a molecule would effectively remove the availability of one donor and one acceptor unit to form intermolecular hydrogen bonds, resulting in increased lipophilicity and membrane permeability and decreased aqueous solubility. Indeed, they observed indicators of these very trends in several different model systems, two of which are presented in Table 2.8. Compound **2.16** has the ability to from an intramolecular hydrogen bond between the benzimidazole NH and the carbonyl oxygen of amide group. Both cell permeability (PAMPA P_e) and lipophilicity (logD) improved compared to those of **2.15** in which the benzimidazole nitrogen is methylated. Similar trends were observed for **2.17**–**2.20**; **2.20** showed a slight increase in cell permeability compared to analogs **2.18** and **2.19**. Water solubility and logD values were comparable throughout the series, except for compound **2.17**, which was considerably less water soluble and more lipophilic.

[29] Kuhn, B.; Mohr, P.; Stahl, M. *J. Med. Chem*. **2010**, *53*, 2601–2611.

Table 2.8 Molecular properties examined in the model ligand sets

	PAMPA P_e (10^{-6} cm/s)	LYSA solubility (μg/ml)	logD
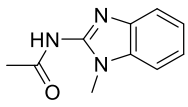 **2.15**	7.4	>220	0.68
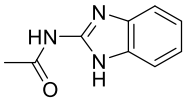 **2.16**	8.0	46	1.39
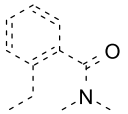 **2.17**	16.3	1	1.29
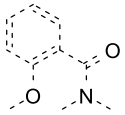 **2.18**	6.0	43	0.63
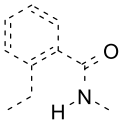 **2.19**	10.0	53	1.32
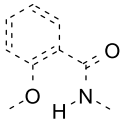 **2.20**	11.3	29	0.85

PAMPA permeation constant P_e. LYSA water solubility. Octanol/water partition coefficient logD

2.2.4 Cavity-Bearing T4 Lysozyme Mutants

The T4 lysozyme consists of 164 amino acids and works to hydrolyze the β-1,4 linkages between the N-acetylmuramic acid (NAM) and N-acetylglucosamine (NAG) units of

bacterial cell walls. The enzyme has been extensively studied as a tool to gain understanding of the general factors that determine the structure and stability of proteins.[30]

2.2.4.1 Origin of T4 Lysozyme Mutants

The first systematic mutation of bacteriophage T4 lysozyme was investigated by Poteete et al. in 1991.[31] They introduced amber mutation using 13 different amino acids at every one of the 164 residues and measured the resulting enzymatic activity. Mutation at 89 of the 164 sites (55%) was found to leave activity equivalent to that of the wild-type. Most of these tolerant sites are distributed on the surface of the protein, consistent with the principle of protein folding: residues on the surface are partially or fully solvated, and therefore have little impact on enzymatic activity. However, residues in or near the catalytic sites (Glu11, Asp20, Asp10, Arg145, Arg148) and a few others (Gly30, Trp 138, Tyr161) were notably sensitive to replacements.

Protein stability was also examined by monitoring changes in the melting temperature brought on by point mutations (Figure 2.9).[30b] Many point mutations decreased protein stability by more than 3 °C, which roughly corresponds to a change in the free energy of stabilization ($\Delta\Delta G$) of about 1 kcal/mol. The most destabilizing point mutants reduced the melting temperature by about 20 °C. These include mutation in the hydrophobic core of the protein: M102K, A98F, A98W, L99G, and R95A.

---

[30] For selected reviews on T4 lysozyme mutants, see: (a) Matthews, B. W. *Biochemistry* **1987**, *26*, 6885–6888. (b) Baase, W. A.; Liu, L.; Tronrud, D. E.; Matthews, B. W. *Protein Sci*. **2010**, *19*, 631–641. (c) Matthews, B. W.; Liu, L. *Protein Sci*. **2009**, *18*, 494–502. (d) Xu, J.; Baase, W. A.; Baldwin, E.; Matthews, B. W. *Protein Sci*. **1998**, *7*, 158–177.

[31] Rennell, D.; Bouvier, S. E.; Hardy L. W. ; Poteete, A. R. *J. Mol. Biol.* **1991**, *222*, 67–87.

Figure 2.9 Distribution of ΔT_m (°C) for 312 known point mutants (This figure has been reproduced from reference 30b)

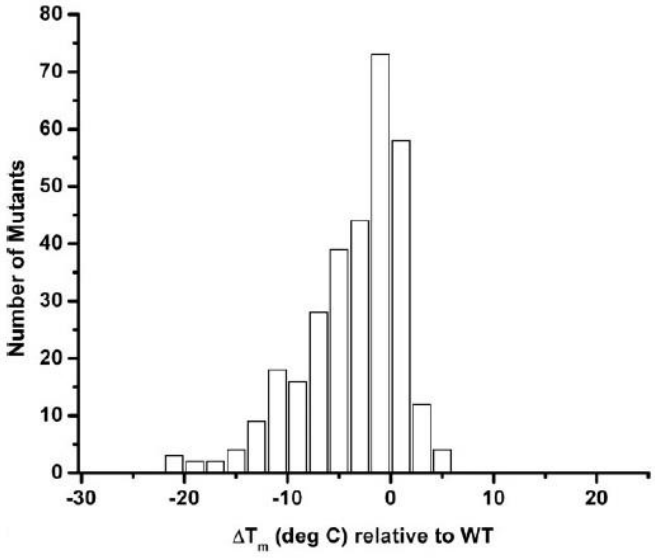

2.2.4.2 Discovery of Cavity-Bearing T4 Lysozyme Mutants

The interiors of proteins are usually tightly packed with little empty space remaining.[32] If a polar cavity exists, it is typically occupied by water molecules; this type of cavity can be up to about 150 $Å^3$ in volume. Apolar cavities appear to be empty and generally have volumes up to about 50 $Å^3$. An artificial cavity can be generated by replacement of a bulky residue (Phe, Leu, Ile, and Met) with a small residue (Ala) in a core of proteins.

In 1992, the Matthews group discovered that the replacement of Leu99 with Ala in T4 lysozyme creates a structurally rigid apolar cavity inside the hydrophobic core of the protein's C-domain.[33] The L99A cavity is unusually large (150 $Å^3$) and well-concealed

[32] Hubbard, S. J.; Gross, K-H.; Argos, P. *Protein Eng*. **1994**, *7*, 613–626.
[33] (a) Eriksson, A. E.; Baase, W. A.; Wozniak, J. A.; Matthews, B. W. *Nature* **1992**, *355*, 371–373. (b) Eriksson, A. E.; Baase, W. A.; Zhang, X-J.; Heinz, D. W.; Blaber, M.; Baldwin, E. P.; Matthews, B. W. *Science* **1992**, *255*, 178–183.

from external solvent molecules. Through crystallographic and thermodynamic analyses, the authors found that the cavity is large enough to bind benzene; this binding notably increases the melting temperature of the protein by 6 °C at pH 3.0.

2.2.4.3 Binding Studies of Cavity-Bearing T4 Lysozyme Mutants

Binding thermodynamics were systematically studied by examining the binding of 91 compounds within the cavity of the L99A T4 lysozyme mutant.[34] In an initial screen, a thermal upshift assay indicated no apparent binding by compounds presumably protonated at pH 3.0, such as aniline, pyridine, and quinoline. Neutral polar compounds including ethanol, furan, phenol, and benzyl alcohol also did not induce thermal upshift. Lastly, binding by sterically bulky ligands, i.e. *t*-butylbenzene, (±)-camphene, and (±)-camphor, was also not detected (Figure 2.10).

Figure 2.10 Examples of compounds for which binding to L99A was not detected

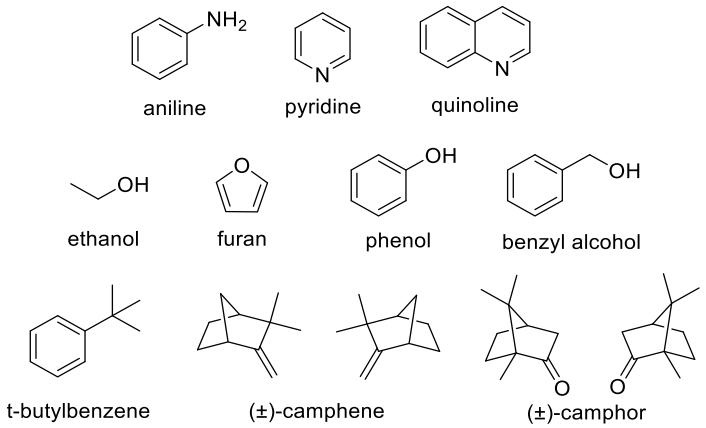

[34] Morton, A.; Baase, W. A.; Matthews, B. W. *Biochemistry*, **1995**, *34*, 8564–8575.

Those ligands that did exhibit binding to the cavity residues were segregated into three separate categories: isophobic ligands of equivalent hydrophobicity to probe possible steric influences in the cavity wall (Class I); isosteric ligands of different hydrophobicities to evaluate hydrophobic contributions to the binding energy (Class II); and alkylbenzenes with different length of side-chains length to determine the effects of ligand size (Class III; Figure 2.11).

Figure 2.11 Classification of ligands used for binding thermodynamic analysis

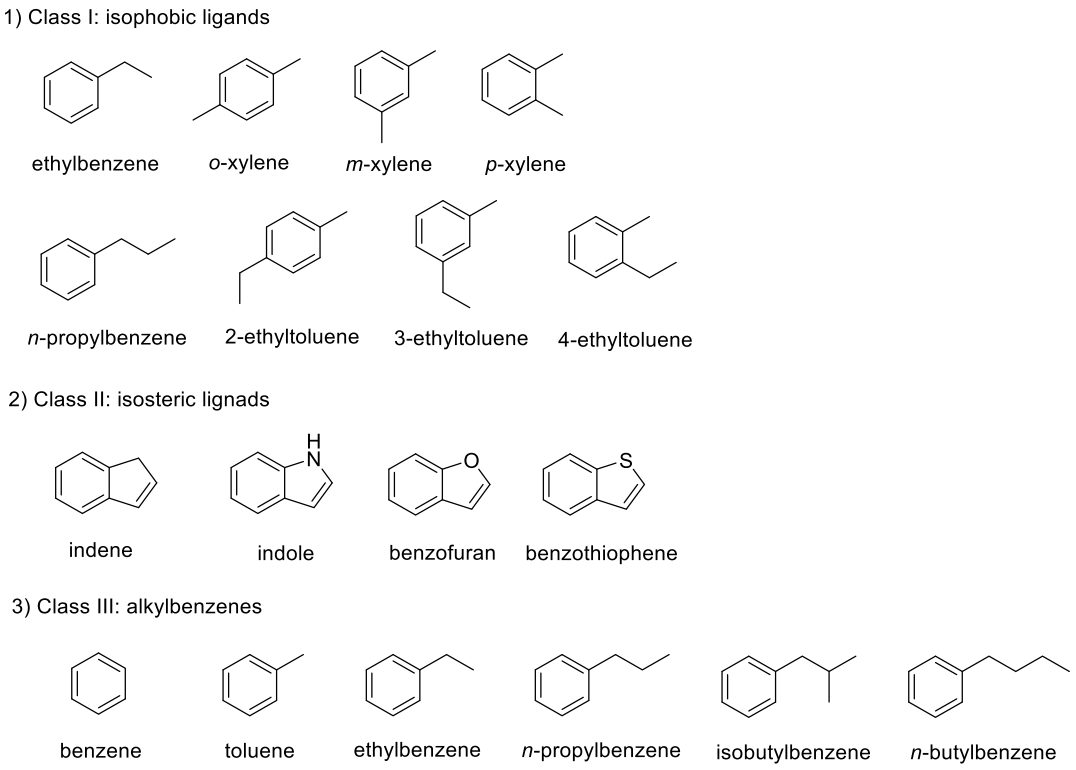

Table 2.9 lists the results of isothermal titration calorimetry (ITC) measurements of the binding thermodynamics of ligand classes I–III. Among the class I ligands, di-substituted

compounds show poorer binding compared to their mono-substituted counterparts (xylenes vs. ethylbenzene and ethyltoluenes vs. propylbenzene). These results indicate sterics strongly influence binding energetics. Later, crystallographic analysis revealed that there is a bulge region in the mutant cavity that can accommodate a single substituent on the aromatic ring.[35] The results for the class II ligands indicate only a rough correlation between hydrophobicitiy and binding free energy. Among the class III compounds, there is a good correlation between the length of the alkyl side-chain and binding strength, with longer chains equating to larger ΔG values.

Table 2.9 Binding thermodynamics of aromatic compounds in L99A cavity

	$\triangle G$ (kcal/mol)	$\triangle H$ (kcal/mol)	K_a (X10^3 M^{-1})
ethylbenzene	–5.76 ± 0.07	–6.76 ± 0.87	14.8 ± 1.7
o-xylene	–4.60 ± 0.06	–8.45 ± 0.96	2.13 ± 0.22
m-xylene	–4.75 ± 0.15	–6.04 ± 0.03	2.75 ± 0.8
p-xylene	–4.61 ± 0.06	–6.97 ± 0.98	2.37 ± 0.25
n-propylbenzene	–6.55 ± 0.02	–9.97 ± 0.05	55.2 ± 2.0
2-ethyltoluene	–4.56 ± 0.06	–7.71 ± 0.74	1.98 ± 0.20
3-ethyltoluene	–5.12 ± 0.02	–7.84 ± 0.02	5.05 ± 0.15
4-ethyltoluene	–5.42 ± 0.01	–8.44 ± 0.03	8.33 ± 0.08
benzofuran	–5.46 ± 0.03	–8.04 ± 0.44	8.9 ± 0.5
indene	–5.13 ± 0.01	–8.31 ± 0.48	5.17 ± 0.09
indole	–4.89 ± 0.06	–11.23 ± 0.94	3.45 ± 0.38
thianaphthene	–5.71 ± 0.05	–7.03 ± 0.04	13.6 ± 1.2
benzene	–5.19 ± 0.16	–6.32 ± 0.37	5.7 ± 1.7
toluene	–5.52 ± 0.04	–6.53 ± 0.73	9.8 ± 0.6
isobutylbenzene	–6.51 ± 0.06	–7.09 ± 0.35	51.0 ± 4.9
n-butylbenzene	–6.70 ± 0.02	–8.06 ± 0.9	69.8 ± 2.9

[35] Morton, A.; Matthews, B. W. *Biochemistry*, **1995**, *34*, 8576–8588.

Crystal structure analyses of the ligand-bound protein complexes indicated a substantial conformational rearrangement occurs during ligand binding.[35] However, the binding cavity remains rigid upon ligand binding, as characterized by low temperature factors and strong protection from hydrogen exchange. Therefore, this part of the protein is mainly responsible for discrimination of ligand shapes. In contrast, significant conformational adjustments (large positional shifts of 1.5–2.5 Å) were found to occur in the flexible region, helix F (residues 108–113) (Figure 2.12). Temperature factors in helix F are significantly higher than those of other regions, which is indicative of great conformational destabilization upon ligand binding.

Figure 2.12 Structure of benzene-bound complex of L99A mutant (PDB: 181L)

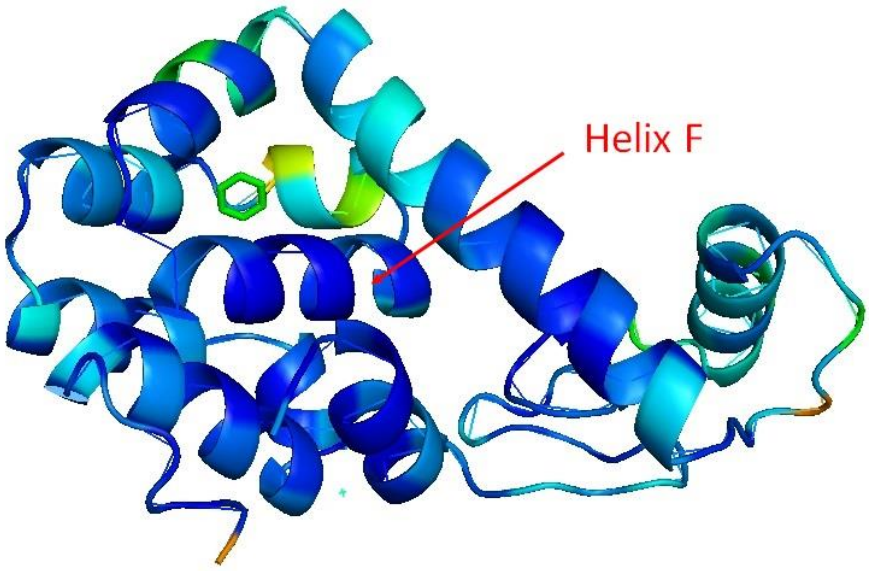

Since their initial discovery, T4 lysozyme mutants have been extensively studied as a model system to verify and test docking predictions generated by different calculation

approaches. The advantages of these systems in this regard include straightforward detection of ligand binding, measurement of affinity, and unambiguous determination of structure by X-ray crystallography.

In the course of developing a docking scoring function, Matthews and Shoichet introduced the T4 lysozyme double mutant L99A/M102Q, which bears a polar binding cavity.[36] The methionine residue was replaced by a polar residue, glutamine. In the binding pocket, a water molecule and β-mercaptoethanol (from the crystallization buffer) were found in the crystal structure in the absence of an added organic compound. The docking calculation was repeated for representative polar organic molecules and verified by experimental results using circular dichroism (CD), ITC, and X-ray crystallography.

Generally, a good agreement was observed between the prediction model and experimental data. Ranking and scoring functions were verified by experimental measurement of thermal denaturation using CD in the binding of a series of polar molecules to the cavity of L99A/M102Q (Table 2.10). These ligands are known not to bind to the apolar binding pocket (L99A). In all cases, binding of the ligands resulted in an increase of protein melting temperature.

[36] Wei, B. Q.; Baase, W. A.; Weaver, L. H.; Matthews, B. W.; Schoichet, B. K. *J. Mol. Biol*. **2002**, *322*, 339−355.

Table 2.10 Representative ligands predicted to bind preferentially to the polar L99A/M102Q cavity

compound	ranking in L99A/M102Q screen	△rank[a]	△score[a] (kcal/mol)	L99A		L99A/M102Q	
				ΔT_m (°C)	binding detected?	ΔT_m (°C)	binding detected?
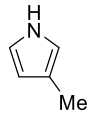	196	–401	–1.5	0.1	No	+2.1	Yes[b]
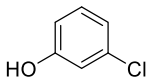	154	–204	–0.7	–0.2	No	+2.7	Yes[b]
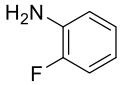	96	–200	–1.1	0.3	No	+1.7	Yes[b]
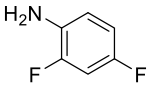	47	–117	–0.8	–0.2	No	+1.3	Yes
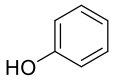	300	–273	–0.7	–0.2	No	+1.9	Yes[b]
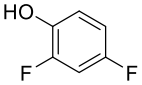	26	–91	–0.9	0.3	No	+1.6	Yes
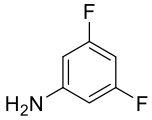	32	–186	–1.8	0	No	+1.7	Yes[b]

[a] △rank or △score: relative to the docking screen against the L99A cavity.
[b] Binding confirmed by crystallography or calorimetry.

Four polar ligands were further examined in calorimetric experiments to determine the binding affinity of each complex with the protein. Among those tested, 3-chlorophenol shows the highest binding affinity (K_a = 18 x 10^3 M^{-1}; Table 2.11, entry 2). An apolar ligand, toluene, was also found to bind to the L99A/M102Q cavity (K_a = 6.4 x 10^3 M^{-1}), but with lesser affinity than for L99A (K_a = 9.8 x 10^3 M^{-1}).

Table 2.11 ITC results of ligand binding to L99A/M102Q

compound	K_a (x 10^3 M^{-1})[a]	$\triangle H$ (kcal/mol)[b]	N[c]
3-methylpyrrole	6.3	–7	0.7
3-chlorophenol	18	–9	0.7
2-fluoroaniline	10	–8	0.6
phenol	11	–8	0.8
toluene	6.4	–6	0.8

[a] Association constant. [b] Calorimetric molar enthalpy.
[c] Apparent stoichiometry of ligand binding to L99A/M102Q.

The binding geometry predicted by the authors' AMSOL charge prediction model was also well-aligned with the actual crystallographic data of the binding of five polar ligands to L99A/M102Q (Figure 2.13). Based on the crystal structures, hydrogen bonds formed between the polar substituents of the ligands and the carbonyl oxygen of Gln102 with the lengths of 2.7–3.3 Å.

Figure 2.13 Comparison of the geometries of binding predicted using the AMSOL charges (carbons in cyan) and the experimentally observed modes (carbons in grey) (This figure has been reproduced from reference 36)

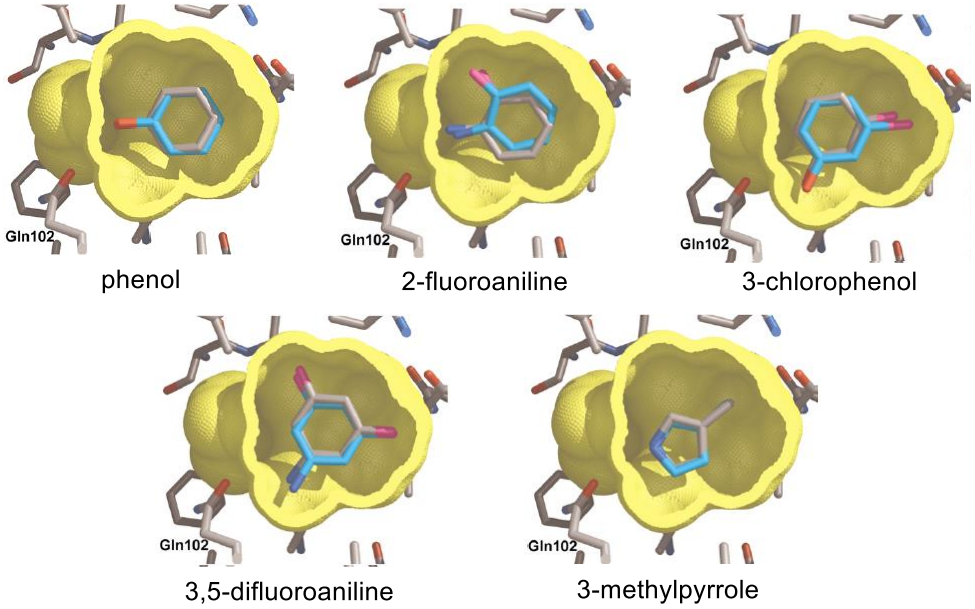

L99A and L99A/M102Q have been repeatedly used in further development of molecular docking prediction methods including testing a flexible-receptor docking algorithm, [37] assembling decoy databases, [38] predicting absolute ligand binding free energy,[39] rescoring docking hit lists,[40] and constructing alchemical free energy methods.[41]

To better understand the effects of protein residues in ligand binding and enzyme activity, Matthews developed another T4 lysozyme double mutant: L99A/M102E. A

[37] Wei, B. Q.; Weaver, L. H.; Ferrari, A. M.; Matthews, B. W.; Shoichet, B. K. *J. Mol. Biol*. **2004**, *337*, 1161–1182.
[38] Graves, A. P.; Brenk, R.; Shoichet, B. K. *J. Med. Chem.* **2005**, *48,* 3714–3728.
[39] Mobley, D. L.; Graves, A. P.; Chodera, J. D.; McReynolds, A. C.; Shoichet, B. K.; Dill, K. A. *J. Mol. Biol*. **2007**, *371*, 1118–1134.
[40] Graves, A. P.; Shivakumar, D. M.; Boyce, S. E.; Jacobson, M. P.; Case, D. A.; Shoichet, B. K. *J. Mol. Biol*. **2008***, 377*, 914–934.
[41] Boyce, S. E.; Mobley, D. L.; Rocklin, G. J.; Graves, A. P.; Dill, K. A.; Shoichet, B. K. *J. Mol. Biol.* **2009**, *394*, 747–763.

negatively charged glutamic acid residue was introduced at the 102 methionine position of the L99A mutant to generate a more polar environment in the binding cavity.[42] The shape of the cavity was found to be essentially the same as in L99A. However, three water molecules were identified in the binding pocket at positions that indicated formation of hydrogen bond network among themselves and with the peptide residues. In addition, binding of both polar and nonpolar benzene analogs was observed in this cavity by crystallographic analysis.

Shoichet also mutated the 102 methionine residue, this time to introduce a positively charged histidine group into the binding pocket.[43] Isolation of the L99A/M102H protein required additional mutations at the residues remote from the binding site to counteract stability issues. Various mutations were introduced and a series of these mutants were used to explore catalysis of Kemp elimination.[43a,43] Notably, certain polar molecules such as 4-nitrophenol that did not or poorly bind to the other mutants (L99A, L99A/M102Q, and L99A/M102E), were accommodated into the L99A/M102H cavity.[43b]

[42] Liu, L.; Baase, W. A.; Matthews, B. W. *Biochemistry,* **2009**, *48*, 8842–8851.
[43] (a) Merski, M.; Shoichet, B. K. *Proc. Natl. Acad. Sci. U. S. A.* **2012**, *109,* 16179−16183. (b) Merski, M.; Shoichet, B. K. *J. Med. Chem*. **2013**, *56*, 2874−2884.

2.3 Hydrogen Bonding of 1,2-Azaborines in the Binding Cavity of T4 Lysozyme Mutants: Structures and Thermodynamics[44]

2.3.1 Previous Evidence of Hydrogen Bonding of 1,2-Azaborines

One of the potential beneficial features of 1,2-azaborines in biological systems is their hydrogen bonding capability. We previously estimated by computation (B3LYP/DZVP2) the pK_a value of the 1,2-azaborine NH to be around 24 (Figure 2.14), which is indicative of modestly protic character.[9d] The protic nature was also confirmed experimentally by deuterium exchange with CD_3OD.[6a] Additionally, the crystal structure of compound **2.21** showed an intramolecular hydrogen bond between the N–H and the carbonyl oxygen of the *B*-phenylacetate substituent (Figure 2.14).[6b]

Figure 2.14 Hydrogen bonding capability of 1,2-azaborines

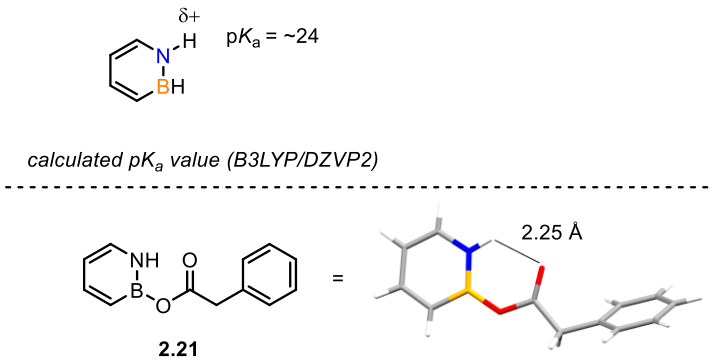

However, no evidence of hydrogen bonding of 1,2-azaborines had been ascertained in a biological context. Hydrogen bonding ability of 1,2-azaborines would have merits over

[44] (a) Lee, H.; Fischer, M.; Shoichet, B. K.; Liu, S.-Y. *J. Am. Chem. Soc.* **2016**, *138*, 12021–12024. (b) Lee, H.; Liu, S.-Y. *J. Vis. Exp.* **2017**, *121*, e55154.

other 6-membered aromatic compounds, especially in the context of potential application in medicinal chemistry. Therefore, we sought to establish a fundamental understanding of the hydrogen bonding capability of 1,2-azaborines in a biological model system: the T4 lysozyme mutant.

2.3.2 Synthesis of 1,2-Azaborines

To prepare the NH-containing 1,2-azaborines required for our binding studies, we employed a modified version of previously reported synthetic routes.[6,10] Triallylborane (**2.22**)[45] was used as a substitute for allyltriphenyl tin or potassium allyltrifluoroborate to prepare the B-N adduct **2.23**. This substitution notably renders the route more atom-economical and environmentally friendly. Conproportionation of triallylborane with boron trichloride generates allylboron dichloride *in situ*, which then reacts with TBS-protected allylamine to afford **2.23**. Subsequent ring closing metathesis, followed by oxidation furnishes the aromatic azaborine core to provide a versatile azaborine intermediate (**2.24)** in a one-pot, two-step sequence. Amide-assisted deprotection of TBS and displacement with the appropriate alcohol results in either precursor **2.25** or **2.26**. Reduction of **2.25** with lithium aluminum hydride gave the unsubstituted azaborine ligand **2.1**. Ethyl lithium was used to complete the synthesis of **2.3**.

[45] Brown, H. C.; Racherla, U. S. *J. Org. Chem*. **1986**, *51*, 427–432.

Scheme 2.1 Synthesis of NH containing 1,2-azaborines used in binding study

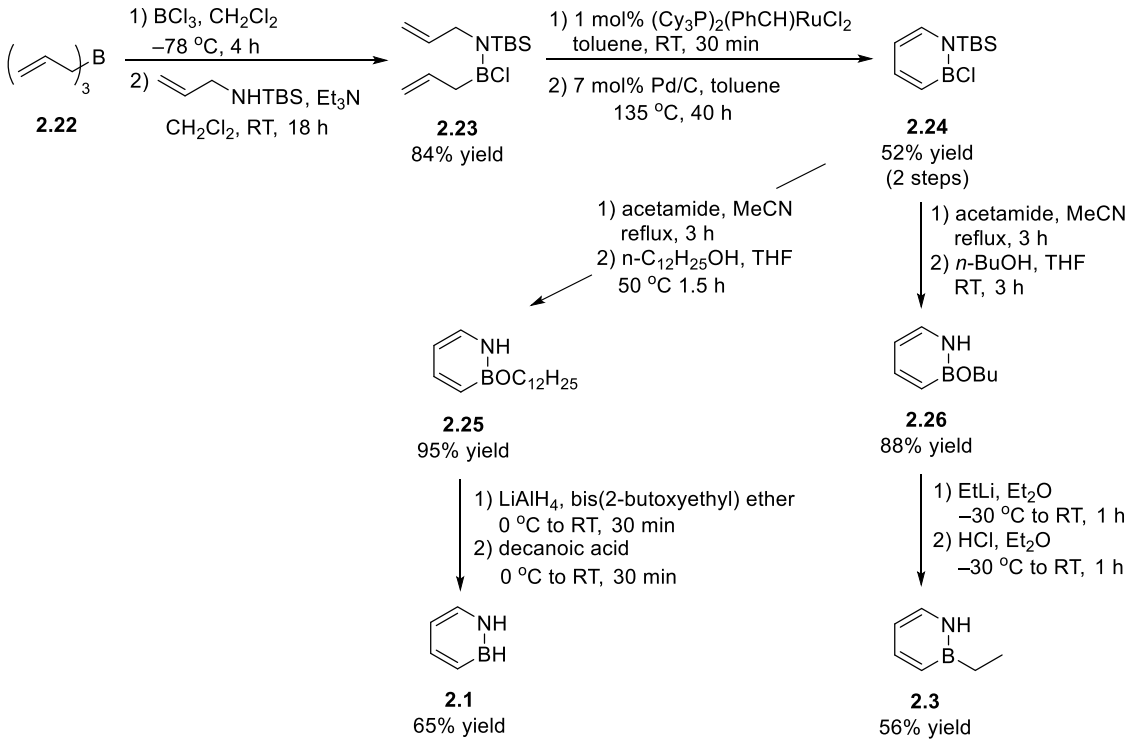

2.3.3 Protein X-Ray Crystal Structures

We chose two engineered cavity-bearing T4 lysozyme mutants, L99A and L99A/M102Q, as a macromolecule binding model. L99A was used as a control protein as it has no residues capable of forming hydrogen bonds inside the binding pocket. A slightly more polar protein, L99A/M102Q was used to determine a potential hydrogen bond between 1,2-azaborines and a polar glutamine residue. Protein X-ray crystallography was utilized to examine this interaction.

In the non-polar cavity (L99A), similar binding modes were observed for the carbonaceous arenes and their corresponding BN analogs, as observed previously.[46] The ethyl group of both ethylbenzene and BN analog **2.3** is oriented towards the bulge region of the cavity, presumably due to shape complementarity. There are two alternative conformations in the binding of **2.1**, ethylbenzene, and **2.3** (Figure 2.15). As expected, in all cases there is no evidence of hydrogen bond formation between the ligands and the surrounding protein residues in the cavity. In addition, the distances between the nitrogen of the azaborine ligands and the sulfur atom of Met102 are 4.0 and 4.5 Å in the **2.1**-L99A complex and 5.9 and 6.2 Å in the **2.3**-L99A complex, all too far to be a hydrogen bond (non-classical sulfur-containing hydrogen bond[47]).

[46] Liu, L.; Marwitz, A. J. V.; Matthews, B. W.; Liu, S.-Y. *Angew. Chem. Int. Ed.* **2009**, *48*, 6817–6819.
[47] (a) Zhou, P.; Tian, F.; Lv, F.; Shang, Z. *Proteins: Struct., Funct., Bioinf.* **2009**, *76*, 151–163. (b) Gregoret, L. M.; Rader, S. D.; Fletterick, R. J.; Cohen, F. E. *Proteins: Struct., Funct., Bioinf.* **1991**, *9*, 99–107.

Figure 2.15 X-ray structures of ligand-bound L99A complexes

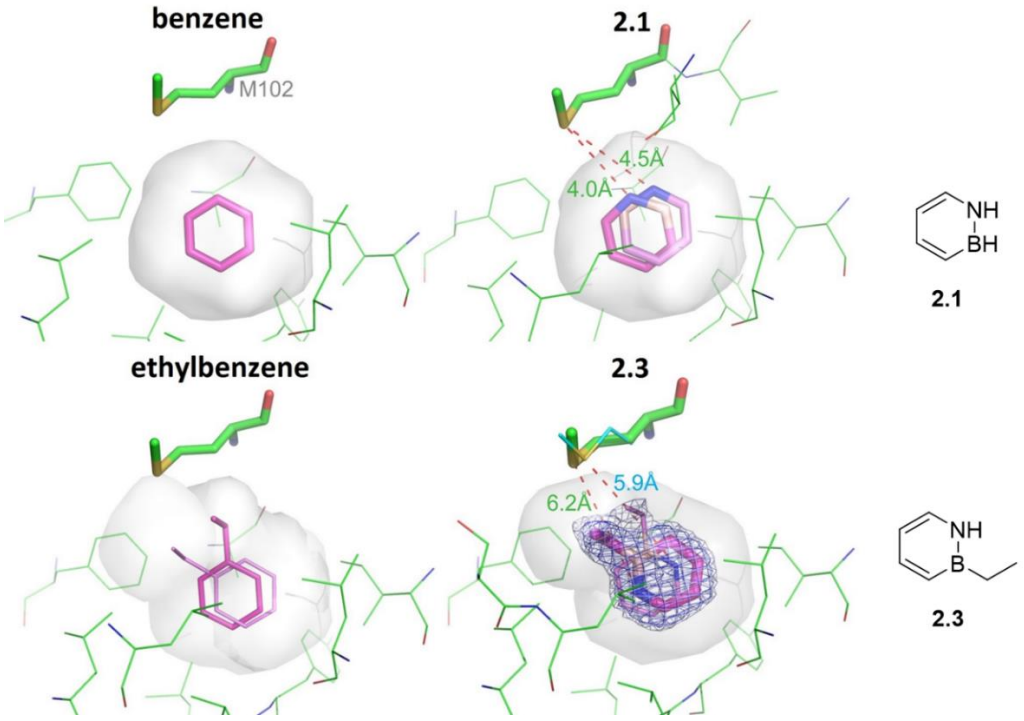

In the polar cavity (L99A/M102Q), a distinctly different interaction is observed between the aryl-bound complexes and the azaborine-bound complexes. In the benzene-L99A/M102Q complex, benzene displaces 2-mercaptoethanol (observed in the previously reported crystal structure; PDB: 1 LGU[36]) to occupy the binding pocket (Figure 2.16, top left). A water molecule is still present in the cavity, forming a hydrogen bond with the carbonyl oxygen of Gln102 with distances of 2.5 and 2.7 Å in the two alternative conformations. In contrast, the crystal structure of the **2.1**-L99A/M102Q complex shows a hydrogen bond between the NH of azaborine **2.1** and the C=O of Gln102 with distances of 3.1 and 3.2 Å in the two alternative conformations of the residue (Figure 2.16, top right). This is the first example of unambiguous structural evidence of an azaborine forming a

hydrogen bond in a biological macromolecule. Similarly, a hydrogen bonding interaction is observed in the **2.3**-L99A/M102Q complex. The distances between the nitrogen of azaborine **2.3** and the carbonyl oxygen of Gln102 are 3.2 and 3.6 Å in the two alternative conformations of the ligand (Figure 2.16, bottom right). The latter could be considered as a very weak hydrogen bond or a polar non-covalent interaction. There is no obvious hydrogen bonding interaction in the ethylbenzene-L99A/M102Q complex (Figure 2.16, bottom left). Additionally, we found a substantial positional change of the Gln102 side chain in the azaborine-bound complexes. Binding of the NH-containing azaborine led to movement of the glutamine residue, resulting in 0.4 and 1.1 Å difference in the position of the oxygen atom compared to the corresponding carbonaceous ligand-bound structures (benzene-L99A/M102Q vs. **2.1**-L99A/M102Q and ethylbenzene-L99A/M102Q vs. **2.3**-L99A/M102Q, respectively). Thus, it appears that the Gln102 side chain undergoes considerable geometric changes upon binding of 1,2-azaborines to accommodate hydrogen bonding.

Figure 2.16 X-ray structures of ligand-bound L99A/M102Q complexes

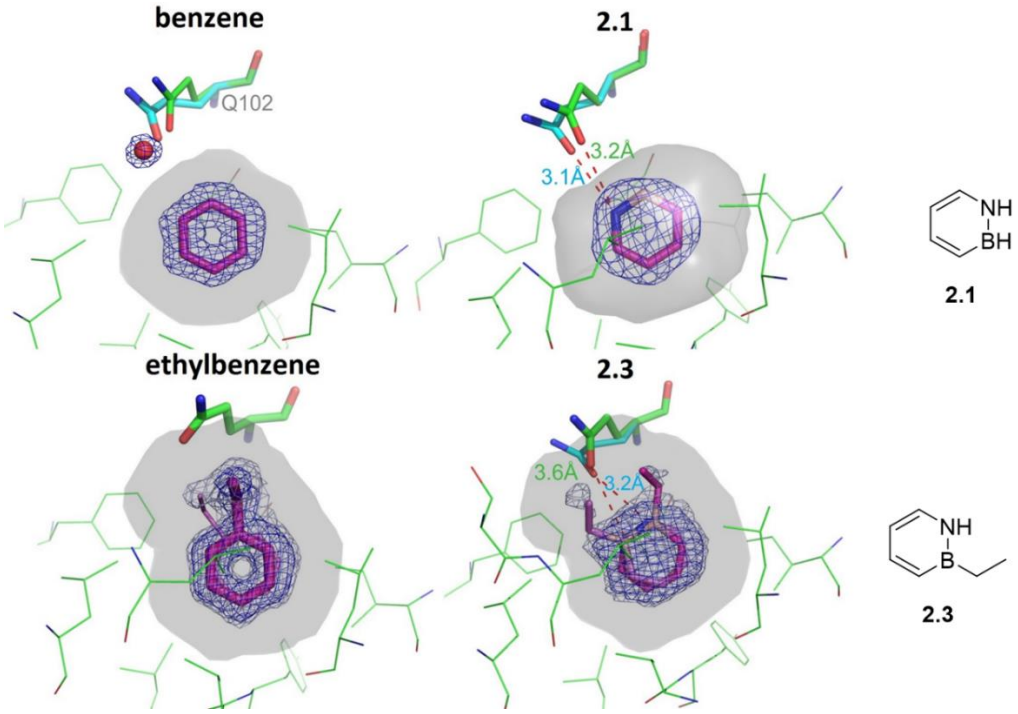

A crystal structure of *N*-ethyl substituted azaborine (**2.2**)-bound L99A/M102Q complex was also obtained (Figure 2.17). Hydrogen bonding capability of this ligand is inhibited by the ethyl substituent, thus it serves as an internal control (binding thermodynamics using this compound as a reference will be discussed in 2.3.5). In the structure, a comparable binding mode was observed as seen in the ethylbenzene-bound complex, with two alternative conformations. There was no indication of hydrogen bonding interactions and we observed BH group of the ligand was positioned away from the carbonyl oxygen of Gln102 in both conformations.

Figure 2.17 X-ray structure of **2.2**-bound L99A/M102Q

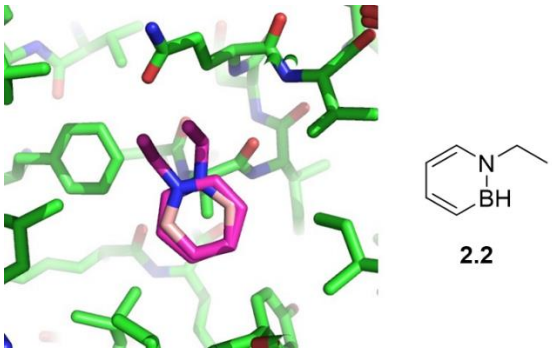

2.3.4 Isothermal Titration Calorimetry Data

To better understand the energetics of the azaborine-protein hydrogen bonding interactions, we determined the binding free energies of each complex using isothermal titration calorimetry (ITC). As expected, in the non-polar cavity (L99A) azaborine ligands **2.1** and **2.3** lost 0.5 and 0.4 kcal/mol, respectively, in binding free energy compared to their arene isosteres (Table 2.12, left column). This is consistent with azaborines having more polar character and thus incurring a higher desolvation penalty.

In contrast, binding of azaborines in the polar cavity (L99A/M102Q) showed 0.2–0.4 kcal/mol stronger binding free energy relative to the carbonaceous analogs (Table 2.12, right column). As observed in the crystal structures, this is due to a hydrogen bonding interaction, which apparently is strong enough to overcome the azaborines' desolvation penalty. We also observed lower binding affinity in the complexes of ethyl-substituted

ligand-bound L99A/M102Q compared to the unsubstituted ligand-bound cases, presumably due to the higher steric demand of the ethyl group.[48]

Table 2.12 Binding free energy and affinity determined by ITC

	L99A		L99A/M102Q	
	$\triangle G$ (kcal/mol)	K_a (x10^4 M^{-1})	$\triangle G$ (kcal/mol)	K_a (x10^4 M^{-1})
benzene	–5.54 ± 0.04	1.89 ± 0.12	–5.96 ± 0.04	3.95 ± 0.29
2.1	–5.04 ± 0.03	0.77 ± 0.05	–6.40 ± 0.02	8.77 ± 0.28
ethylbenzene	–5.54 ± 0.06	1.91 ± 0.18	–5.37 ± 0.03	1.41 ± 0.07
2.3	–5.12 ± 0.02	0.90 ± 0.04	–5.59 ± 0.02	2.08 ± 0.06
2.2	–6.11 ± 0.03	5.19 ± 0.30	–5.73 ± 0.04	2.66 ± 0.17

2.3.5 Thermodynamic Cycle Analysis

In the analysis of energetic contributions of protein-ligand interactions, we need to consider various factors, such as the hydrophobic effect, desolvation cost, hydrogen bonding, electrostatic interactions, etc., that attribute to the observed total energy.[19b] Therefore, it is difficult to determine the energetic contribution of hydrogen bonding by simply comparing a pair of free energy values; e.g. the binding free energies of benzene and **2.1** to the L99A/M102Q mutant. In this simple analysis, the binding free energy difference ($\Delta\Delta G = \Delta G_{\mathbf{2.1}\text{-L99A/M102Q}} - \Delta G_{\text{benzene-L99A/M102Q}} = -6.40 - (-5.96) = -0.44$ kcal/mol) represents the totality of electronic structure differences between benzene and **2.1**, not just hydrogen bonding.

[48] Merski, M.; Fischer, M.; Balius, T. E.; Eidam, O.; Shoichet, B. K. *Proc. Natl. Acad. Sci. U. S. A.* **2015**, *112*, 5039–5044.

To quantify the stabilization energy gained from the hydrogen bonding interactions alone, we turned to double mutant thermodynamic cycle analysis. This method uses "wild-type" and "mutant" versions of both the enzyme and ligand, with each "mutant" lacking the interacting groups of interest. The energetic cost, $\Delta\Delta G$, of removing the ligand functional group both in the presence and the absence of the enzyme residue with which it interacts can be calculated, and the difference between these energies, $\Delta\Delta\Delta G$, is the energy of the interaction. In our case, the wild-type enzyme is the L99A/M102Q T4 lysozyme and the mutant enzyme (lacking the hydrogen bonding interaction) is the L99A T4 lysozyme. The wild-type ligands are the NH-containing 1,2-azaborines, **2.1** and **2.3**, and the mutant ligands are benzene and ethylbenzene.

Using this simple thermodynamic cycle analysis we estimated the free energy of hydrogen bonding between Gln102=O and the NH of **2.1** and **2.3** to be –0.94 and –0.64 kcal/mol, respectively (Figure 2.18). The weaker hydrogen bond interaction for **2.3** compared to **2.1** with the Gln102 residue may arise from a steric penalty induced by the ethyl substituent. This is consistent with the longer average hydrogen bond distance with Gln102 residue in the **2.3**-L99A/M102Q structure compared to the **2.1**-L99A/M102Q structure. The estimated hydrogen bond strengths between the azaborine NH and the glutamine carbonyl oxygen are within a typical range for neutral-neutral hydrogen bonds in an aqueous environment (0.5–1.5 kcal/mol).[49]

[49] Davis, A. A.; Teague, S. J. *Angew. Chem., Int. Ed*. **1999**, *38*, 736–749.

Figure 2.18 Thermodynamic cycle analysis to estimate hydrogen bond strengths

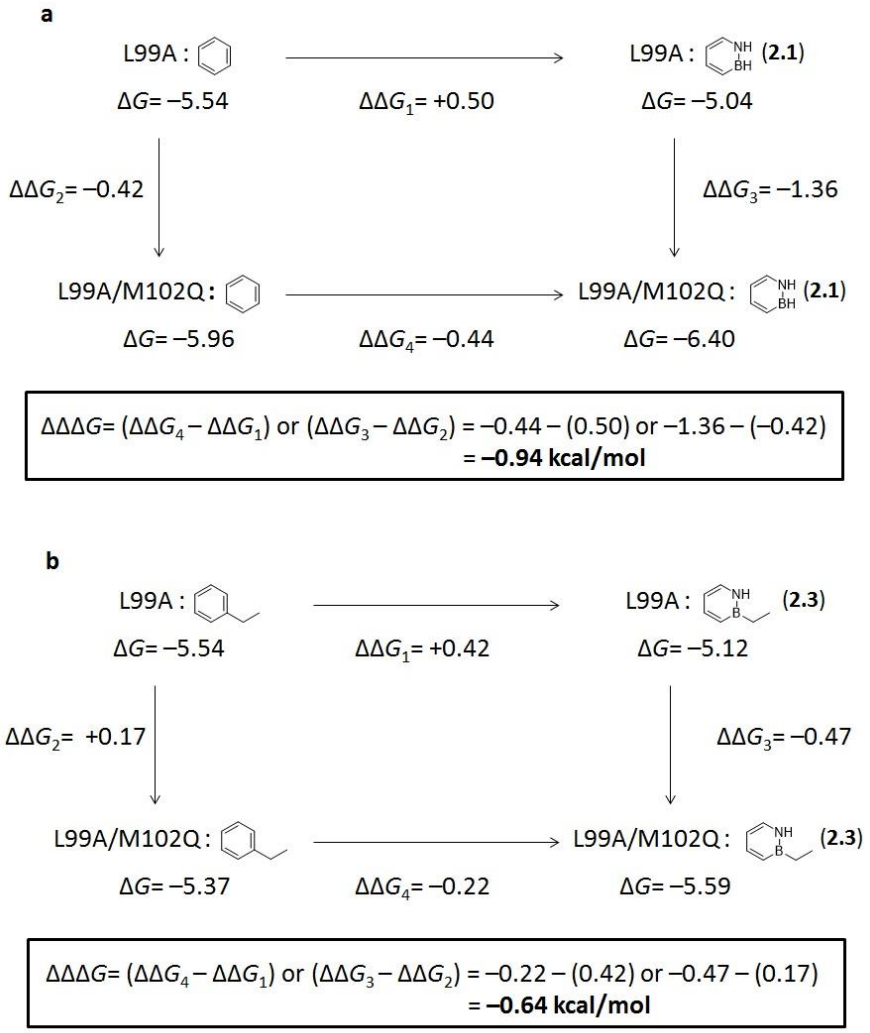

These estimated energetic values may also contain an additional electrostatic contribution between dipolar azaborine molecules and protein binding sites. Therefore, we experimentally determined the binding free energies of *N*-ethyl substituted azaborine (**2.2**) with both L99A and L99A/M102Q to elucidate such interactions (Table 2.12). The resulting thermodynamic cycle analysis with this ligand compared to ethylbenzene is shown in Figure 2.19. The energy derived from the analysis is +0.21 kcal/mol, the energetic

contributions from other polar interactions beyond hydrogen bonding, which turns into rather a repulsive interaction. This may arise from unfavorable interaction between the BH group of the ligand and oxygen of Gln102 as seen in the crystal structure (Figure 2.17). Thus, to better estimate the hydrogen bond strength conferred by **2.3**, we took this energy into account and performed another thermodynamic cycle analysis using **2.2** as the "mutant" ligand (Figure 2.20). The estimated energy from the analysis is –0.85 kcal/mol, slightly higher than the value estimated using ethylbenzene as a control (–0.64 kcal/mol). By the same analogy, the hydrogen bond strength for **2.1** with consideration of the repulsive dipolar interaction leads to –1.15 kcal/mol. Overall, in addition to structural evidences, we conclude that our estimation of hydrogen bond strengths for **2.1** and **2.3** accounts for hydrogen bond as a strong component of the total electrostatic interaction.

Figure 2.19 Thermodynamic cycle analysis using **2.2** as the azaborine ligand

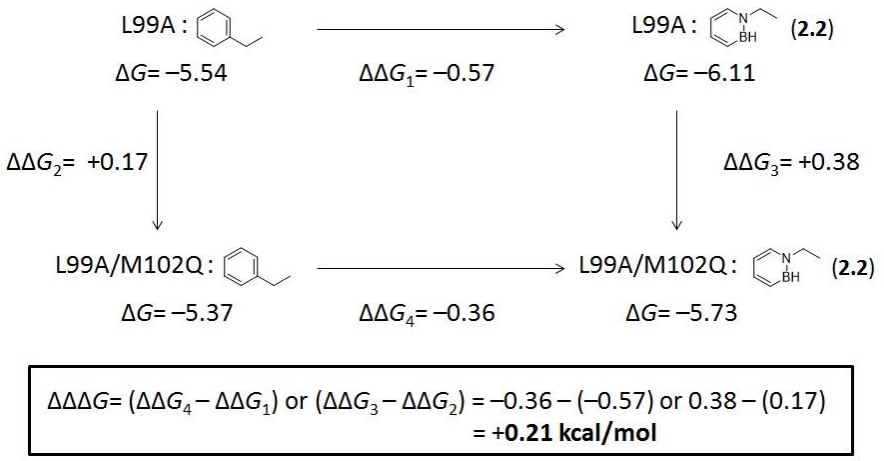

Figure 2.20 Thermodynamic cycle analysis between **2.2** and **2.3**

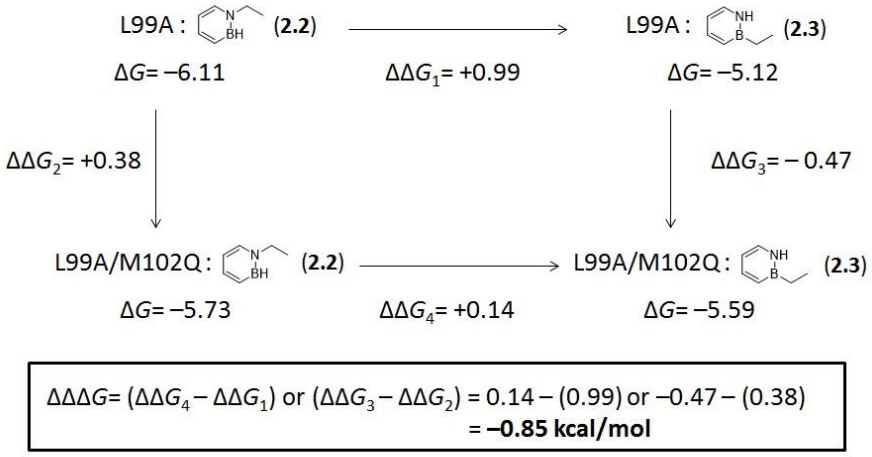

2.4 Conclusions

Aromatic rings are a ubiquitous structural motif in medicinal chemistry, and diversification of chemical structures is a routine practice for medicinal chemists as part of lead compound optimization efforts. Thus, as boron-nitrogen-containing isosteres of arenes, azaborine heterocycles have the potential to expand the chemical space of arenes and generate novel pharmacological activity.

We demonstrated that 1,2- azaborines can be readily accommodated in classic aryl recognition pockets and established one of 1,2- azaborine's distinguishing features from arenes, i.e., its ability to serve as an NH hydrogen bond donor in a biological setting. Specifically, we directly compared NH-containing 1,2-azaborines and their carbonaceous arene analogs in binding to a biological model system, T4 lysozyme mutants-L99A and L99A/M102Q.

We utilized high-resolution protein X-ray crystallography and ITC experiments to achieve a systematic quantitative analysis of hydrogen bonding interactions. A Gln102=O···H–N hydrogen bond was observed in the complexes of 1,2-azaborine in the polar binding pocket of L99A/M102Q. Using a simple thermodynamic cycle analysis with ethylbenzene as the "mutant" ligand lacking the hydrogen bond capability, the strengths of the hydrogen bond were estimated to be 0.94 and 0.64 kcal/mol for **2.1** and **2.3**, respectively. The quantitative structural and thermodynamic binding data of this work will serve as a general reference in future applications of 1,2-azaborines as a pharmacophore.

2.5 Experimental

2.5.1 General Information

All oxygen- and moisture-sensitive manipulations were carried out under an inert atmosphere (N_2) using either standard Schlenk techniques or a glove box. THF, Et_2O, CH_2Cl_2, toluene and pentane were purified by passing through a neutral alumina column under argon. Acetonitrile was dried over CaH_2 and distilled under N_2 prior to use. Pd/C was purchased from Strem and heated under high vacuum at 100°C for 12 hours prior to use. Silica gel (230-400 mesh) was dried for 12 hours at 180 °C under high vacuum. Flash chromatography was performed with this silica gel under an inert atmosphere. All other chemicals and solvents were purchased and used as received.

NMR spectra were recorded on a Varian VNMRS 600 MHz, VNMRS 500 MHz, INOVA 500 MHz, or VNMRS 400 MHz spectrometer. Deuterated solvents were purchased from Cambridge Isotope Labs. ^{11}B NMR spectra were externally referenced to BF_3•Et_2O (δ 0). All NMR chemical shifts are reported in ppm relative to residual solvent for ^{1}H and ^{13}C NMR. Infrared spectroscopy was performed on a Bruker ALPHA-Platinum FT-IR Spectrometer with ATR-sampling module. High-resolution mass spectrometry analyses were performed by direct analysis in real time (DART) on a JEOL AccuTOF DART instrument.

2.5.2 Synthesis of 1,2-Azaborines

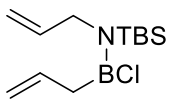

2.23

To an oven-dried 1 L round bottom flask equipped with a stir bar was added triallylborane (6.70 g, 50.0 mmol) and 250 mL CH_2Cl_2. The reaction mixture was cooled to -78 °C. A solution of boron trichloride (100 mL, 100 mmol, 1.0 M in hexane) was added to the reaction mixture via cannula transfer at –78 °C over 30 min, and the mixture was stirred for 3.5 h at this temperature. A solution of N-TBS-allylamine (25.7 g, 150 mmol) in 20 mL CH_2Cl_2 was added to the reaction mixture at –78 °C, followed by triethylamine (21.0 mL, 150 mmol). The reaction mixture was slowly warmed to room temperature and stirred for 16 h. At the conclusion of the reaction, approximately two-third of the solvent was removed under vacuum. The reaction mixture was passed through a medium-porosity frit, and the filtrate was concentrated under reduced pressure. Vacuum distillation (50-60 °C, 350 mTorr) afforded the desired product **2.23** as a colorless liquid (32.3 g, 84%). Spectra of the isolated compound matched published values.[6a]

2.24

In a glove box, Grubbs 1st generation catalyst (1.79 g, 2.17 mmol) was added in portion to a stirring solution of aminoborane **2.23** (56.0 g, 217 mmol) in 500 mL toluene in an oven-dried 1 L round bottom flask. The solution was stirred at room temperature for 20 min. To this solution of the ring-closed product, Pd/C (14.0 g, 13.16 mmol, 10 wt. % on activated carbon) was added. The reaction mixture was refluxed at 135 °C for 16 h. The reaction was monitored by ^{11}B NMR. Usually at this point ^{11}B NMR indicates the reaction is incomplete, with a minor starting material peak (ca. 42.9 ppm) remaining. Additional Pd/C (3.00 g, 2.82 mmol, 10 wt. % on activated carbon) was added to the reaction mixture and refluxed for an additional 24 h. At the conclusion of the

reaction, the reaction mixture was passed through a disposable flash chromatography column packed with paper wipes. The solvent was removed under reduced pressure. Vacuum distillation (65-70 °C, 1000 mTorr) afforded the desired product **2.24** as a colorless liquid (25.8 g, 52% over two steps). Spectra of the isolated compound matched published values.[6]

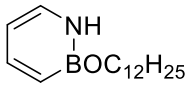

2.25

To an oven-dried 100 mL round bottom flask was added **2.24** (5.00 g, 22.0 mmol), acetamide (1.30 g, 22.0 mmol), and 45 mL acetonitrile. The reaction mixture was refluxed at 85 ºC and stirred for 15 h. After cooling to room temperature, the reaction mixture was concentrated under reduced pressure. The reaction mixture was redissolved in 23 mL THF and added dodecanol (4.09 g, 22.0 mmol). The reaction mixture was heated to 50 ºC and stirred for 1.5 h. The solvent was removed under reduced pressure. Silica gel column chromatography in a glove box using Et_2O as the eluent afforded the desired product **2.25** as a white solid (5.5 g, 95%). Spectra of the isolated compound matched published values.[50]

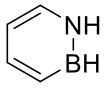

2.1

An oven-dried 250 mL two-neck round bottom flask was charged with **2.25** (5.5 g, 20.9 mmol) and 22 mL bis(2-butoxyethyl) ether. To the reaction flask, lithium aluminum hydride (1.45 g, 38.2 mmol) was added at 0 ºC and the reaction mixture was stirred for 30 min. Decanoic acid (25.8 g, 150 mmol) was added to the reaction mixture to quench at 0 ºC and the reaction mixture was stirred for 30 min. Vacuum transfer

[50] Baggett, A. W. New Strategies Enabling Diverse Functionalization of Aromatic 1,2-Azaborine Motifs. PhD, Boston College, 2016.

afforded the desired product **2.1** as a colorless oil (1.07 g, 65%). Spectra of the isolated compound matched published values.[6]

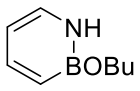

2.26

To an oven-dried 100 mL round bottom flask was added **2.24** (2.27 g, 10.0 mmol), acetamide (650 mg, 11.0 mmol), and 50 mL acetonitrile. The reaction mixture was refluxed at 85 °C and stirred for 15 h. After cooling to room temperature, the reaction mixture was concentrated under reduced pressure. The reaction mixture was redissolved in 10 mL THF and added *n*-butanol (1.83 mL, 20.0 mmol). The reaction mixture was stirred at room temperature for 1 h. The solvent was removed under reduced pressure. Silica gel column chromatography in a glove box using 10% Et_2O/pentane as the eluent afforded the desired product **2.26** as a white solid (1.33 g, 88%). Spectra of the isolated compound matched published values.[6b]

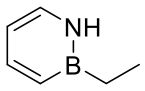

2.3

To an oven-dried 100 mL round bottom flask containing **2.26** (1.00 g, 6.62 mmol) in Et_2O (25 mL) a solution of ethyllithium in Et_2O was added dropwise under nitrogen atmosphere at –30 °C (the ethyllithium solution was prepared from 26.50 mL of 0.5 M solution of EtLi in benzene/cyclohexane, 13.24 mmol, which was concentrated to dryness and then redissolved in 13 mL Et_2O). The reaction mixture was stirred for 1 h as it was allowed to slowly warm up to room temperature. The reaction progress was monitored by ^{11}B NMR until completion. At the end of the reaction, an HCl solution (6.62 mL of 2.0 M solution in Et_2O, 13.2 mmol) was added at –30 °C, and the reaction mixture was allowed to warm to room temperature and stirred for 1h. The solvent was removed under vacuum, and the resulting crude residue was purified by column chromatography with isopentane as the eluent in a glove box. The desired product **2.3** was

isolated as a colorless oil (397 mg, 56%). Spectra of the isolated compound matched published values and are included in Chapter 3.[10]

Synthetic procedures and characterization of compound **2.2** are described in Chapter 3.

2.5.3 Protein Preparation and Crystallization

Escherichia coli strain RR1 (ATCC® 31343™) was transformed with the subcloned plasmids (Addgene plasmids # 18476 and 18477 from Brian Matthews lab, for T4 lysozyme WT* (**L99A**) and T4L mutant (S38D **L99A M102Q** N144D), respectively. Ampicillin-resistant transformants were isolated and stored in 20% glycerol stock solution in LB (lysogeny broth) media.

The bacteria were grown in 200 mL LB media supplemented with 40 mg ampicillin at 37 ºC for 12 h. 160 mL of this culture was added to an Erlenmeyer flask containing 4 liters of LB media with 800 mg ampicillin. The resulting mixture was incubated at 37 ºC at 240 rpm shaking speed with filtered air supply. When the optical density reached 0.7 at 600 nm, the bacterial cultures were cooled to room temperature by removing them from the incubator. Once cooled to room temperature, isopropyl-β-D-1-thiogalactopyranoside (IPTG) was added (final concentration of 0.7 mM) to induce the protein expression. The cultures were incubated for the induction at 110 rpm shaking speed for 21 h at 25 ºC. Then the cultures were centrifuged down at 5000 rpm for 30 min at 4 ºC. The resulting pellet was resuspended in 300 mL of 0.1 M sodium phosphate (pH 6.6), 0.2 M NaCl and added 30 mL of 0.5 M EDTA (pH 8.0) and the suspension was stirred for 17 h at 4 ºC. To the suspension was then added 30 mL of 1.0 M $MgCl_2$ and 0.5 mL of DNaseI, and the mixture

was stirred at room temperature for 8 h. After the lysis and centrifugation at 15000 rpm for 30 min at 4 ºC, the lysate was collected and dialyzed against 20 mM sodium phosphate (pH 6.5 for L99A and pH 6.3 for L99A/M102Q) at 4 ºC overnight. The solution containing protein was then loaded onto a CM Sepharose Fast Flow (GE healthcare) column that was pre-equilibrated with equilibration buffer (50 mM Tris, 1 mM EDTA, pH 7.3). The column was washed with 100 mL of equilibration buffer and eluted with a 600 mL linear gradient of 300 mM NaCl within the equilibration buffer, and the fractions containing pure protein were collected.

For crystallization, the protein sample was dialyzed against 100 mM sodium phosphate, 550 mM NaCl, 0.02% NaN_3 (pH 6.5 for L99A and pH 6.3 for L99A/M102) at 4 ºC overnight. 2- Mercaptoethanol (final concentration of 5 mM) was added to the dialyzed sample, and the protein solution was concentrated to 40 mg/mL using Vivaspin 20 (10,000 mwco (molecular weight cutout)). Protein concentrations were determined by measuring absorption at 280 nm. Any precipitate was removed by spinning prior to crystallization.

The crystals were obtained by vapor-diffusion hanging-drop or sitting-drop method. 5 µL of the 40 mg/mL protein solution was mixed with 5 µL of reservoir solution (2.0-2.2 M sodium/potassium phosphate, pH 6.7-7.1, 50 mM 2-mercaptoethanol, 50 mM 2-hydroxyethyl disulfide), and equilibrated against 1.0 mL of the reservoir solution at 4 ºC. Crystals normally grew within 1-2 weeks.

2.5.4 Complex Preparation

Suitable crystals were picked and transferred into a microcentrifuge tube and maintained in 50 µl of the mother liquor. Crystals were equilibrated with ligands at 4 ºC for 2-7 days by vapor diffusion method by placing a droplet of each ligand inside of the snap-cap of the tube. The complexes were prepared in a glove box for azaborine ligands.

2.5.5 ITC Experiments

Isothermal titration calorimetry (ITC) experiments were carried out with Nano ITC Low Volume calorimeter from TA instruments. Titrations were run by injection of ligand solution to protein solution at 10 ºC and 310 rpm stirring rate with a data collection interval of 4 min/injection. A total of 40 injections of a total volume of 100 uL ligand solution (2.66-3.32 mM) were done with 320 uL protein solution (~0.2 mM). Both ligand and protein were in a degassed buffer solution of 5% PEG400, 0.5 M NaCl, 0.1 M sodium phosphate (pH 6.8). The protein solution was prepared by dialyzing against the degassed buffer and the concentrations were determined by molar absorptivity at 280 nm. Due to the limited solubility of the small molecule ligands in aqueous buffer, accurate concentrations of ligand solution were determined by GC against a calibrated internal standard. Baseline mixing heats were estimated by injection of ligand solution into the buffer and subtracted from individual titration curve. The resulting reaction heat profiles were fit to the independent binding model with the stoichiometry n fixed to 1.0. All data were analyzed using NanoAnalyze software. Experiments were repeated five times and averaged with standard deviation error of the mean.

* Representative ITC data

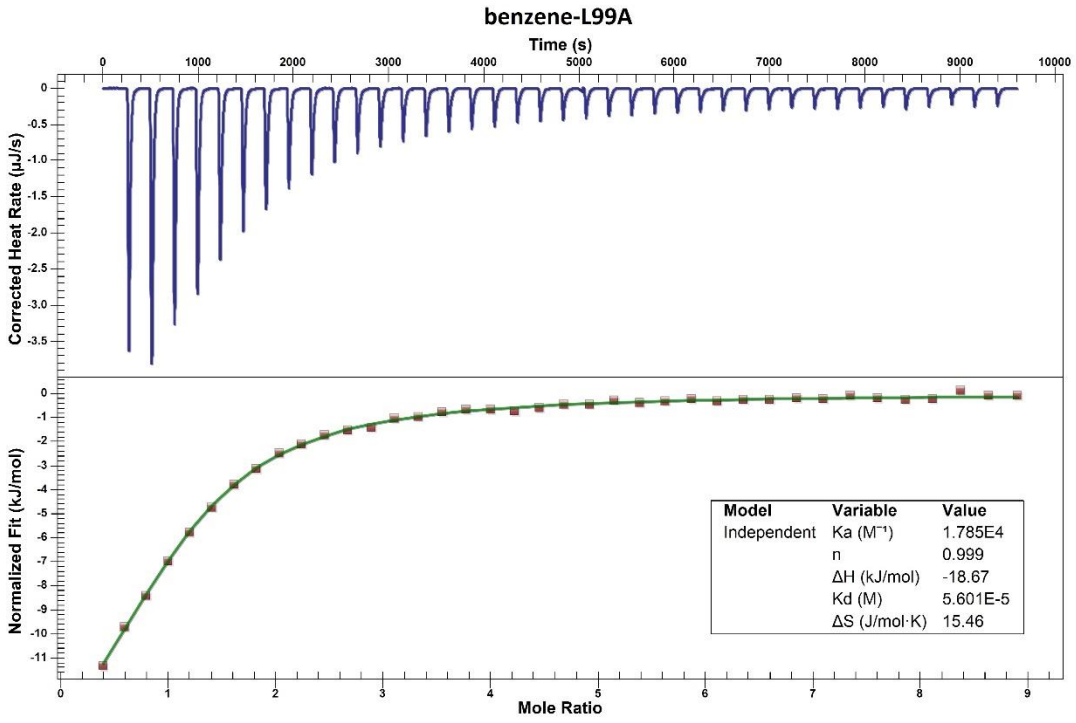

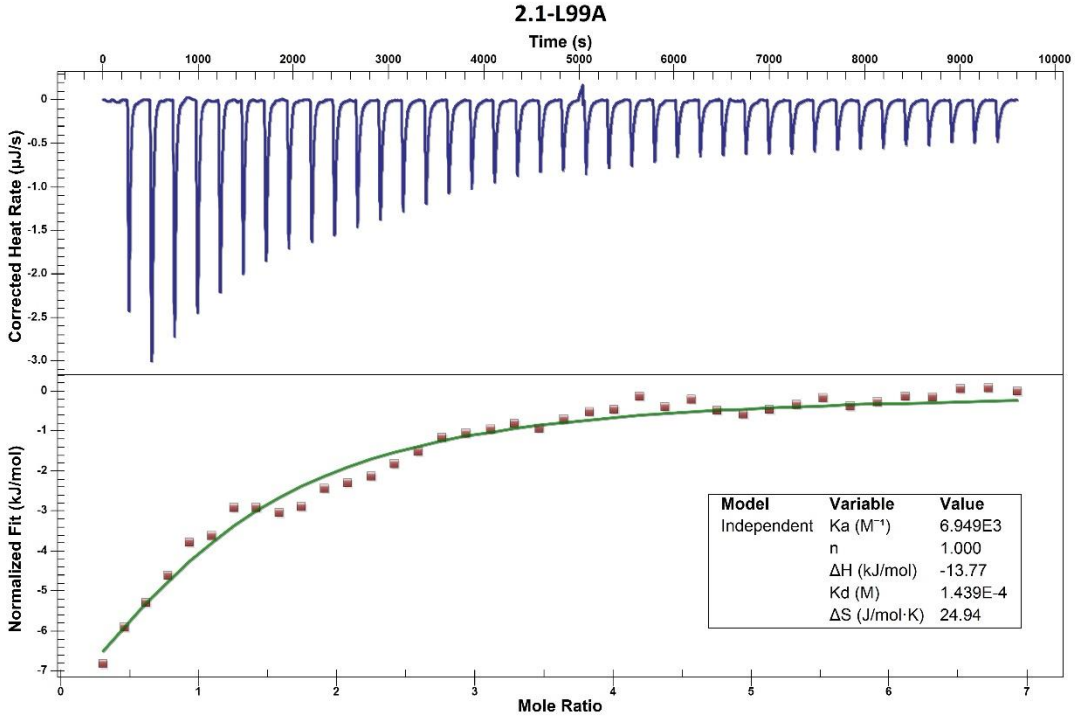

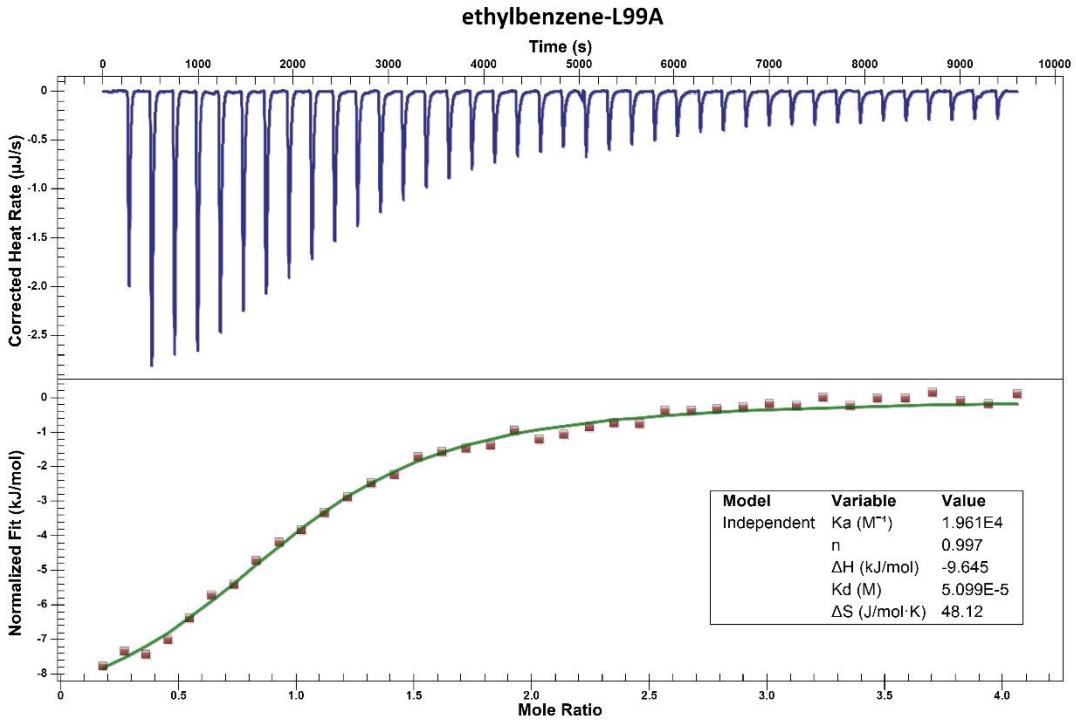
ethylbenzene-L99A
Time (s)
Corrected Heat Rate (µJ/s)
Normalized Fit (kJ/mol)
Mole Ratio
Model Variable Value
Independent Ka (M⁻¹) 1.961E4
n 0.997
ΔH (kJ/mol) -9.645
Kd (M) 5.099E-5
ΔS (J/mol·K) 48.12

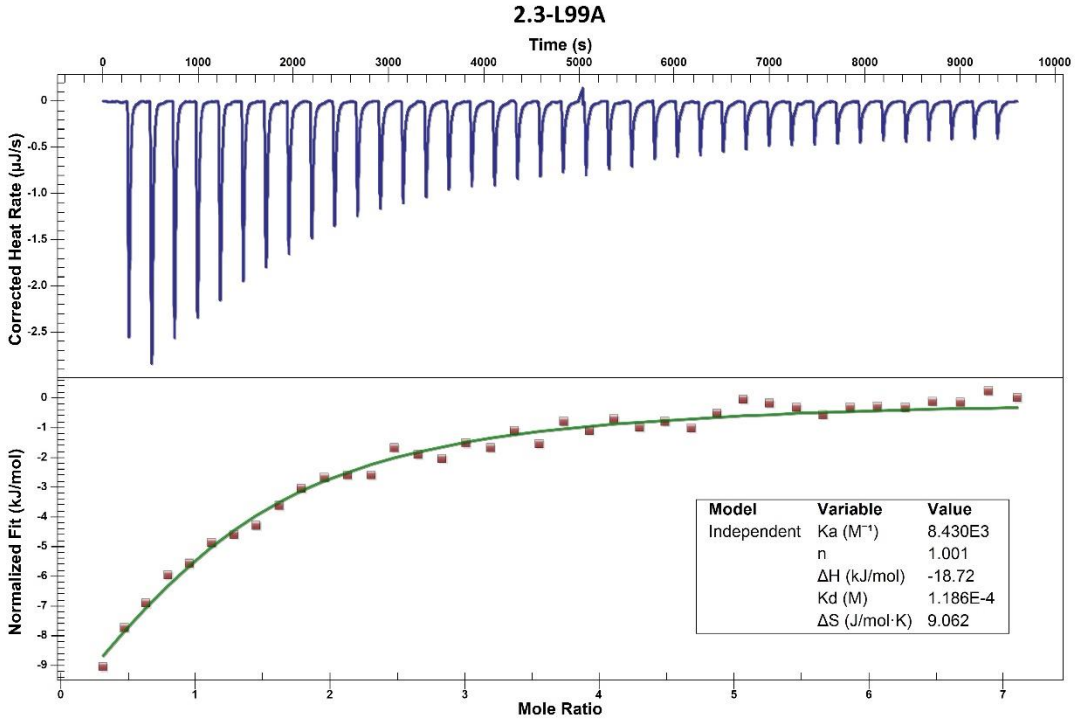
2.3-L99A
Time (s)
Corrected Heat Rate (µJ/s)
Normalized Fit (kJ/mol)
Mole Ratio
Model Variable Value
Independent Ka (M⁻¹) 8.430E3
n 1.001
ΔH (kJ/mol) -18.72
Kd (M) 1.186E-4
ΔS (J/mol·K) 9.062

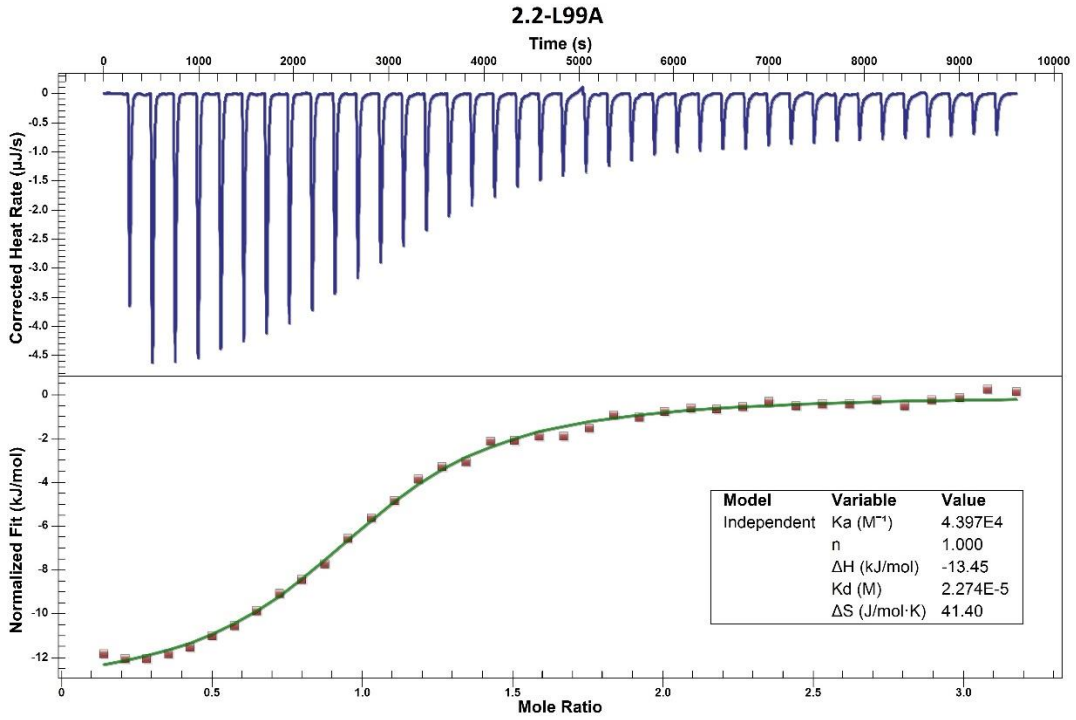
2.2-L99A
Time (s)
Corrected Heat Rate (µJ/s)
Normalized Fit (kJ/mol)
Mole Ratio
Model Variable Value
Independent Ka (M⁻¹) 4.397E4
n 1.000
ΔH (kJ/mol) -13.45
Kd (M) 2.274E-5
ΔS (J/mol·K) 41.40

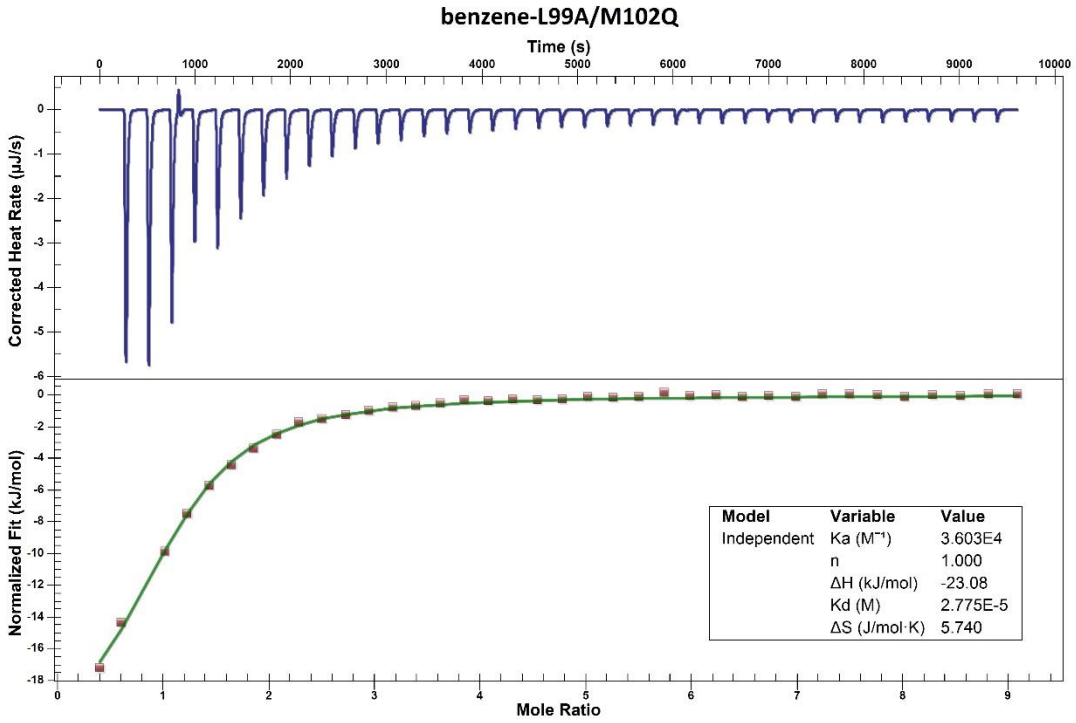
benzene-L99A/M102Q
Time (s)
Corrected Heat Rate (µJ/s)
Normalized Fit (kJ/mol)
Mole Ratio
Model Variable Value
Independent Ka (M⁻¹) 3.603E4
n 1.000
ΔH (kJ/mol) -23.08
Kd (M) 2.775E-5
ΔS (J/mol·K) 5.740

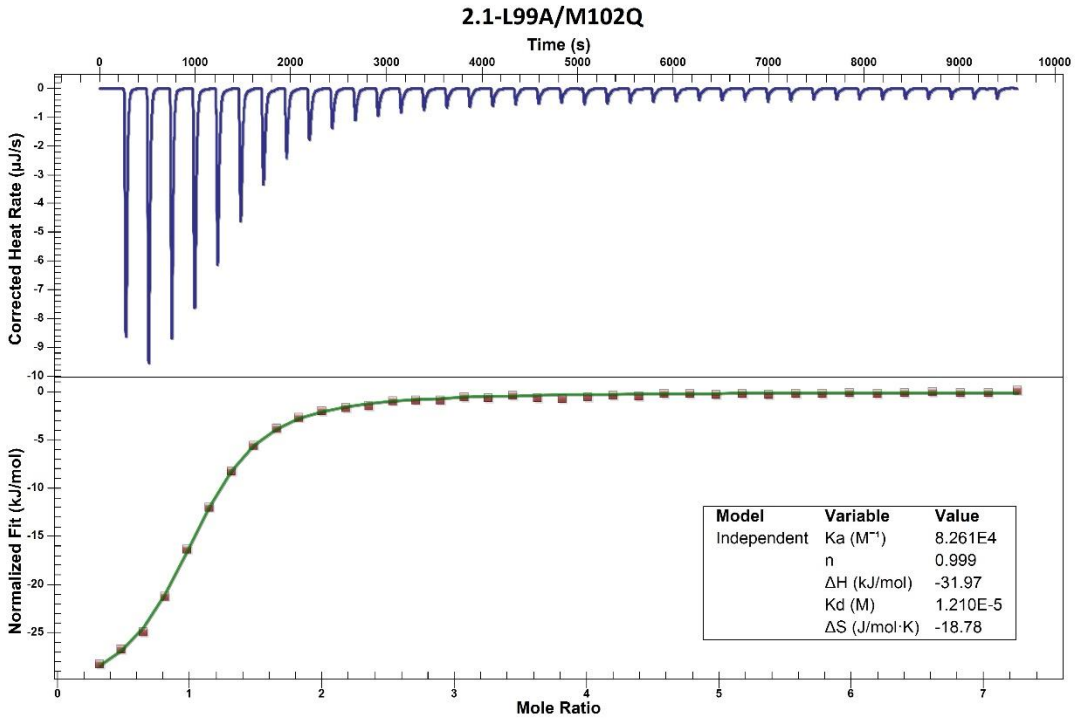
2.1-L99A/M102Q
Time (s)
Corrected Heat Rate (µJ/s)
Normalized Fit (kJ/mol)
Mole Ratio
Model Variable Value
Independent Ka (M⁻¹) 8.261E4
n 0.999
ΔH (kJ/mol) -31.97
Kd (M) 1.210E-5
ΔS (J/mol·K) -18.78

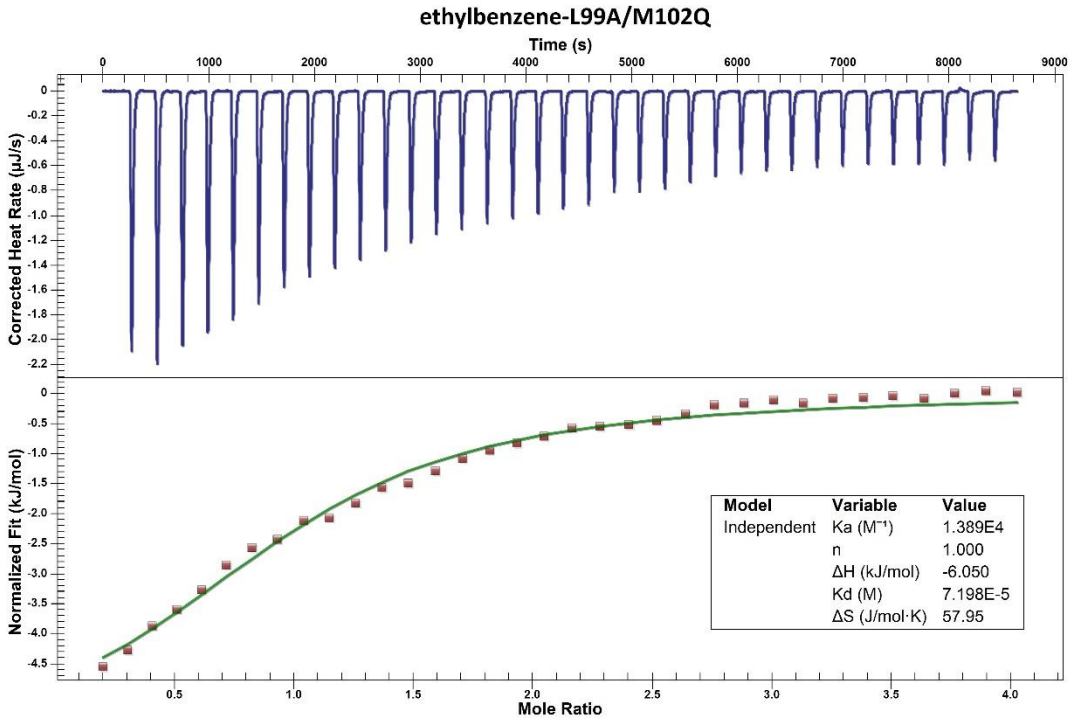
ethylbenzene-L99A/M102Q
Time (s)
Corrected Heat Rate (µJ/s)
Normalized Fit (kJ/mol)
Mole Ratio
Model Variable Value
Independent Ka (M⁻¹) 1.389E4
n 1.000
ΔH (kJ/mol) -6.050
Kd (M) 7.198E-5
ΔS (J/mol·K) 57.95

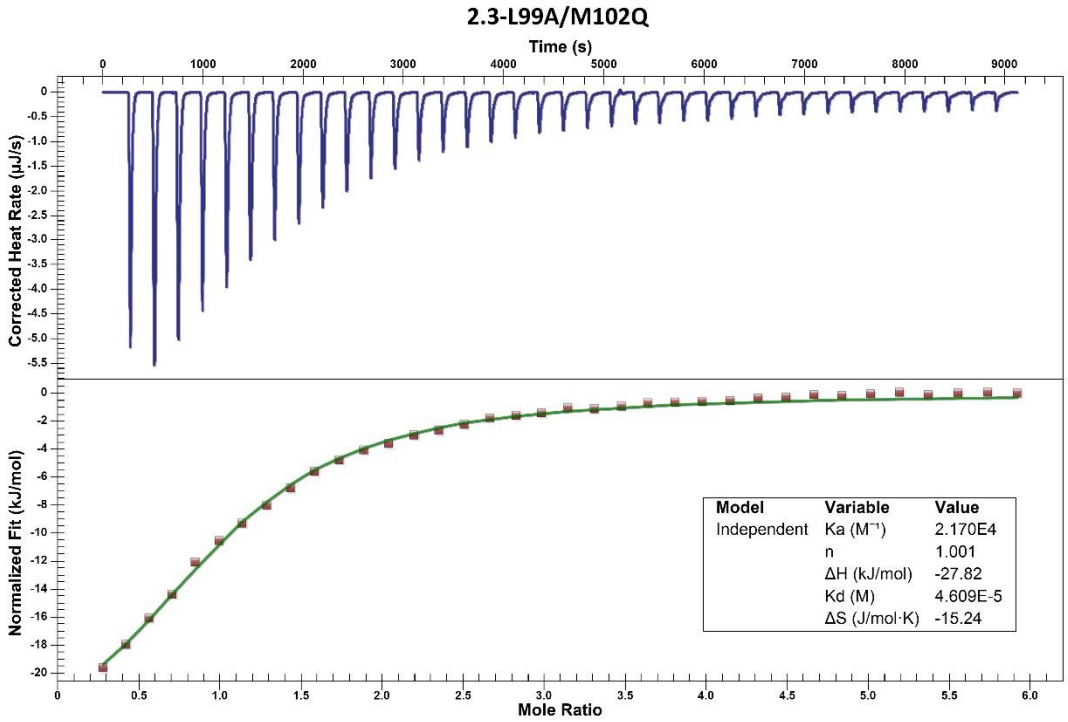
2.3-L99A/M102Q
Time (s)
Corrected Heat Rate (µJ/s)
Normalized Fit (kJ/mol)
Mole Ratio
Model Variable Value
Independent Ka (M⁻¹) 2.170E4
n 1.001
ΔH (kJ/mol) -27.82
Kd (M) 4.609E-5
ΔS (J/mol·K) -15.24

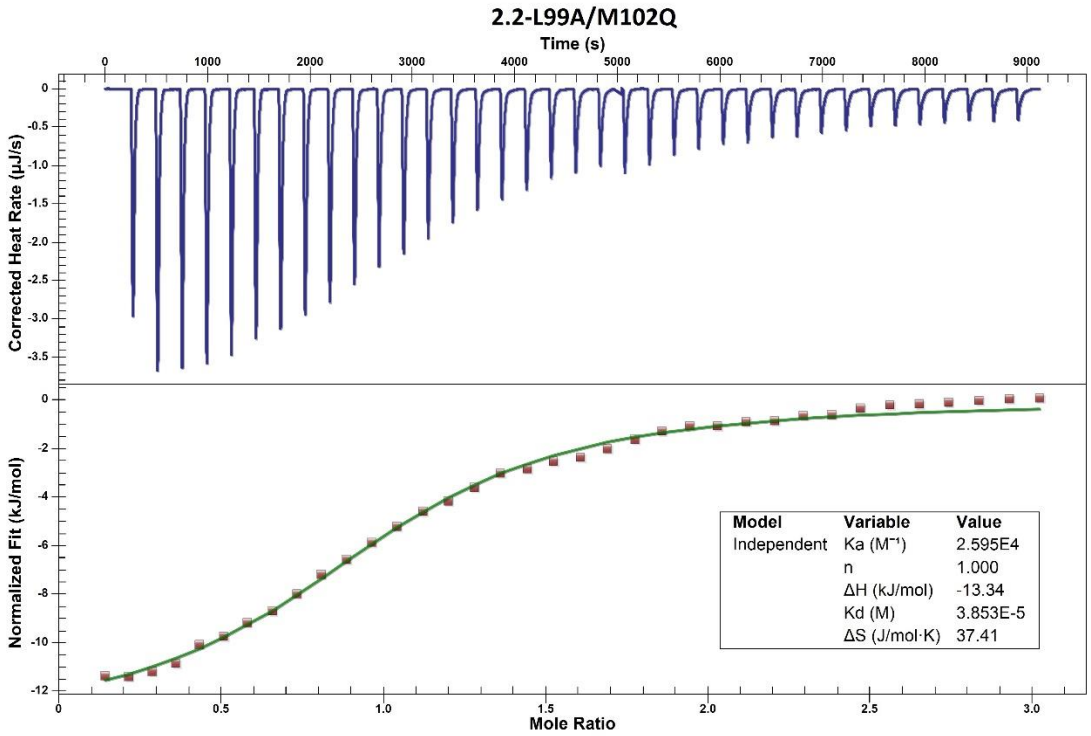
2.2-L99A/M102Q
Time (s)
Corrected Heat Rate (µJ/s)
Normalized Fit (kJ/mol)
Mole Ratio
Model Variable Value
Independent Ka (M⁻¹) 2.595E4
n 1.000
ΔH (kJ/mol) -13.34
Kd (M) 3.853E-5
ΔS (J/mol·K) 37.41

2.5.6 X-ray Structure Data Collection, Structure Determination, and Refinement

Prior to X-ray data collection the crystals were flash-frozen in liquid nitrogen with protection of *N*-paratone (Hampton Research). Data were collected from beamline 8.3.1. at the Advanced Light Source, Berkeley, CA. Reflection data were integrated and scaled with d*TREK.[51] Molecular replacement was performed using PHASER-MR[52] with the ligand-free T4 lysozyme L99A (PDB code: 3DMV[53]) and L99A/M102Q (PDB code: 1LGU[3636]) as the starting models. Initial refinements were carried out with simulated annealing using PHENIX[54] and COOT[55]. Ligand restraints of azaborines were generated by REEL based on knowledge of the crystal structures of the small molecules. All models were checked by MolProbity[56] and the PDB validation tool prior to deposition. Figures were generated with PyMol (The PyMOL Molecular Graphics System, Schrödinger, LLC). The ethyl derivatives were solved to a resolution of 1.3, 1.47 and 1.65 Å for ethylbenzene-L99A/M102Q, **2.3**-L99A/M102Q, and **2.3**-L99A, respectively, allowing alternative conformations, which are visible in the electron density maps, to be modeled explicitly. Their occupancies were refined automatically within phenix.refine using the "strategy=occupancies" flag. Hence occupancies were determined without manual intervention during the final cycles of the structural refinement.

---

[51] Pflugrath, J. W. *Acta Cryst.* **1999**, *D55*, 1718–1725.
[52] McCoy, A. J.; Grosse-Kunstleve, R. W.; Adams, P. D.; Winn, M. D.; Storoni, L. C.; Read, R. J. *J. Appl. Cryst.* **2007***, 40*, 658–674.
[53] Liu, L.; Baase, W. A.; Matthews, B. W. *J. Mol. Biol.* **2009**, *385*, 595–605.
[54] Adams, P. D.; Afonine, P. V.; Bunkóczi, G.; Chen, V. B.; Davis, I. W.; Echols, N.; Headd, J. J.; Hung, L.-W.; Kapral, G. J.; Grosse-Kunstleve, R. W.; McCoy, A. J.; Moriarty, N. W.; Oeffner, R.; Read, R. J.; Richardson, D. C.; Richardson, J. S.; Terwilliger, T. C.; Zwart, P. H. *Acta Cryst.* **2010**, *D66*, 213–221.
[55] Emsley, P.; Lohkamp, B.; Scott, W. G.; Cowtan, K. *Acta Cryst.* **2010**, *D66*, 486–501.
[56] Chen, V. B.; Arendall, W. B.; Headd, J. J.; Keedy, D. A.; Immormino, R. M.; Kapral, G. J.; Murray, L. W.; Richardson, J. S.; Richardson, D. C. *Acta Cryst.* **2010**, *D66*, 12–21.

2.5.7 Data Deposition

The coordinates and structure factors have been deposited in the RCSB Protein Data Bank with PDB ID's 5JWS, 5JWT, 5JWU, 5JWV, and 5JWW for L99A with *B*-Et-1,2-azaborine (**2.3**), L99A/M102Q with benzene, 1,2-dihydro-1,2-azaborine (**2.1**), ethylbenzene, *B*-Et-1,2-azaborine (**2.3**), respectively.

* Overview of PBD codes for ligands in the two T4L cavities

ligand	L99A	L99A/ M102Q
benzene	3HH4[46]	5JWT
2.1	3HH3[46]	5JWU
ethylbenzene	3HH6[46]	5JWV
2.3	5JWS	5JWW

* X-ray Data Collection and Structure Refinement Statistics

Ligand	*B*-Et-1,2-Azaborine (**2.3**)	benzene
Protein	L99A	L99A/M102Q
PDB entry	**5JWS**	**5JWT**
Data collection		
Space group	$P3_221$	$P3_221$
Cell dimensions		
a, *b*, *c* (Å)	60.13, 60.13, 95.61	60.23, 60.23, 96.87
α, β, γ (°)	90, 90, 120	90, 90, 120
Resolution (Å)	31.87-1.65 (1.71 - 1.65)[a]	45.93-1.41 (1.46-1.41) [a]
R_{merge}	0.118 (0.294)	0.058 (0.321)
$I/\sigma(I)$	9.6 (3.3)	10.7 (2.9)
Completeness (%)	96.0 (96.0)	99.6 (99.6)
Redundancy	5.65 (5.54)	5.19 (4.98)
Refinement		
Resolution (Å)	31.87-1.65	45.93-1.41
No. reflections	23691 (2417)	39665 (3884)
R_{work} / R_{free}	0.1944/ 0.2328	0.2201/ 0.2429
No. atoms		
Protein	1402	1371
Ligand/ion	18	6
Water	321	299
B factors		
Protein	15.65	16.40
Ligand/ion	15.72	13.31
Water	31.05	29.11
R.m.s. deviations		
Bond lengths (Å)	0.006	0.005
Bond angles (°)	0.83	0.79

[a] Values in parentheses are for highest-resolution shell.

Ligand	1,2-dihydro-1,2-azaborine (**2.1**)	ethylbenzene
Protein	L99A/M102Q	L99A/M102Q
PDB entry	**5JWU**	**5JWV**
Data collection		
Space group	$P3_221$	$P3_221$
Cell dimensions		
a, *b*, *c* (Å)	60.10, 60.10, 96.77	60.16, 60.16, 96.81
α, β, γ (°)	90, 90, 120	90, 90, 120
Resolution (Å)	45.84-1.70 (1.76-1.70)[a]	45.88-1.30 (1.35-1.30)[a]
R_{merge}	0.084 (0.438)	0.070 (0.327)
$I/\sigma(I)$	8.6 (2.3)	11.0 (4.0)
Completeness (%)	98.1 (98.1)	99.9 (99.9)
Redundancy	5.63 (5.62)	5.72 (5.73)
Refinement		
Resolution (Å)	45.84-1.70	45.88-1.30
No. reflections	22407 (2239)	50443 (4979)
R_{work} / R_{free}	0.2261/ 0.2509	0.1838/ 0.2035
No. atoms		
Protein	1379	1336
Ligand/ion	8	16
Water	144	367
B factors		
Protein	28.82	12.12
Ligand/ion	30.17	10.61
Water	39.74	25.54
R.m.s. deviations		
Bond lengths (Å)	0.007	0.006
Bond angles (°)	1.00	0.83

[a] Values in parentheses are for highest-resolution shell.

Ligand	*B*-Et-1,2-Azaborine (**2.3**)
Protein	L99A/M102Q
PDB entry	**5JWW**
Data collection	
Space group	$P3_221$
Cell dimensions	
a, *b*, *c* (Å)	60.16, 60.16, 97.09
α, β, γ (°)	90, 90, 120
Resolution (Å)	22.95-1.47 (1.52-1.47)[a]
R_{merge}	0.107 (0.527)
$I/\sigma(I)$	8.4 (1.6)
Completeness (%)	98.2 (98.2)
Redundancy	5.25 (5.40)
Refinement	
Resolution (Å)	22.95-1.47
No. reflections	34608 (3459)
R_{work} / R_{free}	0.2139/ 0.2491
No. atoms	
Protein	1370
Ligand/ion	17
Water	297
B factors	
Protein	19.55
Ligand/ion	21.62
Water	34.00
R.m.s. deviations	
Bond lengths (Å)	0.006
Bond angles (°)	0.84

[a] Values in parentheses are for highest-resolution shell.

2.5.8 X-ray Structure Data Refinement Details

2.5.8.1 Modeling of Alternative Positions

We modeled alternative positions in this work where present, based on difference features in the electron density maps. Figure 2.21 illustrates how alternative conformations are engulfed by "wider" electron densities, whereas the single conformation of Q102 in the ethylbenzene structure shows a more "tapered" profile.

Figure 2.21 2Fo-Fc electron density maps, rendered at 1 sigma, showing alternate Q102 conformers for different ligand complexes

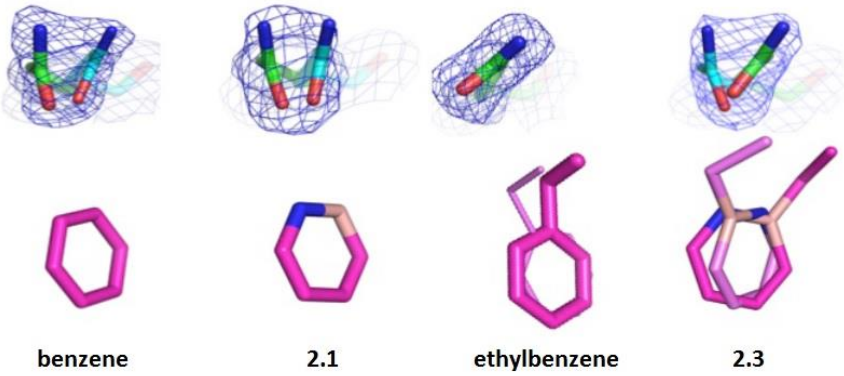

We have re-refined the benzene-L99A/M102Q structure omitting conformers using the same refinement protocol. The resulting Fo-Fc maps show green difference density for the omitted residue in the presence of only one conformer. In addition Rfree values increase from 23.1% for both Q102 conformers to 23.3% for conformer A and 23.4% for conformer B, respectively (Figure 2.22).

Figure 2.22 Positive Fo-Fc difference density (shown as green mesh at 3sigma) and increased Rfree values for structures containing only one conformer (2Fo-Fc maps are shown as blue mesh at 1sigma)

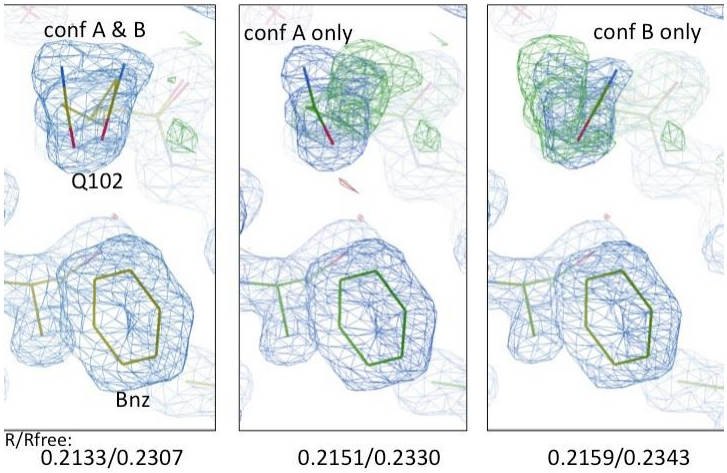

2.5.8.2 Determining the Position of N and B

We determined the positions of N vs. B based on three criteria. First, we inspected electron density maps for differential features, including Fo-Fc difference density in early refinement rounds. Additionally we utilized differences in the number of electrons between B, C and N to determine their relative positions. Figure 2.23 shows that the highest electron density peak (at 4.2 sigma) covers the most electron-rich atom, nitrogen.

Figure 2.23 2Fo-Fc maps shown at 1 and 4.2 sigma to reveal the highest electron density peaks around the nitrogen atom of **2.1**

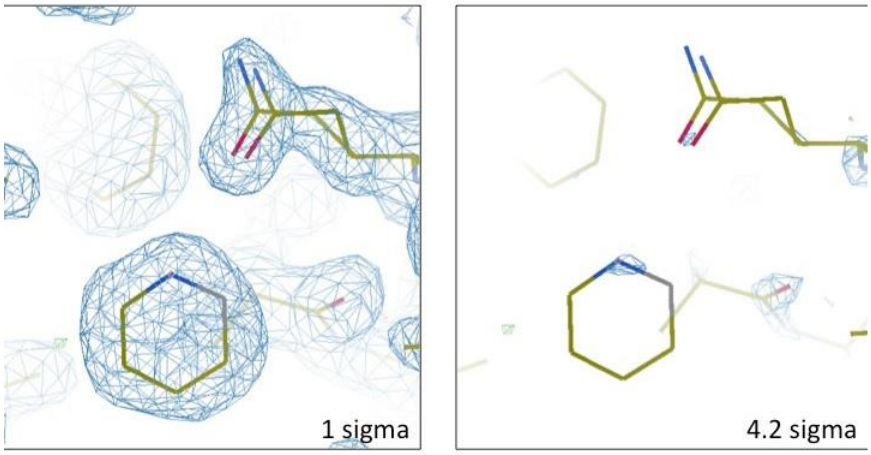

Second, we monitored atomic B factor distribution upon refining different ligand orientations. This approach is based on the expectation that atomic B factors should be homogenously distributed within the ligand and discrepancies can indicate alternative conformations or ligand flips. Third, the hydrogen-bonding ability of N vs. B helps to disambiguate their relative position.

To illustrate the second point, we re-refined the **2.1**-L99A/M102Q structure with two different orientations of the **2.1** ligand using the identical refinement protocol (Figure 2.24). For the correct ligand orientation, no difference density is visible and the B-factors of N and B are of comparable magnitude. For the incorrect ligand orientation, with N and B being swapped, difference density appears and B-factors differ considerably (red box). Rfree values confirm this trend but are expectedly not significantly different.

Figure 2.24 Ligand conformations determined by monitoring the appearance of Fo-Fc difference density (green mesh at 3 sigma on the right) and the B-factor distribution upon re-refinement of alternative ligand positions using an identical refinement protocol

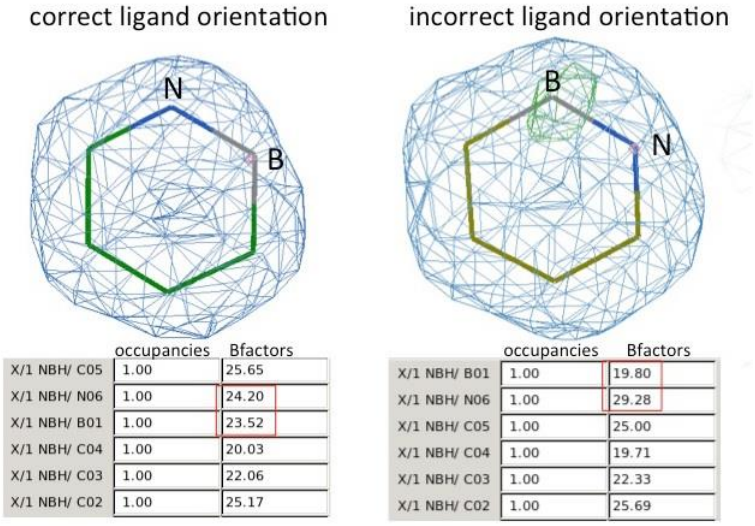

	occupancies	Bfactors
X/1 NBH/ C05	1.00	25.65
X/1 NBH/ N06	1.00	24.20
X/1 NBH/ B01	1.00	23.52
X/1 NBH/ C04	1.00	20.03
X/1 NBH/ C03	1.00	22.06
X/1 NBH/ C02	1.00	25.17

	occupancies	Bfactors
X/1 NBH/ B01	1.00	19.80
X/1 NBH/ N06	1.00	29.28
X/1 NBH/ C05	1.00	25.00
X/1 NBH/ C04	1.00	19.71
X/1 NBH/ C03	1.00	22.33
X/1 NBH/ C02	1.00	25.69

Chapter 3: Binding Study of Ethylbenzene Analogs of 1,2-Azaborines in T4 Lysozyme Mutant Cavity

3.1 Introduction

1,2-Azaborines have unique electronic structures compared to carbon-based arenes due to the presence of a polar B–N bond. In addition, as discussed in 2.1.2, one of the beneficial features of 1,2-azaborines to carbonaceous counterparts is the multiplied number of constitutional isomers possible even when mono-substituted (Figure 2.2). Thus, in the context of our biomedical research efforts, we were interested to see how the binding of different ethyl-substituted 1,2-azaborines to proteins would all compare with that of all-carbon ethylbenzene. For this study, we prepared five 1,2-azaborine regioisomers of ethylbenzene and used them in comparative binding studies to the L99A T4 lysozyme mutant.

3.2 Background

3.2.1 Previous Efforts towards Regio-Selective Functionalization of 1,2-Azaborines

Electronic differences of each position of 1,2-azaborine ring induced by the asymmetric nature of the heterocyclic core has allowed selective functionalization of all six positions. This chapter will treat only functionalization of 1,2-azaborines at C4 and C5; previous works on functionalization at N, B, C3, and C6 will be reviewed in detail in Chapter 4.

Efforts to synthesize C4- and C5-substituted 1,2-azaborines led to the discovery that Ir-catalyzed borylation of *N*-substituted 1,2-azaborines gives a mixture of C4- and C5-

borylated products.[1] The origin of the slight preference for C5 in most cases is unclear; this selectivity was observed regardless of the boron and nitrogen substituents of the substrates (Table 3.1), and the calculated pK_a values[2] for C4–H and C5–H are 45.8 and 46.0, respectively.

Table 3.1 Ir-catalyzed borylation of *N*-substituted 1,2-azaborines

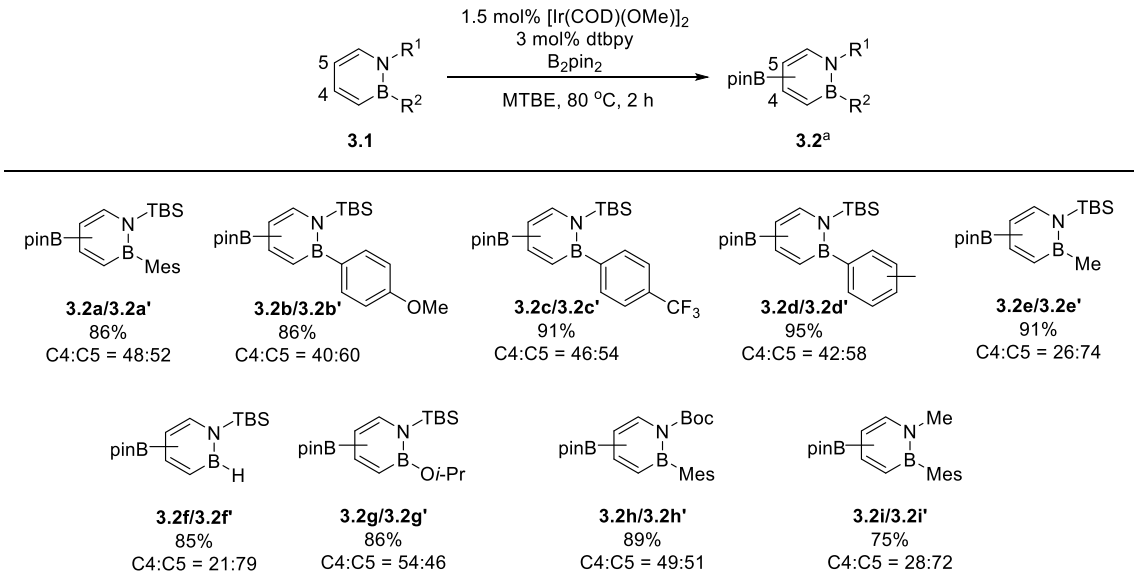

[a]Product yields and ratios are determined by ^{1}H NMR spectroscopy.

Unfortunately, most of the mixtures of borylated products in Table 3.1 were not separable by column chromatography. Selective oxidation of C4-regioisomer in the mixture of C4- and C5-borylated compounds (**3.2 a/3.2a'**) was achieved using *N*-methylmorpholine *N*-oxide (NMO) to afford the corresponding C4-OH product (**3.3**,

[1] Baggett, A. W. New Strategies Enabling Diverse Functionalization of Aromatic 1,2-Azaborine Motifs. PhD, Boston College, 2016.
[2] Baggett, A. W.; Vasiliu, M.; Li, B.; Dixon, D. A.; Liu, S.-Y. *J. Am. Chem. Soc.* **2015**, *137*, 5536–5541.

Scheme 3.1). Using this method, the pure C5-Bpin compound (**3.2a'**) was recovered in 90% yield.

Scheme 3.1 NMO oxidation of a mixture of C4- and C5-borylated 1,2-azaborines

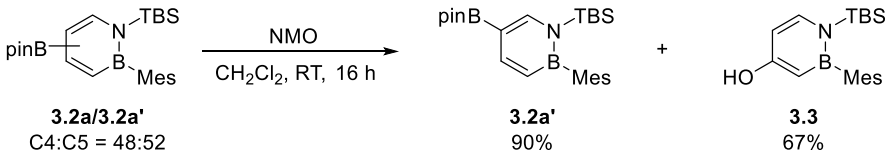

3.2a/3.2a'
C4:C5 = 48:52

3.2a'
90%

3.3
67%

3.3 Syntheses of Ethylbenzene Analogs of 1,2-Azaborines and Their Binding Study in the Cavity of T4 Lysozyme Mutants

3.3.1 Synthesis of Ethylbenzene Derivatives of 1,2-Azaborines

3.3.1.1 Synthesis of *N*-Ethyl-1,2-Azaborine

To prepare *N*-ethyl-1,2-azaborine, we followed the previously reported synthetic method with minor modifications.[3] Addition of *N*-ethylallylamine to *in situ*-generated allylboron dichloride afforded diallyl species **3.5**. Ring-closing metathesis using Grubbs 1st generation catalyst, followed by Pd-mediated oxidation produced 1,2-azaborine **3.7**. Reduction of **3.7** with lithium aluminium hydride ($LiAlH_4$) furnished **3.8** (Scheme 3.2).

[3] Marwitz, A. J. V.; Abbey, E. R.; Jenkins, J. T.; Zakharov, L. N.; Liu, S.-Y. *Org. Lett.* **2007**, *9*, 4905–4908.

Scheme 3.2 Synthesis of *N*-ethyl-1,2-azaborine **3.8**

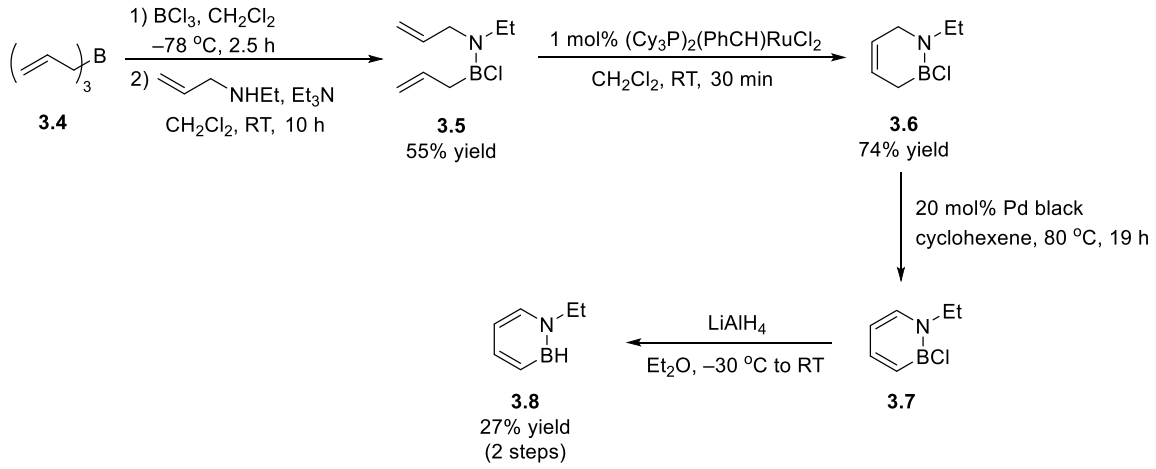

3.3.1.2 Synthesis of *B*-Ethyl-1,2-Azaborine

Synthesis of *B*-ethyl-1,2-azaborine is described in section 2.3.2 (Scheme 2.1).

3.3.1.3 Synthesis of C3-Ethyl-1,2-Azaborine

C3-Ethylated 1,2-azaborine can be accessed starting from C3-brominated compound **3.9**,[4] which first undergoes a two-step boron-substitution/*N*-deprotection[1,5] to give **3.10**. Reaction with $LiAlH_4$, followed by acidic quench results in formation of the 1,2-azaborine equivalent of bromobenzene (**3.11**). Negishi cross-coupling compatible with the BH group in **3.11** was employed to introduce the desired ethyl group in the final product (**3.12**) in moderate yield (Scheme 3.3).

[4] Brown, A. N.; Li, B.; Liu, S.-Y. *J. Am. Chem. Soc.* **2015**, *137*, 8932–8935.
[5] Lamm, A. Fundamental Chemistry of 1,2-Dihydro-1,2-Azaborines. PhD, University of Oregon, 2012.

Scheme 3.3 Synthesis of C3-ethyl-1,2-azaborine **3.12**

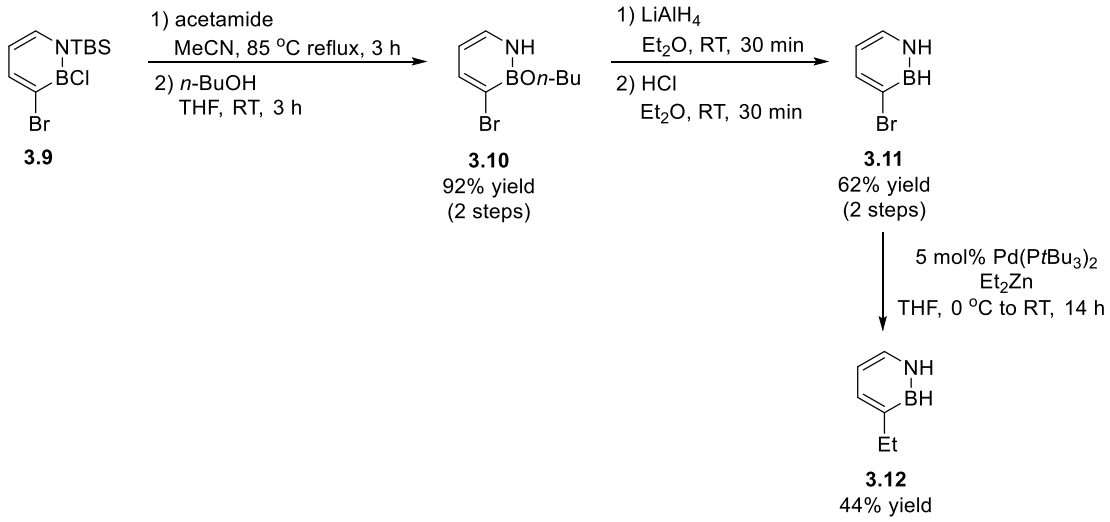

3.9

3.10
92% yield
(2 steps)

3.11
62% yield
(2 steps)

3.12
44% yield

3.3.1.4 Synthesis of C6-Ethyl-1,2-Azaborine

C6-Ethyl-1,2-azaborine was prepared by following the previously reported method.[1] Iridium catalyzed borylation of NH-containing azaborine **3.13** afforded C6-borylated product in good yield and regioselectivity. Suzuki cross coupling of **3.14** with vinylbromide installed a C6-vinyl group that was readily reduced through Pd-catalyzed hydrogenation. Utilizing Cu-catalyzed radical reaction,[1] the benzyl protecting group on boron was transformed into an alkoxy group. Subsequent reduction with $LiAlH_4$ furnished the desired product (**3.18**) in moderate yield (Scheme 3.4).

Scheme 3.4 Synthesis of C6-ethyl-1,2-azaborine **3.18**

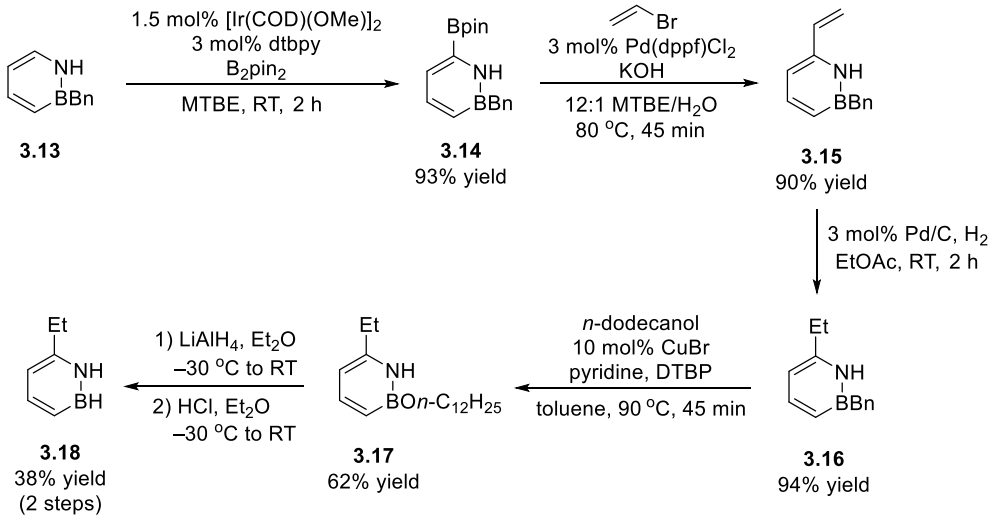

3.3.1.5 Syntheses of C4- and C5-Ethyl-1,2-Azaborines

Synthesis of C4- and C5-substituted 1,2-azaborines is most challenging because those positions are distal from hetero atoms to take advantage of electronic nature for selective transformations to occur. Under conditions similar to those discussed in 3.2.1, Ir-catalyzed borylation of *N*-substituted starting material **3.20** allowed access to both C4- and C5-borylated products in a 36:64 ratio. The steric bulk of the TBS group precludes C6-functionalization. We found that the resulting regioisomers exhibit a key difference in solubility: the majority of C4-borylated product **3.21a** can be precipitated out from the mixture using pentane, while the supernatant becomes correspondingly enriched with the other isomer (**3.21b**). The remaining residual C4-isomer can be separated from the C5-isomer by column chromatography. With pure samples of both regioisomers in hand, we proceeded through a similar reaction sequence as that used in the preparation of C6-ethyl-1,2-azaborine. Suzuki-Miyaura cross-coupling with vinyl bromide followed by

hydrogenation afforded C4- and C5-ethyl substituted products **3.23a** and **3.23b**, respectively. Deprotection on both nitrogen and boron resulted in the requisite precursors (**3.25a** and **3.25b**) to the final products. The final boron substitution reaction of **3.25b** with $LiAlH_4$ afforded the C5-ethyl-1,2-azaborine **3.27**. The C4-isomer (**3.26**), however, proved to be far more susceptible to decomposition during the reaction workup and thus could not be isolated at present (Scheme 3.5).

Scheme 3.5 Synthesis of C4- and C5-ethyl-1,2-azaborines, **3.26** and **3.27**

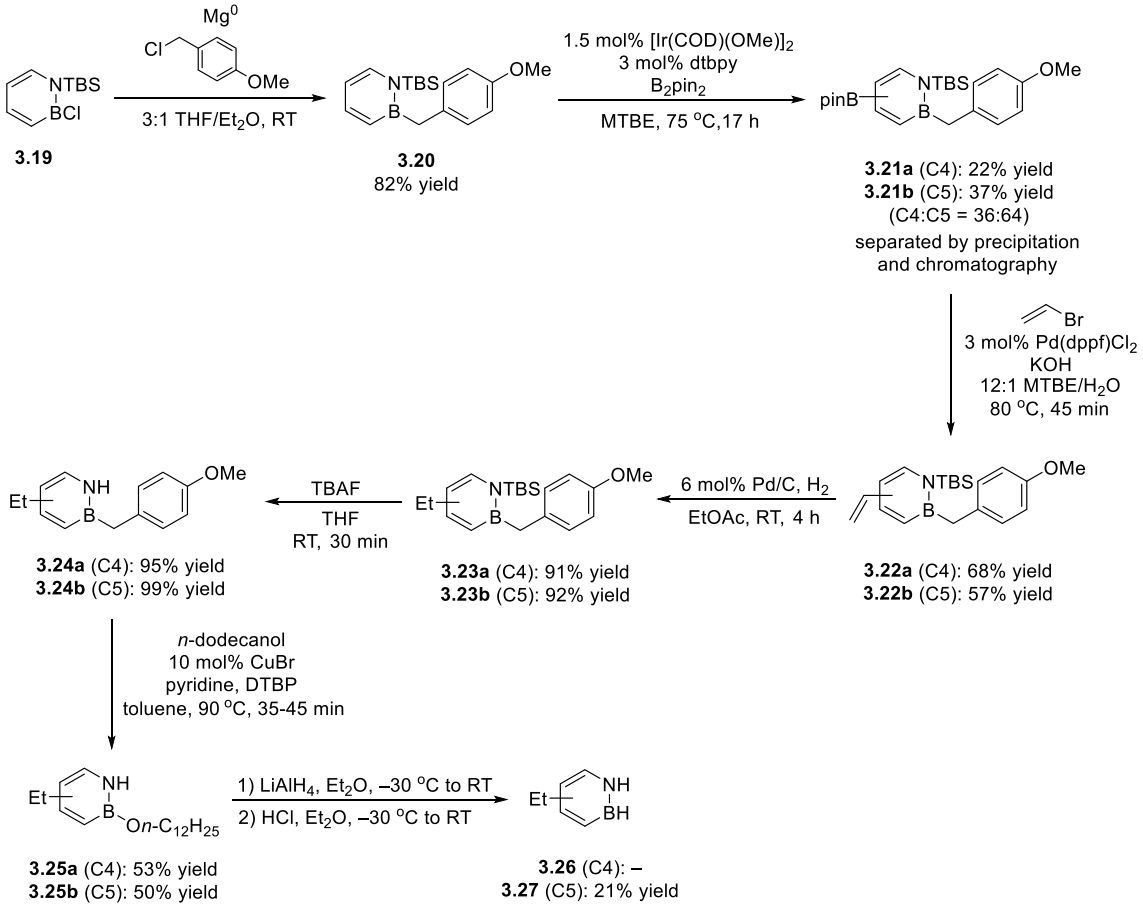

3.3.2 Binding Studies of Ethylbenzene Derivatives in T4 Lysozyme Mutant L99A

3.3.2.1 Isothermal Titration Calorimetry Data

To measure differences in the binding free energy of the regioisomers in the L99A T4 lysozyme binding cavity, we performed ITC experiments. Surprisingly, the more polar *N*-ethyl-1,2-azaborine (**3.8**) gained 0.6 kcal/mol binding free energy in the non-polar pocket of L99A relative to ethylbenzene (Table 3.2, –6.11 vs. –5.55 kcal/mol). The origin of this observation remains unclear at this point. *B*-Ethyl and C3-ethyl-1,2-azaborines (**3.28** and **3.12**) showed relatively weaker binding affinities. However, the binding free energies for C5- and C6-ethyl derivatives (**3.27** and **3.18**) were also about 1.0 kcal/mol stronger in comparison with ethylbenzene.

Table 3.2 Binding free energy and affinity determined by ITC

compound	$\triangle G$ (kcal/mol)	K_a (x10^4 M^{-1})
ethylbenzene	–5.55 ± 0.06	1.91 ± 0.18
N-ethyl-1,2-azaborine (**3.8**)	–6.11 ± 0.03	5.19 ± 0.30
B-ethyl-1,2-azaborine (**3.28**)	–5.12 ± 0.02	0.90 ± 0.04
C3-ethyl-1,2-azaborine (**3.12**)	–5.04 ± 0.03	0.77 ± 0.04
C5-ethyl-1,2-azaborine (**3.27**)	–6.60 ± 0.02	12.4 ± 0.55
C6-ethyl-1,2-azaborine (**3.18**)	–6.54 ± 0.05	11.1 ± 0.94

The position of the ethyl substituent of ligand may have influence on these empirical binding observation. Figure 3.1 (left) shows an electrostatic potential map of the 1,2-azaborine core and the calculated dipole moment value (~ 2.2 D).[6] The ethyl group of

[6] Chrostowska, A.; Xu, S.; Lamm, A. N.; Mazière, A.; Weber, C. D.; Dargelos, A.; Baylère, P.; Graciaa, A.; Liu, S-Y. *J. Am. Chem. Soc*. **2012**, *134*, 10279–10285.

relatively stronger binders (C5, C6, and *N*-ethyl derivatives) is positioned comparatively on the opposite side of that of relatively weaker binders (C3 and *B*-ethyl isomers; Figure 3.1). Thus, we speculate that the observed binding phenomena may originate from dipole interaction induced by dipole moment of ligand and electronic nature of the surrounding protein residue.

Figure 3.1 Dipole moment of 1,2-azaborine and binding trend of BN-ethyl derivatives

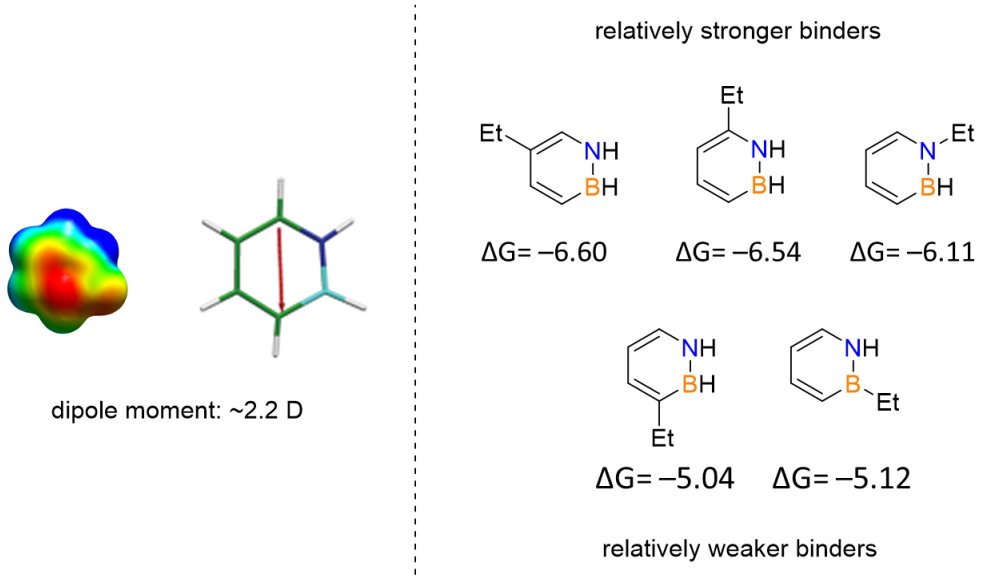

In conclusion, more experimental data (eg. structural determination and binding thermodynamics of C4-ethyl-1,2-azaborine) and computational modeling will need to be performed to give a more in-depth understanding of the observed binding behavior.

3.4 Conclusions

Recent developments in synthetic methods to functionalize the carbon positions of 1,2-azaborines allowed us to selectively substitute each of the six possible positions. Five ethyl-substituted 1,2-azaborines were thereby successfully synthesized.

With these ethylbenzene derivatives in hand, we proceeded to measuring the thermodynamics of their binding to T4 lysozyme mutant L99A. Since the compounds examined here are isosteric, we predicted that the main factors that produce differences in binding energies would originate from electronic differences instead. Specifically, we initially hypothesized that the dipole moment existing in azaborine ring would play a role. This is consistent with our preliminary observation that C5, C6, and *N*-ethyl substituted 1,2-azaborines are relatively stronger binders than the C3 and *B*-ethyl substituted isomers. However, dipole-dipole interactions, for example interactions with the helix macro-dipole, are largely dependent on the distance of the interacting components.[7] As the binding cavity of L99A is relatively large (150 $Å^3$), it may be difficult for dipole-dipole interactions between the bound ligand and the surrounding helix to span the distances involved.

It is also possible that the binding free energy differences observed for each ligand are induced by local dipolar interactions and possibly hydrogen or dihydrogen bonding. We are in the process of computationally calculating the binding energetics of each complex in an effort to develop a model that is consistent with the experimental results.

[7] (a) Le Fèvre, R. J. W. Dipole moments; their measurement and application in chemistry. London, Methuen, 1953. (b) Atkins, P. W. and Paula, J. D. Physical chemistry for the life sciences. New York, Oxford University Press; Freeman, 2006. (c) Bloomfield, M. M. Chemistry and the living organism. New York, Wiley, 1992.

3.5 Experimental

3.5.1 General Information

All oxygen- and moisture-sensitive manipulations were carried out under an inert atmosphere (N_2) using either standard Schlenk techniques or a glove box. THF, Et_2O, CH_2Cl_2, and pentane were purified by passing through a neutral alumina column under argon. Acetonitrile and toluene were dried over CaH_2 and distilled under N_2 prior to use. Pd/C was purchased from Strem and heated under high vacuum at 100 °C for 12 hours prior to use. Silica gel (230-400 mesh) was dried for 12 hours at 180 °C under high vacuum. Flash chromatography was performed with this silica gel under an inert atmosphere. All other chemicals and solvents were purchased and used as received.

NMR spectra were recorded on a Varian VNMRS 600 MHz, VNMRS 500 MHz, INOVA 500 MHz, or VNMRS 400 MHz spectrometer. Deuterated solvents were purchased from Cambridge Isotope Labs. ^{11}B NMR spectra were externally referenced to BF_3•Et_2O (δ 0). All NMR chemical shifts are reported in ppm relative to residual solvent for ^{1}H and ^{13}C NMR. Infrared spectroscopy was performed on a Bruker ALPHA-Platinum FT-IR Spectrometer with ATR-sampling module. High-resolution mass spectrometry analyses were performed by direct analysis in real time (DART) on a JEOL AccuTOF DART instrument or by Agilent 6220 TOF using APPI, and toluene as dopant.

3.5.2 Synthesis of 1,2-Azaborines

N-Ethyl-1,2-Azaborine Synthesis:

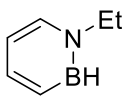

3.8

Compound **3.8** was synthesized following previously reported methods.[3] Spectra of the isolated compound matched published values. ^{1}H NMR (600 MHz, CD_2Cl_2): δ 7.59 (t, *J* = 8.4 Hz, 1H), 7.31 (d, *J* = 6.0 Hz, 1H), 6.83 (d, *J* = 10.8 Hz, 1H), 6.40 (td, *J* = 6.6, 1.2 Hz, 1H), 4.95 (br q, *J* = 138 Hz, 1H), 3.86 (q, *J* = 7.2 Hz, 2H), 1.37 (t, *J* = 7.2 Hz, 3H). ^{11}B NMR (192 MHz, CD_2Cl_2): δ 32.1 (d, *J* = 128 Hz). ^{13}C NMR (151 MHz, CD_2Cl_2): δ 142.8, 138.7, 131.4 (br), 112.3, 53.4, 19.3. FTIR (thin film): 3034, 2977, 2933, 2518, 2476, 1603, 1512, 1473, 1451, 1406, 1378, 1251, 1132, 1008, 954, 879, 803, 741, 603 cm^{-1}. HRMS (DART-TOF) calcd for $C_6H_{11}BN$ ($[M+H]^+$): 108.09845, found: 108.09897.

B-Ethyl-1,2-Azaborine Synthesis:

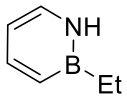

3.28

Synthesis of compound **3.28** was described in Chapter 2. Spectra of the isolated compound matched published values.[8] ^{1}H NMR (600 MHz, CD_2Cl_2): δ 7.86 (br t, *J* = 48.0 Hz, 1H), 7.55 (dd, *J* = 10.5, 6.5 Hz, 1H), 7.25 (t, *J* = 7.5 Hz, 1H), 6.71 (d, *J* = 11.0 Hz, 1H), 6.20 (t, *J* = 6.0 Hz, 1H), 1.18-1.10 (m, 2H), 1.09-1.05 (m, 3H). ^{11}B NMR (160 MHz, CD_2Cl_2): δ 37.5. ^{13}C NMR (151 MHz, CD_2Cl_2): δ 143.8, 134.1, 129.6 (br), 110.1, 26.3, 10.2. FTIR (thin film): 3383, 3022, 2954, 2931, 2870, 1615, 1539, 1507, 1461,

[8] Knack, D. H.; Marshall, J. L.; Harlow, G. P.; Dudzik, A.; Szaleniec, M.; Liu, S.-Y.; Heider, J. *Angew. Chem., Int. Ed.* **2013**, *52*, 2599–2601.

1426, 1397, 1296, 1249, 1157, 1129, 1007, 836, 735 cm^{-1}. HRMS (DART-TOF) calcd for $C_6H_{11}BN$ ($[M+H]^+$): 108.09845, found: 108.09903.

C3-Ethyl-1,2-Azaborine Synthesis:

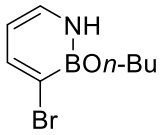

3.10

To a 100 mL round bottom flask containing compound **3.9** (5.70 g, 18.6 mmol) in acetonitrile (40 mL) was added acetamide (1.21 g, 20.5 mmol) under nitrogen atmosphere. The reaction flask was equipped with a reflux condenser and heated to 85 ºC and refluxed for 3 h. After the reaction is cooled to room temperature, the solvent was removed under vacuum. The reaction mixture was dissolved in THF (15 mL), and added *n*-butanol (2.04 mL, 22.3 mmol). The reaction mixture was then stirred at room temperature for 3 h. The solvent was removed under vacuum and the product was isolated by silica gel column chromatography with 5-15% Et_2O/pentane as an eluent, affording the desired product **3.10** as colorless oil (3.93 g, 92%). ^1H NMR (600 MHz, CD_2Cl_2): δ 7.71 (d, J = 6.6 Hz, 1H), 7.05 (t, J = 6.0 Hz, 1H), 6.95 (br s, 1H), 5.81 (td, J = 6.6, 1.8 Hz, 1H), 3.91 (t, J = 7.2 Hz, 2H), 1.71-1.66 (m, 2H), 1.48-1.42 (m, 2H), 0.96 (t, J = 7.8 Hz, 3H). ^{11}B NMR (192 MHz, CD_2Cl_2): δ 25.9. ^{13}C NMR (151 MHz, CD_2Cl_2): δ 146.2, 132.8, 106.5, 64.4, 34.0, 19.6, 14.2 (The carbon adjacent to boron was not observed). FTIR (thin film): 3383, 2957, 2933, 2872, 1621, 1531, 1443, 1288, 968, 694, 671 cm^{-1}. HRMS (DART-TOF) calcd for $C_8H_{14}BBrNO$ ($[M+H]^+$): 230.03518, found: 230.03539.

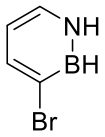

3.11

A 250 mL round bottom flask was charged with compound **3.10** (2.70 g, 11.7 mmol) and Et_2O (120 mL). Lithium aluminium hydride (178 mg, 4.70 mmol) was added in small portions at room temperature under nitrogen atmosphere. The reaction was monitored by ^{11}B NMR and at the completion HCl solution (9.40 mL, 18.8 mmol, 2.0 M in Et_2O) was added dropwise at room temperature and stirred for 30 min. After removing the solvent, silica gel column chromatography using 30% Et_2O/pentane as eluent afforded the desired product **3.11** as colorless oil (1.14g, 62%). ^1H NMR (500 MHz, CD_2Cl_2): δ 8.42 (br t, J = 57 Hz, 1H), 7.91 (d, J = 6.5 Hz, 1H), 7.39 (t, J = 7.0 Hz, 1H), 6.34 (t, J = 6.5 Hz, 1H), 5.02 (br q, J = 139 Hz, 1H). ^{11}B NMR (192 MHz, CD_2Cl_2): δ 31.4 (d, J = 143 Hz). ^{13}C NMR (126 MHz, CD_2Cl_2): δ 145.4, 133.7, 129.2 (br), 112.2. FTIR (thin film): 3385, 25612, 1608, 1520, 1416, 1311, 1238, 988, 863, 734, 646, 593 cm^{-1}. HRMS (DART-TOF) calcd for C_4H_6BBrN ($[M+H]^+$): 157.97767, found: 157.97760.

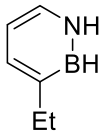

3.12

Compound **3.11** (1.14 g, 7.24 mmol) in THF (100 mL) in a 250 mL round bottom flask was added bis(tri-*tert*-butylphosphine)palladium (185 mg, 0.362 mmol) under nitrogen atmosphere. The reaction was cooled to 0 ºC and diethylzinc solution (10.9 mL, 10.9 mmol, 1.0 M in hexane) was added dropwise. The reaction was slowly warmed to room temperature and stirred for 14 h under nitrogen. The solvent was removed under reduced pressure. Silica gel column chromatography using 100% isopentane afforded the desired product **3.12** as colorless oil (337 mg, 44%). ^1H NMR (500 MHz, CD_2Cl_2): δ 8.32 (br t, J = 57 Hz, 1H), 7.40 (d, J = 6.0 Hz, 1H), 7.22 (t, J = 7.0 Hz, 1H), 6.33 (t, J = 6.5 Hz, 1H), 4.95 (br q, J = 128 Hz, 1H), 2.58 (q, J = 7.5 Hz, 2H), 1.18 (t, J = 7.5 Hz, 3H). ^{11}B NMR (160 MHz, CD_2Cl_2): δ 31.6 (d, J = 127 Hz). ^{13}C NMR (126 MHz, CD_2Cl_2): δ 150.6 (br), 140.4, 131.7, 111.4, 30.3, 17.1. FTIR (thin film): 3389, 2960,

2927, 2869, 2516, 2487, 1611, 1542, 1433, 1209, 1055, 926, 868, 776, 732, 597, 537 cm^{-1}. HRMS (DART-TOF) calcd for $C_6H_{11}BN$ ($[M+H]^+$): 108.09845, found: 108.09897.

C4-Ethyl-1,2-Azaborine Synthesis:

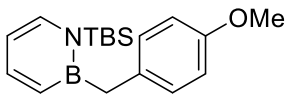

3.20

An oven-dried 250 mL round bottom flask was charged with magnesium turnings (2.40 g, 98.8 mmol) with a crystal of I_2 and 50 mL THF, and a solution of 4-methoxybenzyl chloride (12.0 g, 76.6 mmol) in 100 mL THF was added to the flask. The mixture was allowed to stir at room temperature for 1 h during which time a gentle reflux was observed as the Grignard reagent was formed. This Grignard reagent solution was added in portions to a 250 mL round bottom flask containing **3.19** (15.0 g, 65.9 mmol) dissolved in 50 mL Et_2O until the reaction was judged to be complete by ^{11}B NMR. Pentane was added at this point to precipitate magnesium salts and the reaction mixture was filtered through Celite. The filtrate was concentrated under reduced pressure. The crude material was purified by silica gel column chromatography using 10-100% CH_2Cl_2 in pentane as an eluent to afford the desired product **3.20** as a colorless oil (17.0 g, 82%). ^1H NMR (500 MHz, CD_2Cl_2): δ 7.37 (dd, J = 11.5, 5.5 Hz, 1H), 7.32 (d, J = 7.0 Hz, 1H), 7.01 (d, J = 8.0 Hz, 2H), 6.79 (d, J = 8.0 Hz, 2H), 6.28 (d, J = 11.5 Hz, 1H), 6.22 (t, J = 6.0 Hz, 1H), 3.76 (s, 3H), 2.70 (s, 2H), 0.98 (s, 9H), 0.54 (s, 6H). ^{11}B NMR (160 MHz, CD_2Cl_2): δ 40.9. ^{13}C NMR (151 MHz, CD_2Cl_2): δ 157.3, 143.1, 138.8, 136.5, 131.2 (br), 130.6, 114.1, 111.3, 55.7, 29.6 (br), 27.0, 19.7, –1.0. FTIR (thin film): 2954, 2931, 2858, 1608, 1507, 1391, 1243, 1146, 1039, 985,

842, 811, 711. 689, 571 cm^{-1}. HRMS (DART-TOF) calcd for $C_{18}H_{29}BNOSi$ ($[M+H]^+$): 314.2111, found: 314.2127.

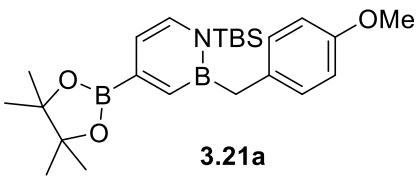

3.21a

Under nitrogen atmosphere, a 150 mL pressure vessel was charged with **3.20** (15.73 g, 50.22 mmol), $[Ir(OMe)(cod)]_2$ (499 mg, 0.753 mmol), 4,4'-di-*tert*-butyl-2,2'-bipyridine (dtbpy) (404 mg, 1.51 mmol), and bis(pinacolato)diboron (B_2pin_2) (12.75 g, 50.22 mmol), and 67.0 mL methyl *tert*-butyl ether (MTBE). The reaction mixture was heated at 75 °C for 17 h. The solvent was removed under reduced pressure. The desired product **3.21a** was precipitated in pentane and filtered off. The remaining mixture of **3.21a** and **3.21b** was purified by silica gel column chromatography using 10% CH_2Cl_2 in pentane as an eluent to afford **3.21a** as a white solid (4.76 g, 22%). ^1H NMR (500 MHz, CD_2Cl_2): δ 7.29 (d, J = 6.5 Hz, 1H), 7.02 (d, J = 8.0 Hz, 2H), 6.87 (s, 1H), 6.67 (d, J = 8.5 Hz, 2H), 6.50 (d, J = 7.0 Hz, 1H), 3.79 (s, 3H), 2.71 (s, 2H), 1.26 (s, 12H), 0.97 (s, 9H), 0.53 (s, 6H). ^{11}B NMR (160 MHz, CD_2Cl_2): δ 40.4, 30.4. ^{13}C NMR (151 MHz, CD_2Cl_2): δ 157.4, 141.1 (br), 137.4, 136.2, 130.7, 129.6 (br), 114.7, 114.1, 84.3, 55.7, 29.4 (br), 26.9, 25.2, 19.6, –1.0. FTIR (thin film): 2977, 2931, 2859, 1611, 1509, 1485, 1388, 1361, 1323, 1244, 1145, 1066, 987, 964, 874, 841, 822, 809, 785, 693 cm^{-1}. HRMS (APPI-TOF) for $C_{24}H_{40}B_2NO_3Si$ ($[M+H]^+$) found: 438.304199.

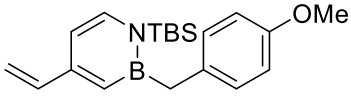

3.22a

Inside a drybox, a 250 mL pressure vessel was charged with **3.21a** (4.76 g, 10.8 mmol), $Pd(dppf)Cl_2 \cdot CH_2Cl_2$ (266 mg, 0.325 mmol), KOH (1.83 g, 32.5 mmol), and a solution of vinyl bromide (43.4 mL, 43.4 mmol, 1 M in THF) in MTBE (37 mL) and H_2O (3.1 mL).

The reaction mixture was heated to 80 °C for 45 min. After cooling the reaction mixture to room temperature, the solvent was removed under reduced pressure. Silica gel column chromatography using 10-50% CH_2Cl_2 in pentane as an eluent afforded the desired product **3.22a** as a colorless liquid (2.49 g, 68%). ^{1}H NMR (500 MHz, CD_2Cl_2): δ 7.31 (d, *J* = 7.5 Hz, 1H), 7.02 (d, *J* = 8.5 Hz, 2H), 6.80 (d, *J* = 8.5 Hz, 2H), 6.46 (dd, *J* = 17.5, 10.5 Hz, 1H), 6.39 (dd, *J* = 7.5, 2.5 Hz, 1H), 6.17 (d, *J* = 2.0 H, 2H), 5.66 (d, *J* = 17.5 H, 1H), 5.21 (d, *J* = 10.5 Hz, 1H), 3.77 (s, 3H), 2.69 (s, 2H), 0.98 (s, 9H), 0.53 (s, 6H). ^{11}B NMR (160 MHz, CD_2Cl_2): δ 41.2. ^{13}C NMR (151 MHz, CD_2Cl_2): δ 157.3, 150.2, 139.6, 139.3, 136.2, 130.6, 129.3 (br), 116.1, 114.1, 108.0, 55.7, 29.5 (br), 26.9, 19.7, –1.2. FTIR (thin film): 2954, 2930, 2858, 1630, 1604, 1509, 1494, 1298, 1243, 1131, 1039, 985, 913, 841, 822, 786, 691, 420 cm^{-1}. HRMS (APPI-TOF) for $C_{20}H_{31}BNOSi$ ([M+H]$^+$) found: 339.231598.

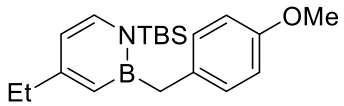

3.23a

Inside a drybox, a 250 mL round bottom flask was charged with **3.22a** (2.76 g, 8.13 mmol), Pd/C (519 mg of 10 wt% Pd, 0.489 mmol) in ethylacetate (70 mL). The reaction mixture was stirred at room temperature for 4 h under 1 atm H_2 atmosphere. The solvent was removed under reduced pressure. Silica gel column chromatography using 15-40% CH_2Cl_2 in pentane as an eluent afforded the desired product **3.23a** as a colorless liquid (2.53 g, 91%). ^{1}H NMR (500 MHz, CD_2Cl_2): δ 7.25 (d, *J* = 6.5 Hz, 1H), 7.16 (d, *J* = 8.5 Hz, 2H), 6.80 (d, *J* = 8.5 Hz, 2H), 6.11 (d, *J* = 7.0 Hz, 1H), 6.06 (s, 1H), 3.77 (s, 3H), 2.68 (s, 2H), 2.36 (q, *J* = 8.0 Hz, 2H), 1.07 (t, *J* = 8.0 Hz, 3H), 0.98 (s, 9H), 0.52 (s, 6H). ^{11}B NMR (160 MHz, CD_2Cl_2): δ 40.6. ^{13}C NMR (151 MHz, CD_2Cl_2): δ 159.4, 157.3, 138.8, 136.5, 130.6, 127.2 (br), 114.0, 112.6, 55.7, 31.7, 29.5 (br), 27.0, 19.7, 14.5, –1.1. FTIR (thin film): 2956,

2931, 2858, 1617, 1508, 1464, 1279, 1243, 1178, 1063, 1039, 994, 866, 841, 808, 751, 693, 485 cm^{-1}. HRMS (APPI-TOF) for $C_{20}H_{33}BNOSi$ ($[M+H]^+$) found: 342.243286.

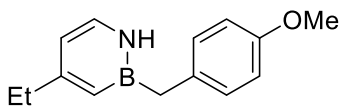

3.24a

To a solution of **3.23a** (2.53 g, 7.42 mmol) in 74 mL THF was added a solution of tetrabutylammonium fluoride (7.42 mL, 7.42 mmol, 1 M in THF) and the reaction mixture was stirred at room temperature for 30 min. The solvent was removed under reduced pressure. Silica gel column chromatography using 30-50% CH_2Cl_2 in pentane as an eluent afforded the desired product **3.24a** as a colorless oil (1.60 g, 95%). ^1H NMR (500 MHz, CD_2Cl_2): δ 7.46 (br s, 1H), 7.12 (t, J = 7.0 Hz, 1H), 7.07 (d, J = 8.5 Hz, 2H), 6.70 (d, J = 8.5 Hz, 2H), 6.48 (s, 1H), 6.11 (d, J = 6.5 Hz, 1H), 3.79 (s, 3H), 2.66 (s, 2H), 2.52 (q, J = 7.5 Hz, 2H), 1.20 (t, J = 7.5 Hz, 3H). ^{11}B NMR (160 MHz, CD_2Cl_2): δ 36.5. ^{13}C NMR (151 MHz, CD_2Cl_2): δ 160.5, 157.5, 135.0, 134.1, 130.1, 125.9 (br), 114.5, 111.6, 55.7, 32.3, 26.6 (br), 14.9. FTIR (thin film): 3378, 2963, 2932, 2833, 1620, 1580, 1532, 1464, 1407, 1296, 1178, 1089, 1037, 874, 834, 725, 532 cm^{-1}. HRMS (APPI-TOF) for $C_{14}H_{19}BNO$ ($[M+H]^+$) found: 227.160294.

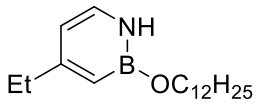

3.25a

Inside a drybox, a 30 mL microwave vial was charged with **3.24a** (1.42 g, 6.25 mmol), *n*-dodecanol (1.63 g, 8.75 mmol) CuBr (90 mg, 0.63 mmol), pyridine (1.01 mL, 12.5 mmol), DTBP (1.38 mL, 7.50 mmol), and 17 mL toluene. The reaction mixture was stirred at 90 °C for 45 min and immediately cooled with chilled water. The solvent was removed under reduced pressure. Silica gel column chromatography using 30-100% CH_2Cl_2 in pentane as an eluent afforded the desired product **3.25a** as a colorless liquid (969 mg, 53% yield of 98% pure product).

Further purification using recycling HPLC with a GPC column afforded the pure desired product. ^{1}H NMR (600 MHz, CD_2Cl_2): δ 6.96 (t, *J* = 7.2 Hz, 1H), 6.75 (br s, 1H), 5.98 (s, 1H), 5.77 (d, *J* = 7.2 Hz, 1H), 3.89 (t, *J* = 7.8 Hz, 2H), 2.46 (q, *J* = 7.8 Hz, 2H), 1.63-1.58 (m, 2H), 1.37-1.25 (m, 18H), 1.17 (t, *J* = 7.8 Hz, 3H), 0.90-0.86 (m, 3H). ^{11}B NMR (160 MHz, CD_2Cl_2): δ 29.0. ^{13}C NMR (151 MHz, CD_2Cl_2): δ 162.9, 133.9, 114.2 (br), 107.7, 65.2, 32.5, 32.4, 30.4, 30.3, 30.2, 30.1, 30.0, 29.9, 27.6, 26.5, 23.3, 14.7, 14.5. FTIR (thin film): 3324, 2958, 2922, 2853, 1623, 1533, 1430, 1387, 1345, 1316, 1266, 1247, 1138, 1104, 944, 844, 768, 720, 689, 427 cm^{-1}. HRMS (DART-TOF) calcd for $C_{18}H_{35}BNO$ ($[M+H]^+$): 292.2812, found: 292.2823.

C5-Ethyl-1,2-Azaborine Synthesis:

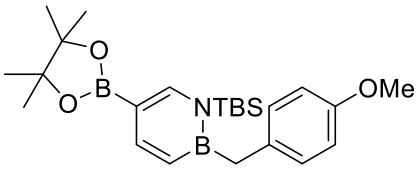

3.21b

C5-borylated product **3.21b** was prepared in the same reaction for the synthesis of **3.21a**. The desired product **3.21b** was isolated as a white solid (8.14 g, 37%) by silica gel column chromatography using 10% CH_2Cl_2 in pentane as an eluent. ^{1}H NMR (500 MHz, CD_2Cl_2): δ 7.86 (s, 1H), 7.62 (d, *J* = 11.0 Hz, 1H), 7.00 (d, *J* = 8.0 Hz, 2H), 6.79 (d, *J* = 8.0 Hz, 2H), 6.26 (d, *J* = 10.5 Hz, H), 3.77 (s, 3H), 2.70 (s, 2H), 1.27 (s, 12H), 0.99 (s, 9H), 0.56 (s, 6H). ^{11}B NMR (160 MHz, CD_2Cl_2): δ 41.8, 30.9. ^{13}C NMR (151 MHz, CD_2Cl_2): δ 157.4, 148.3, 147.0, 140.9 (br), 136.1, 130.6, 130.3 (br), 114.1, 83.7, 55.7, 29.8 (br), 27.0, 25.2, 19.6, –1.0. FTIR (thin film): 2977, 2931, 2859, 1604, 1509, 1499, 1402, 1373, 1259, 1243, 1145, 1091, 1040, 829, 807, 787, 691, 672 cm^{-1}. HRMS (APPI-TOF) for $C_{24}H_{40}B_2NO_3Si$ ($[M+H]^+$) found: 438.303894.

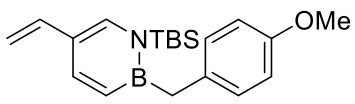

3.22b

Inside a drybox, a 250 mL pressure vessel was charged with **3.21b** (4.31 g, 9.81 mmol), Pd(dppf)Cl_2·CH_2Cl_2 (240 mg, 0.294 mmol), KOH (1.65 g, 29.4 mmol), and a solution of vinyl bromide (39.3 mL, 39.3 mmol, 1 M in THF) in MTBE (33.5 mL) and H_2O (2.8 mL). The reaction mixture was heated to 80 °C for 45 min. After cooling the reaction mixture to room temperature, the solvent was removed under reduced pressure. Silica gel column chromatography using 10-50% CH_2Cl_2 in pentane as an eluent afforded the desired product **3.22b** as a colorless liquid (1.91 g, 57%). ^{1}H NMR (500 MHz, CD_2Cl_2): δ 7.69 (d, *J* = 11.5 Hz, 1H), 7.26 (s, 1H), 7.00 (d, *J* = 8.0 Hz, 2H), 6.79 (d, *J* = 8.0 Hz, 2H), 6.51 (dd, *J* = 17.5, 11.5 Hz, 1H), 6.33 (d, *J* = 11.5 Hz, 1H), 5.40 (d, *J* = 18.0 H, 1H), 4.95 (d, *J* = 11.5 H, 1H), 3.77 (s, 3H), 2.70 (s, 2H), 0.99 (s, 9H), 0.55 (s, 6H). ^{11}B NMR (160 MHz, CD_2Cl_2): δ 41.2. ^{13}C NMR (151 MHz, CD_2Cl_2): δ 157.4, 139.9, 139.6, 139.4, 136.1, 136.1, 131.7 (br), 130.6, 122.1, 114.2, 109.0, 55.7, 29.4 (br), 27.0, 19.6, –1.0. FTIR (thin film): 2954, 2931, 2858, 1632, 1609, 1508, 1463, 1418, 1367, 1283, 1267, 1244, 1174, 1073, 1038, 986, 881, 842, 804, 691, 406 cm^{-1}. HRMS (DART-TOF) calcd for $C_{20}H_{31}BNOSi$ ([M+H]$^+$): 340.2268, found: 340.2285.

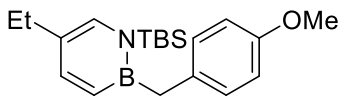

3.23b

Inside a drybox, a 250 mL round bottom flask was charged with **3.22b** (3.83 g, 11.3 mmol), Pd/C (720 mg of 10 wt% Pd, 0.677 mmol) in ethylacetate (100 mL). The reaction mixture was stirred at room temperature for 4 h under 1 atm H_2 atmosphere. The solvent was removed under reduced pressure. Silica gel column chromatography using 10-30% CH_2Cl_2 in pentane as an eluent afforded the desired product **3.23b** as a colorless liquid (3.54 g, 92%). ^{1}H NMR (500 MHz, CD_2Cl_2): δ 7.32 (d, *J* = 11.0 Hz, 1H), 7.10 (s, 1H), 7.00 (d, *J* =

6.5 Hz, 2H), 6.79 (d, J = 6.5 Hz, 2H), 6.25 (d, J = 11.0 Hz, 1H), 3.77 (s, 3H), 2.68 (s, 2H), 2.38 (q, J = 8.0 Hz, 2H), 1.11 (t, J = 8.0 Hz, 3H), 0.98 (s, 9H), 0.54 (s, 6H). ^{11}B NMR (160 MHz, CD_2Cl_2): δ 39.9. ^{13}C NMR (151 MHz, CD_2Cl_2): δ 157.3, 145.1, 136.7, 135.7, 131.9 (br), 130.5, 125.5, 114.1, 55.7, 29.3 (br), 27.2, 26.9, 19.7, 16.3, –1.0. FTIR (thin film): 2956, 2929, 2857, 1623, 1586, 1509, 1450, 1382, 1299, 1245, 1173, 1125, 1081, 1002, 938, 827, 786, 691, 636, 575, 413 cm^{-1}. HRMS (DART-TOF) calcd for $C_{20}H_{33}BNOSi$ ([M+H]$^+$): 342.2424, found: 342.2413.

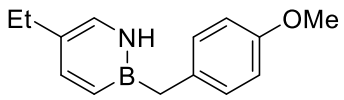

3.24b

To a solution of **3.23b** (3.54 g, 10.4 mmol) in 100 mL THF was added a solution of tetrabutylammonium fluoride (10.4 mL, 10.4 mmol, 1 M in THF) and the reaction mixture was stirred at room temperature for 30 min. The solvent was removed under reduced pressure. Silica gel column chromatography using 30-50% CH_2Cl_2 in pentane as an eluent afforded the desired product **3.24b** as a colorless oil (2.33 g, 99%). ^{1}H NMR (500 MHz, CD_2Cl_2): δ 7.52 (d, J = 12.0 Hz, 1H), 7.50 (br s, 1H), 7.05 (d, J = 8.5 Hz, 2H), 6.99 (d, J = 7.5 Hz, 1H), 6.83 (d, J = 8.5 Hz, 2H), 6.67 (d, J = 11.5 Hz, 1H), 3.78 (s, 3H), 2.64 (s, 2H), 2.40 (q, J = 7.5 Hz, 2H), 1.13 (t, J = 7.5 Hz, 3H). ^{11}B NMR (160 MHz, CD_2Cl_2): δ 35.6. ^{13}C NMR (151 MHz, CD_2Cl_2): δ 157.5, 146.0, 135.0, 131.2, 130.1, 129.8 (br), 125.2, 114.5, 55.7, 26.7, 26.4 (br), 16.3. FTIR (thin film): 3381, 2998, 2961, 2871, 1626, 1610, 1536, 1509, 1456, 1399, 1297, 1243, 1205, 1178, 1085, 1036, 846, 740, 619 cm^{-1}. HRMS (DART-TOF) calcd for $C_{14}H_{19}BNO$ ([M+H]$^+$): 228.1560, found: 228.1568.

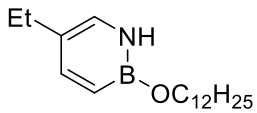

3.25b

Inside a drybox, a 30 mL microwave vial was charged with **3.24b** (1.41 g, 6.20 mmol), *n*-dodecanol (1.62 g, 8.68 mmol) CuBr (89 mg,

0.62 mmol), pyridine (1.00 mL, 12.4 mmol), DTBP (1.37 mL, 7.44 mmol), and 17 mL toluene. The reaction mixture was stirred at 90 °C for 35 min and immediately cooled with chilled water. The solvent was removed under reduced pressure. Silica gel column chromatography using 30-100% CH_2Cl_2 in pentane as an eluent afforded the desired product **3.25b** as a white solid (912 mg, 50% yield of 97% pure product). Further purification using recycling HPLC with a GPC column afforded the pure desired product. ^{1}H NMR (500 MHz, CD_2Cl_2): δ 7.46 (d, J = 12.0 Hz, 1H), 6.83 (d, J = 7.0 Hz, 1H), 6.75 (br s, 1H), 6.22 (d, J = 12.0 Hz, 1H), 3.87 (t, J = 7.0 Hz, 2H), 2.32 (q, J = 7.5 Hz, 2H), 1.63-1.57 (m, 2H), 1.40-1.21 (m, 18H), 1.10 (t, J = 7.5 Hz, 3H), 0.89-0.85 (m, 3H). ^{11}B NMR (160 MHz, CD_2Cl_2): δ 28.5. ^{13}C NMR (151 MHz, CD_2Cl_2): δ 148.5, 130.8, 120.7, 118.6 (br), 65.4, 32.5, 32.4, 31.2, 30.8, 30.6, 30.3, 30.1, 30.0, 26.5, 26.4, 23.3, 16.3, 14.5. FTIR (thin film): 3321, 2958, 2924, 2853, 1632, 1538, 1462, 1409, 1383, 1363, 1274, 1207, 1192, 1140, 1054, 795, 692, 499 cm^{-1}. HRMS (DART-TOF) calcd for $C_{18}H_{35}BNO$ ($[M+H]^+$): 292.2812, found: 292.2824.

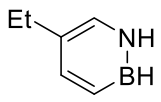

3.27

A 100 mL round bottom flask was charged with compound **3.25b** (1.44 g, 4.94 mmol) and Et_2O (30 mL). Lithium aluminium hydride (195 mg, 5.13 mmol) was added in small portions at –30 °C under nitrogen atmosphere. The reaction was monitored by ^{11}B NMR and at the completion HCl solution (5.00 mL, 10.0 mmol, 2.0 M in Et_2O) was added dropwise at –30 °C and stirred for 30 min. The reaction mixture was filtered through a filter paper and filtrate was concentrated by removing solvent by distillation, silica gel column chromatography using 100% isopentane as eluent afforded the desired product **3.27** as a colorless oil (113 mg, 21%). ^{1}H NMR (600 MHz, CD_2Cl_2): δ 8.30 (br t, J = 50.4 Hz, 1H), 7.66 (d, J = 11.4 Hz, 1H), 7.21 (d, J = 7.2

Hz, 1H), 6.90 (d, J = 10.8 Hz, 1H), 4.80 (br q, J = 135 Hz, 1H), 2.47 (q, J = 7.2 Hz, 2H), 1.17 (t, J = 7.2 Hz, 3H). ^{11}B NMR (160 MHz, CD_2Cl_2): δ 30.1 (d, J = 125 Hz). ^{13}C NMR (126 MHz, CD_2Cl_2): δ 146.4, 132.0, 131.1 (br), 127.0, 26.9, 16.2. FTIR (thin film): 3399, 3024, 2962, 2870, 2528, 1622, 1454, 1308, 1260, 1136, 1094, 1019, 878, 800, 699, 586 cm^{-1}. HRMS (DART-TOF) calcd for $C_6H_{11}BN$ ([M+H]$^+$): 108.0985, found: 108.0988.

C6-Ethyl-1,2-Azaborine Synthesis:

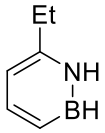

3.18

Compound **3.18** was synthesized following previously reported methods.[1] Spectra of the isolated compound matched published values. ^{1}H NMR (500 MHz, CD_2Cl_2): δ 8.19 (br t, J = 54.0 Hz, 1H), 7.68-7.62 (m, 1H), 6.70 (d, J = 10.5 Hz, 1H), 6.25 (d, J = 6.5 Hz, 1H), 4.84 (br q, J = 130 Hz, 1H), 2.61 (q, J = 7.5 Hz, 2H), 1.26 (t, J = 7.5 Hz, 3H). ^{11}B NMR (160 MHz, CD_2Cl_2): δ 31.3 (d, J = 141 Hz). ^{13}C NMR (151 MHz, CD_2Cl_2): δ 149.4, 145.3, 127.8 (br), 109.5, 29.5, 13.4. FTIR (thin film): 3371, 3023, 2970, 2934, 2875, 2520, 2455, 1611, 1543, 1446, 1402, 1377, 1343, 1194, 1166, 1085, 891, 853, 716, 686, 520, 452 cm^{-1}. HRMS (DART-TOF) calcd for $C_6H_{11}BN$ ([M+H]$^+$): 108.0985, found: 108.0990.

3.5.3 ITC Experiments

Isothermal titration calorimetry (ITC) experiments were carried out with Nano ITC Low Volume calorimeter from TA instruments. Titrations were run by injection of ligand solution to protein solution at 10 ºC and 310 rpm stirring rate with a data collection interval

of 4 min/injection. A total of 20–40 injections of a total volume of 50–100 uL ligand solution (2.66–4.75 mM) were done with 320 uL protein solution (~0.2 mM). Both ligand and protein were in a degassed buffer solution of 5% PEG400, 0.5 M NaCl, 0.1 M sodium phosphate (pH 6.8). The protein solution was prepared by dialyzing against the degassed buffer and the concentrations were determined by molar absorptivity at 280 nm. Due to the limited solubility of the small molecule ligands in aqueous buffer, accurate concentrations of ligand solution were determined by either GC against a calibrated internal standard or UV/VIS. Baseline mixing heats were estimated by injection of ligand solution into the buffer and subtracted from individual titration curve. The resulting reaction heat profiles were fit to the independent binding model with the stoichiometry n fixed to 1.0. All data were analyzed using NanoAnalyze software. Experiments were repeated five times and averaged with standard deviation error of the mean.

* Representative ITC data

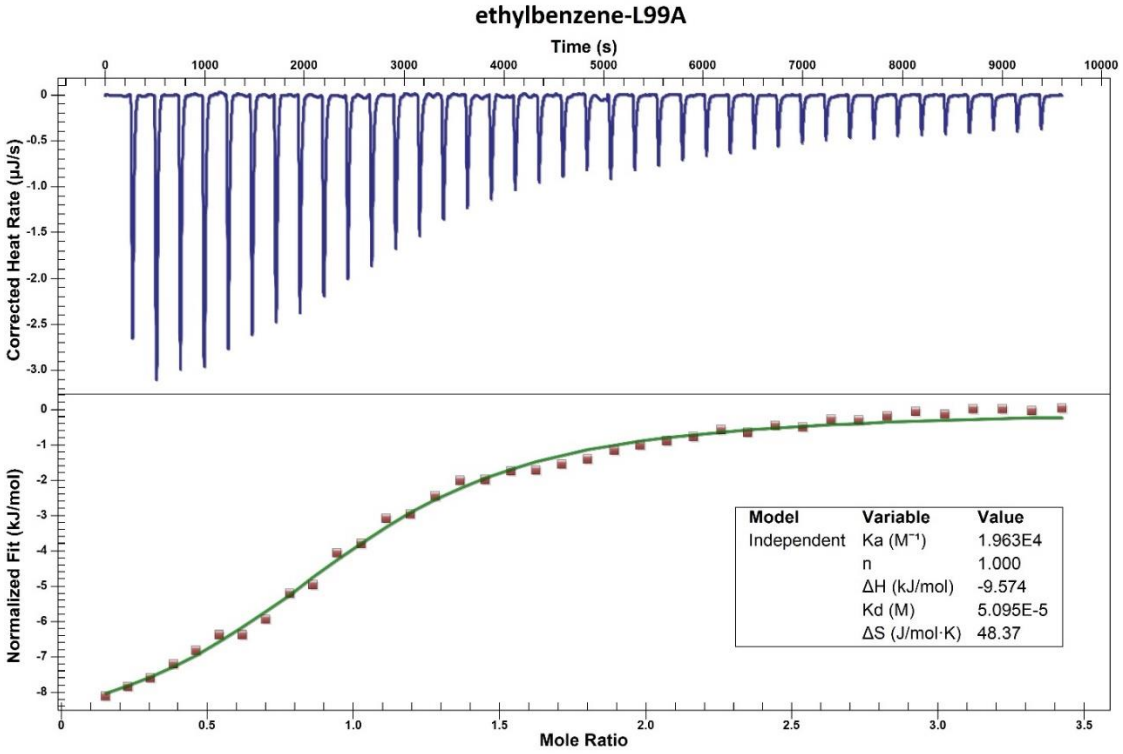

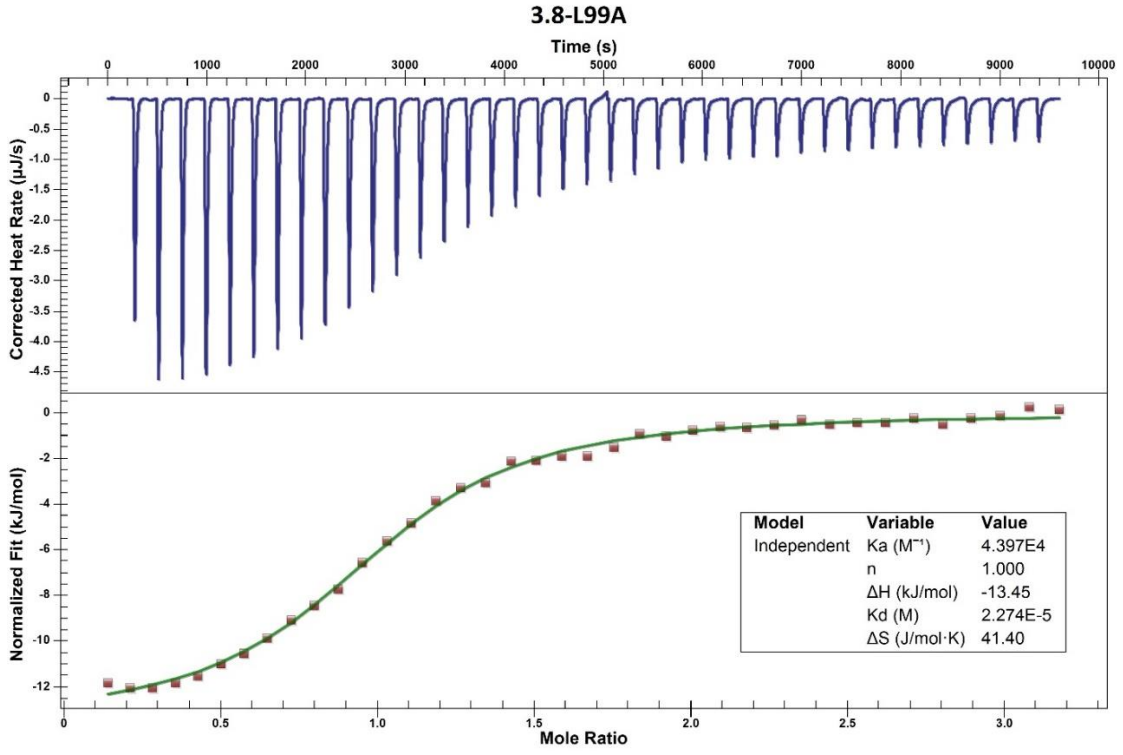

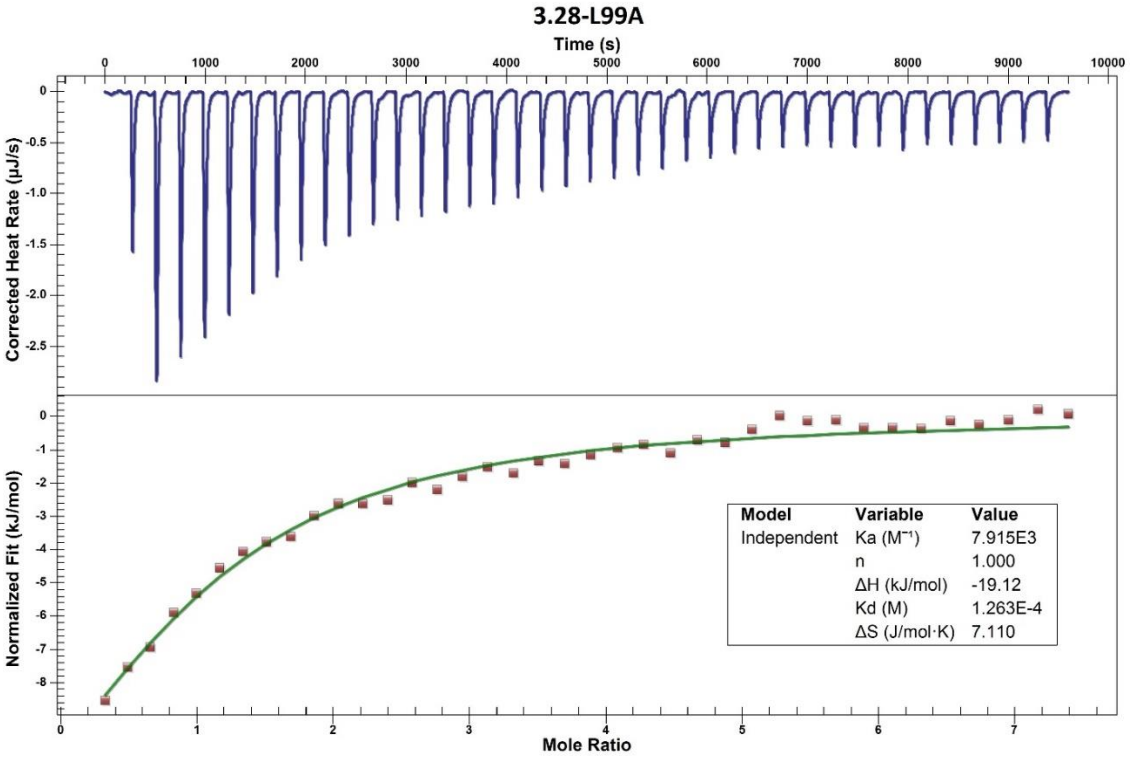
3.28-L99A
Time (s)
Corrected Heat Rate (µJ/s)
Normalized Fit (kJ/mol)
Mole Ratio
Model Variable Value
Independent Ka (M⁻¹) 7.915E3
n 1.000
ΔH (kJ/mol) -19.12
Kd (M) 1.263E-4
ΔS (J/mol·K) 7.110

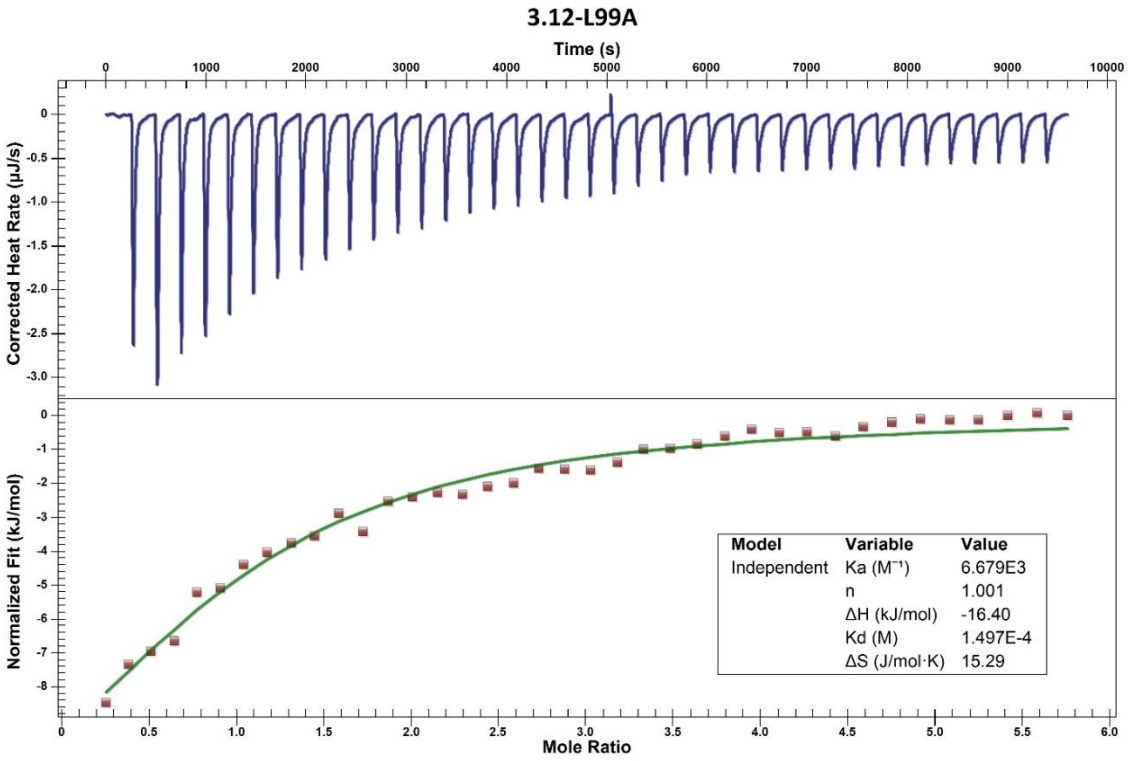
3.12-L99A
Time (s)
Corrected Heat Rate (µJ/s)
Normalized Fit (kJ/mol)
Mole Ratio
Model Variable Value
Independent Ka (M⁻¹) 6.679E3
n 1.001
ΔH (kJ/mol) -16.40
Kd (M) 1.497E-4
ΔS (J/mol·K) 15.29

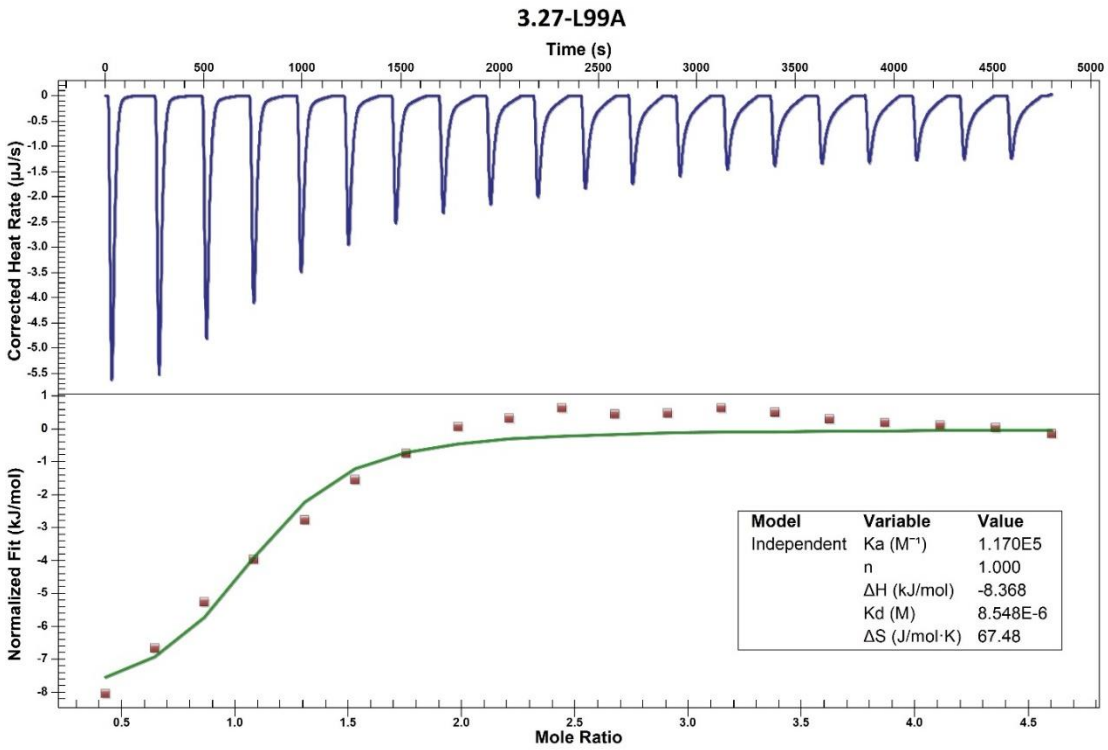
3.27-L99A
Time (s)
Corrected Heat Rate (µJ/s)
Normalized Fit (kJ/mol)
Mole Ratio
Model Variable Value
Independent Ka (M⁻¹) 1.170E5
n 1.000
ΔH (kJ/mol) -8.368
Kd (M) 8.548E-6
ΔS (J/mol·K) 67.48

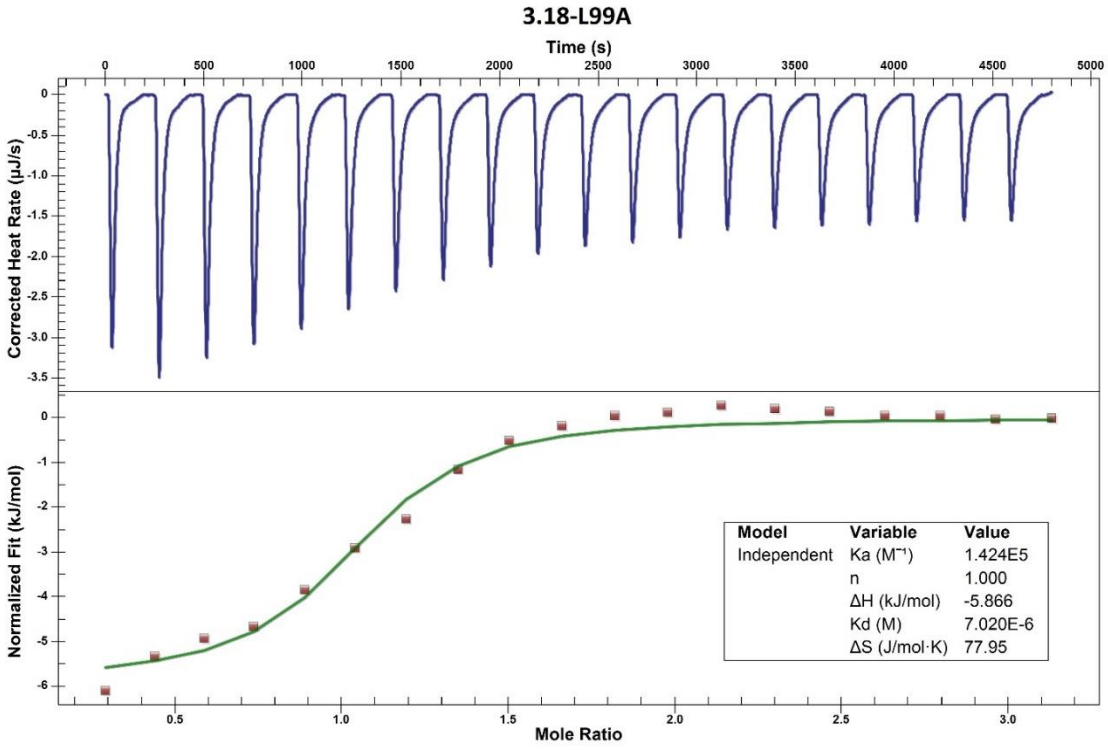
3.18-L99A
Time (s)
Corrected Heat Rate (µJ/s)
Normalized Fit (kJ/mol)
Mole Ratio
Model Variable Value
Independent Ka (M⁻¹) 1.424E5
n 1.000
ΔH (kJ/mol) -5.866
Kd (M) 7.020E-6
ΔS (J/mol·K) 77.95

3.5.4 Spectral Data

HL-II-071-1H

Sample Name HL-II-071-1H
Date collected 2015-04-02

Pulse sequence PROTON
Solvent cd2cl2

Temperature 25
Spectrometer nmr19-vnmrs600

Study owner Liu
Operator Liu

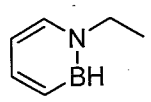

583

Data file /home/ALL/Liu/HL/HL-II-071-1H.fid

Plot date 2017-04-03

HL-II-071-11B

Sample Name HL-II-071-11B
Date collected 2015-04-02

Pulse sequence s2pul
Solvent cd2cl2

Temperature 25
Spectrometer nmr19-vnmrs600

Study owner Liu
Operator Liu

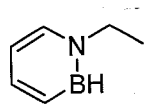

584

Data file /home/ALL/Liu/HL/HL-II-071-11B.fid

Plot date 2017-04-03

HL-II-071-13C

Sample Name HL-II-071-13C
Date collected 2017-04-06

Pulse sequence CARBON
Solvent cd2cl2

Temperature 25
Spectrometer nmr19-vnmrs600

Study owner Liu
Operator Liu

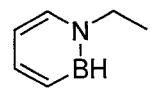

585

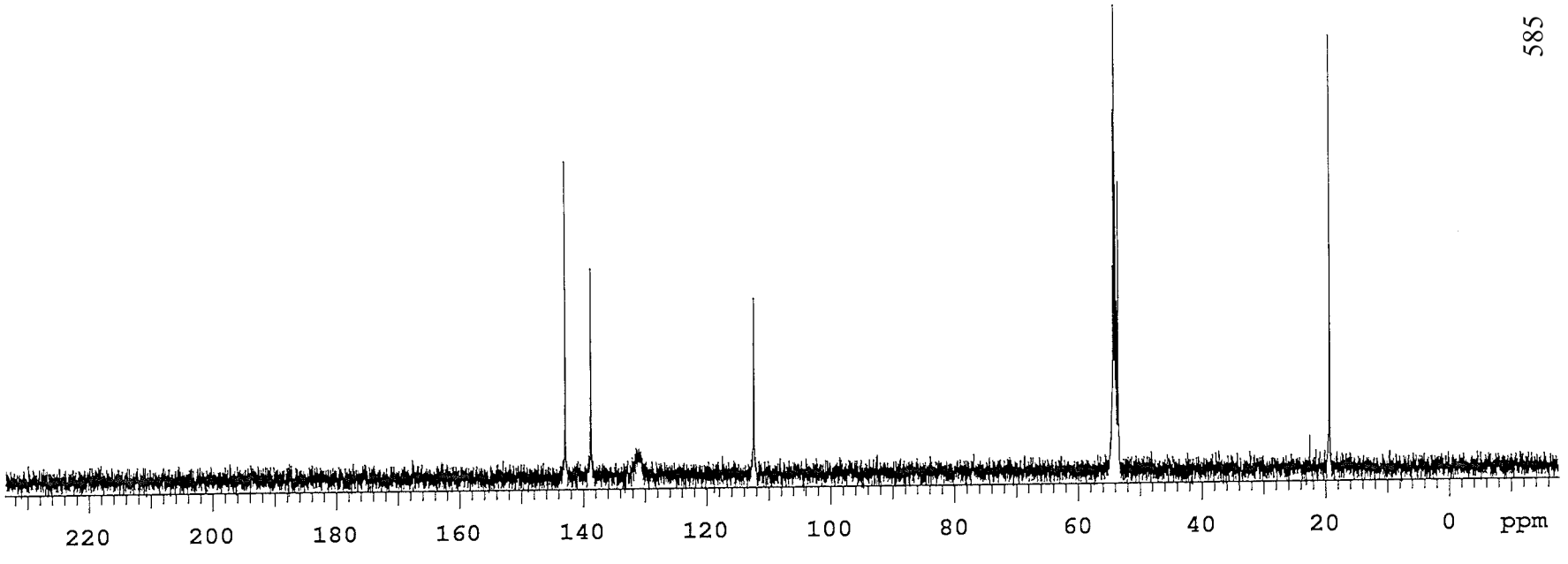

Data file exp

Plot date 2017-04-06

HL-II-062-1H

Sample Name	**HL-II-062-1H**	Pulse sequence	**PROTON**	Temperature	**25**	Study owner	**Liu**
Date collected	**2016-06-06**	Solvent	**cd2cl2**	Spectrometer	**nmr19-vnmrs600**	Operator	**Liu**

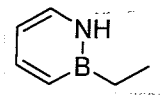

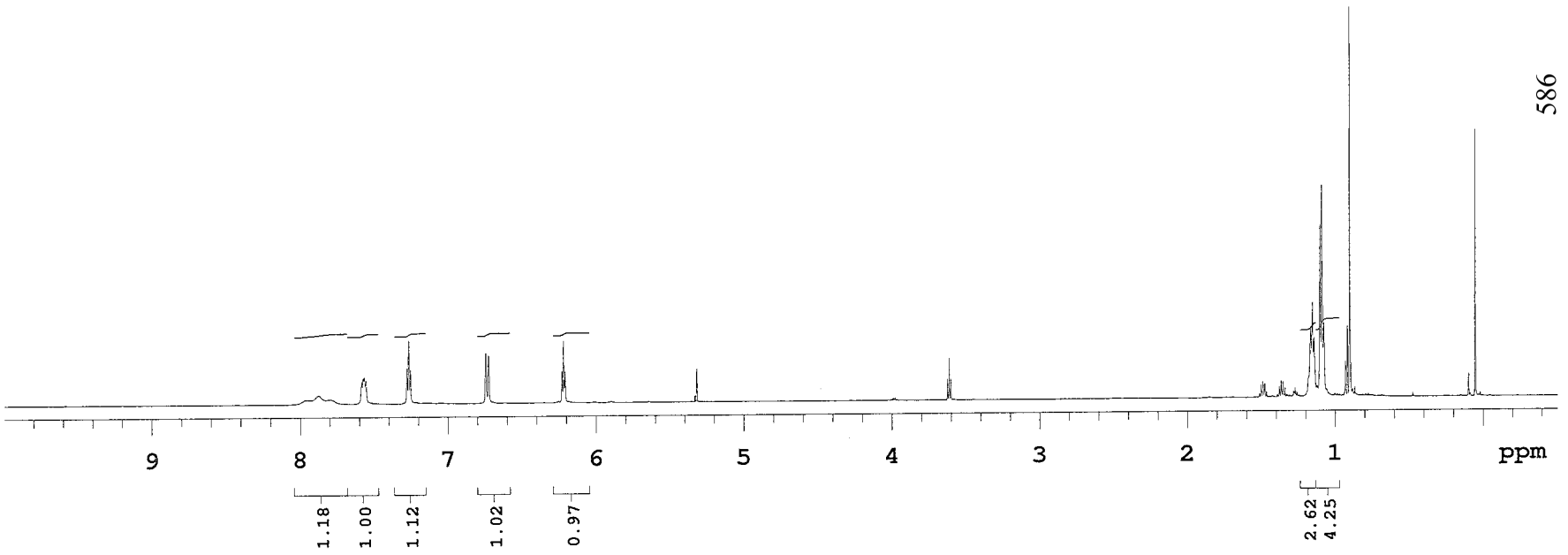

Data file exp

Plot date 2016-06-06

HL-1-051-11B

Sample Name **HL-1-051-11B**	Pulse sequence **BORON_11**	Temperature **25**	Study owner **Liu**
Date collected **2013-12-21**	Solvent **cd2cl2**	Spectrometer **nmr18-vnmrs500**	Operator **Liu**

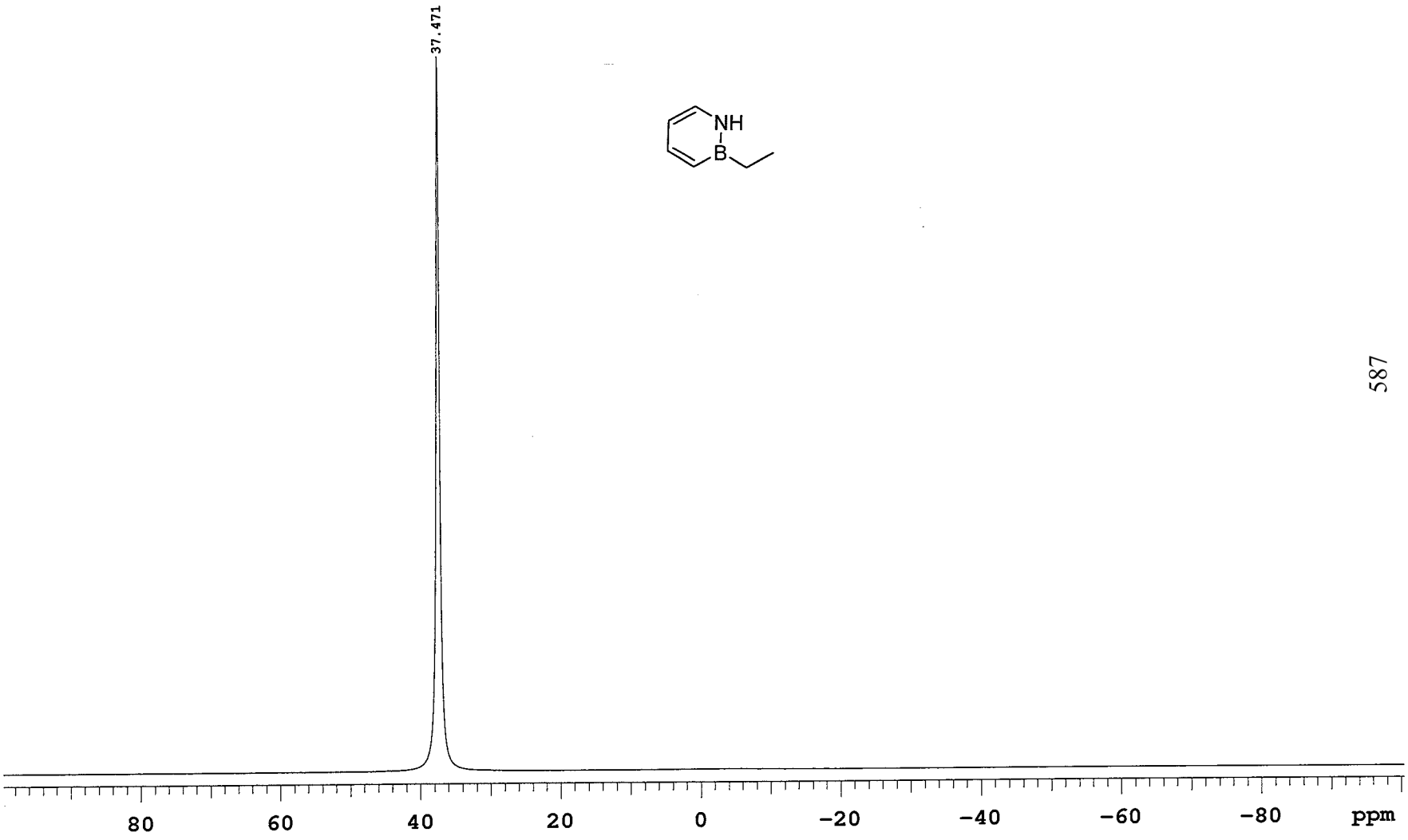

587

Data file /home/All/Liu/Hyelee Lee/HL-1-051-11B.fid

Plot date 2015-12-08

HL-II-062-pure-13C

Sample Name	**HL-II-062-pure-13C**	Pulse sequence	**CARBON**	Temperature	**25**	Study owner	**Liu**
Date collected	**2015-12-11**	Solvent	**cd2cl2**	Spectrometer	**nmr19-vnmrs600**	Operator	**Liu**

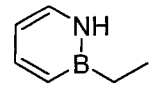

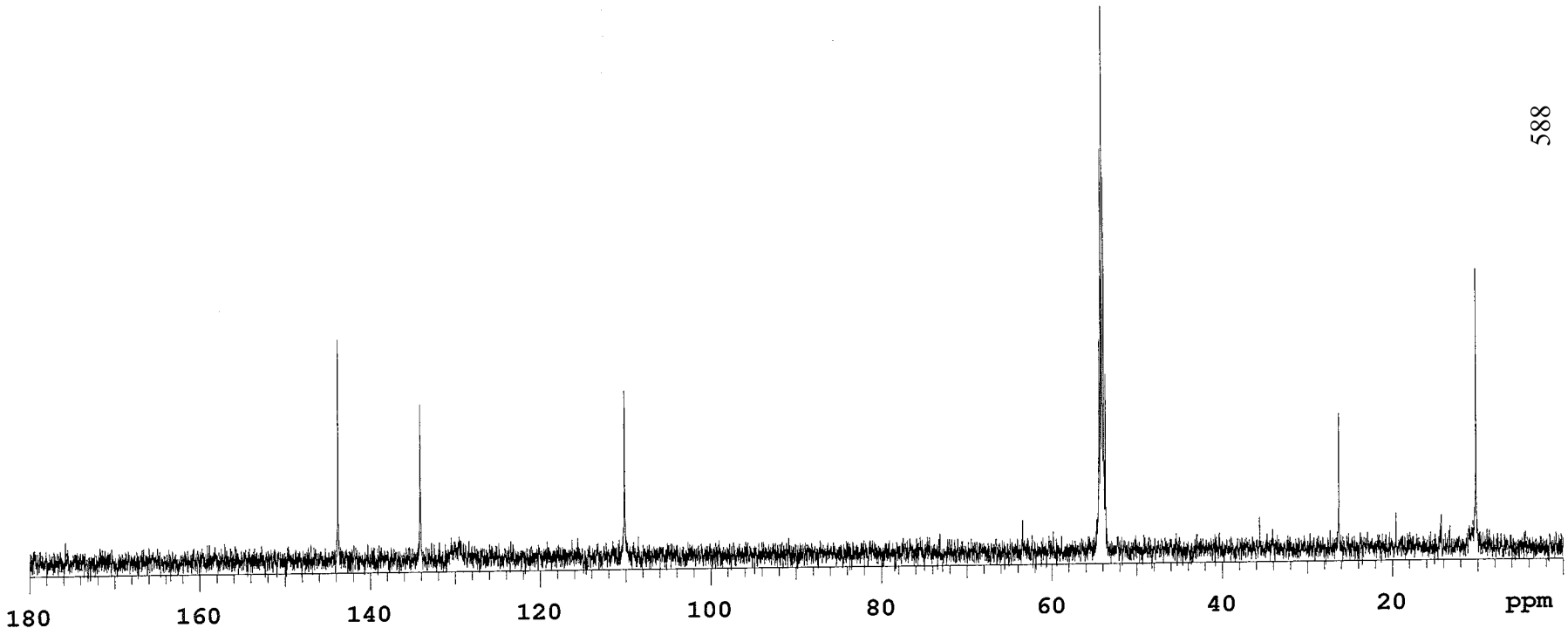

Data file exp

Plot date 2015-12-11

Sample Name:
HL-II-036-1H
Data Collected on:
nmr19-vnmrs600
Archive directory:

Sample directory:

FidFile: PROTON

Pulse Sequence: PROTON (s2pul)
Solvent: cd2cl2
Data collected on: Feb 26 2015

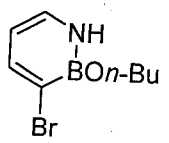

Sample Name:
HL-II-036-11B
Data Collected on:
nmr19-vnmrs600
Archive directory:

Sample directory:

FidFile: B11

Pulse Sequence: s2pul
Solvent: cd2cl2
Data collected on: Feb 26 2015

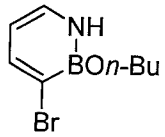

Sample Name:
HL-II-036-13C
Data Collected on:
nmr19-vnmrs600
Archive directory:

Sample directory:

FidFile: CARBON

Pulse Sequence: CARBON (s2pul)
Solvent: cd2cl2
Data collected on: Feb 26 2015

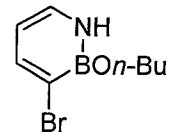

Sample Name:
HL-II-103-1H
Data Collected on:
nmr11-inova500
Archive directory:

Sample directory:

FidFile: PROTON

Pulse Sequence: PROTON (s2pul)
Solvent: cd2cl2
Data collected on: Apr 16 2015

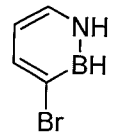

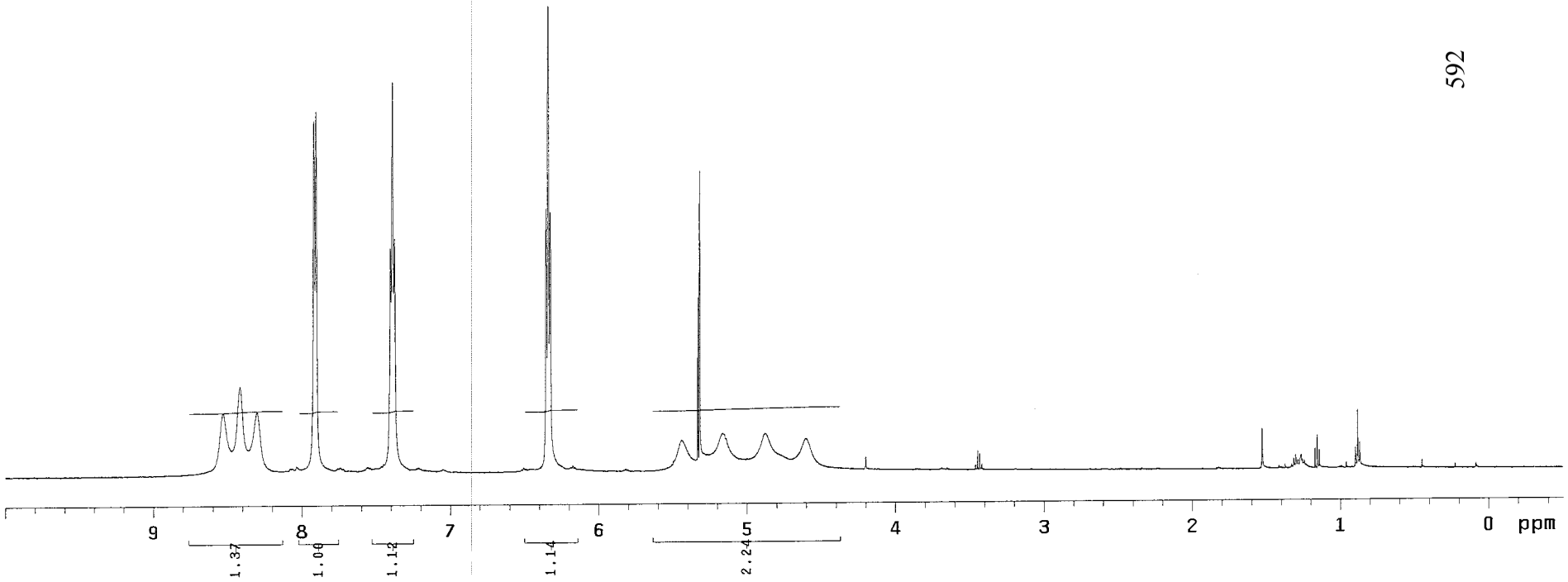

Sample Name:
HL-II-048-11B-coupled
Data Collected on:
nmr19-vnmrs600
Archive directory:

Sample directory:

FidFile: B11

Pulse Sequence: s2pul
Solvent: cd2cl2
Data collected on: Feb 27 2015

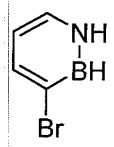

Sample Name:
HL-II-103-13C
Data Collected on:
nmr11-inova500
Archive directory:

Sample directory:

FidFile: CARBON

Pulse Sequence: CARBON (s2pul)
Solvent: cd2cl2
Data collected on: Apr 15 2015

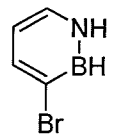

Sample Name:
HL-II-122-pure-1H
Data Collected on:
nmr18-vnmrs500
Archive directory:

Sample directory:

FidFile: PROTON

Pulse Sequence: PROTON (s2pul)
Solvent: cd2cl2
Data collected on: Apr 29 2015

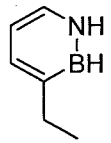

Sample Name:
HL-II-122-11B-pure
Data Collected on:
nmr18-vnmrs500
Archive directory:

Sample directory:

FidFile: BORON_11

Pulse Sequence: BORON_11 (s2pul)
Solvent: cd2cl2
Data collected on: Apr 28 2015

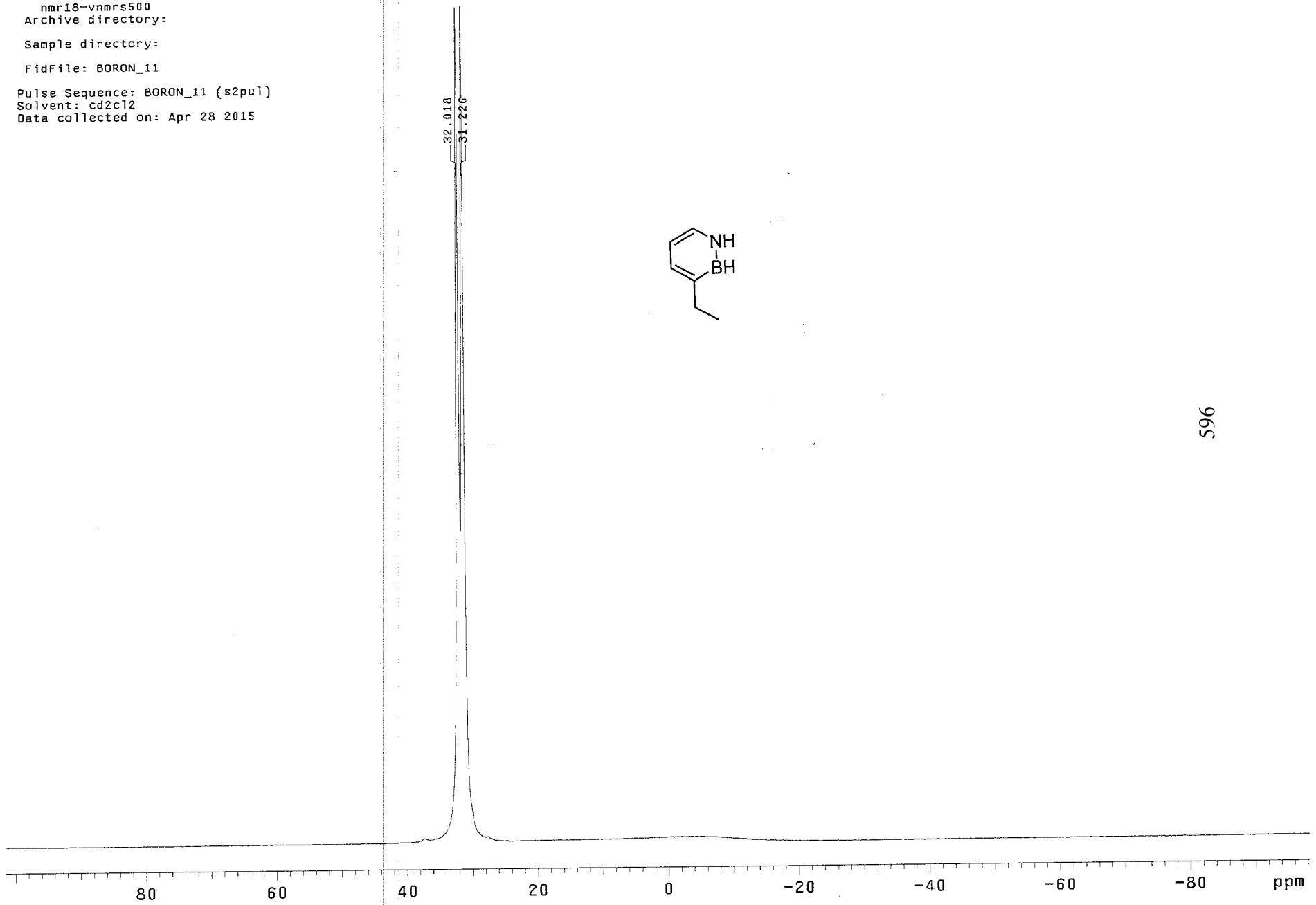

Sample Name:
HL-II-122-13C-pure
Data Collected on:
nmr11-inova500
Archive directory:

Sample directory:

FidFile: CARBON

Pulse Sequence: CARBON (s2pul)
Solvent: cd2cl2
Data collected on: Apr 28 2015

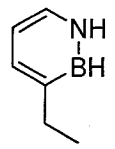

HL-1-091-pure-1H

Sample Name HL-1-091-pure-1H	Pulse sequence PROTON	Temperature 25	Study owner Liu
Date collected 2017-03-09	Solvent cd2cl2	Spectrometer nmr11-inova500	Operator Liu

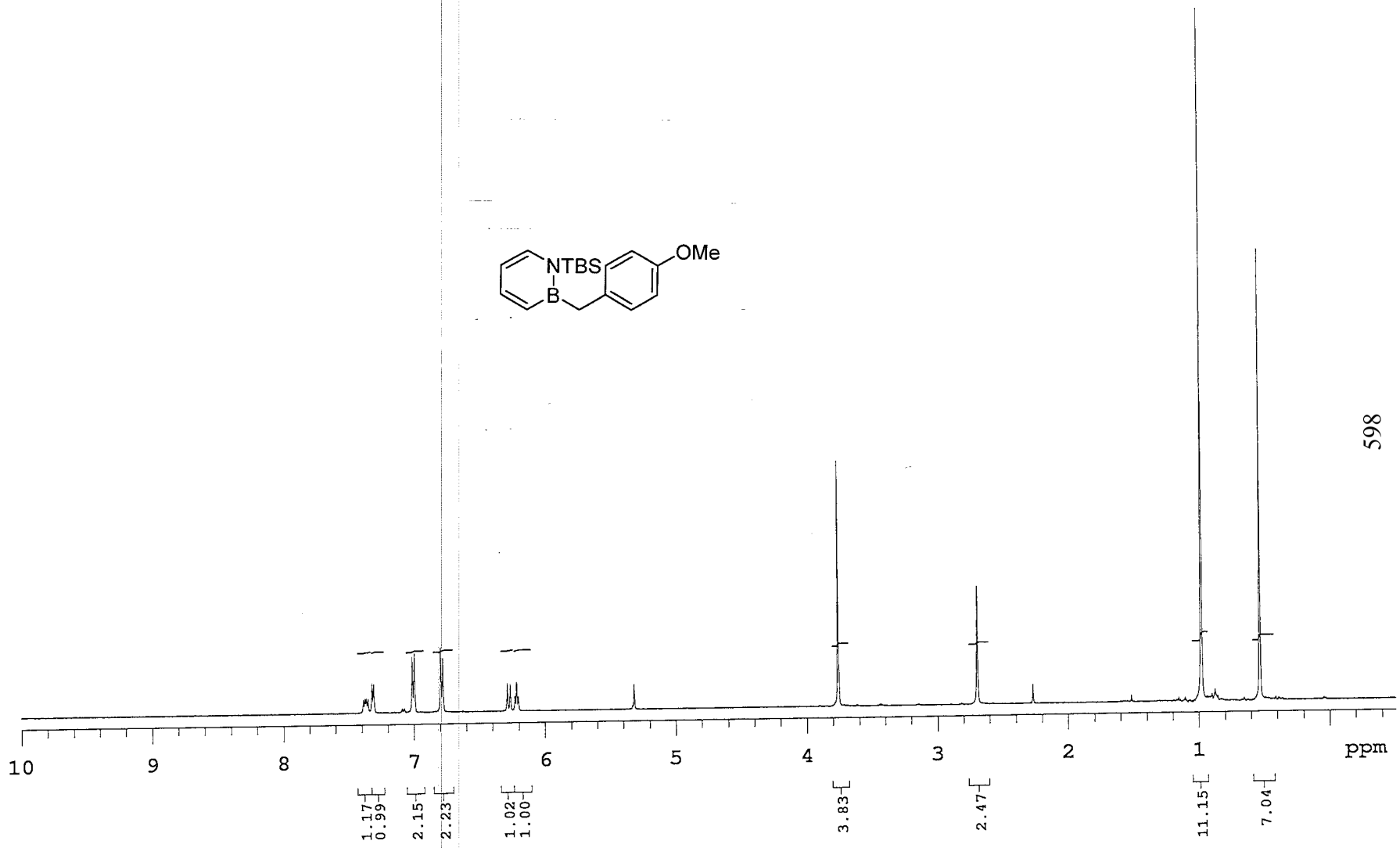

598

Data file exp

Plot date 2017-03-09

HL-1-091-pure-11B

Sample Name HL-1-091-pure-11B
Date collected 2017-03-09

Pulse sequence s2pul
Solvent cd2cl2

Temperature 25
Spectrometer nmr11-inova500

Study owner Liu
Operator Liu

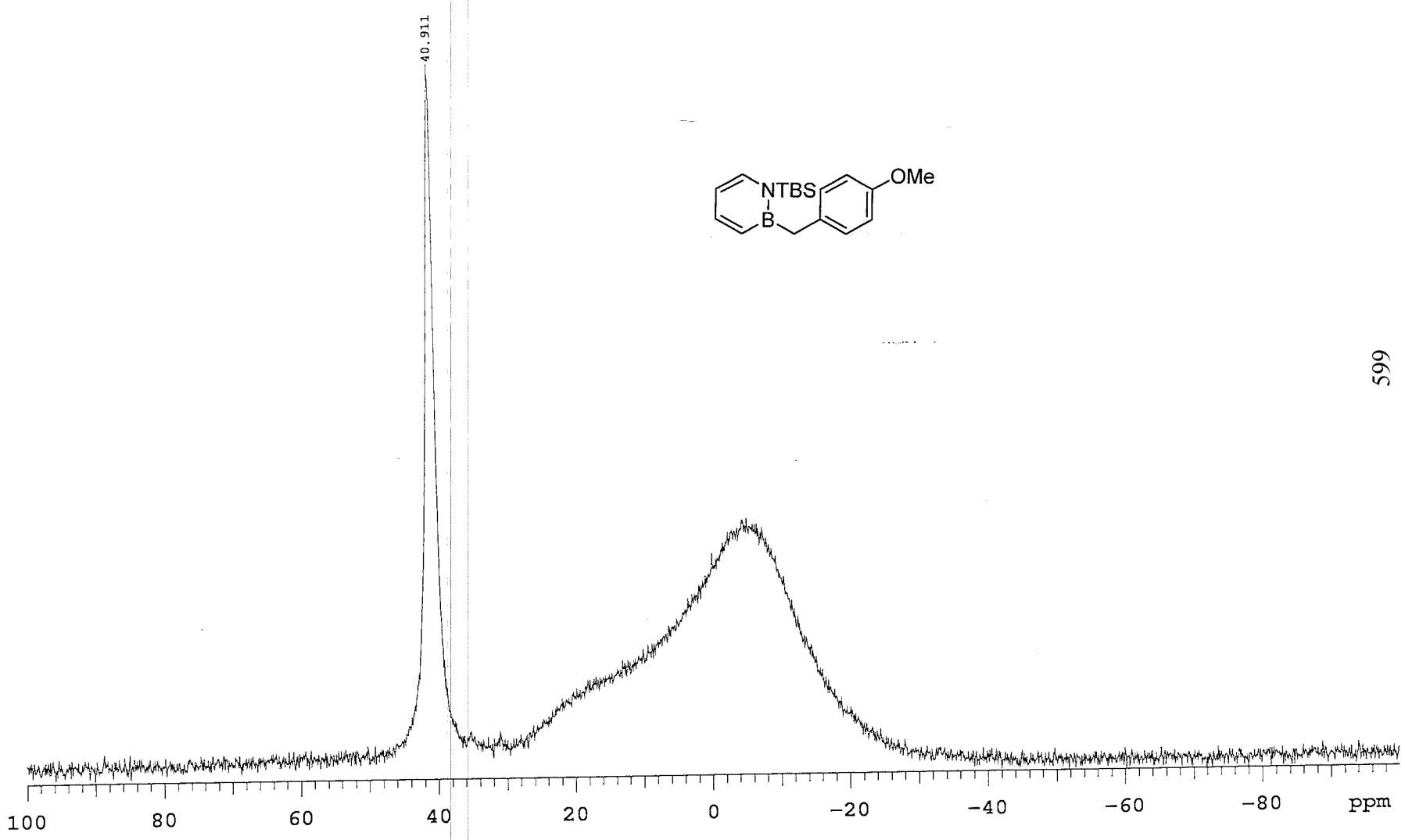

599

Data file exp

Plot date 2017-03-09

HL-1-091-13C

Sample Name	HL-1-091-13C	Pulse sequence	CARBON	Temperature	25	Study owner	Liu
Date collected	2017-03-10	Solvent	cd2cl2	Spectrometer	nmr19-vnmrs600	Operator	Liu

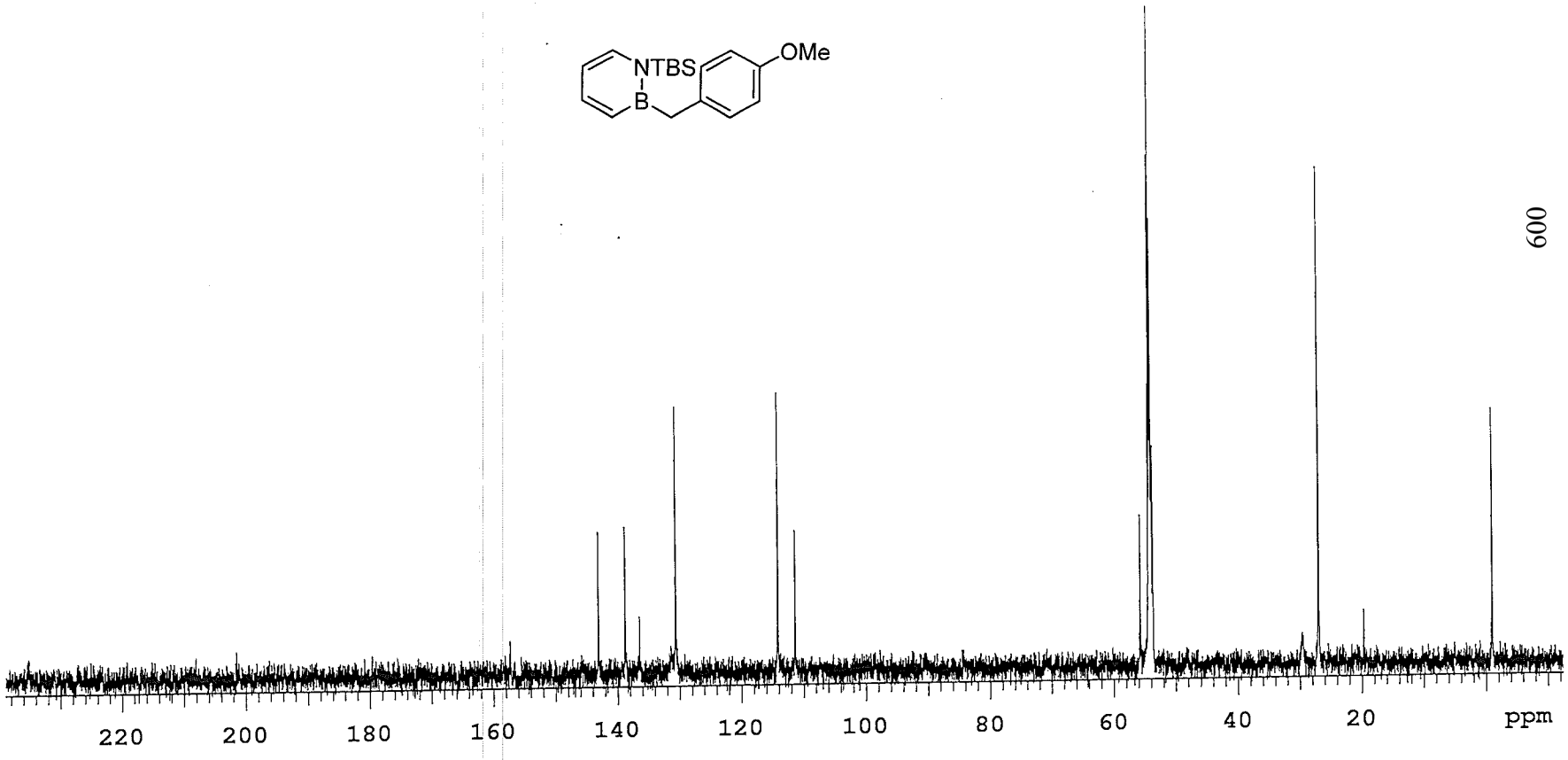

Data file exp

Plot date 2017-03-10

HL-1-036-1H

Sample Name HL-1-036-1H
Date collected 2016-10-03

Pulse sequence PROTON
Solvent cd2cl2

Temperature 25
Spectrometer nmr18-vnmrs500

Study owner Liu
Operator Liu

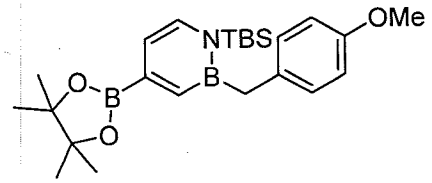

601

Data file /home/ALL/Liu/HL/Chapter 3/new500/HL-1-036-no-pentane-1H.fid

Plot date 2017-03-11

HL-1-032-1-11B

Sample Name HL-1-032-1-11B	Pulse sequence s2pul	Temperature 25	Study owner Liu
Date collected 2016-09-22	Solvent cd2cl2	Spectrometer nmr11-inova500	Operator Liu

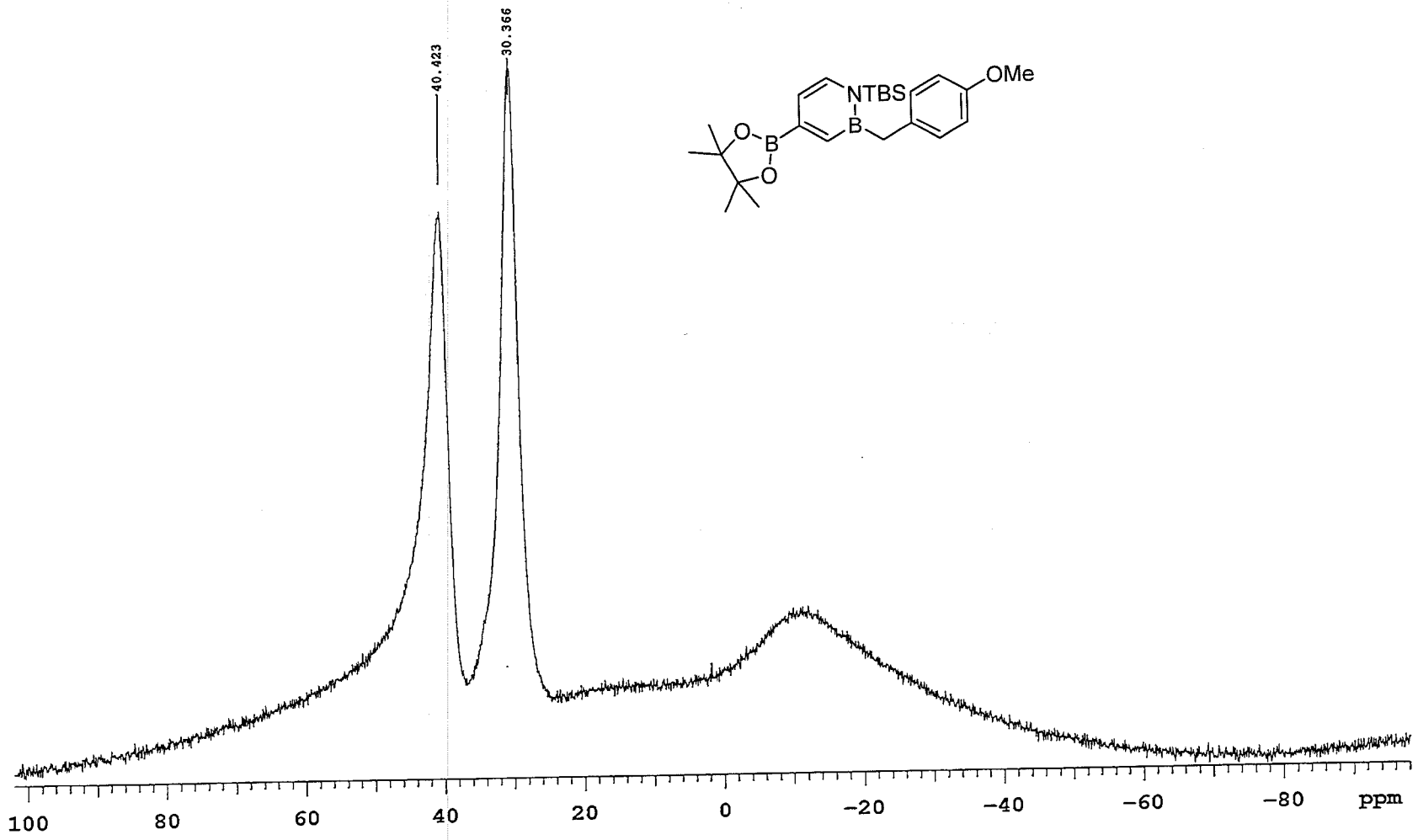

602

Plot date 2016-09-22

Data file exp

HL-1-036-1-13C

Sample Name **HL-1-036-1-13C**	Pulse sequence **CARBON**	Temperature **25**	Study owner **Liu**
Date collected **2016-10-07**	Solvent **cd2cl2**	Spectrometer **nmr19-vnmrs600**	Operator **Liu**

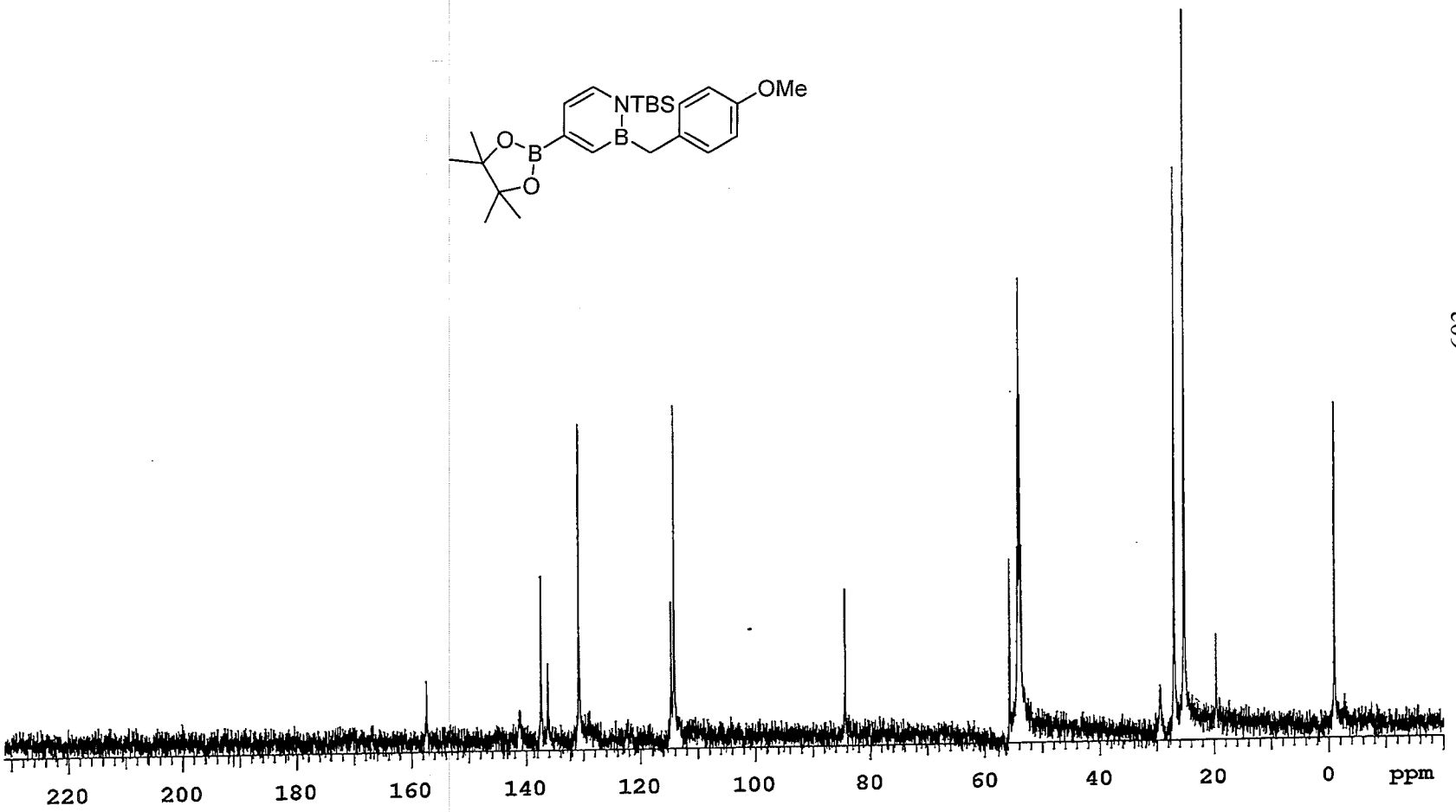

603

Plot date 2016-10-07

Data file exp

HL-1-041-1H

Sample Name HL-1-041-1H
Date collected 2016-10-06

Pulse sequence PROTON
Solvent cd2cl2

Temperature 25
Spectrometer nmr11-inova500

Study owner Liu
Operator Liu

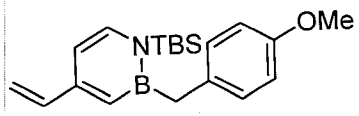

604

Data file /home/ALL/Liu/HL/Chapter 3/HL-1-041-1H.fid

Plot date 2017-03-11

Sample Name HL-1-041-NB
Date collected 2016-10-06

Pulse sequence s2pul
Solvent cd2cl2

Temperature 25
Spectrometer nmr11-inova500

Study owner Liu
Operator Liu

STANDARD PROTON PARAMETERS

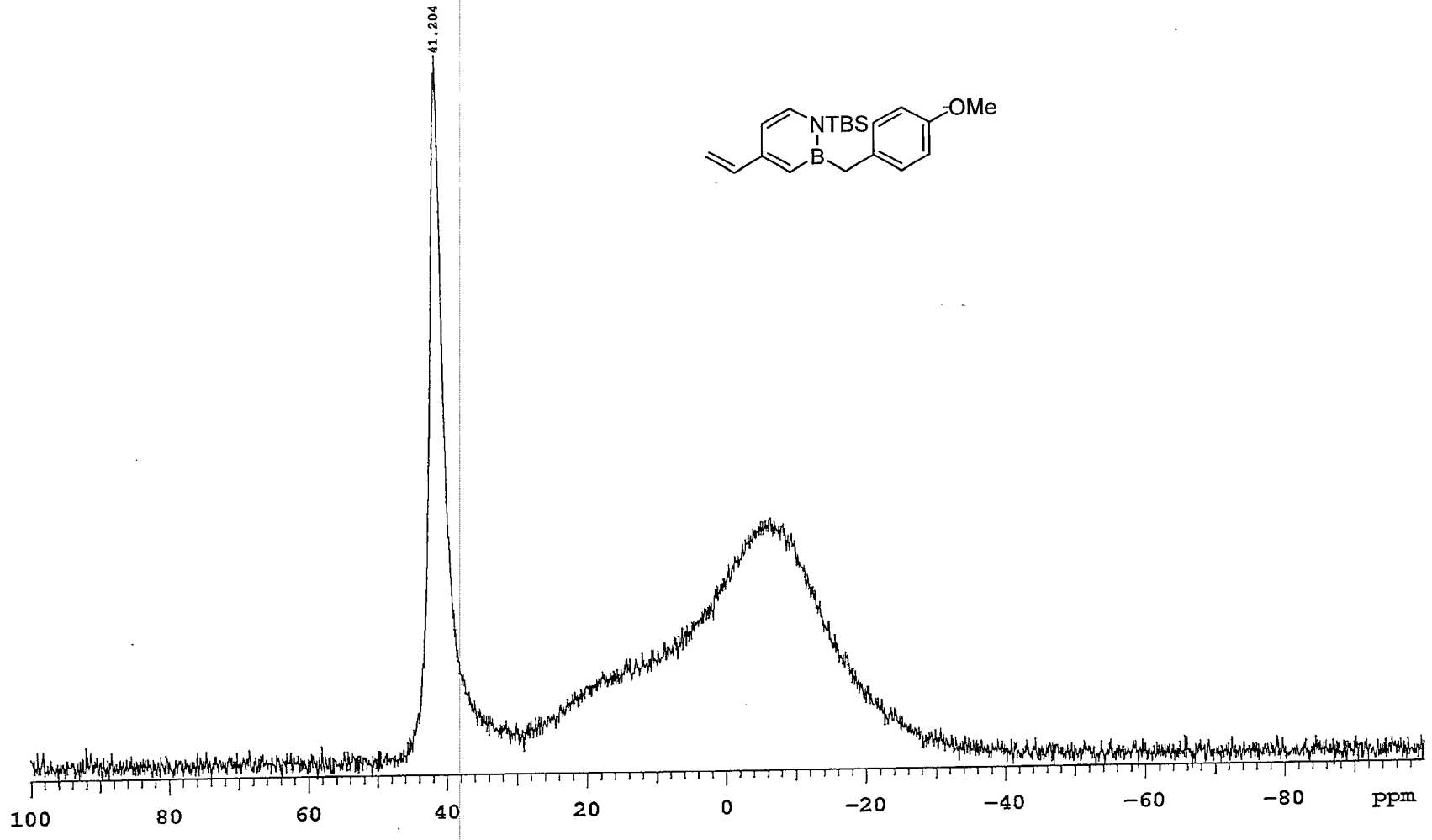

Plot date 2016-10-06

Data file exp

HL-1-041-13C

Sample Name	HL-1-041-13C	Pulse sequence	CARBON	Temperature	25	Study owner	Liu
Date collected	2016-10-06	Solvent	cd2cl2	Spectrometer	nmr19-vnmrs600	Operator	Liu

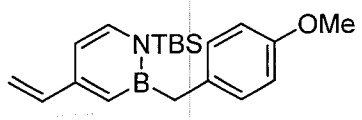

606

Data file exp

Plot date 2016-10-06

HL-2-007-1H

Sample Name HL-2-007-1H	Pulse sequence PROTON	Temperature 25	Study owner Liu
Date collected 2017-02-03	Solvent cd2cl2	Spectrometer nmr11-inova500	Operator Liu

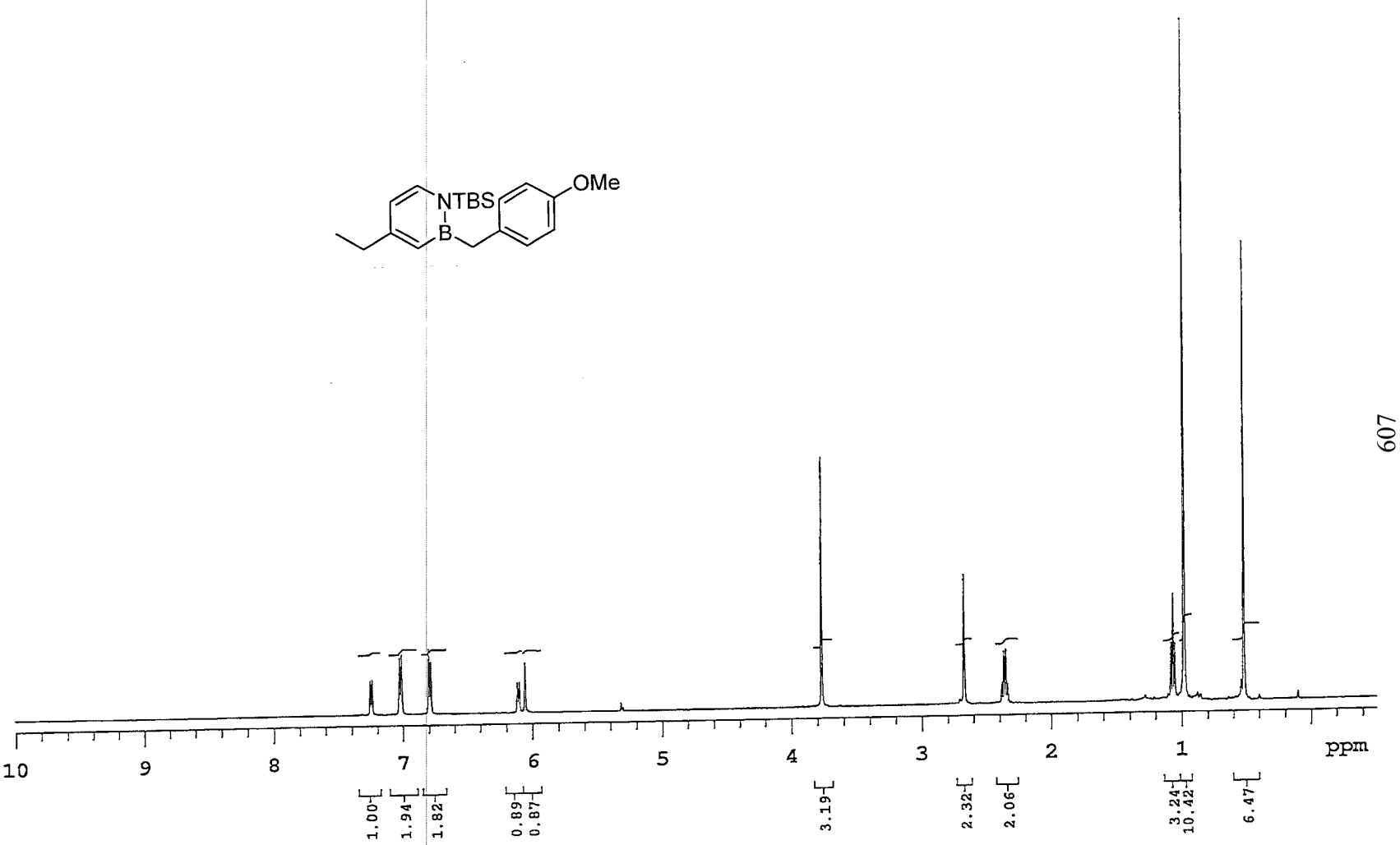

607

Plot date 2017-02-03

Data file exp

HL-2-007-11B

Sample Name HL-2-007-11B	Pulse sequence s2pul	Temperature 25	Study owner Liu
Date collected 2017-02-03	Solvent cd2cl2	Spectrometer nmr11-inova500	Operator Liu

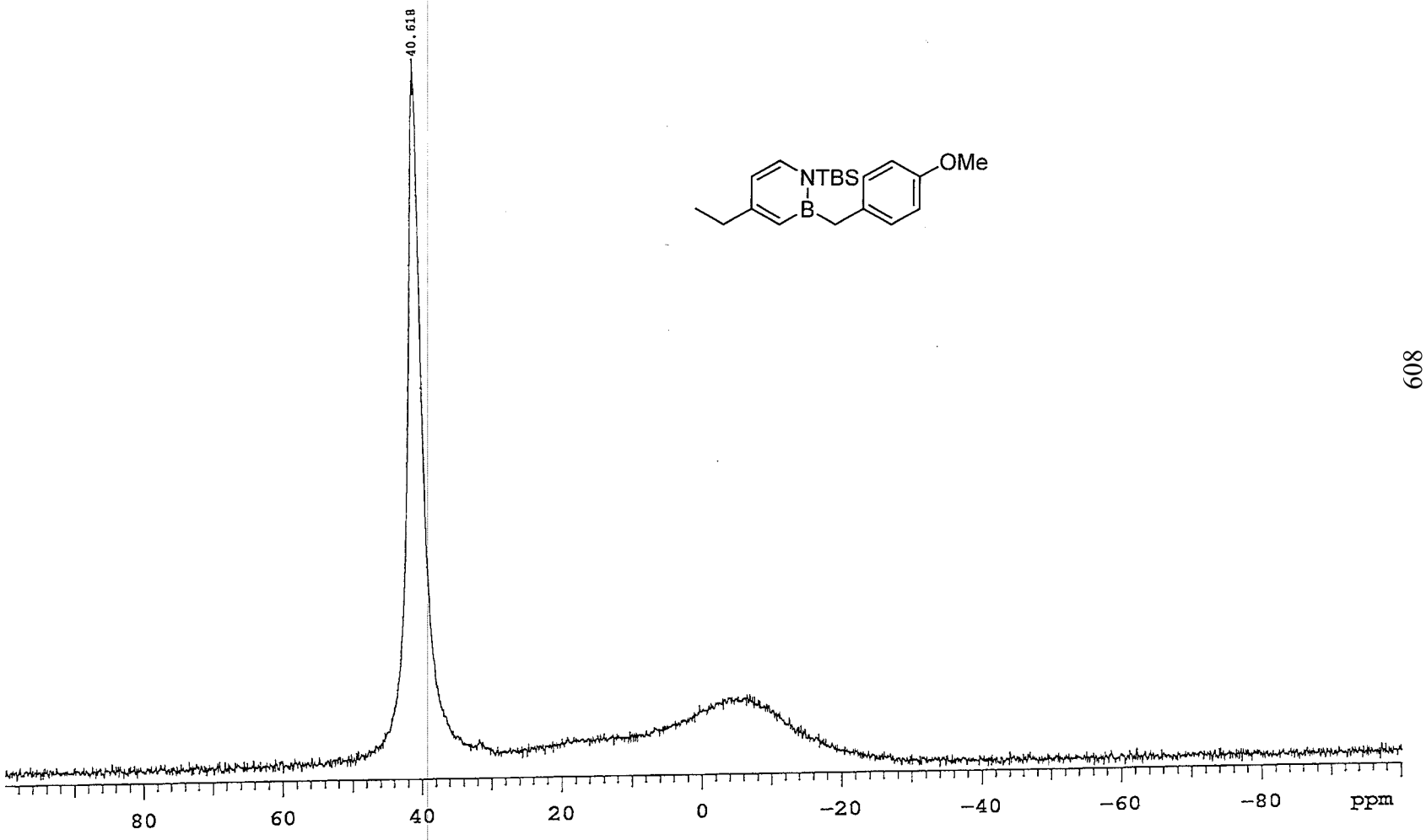

Plot date 2017-02-03

Data file /home/Liu/vnmrsys/data/Hyelee/ELN/HL-2-007-11B.fid

HL-2-007-13C

Sample Name	HL-2-007-13C	Pulse sequence	CARBON	Temperature	25
Date collected	2017-02-03	Solvent	cd2cl2	Spectrometer	nmr19-vnmrs600

Study owner Liu
Operator Liu

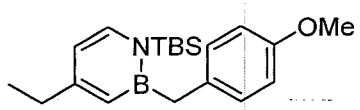

609

Plot date 2017-02-03

Data file exp

HL-1-044-1H

Sample Name HL-1-044-1H
Date collected 2016-10-08

Pulse sequence PROTON
Solvent cd2cl2

Temperature 25
Spectrometer nmr11-inova500

Study owner Liu
Operator Liu

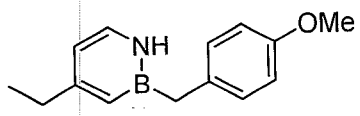

610

Data file /home/ALL/Liu/HL/Chapter 3/HL-1-044-1H.fid

Plot date 2017-03-11

HL-1-044-11B

Sample Name **HL-1-044-11B**
Date collected **2016-10-08**

Pulse sequence **s2pul**
Solvent **cd2cl2**

Temperature **25**
Spectrometer **nmr11-inova500**

Study owner **Liu**
Operator **Liu**

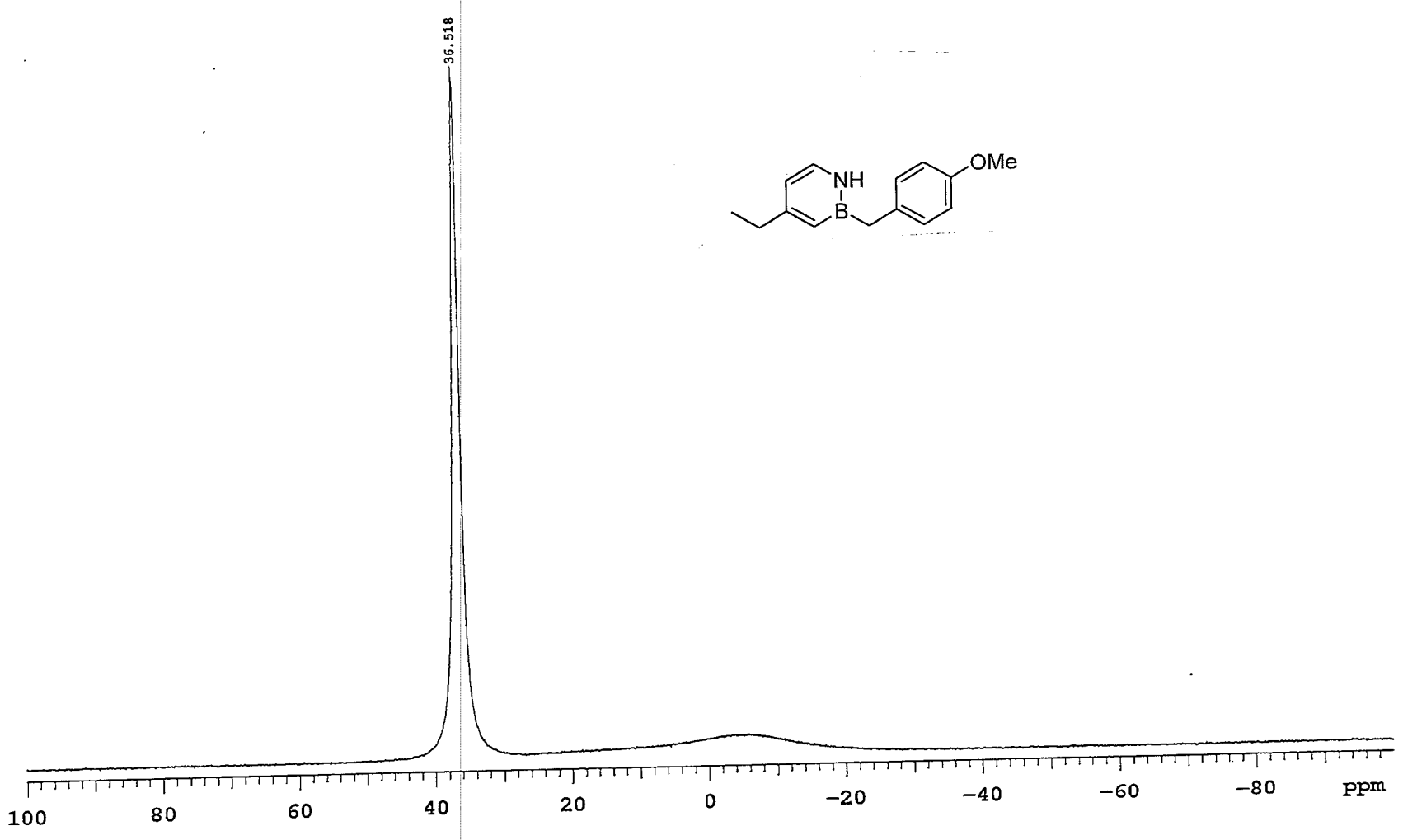

Plot date 2016-10-08

Data file exp

HL-1-044-13C

Sample Name	HL-1-044-13C	Pulse sequence	CARBON	Temperature	25	Study owner	Liu
Date collected	2016-10-08	Solvent	cd2cl2	Spectrometer	nmr19-vnmrs600	Operator	Liu

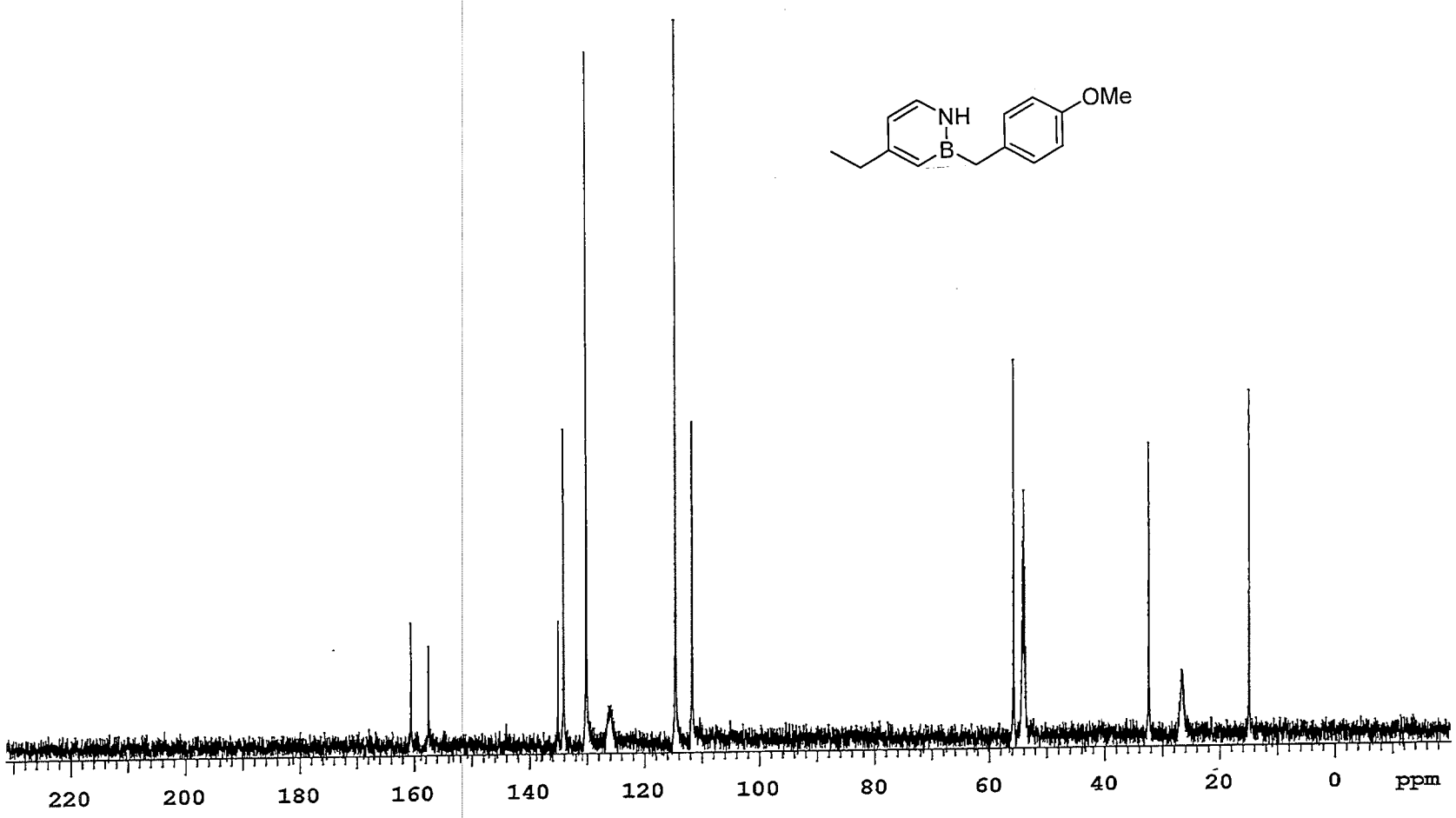

612

Plot date 2016-10-08

Data file exp

HL-2-030-1H

Sample Name HL-2-030-1H
Date collected 2017-04-03

Pulse sequence PROTON
Solvent cd2cl2

Temperature 25
Spectrometer nmr19-vnmrs600

Study owner Liu
Operator Liu

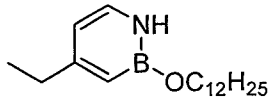

613

Data file exp

Plot date 2017-04-03

HL-2-014-1-11B

Sample Name HL-2-014-1-11B	Pulse sequence s2pul	Temperature 25	Study owner Liu
Date collected 2017-02-24	Solvent cd2cl2	Spectrometer nmr11-inova500	Operator Liu

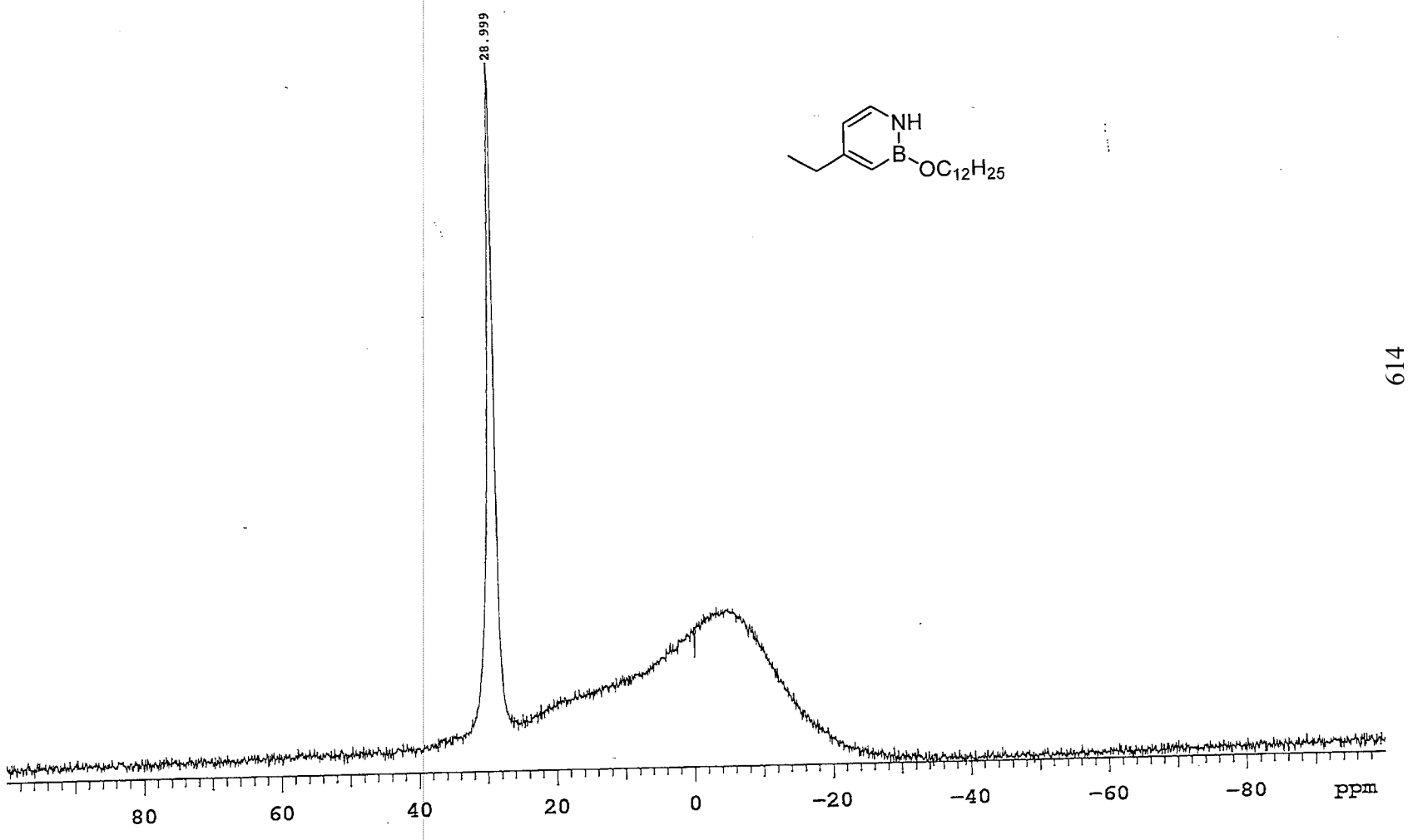

Plot date 2017-02-24

Data file exp

HL-2-014-1-13C

Sample Name	HL-2-014-1-13C	Pulse sequence	CARBON	Temperature	25
Date collected	2017-02-24	Solvent	cd2cl2	Spectrometer	nmr19-vnmrs600
Study owner	Liu				
Operator	Liu				

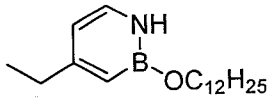

615

Data file

Pur data 2017-02-24

HL-1-036-column3-1H

Sample Name HL-1-036-column3-1H
Date collected 2016-10-08

Pulse sequence PROTON
Solvent cd2cl2

Temperature 25
Spectrometer nmr11-inova500

Study owner Liu
Operator Liu

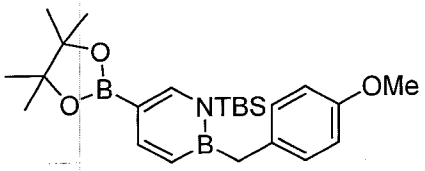

616

Plot date 2016-10-08

Data file exp

HL-1-036-column3-11B

Sample Name HL-1-036-column3-11B	Pulse sequence s2pul	Temperature 25	Study owner Liu
Date collected 2016-10-08	Solvent cd2cl2	Spectrometer nmr11-inova500	Operator Liu

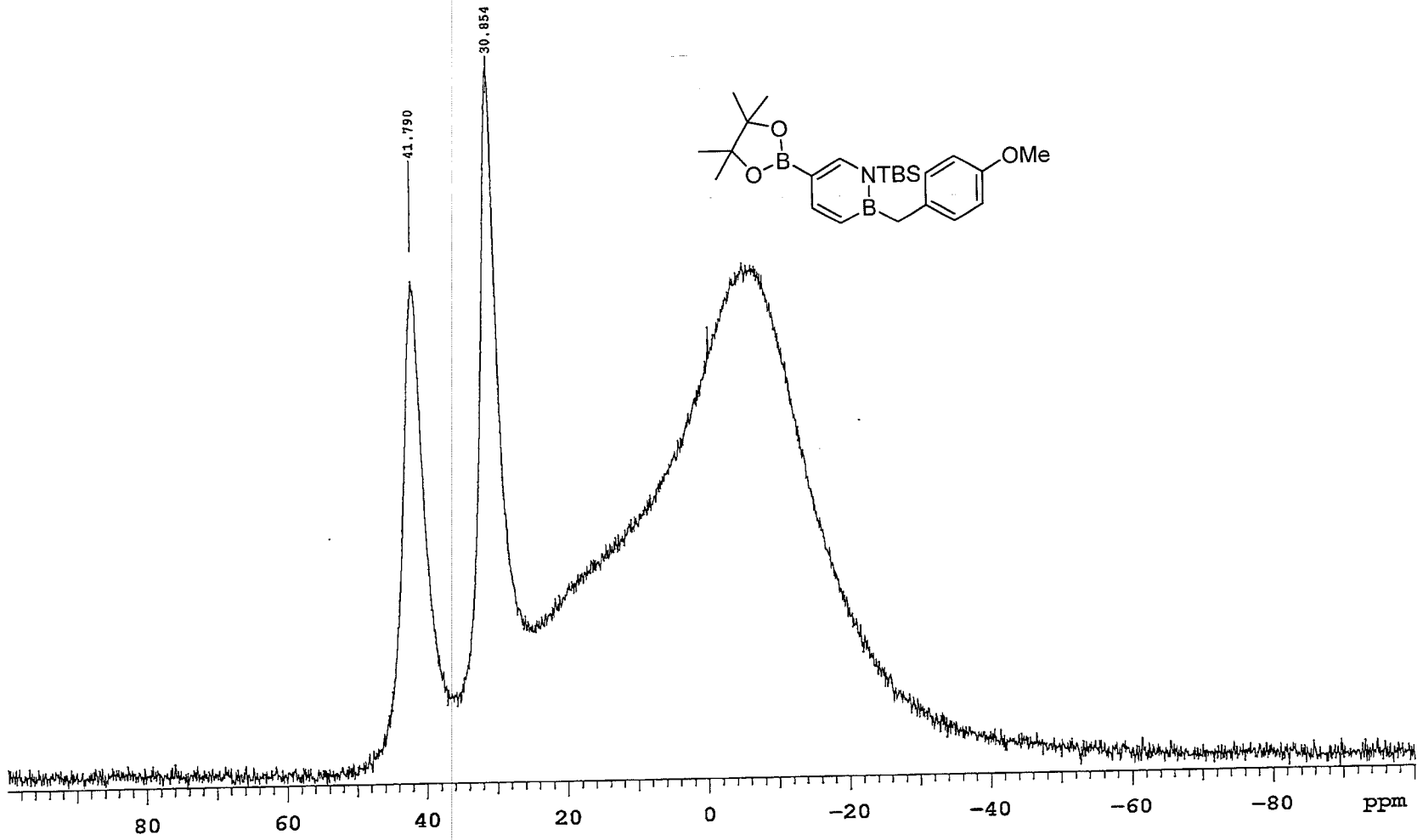

Plot date 2016-10-08

Data file exp

HL-1-036-2-13C

Sample Name **HL-1-036-2-13C**	Pulse sequence **CARBON**	Temperature **25**	Study owner **Liu**
Date collected **2016-10-07**	Solvent **cd2cl2**	Spectrometer **nmr19-vnmrs600**	Operator **Liu**

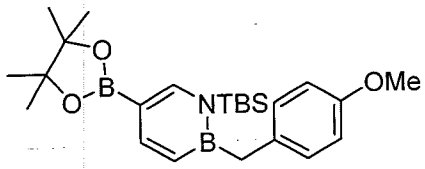

618

Plot date 2016-10-07

Data file exp

HL-2-003-col1-2-1H

Sample Name HL-2-003-col1-2-1H
Date collected 2017-01-26

Pulse sequence PROTON
Solvent cd2cl2

Temperature 25
Spectrometer nmr11-inova500

Study owner Liu
Operator Liu

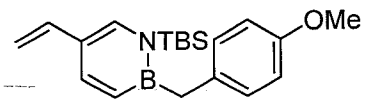

619

Data file /home/ALL/Liu/HL/Chapter 3/HL-2-003-col1-2-1H.fid

Plot date 2017-03-11

HL-1-045-11B

Sample Name HL-1-045-11B	Pulse sequence s2pul	Temperature 25	Study owner Liu
Date collected 2016-10-11	Solvent cd2cl2	Spectrometer nmr11-inova500	Operator Liu

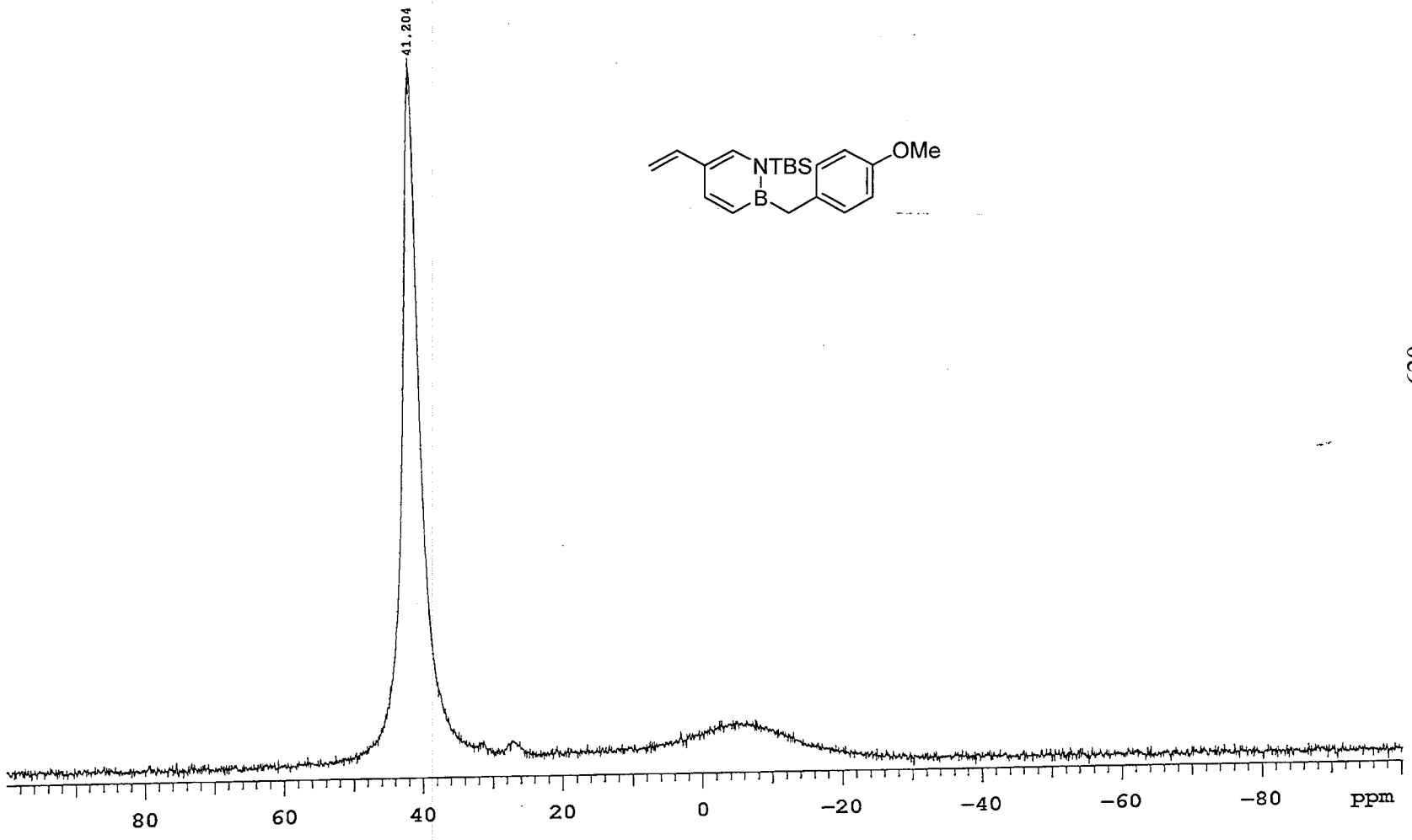

620

Plot date 2016-10-11

Data file exp

HL-1-045-13C

Sample Name **HL-1-045-13C**	Pulse sequence **CARBON**	Temperature **25**	Study owner **Liu**
Date collected **2016-10-11**	Solvent **cd2cl2**	Spectrometer **nmr19-vnmrs600**	Operator **Liu**

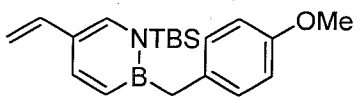

621

Plot date 2016-10-11

Data file exp

HL-2-005-1H

Sample Name HL-2-005-1H	Pulse sequence PROTON	Temperature 25	Study owner Liu
Date collected 2017-01-28	Solvent cd2cl2	Spectrometer nmr11-inova500	Operator Liu

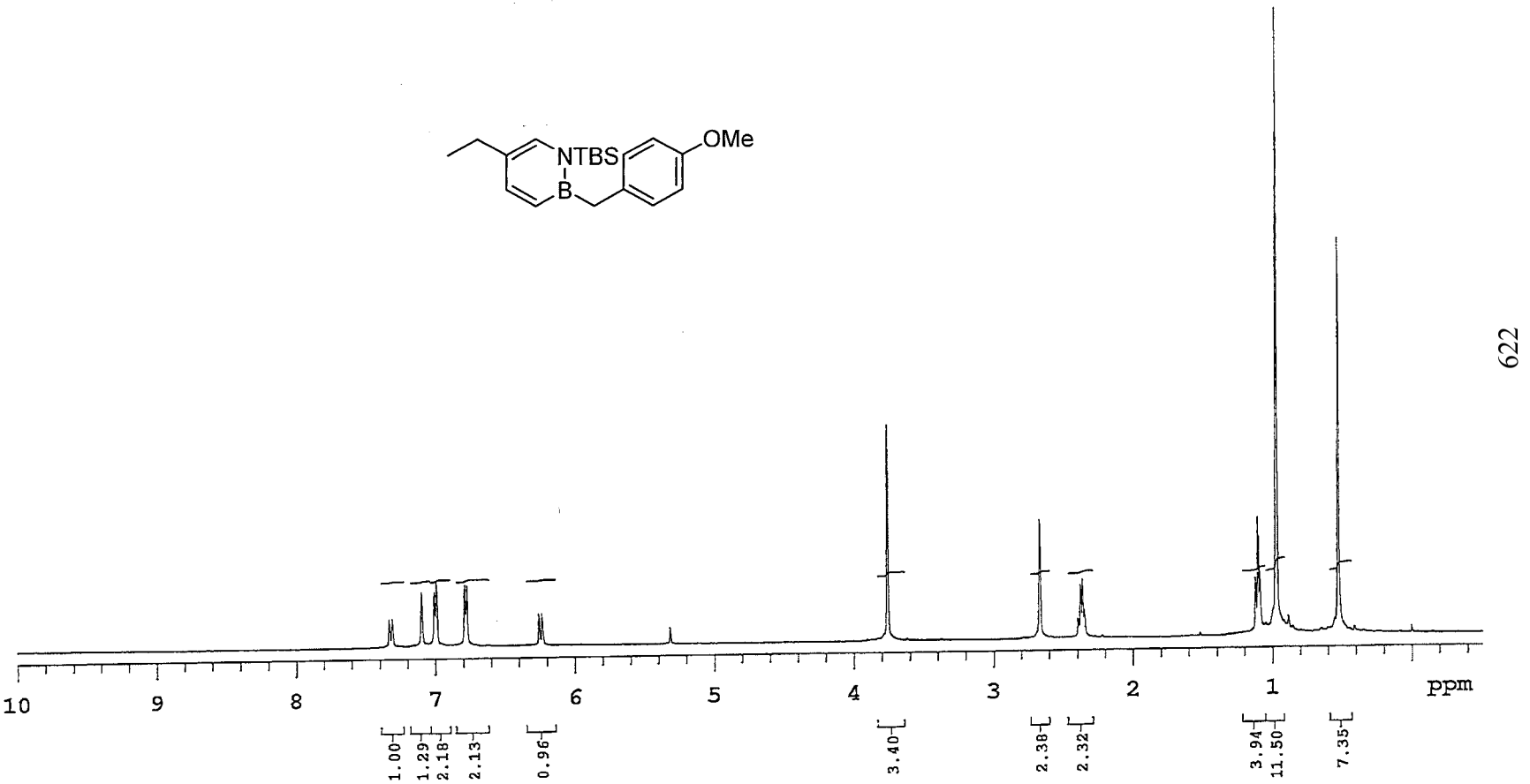

622

Plot date 2017-01-28

Data file exp

HL-2-005-11B

Sample Name HL-2-005-11B	Pulse sequence s2pul	Temperature 25	Study owner Liu
Date collected 2017-01-28	Solvent cd2cl2	Spectrometer nmr11-inova500	Operator Liu

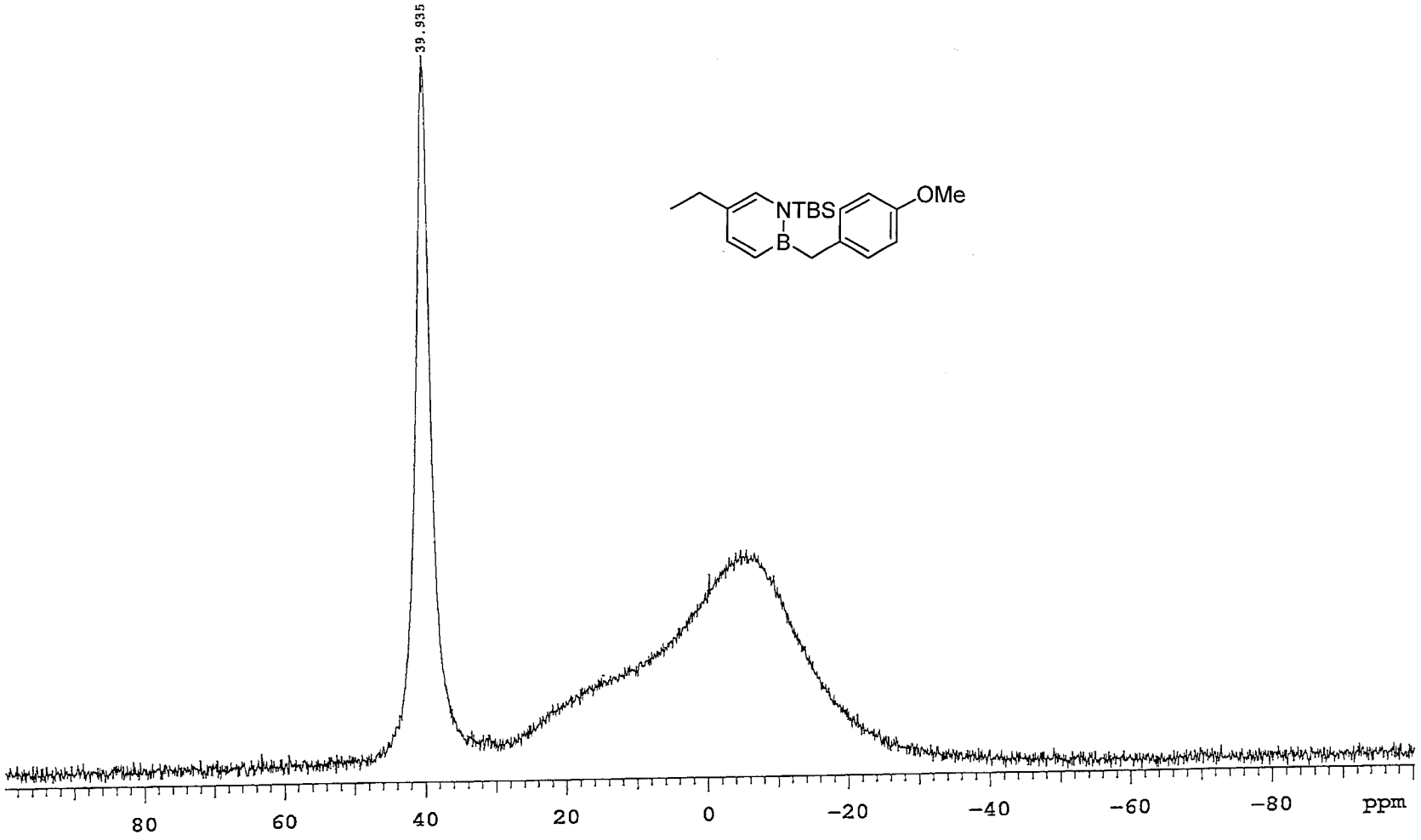

623

Plot date 2017-01-28

Data file exp

HL-2-005-13C

Sample Name HL-2-005-13C	Pulse sequence CARBON	Temperature 25	Study owner Liu
Date collected 2017-01-28	Solvent cd2cl2	Spectrometer nmr19-vnmrs600	Operator Liu

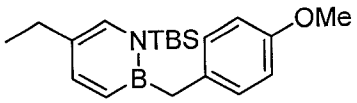

624

Plot date 2017-01-28

Data file exp

HL-1-053-1H

Sample Name HL-1-053-1H	Pulse sequence PROTON	Temperature 25	Study owner Liu
Date collected 2016-10-19	Solvent cd2cl2	Spectrometer nmr11-inova500	Operator Liu

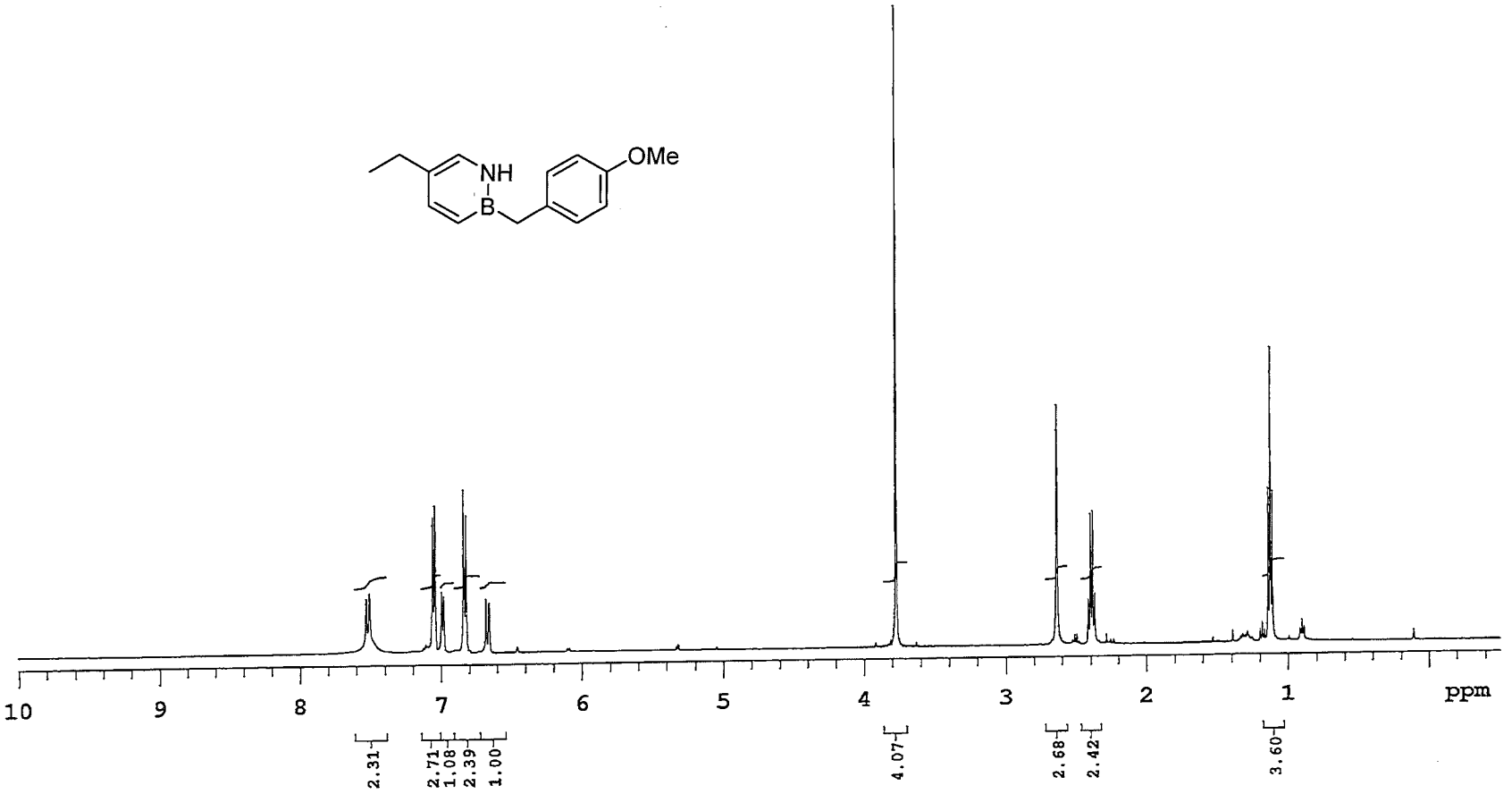

625

Plot date 2016-10-19

Data file exp

HL-1-053-11B

Sample Name HL-1-053-11B	Pulse sequence s2pul	Temperature 25	Study owner Liu
Date collected 2016-10-19	Solvent cd2cl2	Spectrometer nmr11-inova500	Operator Liu

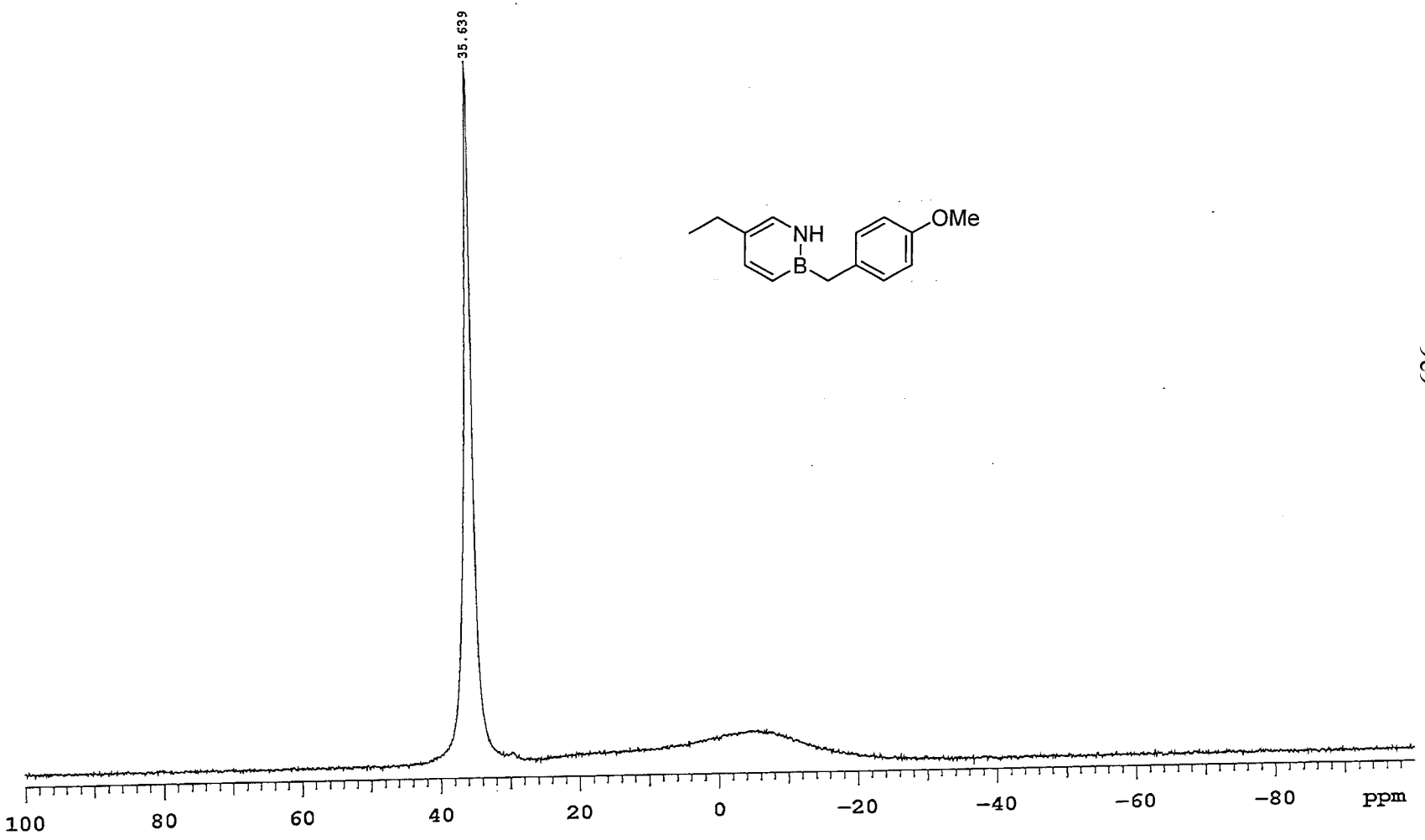

626

Plot date 2016-10-19

Data file exp

HL-1-053-13C

Sample Name	**HL-1-053-13C**	Pulse sequence	**CARBON**	Temperature	**25**	Study owner	**Liu**
Date collected	**2016-10-19**	Solvent	**cd2cl2**	Spectrometer	**nmr19-vnmrs600**	Operator	**Liu**

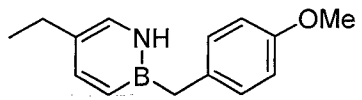

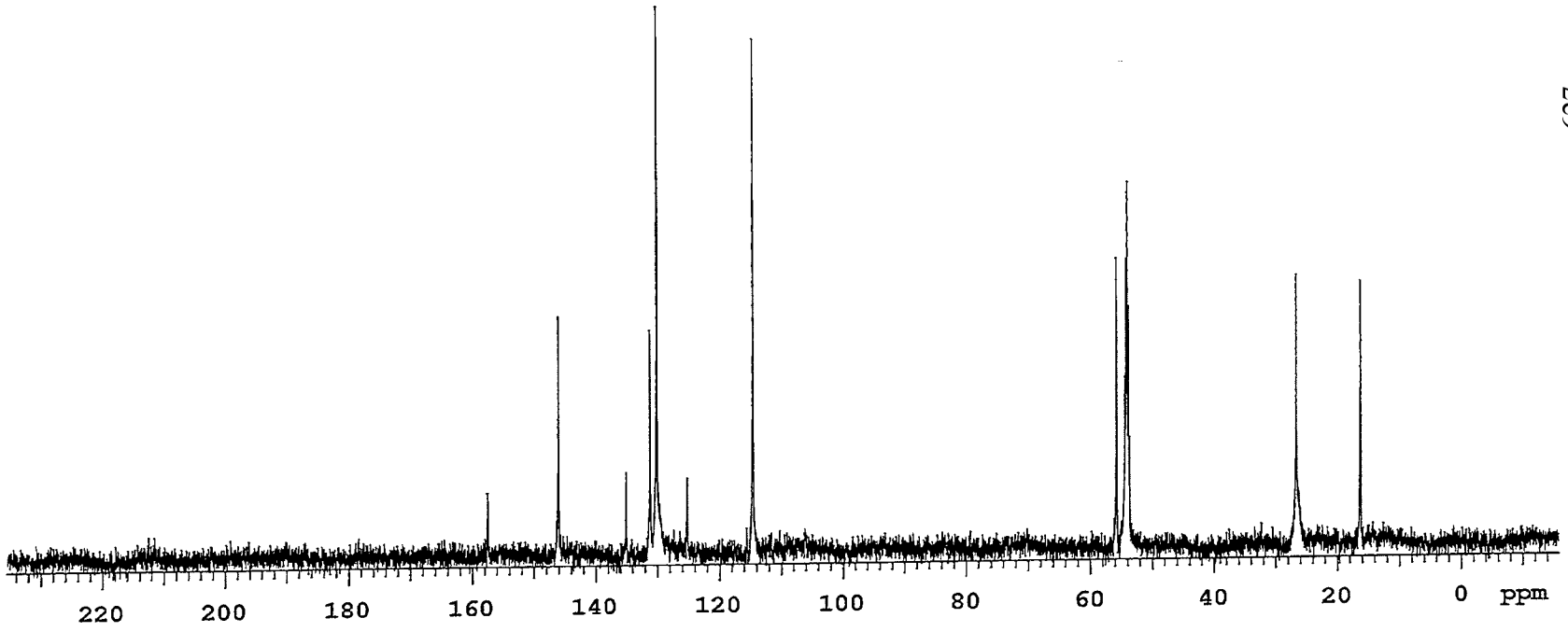

627

Data file exp

Plot date 2016-10-19

HL-2-012-HPLC-2-1-1H

Sample Name HL-2-012-HPLC-2-1-1H	Pulse sequence PROTON	Temperature 25	Study owner Liu
Date collected 2017-03-09	Solvent cd2cl2	Spectrometer nmr11-inova500	Operator Liu

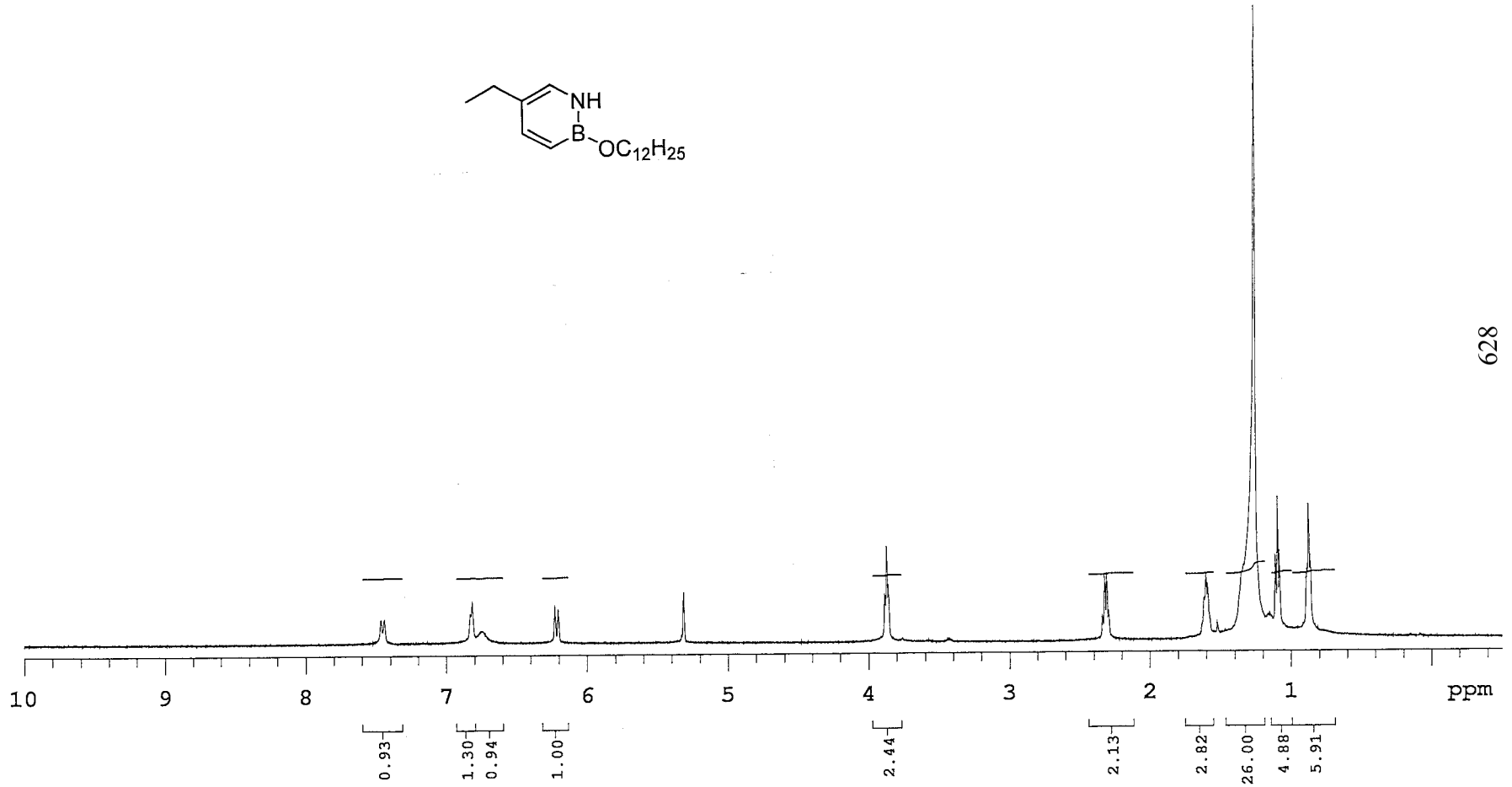

628

Data file /home/Liu/vnmrsys/data/Hyelee/ELN/HL-2-012-HPLC-2-1-1H.fid

Plot date 2017-03-09

HL-2-012-HPLC-2-1-11B

Sample Name	HL-2-012-HPLC-2-1-11B	Pulse sequence	s2pul	Temperature	25	Study owner	Liu
Date collected	2017-03-09	Solvent	cd2cl2	Spectrometer	nmr11-inova500	Operator	Liu

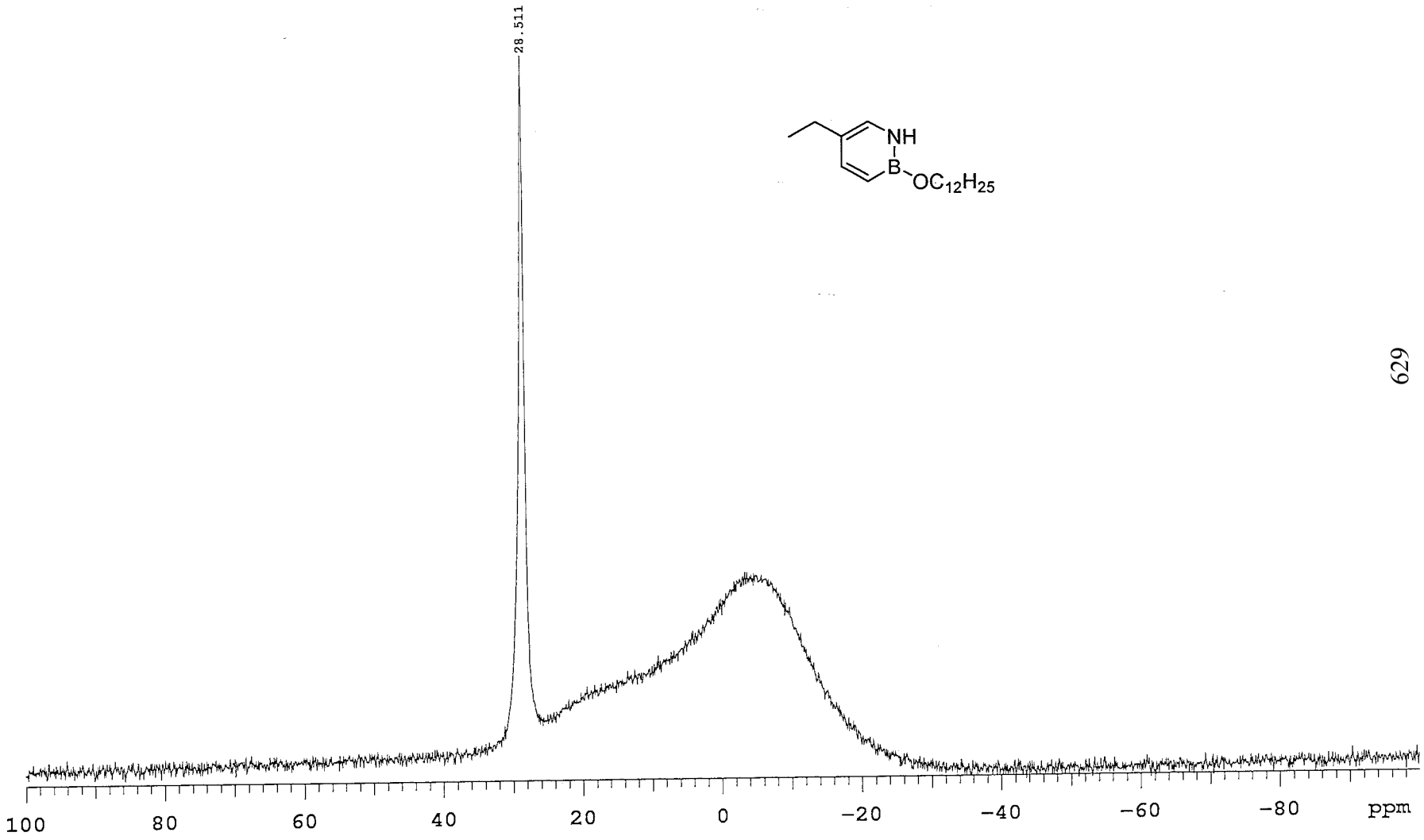

629

Data file /home/Liu/vnmrsys/data/Hyelee/ELN/HL-2-012-HPLC-2-1-11B.fid

Plot date 2017-03-09

HL-2-012-13C

Sample Name HL-2-012-13C	Pulse sequence CARBON	Temperature 25	Study owner Liu
Date collected 2017-02-24	Solvent cd2cl2	Spectrometer nmr19-vnmrs600	Operator Liu

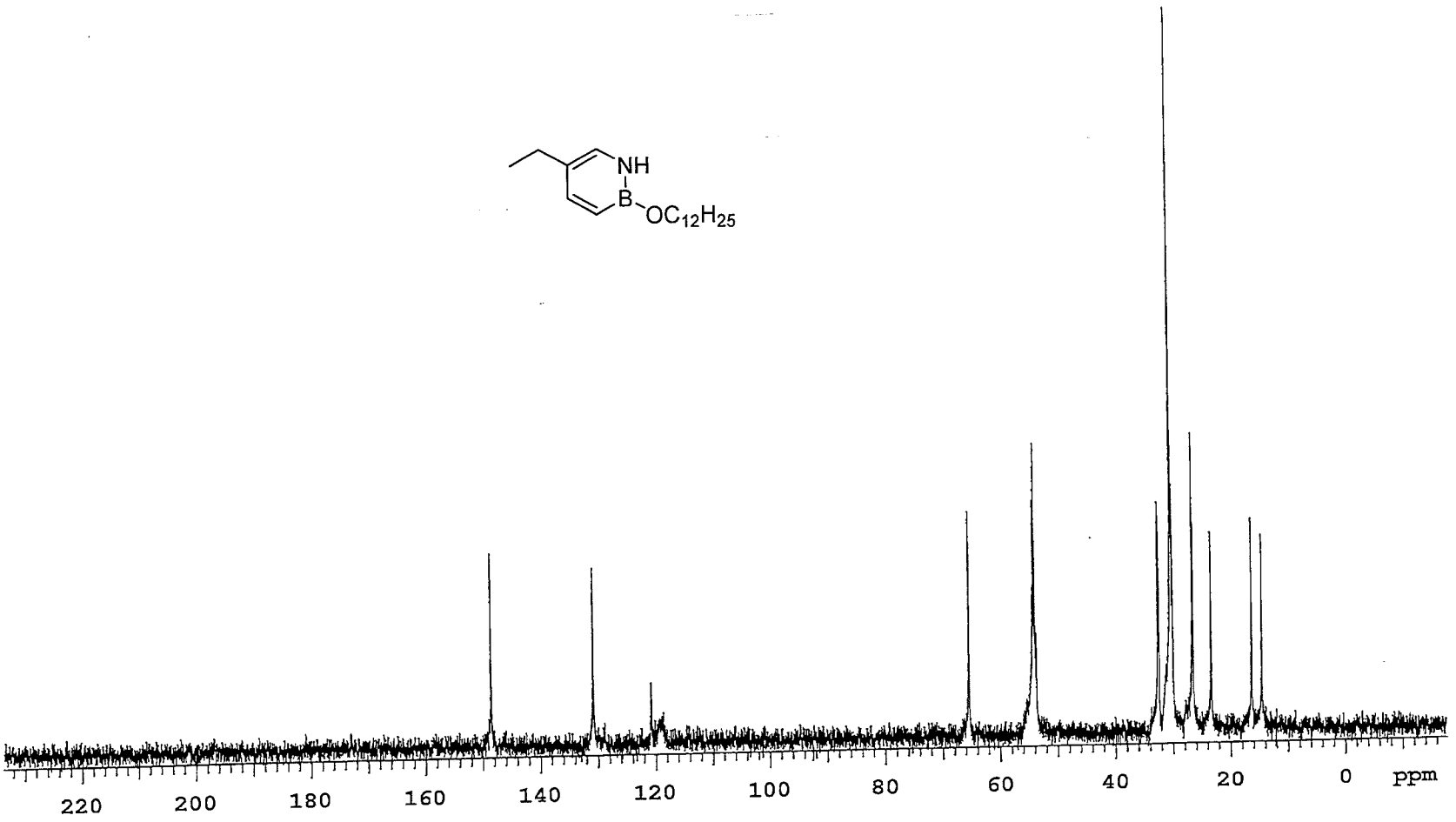

630

Plot date 2017-02-24

Data file exp

HL-2-031-pure-1H

Sample Name HL-2-031-pure-1H
Date collected 2017-04-05

Pulse sequence PROTON
Solvent cd2cl2

Temperature 25
Spectrometer nmr19-vnmrs600

Study owner Liu
Operator Liu

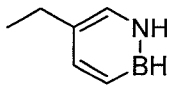

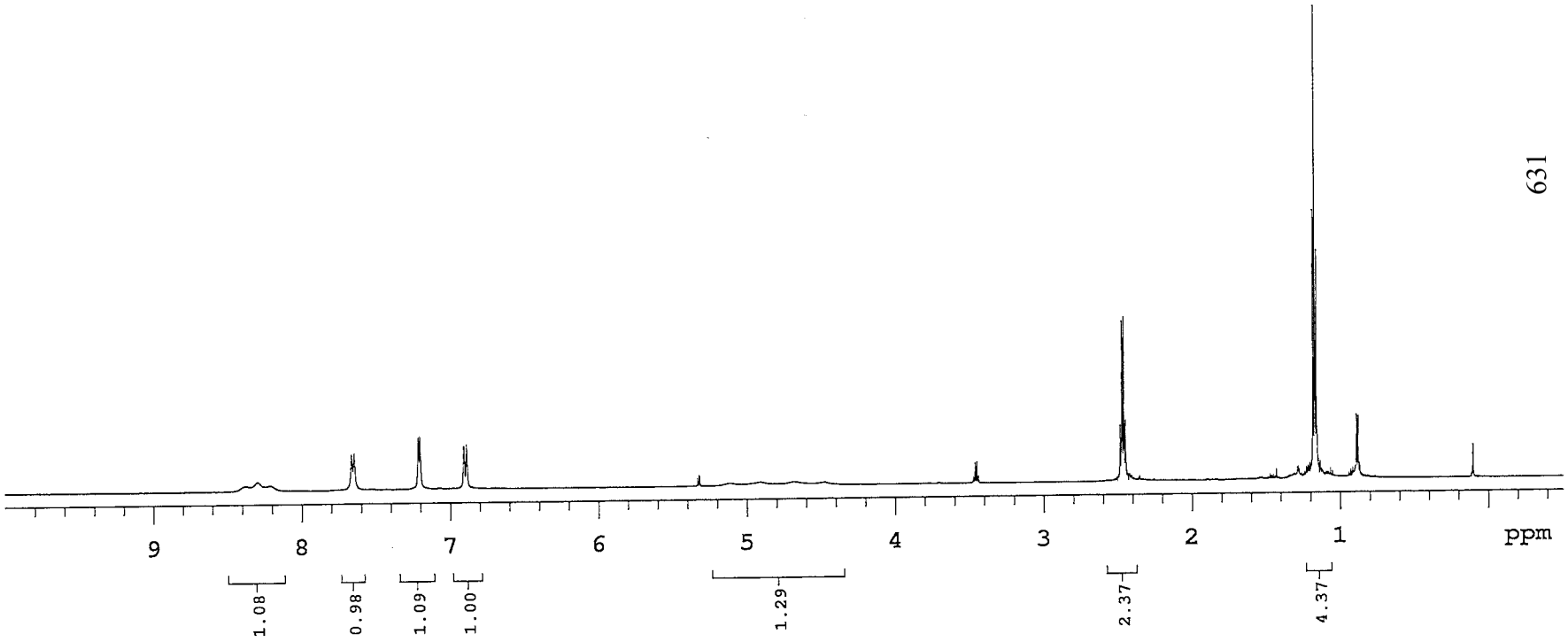

631

Data file exp

Plot date 2017-04-05

HL-2-031-11B

Sample Name HL-2-031-11B
Date collected 2017-03-31

Pulse sequence s2pul
Solvent cd2cl2

Temperature 25
Spectrometer nmr18-vnmrs500

Study owner Liu
Operator Liu

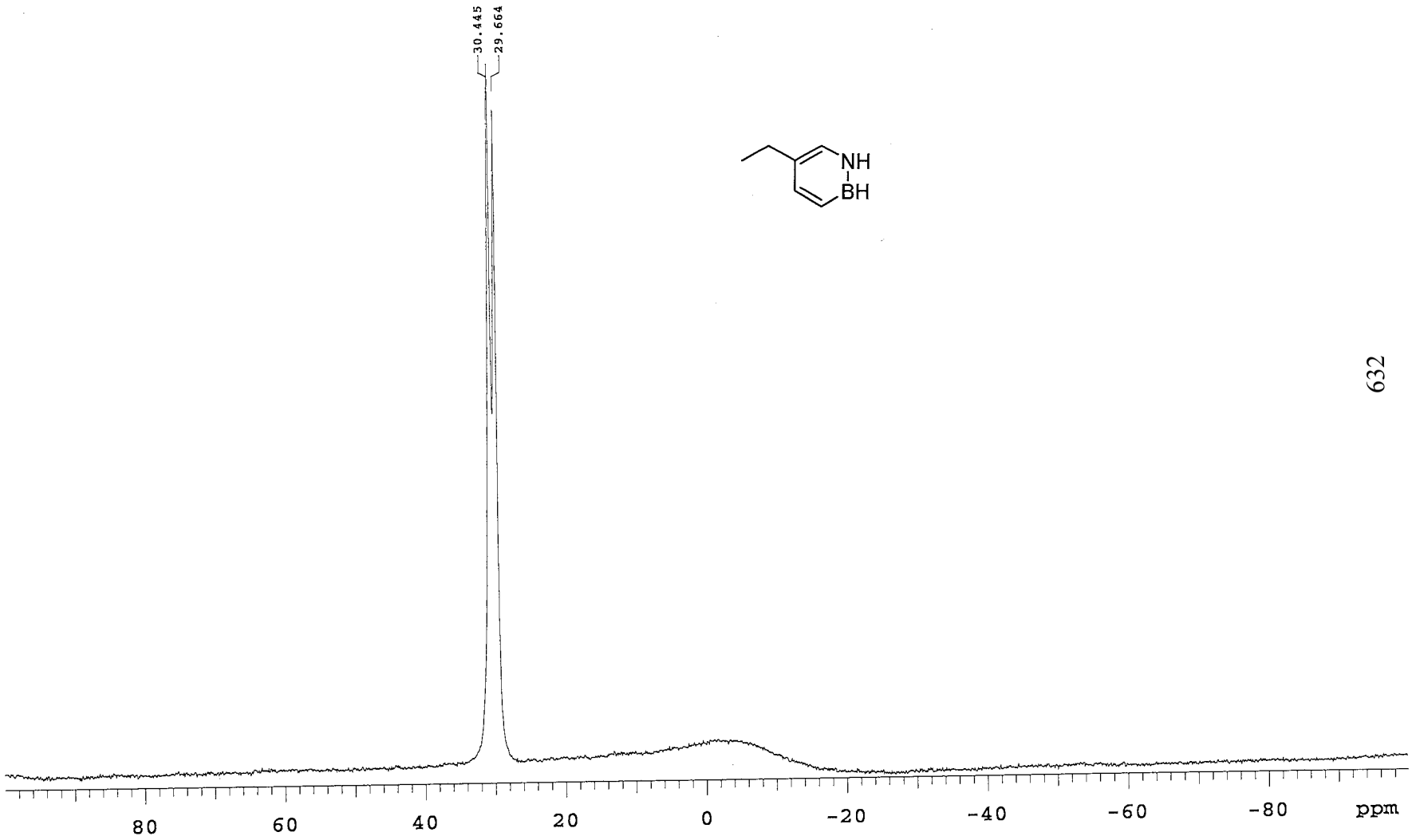

632

Data file /home/ALL/Liu/HL/ELN/HL-2-031-11B.fid

Plot date 2017-04-01

HL-2-031-pure-13C

Sample Name HL-2-031-pure-13C
Date collected 2017-04-05

Pulse sequence CARBON
Solvent cd2cl2

Temperature 25
Spectrometer nmr19-vnmrs600

Study owner Liu
Operator Liu

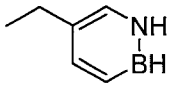

633

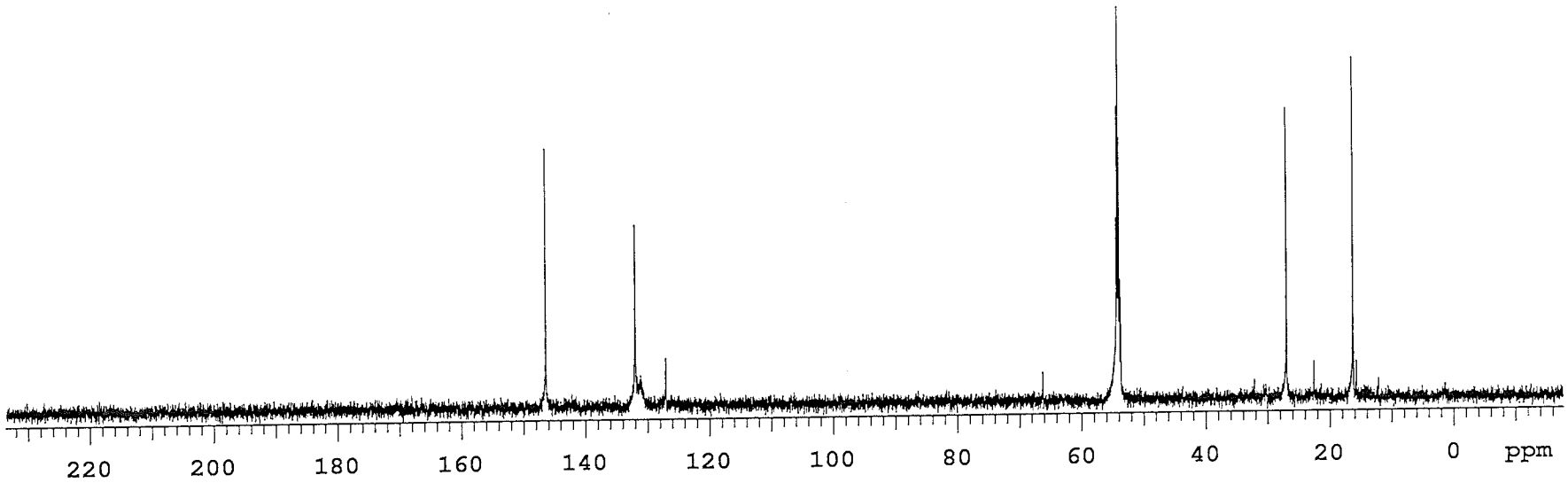

Data file exp

Plot date 2017-04-05

HL-1-086-1H

Sample Name HL-1-086-1H	Pulse sequence PROTON	Temperature 25	Study owner Liu
Data collected 2017-01-16	Solvent cd2cl2	Spectrometer nmr11-inova500	Operator Liu

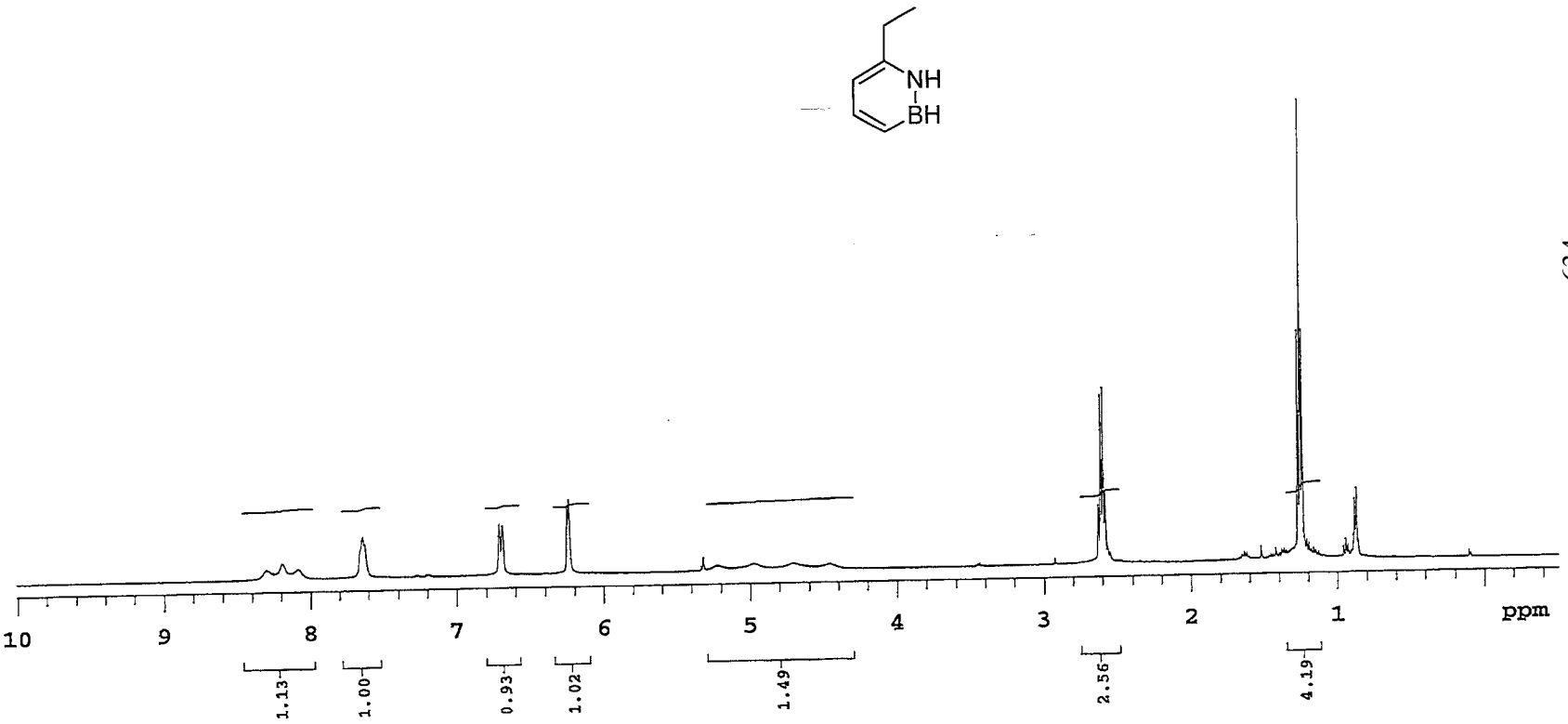

634

Plot date 2017-01-16

Data file exp

HL-1-086-11B

Sample Name HL-1-086-11B	Pulse sequence s2pul	Temperature 25	Study owner Liu
Date collected 2017-01-16	Solvent cd2cl2	Spectrometer nmr11-inova500	Operator Liu

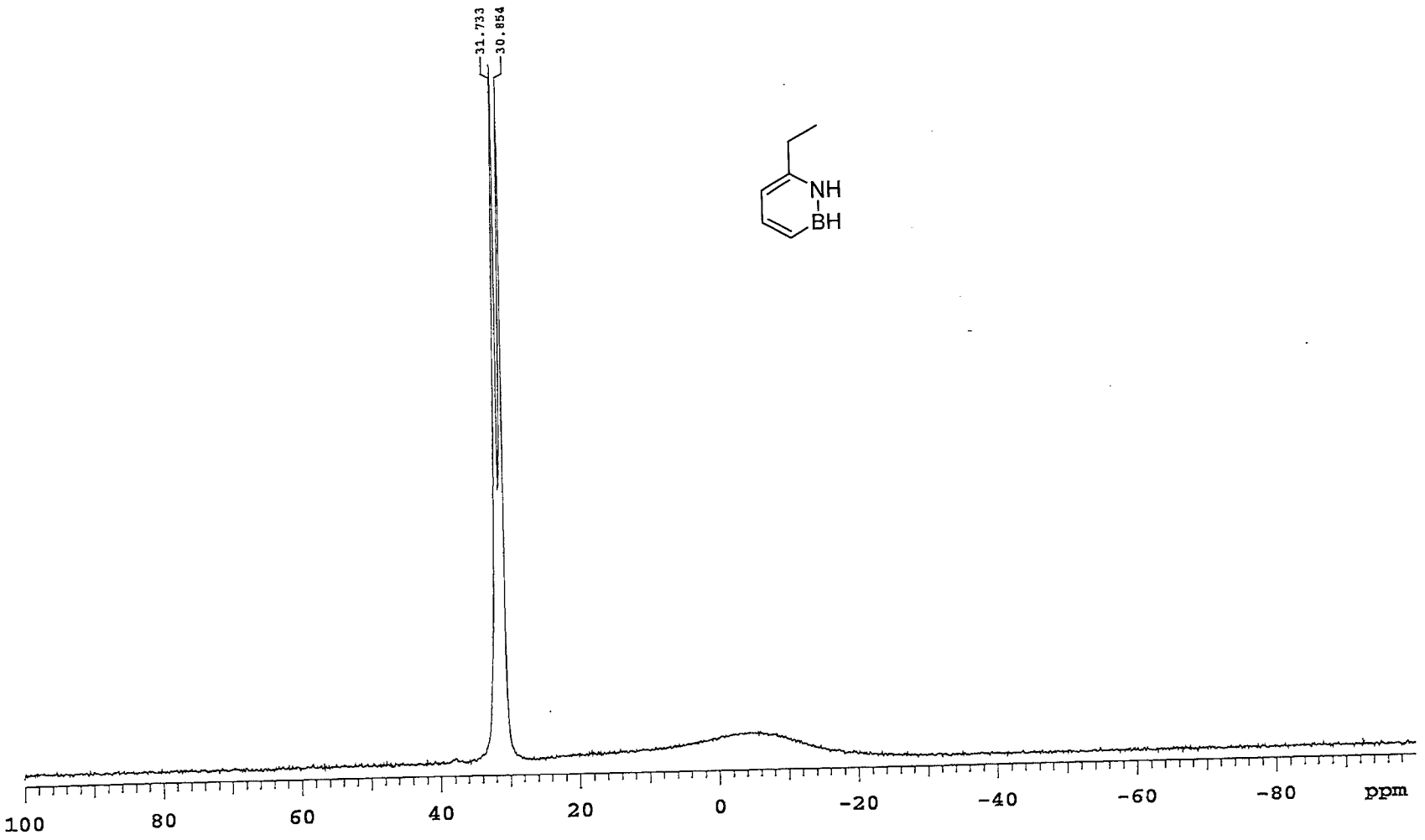

635

Plot date 2017-01-16

Data file exp

HL-1-086-13C

Sample Name	HL-1-086-13C	Pulse sequence	CARBON	Temperature	25
Date collected	2017-01-18	Solvent	cd2cl2	Spectrometer	nmr19-vnmrs600

Study owner Liu
Operator Liu

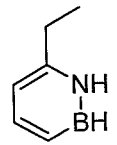

636

Plot date 2017-03-11

Data file /home/ALL/Liu/HL/Chapter 3/HL-1-086-13C.fid

Chapter 4: Late-Stage *N*-Functionalization of 1,2-Azaborines

4.1 Introduction

BN/CC isosterism has been demonstrated to lead to diversification of chemical structures and discovery of unique chemical/physical properties of organic compounds.[1] Late-stage functionalization of 1,2-azaborines, i.e., functionalization after assembly of the azaborine core, provides a general approach to access a library of structurally diversified molecules. However, implementing such a strategy has been challenging until recently due to the scarcity of methodologies that enable selective modification around the aromatic ring.

Recently, Liu and Ashe have demonstrated selective functionalization of monocyclic 1,2-azaborines at the B2 and C3–C6 positions. Nucleophilic substitution, Rh-catalyzed *B*-Cl arylation and *B*–H alkenylation were used to functionalize the boron position.[2] Electrophilic aromatic substitution reactions at C3 and C5 were reported by Ashe in 2007, and the Liu group developed a Negishi cross-coupling procedure involving C3-halogenated 1,2-azaborines in 2015.[3] Ir-catalyzed C–H borylation, followed by Suzuki–Miyaura cross-coupling afforded functionalization of the remaining carbonaceous positions C4, C5, or

[1] (a) Liu, Z.; Marder, T. B. Angew. *Chem., Int. Ed.* **2008**, *47*, 242–244. (b) Bosdet, M. J. D.; Piers, W. E. *Can. J. Chem*. **2009**, *87*, 8–29. (c) Campbell, P. G.; Marwitz, A. J. V.; Liu, S.-Y. *Angew. Chem., Int. Ed*. **2012**, *51*, 6074–6092. (d) Wang, X.-Y.; Wang, J.-Y.; Pei, J. *Chem. Eur. J.* **2014**, *21*, 3528–3539.
[2] (a) Marwitz, A. J. V.; Abbey, E. R.; Jenkins, J. T.; Zakharov, L. N.; Liu, S.-Y. *Org. Lett.* **2007**, *9*, 4905–4908. (b) Lamm, A. N.; Garner, E. B.; Dixon, D. A.; Liu, S.-Y. *Angew. Chem., Int. Ed.* **2011**, *50*, 8157–8160. (c) Rudebusch, G. E.; Zakharov, L. N.; Liu, S.-Y. *Angew. Chem., Int. Ed*. **2013**, *52*, 9316–9319. (d) Brown, A. N.; Zakharov, L. N.; Mikulas, T.; Dixon, D. A.; Liu, S.-Y. *Org. Lett.* **2014**, *16*, 3340–3343.
[3] (a) Pan, J.; Kampf, J. W.; Ashe, A. J. *Org. Lett.* **2007**, *9*, 679–681. (b) Brown, A. N.; Li, B.; Liu, S.-Y. *J. Am. Chem. Soc.* **2015**, *137*, 8932–8935.

C6.[4] To date, only limited examples can be found in literatures for *N*-functionalization of 1,2-azaborines and these transformations generally do not allow for further derivatization because the electrophiles used in the reactions are silyl protecting groups or simple alkyl chains.[5]

Figure 4.1 Late-stage functionalization of 1,2-azaborines

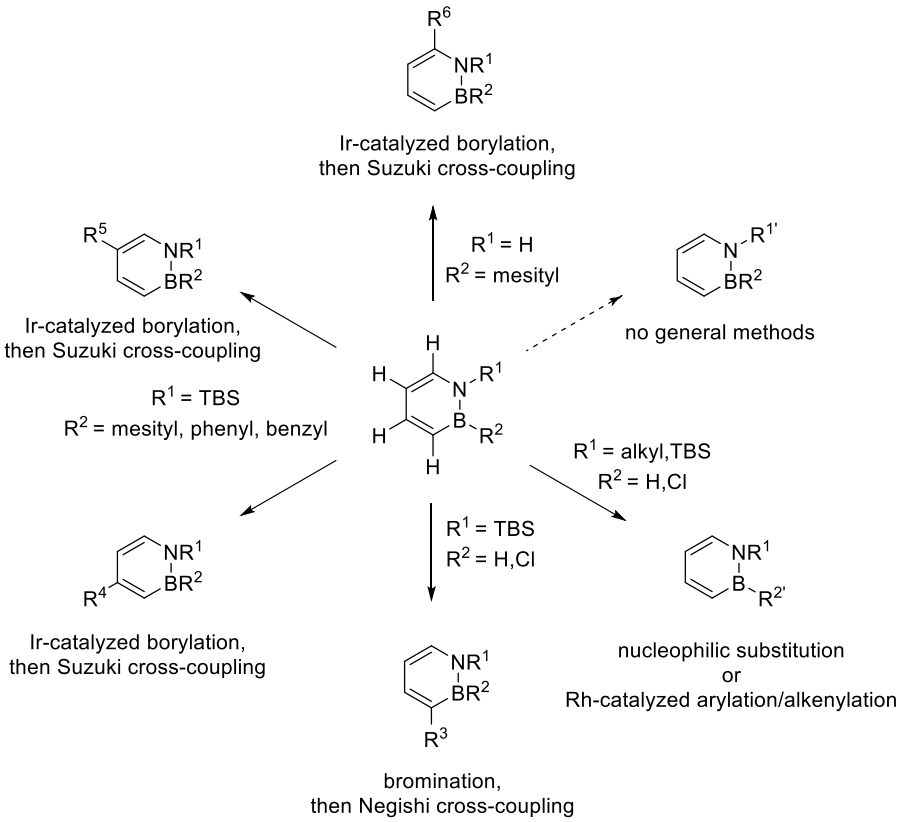

[4] (a) Baggett, A. W.; Vasiliu, M.; Li, B.; Dixon, D. A.; Liu, S.-Y. *J. Am. Chem. Soc.* **2015**, *137*, 5536–5541. (b) Baggett, A. W.; Guo, F.; Liu, S.-Y.; Jäkle, F. *Angew. Chem. Int. Ed.* **2015**, *54*, 11191–11195. See Chapter 3 for C4 and C5 borylation.

[5] (a) Pan, J.; Kampf, J. W.; Ashe, A. J. *Organometallics* **2004**, *23*, 5626–5629. (b) Pan, J.; Kampf, J. W.; Ashe, A. J. *Organometallics* **2008**, *27*, 1345–1347. (c) Abbey, E. R.; Lamm, A. N.; Baggett, A. W.; Zakharov, L. N.; Liu, S.-Y. *J. Am. Chem. Soc.* **2013**, *135*, 12908–12913.

4.2 Background

4.2.1 Functionalization of Polycylic 1,2-Azaborines

While various methods are available to construct the 1,2-azaborine core,[6,7] development of methodologies for functionalization of the resulting BN-heterocycles are still scarce. In Dewar's initial studies of functionalization of 9,10-BN-phenanthrenes, he demonstrated nucleophilic substitution at boron,[8] halogenation, nitration, and Friedel-Crafts acetylation at C6 and C8 through electrophilic aromatic substitution,[9] and *N*-acylation *via* lithiation of NH-containing derivatives.[10]

Research on functionalization of both mono- and polycyclic BN-heterocycles then lay largely dormant until the late 2000s. In 2007, the Piers group utilized Pt-catalyzed alkyne

---

[6] For examples of synthesis of polycyclic 1,2-azaborines, see: (a) Dewar, M. J. S.; Kubba, V. P.; Pettit, R. *J. Chem. Soc.* **1958**, 3073–3076. (b) Dewar, M. J. S.; Dietz, R. *J. Chem. Soc.* **1959,** 2728–2730. (c) Dewar, M. J. S.; Gleicher, G. J.; Robinson, B. P. *J. Am. Chem. Soc.* **1964**, *86*, 5698–5699. (d) Bosdet, M. J. D.; Piers, W. E.; Sorensen, T. S.; Parvez, M. *Angew. Chem. Int. Ed.* **2007**, *46*, 4940–4943. (e) Neue, B.; Araneda, J. F.; Piers, W. E.; Parvez, M. *Angew. Chem. Int. Ed.* **2013**, *52*, 9966–9969. (f) Bettinger, H. F.; Müller, M. *J. Phys. Org. Chem.* **2015**, *28*, 97–103. (g) Lu, J.-S.; Ko, S.-B.; Walters, N. R.; Kang, Y.; Sauriol, F.; Wang, S. *Angew. Chem. Int. Ed.* **2013**, *52*, 4544–4548. (h) Li, G.; Zhao, Y.; Li, J.; Cao, J.; Zhu, J.; Sun, X. W.; Zhang, Q. *J. Org. Chem.* **2015**, *80*, 196–203. (i) Wang, X.; Zhang, F.; Liu, J.; Tang, R.; Fu, Y.; Wu, D.; Xu, Q.; Zhuang, X.; He, G.; Feng, X. *Org. Lett.* **2013**, *15*, 5714–5717. (j) Hashimoto, S.; Ikuta, T.; Shiren, K.; Nakatsuka, S.; Ni, J.; Nakamura, M.; Hatakeyama, T. *Chem. Mater.* **2014**, *26*, 6265–6271. (k) Wang, X.-Y.; Zhuang, F.-D.; Wang, R.-B.; Wang, X.-C.; Cao, X.-Y.; Wang, J.-Y.; Pei, J. *J. Am. Chem. Soc.* **2014**, *136*, 3764–3767. (l) Wisniewski, S. R.; Guenther, C. L.; Argintaru, O. A.; Molander, G. A. *J. Org. Chem.*, **2014**, *79*, 365–378. (m) Ishibashi, J. S. A.; Marshall, J. L.; Maziere, A.; Lovinger, G. J.; Li, B.; Zakharov, L. N.; Dargelos, A.; Graciaa, A.; Chrostowska, A.; Liu, S.-Y. *J. Am. Chem. Soc.* **2014**, *136*, 15414–15421. (n) Fang, X.; Yang, H.; Kampf, J. W.; Holl, M. M. B.; Ashe, A. J. *Organometallics* **2006**, *25*, 513–518.

[7] For examples of synthesis of monocyclic 1,2-azaborines, see: (a) Dewar, M. J. S.; Marr, P. A. *J. Am. Chem. Soc.* **1962**, *84*, 3782. (b) White, D. G. *J. Am. Chem. Soc.* **1963**, *85*, 3634–3636. (c) Ashe, A. J.; Fang. *Org. Lett.* **2000**, *2*, 2089–2091. (d) Ashe, A. J.; Fang, X.; Fang, X.; Kampf, J. W. *Organometallics* **2001**, *20*, 5413–5418. (e) Marwitz, A. J. V.; Matus, M. H.; Zakharov, L. N.; Dixon, D. A.; Liu, S.-Y. *Angew. Chem. Int. Ed.* **2009**, *48*, 973–977. (f) Braunschweig, H.; Geetharani, K.; Jimenez-Halla, J. O. C.; Schäfer, M. *Angew. Chem. Int. Ed.* **2014**, *53*, 3500–3504. (g) Braunschweig, H.; Hörl, C.; Mailänder, L.; Radacki, K.; Wahler, J. *Chem. Eur. J.* **2014**, *20*, 9858–9861. (h) Couchman, S. A.; Thompson, T. K.; Wilson, D. J. D.; Dutton, J. L.; Martin, C. D. *Chem. Commun.* **2014**, *50*, 11724–11726.

[8] Dewar, M. J. S.; Maitlis, P. M. *J. Am. Chem. Soc.* **1961**, *83*, 187–193.

[9] (a) Dewar, M. J. S.; Kubba, V. P. *Tetrahedron* **1959**, *7*, 213–222. (b) Dewar, M. J. S.; Kubba, V. P. *J. Org. Chem.* **1960**, *25*, 1722–1724. (c) Dewar, M. J. S.; Kubba, V. P. *J. Am. Chem. Soc.* **1961**, *83*, 1757–1760.

[10] Dewar, M. J. S.; Maitlis, P. M. *Tetrahedron* **1961**, *15*, 35–45.

cyclization to furnish internally BN-pyrene analogs.[11] B–N bond formation between bis-alkynylated pyridine **4.1** and boracyclohexadienes **4.2** afforded intermediate **4.3**, which underwent spontaneous cyclization to form BN-phenanthrene derivative **4.4**. The second cyclization reaction to complete the formation of the pyrene core, however, required heating in the presence of 5 mol% $PtCl_2$ (Scheme 4.1).

Scheme 4.1 Synthesis of BN-pyrene analog using Pt-catalyzed cyclization

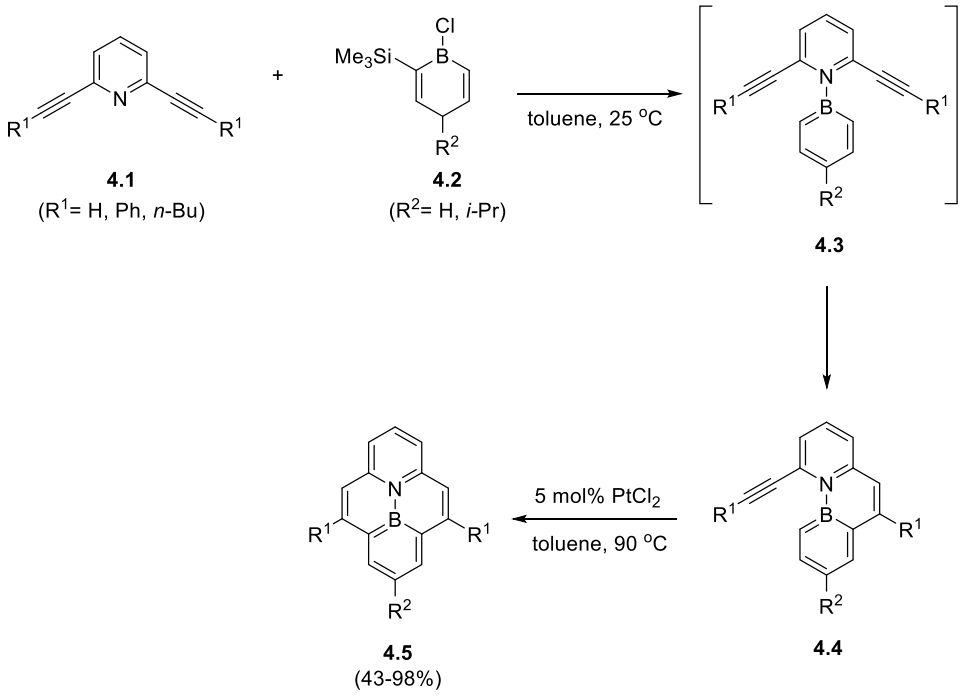

B-Phosphorylation of 9,10-BN-phenanthrene was demonstrated by Pringle in 2014.[12] BN analogues of monoarylphosphine ligands were synthesized by the reaction of the *B*–Cl

[11] Bosdet, M. J. D.; Piers, W. E.; Sorensen, T. S.; Parvez, M. *Angew. Chem. Int. Ed.* **2007**, *46*, 4940–4943.
[12] Bailey, J. A.; Haddow, M. F.; Pringle, P. G. *Chem. Commun.* **2014**, *50*, 1432-1434.

bond in BN-phenanthrene **4.6** and silylphosphines R_2PSiMe_3 (Scheme 4.2). The resulting azaborinylphos-phines demonstrated higher turnover frequencies in Rh-catalyzed hydrogenation reactions of cyclohexene compared to arylphosphine analogs.

Scheme 4.2 Synthesis of the azaborinylphosphines

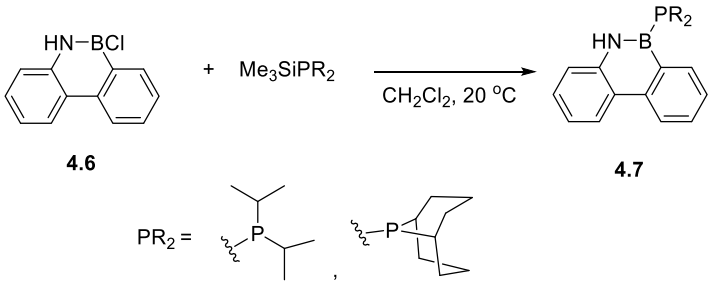

The Molander group contributed to increasing the accessibility of 1,2-BN-naphthalene analogs introducing the use of potassium organotrifluoroborates ($R\text{-}BF_3K$) for their synthesis.[6l] Notably, C3-selective bromination of BN-naphthalene **4.8**, followed by Suzuki–Miyaura cross-coupling with (Het)Ar-BF_3K salts produced derivatives of C3-arylated BN-naphthalenes (Scheme 4.3, eq. 1).[13] C3-Alkenylation was likewise achieved following some minor modifications to the reaction conditions (Scheme 4.3, eq. 2).[14]

[13] Molander, G. A.; Wisniewski, S. R. *J. Org. Chem.* **2014**, *79*, 6663–6678.
[14] Molander, G. A.; Wisniewski, S. R.; Etemadi-Davan, E. *J. Org. Chem.* **2014**, *79*, 11199–11204.

Scheme 4.3 Syntheses of C3-functionalized BN-naphthalenes using potassium organotrifluoroborates

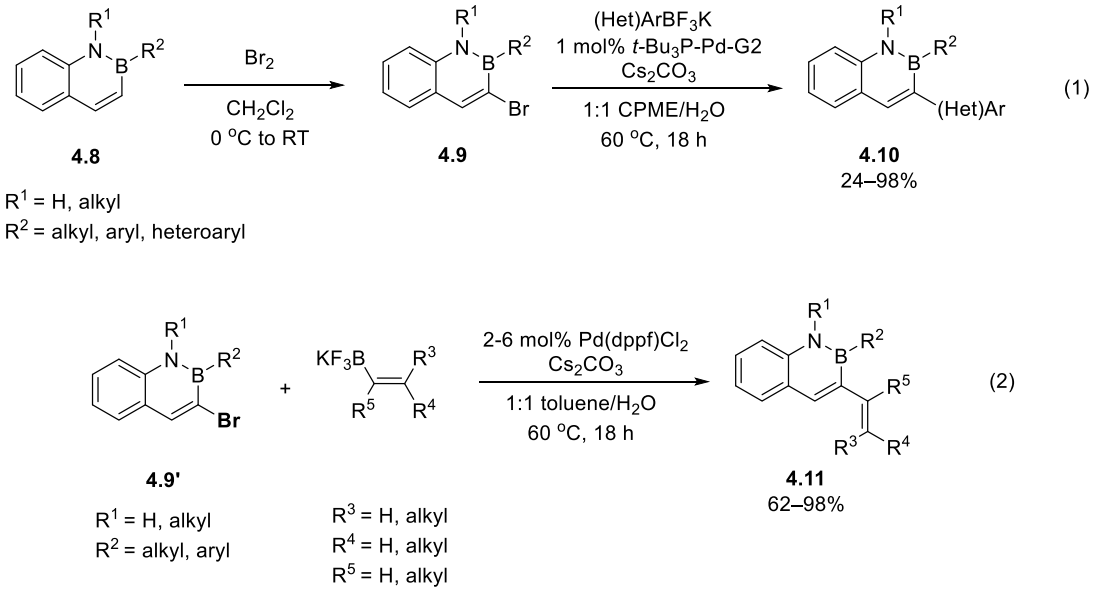

In the course of developing the above cross-coupling reactions of C3-brominated BN-naphthalenes, the Molander group also discovered a unique reaction mode of *N*-substituted, *B*-aryl, C3-brominated substrates involving apparent self-arylation under Suzuki–Miyaura conditions.[15] Using (SPhos)-(aminobiphenyl) palladium chloride (SPhos-Pd-G2) as precatalyst and KOH as base, the self-arylation was found to proceed at ambient temperature to provide B-OH-3-aryl products (Scheme 4.4). A crossover experiment conducted as mechanistic probe revealed that the reaction is actually an intermolecular process (Scheme 4.5, eq. 1). Also of note, the free NH-containing substrate **4.9c** did not undergo self-arylation (Scheme 4.5, eq. 2). Computational studies suggested that the presence of a nitrogen substituent forces the *B*-arly group out of plane relative to the BN-

[15] Molander, G. A.; Wisniewski, S. R. *J. Org. Chem.* **2014**, *79*, 8339–8347.

naphthalene ring, thereby weakening the B–C_{aryl} bond and rendering transmetalation of the aryl group more facile than in NH-containing substrates.

Scheme 4.4 Self-arylation of *B*-aryl, C3-brominated BN-naphthalenes

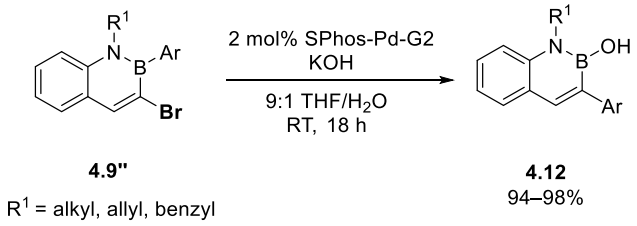

Scheme 4.5 Probing the reaction mechanism of self-arylation

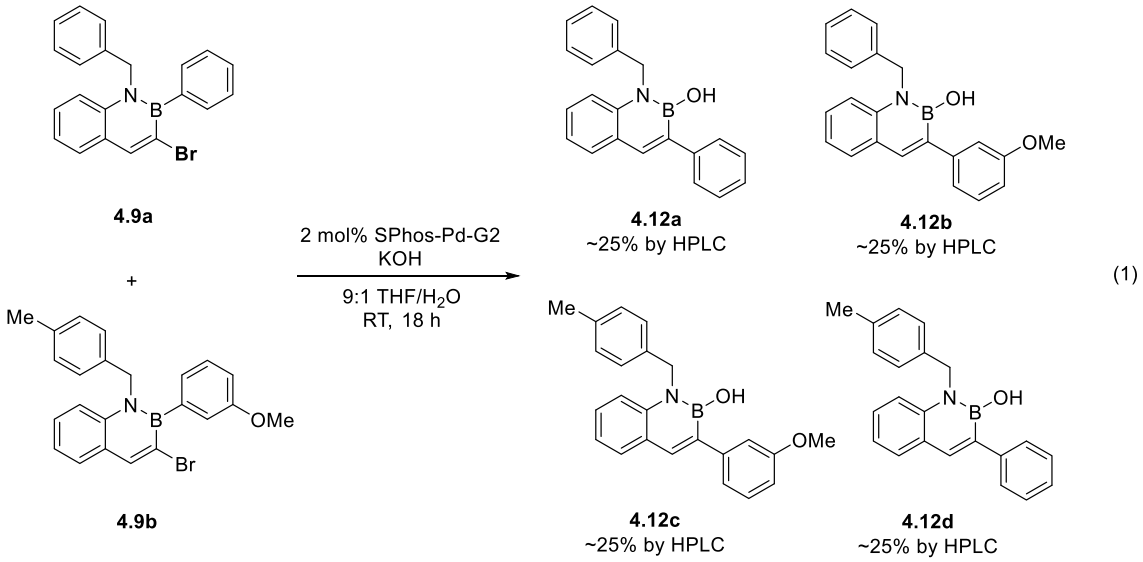

In 2014, Molander also demonstrated alkylation of C3-brominated BN-naphthalenes using Ni-catalyzed reductive cross-coupling reactions. [16] Various primary and secondary alkyl iodides provided the desired sp^2–sp^3 coupling products in good yields (Scheme 4.6).

Scheme 4.6 Ni-catalyzed reductive cross-coupling of BN-naphthalenes

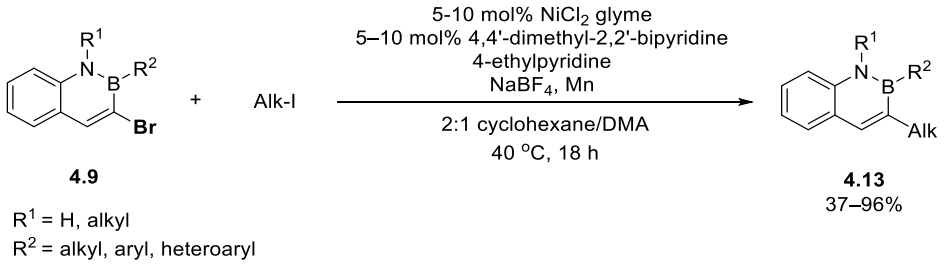

4.9

R^1 = H, alkyl
R^2 = alkyl, aryl, heteroaryl

4.13
37–96%

In 2014, Fang demonstrated iodinated BN-fused naphthalenes can undergo Suzuki–Miyaura, Sonogashira, and Heck cross-coupling reactions.[17] To prepare the halogenated precursors **4.15**–**4.17**, the authors employed Lewis acid-catalyzed electrophilic aromatic substitution reactions. (A second halogenation could also be performed at the α'-carbon adjacent to boron to afford bis-halogenated products **4.18**–**4.21** (Scheme 4.7, eq. 1).) The iodinated BN-naphthalene **4.17** was converted into the corresponding arylated, alkynylated, and alkenylated coupled products under Pd-catalyzed conditions shown in Scheme 4.7 (eq. 2).

[16] Molander, G. A.; Wisniewski, S. R.; Traister, K. M. *Org. Lett.* **2014**, *16*, 3692–3695.
[17] Sun, F.; Lv, L.; Huang, M.; Zhou, Z.; Fang, X. *Org. Lett.* **2014**, *16*, 5024–5027.

Scheme 4.7 Halogenation of **4.14** and Pd-catalyzed cross-coupling reactions of **4.17**.

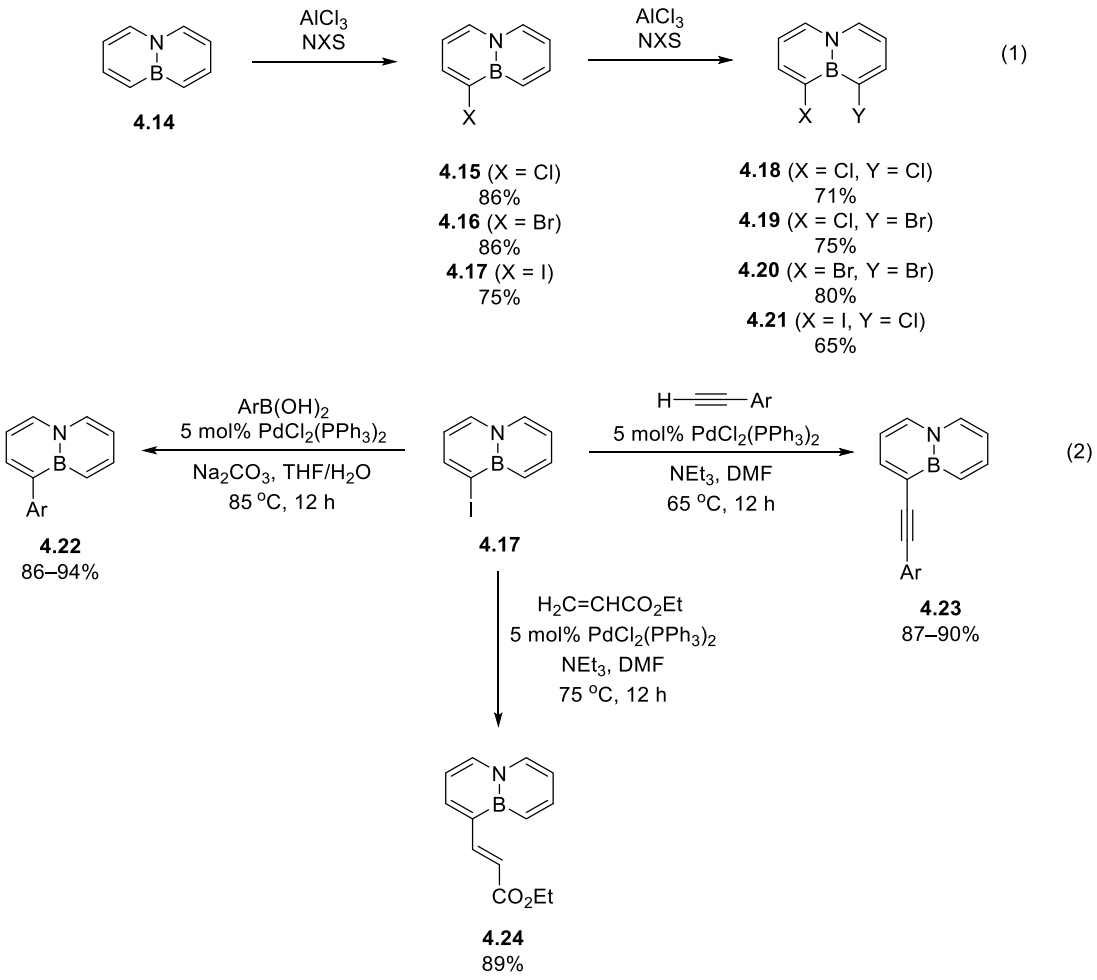

4.2.2 Late-Stage Functionalization of Monocyclic 1,2-Azaborines

4.2.2.1 Functionalization at Boron

The most straightforward derivatization of 1,2-azaborines is nucleophilic substitution at boron as demonstrated in 2007 by Liu.[2a] Direct displacement of the labile *B*-chloro group in **4.25** was successful with a variety of organolithiates and Grignard reagents (Table 4.1, entries 1–4). Heteroatom-based nucleophiles resulted in formation of 1,2-azaborines

bearing B–N, B–S, and B–O bonds (Table 4.1, entries 5–7). Nucleophilic substitution with $LiBEt_3H$ afforded a B–H containing molecule (Table 4.1, entry 8).

Table 4.1 Nucleophilic substitution at the boron center of 1,2-azaborines

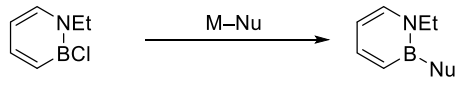

4.25 **4.26**

entry	nucleophile (M–Nu)	product	yield (%)
1	Li–Bu	**4.26a**	79
2	Li–vinyl	**4.26b**	50
3	BrMg–Ph	**4.26c**	76
4	BrMg–≡—Ph	**4.26d**	83
5	Li–NMe_2	**4.26e**	66
6	K–SBn	**4.26f**	80
7	K–O*t*-Bu	**4.26g**	71
8	$LiBEt_3$–H	**4.26h**	92

Isolation of parent 1,2-azaborine (**4.27**)[7e] allowed the group to examine the reactivity of the simplest BN isostere of the arene family. Nucleophilic aromatic substitution of **4.27** was demonstrated; particularly, reactions with various nucleophiles and subsequent quenching with electrophiles generated mono- and bis-functionalized 1,2-azaborines (Table 4.2).[2b] Mechanistic studies revealed that the reaction to form **4.28h** proceeds through the following sequence: 1) deprotonation of the azaborine NH, 2) formation of dianion species by attack of a second equivalent of nucleophile, 3) expulsion of H^- to form anionic species **4.31**, and 4) quenching with electrophile to generate the final product **4.28h** (Scheme 4.8).

Table 4.2 Nucleophilic aromatic substitution of **4.27**

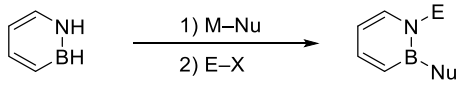

4.27 **4.28**

entry	M–Nu	E–X	product	yield (%)
1	Na–O*t*-Bu	H–Cl	**4.28a**	63
2	K–Oallyl	H–Cl	**4.28b**	79
3	Li–*t*-Bu	H–Cl	**4.28c**	81
4	Li–*n*-Bu	H–Cl	**4.28d**	80
5	Li–Ph	H–Cl	**4.28e**	98
6	BrMg–vinyl	H–Cl	**4.28f**	59
7	BrMg–≡—Ph	H–Cl	**4.28g**	71
8	Li–*n*-Bu	TMS–Cl	**4.28h**	89
9	Li–*n*-Bu	Me–I	**4.28i**	67
10	Li–*n*-Bu	H–Cl	**4.28j**	60

Scheme 4.8 Proposed reaction mechanism of S_NAr of **4.27**

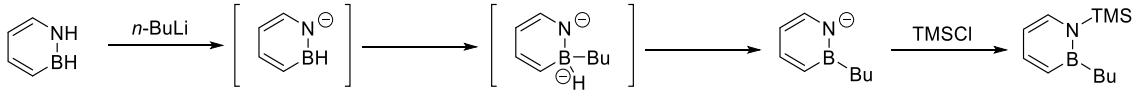

4.27 **4.29** **4.30** **4.31** **4.28h**

In 2013, the Liu group reported Rh-catalyzed *B*-arylation to form BN-biphenyl compounds.[2c] B–Cl containing azaborine **4.25** underwent arylation at boron to form biphenyl products through Rh-catalyzed addition of arylstannanes (Table 4.3). A wide range of functional groups were tolerated under the reaction condition, in marked contrast to the earlier protocols that required organomagnesium and organolithium reagents. The authors demonstrated the utility of this method by synthesizing in just two steps from

azaborine **4.33** a BN-containing version of felbinac, a topical nonsteroidal anti-inflammatory drug (Scheme 4.9).

Table 4.3 Substrate scope of Rh-catalyzed arylation of 1,2-azaborines

4.25 **4.32**

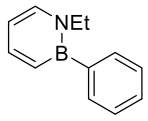

4.32a
77%

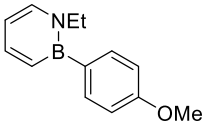

4.32b
78%

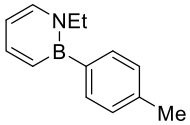

4.32c
74%

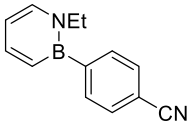

4.32d
81%

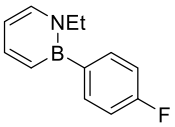

4.32e
80%

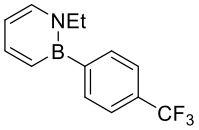

4.32f
56%

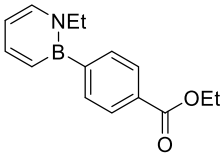

4.32g
75%

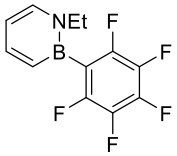

4.32h
40%

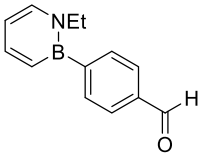

4.32i
41%

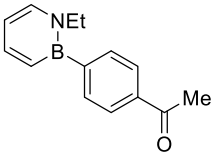

4.32j
66%

Scheme 4.9 Synthesis of BN-felbinac using Rh-catalyzed arylation

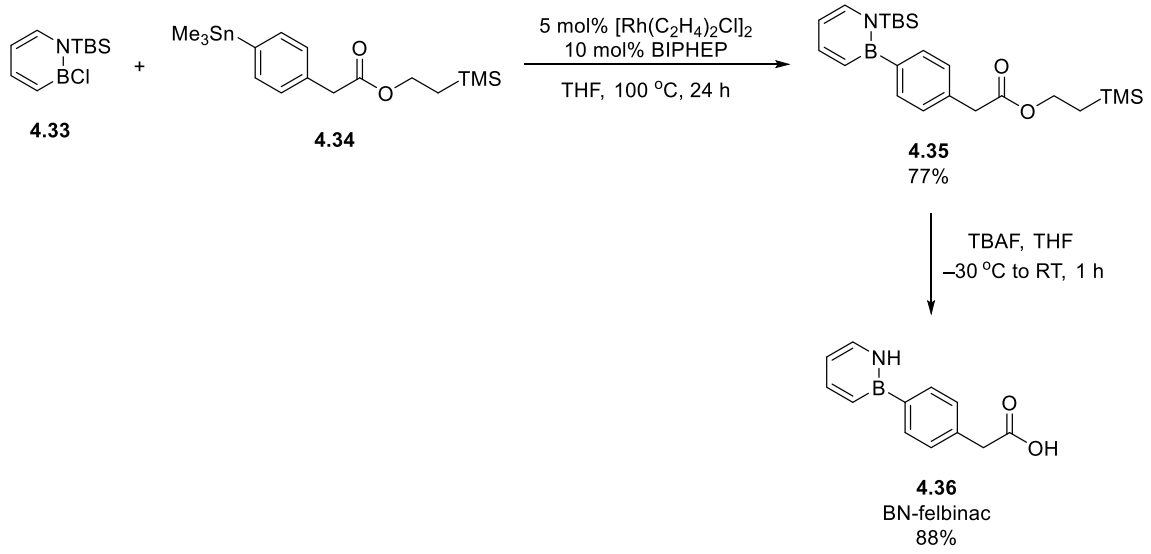

Rh-catalyzed *B*-alkenylation was also reported using B–H containing 1,2-azaborines as starting materials.[2d] The reaction proceeds through B−H activation of the 1,2-azaborine substrate and dehydrogenative borylation of the styrene coupling partner. Using this method, BN-analogs of stilbene were synthesized (Scheme 4.10) and examined for unique photophysical properties in direct comparison with all-carbon analogs.

Scheme 4.10 Synthesis of BN stilbenes by Rh-catalyzed dehydrogenative borylation

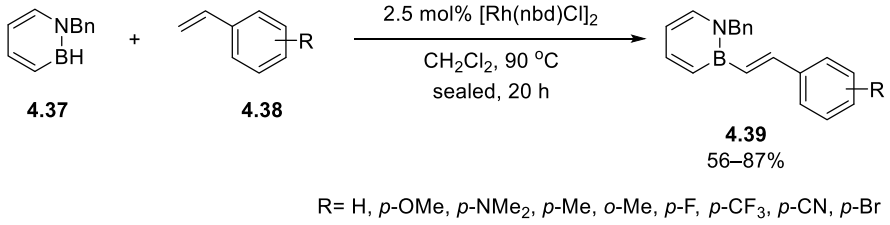

R= H, *p*-OMe, *p*-NMe_2, *p*-Me, *o*-Me, *p*-F, *p*-CF_3, *p*-CN, *p*-Br

In 2013, a protecting group-free synthesis of 1,2-azaborines was demonstrated. The resulting final product **4.40** served as a versatile synthon to access other 1,2-azaborine derivatives. Reaction of **4.40** with lithium aluminum hydride and subsequent acidic quenching allowed isolation of gram quantities of parent 1,2-azaborine **4.27** (Scheme 4.11, eq. 1). Nucleophilic substitution with two equivalents of either vinyl magnesium bromide or *n*-butyllithium produced **4.41** and **4.42**, respectively (Scheme 4.11, eq. 2 and 3). Di-substitution at both boron and nitrogen was also viable to afford **4.43** and **4.44** (Scheme 4.11, eq. 4 and 5).

Scheme 4.11 Functionalization of versatile synthon **4.40**

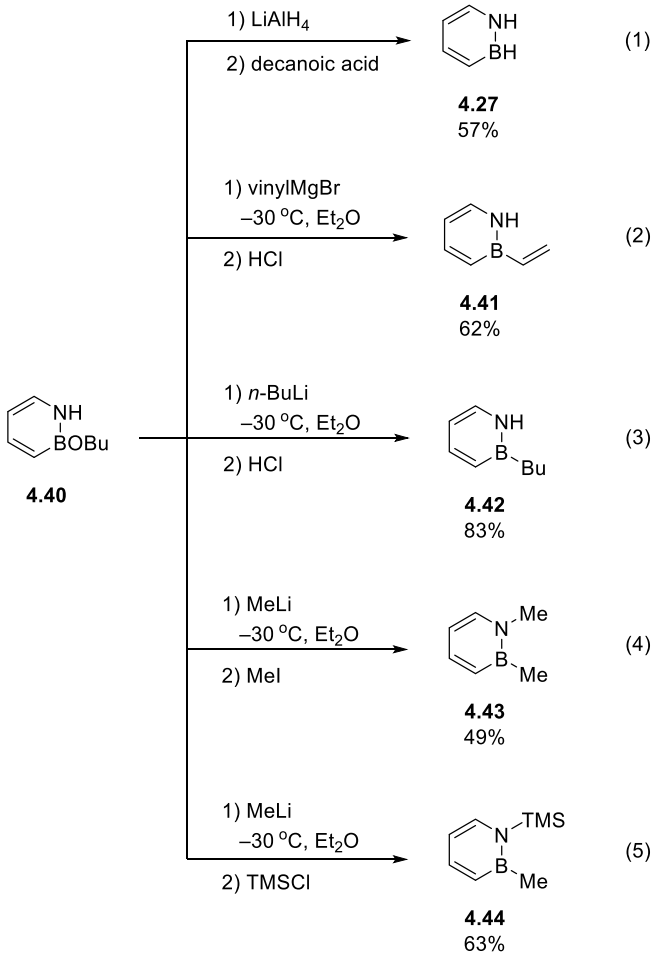

The more reactive azaborine **4.45** was generated *in situ* by the reaction of **4.40** with BCl_3; the resulting *B*-chloro species then subsequently reacted with nucleophiles incapable of directly displacing the -O*n*-Bu group in **4.40** (Scheme 4.12).

Scheme 4.12 Reactions of *in situ*-generated **4.45**

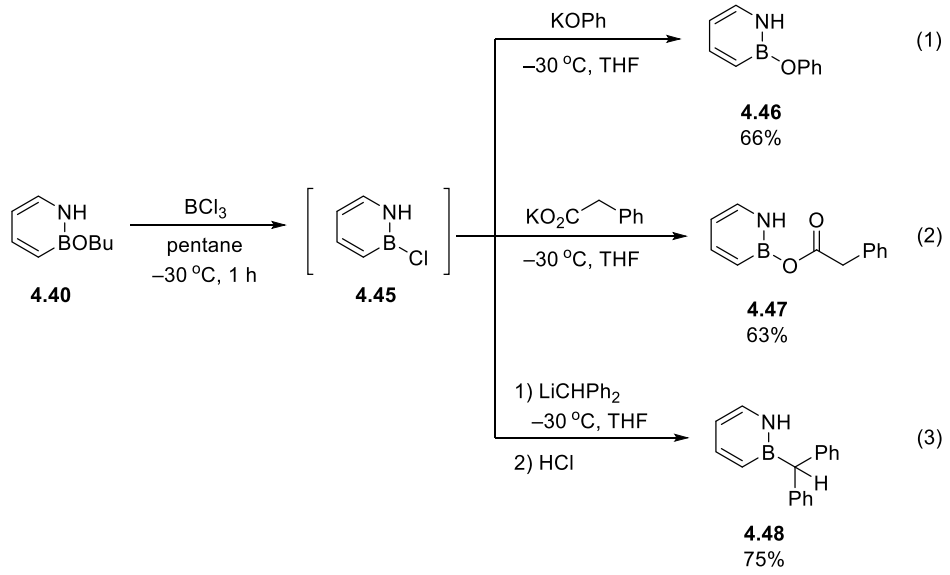

4.2.2.2 Functionalization at Carbon Positions

In 2007, Ashe group reported C3- and C5-selective electrophilic aromatic substitution reactions of monocyclic 1,2-azaborines to afford a variety of 3- and 5-substituted derivatives (Scheme 4.13).[3a] Acid-catalyzed proton-deuterium isotopic exchange afforded the C3-deuterated product. Bromination of **4.32a** occurred at C3, and the resulting brominated product was converted to nitrile **4.51**. Selective iodination of **4.32a** at C3, followed by quenching with aqueous $Na_2S_2O_3$ purportedly gave C3-OH derivative "**4.52**"[18]. Functionalization at C5 was also demonstrated: Friedel-Crafts acetylation of **4.32a** afforded the corresponding C5-acetylated product, while a Mannich reaction with *N*,*N*-dimethylmethyleneiminium chloride gave **4.54** in moderate yield. Molecular orbital calculations indicated that the greatest electron density is localized around C3 and C5, a

[18] Based on our own characterization, the reported compound seems to be a B-OH, C3-Ph isomer.

prediction consistent with the experimental observation of these sites as the most nucleophilic.

Scheme 4.13 Electrophilic aromatic substitution reactions of 1,2-azaborines

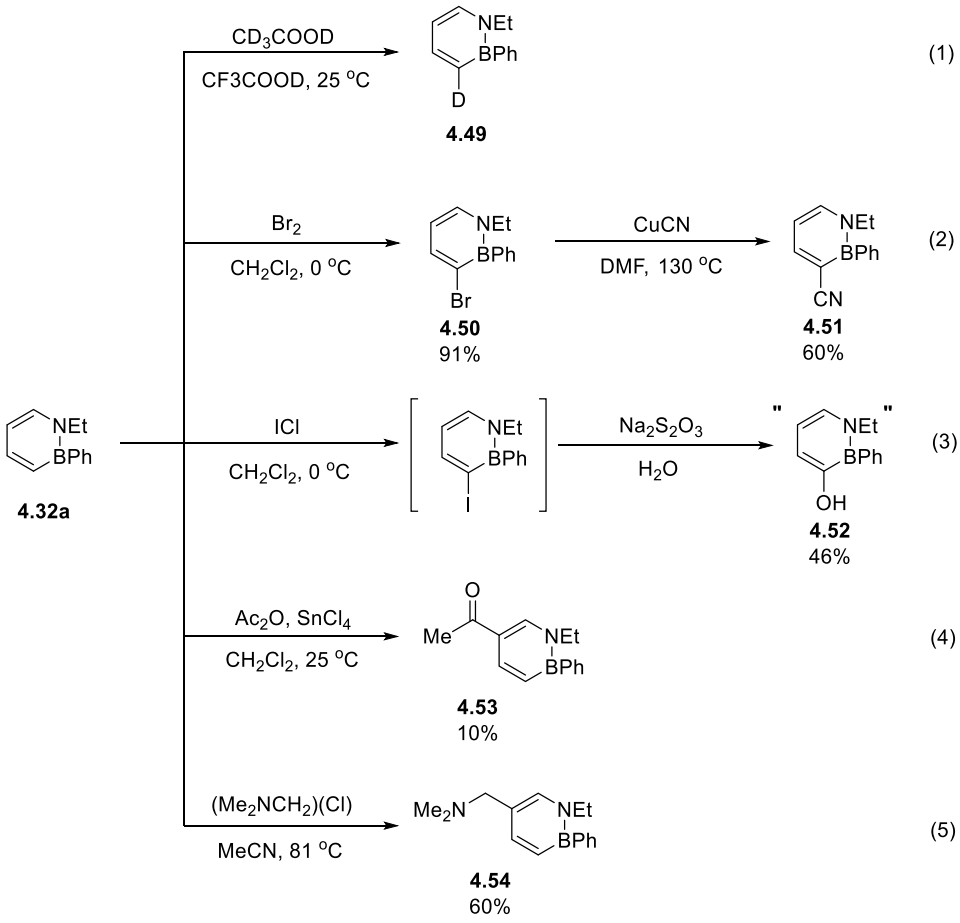

More recently, the Liu group developed a Negishi cross-coupling reaction of 1,2-azaborines in order to introduce functionality at the C3 position.[3b] Bromination of **4.33** occurs selectively at C3, similar to the reactivity observed by Ashe. Cross-coupling of the resulting Br-substituted azaborine is compatible in the presence of a reactive B–Cl bond.

The method was applied to synthesize previously unknown BN isosteres of indenyl and naphthalene; C3-brominated precursor **4.55** underwent regioselective Negishi cross-coupling with vinylzinc bromide to yield **4.56**, which was then utilized in syntheses of BN-indenyl analog **4.57** and a new BN-naphthalene **4.58**.

Scheme 4.14 Negishi cross-coupling of 1,2-azaborine and its application to the synthesis of BN analogs of indenyl and naphthalene

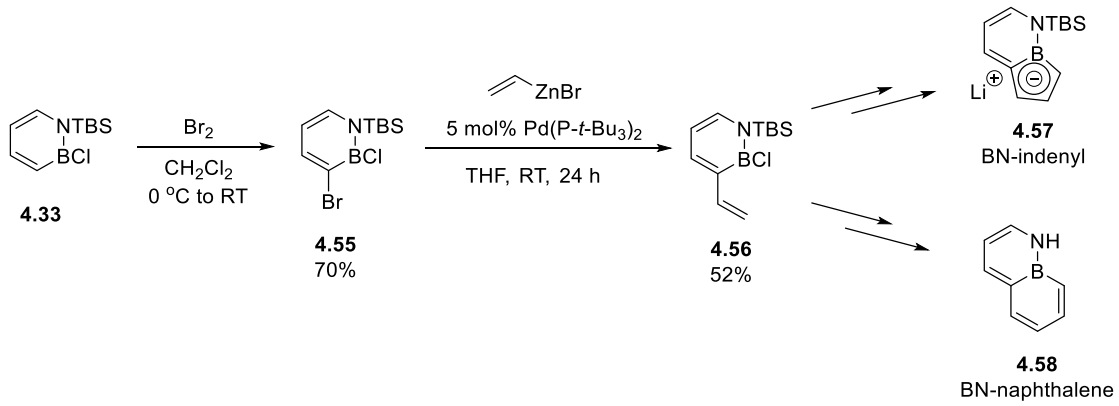

In 2015, the first general method to functionalize C6–H of 1,2-azaborines was established by Ir-catalyzed borylation and subsequent Suzuki–Miyaura cross-coupling.[4a] Regioselective borylation of NH-containing 1,2-azaborines with a number of substituents on boron afforded C6-borylated products (Table 4.4). The observed regioselectivity was attributed primarily to the greater acidity of the C6 proton compared to that of the other carbon positions.

Table 4.4 Regioselective borylation of 1,2-azaborines

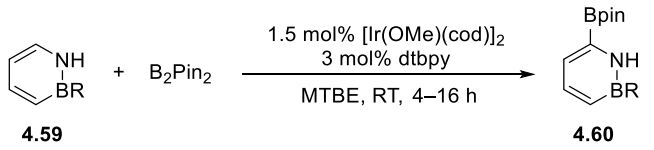

4.59 **4.60**

entry	R	product	yield (%)
1	Me	**4.60a**	67
2	*n*-Bu	**4.60b**	86
3	Mes	**4.60c**	92
4	O-*n*-Bu	**4.60d**	66

The resulting borylated products successfully underwent Suzuki–Miyaura cross-coupling with various (hetero)aryl bromides to afford a library of C6-functionalized 1,2-azaborines. By utilizing this transformation, the authors reported the synthesis of a new type of *N*,*N*-bidentate ligand (Scheme 4.15). This novel ligand after deprotonation forms κ^2-*N*,*N* complex **4.62** with dimesitylboron, demonstrating a potential application of 1,2-azaborines in coordination chemistry.

Scheme 4.15 Synthesis of κ^2-*N*,*N*-bidentate ligand **4.61** and its complex with dimesitylboron

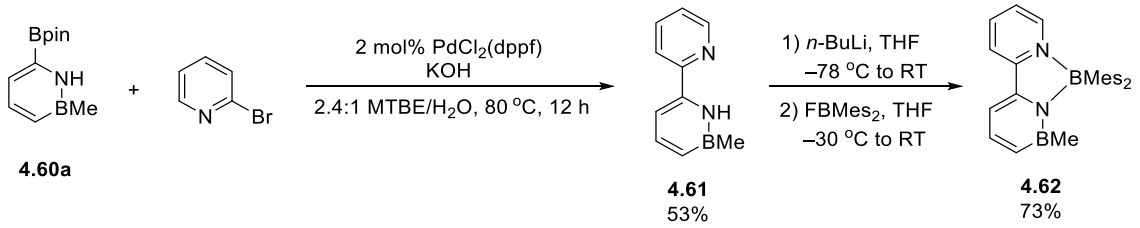

4.60a **4.61** 53% **4.62** 73%

By combining regioselective bromination at C3 of 1,2-azaborines with Ir-catalyzed borylation at C6, the Liu group also demonstrated 1,2-azaborine-based oligomer and polymer syntheses.[4b] C3-brominated azaborine precursor **4.63** was cross-coupled with C6-borylated azaborine **4.60c** to provide dimer **4.64**, which upon further borylation and cross-coupling afforded the trimer **4.66** (Scheme 4.16, eq. 1). An X-ray crystal structure of **4.64** showed a *syn* conformation with respect to *B*-mesityl groups favored by N–H···π interactions. Similarly, regioselective borylation of **4.63** afforded bis-functionalized 1,2-azaborine **4.67,** which served as a monomeric unit for Suzuki–Miyaura polycondensation (Scheme 4.16, eq. 2).

Scheme 4.16 Regioregular synthesis of azaborine oligomers and a polymer

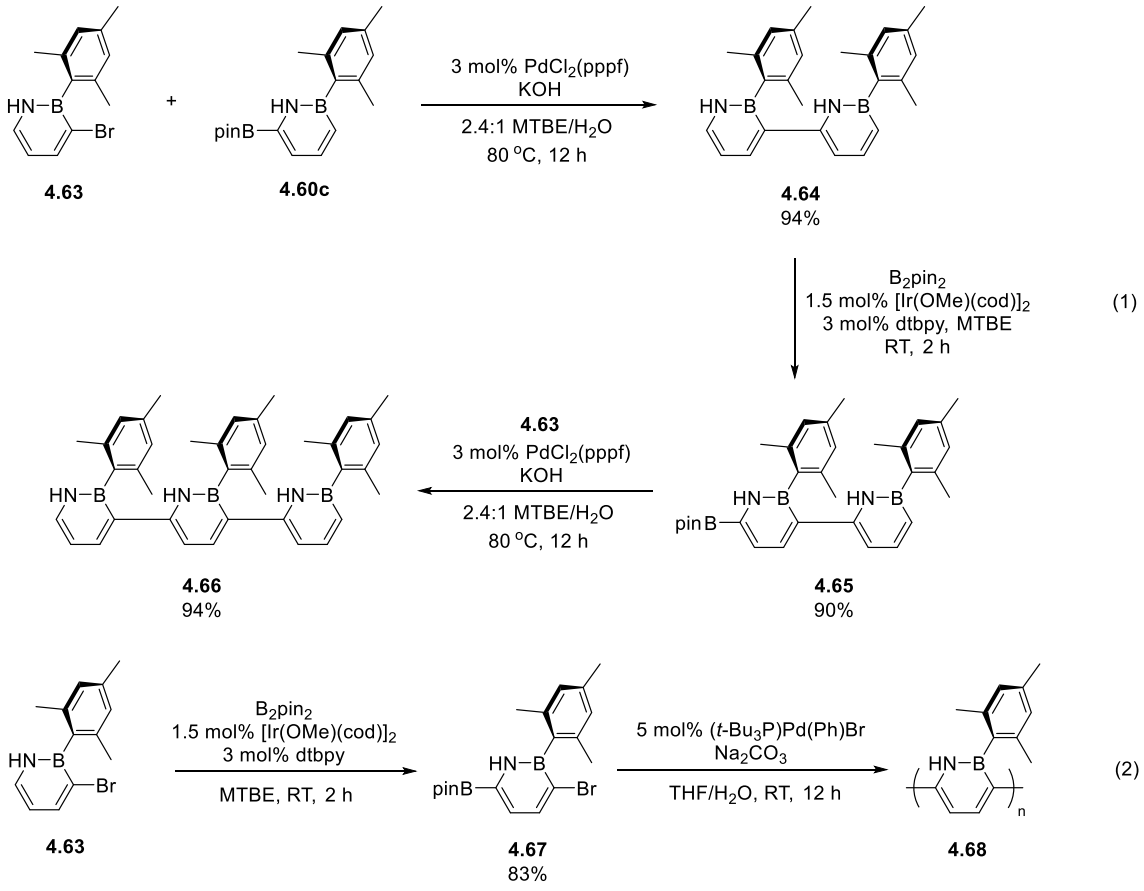

The C4 and C5 positions of 1,2-azaborines remain challenging sites to selectively functionalize. A limited number of examples are discussed in the Chapter 3 for the synthesis of C4- and C5-borylated 1,2-azaborines. In these cases, steric effects play a more significant role compared to C6-borylation due to the presence of the bulky nitrogen TBS substituent (Scheme 4.17).

Scheme 4.17 Diversity-oriented borylation of 1,2-azaborine to functionalize C4 and C5

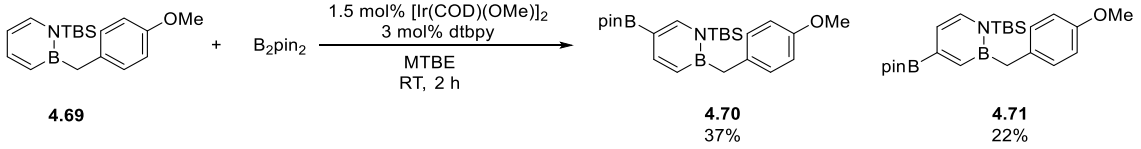

4.3 Late-Stage *N*-Functionalization of 1,2-Azaborines and its Application to the Synthesis of BN Isosteres of *trans*-Stilbene and a Lisdexamfetamine Derivative

4.3.1 Early Syntheses of *N*-Functionalized 1,2-Azaborines

The first example of a direct *N*-functionalization of 1,2-azaborines was demonstrated by the Ashe group during their efforts to synthesize π-coordinated metal complexes of azaborines.[5a] Deprotonation of **4.28e** with potassium bis(trimethylsilyl)amide (KHMDS) afforded the corresponding NK salt **4.72**. Upon treatment of **4.72** with an excess amount of MeI, the authors observed formation of methylated product **4.73**, demonstrating the possibility to render the nitrogen of 1,2-azaborines nucleophilic (Scheme 4.18). In the report, the acid-base properties of the nitrogen atom in **4.28e** and the ruthenium π complex **4.74** were examined. Approximate pK_a value for **4.28e** was estimated to be ~26 whereas a reduced basicity was observed for **4.74** (pK_a = ~9.2) presumably modulated by π-complexation.

Scheme 4.18 Synthesis of **4.7**3 and azaborinyl π-complex **4.74**

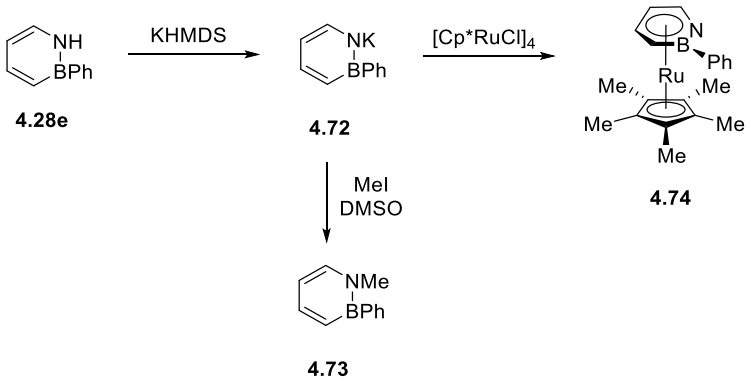

Similarly, in 2008, the Ashe group reported synthesis of an η^1-N bis-(1,2-azaborine).[5b] Anionic azaborine **4.72** reacted with zirconocene dichloride (Cp_2ZrCl_2) to form σ-metal complex **4.76** (Scheme 4.19). To compare the bond lengths and angles from crystal structures, compound **4.75** was prepared by electrophilic substitution of **4.72** with trimethylsilyl chloride (TMSCl).

Scheme 4.19 Synthesis of **4.75** and azaborinyl σ-complex **4.76**

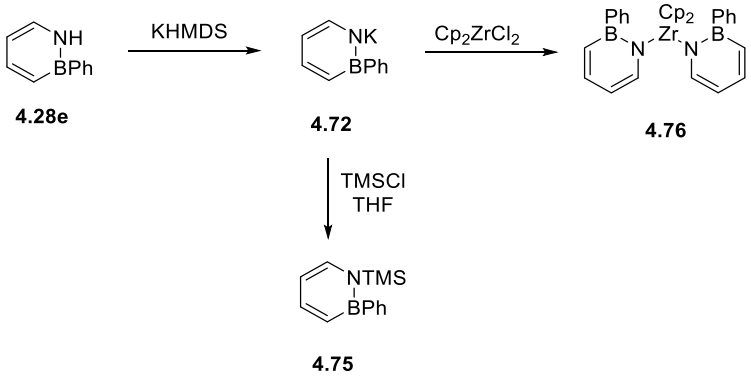

Molander's approach discussed in 4.2.1 enabled modular synthesis of complex BN isosteres of naphthalene with various substituents on nitrogen. However, these complex molecules were assembled from pre-functionalized 2-aminostyrenes. Thus, the scope of nitrogen substituents was limited to a handful of aryl and alkyl groups (Figure 4.2).[6l,13-16,19]

Figure 4.2 Functional groups on nitrogen resulting from Molander's approach to BN-naphthalenes

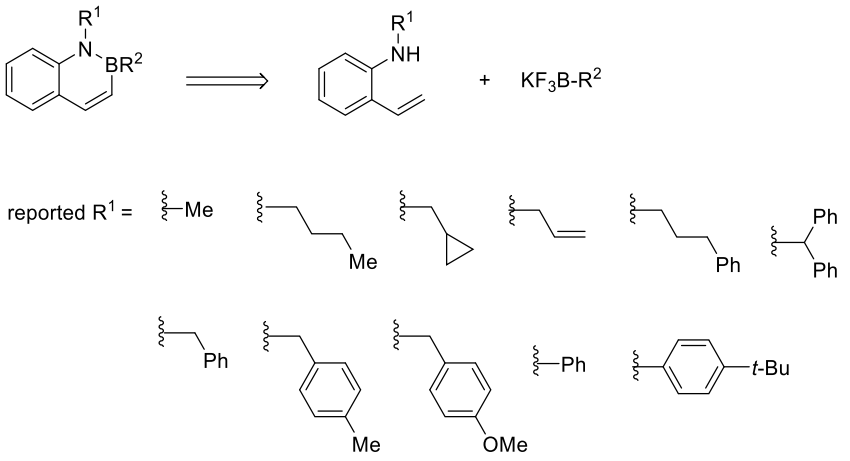

Previously in our laboratory, we have demonstrated a handful of examples of *N*-functionalization of 1,2-azaborines. For example, sequential nucleophlic attack on boron followed by electrophilic quenching on nitrogen gave TMS protection and methylation (Table 4.2 and Scheme 4.11). To expand the scope of possible *N*-substituents, however, we decided to investigate late-stage functionalization of 1,2-azaborines specifically at the nitrogen position alone.

[19] (a) Molander, G. A.; Wisniewski, S. R.; Amani, J. *Org. Lett.* **2014**, *16*, 5636–5639. (b) Davies, G. H. M.; Zhou, Z.-Z.; Jouffroy, M.; Molander, G. A. *J. Org. Chem*. **2017**, *82*, 549–555.

4.3.2 Electrophilic Substitution

First, we investigated electrophilic substitution reactions involving initial deprotonation of NH-containing azaborines followed by reaction with various electrophiles. *N*-H-*B*-phenyl-1,2-azaborine **4.28e** was deprotonated with KHMDS to generate the corresponding NK salt **4.72**, which reacted with numerous electrophiles to afford the desired products in good to excellent yields, including *N*-Boc, *N*-alkyl, and *N*-benzoyl azaborines (Table 4.5, entries 1–4, 6). Only moderate yield was achieved with propargyl bromide presumably due to competing protonation of the NK salt by the relatively acidic propargyl CHs to regenerate the NH azaborine (Table 4.5, entry 5). Electrophilic substitution with another azaborine molecule gave a dimeric species (**4.77g**) in 98% yield (Table 4.5, entry 7).

Table 4.5 Electrophilic substitution of 1,2-azaborines

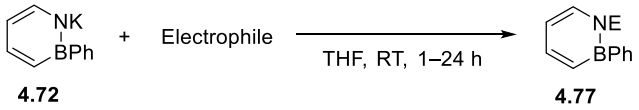

4.72 **4.77**

entry	electrophile	product	yield (%)	entry	electrophile	product	yield (%)
1	Boc_2O	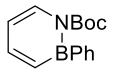 **4.77a**	90	6[a]		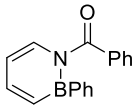 **4.77f**	72
2	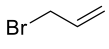	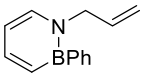 **4.77b**	98	7	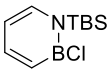	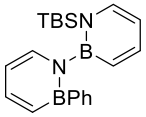 **4.77g**	98
3[a]		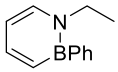 **4.77c**	>99	8[b]		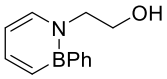 **4.77h**	97
4[a]		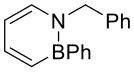 **4.77d**	94	9[b]		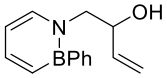 **4.77i**	60
5[a]	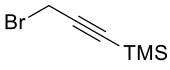	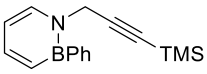 **4.77e**	53	10[b]		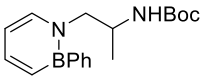 **4.77j**	87

[a]Substrates are generated i*n situ* by reaction of N-H-B-phenyl-1,2-azaborine and potassium bis(trimethylsilyl)amide.
[b]Reactions were quenched with HCl.

Reactions with either epoxides or an aziridine successfully produced the corresponding ring-opened products under ambient temperature without the need for a Lewis acid additive (Table 4.5, entries 8–10).

4.3.3 Synthesis of a BN-Analog of Lisdexamfetamine

To demonstrate the potential utility of the aziridine ring opening reaction in particular to medicinal chemistry, we aimed to synthesize a derivative of a biologically relevant

molecule. Scheme 4.20 illustrates the synthesis of a BN-analog of lisdexamfetamine. Starting with enantiomerically pure (*S*)-2-methylaziridine-1-carboxylic acid *tert*-butyl ester, aziridine ring opening occurred efficiently with NK salt **4.72** (80%) to form **4.77j'**. Boc-deprotection under acidic conditions afforded a BN-analog of amphetamine (**4.78**). Amide coupling of **4.78** with lysine-derived hydroxysuccinimide ester furnished the Boc-protected BN-lisdexamfetamine derivative **4.79** in excellent yield.

Scheme 4.20 Synthesis of BN-lisdexamfetamine analog

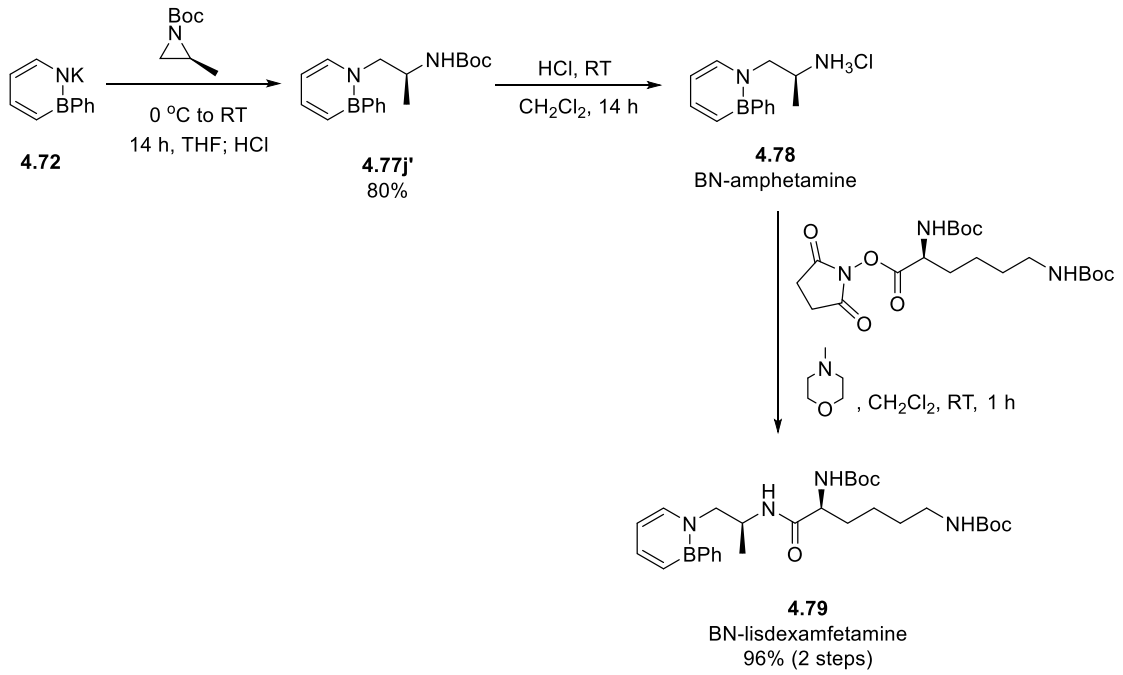

4.3.4 N–C(sp^2) Bond Formation

We next pursued N–C(sp^2) bond formation reactions based on standard Buchwald-Hartwig protocols (see Experimental section 4.5 for ligand studies and optimization

details).[20] The reaction proceeded successfully using a ferrocene-based ligand (QPhos) to generate N–C(sp^2) coupling products (Table 4.6). The reaction with 1,4-dibromobenzene afforded an oligomeric species with five aryl units alternating between phenyl and azaborinyl (Table 4.6, entry 2). This compound in particular has potential applications in synthesis of BN-containing poly(*o*-phenylene) derivatives and extended triphenylene core. Effective *N*-vinylation[21] was achieved using the same catalytic system by switching the base from NaO*t*-Bu to *n*-BuLi.[22] The reaction proved stereospecific to give the corresponding alkenylated products with retention of the configuration of the vinyl bromide starting materials (Table 4.6, entries 3 and 4).

[20] For select examples, see: (a) Paul, F.; Patt, J.; Hartwig, J. F. *J. Am. Chem. Soc.* **1994**, *116*, 5969–5970. (b) Guram, A. S.; Buchwald, S. L. *J. Am. Chem. Soc.* **1994**, *116*, 7901–7902. (c) Guram, A. S.; Rennels, R. A.; Buchwald, S. L. *Angew. Chem., Int. Ed.* **1995**, *34*, 1348–1350. (d) Louie, J.; Hartwig, J. F. *Tetrahedron Lett.* **1995**, *36*, 3609–3612. For selective reviews, see: (e) Muci, A. R.; Buchwald, S. L. *Top. Curr. Chem.* **2002**, *219*, 131–209. (f) Hartwig, J. F. *Angew. Chem. Int. Ed.* **1998**, *37*, 2046–2067. (g) Hartwig, J. F. *Acc. Chem. Res.* **1998**, *31*, 852–860. (h) Wolfe, J. P.; Wagaw, S.; Marcoux, J.-F.; Buchwald, S. L. *Acc. Chem. Res.* **1998**, *31*, 805–818.

[21] For select examples of palladium-catalyzed vinylation, see: (a) Lebedev, A. Y.; Izmer, V. V.; Kazyul'kin, D. N.; Beletskaya, I. P.; Voskoboynikov, A. Z. *Org. Lett.* **2002**, *4*, 623–626. (b) Barluenga, J.; Fernández, M. A.; Aznar, F.; Valdés, C. *Chem. Commun.* **2002**, 2362–2363. (c) Kozawa, Y.; Mori, M. *Tetrahedron Lett.* **2002**, *43*, 111–114. For select examples of copper-catalyzed vinylation, see: (d) Lam, P. Y. S.; Vincent, G.; Clark, C. G.; Deudon. S.; Jadhav, P. K. *Tetrahedron Lett.* **2001**, *42*, 3415–3418. (e) Lam, P. Y. S.; Vincent, G.; Bonne, D.; Clark, C. G. *Tetrahedron Lett.* **2003**, *44*, 4927–4931. (f) Jiang, L.; Job, G. E.; Klapars, A.; Buchwald, S. L. *Org. Lett.* **2003**, *5*, 3667–3669. (g) Pan, X.; Cai, Q.; Ma, D. *Org. Lett.* **2004**, 6, 1809–1812. (h) Taillefer, M.; Ouali, A.; Renard, B.; Spindler, J.-F. *Chem. Eur. J.* **2006**, *12*, 5301–5313. (i) Liao, Q.; Wang, Y.; Zhang, L.; Xi, C. *J. Org. Chem.* **2009**, *74*, 6371–6373.

[22] Vinyl halides are known to undergo elimination by MO*t*-Bu to give the respective alkynes: Huntsman, W. D. *In The Chemistry of the Carbon-Carbon Triple Bond*; Patai, S., Ed.; Wiley: New York, 1978; pp 553–620.

Table 4.6 N–C(sp^2) coupling of 1,2-azaborines

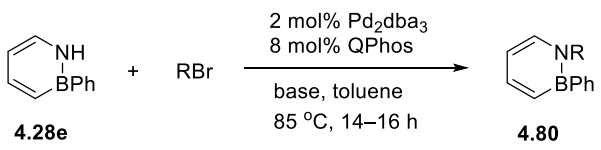

4.28e **4.80**

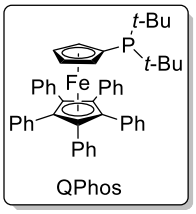

entry	RBr	base	product	yield (%)
1	PhBr	NaO*t*-Bu	**4.80a**	81
2[a]	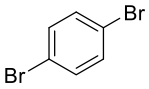	NaO*t*-Bu	**4.80b**	54
3		*n*-BuLi	**4.80c**	92
4	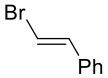	*n*-BuLi	**4.80d**	71

[a]0.6 equiv RBr was used and yield is based on 0.5 equiv **4.28e**.

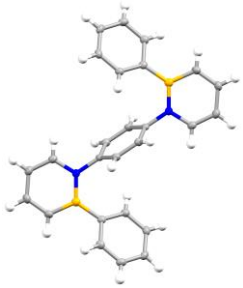

X-ray structure of **4.80b**

4.3.5 Synthesis of a BN Isostere of *trans*-Stilbene

Through the method described above, we were able to synthesize a parental BN isostere of *trans*-stilbene (Scheme 4.21). A benzyl group was chosen to protect the boron to allow for removal through a novel three-step sequence after cross-coupling. Following deprotonation by *n*-BuLi, azaborine **4.81** coupled with β-bromostyrene to give the *N*-alkenylated intermediate **4.82**.[23] Stereochemistry around the newly formed N–C (sp^2) bond was unambiguously determined to be *trans* by an X-ray crystal structure (shown in Scheme 4.21). Copper-mediated oxidation was utilized to remove the benzyl group on boron. Chromatographic purification of the crude materials afforded a mixture of BOR species (dimer and monomer R = *n*-$C_{12}H_{25}$ or R = H), which upon reduction with $LiAlH_4$ furnished

[23] Benzyl displacement by an *n*-butyl group was also observed, producing the corresponding *B*-butyl *N*-alkenyl side product (9% isolated yield).

the desired BN-stilbene in moderate yield (38%) over three steps. The photoluminescence quantum yield of the resulting *trans*-BN-stilbene was determined to be ~4.4 times lower than that of the carbonaceous analog in cyclohexane (0.0388 and 0.179 for BN-stilbene and CC-stilbene, respectively). The solid state quantum yield were 0.127 and 0.324, respectively for BN-stilbene and CC-stilbene (BN-stilbene with ~2.6 times lower yield than that of CC-stilbene). Both absorption and emission peaks of the BN-stilbene are red-shifted compared to carbonaceous stilbene (Figure 4.3).

Scheme 4.21 Synthesis of unsubstituted BN isostere of *trans*-stilbene

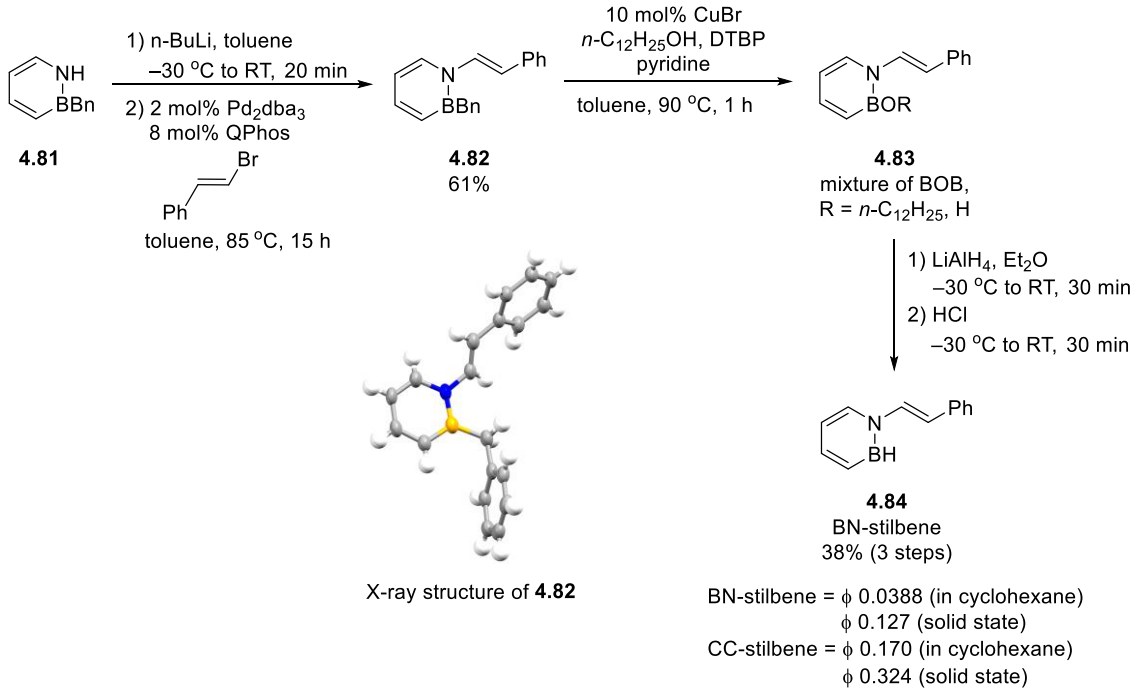

Figure 4.3 Normalized absorption and emission spectra (in cyclohexane) of BN-stilbene in direct comparison with CC-stilbene

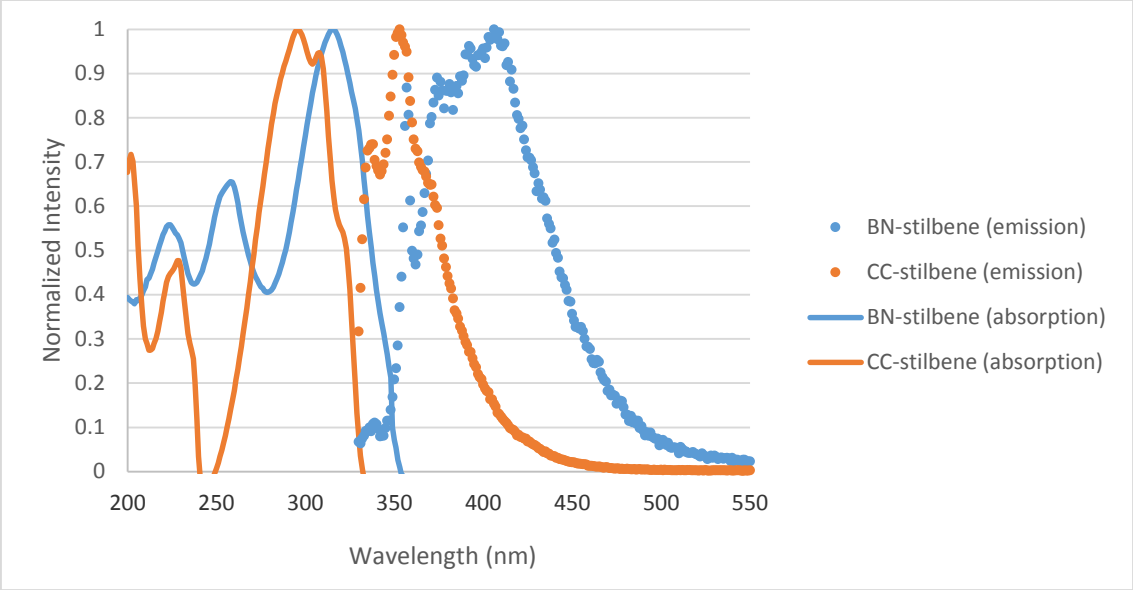

4.3.6 N–C(*sp*) Bond Formation

To access *N*-alkynyl functionality, we chose copper-catalyzed alkynylation reactions with alkynyl bromides under non-oxidative conditions that have been previously applied to either amide, enamide, carbamate, or sulfoximine substrates.[24,25] We hypothesized that reactivity of the azaborine nitrogen atom would be comparable to that of a nitrogen atom in resonance with a carbonyl, sulfonyl, or alkene. Avoidance of dioxygen in particular as a

[24] For select examples of alkynylation with alkynyl bromides, see: (a) Frederick, M. O.; Mulder, J. A.; Tracey, M. R.; Hsung, R. P.; Huang, J.; Kurtz, K. C. M.; Shen, L.; Douglas, C. J. *J. Am. Chem. Soc.* **2003**, *125*, 2368–2369. (b) Dunetz, J. R.; Danheiser, R. L. *Org. Lett.* **2003**, *5*, 4011–4014. (c) Zhang, Y.; Hsung, R. P.; Tracey, M. R.; Kurtz, K. C. M.; Vera, E. L. *Org. Lett.* **2004**, *6*, 1151–1154. (d) Hirano, S.; Tanaka, R.; Urabe, H.; Sato, F. *Org. Lett.* **2004**, *6*, 727–729. (e) Chen, W. Y.; Wang, L.; Frings, M.; Bolm, C. *Org. Lett.* **2014**, *16*, 3796–3799. (f) Zhang, X.; Zhang, Y.; Huang, J.; Hsung, R. P.; Kurtz, K. C. M.; Oppenheimer, J.; Petersen, M. E.; Sagamanova, I. K.; Shen, L.; Tracey, M. R. *J. Org. Chem.* **2006**, *71*, 4170–4177.
[25] For select examples of oxidative cross-coupling reactions, see: (a) Hamada, T.; Ye, X.; Stahl, S. S. *J. Am. Chem. Soc.* **2008**, *130*, 833–835. (b) Jia, W.; Jiao, N. *Org. Lett.* **2010**, *12*, 2000–2003. (c) Laouiti, A.; Rammah, M. M.; Rammah, M. B.; Marrot, J.; Couty, F.; Evano, G. *Org. Lett.* **2012**, *14*, 6–9.

stoichiometric oxidant was also deemed necessary to prevent azaborine decomposition. However, when **4.28e** was subjected to the copper-mediated *N*-alkynylation reaction, we observed only trace amounts of *N*-functionalized side product **4.86a** (Scheme 4.22, in parentheses), with the alkyne homo-coupling product as the major species instead. The side product **4.86a** was produced presumably *via* phenyl group displacement from boron by an excess amount of *n*-BuLi and subsequent *N*-coordination to the active copper complex to undergo alkynylation.

Scheme 4.22 Unexpected results from *N*-alkynylation reaction

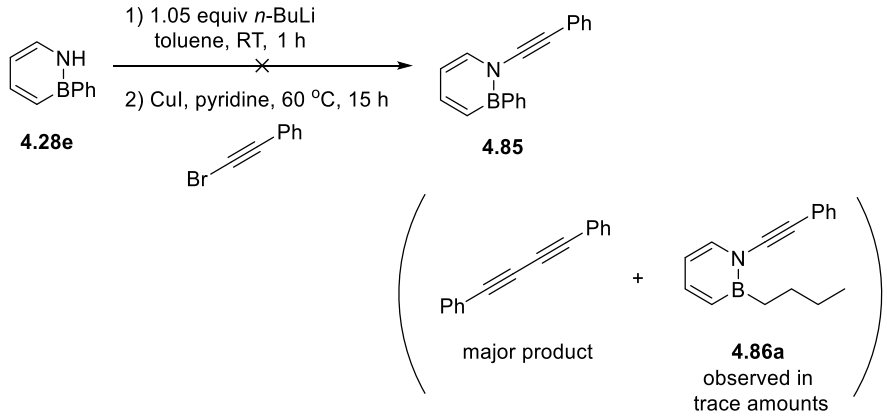

Thus, we decided to change the substituent on boron to more greatly favor the desired reaction path. Under the optimized catalytic condition, *n*-butyl or mesityl substituted azaborines underwent efficient *N*-alkylnylation to furnish the desired products in high yields (Table 4.7).

Table 4.7 *N*-Alkynylation of 1,2-azaborines

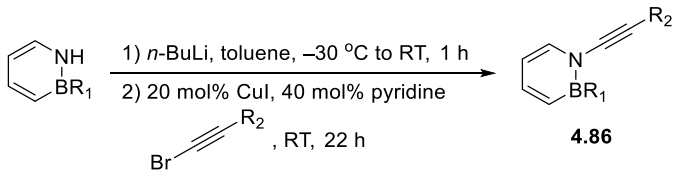

entry	R_1	R_2	product	yield (%)
1	*n*-Bu (**4.28d**)	Ph	**4.86a**	84
2	Mes (**4.87**)	Ph	**4.86b**	98
3	Mes (**4.87**)	TIPS	**4.86c**	79

4.3.7 Discovery of New Reactivity of 1,2-Azaborines

During the electrophilic substitution reactions with epoxides or aziridines before quenching with acid, we observed formation of tetra-coordinated boron species induced by intramolecular cyclization of heteroatom to boron (an example of reaction with ethylene oxide is shown in Scheme 4.23, eq. 1). The ^{11}B NMR peak of the intermediate appeared at 0.4–2.7 ppm, and ^{1}H NMR peaks appeared relatively upfield: 4.4–4.5 ppm and 5.4-5.6 ppm, for C5-H and C3-H, respectively. This observation presents the opportunity to harness a new reaction mode of 1,2-azaborines through the enhanced activity of the boronate species 4.88. For example, we recently published Diels–Alder reactions of 1,2-azaborines, and observed reversible cycloadduct formation, which limited the synthetic utility (Scheme 4.23, eq. 2).[26] We envision that the activated intermediates (such as **4.88**) can potentially serve as electron-rich dienes to undergo Diels–Alder reactions without using Lewis acid catalysts under milder conditions.

[26] Burford, R. J.; Li, B.; Vasiliu, M.; Dixon, D. A.; Liu, S.-Y. *Angew. Chem. Int. Ed*. **2015**, *54*, 7823–7827.

Scheme 4.23 Potential reactivity in Diels-Alder reaction of 1,2-azaborines

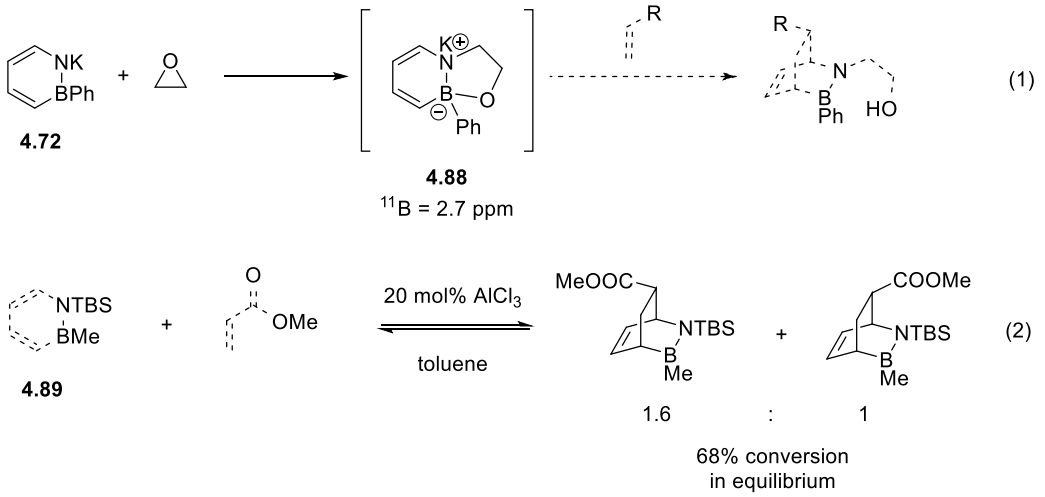

Furthermore, we previously observed self-arylation of C3-bromo-1,2-azaborines under C–O coupling reaction conditions similar to Molander's BN-naphthalene chemistry (Scheme 4.24, eq. 1 and 2).[15] Instead of C–O bond formation, the boron phenyl group in 4.90 migrated to C3 position to form a C–C bond presumably induced by the initial formation of a thermodynamically stable B–O*t*-Bu adduct. By combining this unique reactivity with potential Diels-Alder reaction of activated boronate species 4.95, it is feasible to synthesize a complex chiral molecule 4.96 featuring an oxazaborolidine unit (Scheme 4.24, eq. 3).

Scheme 4.24 Potential application by combination of self-arylation and Diels-Alder reaction

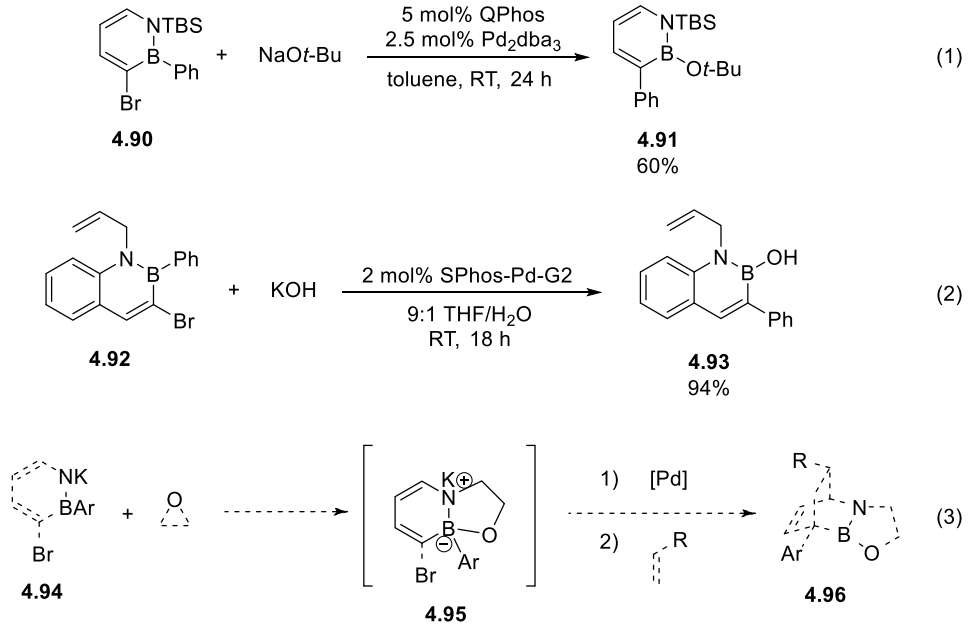

4.4 Conclusions

We have developed an array of chemical transformations to functionalize the nitrogen of 1,2-azaborines. Electrophilic substitution reactions, N–C(sp^2) bond forming reactions under Buchwald-Hartwig amination conditions, and N–C(*sp*) bond forming reactions using copper-catalyzed *N*-alkynylation afforded various *N*-functionalized 1,2-azaborines. This work expands the scope of possible functionality on the azaborine skeleton and enables further elaboration to complex BN-containing molecules applicable to studies in materials science and medicinal chemistry. Specifically, by utilizing an aziridine ring-opening reaction, we successfully prepared a BN-lisdexamfetamine analog. We also described the first example of an unsubstituted BN-isostere of *trans*-stilbene, as prepared by an *N*-alkenylation reactions.

4.5 Experimental

4.5.1 General Information

All oxygen- and moisture-sensitive manipulations were carried out under an inert atmosphere (N_2) using either standard Schlenk techniques or a glove box. THF was purified by distillation from sodium benzophenone ketyl prior to use. Toluene was dried over CaH_2 and distilled under nitrogen atmosphere prior to use. Et_2O, CH_2Cl_2 and pentane were purified by passing through a neutral alumina column under argon. Pd/C was purchased from Strem and heated under high vacuum at 100 °C for 12 hours prior to use. Silica gel (230-400 mesh) was dried for 12 hours at 180 °C under high vacuum. Flash chromatography was performed with this silica gel under an inert atmosphere. Allylbromide, ethyl iodide, benzyl bromide, 3-bromo-1-(trimethylsilyl)-1-propyne, benzoyl chloride were purified by distillation from CaH_2 under nitrogen atmosphere prior to use. 1-Bromo-2-phenylacetylene and 1-bromo-2-(triisopropylsilyl)acetylene were prepared according to the previously reported methods.[24e] All other chemicals and solvents were purchased and used as received.

NMR spectra were recorded on a Varian VNMRS 600 MHz, VNMRS 500 MHz, INOVA 500 MHz, or VNMRS 400 MHz spectrometer. Deuterated solvents were purchased from Cambridge Isotope Labs. ^{11}B NMR spectra were externally referenced to $BF_3 \bullet Et_2O$ (δ 0). All NMR chemical shifts are reported in ppm relative to residual solvent for ^1H and ^{13}C NMR. Signals are quoted as singlet (s), doublet (d), triplet (t), quartet (q), quintet (quint), multiplet (m), and broad singlet (br s). Coupling constants are reported in Hz. Infrared spectroscopy was performed on a Bruker ALPHA-Platinum FT-IR Spectrometer with ATR-sampling module. High-resolution mass spectrometry analyses

were performed by direct analysis in real time (DART) on a JEOL AccuTOF DART instrument. Photoluminescence quantum yields were measured using an integrating sphere instrument.

4.5.2 Synthesis of 1,2-Azaborines

Synthesis of 1,2-Azaborine Starting Materials:

Scheme 4.25 Synthesis of NK salt **4.72**

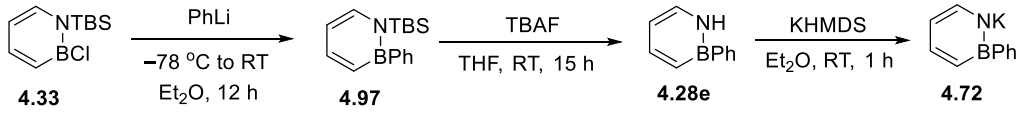

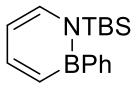

4.97

To a 250 mL round bottom flask containing **4.33** (5.00 g, 22.0 mmol) in Et_2O (100 mL) a solution of phenyllithium (11.6 mL, 22.0 mmol, 1.9 M in dibutylether) was added dropwise under nitrogen atmosphere at –78 °C. The reaction mixture was stirred for 12 h as it was slowly warmed to room temperature. The reaction mixture was filtrated through a glass frit and the solvent was removed under reduced pressure. The crude mixture was purified by silica gel column chromatography with pentane as the eluent. The desired product was isolated as a colorless oil (5.92 g, >99%). The spectra for **4.97** are consistent with the values reported in the literature.[2c]

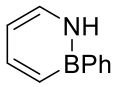

4.28e

To a 500 mL round bottom flask containing **4.97** (9.46 g, 35.2 mmol) in THF (250 mL) a solution of tetrabutylammonium fluoride (38.7 mL, 38.7 mmol, 1.0 M in THF) was added dropwise under nitrogen atmosphere at room temperature. The

reaction mixture was stirred for 15 h. The reaction mixture was concentrated under reduced pressure and dissolved in Et_2O (100 mL). The organic solution was transferred into a separatory funnel containing water (100 mL) and extracted with Et_2O (3 x 50 mL). The combined organic layers were washed with brine (100 mL), dried with $MgSO_4$, filtered and the solvent was removed under reduced pressure. The crude mixture was purified by silica gel column chromatography (100% pentane to 30% Et_2O/pentane). The desired product was isolated as a white solid (4.63 g, 85%). The spectra for **4.28e** are consistent with the values reported in the literature.[5a]

4.72

To a 50 mL round bottom flask containing **4.28e** (500 mg, 3.23 mmol) in Et_2O (15 mL) a solution of potassium bis(trimethylsilyl)amide (7.10 mL, 3.55 mmol, 0.5 M in toluene) was added dropwise under nitrogen atmosphere at room temperature. The reaction mixture was stirred for 1 h. The resulting powder was filtrated and washed with Et_2O, followed by pentane. The white powder was collected as the desired product and dried under reduced pressure (589 mg, 95%). ^{1}H NMR (600 MHz, THF-d_8): δ 8.14 (s, 1H), 7.92 (d, J = 7.2 Hz, 2H), 7.39 (dd, J = 9.6, 6.6 Hz, 1H), 7.21 (t, J = 7.8 Hz , 2H), 7.08 (t, J = 7.8 Hz, 1H), 6.67 (d, J = 10.8 Hz, 1H), 6.14 (t, J = 5.4 Hz, 1H). ^{11}B NMR (160 MHz, THF-d_8): δ 35.2. ^{13}C NMR (151 MHz, THF-d_8): δ 151.1 (br), 150.3, 140.7, 133.2, 128.2, 126.3, 122.5 (br), 112.1. FTIR (thin film): 3072, 3012, 1651, 1612, 1542, 1458, 1414, 1378, 1232, 1166, 980, 884, 713, 593 cm^{-1}. HRMS (DART-TOF) calculated for $C_{10}H_9BN$ ([M]$^-$): 154.0828, found: 154.0831.

Electrophilic Substitution (Table 4.5):

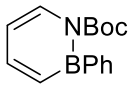

4.77a

In a dry box, an oven-dried 4 mL glass reaction vial was charged with **4.72** (29.0 mg, 0.15 mmol), di-*tert*-butyl dicarbonate (36.0 mg, 0.165 mmol), and THF (2 mL). The reaction was stirred at room temperature for 24 h. The crude mixture was concentrated under reduced pressure and purified by silica gel column chromatography (100% pentane to 10% Et_2O/pentane). The desired product was isolated as a white solid (33.6 mg, 88%). A duplicate reaction gave 91% yield. ^{1}H NMR (500 MHz, CD_2Cl_2): δ 7.80 (d, *J* = 7.5 Hz, 1H), 7.66 (dd, *J* = 11.0, 6.5 Hz, 1H), 7.45 (dd, *J* = 8.5, 2.0 Hz, 2H), 7.37-7.29 (m, 3H), 6.87 (d, *J* = 11.0 Hz, 1H), 6.43 (t, *J* = 6.8 Hz, 1H), 1.22 (s, 9H). ^{11}B NMR (160 MHz, CD_2Cl_2): δ 37.7. ^{13}C NMR (151 MHz, CD_2Cl_2): δ 156.8, 145.5, 143.4 (br), 133.7, 133.0 (br), 132.3, 127.9, 111.9, 84.5, 27.4. FTIR (thin film): 3206, 2981, 1741, 1619, 1513, 1440, 1394, 1258, 1150, 966, 849, 743, 702 cm^{-1}. HRMS (DART-TOF) calculated for $C_{15}H_{19}BNO_2$ ($[M+H]^+$): 256.15088, found: 256.15160.

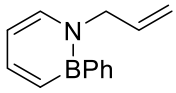

4.77b

In a dry box, an oven-dried 4 mL glass reaction vial was charged with **4.72** (29.0 mg, 0.15 mmol), allylbromide (14.3 μL, 0.165 mmol), and THF (2 mL). The reaction was stirred at room temperature for 2 h. The crude mixture was concentrated under reduced pressure and purified by silica gel column chromatography (100% pentane to 3% CH_2Cl_2/pentane). The desired product was isolated as a colorless oil (29.0 mg, 99%). A duplicate reaction gave 96% yield. ^{1}H NMR (600 MHz, CD_2Cl_2): δ 7.67 (dd, *J* = 10.2, 6.0 Hz, 1H), 7.55 (d, *J* = 7.2 Hz, 2H), 7.40-7.33 (m, 3H), 7.25 (d, *J* = 7.2 Hz, 1H), 6.86 (d, *J* = 10.8 Hz, 1H), 6.44 (t, *J* = 6.9 Hz, 1H), 6.05-5.99 (m, 1H), 5.22 (d, *J* = 11.4 Hz, 1H), 5.02 (d, *J* = 10.0 Hz, 1H), 4.46 (d, *J* = 3.6 Hz, 2H). ^{11}B NMR (192 MHz,

CD_2Cl_2): δ 35.6. ^{13}C NMR (151 MHz, CD_2Cl_2): δ 143.4, 142.0 (br), 139.2, 137.2, 133.4, 131.5 (br), 128.1, 128.0, 116.7, 111.9, 56.3. FTIR (thin film): 3067, 3009, 1643, 1460, 1402, 1205, 1118, 919, 684, 557 cm^{-1}. HRMS (DART-TOF) calculated for $C_{13}H_{15}BN$ ($[M+H]^+$): 196.12975, found: 196.13061.

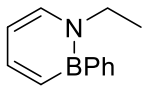

4.77c

In a dry box, an oven-dried 4 mL glass reaction vial was charged with **4.28e** (23.3 mg, 0.15 mmol) and THF (2 mL). A solution of potassium bis(trimethylsilyl)amide (330 μL, 0.165 mmol, 0.5 M in toluene) was added dropwise to the reaction, followed by ethyl iodide (13.2 μL, 0.165 mmol). The reaction was stirred at room temperature for 2 h. The crude mixture was concentrated under reduced pressure and purified by silica gel column chromatography (100% pentane to 5% CH_2Cl_2/pentane). The desired product was isolated as a colorless oil (27.5 mg, >99%). A duplicate reaction gave >99% yield. ^1H NMR (500 MHz, CD_2Cl_2): δ 7.64 (dd, J = 11.0, 7.2 Hz, 1H), 7.53 (d, J = 8.5 Hz, 2H), 7.40-7.32 (m, 4H), 6.79 (d, J = 10.5 Hz, 1H), 6.43 (t, J = 6.5 Hz, 1H), 3.87 (q, J = 7.0 Hz, 2H), 1.31 (t, J = 7.0 Hz, 1H). ^{11}B NMR (160 MHz, CD_2Cl_2): δ 35.4. ^{13}C NMR (151 MHz, CD_2Cl_2): δ 143.1, 142.5 (br), 138.7, 133.3, 131.5 (br), 128.1, 127.8, 111.9, 48.8, 18.8. FTIR (thin film): 3068, 2975, 2897, 1608, 1515, 1405, 1259, 1209, 1114, 801, 781, 597 cm^{-1}. HRMS (DART-TOF) calculated for $C_{12}H_{15}BN$ ($[M+H]^+$): 184.12975, found: 184.13024.

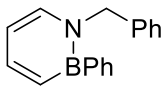

4.77d

In a dry box, an oven-dried 4 mL glass reaction vial was charged with **4.28e** (23.3 mg, 0.15 mmol) and THF (2 mL). A solution of potassium bis(trimethylsilyl)amide (330 μL, 0.165 mmol, 0.5 M in toluene) was added dropwise to the reaction, followed by benzyl bromide (19.6 μL, 0.165 mmol). The reaction was stirred

at room temperature for 2 h. The crude mixture was filtrated through an acro-disc and the filtrate was concentrated under reduced pressure. The crude product was purified by silica gel column chromatography (100% pentane to 3% CH_2Cl_2/pentane). The desired product was isolated as a white solid (35.0 mg, 95%). A duplicate reaction gave 92% yield. ^{1}H NMR (600 MHz, CD_2Cl_2): δ 7.70 (dd, *J* = 11.4, 6.6 Hz, 1H), 7.51 (d, *J* = 7.8 Hz, 2H), 7.36-7.31 (m, 5H), 7.28-7.24 (m, 2H), 7.08 (d, *J* = 6.6 Hz, 1H), 6.92 (d, *J* = 11.4 Hz, 1H), 6.44 (t, *J* = 6.0 Hz, 1H), 5.11 (s, 2H). ^{11}B NMR (192 MHz, CD_2Cl_2): δ 35.8. ^{13}C NMR (151 MHz, CD_2Cl_2): δ 143.5, 142.3 (br), 140.4, 139.4, 133.4, 132.2 (br), 129.2, 128.2, 128.1, 127.8, 127.4, 112.3, 57.2. FTIR (thin film): 3066, 3029, 3008, 1609, 1513, 1403, 1240, 1137, 742, 702, 522 cm^{-1}. HRMS (DART-TOF) calculated for $C_{17}H_{17}BN$ ([M+H]$^+$): 246.14540, found: 246.14551.

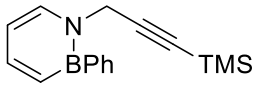

4.77e

In a dry box, an oven-dried 4 mL glass reaction vial was charged with **4.28e** (23.3 mg, 0.15 mmol) and THF (2 mL). A solution of potassium bis(trimethylsilyl)amide (330 μL, 0.165 mmol, 0.5 M in toluene) was added dropwise to the reaction and cooled to 0 °C. 3-Bromo-1-(trimethylsilyl)-1-propyne (27.0 μL, 0.165 mmol) was added to the reaction at this temperature and the reaction was slowly warmed to room temperature while stirring for 17 h. The crude mixture was concentrated under reduced pressure and purified by silica gel column chromatography (100% pentane to 2% Et_2O/pentane). The desired product was isolated as a colorless oil (20.2 mg, 51%). A duplicate reaction gave 55% yield. ^{1}H NMR (500 MHz, CD_2Cl_2): δ 7.66 (dd, *J* = 11.0, 6.5 Hz, 1H), 7.62 (d, *J* = 8.0 Hz, 2H), 7.50 (d, *J* = 7.0 Hz , 1H), 7.42-7.34 (m, 3H), 6.85 (d, *J* = 11.0 Hz, 1H), 6.47 (t, *J* = 6.5 Hz, 1H), 4.59 (s, 2H), 0.19 (s, 9H). ^{11}B NMR (160 MHz, CD_2Cl_2): δ 35.6. ^{13}C NMR (151 MHz, CD_2Cl_2): δ 143.6, 141.7 (br), 138.4, 133.7, 133.5,

131.9 (br), 128.3, 112.4, 103.1, 90.4, 44.3, 0.0. FTIR (thin film): 3070, 3010, 2959, 2180, 1611, 1514, 1404, 1250, 1136, 1011, 841, 747, 683 cm^{-1}. HRMS (DART-TOF) calculated for $C_{16}H_{21}BNSi$ ($[M+H]^+$): 266.15363, found: 266.15356.

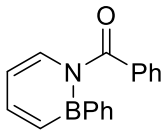

4.77f

In a dry box, an oven-dried 4 mL glass reaction vial was charged with **4.28e** (23.3 mg, 0.15 mmol) and THF (2 mL). A solution of potassium bis(trimethylsilyl)amide (330 µL, 0.165 mmol, 0.5 M in toluene) was added dropwise to the reaction, followed by benzoyl chloride (19.2 µL, 0.165 mmol). The reaction was stirred at room temperature for 16 h. The crude mixture was concentrated under reduced pressure and purified by silica gel column chromatography (100% pentane to 3% Et_2O/pentane). The desired product was isolated as a white solid (29.0 mg, 75%). A duplicate reaction gave 69% yield. ^1H NMR (500 MHz, CD_2Cl_2): δ 7.81 (dd, J = 10.5, 6.0 Hz, 1H), 7.64 (d, J = 8.0 Hz, 2H), 7.57 (d, J = 7.0 Hz, 1H), 7.44-7.38 (m, 3H), 7.27 (t, J = 7.5 Hz, 2H), 7.13 (t, J = 2.5 Hz, 3H), 7.07 (d, J = 11.5 Hz, 1H), 6.55 (t, J = 6.5 Hz, 1H). ^{11}B NMR (160 MHz, CD_2Cl_2): δ 36.6. ^{13}C NMR (126 MHz, CD_2Cl_2): δ 178.8, 145.6, 140.4 (br), 134.6, 134.2, 134.0, 133.7, 132.0 (br), 131.5, 128.9, 128.5, 128.0, 111.9. FTIR (thin film): 3069, 1705, 1612, 1506, 1441, 1262, 1229, 1074, 967, 736, 631 cm^{-1}. HRMS (DART-TOF) calculated for $C_{17}H_{15}BNO$ ($[M+H]^+$): 260.12467, found: 260.12437.

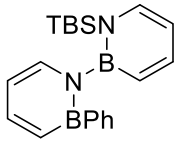

4.77g

In a dry box, an oven-dried 4 mL glass reaction vial was charged with **4.72** (29.0 mg, 0.15 mmol), *N*-TBS-*B*-Cl-1,2-azaborine (**4.33**) (37.6 mg, 0.165 mmol), and THF (2 mL). The reaction was stirred at room temperature for 1 h. The crude mixture was concentrated under reduced pressure and purified by silica gel column chromatography (100% pentane to 2% Et_2O/pentane). The desired product was

isolated as a colorless oil (51.2 mg, 99%). A duplicate reaction gave 97% yield. ^{1}H NMR (500 MHz, CD_2Cl_2): δ 7.73 (dd, *J* = 10.5, 6.5 Hz, 1H), 7.65 (dd, *J* = 10.5, 6.5 Hz, 1H), 7.38 (d, *J* = 6.0 Hz, 1H), 7.33 (d, *J* = 2.5 Hz, 2H), 7.26 (d, *J* = 6.5 Hz, 1H), 7.17 (d, *J* = 3.0 Hz, 2H), 6.97 (d, *J* = 10.5 Hz, 1H), 6.53 (d, *J* = 11.0 Hz, 1H), 6.47 (t, *J* = 6.0 Hz, 1H), 6.42 (t, *J* = 6.0 Hz, 1H). ^{11}B NMR (160 MHz, CD_2Cl_2): δ 36.1. ^{13}C NMR (151 MHz, CD_2Cl_2): δ 146.1, 144.0, 142.6 (br), 138.4, 135.0, 133.6 (br), 130.1 (br), 127.7, 112.3, 111.3, 27.4, 19.6, –3.6. FTIR (thin film): 3067, 2930, 2859, 1604, 1501, 1392, 1272, 1233, 1148, 989, 821, 789, 701 cm^{-1}. HRMS (DART-TOF) calculated for $C_{20}H_{29}B_2N_2O$ ([M+H]$^+$): 347.22861, found: 347.22893.

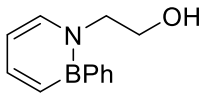

4.77h

In a dry box, an oven-dried 4 mL glass reaction vial was charged with **4.72** (29.0 mg, 0.15 mmol) and THF (2 mL). A solution of ethylene oxide (66 μL, 0.165 mmol, 2.5 M in THF) was added to the reaction. After stirring the reaction at room temperature for 4 h, hydrogen chloride solution (82.5 μL, 0.165 mmol, 2.0 M in diethyl ether) was added and the reaction was stirred for 5 min. The crude mixture was concentrated under reduced pressure and purified by silica gel column chromatography (10% Et_2O/pentane to 100% Et_2O). The desired product was isolated as a colorless oil (29.2 mg, 98%). A duplicate reaction gave 95% yield. ^{1}H NMR (500 MHz, CD_2Cl_2): δ 7.65 (dd, *J* = 10.0, 7.0 Hz, 1H), 7.51 (d, *J* = 7.5 Hz, 2H), 7.39-7.30 (m, 4H), 6.80 (d, *J* = 11.0 Hz, 1H), 6.41 (t, *J* = 6.5 Hz, 1H), 3.98 (t, *J* = 4.0 Hz, 2H), 3.73 (d, *J* = 8.3 Hz, 2H), 1.53 (s, 1H). ^{11}B NMR (192 MHz, CD_2Cl_2): δ 35.9. ^{13}C NMR (151 MHz, CD_2Cl_2): δ 143.5, 142.7 (br), 139.5, 133.4, 131.7 (br), 128.2, 127.9, 111.8, 64.1, 55.9. FTIR (thin film): 3350, 3067, 3007, 2881, 1607, 1513, 1402, 1238, 1142, 1053, 944, 866, 742, 701, 561 cm^{-1}. HRMS (DART-TOF) calculated for $C_{12}H_{15}BNO$ ([M+H]$^+$): 200.12467, found: 200.12457.

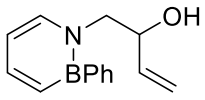

4.77i

In a dry box, an oven-dried 4 mL glass reaction vial was charged with **4.72** (29.0 mg, 0.15 mmol), 3,4-epoxy-1-butene (13.3 μL, 0.165 mmol) and THF (2 mL). After stirring the reaction at room temperature for 4 h, hydrogen chloride solution (82.5 μL, 0.165 mmol, 2.0 M in diethyl ether) was added and the reaction was stirred for 5 min. The crude mixture was concentrated under reduced pressure and purified by silica gel column chromatography (10% Et_2O/pentane to 30% Et_2O/pentane). The desired product was isolated as a colorless oil (20.1 mg, 60%). A duplicate reaction gave 60% yield. ^{1}H NMR (500 MHz, CD_2Cl_2): δ 7.67 (dd, *J* = 11.0, 7.0 Hz, 1H), 7.54 (d, *J* = 7.5 Hz, 2H), 7.41-7.33 (m, 4H), 6.83 (d, *J* = 11.0 Hz, 1H), 6.42 (t, *J* = 5.5 Hz, 1H), 5.76-5.69 (m, 1H), 5.15 (d, *J* = 27.5, 1H), 5.12 (d, *J* = 20.5 Hz, 1H), 4.23 (br s, 1H), 4.03 (dd, *J* = 13.5, 4.0 Hz, 1H), 3.81 (dd, *J* = 13.5, 9.0 Hz, 1H), 1.85 (s, 1H). ^{11}B NMR (160 MHz, CD_2Cl_2): δ 36.2. ^{13}C NMR (151 MHz, CD_2Cl_2): δ 143.6, 142.5 (br), 140.0, 138. 4, 133.4, 131.7 (br), 128.2, 127.9, 116.6, 111.5, 74.5, 59.5. FTIR (thin film): 3394, 3068, 3008, 2930, 1607, 1513, 1403, 1237, 1145, 975, 927, 743, 702 cm^{-1}. HRMS (DART-TOF) calculated for $C_{14}H_{17}BNO$ ($[M+H]^+$): 226.14032, found: 226.14134.

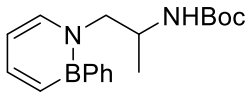

4.77j

In a dry box, an oven-dried 4 mL glass reaction vial was charged with **4.72** (29.0 mg, 0.15 mmol), *tert*-butyl 2-methylaziridine-1-carboxylate (25.9 mg, 0.165 mmol) and THF (2 mL). After stirring the reaction at room temperature for 16 h, hydrogen chloride solution (82.5 μL, 0.165 mmol, 2.0 M in diethyl ether) was added and the reaction was stirred for 5 min. The crude mixture was concentrated under reduced pressure and purified by silica gel column chromatography (5% Et_2O/pentane to 50% Et_2O/pentane). The desired product was isolated as a colorless oil (39.5 mg, 84%). A duplicate reaction gave 89% yield. ^{1}H NMR (500 MHz, CD_2Cl_2): δ 7.65

(dd, J = 11.0, 6.5 Hz, 1H), 7.53 (d, J = 7.5 Hz, 2H), 7.40 (t, J = 7.5 Hz, 2H), 7.36-7.33 (m, 2H), 6.80 (d, J = 11.5 Hz, 1H), 6.43 (t, J = 6.5 Hz, 1H), 4.30 (br s, 1H), 3.90 (d, J = 5.5 Hz, 2H), 3.81 (t, J = 5.5 Hz, 1H), 1.38 (s, 9H), 0.92 (d, J = 5.5 Hz, 3H). ^{11}B NMR (160 MHz, CD_2Cl_2): δ 36.0. ^{13}C NMR (151 MHz, CD_2Cl_2): δ 155.5, 143.4, 142.6 (br), 139.2, 133.3, 131.5 (br), 128.3, 127.8, 111.9, 79.5, 58.5, 49.0, 28.7, 18.7. FTIR (thin film): 3339, 2976, 1693, 1453, 1365, 1116, 1011, 975, 944, 881, 742, 703, 597, 462 cm^{-1}. HRMS (DART-TOF) calculated for $C_{18}H_{26}BN_2O_2$ ($[M+H]^+$): 313.20873, found: 313.21021.

Buchwald-Hartwig Amination:

Table 4.8 Ligand screening

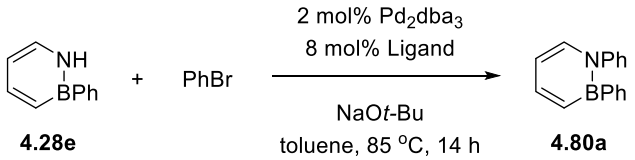

4.28e **4.80a**

entry	ligand	yield (%)[a]	entry	ligand	yield (%)[a]
1	QPhos	67 (86)	8	dppf	ND (6)
2	P(*t*-Bu)$_3$	47 (66)	9	XPhos	13 (19)
3	PtBu$_2$Ph	40 (41)	10	SPhos	30 (50)
4	PPh$_3$	ND (-)	11	JohnPhos	33 (57)
5	PCy$_3$	ND (-)	12	BrettPhos	5 (-)
6	PCy$_2$Ph	ND (-)	13	XPhos PdG2	ND (30)
7	P(*o*-tol)$_3$	ND (-)			

[a]Yields in parentheses are determined by ^{1}H NMR spectroscopy against a calibrated internal standard. 1.0 equiv PhBr and 1.5 equiv NaO*t*-Bu were used. ND= not determined.

Table 4.9 Optimization

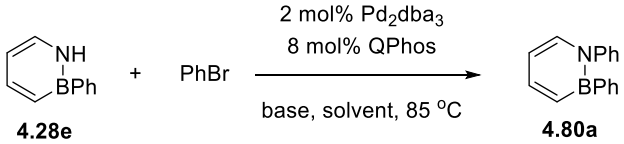

4.28e **4.80a**

entry	variations	yield (%)[a]
1	standard[b]	67 (86)
2	1.5 equiv K_2CO_3	ND (-)
3	2.0 equiv NaO*t*-Bu	51 (78)
4	toluene:DME (5:1)	50 (77)
5	1.2 equiv PhBr	80 (90)
6	1.2 equiv PhBr, 20h	ND (73)
7	1.2 equiv PhBr, 1.2 equiv NaO*t*-Bu	ND (73)

[a]Yields in parentheses are determined by ^{1}H NMR spectroscopy against a calibrated internal standard. [b]Standard condition: 1.0 equiv PhBr, 1.5 equiv NaO*t*-Bu, toluene, 14 h. ND= not determined.

N–C(sp^2) Bond Formation (Table 4.6):

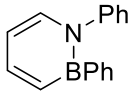

4.80a

In a dry box, an oven-dried 4 mL glass reaction vial was charged with **4.28e** (23.3 mg, 0.150 mmol), Pd_2dba_3 (2.7 mg, 0.0030 mmol), QPhos (8.5 mg, 0.012 mmol), sodium *tert*-butoxide (21.6 mg, 0.225 mmol), bromobenzene (19.2 μL, 0.180 mmol) and toluene (0.7 mL). The reaction mixture was stirred at 85 ºC for 14 h. At the completion of the reaction, the reaction mixture was cooled to room temperature. The crude mixture was filtrated through an acro-disc using CH_2Cl_2 as solvent and the filtrate was concentrated under reduced pressure. The crude product was purified by silica gel column chromatography (3% CH_2Cl_2/pentane to 5% CH_2Cl_2/pentane). The desired product was isolated as a white solid (28.8 mg, 83%). A duplicate reaction gave 79% yield. ^{1}H NMR (500 MHz, CD_2Cl_2): δ 7.76 (dd, *J* = 11.0, 6.5 Hz, 1H), 7.40 (d, *J* = 7.0 Hz, 1H), 7.35-7.30 (m, 3H), 7.22-7.7.12 (m, 7H), 7.03 (d, *J* = 11.5 Hz, 1H), 6.48 (t, *J* = 7.0 Hz, 1H), 4.30 (br s, 1H), 3.90 (d, *J* = 5.5 Hz, 2H), 3.81 (t, *J* = 5.5 Hz, 1H), 1.38 (s, 9H), 0.92 (d, *J* = 5.0 Hz, 3H). ^{11}B NMR (160 MHz, CD_2Cl_2): δ 35.2. ^{13}C NMR (151 MHz, CD_2Cl_2): δ 148.5, 143.9, 141.3 (br), 139.6, 134.4, 131.5 (br), 129.4, 127.9, 127.7, 127.6, 127.3, 111.4. FTIR (thin film): 3068, 3030, 1612, 1507, 1491, 1444, 1396, 1274, 1258, 1156, 1066, 761, 740, 698. 551 cm^{-1}. HRMS (DART-TOF) calculated for $C_{16}H_{15}BN$ ([M+H]$^+$): 232.12975, found: 232.12987.

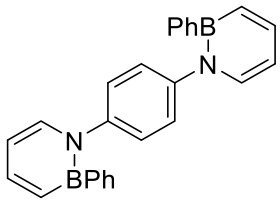

4.80b

In a dry box, an oven-dried 4 mL glass reaction vial was charged with **4.28e** (46.5 mg, 0.300 mmol), Pd_2dba_3 (5.5 mg, 0.0060 mmol), QPhos (17.1 mg, 0.0240 mmol), sodium *tert*-butoxide (43.2 mg, 0.450 mmol), 1,4-dibromobenzene (42.5 mg, 0.180 mmol) and

toluene (1.5 mL). The reaction mixture was stirred at 85 °C for 16 h. At the completion of the reaction, the reaction mixture was cooled to room temperature. The crude mixture was concentrated under reduced pressure and purified by silica gel column chromatography (2% CH_2Cl_2/pentane to 5% CH_2Cl_2/pentane). The desired product was isolated as a white solid (32.3 mg, 56%). A duplicate reaction gave 52% yield. ^{1}H NMR (600 MHz, CD_2Cl_2): δ 7.76 (dd, *J* = 10.8, 6.0 Hz, 2H), 7.37 (d, *J* = 7.2 Hz, 2H), 7.29-7.27 (m, 4H), 7.23-7.21 (m, 6H), 7.12 (s, 4H), 7.04 (d, *J* = 10.2 Hz, 2H), 6.49 (t, *J* = 6.0 Hz, 2H). ^{11}B NMR (160 MHz, CD_2Cl_2): δ 35.4. ^{13}C NMR (151 MHz, CD_2Cl_2): δ 147.0, 144.0, 139.4, 134.5, 131.8 (br), 128.1, 127.9, 127.8, 111.7. FTIR (thin film): 3067, 3031, 1608, 1503, 1445, 1432, 1394, 1254, 1156, 1106, 982, 846, 742, 701, 686 cm^{-1}. HRMS (DART-TOF) calculated for $C_{26}H_{23}B_2N_2$ ($[M+H]^+$): 385.20473, found: 385.20404.

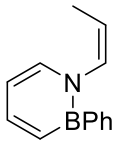

4.80c

In a dry box, an oven-dried 4 mL glass reaction vial was charged with **4.28e** (23.3 mg, 0.150 mmol) and toluene (1.5 mL). A solution of *n*-butyllithium (63.0 μL, 0.158 mmol, 2.5 M in hexane) was added at room temperature and the reaction was stirred for 5 min. To the reaction vial Pd_2dba_3 (2.7 mg, 0.0030 mmol), QPhos (8.5 mg, 0.012 mmol), and *cis*-1-bromo-1-propene (15.3 μL, 0.180 mmol) were added. The reaction mixture was stirred at 85 °C for 16 h. At the completion of the reaction, the reaction mixture was cooled to room temperature. The crude mixture was filtrated through an acro-disc using CH_2Cl_2 as solvent and the filtrate was concentrated under reduced pressure. The crude product was purified by silica gel column chromatography (100% pentane to 2% CH_2Cl_2/pentane). The desired product was isolated as a white solid (27.6 mg, 94%). A duplicate reaction gave 90% yield. ^{1}H NMR (500 MHz, CD_2Cl_2): δ 7.70 (dd, *J* = 11.0, 7.0 Hz, 1H), 7.63 (d, *J* = 6.5 Hz, 2H), 7.37-7.30 (m, 3H), 7.22 (d, *J* = 6.5 Hz, 1H), 6.96 (d, *J* =

11.0 Hz, 1H), 6.78 (dd, *J* = 8.0, 2.0 Hz, 1H), 6.42 (td, *J* = 7.0, 1.5 Hz, 1H), 5.49 (quint, *J* = 6.5 Hz, 1H), 1.56 (dd, *J* = 7.0, 1.5 Hz, 1H). ^{11}B NMR (160 MHz, CD_2Cl_2): δ 34.8. ^{13}C NMR (126 MHz, CD_2Cl_2): δ 144.0, 141.8 (br), 138.9, 135.9, 134.3, 131.6 (br), 128.3, 127.9, 121.4, 111.1, 12.2. FTIR (thin film): 3069, 3031, 1660, 1607, 1509, 1445, 1398, 1295, 1231, 977, 753, 701, 450 cm^{-1}. HRMS (DART-TOF) calculated for $C_{18}H_{26}BN_2O_2$ ($[M+H]^+$): 313.20873, found: 313.21021.

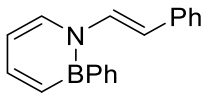

4.80d

In a dry box, an oven-dried 4 mL glass reaction vial was charged with **4.28e** (23.3 mg, 0.150 mmol) and toluene (1.5 mL). A solution of *n*-butyllithium (63.0 μL, 0.158 mmol, 2.5 M in hexane) was added at room temperature and the reaction was stirred for 5 min. To the reaction vial Pd_2dba_3 (2.7 mg, 0.0030 mmol), QPhos (8.5 mg, 0.012 mmol), and β-bromostyrene (23.8 μL, 0.180 mmol) were added. The reaction mixture was stirred at 85 °C for 16 h. At the completion of the reaction, the reaction mixture was cooled to room temperature. The crude mixture was filtrated through an acro-disc using CH_2Cl_2 as solvent and the filtrate was concentrated under reduced pressure. The crude product was purified by silica gel column chromatography (2% CH_2Cl_2/pentane to 5% CH_2Cl_2/pentane). The desired product was isolated as a white solid (25.7 mg, 67%). A duplicate reaction gave 74% yield. ^{1}H NMR (500 MHz, CD_2Cl_2): δ 7.72 (d, *J* = 7.0 Hz, 2H), 7.65 (t, *J* = 6.5 Hz, 3H), 7.44-7.31 (m, 7H), 7.25 (t, *J* = 6.5 Hz, 1H), 6.98 (d, *J* = 11.0 Hz, 1H), 6.71 (d, *J* = 14.0 Hz, 1H), 6.54 (t, *J* = 6.5 Hz, 1H). ^{11}B NMR (160 MHz, CD_2Cl_2): δ 36.3. ^{13}C NMR (151 MHz, CD_2Cl_2): δ 144.3, 140.9 (br), 136.4, 135.4, 134.5, 134.3, 132.0 (br), 129.3, 128.6, 128.2, 127.9, 126.7, 120.5, 112.7. FTIR (thin film): 3068, 3026, 1641, 1609, 1509, 1492, 1402, 1238, 1150, 972, 948,

751, 703, 692 cm^{-1}. HRMS (DART-TOF) calculated for $C_{18}H_{17}BN$ ($[M+H]^+$): 258.14540, found: 258.14438.

Copper-Catalyzed *N*-Alkynylation (Table 4.7):

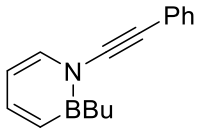

4.86a

In a dry box, an oven-dried 4 mL glass reaction vial was charged with *N*-H-*B*-*n*-butyl-1,2-azaborine (**4.28d**) (28.4 mg, 0.210 mmol) and toluene (1.0 mL) and cooled to –30 ºC. A solution of *n*-butyllithium (80.0 µL, 0.200 mmol, 2.5 M in hexane) was added at –30 ºC and the reaction was stirred for 1h while slowly warming up to room temperature. To the reaction vial CuI (7.6 mg, 0.040 mmol), pyridine (6.4 µL, 0.080 mmol), and a solution of 1-bromo-2-phenylacetylene (114 mg, 0.630 mmol) in toluene (1.0 mL) were added. The reaction was stirred at room temperature for 22 h. The crude mixture was diluted with Et_2O (3.0 mL) and washed with a 2:1 mixture of brine and concentrated NH_4OH (2 x 5.0 mL). The combined aqueous layers were extracted with Et_2O (2 x 5.0 mL). The combined organic layers were washed with brine (10 mL), dried with $MgSO_4$, filtered and the solvent was removed under reduced pressure. The crude product was purified by silica gel column chromatography (100% pentane). The desired product was isolated as a colorless oil (39.0 mg, 83%). A duplicate reaction gave 85% yield. ^{1}H NMR (600 MHz, CD_2Cl_2): δ 7.53 (dd, J = 10.8, 6.0 Hz, 1H), 7.49 (d, J = 6.0 Hz, 2H), 7.39-7.32 (m, 4H), 6.83 (d, J = 12.0 Hz, 1H), 6.30 (t, J = 6.0 Hz, 1H), 1.64 (t, J = 7.2 Hz, 2H), 1.46-1.40 (m, 4H), 0.96 (t, J = 7.2 Hz, 3H). ^{11}B NMR (160 MHz, CD_2Cl_2): δ 41.3. ^{13}C NMR (151 MHz, CD_2Cl_2): δ 143.4, 137.9, 131.8, 129.9 (br), 129.0, 128.4, 123.5, 111.9, 88.7, 68.7, 28.6, 26.3, 18.8 (br), 14.5. FTIR (thin film): 2955,

2922. 2856, 2255, 1617, 1508, 1442, 1400, 1329, 1268, 1149, 1107, 753, 735, 690 cm^{-1}. HRMS (DART-TOF) calculated for $C_{16}H_{19}BN$ ($[M+H]^+$): 236.16105, found: 236.16070.

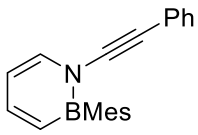

4.86b

In a dry box, an oven-dried 4 mL glass reaction vial was charged with *N*-H-*B*-mesityl-1,2-azaborine (**4.87**) (41.4 mg, 0.210 mmol) and toluene (1.0 mL) and cooled to –30 ºC. A solution of *n*-butyllithium (80.0 µL, 0.200 mmol, 2.5 M in hexane) was added at –30 ºC and the reaction was stirred for 1h while slowly warming up to room temperature. To the reaction vial CuI (7.6 mg, 0.040 mmol), pyridine (6.4 µL, 0.080 mmol), and a solution of 1-bromo-2-phenylacetylene (114 mg, 0.630 mmol) in toluene (1.0 mL) were added. The reaction was stirred at room temperature for 22 h. The crude mixture was diluted with Et_2O (3.0 mL) and washed with a 2:1 mixture of brine and concentrated NH_4OH (2 x 5.0 mL). The combined aqueous layers were extracted with Et_2O (2 x 5.0 mL). The combined organic layers were washed with brine (10 mL), dried with $MgSO_4$, filtered and the solvent was removed under reduced pressure. The crude product was purified by silica gel column chromatography (0.2% Et_2O/pentane). The desired product was isolated as a colorless oil (58.4 mg, 98%). A duplicate reaction gave 98% yield. ^1H NMR (500 MHz, CD_2Cl_2): δ 7.69 (dd, J = 11.0, 6.5 Hz, 1H), 7.56 (d, J = 6.5 Hz, 1H), 7.25-7.23 (m, 3H), 7.09-7.07 (m, 2H), 6.92 (d, J = 11.0 Hz, 1H), 6.89 (s, 2H), 6.48 (t, J = 6.0 Hz, 1H), 2.33 (s, 3H), 2.20 (s, 6H). ^{11}B NMR (160 MHz, CD_2Cl_2): δ 39.8. ^{13}C NMR (151 MHz, CD_2Cl_2): δ 144.0, 140.2, 138.1, 137.9, 137.5 (br), 131.5, 128.8, 128.3, 127.4, 123.2, 112.8, 89.1, 67.9, 22.7, 21.5 (the signal for the mesityl carbon next to boron is not observed). FTIR (thin film): 3031, 2915, 2255, 1614, 1504, 1440, 1396, 1329, 1229, 1125, 936, 849, 753, 691, 515 cm^{-1}. HRMS (DART-TOF) calculated for $C_{21}H_{21}BN$ ($[M+H]^+$): 298.17670, found: 298.17704.

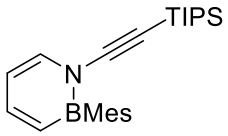

4.86c

In a dry box, an oven-dried 4 mL glass reaction vial was charged with *N*-H-*B*-mesityl-1,2-azaborine (**4.87**) (41.4 mg, 0.210 mmol) and toluene (1.0 mL) and cooled to –30 ºC. A solution of *n*-butyllithium (80.0 µL, 0.200 mmol, 2.5 M in hexane) was added at –30 ºC and the reaction was stirred for 1h while slowly warming up to room temperature. To the reaction vial CuI (7.6 mg, 0.040 mmol), pyridine (6.4 µL, 0.080 mmol), and a solution of 1-bromo-2-(triisopropylsilyl)acetylene (165 mg, 0.630 mmol) in toluene (1.0 mL) were added. The reaction was stirred at room temperature for 22 h. The crude mixture was diluted with Et_2O (3.0 mL) and washed with a 2:1 mixture of brine and concentrated NH_4OH (2 x 5.0 mL). The combined aqueous layers were extracted with Et_2O (2 x 5.0 mL). The combined organic layers were washed with brine (10 mL), dried with $MgSO_4$, filtered and the solvent was removed under reduced pressure. The crude product was purified by silica gel column chromatography (100% pentane). The desired product was isolated as a colorless oil (58.3 mg, 77%). A duplicate reaction gave 81% yield. ^{1}H NMR (500 MHz, CD_2Cl_2): δ 7.63 (dd, J = 11.0, 6.5 Hz, 1H), 7.46 (d, J = 6.5 Hz, 1H), 6.82 (d, J = 11.5 Hz, 1H), 6.76 (s, 2H), 6.40 (t, J = 6.5 Hz, 1H), 2.23 (s, 3H), 2.10 (s, 6H), 0.88 (s, 21H). ^{11}B NMR (160 MHz, CD_2Cl_2): δ 40.0. ^{13}C NMR (126 MHz, CD_2Cl_2): δ 144.1, 139.8, 138.6, 137.7, 131.5 (br), 127.5, 112.5, 102.7, 65.3, 22.7, 21.4, 18.8, 11.9 (the signal for the mesityl carbon next to boron is not observed). FTIR (thin film): 2941, 2891, 2864, 2180, 1615, 1506, 1439, 1393, 1275, 1232, 1078, 976, 883, 827, 667, 496 cm^{-1}. HRMS (DART-TOF) calculated for $C_{24}H_{37}BNSi$ ($[M+H]^+$): 378.27883, found: 378.27837.

Synthesis of BN-Stilbene (Scheme 4.21):

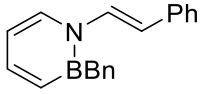

4.82

In a dry box, an oven-dried 50 mL round bottom flask was charged with *N*-H-*B*-benzyl-1,2-azaborine (**4.81**) (507 mg, 3.00 mmol) and toluene (15 mL) and cooled to –30 ºC. A solution of *n*-butyllithium (1.26 mL, 3.15 mmol, 2.5 M in hexane) was added at –30 ºC and the reaction mixture was stirred for 20 min while slowly warming up to room temperature. To the reaction mixture Pd_2dba_3 (55 mg, 0.060 mmol), QPhos (170 mg, 0.240 mmol), and β-bromostyrene (476 μL, 3.60 mmol) were added. The reaction mixture was stirred at 85 ºC for 15 h. At the completion of the reaction, the reaction mixture was cooled to room temperature. The crude mixture was filtrated through an acro-disc using CH_2Cl_2 as solvent and the filtrate was concentrated under reduced pressure. The crude product was purified by silica gel column chromatography (2% CH_2Cl_2/pentane to 10% CH_2Cl_2/pentane). The desired product was isolated as a white solid (497 mg, 61%). ^{1}H NMR (500 MHz, CD_2Cl_2): δ 7.70 (d, *J* = 14.5 Hz, 1H), 7.60-7.54 (m, 2H), 7.48 (d, *J* = 7.5 Hz, 2H), 7.41 (t, *J* = 7.0 Hz, 2H), 7.34-7.29 (m, 3H), 7.25-7.22 (m, 2H), 7.18-7.16 (m, 1H), 6.65 (d, *J* = 14.0 Hz, 1H), 6.58 (d, *J* = 11.5 Hz, 1H), 6.40 (t, *J* = 7.0 Hz, 1H), 2.91 (s, 2H). ^{11}B NMR (160 MHz, CD_2Cl_2): δ 37.9. ^{13}C NMR (151 MHz, CD_2Cl_2): δ 143.8, 143.0, 136.4, 134.1, 133.9, 131.0 (br), 129.7, 129.4, 128.9, 128.1, 126.8, 124.9, 121.5, 111.8, 27.6 (br). FTIR (thin film): 3059, 3025, 1644, 1611, 1511, 1492, 1401, 1356, 1260, 1117, 1008, 801, 751, 693, 517 cm^{-1}. HRMS (DART-TOF) calculated for $C_{19}H_{19}BN$ ($[M+H]^+$): 272.16105, found: 272.16078.

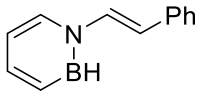

4.84

In a dry box, an oven-dried 20 mL microwave vial was charged with **4.82** (360 mg, 1.33 mmol), n-dodecanol (346 mg, 1.86 mmol), CuBr (19 mg,

0.13 mmol), pyridine (214 μL, 2.66 mmol), di-tert-butyl peroxide (293 μL, 1.59 mmol), and 13 mL toluene. The reaction mixture was stirred at 90 °C for 1 h. At the completion of the reaction, the reaction mixture was cooled to room temperature. The solvent was removed under reduced pressure. The crude oxidized product was purified by silica gel column chromatography (2% Et_2O/pentane to 50% Et_2O/pentane) to isolate a mixture of the desired product, B-OH, and BOB dimer, which was used directly to the next step. In a dry box, an oven-dried 25 mL round bottom flask was charged with the mixture of oxidized products and 10 mL Et_2O and cooled to –30 ºC. To the reaction mixture lithium aluminum hydride (15 mg, 0.40 mmol) was added at –30 ºC and stirred for 30 min. Hydrogen chloride solution (395 μL, 0.790 mmol, 2.0 M in diethyl ether) was added at –30 ºC and the reaction mixture was stirred for 30 min as slowly warmed to room temperature. The solvent was removed under reduced pressure. The crude product was purified by silica gel column chromatography (100% pentane to 2% Et_2O/pentane). The desired product was isolated as a white solid (91.3 mg, 38% over 2 steps). ^{1}H NMR (500 MHz, CD_2Cl_2): δ 7.68-7.64 (m, 2H), 7.48 (d, *J* = 14.5 Hz, 1H), 7.45 (t, *J* = 8.5 Hz, 2H), 7.35 (t, *J* = 7.5 Hz, 2H), 7.26 (t, *J* = 7.5 Hz, 1H), 6.97 (d, *J* = 10.5 Hz, 1H), 6.79 (d, *J* = 14.5 Hz, 1H), 6.51 (t, *J* = 6.5 Hz, 1H), 5.82-4.60 (br, 1H). ^{11}B NMR (160 MHz, CD_2Cl_2): δ 33.2 (d, *J* = 109 Hz). ^{13}C NMR (151 MHz, CD_2Cl_2): δ 144.4, 136.9, 136.4, 134.1, 131.4 (br), 129.3, 127.9, 126.7, 118.8, 113.3. FTIR (thin film): 3063, 3022, 2539, 1650, 1604, 1508, 1404, 1262, 1152, 973, 755, 693, 596 cm^{-1}. HRMS (DART-TOF) calculated for $C_{12}H_{13}BN$ ($[M+H]^+$): 182.11410, found: 182.11324.

Quantum Yield Measurement:

Fluorescence quantum yield, Φ, was measured by using an integrating sphere. Measurements were taken in degassed cyclohexane or directly at solid state with constant slit widths.

Experimental Φ:

BN-stilbene= 0.0388 in cyclohexane/ 0.127 at solid state

CC-stilbene= 0.170 in cyclohexane/ 0.324 at solid state

Synthesis of BN-lisdexamfetamine derivative (Scheme 4.20):

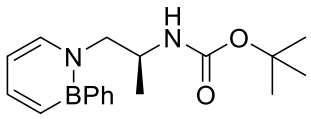

4.77j'

In a dry box, an oven-dried 20 mL scintillation vial was charged with **4.72** (108 mg, 0.561 mmol) and THF (3 mL), and cooled to 0 °C. To the reaction mixture (*S*)-2-methylaziridine-1-carboxylic acid *tert*-butyl ester (97 mg, 0.62 mmol) in THF (1.5 mL) was added and stirred for 14 h as slowly warmed to room temperature. At the completion of the reaction, hydrogen chloride solution (100 μL, 0.200 mmol, 2.0 M in diethyl ether) was added at room temperature and the reaction mixture was stirred for 30 min. The crude mixture was concentrated under reduced pressure and purified by silica gel column chromatography (10% Et_2O/pentane to 75% Et_2O/pentane). The desired product was isolated as a colorless oil (140 mg, 80%). Spectra of the isolated compound **4.77j'** matches the values for compound **4.77j** (racemic product). ^{1}H NMR (500 MHz, CD_2Cl_2): δ 7.64 (dd, *J* = 11.0, 6.5 Hz, 1H), 7.51 (d, *J* = 7.5 Hz, 2H), 7.39 (t, *J* = 7.5 Hz, 2H), 7.35-7.31 (m, 2H), 6.77 (d, *J* = 11.5 Hz, 1H), 6.41 (t, *J* = 6.5 Hz, 1H), 4.25 (br s, 1H), 3.90 (d, *J* = 5.5 Hz, 2H), 3.81 (t, *J* = 5.5 Hz, 1H), 1.36 (s, 9H), 0.91 (d, *J* = 5.5 Hz, 3H). ^{11}B NMR (160 MHz, CD_2Cl_2): δ 35.9. ^{13}C NMR (126 MHz, CD_2Cl_2): δ 155.4, 143.4, 142.8 (br), 139.2, 133.3, 131.6 (br), 128.2, 127.8, 111.9, 79.5, 58.5, 49.0, 28.7, 18.7. FTIR (thin film): 3348, 2977, 2931, 1691, 1609, 1514, 1441, 1404, 1366, 1244, 1031, 976, 743, 704 cm^{-1}. HRMS (DART-TOF) calculated for $C_{18}H_{26}BN_2O_2$ ([M+H]$^+$): 313.20873, found: 313.20959.

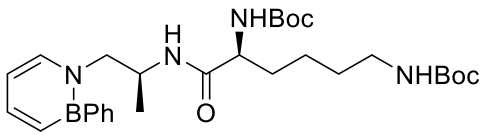

4.79

In a dry box, an oven-dried 20 mL scintillation vial was charged with **4.77j'** (395 mg, 1.27 mmol) and CH_2Cl_2 (10 mL). To the reaction mixture hydrogen

chloride solution (953 μL, 3.81 mmol, 4.0 M in dioxane) was added at room temperature and stirred for 14 h. The crude mixture was concentrated under reduced pressure and directly used for the next step. In a dry box, the crude reaction mixture was transferred to an oven-dried 50 mL round bottom flask and dissolved in CH_2Cl_2 (20 mL) and Boc-Lys(Boc)-OSu (563 mg, 1.27 mmol) and *N*-methylmorpholine (NMM) (838 μL, 7.62 mmol) were added. The reaction mixture was stirred at room temperature for 1 h. The crude mixture was concentrated under reduced pressure and purified by alumina column chromatography (0.25% MeOH/CH_2Cl_2 to 0.50% MeOH/CH_2Cl_2). The desired product was isolated as a white solid (657 mg, 96% over 2 steps). ^{1}H NMR (500 MHz, CD_2Cl_2): δ 7.63 (dd, *J* = 10.5, 6.5 Hz, 1H), 7.51 (d, *J* = 6.5 Hz, 2H), 7.39 (t, *J* = 7.5 Hz, 2H), 7.35-7.31 (m, 2H), 6.77 (d, *J* = 11.0 Hz, 1H), 6.40 (t, *J* = 6.5 Hz, 1H), 5.80 (br s, 1H), 5.02 (br s, 1H), 4.62 (br s, 1H), 4.10 (quint, *J* = 6.5 Hz, 1H), 3.97-3.89 (m, 2H), 3.81 (s, 1H), 3.12-2.98 (m, 2H), 1.69-1.61 (m, 1H), 1.52-1.35 (m, 2H), 1.42 (s, 9H), 1.40 (s, 9H), 1.28-1.19 (m, 3H), 0.92 (d, *J* = 6.5 Hz, 3H). ^{11}B NMR (160 MHz, CD_2Cl_2): δ 36.1. ^{13}C NMR (126 MHz, CD_2Cl_2): δ 172.3, 156.6, 156.3, 143.4, 142.4 (br), 139.2, 133.3, 131.7 (br), 128.3, 127.9, 111.9, 80.2, 79.2, 67.4, 58.0, 56.0, 47.7, 40.4, 32.5, 30.2, 28.7, 23.1, 18.3. FTIR (thin film): 3308, 2976, 2933, 1688, 1656, 1610, 1516, 1455, 1392, 1366, 1247, 1170, 976, 865, 746, 706 cm^{-1}. HRMS (DART-TOF) calculated for $C_{29}H_{46}BN_4O_5$ ($[M+H]^+$): 541.35612, found: 541.35529.

Crystallographic Data for **4.80b**:

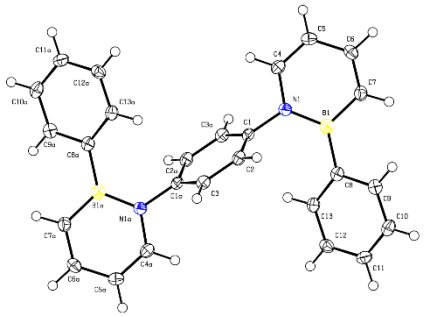

Identification code C26H22B2N2

Empirical formula C26 H22 B2 N2

Formula weight 384.07

Temperature 100(2) K

Wavelength 1.54178 Å

Crystal system Monoclinic

Space group $P2_1/c$

Unit cell dimensions a = 5.8491(3) Å □= 90°.

b = 11.3280(6) Å □= 92.360(3)°.

c = 15.0312(7) Å □ = 90°.

Volume 995.10(9) $Å^3$

Z 2

Density (calculated) 1.282 Mg/m^3

Absorption coefficient 0.559 mm^{-1}

F(000) 404

Crystal size 0.400 x 0.060 x 0.050 mm^3

Theta range for data collection 7.075 to 66.802°.

Index ranges -6<=h<=6, -13<=k<=13, -17<=l<=17

Reflections collected 9940

Independent reflections 1751 [R(int) = 0.0393]

Completeness to theta = 66.802° 99.7 %

Absorption correction Semi-empirical from equivalents

Max. and min. transmission 0.7528 and 0.6758

Refinement method Full-matrix least-squares on F^2

Data / restraints / parameters 1751 / 0 / 136

Goodness-of-fit on F^2 1.029

Final R indices [I>2sigma(I)] R1 = 0.0381, wR2 = 0.0960

R indices (all data) R1 = 0.0468, wR2 = 0.1020

Extinction coefficient na

Largest diff. peak and hole 0.251 and -0.198 e.$Å^{-3}$

Crystallographic Data for **4.82**:

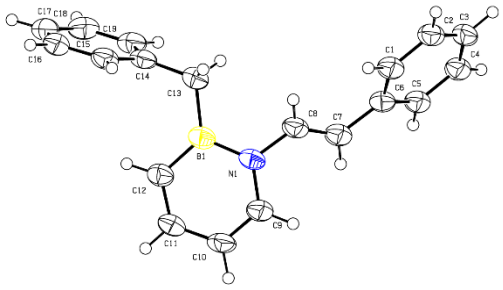

Identification code C19H18BN

Empirical formula C19 H18 B N

Formula weight 271.15

Temperature 100(2) K

Wavelength 1.54178 Å

Crystal system Triclinic

Space group P-1

Unit cell dimensions a = 5.7638(3) Å □= 107.9102(19)°.

b = 10.2966(6) Å □= 91.011(2)°.

c = 13.4006(8) Å □ = 92.945(2)°.

Volume 755.28(7) $Å^3$

Z 2

Density (calculated) 1.192 Mg/m^3

Absorption coefficient 0.512 mm^{-1}

F(000) 288

Crystal size 0.400 x 0.220 x 0.180 mm^3

Theta range for data collection 3.468 to 66.794°.

Index ranges -6<=h<=6, -12<=k<=11, 0<=l<=15

Reflections collected 2664

Independent reflections 2664 [R(int) = ?]

Completeness to theta = 66.794° 98.9 %

Absorption correction Semi-empirical from equivalents

Max. and min. transmission 0.7528 and 0.4502

Refinement method Full-matrix least-squares on F^2

Data / restraints / parameters 2664 / 0 / 192

Goodness-of-fit on F^2 1.068

Final R indices [I>2sigma(I)] R1 = 0.0724, wR2 = 0.2115

R indices (all data) R1 = 0.0750, wR2 = 0.2146

Extinction coefficient	n/a
Largest diff. peak and hole	0.225 and -0.274 e.Å^{-3}

4.5.3 Spectral Data

HL-III-210-1H

Sample Name	**HL-III-210-1H**	Pulse sequence	**PROTON**	Temperature	**25**	Study owner	**Liu**
Date collected	**2015-06-08**	Solvent	**thf**	Spectrometer	**nmr19-vnmrs600**	Operator	**Liu**

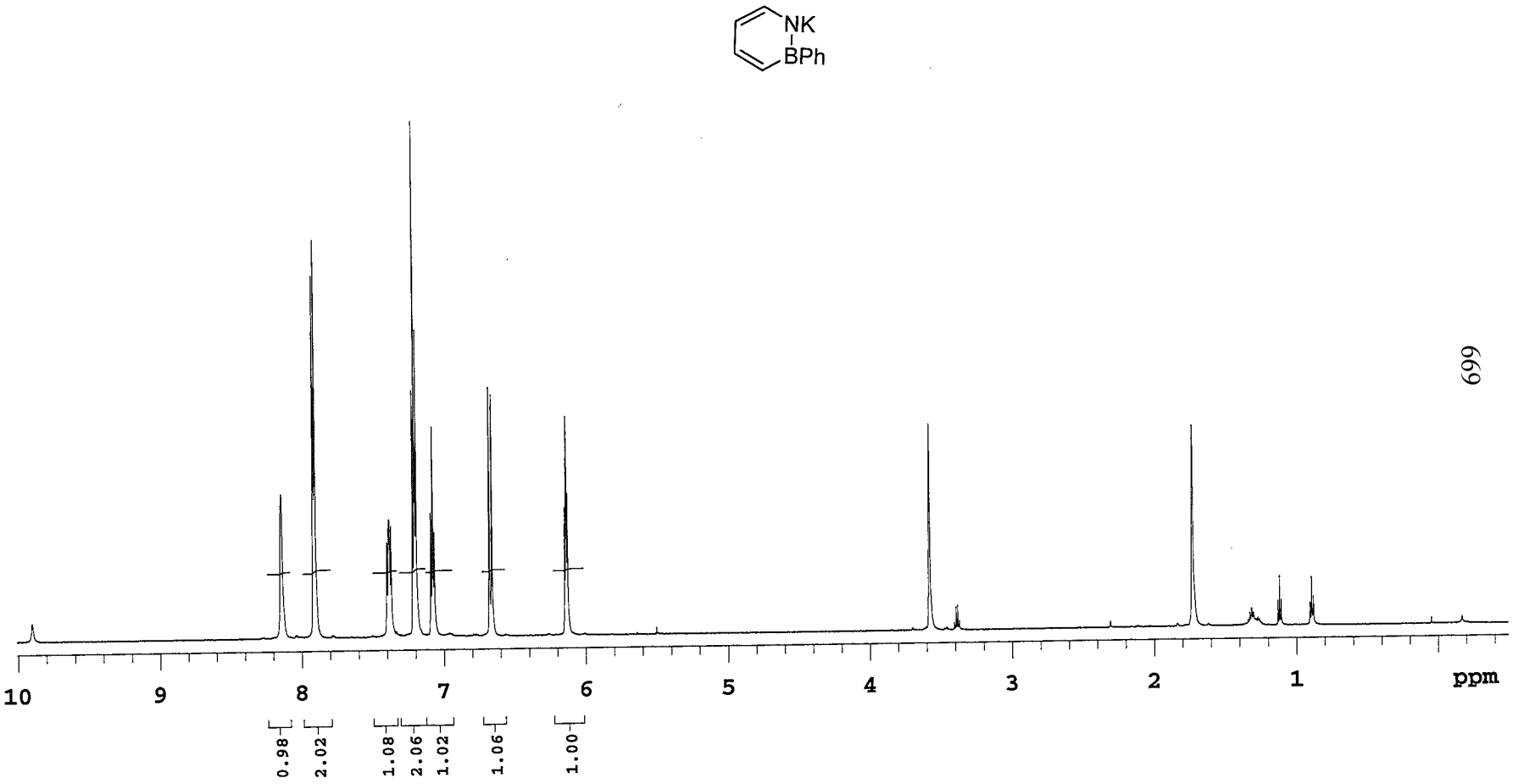

Data file /home/ALL/Liu/HL/N-Substitution/HL-II-159-SM-1H.fid

Plot date 2016-07-22

HL-III-210-11B

Sample Name **HL-III-210-11B**	Pulse sequence **s2pul**	Temperature **25**	Study owner **Liu**
Date collected **2016-07-21**	Solvent **thf**	Spectrometer **nmr11-inova500**	Operator **Liu**

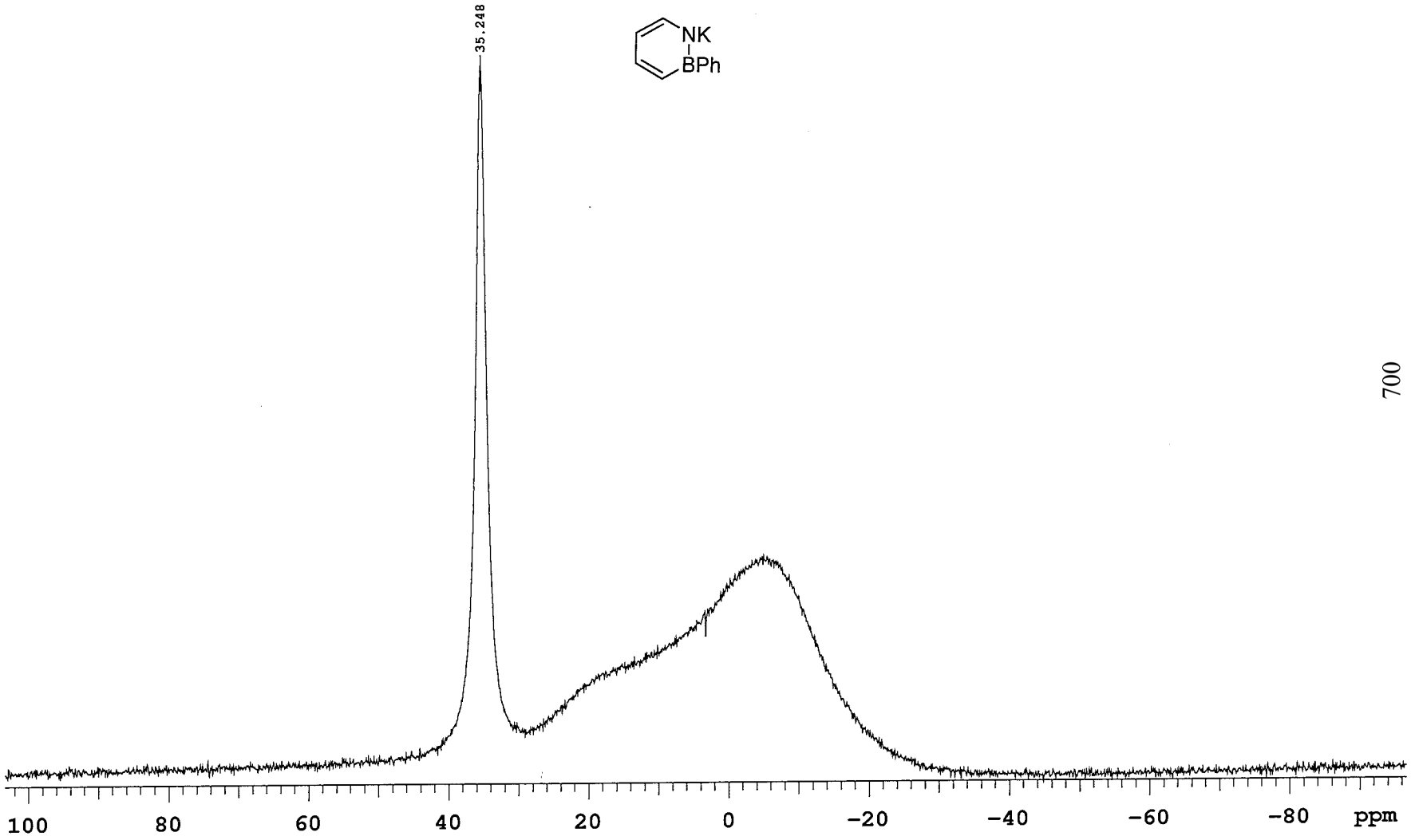

Data file exp

Plot date 2016-07-21

HL-III-210-13C

Sample Name **HL-III-210-13C**	Pulse sequence **CARBON**	Temperature **25**	Study owner **Liu**
Date collected **2016-08-01**	Solvent **thf**	Spectrometer **nmr19-vnmrs600**	Operator **Liu**

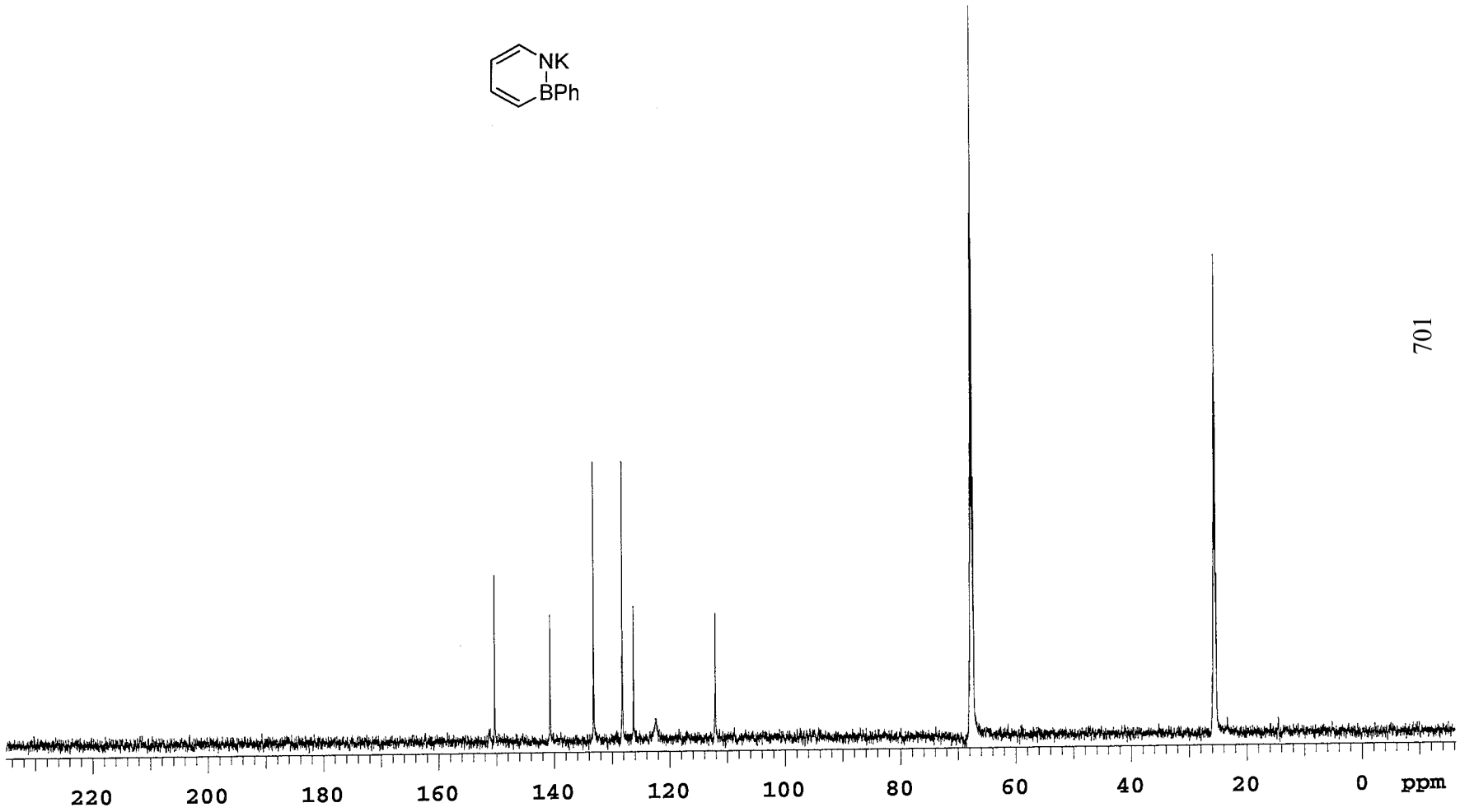

Data file /home/ALL/Liu/HL/N-Substitution/HL-III-210-13C.fid

Plot date 2016-11-03

HL-II-153-1-1H

Sample Name **HL-II-153-1-1H**	Pulse sequence **PROTON**	Temperature **25**	Study owner **Liu**
Date collected **2015-06-04**	Solvent **cd2cl2**	Spectrometer **nmr18-vnmrs500**	Operator **Liu**

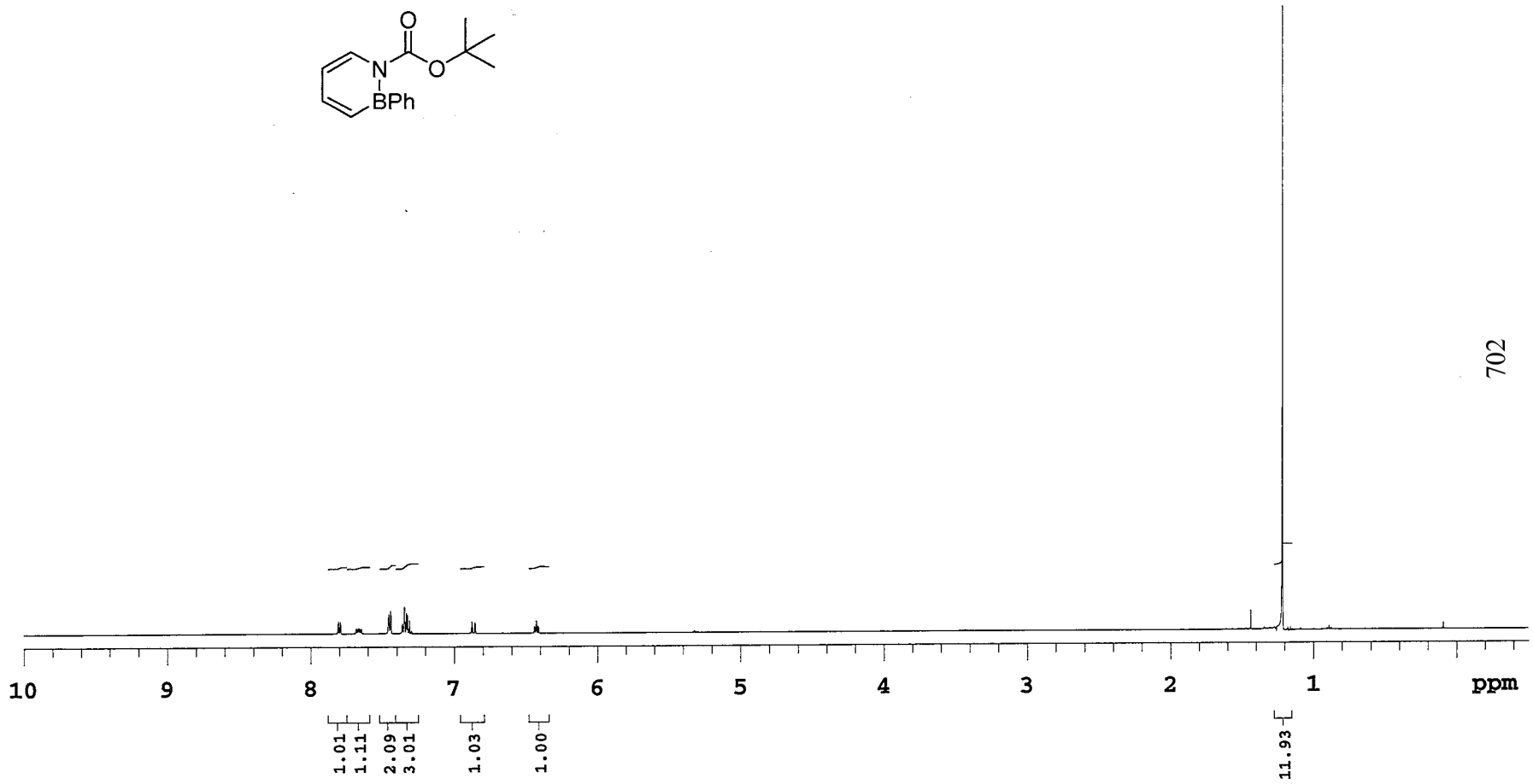

HL-II-153-1-11B

Sample Name	**HL-II-153-1-11B**	Pulse sequence	**BORON_11**	Temperature	**25**	Study owner	**Liu**
Date collected	**2015-06-04**	Solvent	**cd2cl2**	Spectrometer	**nmr18-vnmrs500**	Operator	**Liu**

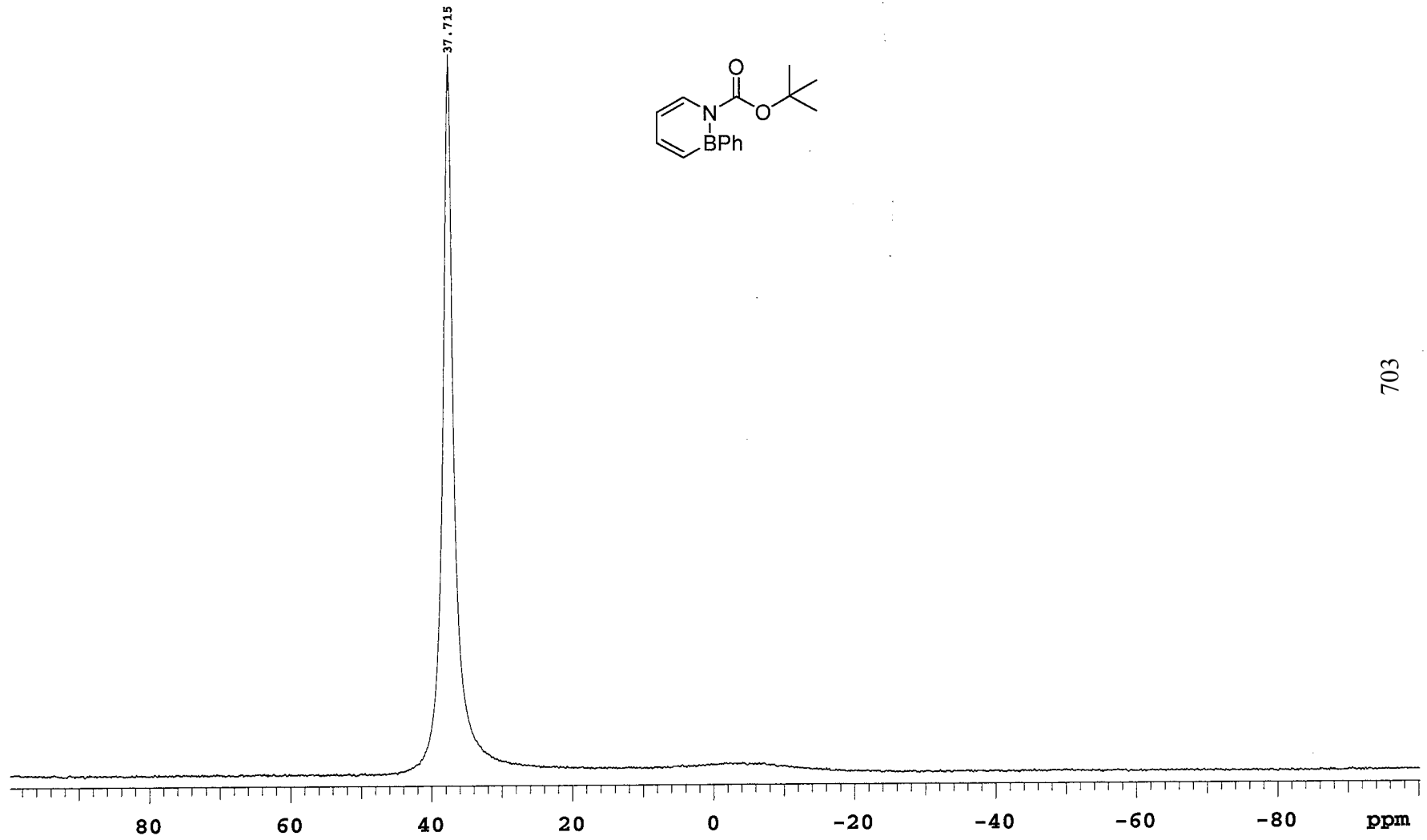

703

Data file /home/ALL/Liu/HL/N-Substitution/Table/HL-II-153-1-11B.fid

Plot date 2015-12-24

HL-III-050-13C

Sample Name	**HL-III-050-13C**	Pulse sequence	**CARBON**	Temperature	**25**	Study owner	**Liu**
Date collected	**2015-12-17**	Solvent	**cd2cl2**	Spectrometer	**nmr19-vnmrs600**	Operator	**Liu**

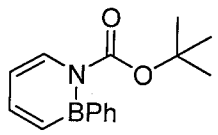

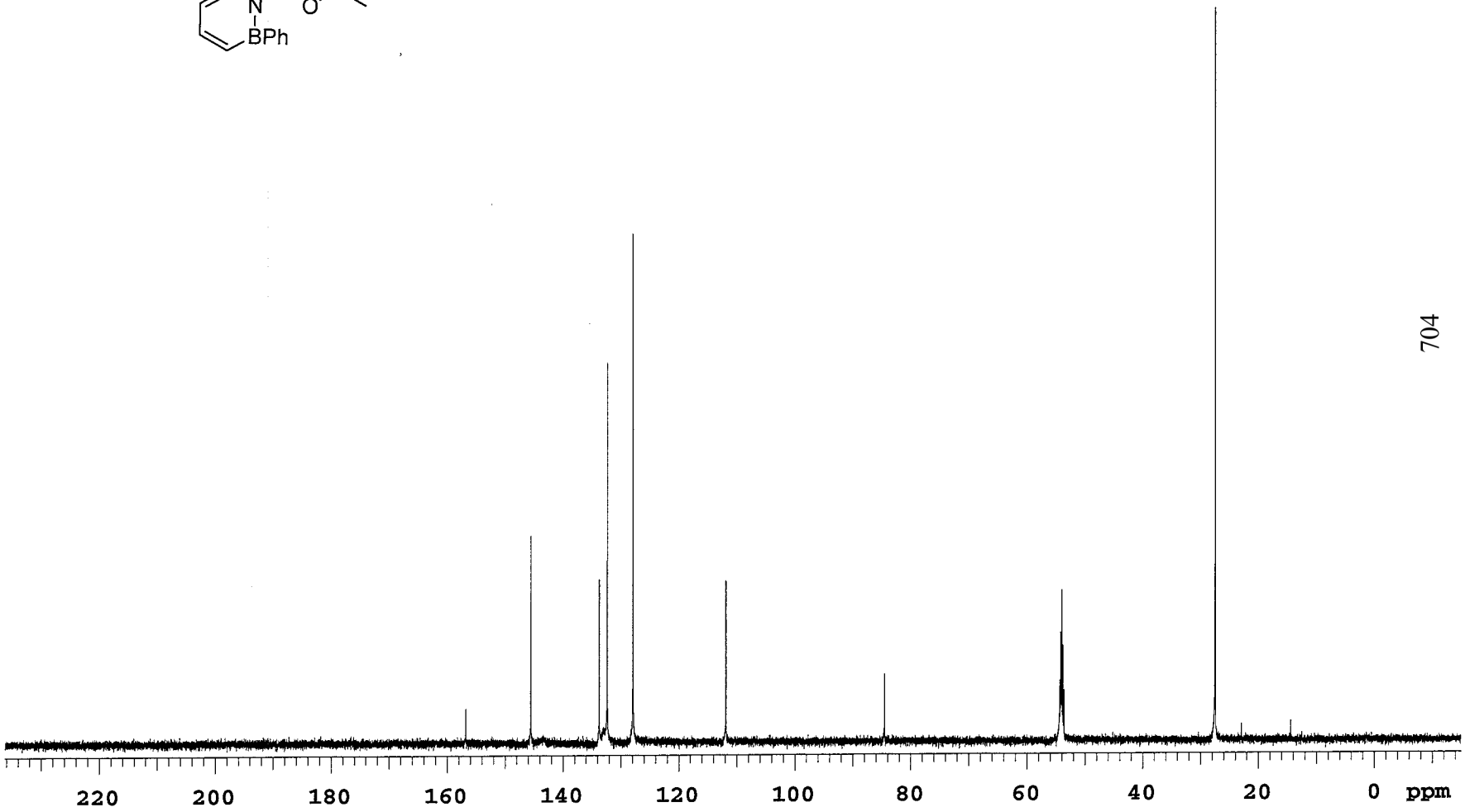

Data file /home/ALL/Liu/HL/N-Substitution/HL-III-050-13C.fid

Plot date 2015-12-24

HL-II-239-1H

Sample Name	**HL-II-239-1H**	Pulse sequence	**PROTON**	Temperature	**25**	Study owner	**Liu**
Date collected	**2015-09-15**	Solvent	**cd2cl2**	Spectrometer	**nmr19-vnmrs600**	Operator	**Liu**

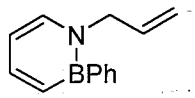

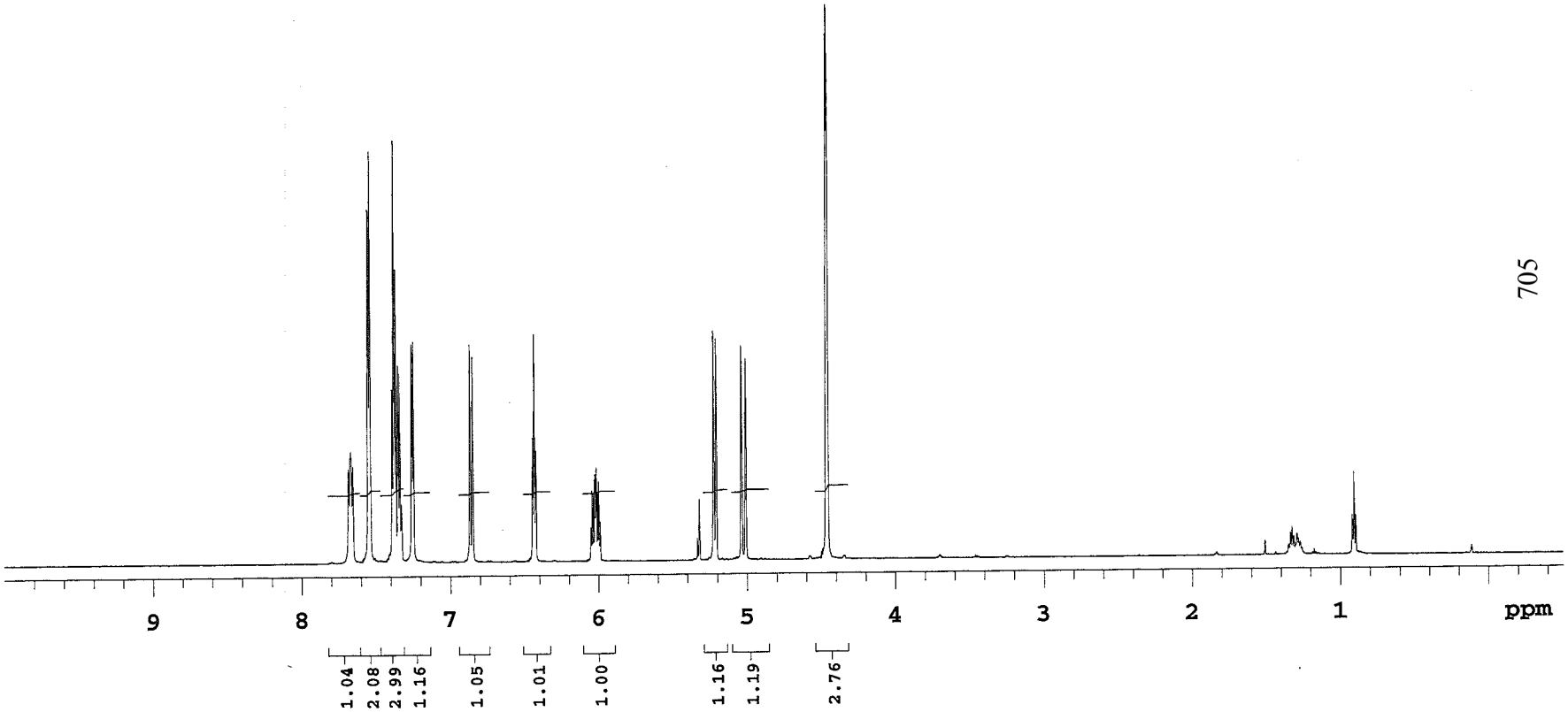

Data file /home/ALL/Liu/HL/N-Substitution/HL-II-239-1H.fid

Plot date 2015-12-24

HL-II-239-11B

Sample Name **HL-II-239-11B**	Pulse sequence **s2pul**	Temperature **25**	Study owner **Liu**
Date collected **2015-09-15**	Solvent **cd2cl2**	Spectrometer **nmr19-vnmrs600**	Operator **Liu**

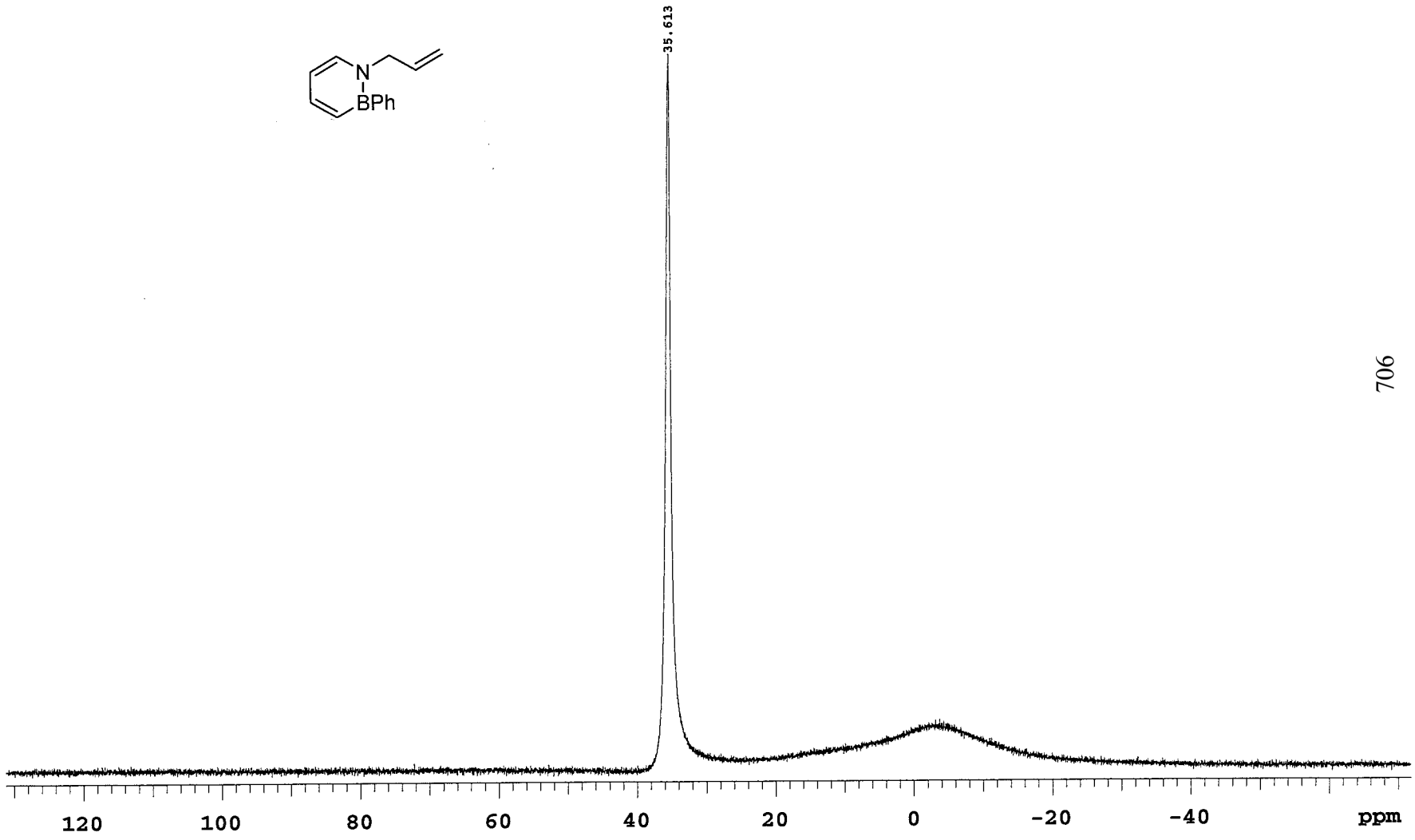

706

Data file /home/ALL/Liu/HL/N-Substitution/HL-II-239-1B.fid

Plot date 2015-12-24

HL-II-239-13C

Sample Name **HL-II-239-13C**	Pulse sequence **CARBON**	Temperature **25**	Study owner **Liu**
Date collected **2015-09-15**	Solvent **cd2cl2**	Spectrometer **nmr19-vnmrs600**	Operator **Liu**

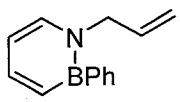

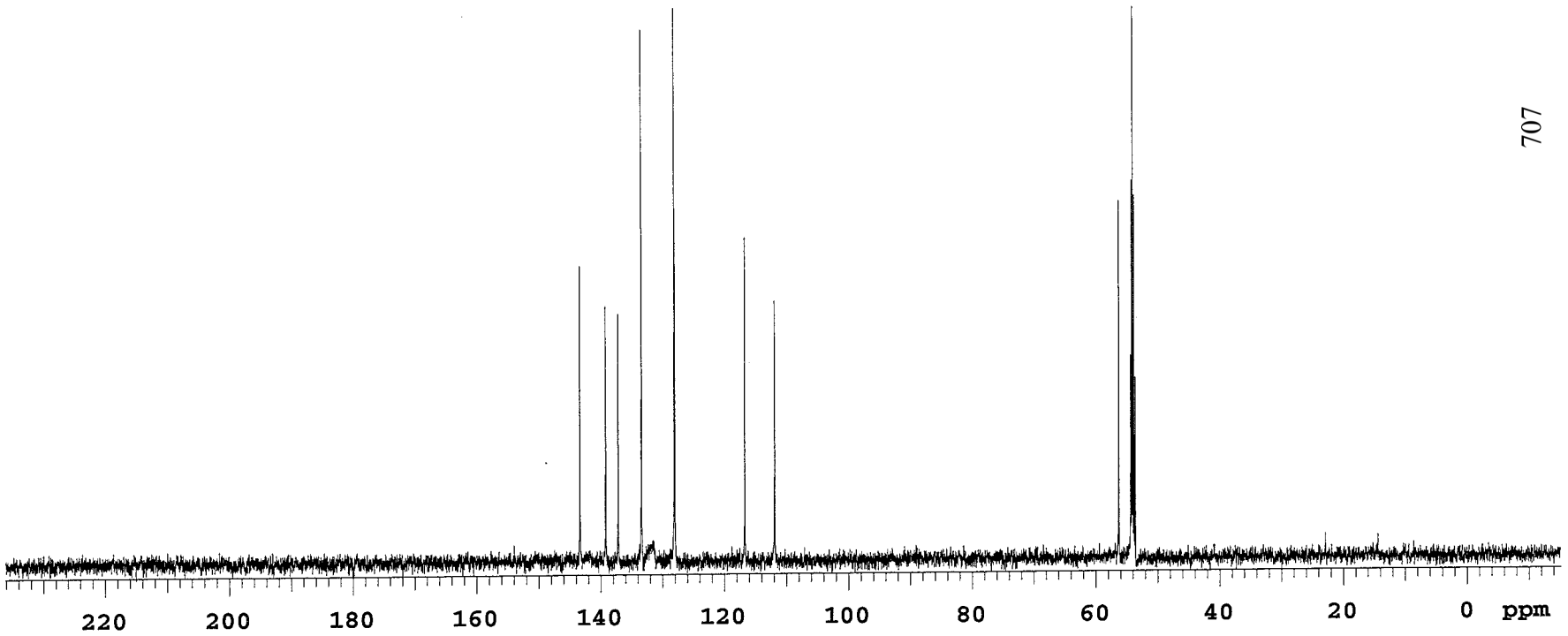

Data file /home/ALL/Liu/HL/N-Substitution/HL-II-239-13C.fid

Plot date 2015-12-24

HL-II-230-1H

Sample Name **HL-II-230-1H**	Pulse sequence **PROTON**	Temperature **25**	Study owner **Liu**
Date collected **2015-09-09**	Solvent **cd2cl2**	Spectrometer **nmr18-vnmrs500**	Operator **Liu**

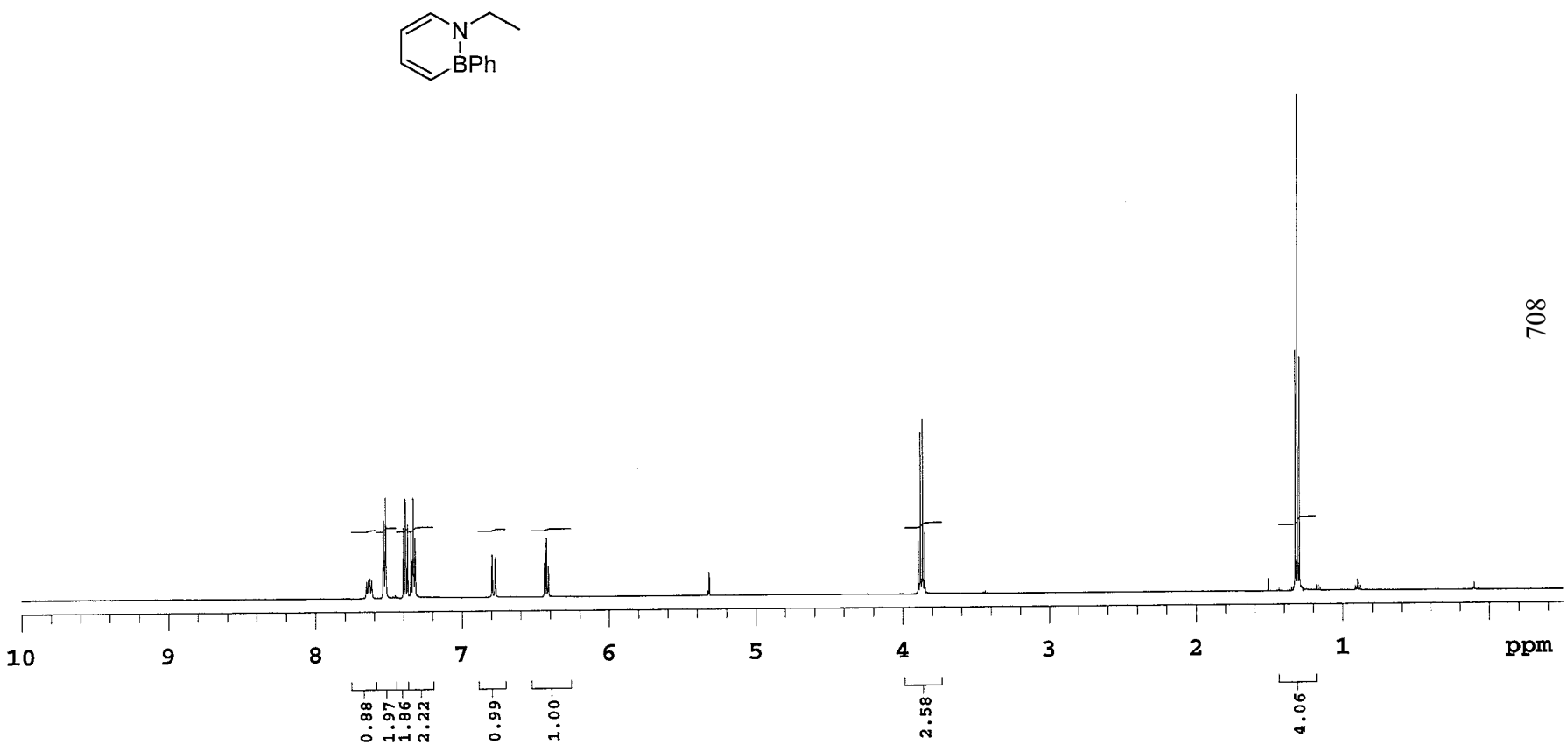

Data file /home/ALL/Liu/HL/N-Substitution/Table/HL-II-230-1H.fid

Plot date 2015-12-24

HL-II-230-11B

Sample Name **HL-II-230-11B**	Pulse sequence **BORON_11**	Temperature **25**	Study owner **Liu**
Date collected **2015-09-09**	Solvent **cd2cl2**	Spectrometer **nmr18-vnmrs500**	Operator **Liu**

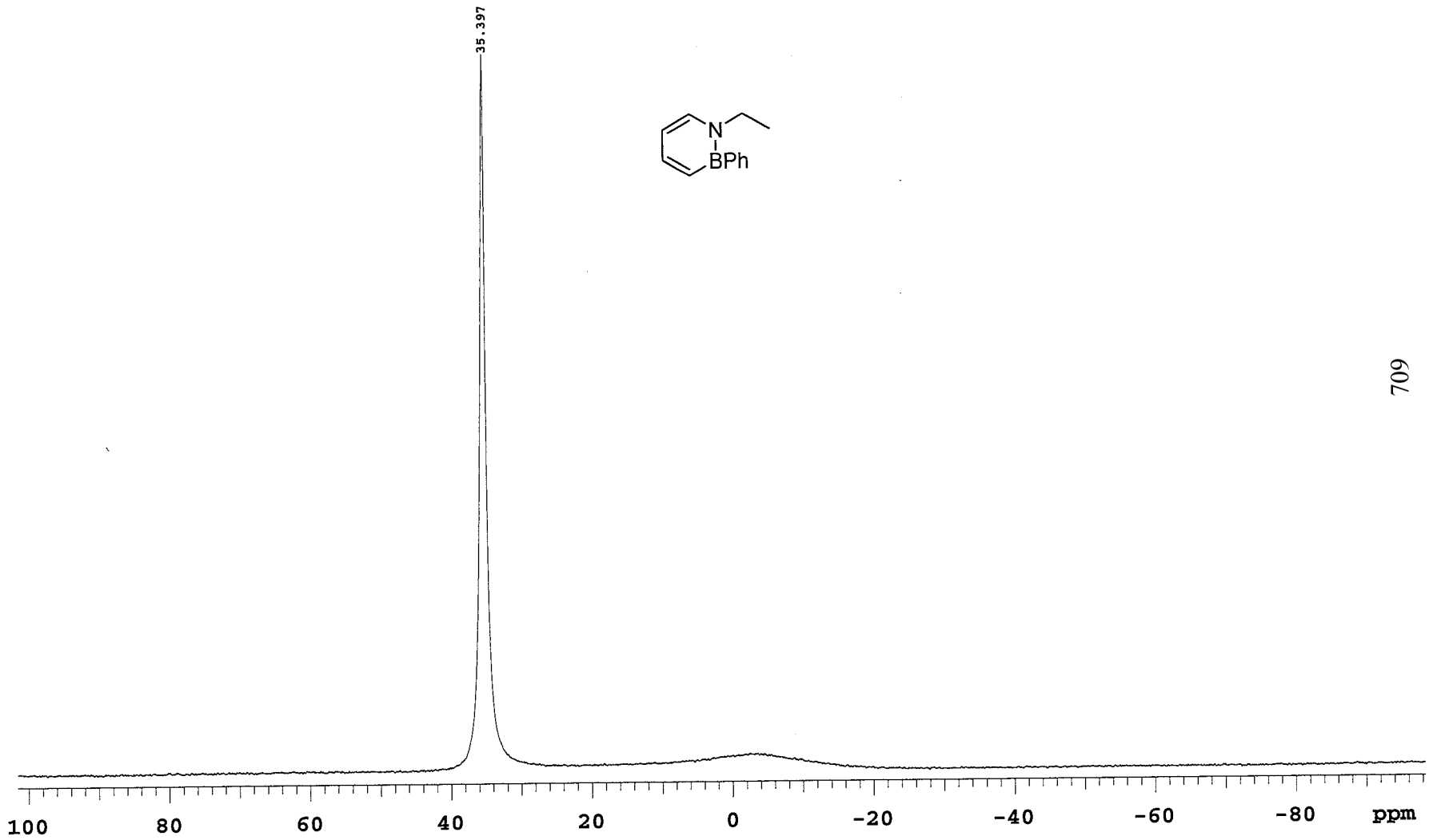

709

Data file /home/ALL/Liu/HL/N-Substitution/Table/HL-II-230-11B.fid

Plot date 2015-12-24

HL-II-230-13C

Sample Name	**HL-II-230-13C**	Pulse sequence	**CARBON**	Temperature	**25**	Study owner	**Liu**
Date collected	**2015-09-10**	Solvent	**cd2cl2**	Spectrometer	**nmr19-vnmrs600**	Operator	**Liu**

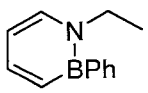

710

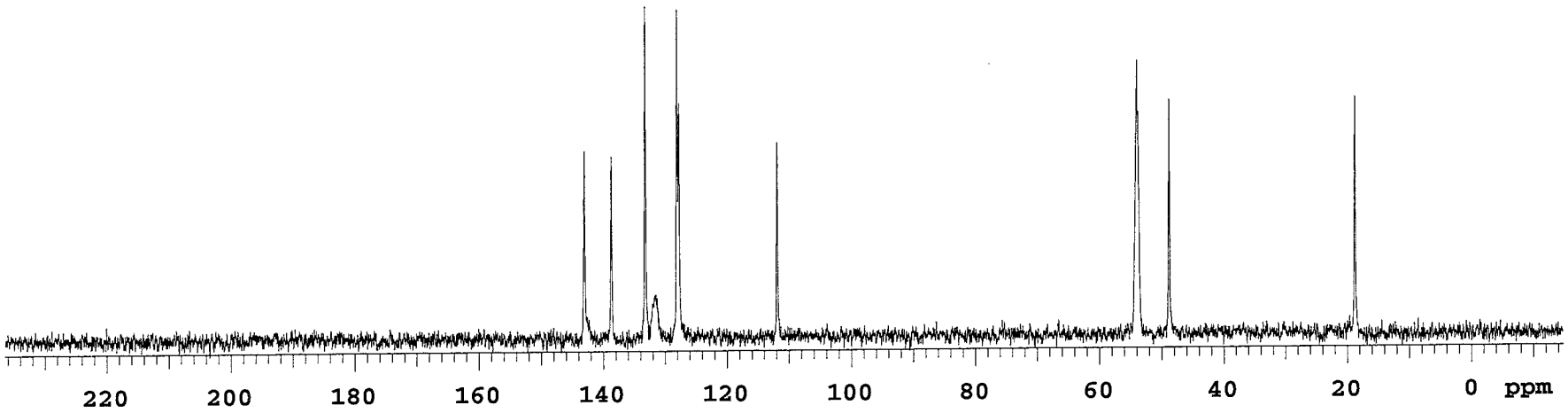

Data file /home/ALL/Liu/HL/N-Substitution/HL-II-230-13C.fid

Plot date 2015-12-24

HL-II-237-1H

Sample Name **HL-II-237-1H**	Pulse sequence **PROTON**	Temperature **25**	Study owner **Liu**
Date collected **2015-09-12**	Solvent **cd2cl2**	Spectrometer **nmr19-vnmrs600**	Operator **Liu**

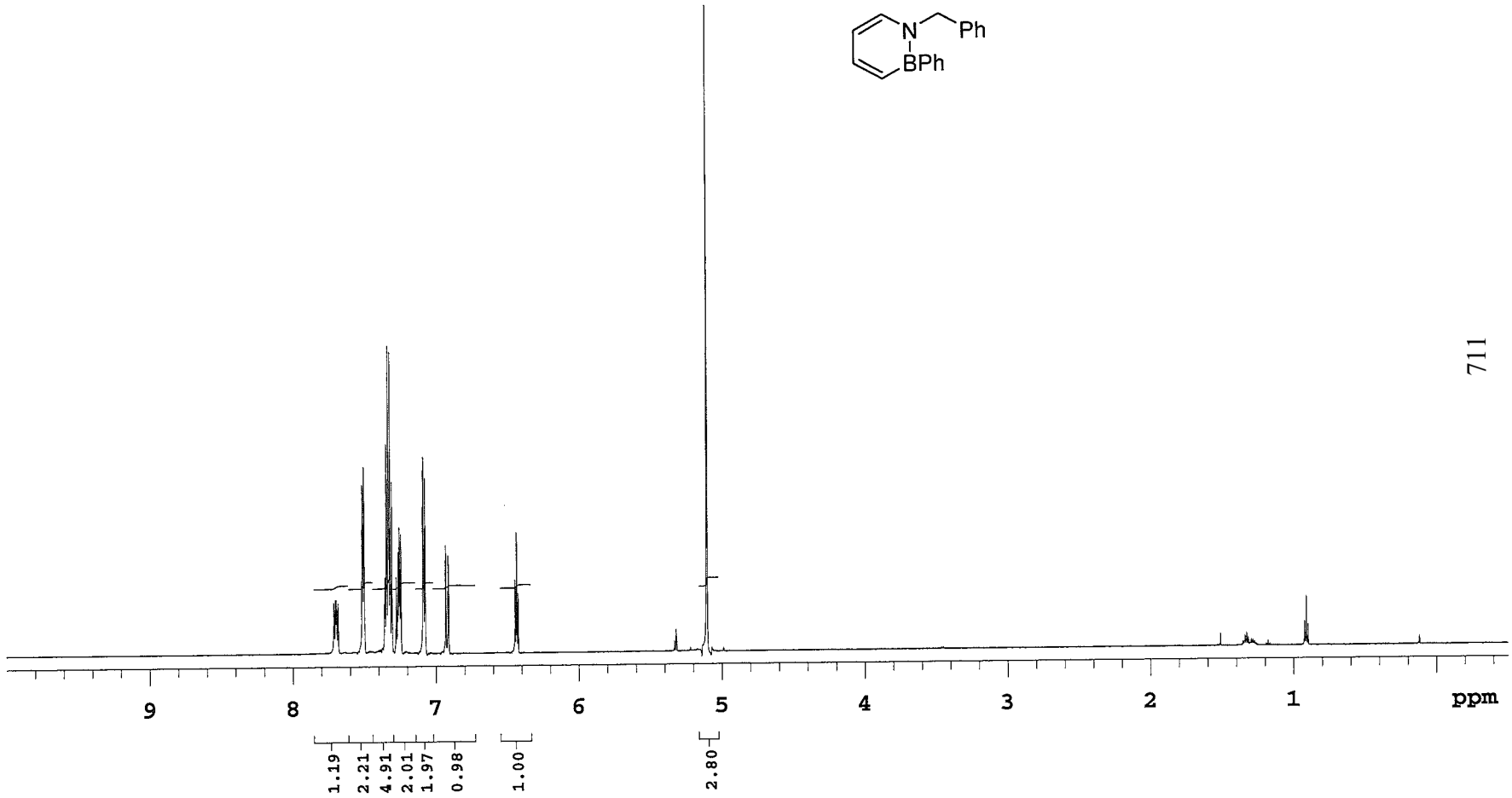

Data file /home/ALL/Liu/HL/N-Substitution/HL-II-237-1H.fid

Plot date 2016-11-03

HL-II-233-11B

Sample Name **HL-II-233-11B**	Pulse sequence **s2pul**	Temperature **25**	Study owner **Liu**
Date collected **2015-09-12**	Solvent **cd2cl2**	Spectrometer **nmr19-vnmrs600**	Operator **Liu**

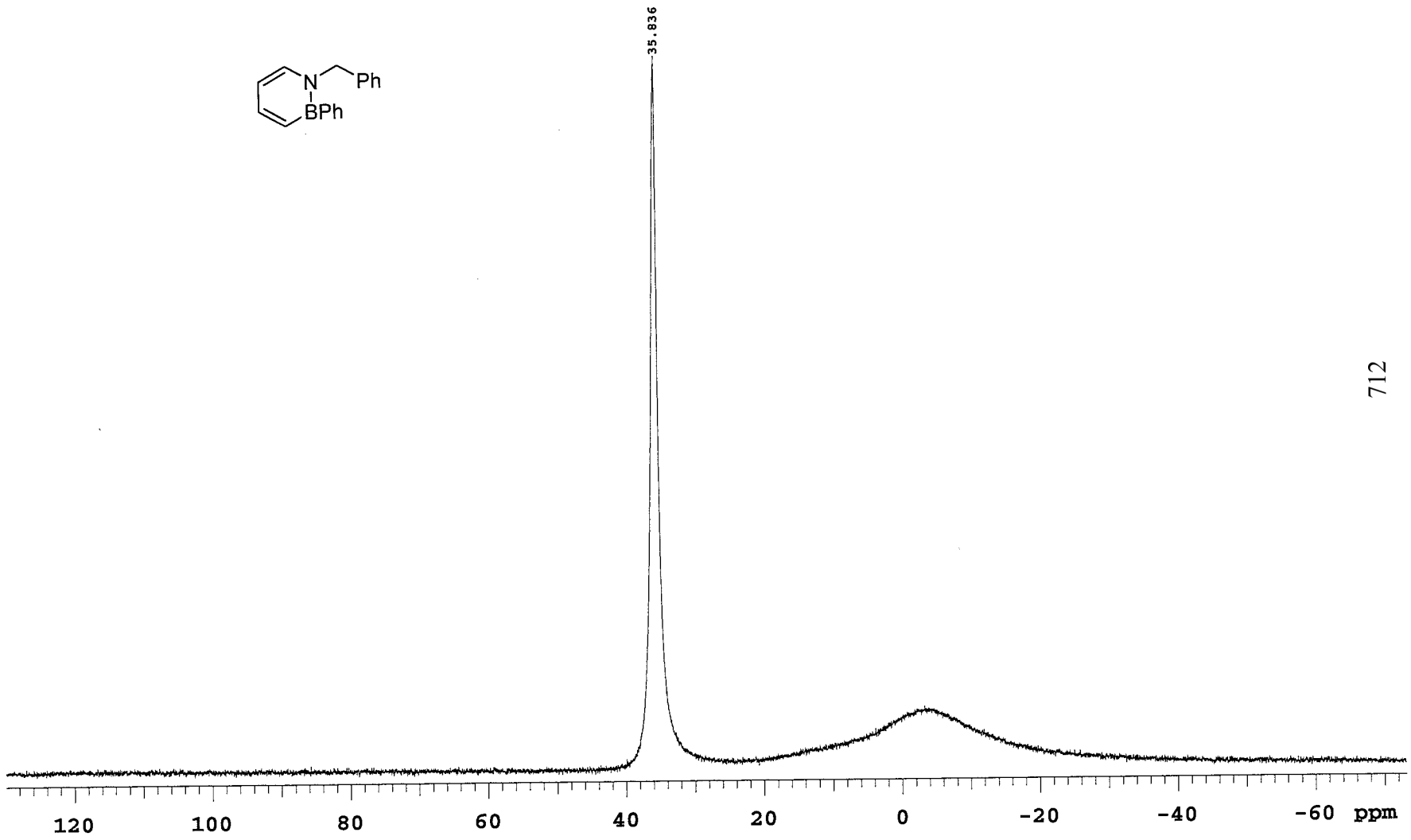

712

Data file /home/ALL/Liu/HL/N-Substitution/HL-II-237-11B.fid

Plot date 2015-12-24

HL-II-237-13C

Sample Name **HL-II-237-13C**	Pulse sequence **CARBON**	Temperature **25**	Study owner **Liu**
Date collected **2015-09-12**	Solvent **cd2cl2**	Spectrometer **nmr19-vnmrs600**	Operator **Liu**

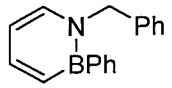

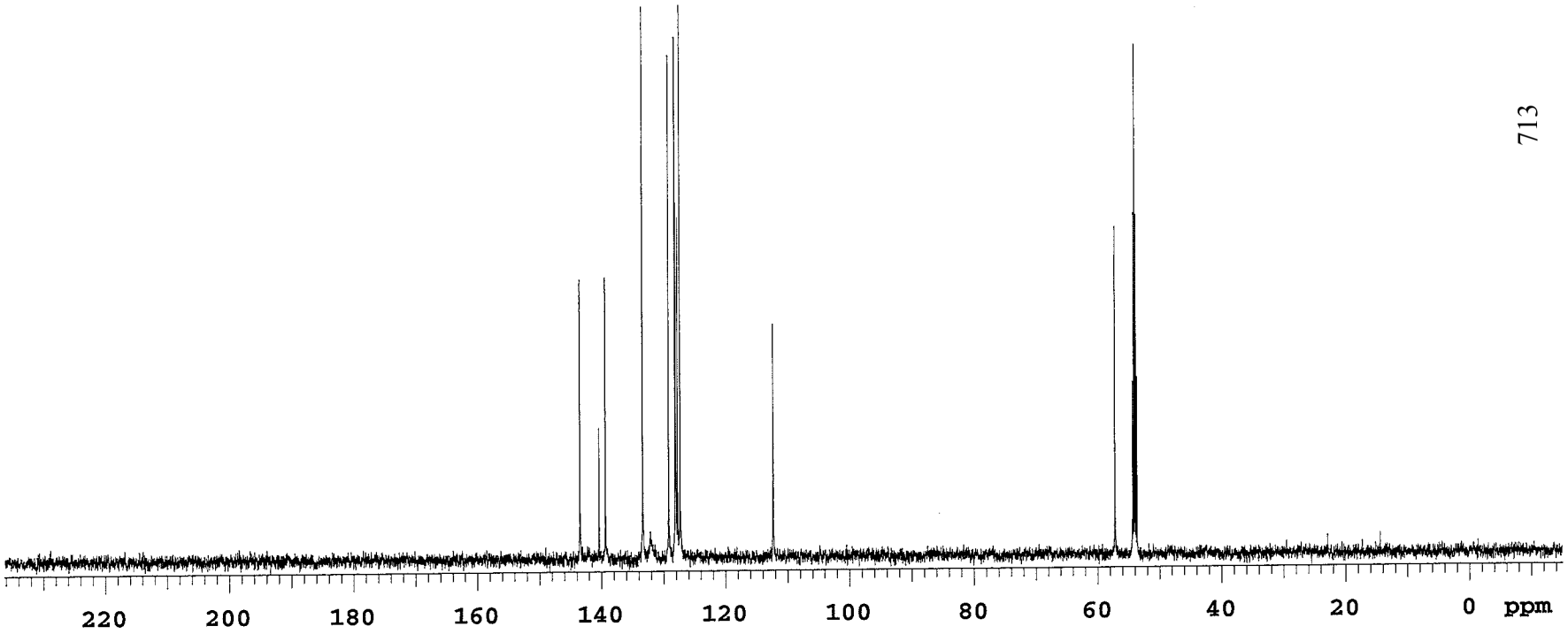

713

Data file /home/ALL/Liu/HL/N-Substitution/HL-II-237-13C.fid

Plot date 2015-12-24

HL-III-052-1-1H

Sample Name **HL-III-052-1-1H**	Pulse sequence **PROTON**	Temperature **25**	Study owner **Liu**
Date collected **2015-12-17**	Solvent **cd2cl2**	Spectrometer **nmr18-vnmrs500**	Operator **Liu**

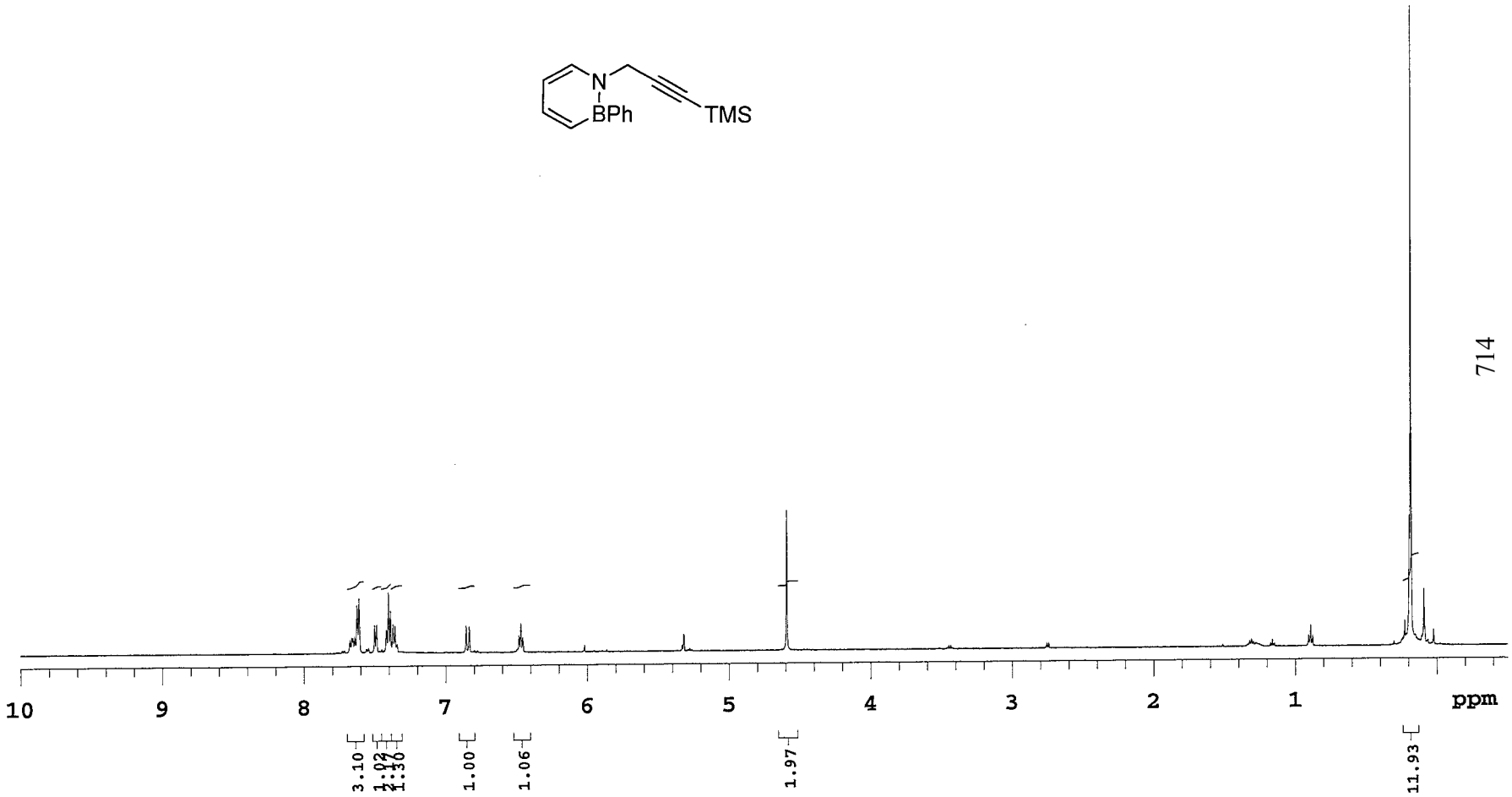

Data file /home/ALL/Liu/HL/N-Substitution/HL-III-052-1-1H.fid

Plot date 2016-11-03

HL-III-052-1-11B

Sample Name	**HL-III-052-1-11B**	Pulse sequence	**BORON_11**	Temperature	**25**	Study owner	**Liu**
Date collected	**2015-12-17**	Solvent	**cd2cl2**	Spectrometer	**nmr18-vnmrs500**	Operator	**Liu**

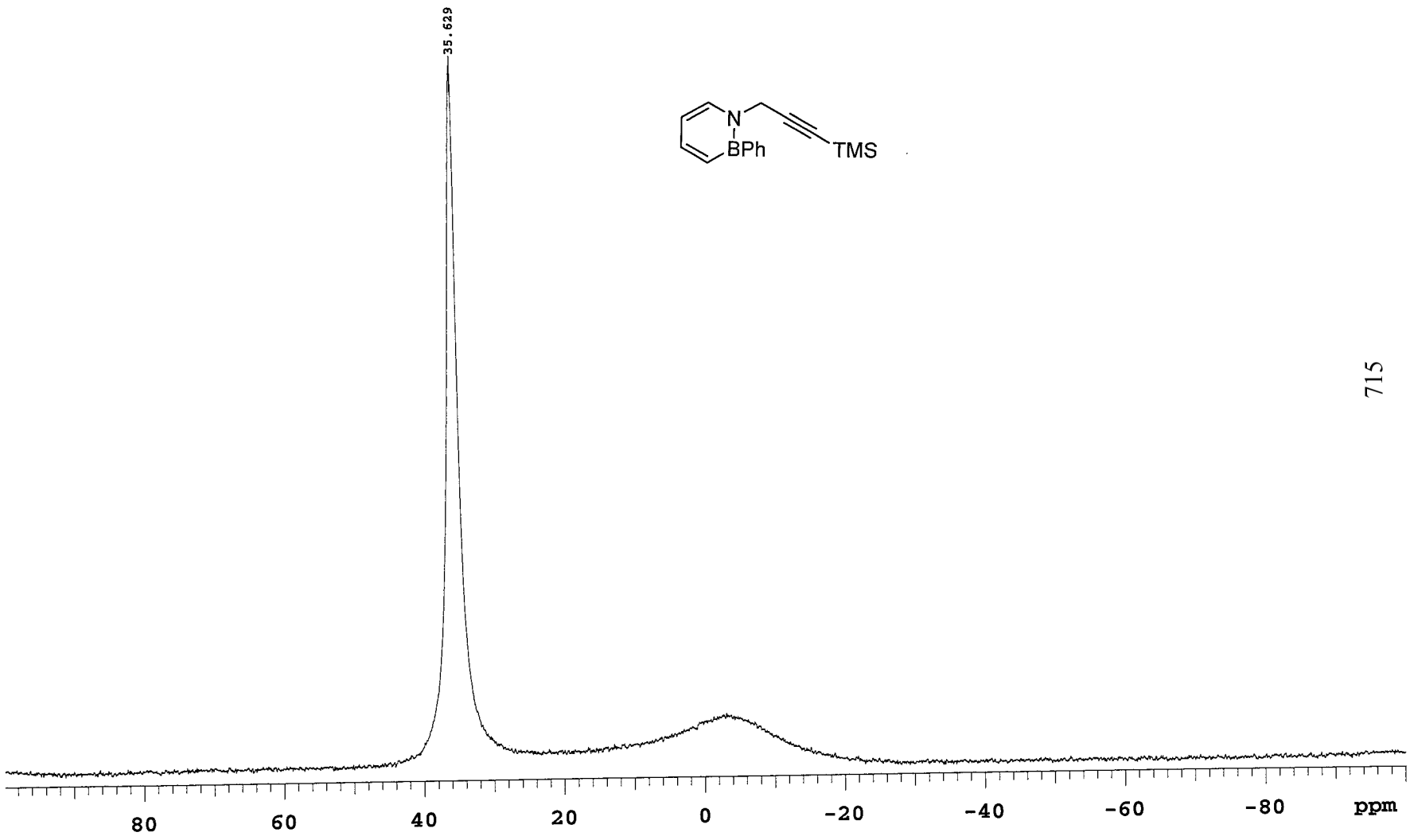

715

Data file /home/ALL/Liu/HL/N-Substitution/Table/HL-III-052-1-11B.fid

Plot date 2015-12-24

HL-III-052-1-13C

Sample Name **HL-III-052-1-13C**	Pulse sequence **CARBON**	Temperature **25**	Study owner **Liu**
Date collected **2015-12-17**	Solvent **cd2cl2**	Spectrometer **nmr19-vnmrs600**	Operator **Liu**

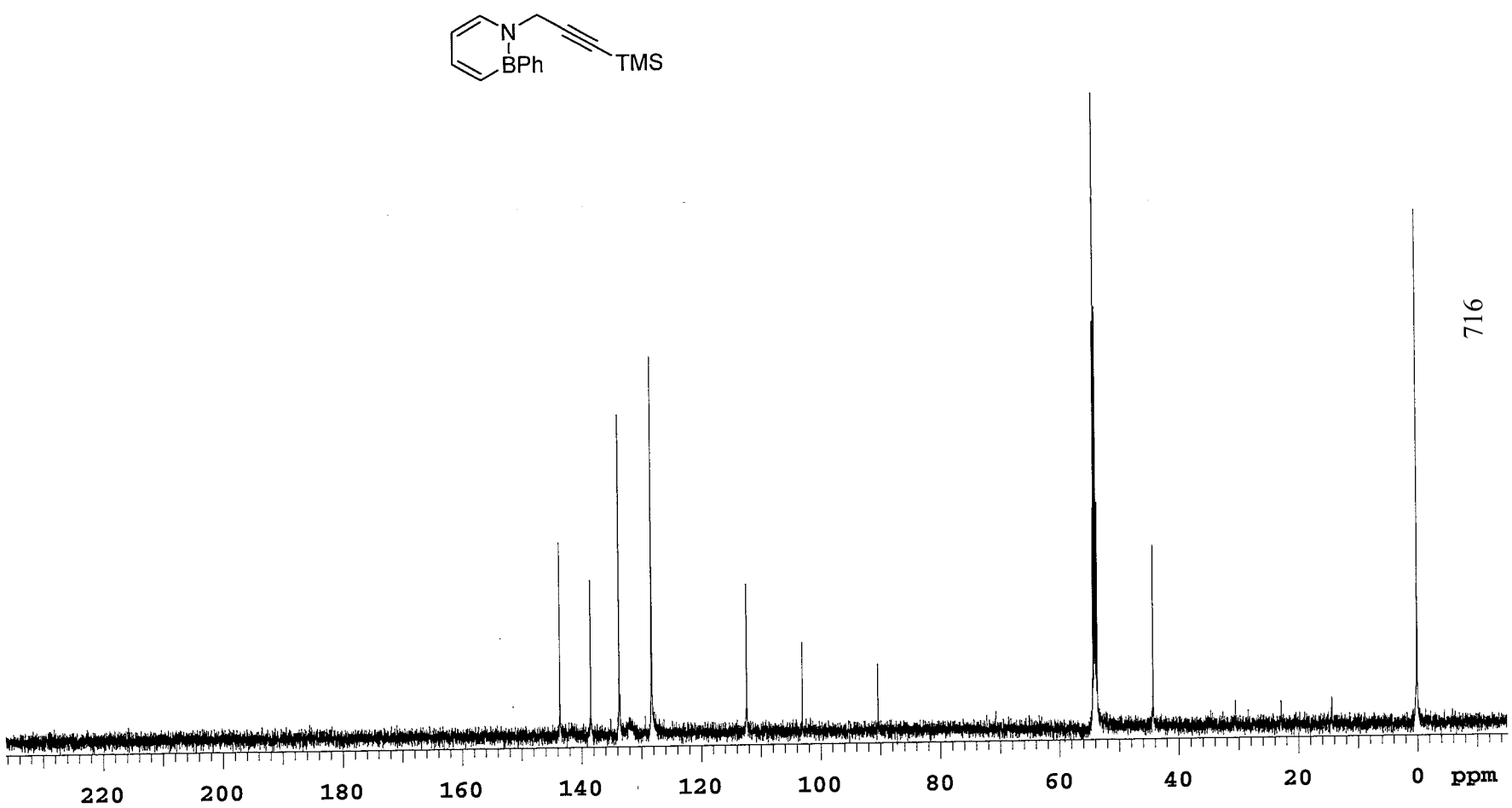

Data file /home/ALL/Liu/HL/N-Substitution/HL-III-052-1-13C.fid

Plot date 2015-12-24

HL-II-193-1H

Sample Name	**HL-II-193-1H**	Pulse sequence	**PROTON**	Temperature	**25**	Study owner	**Liu**
Date collected	**2015-12-15**	Solvent	**cd2cl2**	Spectrometer	**nmr18-vnmrs500**	Operator	**Liu**

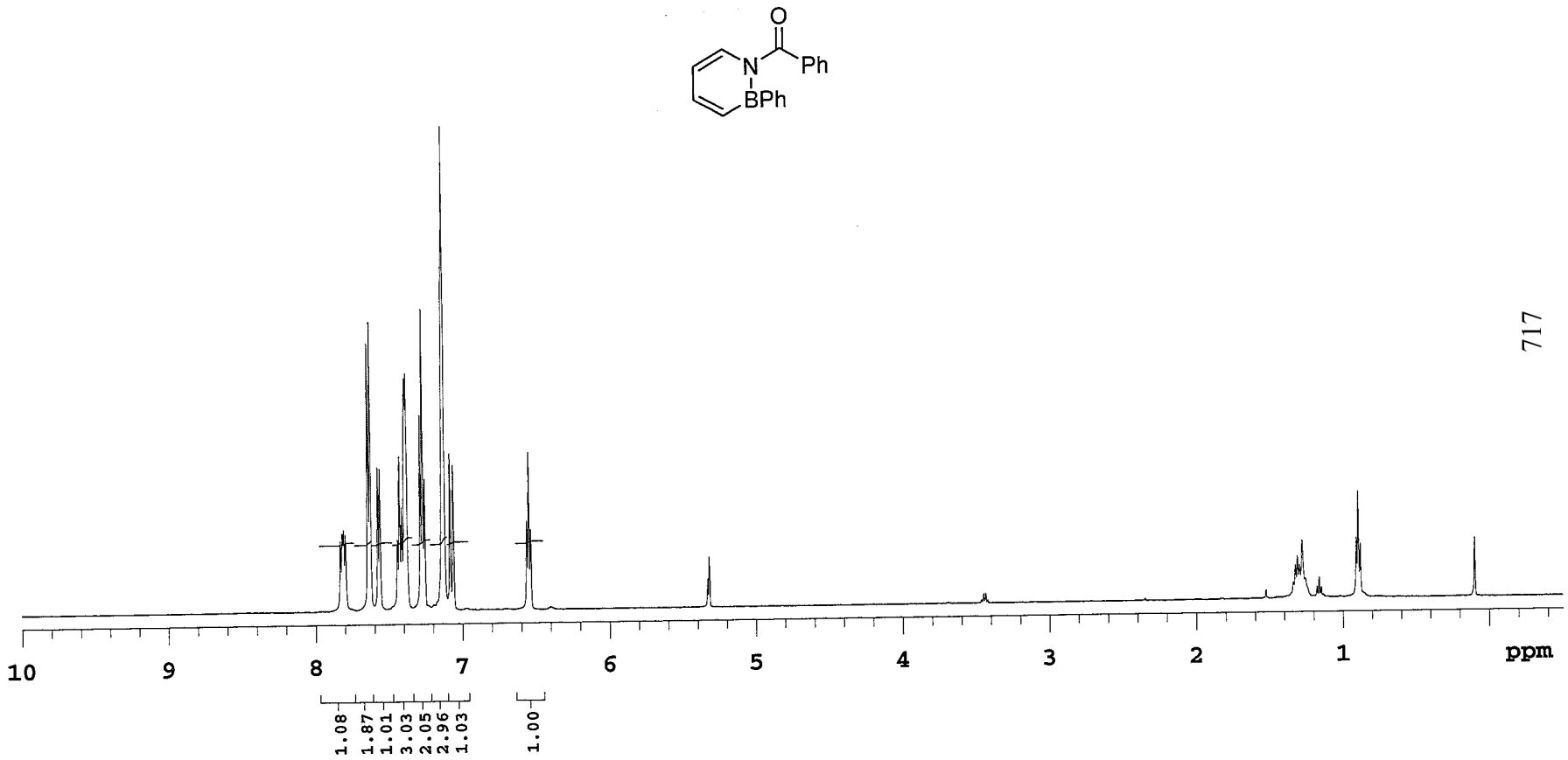

Data file /home/ALL/Liu/HL/N-Substitution/Table/HL-II-193-pure-1H.fid

Plot date 2015-12-24

HL-II-193-11B

Sample Name **HL-II-193-11B**	Pulse sequence **BORON_11**	Temperature **25**	Study owner **Liu**
Date collected **2015-12-15**	Solvent **cd2cl2**	Spectrometer **nmr18-vnmrs500**	Operator **Liu**

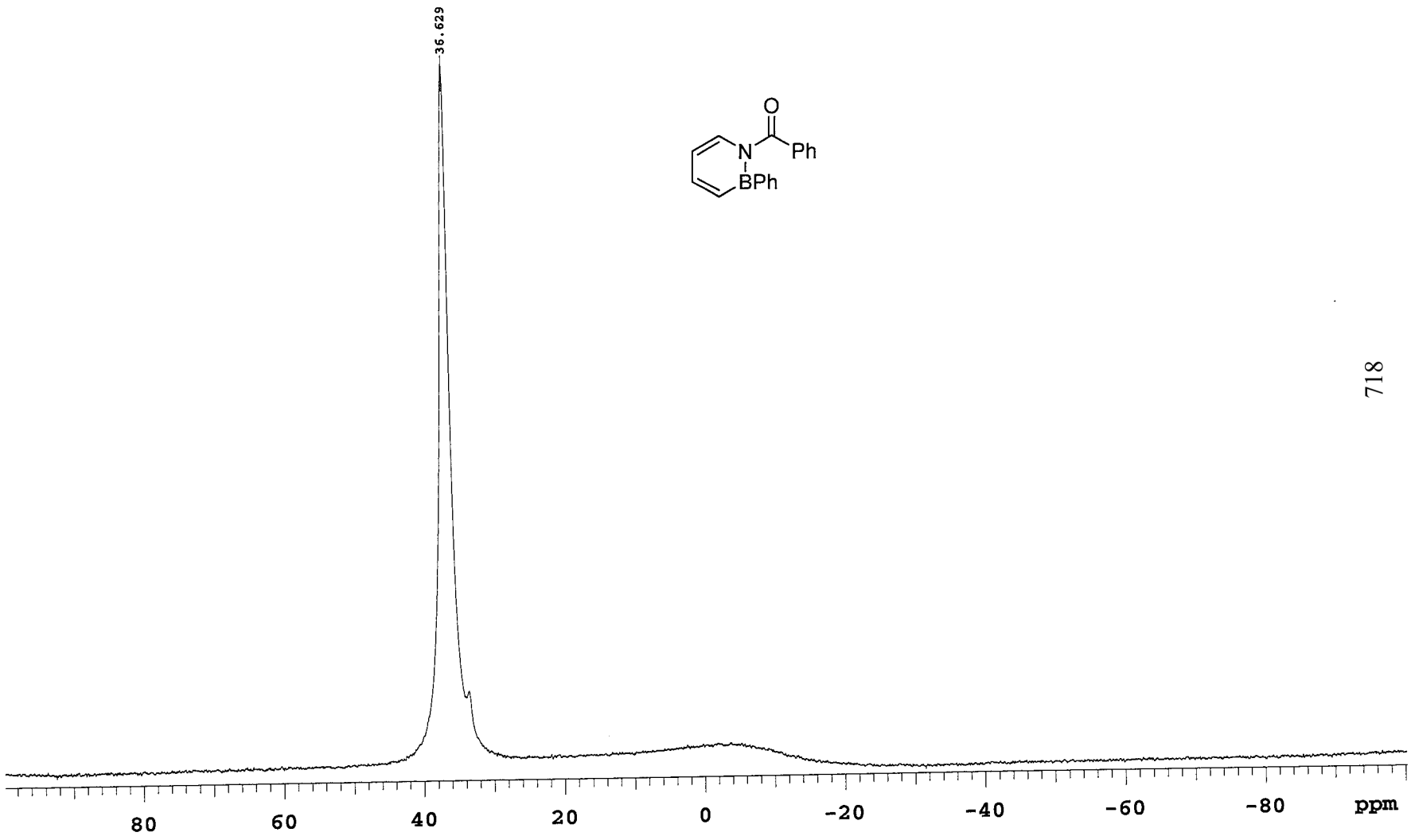

718

Data file /home/ALL/Liu/HL/N-Substitution/Table/HL-II-193-11B.fid

Plot date 2015-12-24

HL-II-193-13C

Sample Name **HL-II-193-13C**	Pulse sequence **CARBON**	Temperature **25**	Study owner **Liu**
Date collected **2015-12-15**	Solvent **cd2cl2**	Spectrometer **nmr18-vnmrs500**	Operator **Liu**

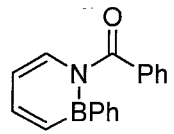

719

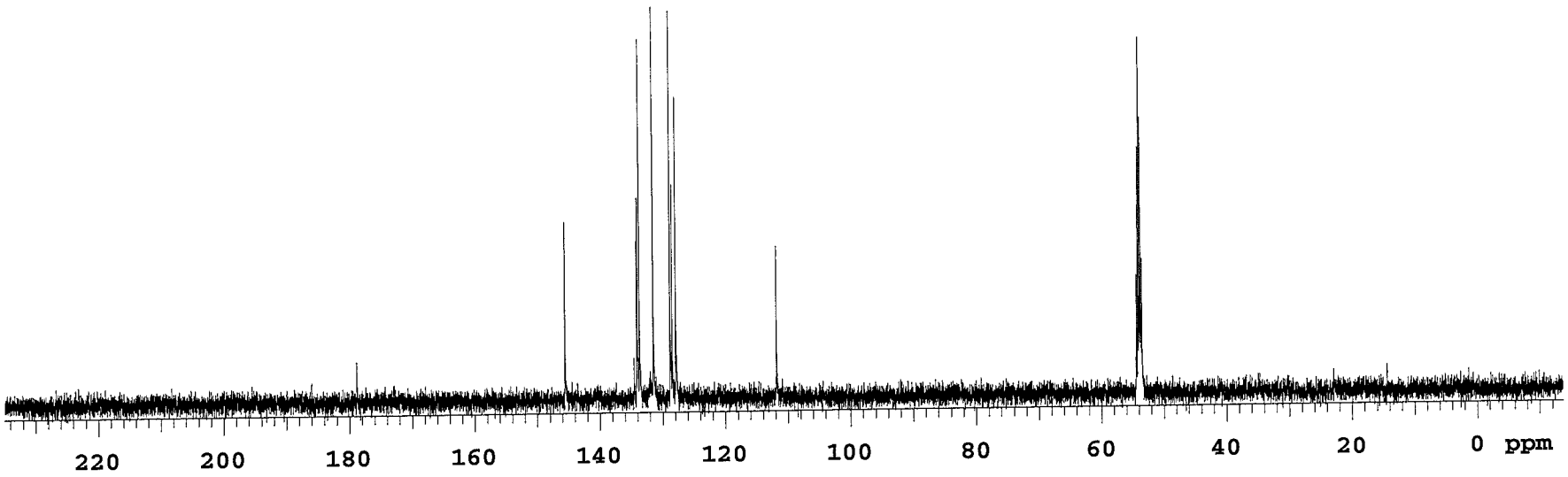

Data file /home/ALL/Liu/HL/N-Substitution/Table/HL-II-193-13C.fid

Plot date 2015-12-24

HL-III-051-1H

Sample Name	**HL-III-051-1H**	Pulse sequence	**PROTON**	Temperature	**25**	Study owner	**Liu**
Date collected	**2015-12-17**	Solvent	**cd2cl2**	Spectrometer	**nmr18-vnmrs500**	Operator	**Liu**

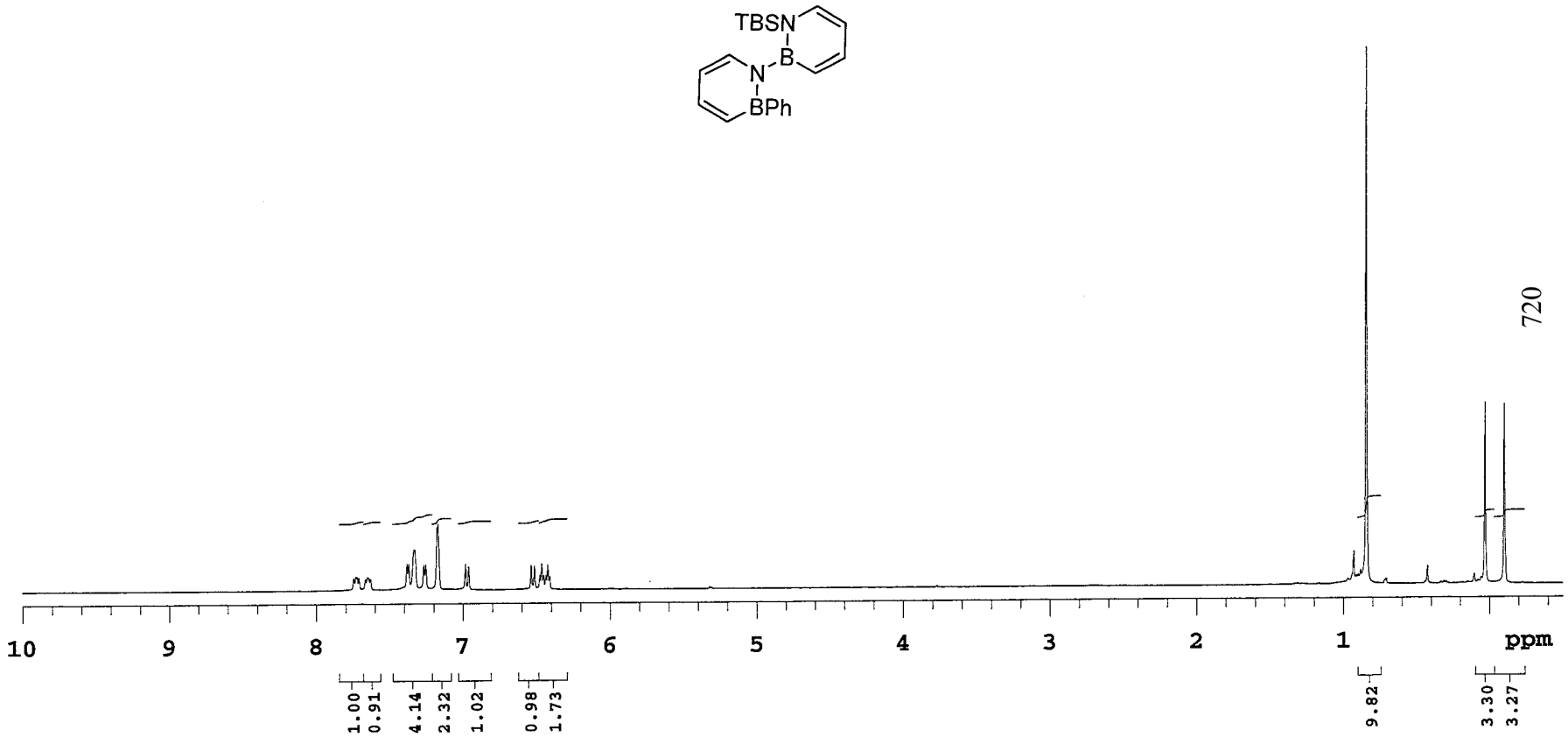

Data file /home/ALL/Liu/HL/N-Substitution/Table/HL-III-051-1H.fid

Plot date 2015-12-24

HL-II-146-11B

Sample Name	**HL-II-146-11B**	Pulse sequence	**BORON_11**	Temperature	**25**	Study owner	**Liu**
Date collected	**2015-05-29**	Solvent	**cd2cl2**	Spectrometer	**nmr18-vnmrs500**	Operator	**Liu**

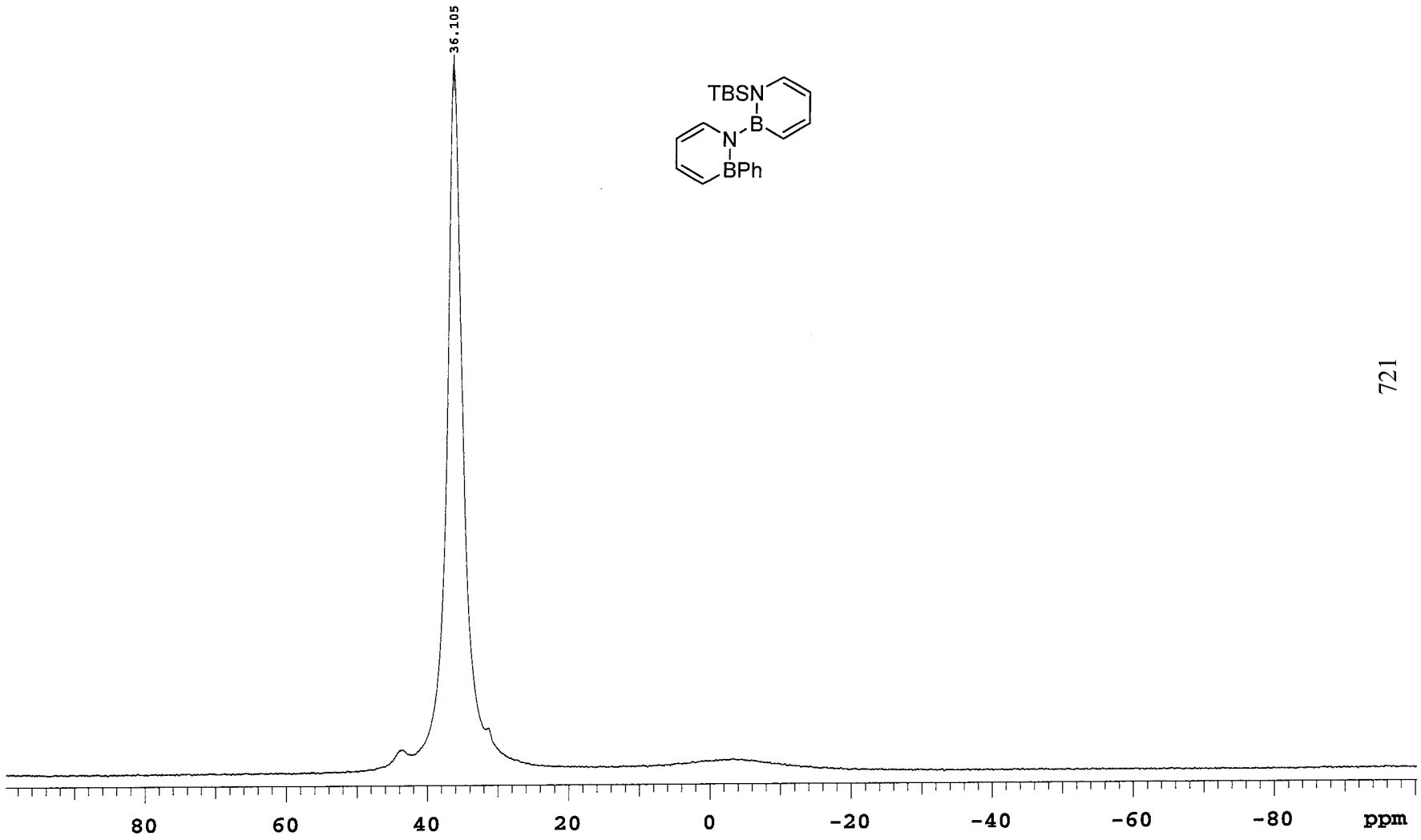

721

Data file /home/ALL/Liu/HL/N-Substitution/Table/HL-II-146-11B.fid

Plot date 2015-12-24

HL-III-051-13C

Sample Name	**HL-III-051-13C**	Pulse sequence	**CARBON**	Temperature	**25**	Study owner	**Liu**
Date collected	**2015-12-17**	Solvent	**cd2cl2**	Spectrometer	**nmr19-vnmrs600**	Operator	**Liu**

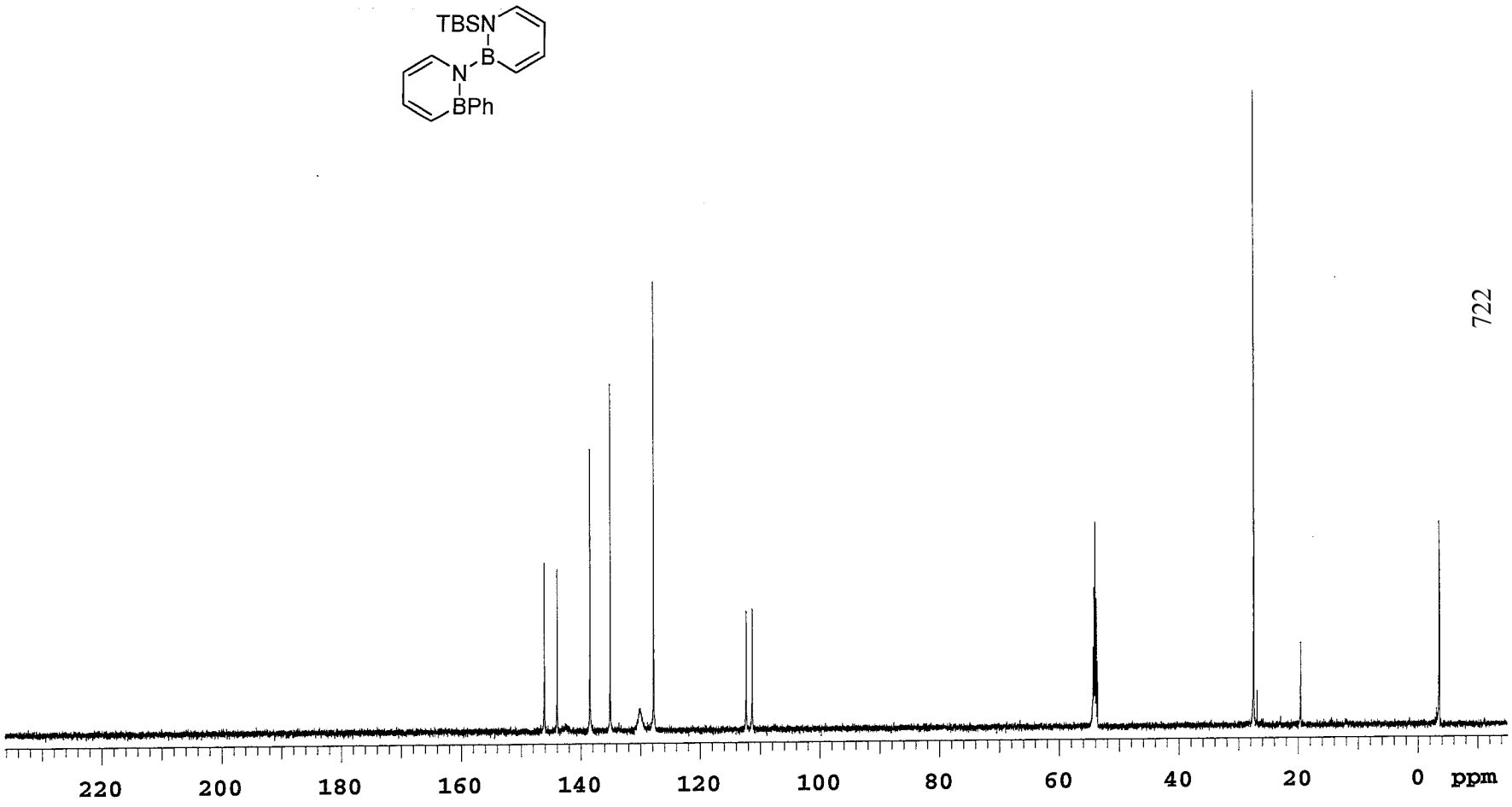

Data file /home/ALL/Liu/HL/N-Substitution/HL-III-051-13C.fid

Plot date 2015-12-24

HL-II-290-1H

Sample Name **HL-II-290-1H**	Pulse sequence **PROTON**	Temperature **25**	Study owner **Liu**
Date collected **2015-12-03**	Solvent **cd2cl2**	Spectrometer **nmr18-vnmrs500**	Operator **Liu**

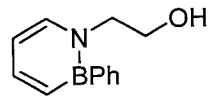

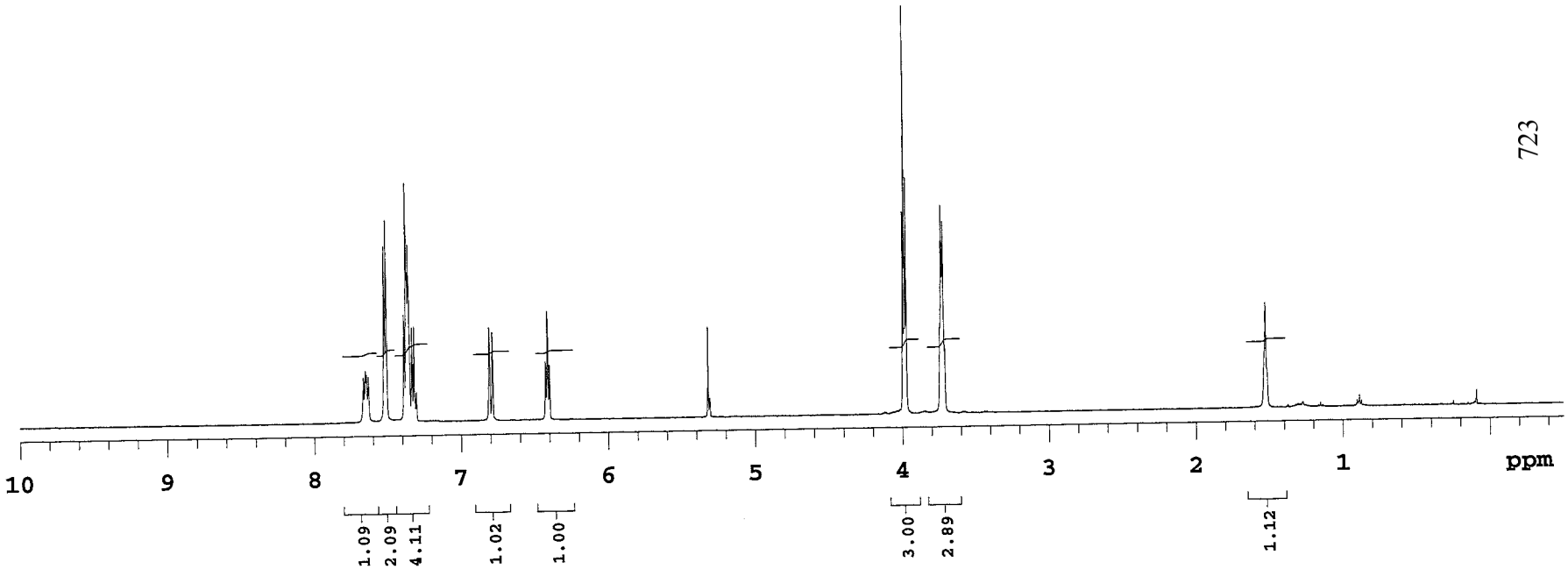

Data file /home/ALL/Liu/HL/N-Substitution/Table/HL-II-290-1H.fid

Plot date 2015-12-24

Sample Name	Pulse sequence **s2pul**	Temperature **25**	Study owner **Liu**
Date collected **2015-04-25**	Solvent **cd2cl2**	Spectrometer **nmr19-vnmrs600**	Operator **Liu**

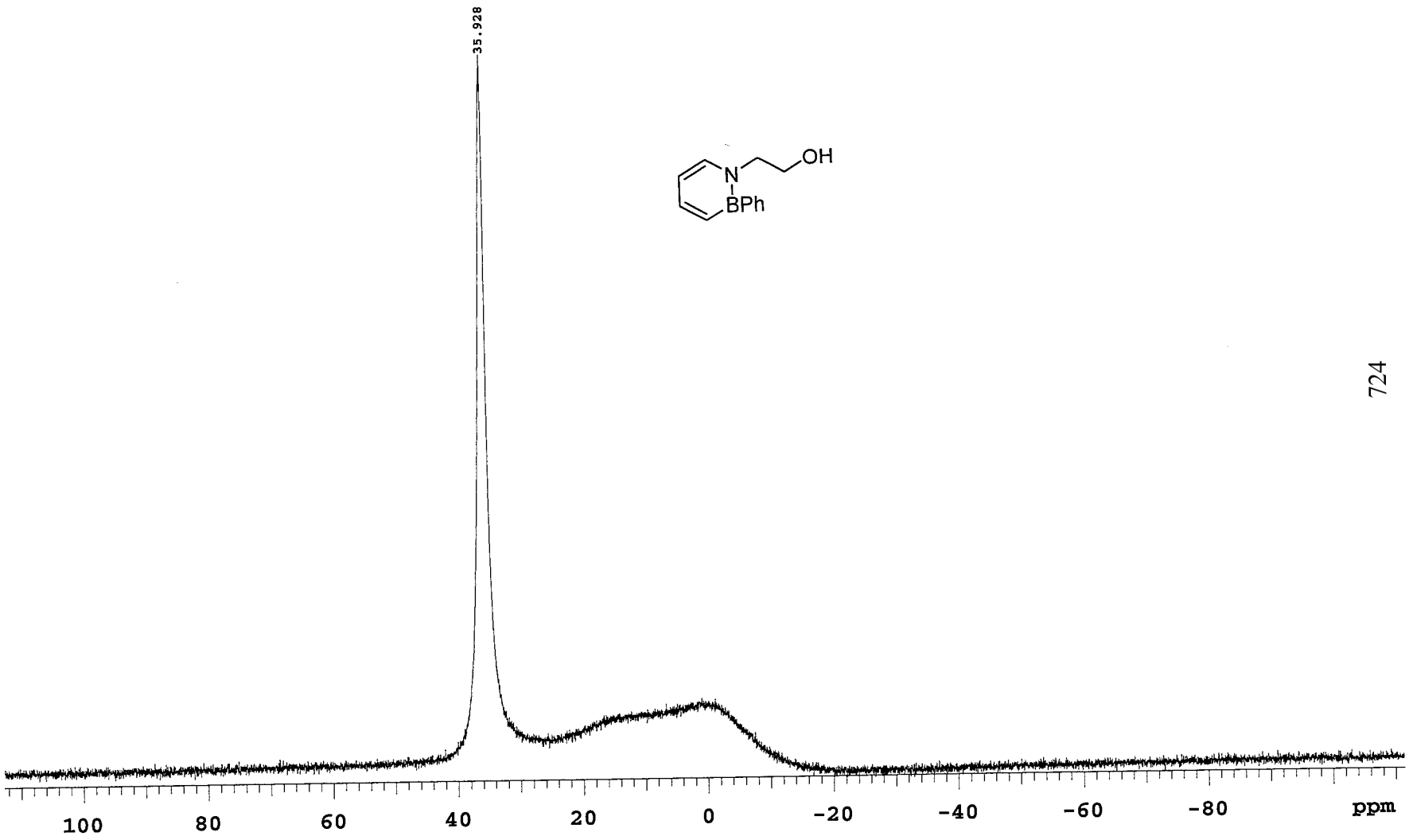

724

Data file /home/ALL/Liu/HL/N-Substitution/Table/SI-1-076-pure-11B.fid

Plot date 2015-12-24

Sample Name	Pulse sequence **CARBON**	Temperature **25**	Study owner **Liu**
Date collected **2015-04-25**	Solvent **cd2cl2**	Spectrometer **nmr19-vnmrs600**	Operator **Liu**

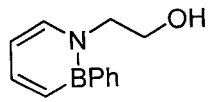

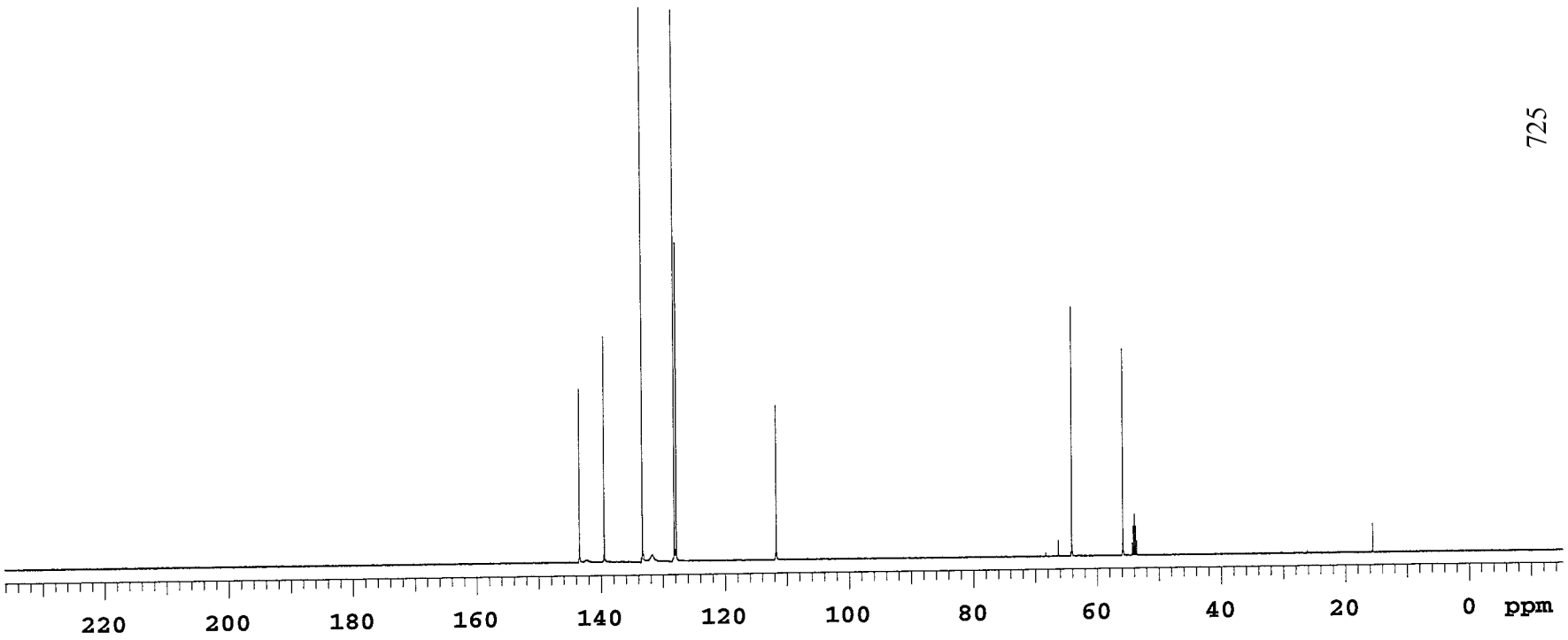

725

Data file /home/ALL/Liu/HL/N-Substitution/Table/SI-1-076-pure-13C.fid

Plot date 2015-12-24

Sample Name	Pulse sequence **PROTON**	Temperature **25**	Study owner **Liu**
Date collected **2015-04-18**	Solvent **cd2cl2**	Spectrometer **nmr18-vnmrs500**	Operator **Liu**

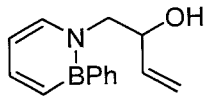

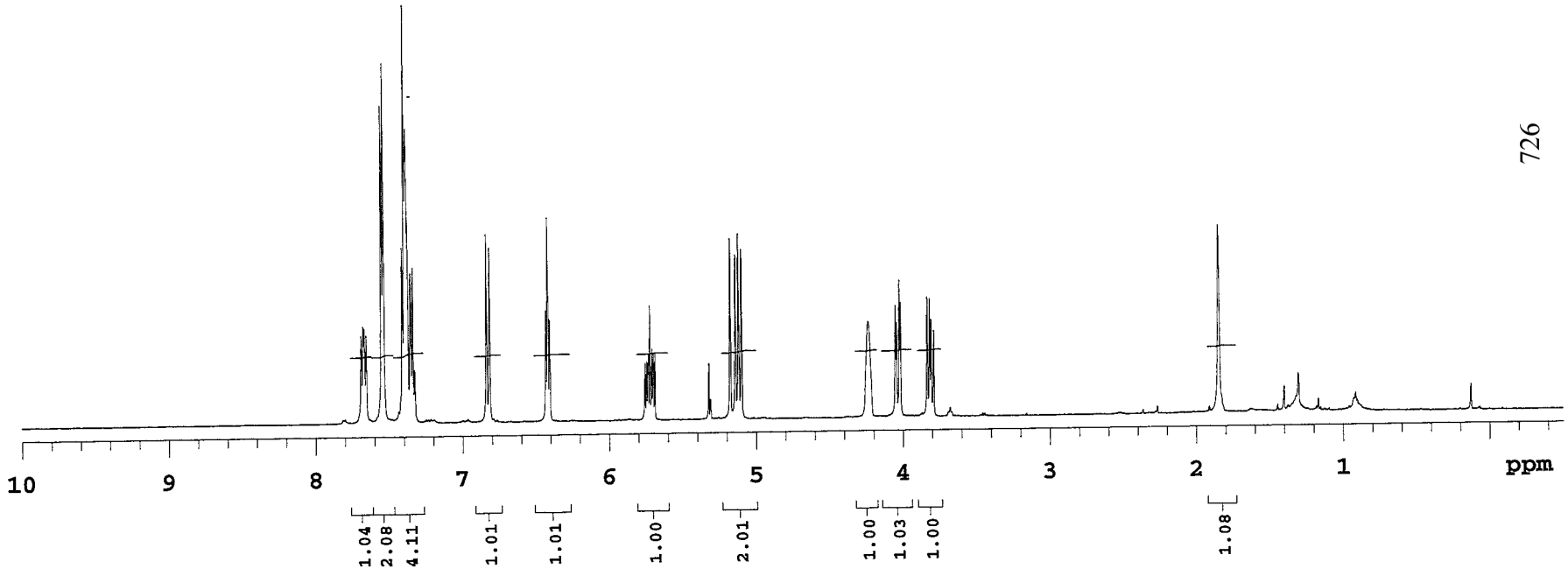

726

Data file /home/ALL/Liu/HL/N-Substitution/Table/Si-1-074-1H-pure.fid

Plot date 2015-12-24

Sample Name	Pulse sequence **s2pul**	Temperature **25**	Study owner **Liu**
Date collected **2015-04-18**	Solvent **cd2cl2**	Spectrometer **nmr18-vnmrs500**	Operator **Liu**

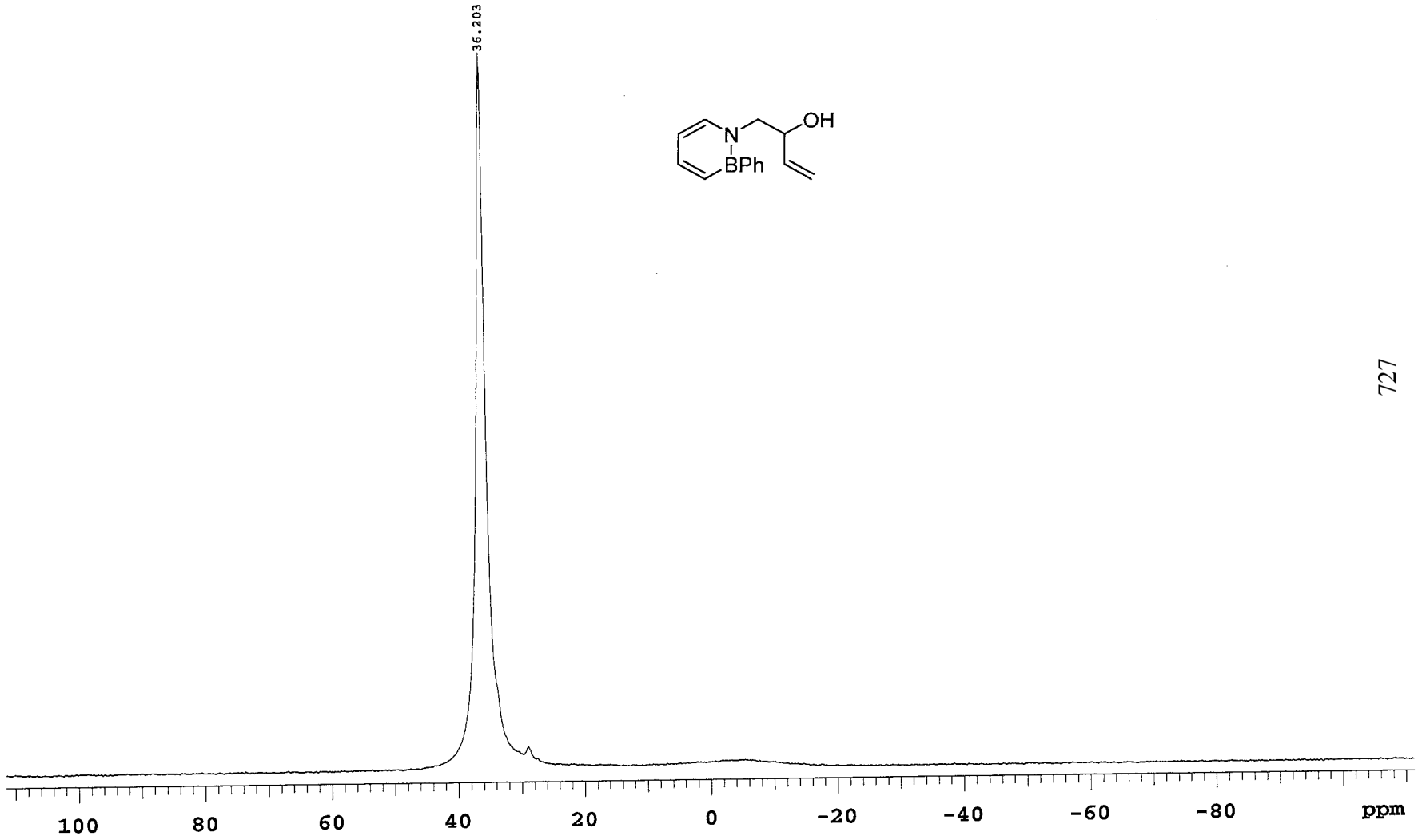

727

Data file /home/ALL/Liu/HL/N-Substitution/Table/Si-1-074-11B-pure.fid

Plot date 2015-12-24

Sample Name	Pulse sequence **CARBON**	Temperature **25**	Study owner **Liu**
Date collected **2015-04-15**	Solvent **cd2cl2**	Spectrometer **nmr19-vnmrs600**	Operator **Liu**

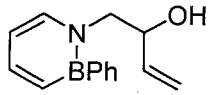

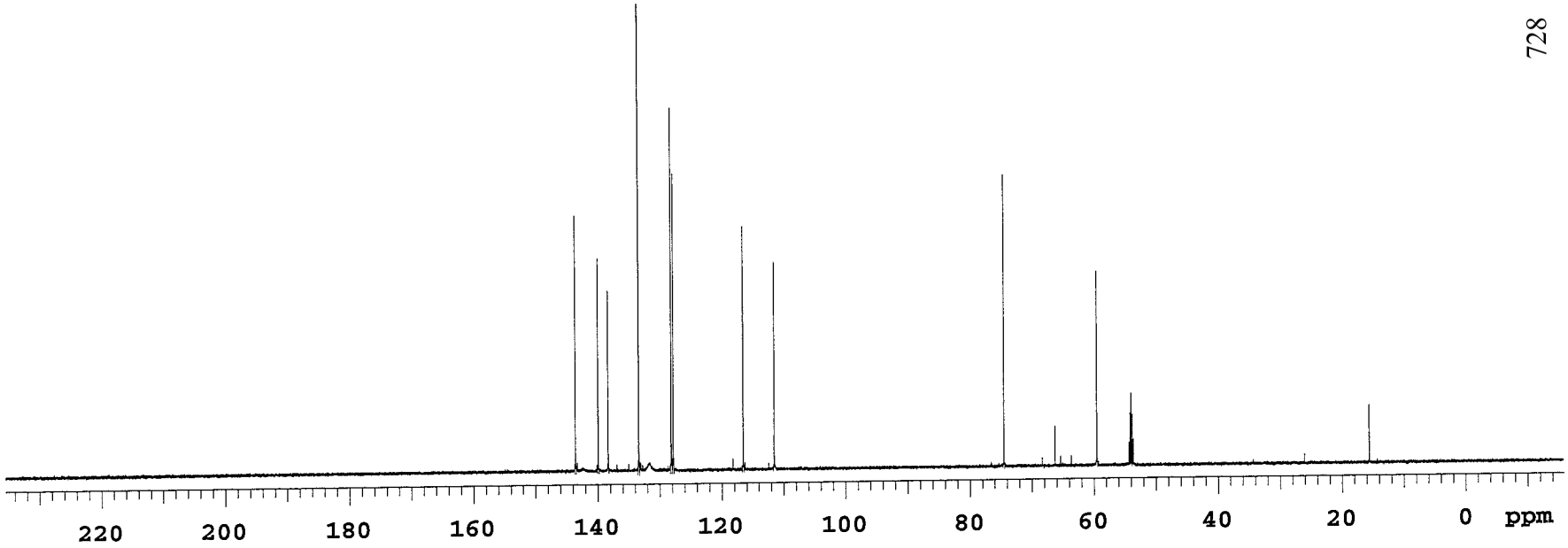

Data file /home/ALL/Liu/HL/N-Substitution/Table/Si-1-074-13C.fid

Plot date 2015-12-24

HL-II-279-1H

Sample Name	**HL-II-279-1H**	Pulse sequence	**PROTON**	Temperature	**25**	Study owner	**Liu**
Date collected	**2015-12-15**	Solvent	**cd2cl2**	Spectrometer	**nmr18-vnmrs500**	Operator	**Liu**

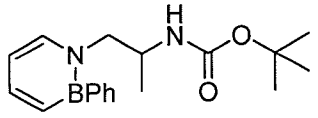

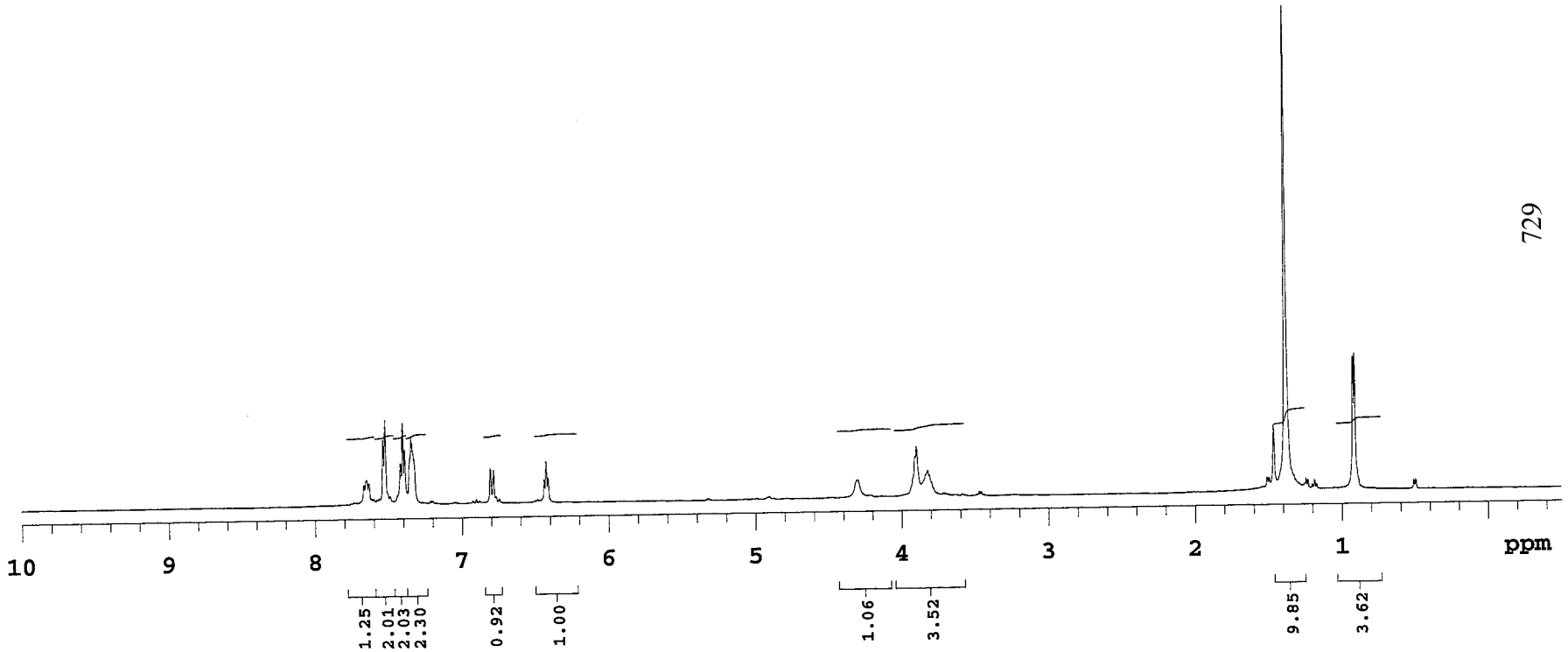

729

Data file /home/ALL/Liu/HL/N-Substitution/Table/HL-II-279-pure-1H.fid

Plot date 2015-12-24

HL-II-279-11B

Sample Name	**HL-II-279-11B**	Pulse sequence	**BORON_11**	Temperature	**25**	Study owner	**Liu**
Date collected	**2015-12-15**	Solvent	**cd2cl2**	Spectrometer	**nmr18-vnmrs500**	Operator	**Liu**

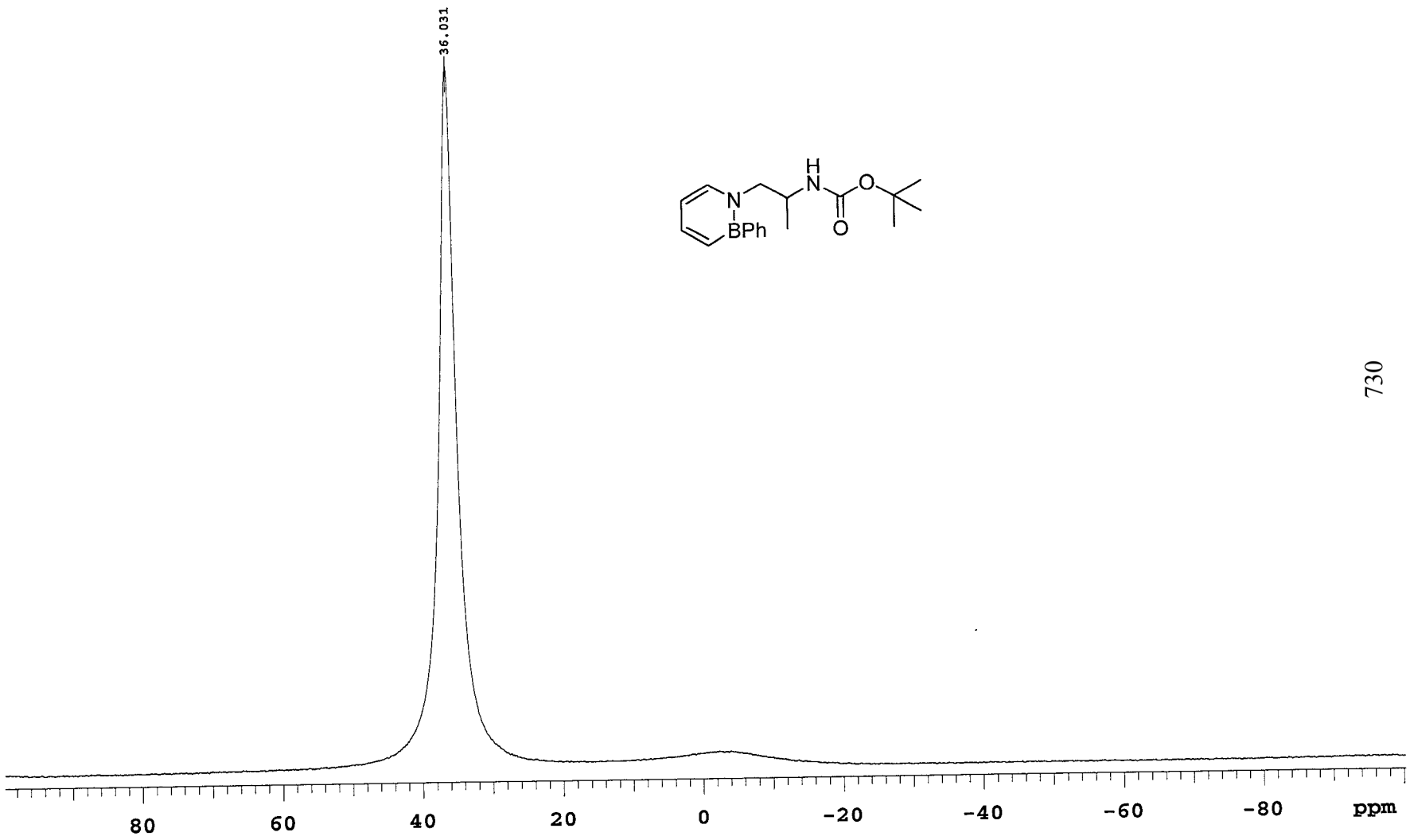

Data file /home/ALL/Liu/HL/N-Substitution/Table/HL-II-279-pure-11B.fid

Plot date 2015-12-24

HL-II-279-13C

Sample Name **HL-II-279-13C**	Pulse sequence **CARBON**	Temperature **25**	Study owner **Liu**
Date collected **2015-12-15**	Solvent **cd2cl2**	Spectrometer **nmr19-vnmrs600**	Operator **Liu**

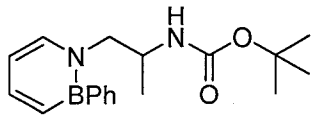

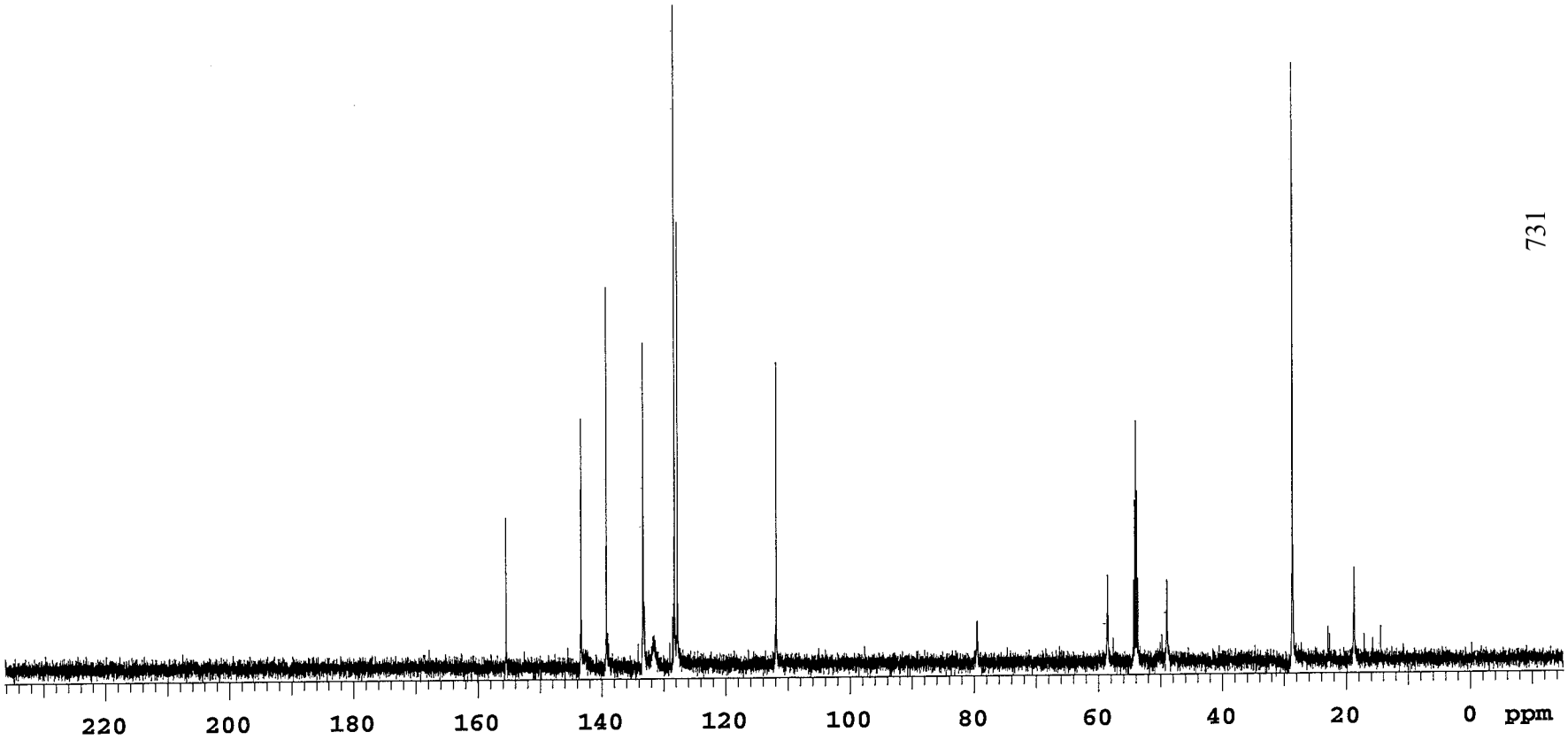

Data file /home/ALL/Liu/HL/N-Substitution/HL-II-279-13C.fid

Plot date 2016-06-15

HL-II-018-1H

Sample Name	**HL-II-018-1H**	Pulse sequence	**PROTON**	Temperature	**25**	Study owner	**Liu**
Date collected	**2015-11-19**	Solvent	**cd2cl2**	Spectrometer	**nmr18-vnmrs500**	Operator	**Liu**

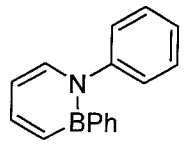

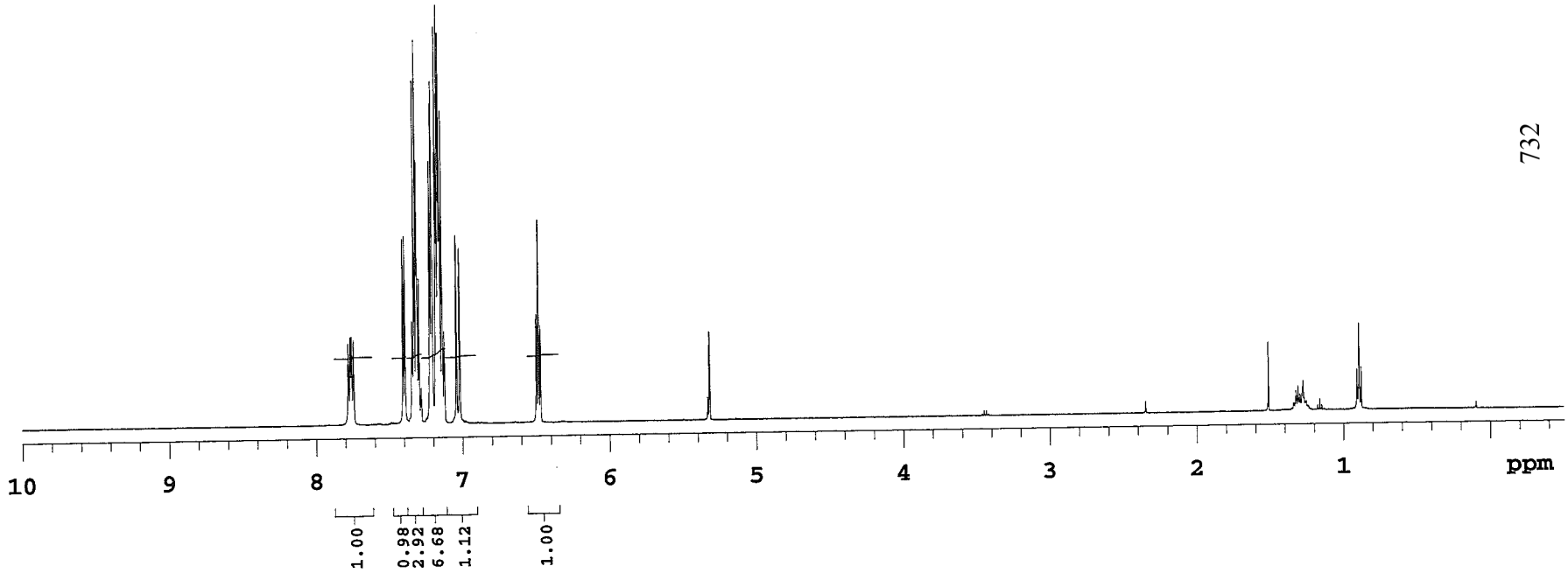

732

Data file /home/ALL/Liu/HL/N-Substitution/Table/HL-II-018-1H.fid

Plot date 2015-12-24

HL-II-018-11B

Sample Name	**HL-II-018-11B**	Pulse sequence	**BORON_11**	Temperature	**25**	Study owner	**Liu**
Date collected	**2015-11-19**	Solvent	**cd2cl2**	Spectrometer	**nmr18-vnmrs500**	Operator	**Liu**

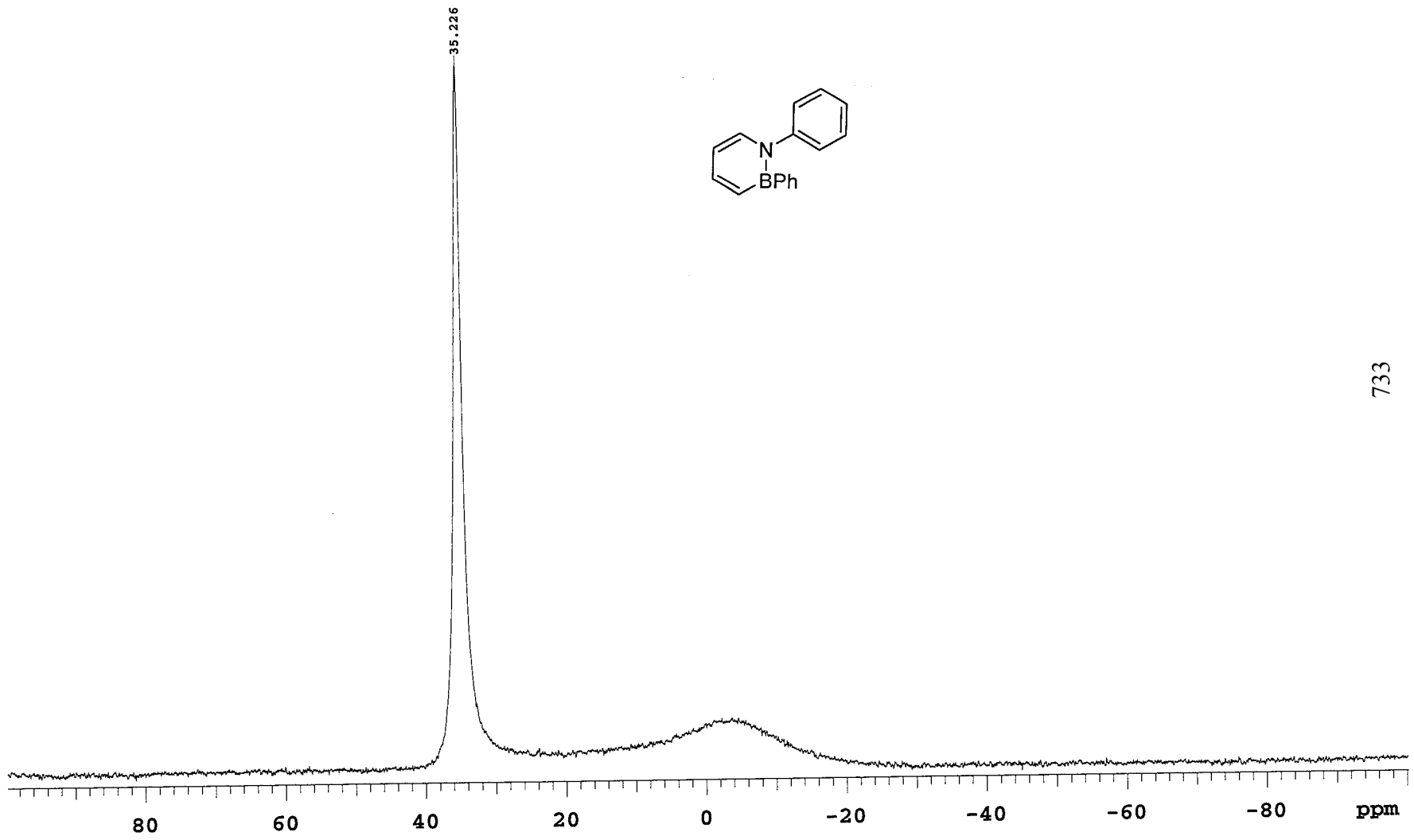

733

Data file /home/ALL/Liu/HL/N-Substitution/Table/HL-II-018-11B.fid

Plot date 2015-12-24

HL-III-018-13C

Sample Name	**HL-III-018-13C**	Pulse sequence	**CARBON**	Temperature	**25**	Study owner	**Liu**
Date collected	**2015-11-21**	Solvent	**cd2cl2**	Spectrometer	**nmr19-vnmrs600**	Operator	**Liu**

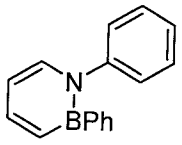

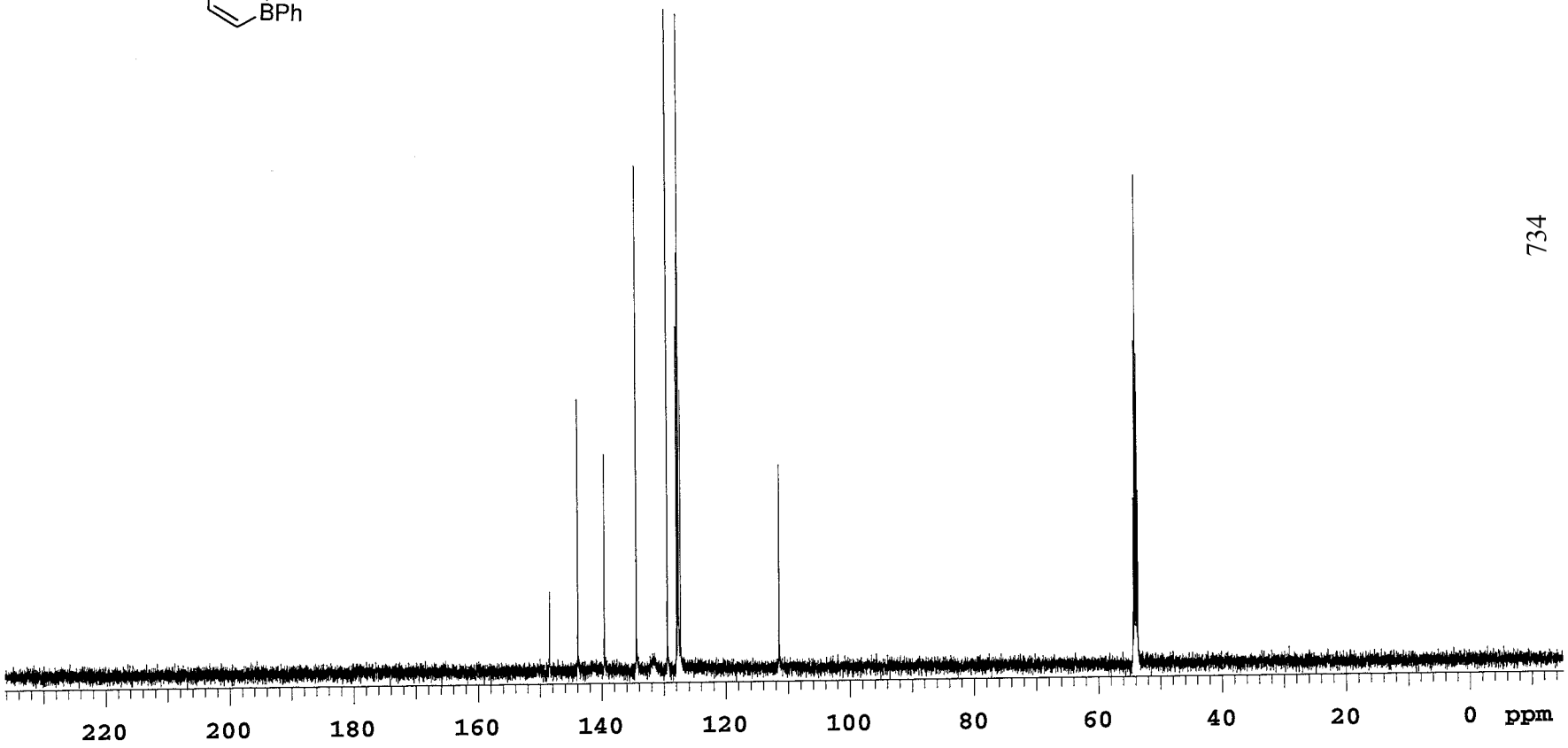

734

Data file /home/ALL/Liu/HL/N-Substitution/HL-III-018-13C.fid

Plot date 2015-12-24

HL-III-279-1H

Sample Name HL-III-279-1H
Date collected 2016-07-18

Pulse sequence PROTON
Solvent cd2cl2

Temperature 25
Spectrometer nmr19-vnmrs600

Study owner Liu
Operator Liu

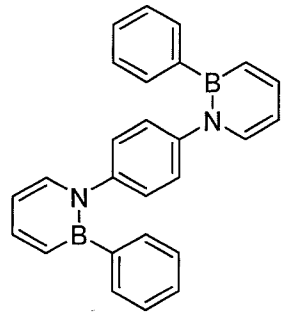

735

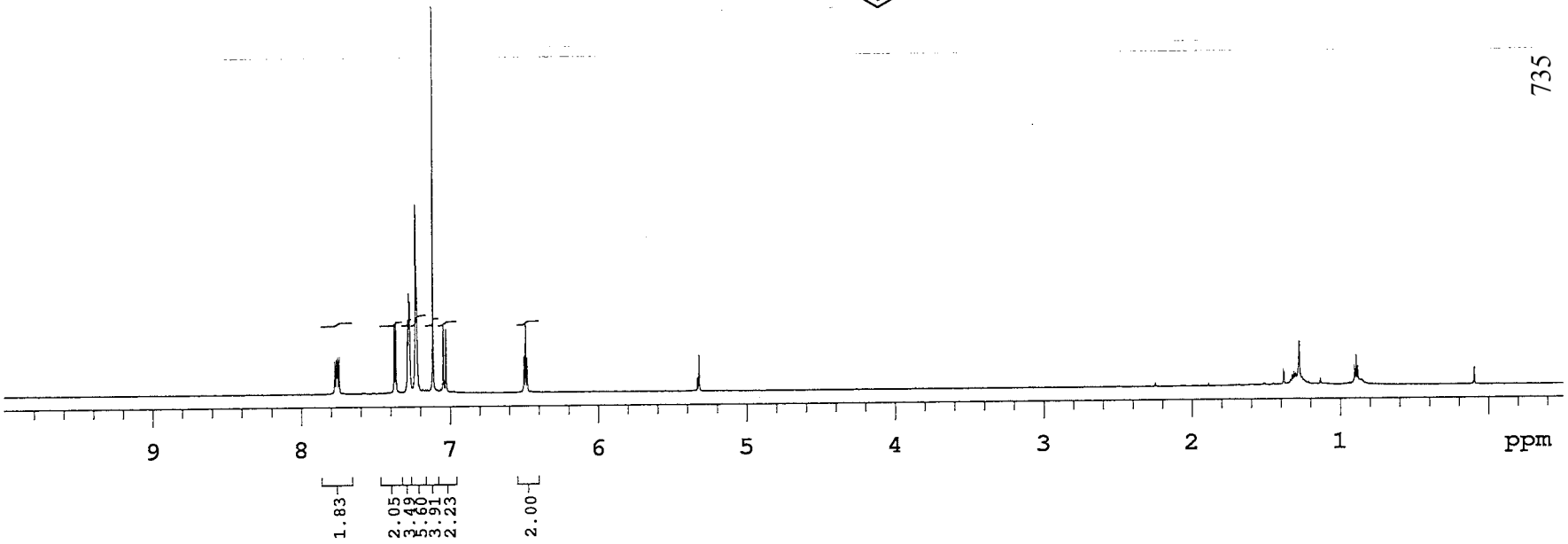

Data file /home/Liu/vnmrsys/data/Hyelee/HL-III-279-1H.fid

Plot date 2016-07-18

HL-III-275-11B

Sample Name **HL-III-275-11B**	Pulse sequence **s2pul**	Temperature **25**	Study owner **Liu**
Date collected **2016-07-14**	Solvent **cd2cl2**	Spectrometer **nmr11-inova500**	Operator **Liu**

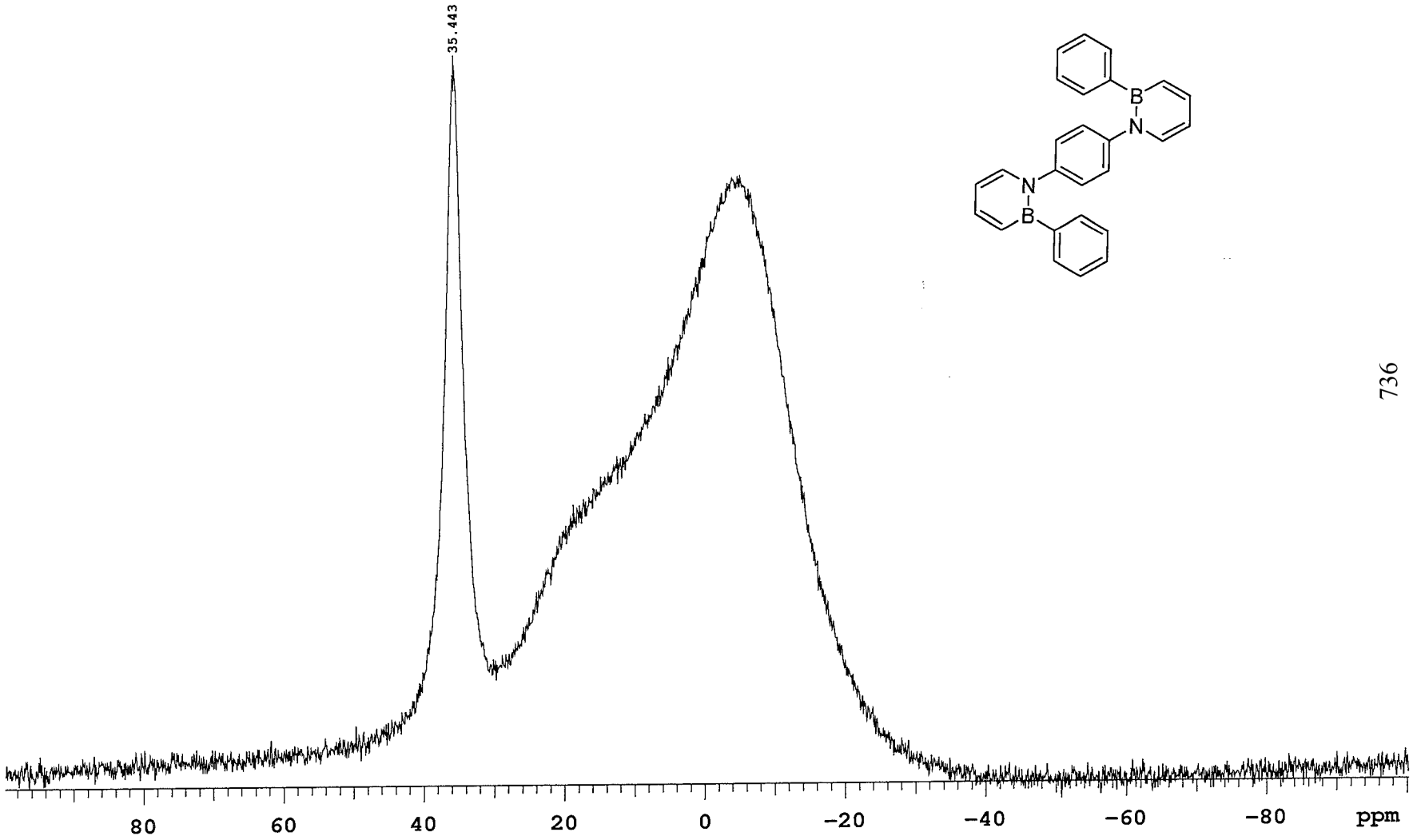

736

Data file exp

Plot date 2016-07-14

HL-III-279-1H

Sample Name	**HL-III-279-1H**	Pulse sequence	**CARBON**	Temperature	**25**	Study owner	**Liu**
Date collected	**2016-07-18**	Solvent	**cd2cl2**	Spectrometer	**nmr19-vnmrs600**	Operator	**Liu**

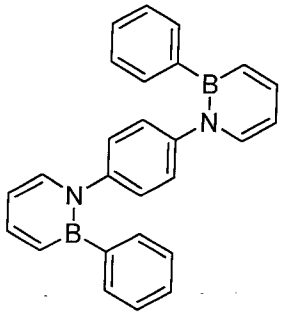

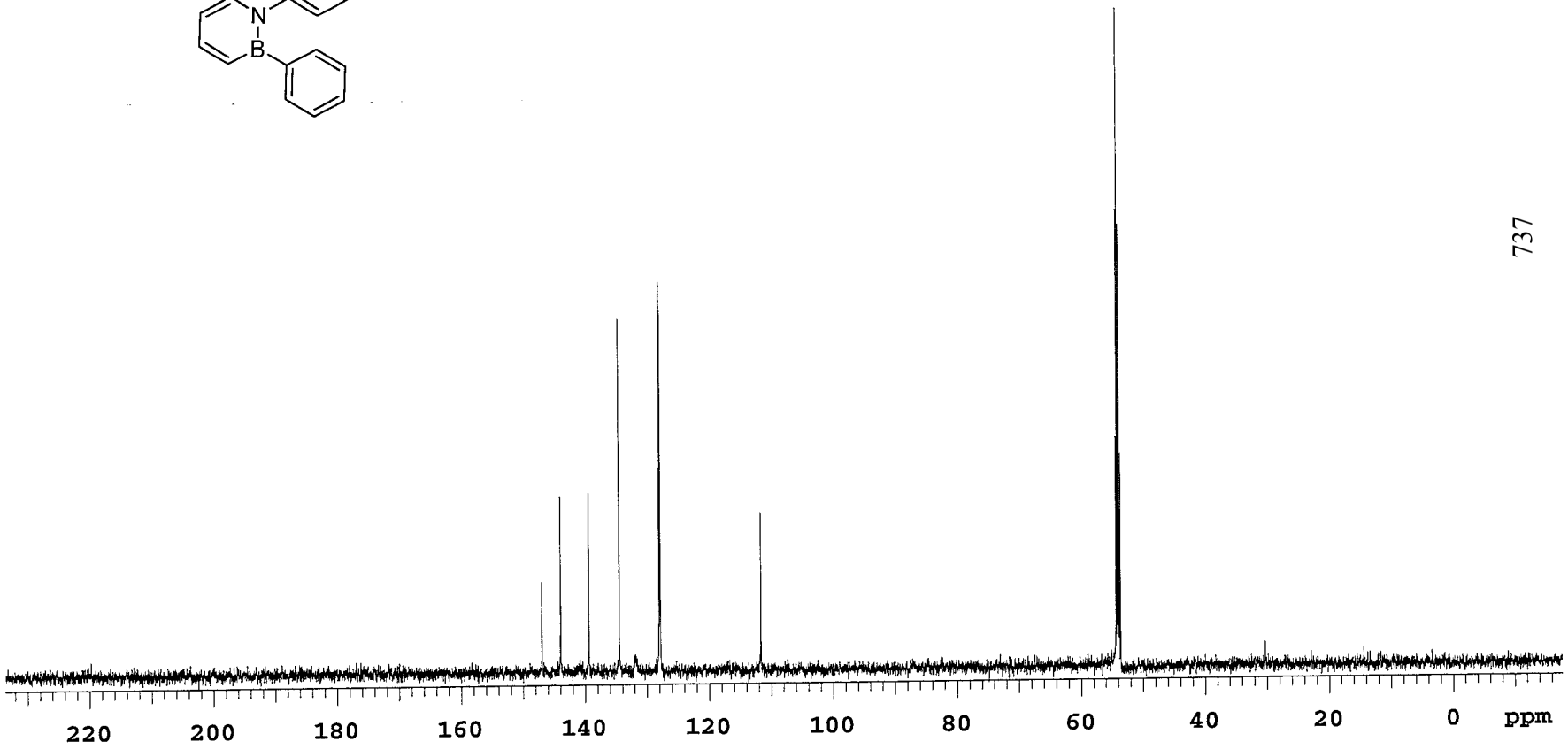

Data file /home/ALL/Liu/HL/N-Substitution/HL-III-279-13C.fid

Plot date 2016-07-18

HL-II-022-1H

Sample Name **HL-II-022-1H**	Pulse sequence **PROTON**	Temperature **25**	Study owner **Liu**
Date collected **2015-11-19**	Solvent **cd2cl2**	Spectrometer **nmr18-vnmrs500**	Operator **Liu**

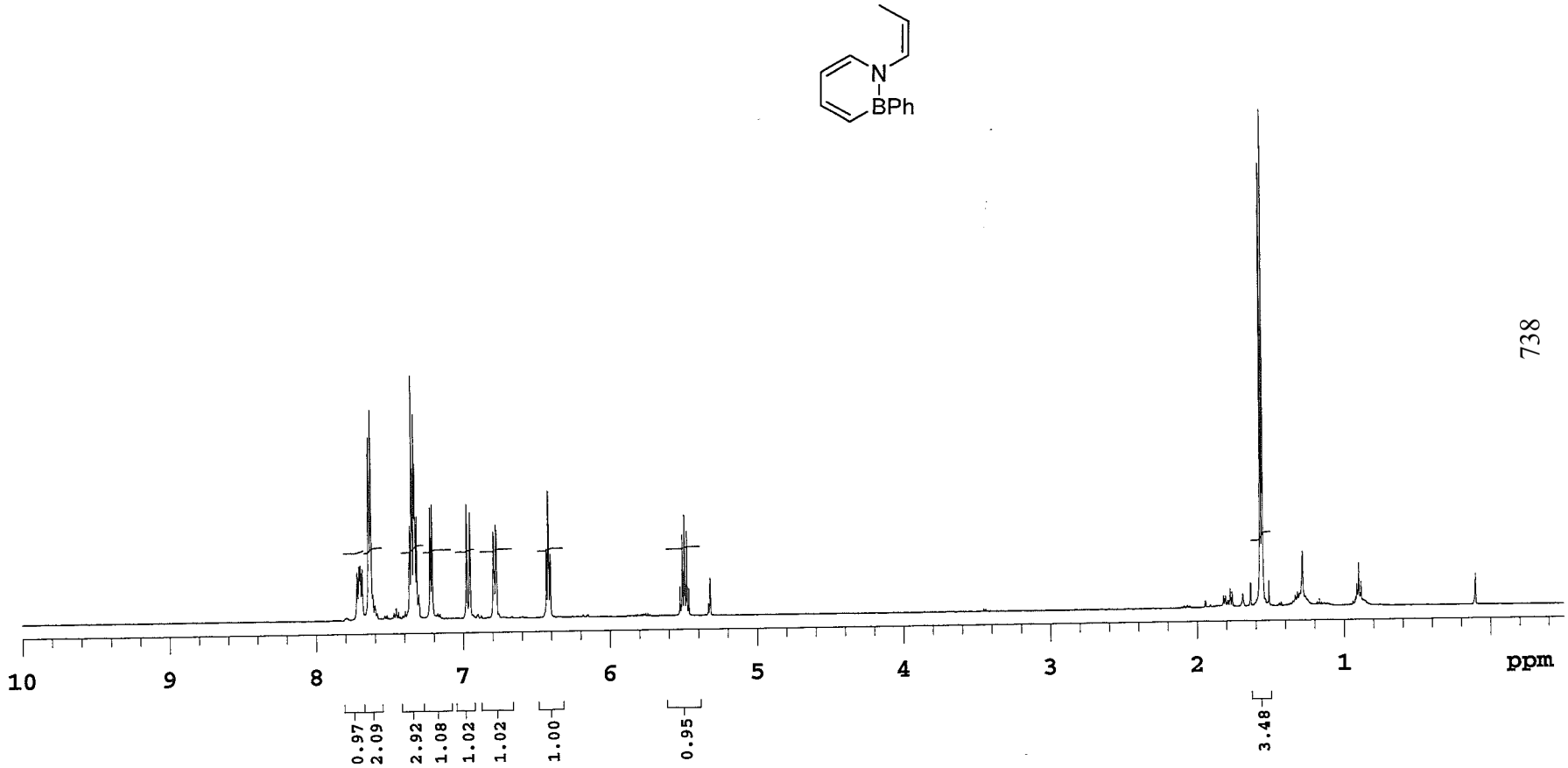

Data file /home/ALL/Liu/HL/N-Substitution/Table/HL-II-022-1H.fid

Plot date 2015-12-24

HL-II-022-11B

Sample Name	**HL-II-022-11B**	Pulse sequence	**BORON_11**	Temperature	**25**	Study owner	**Liu**
Date collected	**2015-11-19**	Solvent	**cd2cl2**	Spectrometer	**nmr18-vnmrs500**	Operator	**Liu**

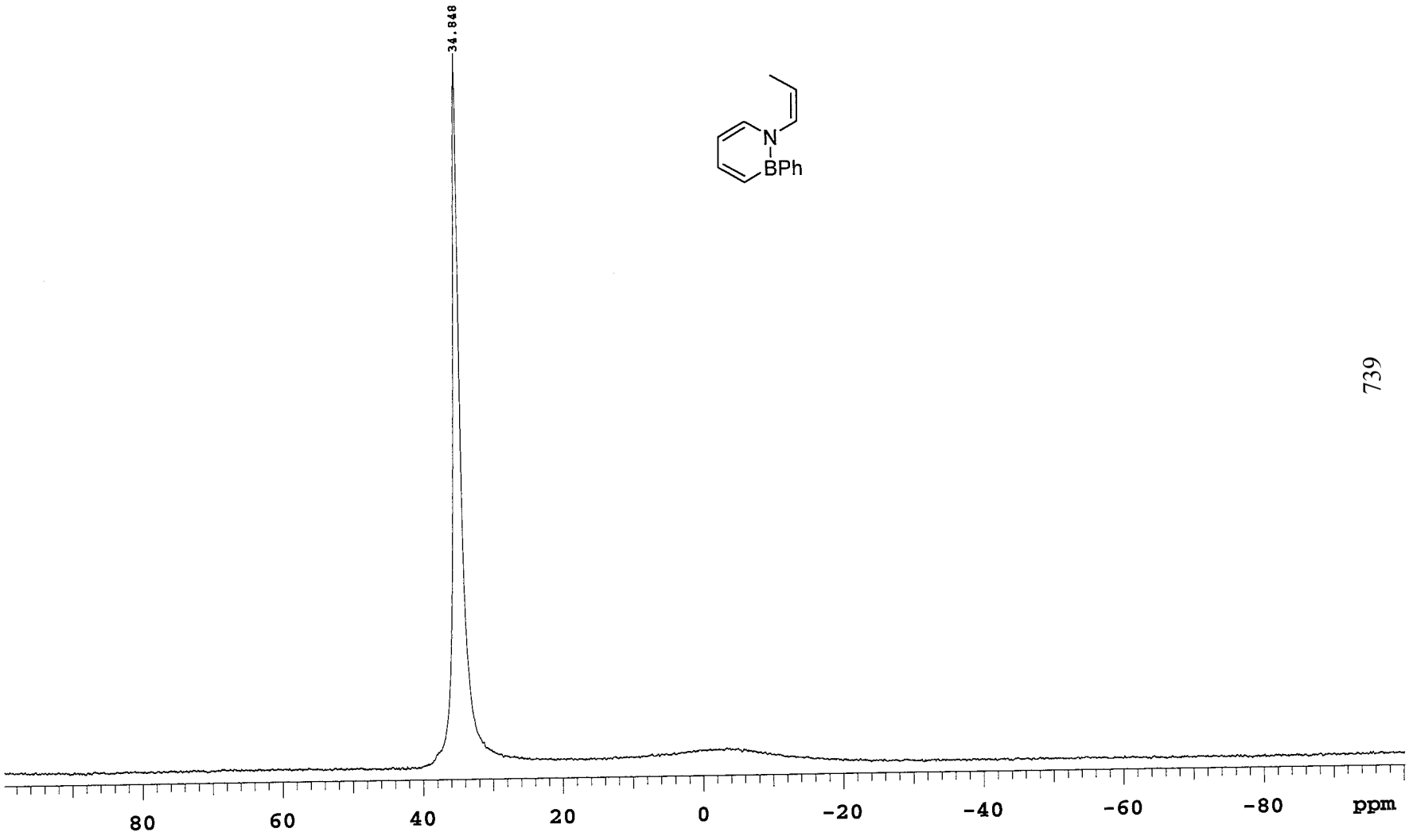

739

Data file /home/ALL/Liu/HL/N-Substitution/Table/HL-II-022-11B.fid

Plot date 2015-12-24

HL-III-022-13C

Sample Name **HL-III-022-13C**	Pulse sequence **CARBON**	Temperature **25**	Study owner **Liu**
Date collected **2015-11-20**	Solvent **cd2cl2**	Spectrometer **nmr18-vnmrs500**	Operator **Liu**

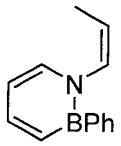

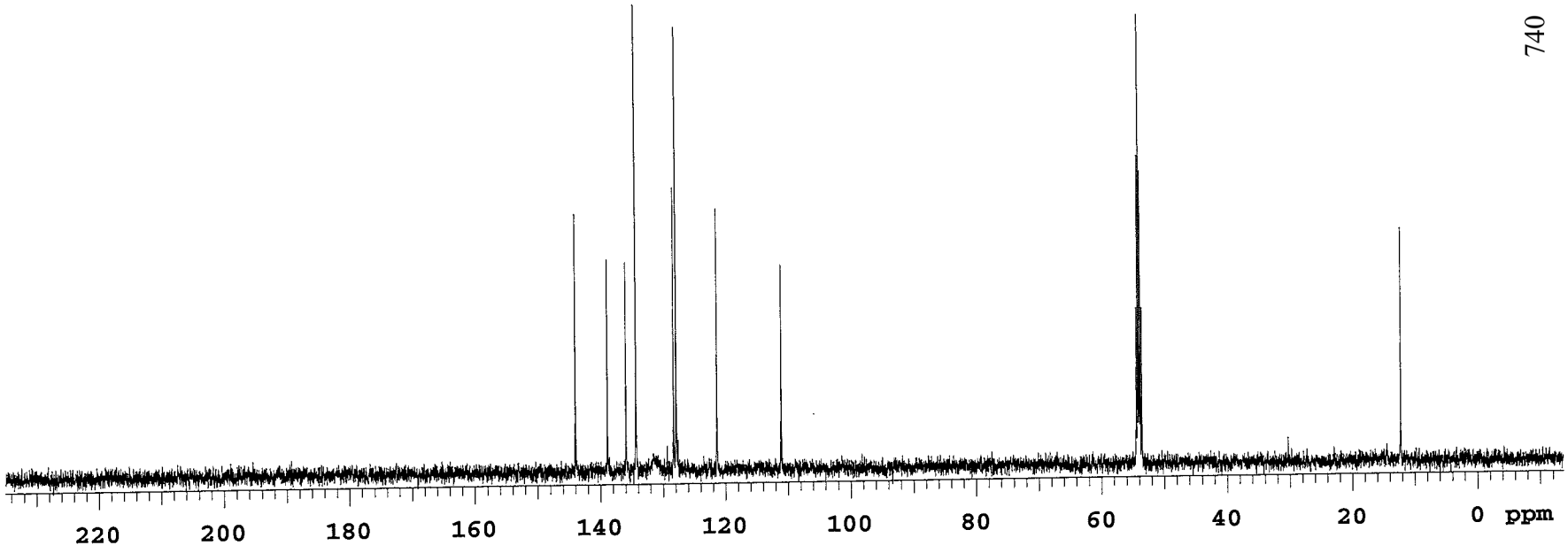

Data file /home/ALL/Liu/HL/N-Substitution/Table/HL-III-022-13C.fid

Plot date 2015-12-24

HL-III-226-1H

Sample Name **HL-III-226-1H**	Pulse sequence **PROTON**	Temperature **25**	Study owner **Liu**
Date collected **2016-05-26**	Solvent **cd2cl2**	Spectrometer **nmr11-inova500**	Operator **Liu**

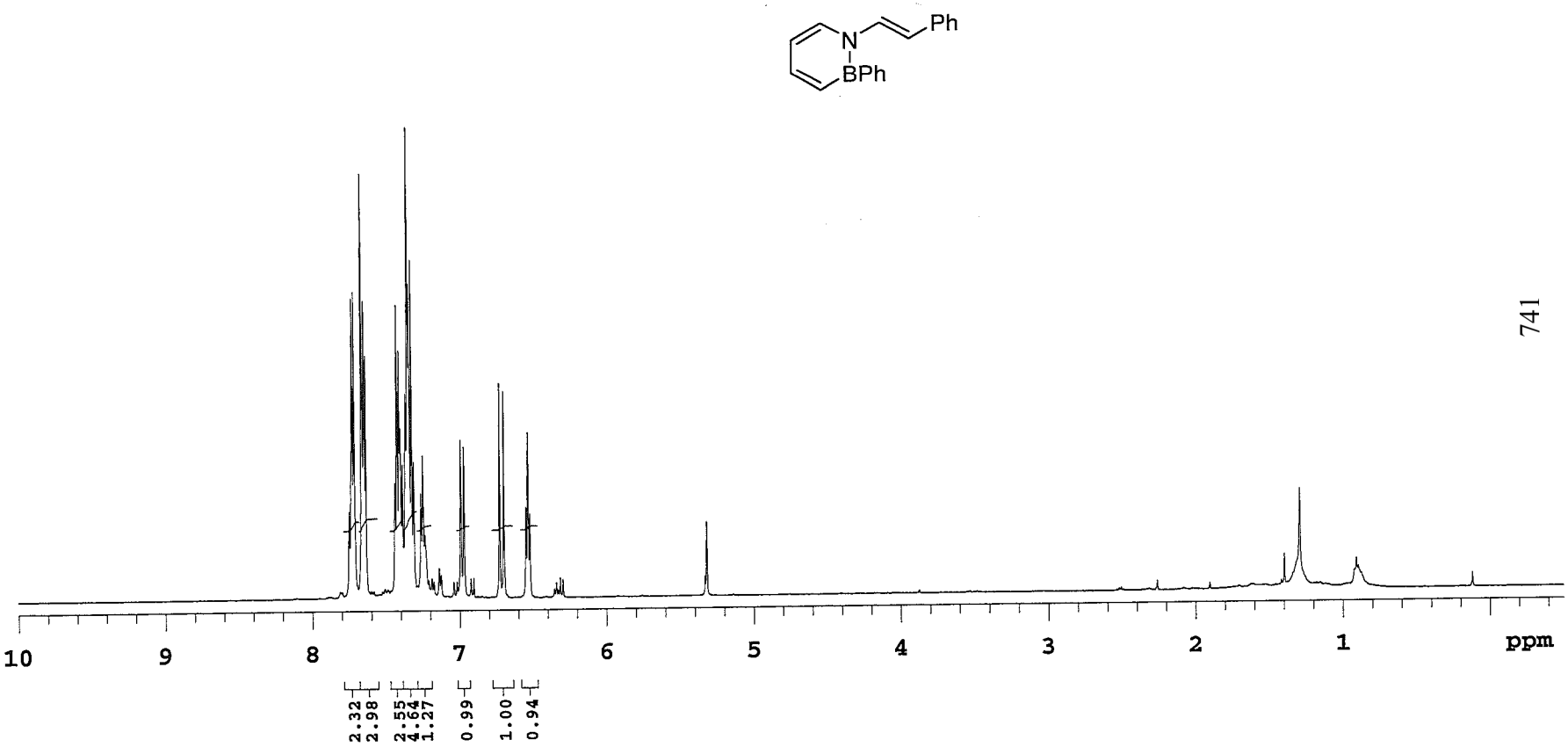

Data file /home/ALL/Liu/HL/N-Substitution/HL-III-226-1H.fid

Plot date 2016-07-13

HL-III-055-2-11B

Sample Name **HL-III-055-2-11B**	Pulse sequence **BORON_11**	Temperature **25**	Study owner **Liu**
Date collected **2015-12-19**	Solvent **cd2cl2**	Spectrometer **nmr18-vnmrs500**	Operator **Liu**

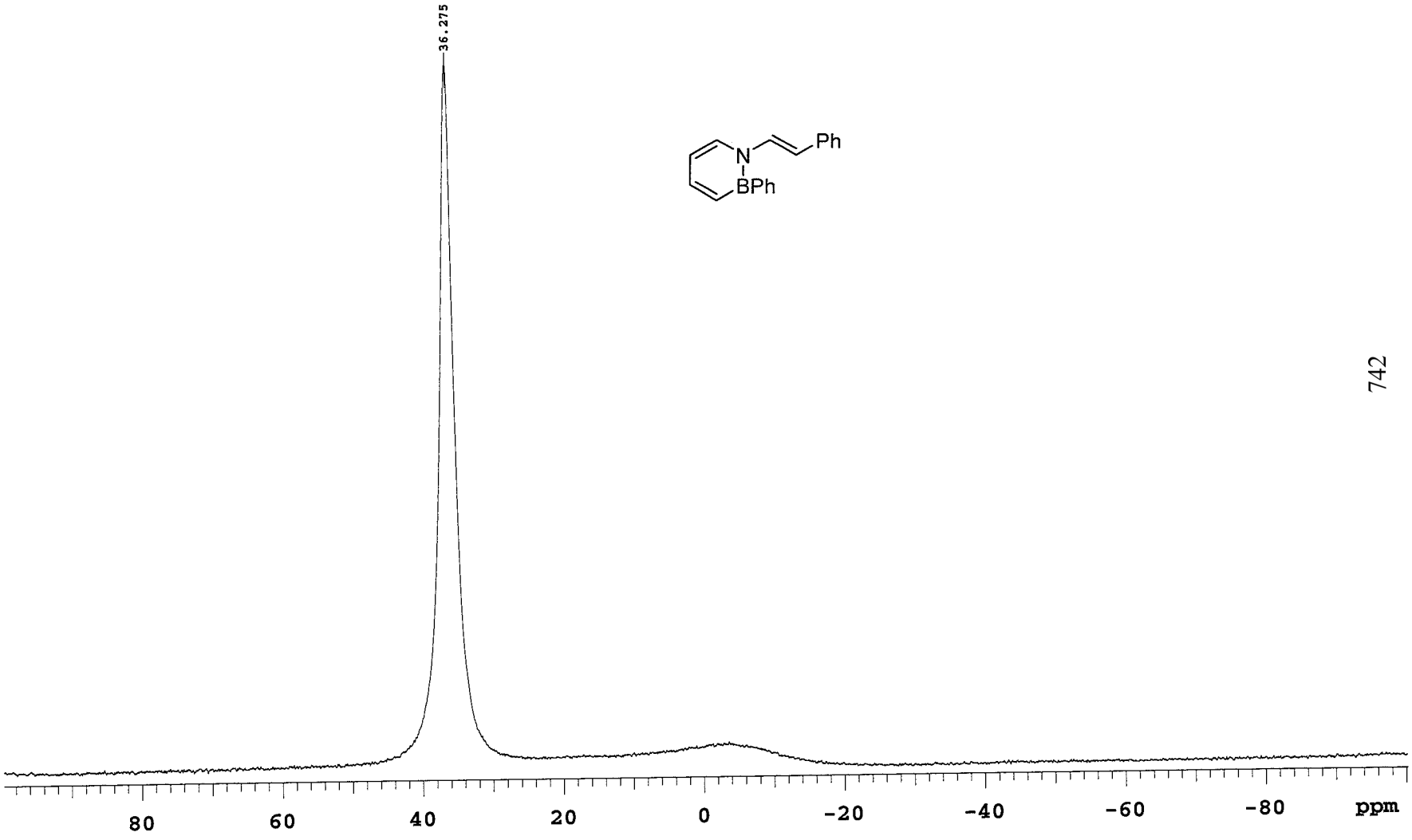

742

Data file /home/ALL/Liu/HL/N-Substitution/Table/HL-III-055-2-11B.fid

Plot date 2015-12-24

HL-III-055-pure-13C

Sample Name	**HL-III-055-pure-13C**	Pulse sequence	**CARBON**	Temperature	**25**	Study owner	**Liu**
Date collected	**2015-12-19**	Solvent	**cd2cl2**	Spectrometer	**nmr19-vnmrs600**	Operator	**Liu**

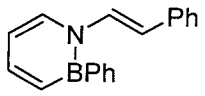

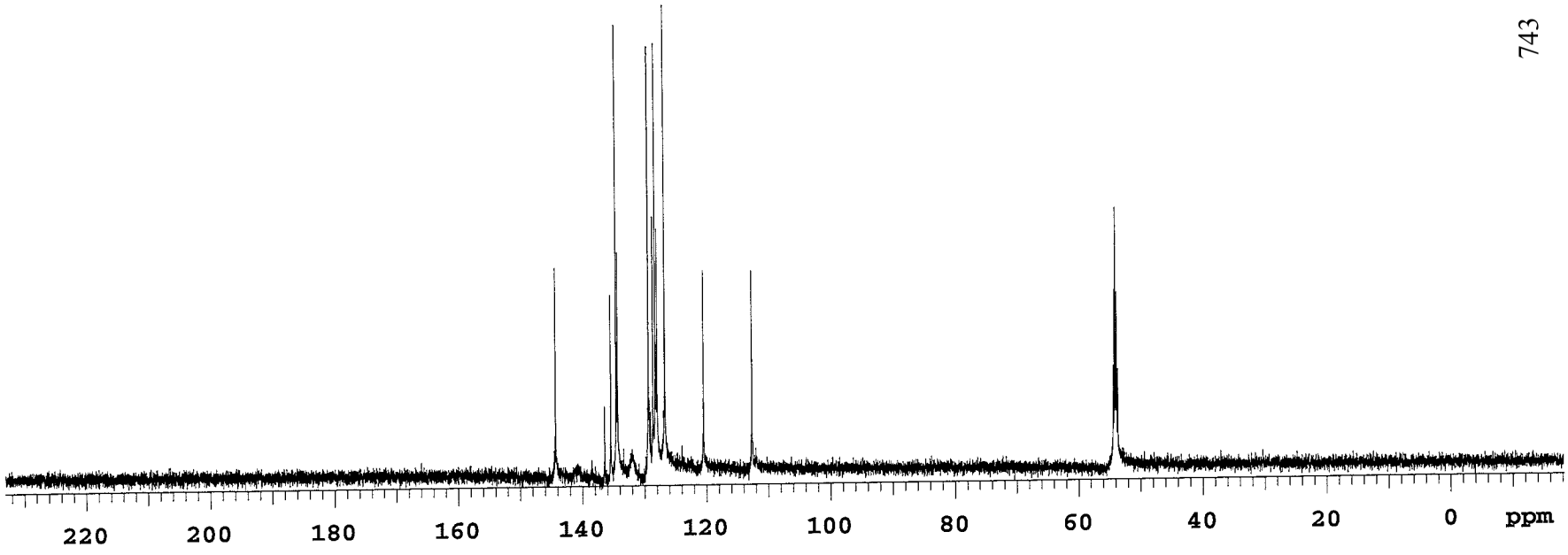

Data file /home/ALL/Liu/HL/N-Substitution/HL-III-055-pure-13C.fid

Plot date 2015-12-24

HL-III-162-1H

Sample Name	**HL-III-162-1H**	Pulse sequence	**PROTON**	Temperature	**25**	Study owner	**Liu**
Date collected	**2016-03-03**	Solvent	**cd2cl2**	Spectrometer	**nmr19-vnmrs600**	Operator	**Liu**

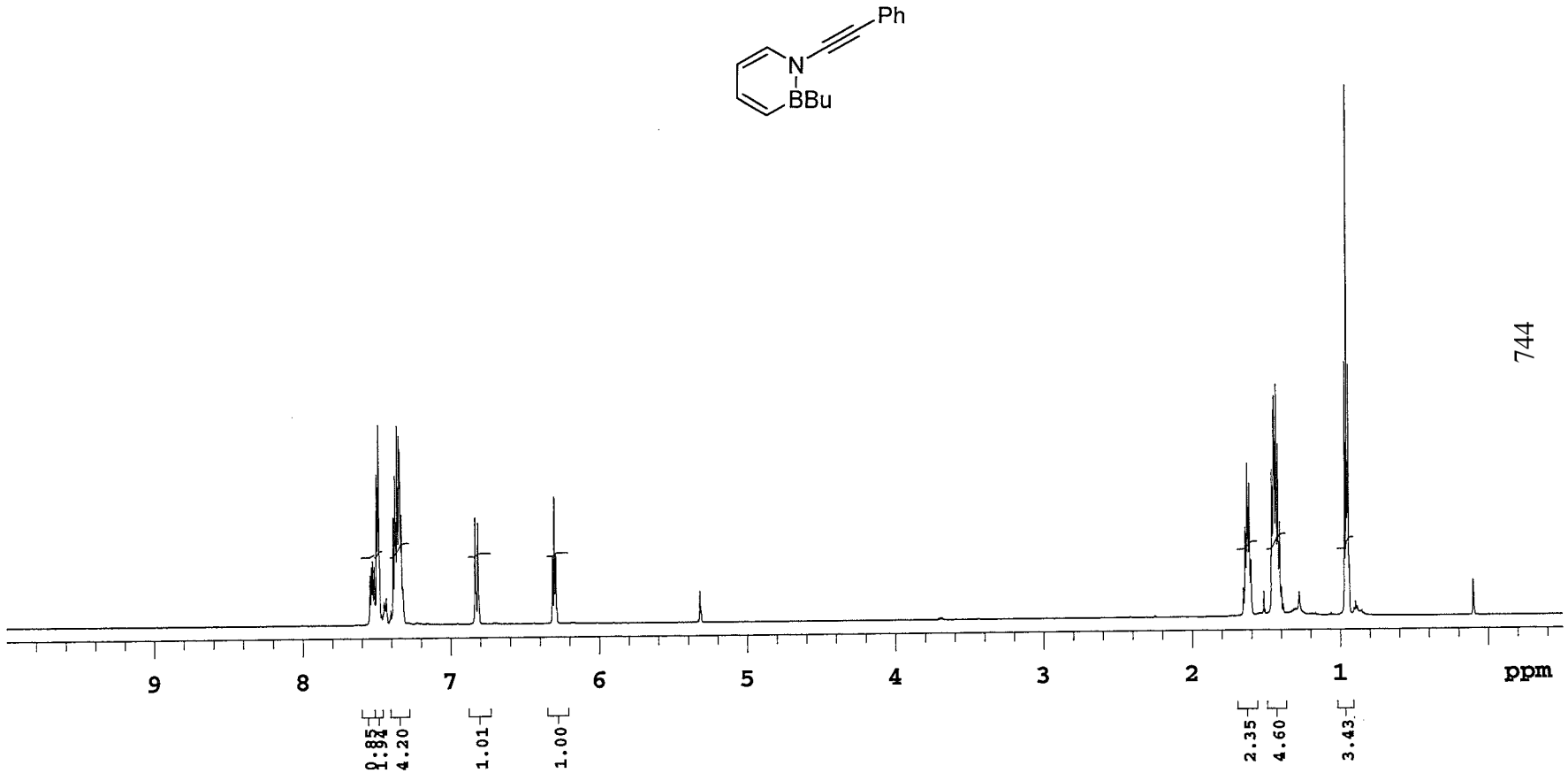

Data file /home/ALL/Liu/HL/N-Substitution/HL-III-162-1H.fid

Plot date 2016-06-15

HL-III-163-11B

Sample Name	**HL-III-163-11B**	Pulse sequence	**BORON_11**	Temperature	**25**	Study owner	**Liu**
Date collected	**2016-03-16**	Solvent	**cd2cl2**	Spectrometer	**nmr18-vnmrs500**	Operator	**Liu**

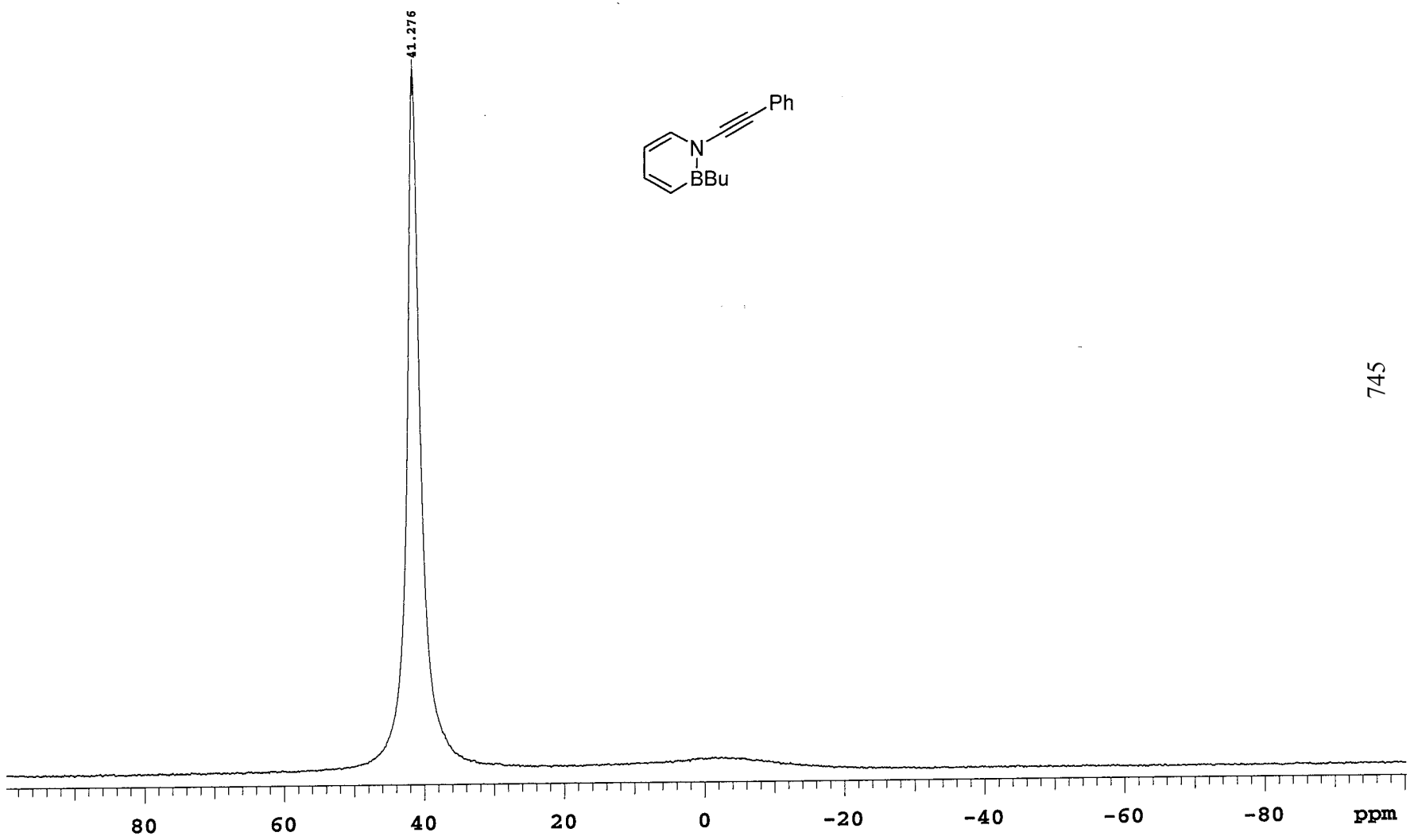

745

Data file /home/ALL/Liu/HL/N-Substitution/HL-III-163-11B.fid

Plot date 2016-06-15

HL-III-162-13C

Sample Name **HL-III-162-13C**	Pulse sequence **CARBON**	Temperature **25**	Study owner **Liu**
Date collected **2016-06-15**	Solvent **cd2cl2**	Spectrometer **nmr19-vnmrs600**	Operator **Liu**

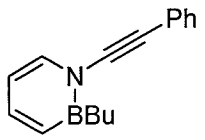

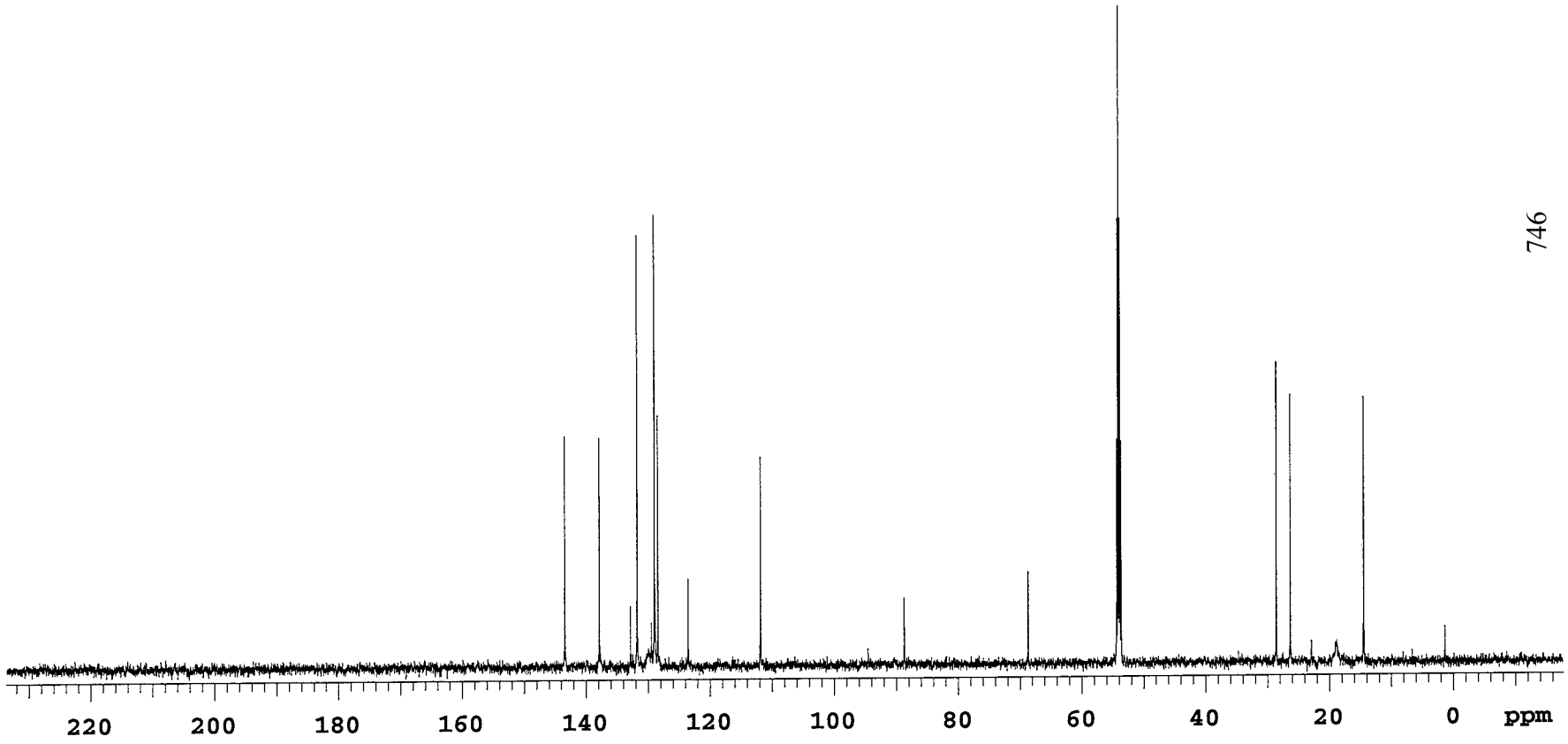

Data file /home/ALL/Liu/HL/N-Substitution/HL-III-162-13C.fid

Plot date 2016-06-15

HL-III-203-1H

Sample Name **HL-III-203-1H**	Pulse sequence **PROTON**	Temperature **25**	Study owner **Liu**
Date collected **2016-05-04**	Solvent **cd2cl2**	Spectrometer **nmr18-vnmrs500**	Operator **Liu**

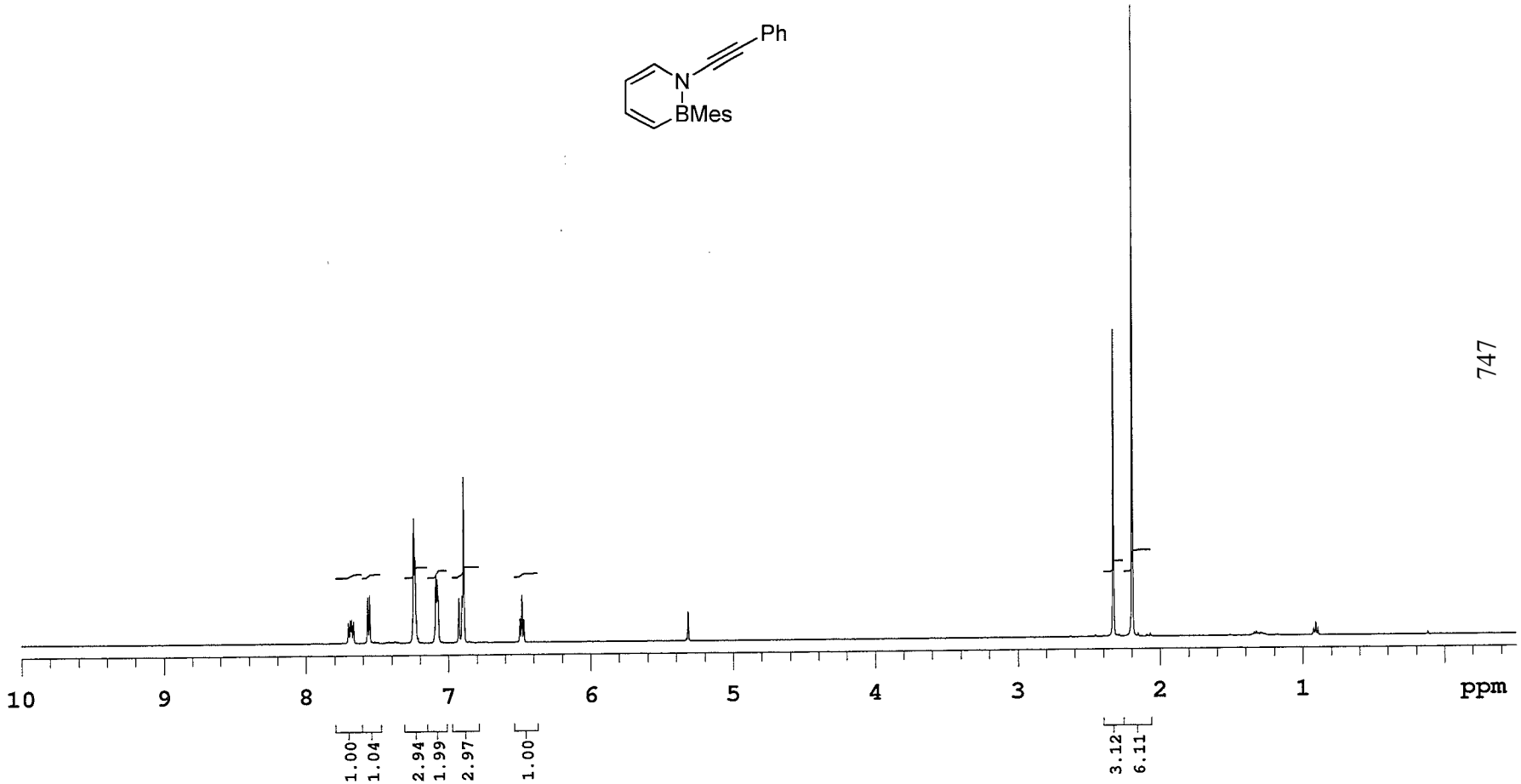

Data file /home/All/Liu/Hyelee Lee/HL-III-203-1H.fid

Plot date 2016-07-14

HL-III-203-11B

Sample Name	**HL-III-203-11B**	Pulse sequence	**s2pul**	Temperature	**25**	Study owner	**Liu**
Date collected	**2016-05-04**	Solvent	**cd2cl2**	Spectrometer	**nmr18-vnmrs500**	Operator	**Liu**

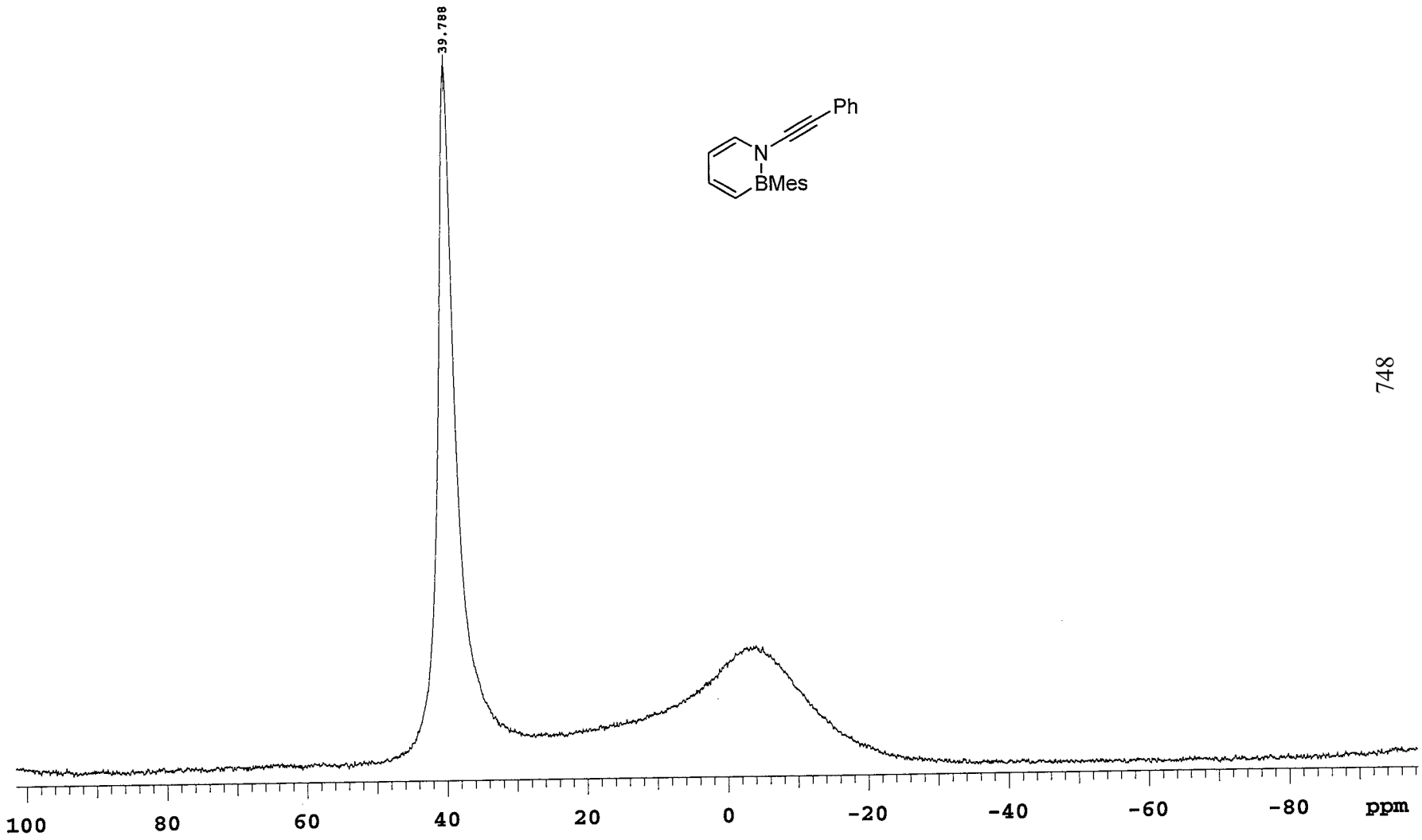

748

Data file /home/ALL/Liu/HL/N-Substitution/HL-III-203-11B.fid

Plot date 2016-06-16

HL-III-203-13C

Sample Name **HL-III-203-13C**	Pulse sequence **CARBON**	Temperature **25**	Study owner **Liu**
Date collected **2016-05-04**	Solvent **cd2cl2**	Spectrometer **nmr19-vnmrs600**	Operator **Liu**

STANDARD PROTON PARAMETERS

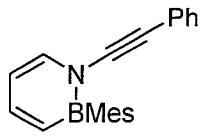

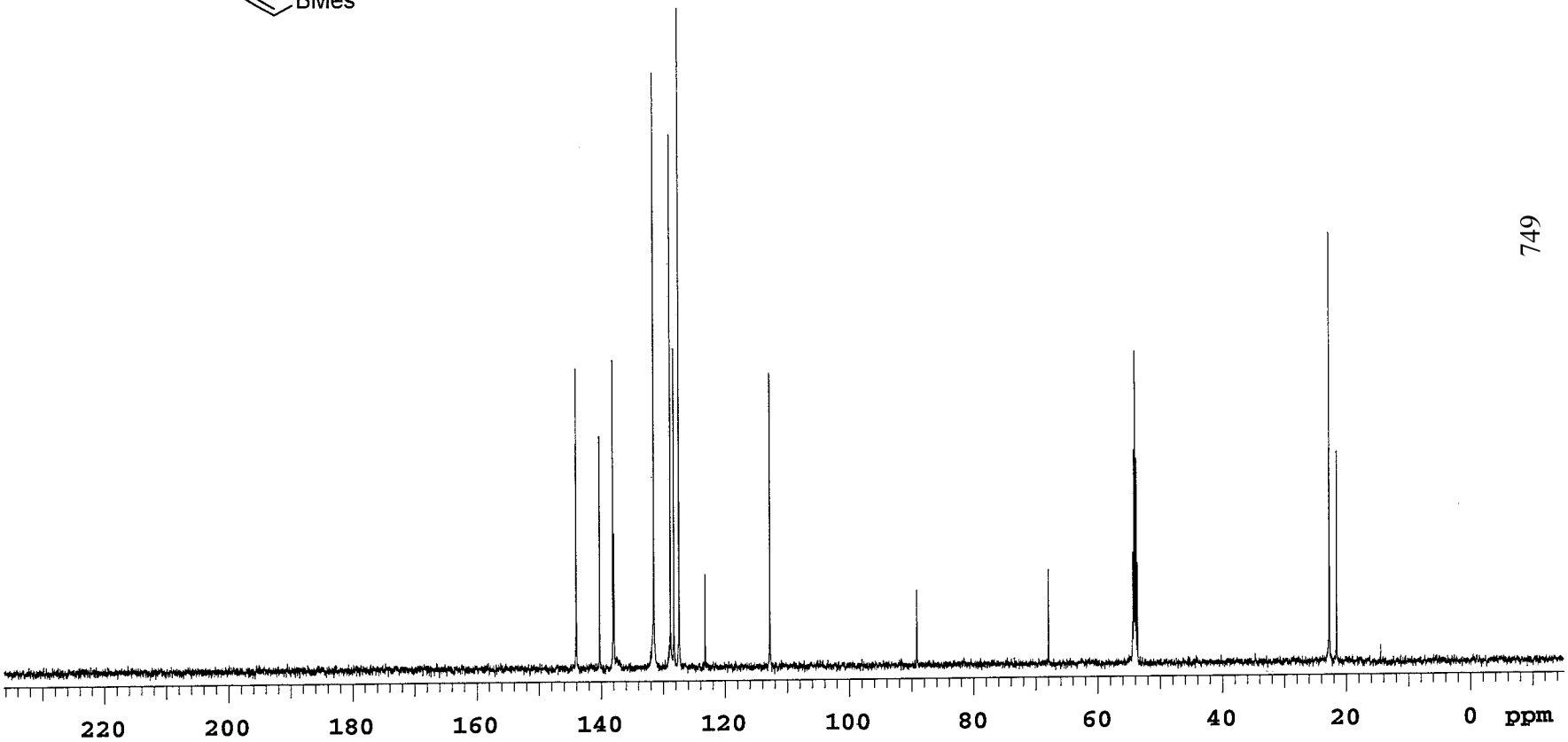

Data file /home/ALL/Liu/HL/N-Substitution/HL-III-203-13C.fid

Plot date 2016-06-16

HL-III-240-1H

Sample Name **HL-III-240-1H**	Pulse sequence **PROTON**	Temperature **25**	Study owner **Liu**
Date collected **2016-06-03**	Solvent **cd2cl2**	Spectrometer **nmr11-inova500**	Operator **Liu**

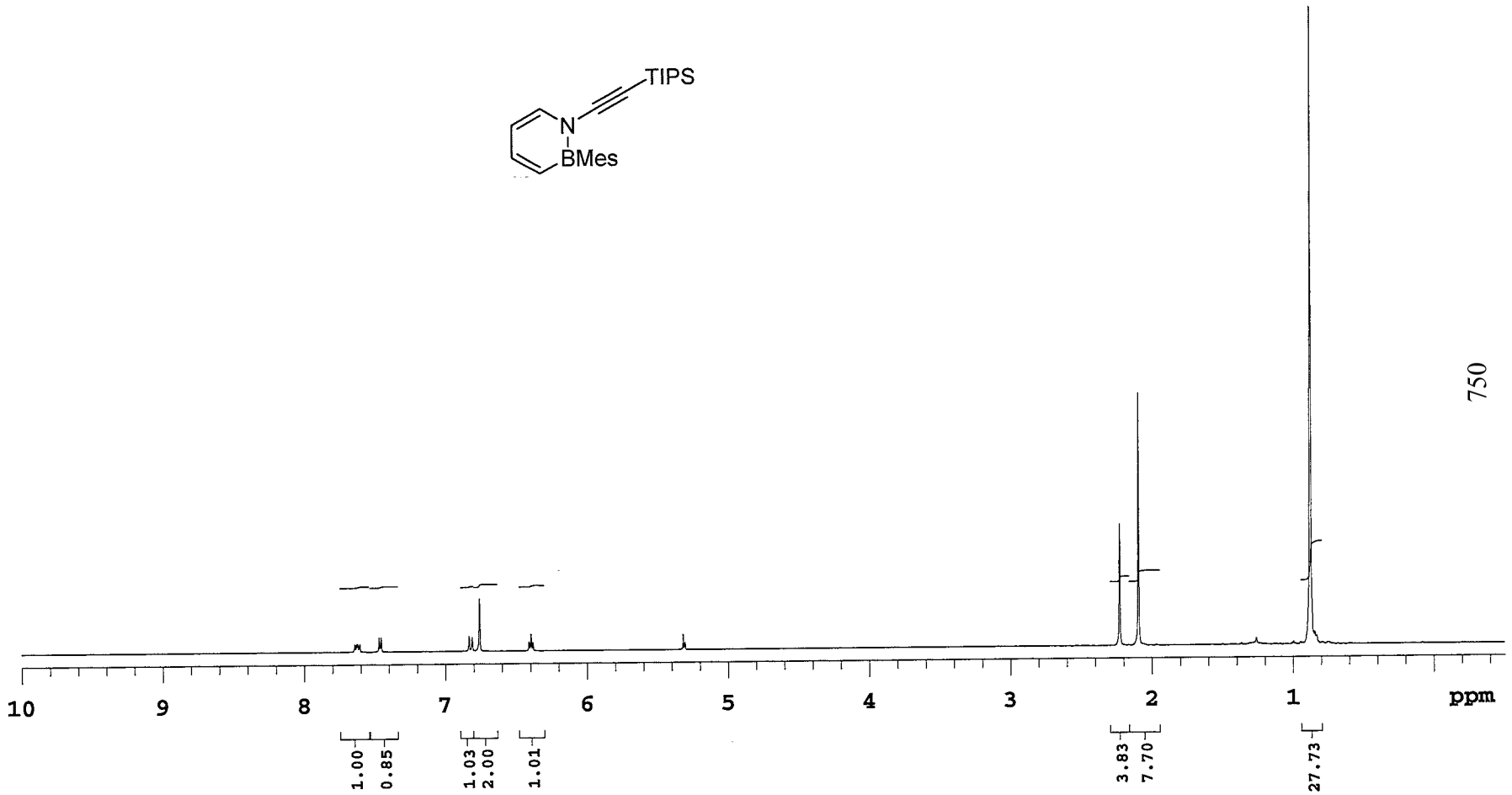

Data file /home/ALL/Liu/HL/N-Substitution/HL-III-240-1H.fid

Plot date 2016-06-15

HL-III-240-11B

Sample Name **HL-III-240-11B**	Pulse sequence **s2pul**	Temperature **25**	Study owner **Liu**
Date collected **2016-06-03**	Solvent **cd2cl2**	Spectrometer **nmr11-inova500**	Operator **Liu**

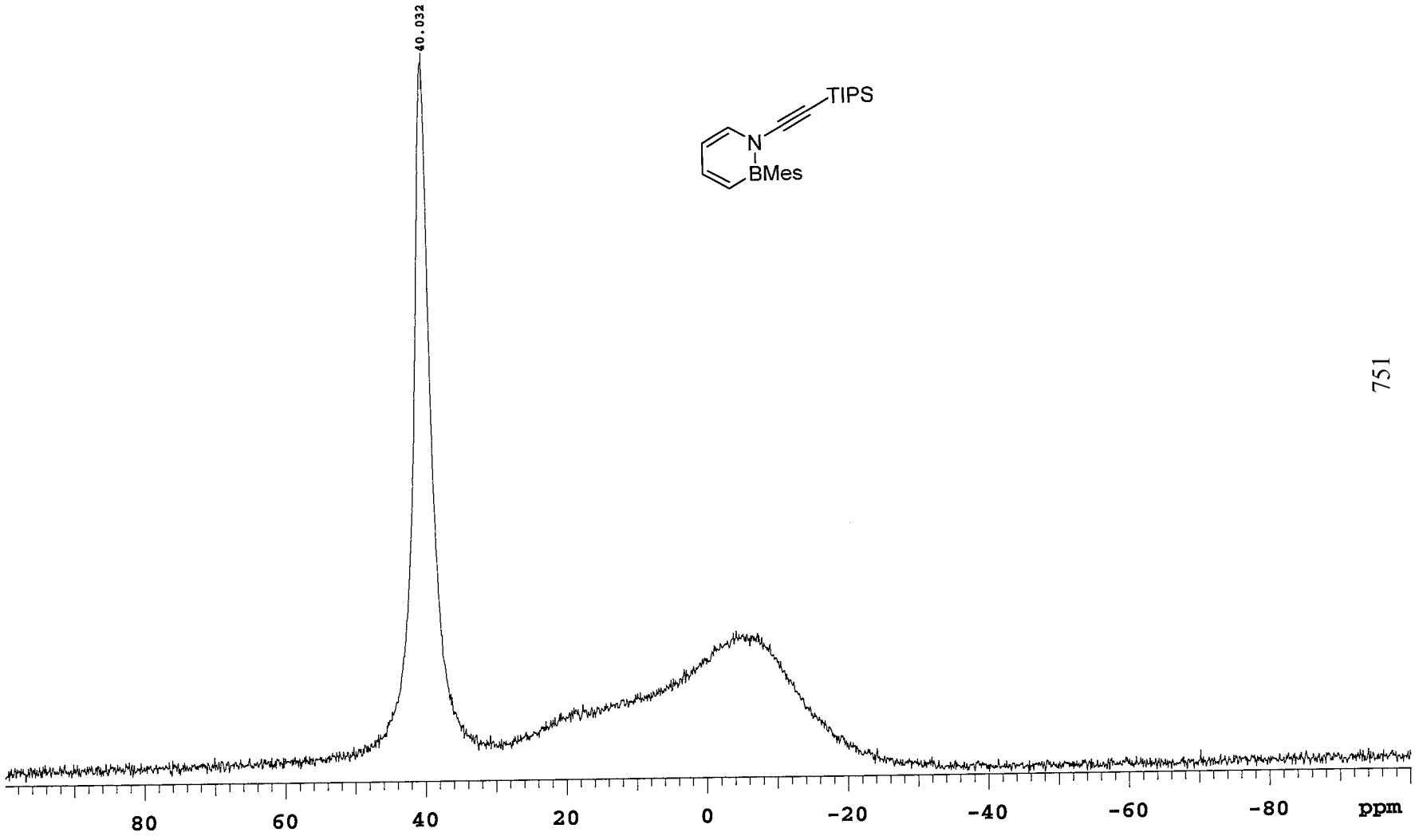

751

Data file /home/ALL/Liu/HL/N-Substitution/HL-III-240-11B.fid

Plot date 2016-06-15

HL-III-240-13C

Sample Name **HL-III-240-13C**	Pulse sequence **CARBON**	Temperature **25**	Study owner **Liu**
Date collected **2016-06-15**	Solvent **cd2cl2**	Spectrometer **nmr18-vnmrs500**	Operator **Liu**

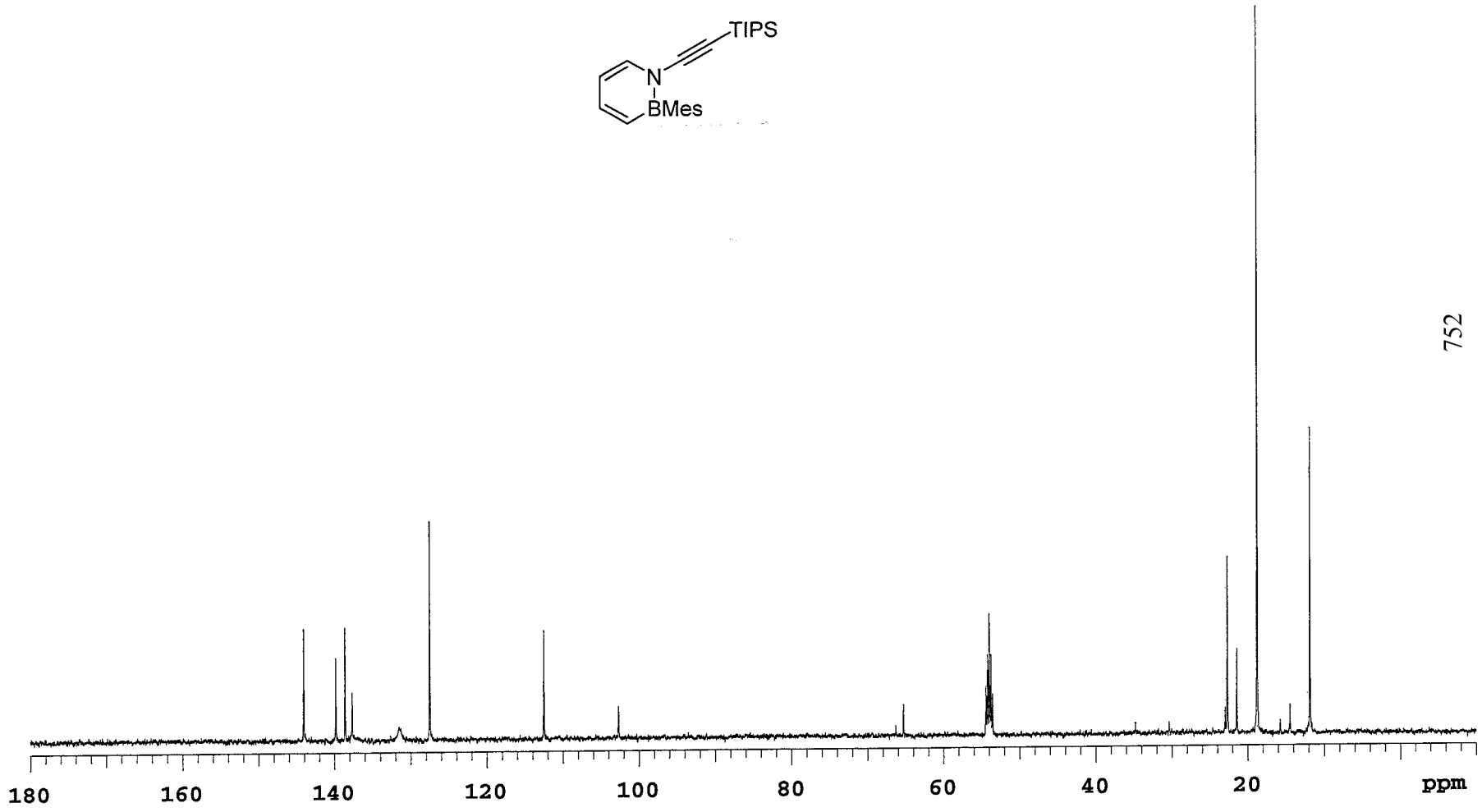

HL-III-188-3-1H

Sample Name	**HL-III-188-3-1H**	Pulse sequence	**PROTON**	Temperature	**25**	Study owner	**Liu**
Date collected	**2016-04-04**	Solvent	**cd2cl2**	Spectrometer	**nmr18-vnmrs500**	Operator	**Liu**

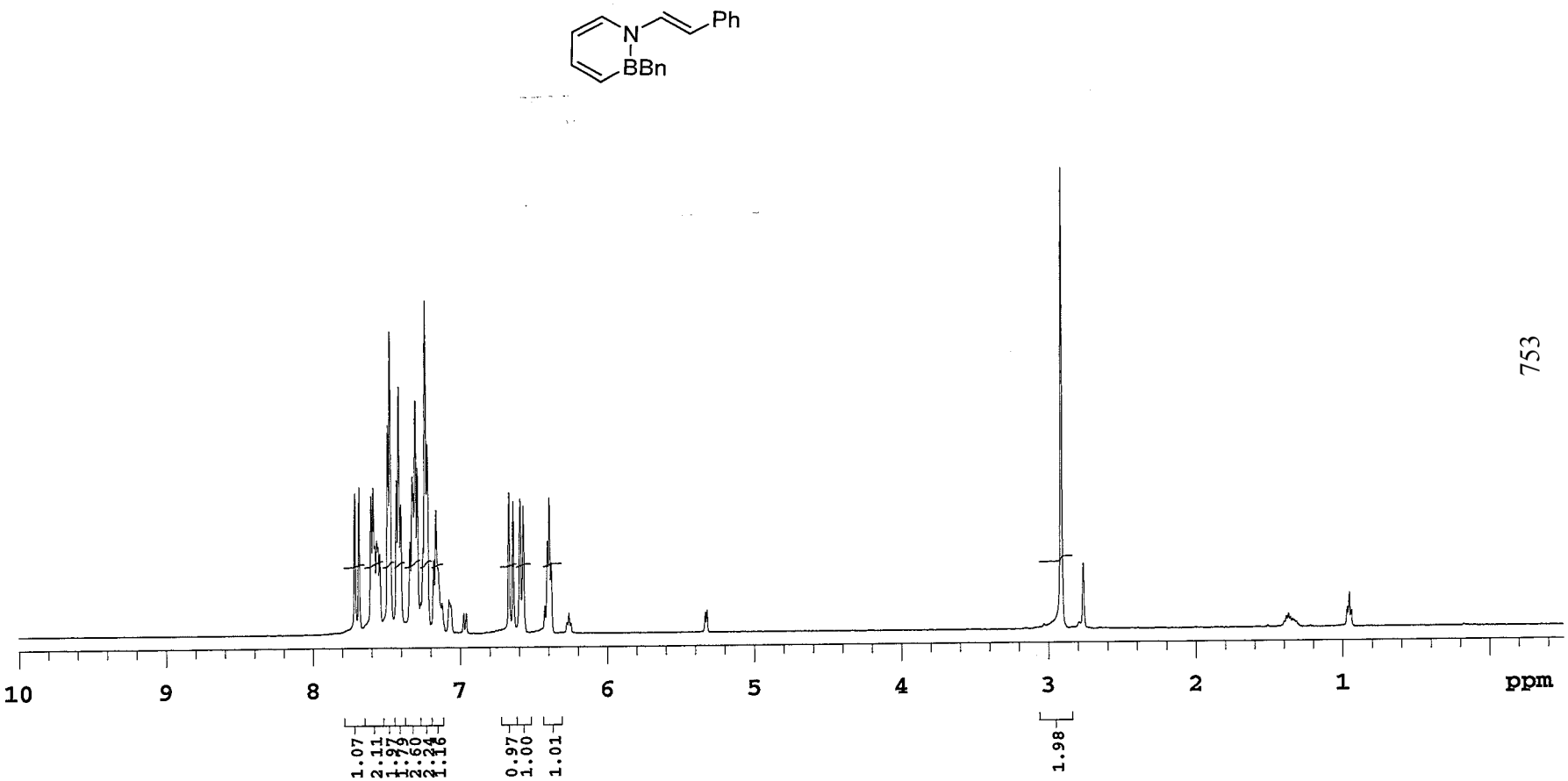

Data file /home/ALL/Liu/HL/N-Substitution/HL-III-188-3-1H.fid

Plot date 2016-07-21

HL-III-075-11B

Sample Name **HL-III-075-11B**	Pulse sequence **BORON_11**	Temperature **25**	Study owner **Liu**
Date collected **2015-12-24**	Solvent **cd2cl2**	Spectrometer **nmr18-vnmrs500**	Operator **Liu**

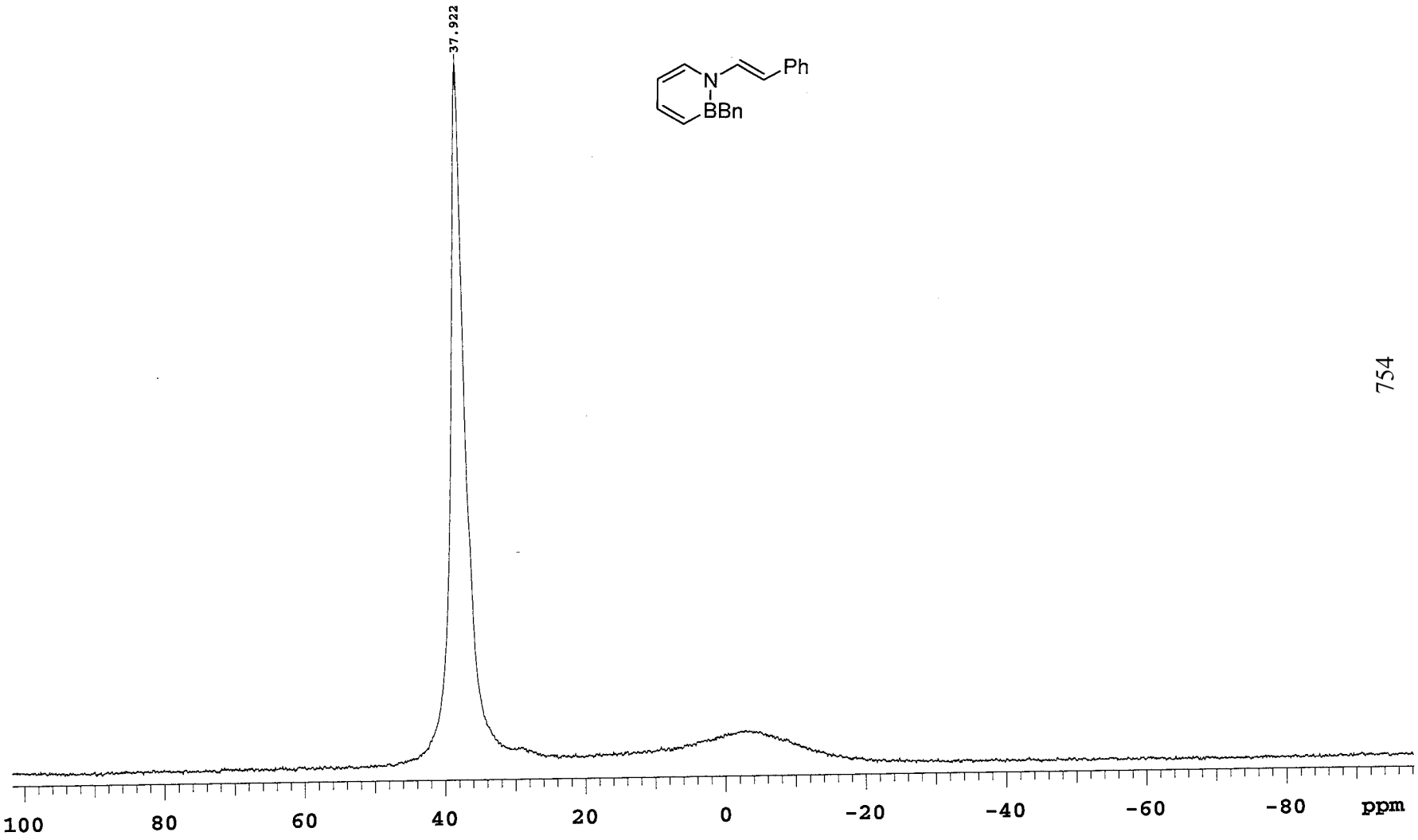

754

Data file /home/ALL/Liu/HL/N-Substitution/Table/HL-III-075-11B.fid

Plot date 2015-12-24

HL-III-188-3-13C

Sample Name	**HL-III-188-3-13C**	Pulse sequence	**CARBON**	Temperature	**25**	Study owner	**Liu**
Date collected	**2016-04-04**	Solvent	**cd2cl2**	Spectrometer	**nmr19-vnmrs600**	Operator	**Liu**

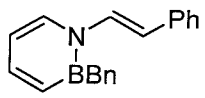

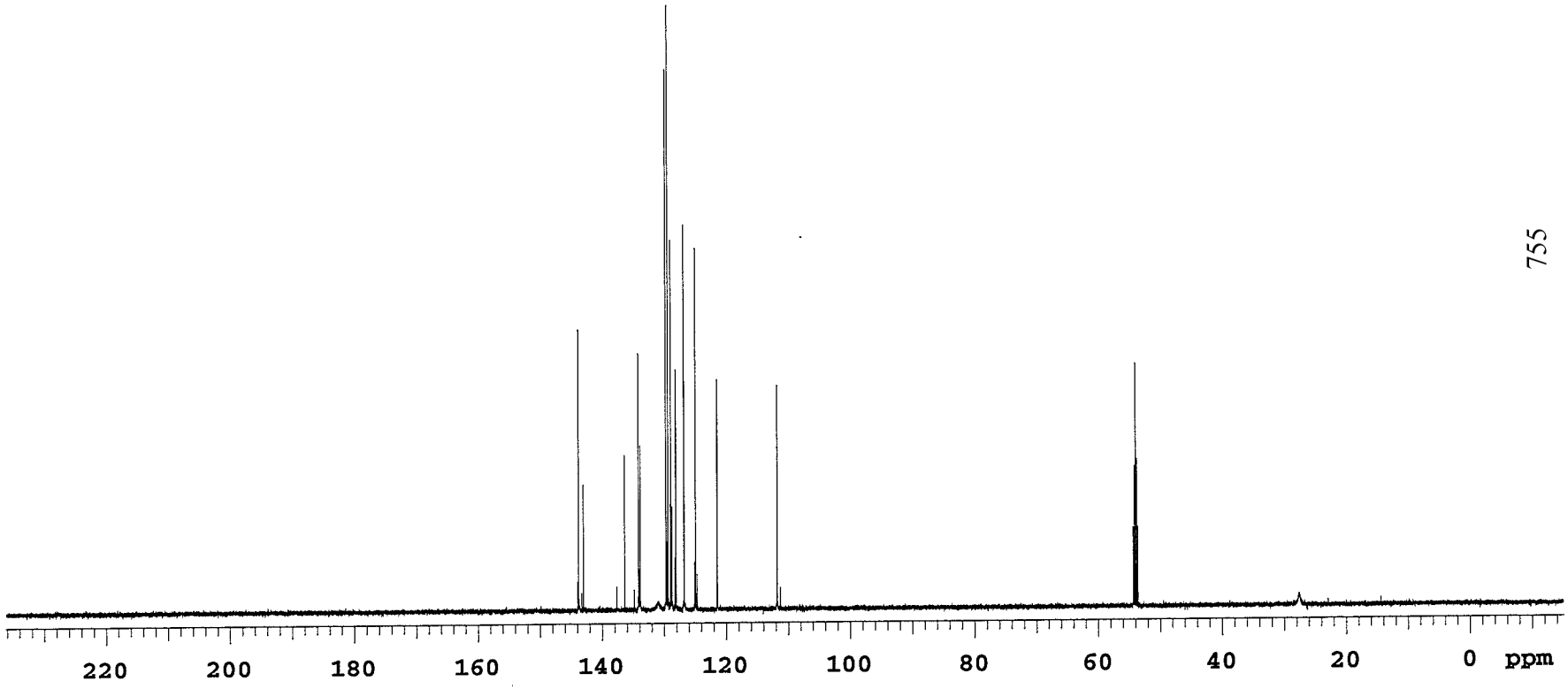

HL-III-128-1H

Sample Name	**HL-III-128-1H**	Pulse sequence	**PROTON**	Temperature	**25**	Study owner	**Liu**
Date collected	**2016-02-22**	Solvent	**cd2cl2**	Spectrometer	**nmr18-vnmrs500**	Operator	**Liu**

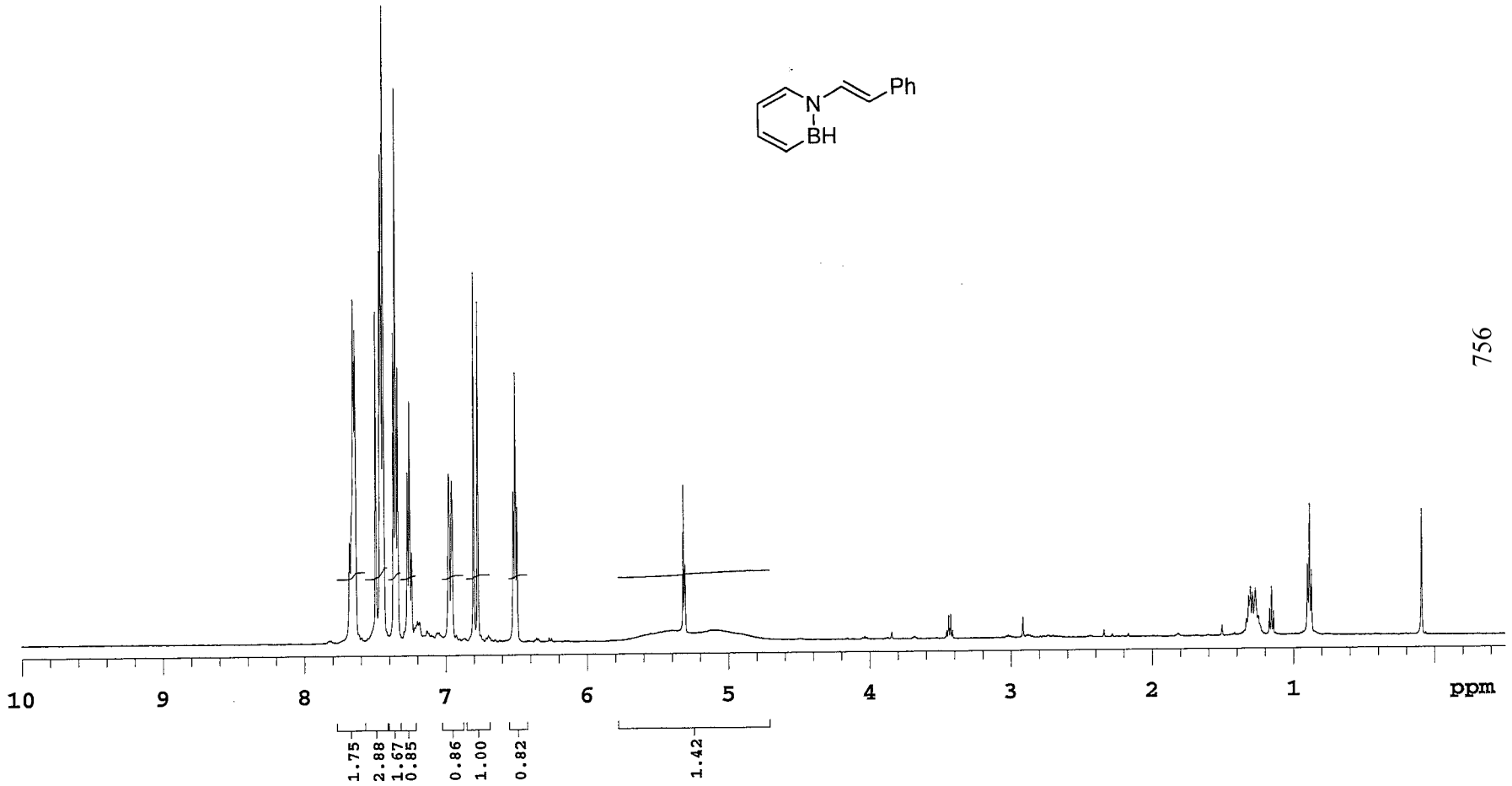

Data file /home/ALL/Liu/HL/N-Substitution/HL-III-128-1H.fid

Plot date 2016-11-03

HL-III-128-11B

Sample Name	**HL-III-128-11B**	Pulse sequence	**BORON_11**	Temperature	**25**	Study owner	**Liu**
Date collected	**2016-02-22**	Solvent	**cd2cl2**	Spectrometer	**nmr18-vnmrs500**	Operator	**Liu**

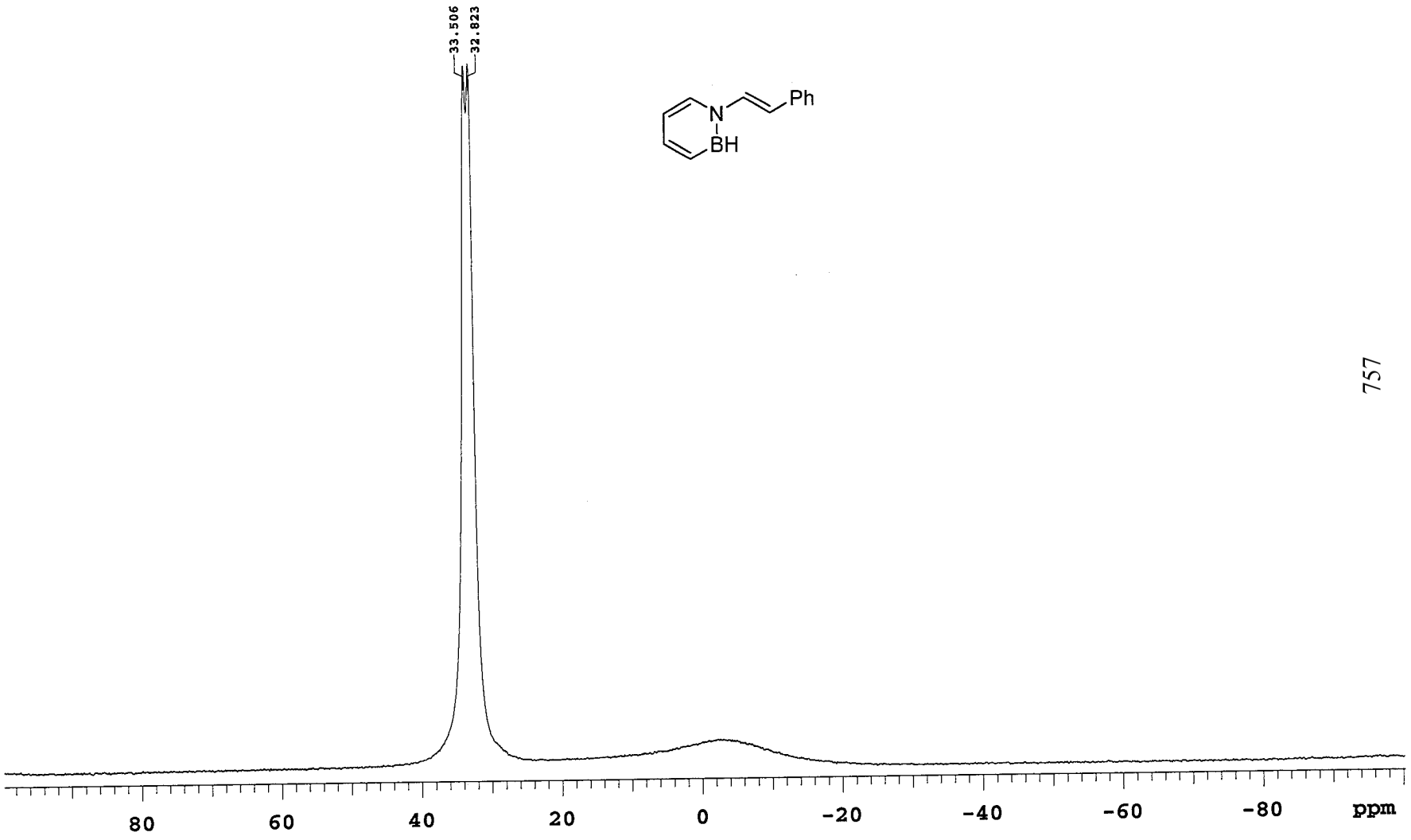

757

Data file /home/ALL/Liu/HL/N-Substitution/HL-III-128-11B.fid

Plot date 2016-05-15

HL-III-128-13C

Sample Name	**HL-III-128-13C**	Pulse sequence	**CARBON**	Temperature	**25**	Study owner	**Liu**
Date collected	**2016-02-22**	Solvent	**cd2cl2**	Spectrometer	**nmr19-vnmrs600**	Operator	**Liu**

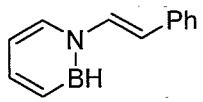

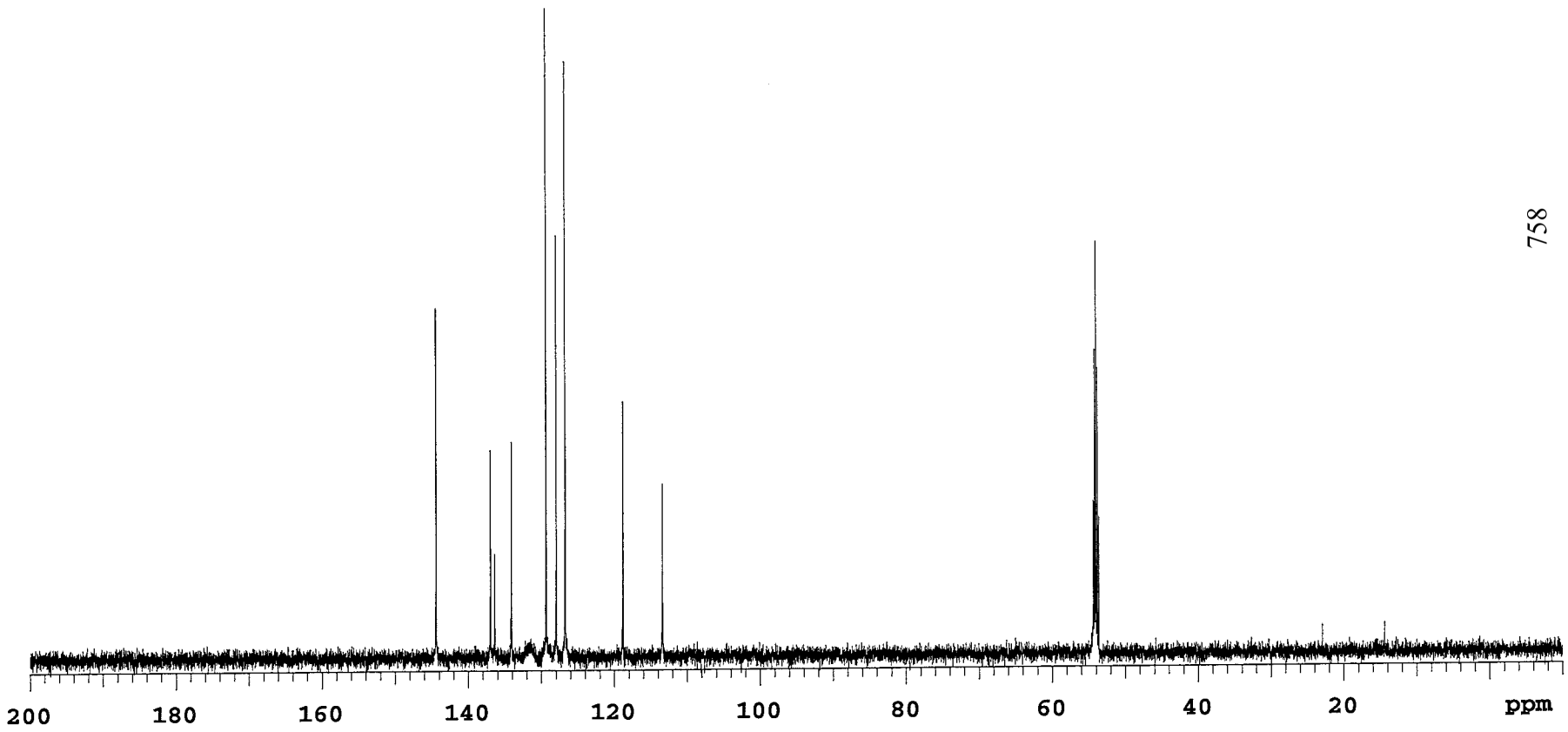

HL-III-273-1H

Sample Name **HL-III-273-1H**	Pulse sequence **PROTON**	Temperature **25**	Study owner **Liu**
Date collected **2016-07-13**	Solvent **cd2cl2**	Spectrometer **nmr18-vnmrs500**	Operator **Liu**

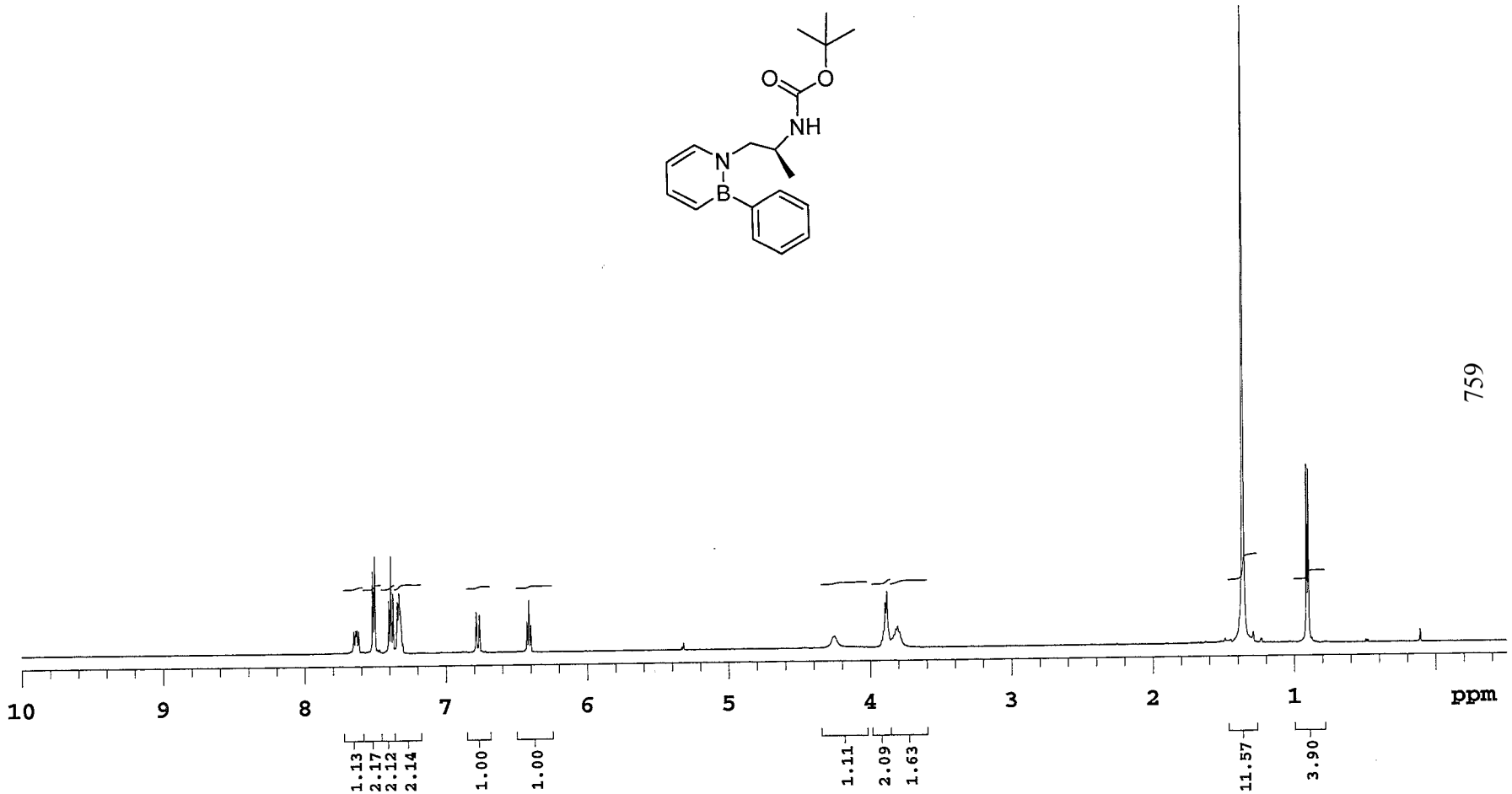

Data file /home/ALL/Liu/HL/N-Substitution/HL-III-273-1H.fid

Plot date 2016-07-13

HL-III-242-11B

Sample Name	**HL-III-242-11B**	Pulse sequence	**s2pul**	Temperature	**25**	Study owner	**Liu**
Date collected	**2016-06-08**	Solvent	**cd2cl2**	Spectrometer	**nmr18-vnmrs500**	Operator	**Liu**

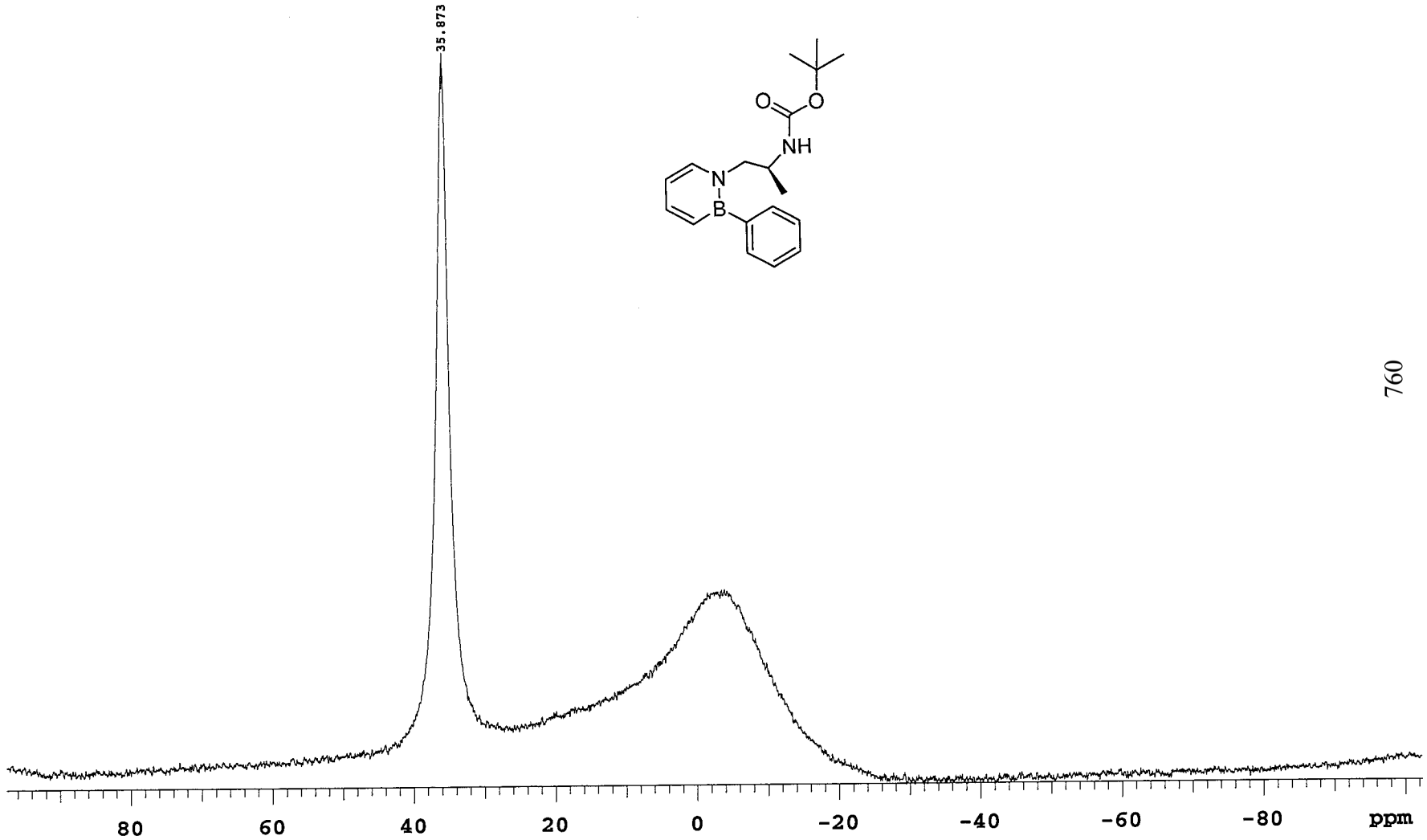

Data file /home/ALL/Liu/HL/N-Substitution/HL-III-242-11B.fid

Plot date 2016-06-15

HL-III-242-13C

Agilent Technologies

Sample Name	HL-III-242-13C	Pulse sequence	CARBON	Temperature	25	Study owner	Liu
Date collected	2016-07-02	Solvent	cd2cl2	Spectrometer	nmr18-vnmrs500	Operator	Liu

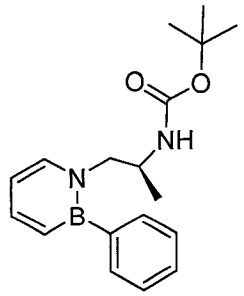

761

Data file exp

Plot date 2016-07-02

HL-III-269-crystal-1H

Sample Name	**HL-III-269-crystal-1H**	Pulse sequence	**PROTON**	Temperature	**25**	Study owner	**Liu**
Date collected	**2016-08-18**	Solvent	**thf**	Spectrometer	**nmr18-vnmrs500**	Operator	**Liu**

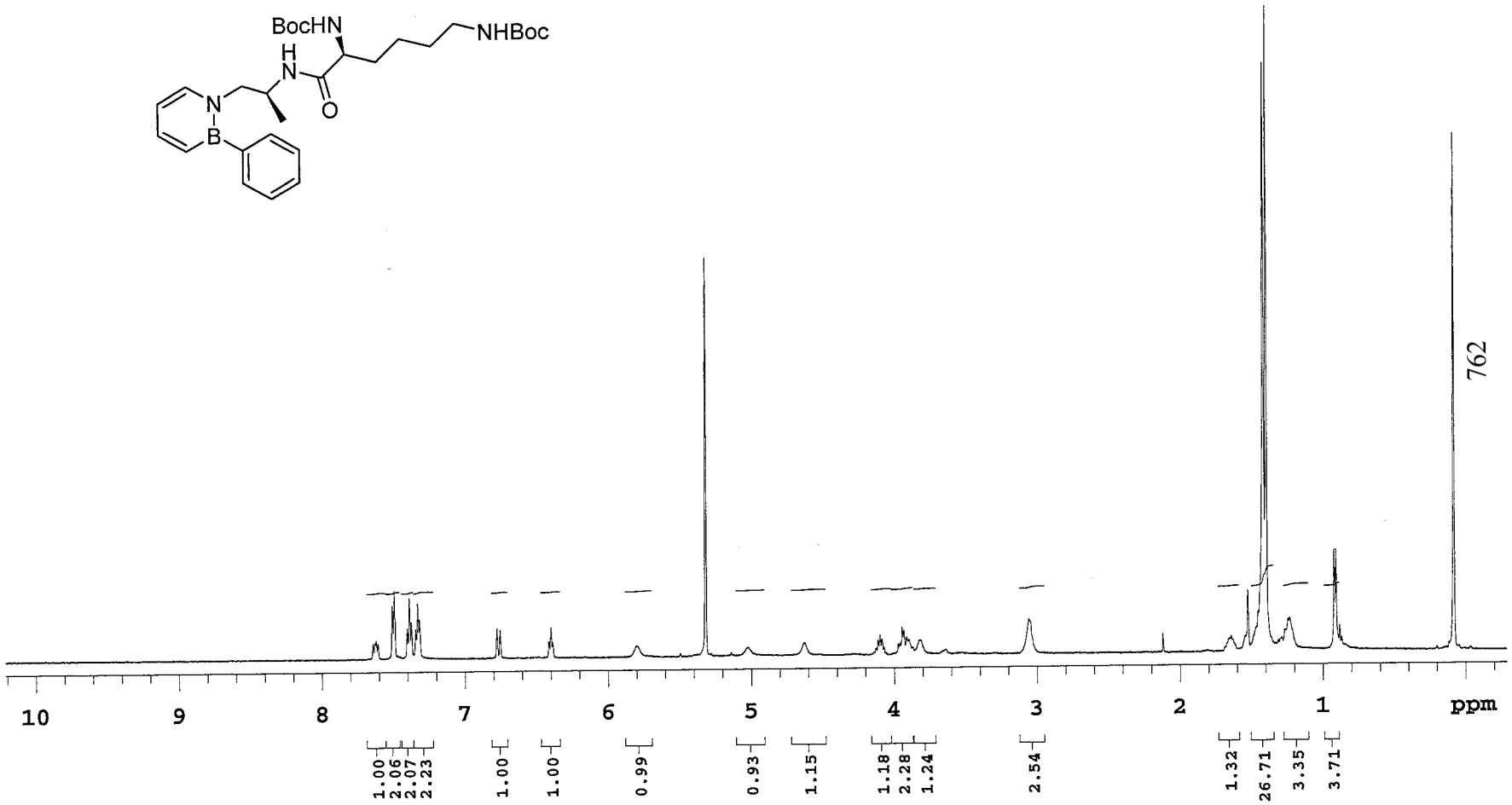

Data file /home/ALL/Liu/HL/N-Substitution/HL-III-269-crystal-1H.fid

Plot date 2016-11-03

HL-III-269-11B

Sample Name **HL-III-269-11B**	Pulse sequence **s2pul**	Temperature **25**	Study owner **Liu**
Date collected **2016-07-07**	Solvent **cd2cl2**	Spectrometer **nmr11-inova500**	Operator **Liu**

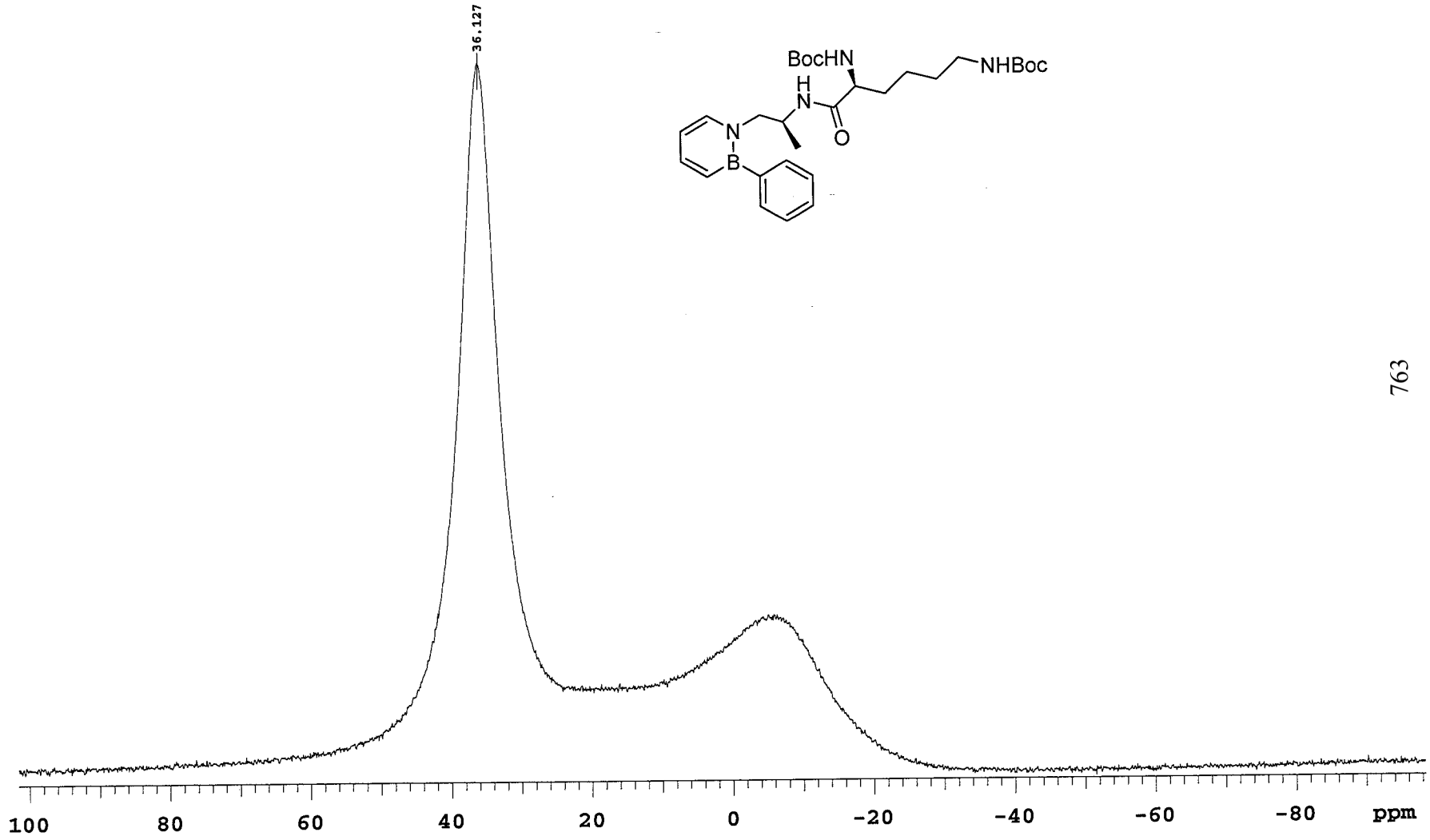

763

Data file /home/ALL/Liu/HL/HL-III-269-11B.fid

Plot date 2016-07-07

HL-III-269-13C

Agilent Technologies

Sample Name	HL-III-269-13C	Pulse sequence	CARBON	Temperature	25	Study owner	Liu
Date collected	2016-07-07	Solvent	cd2cl2	Spectrometer	nmr18-vnmrs500	Operator	Liu

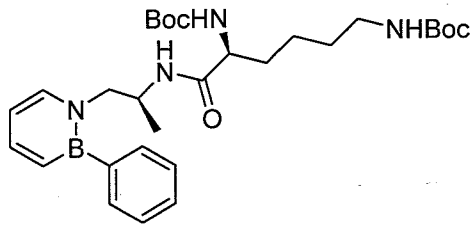

764

Data file exp

Plot date 2016-07-07